Concessionaria per la progettazione, realizzazione e gestione del collegamento stabile tra la Sicilia e il Continente Organismo di Diritto Pubblico
(Legge n° 1158 del 17 dicembre 1971, modificata dal D.Lgs. n°114 del 24 aprile 2003)

PONTE SULLO STRETTO DI MESSINA

PROGETTO DEFINITIVO

EUROLINK S.C.p.A.

IMPREGILO S.p.A. (MANDATARIA)
SOCIETÀ ITALIANA PER CONDOTTE D'ACQUA S.p.A. (MANDANTE)
COOPERATIVA MURATORI E CEMENTISTI - C.M.C. DI RAVENNA SOC. COOP. A.R.L. (MANDANTE)
SACYR S.A.U. (MANDANTE)
ISHIKAWAJIMA - HARIMA HEAVY INDUSTRIES CO. LTD (MANDANTE)
A.C.I. S.C.P.A. - CONSORZIO STABILE (MANDANTE)

IL PROGETTISTA	IL CONTRAENTE GENERALE	STRETTO DI MESSINA	STRETTO DI MESSINA
COWI Ing. E.M. Veje Dott. Ing. E. Pagani Ordine Ingegneri Milano n° 15408 EurolinK	Project Manager (Ing. P.P. Marcheselli)	Direttore Generale e RUP Validazione (Ing. G. Fiammenghi)	Amministratore Delegato (Dott. P. Ciucci)

Unità Funzionale	OPERA DI ATTRAVERSAMENTO	PB0033_F0
Tipo di sistema	STUDI DI BASE	
Raggruppamento di opere/attività	STUDI AERODINAMICI	
Opera - tratto d'opera - parte d'opera	Generale	
Titolo del documento	Prove in galleria del vento, torri	

CODICE: C G 1 0 0 0 P R G D P S B S 3 0 0 0 0 0 0 0 0 0 1 F0

REV	DATA	DESCRIZIONE	REDATTO	VERIFICATO	APPROVATO
F0	20/06/2011	EMISSIONE FINALE	ADME	ALN	ALN/EYA

NOME DEL FILE: PB0033_F0_ITA.doc

INDICE

1 Relazione di sintesi

Prove in galleria del vento del modello sezionale sono state condotte con un modello in scala 1:100 della struttura della torre del Ponte sullo stretto di Messina al fine di determinare i coefficienti di carico da vento in relazione al progetto strutturale e per fornire una valutazione indicativa degli effetti del vento sulle torre, come vibrazioni indotte da vortice e stabilità aerodinamica.

Prove su modello aeroelastico sono state inoltre condotte in scala 1:200 in due diverse strutture di galleria del vento, al fine di esaminare gli effetti del vento e verificare la risposta della torre al flusso di vento di strato limite. Il punto di interesse principale dell'indagine condotta al The Boundary Layer Wind Tunnel Laboratory (BLWTL), presso la University of Western Ontario in Canada, era quello di verificare il comportamento della torre secondo quanto riscontrato al BMT Fluid Mechanics, Inghilterra.

Uno degli obiettivi principali delle prove in galleria del vento era quello di individuare il livello di smorzamento strutturale necessario al fine di mitigare la risposta di distacco dei vortici.

Le prove dettagliate della struttura delle torri, hanno condotto alle seguenti conclusioni:

- Con un flusso calmo, il modello sezionale della torre ha mostrato oscillazioni indotte dal vortice nel range di velocità non- dimensionale del vento 5 < V/fbB < 10.0.
- La risposta RMS per il modello sezionale della torre può essere mitigata incrementando il livello di smorzamento strutturale.
- Il modello sezionale della torre è aerodinamicamente stabile fino, e al di sopra della massima velocità di progetto alla punta della torre.
- I coefficienti di carico da vento statico sembrano essere indipendenti dal numero di Reynolds per il modello sezionale in scala 1:100 nel range di velocità del vento testato ed esso resta immutato con turbolenza.
- Le vibrazioni indotte da vortice per il modello aeroelastico della torre sono osservate sia nel grado di libertà di piegamento che di torsione.
- La risposta aeroelastica della torre riscontrata a BMT è pressoché inalterata dalla turbolenza, mentre le indagini BLWTL indicano che la turbolenza risulta generalmente in una riduzione della magnitudo dei picchi indotti da distacco dei vortici, ma con velocità di

vento superiori, le risposte al buffeting incrementano. L'intensità della turbolenza al BLWTL era maggiore di circa il 3%.

- La risposta di distacco dei vortici del modello aeroelastico della torre - configurazione in-service, lungo gli assi del ponte, modalità di piegamento primaria - è stata misurata per tutte le configurazioni fra 0° e 20° per velocità di vento inferiori rispetto alla velocità di vento di progetto.
- Incrementando il livello di smorzamento strutturale della modalità di piegamento fino al 4% rispetto alla criticità, per la configurazione in-service della torre, la risposta può essere mitigata ad un livello di accelerazione RMS di circa 0.5 m/s2, come richiesto dalle specifiche.

2 Geometria delle Torri e Caratteristiche Dinamiche

Il modello di torre preso in esame per i sub-test T1, T2 e T3 inclusi nel programma di prove in galleria del vento. Figura 1, è identico a quello presentato nel Progetto d'Offerta ad eccezione dell'altezza delle torri che è stata aumentata di 16,4 m (Progetto Definitivo). Le due torri a doppia gamba, entrambe a sezione ottagonale costante, sono inclinate verso l'interno sulla sommità , Figura 2.

Figura 1 Lato sinistro: geometria sezionale della torre verificata nel tunnel del vento, lato destro: geometria sezionale del traverso.

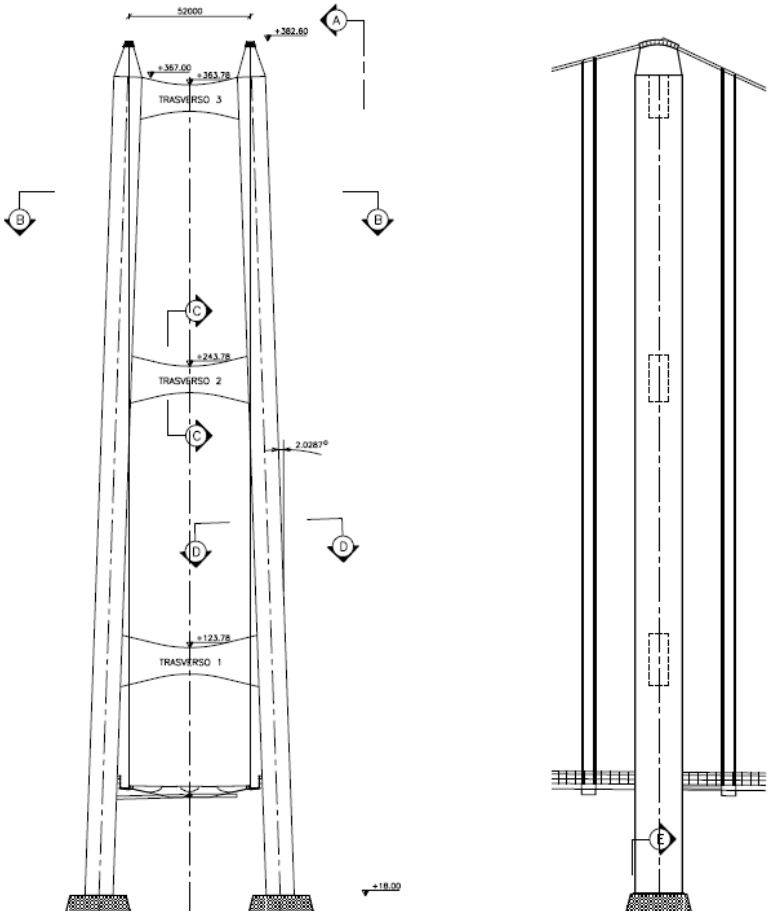

Figura 2 Geometria della torre verificata in galleria del vento, vista lungo ed attraverso l'impalcato.

2.1 Sub-test T1 e T2, modello sezionale

I sub-test T1 e T2 effettuati in galleria del vento sul modello della torre sono stati eseguiti presso la BMT Fluid Mechanics UK. L'assetto delle prove ed i risultati sono riportati in [1].

Il modello delle gambe delle torri del Ponte sullo Stretto di Messina è stato costruito in scala geometrica di 1:λ_L = 1:100 generando una larghezza delle gambe B = 20 m / 100 = 0,2 m. Le verifiche vengono eseguite in una galleria del vento della larghezza di 2,7m con sezioni trasversali di una gamba e un insieme di sezioni trasversali delle due gambe rappresentative del 70% dell'intera altezza delle torri.

Una foto del modello delle gambe è riportata in Figura 3.

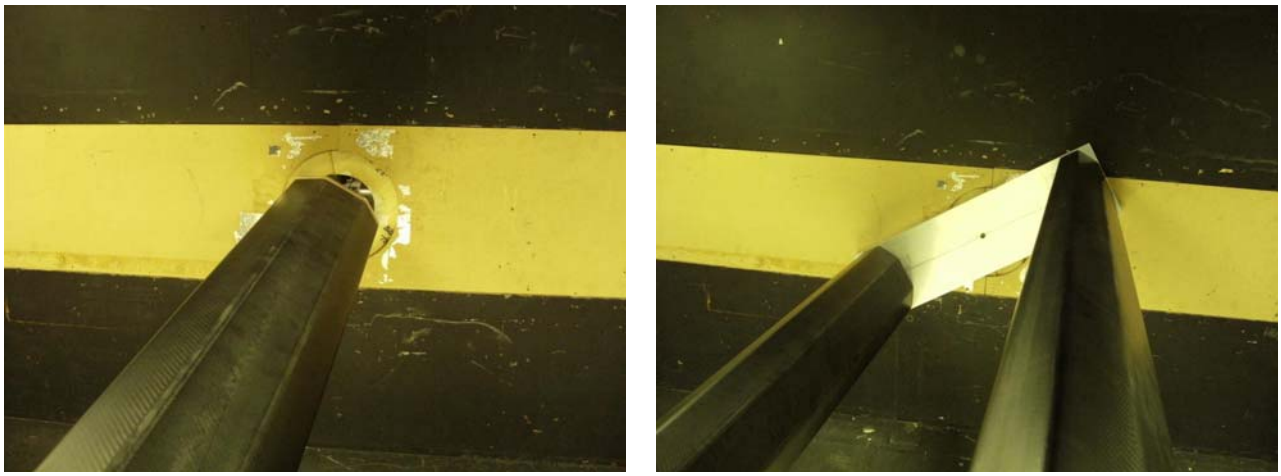

Figura 3 Modello sezionale della torre in scala 1:100. Il lato sinistro della figura mostra la configurazione di una sola gamba, quello destro il sistema a due gambe .

2.1.1 Rappresentazione su scala dinamica del modello sezionale in galleria del vento

Un insieme di considerazioni sulla geometria, la massa e la robustezza ha portato alla scelta di una scala geometrica di λ_L = 1:100 per il modello della torre del Ponte di Messina. Il modello a sezione lunga rappresenta 270 m di torre e tutti i dettagli geometrici che si pensa abbiano un'influenza sull'aerodinamica della struttura. Per le prove statiche si può applicare solo la scala geometrica.

2.2 Sub-test T3, Modello aeroelastico

Il sub-test T3 sul modello della torre in galleria del vento è stato effettuato presso la BMT Fluid Mechanics ed il The Boundary Layer Wind Tunnel Laboratory BLWTL. L'assetto di prova ed i risultati sono riportati rispettivamente in [2] e [3].

2.2.1 Prove BMT

La verifica del modello della torre del Ponte sullo Stretto di Messina è stata eseguita presso la BMT in galleria del vento allo stato limite su una sezione trasversale di 4,8x2,4m. Per garantire una

descrizione precisa degli effetti del vento ed una verifica della risposta della torre sono stati testati tre modelli differenti. I modelli sono geometricamente identici alle diverse caratteristiche dinamiche.

Sono state verificate quattro condizioni strutturali

- Torre finita, posizione verticale
- Torre finita, fissata sulla sommità per simulare l'effetto dei cavi principali prima dell'installazione dell'impalcato
- Fase di costruzione subito prima del montaggio del traverso superiore
- Torre finita, condizione in service, fissata sulla sommità per simulare l'effetto del cavo principale, con impalcato installato

Le caratteristiche dinamiche dei modelli tipo ed aeroelastico sono riportate in [2], Appendice B.

Una foto del modello sezionale della torre presso BMT è rappresentata in Figura 4.

Figura 4 Modello aeroelastico completo prima delle prove BMT. A sinistra, la torre in verticale a destra la torre in service fissata in sommità.

2.2.2 Prove BLWTL

I modelli aeroelastici completi della torre del ponte sono stati studiati presso la sezione di prova principale dello stato limite di BLWT II. Sono stati progettati e costruiti due modelli aeroelastici completi, un modello Froude ed un modello in scala non Froude.

Le prove comprendono le misurazioni della risposta del modello aeroelastico completo al vento calmo ed a quello turbolento su due configurazioni:

- Torre finita, posizione verticale
- Torre finita, fissata alla sommità per simulare gli effetti dei cavi principali e del tiro all'indietro.

Le caratteristiche dinamiche dei modelli tipo ed aeroelastico sono riportate in [3].

2.2.3 Rappresentazione in scala dinamica del modello aeroelastico completo in galleria del vento

Le configurazioni di prova sono state verificate usando modelli aeroelastici in scale differenti. Un insieme di considerazioni sulla geometria, la massa e la robustezza ha portato alla scelta di una scala geometrica di λ_L = 1:200 per tutti i modelli di torre aeroelastici del Ponte di Messina.

Le specifiche SdM richiedono che le prove su modello con un sistema aeroelastico obbediscano alla rappresentazione in scala di Froude. Ciò significa che il rapporto tra le frequenze del modello e le frequenze tipo venga indicato come radice quadrata della scala geometrica $f_m / f_p = \sqrt{\lambda_L}$, il che richiede a sua volta che le velocità tipo del vento vengano ottenute sotto forma di velocità del vento del modello moltiplicate per la radice quadrata della scala geometrica $V_p = V_m \cdot \sqrt{\lambda_L}$.

Mentre la rappresentazione in scala di Froude è una condizione necessaria per la corretta rappresentazione dei sistemi fluido/struttura nei quali la gravità gioca un ruolo significativo, come nel caso del modello aeroelastico completo di un ponte sospeso, tale rappresentazione non è richiesta per un modello sezionale elasticamente sospeso in galleria del vento che funziona indipendentemente dalla gravità. L'analisi dimensionale delle forze importanti che agiscono sul modello sezionale elastico dimostra che il rapporto di frequenza f_m / f_p può essere scelto indipendentemente dalla scala geometrica e che le velocità tipo del vento vengono ottenute sotto forma di velocità del vento del modello moltiplicate per la scala geometrica e l'inverso della frequenza $V_p = V_m \, \lambda_L \cdot f_p / f_m = V_m \cdot \lambda_V$.

Per il presente sub-test T3, la BMT e la BLWTL hanno scelto rispettivamente il fattore di scala della velocità del vento λ_V = 4.1 e λ_V = 6.0 per le prove di stabilità onde garantire il pieno utilizzo del campo delle velocità della galleria del vento e quindi dei numeri di Reynolds più alti possibili.

Per le prove del distacco dei vortici presso la BMT, il fattore di scala λ_V = 2.2 della velocità del vento è stato scelto per garantire che il distacco dei vortici venisse captato in presenza di velocità in galleria del vento superiori a 2 m/s.

Per le prove del distacco dei vortici in-service è stata scelta la rappresentazione in scala di Froude indicando λ_V = 14,2 per il modo di flessione .

3 Risultati, Sub-test T1

Il sub-test T1 è stato suddiviso in tre parti conformemente allo scopo, vale a dire una fase di distacco dei vortici avente lo scopo di identificare gli effetti del vento sul modello della torre, una fase di smorzamento per verificare l'effetto dell'aumentato smorzamento strutturale e una fase di verifica in grado di documentare la stabilità aerodinamica della configurazione della torre a due gambe.

Sono state verificate configurazioni diverse di gamba della torre come indicato in [2], Tabella 2.2. La mitigazione dell'eccitazione di distacco dei vortici viene realizzata aumentando lo smorzamento strutturale.

3.1 Risposta indotta dai vortici

Le oscillazioni indotte dai vortici della gamba della torre in flusso calmo sono state misurate per entrambe le configurazioni, gamba singola e doppia, in corrispondenza di ciascun angolo di attacco.

Le misurazioni sono state eseguite variando la velocità del vento nel campo non dimensionale $1{,}0 < V/f_bB < 10$ con incrementi di ca. 1,0. Alle velocità del vento, alle quali il modello sezionale mostrava una risposta oscillatoria, gli incrementi di velocità sono stati ridotti per garantire la captazione dell'intero campo di sincronizzazione.

In flusso calmo, il modello sezionale della torre ha mostrato delle oscillazioni indotte dai vortici nel campo di velocità del vento non dimensionale $5 < V/f_bB < 10.0$.

Nella configurazione ad una sola gamba, il peggior caso di spostamento rms di ca. 1,16 m con un livello di smorzamento di 0,1% rispetto alla criticità si verifica in corrispondenza dell'angolo di attacco 0º e 5º.

Le ampiezze misurate per una configurazione a due gambe sono maggiori di quelle della configurazione ad una gamba. A 0º, con livello di smorzamento di 0,1% rispetto alla criticità, la doppia gamba ha raggiunto un'ampiezza di 1,54m.

3.2 Mitigazione della risposta indotta dai vortici

Per mitigare l'eccitazione di distacco dei vortici, ad entrambe le configurazioni è stato aggiunto uno smorzamento strutturale supplementare mediante pala in rame supportata dai bracci del banco di prova dinamico, tra i poli dell'elettromagnete. Variando l'alimentazione di corrente all'elettromagnete si possono ottenere livelli differenti di smorzamento.

A 0º, con configurazione ad una sola gamba, gli spostamenti RMS vengono ridotti a 0,24m con livello di smorzamento del 2% rispetto alla criticità, mentre con configurazione a due gambe gli spostamenti RMS a 5° vengono ridotti a 0,13m con livello di smorzamento del 2,5% rispetto alla criticità.

3.3 Stabilità aerodinamica

La velocità critica del vento di T1 nella configurazione della torre a due gambe è stata misurata per angoli di attacco tra 0^0 e 90^0 in flusso calmo (I = 0.3%) usando lo stesso banco di prova dinamico applicato nelle prove di distacco dei vortici ed è riportata in [1].

Dai risultati si evince che la sezione della torre a due gambe T1 è stabile dal punto di vista aerodinamico a velocità del vento di fondo scala in flusso calmo fino alla e al di sopra della massima velocità di progetto di $80ms^{-1}$ sulla sommità della torre.

4 Risultati, Sub-test T2

Le configurazioni delle gambe della torre sono state sottoposte alle prove di carico da vento in flusso calmo ($I_{u,w}$ = 0,3%) e in flusso turbolento (I_u = 4,8% and I_v = 3,7%) per la verifica della prestazione aerodinamica [1]. Queste prove comprendono:

. Configurazione ad una ed a due gambe, misurazione dei coefficienti di carico del vento C_L, C_D, C_M quali funzioni dell'angolo di attacco η.

4.1 Coefficienti di carico del vento

I coefficienti di carico del vento vengono definiti come forza di portanza e di resistenza $F_{L,D}$ e come momento di ribaltamento F_M che agiscono sul modello sezionale reso non dimensionale tramite normalizzazione con carico dinamico $½\rho V^2$, e larghezza del modello della torre B (portanza e resistenza) o larghezza della torre al quadrato B^2:

$$C_{L,D} = \frac{F_{L,D}}{\frac{1}{2}\rho V^2 B}$$

$$C_M = \frac{F_M}{\frac{1}{2}\rho V^2 B^2}$$

La misurazione di verifica di C_L, C_D, C_M è stata eseguita con il modello sezionale sospeso in una bilancia di forza a 6 componenti ad alta frequenza. I tracciati di C_L, C_D, C_M rispetto all'angolo di attacco nel campo $0^0 < \eta < 90^0$ ottenuti in flusso calmo e turbolento estratti da [1], figura 3.2 sono indicati in Angolo del vento (gradi) Angolo del vento (gradi)

Figura 5 **Errore. L'origine riferimento non è stata trovata.** e Angolo del vento (gradi)

Angolo del vento (gradi)

Figura 6.

T2 calmo T2 turbolento

Medio

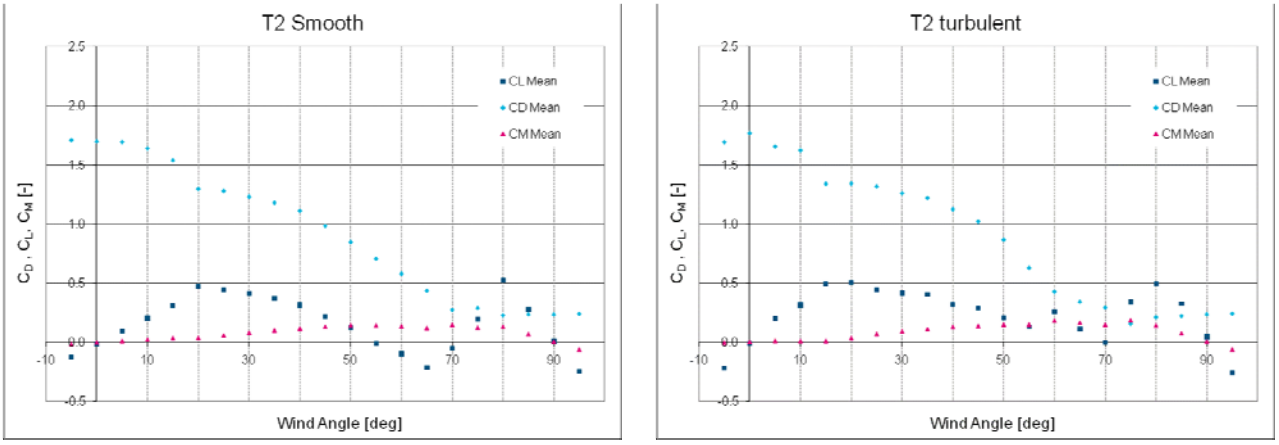

Angolo del vento (gradi) Angolo del vento (gradi)

Figura 5 Coefficienti di carico del vento nella configurazione ad una gamba T2 ottenuti in flusso calmo e turbolento con numero di Reynolds di $5 \cdot 10^5$.

Dalla Figura 5 si evince che il coefficiente di resistenza non cambia in maniera significativa con il variare delle condizioni di flusso da calmo a turbolento.

T2 calmo

T2 turbolento

Medio

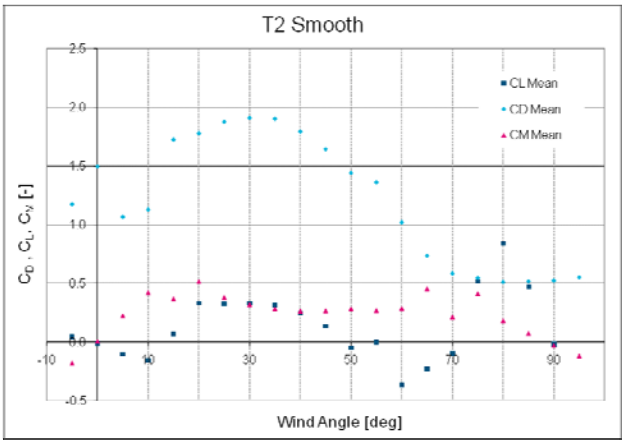

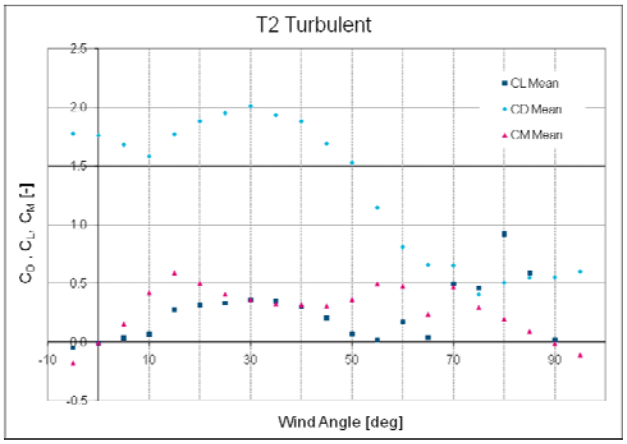

Angolo del vento (gradi)

Angolo del vento (gradi)

Figura 6 Coefficienti di carico del vento nella configurazione a due gambe T2 ottenuti in flusso calmo e turbolento con numero di Reynolds di $5 \cdot 10^5$.

Dalla Angolo del vento (gradi)

Angolo del vento (gradi)

Figura 6 si evince che la tendenza dei coefficienti di portanza e di momento misurati è la stessa della configurazione ad una gamba con un angolo di attacco maggiore di 30º. Con angoli di attacco inferiori, dove la gamba a valle si trova nella scia diffusa dalla gamba a monte, si nota qualche discrepanza. Inoltre, il coefficiente di resistenza risulta essere ampiamente non interessato dai livelli di turbolenza con tutti gli angoli di attacco superiori a 10º.

Per stabilire fino a che punto i coefficienti di resistenza statica sono soggetti ad effetti di scala, due ulteriori modelli ad una gamba, uno in scala 1:50 e uno in scala 1:200, sono stati sottoposti a verifica a velocità del vento più elevate con numero di Reynolds fino a $1x10^6$ per 4 angoli di attacco, 0º, 30º, 60º e 90º [1]. Tale osservazione indica che i carichi da vento sono ragionevolmente indipendenti dal numero di Reynolds nel modello in scala 1:100.

5 Risultati, Sub-test T3

Il modello aeroelastico è stato sottoposto a prove più dettagliate in flusso calmo ($I_{u,w}$ = 0,3% presso BMT e I_u = 1% presso BLWTL) e flusso turbolento (I_u = 6,9% e I_v = 5,2% presso BMT e I_u = 10% presso BLWTL) per verificare la prestazione aerodinamica, [2] e [3]. Per le condizioni strutturali indicate al punto 2.2, queste prove comprendevano:

- Misurazione della risposta strutturale a velocità del vento incrementali nel campo compreso tra 5m/s-80m/s di fondo scala in direzioni del vento tra 0º-90º con incrementi di 10º. L'incremento dell'angolo di attacco viene ridotto a 2,5º tra le due direzioni generando la risposta più alta.
- Misurazione della velocità critica del vento sul modello della torre e conferma della stabilità aerodinamica.

5.1 Risposta indotta dai vortici

Le misurazioni sono state eseguite variando la velocità del vento nel campo di scala del modello 1,0< V_{MS} < 15 con incrementi di ca. 1,0. Con velocità del vento, alle quali il modello sezionale mostrava una risposta oscillatoria, gli incrementi di velocità sono stati ridotti per garantire la captazione dell'intero campo di sincronizzazione.

Secondo i risultati delle prove sulla torre in verticale p.18 [2], la risposta della torre non risente dell'effetto della turbolenza, che però si osserva confrontando la figura 3.1 e la figura 3.7 in [3]. Il secondo picco in direzione longitudinale, vento 0º, viene mitigato attorno a V_{FS}=40m/s. Il primo picco in direzione longitudinale di ca. V_{FS}=17m/s è della stessa grandezza e non risente dell'effetto della turbolenza.

Nella condizione in service, il confronto con le risposte longitudinali in figura 3.4 e figura 3.8 in [3], dimostra che la risposta della torre non risente dell'effetto della turbolenza.

La risposta al distacco dei vortici della torre lungo l'asse del ponte, modalità flessionale primaria, è stata misurata su tutte le configurazioni tra 0º e 20º a velocità del vento inferiori alla velocità di progetto.

Per le prime tre configurazioni di cui al punto 2.2, il peggior picco di distacco dei vortici nella flessione lungo l'asse del ponte, flusso calmo, riscontrato presso la BMT Fluid Mechanics [2] è indicato in

Tabella 1 Peggiori picchi di distacco dei vortici, flusso calmo, flessione lungo l'asse del ponte, BMT.

Configurazione	Direzione del vento [°]	Accelerazione RMS MS [m/s^2]	Smorzamento rispetto alla criticità [%]
Torre in verticale	0	60	0.16
Prima dell'installazione del traverso	15	35	0.32
Torre finita, con cavi installati	20	12	0.32

Le verifiche di BLWTL mostrano che la risposta massima in fase di costruzione (torre in verticale) durante quasi tutte le prove si verifica con la torsione della torre. La risposta massima della torre si ha nelle prove con direzione del vento a 20° in flusso turbolento con una velocità del vento di V_{FS}=46m/s, che ha portato ad un'interruzione delle prove per elevate risposte al buffeting.

Velocità del vento tra 50-63 m/s sono state saltate nelle prove BLWTL sulla configurazione in-service a causa delle grosse risposte della torre.

Con la configurazione in service di un modello di torre in scala Froude sembra che un grave distacco dei vortici sulle gambe della torre nella flessione lungo l'asse della torre stessa si verifichi ad una velocità del vento inferiore a V=71 m/s corrispondente alla condizione SILS con z=250m di livello. La peggior risposta in flusso calmo si è avuta con una direzione del vento di 2,5° e 5° con la perpendicolare verso la linea del ponte.

La prima serie di prove del distacco dei vortici eseguita presso la BMT per la configurazione in service non ha dato la stessa risposta ottenuta dal modello in scala Froude. Per una verifica di tale

aspetto, il modello in scala di Froude è stato testato sotto forma di torre in verticale onde valutare l'effetto del numero di Reynolds sulla risposta della torre. La torre nella scala di Froude e non in posizione verticale ha generato una risposta identica, Figura 7.

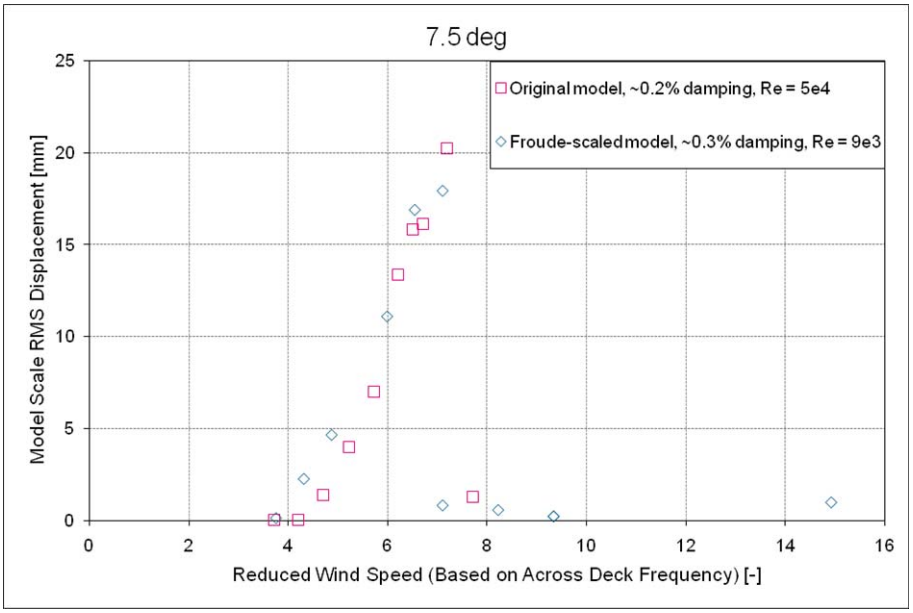

Spostamento RMS nel modello in scala

Modello originario, ca. 0,2% di smorzamento, Re =

Modello in scala di Froude, ca. 0.3% di smorzamento, Re =9e3

Ridotta velocità del vento (basata sulla frequenza attraverso l'impalcato

Figura 7 Confronto tra la torre in verticale ed il modello originario e in scala Froude [2].

Il confronto tra i numeri di Reynolds per le configurazioni in verticale e in service del modello nuovo e vecchio indicano l'insensibilità del modello agli effetti del numero di Reynolds, Tabella 2 e Figura 8. Le vecchie prove si sono rivelate non corrette.

Tabella 2 Confronto dei numeri di Reynolds per la 1^ modalità di flessione lungo l'asse del ponte.

Configurazione	Numero di Reynolds
Verticale, vecchio modello rigido	$9.0 \cdot 10^3$
Verticale, modello in scala di Froude	$5.0 \cdot 10^4$
In service, modello in scala di Froude	$3.1 \cdot 10^4$

In service, vecchio modello rigido	$6.5 \cdot 10^4$

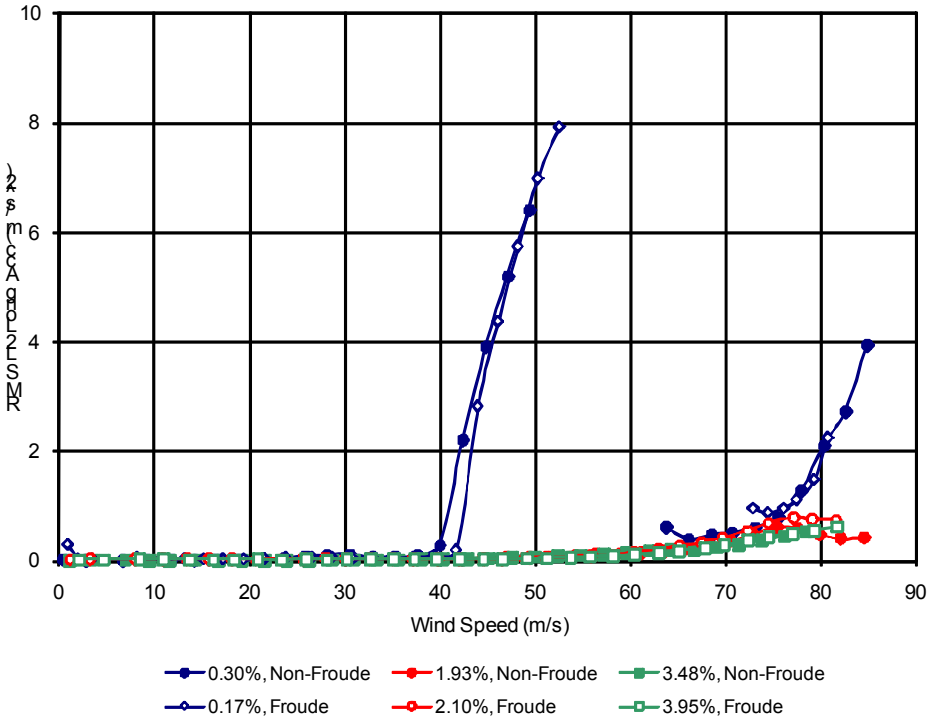

Figura 8 Confronto tra le risposte della torre in flusso calmo con vento a 0º, condizione in-service, BLWTL.

5.2 Mitigazione della risposta indotta dai vortici

Per mitigare l'eccitazione del distacco dei vortici è stato aggiunto uno smorzamento strutturale presso la BMT mediante una pala in rame supportata da un'asta in fibra di carbonio proveniente dalla torre, tra i poli dell'elettromagnete. Variando l'alimentazione della corrente si potevano ottenere livelli di smorzamento diversi.

Nelle prime tre configurazioni, il peggior picco di distacco dei vortici in flusso calmo nella flessione lungo l'asse del ponte indicata in ha potuto essere ridotto ad un livello quale indicato in Tabella 3.

Tabella 3 Peggiori picchi di distacco dei vortici, flessione lungo l'asse del ponte con aggiunta di smorzamento strutturale supplementare, BMT.

Configurazione	Direzione del vento [º]	Accelerazione RMS MS [m/s^2]	Smorzamento rispetto alla criticità. [%]
Torre in verticale	0	10	0.47
Prima dell'installazione del traverso	15	<5	0.47
Torre finita, con cavi installati	20	-	-

Aumentando il livello di smorzamento strutturale della modalità di flessione fino al 4% rispetto alla criticità nella configurazione in service della torre, la risposta può essere mitigata ad un livello di accelerazione RMS di ca. 0,5 m/s^2 come richiesto dalle specifiche. Il peggior caso di distacco dei vortici in fondo scala con smorzamento strutturale supplementare è indicato in Figura 9.
Le figure sono indicate in [2] (figura 3.11) nella scala del modello e in fondo scala. I fattori di rappresentazione in scala usati sono dati da $\lambda_{acc} = \left(f_{FS} / f_{MS}\right)^2 \cdot \lambda_L$ e $\lambda_v = \left(f_{FS} / f_{MS}\right) \cdot \lambda_L$.

Usando le prime frequenze di flessione $f_{FS} = 0.477Hz$ e $f_{MS} = 6.7Hz$ si ottengono fattori di scala di $\lambda_{acc} = 1.01$ e $\lambda_v = 14.24$.

Incidenza del vento 2.5°

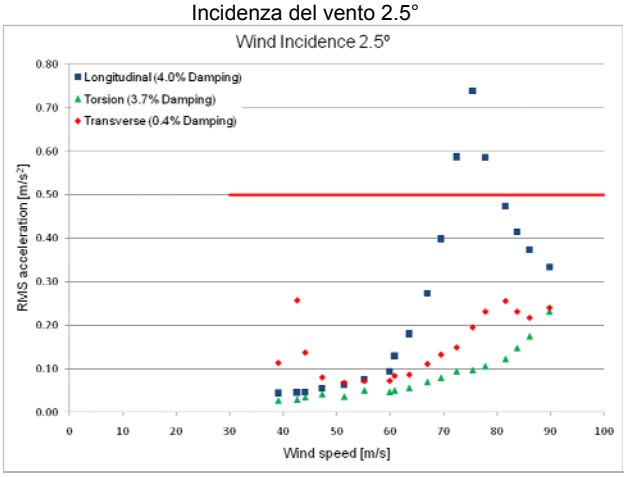

Incidenza del vento 5.0°

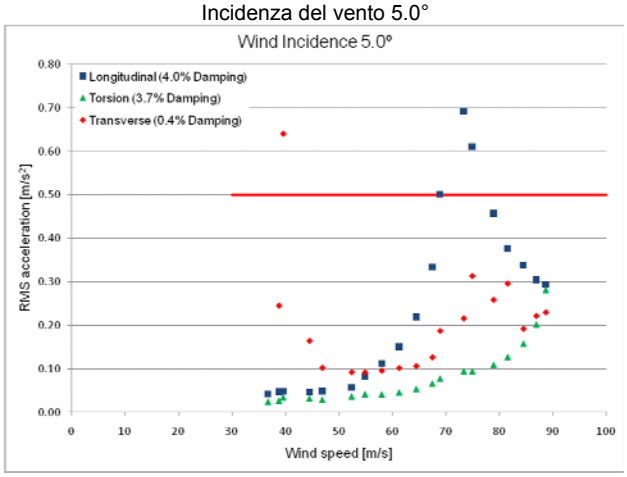

RMS L2 Acc. Lunga (m/s'2)

Velocità del vento

Velocità del vento

Longitudinale (4,0% di smorzamento)

Torsionale (3,7% di smorzamento)

Trasversale (0,4% di smorzamento)

Figura 9 Peggior caso di distacco dei vortici con smorzamento strutturale supplementare del 4% rispetto alla criticità , BMT.

La risposta trasversale della configurazione in service con un vento a 5º supera leggermente il requisito SdM di 0,5 m/s^2. Tuttavia, questa modalità non è fedelmente rappresentata nel modello in galleria del vento in quanto la massa del modello della struttura completa del ponte in service è oltre tre volte più alta di quella della torre fissata con impedimento del movimento in sommità nella direzione lungo l'asse. Tenendo conto della differenza della massa modale, si ottiene una risposta RMS massima di ca. 0,2 m/s in direzione trasversale.

Dalle prove BLWTL si può vedere che il flusso turbolento allo stato limite con un'intensità di turbolenza del 10% risulta efficace nell'eliminazione di quasi tutti i picchi di distacco dei vortici. Fa eccezione a tale conclusione il picco tra 53-60m/s, che è stato omesso nelle prove a flusso calmo e a flusso turbolento per l'eccessiva risposta della torre.

La turbolenza comporta in genere una riduzione della grandezza dei picchi indotti dal distacco dei vortici, ma aumenta le risposte al buffeting con velocità del vento più elevate.

Si è osservato dalle prove in flusso calmo che i picchi di distacco dei vortici tra 53-60m/s possono effettivamente essere eliminati aggiungendo uno smorzamento strutturale extra, Figura 10.

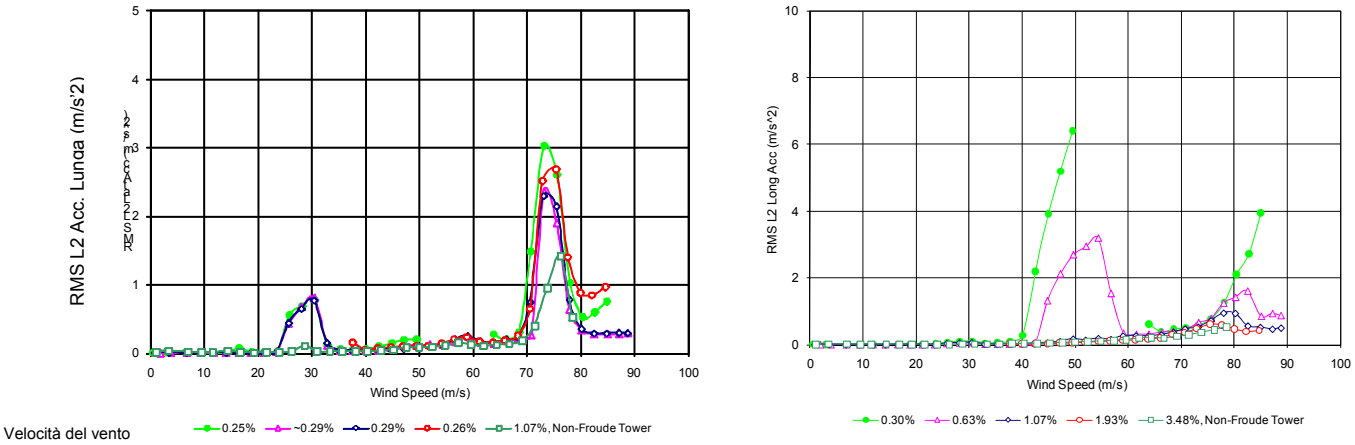

Figura 10 Risposta della torre in flusso calmo con vento a 0º, condizione in service con smorzamento strutturale supplementare, BLWTL.

In generale, con uno smorzamento strutturale del 4% rispetto alla criticità, le verifiche condotte dalla BLWTL indicano che la risposta della torre è inferiore al requisito SdM di 0,5 m/s^2 con velocità del vento fino alla velocità di progetto di 80 m/s.

Lo smorzamento strutturale in direzione laterale (attraverso l'impalcato) è stato ampiamente non interessato dallo smorzamento supplementare nelle direzioni longitudinale (lungo l'impalcato) e torsionale. Il livello di smorzamento in direzione laterale è dell'1% nelle prove con smorzamento supplementare del 4% in direzione longitudinale. La risposta laterale supera leggermente il requisito SdM di 0,5 m/s^2.

5.3 Stabilità aerodinamica

La velocità critica del vento di T3 nelle due configurazioni, torre in verticale e torre prima dell'installazione del traverso, è stata misurata per angoli di attacco compresi tra 0^0 e 90^0 in flusso calmo (I = 0,3%) e riportata in [2].

Dalla verifica in [2] si nota che la torre è aerodinamicamente stabile a velocità del vento in flusso calmo a fondo scala fino alla massima velocità di progetto di 80ms^{-1} sulla sommità della torre.

La maggior parte delle prove condotte in BLWTL sulla configurazione in fase di costruzione [3] ha raggiunto una velocità del vento media oraria ad altezza torre di 50m/s. Alcune prove sono state terminate anticipatamente a causa della significativa risposta al buffeting.

Dalla verifica in-service in [3] si nota che la torre è aerodinamicamente stabile fino alla velocità del vento di progetto di 80m/s ad altezza torre. A causa dell'ampia risposta della torre nei testi con smorzamento intrinseco, le velocità tra 50-63 m/s sono state omesse.

6 Riferimenti

1 BMT Fluid Mechanics, Project No. 431163/00 Messina Straits Crossing, Towers, Section Model Studies, 10th November 2010

2 BMT Fluid Mechanics, Project No. 431163/00 Messina Straits Crossing, Towers, Full Aeroelastic Studies, 10th November 2010

3 BLWTL The University of Western Ontario, BLWT-SS1-2011 Messina Strait Bridge, Italy, Non-Froude and Froude Scaled Aeroelastic Models of Tower - Sub-Test T3

Appendice e Scopo del Lavoro

COWI

Memo

	Eurolink s.c.p.a.
Title	Scope of work, Tower wind tunnel tests, Sub-tests T1,T2 and T3
Date	16 June 2010
To	Eurolink, EYA
Copy	SAMI
From	ALN

COWI A/S

Parallelvej 2
DK-2800 Kongens Lyngby
Denmark

Tel +45 45 97 22 11
Fax +45 45 97 22 12
www.cowi.com

1 Introduction

This memo details the scope of work for the tower wind tunnel tests, sub-tests T1, T2 and T3, following the overall aerodynamic design methodology for the Progetto Definitivo phase.

The objectives of the tests are as follows:

Identify the level of structural damping necessary to mitigate vortex shedding excitation.

Establish wind load coefficients for the tower leg cross section.

Verify tower responses to boundary layer wind flow for the free-standing tower and two erection stages.

2 Wind Tunnel Test Programme

The wind tunnel test programme is split into three sub-tests according to the above objectives and methods of testing.

2.1 Sub-test T1. Response Measurements, Spring Suspended Section Model

Sub-test T1shall investigate the proneness of the tower to vortex shedding excitation and establish a level of structural damping necessary for mitigation of the vortex shedding response.

The tests are to be carried out using spring suspended section models of one tower leg cross section and an assembly of two tower leg cross sections representative of the tower at 70% of full height.

2.1.1 Methodology

Sub-test T1 is carried out by subjecting the suspended tower leg section or assembly to increasing wind speeds in the range 5 m/s - 80 m/s full scale and recording the response of the section.

For the two model configurations, the angle of incidence of the wind is varied from 0 deg. (flow perpendicular to bridge line) to 90 deg. in steps of 10 deg. The inflow angle increment is decreased to 2 deg. between the two inflow angles yielding the highest responses.

The mechanical damping of the suspension rig is increased from approximately 0.4% rel-to-crit. to approximately 4% rel-to-crit. in five steps.

The tests are to be carried out in smooth flow with turbulence intensity < 2%.

Suggested model scale: 1:100 - 1:150

2.1.2 Test results
The results are to be presented as diagrams of root mean square response as function of wind speed.

2.2 Sub-test T2. Force Measurements, Fixed Section Model
Sub-test T2 shall measure wind forces lift, drag and twisting moment on the section model of one tower leg and the two leg assembly. The results shall be presented as lift, drag and moment coefficients C_L, C_D, C_M, through normalization with section length, characteristic dimension and dynamic head.

2.2.1 Methodology
The angle of incidence of the wind is varied from 0 deg. (flow perpendicular to bridge line) to 90 deg. in steps of 5 deg and the measured forces are measured.

For one of the wind inflow angles the wind forces are measured at a range of wind speeds to demonstrate that the wind load coefficients are independent of Reynolds Number.

Tests are to be carried out in smooth flow with turbulence intensity < 2% as well as in turbulent flow of 10% intensity.

Suggested model scale: 1:100 - 1:150

2.2.2 Test results
The results are to be presented as diagrams giving wind load coefficients as function of the angle of wind incidence.

2.3 Sub-test T3, Response Measurements, Full Aeroelastic Model
Sub-test T3 shall measure the response of a full aeroelastic model of the tower to turbulent wind. Four structural conditions shall be tested:

- Completed tower, free standing condition.
- Completed tower, pinned at top simulating the effects of main cables and tie back.
- Construction phase immediately before mounting of third cross beam.

The tests shall measure the horizontal response along the bridge line and across the bridge line of each tower leg at the tower top as well as at the position of the second cross beam. The bending moments at the base of each leg along the bridge line and across the bridge shall also be measured.

2.3.1 Methodology

Sub-test T3 is carried out by subjecting the aeroelastic tower model to increasing wind speeds in the range 5 m/s - 80 m/s full scale and recording the structural response.

For all three structural configurations the wind direction is varied from 0 deg. (flow perpendicular to bridge line) to 90 deg. in steps of 10 deg. The inflow angle increment is decreased to 2 deg. between the two wind directions yielding the highest responses.

The tests shall be carried out at three levels of mechanical damping of the aeroelastic model. The lowest damping level shall be approximately 0.5% rel-to -crit. The remaining damping levels will be chosen upon evaluation of the sub-test T1 results.

The tests are to be carried out in smooth flow with turbulence intensity less tan 2% and in a simulated atmospheric boundary layer with the following mean wind speed and turbulence profiles:

$$u(z) \approx ln\frac{z}{0.01}$$

$$I_u(z) = \frac{1}{ln\frac{z}{0.01}}$$

Where z is the elevation above ground level

The power spectrum of the longitudinal turbulence is given as follows:

$$\frac{nS_u(n,z)}{I_u^2 u(z)^2} = \frac{6.868\frac{nL_u(z)}{u(z)}}{\left(1+10.302\frac{nL_u(z)}{u(z)}\right)^{5/3}}$$

$$L_u(z) = 300\left(\frac{z}{200}\right)^{0.5}$$

Where n is frequency in Hz.

Suggested model scale: 1:200 - 1:250

2.3.2 Results

The results are to be presents in diagrams giving root mean square and mean values of structural response as function of wind speed

3 Model Parameters

The section and full aeroelastic models shall be built to faithfully replicate the geometry given in the attached drawing.

Preliminary mass and frequency to be modelled in the section model sub-test T1 are as follows:

- Tower leg: mass / unit length m = 73000 kg/m
- Free standing tower, 1 mode along axis bending bending: $f_1 \approx 0.1$ Hz
- Free standing tower, 1 mode cross axis bending bending: $f_2 \approx 0.3$ Hz

Adjustments to the above data shall be given prior to start of the section model tests and start of the building of the full aeroelastic model.

4 Data Analysis and Reporting

The results of the individual sub-tests shall be given in individual test reports, which also document the particulars of the models and the wind tunnel flow.

For the full aeroelastic tests, the report shall document that the modelled atmospheric boundary layer matches the mean wind, turbulence intensity and power spectral density required in section 2.3.1.

The results of the analyses shall be reported with a complete documentation of the applied procedures and observations made in course of the tests.

High quality video recordings of selected test runs shall accompany each of the individual reports.

Test data shall be provided in digital form upon request.

BMT Fluid Mechanics

Project No. 431163/00
Messina Straits Crossing
Towers
Italy

Wind Tunnel Testing

Full Aeroelastic Studies

(21st December 2010)

For

Eurolink S.C.p.A

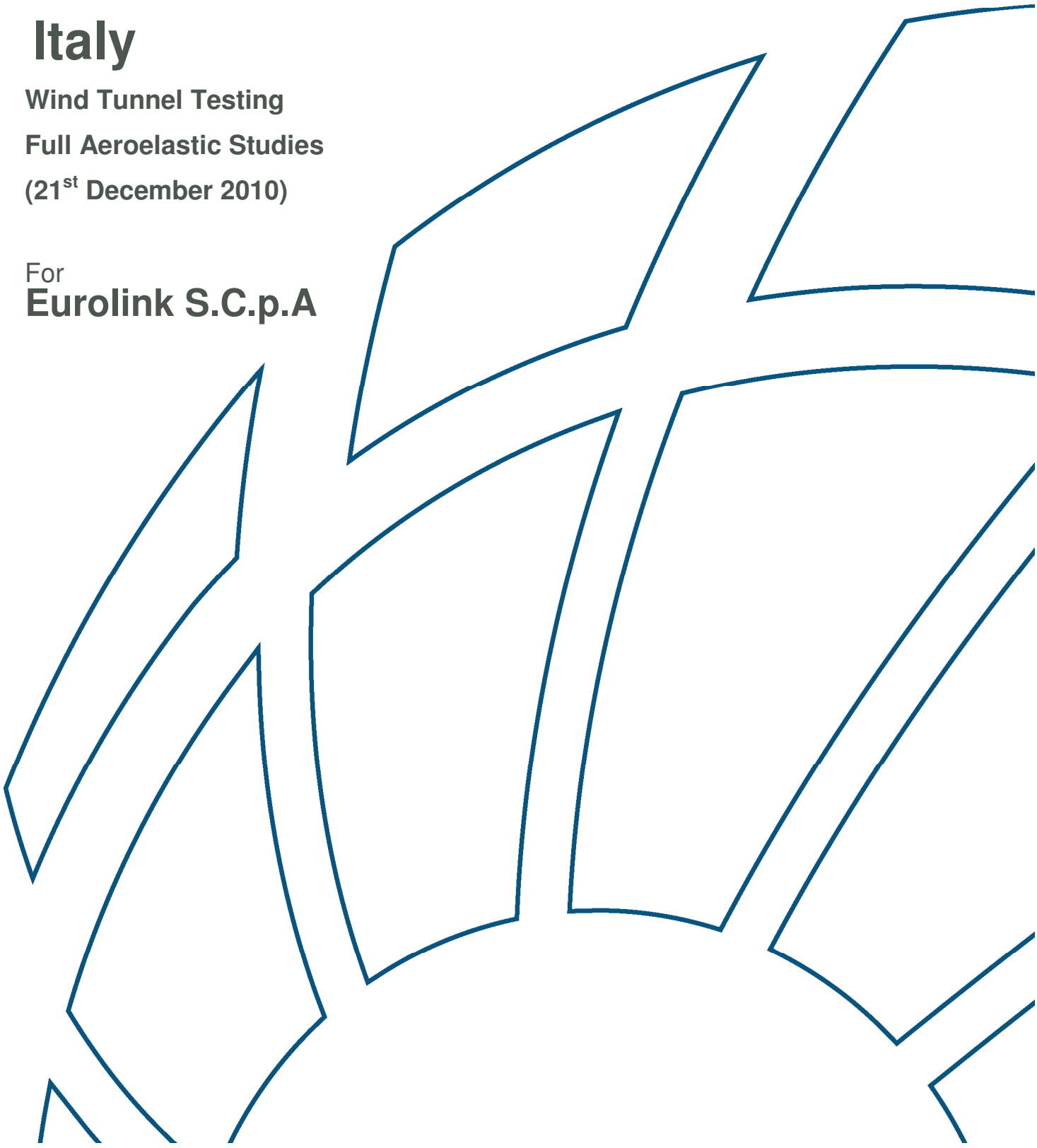

Report Title	**Messina Straits Crossing Towers** **Wind Tunnel Testing,** **Full Aeroelastic Studies**		
Client:	**Eurolink S.C.p.A**		
Document No:	**431163rep1v5**	**Release: 5**	**Copy No:**
Status	**Final**		
Report Date:	**21st December 2010**		
Holds:			

	Name:	Signature:	Date:
Prepared by:	**Mr J Osman**		21-12-10
Checked by:	**Miss A Bagnara**	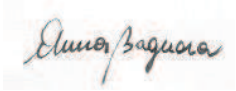	21-12-10
Approved by:	**Dr V Buttgereit**		21-12-10

Distribution:	

Previous Release History:	Release No:	Status:	Date:
431163rep1v1	**1**	**Draft Report for Internal Review**	**20/09/2010**
431163rep1v2	**2**	**Draft Report for Client Review**	**05/10/2010**
431163rep1v3	**3**	**Draft Report for Client Review**	**1/12/2010**
431163rep1v4	**4**	**Draft Report for Client Review**	**9/12/2010**

Messina Straits Crossing Towers
Wind Tunnel Testing
Full Aeroelastic Studies

Contents

EXECUTIVE SUMMARY

Background

This document has been prepared by BMT Fluid Mechanics Limited (BMT) for Cowi acting on behalf of Eurolink S.C.p.A. to summarise the results of full aeroelastic testing commissioned to study the wind effects relevant to the design of the towers of the Messina Straits Crossing in Italy.

This report describes the results from the full aeroelastic model tests carried out at 1:200 scale for the following erection conditions of the towers:

- Completed Free-Standing Tower
- Tower Prior to Top Crossbeam Installation
- Tower In-Service
- Tower With Cables Installed, Prior to Deck Installation

The study has provided an assessment of the aerodynamic stability with respect to vortex-shedding and divergent responses of the towers as well as a quantification of the wind loads applicable to the structural design.

Conclusion

The main results of the studies, which are presented in Model Scale, are summarised below:

FREE-STANDING TOWER

Vortex Shedding

- The peak accelerations for an estimated damping level of 0.16% (of critical), are as follows:

Flow	Wind Angle [deg]	Wind Speed [m/s]	RMS Acceleration [m/s^2]
Smooth	7.5	7.0	76
Turbulent	0	7	61

Aerodynamic Stability

- The free-standing tower was found stable up to and above the maximum design wind speed of 80 ms^{-1} at the top of the tower in smooth flow.

TOWER PRIOR TO CROSSBEAM INSTALLATION

Vortex Shedding

- The peak accelerations for an estimated damping level of 0.16% (of critical), are as follows:

Flow	Wind Angle [deg]	Wind Speed [m/s]	RMS Acceleration [m/s^2]
Smooth	10	7.6	37
Turbulent	20	6.8	29

Aerodynamic Stability

- The tower prior to top crossbeam installation was found stable up to and above the maximum design wind speed of $80ms^{-1}$ at the tip of the tower.

TOWER IN-SERVICE

Vortex Shedding

- The peak accelerations for an estimated damping level of 4% (of critical), are as follows:

Flow	Wind Angle [deg]	Wind Speed [m/s]	RMS Acceleration [m/s^2]
Smooth	2.5	5.3	0.74

TOWER WITH CABLES INSTALLED, PRIOR TO DECK INSTALLATION

Vortex Shedding

- The peak accelerations for an estimated damping level of 0.32% (of critical), are as follows:

Flow	Wind Angle [deg]	Wind Speed [m/s]	RMS Acceleration [m/s^2]
Smooth	20	10	12

Messina Straits Crossing Towers Wind Tunnel Testing, Full Aeroelastic Studies

1. Introduction

1.1. Background

This document has been prepared by BMT Fluid Mechanics Limited (BMT) for Eurolink S.C.p.A. to summarise the results of full aeroelastic testing commissioned to study the wind effects relevant to the design of the towers of the Messina Straits Crossing in Italy.

This report describes the results from the full aeroelastic model tests carried out at 1:200 scale for the following erection conditions of the towers:

- Completed Free-Standing Tower
- Tower Prior to Top Crossbeam Installation
- Tower In-Service
- Tower With Cables Installed, Prior to Deck Installation

The study has provided an assessment of the aerodynamic stability with respect to vortex shedding and divergent responses of the 4 configurations of the towers as well as a quantification of the wind loads applicable to the structural design for the freestanding configuration.

The general scope of the study includes a series of section model tests at a scale of 1:100 aimed at deriving an indicative assessment of the dynamic response of the towers. The results of these studies are reported on BMT report 2 dated 29th November 2010.

1.2. Details of the Proposed Structure

The Messina Straits Crossing is a suspension bridge linking the Island of Sicily with mainland Italy, and has a total length of ~3300m. Two twin-leg towers, 399m tall, support the suspension cables. Each leg is of constant octagonal section, 20m by 12m, and they are canted in towards each other at the tip. Figure 1.1 shows the arrangement of the tower and the relevant geometrical features.

2. Methodology

2.1. Objective of the studies

The key objectives of the studies were to:

- Define the worst case vortex-shedding responses and corresponding critical wind speeds of the four erection configurations of the towers.
- Confirm that the towers are stable with respect to divergent responses within the design wind speed range (up to 80ms^{-1} at the top the towers).
- Derive the variation of wind loading with wind speed of the freestanding condition within the design wind speed range.

To ensure that the aeroelastic tests would define accurately the vortex-shedding motions and cover the full design wind speed range to validate the aerodynamic tests, BMT have designed and constructed 3 full aeroelastic with the following characteristics:

1) ***Stiff Model –*** A "Stiff", (high frequency) model with a speed scale of ~2:1 was used for the vortex-shedding studies of freestanding configuration with and without crossbeam. The speed scale was chosen to maximize the Reynolds number at which vortex-shedding would occur, maintaining a frequency scale within a measurable signal range.

2) ***Soft Model -*** "Soft" (low frequency) model with a speed scale of ~4:1 was used to allow the aerodynamic stability studies of the freestanding configuration with and without top beam.

3) ***Froude Scaled Model –*** A Soft (low frequency) model with a speed scale of ~ 12:1 was used for the vortex shedding studies of the in service condition following a request by the design team.

Details of how the 3 aeroelastic models were adapted to study the 4 tower configurations are given in section 2.3 and Appendix B.

2.2. Model Configurations & Tests Matrix

The four tower configurations subject of these studies and the test matrices for each of these configurations are provided below:

COMPLETED FREE STANDING TOWER

Test Description	Wind Angles [deg]	Flow Condition	Reduced Wind Speeds	Damping Level [%]
Vortex Shedding	0-90	Smooth & Turbulent	~7	0.16
Vortex Shedding - Sensitivity to Damping	0	Smooth & Turbulent	~7	0.32 – 1.1
Aerodynamic Stability	0-90	Smooth	~40 ($80ms^{-1}$ FS)	0.16
Wind Loading	0-90	Turbulent	Full Range	0.16

Wind speeds are quoted as reduced wind speeds (U/ND), based on the first longitudinal frequency of the configuration and the reference dimension of 20m.

TOWER PRIOR TO TOP CROSSBEAM INSTALLATION

Test Description	Wind Angles [deg]	Flow Condition	Reduced Wind Speeds	Damping Level [%]
Vortex Shedding	0-90	Smooth & Turbulent	~6	0.32
Vortex Shedding - Sensitivity to Damping	15	Smooth & Turbulent	~6	0.32 & 0.48
Aerodynamic Stability	0-90	Smooth	~40 ($80ms^{-1}$ FS)	0.32

BRIDGE IN-SERVICE CONFIGURATION

Test Description	Wind Angles [deg]	Flow Condition	Reduced Wind Speeds	Damping Level [%]
Vortex Shedding	0-20	Smooth	~6	2
Vortex Shedding	0-30	Smooth	~6	4
Vortex Shedding	2.5 & 5	Smooth	~6	5

TOWER WITH CABLES INSTALLED, PRIOR TO DECK INSTALLATION

Test Description	Wind Angles [deg]	Flow Condition	Reduced Wind Speeds	Damping Level [%]
Vortex Shedding	0-90	Smooth	~5	0.32

2.3. Wind Tunnel Models

Three geometrically similar full aeroelastic models of the tower were designed and constructed at a scale of 1:200 based on structural and drawing information supplied by COWI.

The three models were designed to allow the different configurations to be tested as follows:

Configuration	Testing Scenario	Speed Scale	Model	Modification
Freestanding	Vortex Shedding	~2.2	Stiff	None
Freestanding	Aerodynamic Stability	~4.1	Soft	None
Freestanding	Wind Loading	~4.1	Soft	None
Prior to Top Crossbeam Installation	Vortex Shedding	~2.2	Stiff	Top crossbeam removed
Prior to Top Crossbeam Installation	Aerodynamic Stability	~4.4	Soft	Top crossbeam removed
In-Service	Vortex Shedding	~12	Froude	Top of tower "pinned" by tether cables
With Cables Installed	Vortex Shedding	~4	Soft	Top of tower connected to dynamic mass rig

Appendix B contains further details on each of the configurations, as well as details on the model scale and construction. Also presented in Appendix B are photographs of the models and wind tunnel set-up, and details of the target and measured mode shapes and frequencies.

The aeroelastic model tests were conducted in BMT's Boundary Layer Wind Tunnel facility, the specification of the facility is also included in Appendix A.

2.4. Measurement and Analysis

2.4.1. Vortex Shedding & Divergent Responses

For the vortex-shedding tests, measurements were taken in fine wind speed increments around the reduced wind speed of 6 in order to define the vortex-shedding peak and quantify the maximum response. The testing wind speed range was chosen based on the results of the section model studies.

For the aerodynamic stability assessment, the general approach to the tests was to observe the behaviour of the towers over a range of wind speeds, up and above the maximum design wind speed.

Measurements were taken for all wind directions in the sector 0° to 90° using 8 accelerometers located, according to the specification[1] at the height of the top and centre crossbeams, measuring parallel and perpendicular to the bridge deck axis for both legs. The accelerometer output was recorded as a time history, and then filtered to derive the root mean square (RMS) resonant component of the signal corresponding to the modes of interest. Peak vortex-shedding responses were also derived for the worst case wind directions.

Further details on the measurements and analysis of the data are provided in Appendix C.

2.4.2. Wind Loading

Time histories of base loads acting on both legs of the freestanding tower in isolation were measured simultaneously using a six-component high frequency force balance connected at the base of each leg.

The mean, resonant and background wind loads were determined from the time histories by the filtering process. Further details on the measurements and analysis of the data are provided in Appendix C.

2.5. Design Wind Properties & Model Scale Simulation of the Atmospheric Boundary Layer

The design wind speeds and the target characteristics of the atmospheric boundary layer used in this study were provided by COWI and are detailed in Appendix A.

The tests were carried out in smooth flow and in turbulent flow. The set up of the wind tunnel for both flow conditions is detailed in Appendix A.

2.6. Definition of Wind Direction and Axis System

The 0° wind direction has been chosen to coincide with winds blowing transversely across the deck. As the tower has two perpendicular planes of symmetry, results are quoted wind angles from one sector: 0 to 90°. Figures 2.2 and 2.3 show the axis system on which the wind forces are based.

3. Results

The results of all the tests are presented in a series of plots in Electronic Appendix E. To highlight the key results of the tests and to illustrate some of the main conclusions, a selection of data is reproduced as figures and tables in the main body of this report. All results are presented in model scale (MS) as requested by Stretto di Messina.

3.1. Vortex Shedding

3.1.1. Completed Free-Standing Tower

The model scale results of the dynamic response measurement are presented in form of:

- Variation of MS RMS accelerations at the heights of the upper two crossbeams of leg 1 with MS wind speed for the first longitudinal and transverse modes, in smooth flow for wind angles 0° - 90° (Figure 3.1).
- Variation of MS RMS accelerations at the heights of the upper two crossbeams of leg 1 with MS wind speed for the first torsion mode, in smooth flow for wind angles 0° - 90° (Figure 3.2).
- Variation of MS RMS accelerations at the heights of the upper crossbeam of leg 1 and 2 with damping for the first longitudinal mode, in smooth and turbulent flow for the worst-case wind angle of 0° (Figure 3.3).
- Variation of MS RMS & Peak displacements at the heights of the upper crossbeam of leg 1 with Scruton number for the first longitudinal mode, in smooth flow for the worst-case wind angle of 0° (Figure 3.4).

3.1.2. Tower Prior to Cross-beam Installation

The model scale results of the dynamic response measurement are presented in form of:

- Variation of MS RMS accelerations at the heights of the upper two crossbeams of leg 1 with MS wind speed for the first longitudinal and transverse modes, in smooth flow for wind angles 0° - 90° (Figure 3.5).
- Variation of MS RMS accelerations at the heights of the upper two crossbeams of leg 1 with MS wind speed for the first torsion mode, in smooth flow for wind angles 0° - 90° (Figure 3.6).
- Variation of MS RMS accelerations at the heights of the upper crossbeam of leg 1 and 2 with damping for the first longitudinal mode, in smooth and turbulent flow for the worst-case wind angle of 15° (Figure 3.7).
- Variation of MS RMS & Peak displacements at the heights of the upper crossbeam of leg 1 with Scruton number for the first longitudinal mode, in smooth flow for the worst-case wind angle of 15° (Figure 3.8).

3.1.3. Bridge In-Service

- Variation of MS RMS accelerations at the middle crossbeam with MS wind speed for the first longitudinal, torsional and transverse modes, in smooth flow for wind angle 0°, with a damping level of ~0.3% (Figure 3.9).
- Variation of MS RMS accelerations at the middle crossbeam with MS wind speed for the first longitudinal, torsional and transverse modes, in smooth flow for wind angles 0° - 20°, with a damping level of ~2% (Figure 3.10).
- Variation of MS RMS accelerations at the middle crossbeam with MS wind speed for the first longitudinal, torsional and transverse modes, in smooth flow for wind angles 0° - 30°, with a damping level of ~4% (Figure 3.11).
- Variation of MS RMS accelerations at the middle crossbeam with MS wind speed for the first longitudinal, torsional and transverse modes, in smooth flow for wind angles 2.5° & 50°, with a damping level of ~5% (Figure 3.12).
- Variation of MS RMS accelerations at the middle crossbeam with MS wind speed for the first longitudinal, torsional and transverse modes, in smooth flow for wind angle 5°, with a damping level for the transverse mode of ~1% (Figure 3.13).

3.1.4. Bridge with Cables Installed

The model scale results of the dynamic response measurement are presented in form of:

- Variation of MS RMS accelerations at the heights of the upper two crossbeams of leg 1 with MS wind speed for the first longitudinal and transverse modes, in smooth flow for wind angles 0° - 90° (Figure 3.14).

3.2. Aerodynamic Stability

3.2.1. Completed Free-Standing Tower

The model scale results of the dynamic response measurement are presented in form of:

- Variation of MS RMS accelerations at the heights of the upper two crossbeams of leg 1 with MS wind speed for the first lateral and transverse modes, in smooth flow for wind angles 0° - 90° in the region of the design wind speed (Figure 3.15).

3.2.2. Tower Prior to Top Crossbeam Installation

The model scale results of the dynamic response measurement are presented in form of:

- Variation of MS RMS accelerations at the heights of the upper two crossbeams of leg 1 with MS wind speed for the first lateral and transverse modes, in smooth flow for wind angles 0° - 90° in the region of the design wind speed (Figure 3.16).

3.3. Wind Loading Studies – Completed Free-Standing Tower

The MS results of the dynamic response measurement are presented in form of:

- Variation of mean, resonant and background wind load coefficients at the base of leg 1 with reduced wind speed for wind angles 0° - 90°. (Figure 3.17).
- Variation of mean, resonant and background wind load coefficients at the base of leg 2 with reduced wind speed for wind angles 0° - 90°. (Figure 3.18).

It should be noted that:

- All load coefficients are non-dimensionalised using the characteristic frontal area of one single leg at 0° wind angle (8000m^2).
- All Moment coefficients are non-dimensionalised using the characteristic length as the height of the tower (400m).

3.4. Interpretation/Discussion of Results

The main results of the studies are summarised below:

Vortex Shedding

- Vortex-shedding response in the primary bending mode of the tower were measured for all configurations at reduced wind speeds in the range 6 to 7 for the worst case angles, which are 0ºto 20º for all configurations.
- These values are consistent with the prediction of a reduced velocity of 6 from the section model tests. A slight departure from the value of 6 is expected and is due to differences in mode shapes, geometry of the model, profile of the wind speed, modal mass etc. The first configuration, the freestanding tower exhibits a response which is typical of a tall building. The worst-case vortex-shedding peak occurs at ~0°, with an associated RMS resonant displacement of the order of ~3m (at a damping level of 0.16%): this can be mitigated down to ~0.5m with a total level of damping of the order of ~0.5%. The configuration without the top cross-beam installed is characterised by a weaker, more disorganised and more broadband response: the associated worst-case response occurs this time at ~15°. The structural system with the upper cross-beam installed has greater potential to feed

energy directly from the upstream to the downstream leg (the system behaves like a single cantilever structure) - In the structural system prior to the installation of the upper cross-beam, the upper part of the two legs do appear to behave more independently and definitely in a less correlated manner: this is believed to reduce the potential for the 'lock-on' to take place. The configurations that simulate the presence of the cables and the deck are characterised by modeshapes that have maxima well below the top due to the restrain imposed by the cables. For both configurations the key phenomenon to be investigated was vortex-shedding in the weaker direction (along the deck axis). The results have shown that the peak displacements are lower than those of the first two configurations and occur for wind angles of 20°.

- In all cases investigated, the upstream and downstream leg display similar responses.

- The effect of turbulence in mitigating the vortex-shedding responses was seen to be negligible. This is consistent with the relatively low level of turbulence in the boundary-layer setup, and therefore there is similarity between the results of two flow regimes. Displayed in the plots below are comparisons of the responses in the longitudinal (crosswind) direction for the worst cases: freestanding tower at 0°, and tower prior to crossbeam installation at 20°, both with nominal damping in smooth and turbulent flow.

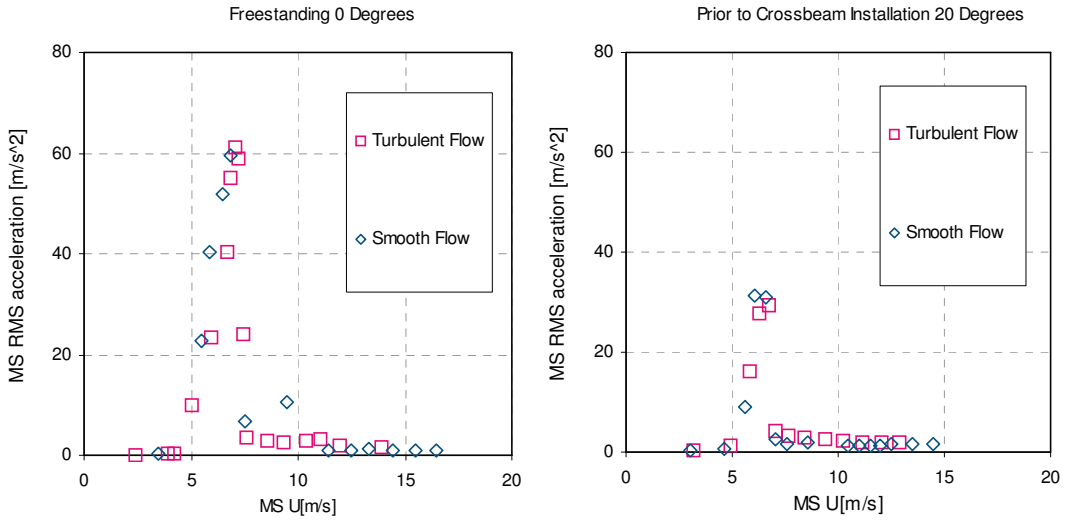

Based on the freestanding tower data with and without top cross beam, it can be concluded that the response of the tower is unaffected by the turbulence specified for the tests. As a result, for the in service condition and the configuration with cables in place the smooth flow data can be directly used for design.

- The Froude-scaled model was also tested at 7.5° with the tethers removed in order to provide a repeat of the free-standing configuration, and assess the effect of Reynolds number on the response of the tower. The comparison displayed below demonstrates good repeatability between the two models, and hence the insensitivity of the section to Reynolds-number effects for the Reynolds number range considered. The peak is at a Reynolds number of 5×10^4 for the original (stiff) model, and 9×10^3 for the Froude model.

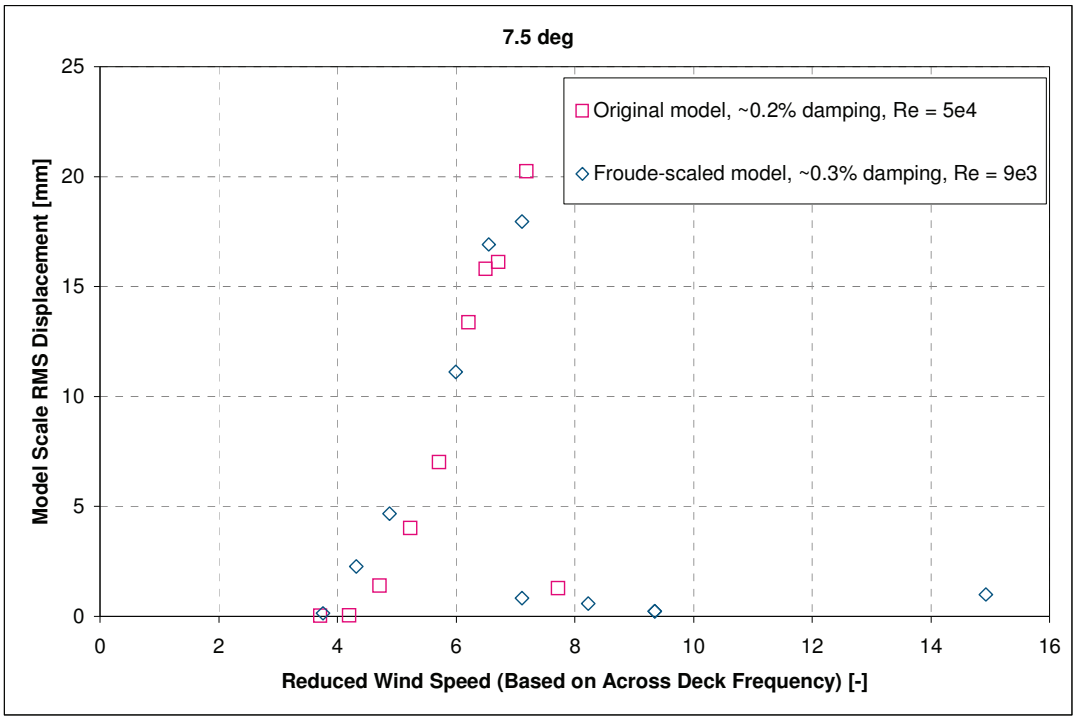

Aerodynamic Stability

- The freestanding tower and prior to crossbeam installation configurations were both found to be stable up to and above the design wind speed of 80ms^{-1} for all wind angles.

4. References

[1] Scope of work, Tower wind tunnel tests, Sub-tests T1, T2 and T3. ALN0002122.doc

5. Figures

Figure 1.1 Messina Straits Crossing – Tower Arrangement

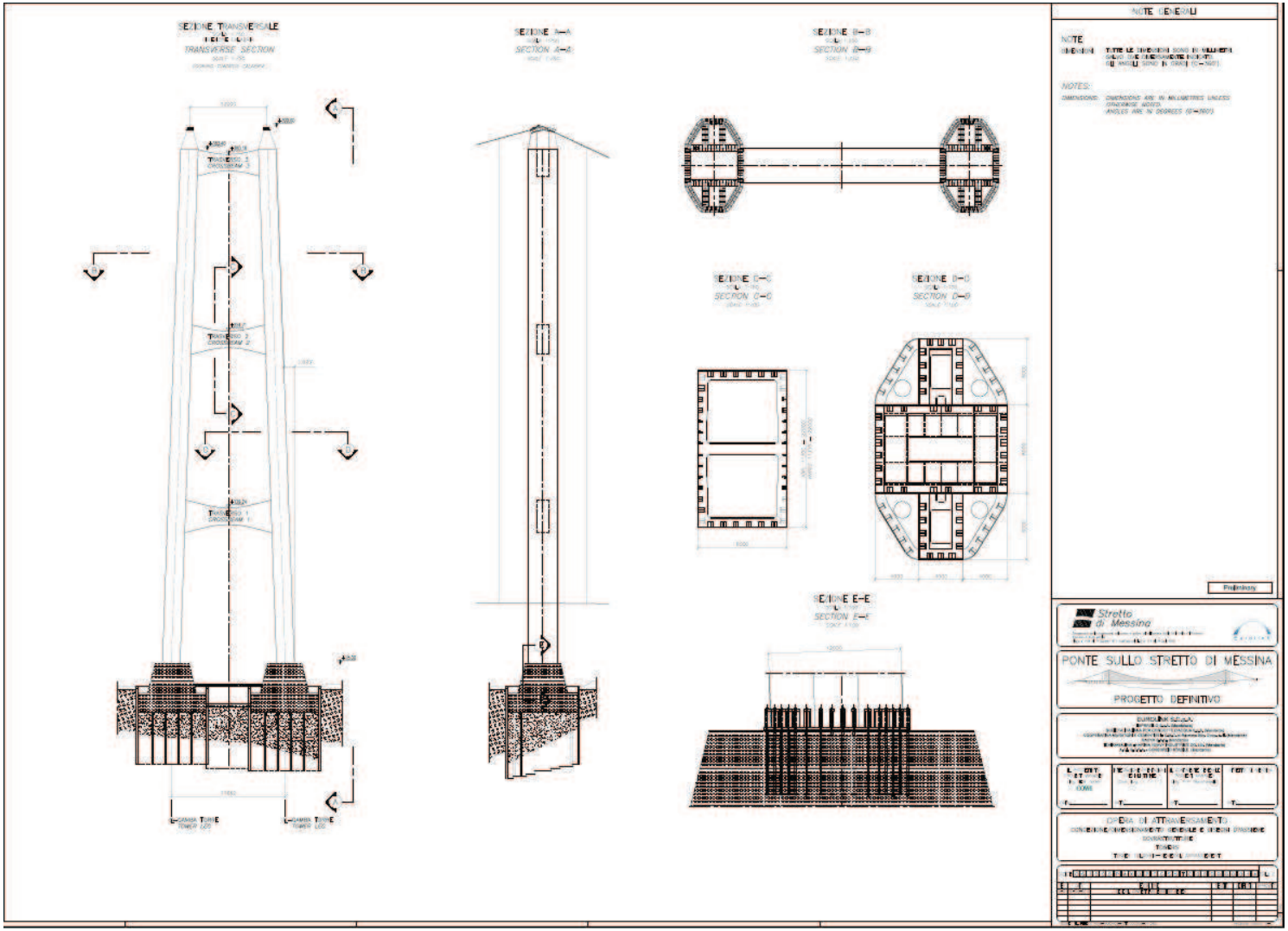

Figure 2.2 Messina Straits Crossing Tower – Axis Systems: Plan

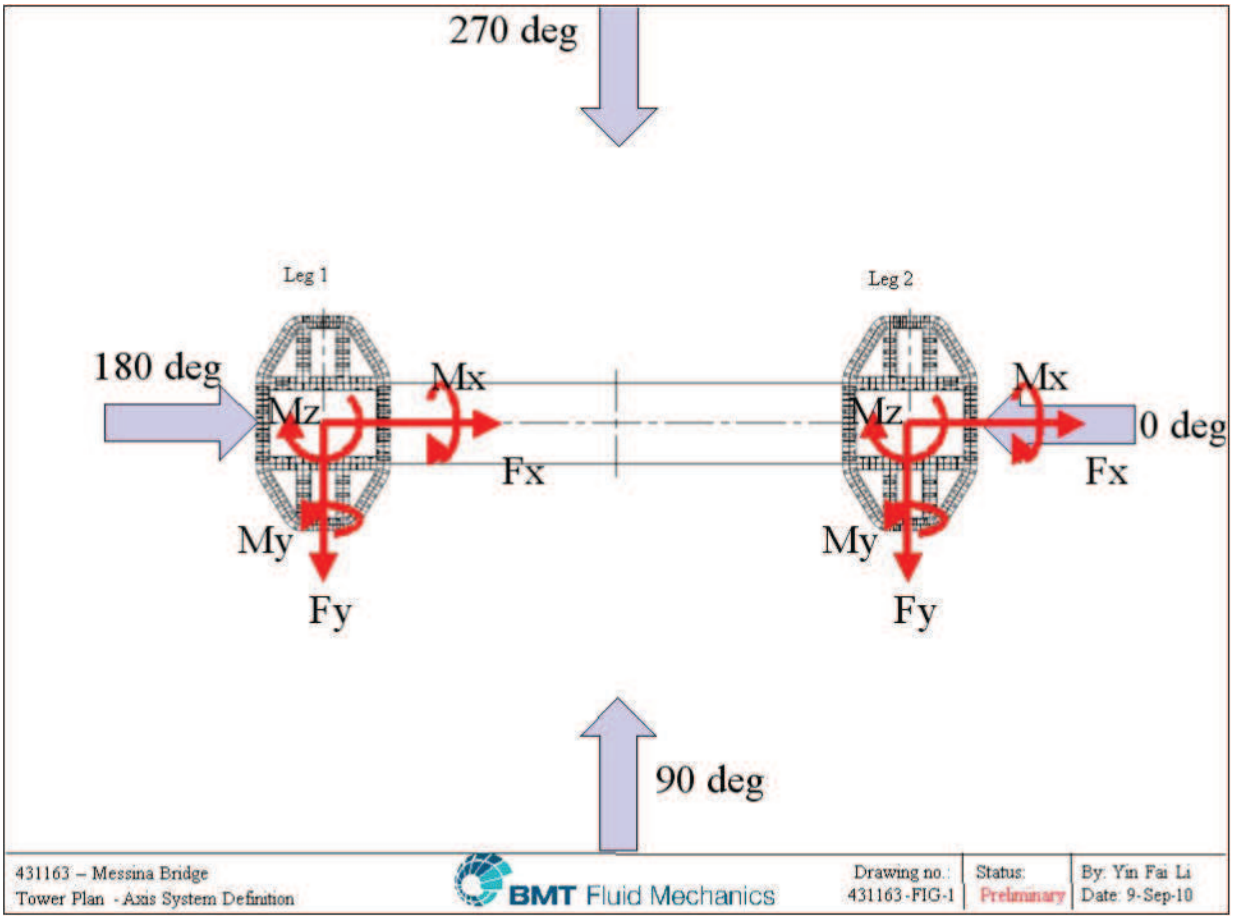

Figure 2.3 Messina Straits Crossing Tower - Axis Systems: Elevation

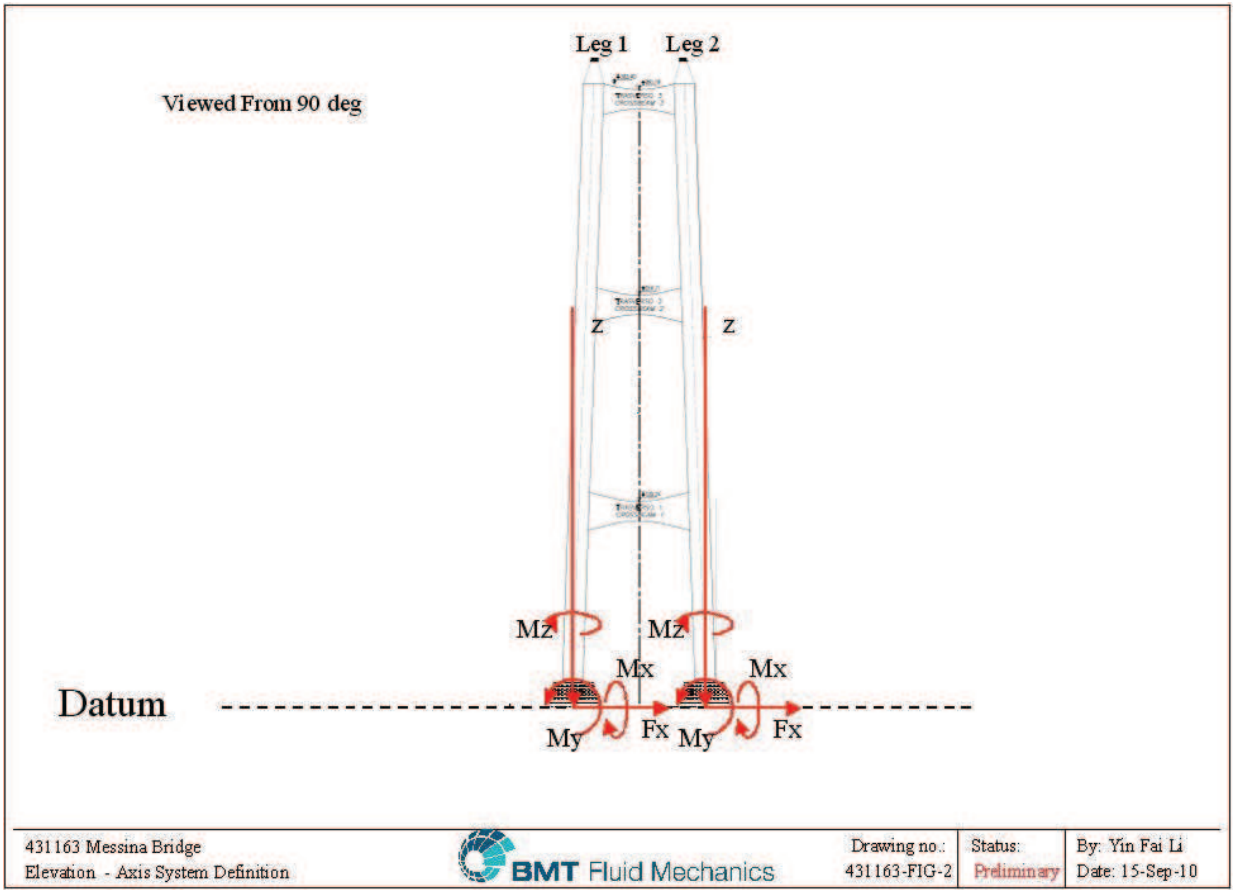

Figure 2.4 Measurement Location Scheme

a) In-service Condition

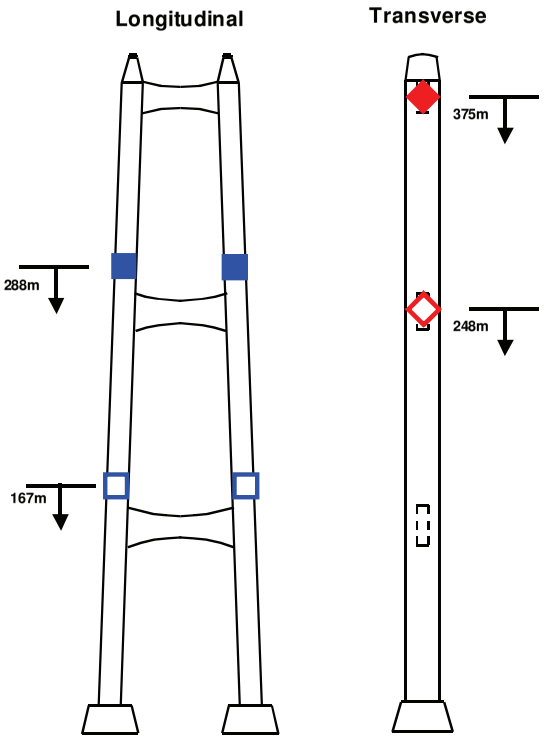

N.B. Measurement axis is normal to the surface on which they are mounted

b) All other Configurations

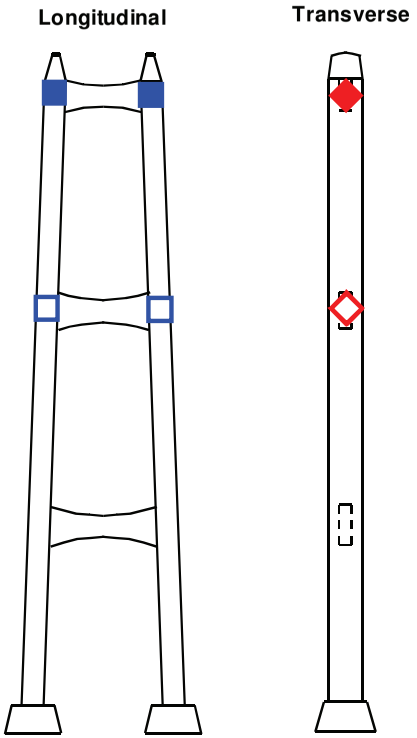

N.B. Measurement axis is normal to the surface on which they are mounted

Figure 3.1 Leg 1 MS Accelerations vs Wind Speed; Freestanding Tower in Smooth Flow with Damping Level 0.16% of Critical (Transverse & Longitudinal Modes)

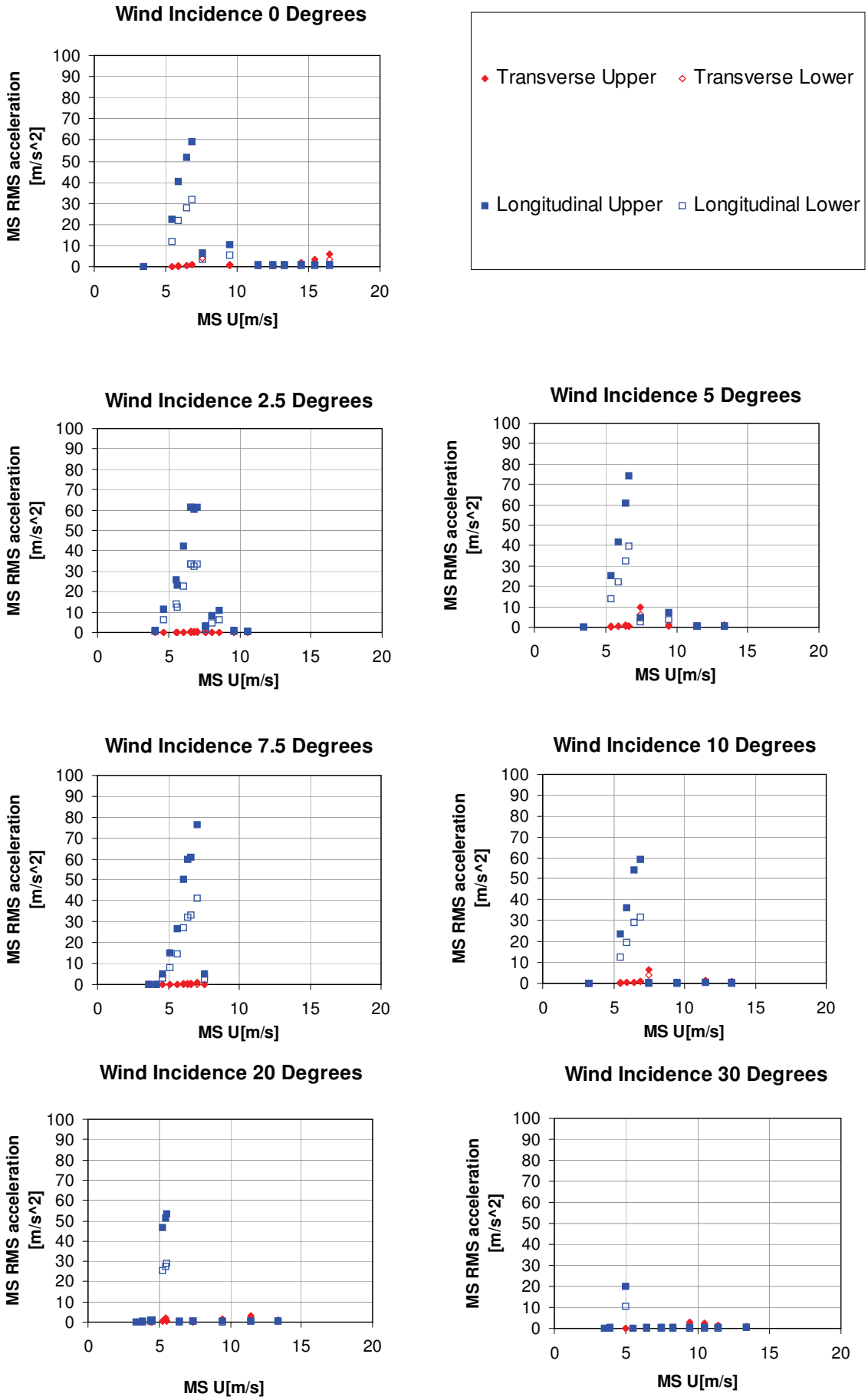

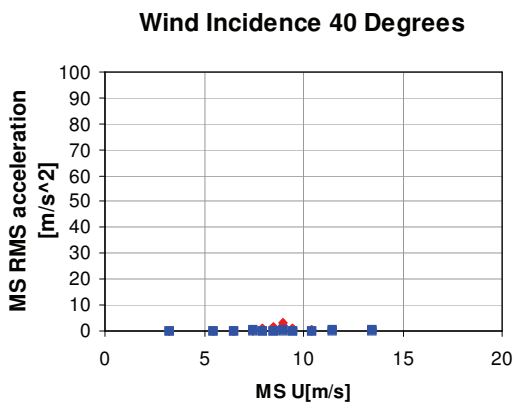
Wind Incidence 40 Degrees
MS RMS acceleration [m/s^2]
MS U[m/s]

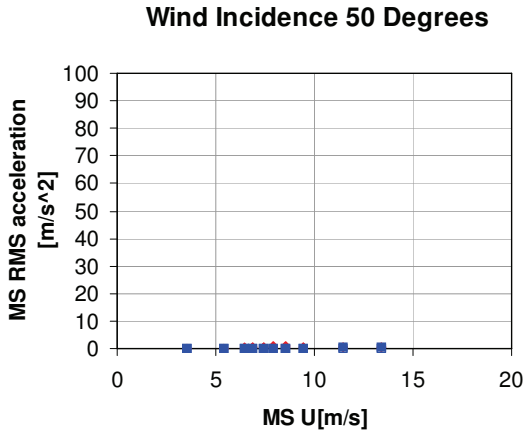
Wind Incidence 50 Degrees
MS RMS acceleration [m/s^2]
MS U[m/s]

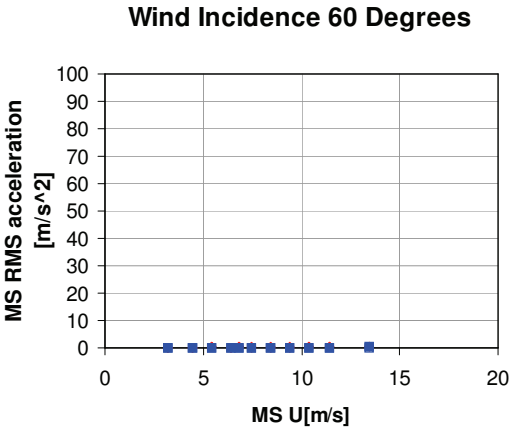
Wind Incidence 60 Degrees
MS RMS acceleration [m/s^2]
MS U[m/s]

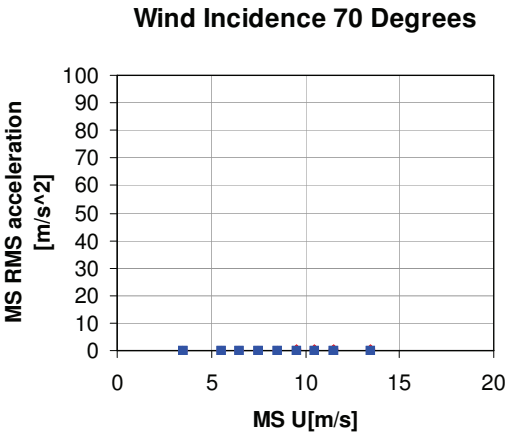
Wind Incidence 70 Degrees
MS RMS acceleration [m/s^2]
MS U[m/s]

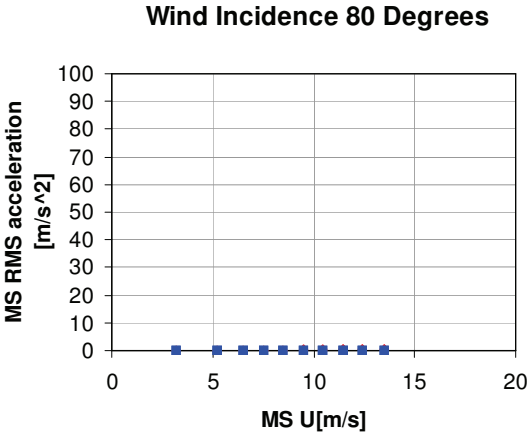
Wind Incidence 80 Degrees
MS RMS acceleration [m/s^2]
MS U[m/s]

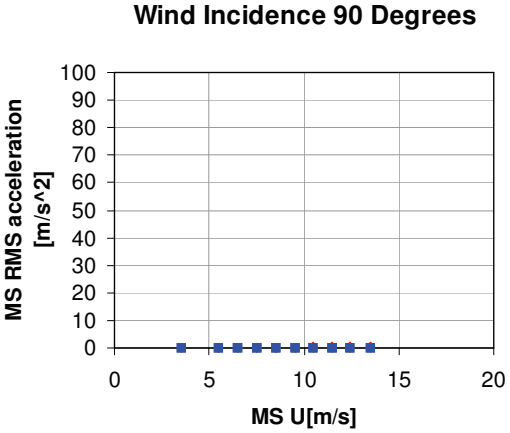
Wind Incidence 90 Degrees
MS RMS acceleration [m/s^2]
MS U[m/s]

Figure 3.2 Leg 1 MS Accelerations vs Wind Speed; Freestanding Tower in Smooth Flow with Damping Level 0.16% of Critical (Torsional Mode)

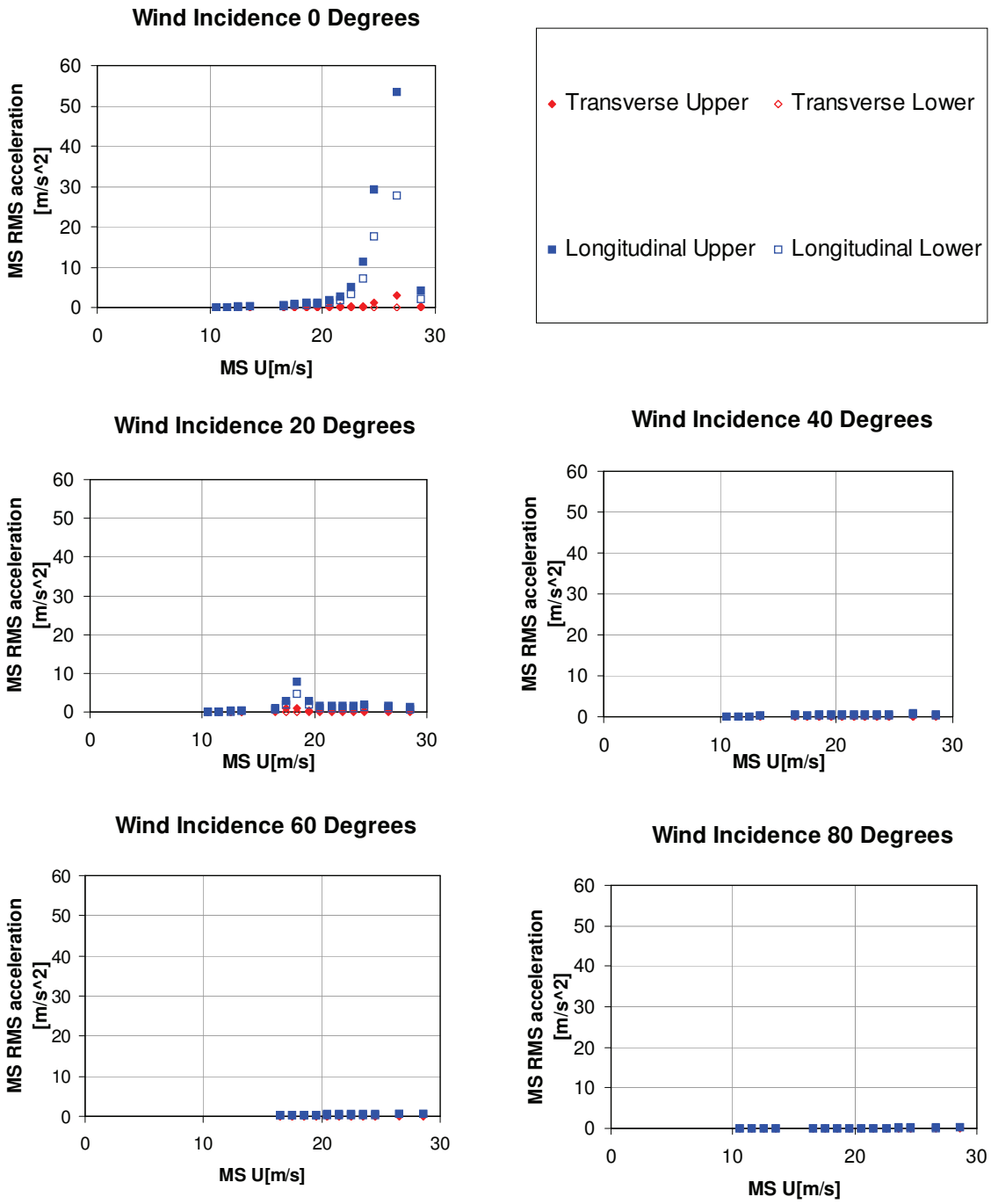

Figure 3.3 Worst Case MS Accelerations vs Wind Speed Sensitivity to Damping; Freestanding Tower

Smooth Flow Leg 1

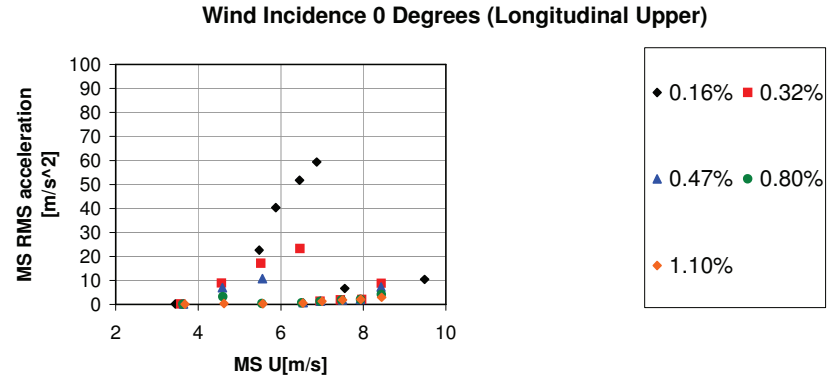

Smooth Flow Leg 2

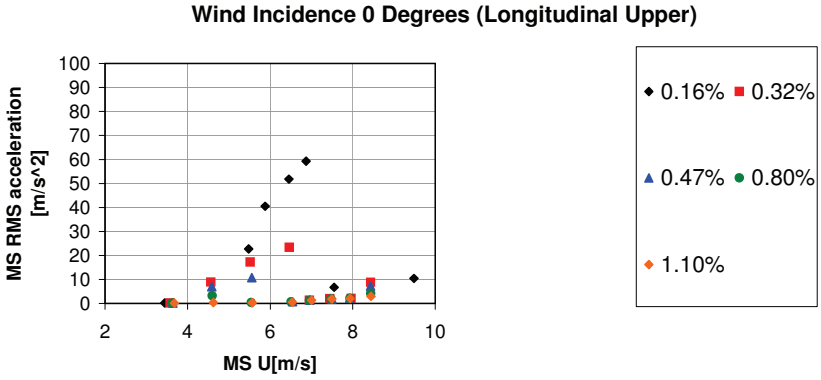

Turbulent Flow Leg 1

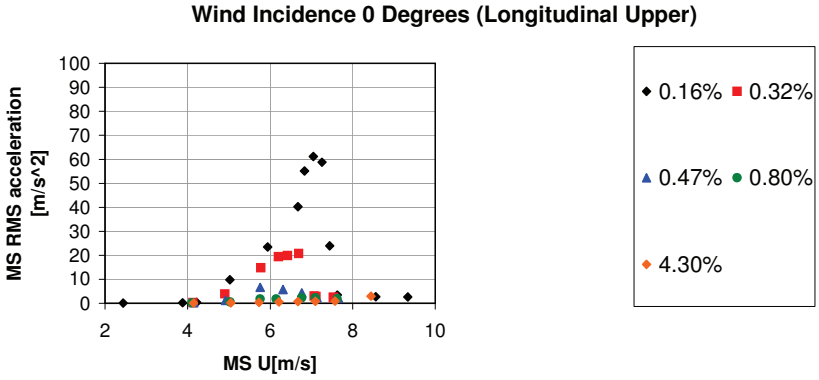

Turbulent Flow Leg 2

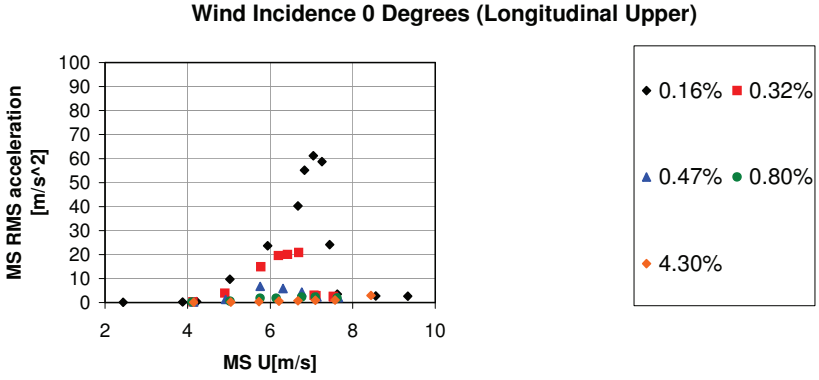

Figure 3.4 Worst Case MS Displacements & Peak Factors vs Scruton Number[1]: Freestanding Tower Leg 1 in Smooth Flow

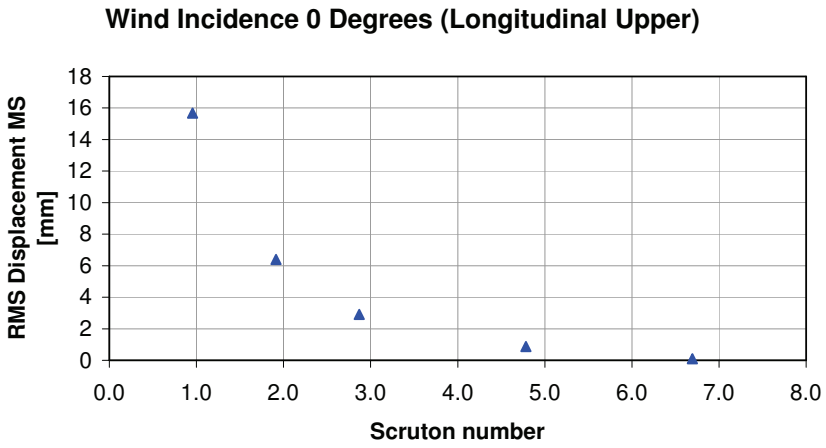

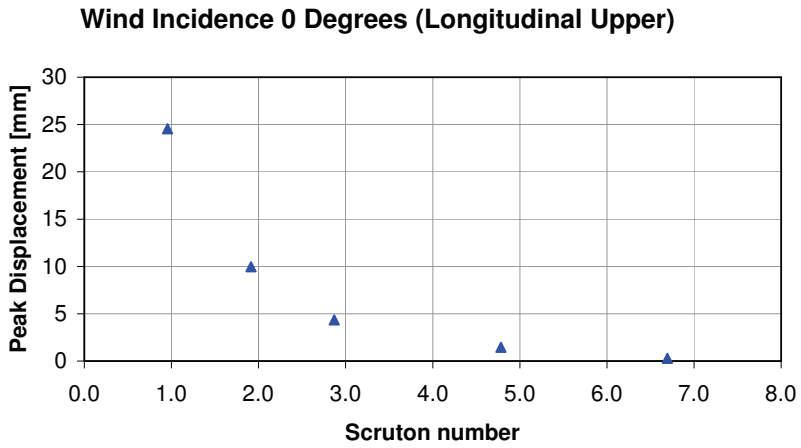

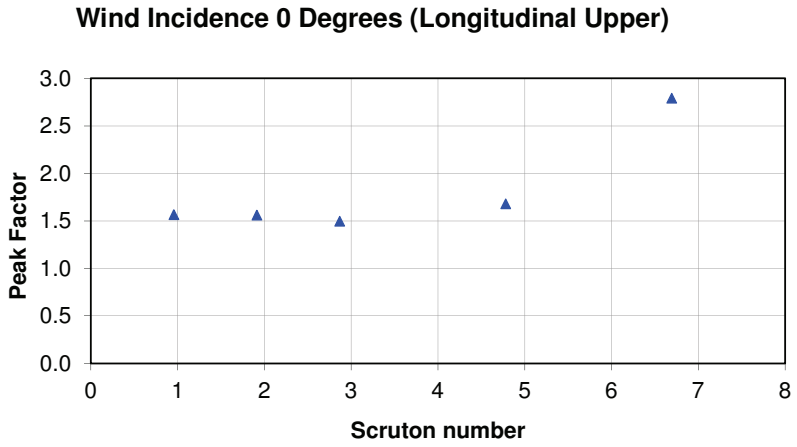

[1] $Sc = 2 \cdot \delta \cdot M / (\rho_a \cdot D^2)$
Where:
δ is the damping ratio [%crit]
M is the mode-generalised mass [tm^{-1}]
ρ_a is the density of air [tm^{-2}]
D is the reference dimension [m]

Figure 3.5 Leg 1 MS Accelerations vs Wind Speed; Tower Prior to Crossbeam Installation in Smooth Flow with Damping Level of 0.16% of Critical (Transverse & Longitudinal Modes)

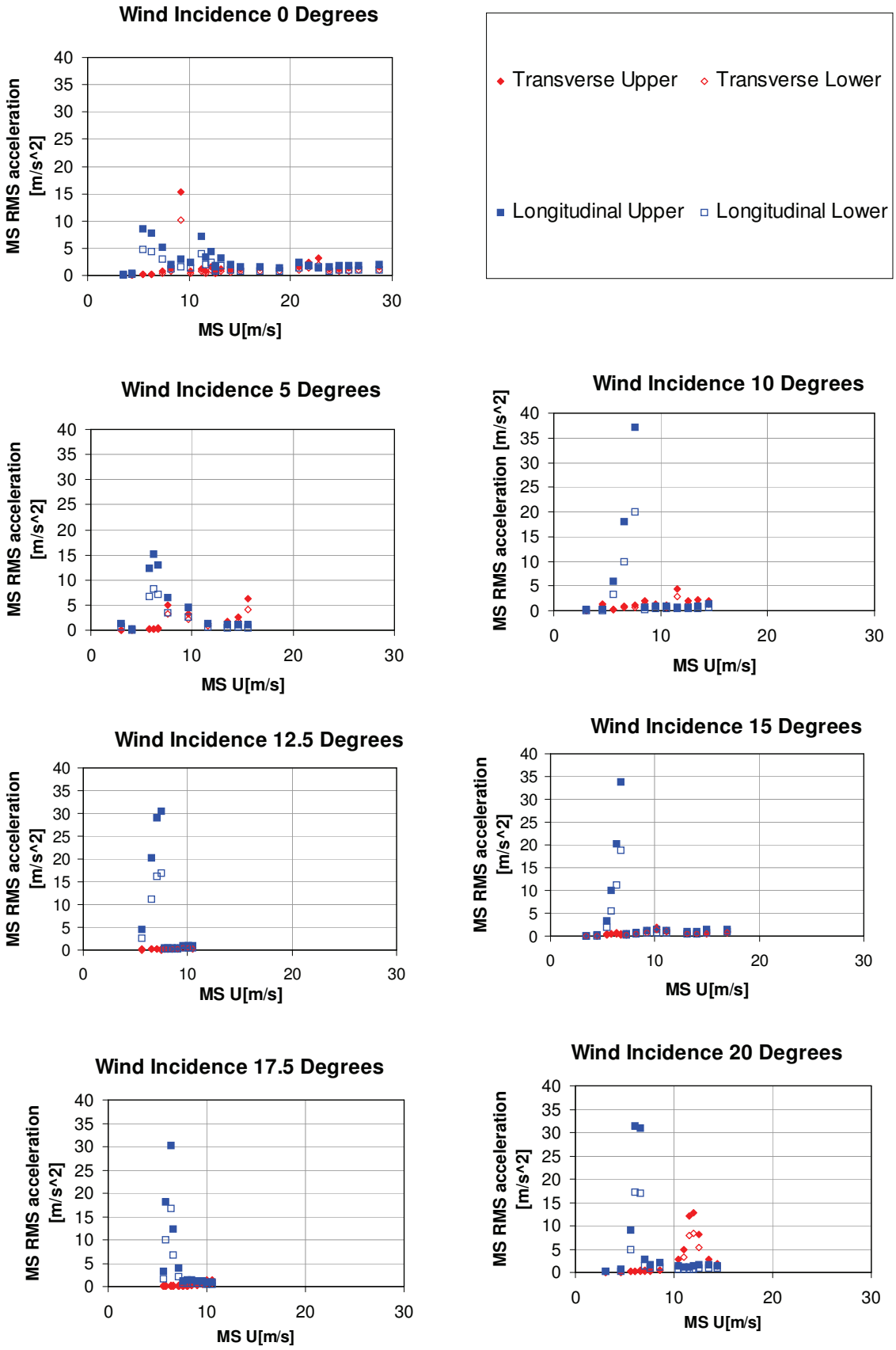

Wind Incidence 30 Degrees

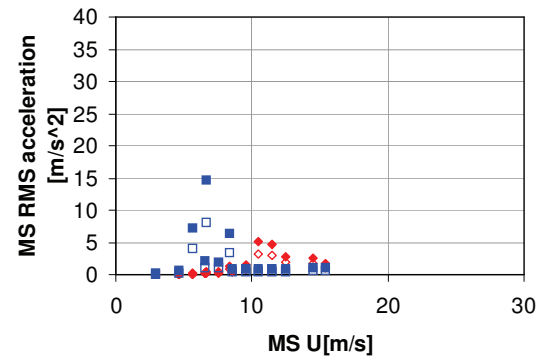

Wind Incidence 40 Degrees

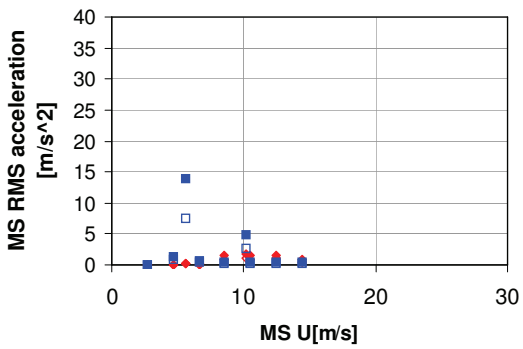

Wind Incidence 50 Degrees

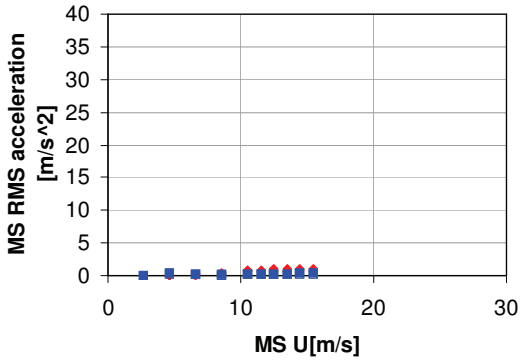

Wind Incidence 60 Degrees

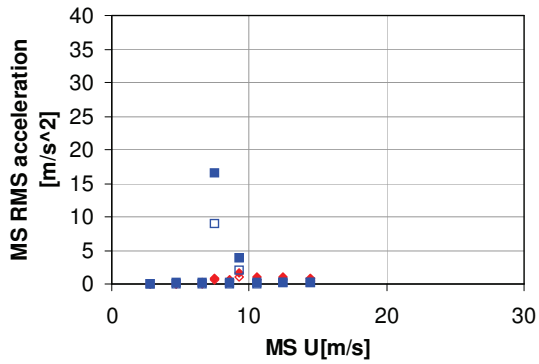

Wind Incidence 70 Degrees

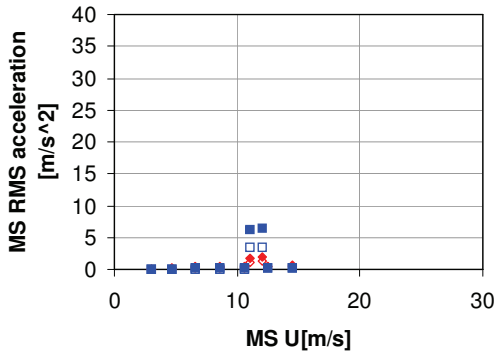

Wind Incidence 80 Degrees

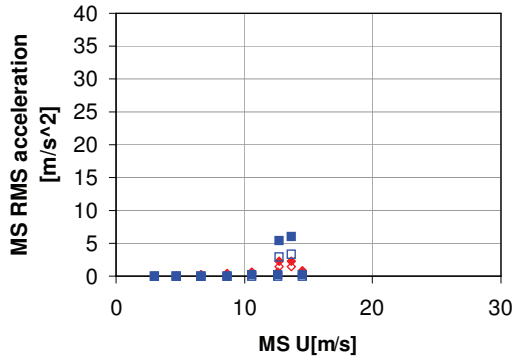

Wind Incidence 90 Degrees

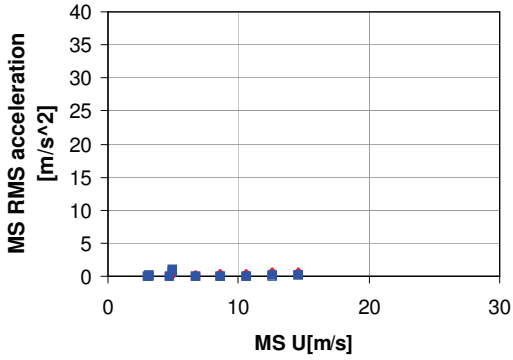

Figure 3.6 Leg 1 MS Accelerations vs Wind Speed; Tower Prior to Crossbeam Installation in Smooth Flow with Damping Level 0.16% of Critical (Torsional Mode)

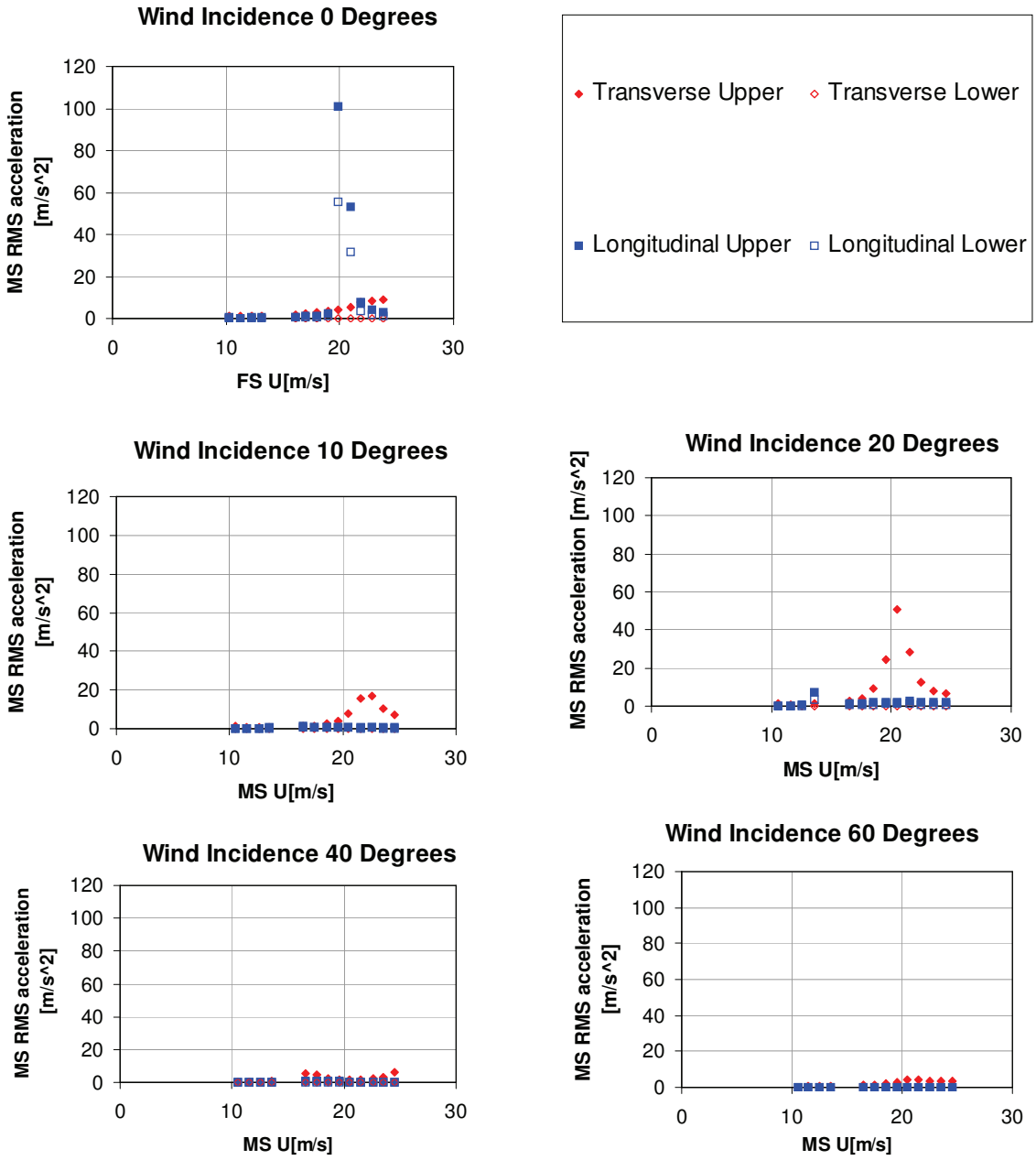

Figure 3.7 Worst Case FS Accelerations vs Wind Speed Sensitivity to Damping; Tower Prior to Crossbeam Installation

Smooth Flow Leg 1

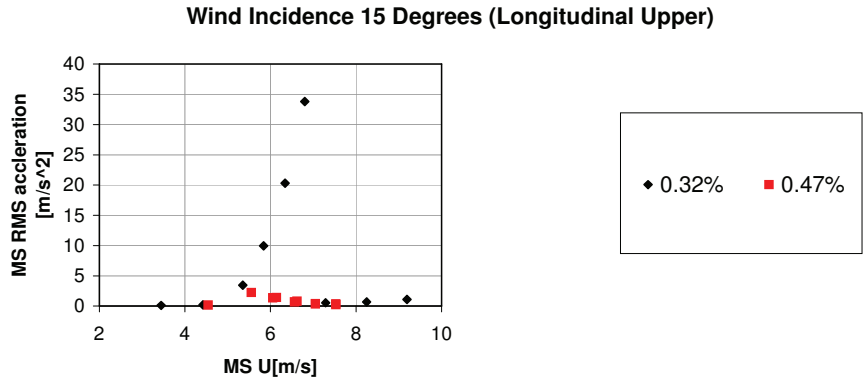

Smooth Flow Leg 2

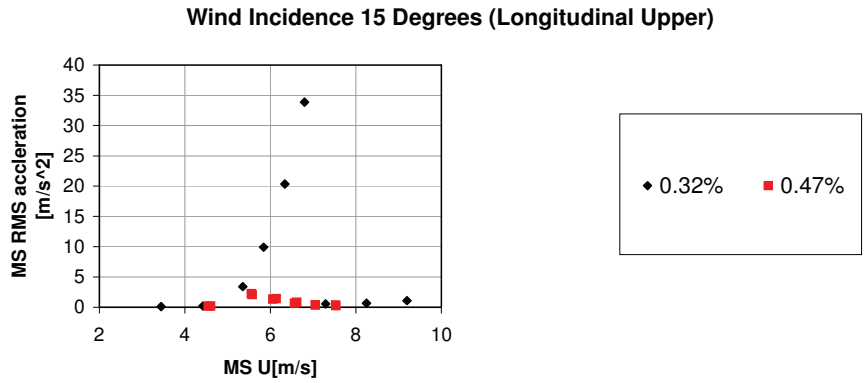

Turbulent Flow Leg 1

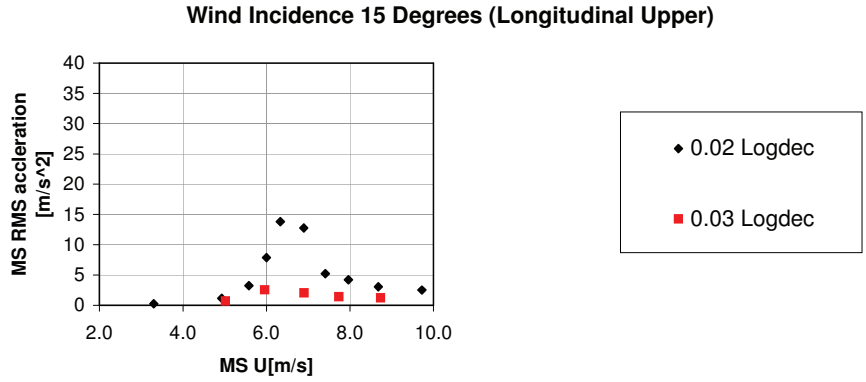

Turbulent Flow Leg 2

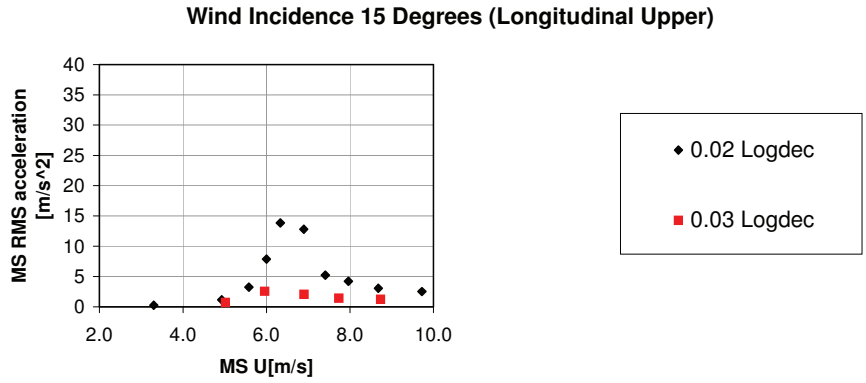

Figure 3.8 Worst Case FS Displacements vs Scruton Number[2] : Tower Prior to Crossbeam Installation Leg 1 in Smooth Flow

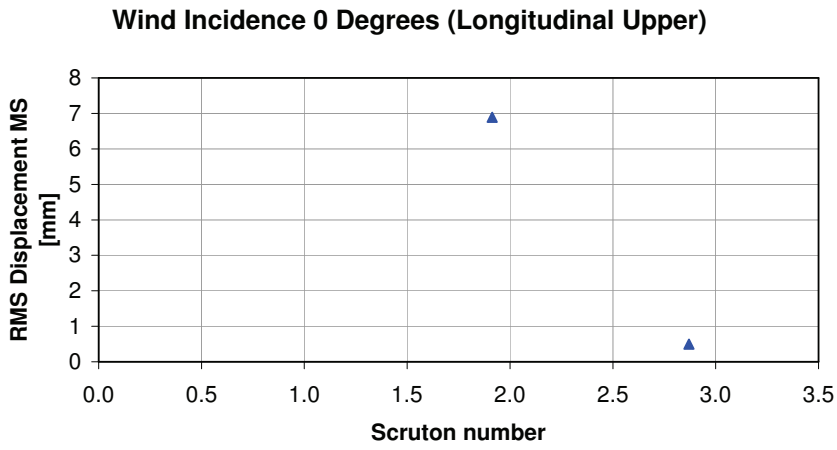

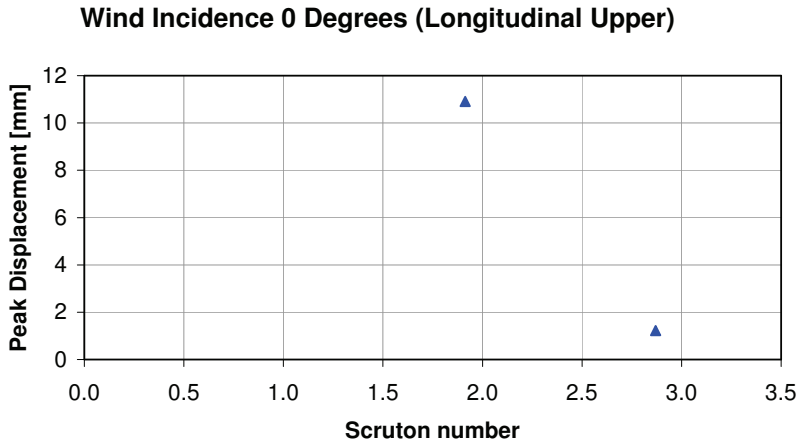

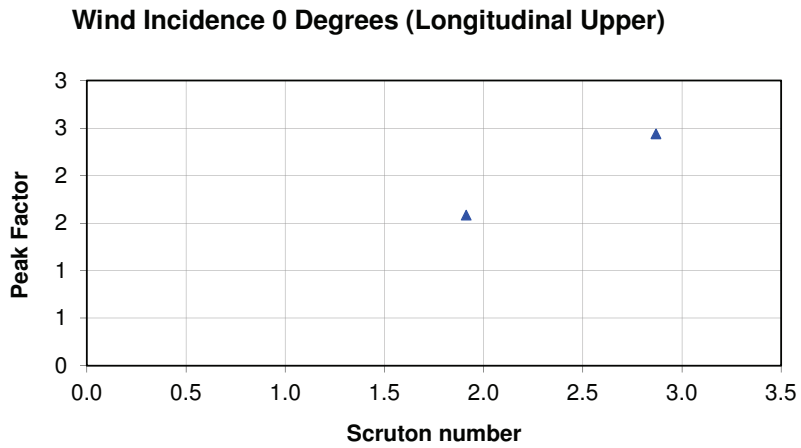

[2] $Sc = 2 \cdot \delta \cdot M / (\rho_a \cdot D^2)$
Where:
δ is the damping ratio [%crit]
M is the mode-generalised mass [tm^{-1}]
ρ_a is the density of air [tm^{-2}]
D is the reference dimension [m]

Figure 3.9 Leg 1 MS Accelerations vs Wind Speed; Tower In-Service in Smooth Flow, with ~0.3% Damping (Longitudinal, Torsional and Transverse Modes)

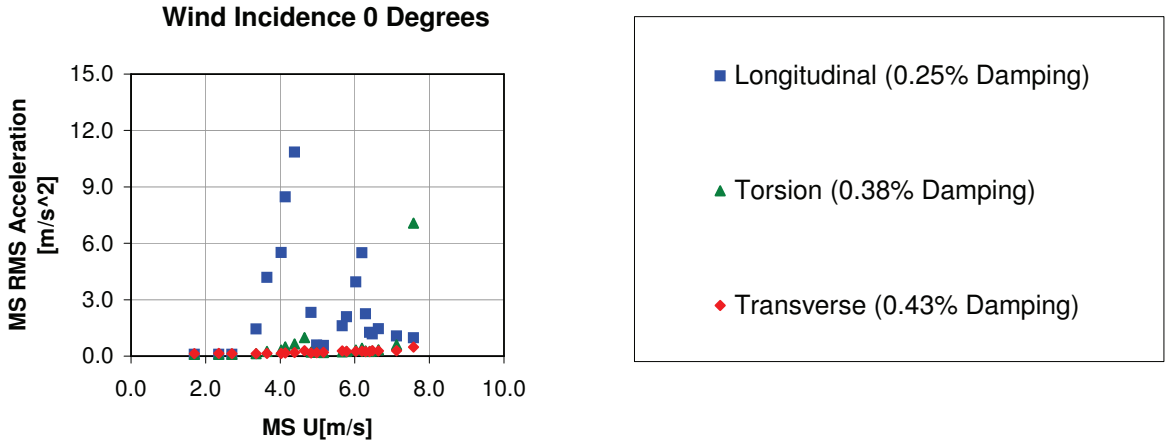

Figure 3.10 Leg 1 MS Accelerations vs Wind Speed; Tower In-Service in Smooth Flow, with ~2% Damping (Longitudinal, Torsional and Transverse Modes)

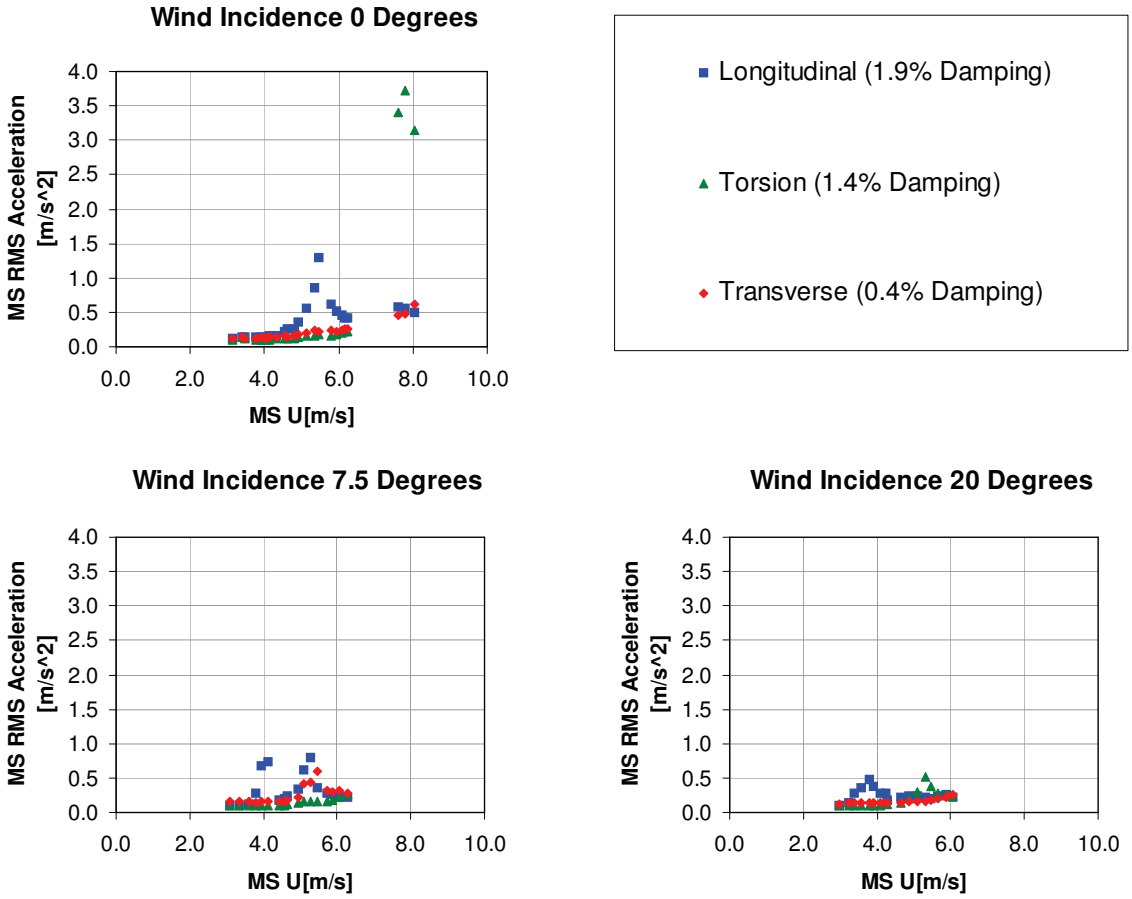

Figure 3.11 Leg 1 MS Accelerations vs Wind Speed; Tower In-Service in Smooth Flow, with ~4% Damping (Longitudinal, Torsional and Transverse Modes)

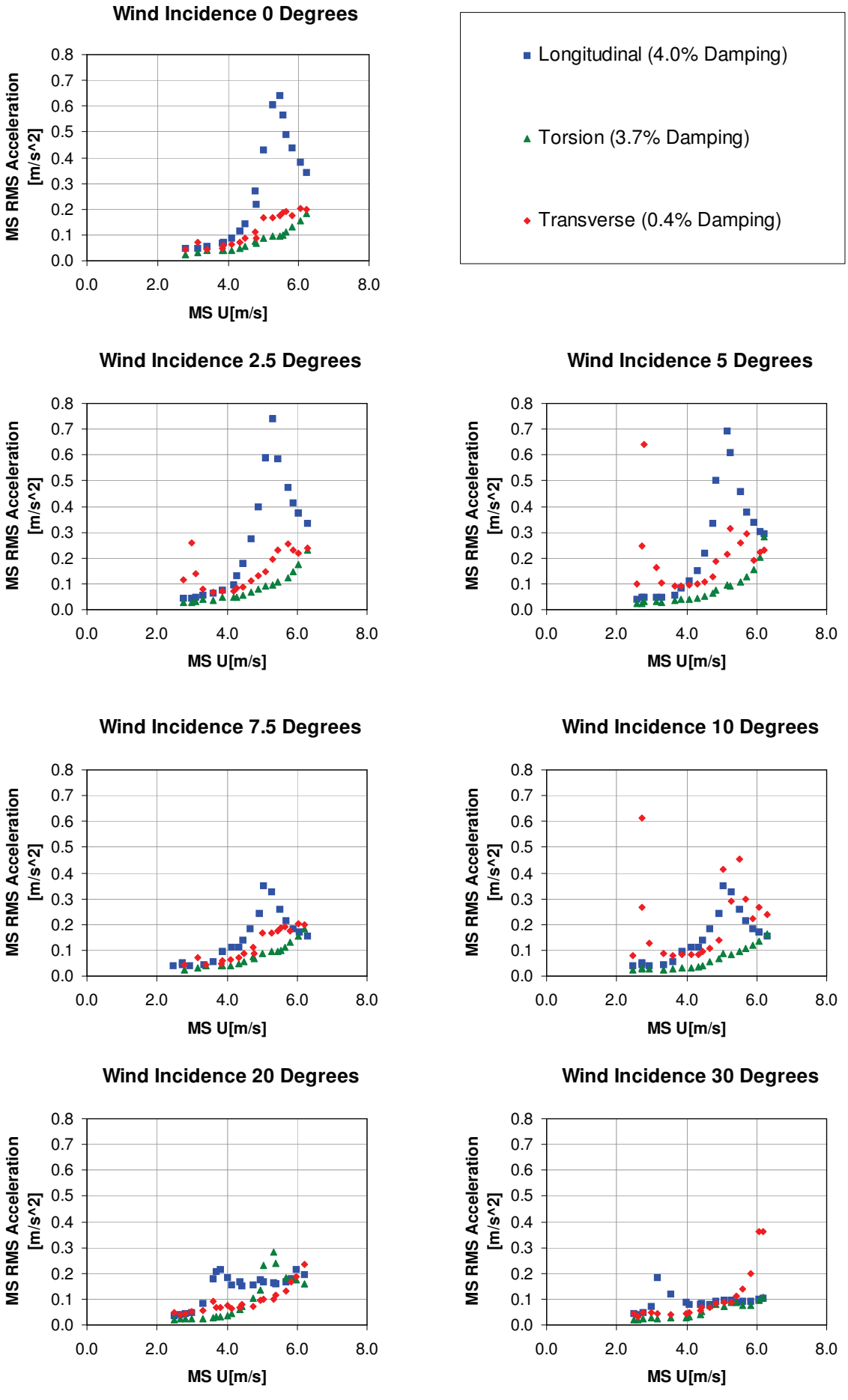

Figure 3.12 Leg 1 MS Accelerations vs Wind Speed; Tower In-Service in Smooth Flow, with ~5% Damping (Longitudinal, Torsional and Transverse Modes)

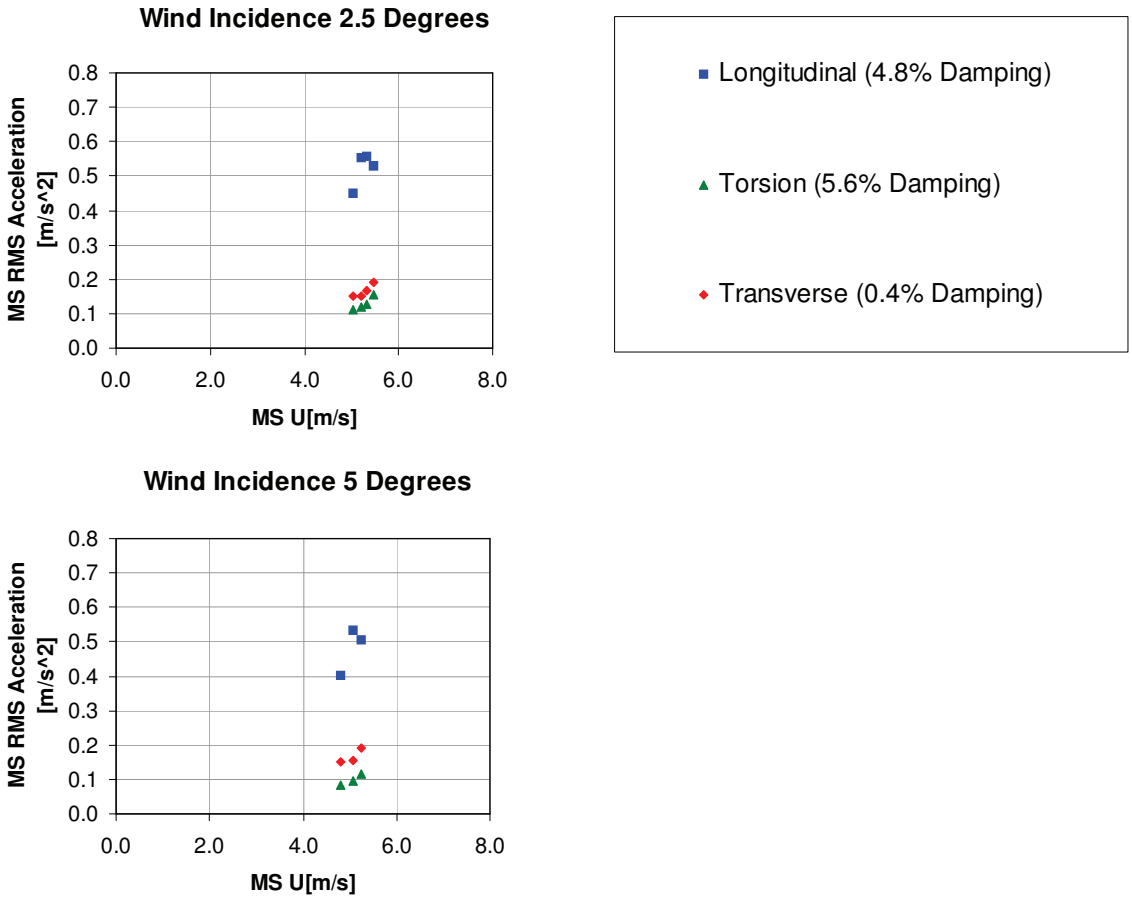

Figure 3.13 Leg 1 MS Accelerations vs Wind Speed; Tower In-Service in Smooth Flow, with ~1% Damping (Longitudinal, Torsional and Transverse Modes) (Damping Applied to Transverse Mode)

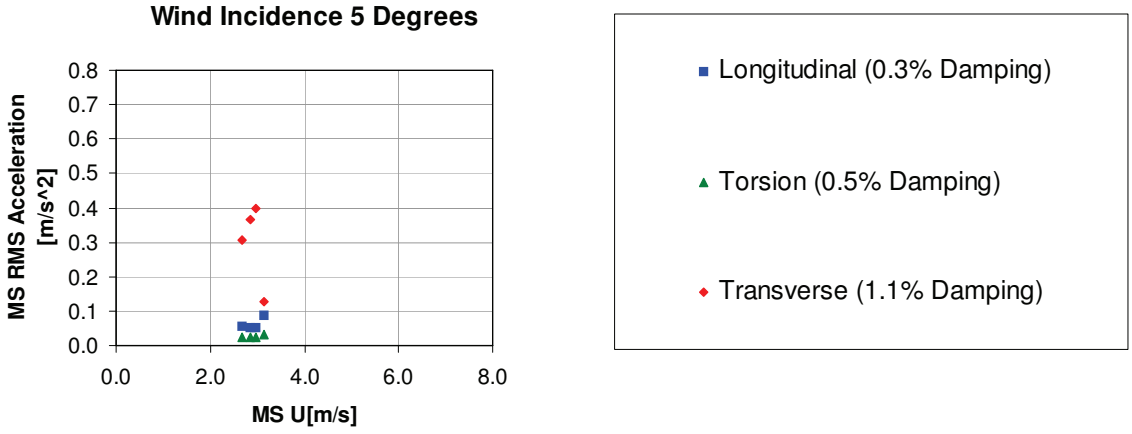

Figure 3.14 Leg 1 FS Accelerations vs Wind Speed; Tower With Cables Installed, Prior to Deck Installation in Smooth Flow with Damping Level 0.32% of Critical (Transverse & Longitudinal Modes)

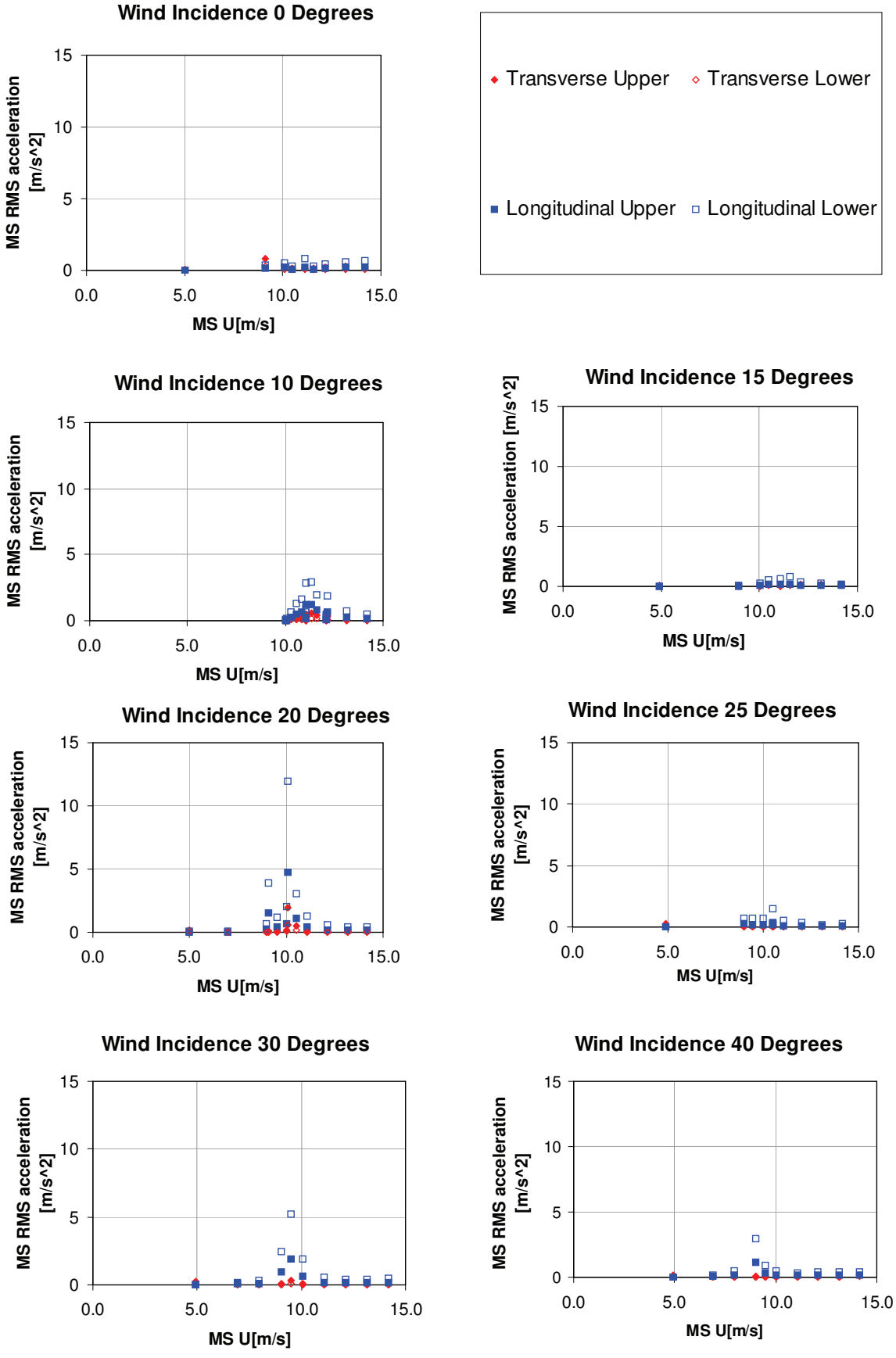

Wind Incidence 50 Degrees

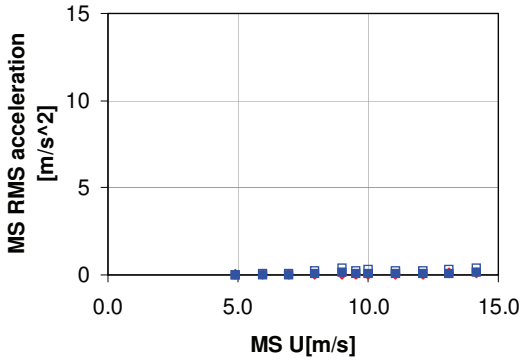

Wind Incidence 60 Degrees

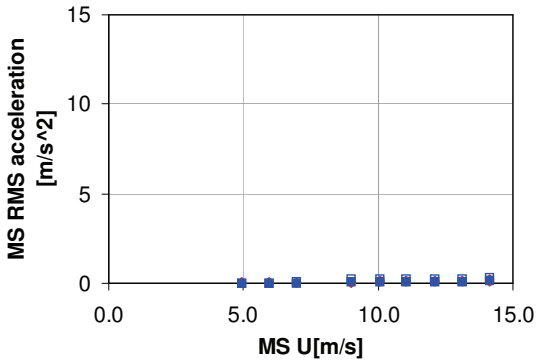

Wind Incidence 70 Degrees

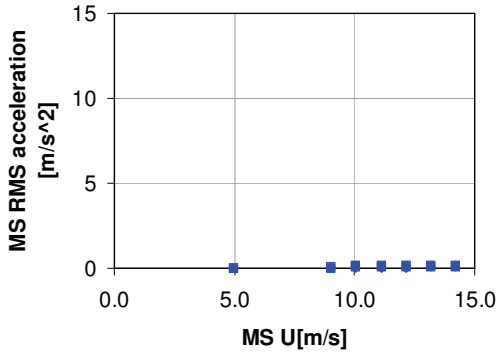

Wind Incidence 80 Degrees

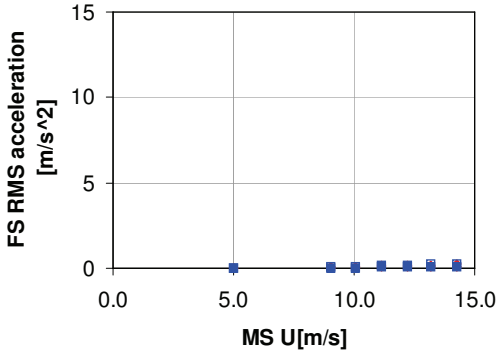

Wind Incidence 90 Degrees

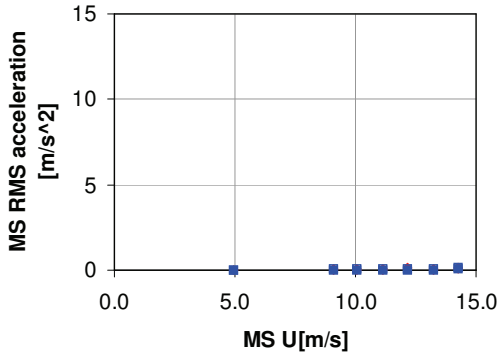

Figure 3.15 Leg 1 FS Accelerations vs Wind Speed; Freestanding Tower in Smooth Flow with Damping Level 0.16% of Critical (Transverse & Longitudinal Modes)

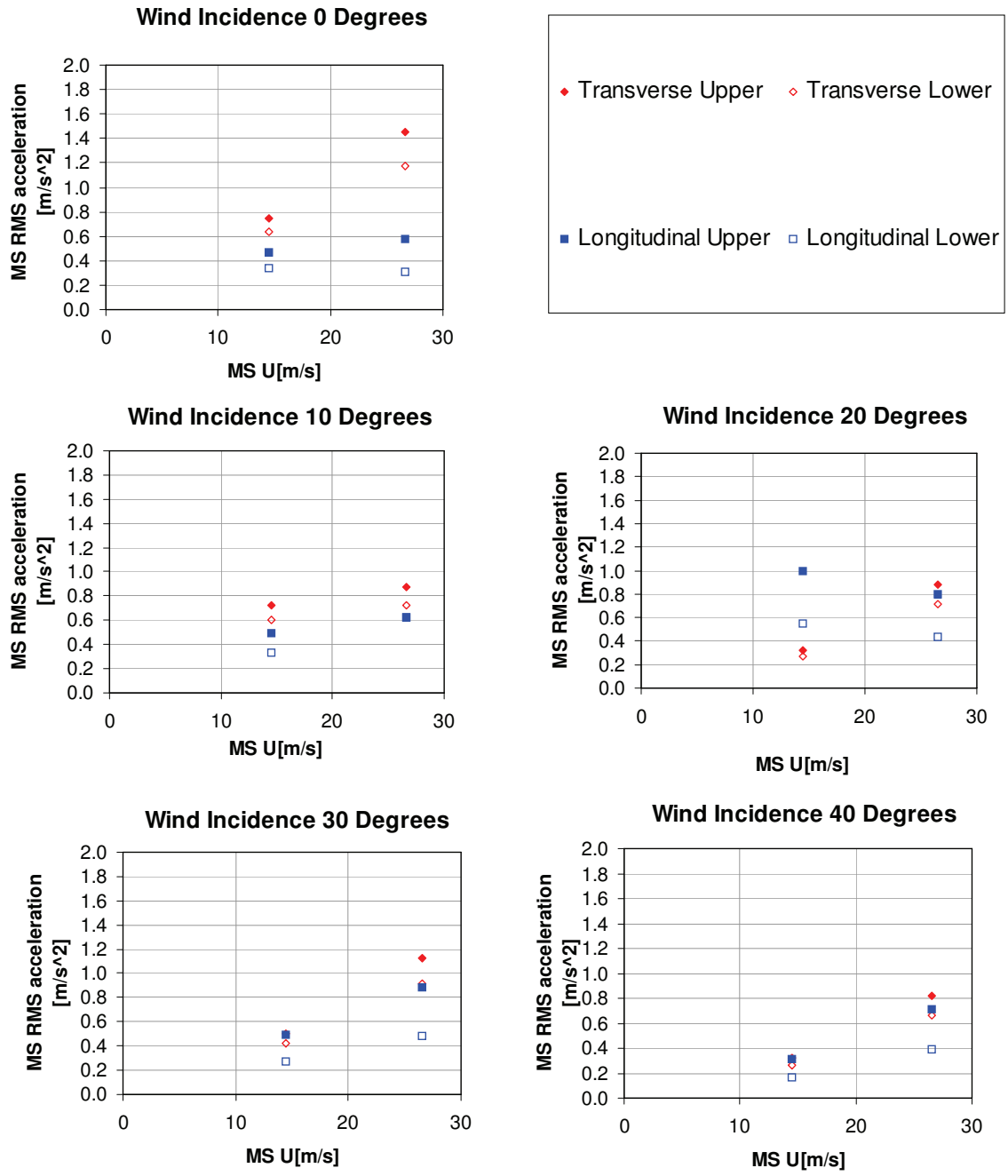

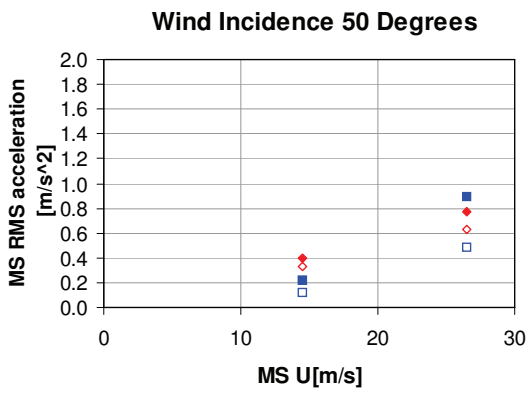
Wind Incidence 50 Degrees
MS RMS acceleration [m/s^2]
MS U[m/s]

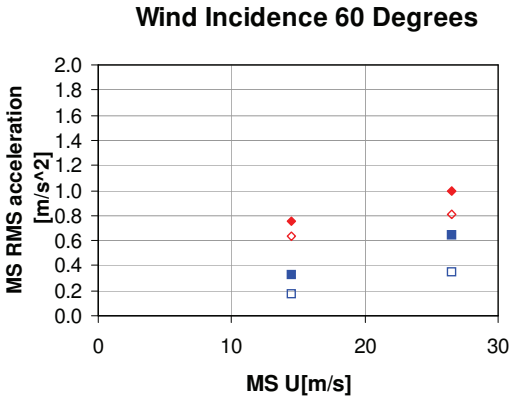
Wind Incidence 60 Degrees
MS RMS acceleration [m/s^2]
MS U[m/s]

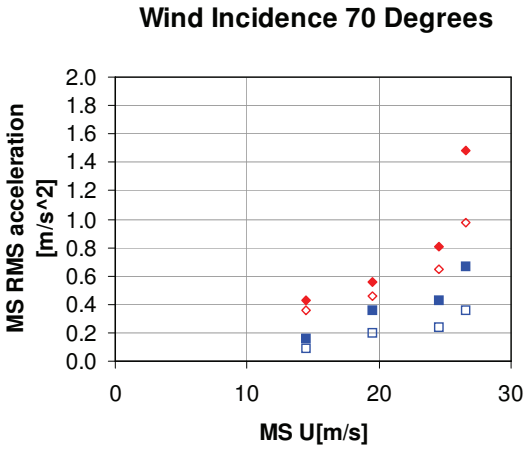
Wind Incidence 70 Degrees
MS RMS acceleration [m/s^2]
MS U[m/s]

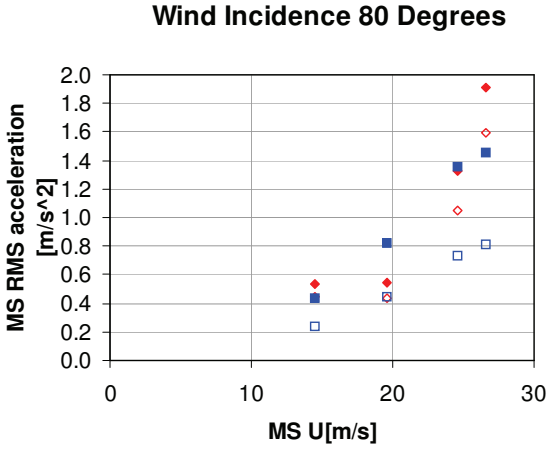
Wind Incidence 80 Degrees
MS RMS acceleration [m/s^2]
MS U[m/s]

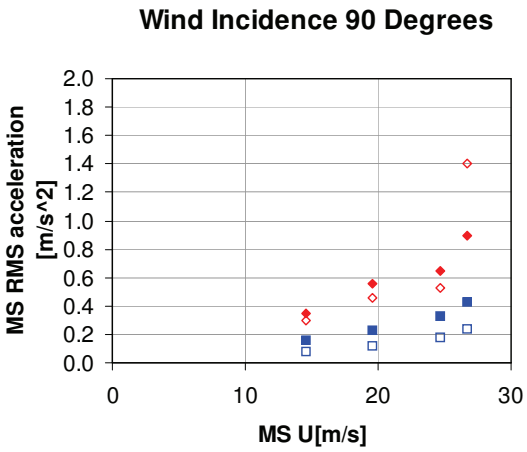
Wind Incidence 90 Degrees
MS RMS acceleration [m/s^2]
MS U[m/s]

Figure 3.16 Leg 1 FS Accelerations vs Wind Speed; Tower Prior to Crossbeam Installation in Smooth Flow with Damping Level 0.16% of Critical (Transverse & Longitudinal Modes)

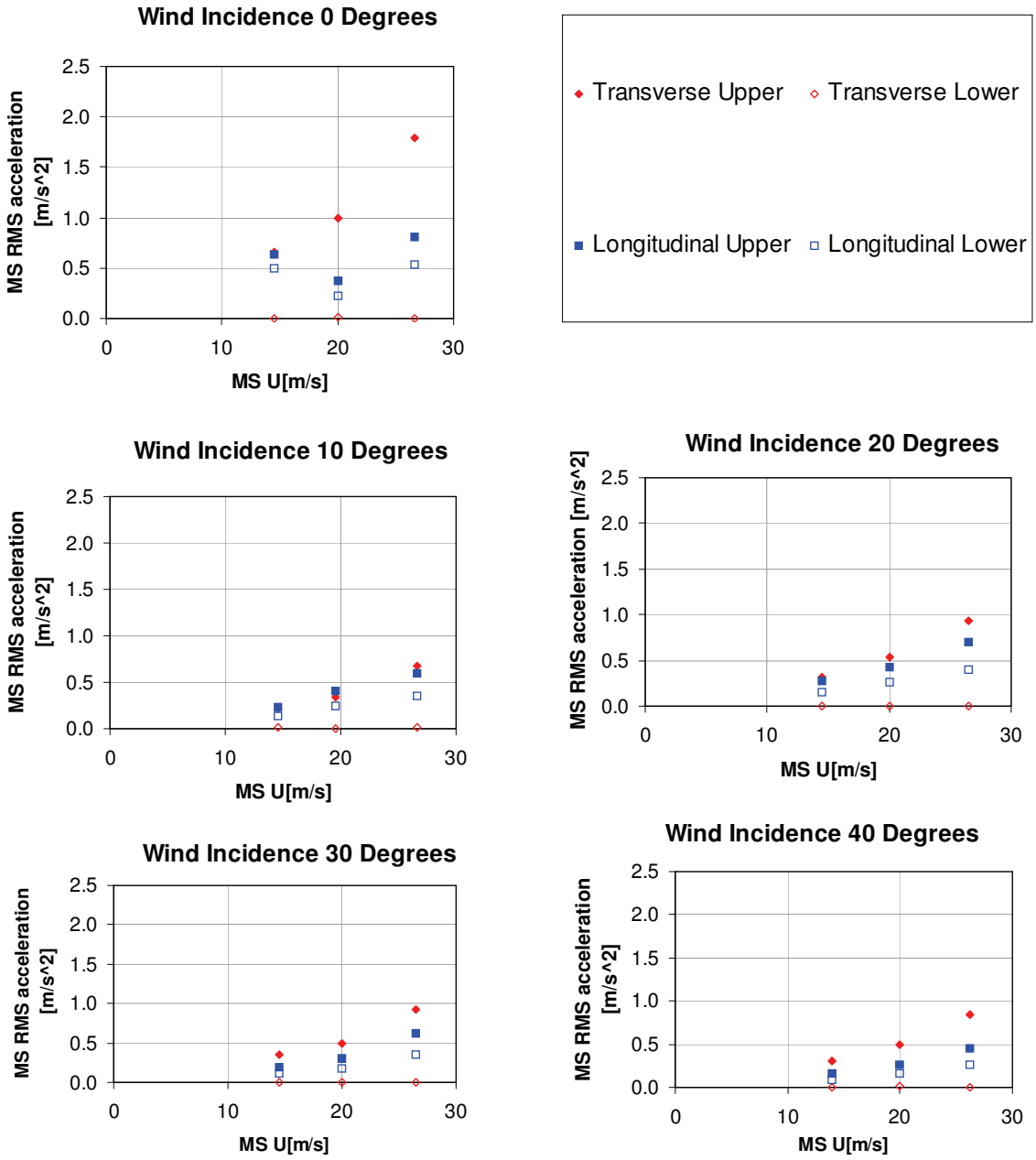

Wind Incidence 50 Degrees

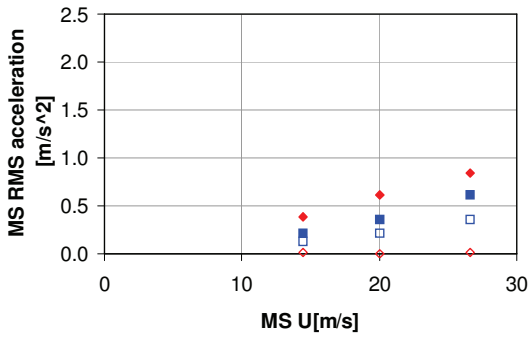

Wind Incidence 60 Degrees

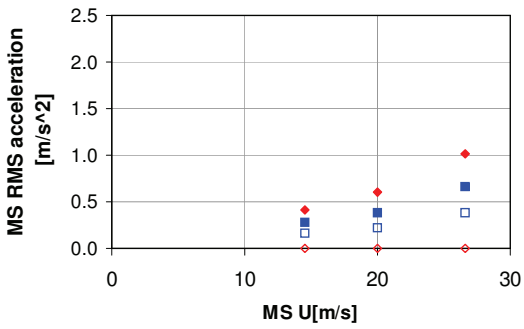

Wind Incidence 70 Degrees

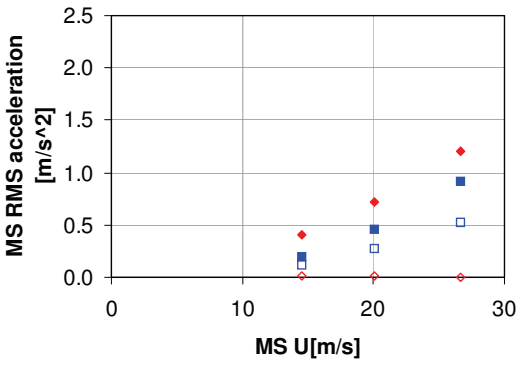

Wind Incidence 80 Degrees

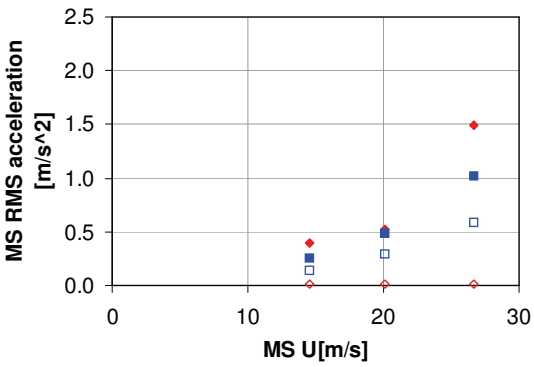

Wind Incidence 90 Degrees

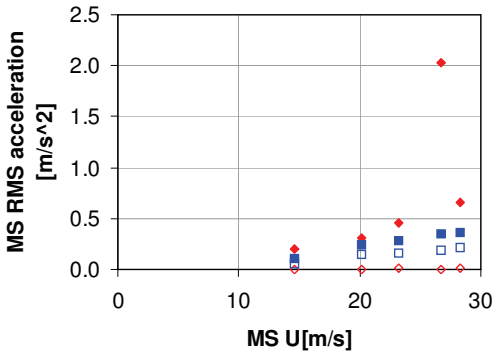

Figure 3.17 Leg 1 Base Loads and Moments, Freestanding Configuration in Turbulent Flow at 0°

FY – Mode 1

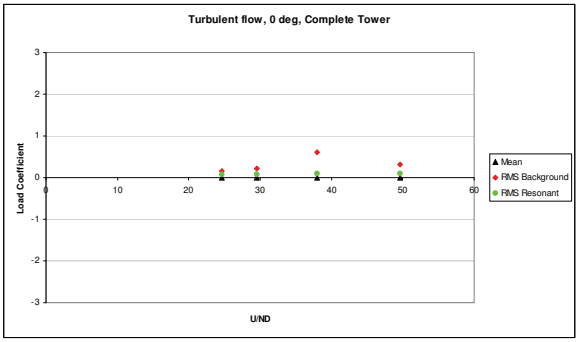

MX – Mode 1

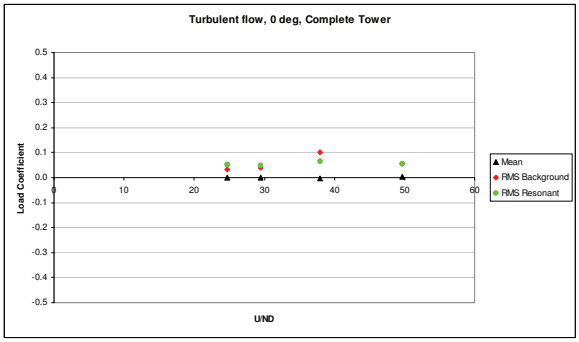

FZ – Mode 2

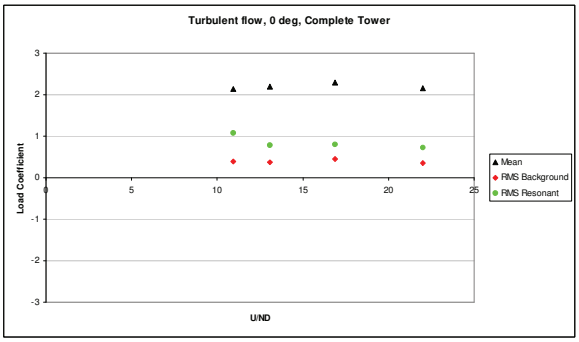

MY – Mode 2

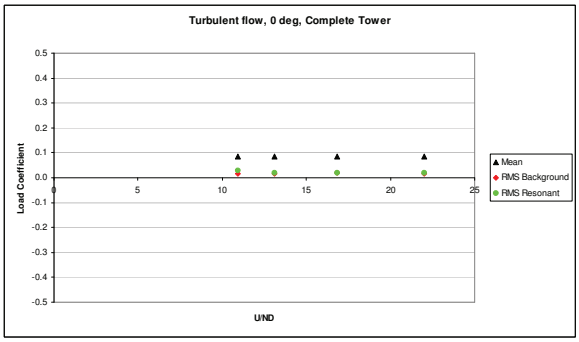

FX – Mode 2

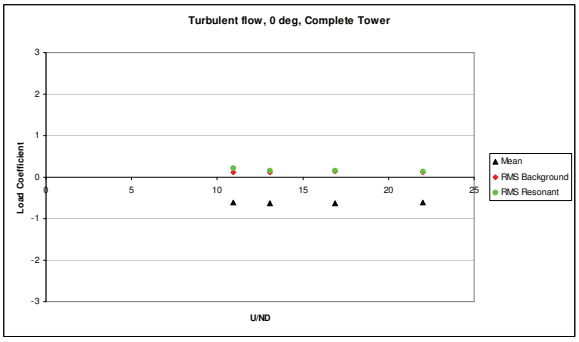

FY – Mode 3

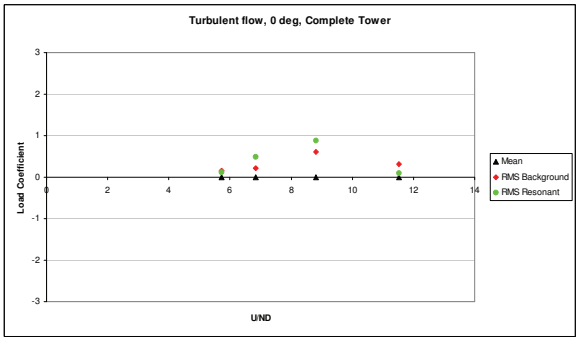

MZ – Mode 3

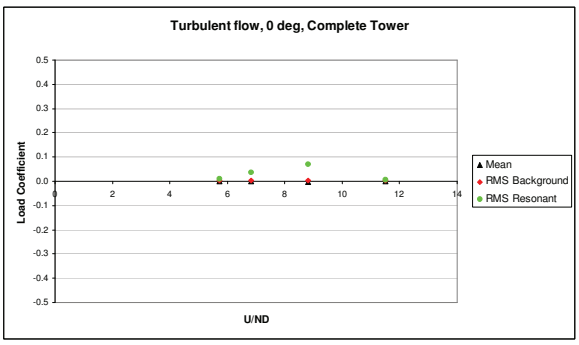

MX – Mode 3

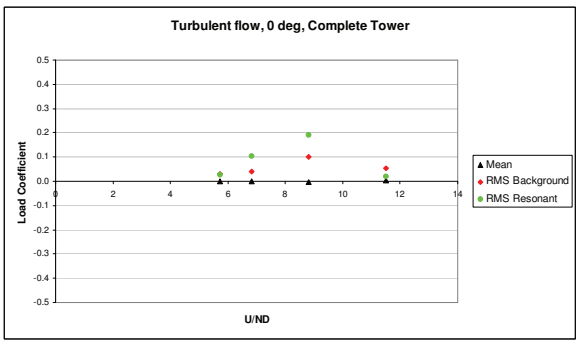

Figure 3.18 Leg 2 Base Loads and Moments, Freestanding Configuration in Turbulent Flow at 0°

FY – Mode 1

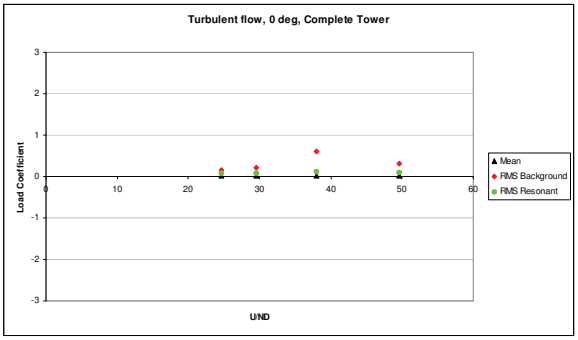

MX - Mode 1

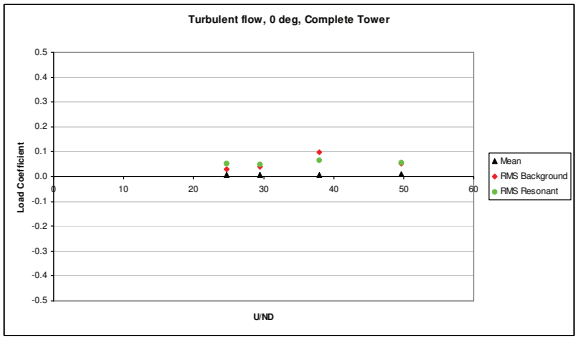

FZ – Mode 2

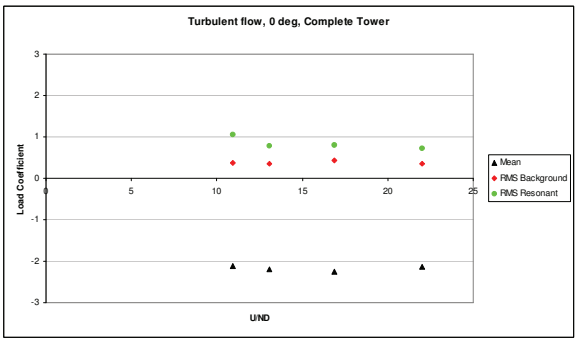

MY – Mode 2

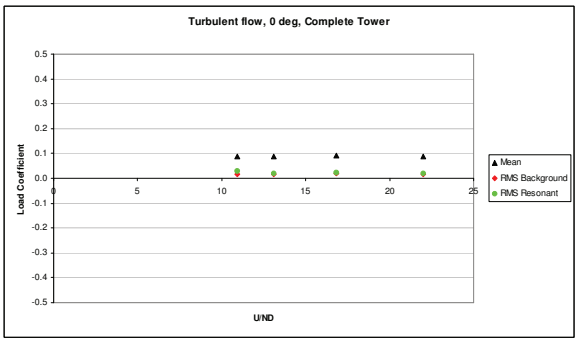

FX – Mode 2

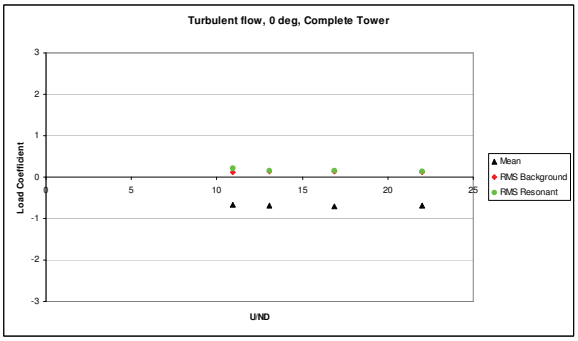

FY – Mode 3

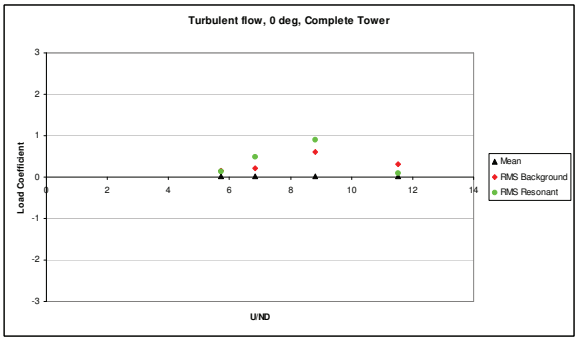

MZ – Mode 3

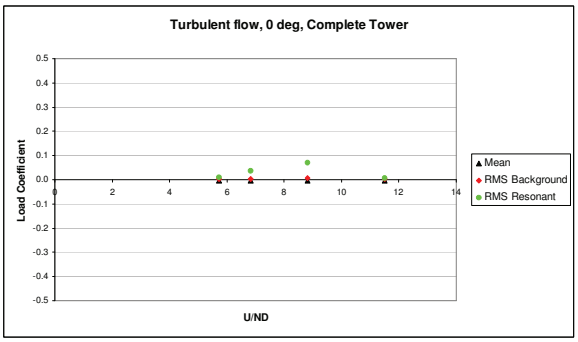

MX – Mode 3

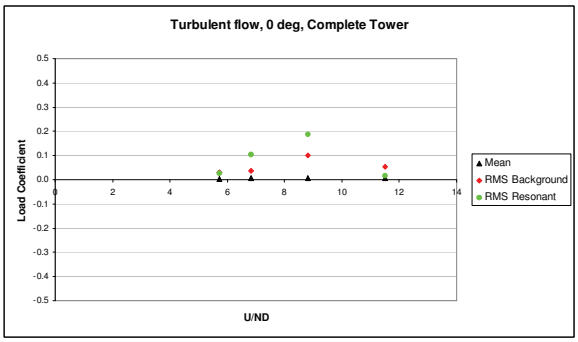

APPENDIX A. DESIGN WIND PROPERTIES & BOUNDARY LAYER SIMULATION

A.1. Design Wind Properties

The wind characteristics at the site were derived in accordance with the Specification [1] provided by COWI, and are summarised in the following sections.

A.1.1. Design Wind Speed Profile

The design wind speed profile for all wind directions is as follows:

$$u(z) = \frac{\ln z}{0.01}$$

Where u is the mean wind speed at elevation z above ground level

A.1.2. Design Turbulence Intensity Profiles

The turbulence intensity I profiles of the longitudinal (u), vertical (w) and lateral (v) components for the ocean and the land fetch respectively are defined as follows:

$$I_u(z) = \frac{1}{\ln\left(\frac{z}{z_0}\right)} \qquad I_v(z) = 0.75 I_u(z)$$

A.1.3. Design Power Spectra

The wind spectra are defined according to the Von Karman spectral model as follows:

$$\frac{nS_u(z,n)}{I_u^2(z)\overline{u}^2(z)} = \frac{6.868nL_u(z)/\overline{u}(z)}{[1+10.302nL_u(z)/\overline{u}(z)]^{5/3}}$$

$$\frac{nS_v(z,n)}{I_v^2(z)\overline{u}^2(z)} = \frac{9.434nL_v(z)/\overline{u}(z)}{[1+14.15nL_v(z)/\overline{u}(z)]^{5/3}}$$

Where

n is the frequency in Hz

L_u is the longitudinal length scale defined as follows: $L_u(z) = 300\left(\frac{z}{200}\right)^{0.5}$

L_v is the lateral length scale defined as follows: $L_v(z) = 0.25 L_u(z)$

A.2. BMT's Wind Tunnel – Technical Specification

The aeroelastic wind tunnel studies were carried out in BMT's Boundary Layer Wind Tunnel which has a test section 4.8 m wide, 2.4 m high and 15 m long with a 4.4 m diameter multiple plate turntable and a remotely controlled 3-dimensional traversing system. The operating wind speed range is 0.2 - 45 ms^{-1}. This wind tunnel facility is equipped state-of-the-art instrumentation for a wide range of applications and measurement techniques. The airline of the wind tunnel is indicated below in schematic form in Figure A.1.

Figure A.1 BMT's Boundary Layer Wind Tunnel – Airline

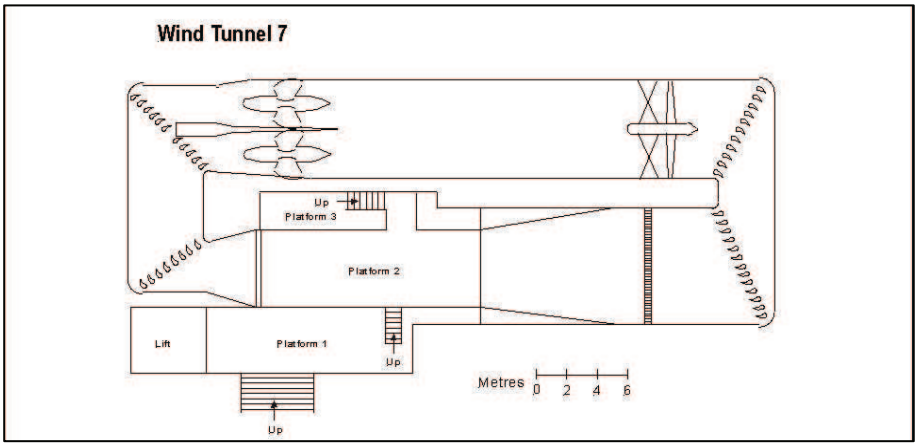

A.3. Experimental Conditioning

The full aeroelastic tower model tests were carried for the following flow conditions:

- Smooth Flow
- Turbulent Flow

A.3.1. Smooth Flow Test – Air Flow Generation

The maximum level of turbulence inherent in smooth flow in the wind tunnel is less than 0.3% and is consistent with best industry standard for aeroelastic testing for long span bridges. Figure A.2 presents the profiles of mean wind speed and turbulence intensity (I_u) that BMT used in the tests. The mean is normalised by the wind speed at the highest point measured (160m)

Figure A.2: Smooth Flow Velocity and Turbulence Profiles

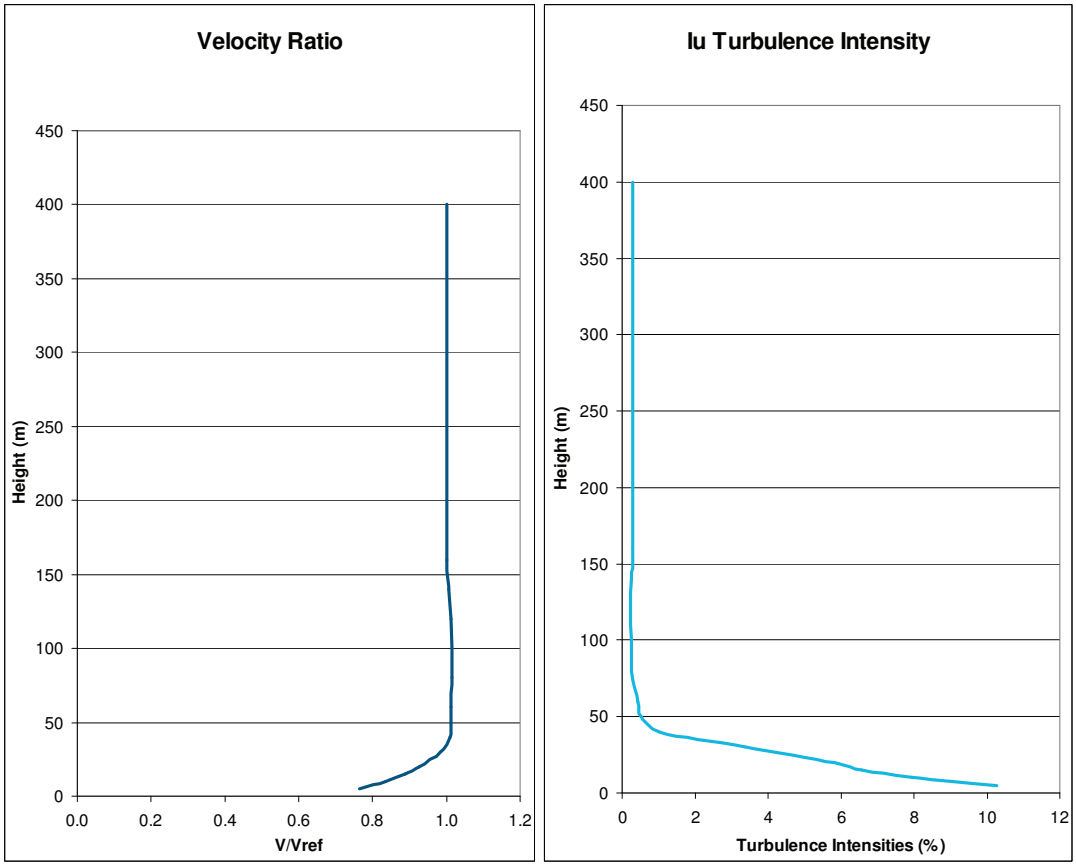

A.3.2. Turbulent Flow Test – Air Flow Generation

The turbulent boundary layer was set up using an arrangement of roughness elements distributed over the floor of the wind tunnel and a 2-dimensional barrier, with square vortex generating posts, placed at the entrance to the test section

The properties of the boundary layer were measured at the centre of the turntable (in absence of the model) using hot-wire anemometry.

The mean wind speed, the turbulence intensities (longitudinal and lateral component) and the wind spectra were measured at a range of full-scale heights up to 400m. Measurements were also carried out for two wind speeds, $5ms^{-1}$ and $17ms^{-1}$ at the top of the tower (400m), to ensure that no significant variation of the wind characteristic would occur within the wind speed range of the tests.

Results of the turbulence simulation are presented in terms of wind profile, turbulence intensities profiles and u-, v-component of the wind spectra at a number of heights along the tower.

Figure A.3 presents the profiles of mean wind speed and turbulence intensities (I_u I_v) that BMT used in the tests compared against the target site profile. The mean is normalised by the mean wind speed at a reference height at the top of the tower (400m).

Figure A.3: Target and Achieved Velocity and Turbulence Profiles

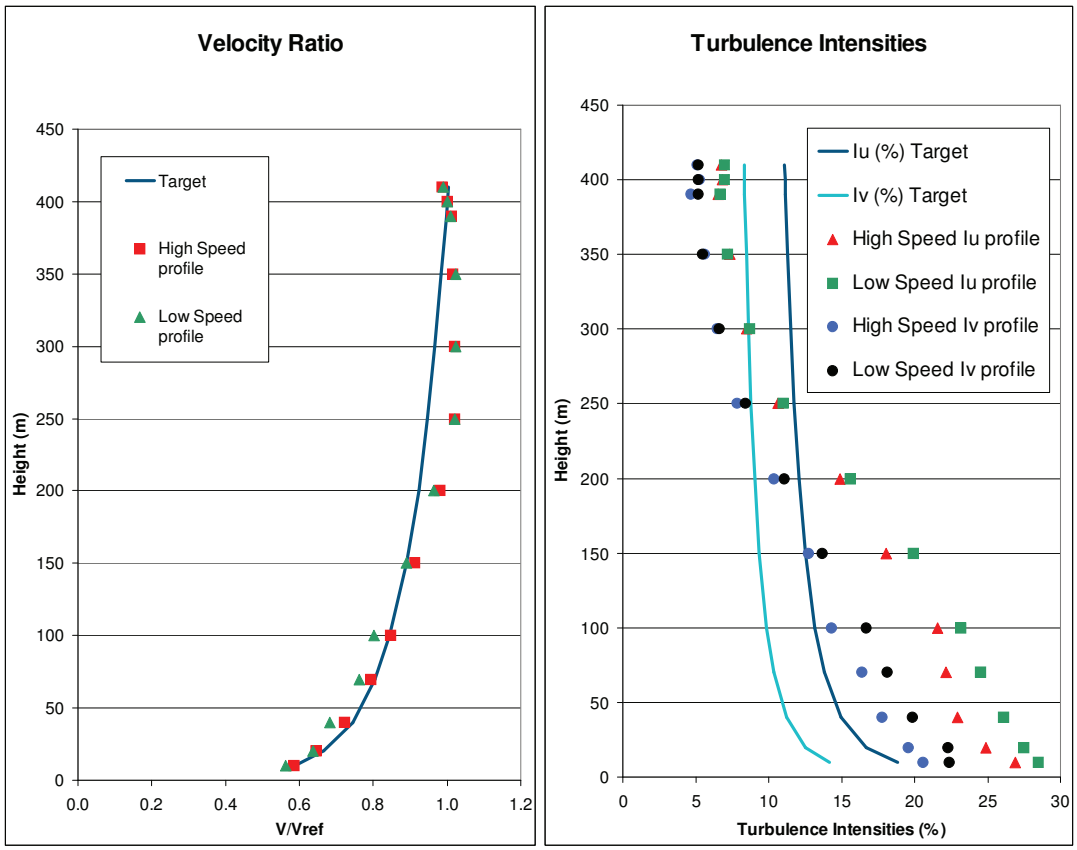

The wind spectra measured for the u and v component (S_{uu} and S_{vv}) are presented and compared to von Karman wind spectra in Figures A.4 to A.7 for 200m and 400m. The reference dimension B is taken as 20m full scale. Measurements were taken at model-scale speeds of $18ms^{-1}$ and $5ms^{-1}$, in order to quantify the properties in the region of the two wind regimes associated to vortex-shedding responses and wind loading / divergent responses. It is clear from the graphs presented that the wind spectra and the wind profiles and turbulence intensities thereof do not vary within the testing wind speed range.

Figure A.4: Target and Achieved Spectra, High Speed, 200m

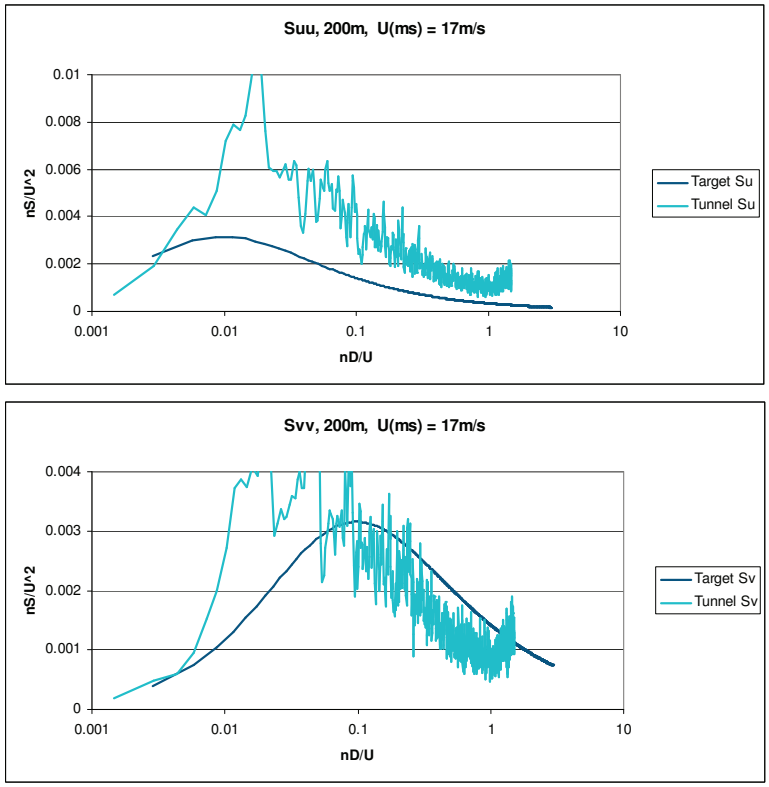

Figure A.5: Target and Achieved Spectra, High Speed, 400m

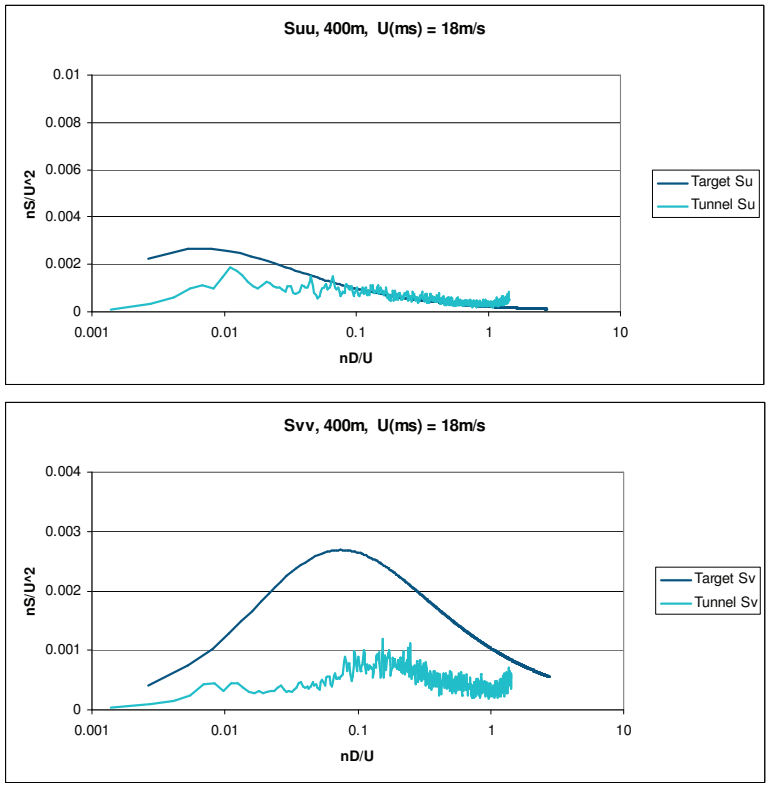

Figure A.6: Target and Achieved Spectra, Low Speed, 200m

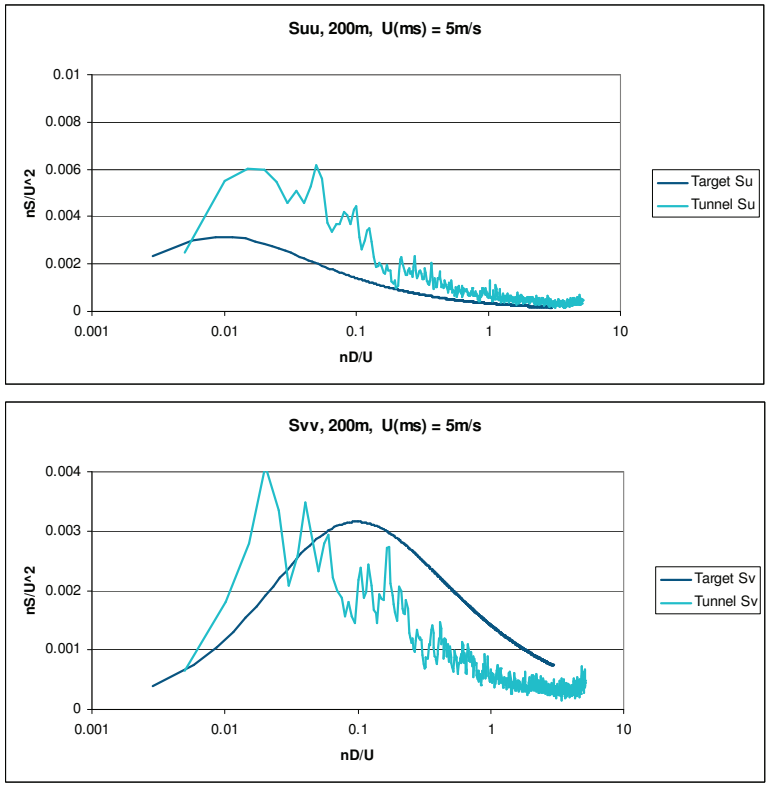

Figure A.7: Target and Achieved Spectra, Low Speed, 400m

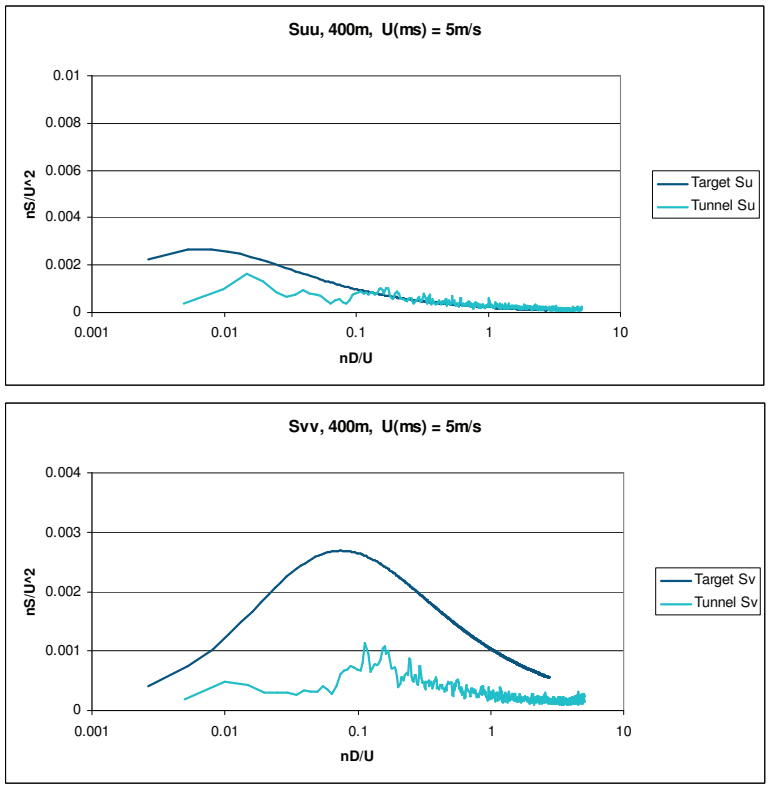

APPENDIX B. MODELS DESIGN AND CONSTRUCTION

B.1. General

The full aeroelastic models, as designed, were suitable for aeroelastic wind tunnel testing.

B.2. Basis for Design and Construction of the Wind Tunnel Model

The models of the tower were constructed based on information supplied by COWI, as follows:

Drawing Name/No.	Date	Description
CG1000-PAXDPCG-S5TC000000-01_A.dwg	16-07-10	Tower Drawing
CG1000-PAXDPCG-S5TOT00000-01_A.dwg	16-07-10	Crossbeam Detail
Tower Mode Information_July12_to BMT.xlsx	16-07-10	Modal Data

The models were reviewed and approved by the design team, prior to testing.

B.3. Model Scale

A model scale of *1:200* has been adopted. At this scale the model allowed a detailed representation of all geometric features of the tower that are expected to affect the wind flows around the structure at full scale. In addition, this scale enables a good simulation of the turbulence properties of the wind to be achieved.

B.4. Model Configurations

The four model configuration were represented and tested using the three full aeroelastic models, namely *stiff, soft* and *Froude scaled* as follows:

Configuration	Testing Scenario	Speed Scale	Model	Modification
Freestanding	Vortex Shedding	~2.2	Stiff	None
Freestanding	Aerodynamic Stability	~4.1	Soft	None
Freestanding	Wind Loading	~4.1	Soft	None
Prior to Top Crossbeam Installation	Vortex Shedding	~2.2	Stiff	Top crossbeam removed
Prior to Top Crossbeam Installation	Aerodynamic Stability	~4.4	Soft	Top crossbeam removed
In-Service	Vortex Shedding	~12	Froude Scaled	Top of tower "pinned" by tether cables
With Cables Installed	Vortex Shedding	~4	Soft	Top of tower connected to dynamic mass rig

B.5. Details of Model Design & Construction

B.5.1. Governing Criteria and Scaling Requirements

The governing criteria for full aeroelastic model design were as follows:

- Geometric representation of the aerodynamic envelope at scale 1:200
- Conservation of the following non-dimensional parameters defined below:

Bending stiffness - $$\frac{EI}{\rho_a V^2 B^4} \quad (1)$$

Extensional stiffness - $$\frac{EA}{\rho_a V^2 B^2} \quad (2)$$

Mass - $$\frac{M}{\rho_a B^2} \quad (3)$$

Where I is the second moment of inertia, J is the polar second moment of area, A is the cross sectional area, and M is the mass per meter.

- Replication of those key modes likely to have influence in the dynamic response of the tower. These are the primary bending modes of the tower for each configuration.
- Operating speed capability to cover the design wind speed range and allow accurate assessment of the vortex-shedding responses.

B.5.2. Details of Model Construction

Stiff Model (Freestanding Tower With/Without Crossbeam - Vortex Shedding)

The spine of the tower was manufactured from rectangular cross section steel tube. The tower shape was generated using foam and lightweight wood arranged into 4 sections to ensure that the stiffness of the structures (given by the spine) was not affected by the presence of the cladding. Each cladding panel was fixed to the spine at a discreet contact point in the centre of each section, therefore the motion of the spine and cladding is matched. The gap size between two adjoining cladding section was approximately 1-1.5mm. All elements were chosen to have to correctly scaled mass. The spines were connected to the BMT High Frequency Force Balances (HFFB) via purposely-machined steel plates. The top crossbeam was designed to be detachable, bolted securely to the steel spine.

Figure B.1: Stiff Model – Freestanding Tower and with Crossbeam Removed

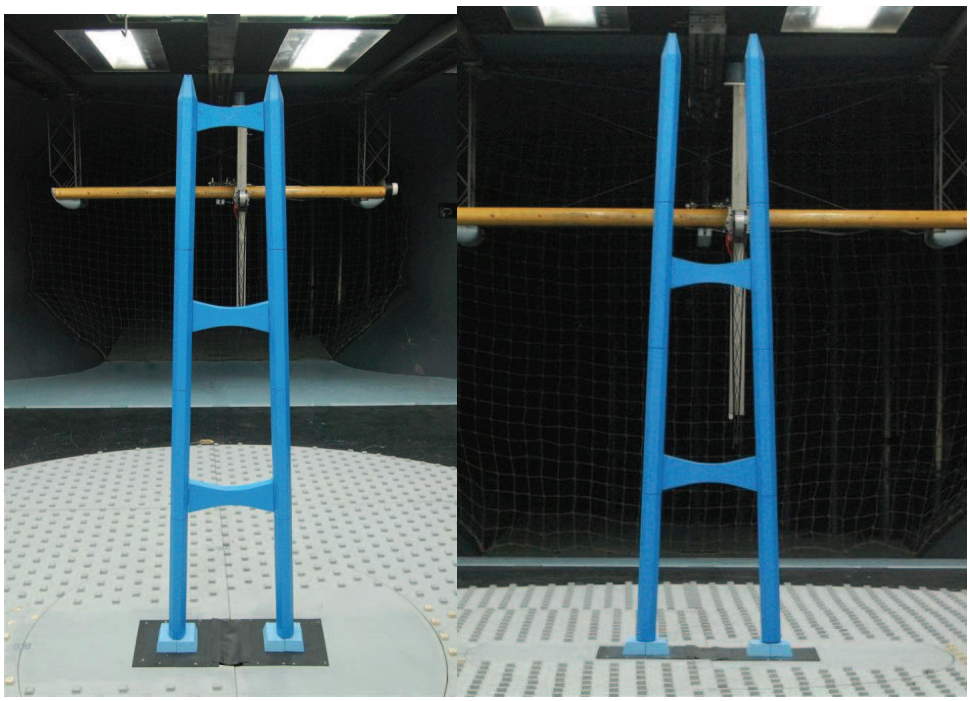

Soft Model (Freestanding Tower With/Without Crossbeam - Stability and Wind Loading)

The *soft* aeroelastic model was constructed in a similar fashion to the stiff model, but used a spine constructed from a thinner cross section rectangular tube. The tower shape was generated using foam and lightweight wood, arranged into 6 sections. As with the stiff model, the gap size between two adjoining cladding sections was approximately 1-1.5mm, and they were fixed at their centres to the spine. All elements were chosen to have correctly scaled mass. The spines were connected to the BMT High Frequency Force Balance (HFFB) via a purposely machine steel plate.

Figure B.2: Soft Model – Freestanding Tower

Froude Scaled Model (Pinned) (Complete bridge – Vortex Shedding)

The spine of the tower was manufactured from rectangular cross section brass tube. The tower shape was generated using lightweight wood arranged into 12 sections to ensure that the stiffness of the structures (given by the spine) was not affected by the presence of the cladding. Each panel was joined to the spine at its centre. The gap size between two adjoining cladding section was approximately 1-1.5mm. All elements were chosen to have to correctly scaled mass. The spines were connected to the BMT High Frequency Force Balances (HFFB) via purposely-machined steel plates. In order to replicate the mode shape of the bridge in service, the *Froude Scaled* model was pinned at the top, using tensioned steel cables. The cables were connected to a stiff interface at the top of the brass spine, and firmly anchored to the wind tunnel floor at the other end.

Figure B.3: Froude Scaled Model Pinned

Soft Model and Rig to Model Cable Mass (Tower With Cables Installed, Prior to Deck Installation - Vortex Shedding)

The intermediate erection stage highlighted modes in which tower motion accounted for only a modest part of the total kinetic energy of the oscillation, as expressed by the modal effective mass. The critical mode was identified as equal spanwise motion of the two legs of the tower, with significant restraint at the top enhancing the relative importance of movements at part-height.

The manner in which the key features of this mode were reproduced is shown in Figure B.4. The additional mass was incorporated as a single block (B), approximately 25kg, located for convenience on the tunnel floor. This was constrained to move in the horizontal spanwise direction by a set of vertical leaf springs (C), and connected to the tower top by a steel-rod 'forestay' (D) selected to give the appropriate elasticity between tower and supplementary mass. An appropriate initial ('static') tension to cover the inertial stressing in oscillation was provided by a turnbuckle action through a relatively soft coil spring (G).

Twin backstays (E) were provided, which restrained torsion in plan as well as providing the controlled elasticity required for the spanwise mode. Solid rods were again chosen, to avoid the risk of damping inherent in helical-laid cables. As twin rods developed a greater stiffness than required to simulate this mode, they were connected to the foundation bed (H) through leaf springs (F). These were adjustable to allow compensation for compliance in joints and connections not explicitly included in the design model. Note that this arrangement did not provide supplementary mass for the torsion or lateral-action modes.

A response of magnitude as small as 1mm rms (model scale) would develop peak inertia forces likely to exceed ±1kN the model was assembled on a robust welded foundation bed (H) comprising two longitudinal steel I-section beams and RHS cross-members.

Figure B.4: Cable Mass Rig Arrangement

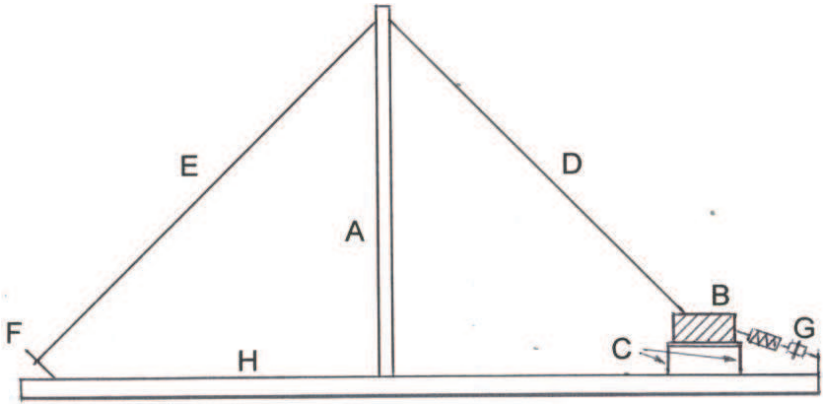

Where:

A	Aeroelastic model of tower
B	Supplementary mass
C	Leaf spring array
D	Forestay: single rod on centre-line in plan
E	Backstays: twin rods on line of bridge cables
F	Leaf spring anchorage for each backstay
G	Tensioning coil spring and turnbuckle
H	Foundation bed

Figure B.5: Cable Mass Rig

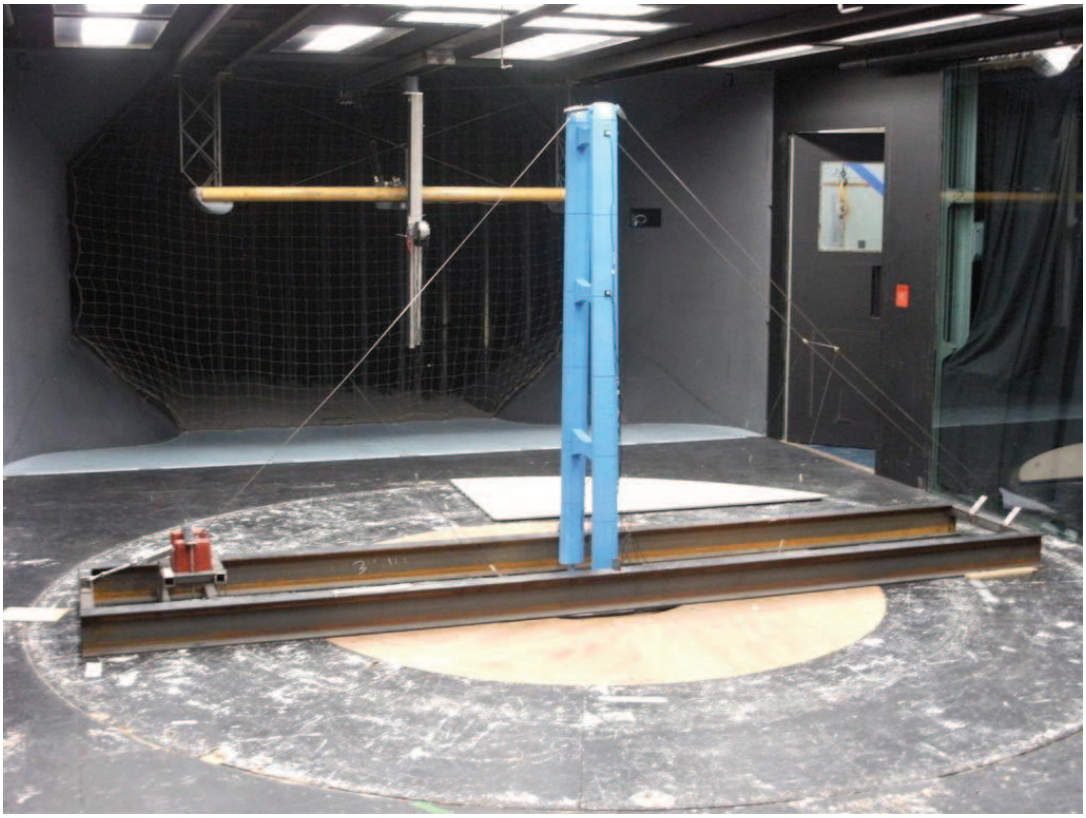

Figure B.6: Closeup of Supplementary Mass of Dynamic Rig

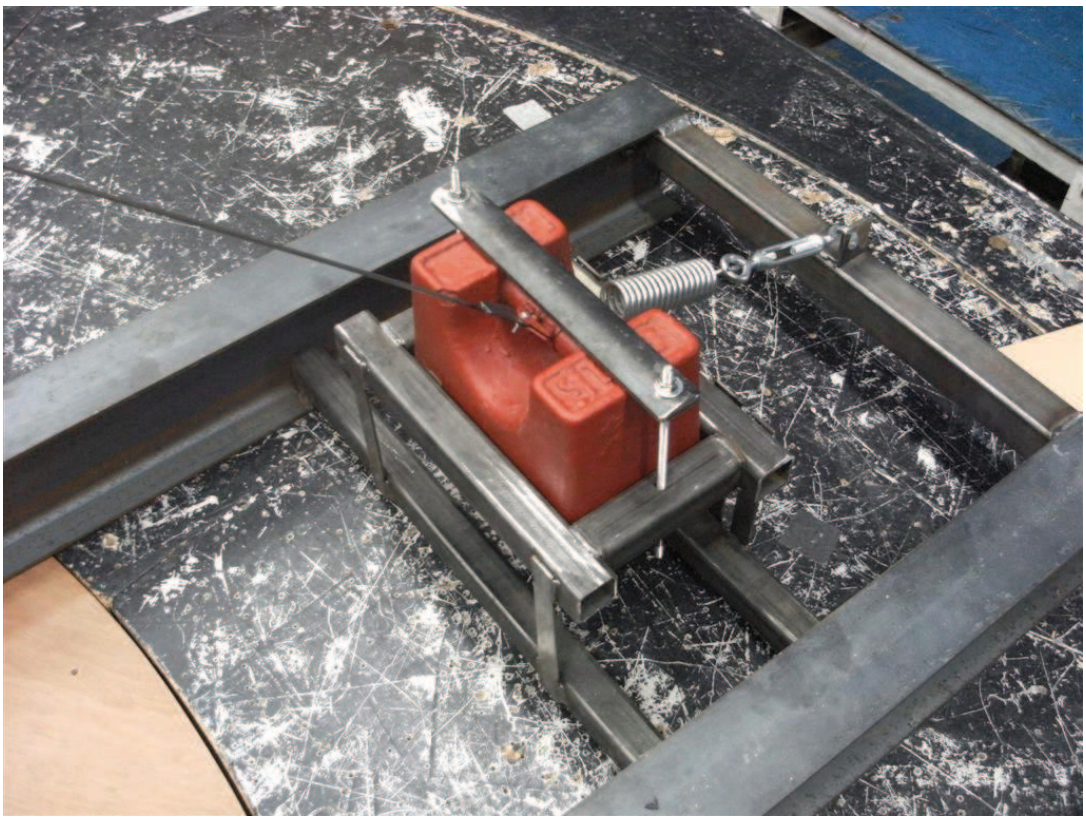

Figure B.7: Close Up View of Gap Between Cladding Panels

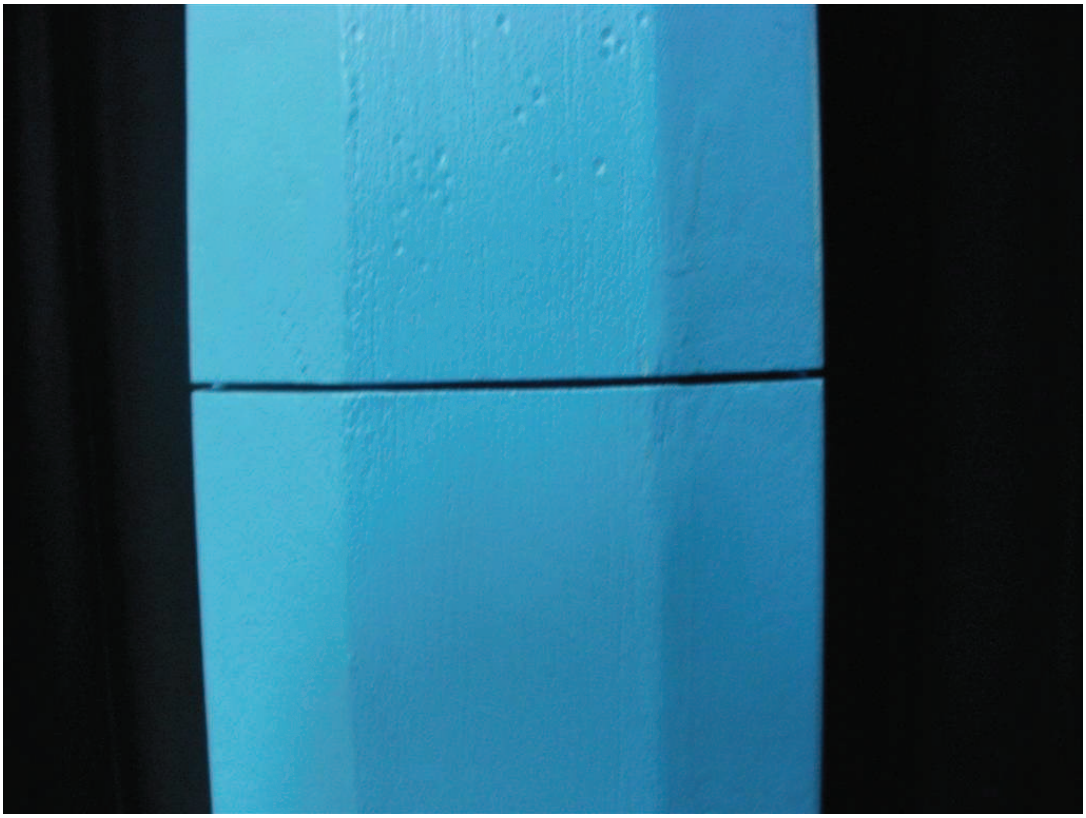

Figure B.8: Close Up View of Gap Between Cladding Panels Sealed

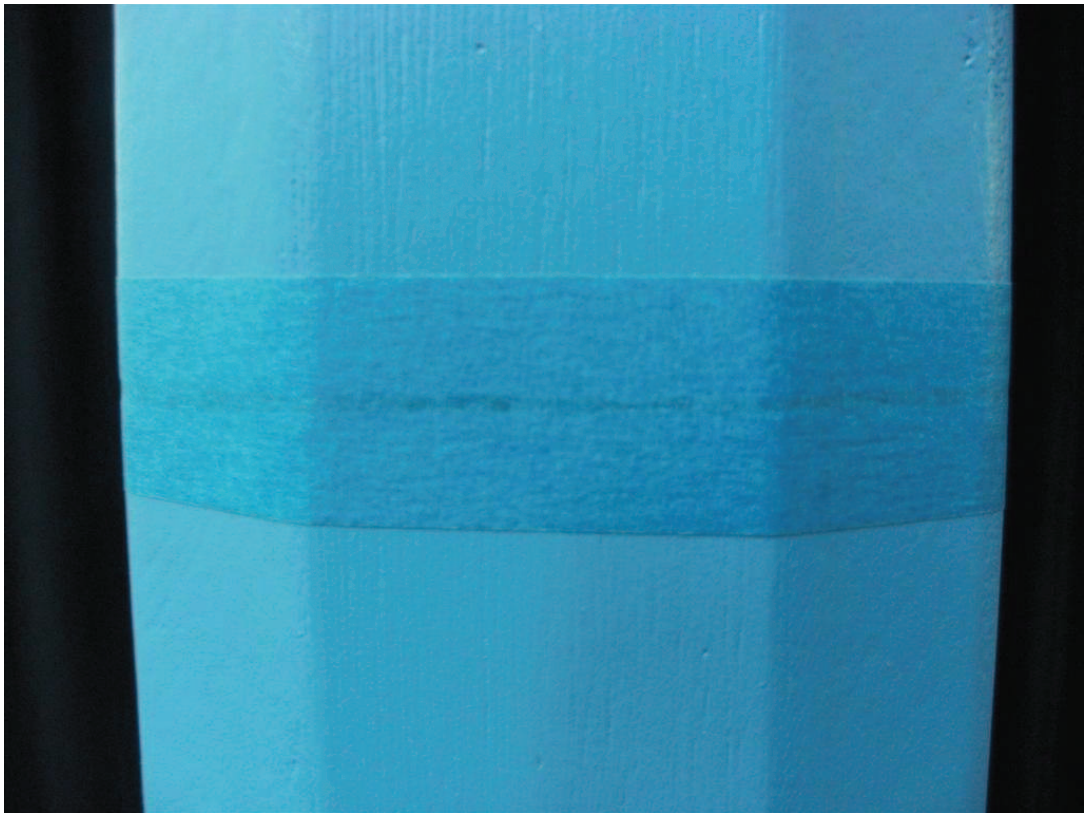

B.6. Dynamic Properties of the Aeroelastic Models

The models were specifically designed to provide a best match to the modes anticipated to be most susceptible to excitation by vortex shedding, as defined in the specification [(1)]. These are the primary bending modes of the tower.

B.7. Calibration of the Aeroelastic Models

The frequencies, the mode shapes and the damping values of the models for each tested configuration were measured prior to testing by resonating the models in a natural mode using an electromagnetic vibrator attached to the towers through a light spring.

The mode shapes and frequencies were measured by oscillating the models at constant amplitude. The mode shapes were determined by measuring the resonant accelerations at a number of points relative to an accelerometer at a fixed reference location. The structural damping of each mode was measured in amplitude decay tests.

The dynamic properties of the models in terms of frequencies, speed scales, mode shapes and damping for each mode are shown in Figures B.8 to B.11 for all configurations. Figures B.5 and B.6 show a comparison between the measured and target modes of shape.

B.7.1. Damping Measurements

The level of structural damping present in each of the aeroelastic models was measured through a series of amplitude decay tests. Each mode was first excited by use of an electromagnetic vibrator connected to a signal generator, then the excitation was halted and the motion was allowed to decay naturally. Time traces of the accelerometer output were recorded and analyzed to derive the damping level by comparing the ratio of successive peaks.

Figure B.9 Example Decay Time Trace:

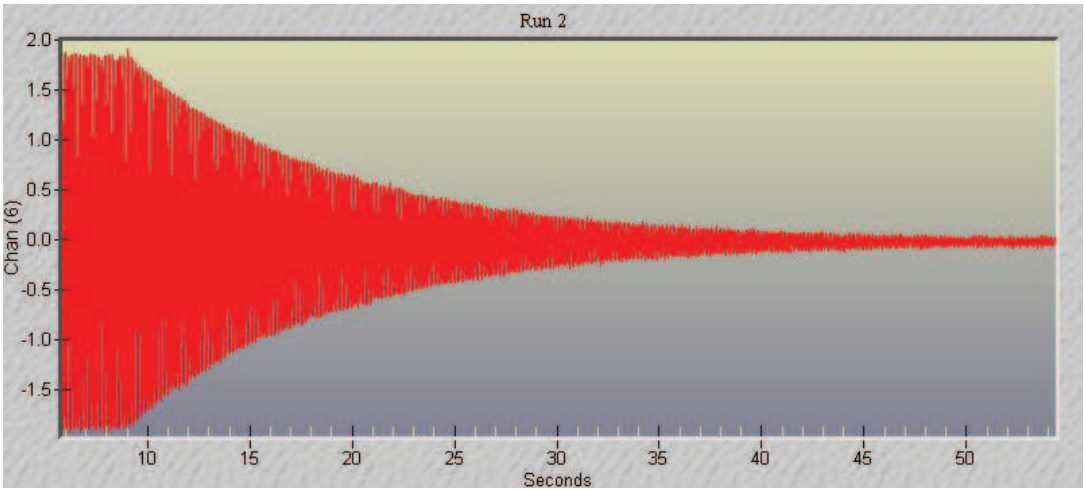

Measurements were taken at different amplitudes of vibration in order to assess the sensitivity of the damping level to the amplitude of the motion. As illustrated in the picture below, the level of damping is seen to increase slightly with displacement amplitude, and drops off rapidly at low amplitudes. Damping levels quoted in this report have been measured for amplitudes comparable to those observed at the vortex shedding peaks for each aeroelastic model.

Figure B.10 Example Plot of Damping Level vs MS Displacement amplitude:

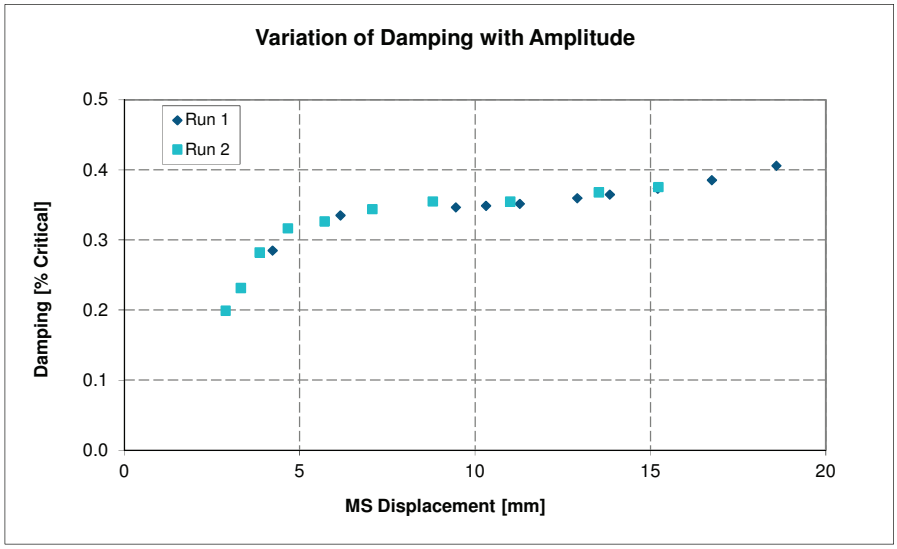

Fig B.11: Freestanding Tower: Comparison between FS and MS Natural Frequencies, Speed Scale, Mode Shape and Basic Damping Ratio – STIFF MODEL

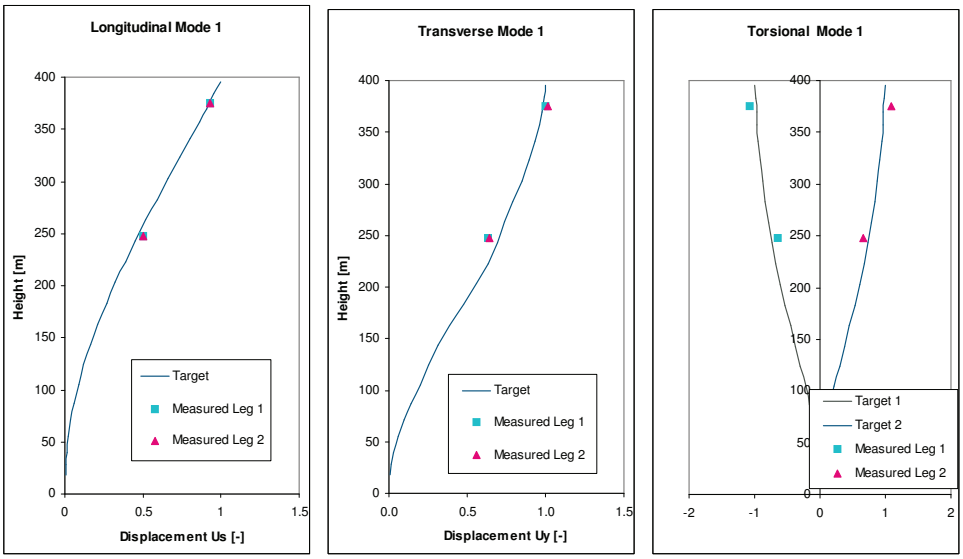

	First Longitudinal	First Transverse	First Torsional
FS Frequency [Hz]	0.11	0.22	0.36
MS Frequency [Hz]	9.8	20.2	33.1
Damping Ratio [%]	0.16	0.16	0.16
Speed Scale	2.2	2.2	2.2

Fig B.12: Freestanding Tower: Comparison between FS and MS Natural Frequencies, Speed Scale, Mode Shape and Basic Damping Ratio – SOFT MODEL

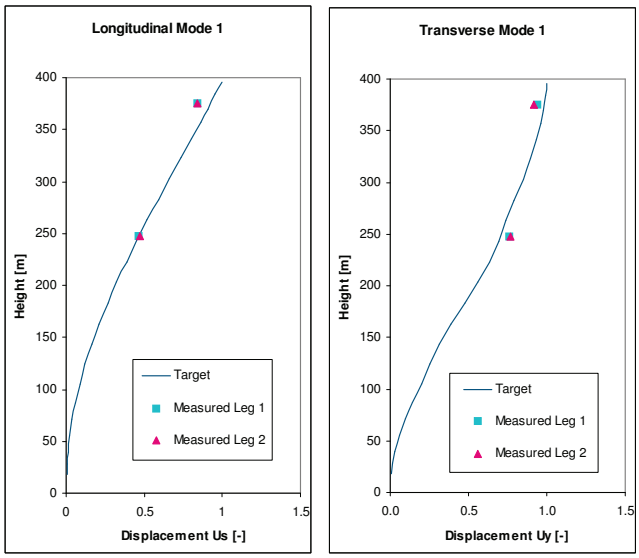

	First Longitudinal	First Transverse	First Torsional
FS Frequency [Hz]	0.11	0.22	[-]
MS Frequency [Hz]	5.1	11.5	[-]
Damping Ratio [%]	0.16	0.16	[-]
Speed Scale	4.1	3.8	[-]

Fig B.13: Freestanding Tower: Comparison between FS and MS Natural Frequencies, Speed Scale, and Basic Damping Ratio – FROUDE MODEL

	First Longitudinal	First Transverse	First Torsional
FS Frequency [Hz]	0.11	0.22	0.36
MS Frequency [Hz]	1.9	7.1	3.71
Damping Ratio [%]	0.40	0.40	0.40
Speed Scale	11.2	6.2	19.2

Fig B.14: Tower Prior To Crossbeam Installation: Comparison between FS and MS Natural Frequencies, Speed Scale, Mode Shape and Basic Damping Ratio – STIFF MODEL

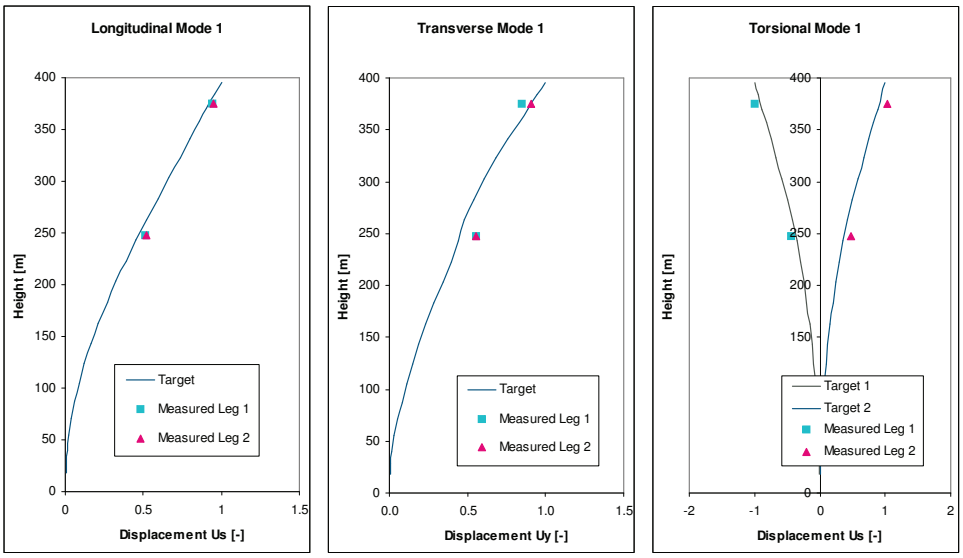

	First Longitudinal	First Transverse	First Torsional
FS Frequency [Hz]	0.11	0.19	0.24
MS Frequency [Hz]	10.0	20.5	27.2
Damping Ratio [%]	0.16	0.32	0.32
Speed Scale	2.2	1.9	1.7

Fig B.15: Tower Crossbeam Removed: Comparison between FS and MS Natural Frequencies, Speed Scale, Mode Shape and Basic Damping Ratio – SOFT MODEL

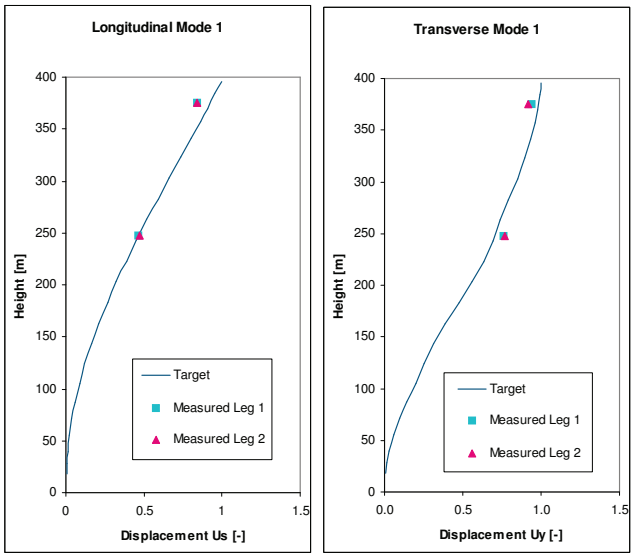

	First Longitudinal	First Transverse	First Torsional
FS Frequency [Hz]	0.11	0.19	[-]
MS Frequency [Hz]	5.0	9.4	[-]
Damping Ratio [%]	0.16	0.16	[-]
Speed Scale	4.4	4.1	[-]

Fig B.16: Tower In-Service: Comparison between FS and MS Natural Frequencies, Speed Scale, Mode Shape and Basic Damping Ratio

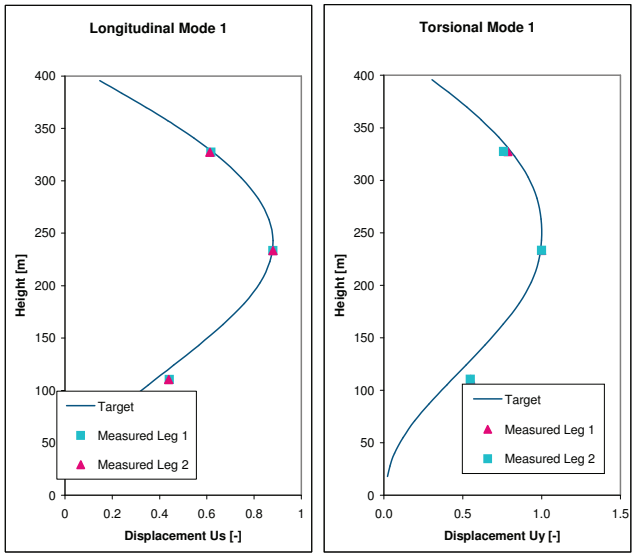

	First Longitudinal	First Transverse	First Torsional
FS Frequency [Hz]	0.48	0.22	0.63
MS Frequency [Hz]	6.7	3.80	10.0
Damping Ratio [%]	0.32	0.40	0.5
Speed Scale	14.2	11.5	12.7

Fig B.17: Tower With Cables Installed: Comparison between FS and MS Natural Frequencies, Speed Scale, Mode Shape and Basic Damping Ratio

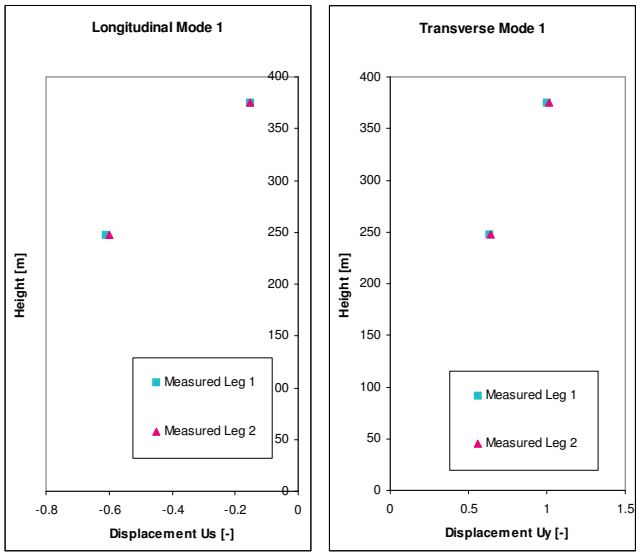

	First Longitudinal	First Transverse	First Torsional
FS Frequency [Hz]	0.40	0.22	[-]
MS Frequency [Hz]	20.0	10.4	[-]
Damping Ratio [%]	0.32	0.32	[-]
Speed Scale	4.0	4.2	[-]

B.7.2. Damping Devices

Controlled additional damping to simulate the effect of a damping device was also provided for the vortex-shedding tests. For the longitudinal mode, two damping systems, coupled to an eddy-current damper, were designed. The system transforms the longitudinal motion of the tower through a carbon-fibre pushrod into a copper vane supported between the poles of an electromagnet. The current generated in the copper vane interacts electromagnetically to provide additional damping. By varying the current feeding the electromagnet, different levels of damping can be obtained.

For the freestanding tower, the electromagnet is mounted 1m to the side at the height of the top crossbeam. The pushrod is mounted to a flexure in the centre of the upper crossbeam, and runs horizontally to the electromagnet, where it is mounted on another flexible support.

For the case where the top crossbeam is removed, and for the in-service configuration, the pushrod was mounted to the centre crossbeam and angled down towards the floor. The electromagnet was placed on the floor, again with a flexible support for the other end of the pushrod.

The damping system is shown in Figures B.18 and B.19.

Fig B.18: Damping System, as Mounted to Freestanding Tower

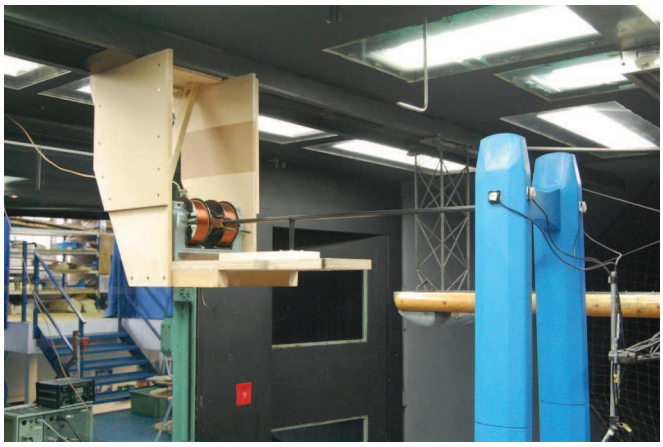

Fig B.19: Damping System, as Mounted to Tower In-Service

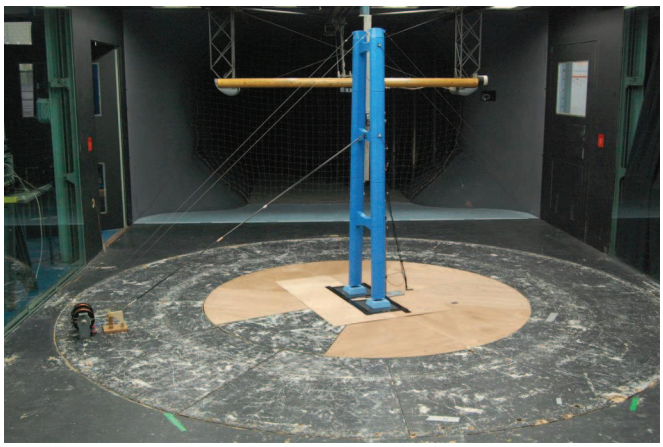

APPENDIX C. WIND TUNNEL TESTS- MEASUREMENT AND ANALYSIS

C.1. Measurement Details

The models were instrumented with:

- Low-range high-resolution accelerometers to measure main responses in the location of interest. The location of the accelerometers is presented in Figures 2.4.

Fig C.1: Accelerometers, as mounted during testing

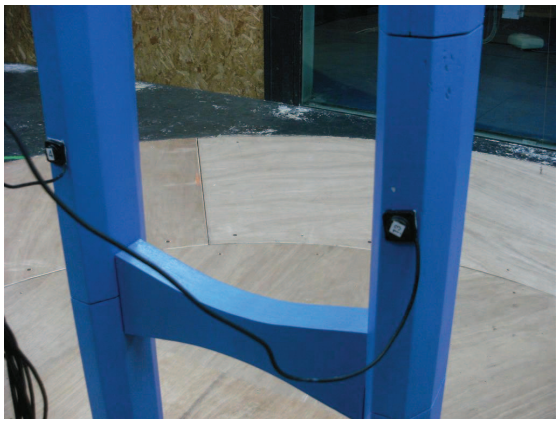

- High-frequency six-component force balances in conjunction with a signal-conditioning unit to measure the shear forces and moments acting at the base of each leg

Data records were of sufficient length to enable the probability statistics and spectra to be computed in addition to the mean values.

From the acceleration time histories, the RMS resonant component of the dynamic response can be derived. From the force and moment time histories, mean and RMS background components of the dynamic response can be derived.

C.2. Analysis Details

C.2.1. Vortex Shedding & Aerodynamic Stability

Time histories of accelerometer data were recorded at a number of wind speeds in the range of interest. These were then processed by evaluating the spectra, in order to isolate the contribution from the modes of interest. Then, using a mechanical admittance type filter, the RMS resonant component from each mode was derived. Figure C.2 shows an example of a raw spectra, along with the same data, filtered for the first mode of longitudinal bending. The difference between the two is the RMS resonant contribution from that mode.

From the accelerometer data, the FS RMS accelerations for each mode can be calculated as follows:

$$\ddot{y}_{FS,k} = MS \cdot \ddot{y}_{MS,k} \cdot \frac{fr^2_{FS,k}}{fr^2_{MS,k}}$$

Where MS is the model scale, $\ddot{y}_{FS,k}$ are the full-scale RMS accelerations for mode *k*, $\ddot{y}_{MS,k}$ are the model-scale RMS accelerations for mode *k* and $fr_{FS,k}$ and $fr_{MS,k}$ are the bending frequencies for mode *k* in full-scale and model-scale respectively.

Fig C.2: Example of filtered and unfiltered spectrum

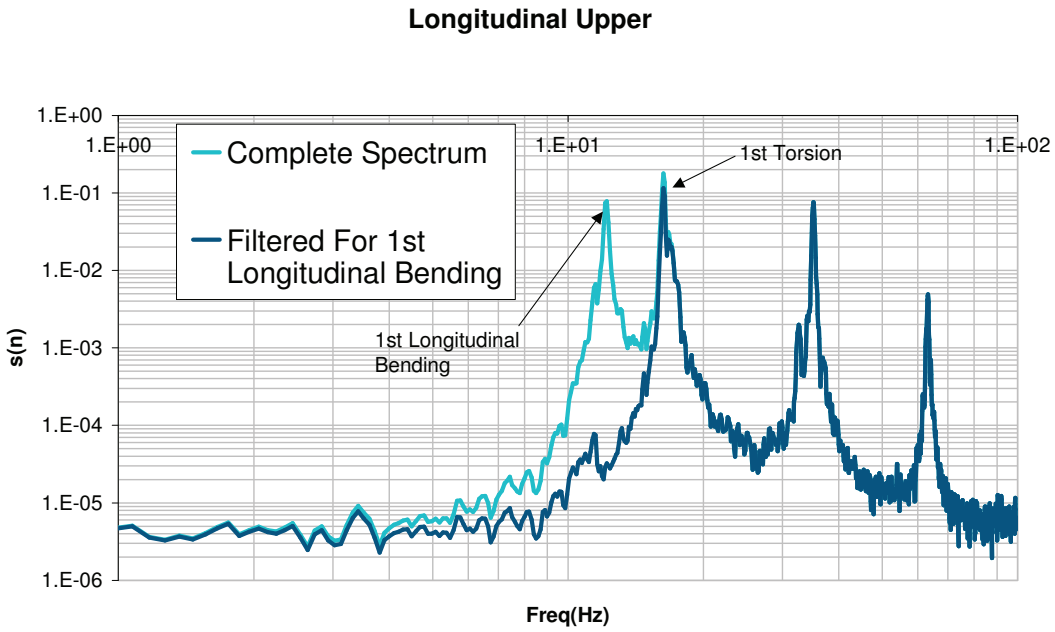

C.2.2. Wind Loading

Time histories were recorded at 4 wind speeds in order to provide good coverage of the design wind speed range. Each time history was processed by evaluation of the spectrum, permitting the isolation of the narrow-band responses and thus the RMS model-scale value thereof for each mode independently. The background and resonant component was then determined from the loads by filtering the peaks corresponding to the resonant components of the loads using a MA (Mechanical Admittance) type filter. The wind loads were measured using a six-component high frequency piezo-electric force balance. The fluctuating wind loads were measured in terms of the shear forces and moments (5 components: Fx, Fy, Mx, My & Mz).

APPENDIX D. WIND TUNNEL TEST RESULTS

The main results of the study are provided in a series of Excel Spread Sheet tables and plots attached:

431163_Free Standing_Leg 1_Smooth_Stablilty.xls

431163_Free Standing_Leg 1_Smooth_Torsion.xls

431163_Free Standing_Leg 1_Smooth_VS.xls

431163_Free Standing_Leg 1_Smooth_VS-SC.xls

431163_Free Standing_Leg 1_Turbulent_Loads.xls

431163_Free Standing_Leg 1_Turbulent_VS.xls

431163_Free Standing_Leg 1_Turbulent_VS-SC.xls

431163_Free Standing_Leg 2_Smooth_VS.xls

431163_Free Standing_Leg 2_Turbulent_Loads.xls

431163_Free Standing_Leg 2_Turbulent_VS.xls

431163_Crossbeam Removed Leg 1 Smooth_Stability.xls

431163_Crossbeam Removed Leg 1 Smooth_Torsion.xls

431163_Crossbeam Removed Leg 1 Smooth_VS.xls

431163_Crossbeam Removed Leg 1 Smooth_VS_SC.xls

431163_Crossbeam Removed Leg 1 Turbulent_VS.xls

431163_Crossbeam Removed Leg 1 Turbulent_VS_SC.xls

431163_Crossbeam Removed Leg 2 Smooth_VS.xls

431163_Crossbeam Removed Leg 2 Turbulent_VS.xls

431163_In Service Smooth Flow_VS.xls

431163_Cables in Place Leg 1 Smooth_VS.xls

431163_Cables in Place Leg 2 Smooth_VS.xls

BMT Fluid Mechanics

Project No. 431163/00
Messina Straits Crossing
Towers
Italy

Wind Tunnel Testing

Section Model Studies

(10th Novemberer 2010)

For

Eurolink S.C.p.A.

Report Title	**Messina Straits Crossing Towers** **Wind Tunnel Testing,** **Section Model Studies**		
Client:	**Eurolink S.C.p.A.**		
Document No:	**431163rep2v2**	**Release: 2**	**Copy No:**
Status	**Draft Report for Client Review**		
Report Date:	**10th November 2010**		
Holds:			

	Name:	Signature:	Date:
Prepared by:	**Mr J Osman**	_____	_____
Checked by:	**Miss A Bagnara**	_____	_____
Approved by:	**Dr V Buttgereit**	_____	_____

Distribution:	

Previous Release History:	Release No:	Status:	Date:
431163rep2v1	**1**	**Draft Report for Internal Review**	**9-11-10**

Messina Straits Crossing Towers
Wind Tunnel Testing
Section Model Studies

Contents

EXECUTIVE SUMMARY

Background

This document has been prepared by BMT Fluid Mechanics Limited (BMT) for Cowi acting on behalf of Eurolink S.C.p.A. to summarise the results of section model testing commissioned to study the wind effects relevant to the design of the towers of the Messina Straits Crossing in Italy.

This report describes the results from the dynamic and static section model tests carried out in BMT's aeronautical wind tunnel using 2-dimensional models of the tower section at a scale of 1:100, in two configurations:

- Single leg in isolation
- Double leg system

The study has provided a qualitative assessment of the aerodynamic stability of the tower cross section with respect to vortex-shedding and divergent responses as well as a quantification of the mean wind load coefficients applicable to the structural design.

Conclusion

The main results of the studies are summarised below:

Single Leg

Vortex Shedding

- The worst-case RMS displacement for a damping level of 0.006 Logdec, is *1.16m*, occurring at a reduced wind speed of 5.6 (based on the frequency of the first longitudinal bending mode and the major width of the section of 20m).

Double Leg

Vortex Shedding

- The worst-case RMS displacement for a damping level of 0.008 Logdec, is *1.57m*, occurring at a reduced wind speed of 6.4 (reduced using the frequency of the first longitudinal bending mode and the major width of the section of 20m).

Aerodynamic Stability

- The double leg configration was found stable up to and above the maximum design wind speed of 80ms^{-1} at the tip of the tower.

Messina Straits Crossing Towers Wind Tunnel Testing, Section Model Studies

1. Introduction

1.1. Background

This document has been prepared by BMT Fluid Mechanics Limited (BMT) for Cowi acting on behalf of Eurolink S.C.p.A. to summarise the results of section model testing commissioned to study the wind effects relevant to the design of the towers of the Messina Straits Crossing in Italy.

This report describes the results from the dynamic and static section model tests carried out in BMT's aeronautical wind tunnel using 2-dimensional models of the tower section at a scale of 1:100, in two configurations:

- Single leg in isolation
- Double leg system

The study has provided a qualitative assessment of the aerodynamic stability of the tower cross section with respect to vortex-shedding and divergent responses as well as a quantification of the wind loads applicable to the structural design.

1.2. Details of the Proposed Structure

The Messina Straits Crossing is a suspension bridge linking the Island of Sicily with mainland Italy, and has a total length of ~3300m. Two twin-leg towers, 399m tall, support the suspension cables. Each leg is of constant octagonal section, 20m by 12m, and they are canted in towards each other at the tip – the double leg sytsem models the separation at 70% of the full height of the tower. Figure 1.1 shows the arrangement of the tower and the relevant geometrical features.

2. Methodology

2.1. Objective of the studies

The key objectives of the studies were to:

- Define the worst-case vortex-shedding responses and corresponding critical wind speeds of the two configurations of the towers in smooth flow.
- Determine whether the tower section is stable with respect to divergent responses within the design wind speed range (up to 80ms^{-1}).
- Determine the steady-state mean load coefficients for both configurations in smooth and turbulent flow.

The tests were carried out up to the maximum design wind speed of 80ms^{-1}, as defined by COWI.

To ensure that the section model tests would define accurately the vortex-shedding motions and cover the full design wind speed range to validate the aerodynamic tests, the dynamic tests were run with two different rig setups with the following characteristics:

1) ***Stiff Spring Setup–*** A "Stiff", (high frequency) rig setup with a speed scale of ~1:1 was used for the vortex-shedding studies. The speed scale was chosen to maximize the Reynolds number at which vortex-shedding would occur, maintaining a frequency scale within a measureable signal range.

2) ***Soft Spring Setup -*** "Soft" (low frequency) rig setup with a speed scale of ~3:1 was used to allow coverage of the full design wind speed range.

2.2. Model Configurations & Tests Matrix

The test matrices for the two configurations are provided below:

Table 2.1: Static Rig Test Matrix

Configuration	Testing Scenario	Flow Condition	Wind Angles	Reynolds Number
Single Leg	Re Sensitivity	Smooth	0°, 30°, 60°, 90°	4.0E+04 to 6.4E+05
Single Leg	Wind Loads	Smooth	0°-90°, 5° steps	5.0E+05
Single Leg	Wind Loads	Turbulent	0°-90°, 5° steps	5.0E+05
Double Leg	Wind Loads	Smooth	0°-90°, 5° steps	5.0E+05
Double Leg	Wind Loads	Turbulent	0°-90°, 5° steps	5.0E+05

Table 2.2: Dynamic Rig Test Matrix

Configuration	Testing Scenario	Flow Condition	Wind Angles	Reduced Wind Speeds
Single Leg	Vortex Shedding	Smooth	0°-90°, 10° steps	5 - 10
Double Leg	Vortex Shedding	Smooth	0°-90°, 10° steps	5 - 10
Single Leg	Vortex Shedding - Damping Studies	Smooth	Worst-Case Angles	5 - 10
Double Leg	Vortex Shedding - Damping Studies	Smooth	Worst-Case Angles	5 - 10
Single Leg	Vortex Shedding - Mitigation Studies	Smooth	Worst-Case Angles	5 - 10
Double Leg	Aerodynamic Stability	Smooth	0°-90°, 10° steps	Up to & Above 40

Wind speeds are quoted as reduced windspeeds (U/ND), based on the first longitudinal frequency of 0.1Hz of the free-standing configuration and the reference dimension of 20m.

2.2.1. Evaluation of Scale Effects

In order to quantify the sensitivity of the tower cross section to scale effects, two additional models were constructed, at scales of 1:50 and 1:200. The 1:50 scale model was used to derive drag coefficient and the strouhal number for Reynolds numbers up to XX. The 1:200 model was used to investigate the drag coeff and the struhal number at the Reynols number range of the aeroelastic studies Full details of this testing can be found in Appendix E.

Table 2.3: Reynolds Number Sensitivity Test Matrix

Configuration	Testing Scenario	Model Scale	Flow Condition	Wind Angles	Reynolds Number
Single Leg	Static	1:50	Smooth	0°, 30°, 60°, 90°	1.8E+05 to 1.3E+06
Single Leg	Static	1:200	Smooth	0°, 30°, 60°, 90°	2.1E+04 to 3.4E+05

2.3. Wind Tunnel Models

The wind tunnel model was designed and constructed at scale of 1:100 based on structural and drawing information supplied by COWI. The legs were constructed so that they could both be mounted simultaneously, linked by a stiff support to simulate the double leg system, or individually in order to model the single leg in isolation.

The models were designed to allow the different configurations and scenarios to be tested as follows:

1:100 Single Leg in Isolation

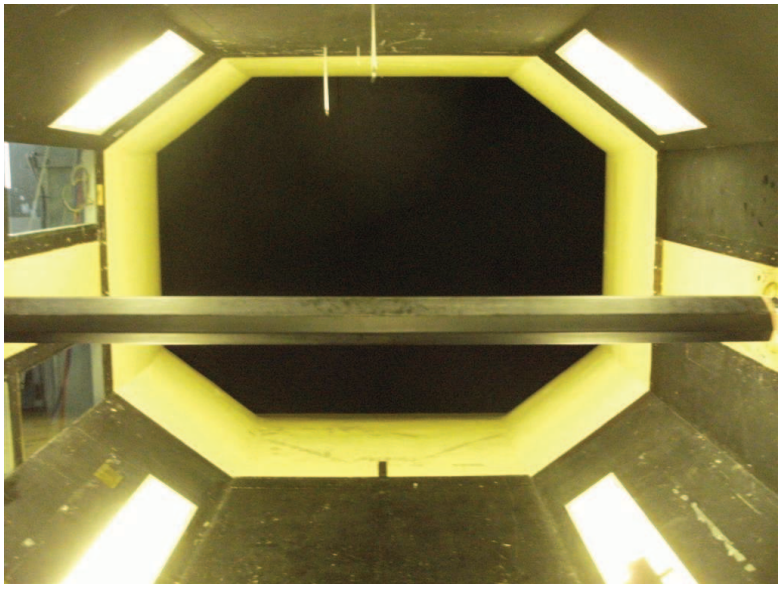

1:100 Double Leg System

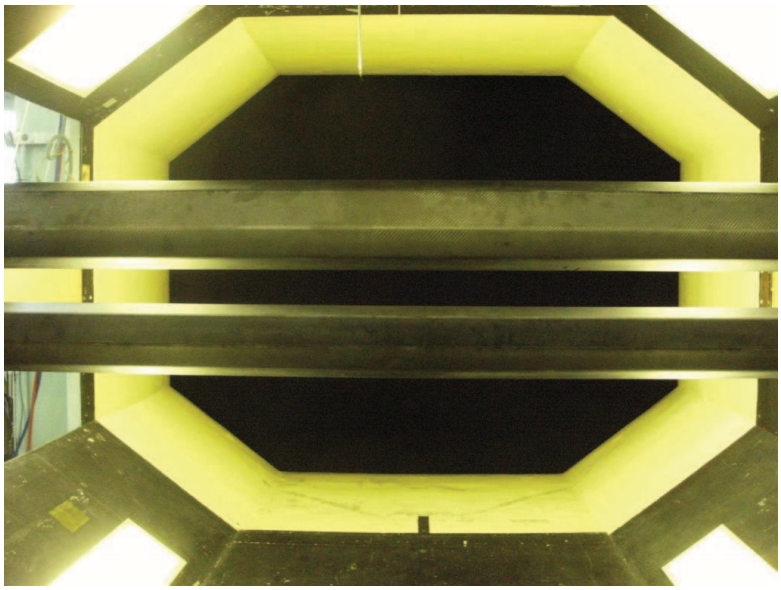

Appendix B contains further details on each of the configurations, as well as details on the model scale and construction. Also presented in Appendix B are photographs of the models and wind tunnel set-up.

2.4. Measurement and Analysis

2.4.1. Wind Loading

Time histories of forces and moments were measured simultaneously using a six - component high frequency force balance rig, mounted at each end of the section. Measurements were taken for the single leg configuration in smooth flow at a range of speeds for the angles of 0°, 30°, 60° and 90° in order to assess the sensitivity to Reynolds number. Measurements were then taken at highest Reynolds number achievable in the wind tunnel for both the single and double leg models, in both smooth and turbulent flow, for the sector of 0° - 90° in increments of 5°.

Steady-state mean load and moment coefficients were then calculated in order to quantify the sensitivity of the section to Reynolds number effects, and the variation with wind angle. Each time history was also processed by evaluation of the spectrum, permitting the isolation of the narrow-band responses, and was used to determine the Strouhal number at which the vortex-shedding response would occur.

Further details on the measurements and analysis of the data are provided in Appendix C.

2.4.2. Vortex Shedding

For the vortex-shedding tests, measurements were taken in fine wind speed increments between the reduced wind speeds of 5 and 10 (based on the bending frequency of the tower and the dimension of 20m), in order to define the vortex-shedding critical wind speed and quantify the maximum response. Measurements were taken for all wind directions in the sector 0° to 90° using 2 accelerometers configured to measure vertical motion of the section. The accelerometer output was recorded as a time history, and then filtered to derive the root mean square (RMS) resonant component of the signal corresponding to the vertical modes of vibration of the rig. Further details on the measurements and analysis of the data are provided in Appendix D.

2.4.3. Divergent Responses

For the aerodynamic stability assessment, the general approach to the tests was to observe the behaviour of the towers over a range of wind speeds, up and above the maximum design wind speed.

Measurements were taken for all wind directions in the sector 0° to 90° using 2 accelerometers configured to measure vertical motion of the section. The accelerometer output was recorded as a time history, and then filtered to derive the root mean square (RMS) resonant component of the signal corresponding to the vertical modes of vibration of the rig. Further details on the measurements and analysis of the data are provided in Appendix D.

2.5. Design Wind Properties & Model Scale Simulation of the Atmospheric Boundary Layer

The design wind speeds and the target turbulence properties used in this study were provided by COWI and are detailed in Appendix A.

The tests were carried out in smooth flow and in turbulent flow.

2.6. Definition of Wind Direction and Axis System

The 0° wind direction has been chosen to coincide with winds blowing transversely across the deck. As the tower has two perpendicular planes of symmetry, results are quoted wind angles from one sector: 0 to 90°. Figures 2.2 and 2.3 show the axis system on which the wind forces are based.

3. Results

3.1. Reynolds Number Sensitivity

The results of the static load measurements are presented in form of:

- Variation of Drag Coefficients with Reynolds number for the single leg model at wind angles of: 0°, 30°, 60° & 90° (Figure 3.1).

3.2. Wind Loading

The results of the static load measurements are presented in form of:

- Variation of Lift, Drag and Moment Coefficients with wind angle for both the single leg and double leg configurations in smooth and turbulent flow for wind angles of 0° - 90° (Figure 3.2).

3.3. Vortex Shedding

The results of the dynamic tests are presented in form of:

- Variation of FS RMS displacements with reduced wind speed for the single leg configuration in smooth flow for wind angles 0° - 90°, at various levels of damping (Figure 3.3).
- Variation of FS RMS displacements with reduced wind speed for the double leg configuration in smooth flow for wind angles 0° - 90°, at various levels of damping (Figure 3.4).

- Variation of FS RMS displacements with reduced wind speed for the single leg configuration in smooth flow for a wind angle of 0° for various mitigation options with a level of damping of 0.004 Logdec (Figure 3.5).
- Variation of FS RMS displacements with wind speed for the single leg configuration with a mitigation option of semi-circular nosing in smooth flow for wind angles of 0°, 30°, 60° & 90° with a level of damping of 0.03 Logdec (Figure 3.6).

3.4. Aerodynamic Stability

The results of the static load measurements are presented in form of:

- Variation of FS RMS displacements with reduced wind speed for the double leg configuration in smooth flow for wind angles 0° - 90°, with a level of damping of 0.01 Logdec (Figure 3.12).

3.5. Interpretation/Discussion of Results

The main results of the studies are summarised below:

Vortex Shedding

- Vortex shedding was measured for both configurations, at each angle tested. The greatest responses were measured at 0° and 5°.
- The amplitudes measured for the double leg configuration are greater than those for the single leg configuration; at 0°, with a level of damping of 0.03 Logdec, the single leg reached an amplitude of 794mm, compared to 1305mm for the double leg.
- Vortex shedding occurs for both configurations at a Strouhal number of around 0.17 (normalised using the major dimension of one leg of 20m for both cases).
- The response is at a minimum of 40mm (0.006 Logdec) at 70° for the single leg configuration.
- The response is at a minimum of 47mm (0.015 Logdec) at 80° for the double leg configuration.
- The response is largely mitigated by the introduction of additional structural damping. At 0° the single leg displacements are reduced to 236mm by a damping level of 0.11 logdec, and the double leg displacements at 5° are reduced to 129mm by a damping level of 0.15 logdec.

- A number of aerodynamic mitigation options were trialled for the single leg configuration, however none was found to offer a significant reduction in the displacement amplitudes with no additional damping. It was found that a porous semi-circular nosing combined with a damping level of 0.03 logdec could reduce the amplitude of the response to 443mm for 0°.

- At 60°, a second peak is observed at a Strouhal number of 0.11 for the single leg configuration. For the double leg configuration, a very broadband peak is found, spanning the Strouhal number range from 0.24 to 0.11. It is believed that this is due to a scale effect, and noted that two of the chamfered edges of the section are aligned with the upstream wind direction for this case.

Wind Loading

- The drag coefficent of the section is found to be largely unaffected by the levels of turbulence for all wind angles for the single leg configuration.

- For the double leg configuration, the drag coefficent of the section is found to be largely unaffected by the levels of turbulence for all wind angles, except for in the range of 0° and 10° (where one leg is directly upstream of the other).

- The lift and drag coefficients of the double leg configuration follow the same trend as the single leg configuration, except in the range of 0° to 30°, where the downstream leg is in the wake shed from the upstream leg.

Aerodynamic Stabililty

- The double leg configuration was found to be stable up to and above the design wind speed of 80ms^{-1} for all wind angles.

4. References

[1] Scope of work, Tower wind tunnel tests, Sub-tests T1, T2 and T3. ALN0002122.doc

5. Figures

Figure 1.1 Messina Straits Crossing – Tower Arrangement

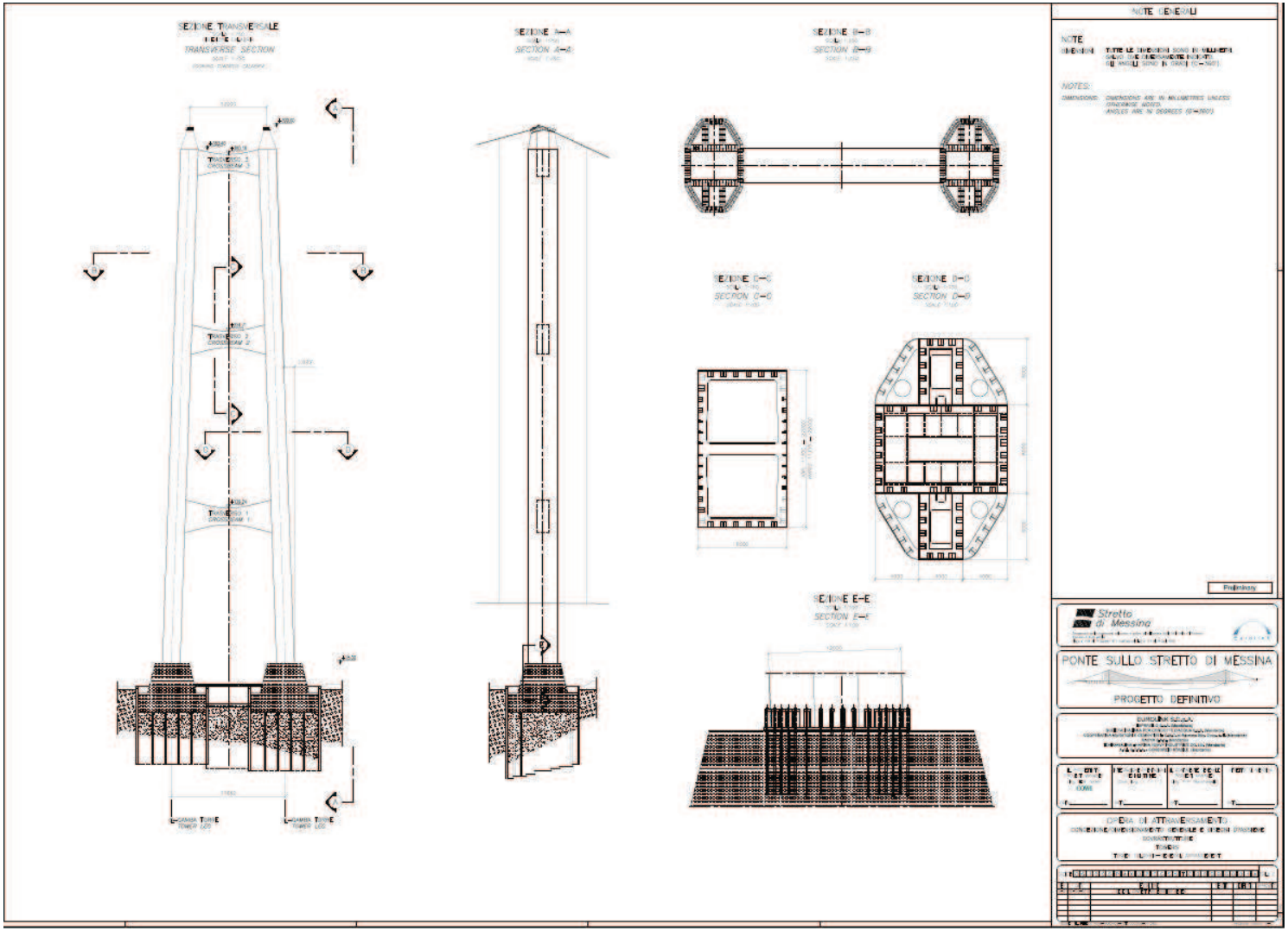

Figure 2.2 Messina Straits Crossing Tower Section Test– Axis System

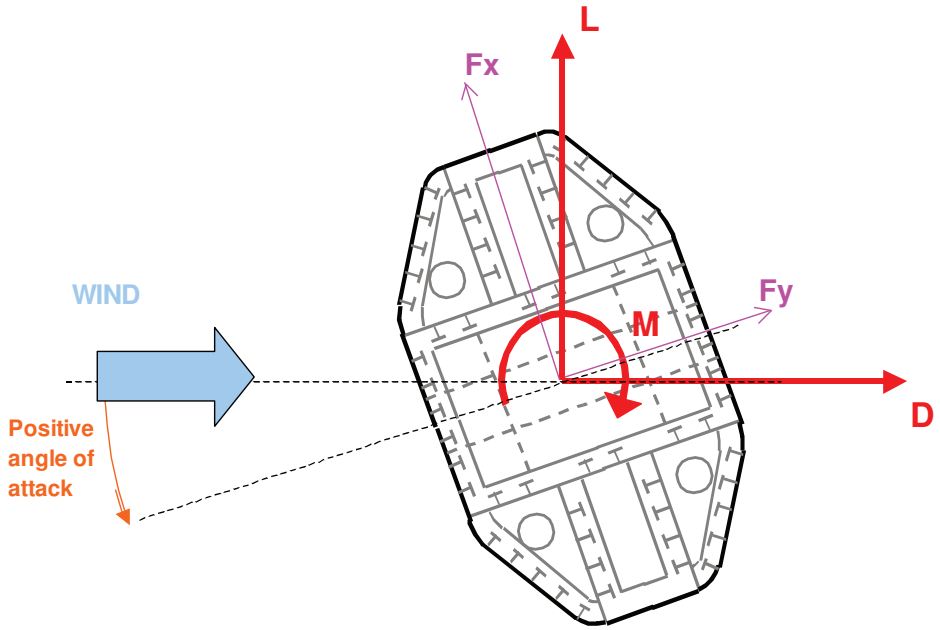

Figure 3.1: Variation of Drag Coefficients with Reynolds number for each of the three single leg model scales at wind angles of: 0°, 30°, 60° & 90°

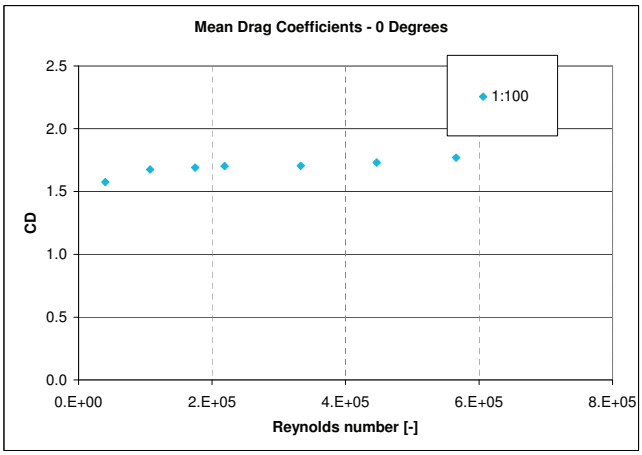

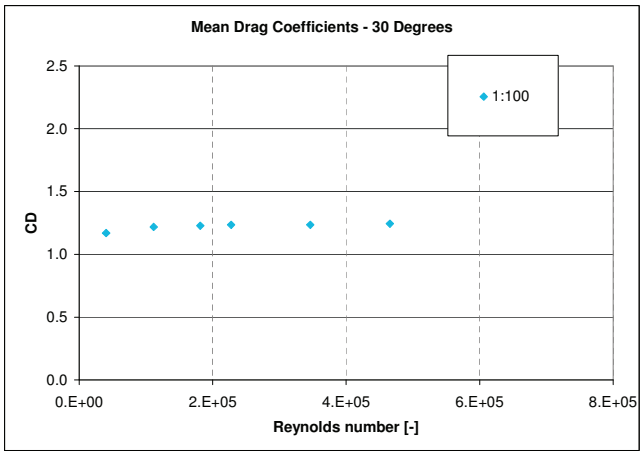

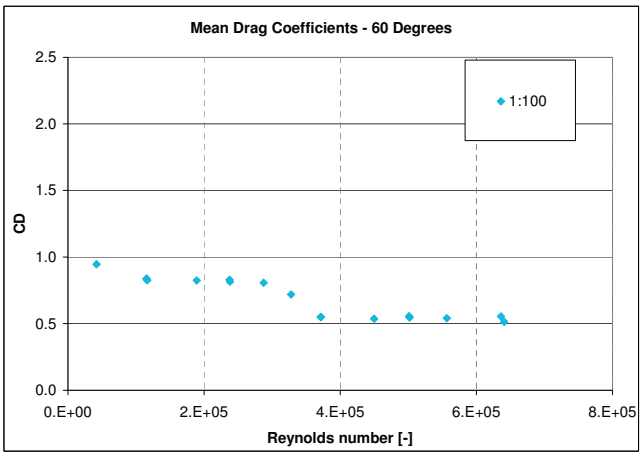

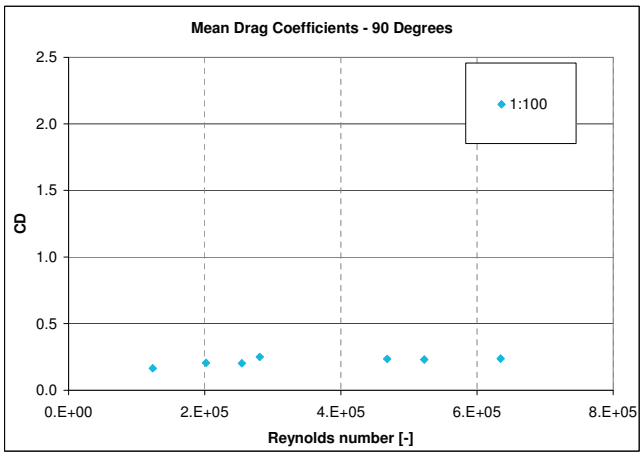

Figure 3.2: Variation of Lift, Drag and Moment Coefficients with wind angle for both the single leg and double leg configurations in smooth and turbulent flow for wind angles of 0° - 90°

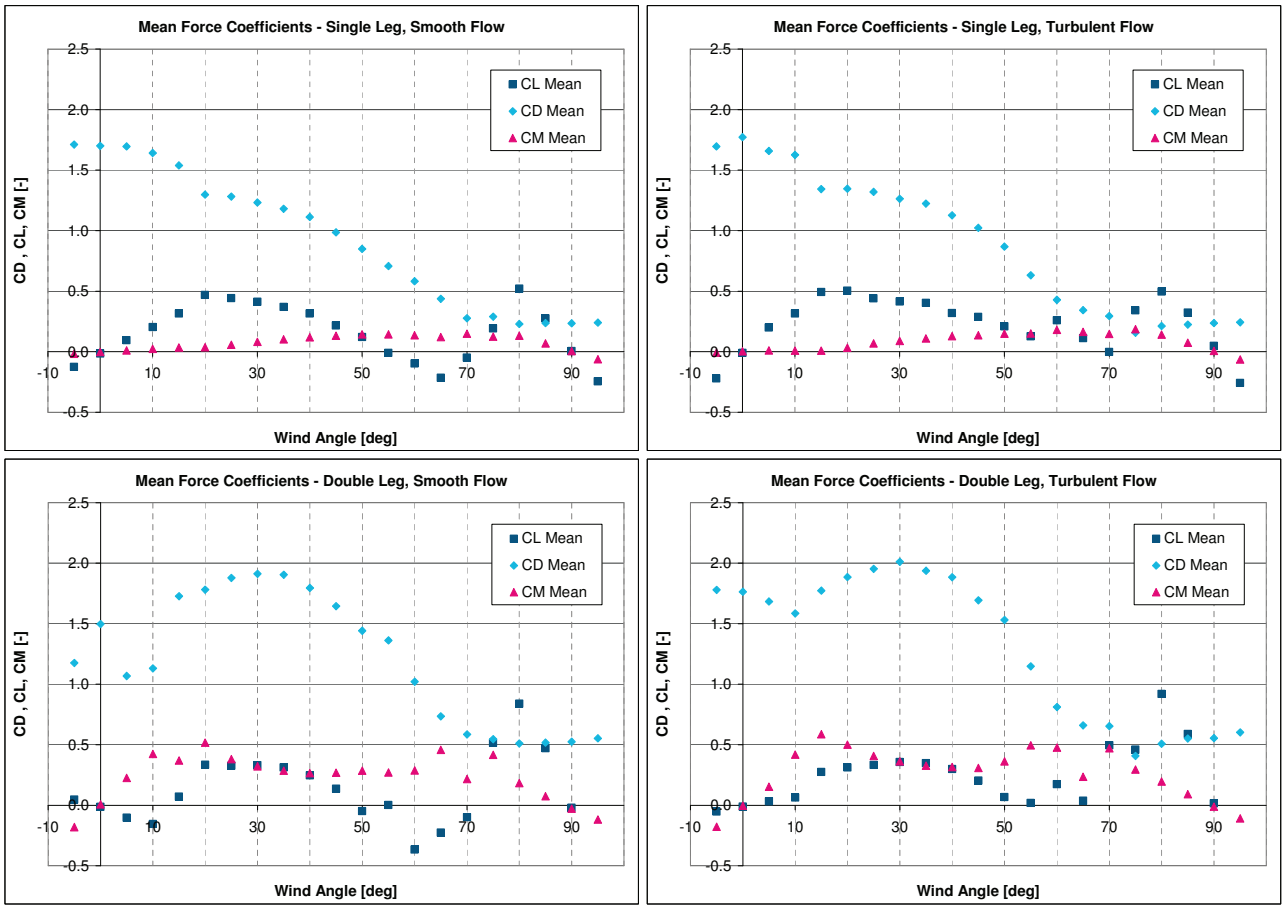

Figure 3.3: Variation of FS RMS displacements with reduced wind speed for the single leg configuration in smooth flow for wind angles 0° - 90°, at various levels of damping

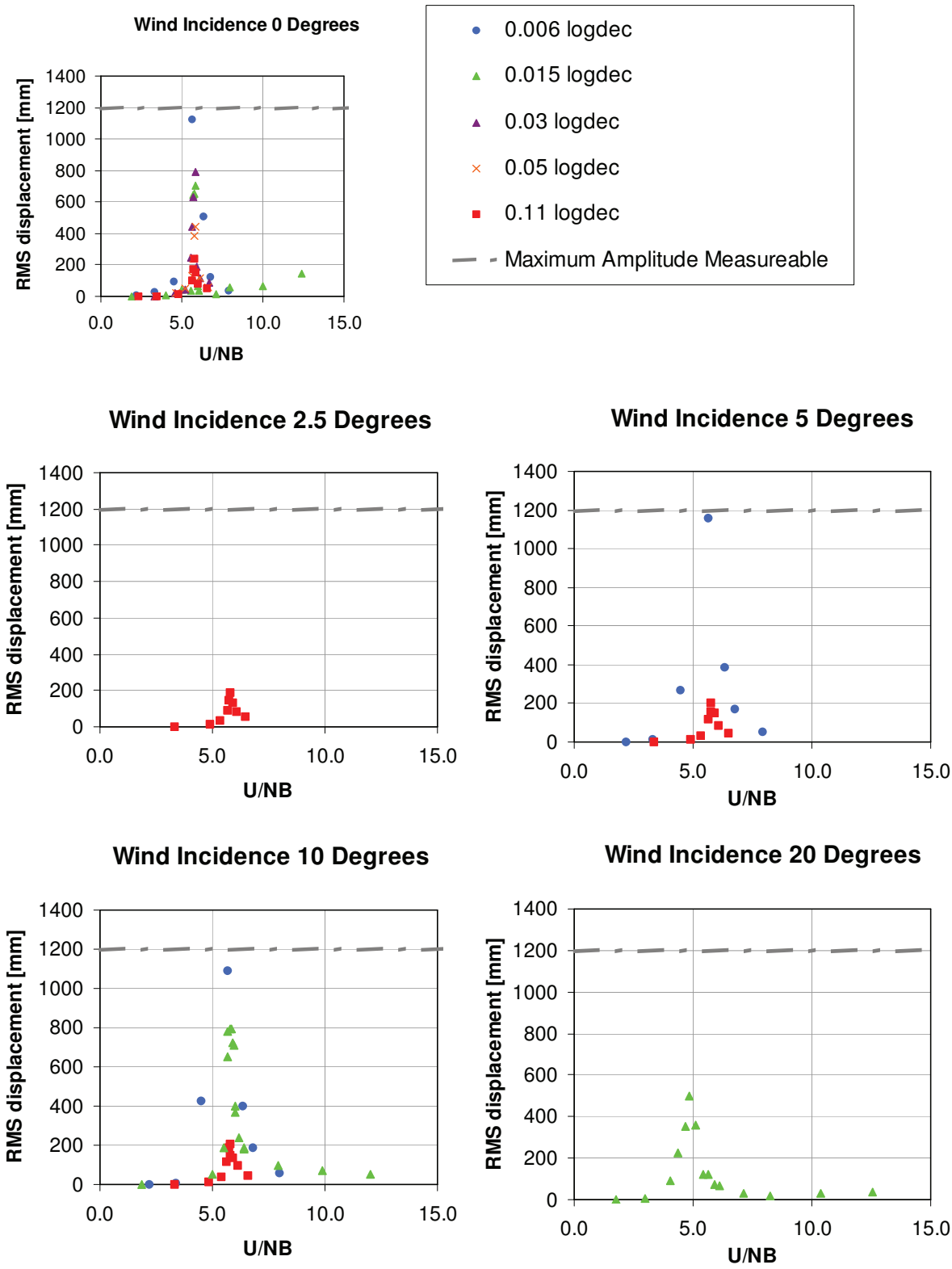

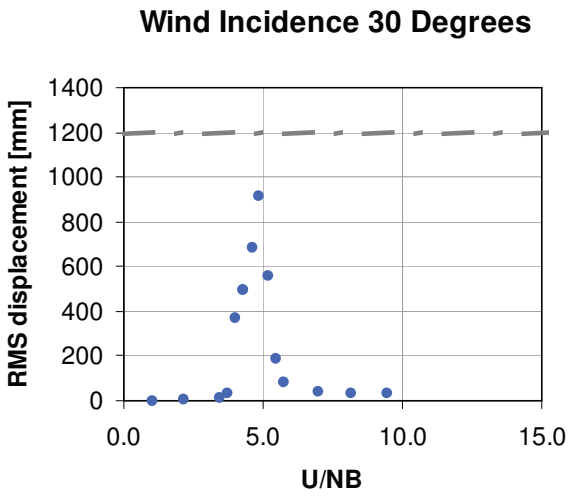
Wind Incidence 30 Degrees
RMS displacement [mm]
1400
1200
1000
800
600
400
200
0
0.0
5.0
10.0
15.0
U/NB

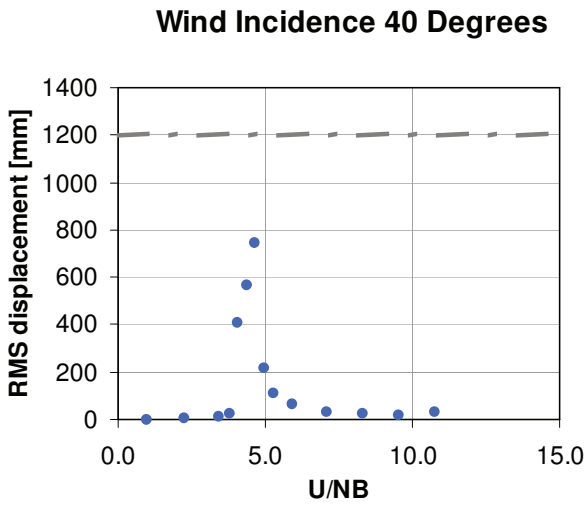
Wind Incidence 40 Degrees
RMS displacement [mm]
1400
1200
1000
800
600
400
200
0
0.0
5.0
10.0
15.0
U/NB

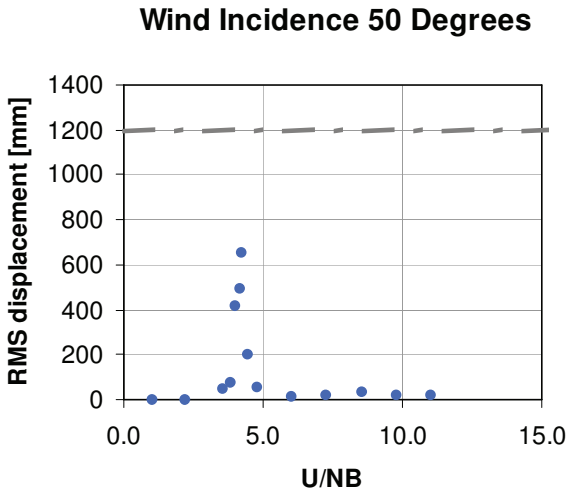
Wind Incidence 50 Degrees
RMS displacement [mm]
1400
1200
1000
800
600
400
200
0
0.0
5.0
10.0
15.0
U/NB

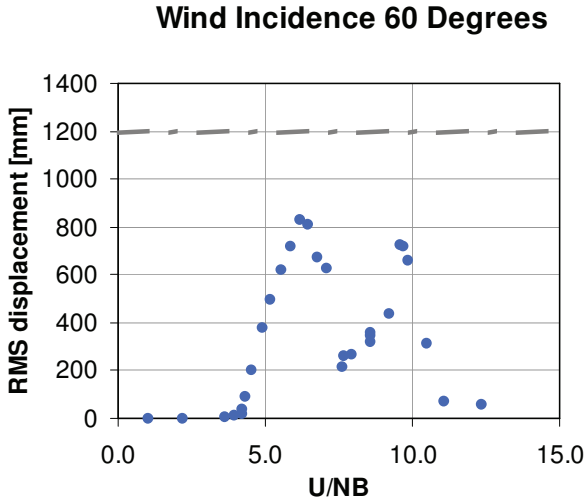
Wind Incidence 60 Degrees
RMS displacement [mm]
1400
1200
1000
800
600
400
200
0
0.0
5.0
10.0
15.0
U/NB

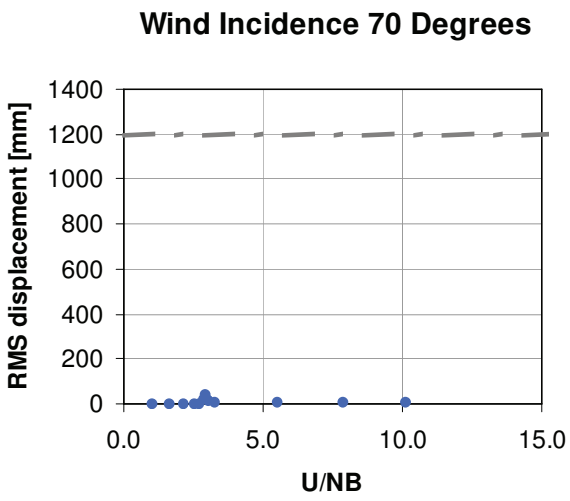
Wind Incidence 70 Degrees
RMS displacement [mm]
1400
1200
1000
800
600
400
200
0
0.0
5.0
10.0
15.0
U/NB

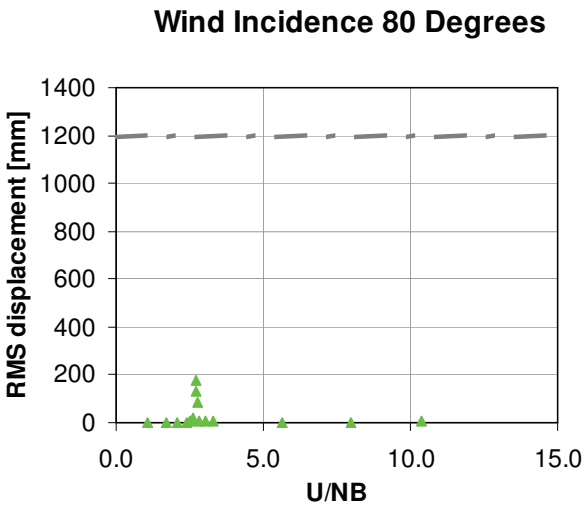
Wind Incidence 80 Degrees
RMS displacement [mm]
1400
1200
1000
800
600
400
200
0
0.0
5.0
10.0
15.0
U/NB

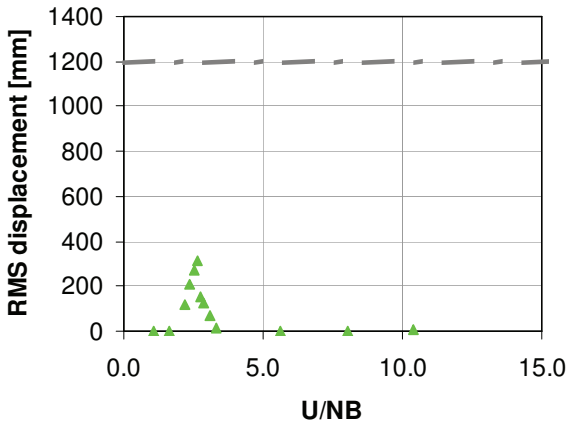
Wind Incidence 90 Degrees
RMS displacement [mm]
1400
1200
1000
800
600
400
200
0
0.0
5.0
10.0
15.0
U/NB

Figure 3.4: Variation of FS RMS displacements with reduced wind speed for the double leg configuration in smooth flow for wind angles 0° - 90°, at various levels of damping

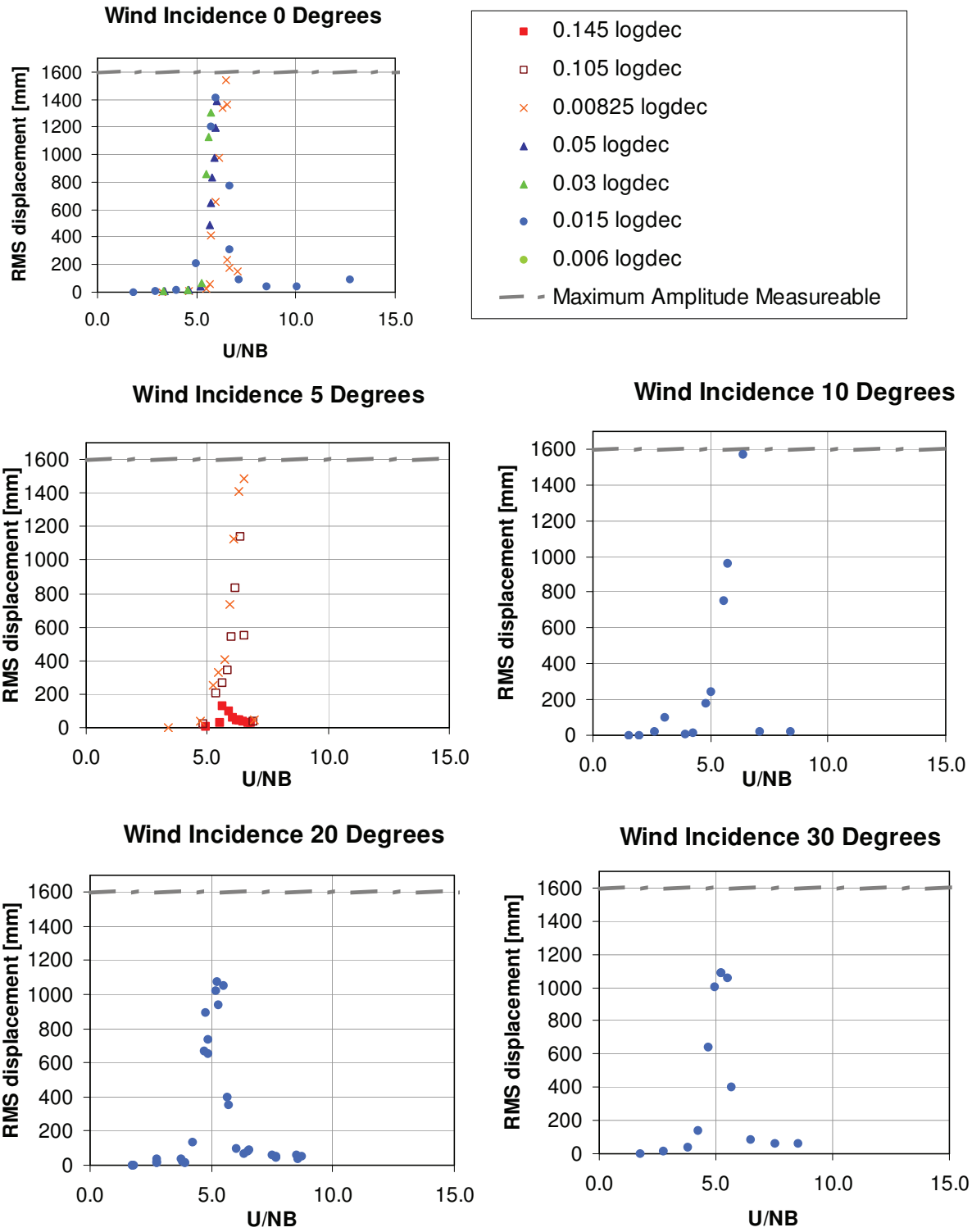

Wind Incidence 40 Degrees

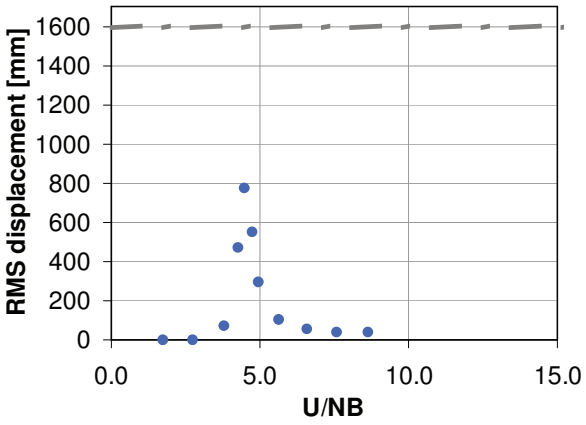

Wind Incidence 50 Degrees

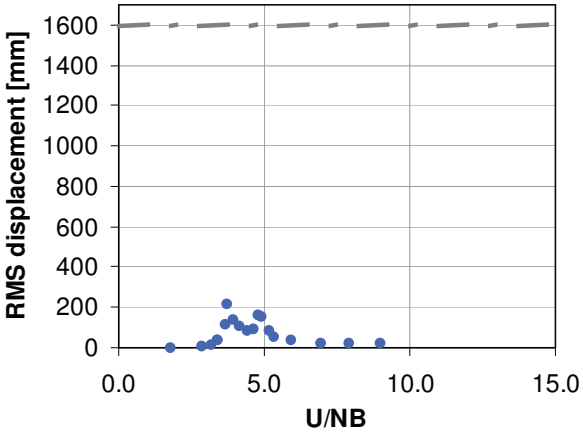

Wind Incidence 60 Degrees

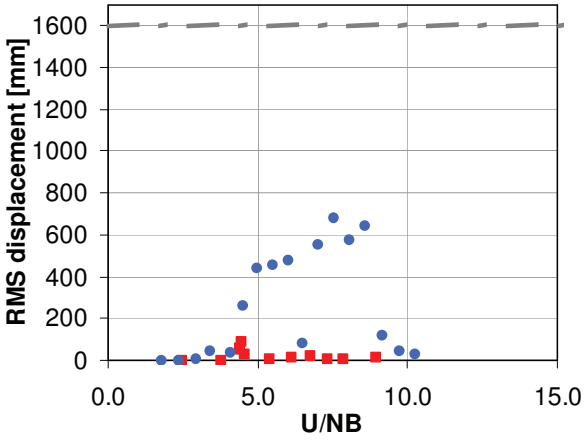

Wind Incidence 70 Degrees

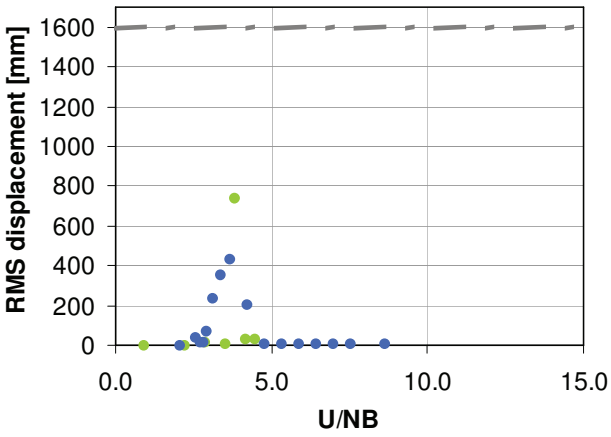

Wind Incidence 80 Degrees

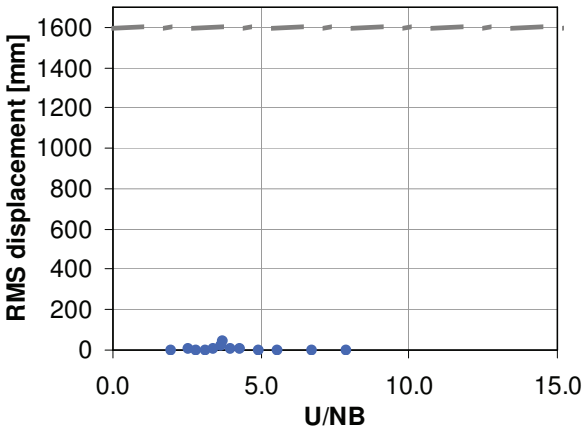

Wind Incidence 90 Degrees

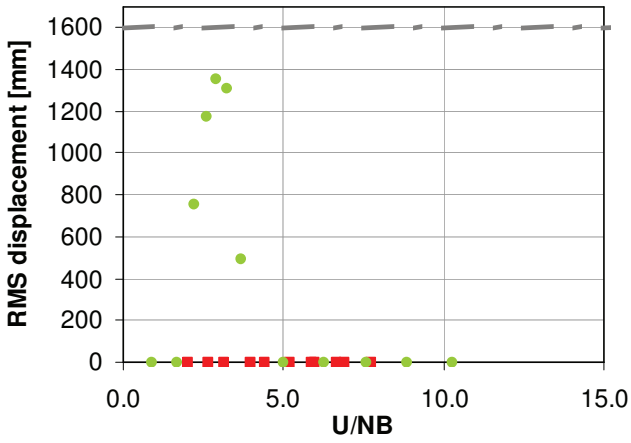

Figure 3.5 Variation of FS RMS displacements with reduced wind speed for the single leg configuration in smooth flow for a wind angle of 0° for various mitigation options with a level of damping of 0.004 Logdec.

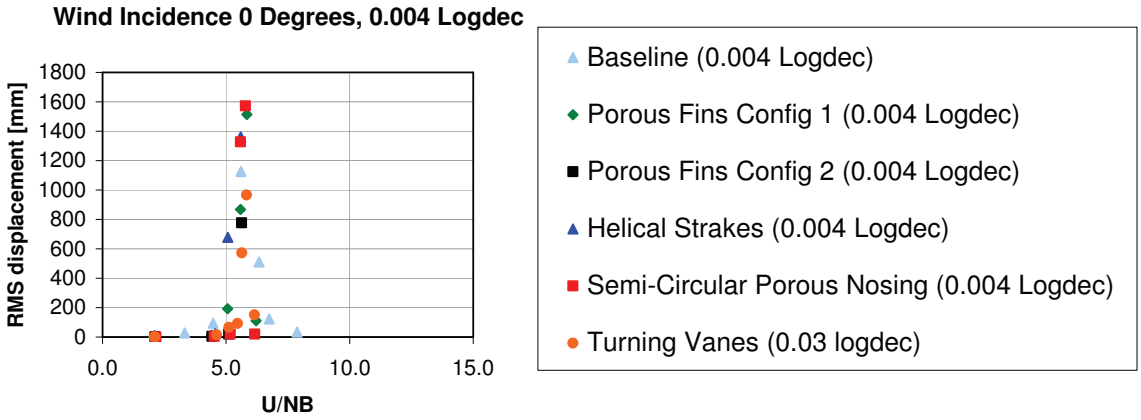

Figure 3.6 Variation of FS RMS displacements with wind speed for the single leg configuration with a mitigation option of semi-circular nosing in smooth flow for wind angles of 0°, 30°, 60° & 90° with a level of damping of 0.03 Logdec.

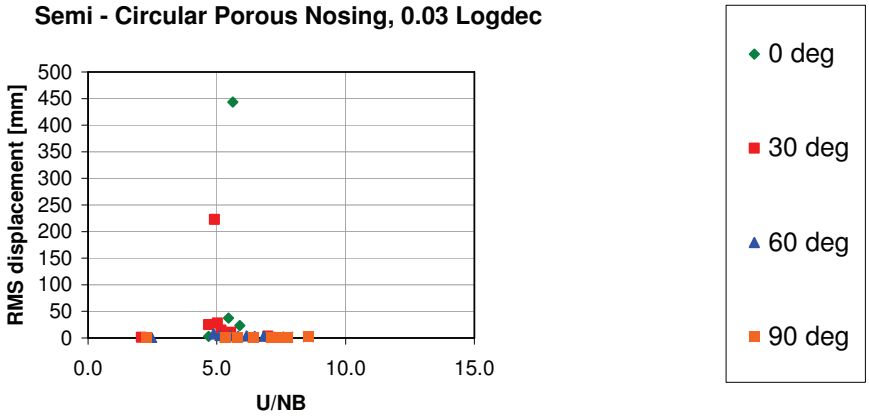

Figure 3.7: Mitigation Option: Porous Fins Config 1

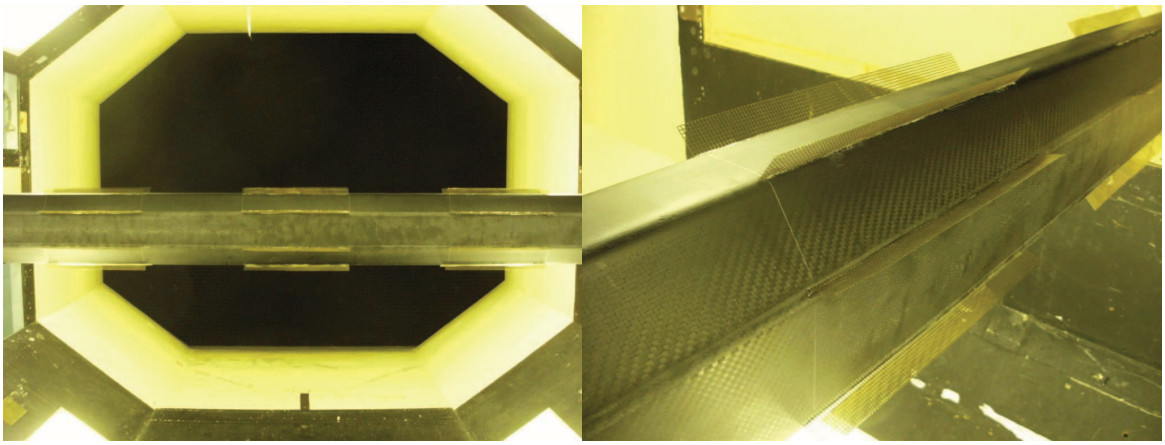

Figure 3.8: Mitigation Option: Porous Fins Config 2

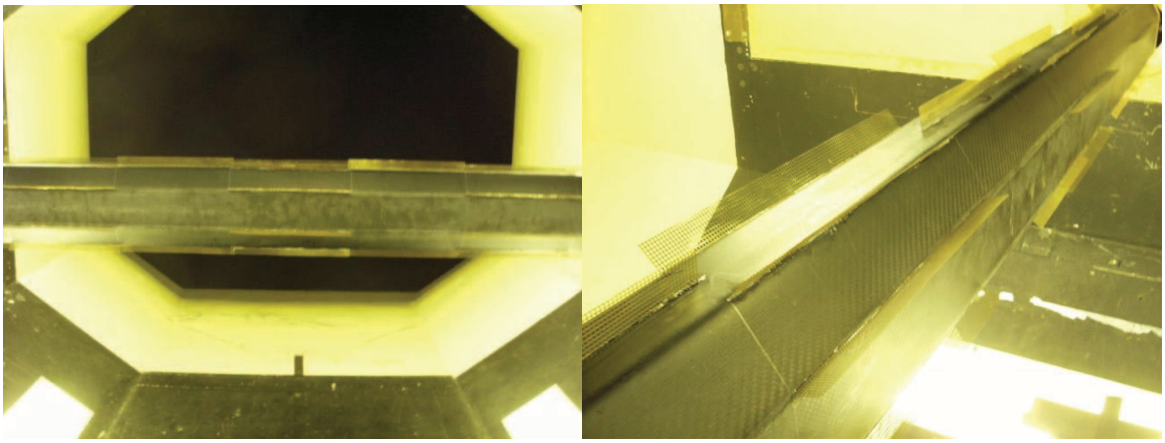

Figure 3.9: Mitigation Option: Helical Strakes

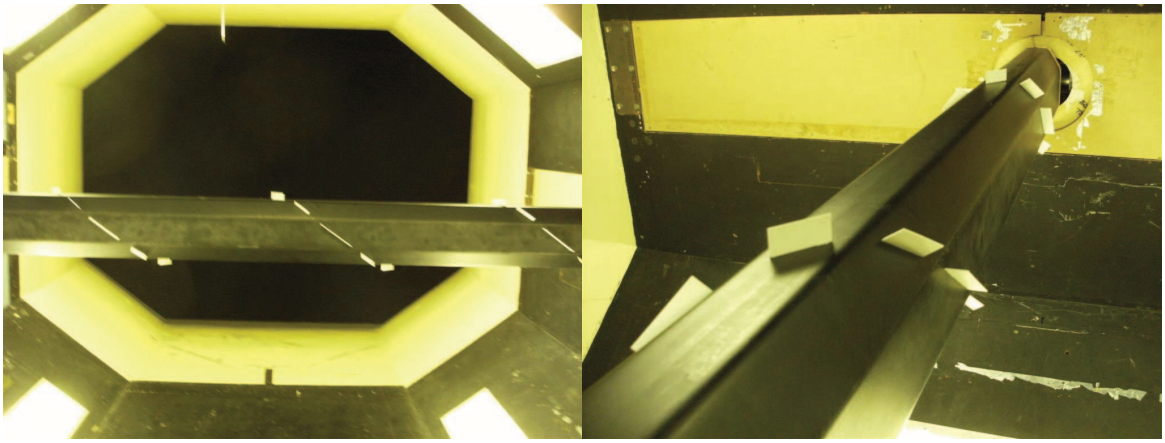

Figure 3.10: Mitigation Option: Semi-Circular Porous Nosing

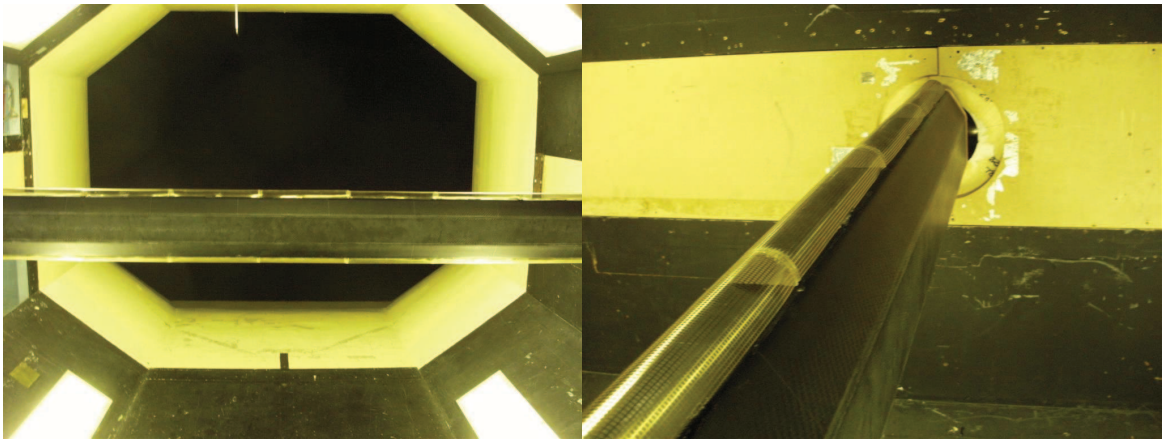

Figure 3.11: Mitigation Option: Turning Vanes

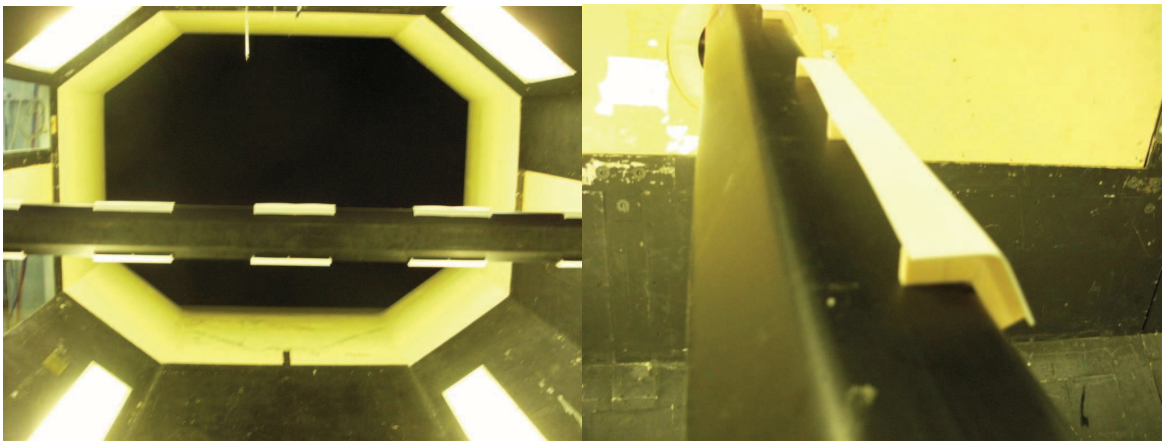

Figure 3.12: Variation of FS RMS displacements with reduced wind speed for the double leg configuration in smooth flow for wind angles 0° - 90°, with a level of damping of 0.01 Logdec.

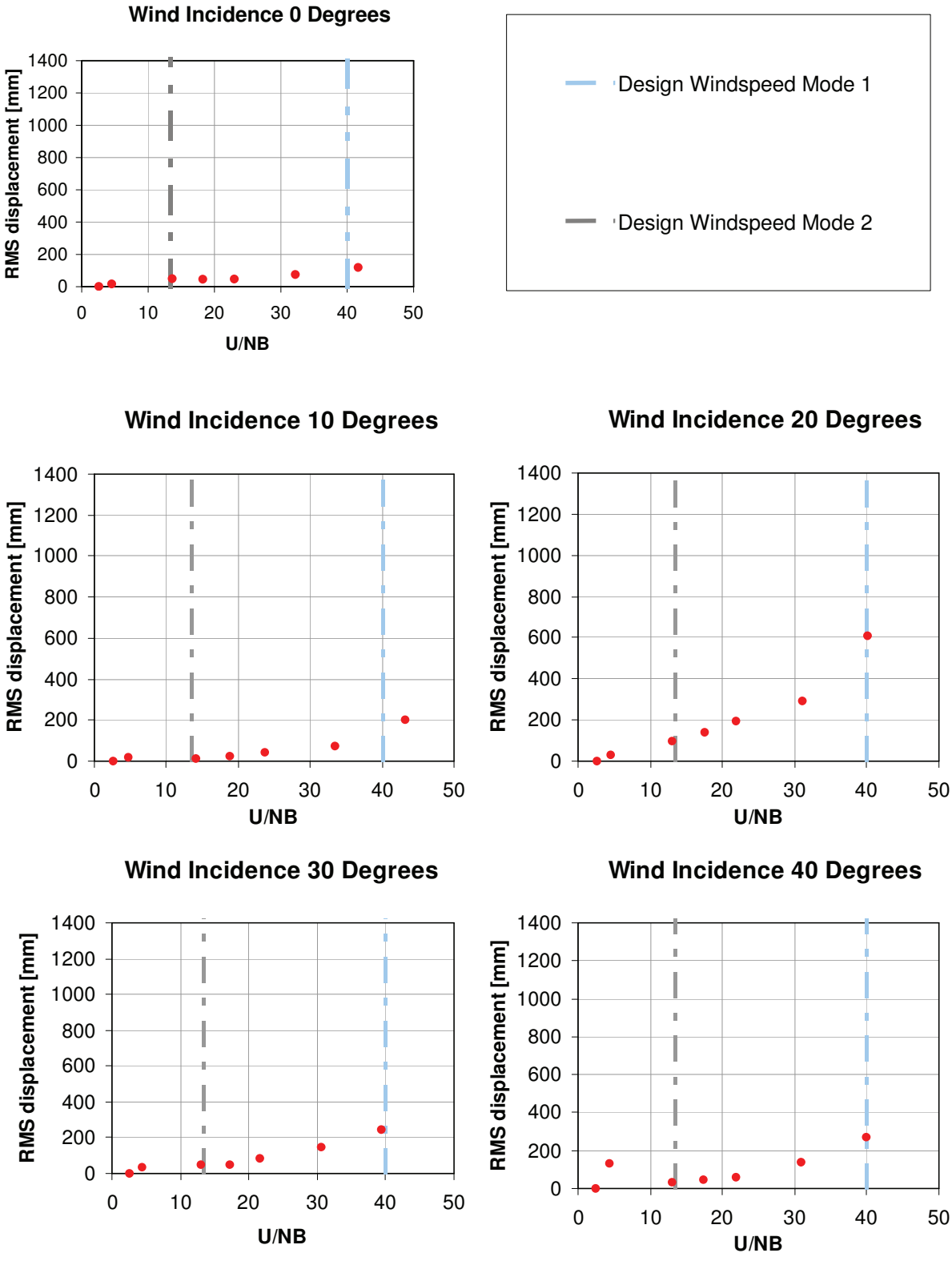

Wind Incidence 50 Degrees

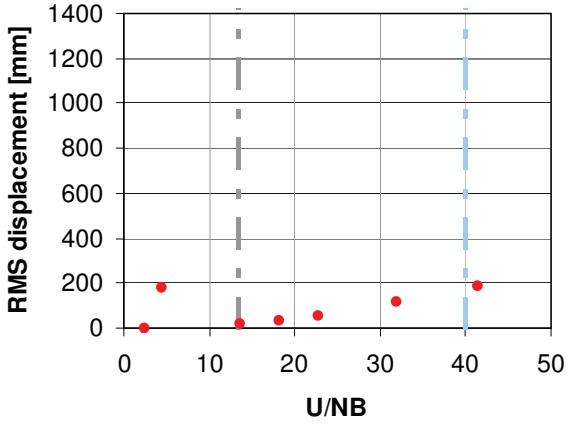

Wind Incidence 60 Degrees

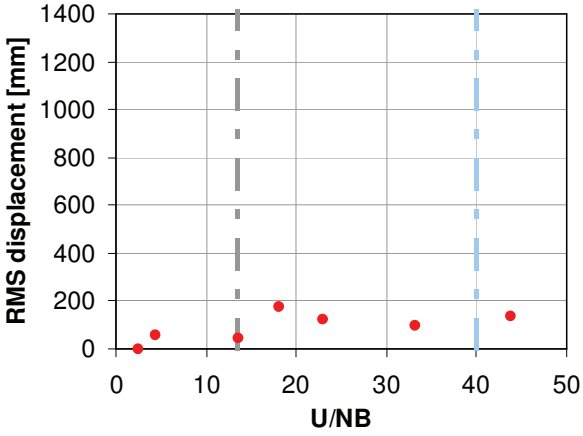

Wind Incidence 70 Degrees

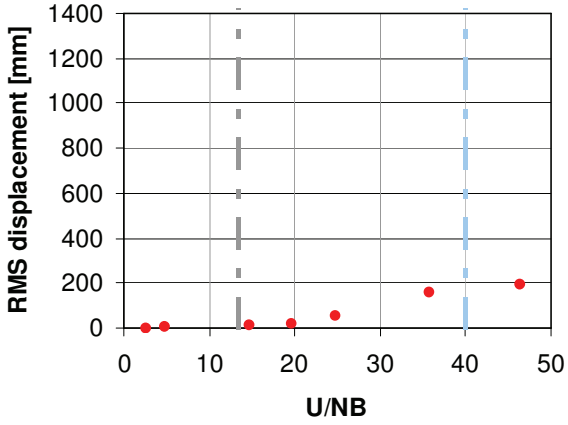

Wind Incidence 80 Degrees

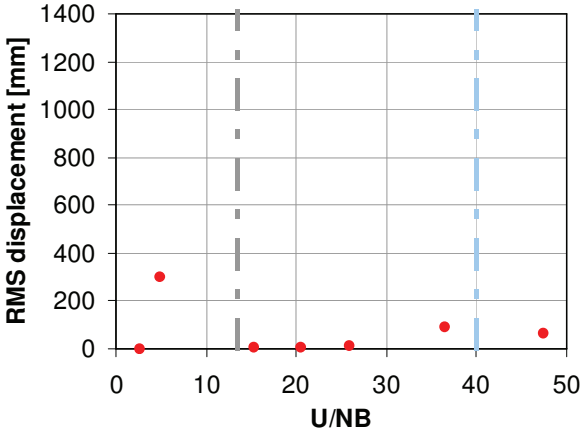

Wind Incidence 90 Degrees

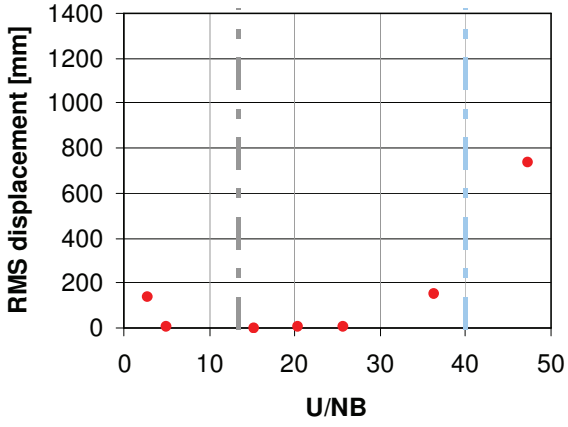

APPENDIX A. DESIGN WIND PROPERTIES & BOUNDARY LAYER SIMULATION

A.1. Design Wind Properties

The wind characteristics at the site were derived in accordance with the Specification [1] provided by COWI, and are summarised in the following sections.

A.1.1. Design Wind Speed Profile

The design wind speed profile for all wind directions is as follows:

$$u(z) = \frac{\ln z}{0.01}$$

Where u is the mean wind speed at elevation z above ground level

A.1.2. Design Turbulence Intensity Profiles

The turbulence intensity I profiles of the longitudinal (u), vertical (w) and lateral (v) components for the ocean and the land fetch respectively are defined as follows:

$$I_u(z) = \frac{1}{\ln\left(\frac{z}{z_0}\right)} \qquad I_v(z) = 0.75 I_u(z)$$

A.1.3. Design Power Spectra

The wind spectra are defined according to the Von Karman spectral model as follows:

$$\frac{nS_u(z,n)}{I_u^2(z)\overline{u}^2(z)} = \frac{6.868nL_u(z)/\overline{u}(z)}{\left[1+10.302nL_u(z)/\overline{u}(z)\right]^{5/3}}$$

$$\frac{nS_v(z,n)}{I_v^2(z)\overline{u}^2(z)} = \frac{9.434nL_v(z)/\overline{u}(z)}{\left[1+14.15nL_v(z)/\overline{u}(z)\right]^{5/3}}$$

Where

n is the frequency in Hz

L_u is the longitudinal length scale defined as follows: $L_u(z) = 300\left(\frac{z}{200}\right)^{0.5}$

L_v is the lateral length scale defined as follows: $L_v(z) = 0.25 L_u(z)$

A.2. BMT's Wind Tunnel – Technical Specification

The sectional wind tunnel studies were carried out in BMT's Aeronautic Wind Tunnel which has a test section 2.7 m wide and 2.1 m high. The operating wind speed range is 0.2 - 65 ms^{-1}. This wind tunnel facility is equipped state-of-the-art instrumentation for a wide range of applications and measurement techniques.

A.3. Experimental Conditioning

The section model tests were carried for the following flow conditions:

- Smooth Flow
- Turbulent Flow

A.3.1. Smooth Flow Test – Air Flow Generation

The maximum level of turbulence inherent in smooth flow in the wind tunnel is less than 0.3% and is consistent with best industry standard for aeroelastic testing for long span bridges.

A.3.2. Turbulent Flow Test – Air Flow Generation

The turbulent flow regime was set up using a 2-dimensional aluminium grid, placed at the entrance to the test section.

The properties of the flow were measured at the centre of the test section (in absence of the model) using hot-wire anemometry.

The mean wind speed, the turbulence intensities (longitudinal and lateral component) and the wind spectra were measured. Measurements were also carried out for two wind speeds, 10ms^{-1} and 20ms^{-1}, to ensure that no significant variation of the wind characteristic would occur within the wind speed range of the tests.

Results of the turbulence simulation are presented in terms of u-component and v-component of the wind spectra, and compared to the target values at a height of 70% of the overall tower height.

The wind spectra measured for the u and v component (S_{uu} and S_{vv}) are presented and compared to von Karman wind spectra in Figure A.1. The reference dimension B is taken as 20m full scale. Measurements were taken at model-scale speeds of 10ms^{-1} and 20ms^{-1}, in order to quantify the properties in the region of the two wind regimes associated to vortex-shedding responses and divergent responses.

Figure A.1: Target and Achieved Spectra, Turbulent Flow Setup

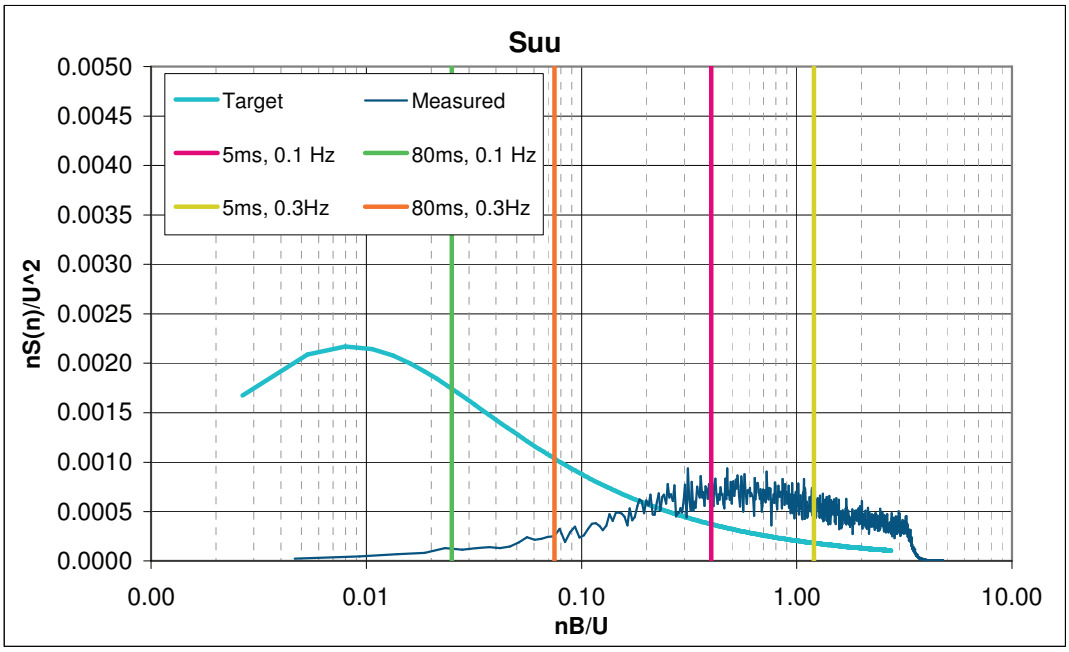

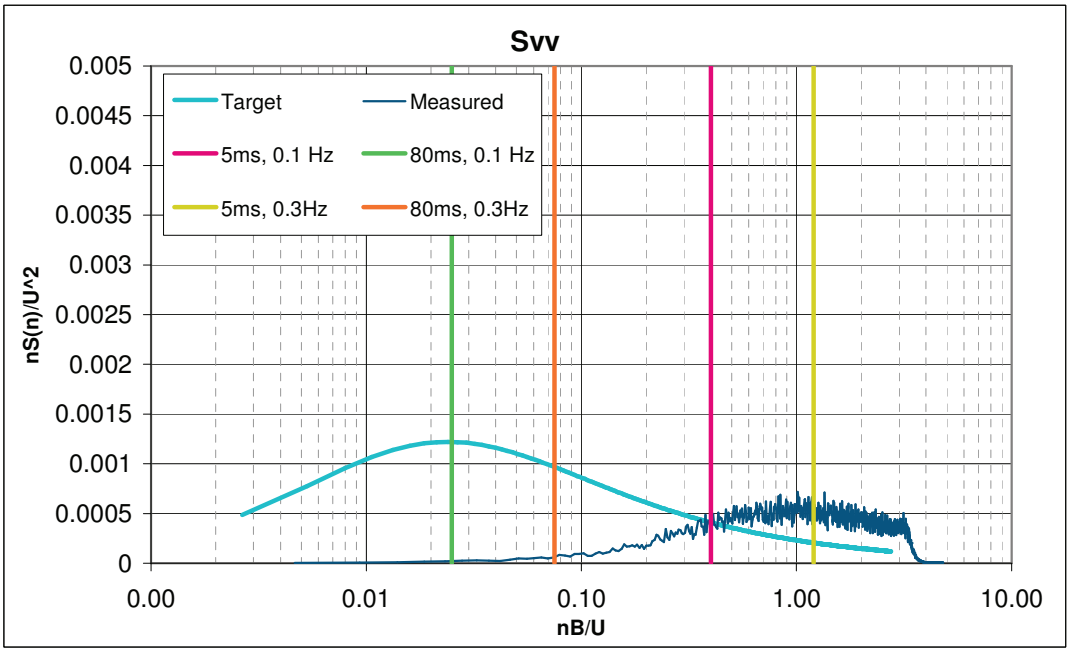

APPENDIX B. MODELS DESIGN AND CONSTRUCTION

B.1. General

The section models, as designed, were suitable for sectional wind tunnel testing.

B.2. Basis for Design and Construction of the Wind Tunnel Model

The models of the tower were constructed based on information supplied by COWI, as follows:

Drawing Name/No.	Date	Description
CG1000-PAXDPCG-S5TC000000-01_A.dwg	16-07-10	Tower Drawing
Tower Mode Information_July12_to BMT.xlsx	16-07-10	Modal Data

The models were reviewed and approved by the design team, prior to testing.

B.3. Model Scale

A model scale of 1:100 has been adopted for the main objectives of this study. At this scale the model allowed a detailed representation of all geometric features of the tower that are expected to affect the wind flows around the structure at full scale. In addition, this scale enables a good simulation of the turbulence properties of the wind to be achieved.

B.4. Model Configurations

As described in section 2, a multi-purpose section model was built which could be configured as either the single leg in isolation or the double leg system. Two identical sections were constructed from carbon fibre, along with two types of support:

1. A pair of aluminium interface plates in order to securely mount each end of one leg to the centre of the measurement rig in order to measure the forces and accelerations on one leg.

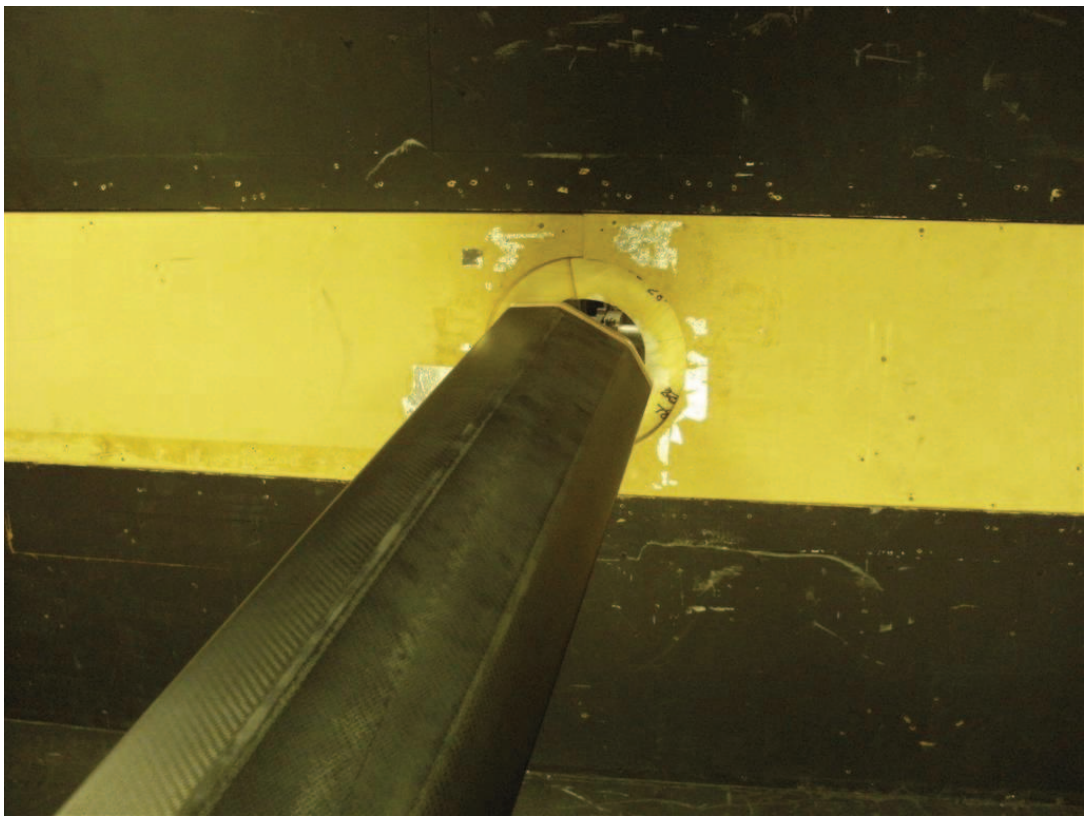

2. A longer pair of aluminium interface plates, configured to mount the pair of legs at the correct separation, as specified in the scope of work[1]. The system is mounted to the measurement rig through the centre of this plate.

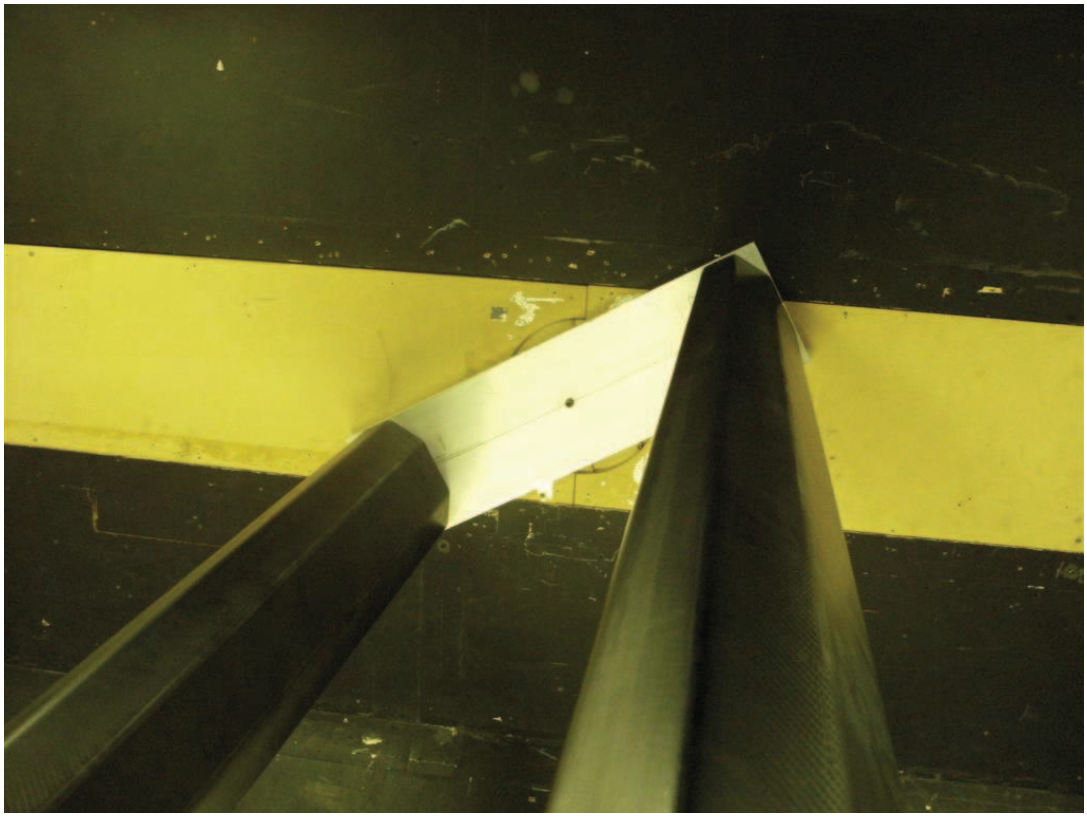

APPENDIX C. WIND LOADING MEASUREMENTS

C.1. Model Mounting & Instrumentation

For measurement of the static wind load coefficients the model was mounted across the 2.74 m width of the wind tunnel on a force balance rig. Data records were of sufficient length to enable the probability statistics and spectra to be computed in addition to the mean values.

The force balance rig consists of a pair of high-frequency six-component force balances in conjunction with a signal-conditioning unit to measure the shear forces and moments at either side of the wind tunnel test section and on which the wind tunnel model is accurately rigged via precision-machined fittings. The model is rotated through the test wind angles on the balances so that the wind loads are measured directly in model axes.

Load balance checks were carried out prior to the experiments over the expected range of forces and moments coefficients. Further checks including repeatability checks, showing agreement on forces and moments, and symmetry checks were carried out to ensure the reliability of the data.

APPENDIX D. DYNAMIC RESPONSE MEASURMENTS

D.1. Model Mounting & Instrumentation

For the dynamic response tests the model was mounted across the 2.74 m width of the wind tunnel on a dynamic rig consisting of a system of springs allowing the vertical bending degree of freedom. The model was restrained from moving in the other directions by a combination of light steel wires.

The layout of the dynamic rig for this configuration is shown in Figure D.1 below.

Figure D.1: Layout of the Dynamic Rig

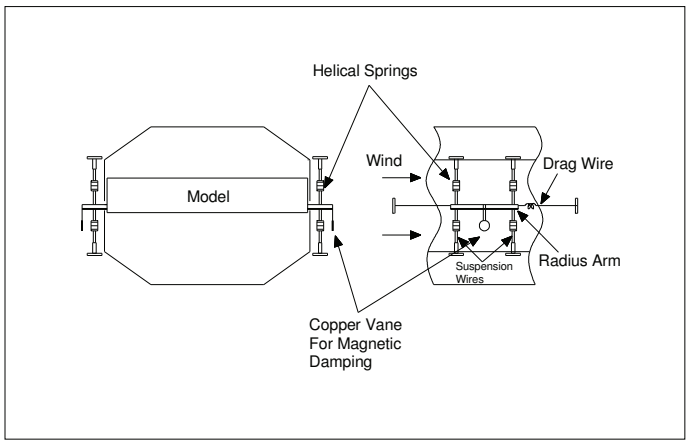

For dynamic response measurements, the test rig was instrumented with four small accelerometers mounted on the suspension arm external to the wind tunnel and positioned to resolve the vertical bending motion through the sum of the signals digitized simultaneously. From the accelerations time histories the amplitude response of the model was determined.

D.2. Experimental Conditioning

For the dynamic rig tests it was required to reproduce the full-scale behaviour of the tower by imposing the correct structural properties on the wind tunnel model subject to scaling laws detailed below. For dynamic similarity, equality of the following non-dimension parameters is required between model-scale and full-scale:

$$i)\ \frac{I_z}{\rho B^2}$$

$$ii)\ \frac{U}{f_b B}$$

$$iii)\ \delta_z$$

Where:

I_z is the mass per unit length of the tower

B is the reference dimension taken as the tower width

ρ is the density of air

U is the mean hourly wind speed

f_b is the bending natural frequency

δ_z is the logarithmic decrement of the structural damping corresponding to the bending frequency

The combined damping and inertial parameters for single degree of freedom sinusoidal motions are as follows:

$$iv)\ \frac{I_z \delta_z}{\rho B^2}$$

With the above parameters correctly modelled, values of U/f_bB obtained from wind tunnel measurements will be directly applicable to full scale. The responses measured in the wind tunnel can be related via the model scale.

The comparison between full scale and model scale achieved quantities is shown below:

	Full Scale	Model Scale
Modal Mass [Kg/m]	147550	12.7
Bending Frequency [Hz]	0.11	3.71

D.3. Model Calibration

The model dynamic properties in terms of natural bending frequency and structural damping were measured prior to each set of tests. The dynamic properties of the model were measured by resonating the model in a natural mode via using a vibrator through a light spring or by hand. The bending frequency was measured by oscillating the model at constant amplitude. The structural damping associated with the rig system was measured in amplitude decay tests.

In order to cover the two wind speed ranges of interest (relevant to vortex-shedding and stability) at a reasonable wind speed in the tunnel, two dynamic rig setups were used, one stiff with a speed scale of 1.3 for vortex shedding, and one soft with a speed scale of 2.9 to allow the maximum design wind speed to be reached in the tunnel.

The structural damping of the rig was measured in amplitude decay tests.

D.4. Derivation of Full-Scale Displacement

Time histories of accelerometer data were recorded at a number of wind speeds in the range of interest. These were then processed by evaluating the spectra, in order to isolate the contribution from the mode of interest. Then, using a mechanical admittance type filter, the RMS resonant component from each mode was derived. Figure C.2 shows an example of a raw spectra, along with the same data, filtered for the first mode of longitudinal bending. The difference between the two is the RMS resonant contribution from that mode.

The full-scale bending RMS displacements are determined from the RMS model accelerations as follows:

$$y_{FS} = 100 \frac{\ddot{y}_{MS}}{(2\pi f_b)^2}$$

Where y_{FS} is the full-scale RMS bending displacement, $\ddot{y}_{MS}$ is the vertical RMS model acceleration and f_b is the vertical frequency

D.5. Damping Devices

Controlled additional damping to simulate the effect of a damping device was also provided for the vortex-shedding tests. A copper vane was supported from the arms of the rig, between the poles of an electromagnet. The current generated in the copper vane interacts electromagnetically to provide additional damping. By varying the current feeding the electromagnet, different levels of damping can be obtained.

APPENDIX E. ASSESSMENT OF SCALE EFFECTS

E.1. Background

Additional testing has been undertaken by BMT, in order to quantify the sensitivity of the cross section to scale effects, as the maximum achievable Reynolds number for the 1:100 model in the BMT wind tunnel is 6×10^5 and the full scale Reynolds number is 1.1×10^8. Two further models of the single leg, at scales of 1:50 and 1:200 were constructed. The 1:50 model was used to investigate the variation of wind loading and Strouhal number with Reynolds number up to 1×10^6. The 1:200 model was used to inform the aeroelastic studies of the Strouhal number and wind loading coefficient of the section.

E.2. Methodology

E.2.1. Objective of the Studies

The key objectives of the studies were to:

- Determine to what extent the static load coefficients measured on the 1:100 model are subject to scale effects, based on the results of the 1:50 scale model.
- Determine to what extent the full aeroelastic 1:200 model will be subject to scale effects.

The 1:50 and 1:200 models were tested 'as built' as per the 1:100 scale model on the static rig in order to measure static load coefficients over an extended Reynolds number range (up to $\sim1\times10^6$).

E.2.2. Wind Tunnel Models

1:50 Scale Static Model

The 1:50 scale static model was constructed from MDF formers attached to an aluminium spine. The shape of the tower was generated from foam.

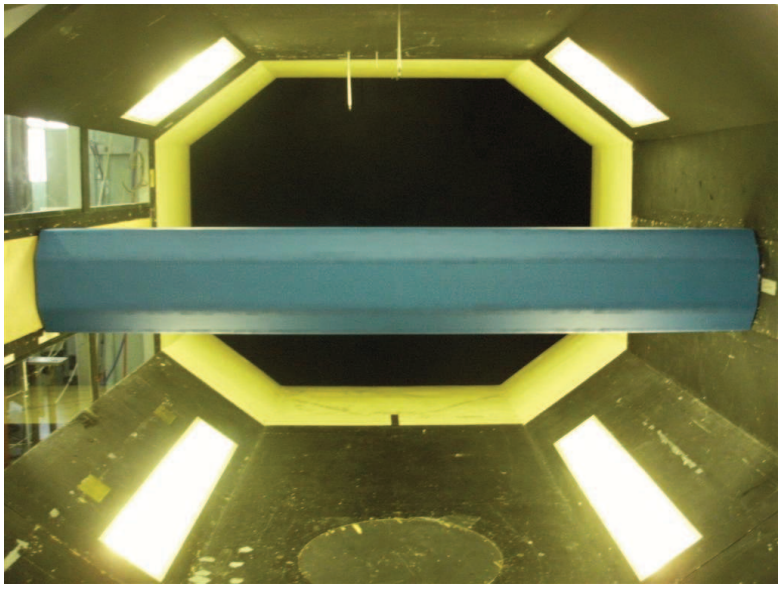

1:200 Scale Static Model

The 1:200 scale model was constructed from a 40mm square aluminum tube, clad with foam, shaped to give an accurate representation of the section.

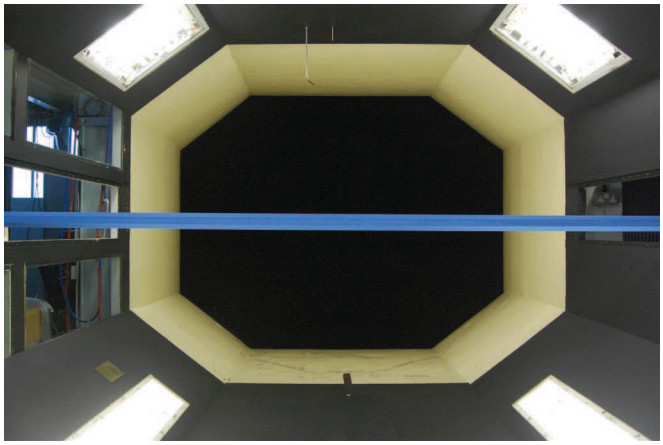

E.2.3. Test Matrix

Configuration	Testing Scenario	Model Scale	Flow Condition	Wind Angles	Reynolds Number
Single Leg	Static	1:50	Smooth	0°, 30°, 60°, 90°	1.8E+05 to 1.3E+06
Single Leg	Static	1:200	Smooth	0°, 30°, 60°, 90°	2.1E+04 to 3.4E+05

E.2.4. Measurements and Analysis

Time histories of load and moments were measured simultaneously using a three-component high frequency force balance rig, mounted at each end of the section. Measurements were taken for the single leg configuration in smooth flow at a range of speeds for the angles of 0°, 30°, 60° and 90° in order to assess the sensitivity to Reynolds number.

Steady-state mean load and moment coefficients were then calculated in order to quantify the sensitivity of the section to Reynolds number effects.

E.3. Results

Figure E.1: Variation of Drag Coefficients with Reynolds number for each of the three single leg model scales at wind angles of: 0°, 30°, 60° & 90°

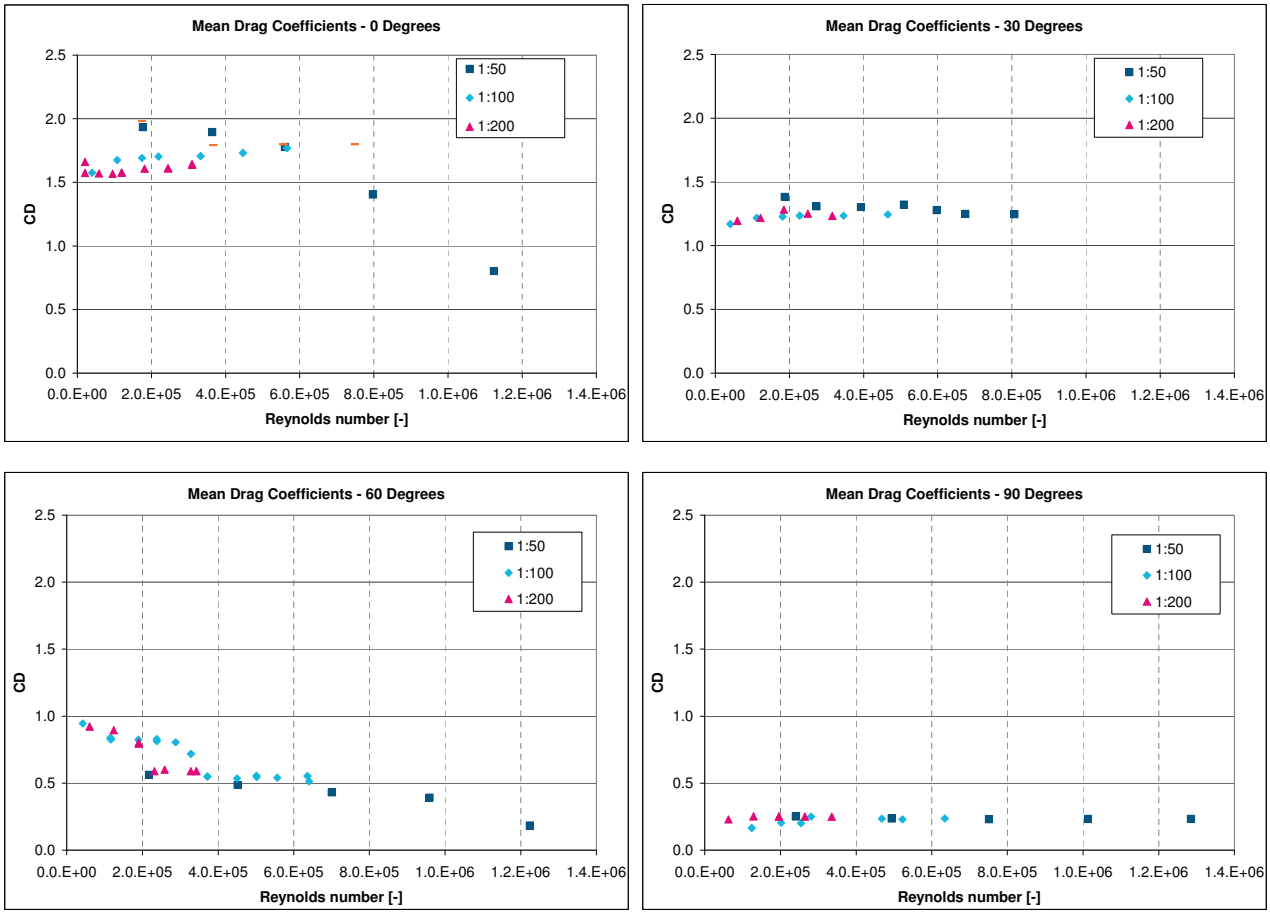

E.3.1. Interpretation / Discussion of results

- At 0°, the calculated wind load coefficient is seen to be largely independent of Reynolds number up to 6×10^5.
- At 30°, the calculated wind load coefficient is seen to be largely independent of Reynolds number up to 8×10^5.
- At 60°, Load coefficients are largely independant of Reynolds number between 4×10^5 and 1×10^6.
- At 90°, the calculated wind load coefficient is seen to be largely independent of Reynolds number up to 1.3×10^6.

Alan G. Davenport Wind Engineering Group

A STUDY OF WIND EFFECTS FOR THE

MESSINA STRAIT BRIDGE, ITALY

Non-Froude and Froude Scaled Aeroelastic Models of Tower - Sub-Test T3

J.P.C. KING / L. KONG / B. BAKHT

BLWT-SS1-2011 / DRAFT 1 / JANUARY 2011

The Boundary Layer Wind Tunnel Laboratory
The University of Western Ontario, Faculty of Engineering
London, Ontario, Canada N6A 5B9; Tel: (519) 661-3338; Fax: (519) 661-3339
Internet: www.blwtl.uwo.ca; E-mail: info@blwtl.uwo.ca

TABLE OF CONTENTS

LIST OF TABLES

LIST OF FIGURES

ACKNOWLEDGEMENTS

The full aeroelastic model studies of wind effects for the tower of the Messina Straits Crossing between Sicily and Reggio Calabria, Italy was initiated by Dr. Allan Larsen of COWI A/S, Denmark. The co-operation and support of Dr. Larsen throughout the study is greatly appreciated. Acknowledgement is also made of the support of Mr. Sandro Ordanini of Eurolink S.C.p.A.

Acknowledgment is made of the contributions by various members of the engineering and technical staff of the Laboratory, particularly: Mr. Gerry Dafoe and Mr. Anthony Burggraaf who carried out the experimental phases of the study. The section model was constructed by members of the University Machine Shop under the direction of Mr. Doug Phillips.

DETAILS OF THE STUDY

Project Name:	Messina Strait Bridge
Project Location:	Straits of Messina – between Sicily and Reggio Calabria Italy
Project Description:	The proposed suspension bridge across the Straits of Messina is situated over a narrow section of water between the eastern tip of Sicily and Reggio Calabria on the mainland of Italy. With a length of 3.3km and a width of 60m, the bridge will be supported by two 382 m high towers. There will be three motorway lanes and one emergency lane in each direction and a two-track railway.
Test Dates:	Froude Scaled Aeroelastic Model – December 2010 Non-Froude Scaled Aeroelastic Model – December 2010 & January 2011
Preliminary Reporting:	Froude Scaled Aeroelastic Model – December 2010 Non-Froude Scaled Aeroelastic Model – December 2010 & January 2011
Report Scope and Format:	The report is organized as follows: Section 1 – Introduction Section 2 – Full Aeroelastic Model Studies of the Tower Section 3 – Froude Tower Aeroelastic Model Study Section 4 – Non-Froude Tower Aeroelastic Model Study
General Reference:	Discussion and details of the general methodology used by the Alan G Davenport Wind Engineering Group can be found in “Wind Tunnel Testing – A General Outline” [Reference 3].

1 INTRODUCTION

1.1 General

This report describes the full aeroelastic model studies of the tower for the Messina Strait Bridge in Italy. The proposed bridge is located between the island of Sicily and Reggio Calabria on the mainland. The bridge will feature a six-lane highway, two service lanes and a double-track railway. It is a steel suspension bridge with a central span of 3,300 m between the two towers and two side spans of different lengths and arrangements, for an additional 960 m to the Sicily anchorage and 810 m to the Reggio Calabria anchorage. The steel towers, standing at a height of 382 m, each consist of two vertical legs linked by three cross beams. The deck has a total width of about 60 m and comprises a central double-track railway deck flanked on either side by a 3-lane road deck. The suspension system consists of two pair of steel cables, each with a diameter of 120 cm. The deck is suspended from the cables by a system of vertical steel hangers at 30 m intervals.

The site of the bridge is shown in Figure 1.1. The overall dimensions of the prototype bridge are given in Figure 1.2. Figures 1.3 through 1.6 provide general details of the bridge towers which the design of the full aeroelastic models was based.

The full aeroelastic models of the bridge tower were studied at the main boundary layer (high speed) test section of BLWT II, located at the University of Western Ontario.

1.2 Scope of Report

This report includes results from the dynamic tests of the two aeroelastic models of the tower for the Messina Straits Bridge. The series of tests follows as closely as possible, the outline test specification documents referenced in [1], provided by COWI A/S. The wind tunnel tests addressed Sub-test T3 as defined by Eurolink s.c.p.a "Overall Aerodynamic Design Methodology and Plan for Aerodynamic Testing [2]. The full aeroelastic model tests included:

Sub-Test T3:

a) the measurement of the response of the full aeroelastic model to turbulent wind, where two structural configurations were investigated:
   - Completed Tower, free standing condition
   - Completed Tower, pinned at top simulating the effects of the main cables and tie back.

The tests were intended to measure the horizontal response along the bridge line and across the bridge line of each tower leg at the tower top as well as at the position of the second cross beam as well as the along axis and cross axis bending moments at the base of each leg.

The primary focus of the investigation was to provide verification of the tower behavior as reported elsewhere. A full aeroelastic model of the tower was designed and constructed at a geometric scale of 1 to 200. The full aeroelastic model was designed as a non-Froude scaled model, in order to utilize a greater range of the wind speed of the wind tunnel and to increase the Reynolds number associated with vortex shedding induced oscillation to as high a value as practical. The model structural members were designed to replicate the longitudinal, lateral and torsional stiffness and the cladding elements were ballasted to the scaled mass and fixed to the various structural members. As a precaution against mis-interpreting the results of the non-Froude scaled model tests, a second model was designed and constructed using Froude number scaling. The identical geometric scale of 1 to 200 was utilized and the models were tested in a similar fashion. The primary differences in the model tests were in the extent of the instrumentation used and the model to prototype wind speed scaling, which in the case of the non-Froude scaled model was approximately 1 to 6 and for the Froude scaled model was 1 to 14.1.

The methodology and test results for Sub Test T3 for the non-Froude scaled tower model are detailed in Section 3, while those for the Froude scaled tower are given in Section 4 of this report.

2 FULL AEROELASIC MODEL STUDIES

2.1 General

Two full aeroelastic models of the Messina Tower were designed and constructed at a geometric scale of 1 to 200 relative to the prototype. The first model constructed was designed without preserving Froude number and is termed the “non-Froude scaled model”. The second model preserved the Froude number and is termed the “Froude scaled model”. The approach taken for the full aeroelastic model study has been discussed in [3], and has been used in a variety of long and short span bridge studies [4,5,6,7 and 8].

The behaviour of the Messina Tower aeroelastic models were studied at the main boundary layer test section of the High-Speed Test Section of Boundary Layer Wind Tunnel II (BLWT II). The response of the tower was examined under two general wind conditions: a) a “smooth” flow and b) a turbulent boundary layer flow.

Sub-test T3 was carried out by subjecting the s aeroelastic model of the tower to increasing wind speeds in the range of 5 m/s to 80 m/s full scale and recording the structural response. For the two structural configurations examined, the wind direction was varied from 0 deg. (flow perpendicular to bridge line) to 90 degrees in steps of 10 deg. The inflow angle increment was decreased to 2.5 degrees in the range of 0 to 10 degrees, as these directions were expected to yield the highest responses. The tests were to be carried out at three levels of mechanical damping in the aeroelastic model, with the lowest level approximately 0.5% relative to critical and the remaining damping levels 2% and 4% of critical. The tests were to be carried out in smooth flow with turbulence intensity less than 2% and in a simulated boundary layer representative of the conditions to be expected at the project site.

Examples of the aeroelastic model test set-up are shown in Figure 2.1. The model is situated on the turntable of the High Speed Test Section. The two upstream terrain conditions modeled in the test can be seen in the figure. Figure 2.2 presents the in-service condition and the construction stage test configurations of the model. The anchored cable ties used in simulating the in-service condition of the tower can be seen in the figure. Views of the non-Froude scaled aeroelastic model are given in Figures 2.3 and 2.4 while those for the Froude scaled aeroelastic model are given in Figures 2.5 and 2.6. The instrumentation used as well as the damper configuration can be seen in the figures. The definition of wind directions used in the tests is given in Figure 2.7. Prototype values of the relevant structural properties for the main members of the tower, as provided by the Client are given in Table 2.1.

2.2 Dynamic Similarity of Aeroelastic Models

The aeroelastic modelling of structures generally requires equality of the following non-dimensional quantities in addition to an overall geometric similarity:

- Froude number (ratio of the gravitational to the inertia forces);
- Cauchy number (ratio of the elastic to inertia forces);
- Density Ratio (ratio of the inertia force of the structure to that of the flow);
- Damping Ratio;
- Reynolds number (based on the dimensions of the structure).

The full aeroelastic models included: a) Model 1, where Froude number ($Fr = gL/V^2$) was not preserved (termed the “non-Froude Model”) and b) Model 2 Froude number was preserved (termed the “Froude Model”). Eliminating the requirement to preserve Froude number enables the selection of the velocity scaling between model and prototype to be undertaken independently of the length scale and usually results in tests performed at higher test wind speeds. The latter design methodology requires tests to be conducted at low wind speeds since the velocity scaling is fixed as the square-root of the

length scale. With the selected length scale of 1:200 for the aeroelastic model, the resulting Froude scaled velocity ratio of 14.14:1 between prototype and model is well suited to the scaling of the turbulent boundary layer in the High Speed Test Section of BLWTII. The non-Froude scaled model utilised a nominal velocity ratio of 6:1 between prototype and model.

Cauchy number is a non-dimensional parameter which represents the ratio of the elastic forces of the bridge to the inertia forces of the flow ($Ca = E / \rho V^2$). This parameter is preserved in the design of the model.

The density ratio ($\rho_{\mathrm{mod}\,el} / \rho_{air}$) fixes the mass of the model with respect to the air in the wind tunnel. Since the air density of the prototype is assumed the same as that of the model, the density of the model must be identical to that of the prototype.

The damping ratio ($\delta_{\mathrm{mod}\,el} / \delta_{prototype}$) is an important quantity to preserve, since it has a direct effect on the resonant motions. In the majority of cases, the damping is approximately that which may be (conservatively) expected to be found in the prototype tower. The design of aeroelastic models does not easily allow for the adjustment of the structural damping and in order to identify possible instabilities under the action of wind, the model is designed to have as low a value of structural damping as possible. This also has the effect of providing conservative estimates of the structural responses. The effect of increased damping in the prototype can usually be estimated through an analytical correction to the test results, or through tests where discrete dampers are used to augment the structural damping in specific modes of vibration.

Reynolds number similarity ($Re = VL / \nu$) is not practical in most cases and aeroelastic tests are usually carried out at a Reynolds number several orders of magnitude lower than that of full scale. For sharp edged bodies such as bridge decks, the effects of this relaxation of Re scaling is not severe for overall wind induced forces and responses. Reynolds number effects can be significant in the modelling of circular or rounded edge objects such as cables or in this case, the legs of the tower. In the cases of the bridge cable, the model cable diameter is adjusted to equate to the mean drag wind effects using an equivalent C_dDL approach and in other cases where adjustment is not practical, the surface of the model is roughened to ensure a turbulent boundary layer and tests are performed at varying velocities to investigate the potential for Reynolds number dependence on the response of the model.

2.3 Design of Aeroelastic Models

The full aeroelastic models were designed using the scaling parameters listed in Table 2.2. The CNC (Computer Numeric Control) facilities at the University Machine Services were used in the construction of the full aeroelastic model. The elastic properties of the tower members were modelled by a continuous central "spine" providing the appropriate longitudinal, lateral and torsional stiffness of each tower leg. A similar approach was taken for the design of the cross beams. A high-strength aluminum section was machined to develop a channel shape in order to simulate the three degrees of freedom in the primary bending and torsional directions of each member. The section properties were varied in a step-wise fashion, to replicate as closely as possible the variation with the length of the member of the moments of inertia and torsional constant. A fixed clamp-type connection was designed to connect the tower cross beams to the legs of the towers. The base plate of the model provided a fixed end condition for the tower leg members, restraining bending and torsional moments as well as shear forces. An aluminum “saddle” was clamped to the top of the tower leg members to provide a rigid point to attach the restraining cables to the tower top in the in-service tests.

The cladding modules were constructed out of “Rohacell” Structural Foam using CNC machining techniques and ballasted with brass weights to provide the scaled value of mass per unit length of the tower members. The cladding segments were affixed to the spine at the centre of each segment using a machined clamp, which also provided the required lumped mass for the appropriate portion of cladding The clamp was constructed of magnesium, aluminum, brass or steel, depending upon the required mass properties of the particular segment. The cladding modules provide no significant additional stiffness to the structural spine of the tower members, yet provide the necessary mass and geometric shape for the

proper simulation of the aerodynamic forces. The individual tower modules were separated from each other through a small gap (~1 mm), which has been shown to be aerodynamically insignificant.

A complete set of model drawings for the non-Froude and Froude scaled tower aeroelastic models are given in Figures 2.8 to 2.11.

2.4 Instrumentation

2.4.1 Non-Froude Scaled Aeroelastic Model

The model tower spine was instrumented with strain gauges at three locations in each of the two legs of the tower. Strain gauges were located at the base of each leg near the foundation level where lateral and longitudinal bending moments, as well as tower leg torque were measured and above Levels 1 and 2 with measurements of leg lateral and longitudinal bending moments. In addition, strain gauges were installed on the crossbeams near Leg A where longitudinal and vertical bending moments were measured.

The tower model was fitted with two non-contacting laser displacement transducers to monitor tower displacements at Level 2. The two transducers were oriented in a horizontal manner separated by a fixed distance at each tower leg. The time history output of these two channels was digitally summed and differenced to provide measures of the tower longitudinal motion and rotation. The resolution of the displacement measuring system was 0.05mm in model scale (or 10mm in full scale). This translates into a resolution of the angular motion of approximately 0.05 degrees. All displacements and rotations presented in the plots are well within the resolution of the instrumentation.

Three pairs of high sensitivity accelerometers were placed on each of the two tower legs at Levels 1, 2 and 3, oriented to provide longitudinal accelerations of the tower at each leg. The time history outputs of these paired accelerometers were digitally summed and differenced to obtain the longitudinal and rotational accelerations. Additional accelerometers were located in the transverse direction of the tower at these three levels to provide a measure of the tower lateral accelerations.

The wind speeds at the full tower height, the mid height, as well as the deck height were monitored throughout the tests. The tower height wind speed was used as the reference wind speed for all subsequent analyses of the experimental data. In addition, wind speeds at standard reference heights were recorded for redundancy.

In summary, a total of 42 channels were used in the tests for the Non-Froude Tower model. An additional 8 “virtual” channels were digitally formed during the analysis of the recorded time histories. These formed channels included: the longitudinal displacement and rotation of the tower at Level 2, the longitudinal and rotational accelerations of the tower at Levels 1, 2 and 3. Details of the instrumentation used and their locations for the Non-Froude Tower model are summarized in Table 2.4. They are also given schematically in Figure 2.12.

The scaling of the model responses was performed using the scaling parameters given in Table 2.2. The nominal value for the velocity scaling of 1 to 6 was adjusted to a value of 1 to 7.2 in the scaling of all responses. This adjustment was made considering the natural frequencies of the fundamental longitudinal mode of vibration of the prototype and non-Froude scaled model tower in the in-service condition. The nominal velocity scaling of 1 to 6 was used for the free standing construction stage.

2.4.2 Froude Scaled Aeroelastic Model

The model was fitted with two non-contacting laser displacement transducers to monitor tower displacements at Level 2 as was the case for the non-Froude scaled aeroelastic model. A similar summation and differencing was performed to provide measures of the tower longitudinal motion and rotation. Strain gauges were not used in the Froude scaled model. Accelerometers were placed on each of the two tower legs at Levels 1, 2 and 3 as with the non-Froude scaled tower and the summation and differencing performed to obtain the longitudinal and rotational accelerations. Additional accelerometers

were also located in the transverse direction of the tower at these three levels to provide a measure of the tower lateral accelerations. The same wind speed measurements as described above were employed.

In summary, a total number of 22 channels were used in the tests for the Froude scaled aeroelastic model. An additional 8 channels were formed during the analysis using the recorded time histories. These formed channels included: the longitudinal displacement and rotation of the tower at Level 2, the longitudinal and rotational accelerations of the tower at Levels 1, 2 and 3. Details of the instrumentation used and their locations for the Froude Tower model are summarized in Table 2.5. They are also given schematically in Figure 2.13.

The scaling of the model responses was performed using the scaling parameters given in Table 2.2. The nominal value for the velocity scaling for the Froude scaled model of 1 to 14.14 was used in the scaling of all responses.

2.5 Wind Simulation

The tests were to be carried out in smooth flow with turbulence intensity less than 2% and in a simulated boundary layer representative of the conditions to be expected at the project site. Properties of the target mean wind speed, $\bar{u}(z)$ and turbulence intensity, $I_u(z)$, with a logarithmic variation with height as given in reference [1] is:

$$\bar{u}(z) \approx \frac{1}{k} u_* \ln\frac{z}{z_o} \;;\; I_u(z) = \frac{1}{\ln\frac{z}{z_o}} \tag{2.1}$$

where z is the elevation above ground level, $k = 0.4$ and u_* is the shear velocity of the flow. The target power spectrum of the longitudinal component of turbulence was given as follows:

$$\frac{nS_u(n,z)}{I_u^2\bar{u}(z)^2} = \frac{6.868\frac{nL_u(z)}{\bar{u}(z)}}{\left(1+10.302\frac{nL_u(z)}{\bar{u}(z)}\right)^{5/3}} \tag{2.2}$$

$$L_u(z) = 300\left(\frac{z}{200}\right)^{0.5} \tag{2.3}$$

where n is frequency in Hz and $L_u(z)$ is the integral length scale of turbulence (in metres) at elevation z.

Measurements were performed for the two exposures selected, using Hot-wire anemometry of the variation in the mean wind speed and turbulence intensity with height above the wind tunnel floor. were made selected. Figures 2.14 and 2.15 present the profiles of the variation in the mean wind speed and the intensity of the longitudinal component of turbulence obtained in the wind tunnel.

The first exposure was a nominal “smooth flow” condition, where no additional roughness was present on the wind tunnel floor or at the inlet to the test section. This wind tunnel simulation results a relatively “smooth” flow condition with a longitudinal turbulence intensity of 1% at the 300m level of the tower and corresponding to a roughness length of $z_o = 0.0005\text{m}$. The turbulent boundary layer specified above was modelled in the wind tunnel with turbulence generating devices (including a transverse barrier and spires at the inlet and floor roughness elements upwind of the model, which can be seen in Figure 2.1). The corresponding turbulence intensity at the top of the tower with the turbulent boundary layer flow condition was about 10%, corresponding to a roughness length of $z_o = 0.01\text{m}$.

Time histories of the longitudinal component so the wind were measured at various heights and the power spectrum evaluated. Figure 2.16 shows the resulting power spectra with a comparison to the target

spectrum given in equation 2.2, above. There is good agreement between the simulation and the target spectrum.

2.6 Aeroelastic Model Test Procedure

The tests of the aeroelastic models were comprised of taking measurements and records of time histories of all channels for various responses at each wind speed for a selected range of wind speeds. The responses at approximately 30 to 40 wind speeds were examined in each test. The mean, root-mean-square (RMS), maximum and minimum values of all measured bridge responses were obtained in a subsequent analysis of the time histories. A total of 42 channels for the Non-Froude Tower model and 22 channels for the Froude Tower model, were recorded for a scaled time period of between 15 to 30 minutes at each wind speed.

The inherent structural damping of the model as well as nominal target values of 2% of critical and 4% of critical (in the longitudinal direction) were used in the test. Two additional nominal damping levels of 0.6% and 1% (in the longitudinal direction) were also used for the Non-Froude model test. A sample plot of the free vibration response to an impact load and damping estimation for the three fundamental modes of vibration (longitudinal, lateral and torsional) is given in Figure 2.17. The free vibration plots used in determining the damping values are presented in Appendix F. The nominal damping levels indicated in the text, tables and plots in this report refer primarily to the tower longitudinal direction unless otherwise stated.

The responses as presented contain all responses up to 50 Hz in model scale or up to 1.8 ~ 3.5 Hz prototype. Mean and RMS (Root Mean Square) responses are plotted separately in the plots of equivalent prototype response. If the maximum response of the tower is desired, the following principle should be applied.

Peak response is defined as the RMS multiplied by a statistically-based Peak Factor (g) for random vibration (i.e. turbulent buffeting), which can be assumed to be approximately 3.5. Since the peak factor during sinusoidal motion (arising from response to vortex shedding excitation) decreases and approaches a value of $\sqrt{2}$, the use of a constant value of 3.5 for these wind speeds would over-estimate the dynamic response when vortex induced peak occurs. Thus, for the range of wind speeds where the model has shown a large vortex shedding response peak, the actual peak factor calculated from the test for the corresponding wind speed should be used rather than the random response peak factor of 3.5. The total response can then be estimated as the mean response, plus or minus the peak response, as shown below,

$$\begin{aligned} y_{\max} &= \bar{y} + y_{RMS} \times g \\ y_{\min} &= \bar{y} - y_{RMS} \times g \end{aligned} \tag{2.4}$$

where $y_{\max}, y_{\min}$, $\bar{y}$ and y_{RMS} are the maximum, minimum, mean and RMS components of the responses. A generally accepted definition of the flutter instability criteria based on the measured peak factor can be found in Appendix A.

3 NON-FROUDE SCALED AEROELASTIC MODEL STUDY

3.1 General

The Non-Froude Scaled Aeroelastic Model test was performed in the High Speed Test Section of the Boundary Layer Wind Tunnel II. The tests performed are summarized in Tables 3.1 and 3.2 for the construction stage and the in-service condition respectively. The test conditions corresponding to each test, the maximum wind speeds reached, the maximum accelerations and any instability characteristics observed and their associated response directions and wind speeds are summarized in the tables.

The "smooth" flow tests were conducted for wind angles between 0^o (wind perpendicular to the bridge axis) and 10^o in increments of 2.5^o at different damping levels. The turbulent boundary layer flow tests were performed for the inherent damping case, at angles from 0^o and 90^o in increments of 10^o.

Figures 3.1 to 3.6 presents a comparison of tower accelerations at Levels 2 and 3 for different damping levels in smooth flow for wind angles of 0^o, 2.5^o and 10^o. Figures 3.7 and 3.8 present a comparison of tower responses for selected wind angles in turbulent flow under inherent damping. The nominal damping levels indicated in the text, tables and plots refer to that for the longitudinal direction.

A complete set of response plots for all tests performed for the Non-Froude scaled tower is contained in Appendix B for the construction stage configuration and in Appendix C for the in-service condition.

3.2 Construction Stage

Most of the tests conducted for the construction stage configuration reached a mean hourly wind speed at tower height of 50 m/s. Several of the tests performed in turbulent boundary layer flow for wind angles between 0^o and 20^o, were terminated early due to significant buffeting response and resulted in a reduced maximum wind speed of 45 m/s being achieved.

The behaviour of the Non-Froude Tower in the construction stage condition can be summarized as follows.

3.2.1 "Smooth" Flow Test

- Table 3.1 shows that the maximum tower response in the under construction condition in smooth flow for all but one test occurred in the tower torsional direction. The exception was the test with a 2% nominal damping at a wind angle of 10^o in which the maximum tower response was in the lateral direction.

- Vortex shedding peaks were observed in each of the three degrees of freedom for the inherent damping case, at wind angles between 0^o and 10^o in smooth flow, as shown in Figures 3.1 to 3.3. The inherent damping values in the longitudinal and torsional directions were 0.33% and 0.11% respectively.

- The inherent damping in the lateral direction was not measured directly for all test conditions and in some cases was inferred from the time history of lateral response due to impacts in the longitudinal direction. An analysis of the time histories indicated that the lateral structural damping values were generally less than 0.95%. However, since the signal level in the lateral response was extremely small (<5% of that in the longitudinal direction), the reliability of the damping estimate in the lateral direction is in question.

- Vortex shedding peaks for a nominal damping level of 2% in the longitudinal and torsional directions (with measured values of 2.45% and 1.24% respectively) were eliminated up to a wind speed of 50 m/s for wind angles between 0^o and 10^o. The longitudinal and torsional responses are seen to be extremely small for wind speeds less than 50 m/s for nominal damping values of 2% and 4%.

- Small vortex shedding induced response peaks were observed in the tower lateral responses near full scale wind speeds of 40 m/s with a nominal structural damping of 2% and 4%. This is not surprising as the structural damping in the lateral direction was largely unaffected by the additional damping in the longitudinal and torsional directions. The actual damping value in the lateral direction was about 1% for these two tests.

3.2.2 Turbulent Boundary Layer Flow Test

- Table 3.1 shows that for the turbulent boundary layer flow test of the construction stage, the maximum response also occurred in the torsional direction for most wind angles. The only exception is for the tests at wind angles of 80^o and 90^o in which the maximum response was found to occur in the lateral direction.

- Vortex shedding peaks were observed in the responses at wind angles of 0^o, 10^o and 20^o, as shown in Figure 3.7. The largest tower responses in were found to occur in the 20^o wind angle test at mean wind speeds of 46 m/s, where the test was stopped due to large buffeting response. The turbulent buffeting responses of the tower were generally small at wind angles greater than 20^o.

3.3 In-Service Condition

All tests conducted for the in-service condition reached a mean hourly wind speed at the tower height of 80 m/s. Wind speeds between 50 and 63 m/s were omitted for the inherent damping tests in the smooth flow tests, as well as in the turbulent boundary layer flow tests for 0^o and 10^o wind angles due to large tower responses.

The behaviour of the Non-Froude Tower under the in-service condition can be summarized as follows.

3.3.1 "Smooth" Flow Test

- Table 3.2 shows that the maximum tower response in smooth flow occurred in the longitudinal direction for all tests in the inherent damping case, as well as for the 0.6% nominal damping test at a wind angle of 0^o. Tests with nominal structural damping values of 1%, 2% and 4% resulted in maximum tower response in the lateral direction.

- Vortex shedding peaks were found in all three degrees of freedom, for the inherent damping case in all wind angles tested between 0^o and 10^o, as shown in Figures 3.4 to 3.6. The inherent damping values were all less than 0.3% in the three directions. Wind speeds between 50 m/s and 63 m/s were skipped in the test due to large tower responses.

- With a 2% nominal damping in the longitudinal direction, vortex peaks in the longitudinal and torsional directions (with measured damping of 1.93% and 1.44% respectively) were eliminated for all wind speeds in up to at least 80 m/s for wind angles tested between 0^o and 10^o.

- The lateral direction damping was unaffected by the dampers in the longitudinal direction for the 2% nominal damping case. Therefore the vortex peaks observed at 30 m/s and 75 m/s in the lateral direction for wind angles between 0^o and 10^o were about the same amplitude as those observed in the inherent damping result.

- With a 4% nominal damping, the measured damping in the lateral direction was 1.07%. The vortex peak at 30 m/s in the lateral response was eliminated, and the other peak at 75 m/s was also reduced. However the peak at 75 m/s was still significant with accelerations ranging from 1.5 m/s^2 for 0^o wind to about 3 m/s^2 for 10^o wind.

- Under conditions with 4% nominal damping, the longitudinal (3.48% damping) and torsional (~1.35% damping) accelerations in smooth flow for wind angles between 0^o and 10^o were

observed to be less than 0.5 m/s^2 up to a mean wind speed of 80 m/s. However, the lateral acceleration (where the structural damping was only 1.07% of critical) was still much higher than 0.5 m/s^2.

3.3.2 Turbulent Boundary Layer Flow Test

- Table 3.2 shows that for the tests in turbulent boundary layer flow, the maximum tower response at 0^o and 10^o occurred in the longitudinal direction, in the torsional direction for wind angles between 20^o and 60^o and in the lateral direction for wind angles of 70^o, 80^o and 90^o.

- Vortex shedding peaks were observed in the responses for tests at 0^o, 10^o and 20^o, as shown in Figure 3.8. The inherent damping values were all less than 0.3% in the three directions. Wind speeds between 52 m/s and 67 m/s were omitted from the 0^o and 10^o tests due to large tower responses. The turbulent buffeting responses were generally small at increased wind angles (i.e. approaching a longitudinal wind condition).

4 FROUDE SCALED AEROELASTIC MODEL STUDY

4.1 General

The Froude Scaled Aeroelastic Model test was also performed in the High Speed Test Section of the Boundary Layer Wind Tunnel II. The tests performed are summarized in Tables 4.1 and 4.2 for the construction stage and the in-service condition, respectively. The test conditions corresponding to each test, the maximum wind speed reached, the maximum acceleration and any instability characteristics observed are summarized in the tables.

The "smooth" flow tests were conducted for wind angles between 0^o (wind perpendicular to the bridge axis) and 10^o in increments of 2.5^o at different damping levels. The turbulent boundary layer flow tests were performed for the inherent damping case, at angles from 0^o and 90^o in increments of 10^o.

Figures 4.1 to 4.6 show the comparison of tower acceleration at Levels 2 and 3 for different damping levels at wind angles of 0^o, 5 and 10^o. Figures 4.7 and 4.8 show the comparison of tower responses for different wind angles in turbulent flow under inherent damping. The nominal damping levels indicated in the text, tables and plots refer to the tower longitudinal direction.

A complete set of response plots for all tests performed for the Froude scaled tower is contained in Appendix D for the construction stage configuration and in Appendix E for the in-service condition. Note that strain gauges, thus tower bending moments and torques, were not installed for the Froude scaled tower model.

4.2 Construction Stage

All tests conducted for the construction stage configuration reached a mean hourly wind speed at tower height of at least 50 m/s.

The behaviour of the Froude Tower under the construction stage condition can be summarized as follows.

4.2.1 "Smooth" Flow Test

- Table 4.1 shows that the maximum tower response in smooth flow occurred in the torsional direction for all tests.
- Vortex shedding peaks were found in all three degrees of freedom for the inherent damping case for wind angles between 0^o and 10^o in smooth flow, as shown in Figures 4.1 to 4.3. The inherent damping values were about 0.35% in the lateral direction, and less than 0.3% in the longitudinal and torsional directions.
- With 2% nominal damping, the vortex peaks in the longitudinal and torsional directions (with measured structural damping of 1.92% and 1.01% respectively) were eliminated for wind speeds up to 50 m/s for wind angles between 0^o and 10^o. The longitudinal and torsional responses were observed to be very small for wind speeds less than 50 m/s for nominal damping values of 2% and 4%.
- With 2% and 4% nominal damping values, vortex shedding induced response peaks were still present in the lateral responses for wind speeds near 30 m/s for angles of 0^o and 5^o. A second small peak was also visible for these two tests at about 42 m/s. The actual damping value in the lateral direction was about 0.85% for these tests.

4.2.2 Turbulent Boundary Layer Flow Test

- Table 4.1 shows that the maximum response for the construction stage in the turbulent flow tests also occurred in the torsional direction for most wind angles. The only exception was at wind angles of 70^o, 80^o and 90^o in which the largest response was observed in the lateral direction.

- Vortex shedding peaks were observed in the responses for wind angles of 0^o, 10^o and 20^o, as shown in Figure 4.7. The turbulent buffeting responses of the tower were generally small at wind angles approaching the longitudinal direction.

4.3 In-Service Condition

All tests conducted for the in-service condition reached mean hourly wind speeds at the tower height of 80 m/s in both "smooth" and turbulent boundary layer flow. However, tests for a range of wind speeds between 54 and 72 m/s were skipped in the inherent damping tests due to large tower responses.

The behaviour of the Froude scaled aeroelastic model of the tower under the in-service condition can be summarized as follows.

4.3.1 "Smooth" Flow Test

- Table 4.2 shows that the maximum response in smooth flow occurred in the longitudinal direction for all tests in the inherent damping case. This was also the observation for the tests with 2% nominal damping at 10^o. Maximum response was observed in the lateral direction under the remainder of the nominal damping tests at 2% and 4%.

- Vortex shedding peaks were found in all three directions for the inherent damping case for wind angles between 0^o and 10^o in smooth flow, as shown in Figures 4.4 to 4.6. The inherent damping values were about 0.35% in the lateral direction, and less than 0.3% in the longitudinal and torsional directions. Tests for a range of wind speeds between 54 m/s and 72 m/s were skipped due to large tower responses.

- With 2% nominal damping, vortex shedding induced response peaks in the longitudinal and torsional directions (with measured damping of 2.10% and 1.60% respectively) were eliminated for wind speeds up to 80 m/s for wind angles between 0^o and 10^o.

- The measured structural damping in the lateral direction was not affected by the addition of the dampers in the longitudinal and torsional directions. Therefore the vortex shedding response peaks fount at 30 m/s and 75 m/s in the lateral directions for wind angles between 0^o and 10^o were essentially at the same level of amplitude as those observed in the inherent damping test.

- In summary, with a 4% nominal damping (with measured structural damping of 3.95% and 2.06% respectively), the longitudinal and torsional accelerations in smooth flow for wind angles between 0^o and 10^o are less than 0.5 m/s^2 up to mean wind speeds at tower height of 80 m/s. However, the lateral acceleration (with measured structural damping of 0.34% of critical) was much higher than 0.5 m/s^2 for wind speeds over 67 m/s.

4.3.2 Turbulent Boundary Layer Flow Test

- Table 4.2 indicates that for the turbulent flow test, the maximum response occurred in the longitudinal direction at 0^o and 10^o, as well as 30^o. Maximum response occurred in the lateral direction at wind angles of 80^o and 90^o, and in the torsional direction for the remaining wind angles of 20^o, 40^o, 50^o and 60^o.

- Vortex shedding response peaks were observed for wind angles of 0^o, 10^o and 20^o, as shown in Figure 4.8. The inherent damping values were about 0.35% in the lateral direction, and less than 0.3% in the longitudinal and torsional directions. The turbulent buffeting responses of the tower were generally small at wind angles approaching the longitudinal direction.

- Large buffeting responses were observed in the tower lateral direction for wind angles of 0^o and 10^o, as well as in the torsional direction at 20^o.

5 CONCLUDING REMARKS

Tower responses in smooth flow at Level 2 for the Froude scaled and Non-Froude scaled models at 0^o wind are shown for comparative purposes in Figure 5.1. Good agreement between the tests of the two models are observed and thus lend confidence to the test results. All vortex peaks observed in the tests of the two models occurred in the same range of scaled prototype wind speed. The amplitudes of the responses in these peaks are also seen to be comparable. The magnitude of the response in the longitudinal and torsional directions are seen to be consistent with the level of the damping in the test.

Figures 5.2 and 5.3 present a comparison of tower response and the effect of smooth and turbulent flows at Level 2 for the Non-Froude Tower model for 0^o and 10^o wind respectively. The results are presented for the tests with the inherent damping. It can be seen that the turbulent boundary layer flow with $z_o = 0.01$ m is effective in eliminating nearly all of the vortex shedding peaks. The exception to this conclusion was the peak between 50 and 63 m/s, which was omitted in both the smooth and turbulent flow tests due to excessive tower response. Turbulence generally results in a reduction in the magnitude of vortex shedding induced peaks, but increases buffeting responses at higher wind speeds. The turbulent flow test at a 10^o incidence angle in Figure 5.3 was allowed to pass through the omitted wind speeds, which again indicates the effectiveness of turbulence in reducing the magnitude of the vortex peak. It has been observed from the smooth flow tests with 2% and 4% nominal damping levels that the vortex peaks between 50 and 63 m/s can effectively be eliminated with added damping. However, the vortex shedding peak in the lateral response between 70 and 80 m/s is sufficiently strong that additional damping is ineffective in reducing the peak. Figure 3.4 indicated that this peak was still quite significant with lateral structural damping of 1.07%. The fact that the turbulent flow condition used in the current study eliminated this peak completely again proves the effectiveness of turbulence with regard to the tower stability characteristics.

These observations were further confirmed from Figures 5.4 and 5.5, which provides a comparison of the Froude Tower model test results in smooth and turbulent flow conditions.

In general, with a 4% nominal damping, the longitudinal direction (3.48% and 3.95% damping for the non-Froude and Froude scaled model tests, respectively) and torsional direction (~1.35% and 2.07% damping for the non-Froude and Froude scaled model tests, respectively) responses were below 0.5 m/s^2 for mean wind speeds up to about 80 m/s. The lateral response was higher than 0.5 m/s^2 for wind speeds over 70 m/s, however the actual lateral damping was about 1.07% for the Non-Froude tower test.

REFERENCES

1. “Scope of Work, Tower wind tunnel tests, Sub-tests T1, T2 and T3”, 7 May, 2010, COWI, Denmark.
2. “Messina Strait Bridge, Tender Design - Overall Aerodynamic Design Methodology and Plan for Aerodynamic Testing”, Eurolink s.p.c.a., May 2009.
3. BLWTL, May 2007, “Wind Tunnel Testing: A General Outline”, The University of Western Ontario, Boundary Layer Wind Tunnel Laboratory General Outline Report.
4. King, J.P.C., Ho, E. and Davenport, A.G., "A Study of Wind Effects for the Helgelands Bridge, Norway, Cable Stayed Alternate", The University of Western Ontario, Faculty of Engineering Science Research Report, BLWT-SS17-1988, The University of Western Ontario, London, Ontario, Canada, 1988.
5. King, J.P.C., Larose, G.L. and Davenport, A.G., "A Study of Wind Effects for the New Bridge Over Johnston's Bay, Sydney, Australia", The University of Western Ontario, Faculty of Engineering Science Research Report, BLWT-SS11-1990, The University of Western Ontario, London, Ontario, Canada, 1990.
6. King, J.P.C. and Davenport, A.G., "A Study of Wind Effects for the Seo Hae Grand Bridge, Korea”, The University of Western Ontario, Faculty of Engineering Science Research Report, BLWT-SS25-1992, The University of Western Ontario, London, Ontario, Canada, 1992.
7. Davenport, A.G. and King, J.P.C., "A Study of Wind Effects for the Sunshine Skyway Bridge, Tampa, Florida - Concrete Alternate", The University of Western Ontario, Faculty of Engineering Science Research Report, BLWT-SS24-1982, London, Ontario, Canada, 1982.
8. Davenport, A.G. and King, J.P.C., "A Study of Wind Effects for the Sunshine Skyway Bridge, Tampa, Florida - Steel Alternate", The University of Western Ontario, Faculty of Engineering Science Research Report, BLWT-SS25-1982, The University of Western Ontario, London, Ontario, Canada, 1982.
9. Holmes, J.D., “Wind Loading of Structures – First Edition”, Spon Press, New York, NY, 2001.

TABLES

TABLE 2.1 PARAMETERS FOR DESIGN OF THE AEROELASTIC TOWER MODEL

Messina Strait Bridge - Progetto Definitivo

Tower Leg Section Properties

Calculation of torsional constant, J, is approximate, and corresponds to that considering only the closed cell formed by the skin plates (A, B, C, D).

Section	h (m)	El. 1 (m)	El. 2 (m)	Calabria			
				$A\ (m^2)$	$I_Y\ (m^4)$	$I_Z\ (m^4)$	$J\ (m^4)$
1	10	18.25	28.24	9.14	424	140	261
2	12	28.24	40.24	8.60	412	129	234
3	15	40.24	55.23	8.09	386	120	216
4	16	55.23	71.22	7.53	362	110	190
5	16	71.22	87.21	7.03	330	101	165
6	18	87.21	105.20	6.59	292	98	150
7	19	105.20	124.19	6.95	288	110	160
8	19	124.19	143.18	7.41	296	123	181
9	20	143.18	163.17	6.91	280	113	164
10	20	163.17	183.16	6.61	279	102	153
11	20	183.16	203.15	6.58	297	94	144
12	20	203.15	223.13	6.83	305	100	157
13	20	223.13	243.12	7.10	305	108	164
14	20	243.12	263.11	7.28	312	112	171
15	20	263.11	283.10	6.99	321	101	161
16	20	283.10	303.09	6.81	318	96	151
17	20	303.09	323.08	6.57	303	93	147
18	18	323.08	341.07	6.39	284	93	142
19	16.4	341.07	357.46	6.65	278	105	156
20	12.5	357.46	369.95	6.88	280	108	155
21	14.474	369.95	384.42	7.24	298	108	156
			Average	7.15	317	108	170

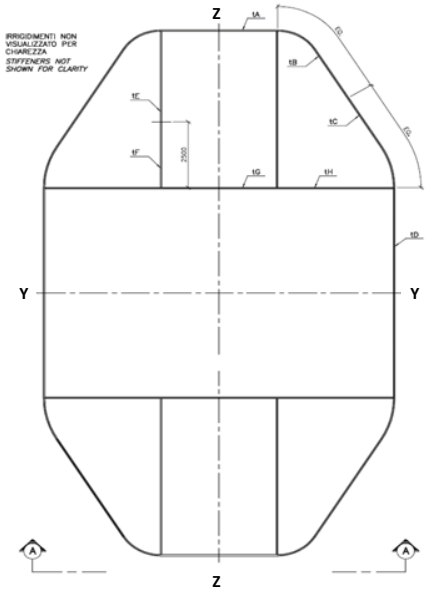

TABLE 2.1(CONT.) PARAMETERS FOR DESIGN OF THE AEROELASTIC TOWER MODEL

Cross Beam Section Properties

Cross Beam 1

Section	Distance from Bridge Centreline (m)	Depth (m)	$A\ (m^2)$	$I_Y\ (m^4)$	$I_Z\ (m^4)$	$J\ (m^4)$
1	-29.531	21.793	2.442	31	150	58
2	-19.685	17.234	2.282	27	93	43
3	-9.842	12.738	2.052	24	48	30
4	0.000	11.500	1.880	21	36	26
5	9.842	12.738	2.052	24	48	30
6	19.685	17.234	2.282	27	93	43
7	29.531	21.793	2.442	31	150	58

Cross Beam 2

Section	Distance from Bridge Centreline (m)	Depth (m)	$A\ (m^2)$	$I_Y\ (m^4)$	$I_Z\ (m^4)$	$J\ (m^4)$
1	-25.136	19.721	2.842	35	143	69
2	-16.755	15.785	2.666	32	91	51
3	-8.378	12.317	2.285	27	48	33
4	0.000	11.500	2.110	25	39	29
5	8.378	12.317	2.285	27	48	33
6	16.755	15.785	2.666	32	91	51
7	25.136	19.721	2.842	35	143	69

Cross Beam 3

Section	Distance from Bridge Centreline (m)	Depth (m)	$A\ (m^2)$	$I_Y\ (m^4)$	$I_Z\ (m^4)$	$J\ (m^4)$
1	-20.742	17.649	2.565	30	109	57
2	-13.826	14.338	2.388	27	74	43
3	-6.913	11.984	2.215	25	46	32
4	0.000	11.500	2.075	23	40	31
5	6.913	11.984	2.215	25	46	32
6	13.826	14.338	2.388	27	74	43
7	20.742	17.649	2.565	30	109	57

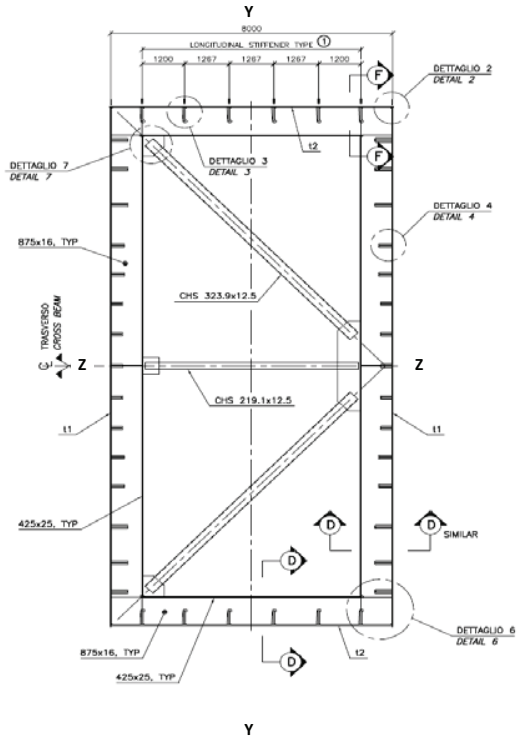

TABLE 2.1(CONT.) PARAMETERS FOR DESIGN OF THE AEROELASTIC TOWER MODEL

Messina Strait Bridge - Progetto Definitivo

Tower Leg Masses (all masses are per leg) - Rev 3

Base weight includes all components other than splices and non-structural equipment.
Total weight includes the base weight and weight of splices and all non-structural elements.
Mass is given in metric tonnes (1000 kg) per metre.

Diaphragms:		0	kN/m	included in base weigh
Splices:	Calabria	47.1	kN/m	
Equipment:		10	kN/m	
Crossbeam Weight:		15843	kN	Total/leg
			kN	
			kN	
	Total	15843	kN	
Spread total crossbeam weight over tower height:		41.6	kN/m	
Saddle weight:		11000	kN	
Spread total saddle weight over tower height:		28.9	kN/m	

				Calabria					
Segment	**h (m)**	**El. 1 (m)**	**El. 2 (m)**	*Base Weight (kN/m)*	*Base Weight plus splices & equip (kN/m)*	*Mass excl Crossbeam & Saddle (t/m)*	*Total Weight (kN/m)*	*Total Mass (t/m)*	*Segment Weight (kN)*
1	10	18.25	28.24	1073	1130	115	1197	122	11965
2	12	28.24	40.24	717	774	79	840	86	10082
3	15	40.24	55.23	675	732	75	799	81	11985
4	16	55.23	71.22	660	717	73	784	80	12537
5	16	71.22	87.21	589	647	66	713	73	11409
6	18	87.21	105.20	557	614	63	681	69	12251
7	19	105.20	124.19	638	695	71	761	78	14462
8	19	124.19	143.18	674	731	75	797	81	15148
9	20	143.18	163.17	578	635	65	702	72	14032
10	20	163.17	183.16	553	610	62	677	69	13539
11	20	183.16	203.15	552	609	62	675	69	13507
12	20	203.15	223.13	570	627	64	694	71	13877
13	20	223.13	243.12	636	693	71	760	77	15197
14	20	243.12	263.11	655	713	73	779	79	15581
15	20	263.11	283.10	584	641	65	708	72	14152
16	20	283.10	303.09	570	627	64	694	71	13873
17	20	303.09	323.08	551	608	62	675	69	13497
18	18	323.08	341.07	541	598	61	665	68	11965
19	16.4	341.07	357.46	559	616	63	683	70	11196
20	12.5	357.46	369.95	639	696	71	762	78	9531
21	14.474	369.95	384.42	678	735	75	801	82	11599
Saddle	14.575	384.42	399.00	504	561	57	628	64	9148
			Average	604	661	67	727	74	
								Total	**280534**

Average weights do not include Segment 1

TABLE 2.2 AEROELASTIC MODEL SCALING PARAMETERS, NON-FROUDE AND FROUDE SCALED AEROELASTIC MODELS

		NON-FROUDE SCALED		FROUDE SCALED
PARAMETER	**SIMILITUDE REQUIREMENT**	**NOMINAL**	**ADJUSTED**	
Length*	$\lambda_L = \mathbf{L}_m / \mathbf{L}_p$	5.000E-03	5.000E-03	5.000E-03
Density	$\lambda\rho = \rho_m / \rho_p$	1.000E+00	1.000E+00	1.000E+00
Velocity**	$\lambda_v = \mathbf{V}_m / \mathbf{V}_p$	1.667E-01	1.389E-01	7.071E-02
Mass per Unit Length	$\lambda_m = \lambda_\rho \lambda_L^2$	2.500E-05	2.500E-05	2.500E-05
Mass	$\lambda_M = \lambda_\rho \lambda_L^3$	1.250E-07	1.250E-07	1.250E-07
Mass Moment of Inertia per Unit Length	$\lambda_i = \lambda_m \lambda_L^2$	6.250E-10	6.250E-10	6.250E-10
Mass Moment of Inertia	$\lambda_I = \lambda_M \lambda_L^2$	3.125E-12	3.125E-12	3.125E-12
Time	$\lambda_T = \mathbf{T}_m / \mathbf{T}_p = \lambda_L / \lambda_V$	3.000E-02	3.600E-02	7.071E-02
Acceleration	$\lambda_a = a_m / a_p = \lambda_v / \lambda_T$	5.556E+00	3.858E+00	1.000E+00
Damping	$\lambda_\zeta = \zeta_m / \zeta_p$	1.000E+00	1.000E+00	1.000E+00
Elastic Stiffness	$\lambda_{EI} = \lambda_{GC} = \lambda_V^2 \lambda_L^4$	1.736E-11	1.206E-11	3.125E-12
	$\lambda_{EA} = \lambda_V^2 \lambda_L^2$	6.944E-07	4.823E-07	1.250E-07
Force per Unit Length	$\lambda_f = \lambda_V^2 \lambda_L = \lambda_L^3 / \lambda_T^2$	1.389E-04	9.645E-05	2.500E-05
Force	$\lambda_F = F_m / F_p = \lambda_V^2 \lambda_L^2$	6.944E-07	4.823E-07	1.250E-07
Bending and Torsional Moment	$\lambda_{BM} = \lambda_V^2 \lambda_L^3$	3.472E-09	2.411E-09	6.250E-10
Warping Stiffness	$\lambda_{CwE} = \lambda_V^2 \lambda_L^6$	4.340E-16	3.014E-16	7.813E-17

* Length Scale 1: 200	1: 200	1: 200
** Velocity Scale 1: 6.00	1: 7.20	1: 14.14

Note: The adjusted velocity scaling of 1:7.2 for the Non-Froude scaled model was utilised for the in-service condition only and was a consequence of the imperfect pinned-end condition formed by the tensioned tie-down cables from the turntable to tower saddle.

TABLE 2.4 NON-FROUDE SCALED AEROELASTIC MODEL DIMENSIONS OF LEG AND CROSSBEAM MEMBERS

MESSINA LEGS

Leg Section #	Z-coord (mm)	b (mm)	d (mm)	bf (mm)	df (mm)	y-bar (mm)	Mass (kg/m
1	91.3	25.2	18.1	4.0	6.5	7.2	2.88
2	141.2	26.4	17.9	4.0	6.7	7.0	1.97
3	201.2	26.1	17.4	4.0	6.5	6.8	1.87
4	276.1	25.7	16.8	4.0	6.5	6.5	1.83
5	356.1	25.0	16.5	4.0	6.5	6.4	1.65
6	436.1	24.1	16.5	4.0	6.5	6.5	1.57
7	526.0	23.2	17.3	4.0	7.0	6.8	1.77
8	620.9	22.6	18.1	4.0	7.5	7.1	1.86
9	715.9	22.4	17.7	4.0	7.3	7.0	1.62
10	815.8	22.5	16.9	4.0	6.9	6.7	1.56
11	915.8	22.8	16.6	4.0	6.7	6.5	1.55
12	1015.7	23.1	16.7	4.0	6.6	6.6	1.60
13	1115.7	23.1	17.2	4.0	6.8	6.8	1.77
14	1215.6	23.5	17.2	4.0	6.7	6.8	1.82
15	1315.6	23.8	16.6	4.0	6.4	6.5	1.63
16	1415.5	24.2	16.2	4.0	6.3	6.4	1.60
17	1515.4	23.9	16.0	4.0	6.2	6.3	1.55
18	1615.4	23.5	16.3	4.0	6.3	6.4	1.52
19	1705.3	22.7	16.7	4.0	6.6	6.6	1.57
20	1787.3	22.6	17.2	4.0	7.0	6.8	1.77
21	1849.8	22.9	17.2	4.0	7.1	6.7	1.87
					average Y-bar	6.7	

MESSINA CROSSBEAMS

TARGET MASS OF CROSSBEAM #1 = 0.1483 kg

MODEL X (mm)	b (mm)	d(mm)	bf(mm)	df (mm)
-147.7	20.60	11.25	4.00	3.85
-123.0	20.60	11.25	4.00	3.85
-73.8	17.50	11.20	4.00	4.25
-24.6	13.90	11.15	4.00	4.55
24.6	12.70	10.85	4.00	4.40
73.8	13.90	11.15	4.00	4.55
123.0	17.50	11.20	4.00	4.25
147.7	20.60	11.25	4.00	3.85

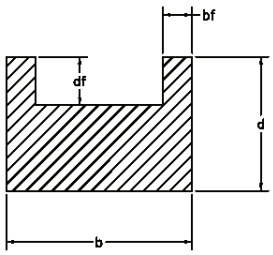

TARGET MASS OF CROSSBEAM #2 = 0.1448 kg

FULL SCALE X (m)	MODEL X (mm)	b (mm)	d(mm)	bf(mm)	df (mm)
	-125.7	19.90	11.85	4.00	3.90
	-104.7	19.90	11.85	4.00	3.90
	-62.8	17.05	11.85	4.00	4.35
	-20.9	13.65	11.70	4.00	4.90
	20.9	12.75	11.45	4.00	4.75
	62.8	13.65	11.70	4.00	4.90
	104.7	17.05	11.85	4.00	4.35
	125.7	19.90	11.15	4.00	4.40

TARGET MASS OF CROSSBEAM #3 = 0.1108 kg

FULL SCALE X (m)	MODEL X (mm)	b (mm)	d(mm)	bf(mm)	df (mm)
	-103.7	18.30	11.40	4.00	3.80
	-86.4	18.30	11.40	4.00	3.80
	-51.8	16.10	11.25	4.00	4.05
	-17.3	13.60	11.45	4.00	4.65
	17.3	13.05	11.15	4.00	4.40
	51.8	13.60	11.45	4.00	4.65
	86.4	16.10	11.25	4.00	4.05
	103.7	18.30	11.40	4.00	3.80

TABLE 2.5 FROUDE SCALED AEROELASTIC MODEL DIMENSIONS OF LEG AND CROSSBEAM MEMBERS

MESSINA LEGS

Leg Section #	From Z-cc	b (mm)	d (mm)	bf (mm)	df (mm)	y-bar (mm	Mass (kg/m)
1	91.3	16.4	11.2	3.5	3.7	4.7	2.88
2	141.2	17.2	11.1	3.5	3.9	4.6	1.97
3	201.2	16.9	10.8	3.5	3.8	4.5	1.87
4	276.1	16.7	10.4	3.5	3.7	4.3	1.83
5	356.1	16.2	10.2	3.5	3.7	4.3	1.65
6	436.1	15.7	10.2	3.5	3.8	4.3	1.57
7	526.0	15.1	10.7	3.5	4.1	4.5	1.77
8	620.9	14.7	11.1	3.5	4.3	4.7	1.86
9	715.9	14.5	10.9	3.5	4.2	4.6	1.62
10	815.8	14.6	10.5	3.5	4.1	4.4	1.56
11	915.8	14.8	10.2	3.5	3.8	4.3	1.55
12	1015.7	15.0	10.3	3.5	3.8	4.4	1.60
13	1115.7	15.0	10.6	3.5	3.9	4.5	1.77
14	1215.6	15.3	10.6	3.5	3.8	4.5	1.82
15	1315.6	15.5	10.2	3.5	3.6	4.3	1.63
16	1415.5	15.7	10.0	3.5	3.6	4.2	1.60
17	1515.4	15.5	9.9	3.5	3.6	4.2	1.55
18	1615.4	15.3	10.1	3.5	3.7	4.3	1.52
19	1705.3	14.8	10.3	3.5	3.8	4.4	1.57
20	1787.3	14.7	10.6	3.5	4.1	4.5	1.77
21	1849.8	14.9	10.6	3.5	4.1	4.5	1.87
				average Y-bar		4.4	

MESSINA CROSSBEAMS

TARGET MASS OF CROSSBEAM # 0.1483 kg

FULL SCALE MODEL

X (mm)	b (mm)	d(mm)	bf(mm)	df (mm)	y-bar (mm)
-147.7	13.45	7.15	3.00	2.40	3.03258
-123.0	11.40	7.15	3.00	2.70	3.09031
-73.8	9.05	7.10	3.00	2.90	3.21478
-24.6	8.30	6.90	3.00	2.85	3.18827
24.6	9.05	7.10	3.00	2.90	3.21478
73.8	11.40	7.15	3.00	2.70	3.09031
123.0	13.45	7.15	3.00	2.40	3.03258
147.7	13.45	7.15	3.00	2.40	3.03258

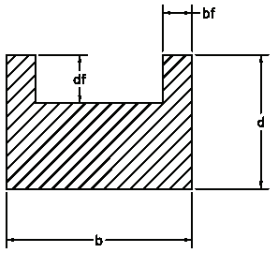

TARGET MASS OF CROSSBEAM # 0.1448 kg

FULL SCALE MODEL

X (m)	X (mm)	b (mm)	d(mm)	bf(mm)	df (mm)	y-bar (mm)
	-125.7	12.95	7.60	2.85	2.45	3.23293
	-104.7	11.10	7.60	2.85	2.75	3.28193
	-62.8	8.90	7.50	2.85	3.10	3.36598
	-20.9	8.35	7.30	2.85	3.00	3.32753
	20.9	8.90	7.50	2.85	3.10	3.36598
	62.8	11.10	7.60	2.85	2.75	3.28193
	104.7	12.95	7.15	2.85	2.80	3.23293
	125.7	12.95	7.15	2.85	2.80	3.23293

TARGET MASS OF CROSSBEAM # 0.1108 kg

FULL SCALE MODEL

X (m)	X (mm)	b (mm)	d(mm)	bf(mm)	df (mm)	y-bar (mm)
	-103.7	11.95	7.35	2.85	2.45	3.15769
	-86.4	10.45	7.25	2.85	2.60	3.17219
	-51.8	8.90	7.30	2.85	2.90	3.2834
	-17.3	8.50	7.15	2.85	2.80	3.25287
	17.3	8.90	7.30	2.85	2.90	3.2834
	51.8	10.45	7.25	2.85	2.60	3.17219
	86.4	11.95	7.35	2.85	2.45	3.15769
	103.7	11.95	7.35	2.85	2.45	3.15769

TABLE 2.4 INSTRUMENTATION LOCATIONS, NON-FROUDE SCALED MODEL

Instrumentation	Instrumentation Locations
Strain Gauges (Tower Legs):	
M_x, M_y and $M_{Z,}$, Base of Leg A	Bending moments measured on Leg A at ??? m above Leg A base (or ground??)
M_x and M_y, Level 1 of Leg A	Bending moments measured on Leg A, ??? m above ???
M_x and M_y, Level 2 of Leg A	Bending moments measured on Leg A, ??? m above ???
M_x, M_y and $M_{Z,}$, Base of Leg B	Bending moments measured on Leg B at ??? m above Leg B base (or ground??)
M_x and M_y, Level 1 of Leg B	Bending moments measured on Leg B, ??? m above ???
M_x and M_y, Level 2 of Leg B	Bending moments measured on Leg B, ??? m above ???
Strain Gauges (X-Beams):	
M_z and M_x, Level 1	Bending moments measured on X-beam, ??? m from Mid location towards to Leg A
M_z and M_x, Level 2	Bending moments measured on X-beam, ??? m from Mid location towards to Leg A
M_z and M_x, Level 3	Bending moments measured on X-beam, ??? m from Mid location towards to Leg A
Accelerometers:	
x, y and Torsional accelerations, Level 2	Accelerations measured at 246.4 m above ground
x, y and Torsional accelerations, Level 3	Accelerations measured at 373.4 m above ground
Lasers (January 2011 Test only):	
x displacement and rotation, Level 2	Tower displacement along bridge axis and tower rotation measured at 238.7 m above ground
Wind Speeds:	
Deck Height	At a height of 66 m full scale above ground
Tower Height	At a height of 399 m full scale above ground
Mid Tower Height	At a height of 199 m full scale above ground
Reference Height	Where the wind speed not affected by the boundary layer of the wind tunnel floor

Notes:

1. Right-hand rule used for sign convention.
2. x – along bridge axis; y – perpendicular to bridge axis (lateral to tower)

TABLE 2.5 INSTRUMENTATION LOCATIONS, FROUDE SCALED MODEL

Instrumentation	Instrumentation Locations
Accelerometers:	
x, y and Torsional accelerations, Level 1	Accelerations measured at 119.4 m above ground
x, y and Torsional accelerations, Level 2	Accelerations measured at 243.8 m above ground
x, y and Torsional accelerations, Level 3	Accelerations measured at 370.8 m above ground
Laser Deflection Transducers:	
x displacement and Rotation θ, Level 2	Displacements measured at 238.7 m above ground
Wind Speeds:	
Deck Height	At a height of 66 m full scale above ground
Tower Height	At a height of 399 m full scale above ground
Mid Tower Height	At a height of 199 m full scale above ground
Reference Height	Where the wind speed not affected by the boundary layer of the wind tunnel floor

Notes:
1. Right-hand rule used for sign convention.
2. x – along bridge axis; y – perpendicular to bridge axis (lateral to tower)

TABLE 3.1 SUMMARY OF NON-FROUDE SCALED MODEL TESTS, CONSTRUCTION STAGE

Test Configuration	Test No.	Test Files	Modal Frequency (Hz) and Damping (%)			Wind Angle	Maximum Wind Speed	Level 3 Maximum Acceleration Observed		
			Long.	Lat.	Tor.	Deg	m/s	m/s^2	Direction occurred	Wind speed (m/s)
Smooth flow, inherent damping	1	M075a1E01R002	4.1 (0.33~0.35)	10.02 (1.10~1.17)	12.26 (0.10~0.11)	0 (Lat.)	51	6.759	Tor	31
	2	M075a1E01R003				2.5	51	7.481	Tor	30
	3	M075a1E01R004				5	51	7.831	Tor	31
	4	M075a1E01R005				7.5	51	8.611	Tor	33
	5	M075a1E01R006				10	50	9.312	Tor	33
Smooth flow, 2% nominal damping	6	M075a2E01R002	4.1 (2.45~2.51)	10 (0.91~0.96)	11.93 (1.24~1.34)	0 (Lat.)	55	6.357	Tor	55
	7	M075a2E01R003				2.5	55	6.371	Tor	55
	8	M075a2E01R004				10	55	0.496	Lat	40
Smooth flow, 4% nominal damping	9	M075a3E01R002	4.1 (3.77~3.81)	10 (0.96~1.08)	12.03 (1.73~1.81)	0 (Lat.)	53	0.612	Tor	53
	10	M075a3E01R003				2.5	52	0.600	Tor	52
	11	M075a3E01R004				10	52	0.216	Tor	52
Turbulent boundary layer flow, inherent damping	12	M075a4E02R002	4.1 (0.33~0.35)	10.02 (1.10~1.17)	12.26 (0.10~0.11)	0 (Lat.)	49	4.186	Tor	29
	13	M075a4E02R003				2.5	48	4.480	Tor	29
	14	M075a4E02R004				5	48	5.216	Tor	29
	15	M075a4E02R005				7.5	46	6.804	Tor	31
	16	M075a4E02R006				10	46	7.586	Tor	33
	17	M075a4E02R015				20	46	20.243	Tor	46
	18	M075a4E02R022				30	50	6.180	Tor	47
	19	M075a4E02R023				40	50	0.673	Tor	45
	20	M075a4E02R024				50	50	0.473	Tor	40
	21	M075a4E02R025				60	49	0.505	Tor	40
	22	M075a4E02R026				70	50	0.331	Tor	50
	23	M075a4E02R027				80	50	0.478	Lat	50
	24	M075a4E02R028				90 (Long.)	50	0.517	Lat	50

Notes:

1. Maximum wind speed is the equivalent hourly mean wind speed at the top of the tower using a velocity scale of 1:6.
2. Long. = Longitudinal direction (along deck), Lat. = Transverse direction with respect to the axis of the bridge deck

TABLE 3.2 SUMMARY OF NON-FROUDE SCALED MODEL TESTS, IN SERVICE

Test Configuration	Test No.	Test Files (January 2011)	Modal Frequency (Hz) and Damping (%)			Wind Angle	Maximum Wind Speed	Level 2 Maximum Acceleration Observed		
			Long.	Lat.	Tor.	Deg	m/s	m/s^2	Direction occurred	Wind speed (m/s)
Smooth flow, inherent damping	1	M075b1E01R013 M075b1E01R036	12.95 (0.29~ 0.30)	10.10 (0.23~ 0.26)	17.99 (0.17~ 0.18)	0 (Lat.)	85	6.403	Long	50
	2	M075b1E01R014 M075b1E01R037				2.5	89	6.471	Long	50
	3	M075b1E01R015 M075b1E01R038				5	89	7.129	Long	52
	4	M075b1E01R016 M075b1E01R039				7.5	89	6.213	Long	52
	5	M075b1E01R017 M075b1E01R040				10	89	6.474	Long	54
Smooth, 0.6%	6	M075b5E01R002	12.81 (0.62~ 0.63)	10.03 (0.17~ 0.19)	17.53 (0.38~ 0.43)	0 (Lat.)	89	3.185	Long	54
Smooth flow, 1% nominal damping	7	M075b6E01R004	12.9 (1.06~ 1.08)	10.01 (0.29~ 0.34)	17.64 (0.99~ 1.10)	0 (Lat.)	89	2.295	Lat	73
	8	M075b6E01R005				2.5	89	2.423	Lat	76
	9	M075b6E01R006				5	89	3.930	Lat	76
	10	M075b6E01R007				7.5	89	4.805	Lat	76
	11	M075b6E01R008				10	89	4.289	Lat	76
Smooth flow, 2% nominal damping	12	M075b7E01R002	12.9 (1.90~ 1.93)	9.97 (0.27~ 0.33)	16.8 (1.32~ 1.66)	0 (Lat.)	85	2.687	Lat	75
	13	M075b7E01R003				2.5	88	2.374	Lat	75
	14	M075b7E01R004				5	88	4.086	Lat	75
	15	M075b7E01R005				7.5	88	4.500	Lat	75
	16	M075b7E01R006				10	88	4.181	Lat	75
Smooth flow, 4% nominal damping	17	M075b3E01R002	13.21 (3.45~ 3.64)	9.83 (1.07~ 1.12)	17.0 (1.26~ 1.40)	0 (Lat.)	79	1.418	Lat	76
	18	M075b3E01R003				2.5	79	1.138	Lat	76
	19	M075b3E01R004				10	79	3.050	Lat	79
Turbulent boundary layer flow, inherent damping	20	M075b4E02R002 M075b4E02R014	12.95 (0.29~ 0.30)	10.10 (0.23~ 0.26)	17.99 (0.17~ 0.18)	0 (Lat.)	86	5.650	Long	52
	21	M075b2E02R003 M075b2E02R018				10	84	5.250	Long	54
	22	M075b4E02R004				20	82	6.886	Tor	81
	23	M075b4E02R005				30	86	2.151	Tor	85
	24	M075b4E02R006				40	87	1.035	Tor	79
	25	M075b4E02R007				50	87	0.573	Tor	73
	26	M075b4E02R008				60	87	0.697	Tor	76
	27	M075b4E02R009				70	87	0.734	Lat	83
	28	M075b4E02R010				80	87	0.739	Lat	87
	29	M075b4E02R011				90 (Long.)	87	0.685	Lat	87

Notes:

1. Maximum wind speed is the equivalent hourly mean wind speed at the top of the tower using a velocity scale of 1:7.20, based on the longitudinal direction frequency scaling.
2. Long. = Longitudinal direction (along deck), Lat. = Transverse direction with respect to the axis of the bridge deck
3. Tests between 50 m/s and 63 m/s were skipped due to large tower responses for the inherent damping tests in smooth flow as well as Test No. 20 & 21 in turbulent boundary layer flow.

TABLE 4.1 SUMMARY OF FROUDE SCALED MODEL TESTS, CONSTRUCTION STAGE

Test Configuration	Test No.	Test Files	Modal Frequency (Hz) and Damping (%)			Wind Angle	Maximum Wind Speed	Level 3 Maximum Acceleration Observed		
			Long.	Lat.	Tor.	Deg	m/s	m/s^2	Direction occurred	Wind speed (m/s)
Smooth flow, inherent damping	1	M075c1E01R002	1.72 (0.16~ 0.20)	4.73 (1.21~ 1.27)	5.46 (0.08~ 0.09)	0 (Lat.)	58	7.896	Tor	34
	2	M075c1E01R003				2.5	58	8.074	Tor	36
	3	M075c1E01R009				5	58	8.659	Tor	37
	4	M075c1E01R010				7.5	58	12.629	Tor	36
	5	M075c1E01R004				10	58	12.569	Tor	36
Smooth flow, 2% nominal damping	6	M075c2E01R002	1.71 (1.90~ 1.92)	4.78 (1.25~ 1.30)	5.4 (0.97~ 1.03)	0 (Lat.)	57	3.126	Tor	57
	7	M075c2E01R003				5	57	3.384	Tor	57
	8	M075c2E01R004				10	57	0.473	Tor	57
Smooth flow, 4% nominal damping	9	M075c3E01R009	1.72 (3.98~ 3.99)	4.78 (1.24~ 1.27)	5.4 (2.14~ 2.18)	0 (Lat.)	58	1.290	Tor	58
	10	M075c3E01R010				5	57	1.487	Tor	57
	11	M075c3E01R011				10	57	0.480	Tor	57
Turbulent boundary layer flow, inherent damping	12	M075c4E02R002	1.72 (0.16~ 0.20)	4.73 (1.21~ 1.27)	5.46 (0.08~ 0.09)	0 (Lat.)	54	8.006	Tor	36
	13	M075c4E02R003				10	55	10.461	Tor	55
	14	M075c4E02R004				20	54	12.603	Tor	54
	15	M075c4E02R005				30	54	11.550	Tor	48
	16	M075c4E02R006				40	54	2.965	Tor	48
	17	M075c4E02R007				50	55	2.004	Tor	46
	18	M075c4E02R008				60	53	2.113	Tor	44
	19	M075c4E02R009				70	54	0.594	Lat	54
	20	M075c4E02R010				80	55	0.660	Lat	51
	21	M075c4E02R011				90 (Long.)	55	0.567	Lat	55

Notes:

b) Maximum wind speed is the equivalent hourly mean wind speed at the top of the tower using a velocity scale of 1:14.14.

c) Long. = Longitudinal direction (along deck), Lat. = Transverse direction with respect to the axis of the bridge deck

TABLE 4.2 SUMMARY OF FROUDE SCALED MODEL TESTS, IN SERVICE

Test Configuration	Test No.	Test Files	Modal Frequency (Hz) and Damping (%)			Wind Angle	Maximum Wind Speed	Level 2 Maximum Acceleration Observed		
			Long.	Lat.	Tor.	Deg	m/s	m/s^2	Direction occurred	Wind speed (m/s)
Smooth flow, inherent damping[3.]	1	M075d1E01R002	6.7 (0.17~ 0.18)	4.67 (0.34~ 0.35)	9.25 (0.14~ 0.16)	0 (Lat.)	81	7.938	long	53
	2	M075d1E01R003				2.5	81	8.157	long	53
	3	M075d1E01R004				5	81	8.193	long	53
	4	M075d1E01R005				7.5	81	7.441	long	53
	5	M075d1E01R006				10	81	6.418	long	53
Smooth flow, 2% nominal damping	6	M075d2E01R002	6.7 (2.07~ 2.12)	4.64 (0.30~ 0.32)	9.10 (1.58~ 1.66)	0 (Lat.)	82	2.181	Lat	77
	7	M075d2E01R003				5	82	1.637	Lat	77
	8	M075d2E01R004				10	82	0.949	Long	79
Smooth flow, 4% nominal damping	9	M075d3E01R002	6.97 (3.92~ 3.97)	4.64 (0.30~0 .34)	9.3 (2.06~ 2.08)	0 (Lat.)	82	2.126	Lat	77
	10	M075d3E01R003				5	82	1.759	Lat	77
	11	M075d3E01R004				10	82	0.898	Lat	77
Turbulent boundary layer flow, inherent damping	12	M075d4E02R002	6.7 (0.17~ 0.18)	4.67 (0.34~ 0.35)	9.25 (0.14~ 0.16)	0 (Lat.)	79	32.694	long	64
	13	M075d4E02R003				10	79	32.443	long	64
	14	M075d4E02R004				20	79	15.481	Tor	79
	15	M075d4E02R005				30	79	9.098	long	51
	16	M075d4E02R006				40	79	2.584	Tor	79
	17	M075d4E02R007				50	78	1.981	Tor	67
	18	M075d4E02R008				60	79	1.877	Tor	70
	19	M075d4E02R009				70	79	0.851	Tor	72
	20	M075d4E02R010				80	79	0.838	Lat	79
	21	M075d4E02R011				90 (Long.)	79	0.675	Lat	76

Notes:

1. Maximum wind speed is the equivalent hourly mean wind speed at the top of the tower using a velocity scale of 1:14.14.
2. Long. = Longitudinal direction (along deck), Lat. = Transverse direction with respect to the axis of the bridge deck
3. Tests between 54 m/s and 72 m/s were skipped due to large tower responses for the inherent damping tests in smooth flow.

FIGURES

FIGURE 1.1 SITE OF THE MESSINA BRIDGE

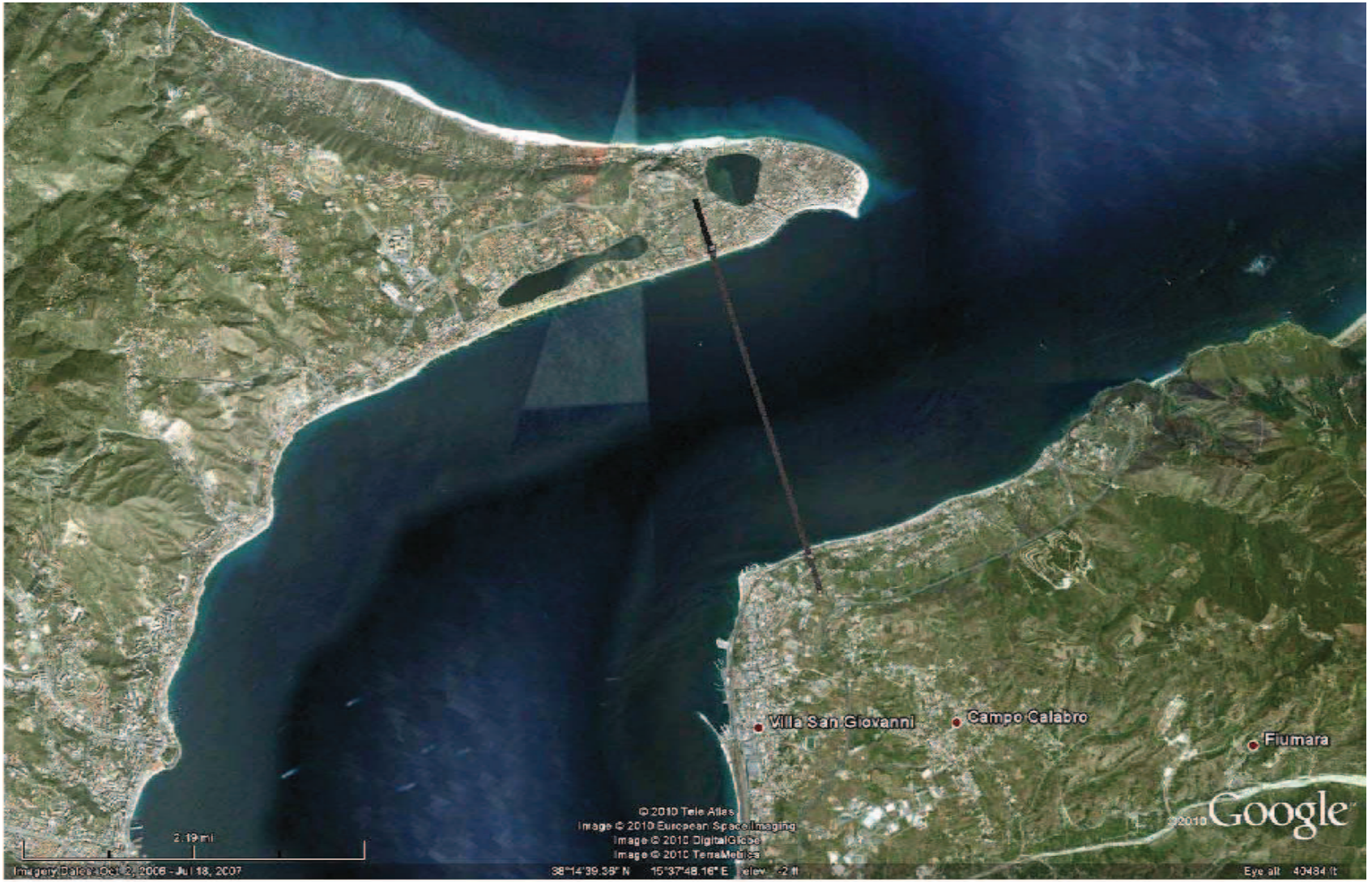

FIGURE 1.1 (CONT.) SITE OF THE MESSINA BRIDGE

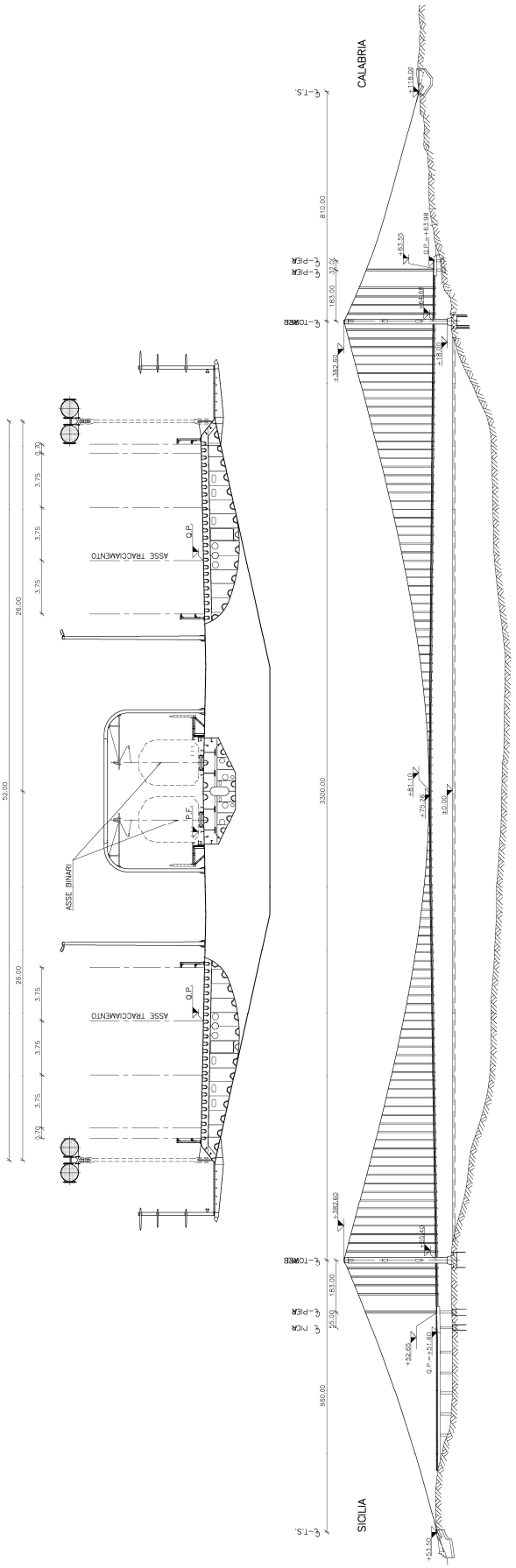

FIGURE 1.2 PROTOTYPE DIMENSIONS OF THE MESSINA BRIDGE

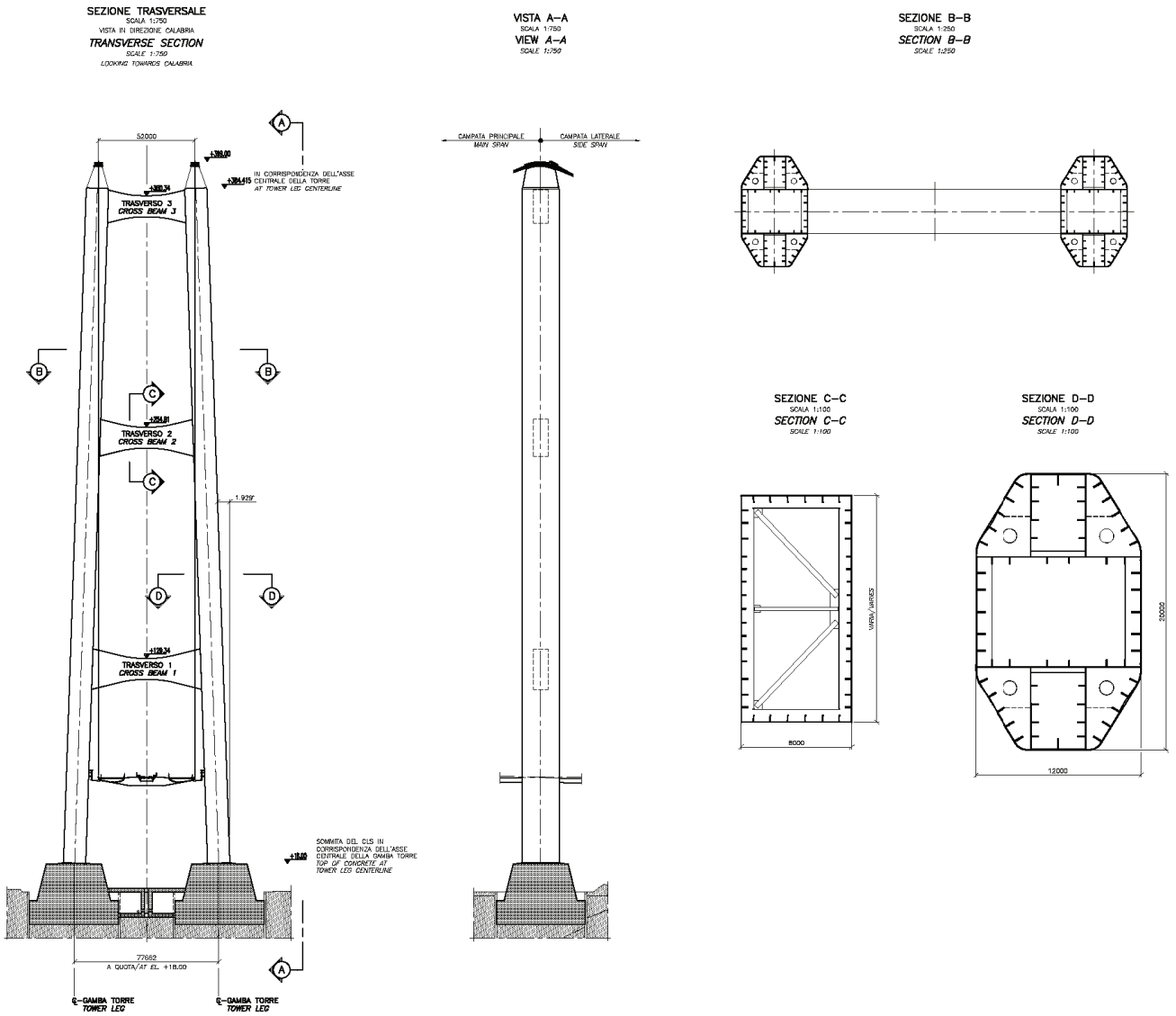

FIGURE 1.3 PROTOTYPE DIMENSIONS OF TOWER

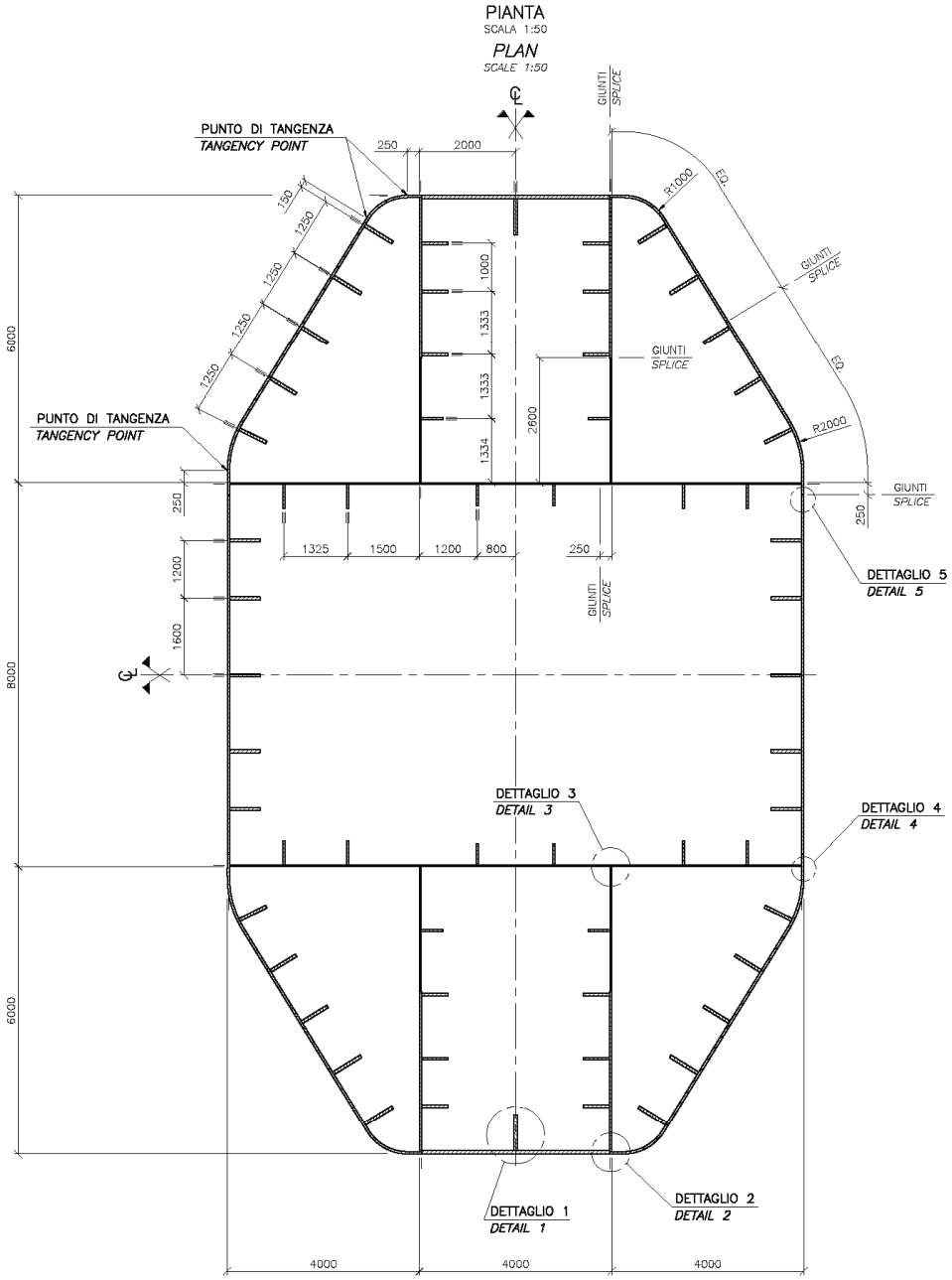

FIGURE 1.4 PROTOTYPE DIMENSIONS OF TOWER LEG

NOTE:

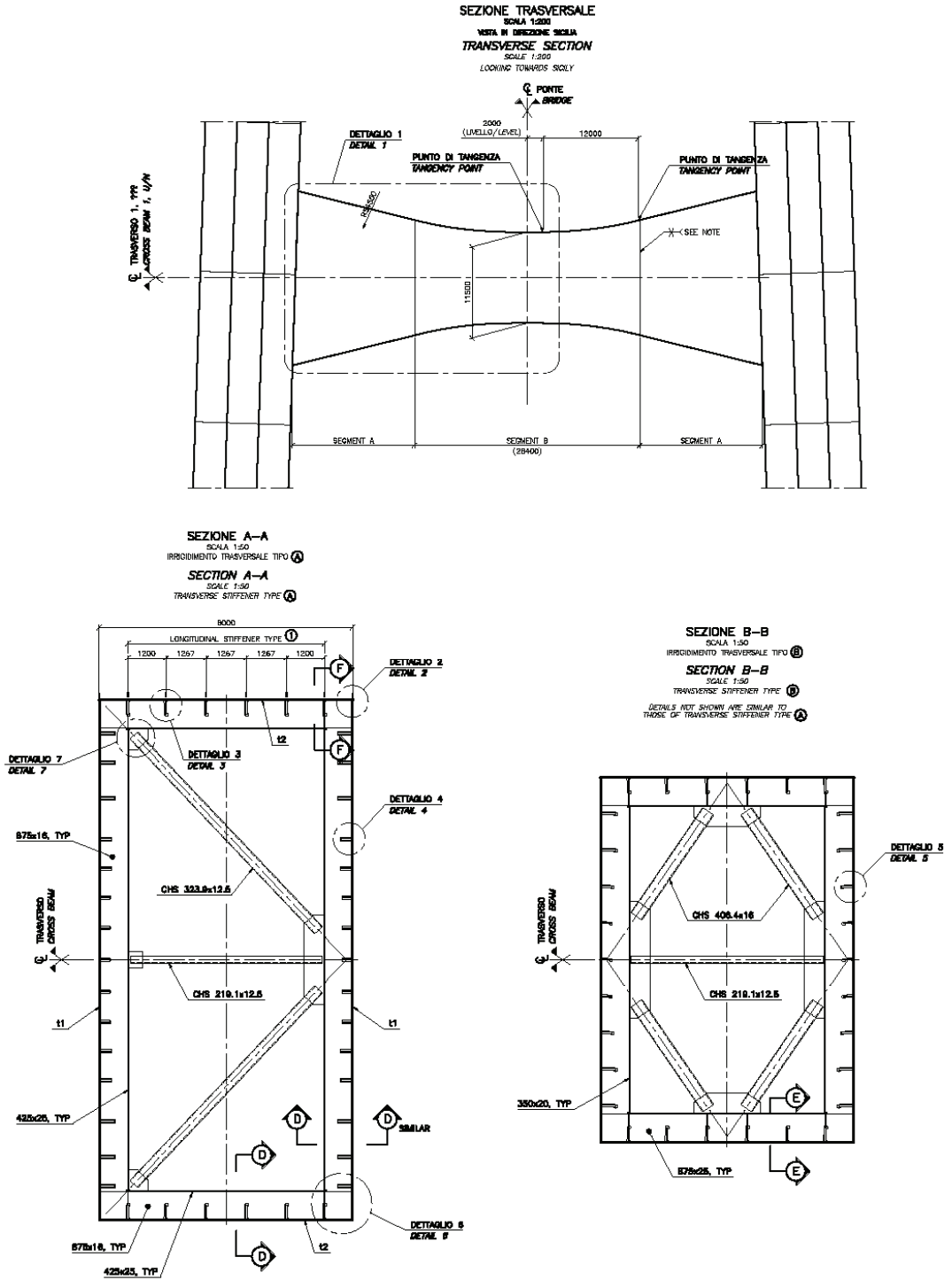

NOTE: CB1 Shown in Figure, maximum vertical dimension of Segment A varies between CB1, CB2, CB3

FIGURE 1.5 PROTOTYPE DIMENSIONS OF CROSS BEAM

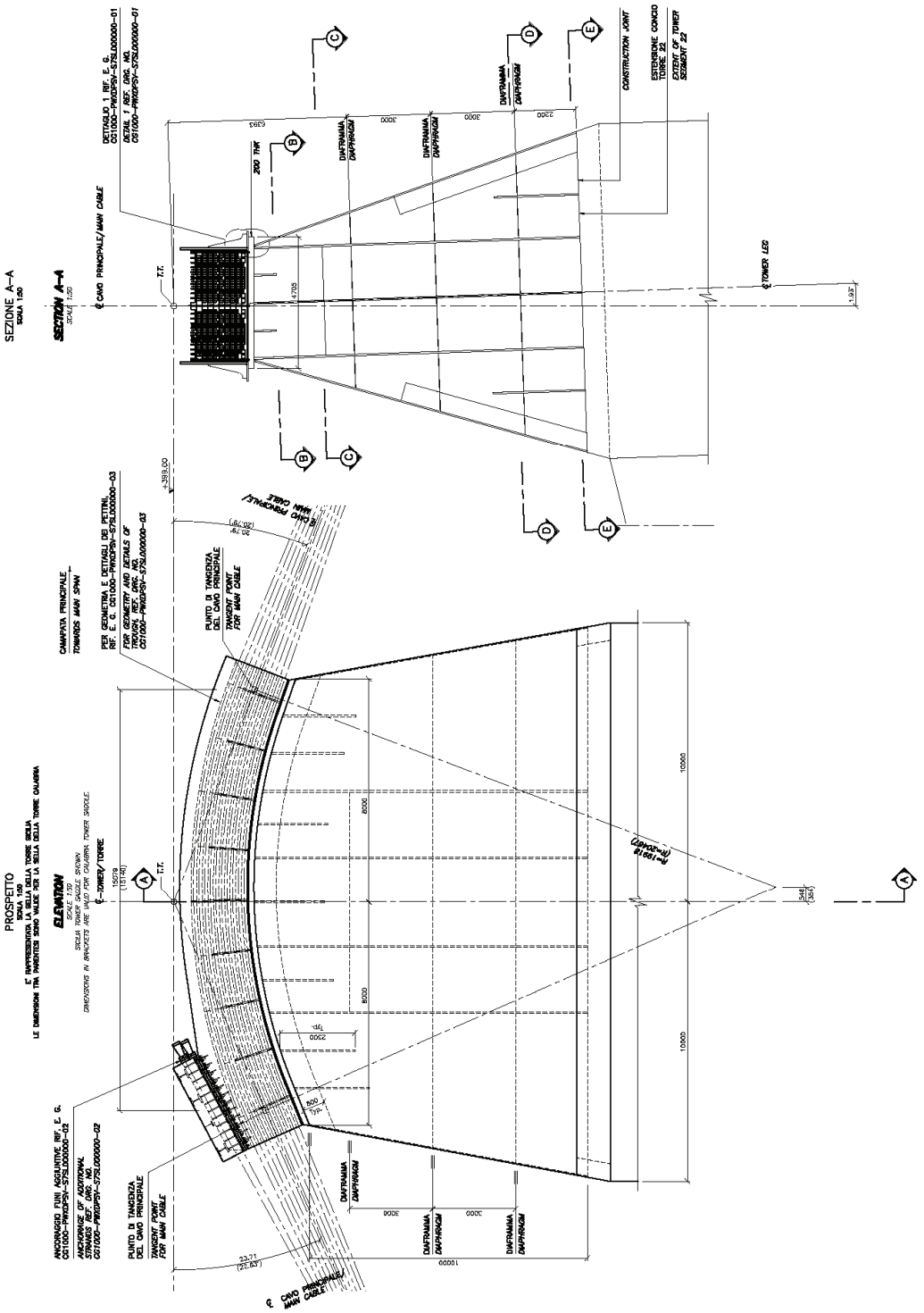

FIGURE 1.6 PROTOTYPE DIMENSIONS OF TOWER SADDLE

a) “Smooth” Flow

b) Turbulent Boundary Layer Flow

FIGURE 2.1 FULL AEROELASTIC MODEL IN THE WIND TUNNEL SHOWING THE UPSTREAM TERRAIN MODELS

a) In-service condition

b) Free-standing Construction Stage

FIGURE 2.2 TWO TEST CONFIGURATIONS OF AEROELASTIC MODEL

FIGURE 2.3 NON-FROUDE SCALED AEROELASTIC MODEL, CONFIGURATION AND INSTRUMENTATION

a) View of Level 3

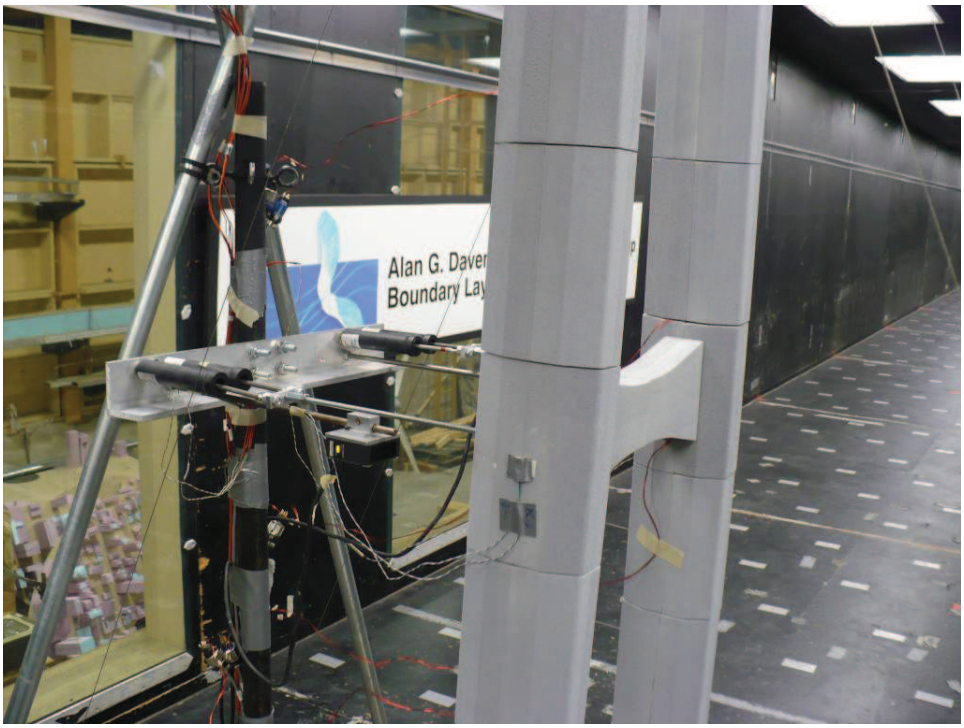

b) View of Level 2

FIGURE 2.4 DETAILS OF NON-FROUDE SCALED AEROELASTIC MODEL

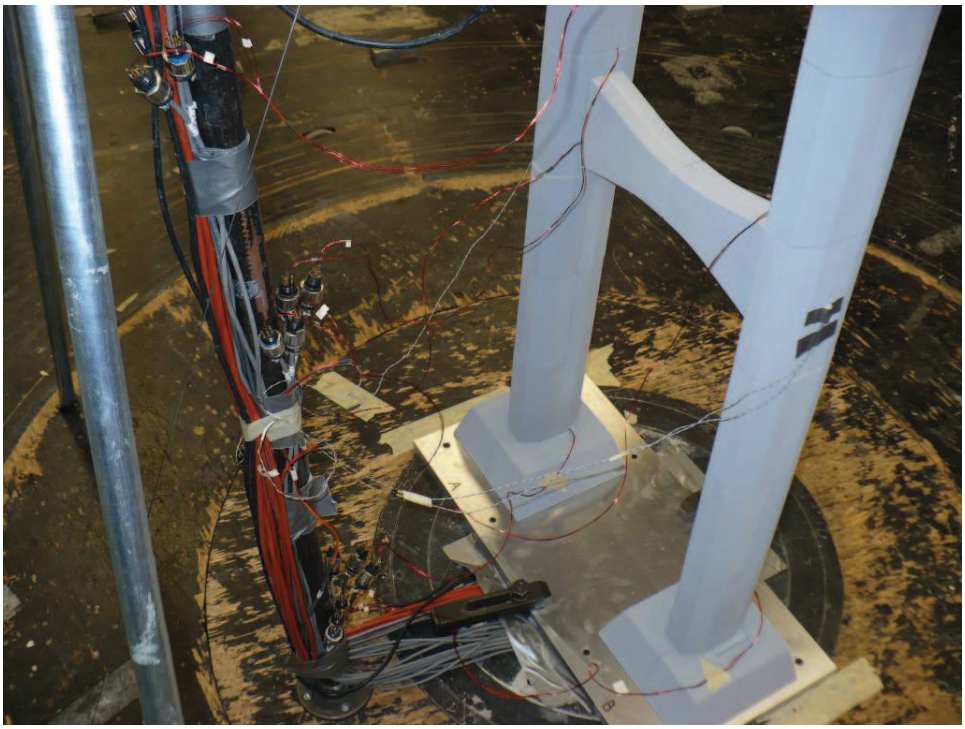

c) View of Base and Level 1

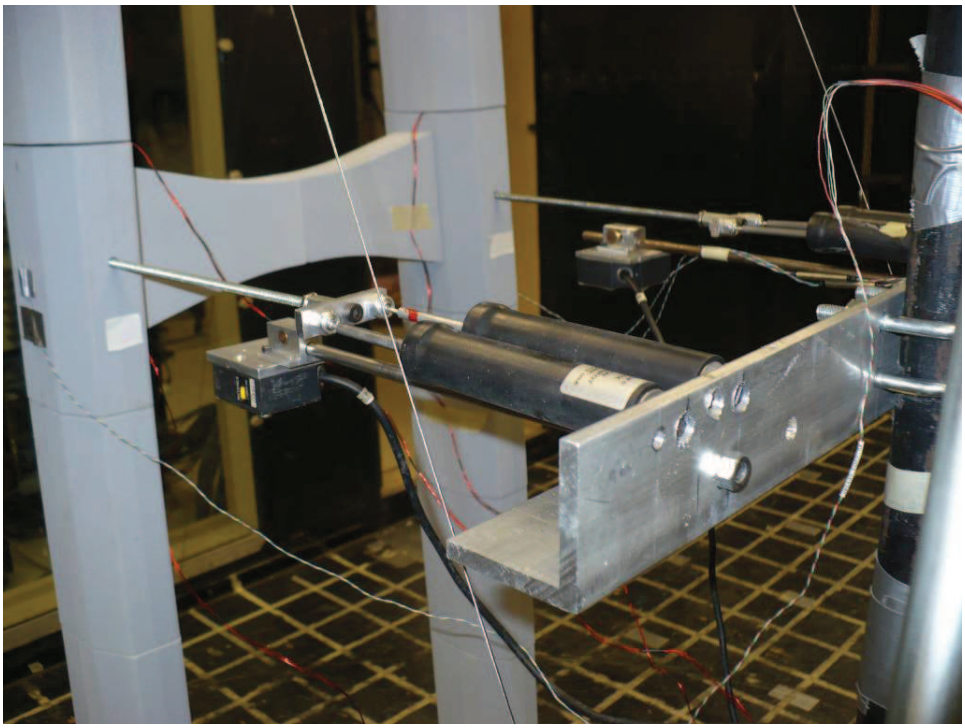

d) View of Pneumatic Dampers at Level 2

FIGURE 2.4 (CONT.) DETAILS OF NON-FROUDE SCALED AEROELASTIC MODEL

FIGURE 2.5 FROUDE SCALED AEROELASTIC MODEL, CONFIGURATION AND INSTRUMENTATION

a) View of Level 3

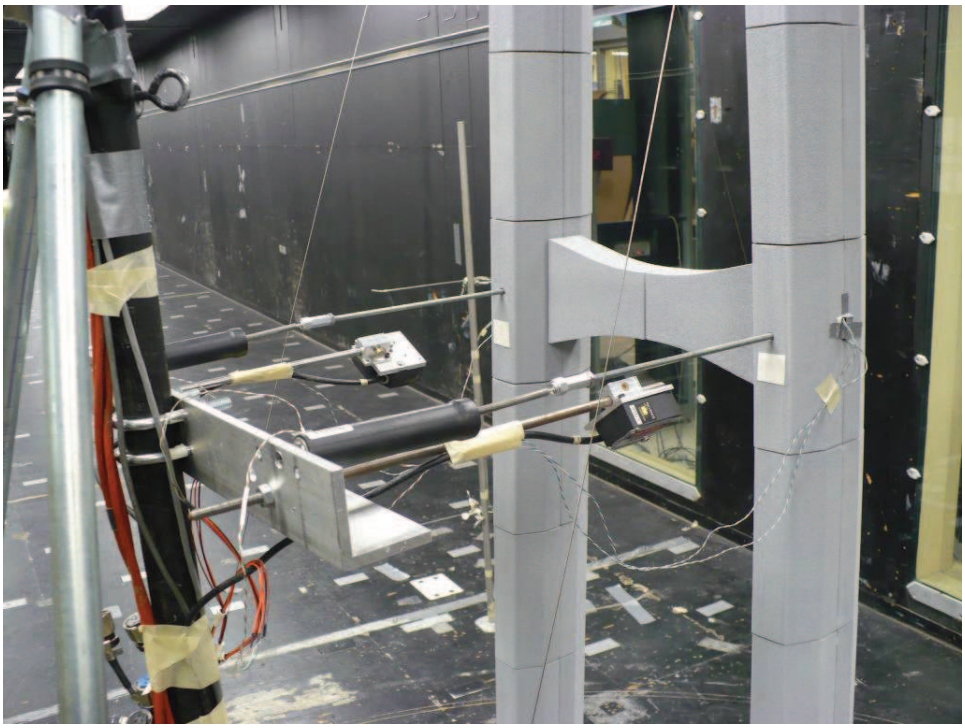

b) View of Level 2

FIGURE 2.6 DETAILS OF FROUDE SCALED AEROELASTIC MODEL

c) View of Base and Level 1

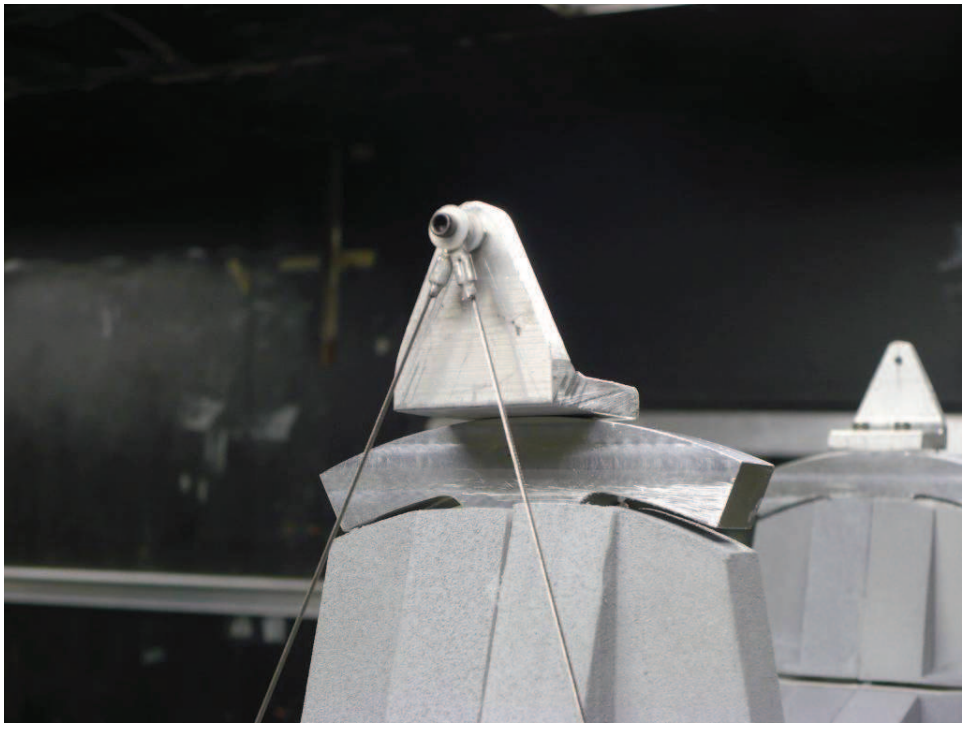

d) View of Cable Tie at Saddle

FIGURE 2.6 (CONT.) DETAILS OF FROUDE AEROELASTIC MODEL

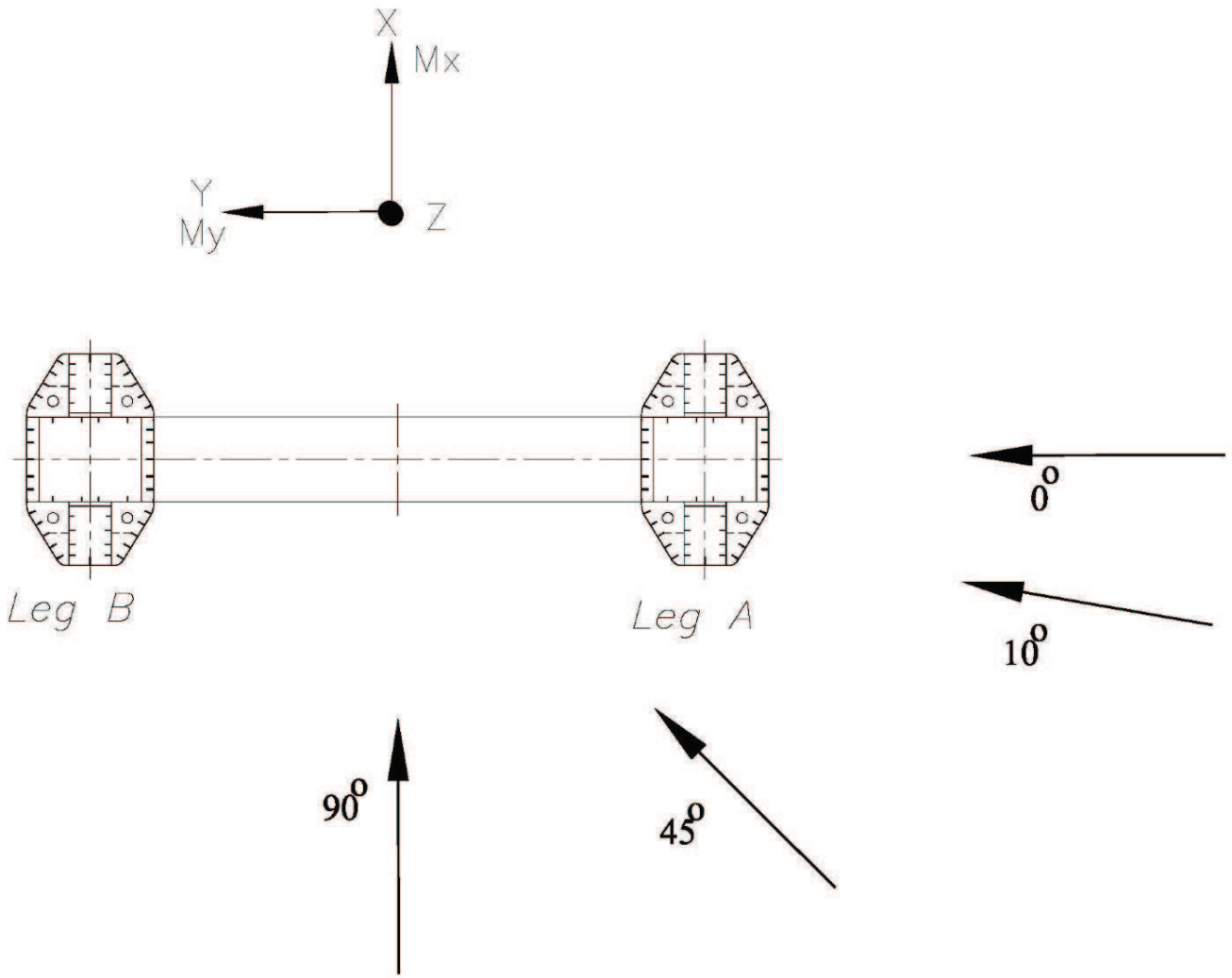

FIGURE 2.7 DEFINITION OF WIND ANGLES USED IN THE MESSINA TOWER TEST

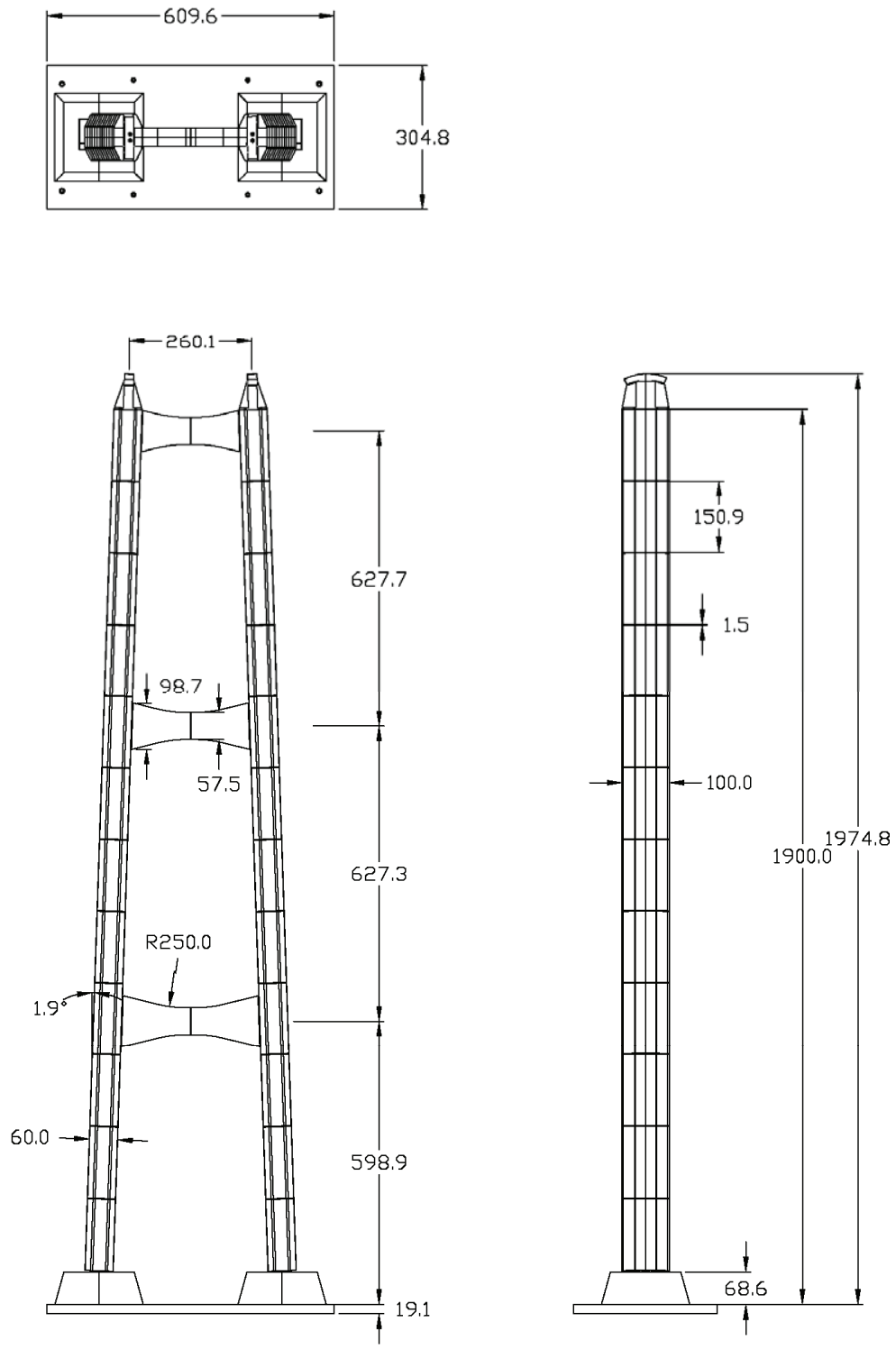

FIGURE 2.8 1:200 SCALE AEROELASTIC MODEL – BASIC DIMENSIONS

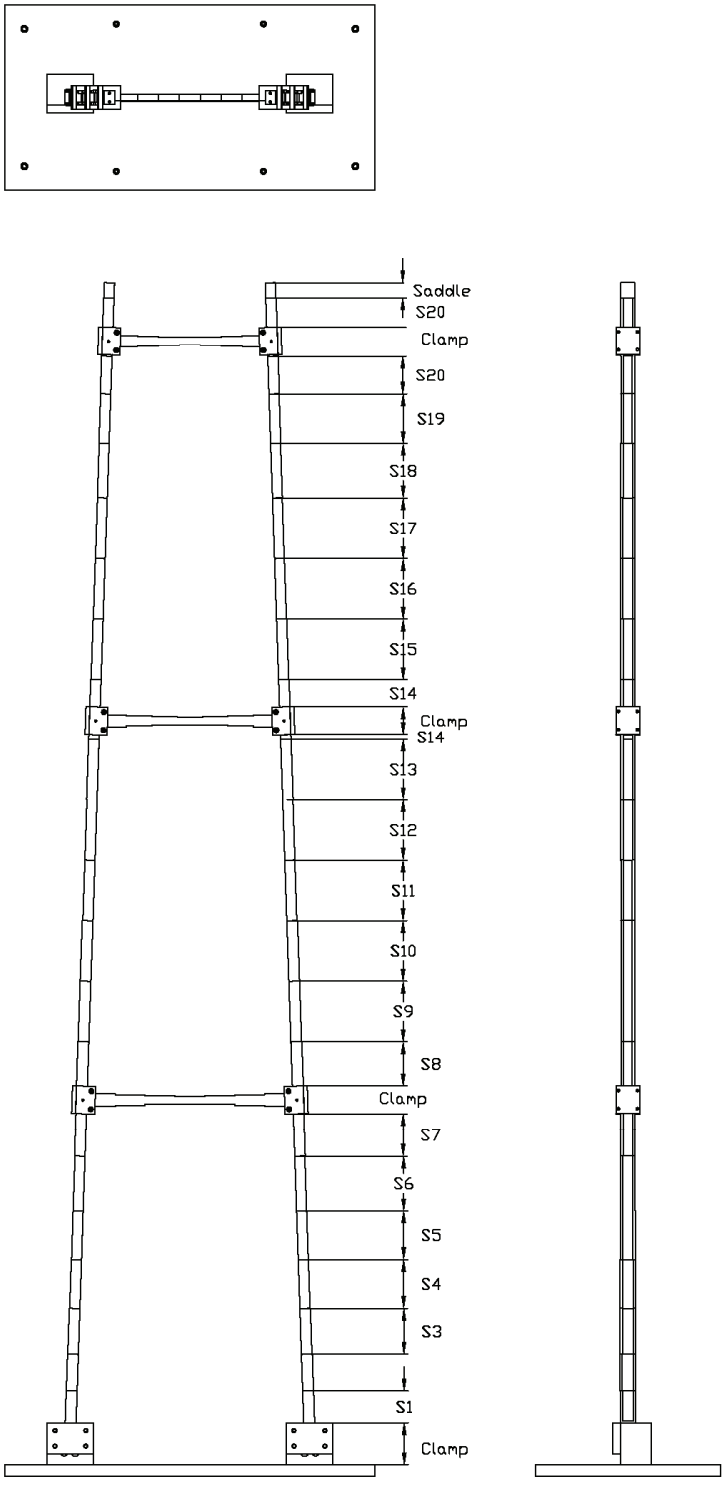

FIGURE 2.9 1:200 SCALE AEROELASTIC MODEL – MODEL 1 - NON-FROUDE SCALED STRUCTURAL MEMBERS

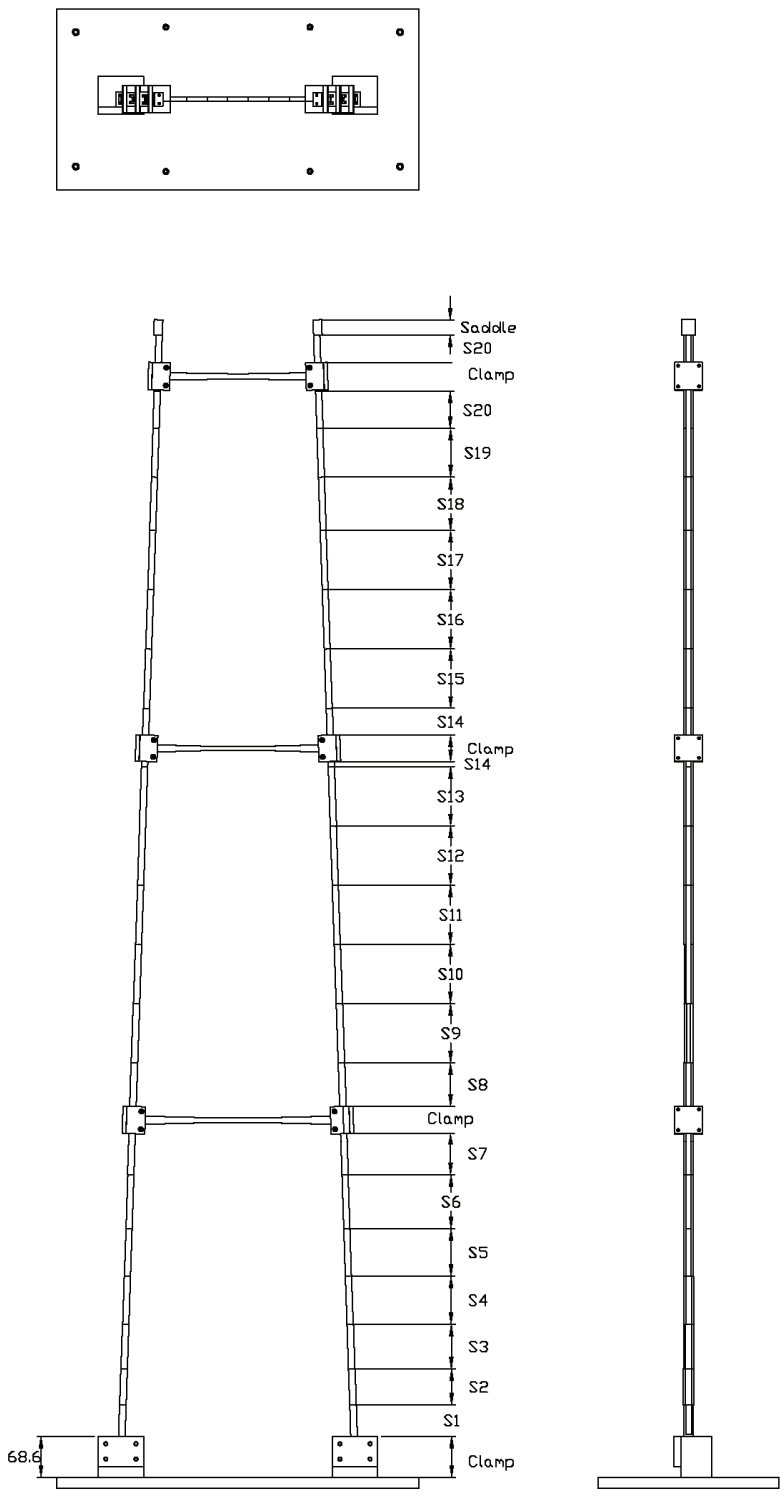

FIGURE 2.10 1:200 SCALE AEROELASTIC MODEL – MODEL 2 - FROUDE SCALED STRUCTURAL MEMBERS

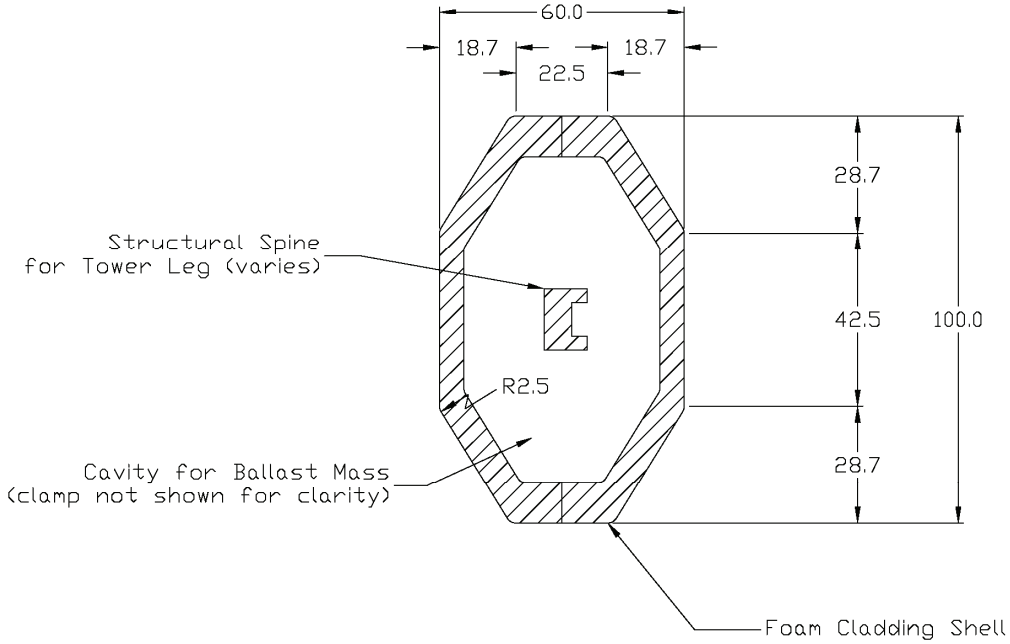

FIGURE 2.11 TYPICAL FOAM CLADDING FOR AEROELASTIC MODELS

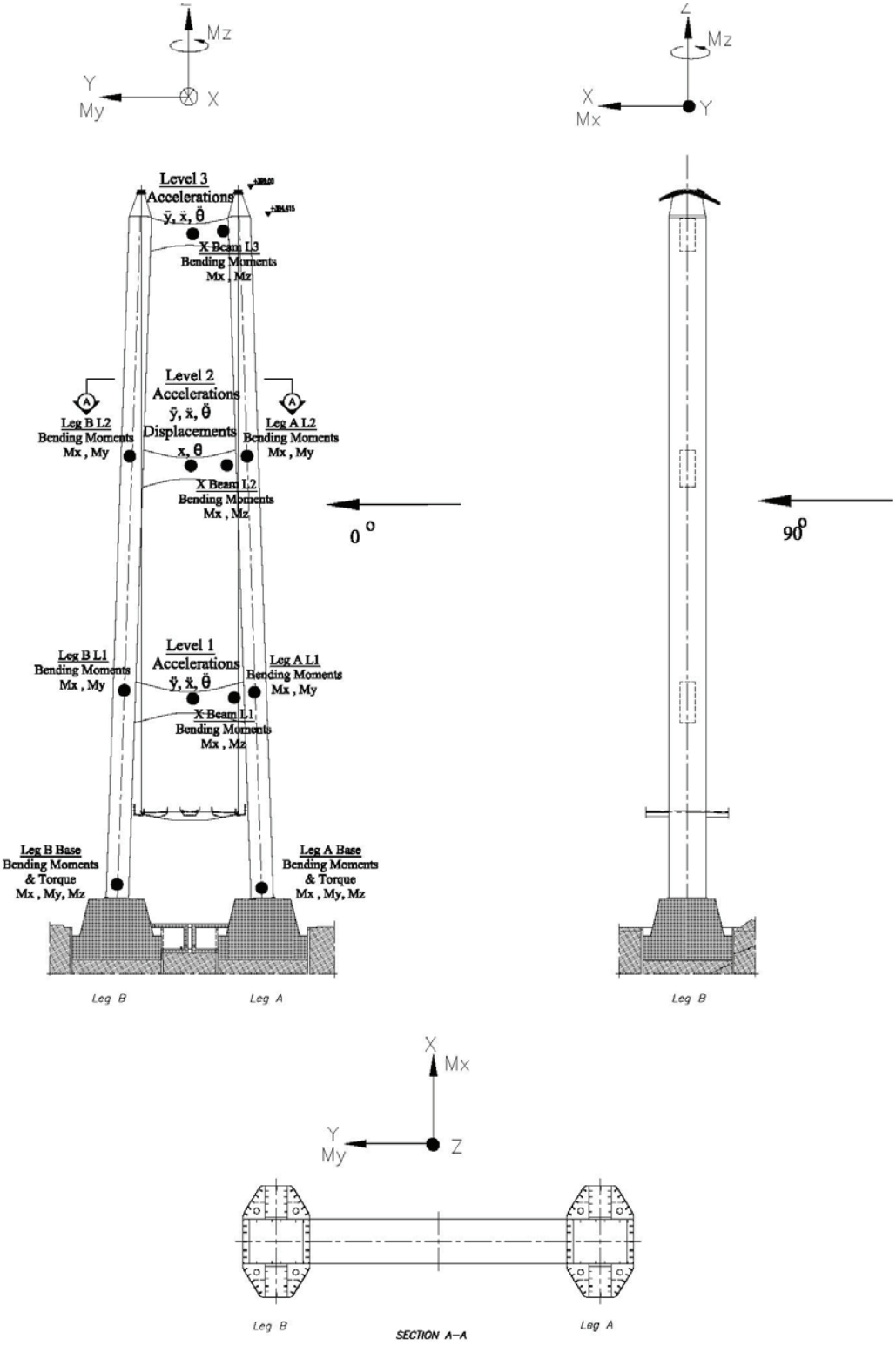

FIGURE 2.12 INSTRUMENTATION LOCATIONS AND SIGN CONVENTION FOR NON-FROUDE MODEL

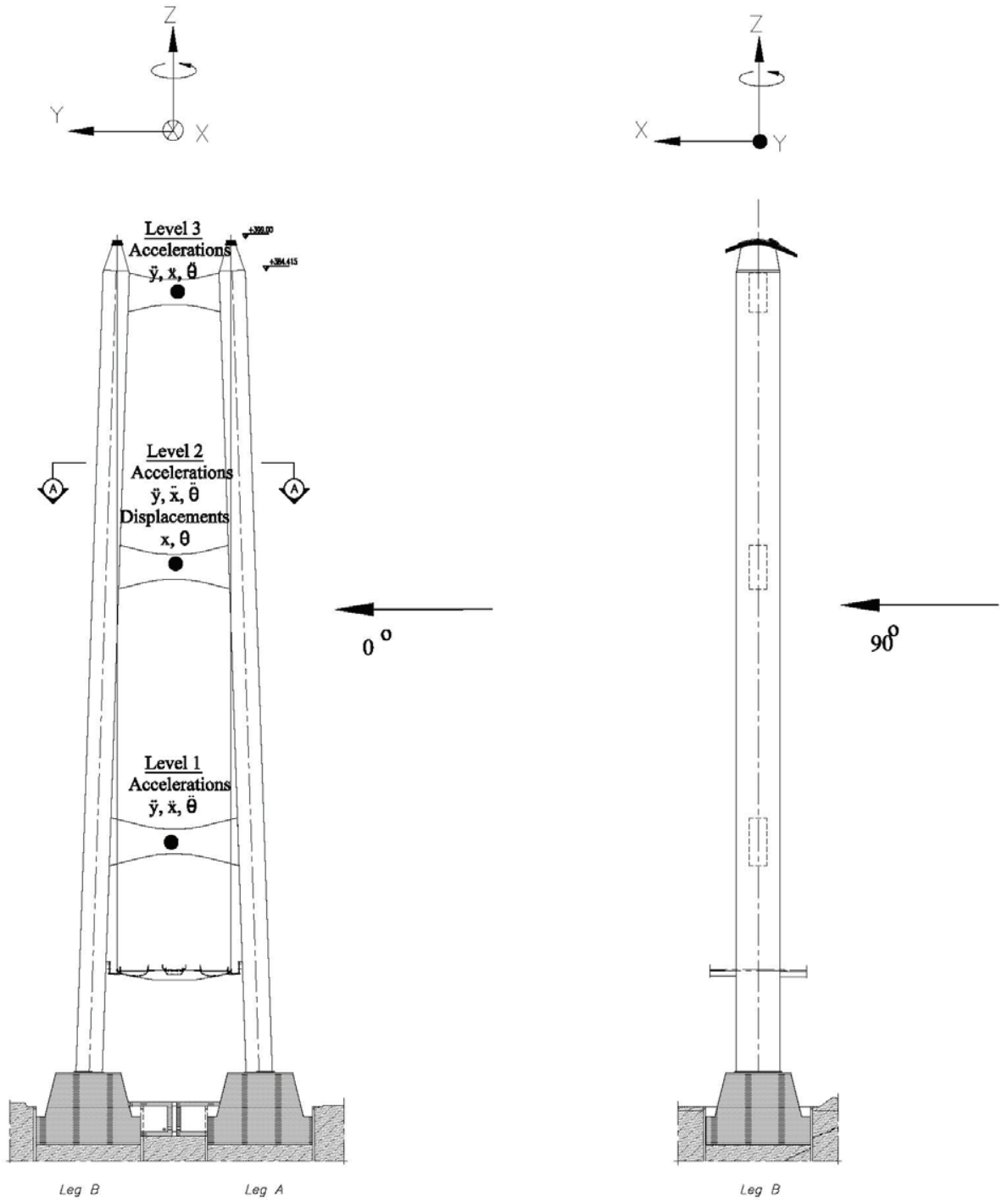

FIGURE 2.13 INSTRUMENTATION LOCATIONS AND SIGN CONVENTIONS FOR FROUDE MODEL

"Smooth Flow"

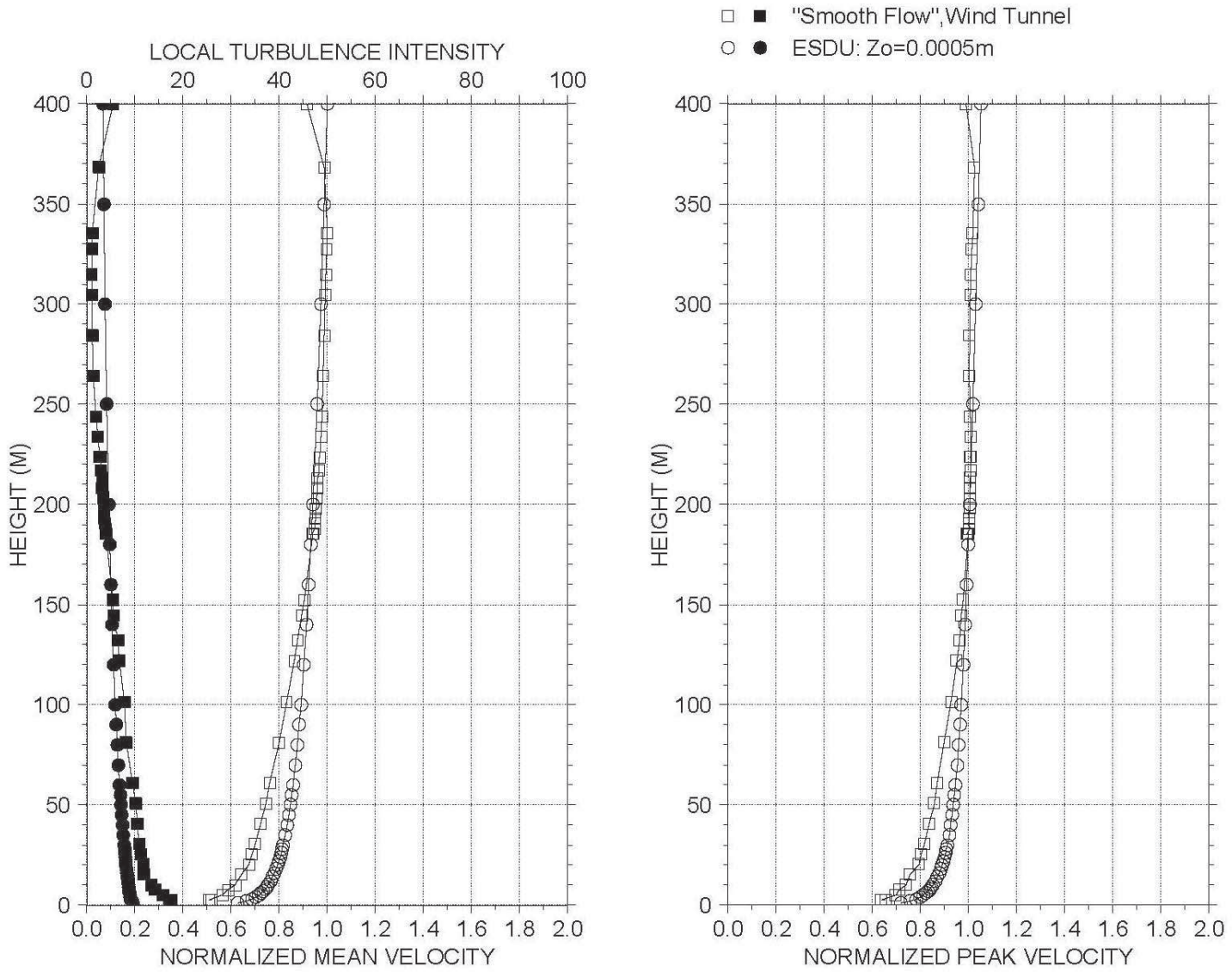

FIGURE 2.14 VERTICAL PROFILES OF THE LONGITUDINAL COMPOENNT OF WIND – SMOOTH FLOW

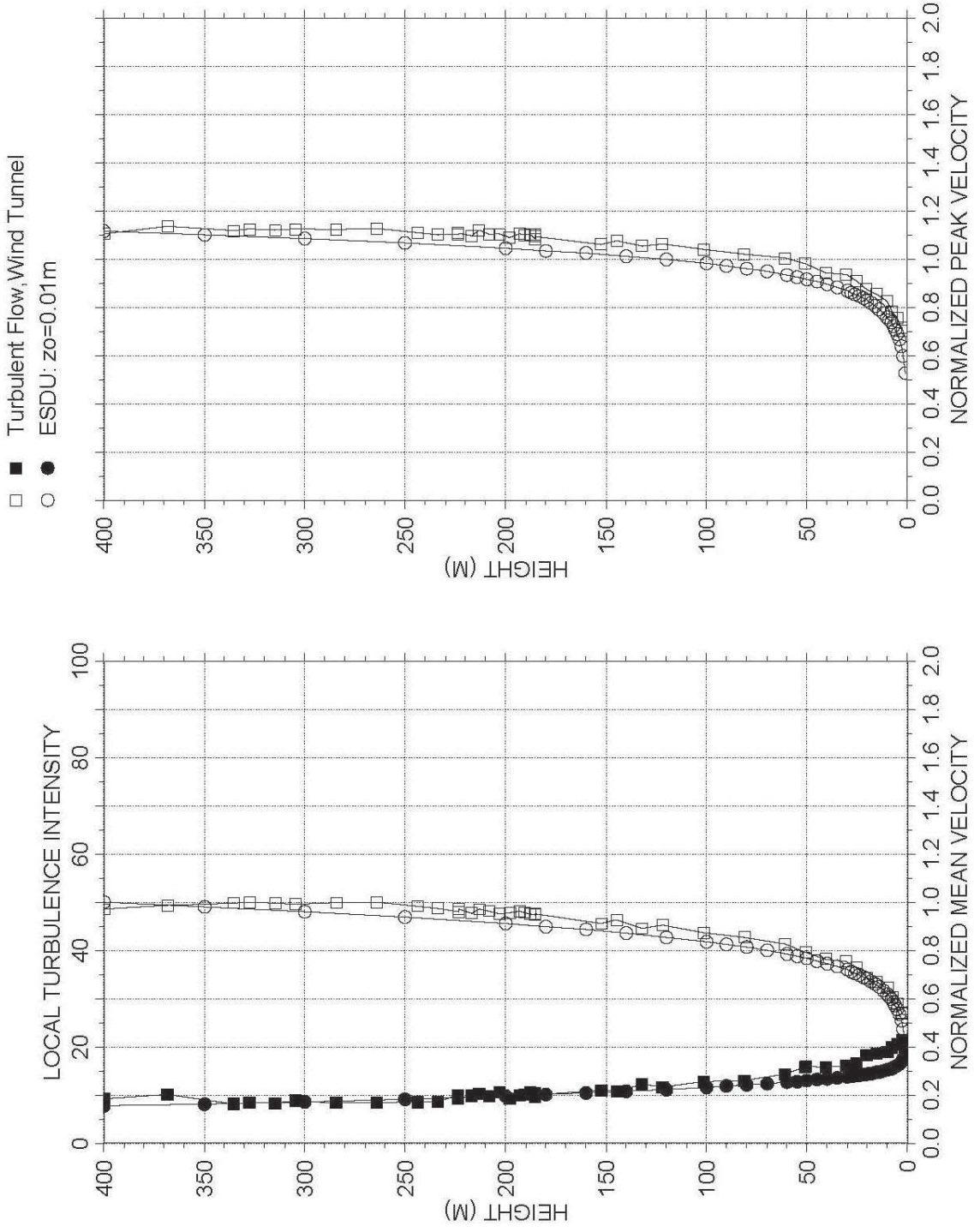

FIGURE 2.15 VERTICAL PROFILES OF THE LONGITUDINAL COMPOENNT OF WIND – TURBULENT FLOW

FIGURE IN PREPARATRION

FIGURE 2.16 POWER SPECTRA OF THE LONGITUDINAL COMPOENT OF THE WIND

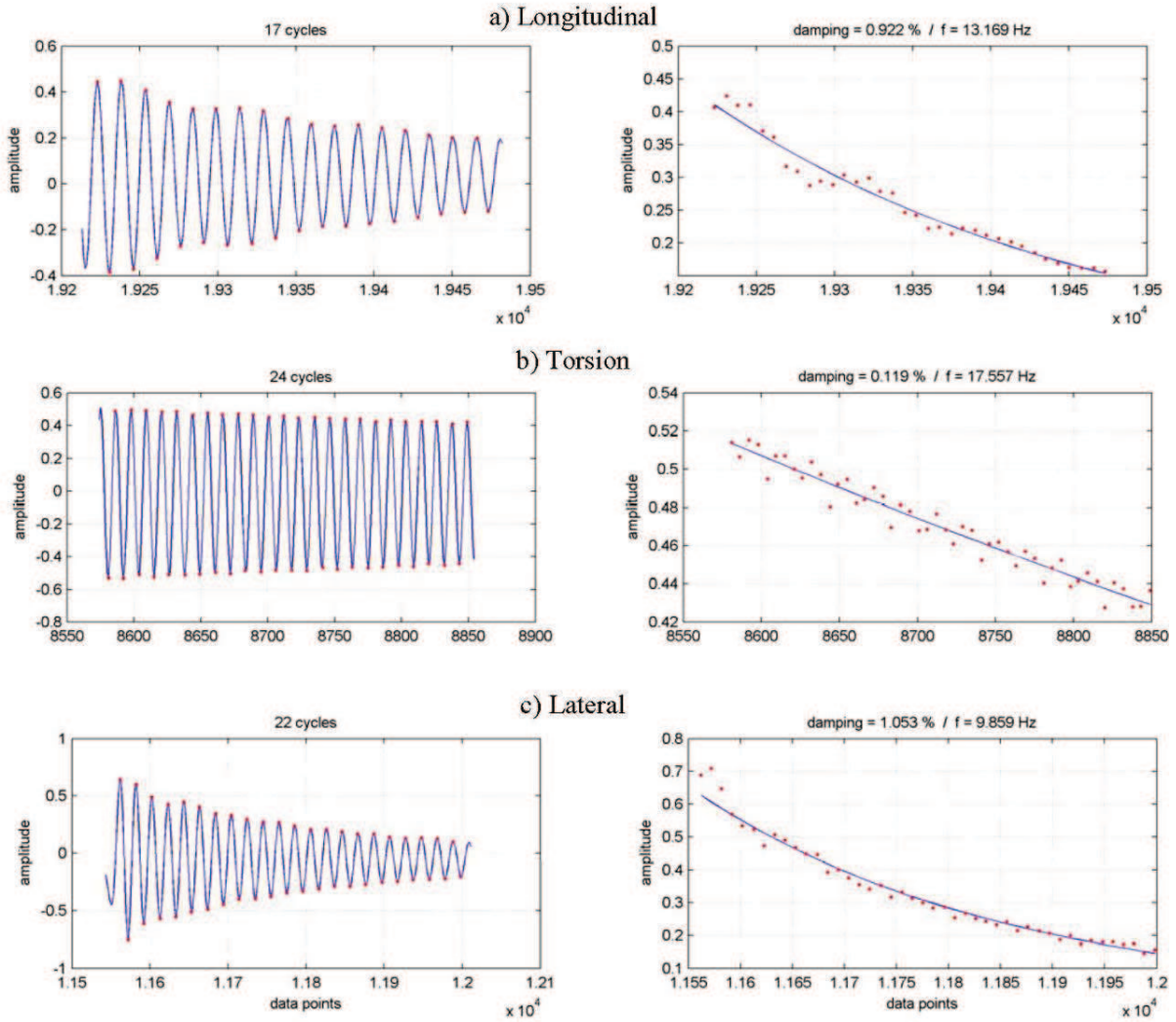

FIGURE 2.17 A SAMPLE PLOT OF DAMPING ESTIMATE, NON-FROUDE TOWER MODEL, IN-SERVICE CONDITION

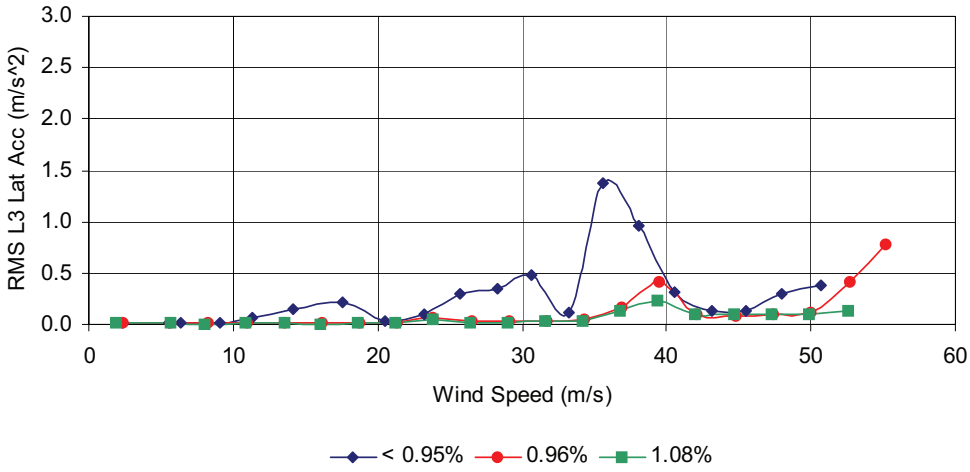

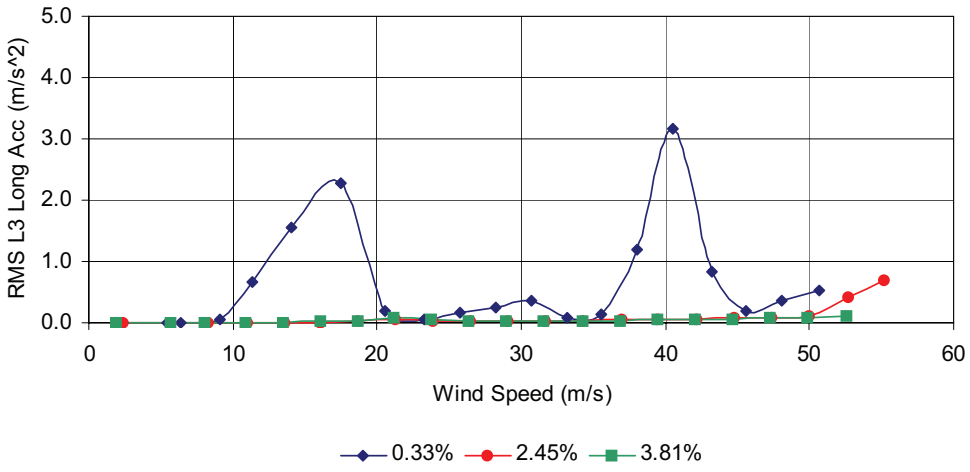

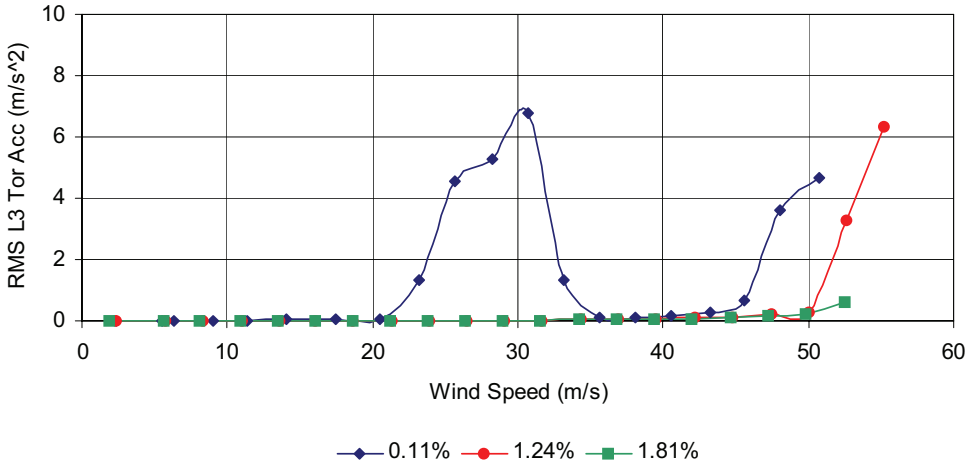

FIGURE 3.1 TOWER RESPONSE IN SMOOTH FLOW AT LEVEL 3 FOR 0^{O} WIND, CONSTRUCTION STAGE, NON-FROUDE TOWER

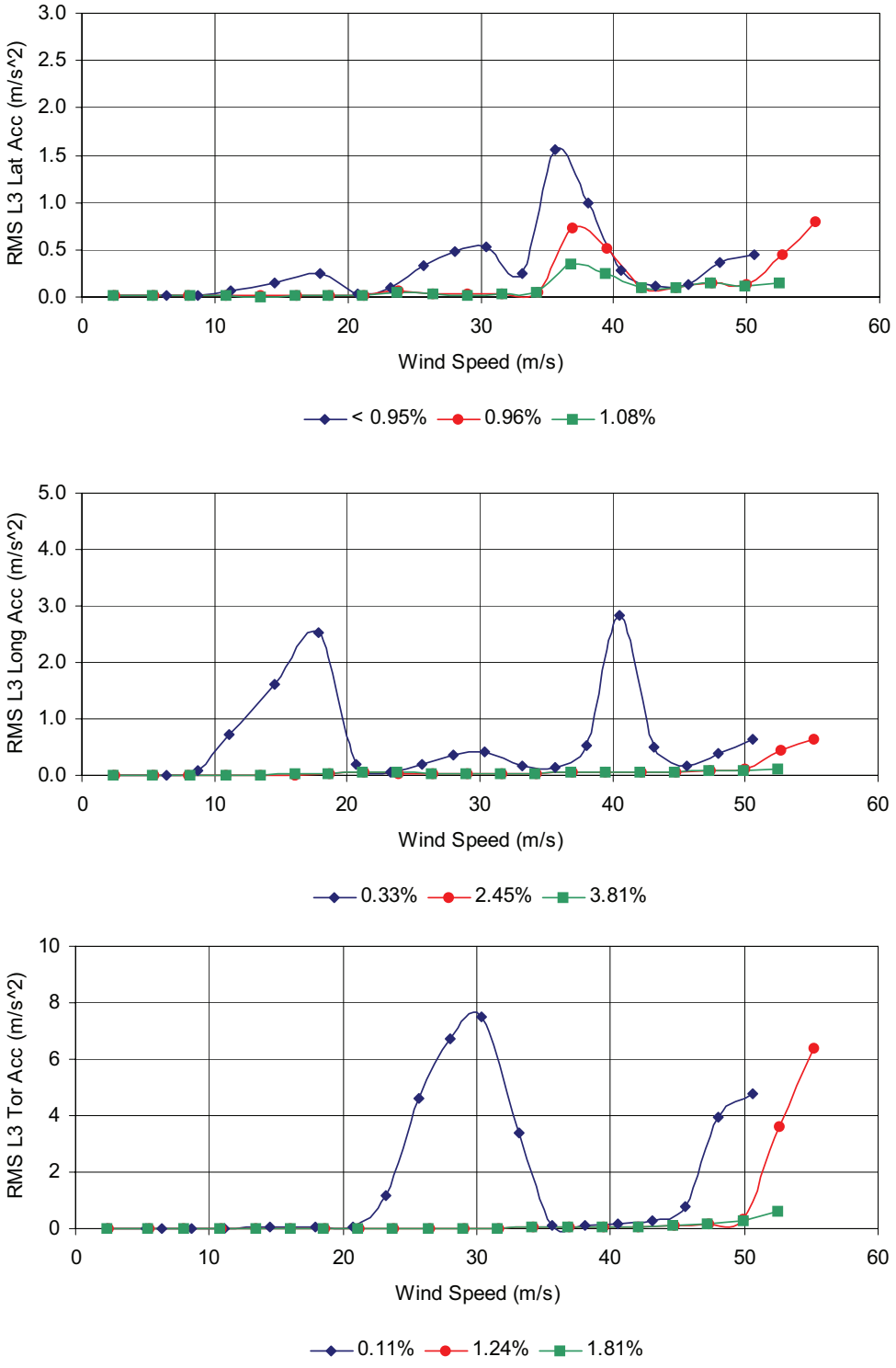

FIGURE 3.2 TOWER RESPONSE IN SMOOTH FLOW AT LEVEL 3 FOR 2.5^{O} WIND, CONSTRUCTION STAGE, NON-FROUDE TOWER

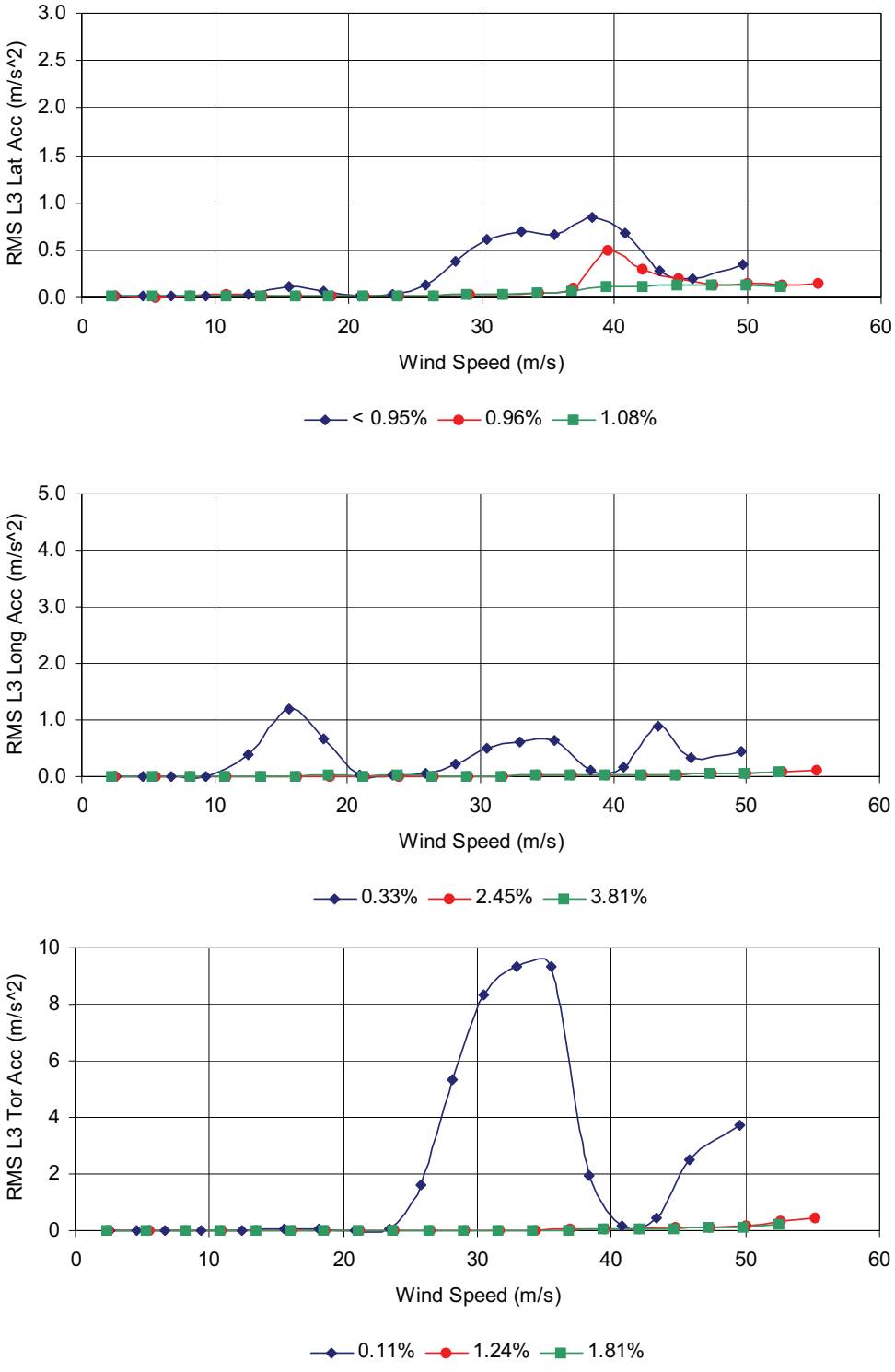

FIGURE 3.3 TOWER RESPONSE IN SMOOTH FLOW AT LEVEL 3 FOR 10^{O} WIND, CONSTRUCTION STAGE, NON-FROUDE TOWER

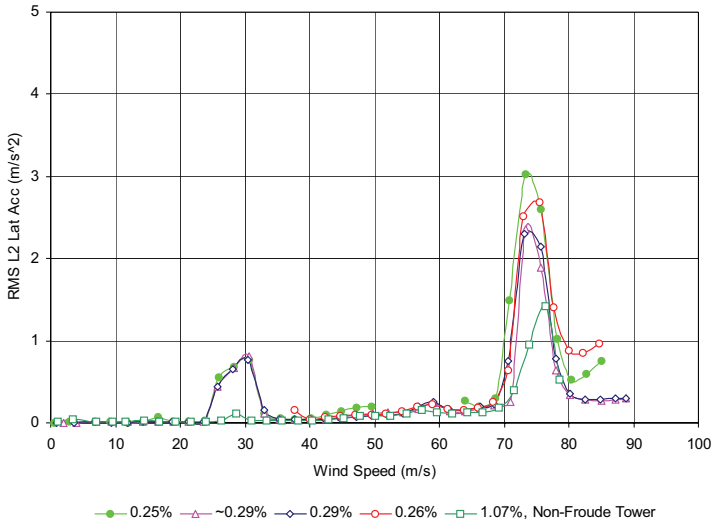

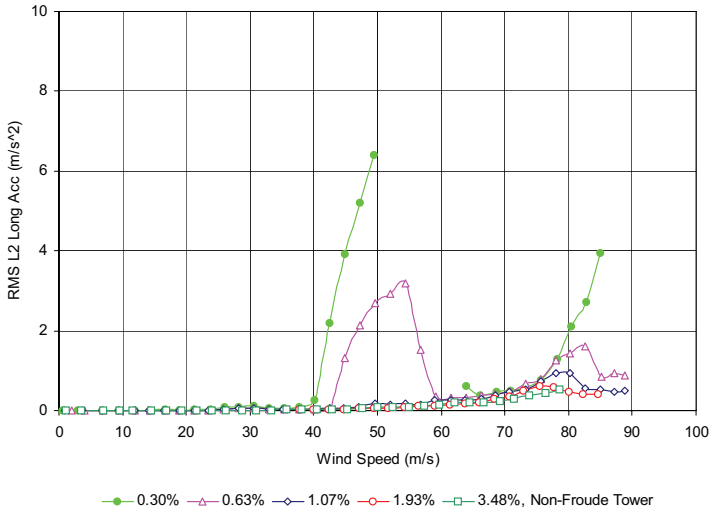

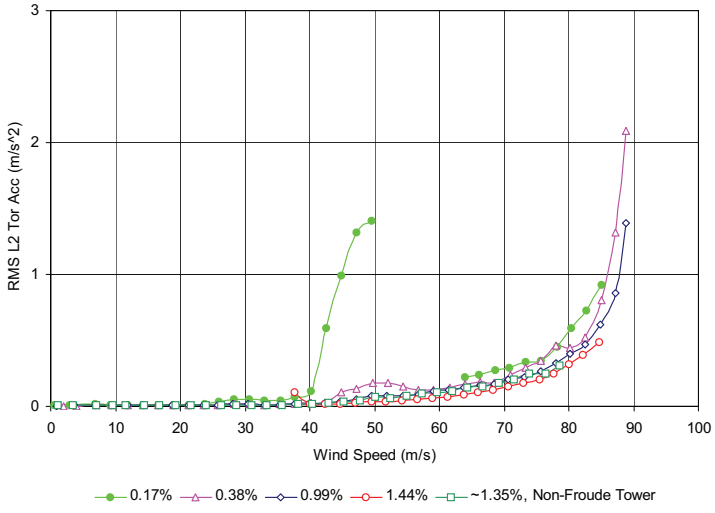

FIGURE 3.4 TOWER RESPONSE IN SMOOTH FLOW AT LEVEL 2 FOR 0^{O} WIND, IN SERVICE CONDITION, NON-FROUDE TOWER

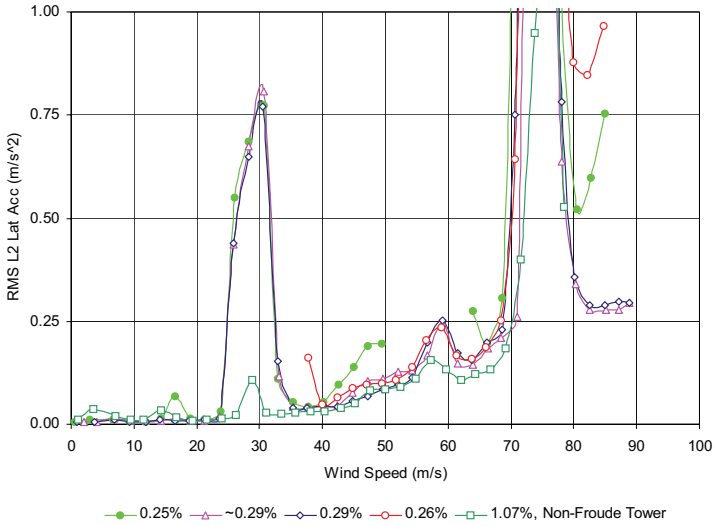

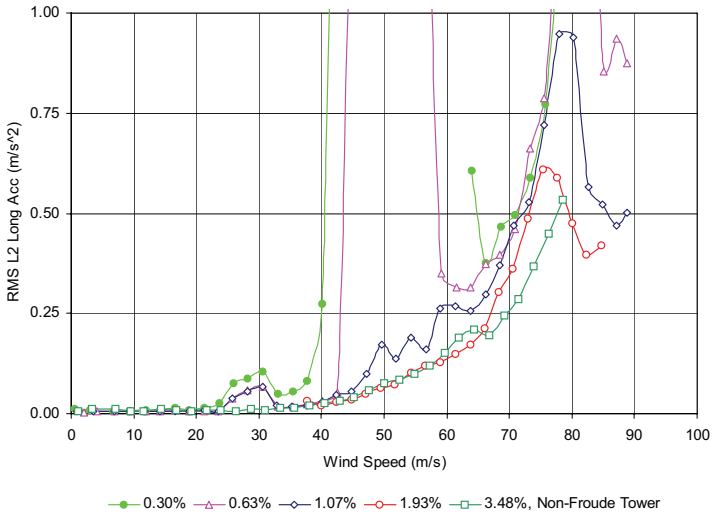

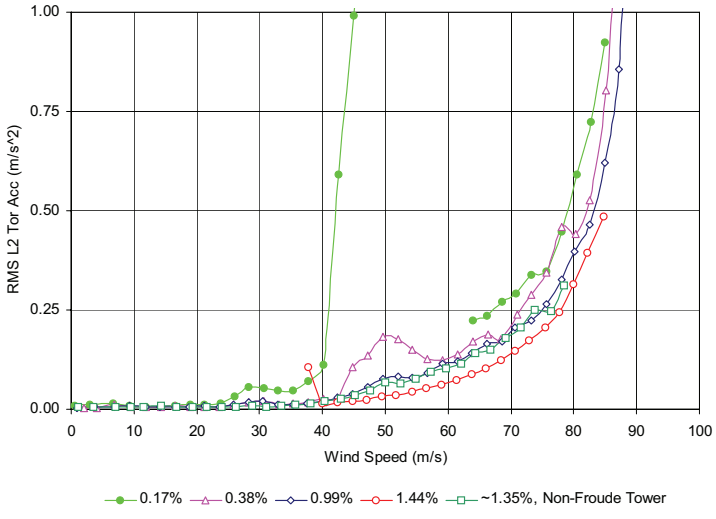

FIGURE 3.4 (CONT.) TOWER RESPONSE IN SMOOTH FLOW AT LEVEL 2 FOR 0^{O} WIND, IN SERVICE CONDITION, NON-FROUDE TOWER

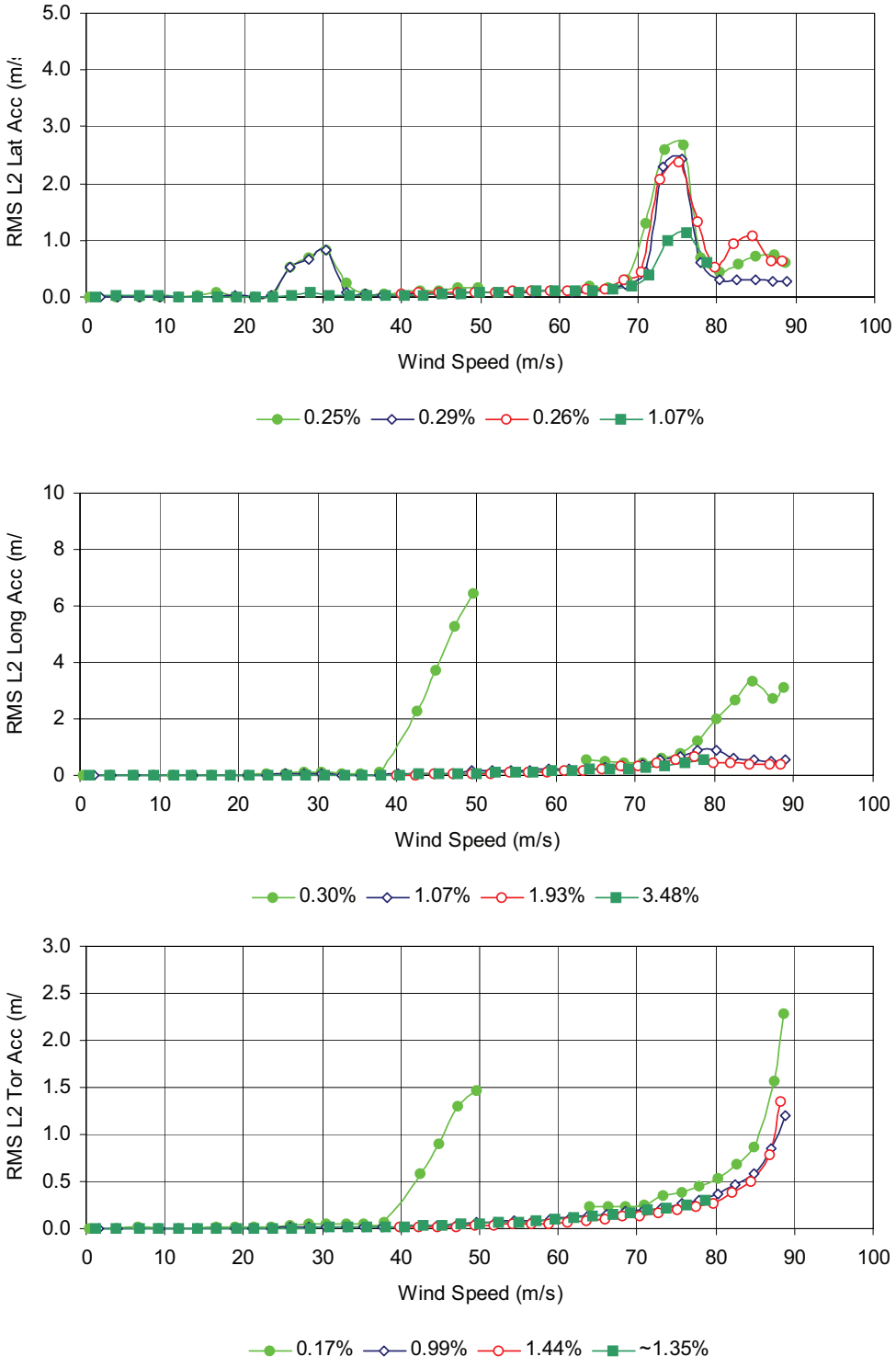

FIGURE 3.5 TOWER RESPONSE IN SMOOTH FLOW AT LEVEL 2 FOR 2.5^{O} WIND, IN SERVICE CONDITION, NON-FROUDE TOWER

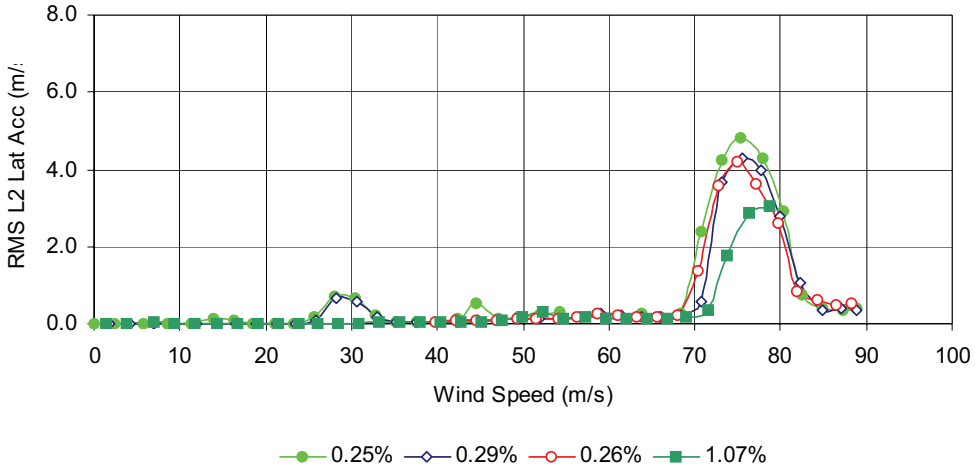

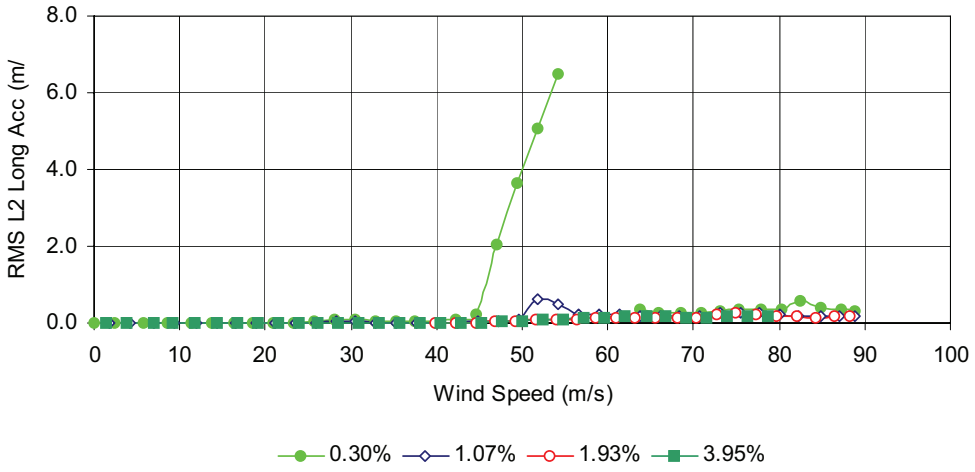

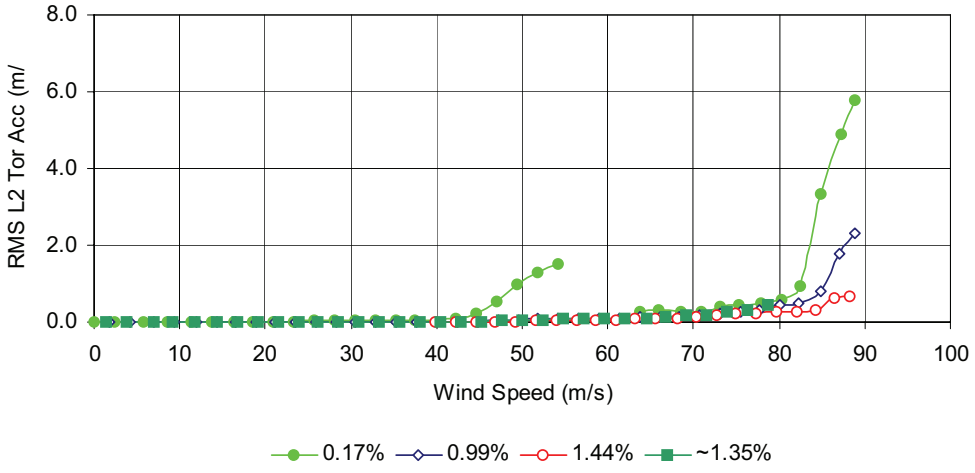

FIGURE 3.6 TOWER RESPONSE IN SMOOTH FLOW AT LEVEL 2 FOR 10^{O} WIND, IN SERVICE CONDITION, NON-FROUDE TOWER

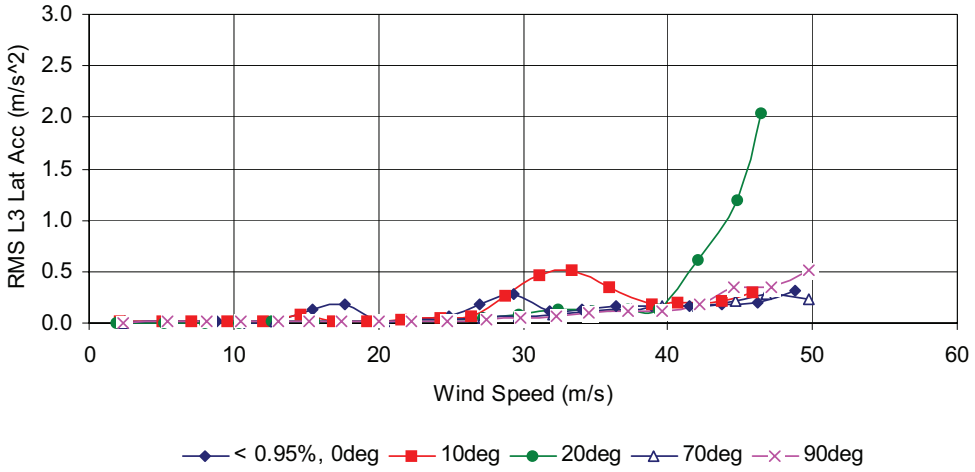

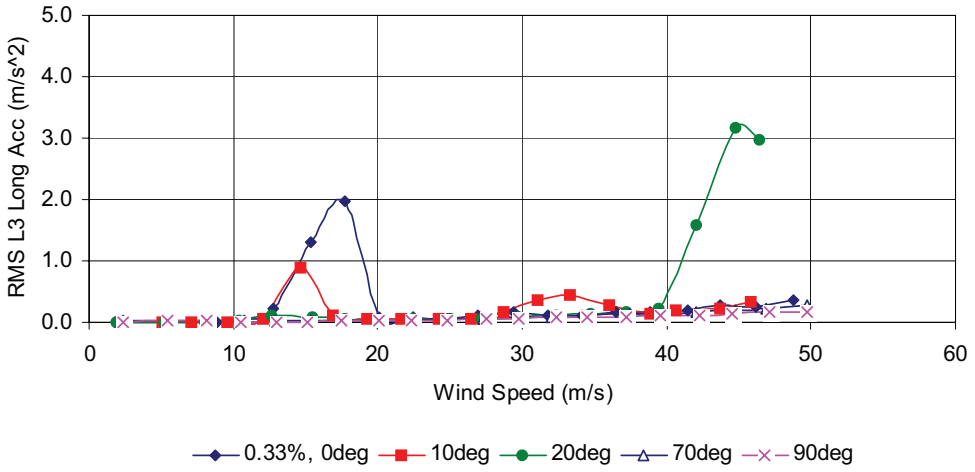

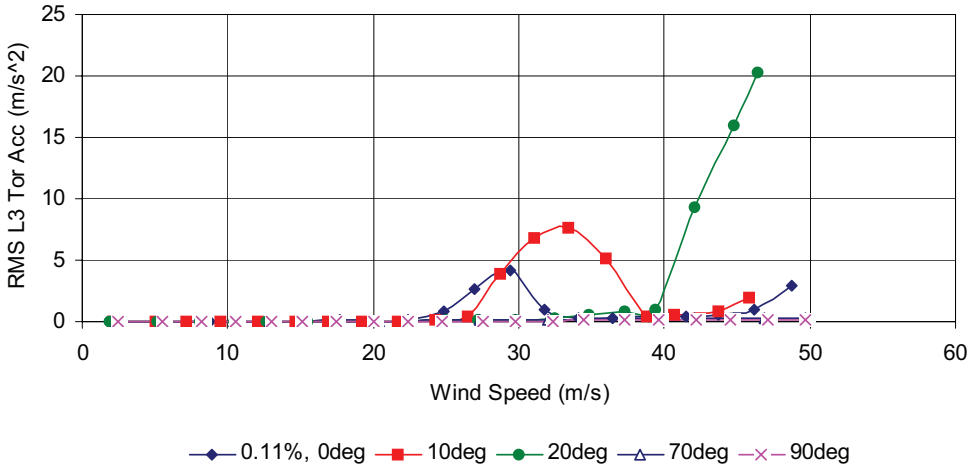

FIGURE 3.7 TOWER RESPONSE IN TURBULENT FLOW AT LEVEL 3 FOR SELECTED WIND ANGLES WITH INHERENT DAMPING, CONSTRUCTION STAGE, NON-FROUDE TOWER

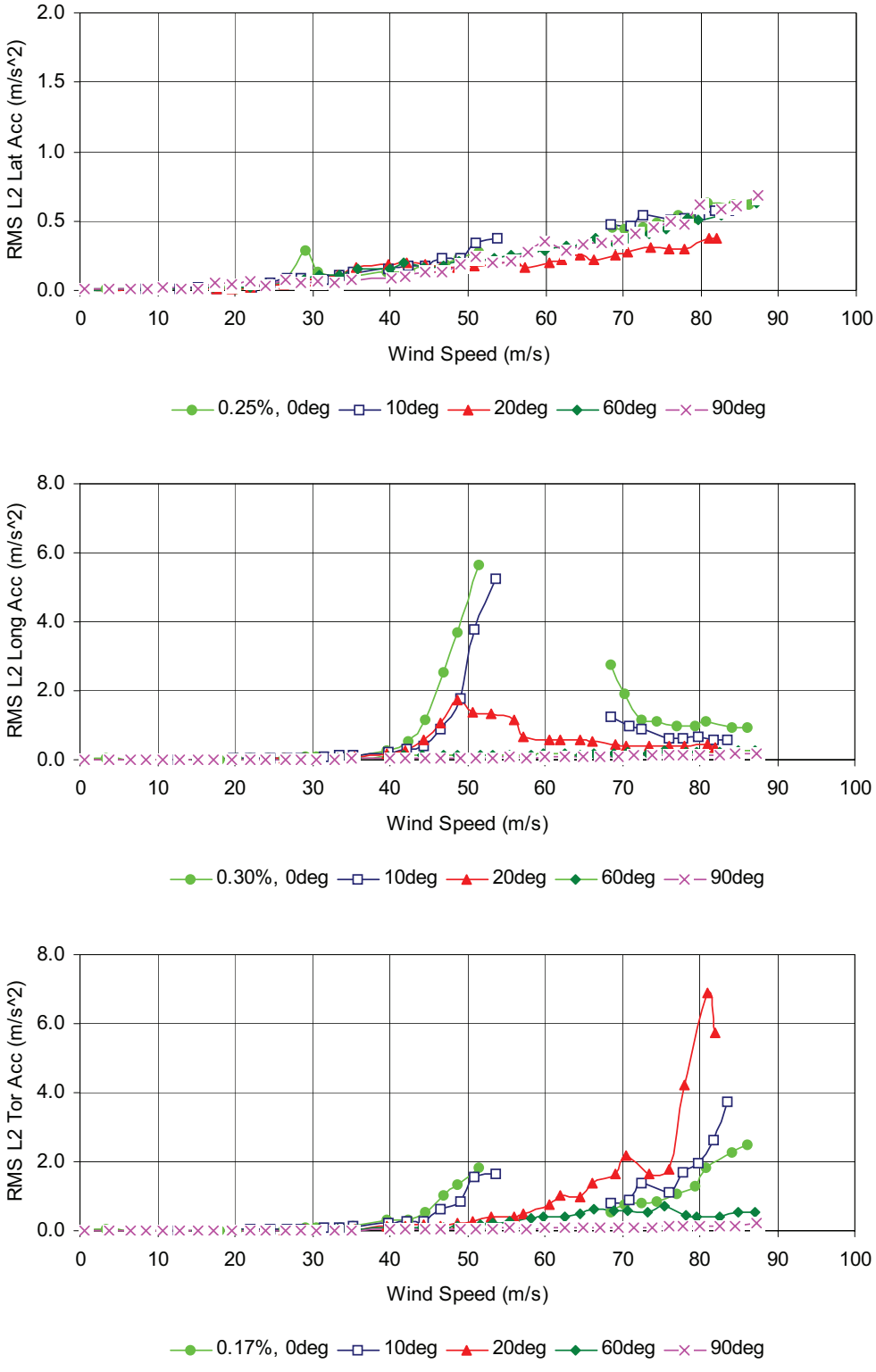

FIGURE 3.8 TOWER RESPONSE IN TURBULENT FLOW AT LEVEL 2 FOR SELECTED WIND ANGLES WITH INHERENT DAMPING, IN SERVICE CONDITION, NON-FROUDE TOWER

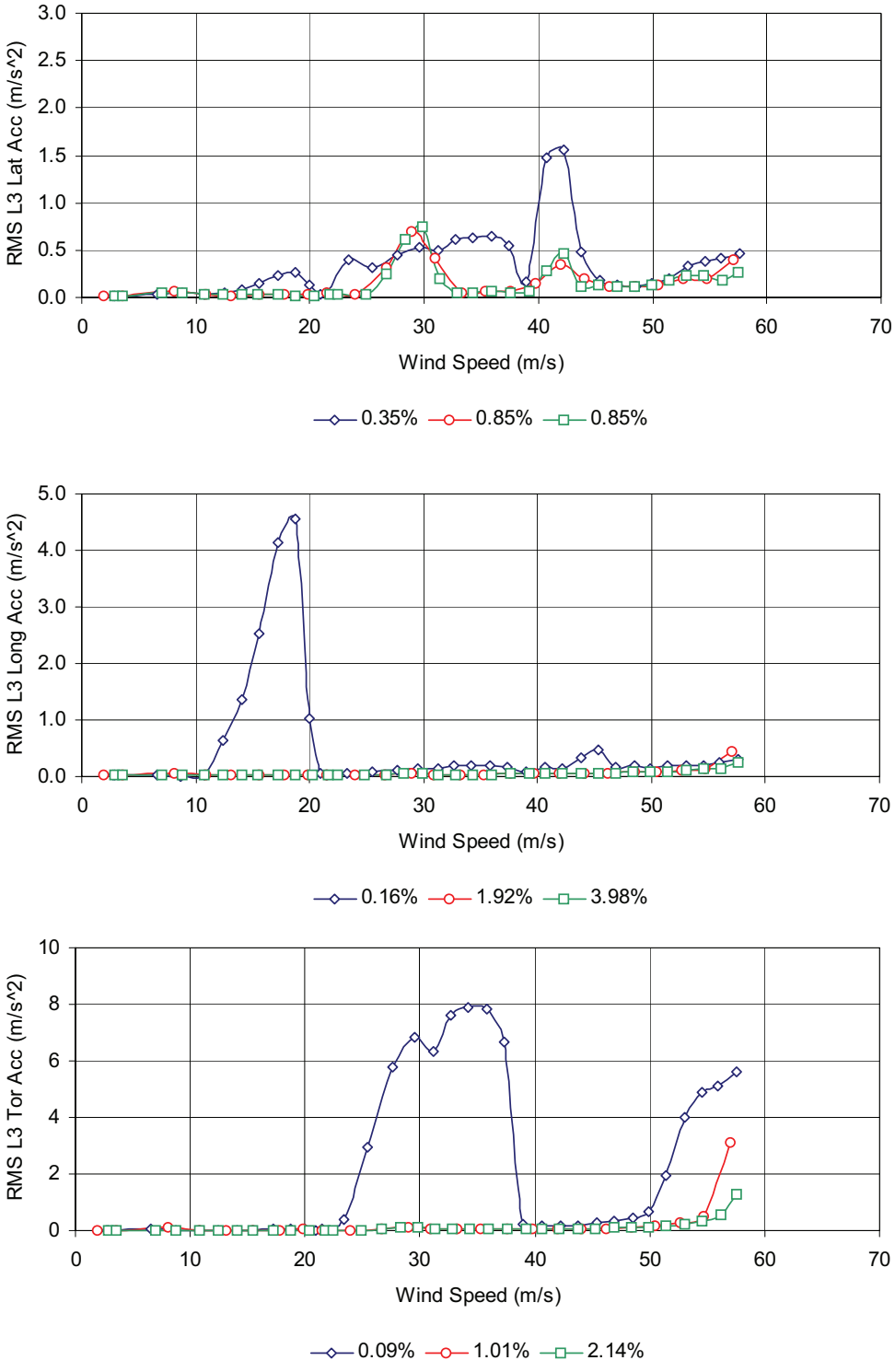

FIGURE 4.1 TOWER RESPONSE IN SMOOTH FLOW AT LEVEL 3 FOR 0^{O} WIND, CONSTRUCTION STAGE, FROUDE TOWER

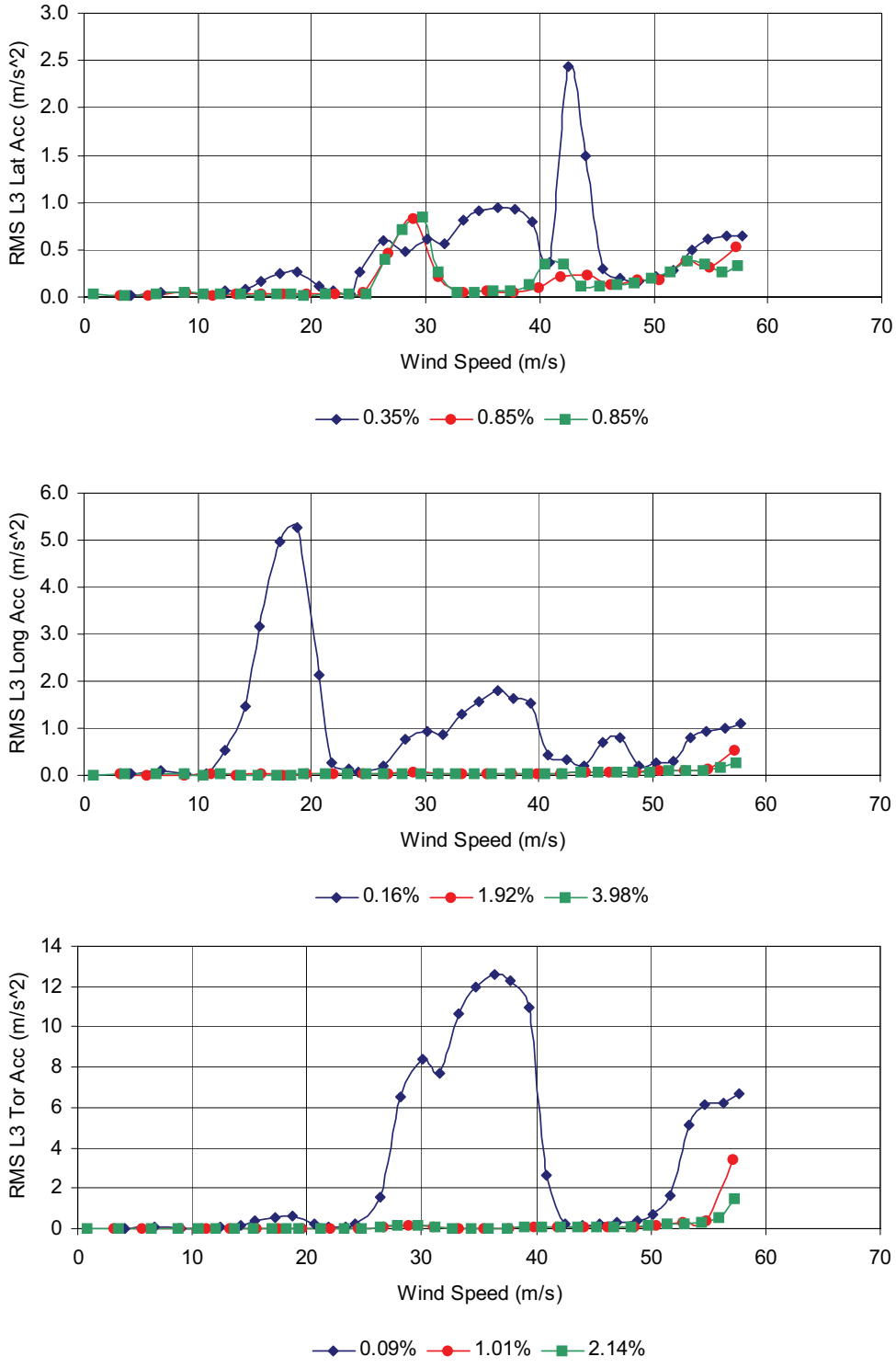

FIGURE 4.2 TOWER RESPONSE IN SMOOTH FLOW AT LEVEL 3 FOR 5^{O} WIND, CONSTRUCTION STAGE, FROUDE TOWER

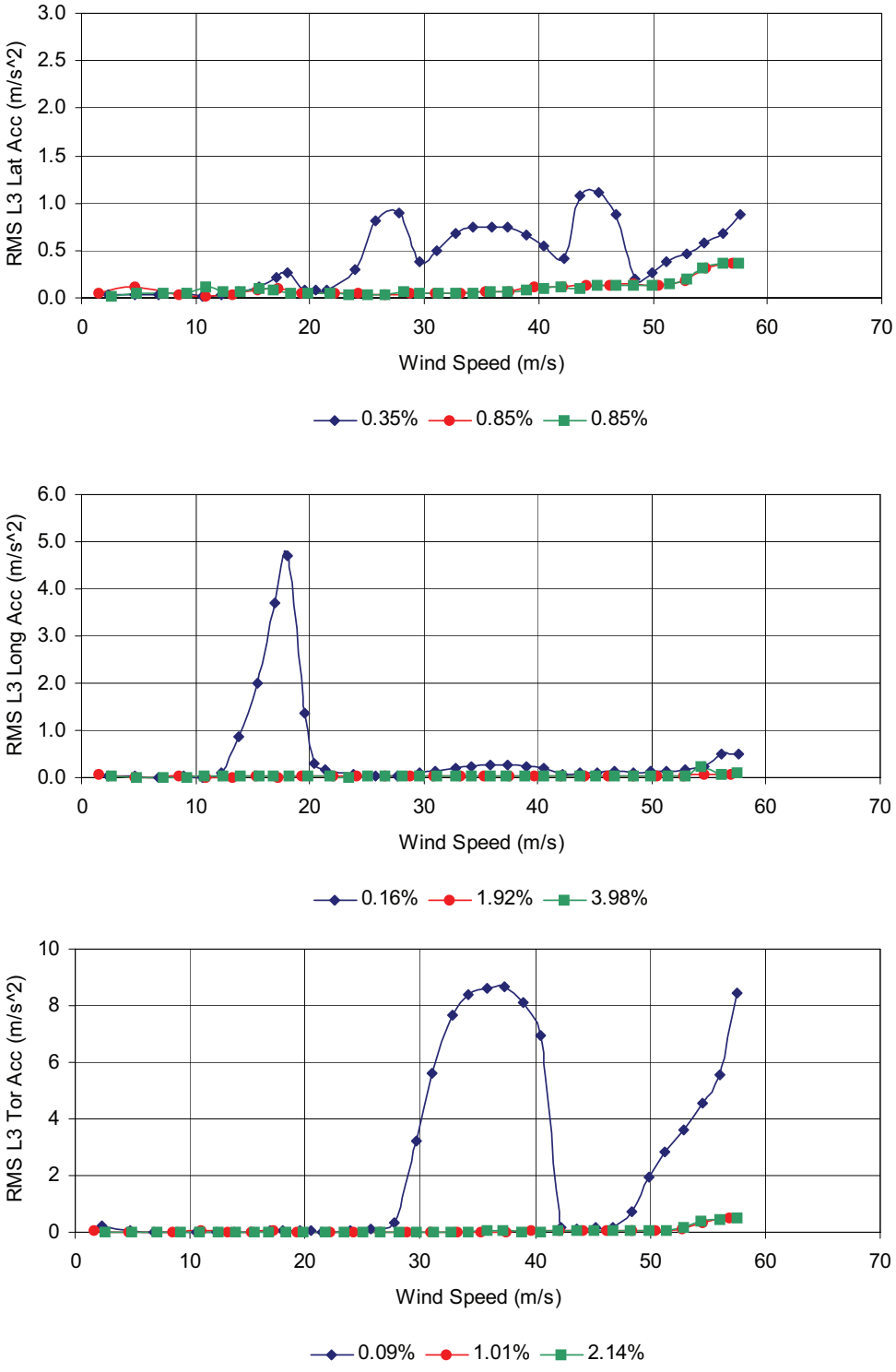

FIGURE 4.3 TOWER RESPONSE IN SMOOTH FLOW AT LEVEL 3 FOR 10^{O} WIND, CONSTRUCTION STAGE, FROUDE TOWER

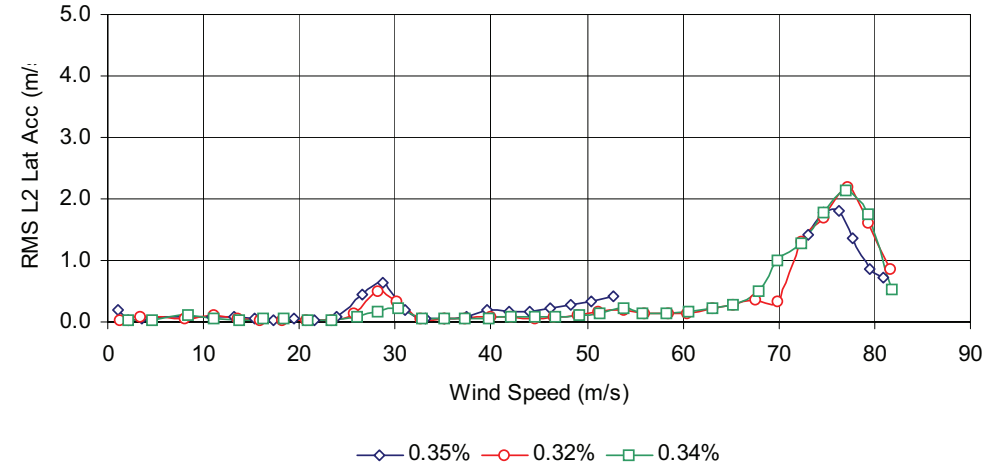

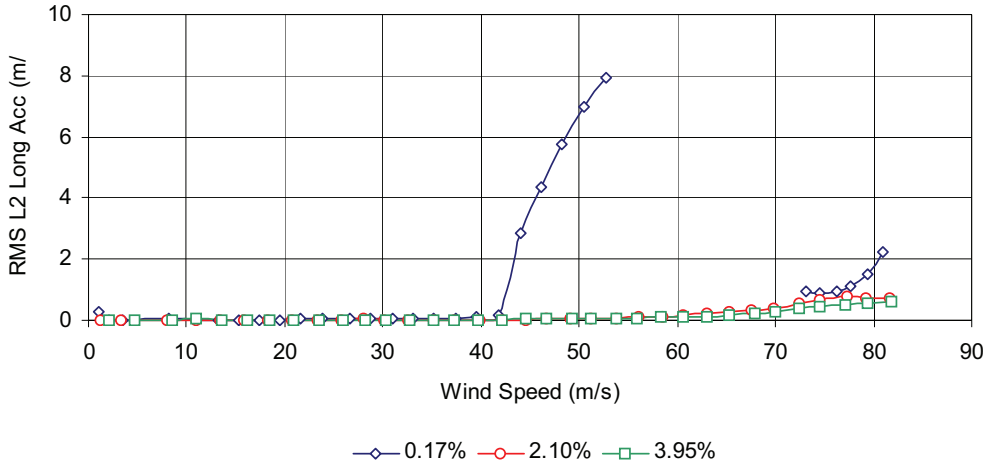

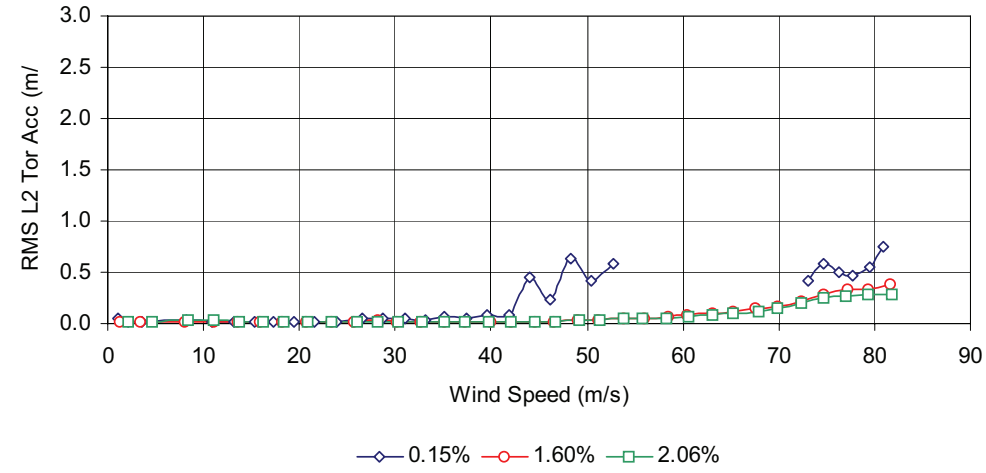

FIGURE 4.4 TOWER RESPONSE IN SMOOTH FLOW AT LEVEL 2 FOR 0^{O} WIND, IN SERVICE CONDITION, FROUDE TOWER

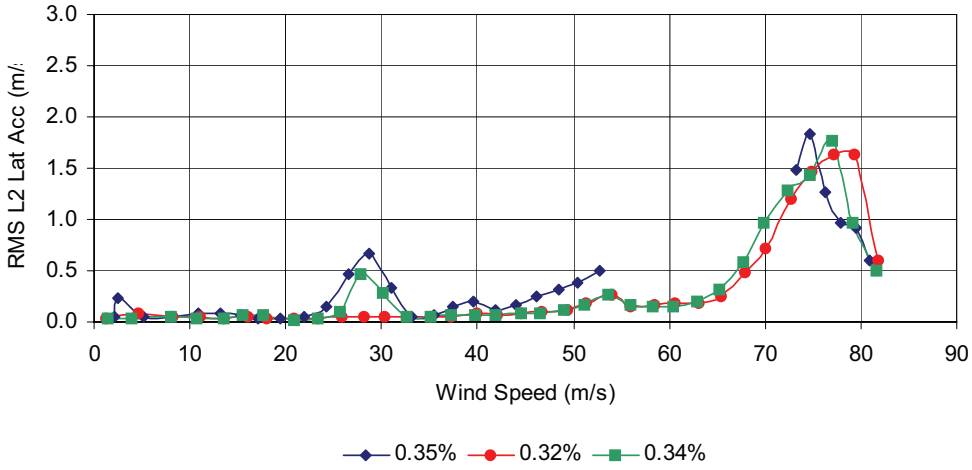

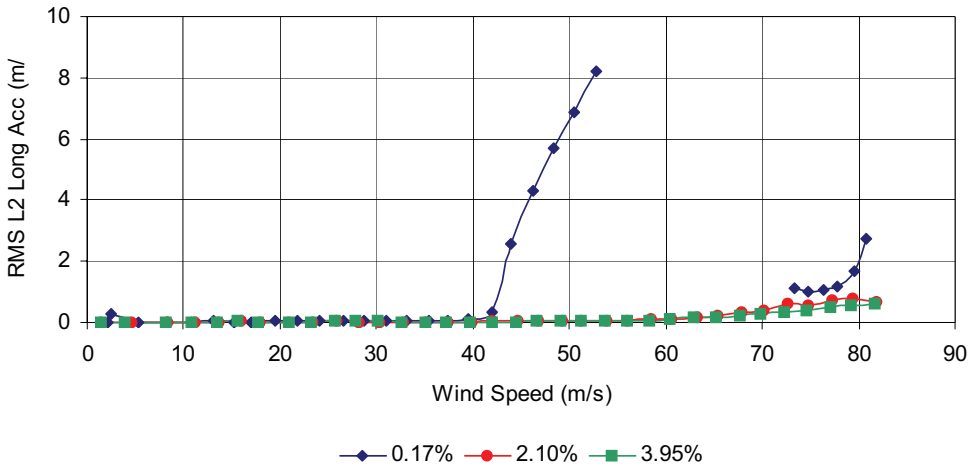

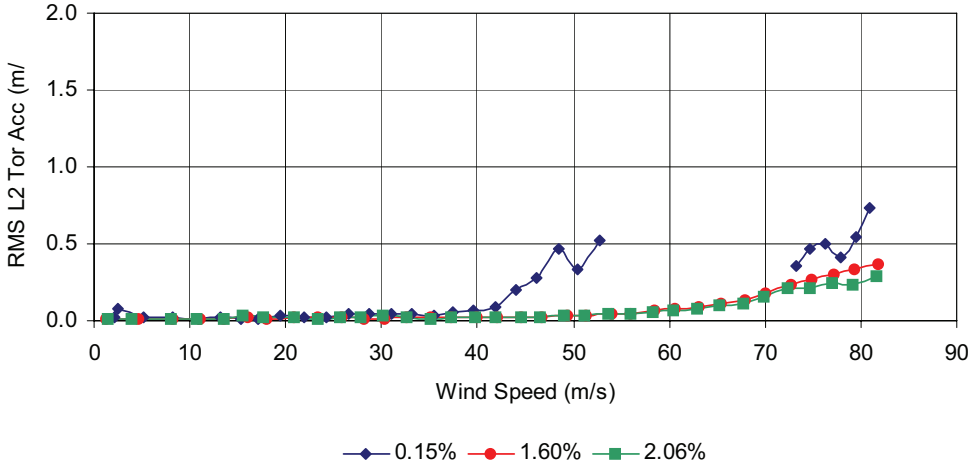

FIGURE 4.5 TOWER RESPONSE IN SMOOTH FLOW AT LEVEL 2 FOR 5^{O} WIND, IN SERVICE CONDITION, FROUDE TOWER

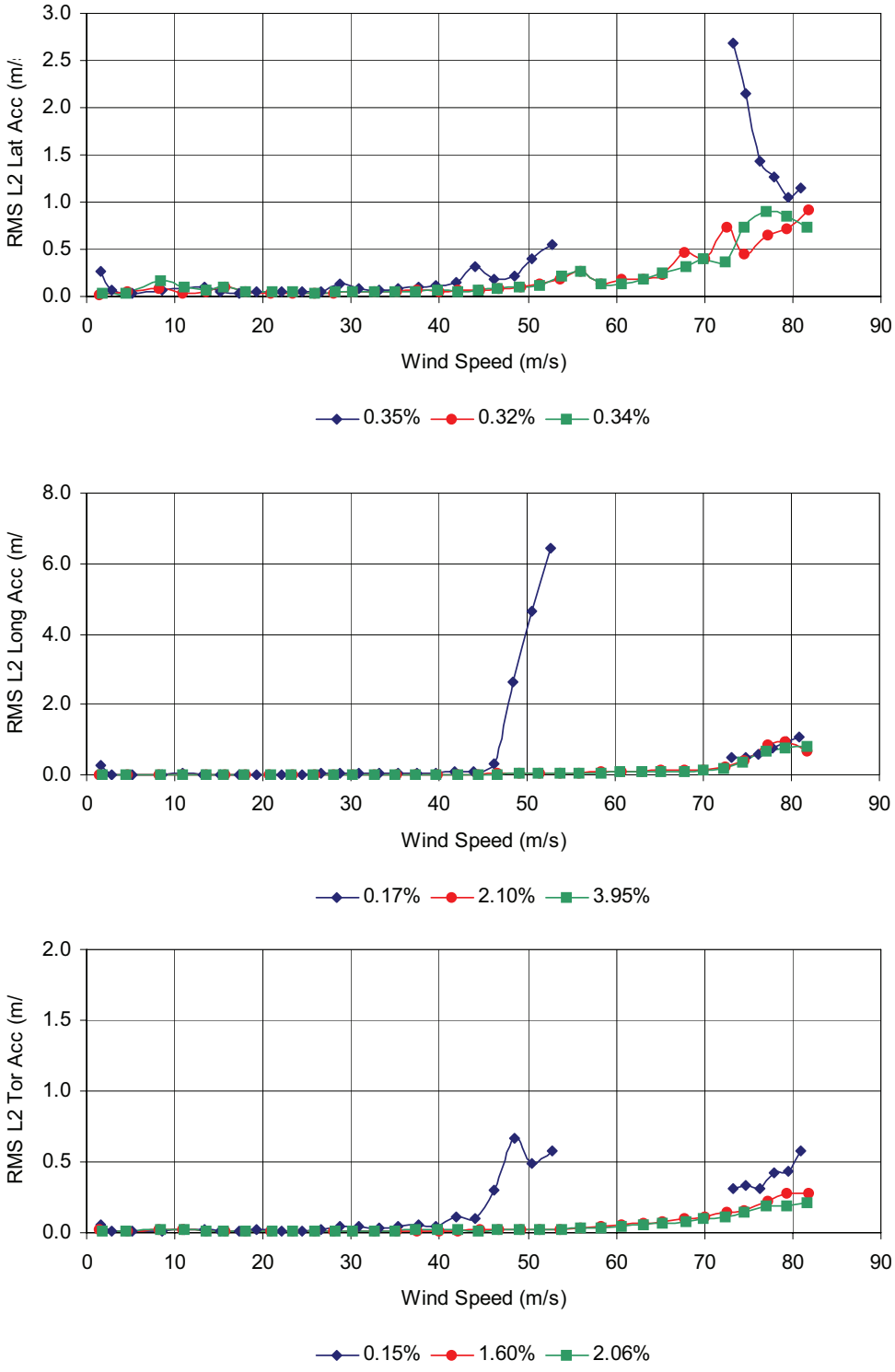

FIGURE 4.6 TOWER RESPONSE IN SMOOTH FLOW AT LEVEL 2 FOR 10^{O} WIND, IN SERVICE CONDITION, FROUDE TOWER

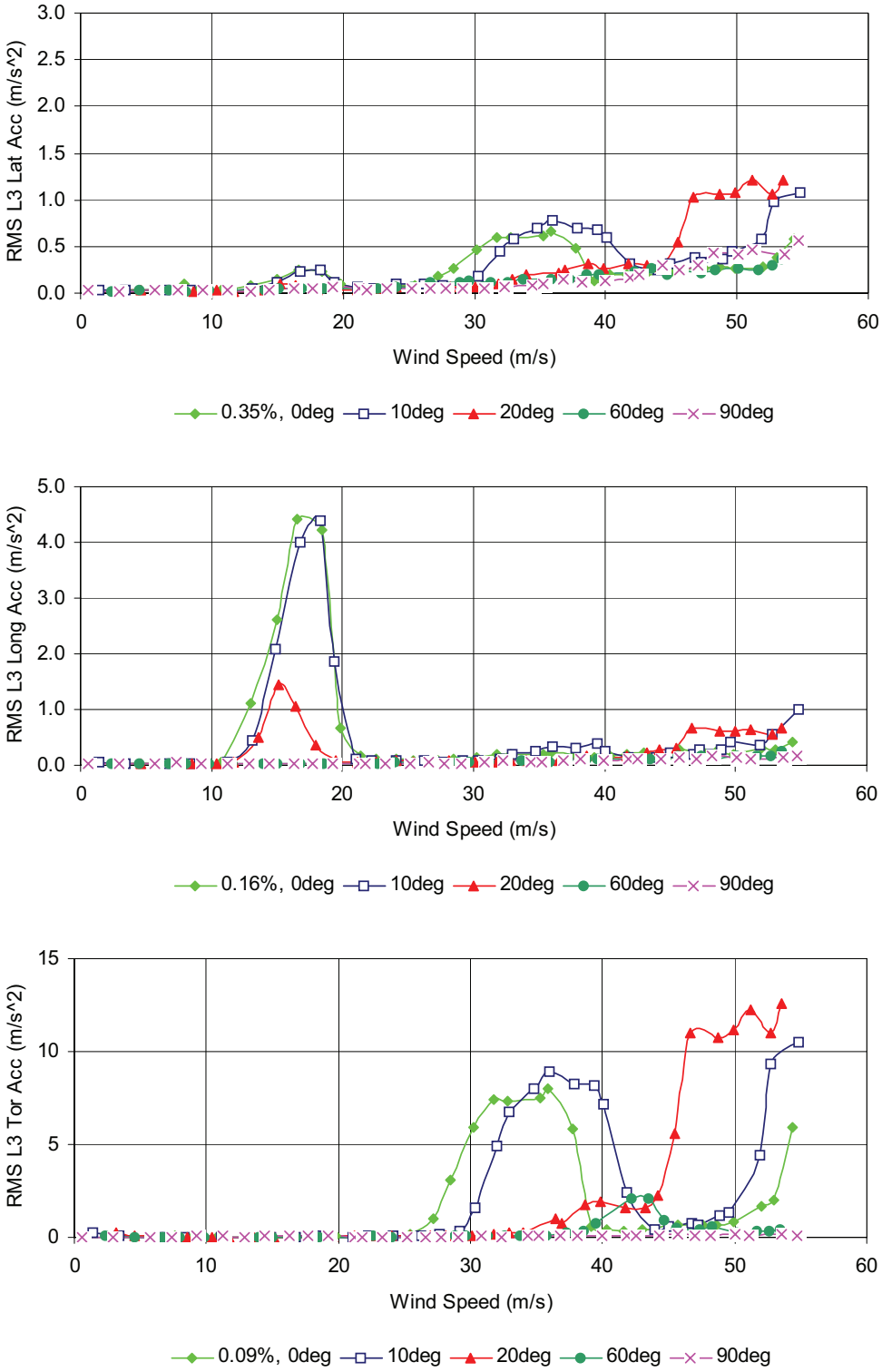

FIGURE 4.7 TOWER RESPONSE IN TURBULENT FLOW AT LEVEL 3 FOR SELECTED WIND ANGLES WITH INHERENT DAMPING, CONSTRUCTION STAGE, FROUDE TOWER

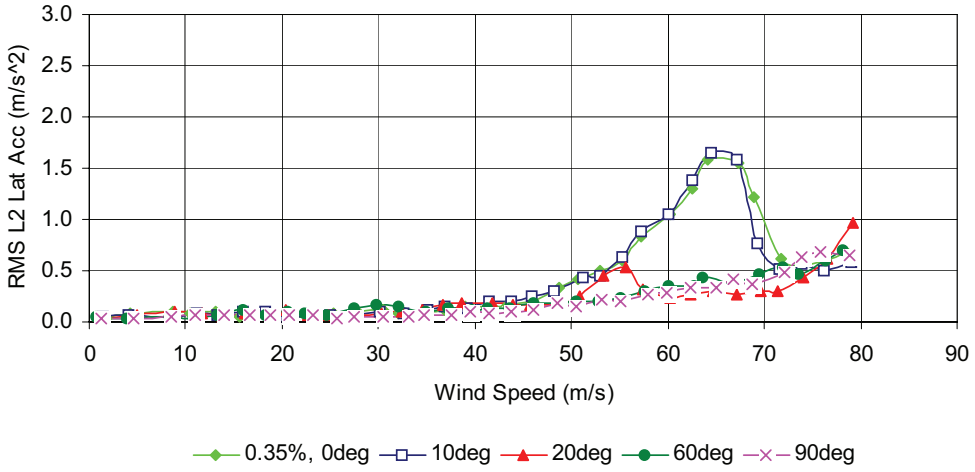

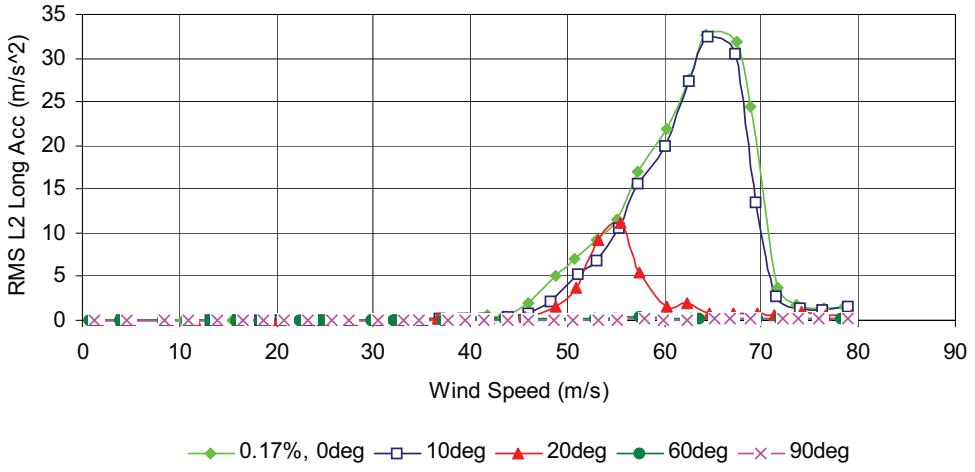

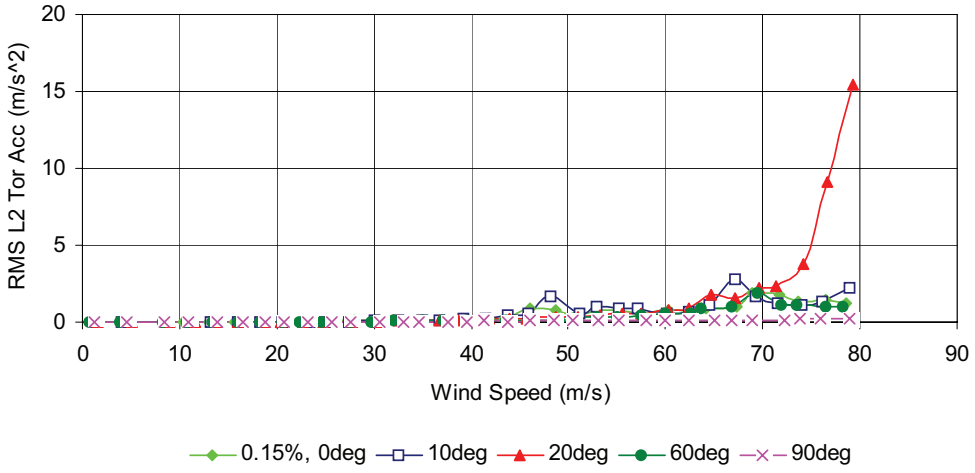

FIGURE 4.8 TOWER RESPONSE IN TURBULENT FLOW AT LEVEL 2 FOR SELECTED WIND ANGLES WITH INHERENT DAMPING, IN-SERVICE CONDITION, FROUDE TOWER

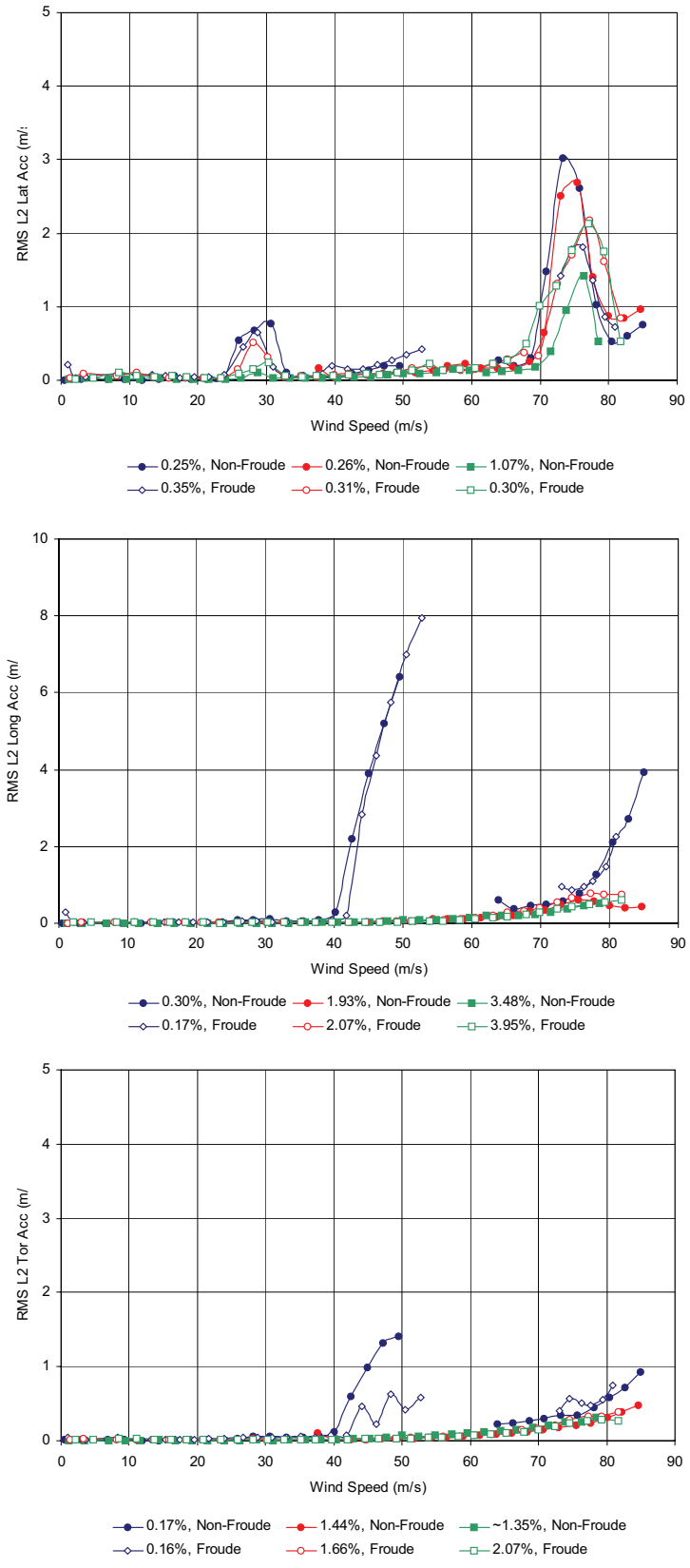

FIGURE 5.1 COMPARISON OF TOWER RESPONSES IN SMOOTH FLOW (LEVEL 2) FOR 0^{O} WIND, IN-SERVICE CONDITION

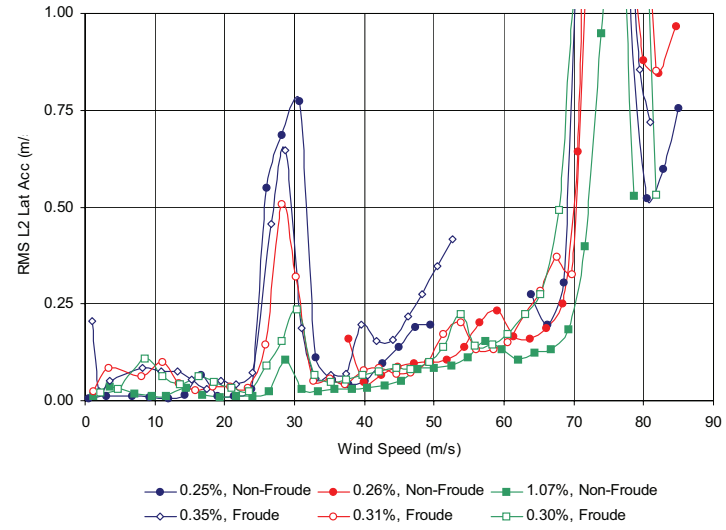

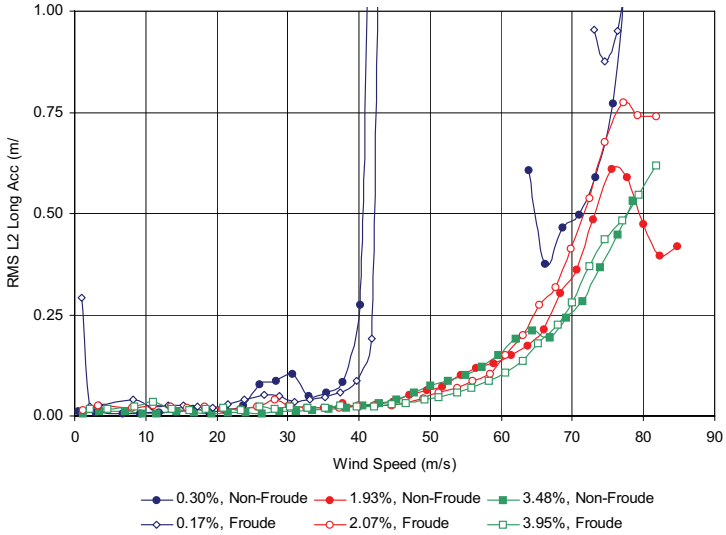

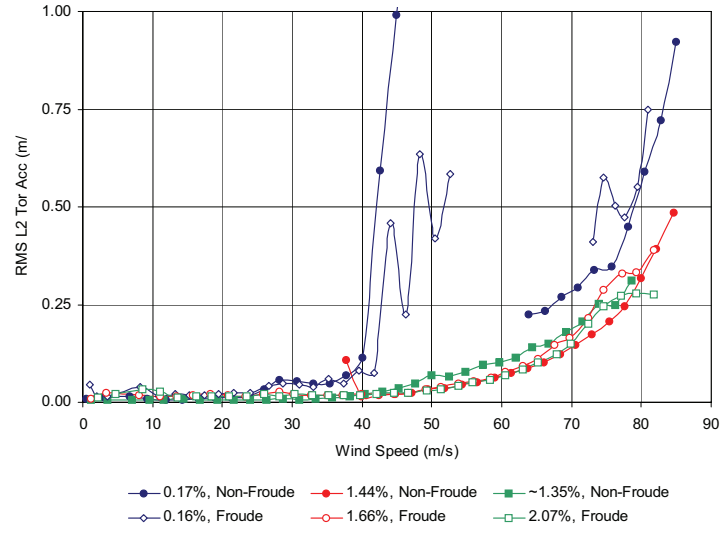

FIGURE 5.1 (CONT.) COMPARISON OF TOWER RESPONSES IN SMOOTH FLOW (LEVEL 2) FOR 0^{O} WIND, IN-SERVICE CONDITION

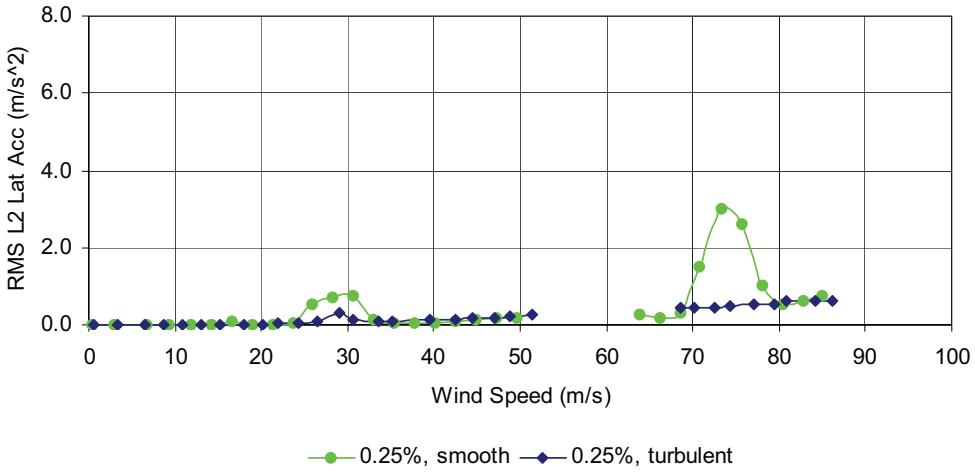

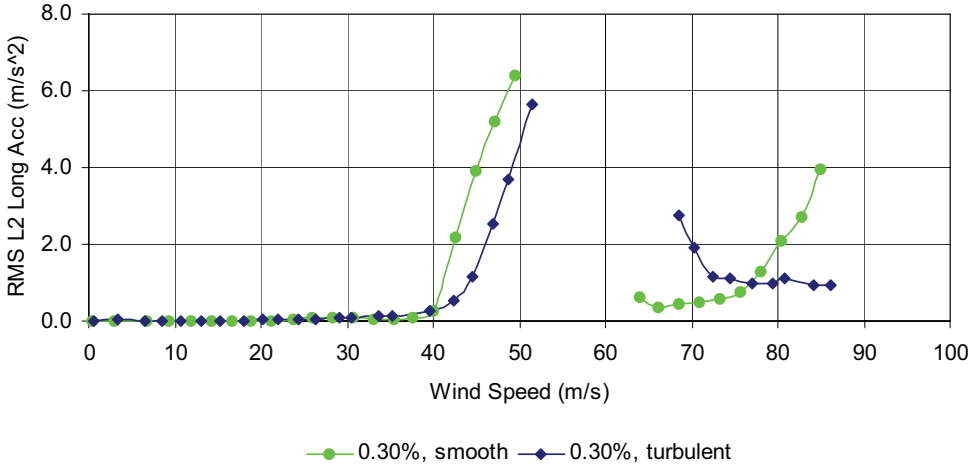

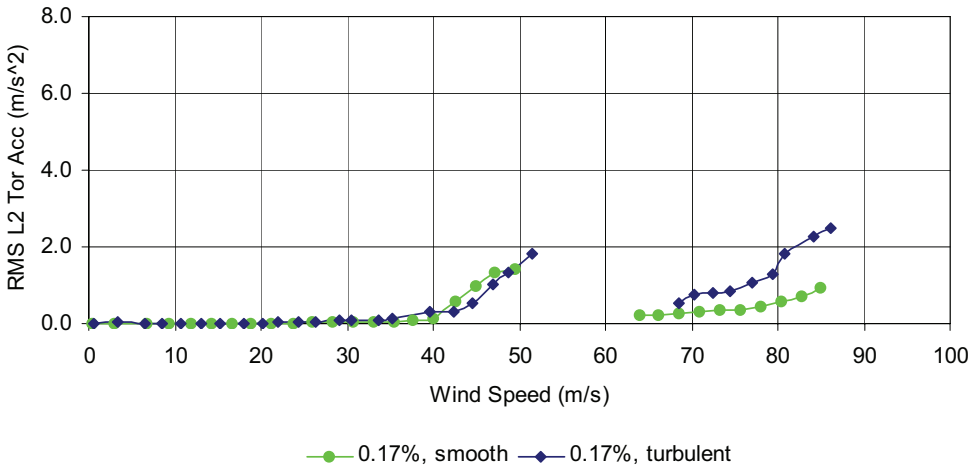

FIGURE 5.2 COMPARISON OF TOWER RESPONSES (LEVEL 2) FOR 0^{O} WIND IN SMOOTH AND TURBULENT FLOW CONDITIONS, IN-SERVICE NON-FROUDE TOWER

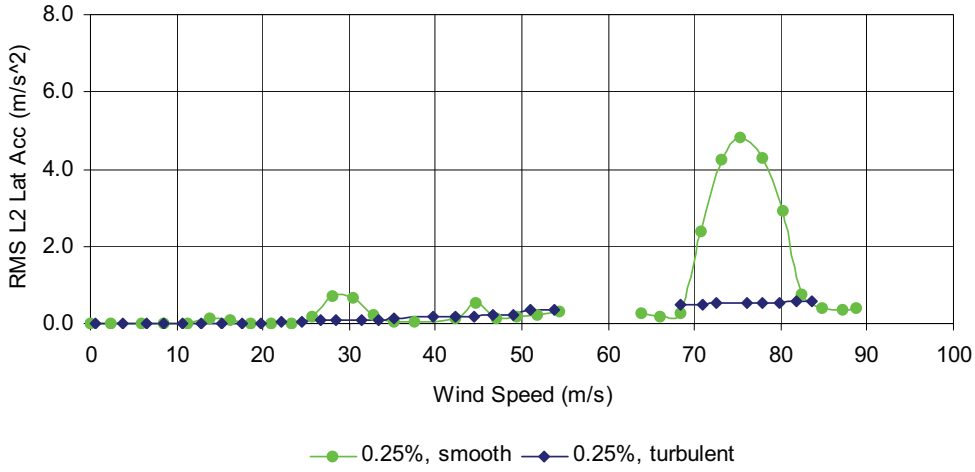

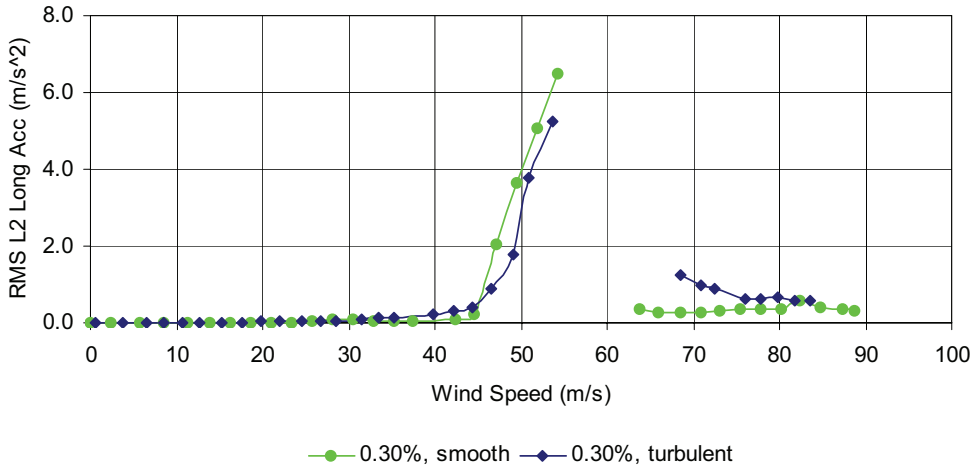

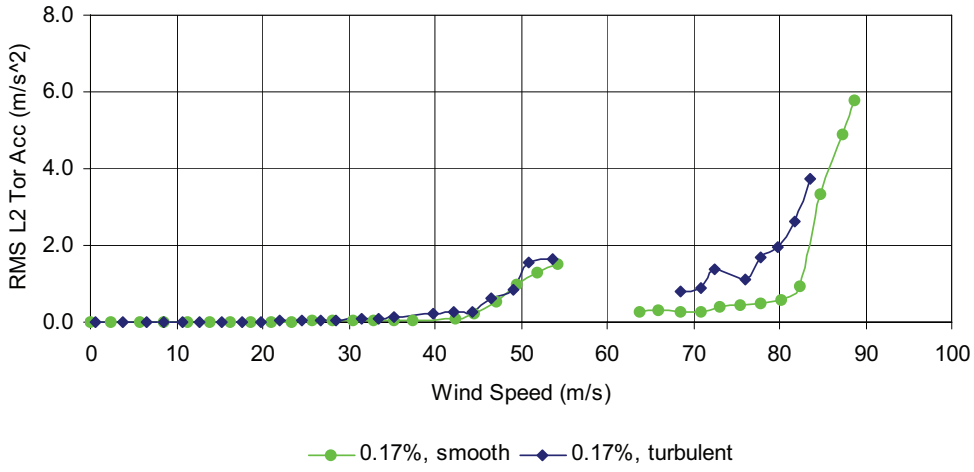

FIGURE 5.3 COMPARISON OF TOWER RESPONSES (LEVEL 2) FOR 10^{O} WIND IN SMOOTH AND TURBULENT FLOW CONDITIONS, IN-SERVICE NON-FROUDE TOWER

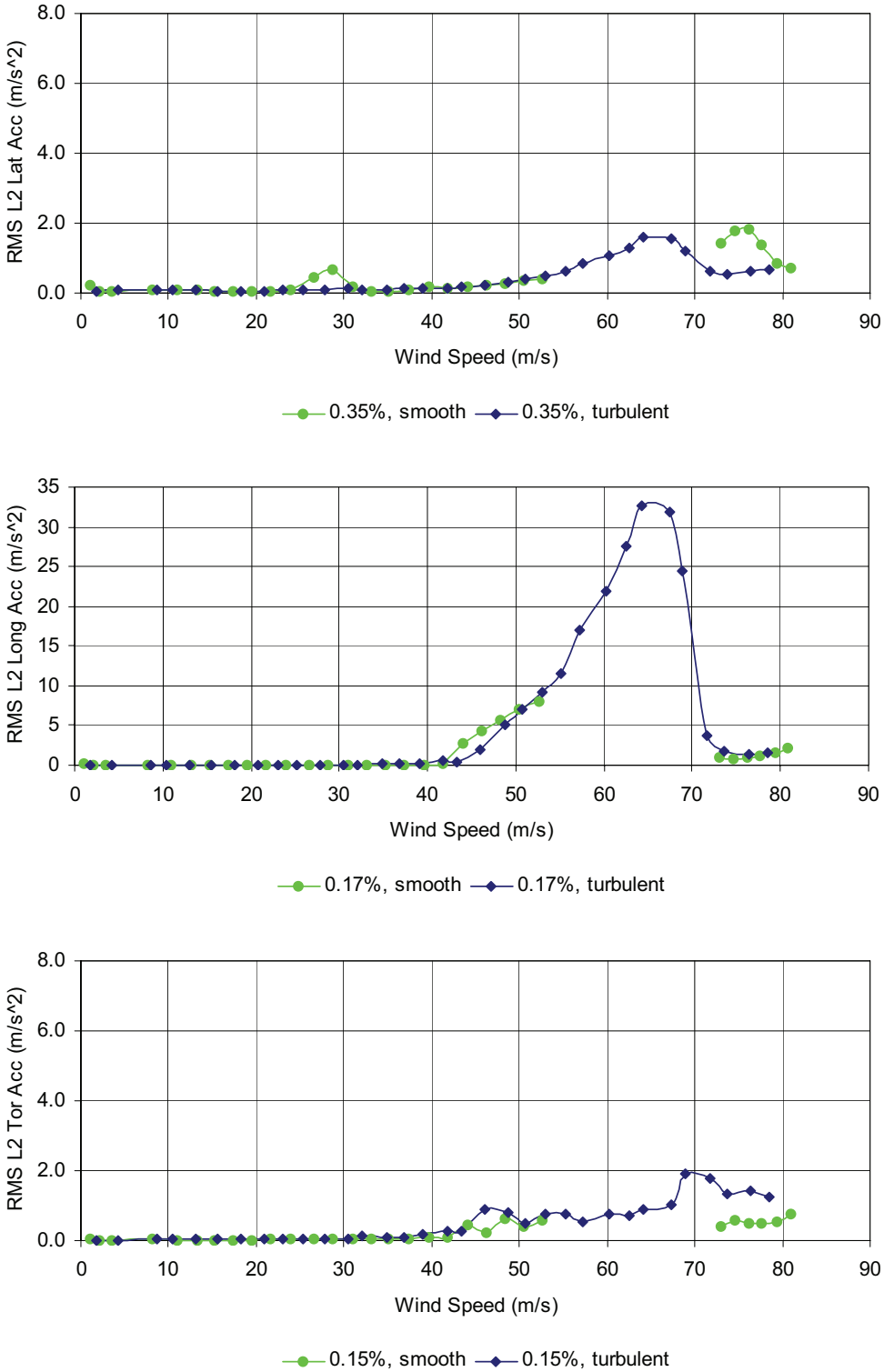

FIGURE 5.4 COMPARISON OF TOWER RESPONSES (LEVEL 2) FOR 0^{O} WIND IN SMOOTH AND TURBULENT FLOW CONDITIONS, IN-SERVICE FROUDE TOWER

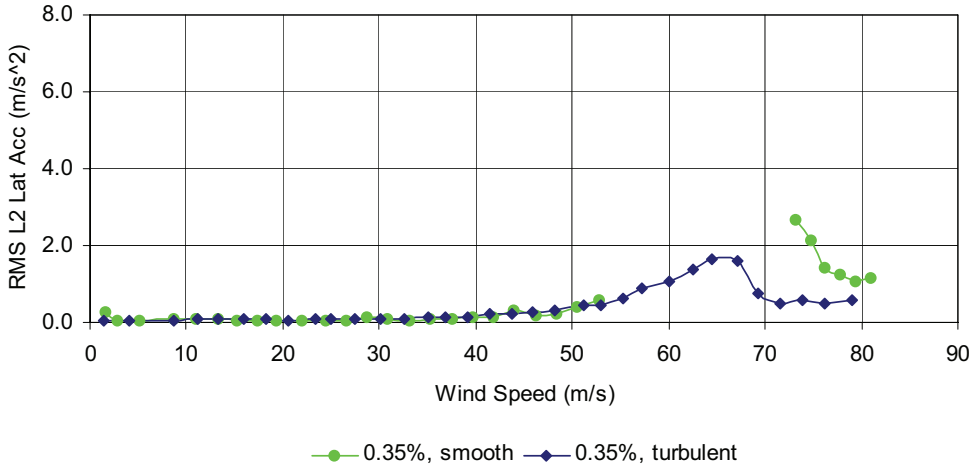

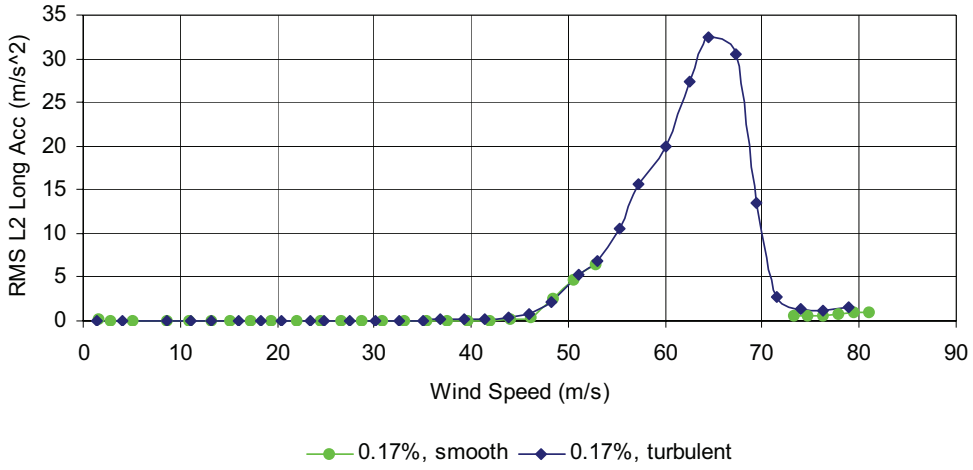

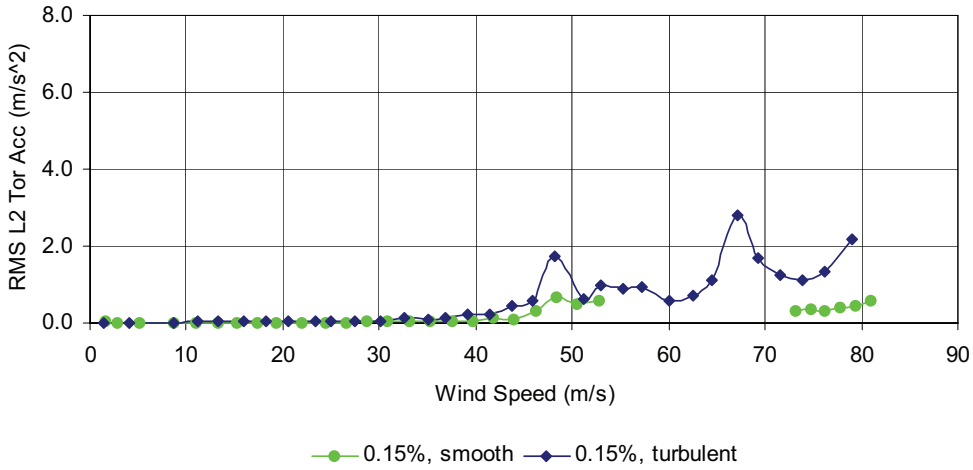

FIGURE 5.5 COMPARISON OF TOWER RESPONSES (LEVEL 2) FOR 10^{O} WIND IN SMOOTH AND TURBULENT FLOW CONDITIONS, IN-SERVICE FROUDE TOWER

Alan G. Davenport Wind Engineering Group

A STUDY OF WIND EFFECTS FOR THE

MESSINA STRAIT BRIDGE, ITALY

Non-Froude and Froude Scaled Aeroelastic Models of Tower - Sub-Test T3
APPENDICES

J.P.C. KING / L. KONG / B. BAKHT

BLWT-SS1-2011 / DRAFT 1 / JANUARY 2011

The Boundary Layer Wind Tunnel Laboratory
The University of Western Ontario, Faculty of Engineering
London, Ontario, Canada N6A 5B9; Tel: (519) 661-3338; Fax: (519) 661-3339
Internet: www.blwtl.uwo.ca; E-mail: info@blwtl.uwo.ca

TABLE OF CONTENTS

APPENDIX A

FLUTTER INSTABILITY CRITERIA

The definition of “flutter” used in this report is related to the “peak factor”, which is defined as the ratio of the largest observed reading during the sample period to the Root Mean Square (RMS) of the sample. Each of the data points on the response plots result from the measurements of real, stable, limited amplitude motion as opposed to a negative total damping case where the amplitude continues to grow in magnitude for the same wind speed. The peak factor can be used to see whether the motion is in a “locked-in” state of sinusoidal motion or only a random type motion.

The onset of a “flutter instability” is defined as when the character of the response changes from a random type motion to that of a regular, sinusoidal motion, involving either pure torsional or a coupled vertical-torsional vibration. This can be clearly identified through an examination of the peak factor. A random signal has peak factors in the 3-4 range, while a sinusoid has a peak factor of $\sqrt{2}$ or 1.41. For the purposes of this investigation, a peak factor of less than 2 was selected as the governing criteria.

There are other definitions of flutter that have been used by this Laboratory and other researchers. One could determine a limiting amplitude beyond which the response is unacceptable. This criterion was used for the Tsing Ma Bridge [A1] and Ting Kau Bridge [A2] studies with a limiting RMS torsional amplitude of 0.5^{o} (or a peak amplitude of 3.5^{o} on the response plots).

Another method, has been also used, is based on the steepness of the response curves with wind speed to determine flutter instability. This has some logic associated with it since there is a very definite chance in the character of the response from a uniform, steady growth with wind speed to that which is becoming alarmingly violent. However, the steepness of the curves is highly dependent on the total damping of the structure (structure plus aerodynamic damping). In the low wind speed areas, the structural term dominates (or the aerodynamic term is positive). In the high wind speed range, the aerodynamic term dominates and is negative, but does not yet exceed the structural term in magnitude. Infinite amplitudes occur when the total damping becomes equal to zero or negative, since response is inversely proportional to the total damping.

REFERENCES - APPENDIX A

A1. King, J.P.C. and Davenport, A.G., "Lantau Fixed Crossing - Tsing Ma Bridge, Full Aeroelastic Model Tests of Completed Bridge", The University of Western Ontario, Faculty of Engineering Science Research Report, BLWT-SS11-1997, London, Ontario, Canada, 1997.

A2. King, J.P.C. and Davenport, A.G., "Ting Kau Bridge - Wind Tunnel Report", The University of Western Ontario, Faculty of Engineering Science Research Report, BLWT-SS29-1995, London, Ontario, Canada, 1995.

APPENDIX B

RESULTS OF NON-FROUDE TOWER MODEL, CONSTRUCTION STAGE

Notes:

B1. The wind speed indicated is the mean hourly wind speed in m/s at the tower height. The bending moments and torques given in the plots have the unit of kN-m. The accelerations have the unit of m/s^2. The displacements have the units of m in the longitudinal direction and degree for tower rotation.

B2. The mean and RMS (root mean square) responses are given separately in the plots. The total responses should be calculated as the mean plus or minus the RMS multiplied by the appropriate peak factor.

B3. Refer to Figure B1 for the definition of test wind angles.

B4. Refer to Figure B2 and Table B1 for the instrumentation locations and sign convention used.

B5. Table B2 summarizes the test results and corresponding test conditions.

TABLE B1 INSTRUMENTATION LOCATIONS, NON-FROUDE TOWER MODEL

Instrumentation	Instrumentation Locations
Strain Gauges (Tower Legs):	
M_x, M_y and M_Z,, Base of Leg A	Bending moments measured on Leg A at ??? m above Leg A base (or ground??)
M_x and M_y, Level 1 of Leg A	Bending moments measured on Leg A, ??? m above ???
M_x and M_y, Level 2 of Leg A	Bending moments measured on Leg A, ??? m above ???
M_x, M_y and M_Z,, Base of Leg B	Bending moments measured on Leg B at ??? m above Leg B base (or ground??)
M_x and M_y, Level 1 of Leg B	Bending moments measured on Leg B, ??? m above ???
M_x and M_y, Level 2 of Leg B	Bending moments measured on Leg B, ??? m above ???
Strain Gauges (X-Beams):	
M_z and M_x, Level 1	Bending moments measured on X-beam, ??? m from Mid location towards to Leg A
M_z and M_x, Level 2	Bending moments measured on X-beam, ??? m from Mid location towards to Leg A
M_z and M_x, Level 3	Bending moments measured on X-beam, ??? m from Mid location towards to Leg A
Accelerometers:	
x, y and Torsional accelerations, Level 2	Accelerations measured at 246.4 m above ground
x, y and Torsional accelerations, Level 3	Accelerations measured at 373.4 m above ground
Lasers (January 2011 Test only):	
x displacement and rotation, Level 2	Tower displacement along bridge axis and tower rotation measured at 238.7 m above ground
Wind Speeds:	
Deck Height	At a height of 66 m full scale above ground
Tower Height	At a height of 399 m full scale above ground
Mid Tower Height	At a height of 199 m full scale above ground
Reference Height	Where the wind speed not affected by the boundary layer of the wind tunnel floor

Notes:

1. Right-hand rule used for sign convention.
2. x – along bridge axis; y – perpendicular to bridge axis (lateral to tower)

TABLE B2 SUMMARY OF NON-FROUDE TOWER MODEL TESTS, CONSTRUCTION STAGE

Test Configuration	Test No.	Test Files	Modal Frequency (Hz) and Damping (%)			Wind Angle	Maximum Wind Speed	Level 3 Maximum Acceleration Observed		
			Long.	Lat.	Tor.	Deg	m/s	m/s^2	Direction occurred	Wind speed (m/s)
Smooth flow, inherent damping	1	M075a1E01R002	4.1 (0.33~0.35)	10.02 (1.10~1.17)	12.26 (0.10~0.11)	0 (Lat.)	51	6.759	Tor	31
	2	M075a1E01R003				2.5	51	7.481	Tor	30
	3	M075a1E01R004				5	51	7.831	Tor	31
	4	M075a1E01R005				7.5	51	8.611	Tor	33
	5	M075a1E01R006				10	50	9.312	Tor	33
Smooth flow, 2% nominal damping	6	M075a2E01R002	4.1 (2.45~2.51)	10 (0.91~0.96)	11.93 (1.24~1.34)	0 (Lat.)	55	6.357	Tor	55
	7	M075a2E01R003				2.5	55	6.371	Tor	55
	8	M075a2E01R004				10	55	0.496	Lat	40
Smooth flow, 4% nominal damping	9	M075a3E01R002	4.1 (3.77~3.81)	10 (0.96~1.08)	12.03 (1.73~1.81)	0 (Lat.)	53	0.612	Tor	53
	10	M075a3E01R003				2.5	52	0.600	Tor	52
	11	M075a3E01R004				10	52	0.216	Tor	52
Turbulent boundary layer flow, inherent damping	12	M075a4E02R002	4.1 (0.33~0.35)	10.02 (1.10~1.17)	12.26 (0.10~0.11)	0 (Lat.)	49	4.186	Tor	29
	13	M075a4E02R003				2.5	48	4.480	Tor	29
	14	M075a4E02R004				5	48	5.216	Tor	29
	15	M075a4E02R005				7.5	46	6.804	Tor	31
	16	M075a4E02R006				10	46	7.586	Tor	33
	17	M075a4E02R015				20	46	20.243	Tor	46
	18	M075a4E02R022				30	50	6.180	Tor	47
	19	M075a4E02R023				40	50	0.673	Tor	45
	20	M075a4E02R024				50	50	0.473	Tor	40
	21	M075a4E02R025				60	49	0.505	Tor	40
	22	M075a4E02R026				70	50	0.331	Tor	50
	23	M075a4E02R027				80	50	0.478	Lat	50
	24	M075a4E02R028				90 (Long.)	50	0.517	Lat	50

Notes:

1. Maximum wind speed is the equivalent hourly mean wind speed at the top of the tower using a velocity scale of 1:6.
2. Long. = Longitudinal direction (along deck), Lat. = Transverse direction with respect to the axis of the bridge deck

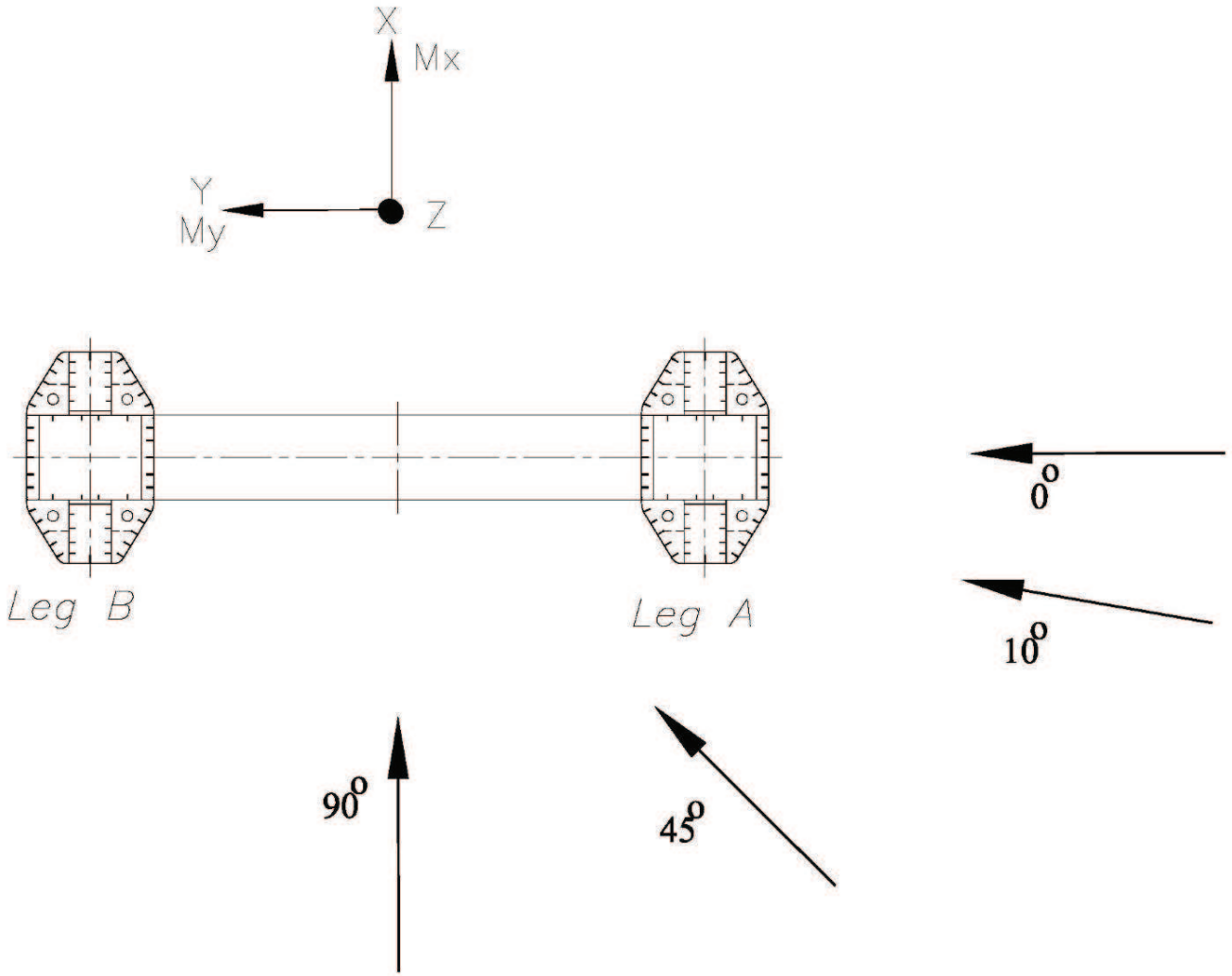

FIGURE B1 DEFINITION OF WIND ANGLES USED IN THE MESSINA TOWER TEST

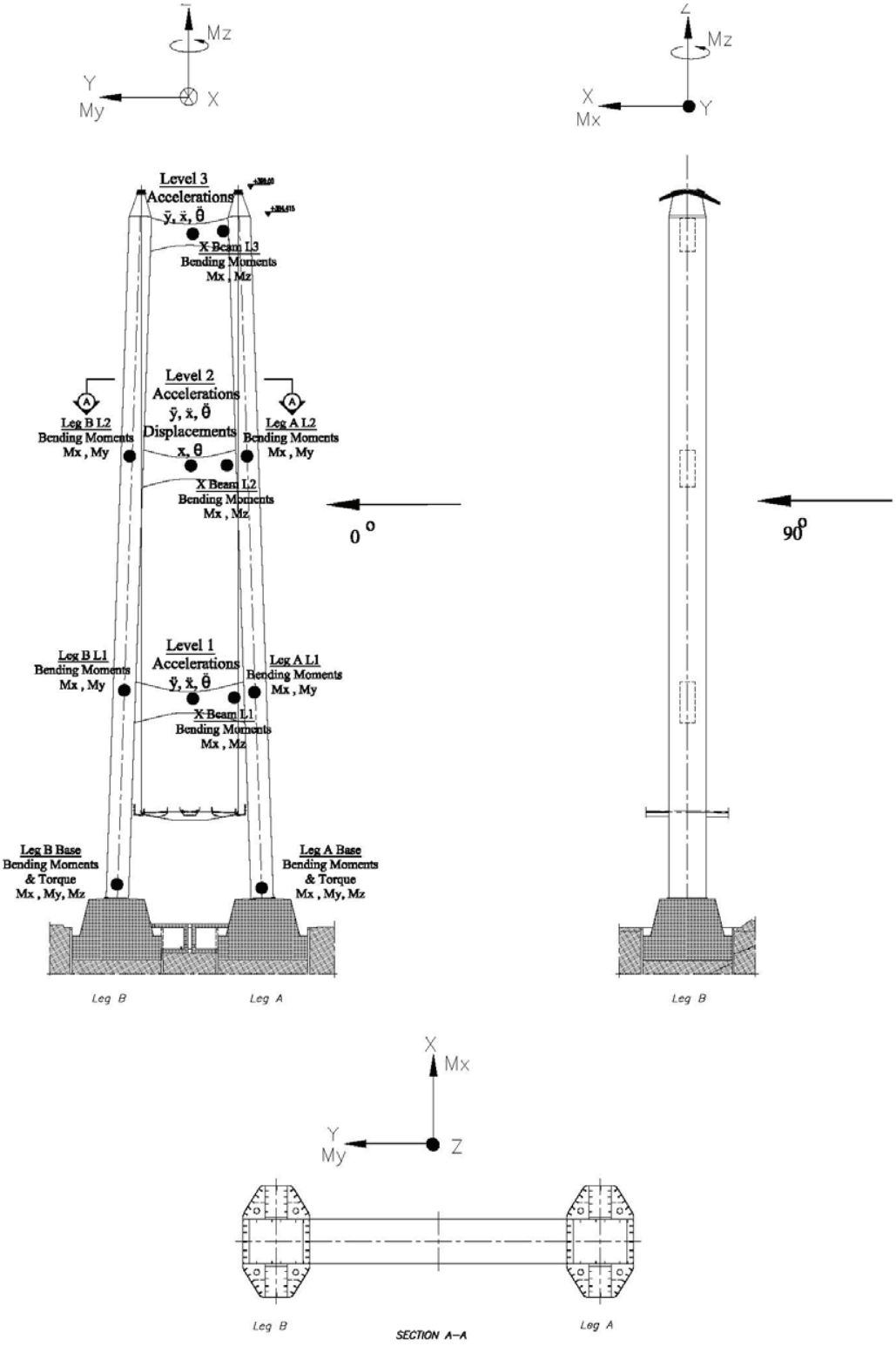

FIGURE B2 INSTRUMENTATION LOCATIONS AND SIGN CONVENTIONS USED IN THE NON-FROUDE TOWER TEST

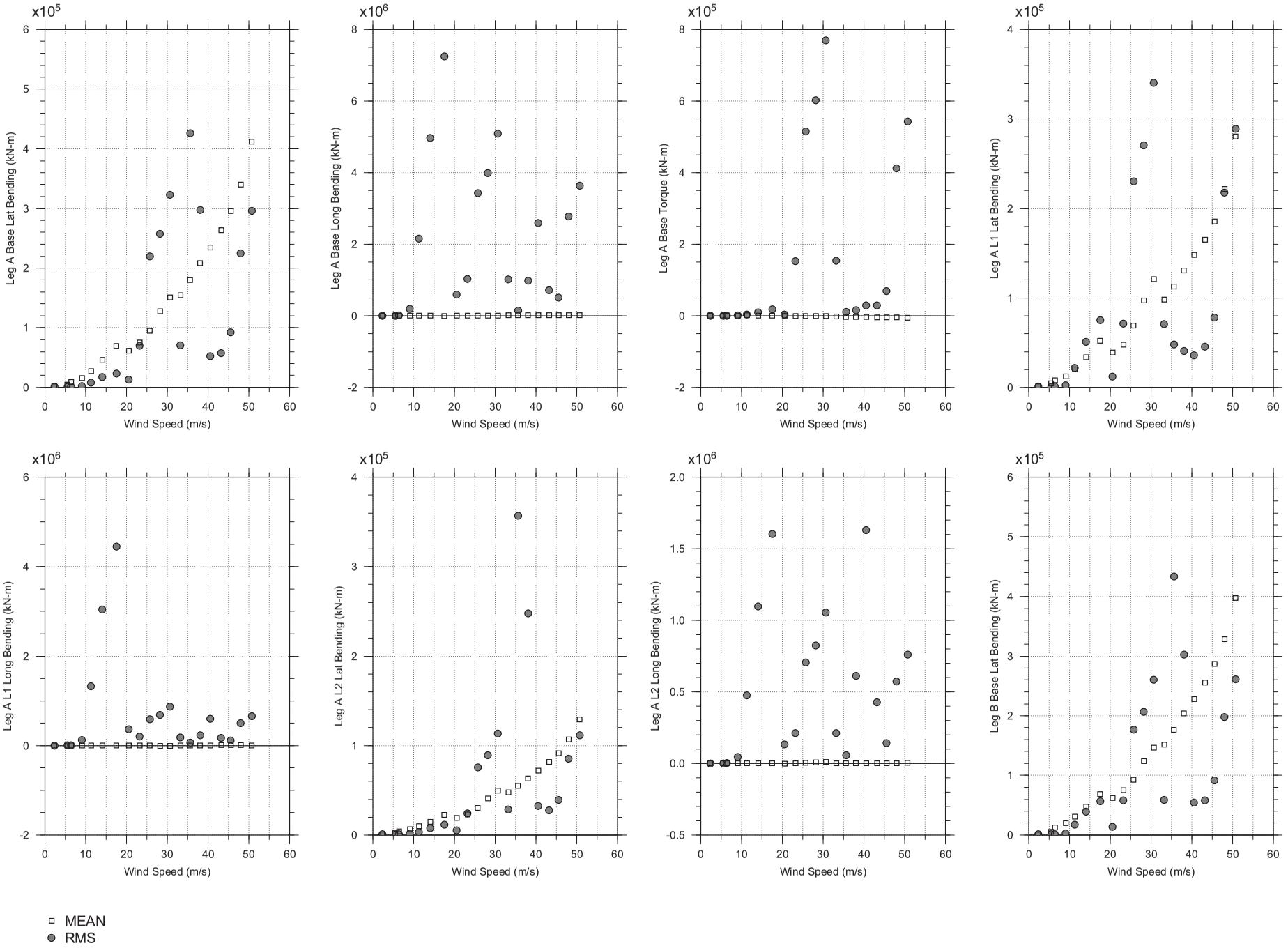

Messina Bridge, Free Standing Tower, 0 degree, Smooth Flow

Dec. 13, 2010
tf11abdg.cl

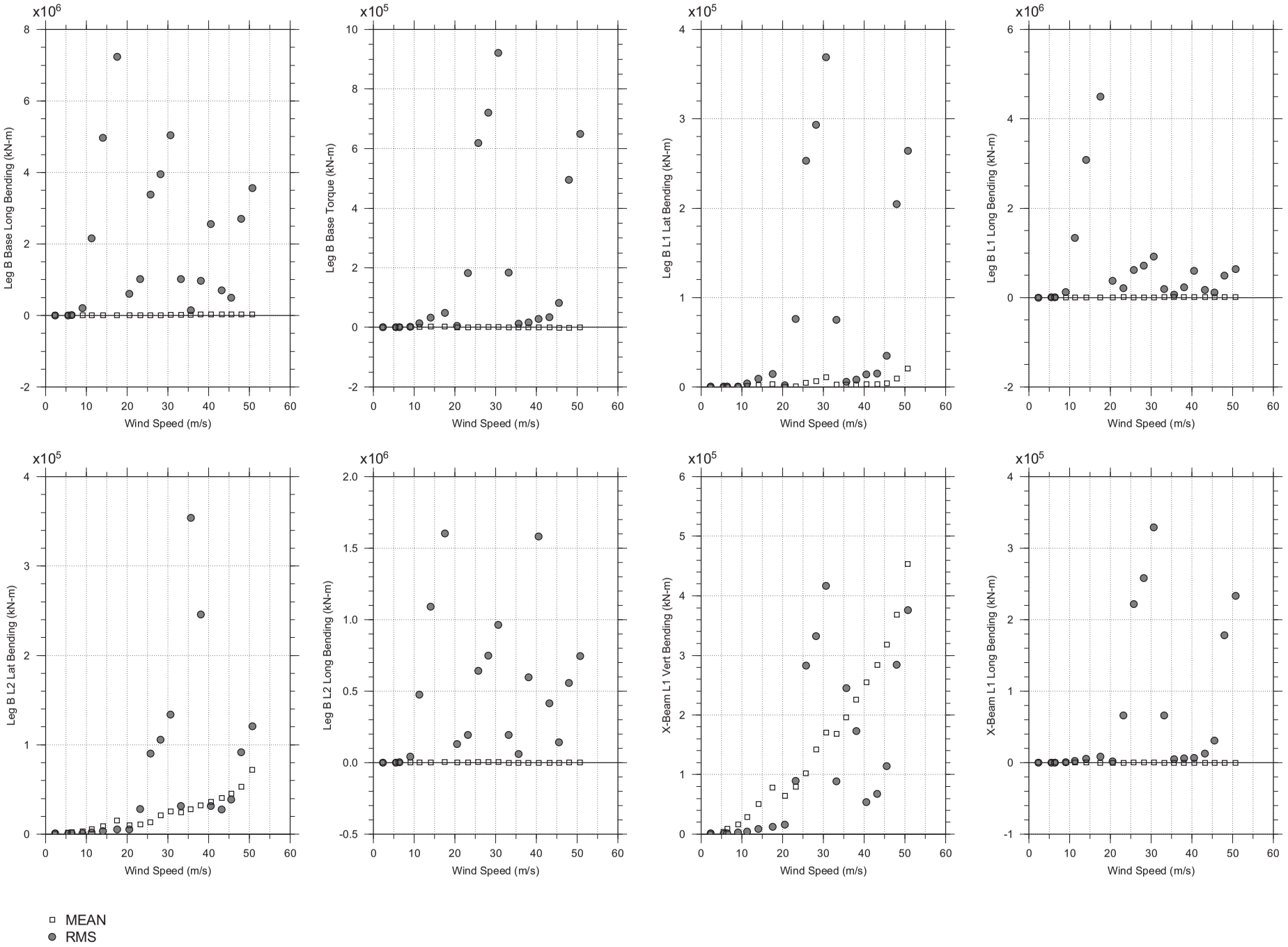

Messina Bridge, Free Standing Tower, 0 degree, Smooth Flow

Dec. 13, 2010
tf11abdg.cl

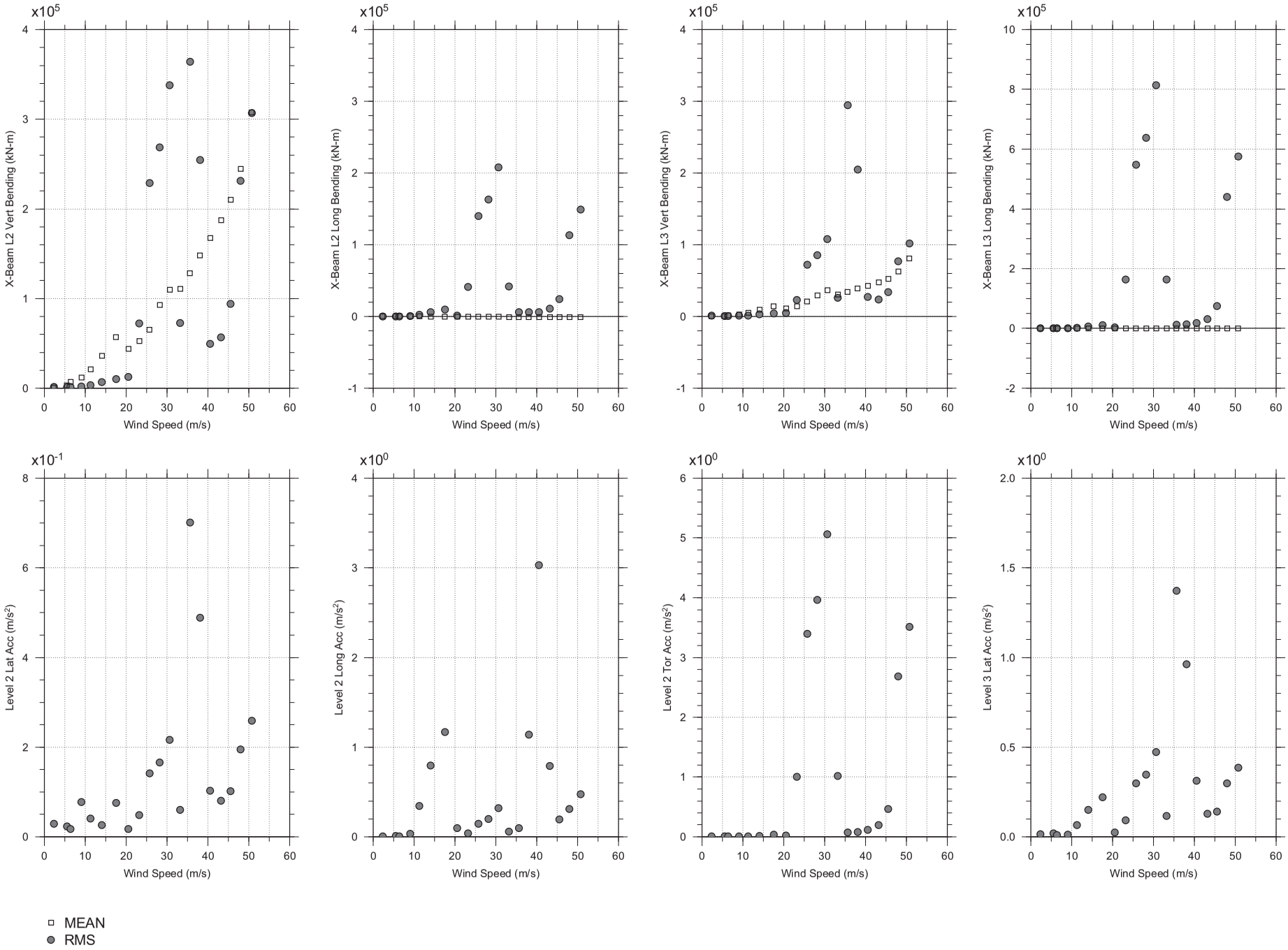

Messina Bridge, Free Standing Tower, 0 degree, Smooth Flow

Dec. 13, 2010
tf11abdg.cl

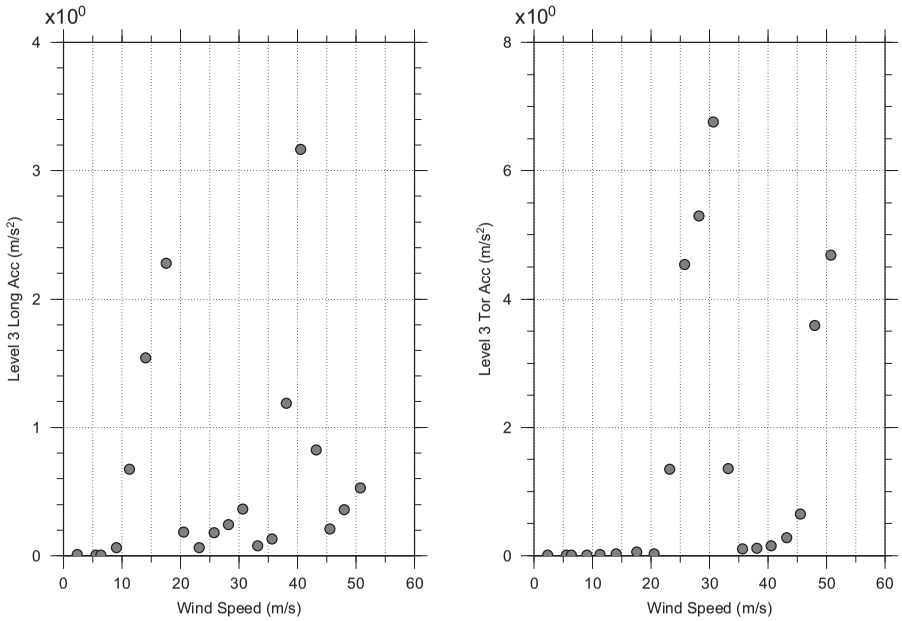

MEAN
RMS

Messina Bridge, Free Standing Tower, 0 degree, Smooth Flow

Dec. 13, 2010
tf11abdg.cl

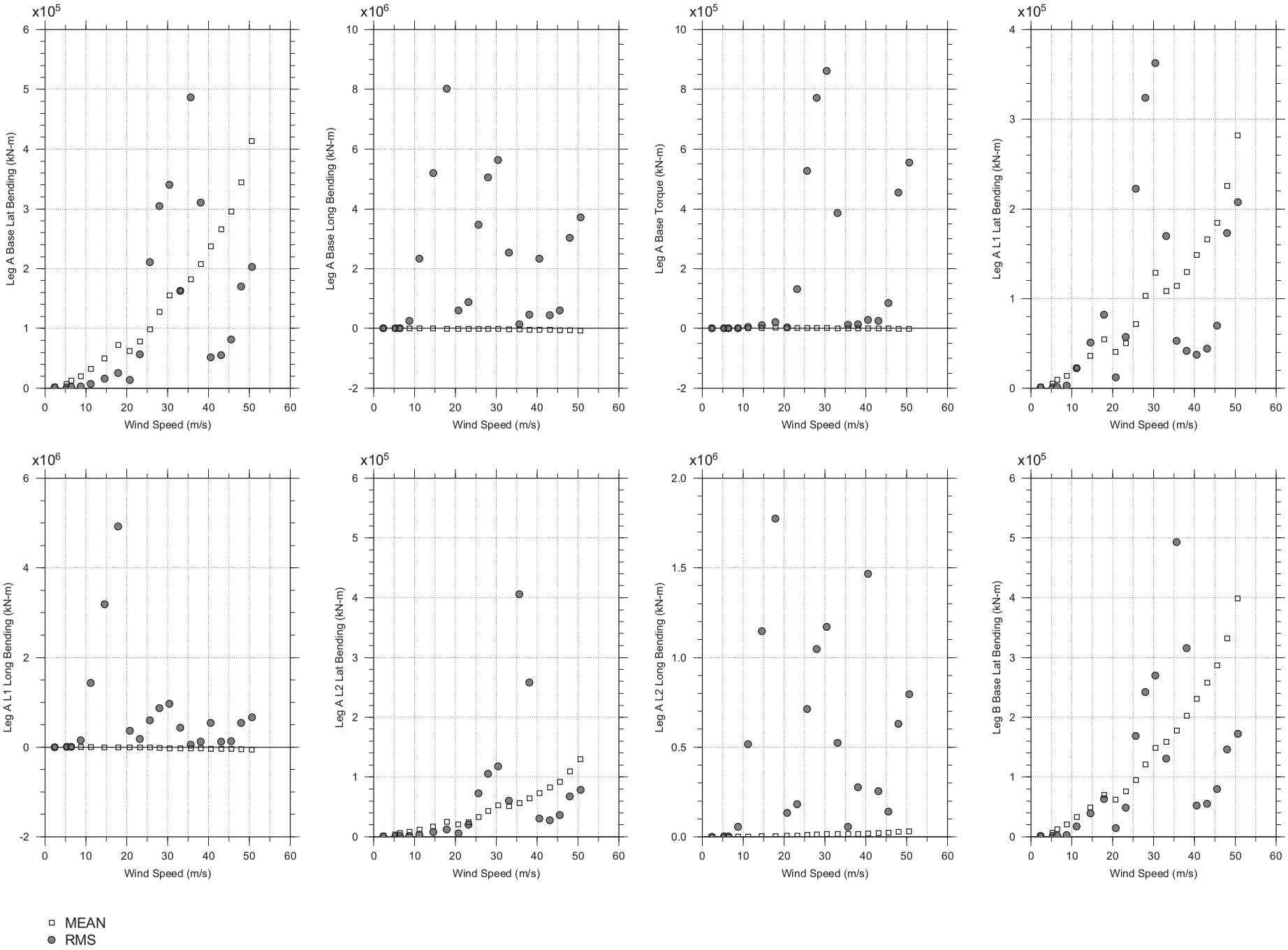

Messina Bridge, Free Standing Tower, 2.5 degree, Smooth Flow

Dec. 13, 2010
tf12abdg.cl

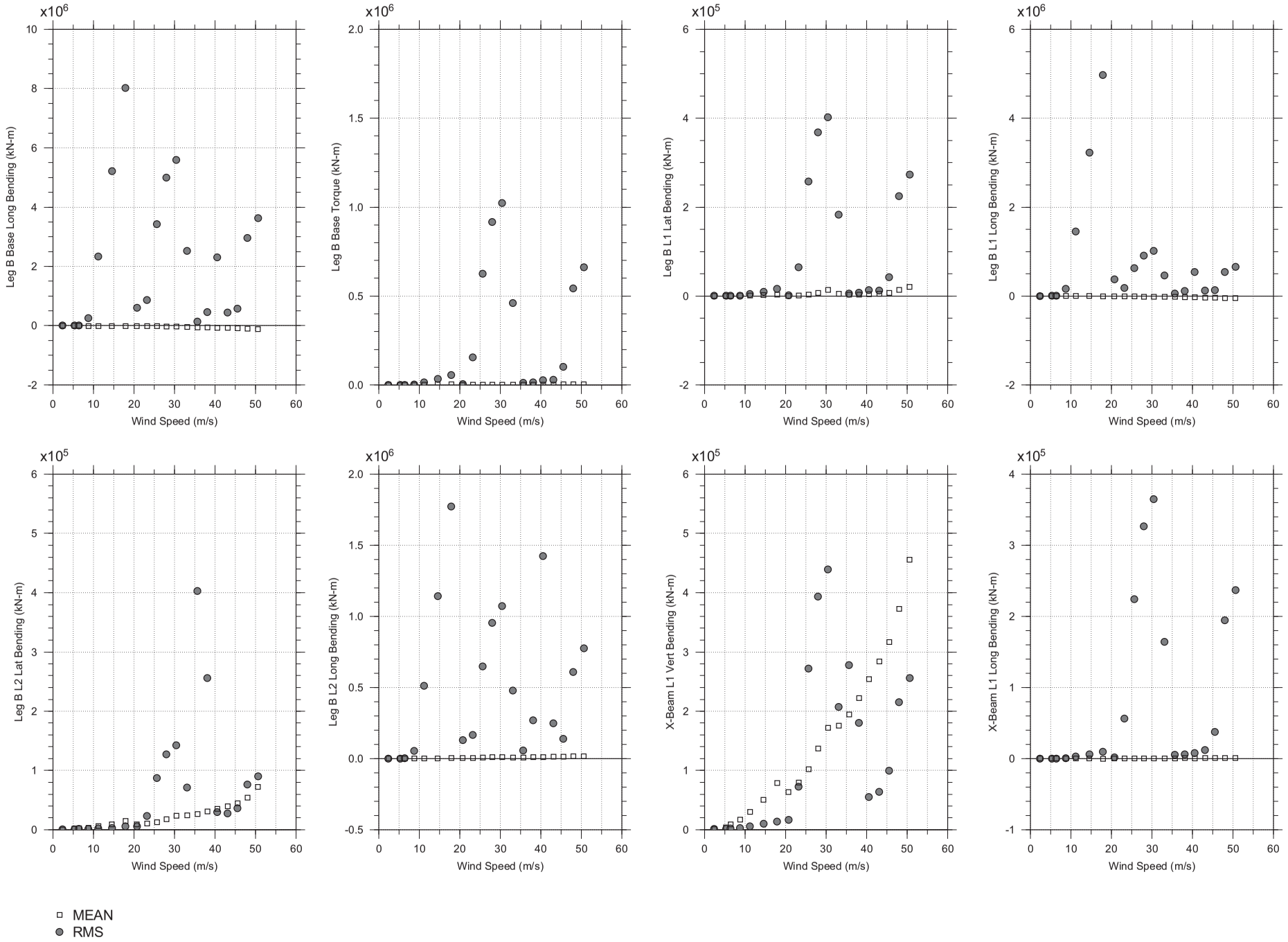

Messina Bridge, Free Standing Tower, 2.5 degree, Smooth Flow

Dec. 13, 2010
tf12abdg.cl

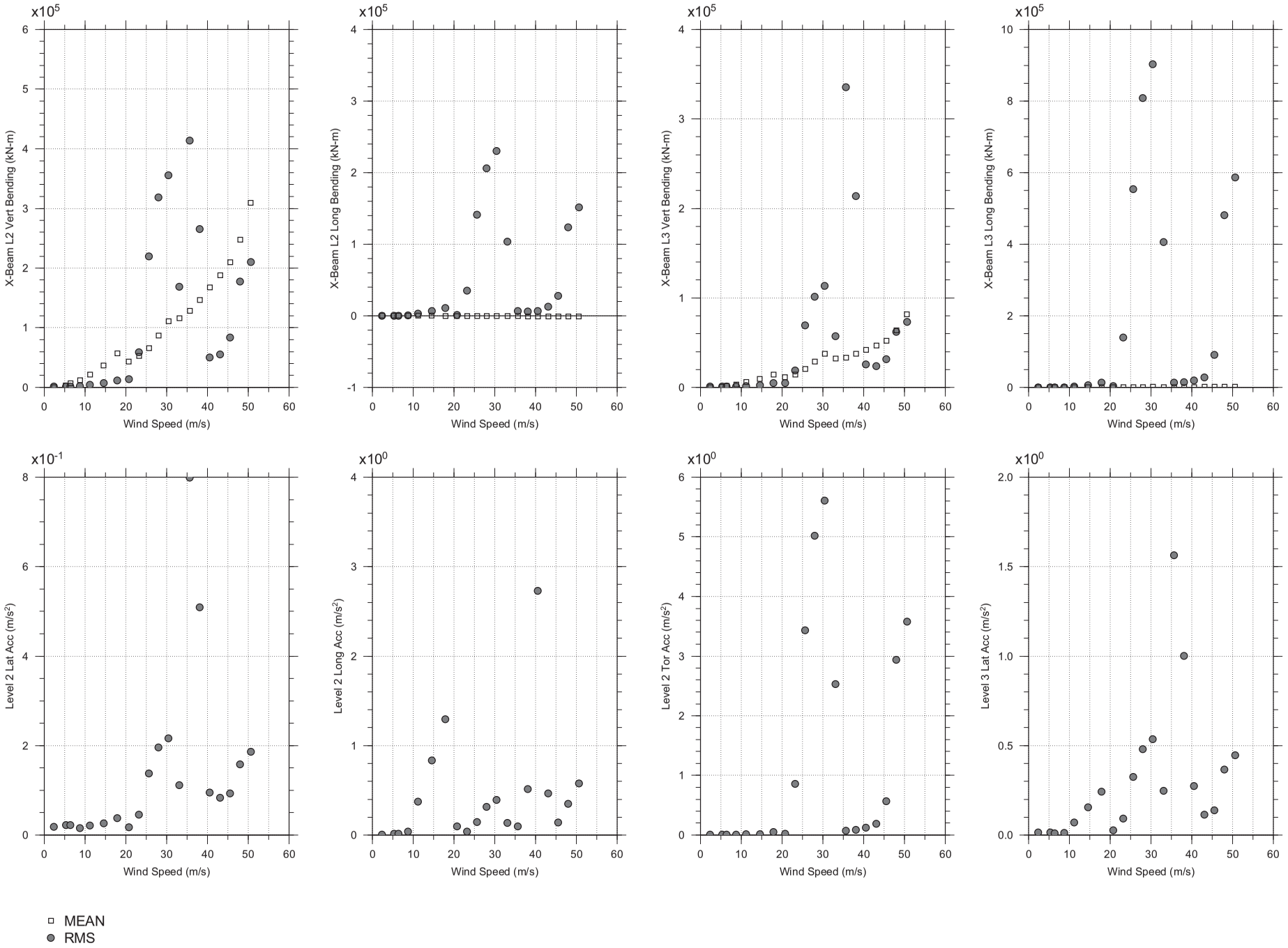

Messina Bridge, Free Standing Tower, 2.5 degree, Smooth Flow

Dec. 13, 2010
tf12abdg.cl

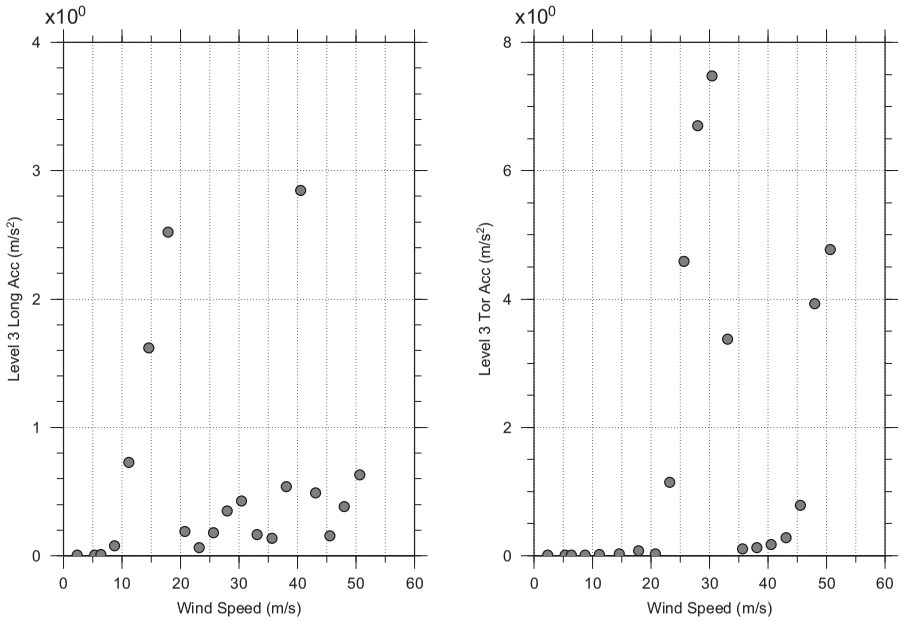

MEAN
RMS

Messina Bridge, Free Standing Tower, 2.5 degree, Smooth Flow

Dec. 13, 2010
tf12abdg.cl

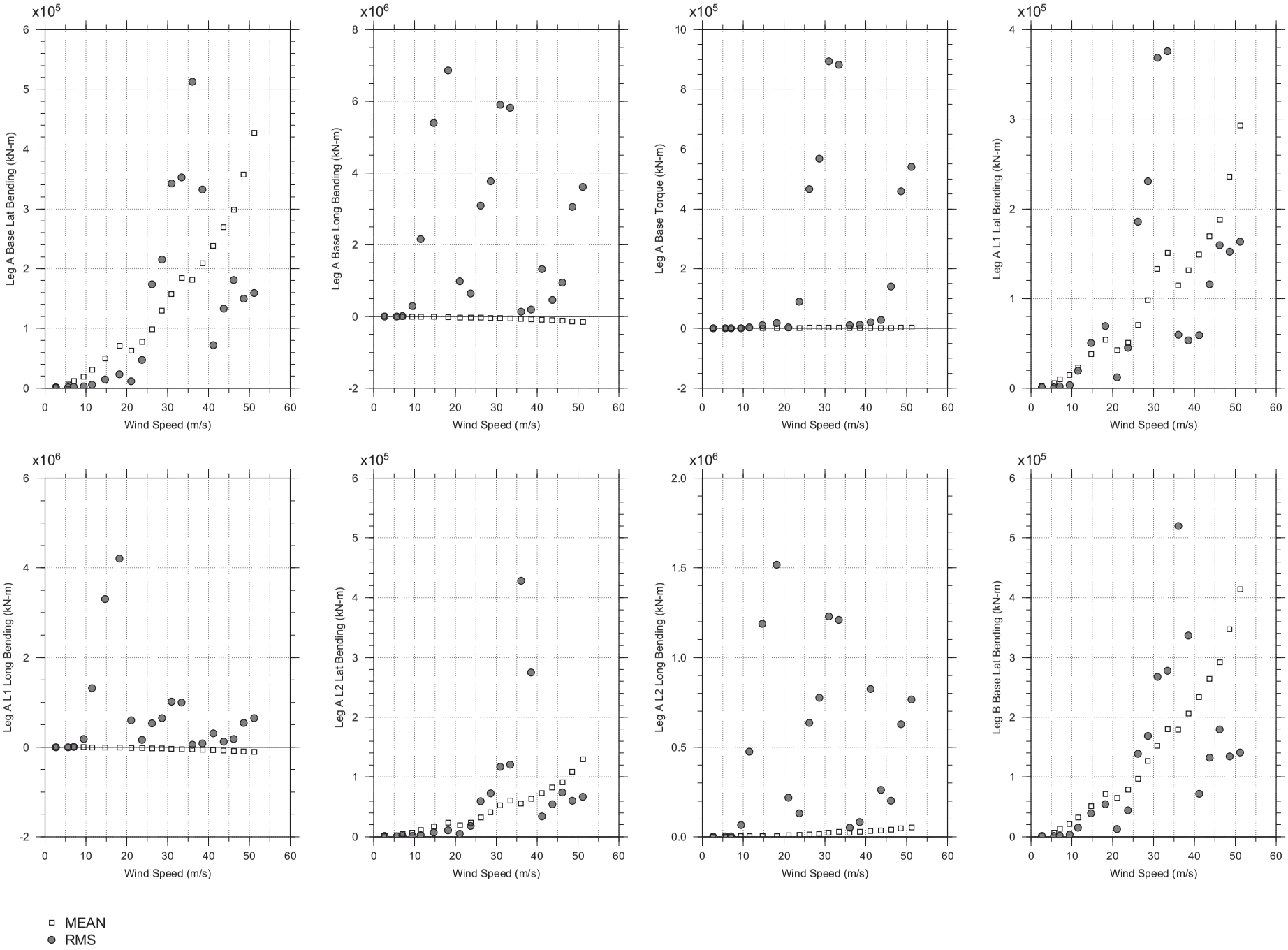

Messina Bridge, Free Standing Tower, 5 degree, Smooth Flow

Dec. 13, 2010
tf13abdg.cl

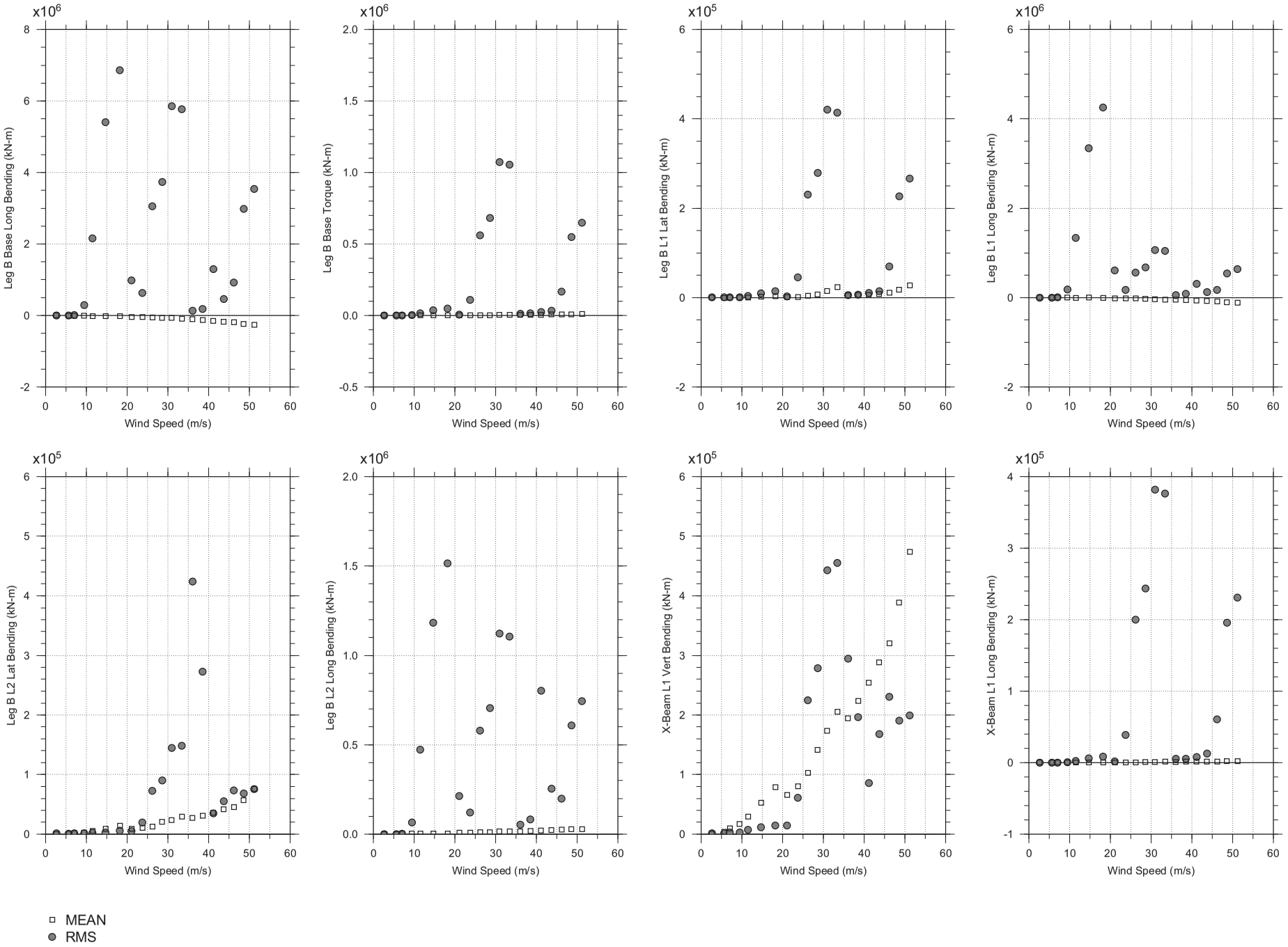

Messina Bridge, Free Standing Tower, 5 degree, Smooth Flow

Dec. 13, 2010
tf13abdg.cl

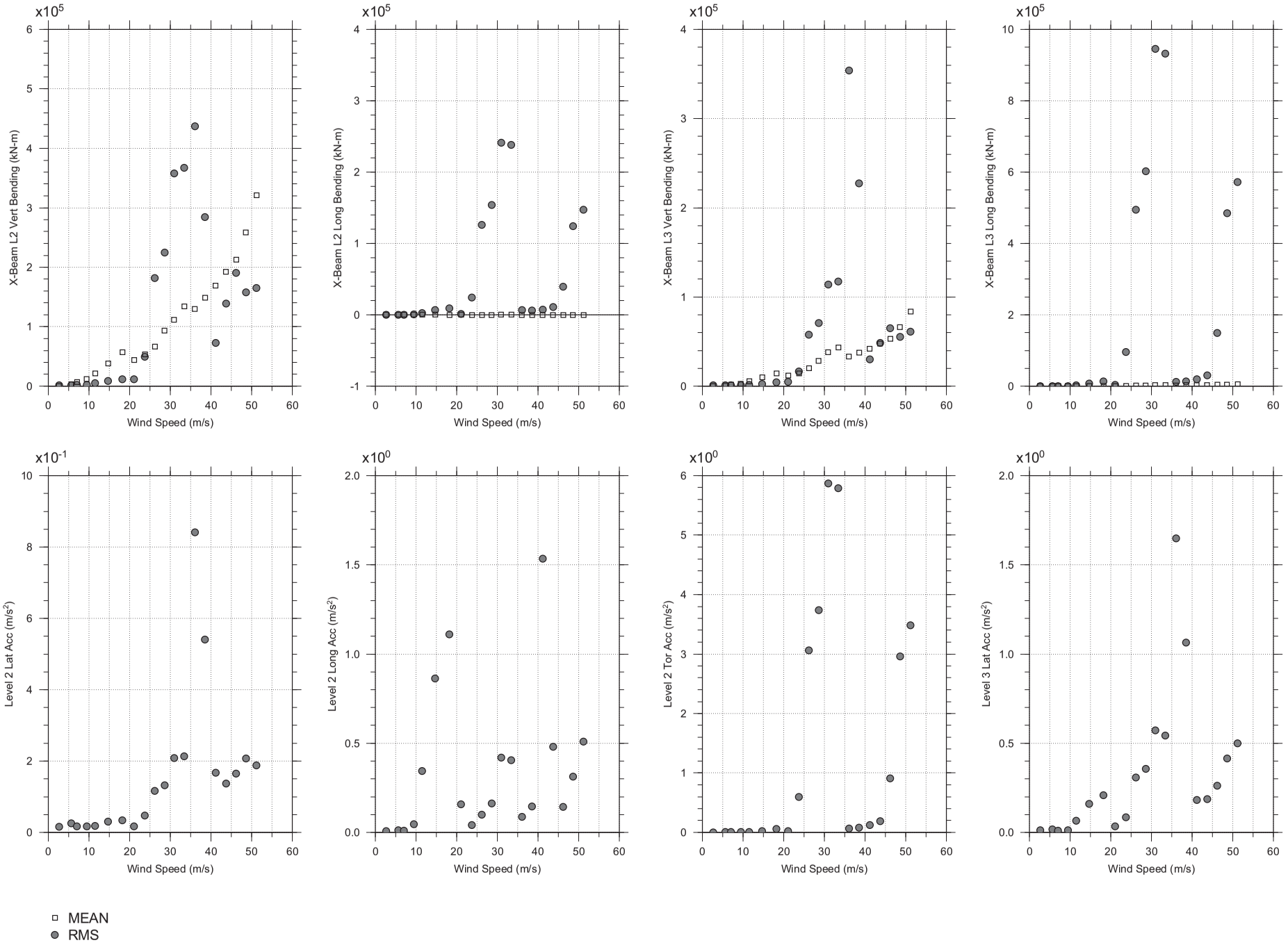

Messina Bridge, Free Standing Tower, 5 degree, Smooth Flow

Dec. 13, 2010
tf13abdg.cl

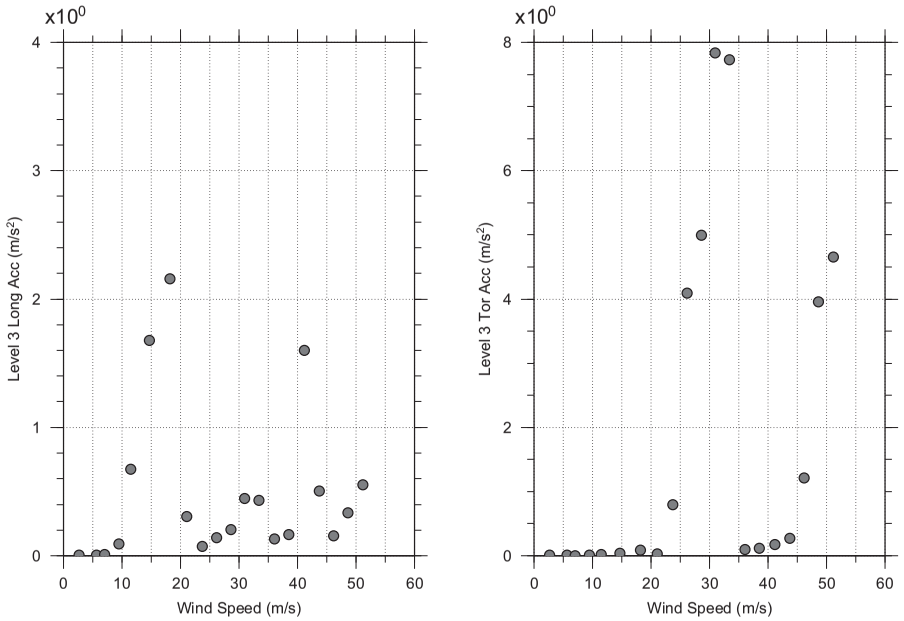

MEAN
RMS

Messina Bridge, Free Standing Tower, 5 degree, Smooth Flow

Dec. 13, 2010
tf13abdg.cl

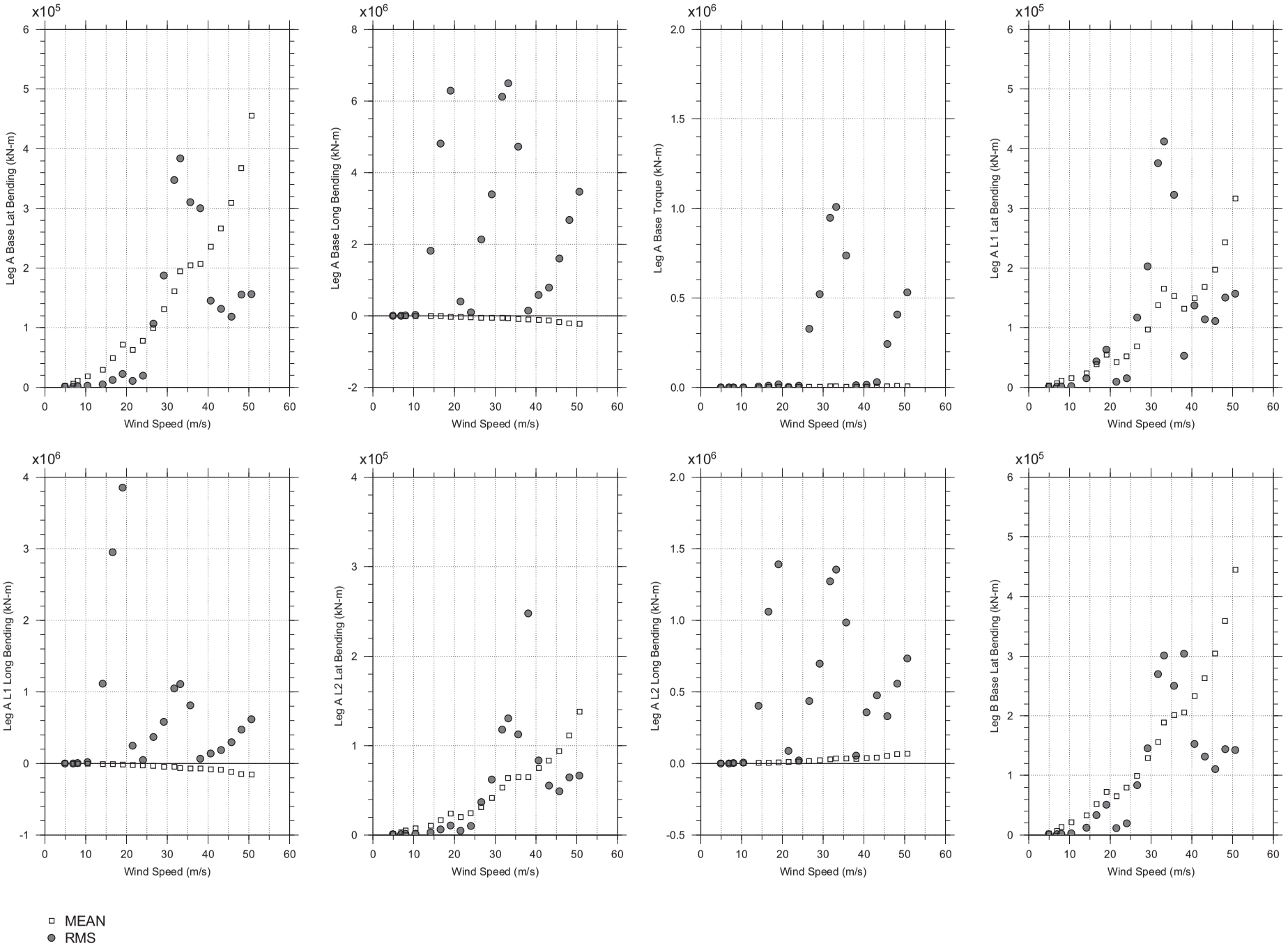

Messina Bridge, Free Standing Tower, 7.5 degree, Smooth Flow

Dec. 13, 2010
tf14abdg.cl

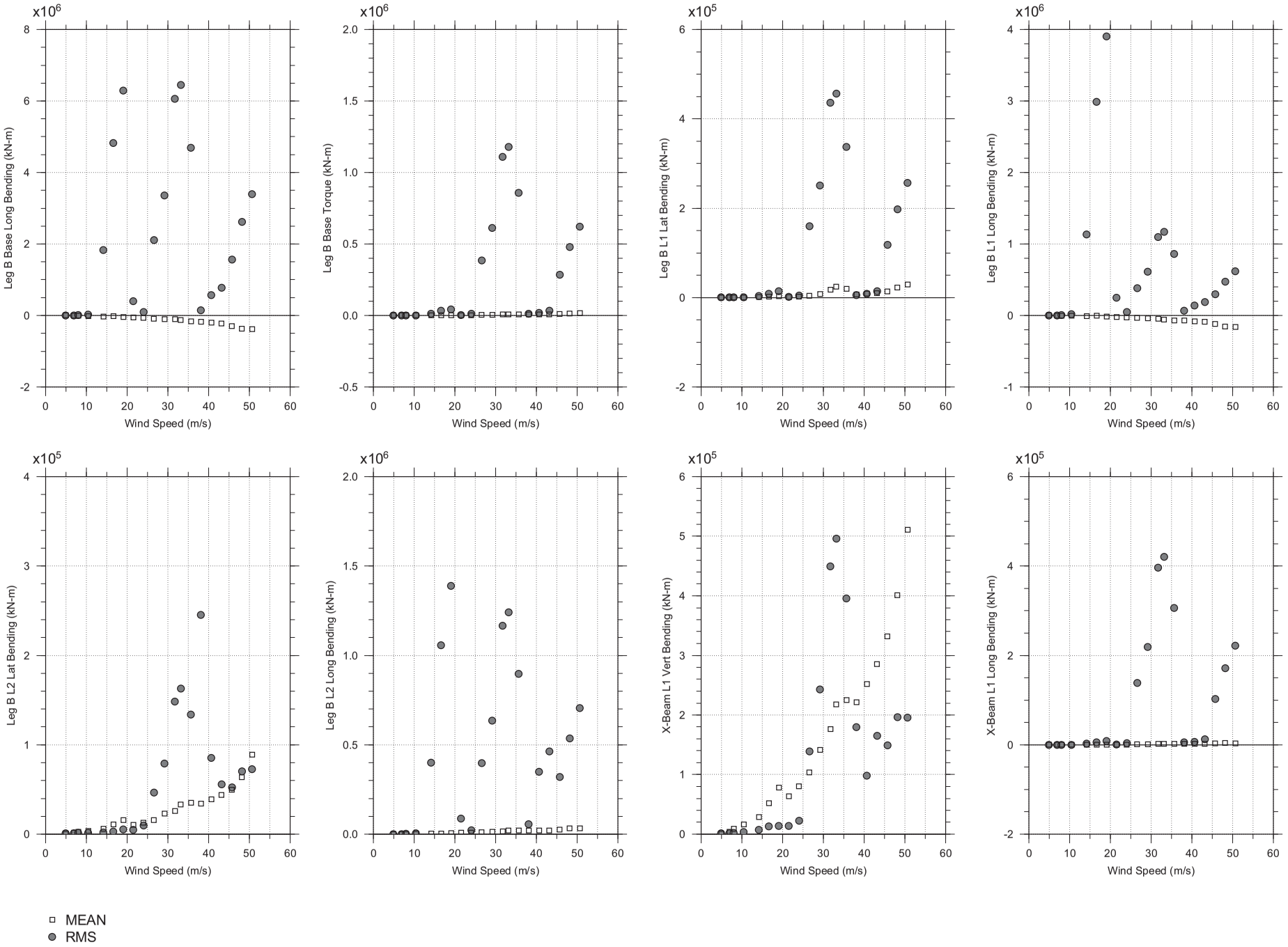

Messina Bridge, Free Standing Tower, 7.5 degree, Smooth Flow

Dec. 13, 2010
tf14abdg.cl

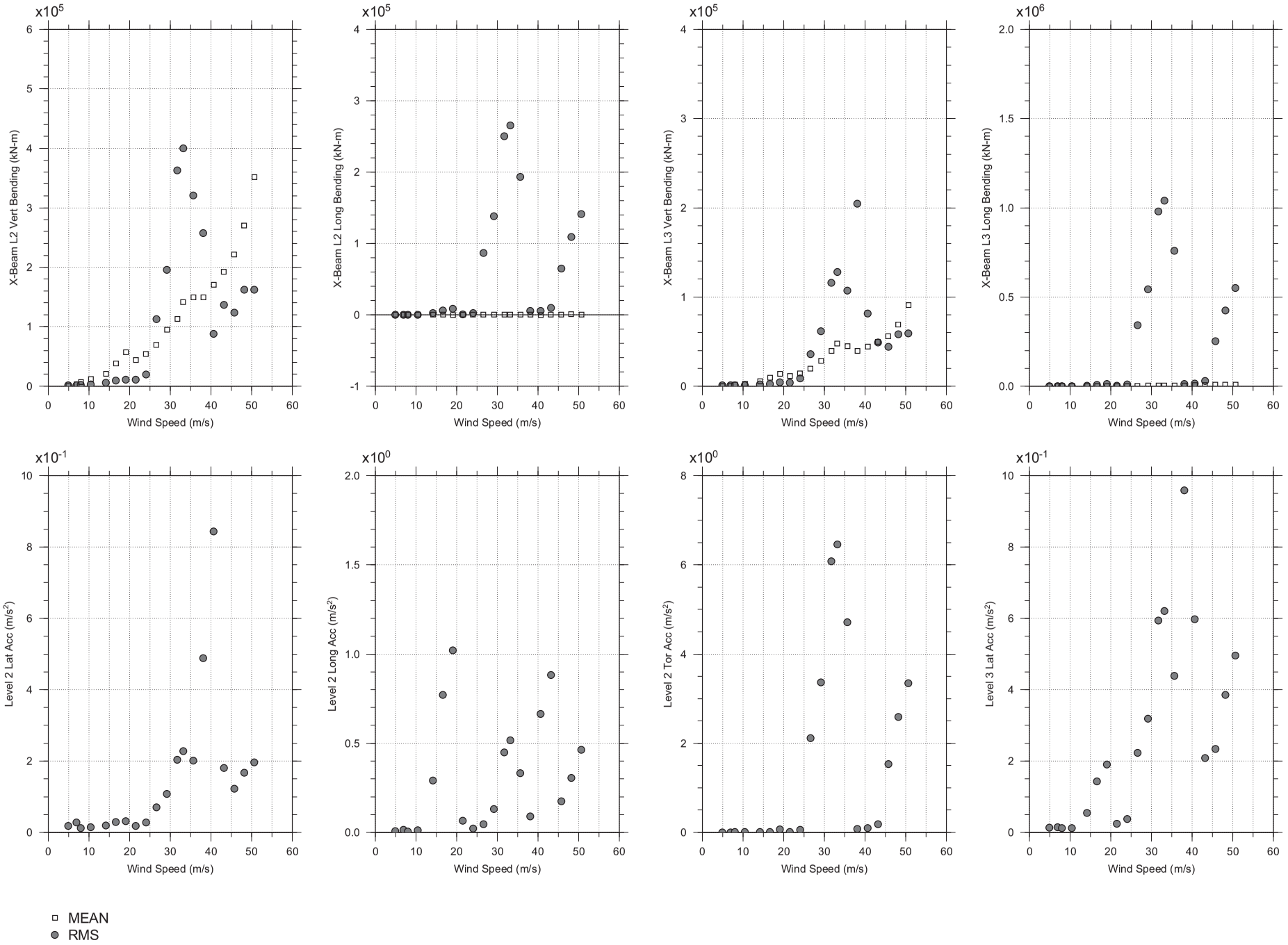

Messina Bridge, Free Standing Tower, 7.5 degree, Smooth Flow

Dec. 13, 2010
tf14abdg.cl

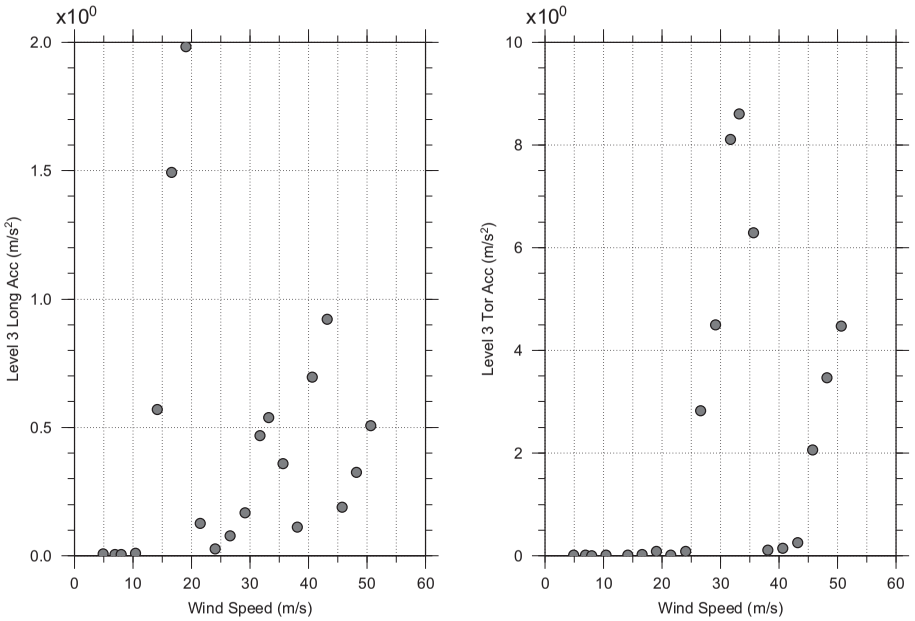

MEAN
RMS

Messina Bridge, Free Standing Tower, 7.5 degree, Smooth Flow

Dec. 13, 2010
tf14abdg.cl

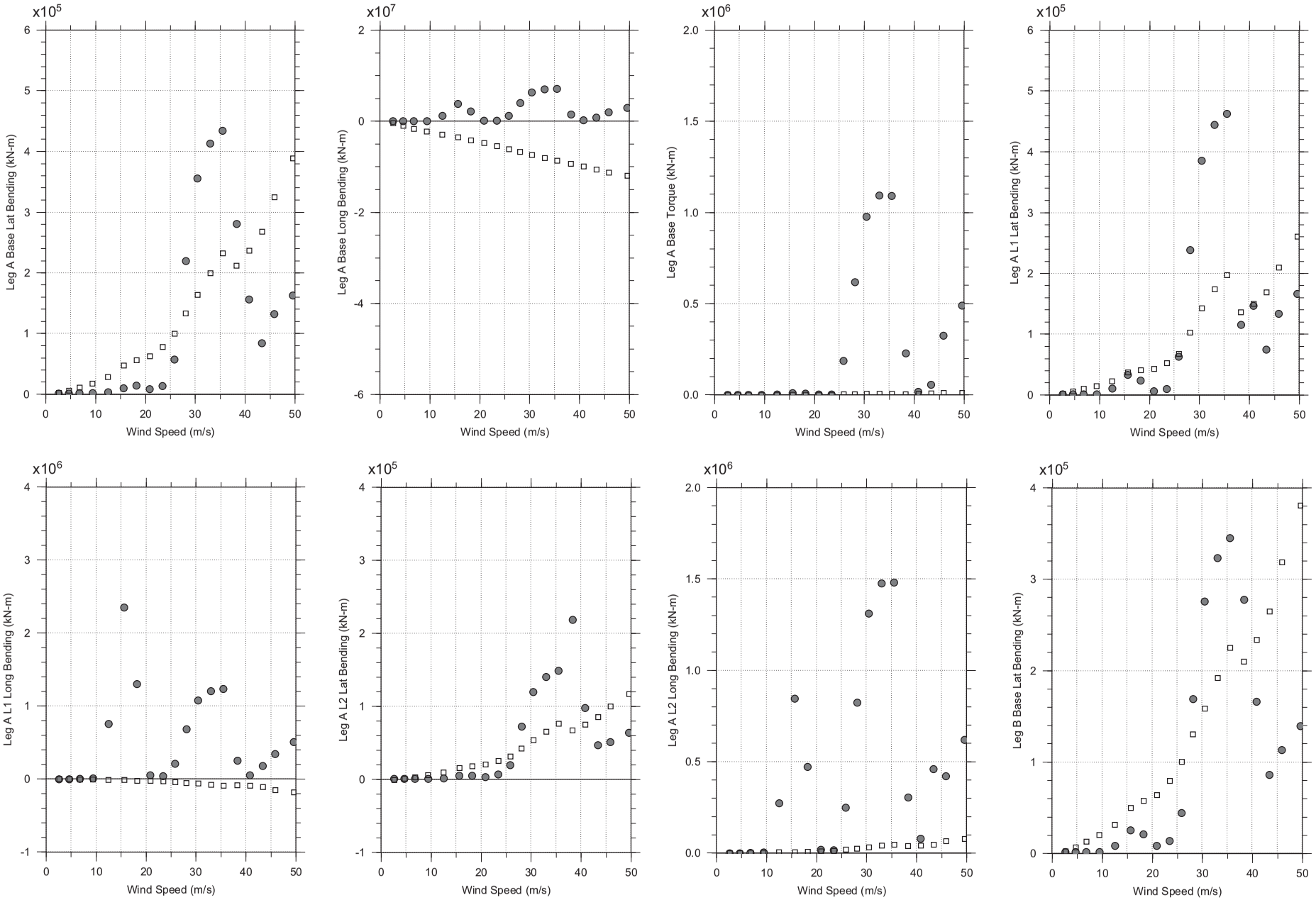

Messina Bridge, Free Standing Tower, 10 degree, Smooth Flow

Dec. 15, 2010
tf15abdg.cl

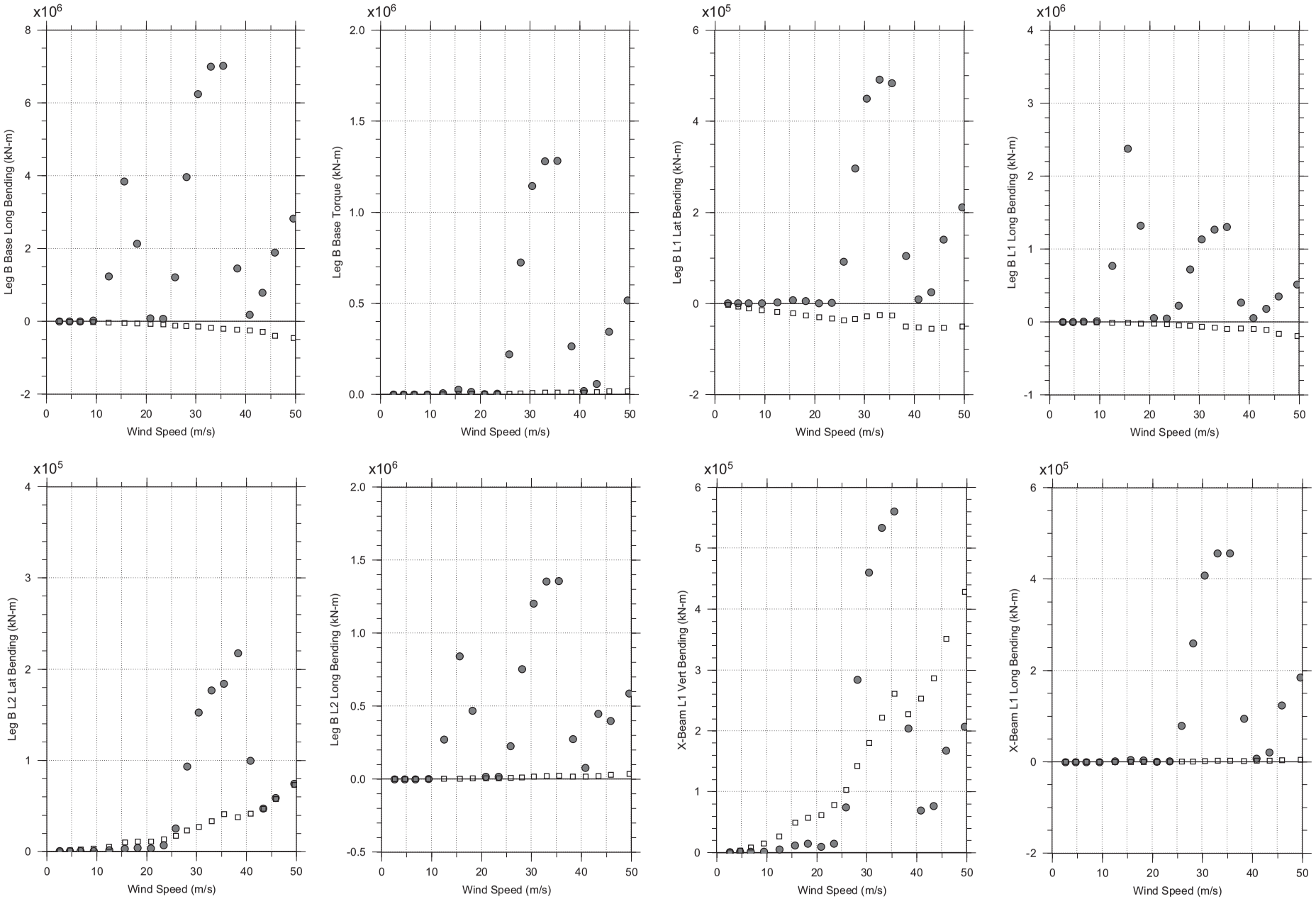

Messina Bridge, Free Standing Tower, 10 degree, Smooth Flow

Dec. 15, 2010
tf15abdg.cl

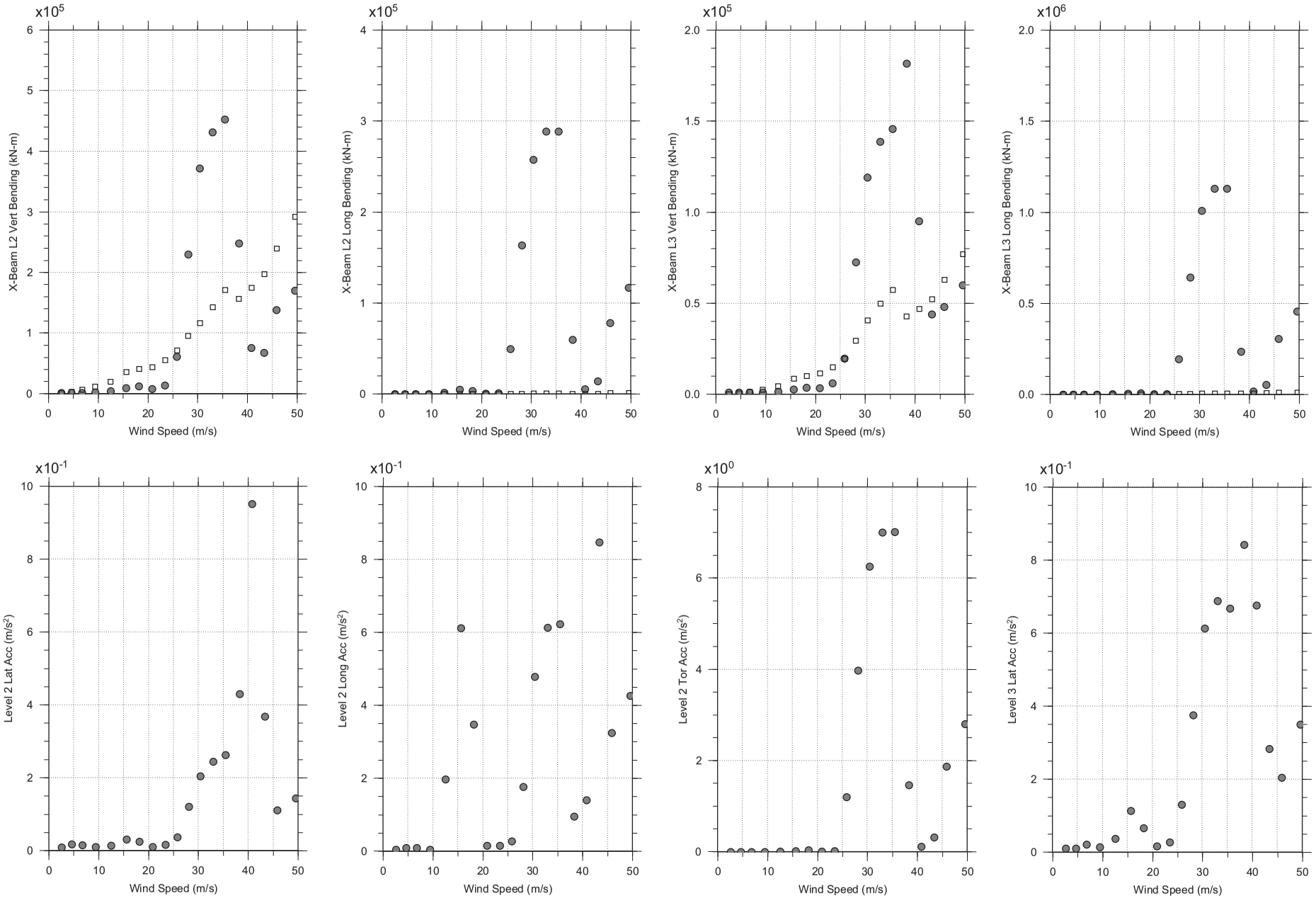

Messina Bridge, Free Standing Tower, 10 degree, Smooth Flow

Dec. 15, 2010
tf15abdg.cl

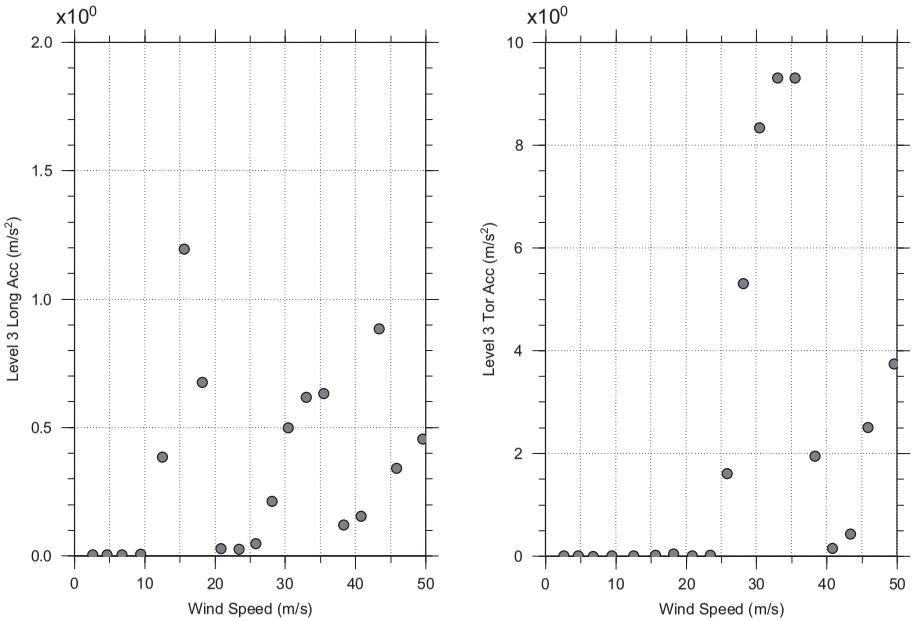

MEAN
RMS

Messina Bridge, Free Standing Tower, 10 degree, Smooth Flow

Dec. 15, 2010
tf15abdg.cl

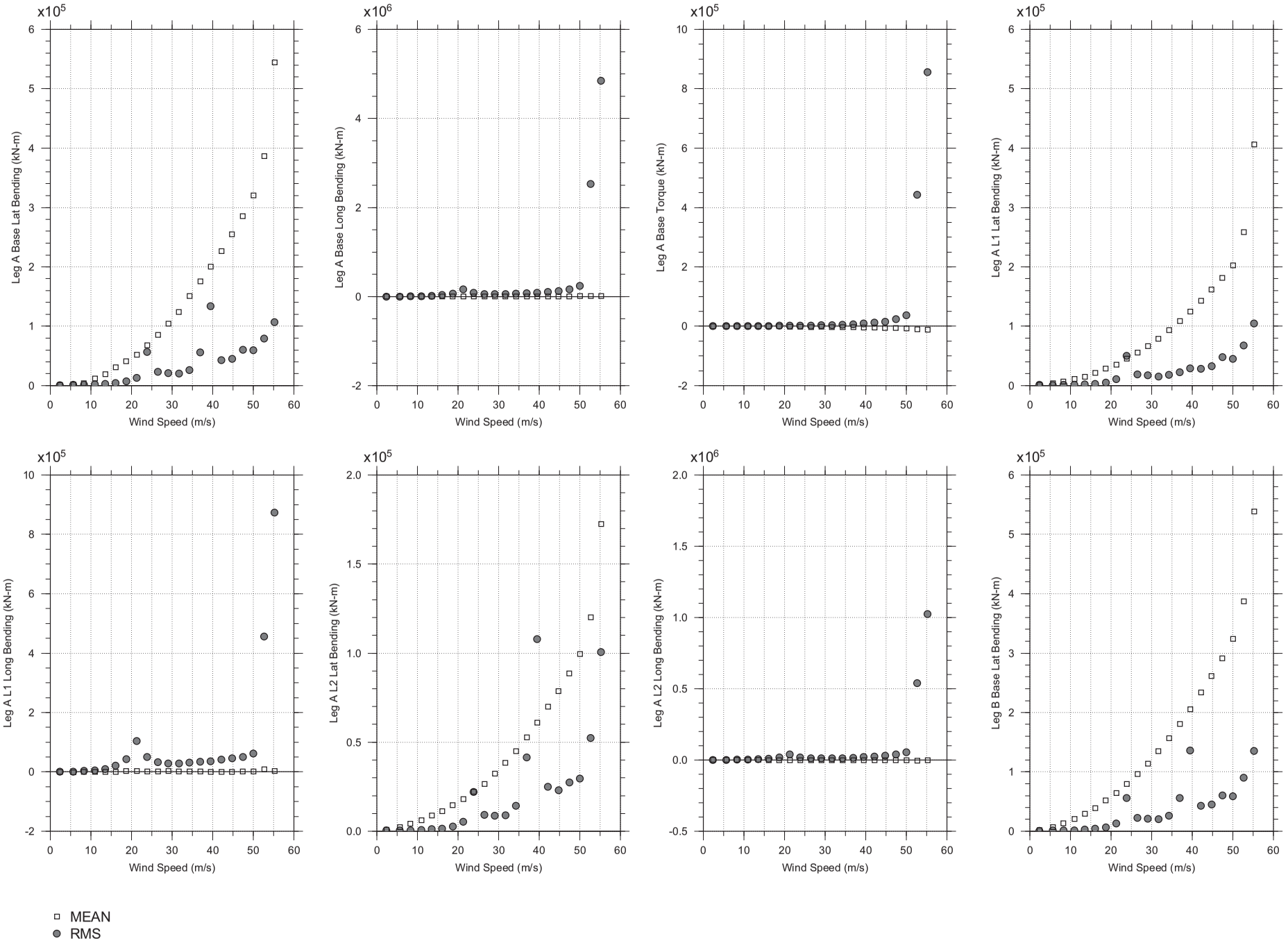

Messina Bridge, Free Standing Tower, 0 degree, 2% Damping, Smooth Flow

Dec. 13, 2010
tf21abdg.cl

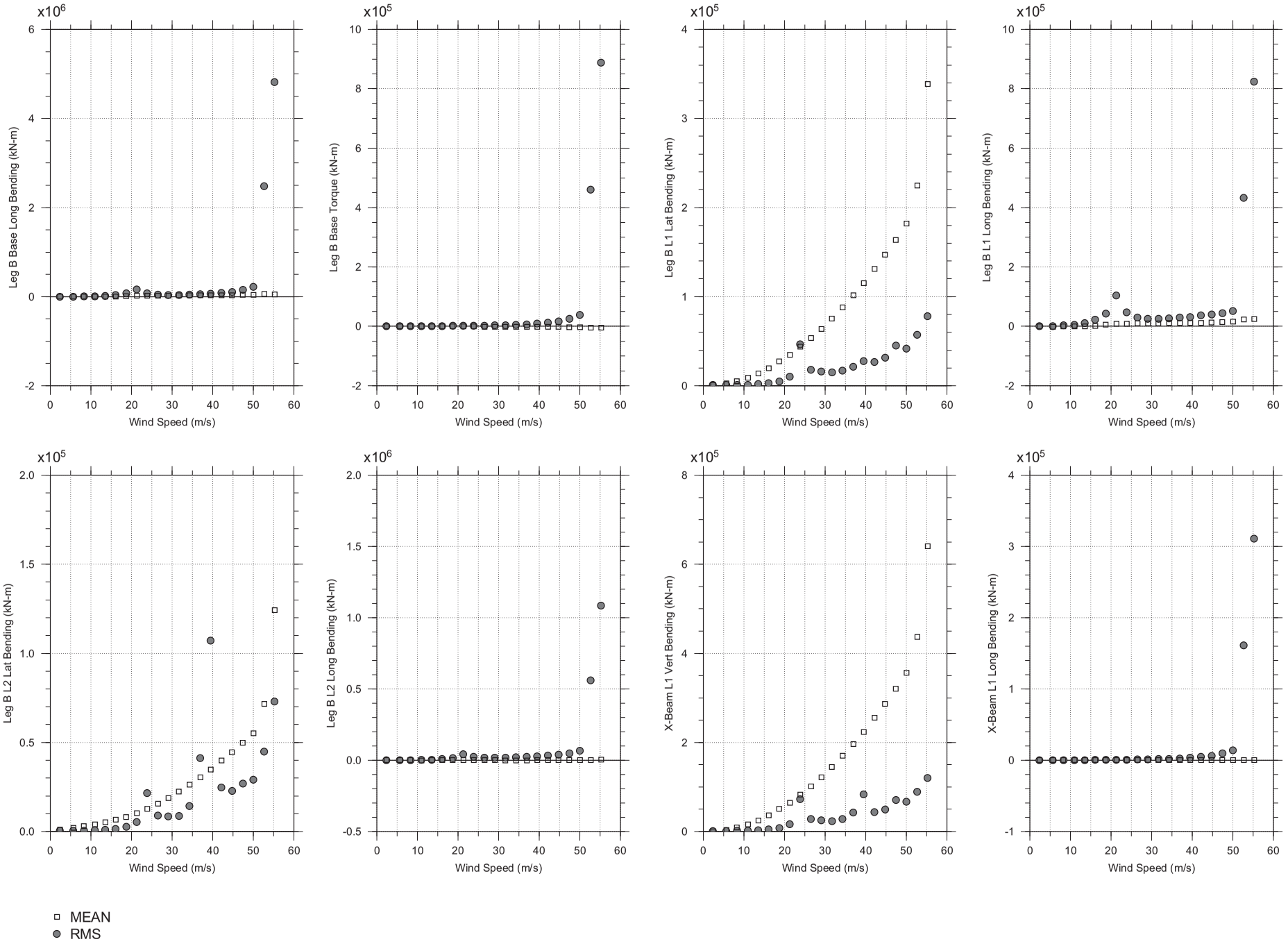

Messina Bridge, Free Standing Tower, 0 degree, 2% Damping, Smooth Flow

Dec. 13, 2010
tf21abdg.cl

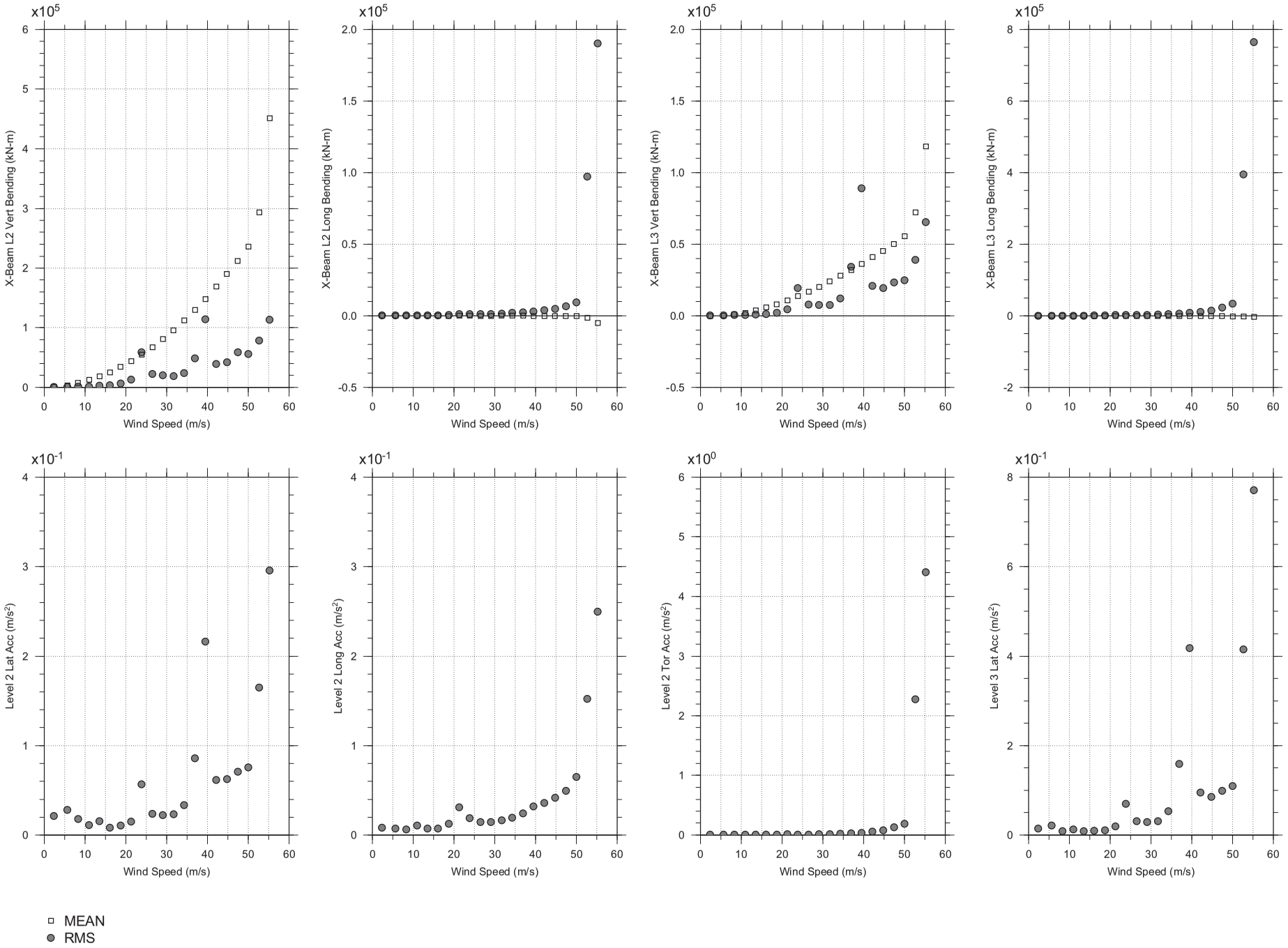

Messina Bridge, Free Standing Tower, 0 degree, 2% Damping, Smooth Flow

Dec. 13, 2010
tf21abdg.cl

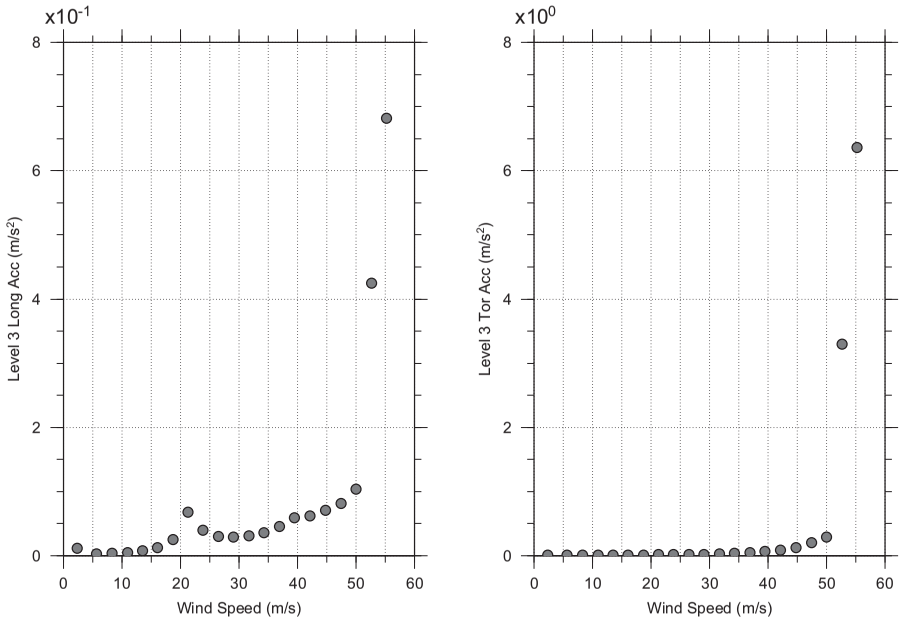

MEAN
RMS

Messina Bridge, Free Standing Tower, 0 degree, 2% Damping, Smooth Flow

Dec. 13, 2010
tf21abdg.cl

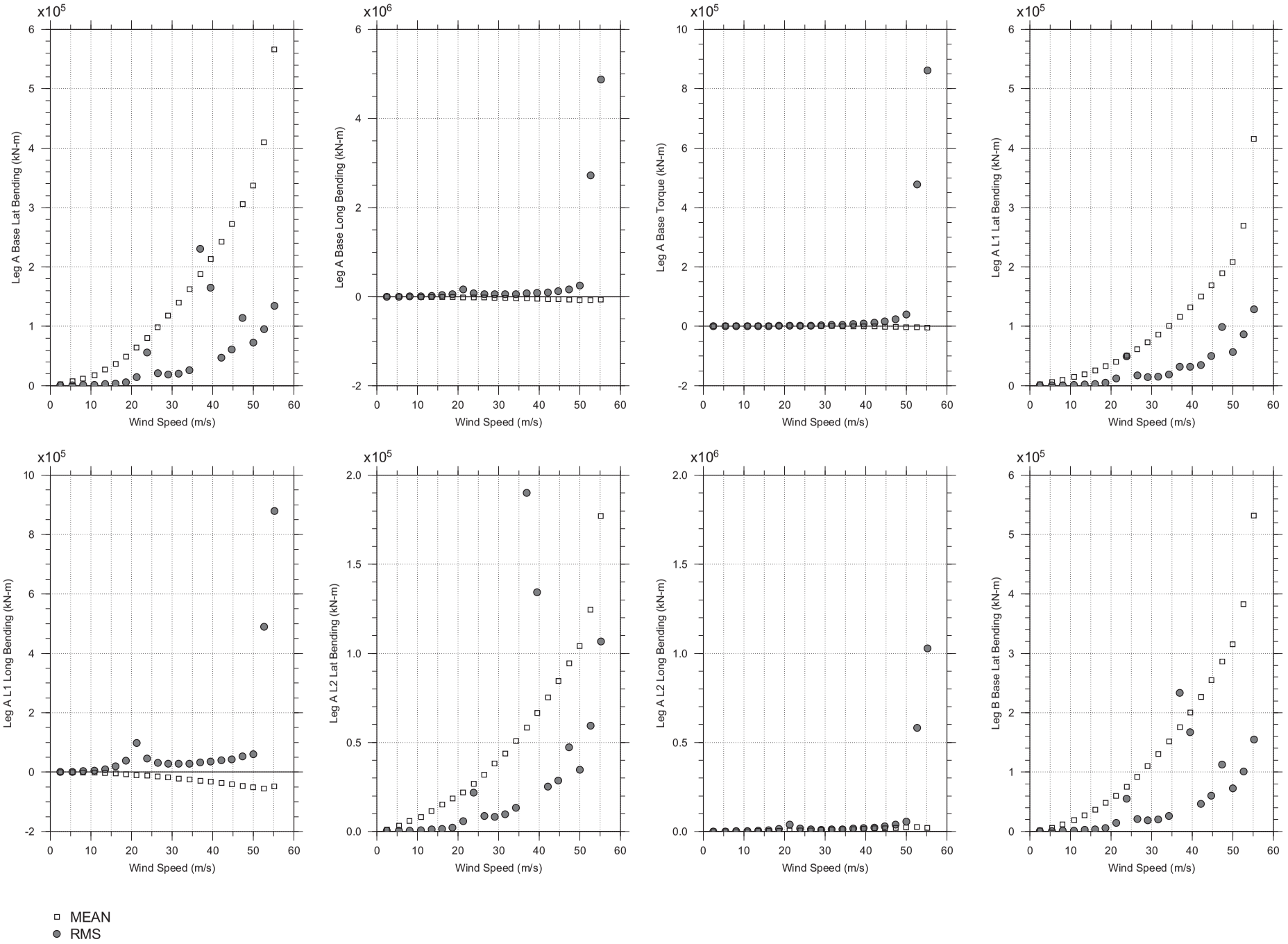

Messina Bridge, Free Standing Tower, 2.5 degree, 2% Damping, Smooth Flow

Dec. 13, 2010
tf22abdg.cl

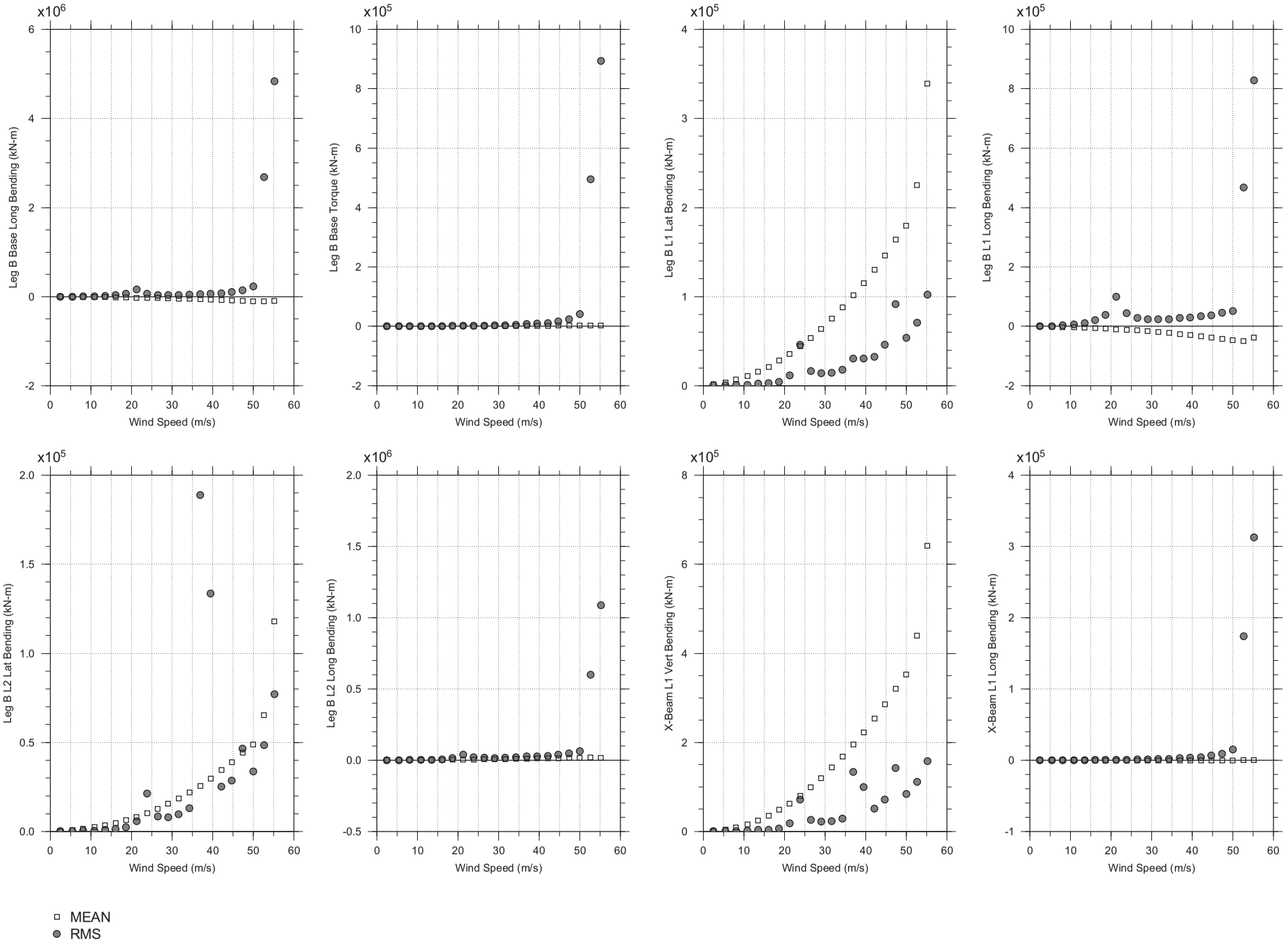

Messina Bridge, Free Standing Tower, 2.5 degree, 2% Damping, Smooth Flow

Dec. 13, 2010
tf22abdg.cl

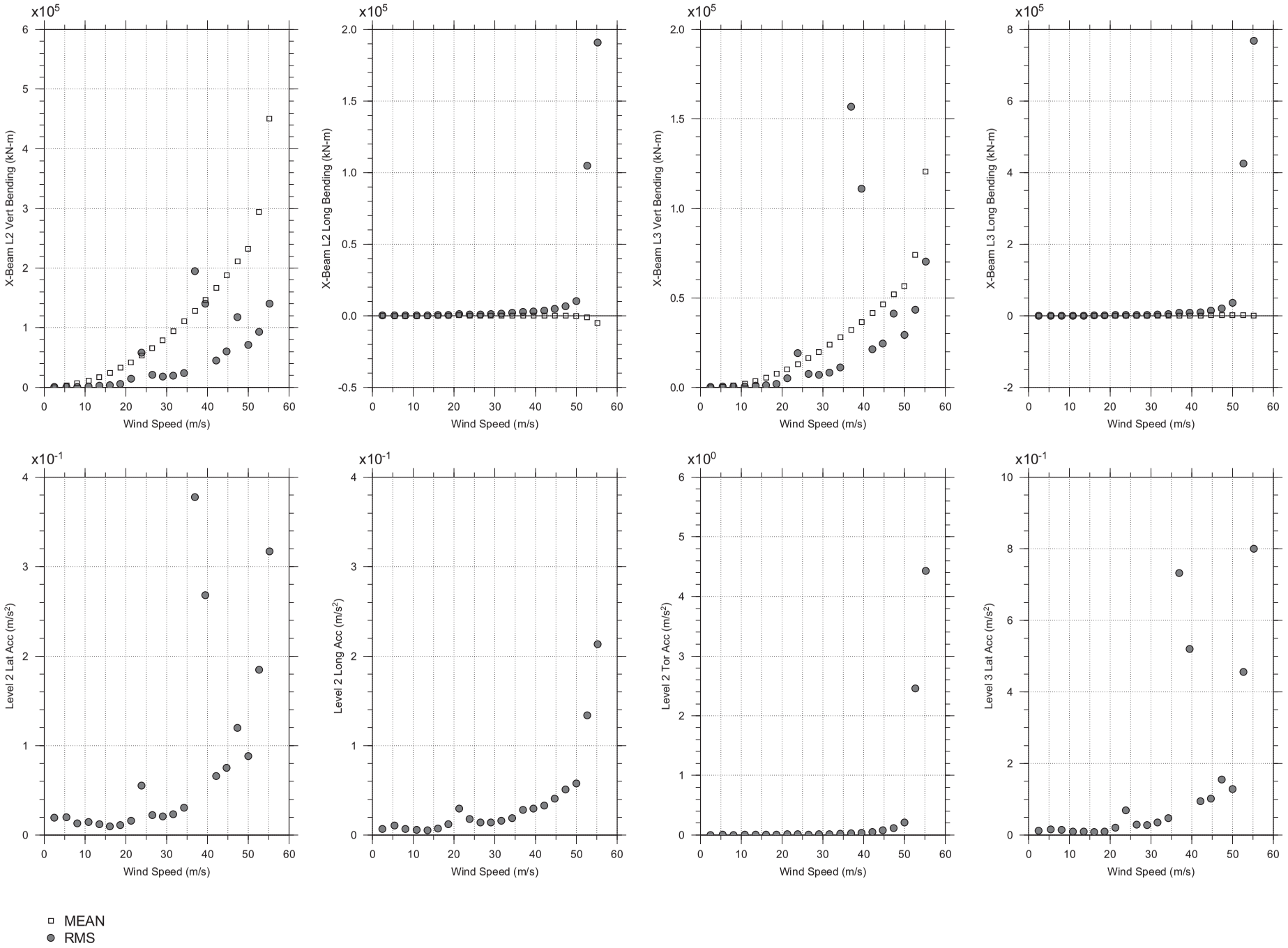

Messina Bridge, Free Standing Tower, 2.5 degree, 2% Damping, Smooth Flow

Dec. 13, 2010
tf22abdg.cl

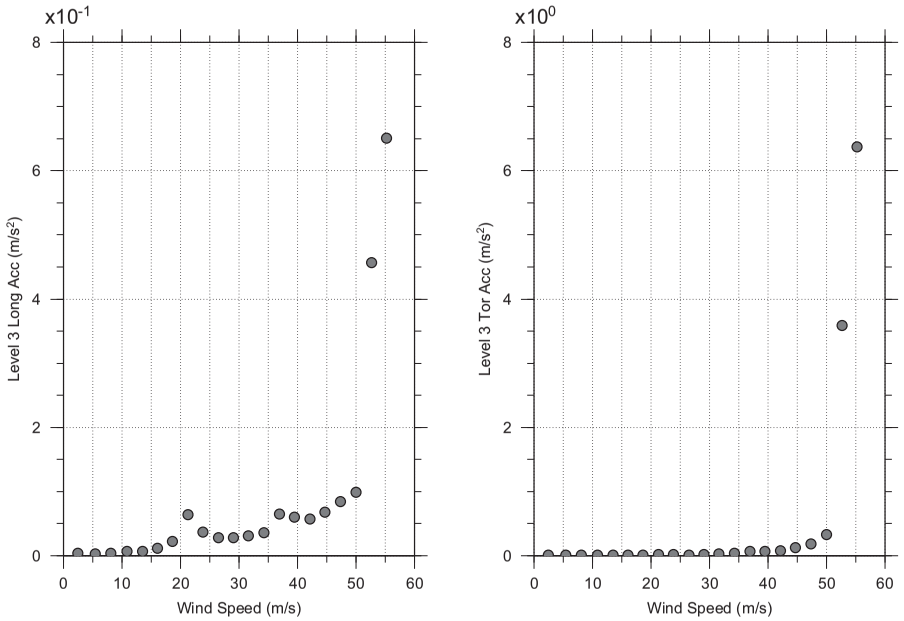

MEAN
RMS

Messina Bridge, Free Standing Tower, 2.5 degree, 2% Damping, Smooth Flow

Dec. 13, 2010
tf22abdg.cl

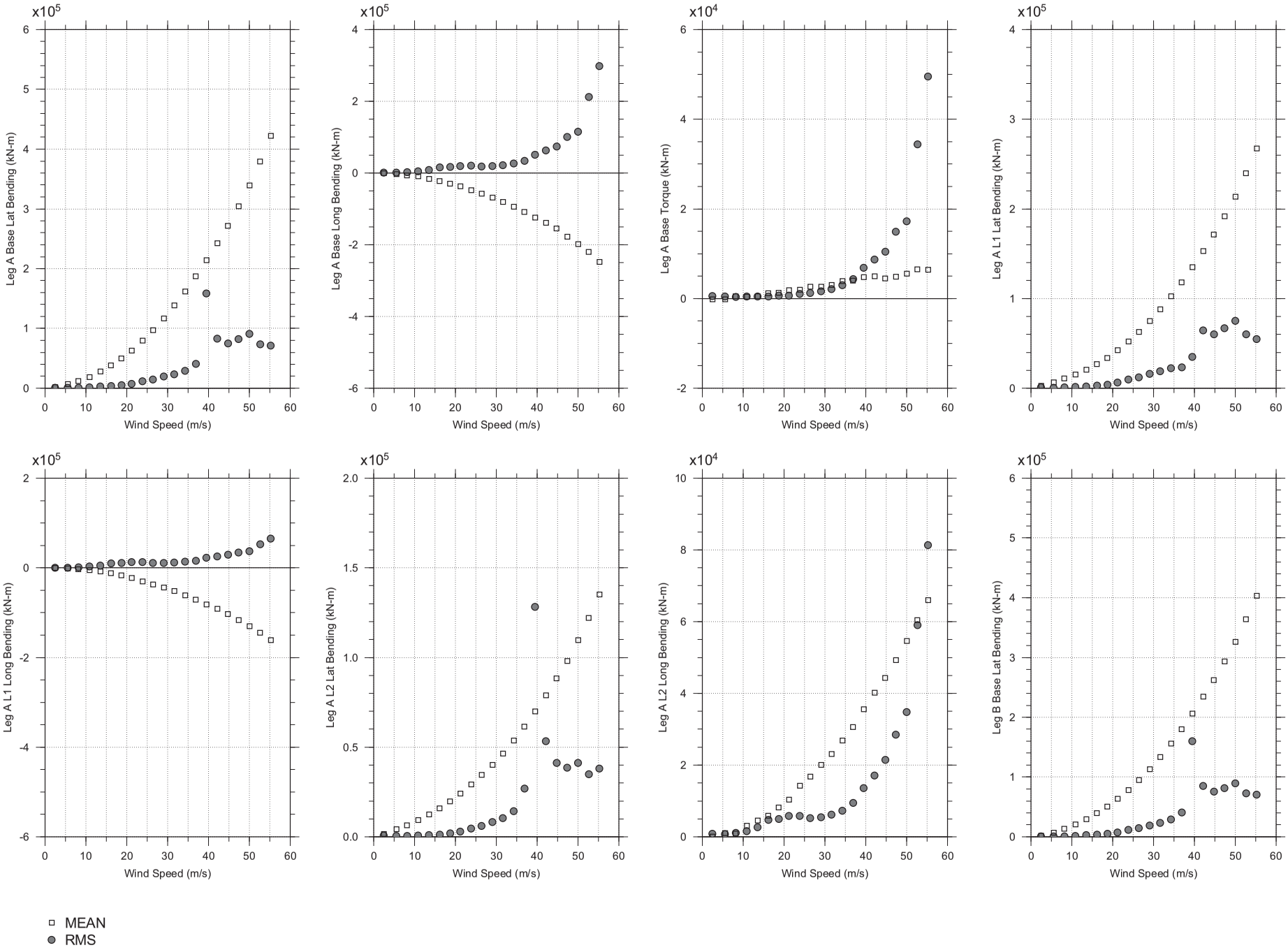

Messina Bridge, Free Standing Tower, 10 degree, 2% Damping, Smooth Flow

Dec. 13, 2010
tf23abdg.cl

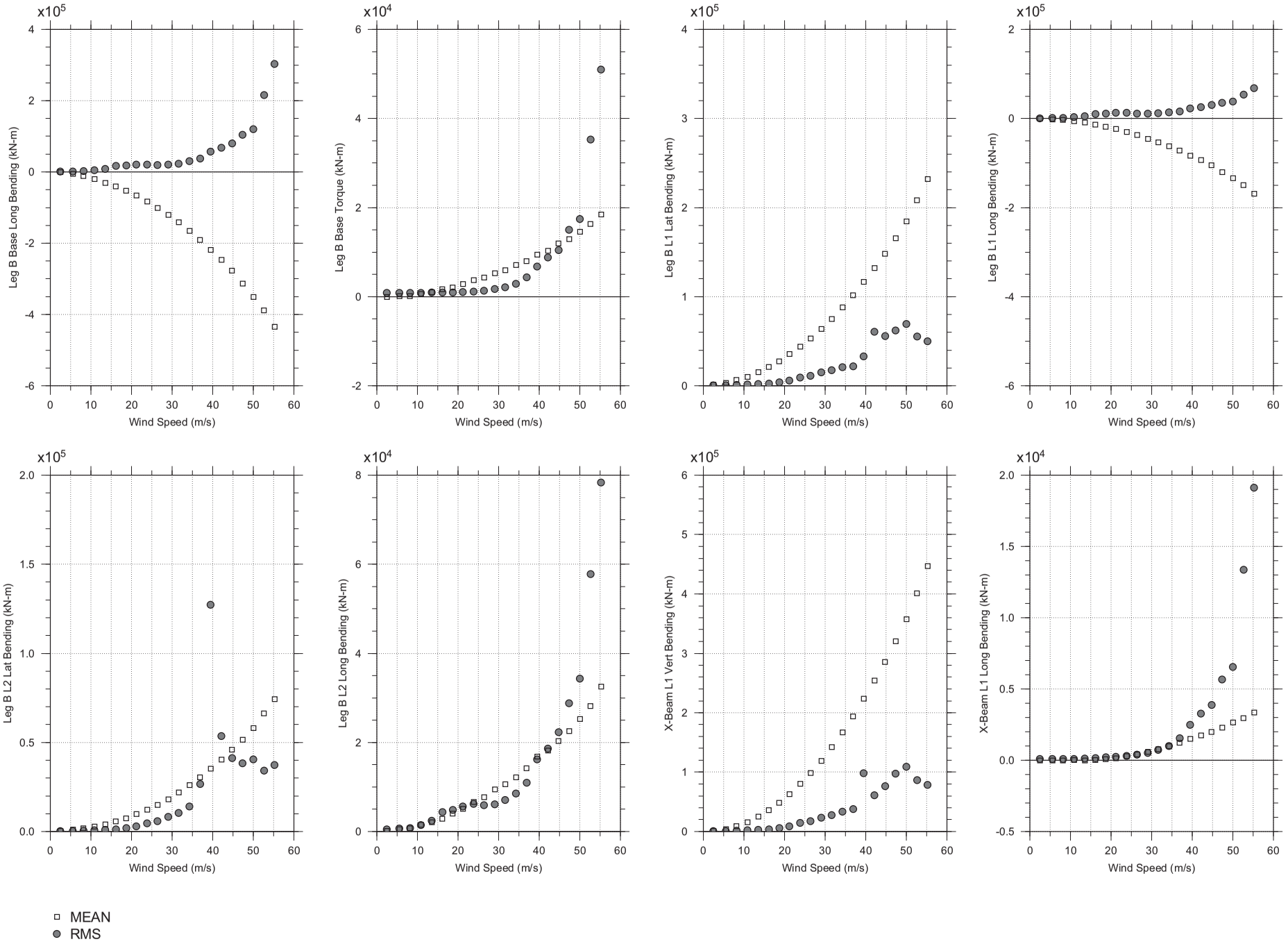

Messina Bridge, Free Standing Tower, 10 degree, 2% Damping, Smooth Flow

Dec. 13, 2010
tf23abdg.cl

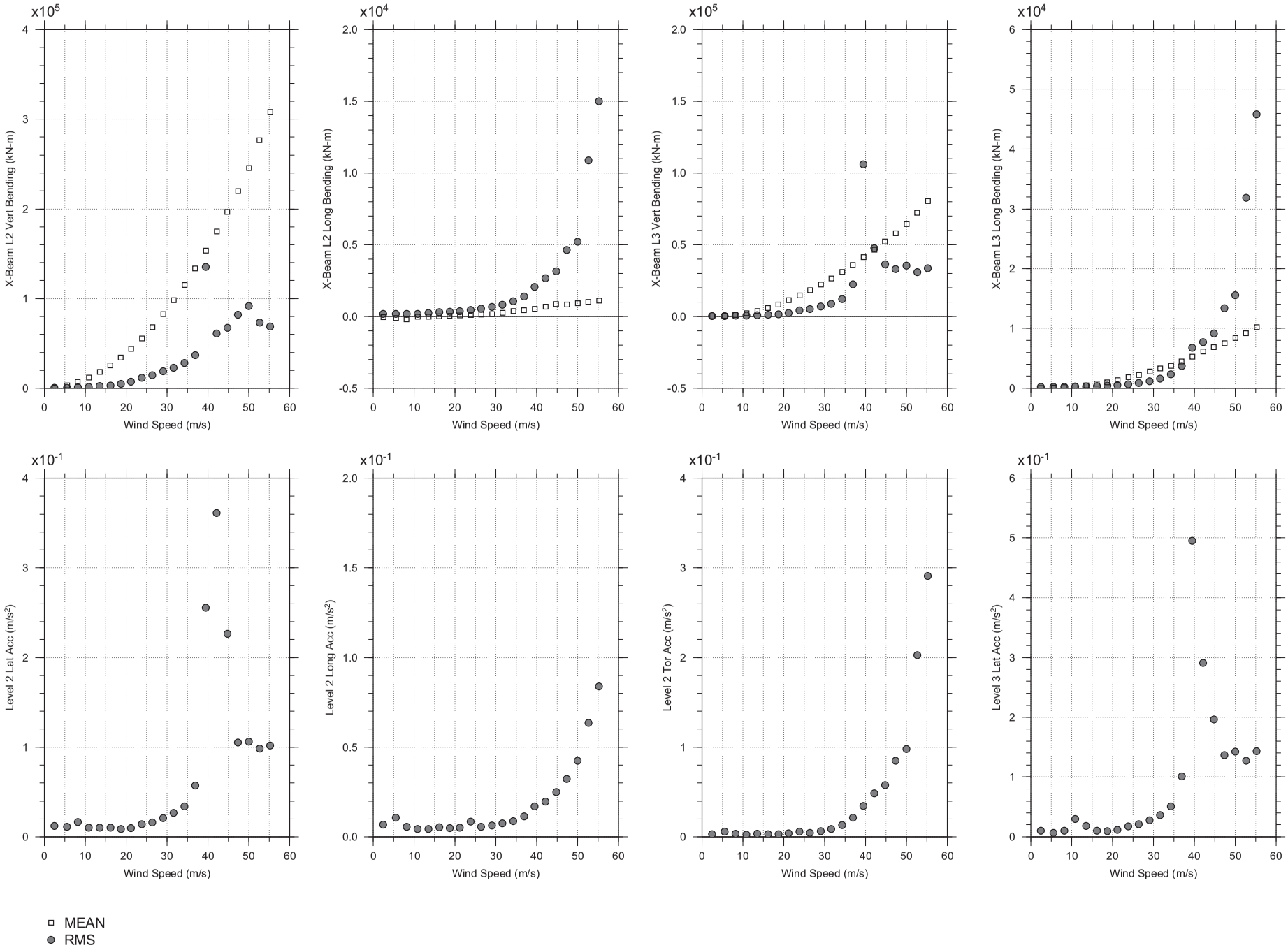

Messina Bridge, Free Standing Tower, 10 degree, 2% Damping, Smooth Flow

Dec. 13, 2010
tf23abdg.cl

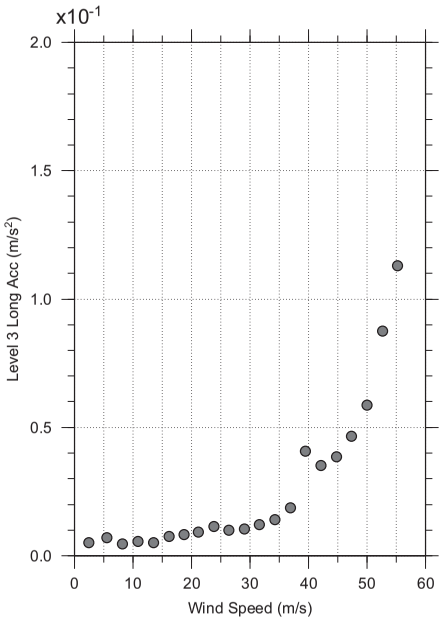

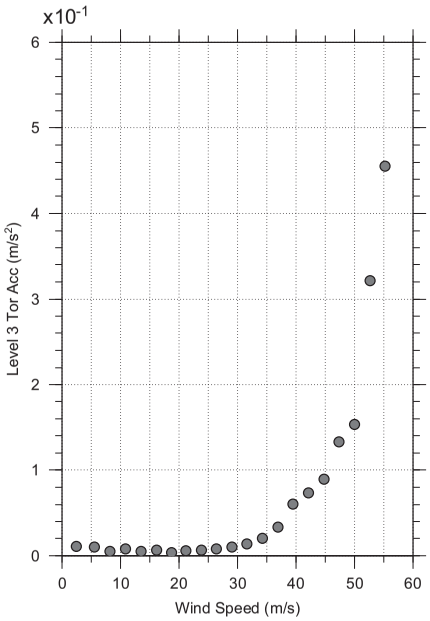

□ MEAN
● RMS

Messina Bridge, Free Standing Tower, 10 degree, 2% Damping, Smooth Flow

Dec. 13, 2010
tf23abdg.cl

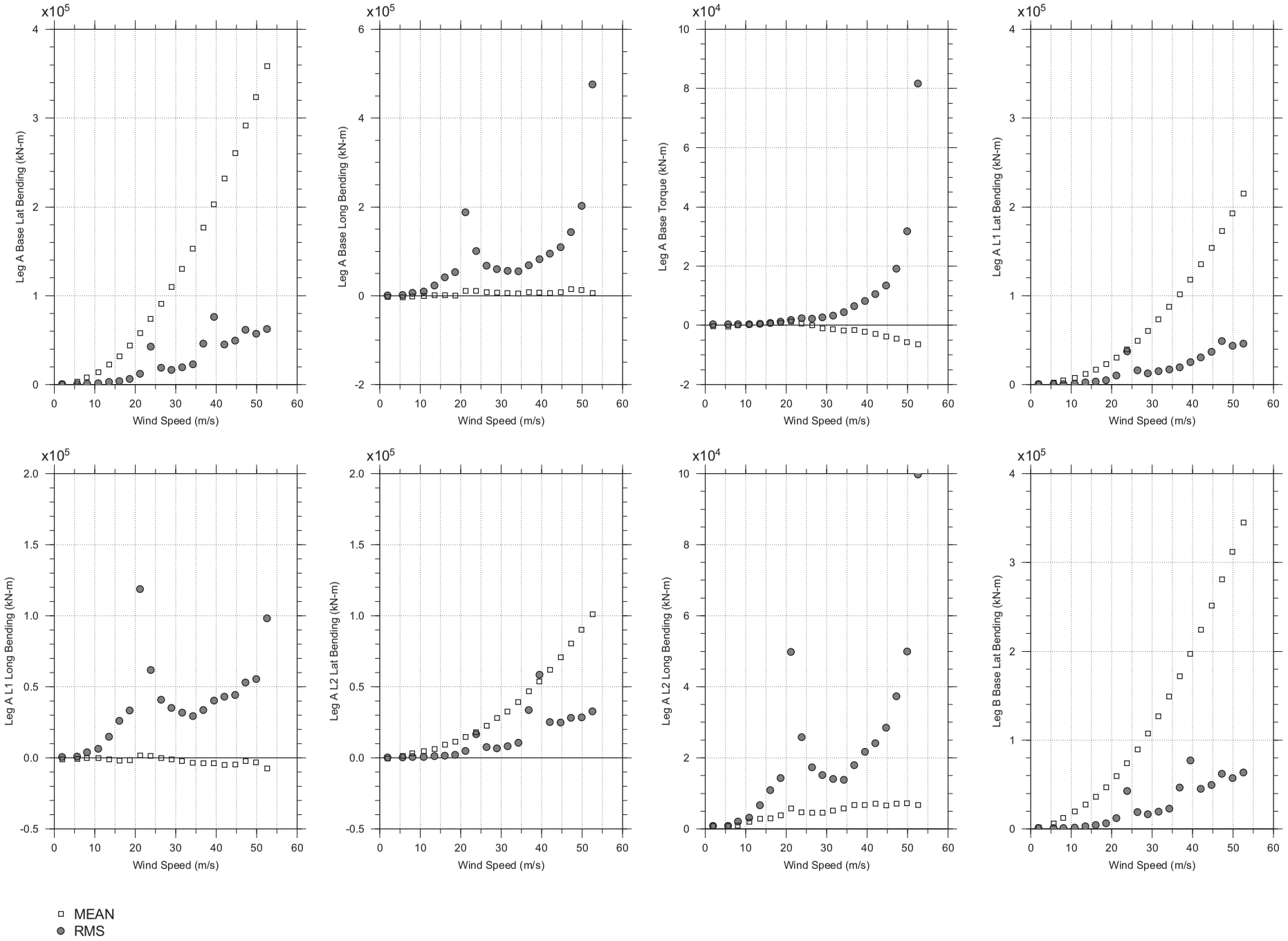

Messina Bridge, Free Standing Tower, 0 degree, 4% Damping, Smooth Flow

Dec. 13, 2010
tf31abdg.cl

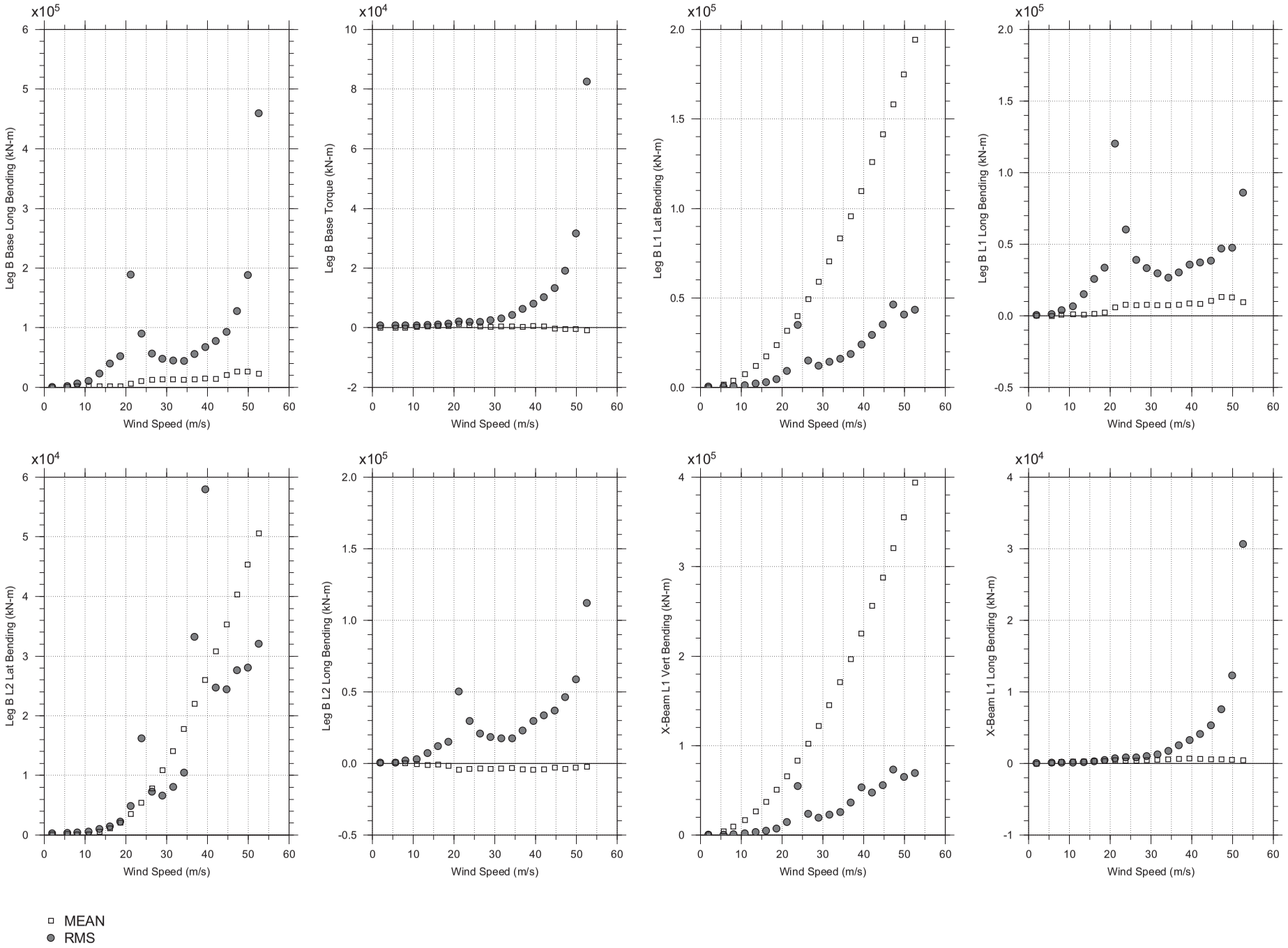

Messina Bridge, Free Standing Tower, 0 degree, 4% Damping, Smooth Flow

Dec. 13, 2010
tf31abdg.cl

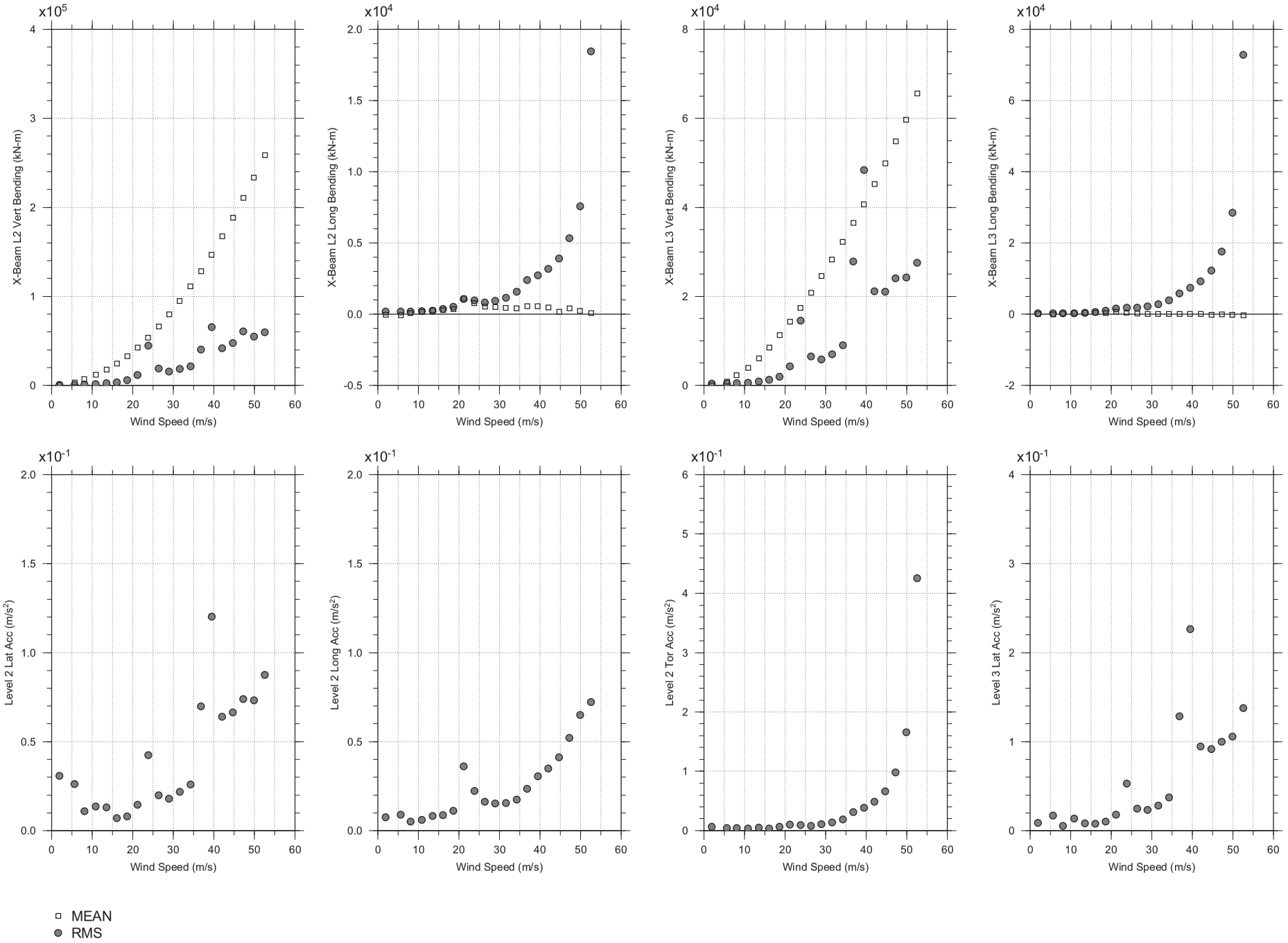

Messina Bridge, Free Standing Tower, 0 degree, 4% Damping, Smooth Flow

Dec. 13, 2010
tf31abdg.cl

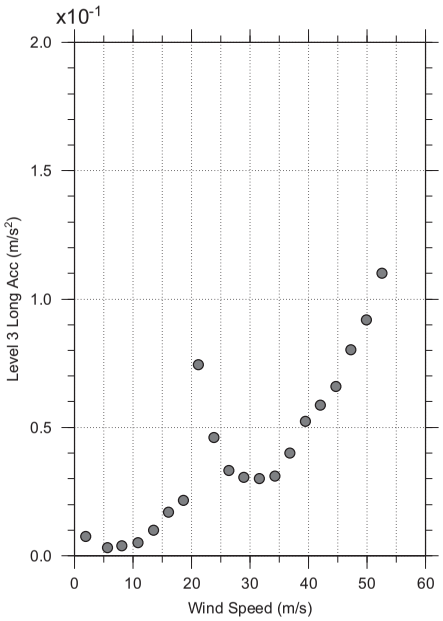

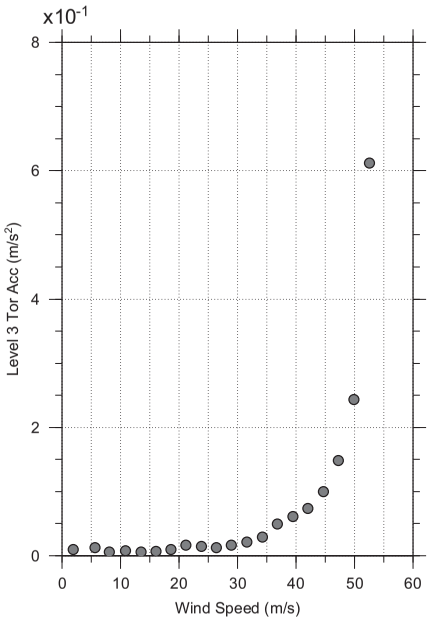

□ MEAN
● RMS

Messina Bridge, Free Standing Tower, 0 degree, 4% Damping, Smooth Flow

Dec. 13, 2010
tf31abdg.cl

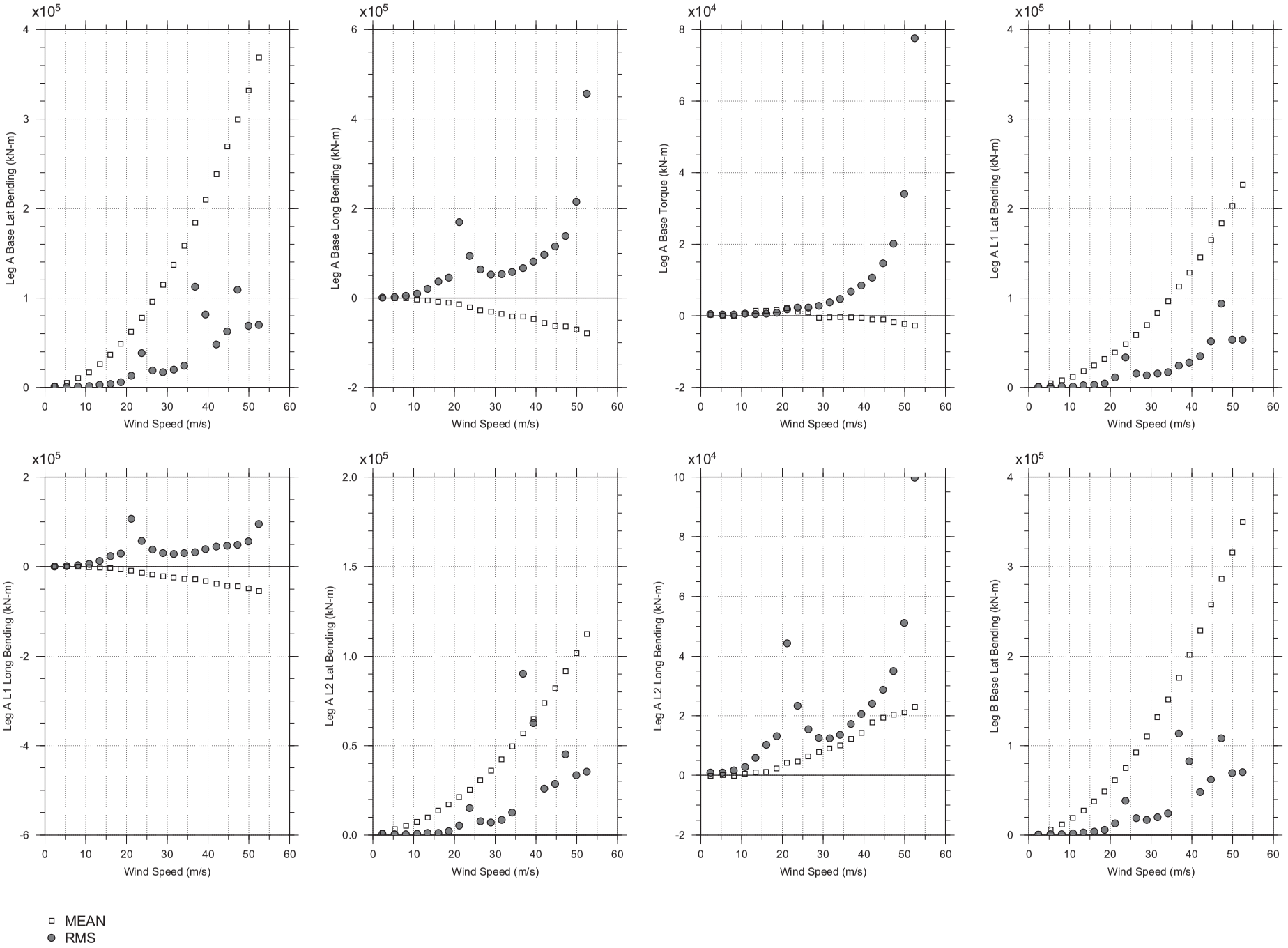

Messina Bridge, Free Standing Tower, 2.5 degree, 4% Damping, Smooth Flow

Dec. 13, 2010
tf32abdg.cl

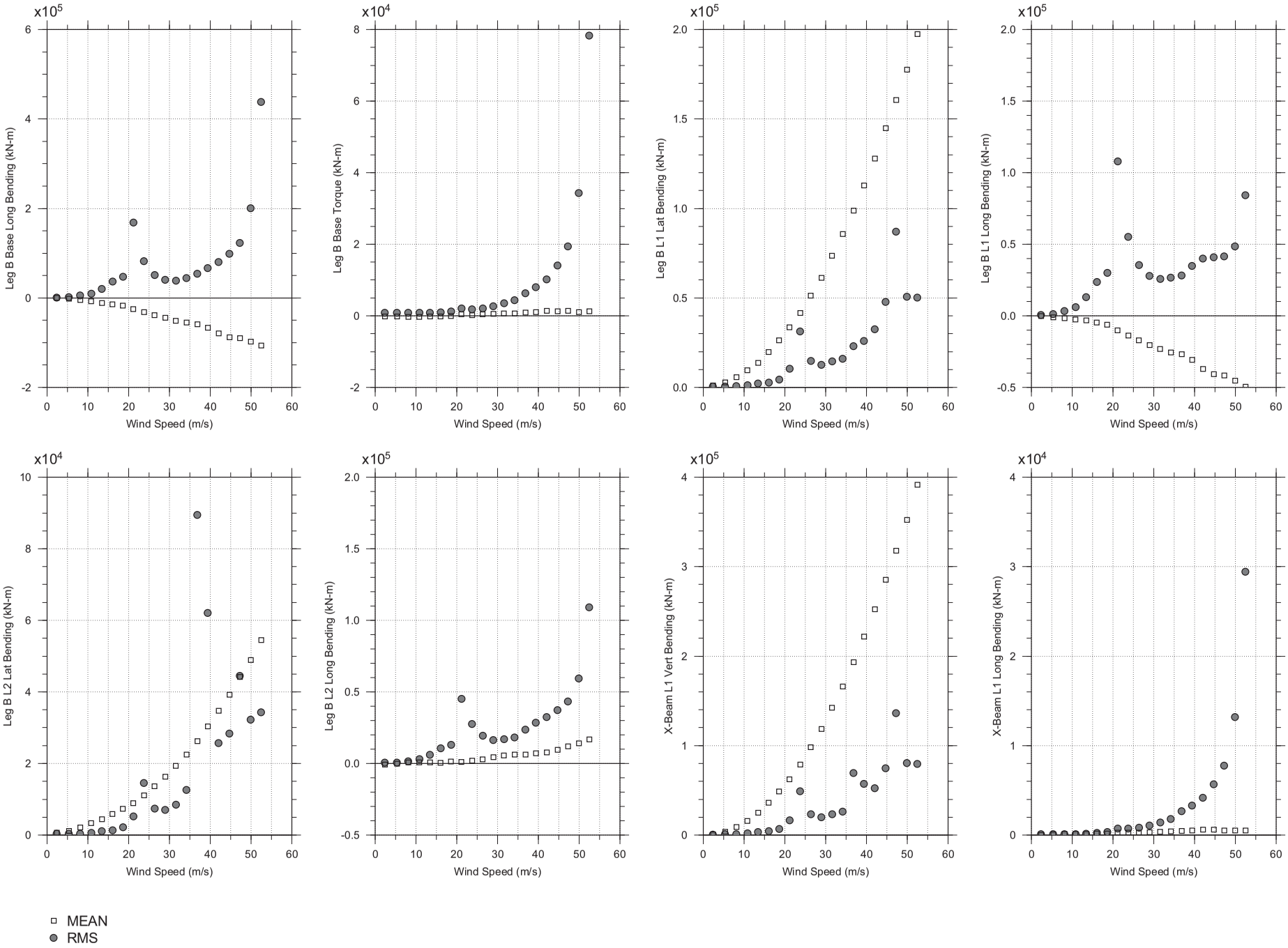

Messina Bridge, Free Standing Tower, 2.5 degree, 4% Damping, Smooth Flow

Dec. 13, 2010
tf32abdg.cl

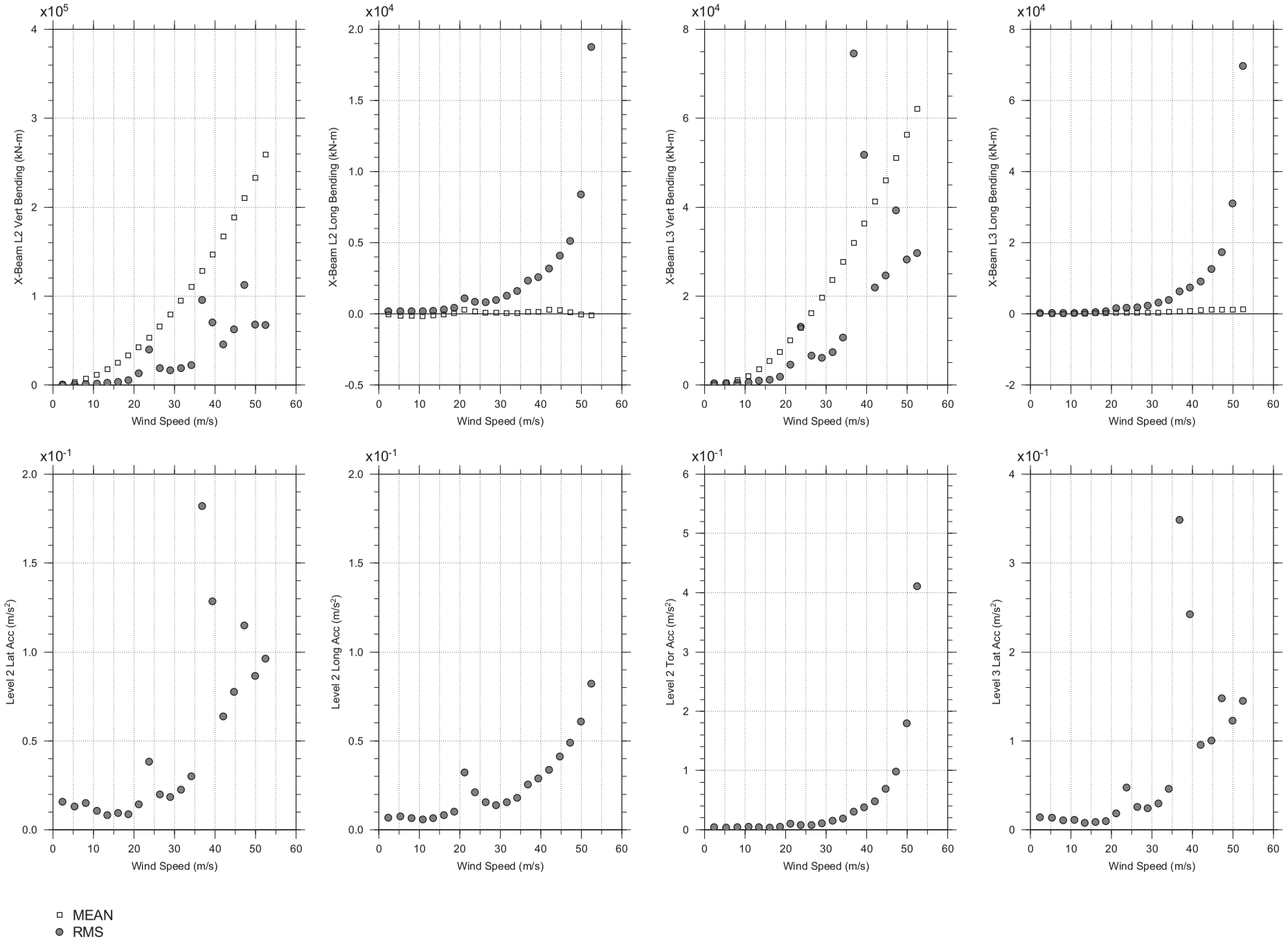

Messina Bridge, Free Standing Tower, 2.5 degree, 4% Damping, Smooth Flow

Dec. 13, 2010
tf32abdg.cl

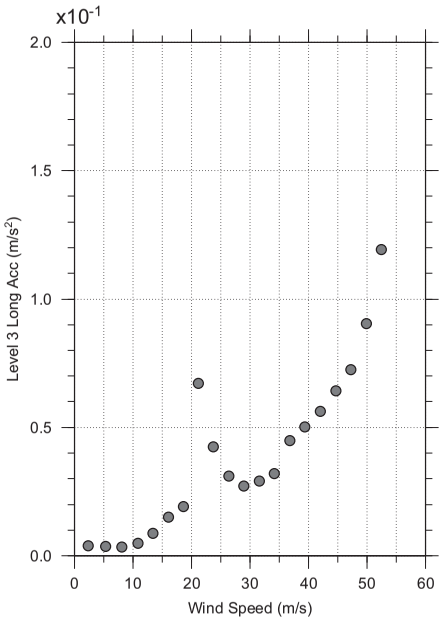

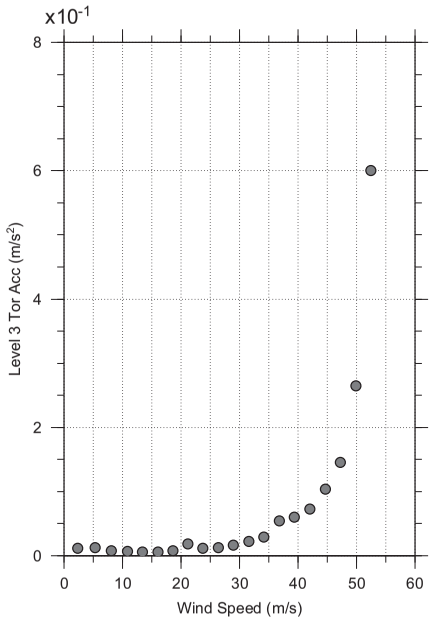

□ MEAN
● RMS

Messina Bridge, Free Standing Tower, 2.5 degree, 4% Damping, Smooth Flow

Dec. 13, 2010
tf32abdg.cl

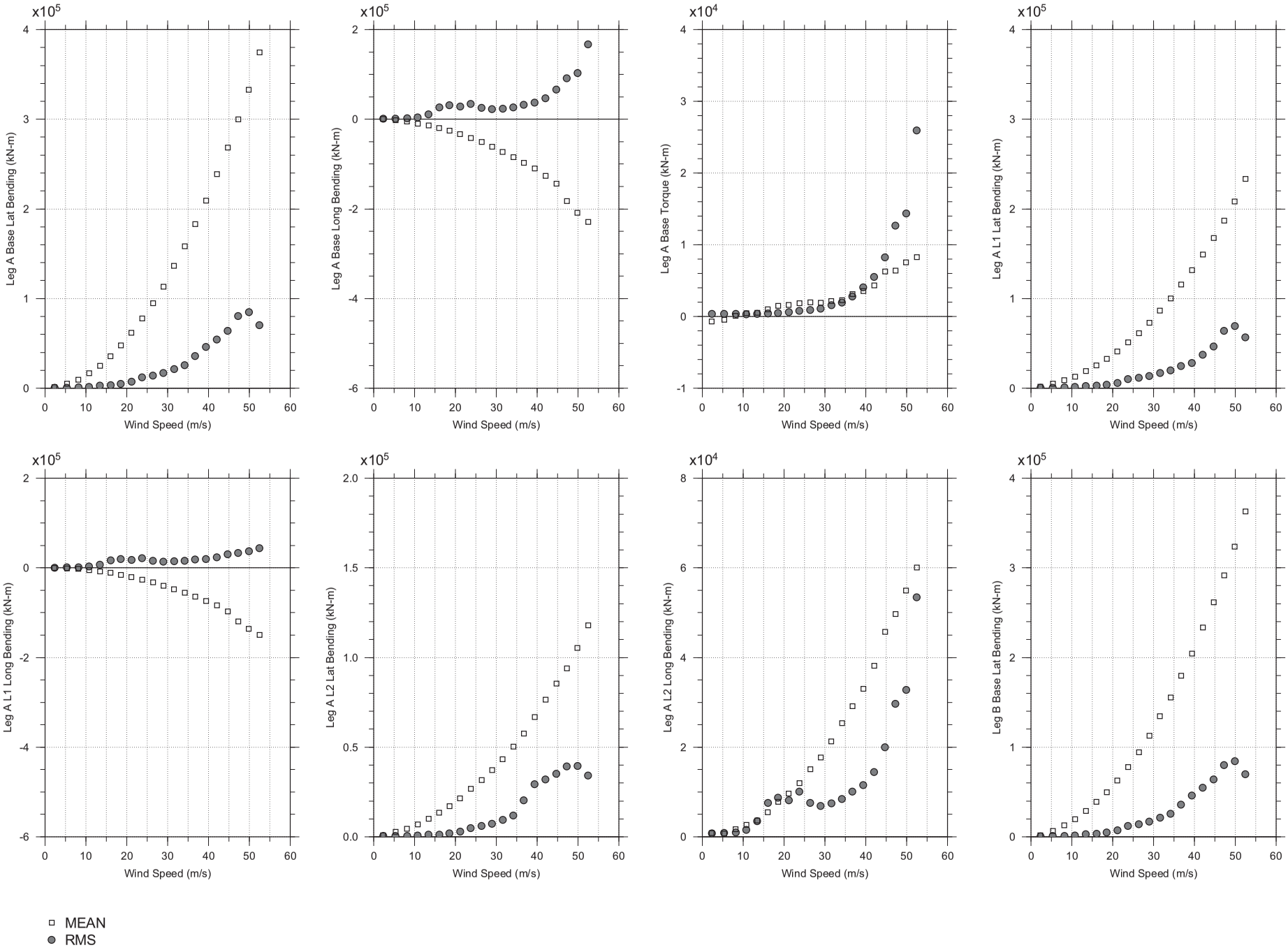

Messina Bridge, Free Standing Tower, 10 degree, 4% Damping, Smooth Flow

Dec. 13, 2010
tf33abdg.cl

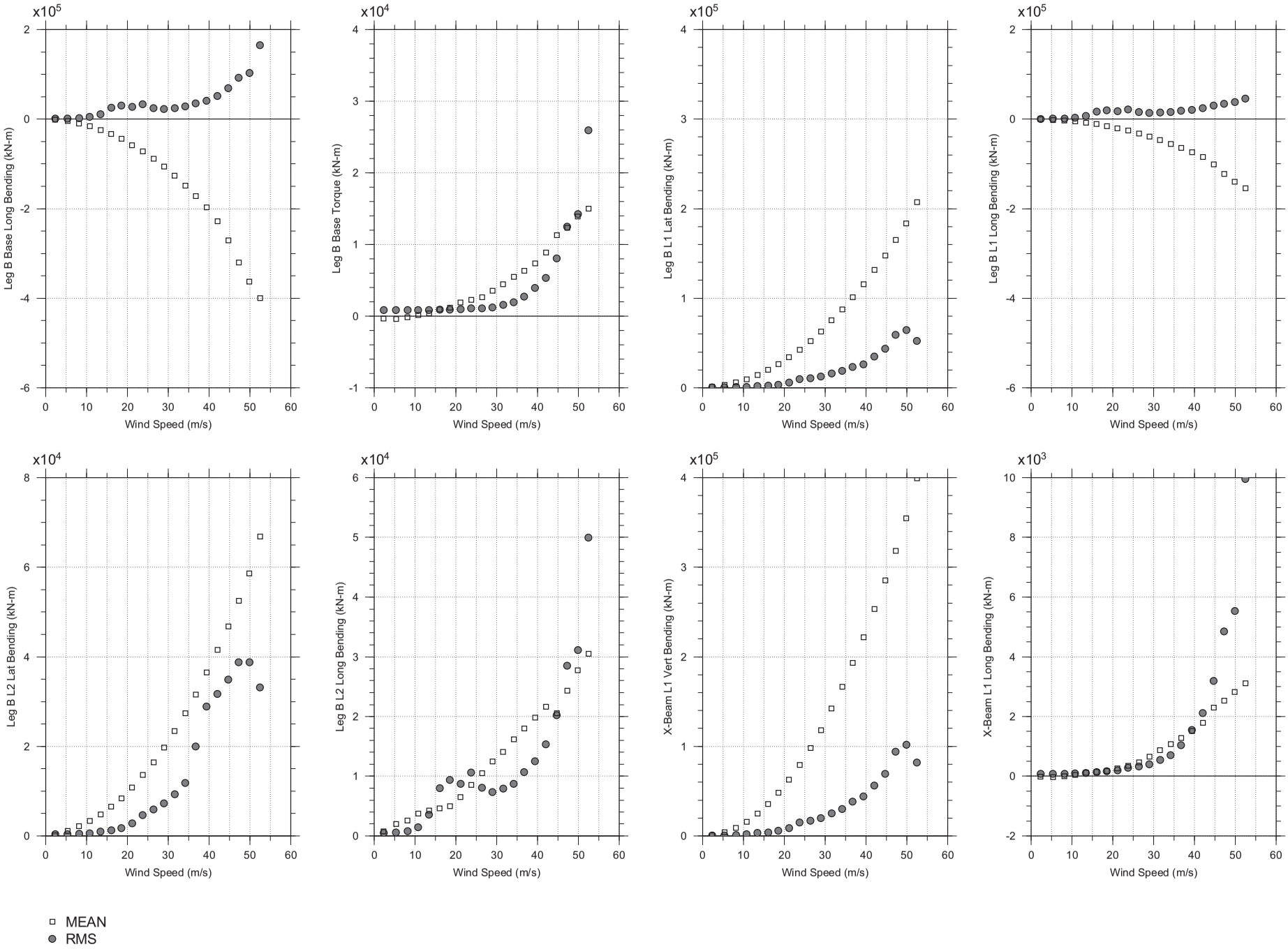

Messina Bridge, Free Standing Tower, 10 degree, 4% Damping, Smooth Flow

Dec. 13, 2010
tf33abdg.cl

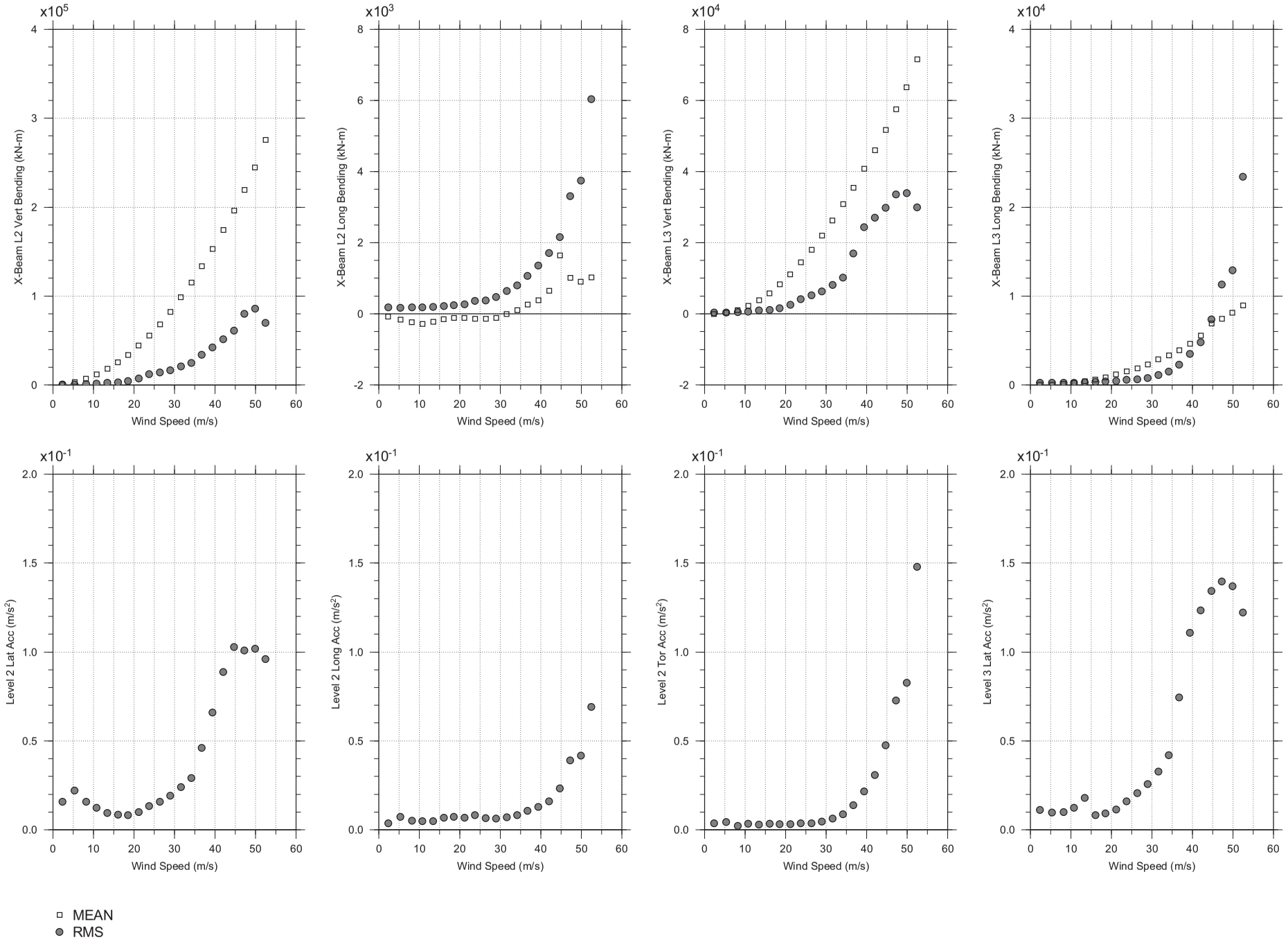

Messina Bridge, Free Standing Tower, 10 degree, 4% Damping, Smooth Flow

Dec. 13, 2010
tf33abdg.cl

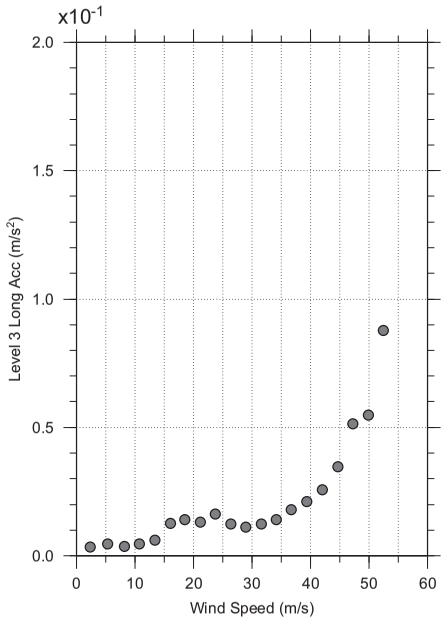

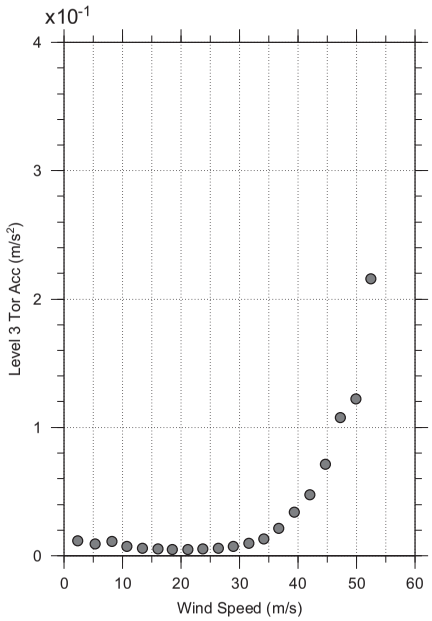

□ MEAN
● RMS

Messina Bridge, Free Standing Tower, 10 degree, 4% Damping, Smooth Flow

Dec. 13, 2010
tf33abdg.cl

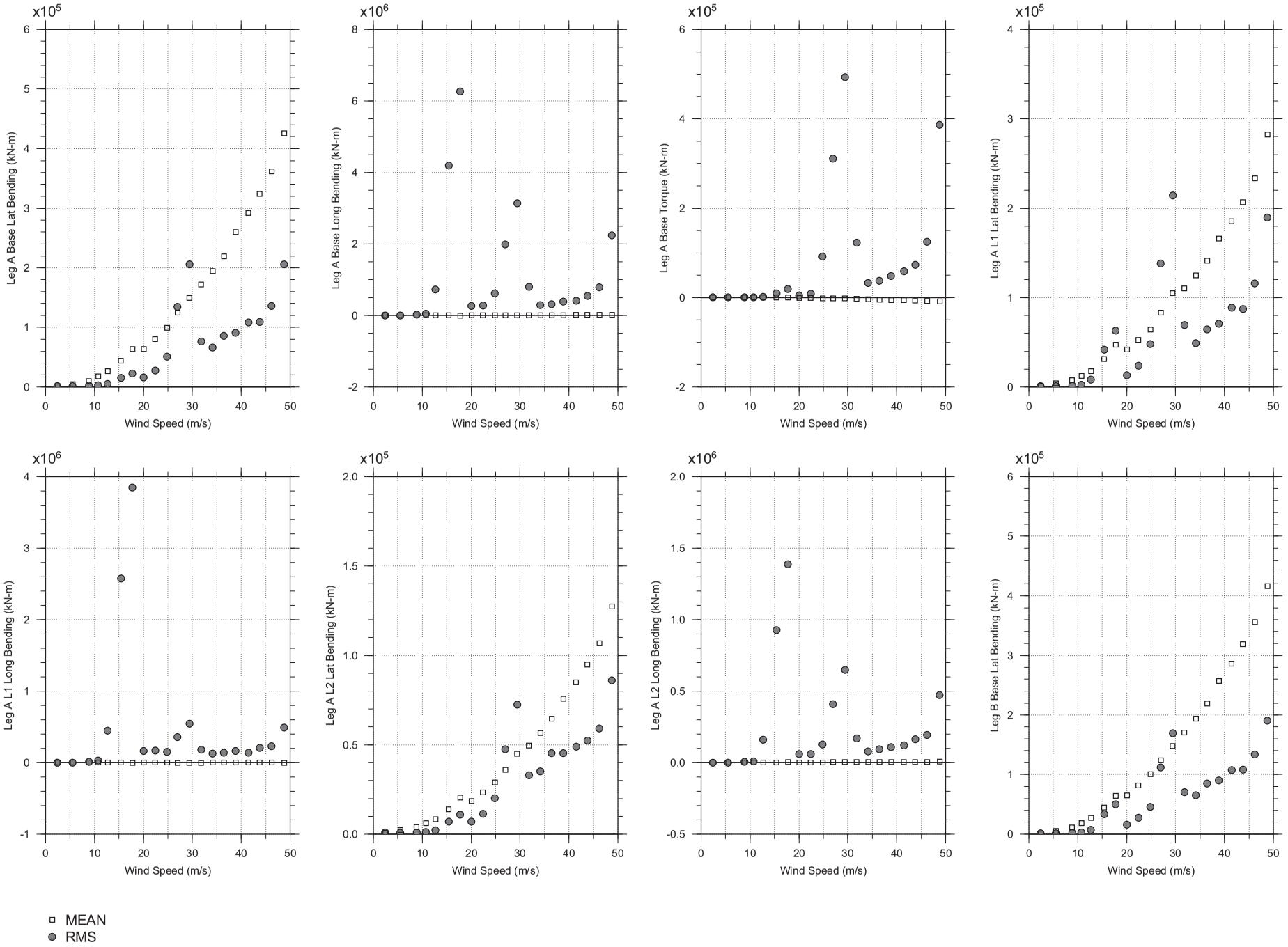

Messina Bridge, Free Standing Tower, 0 degree, Turbulent Flow

Dec. 13, 2010
tf41abdg.cl

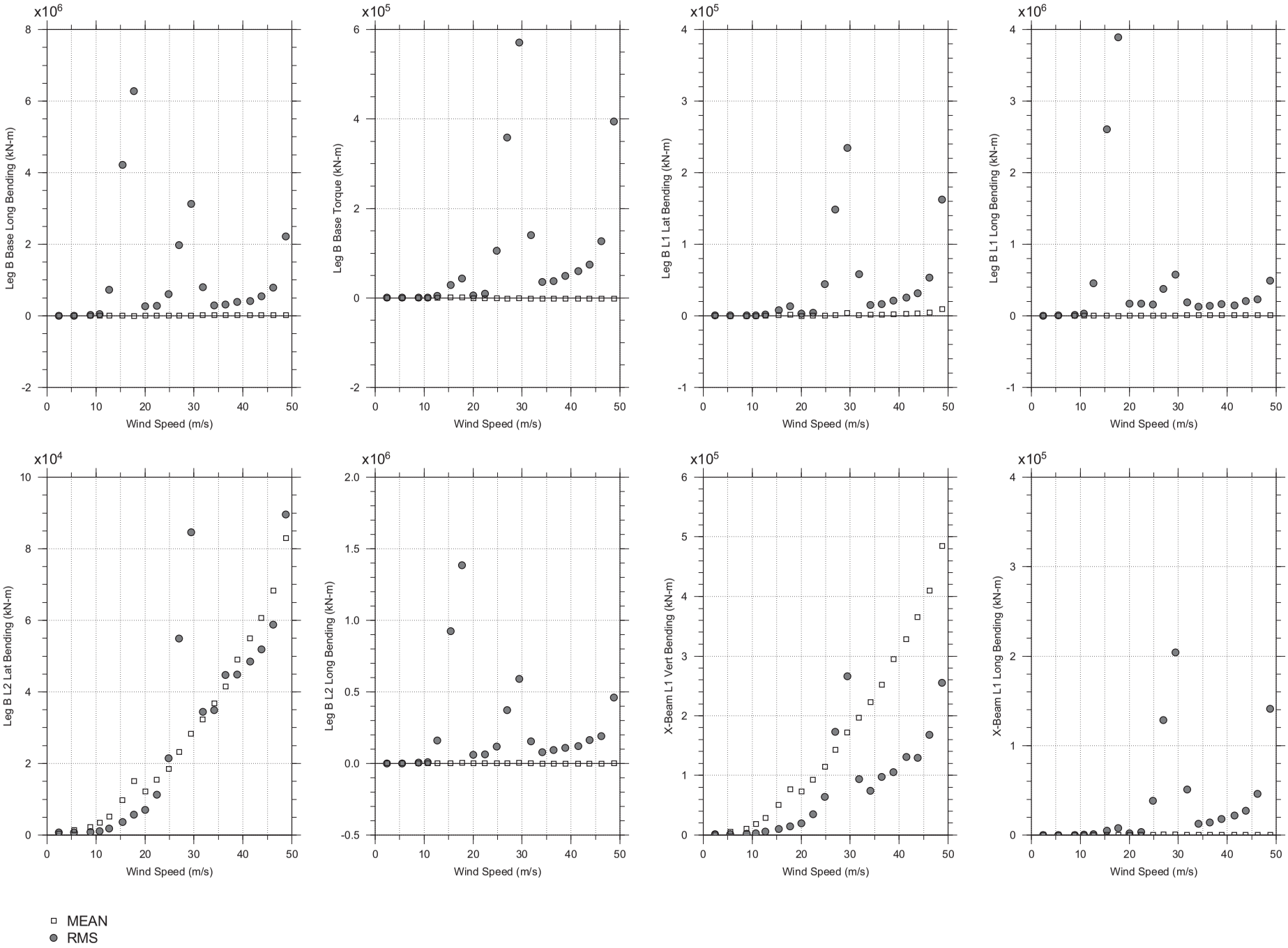

Messina Bridge, Free Standing Tower, 0 degree, Turbulent Flow

Dec. 13, 2010
tf41abdg.cl

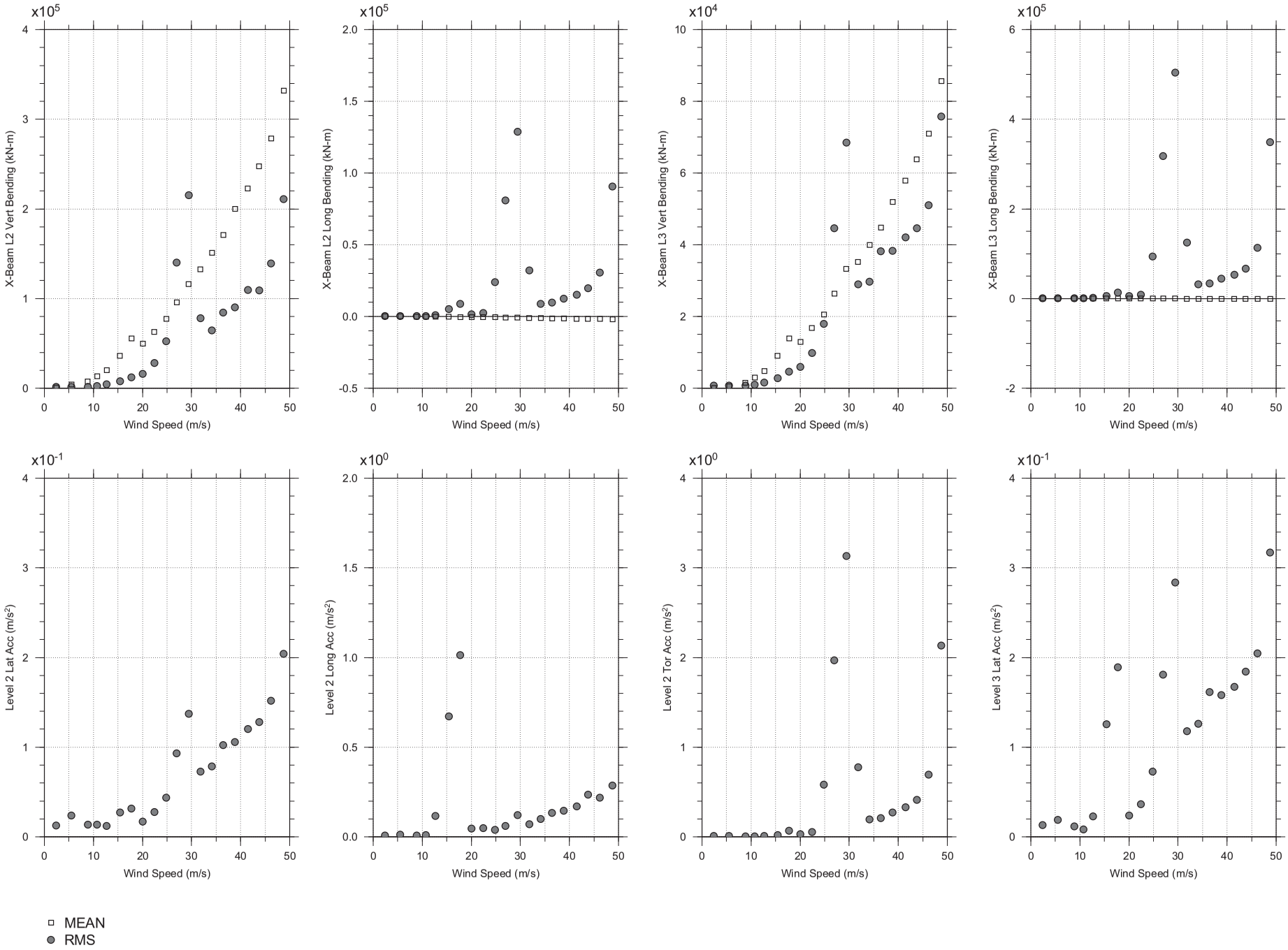

Messina Bridge, Free Standing Tower, 0 degree, Turbulent Flow

Dec. 13, 2010
tf41abdg.cl

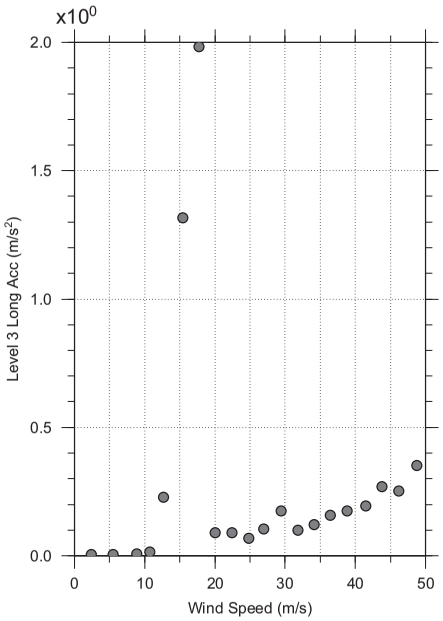

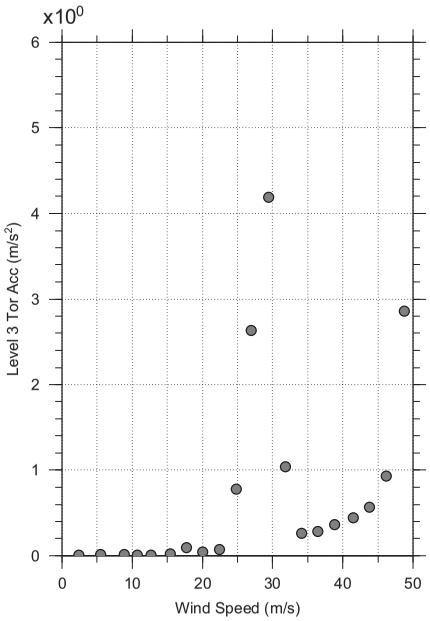

□ MEAN
● RMS

Messina Bridge, Free Standing Tower, 0 degree, Turbulent Flow

Dec. 13, 2010
tf41abdg.cl

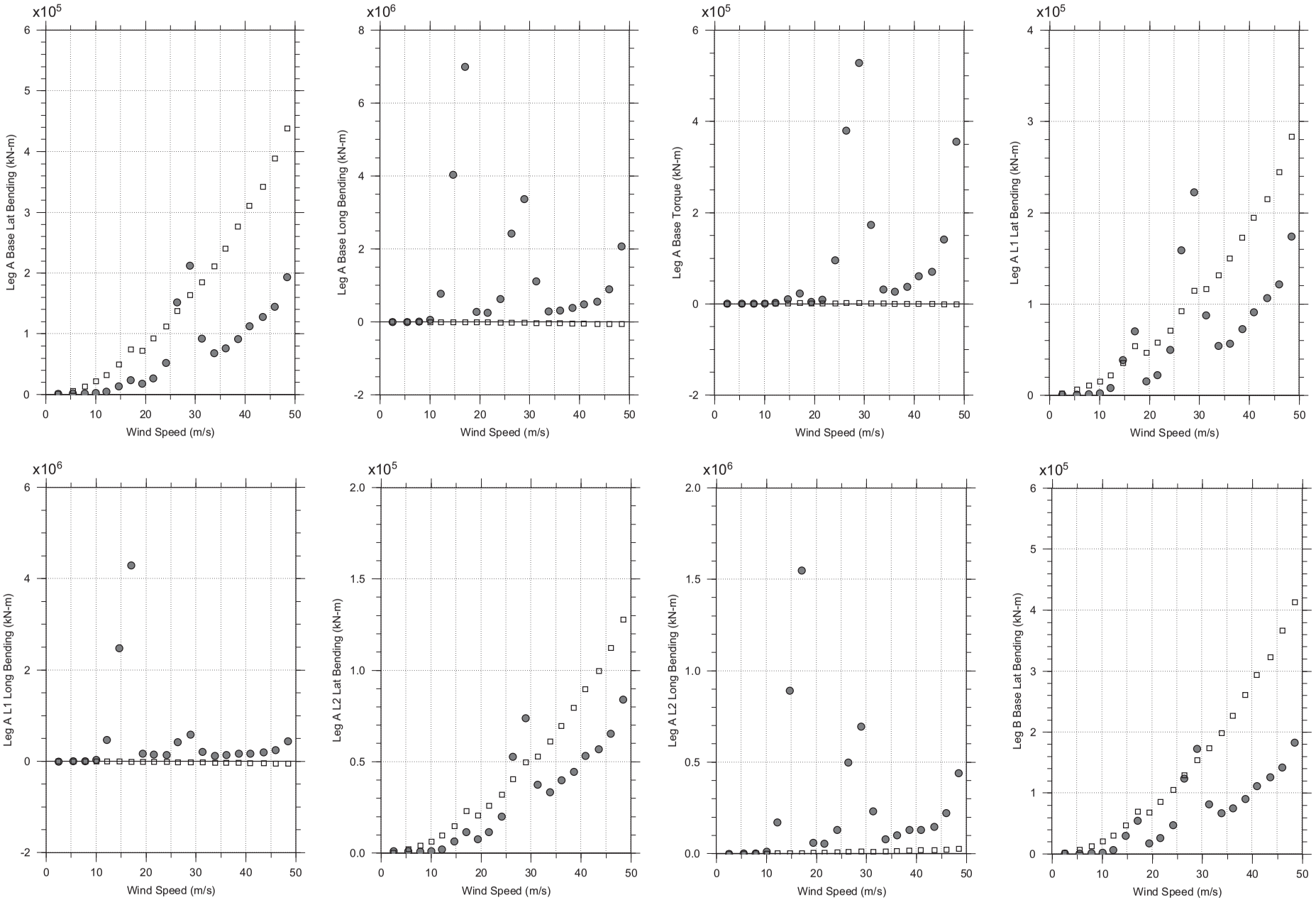

Messina Bridge, Free Standing Tower, 2.5 degree, Turbulent Flow

Dec. 15, 2010
tf42abdg.cl

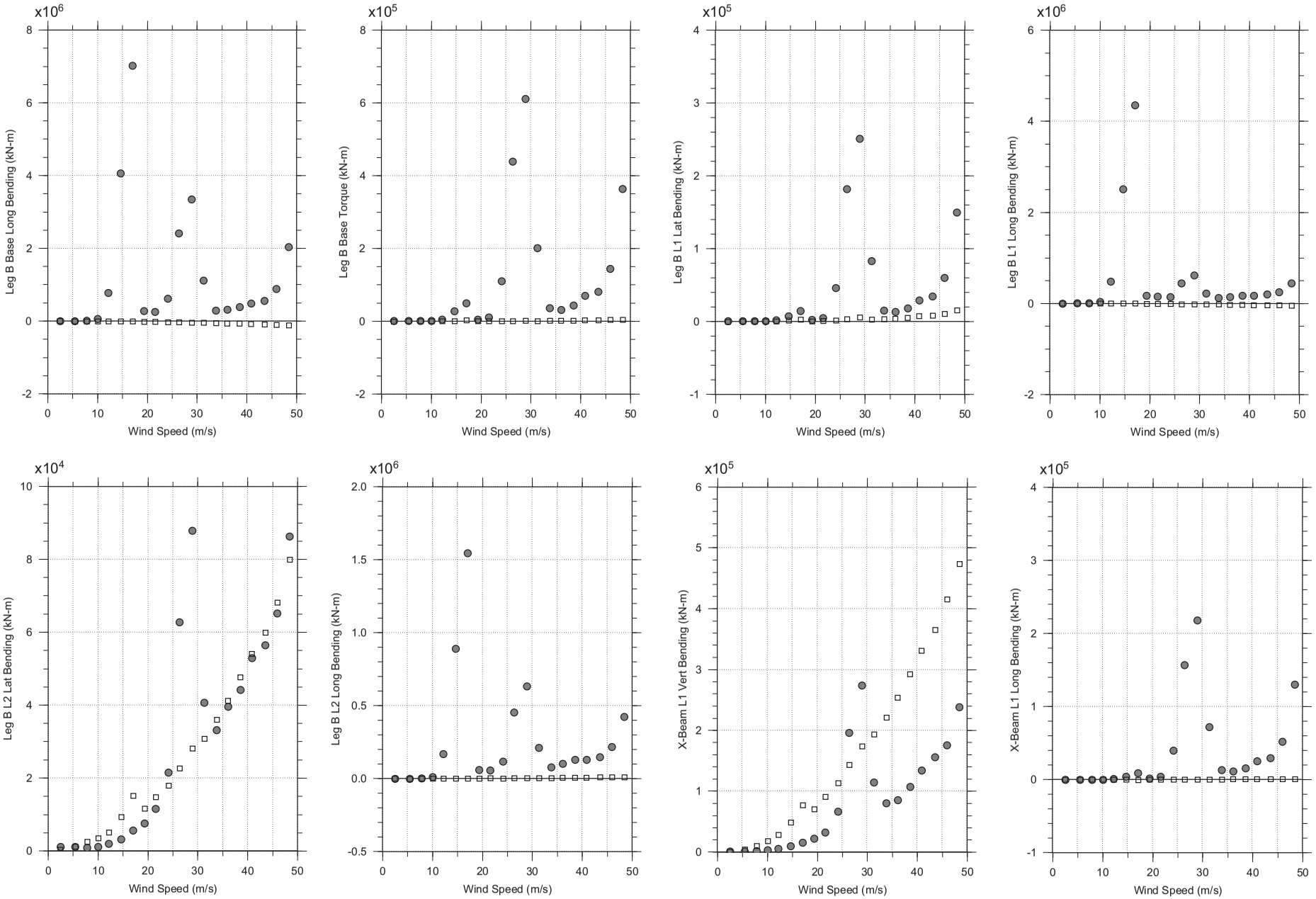

Messina Bridge, Free Standing Tower, 2.5 degree, Turbulent Flow

Dec. 15, 2010
tf42abdg.cl

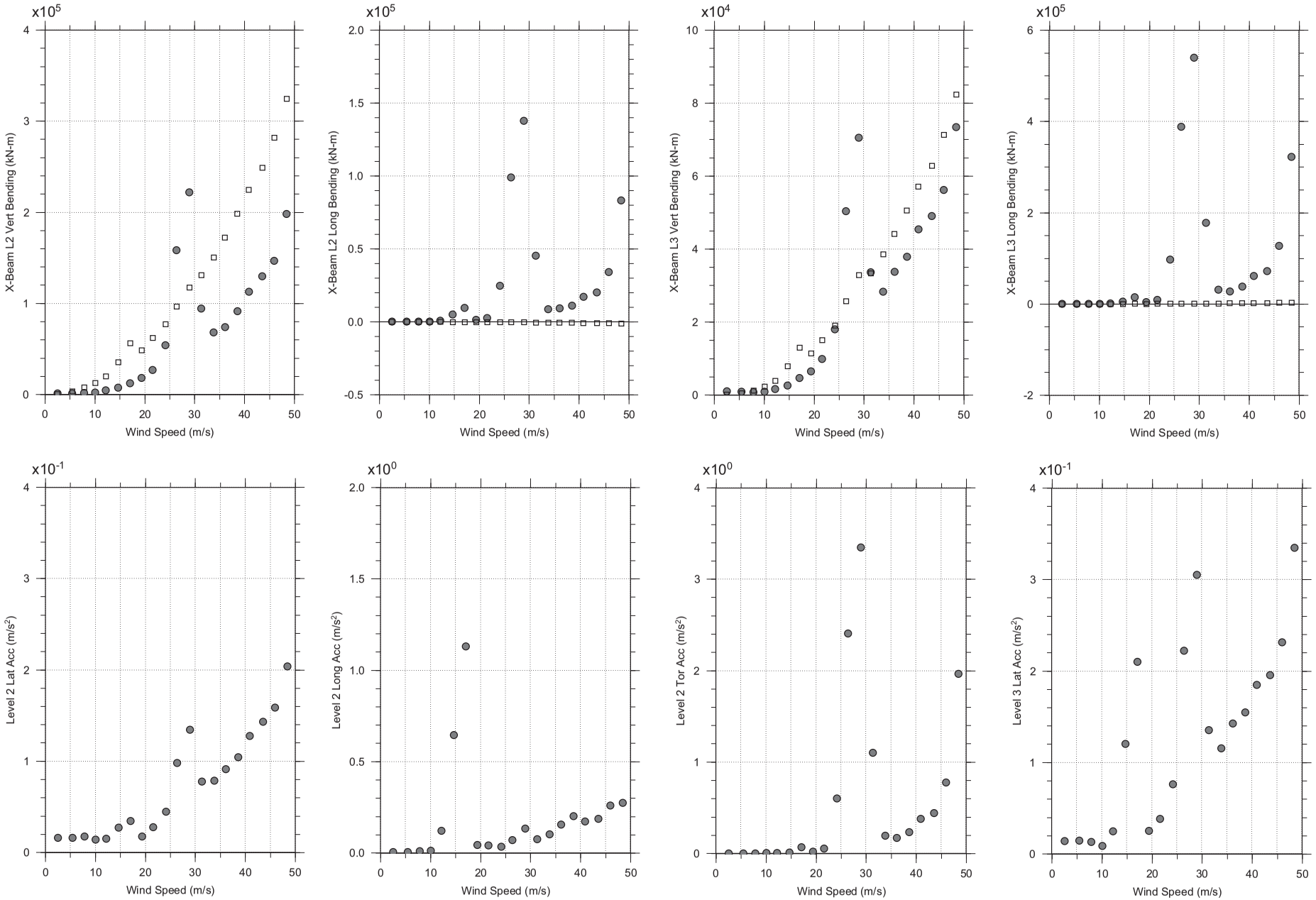

Messina Bridge, Free Standing Tower, 2.5 degree, Turbulent Flow

Dec. 15, 2010
tf42abdg.cl

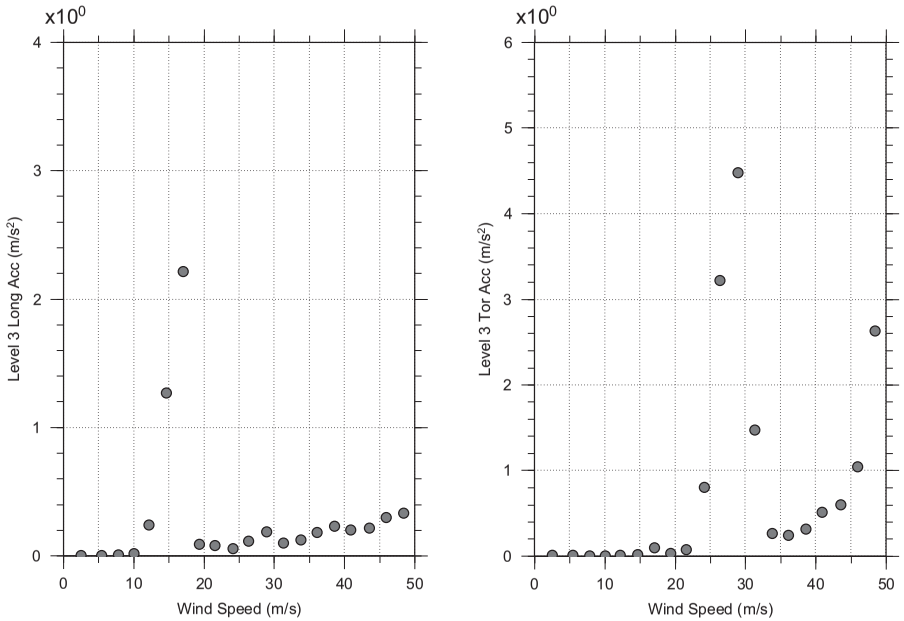

□ MEAN
● RMS

Messina Bridge, Free Standing Tower, 2.5 degree, Turbulent Flow

Dec. 15, 2010
tf42abdg.cl

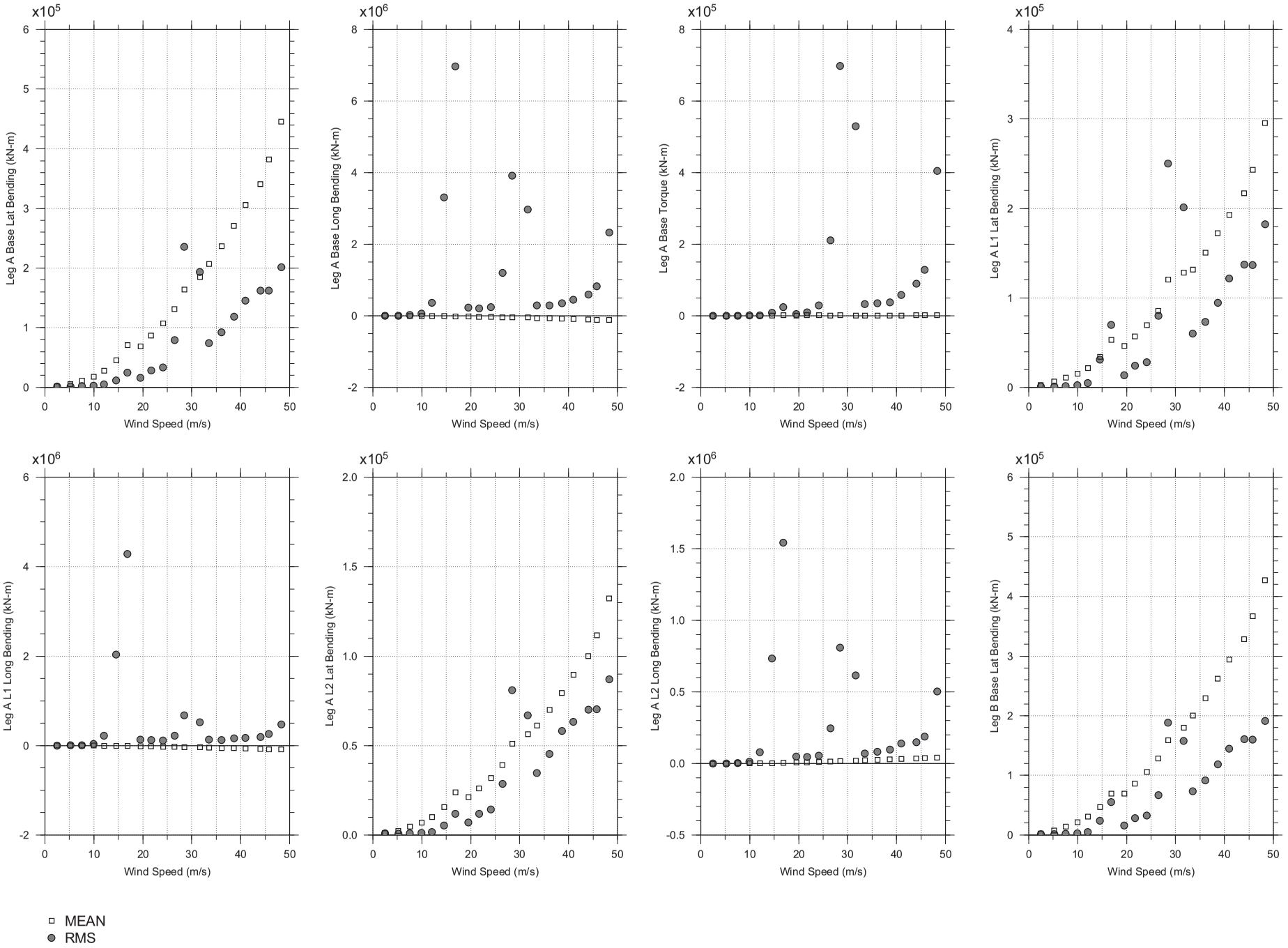

Messina Bridge, Free Standing Tower, 5 degree, Turbulent Flow

Dec. 13, 2010
tf43abdg.cl

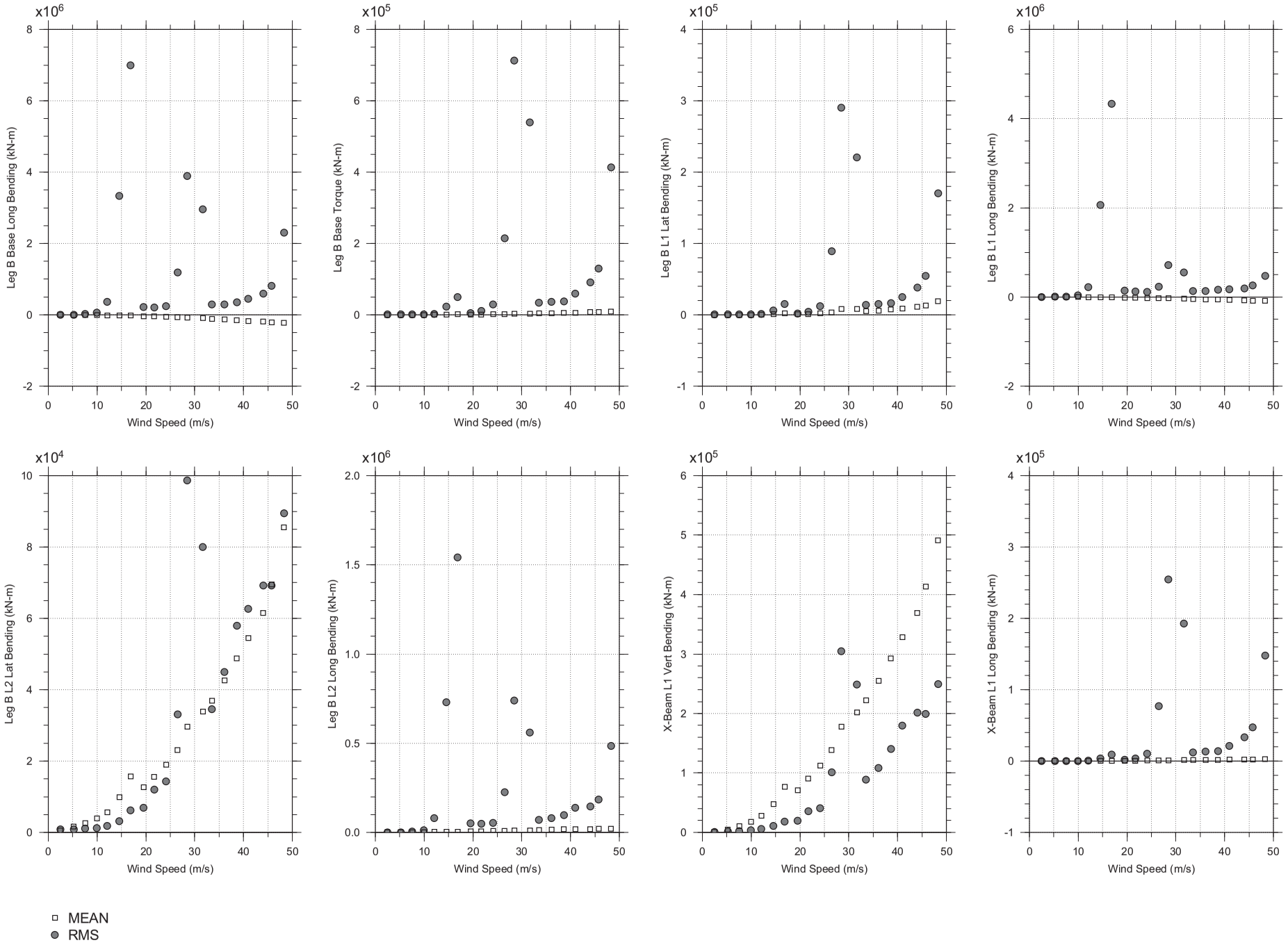

Messina Bridge, Free Standing Tower, 5 degree, Turbulent Flow

Dec. 13, 2010
tf43abdg.cl

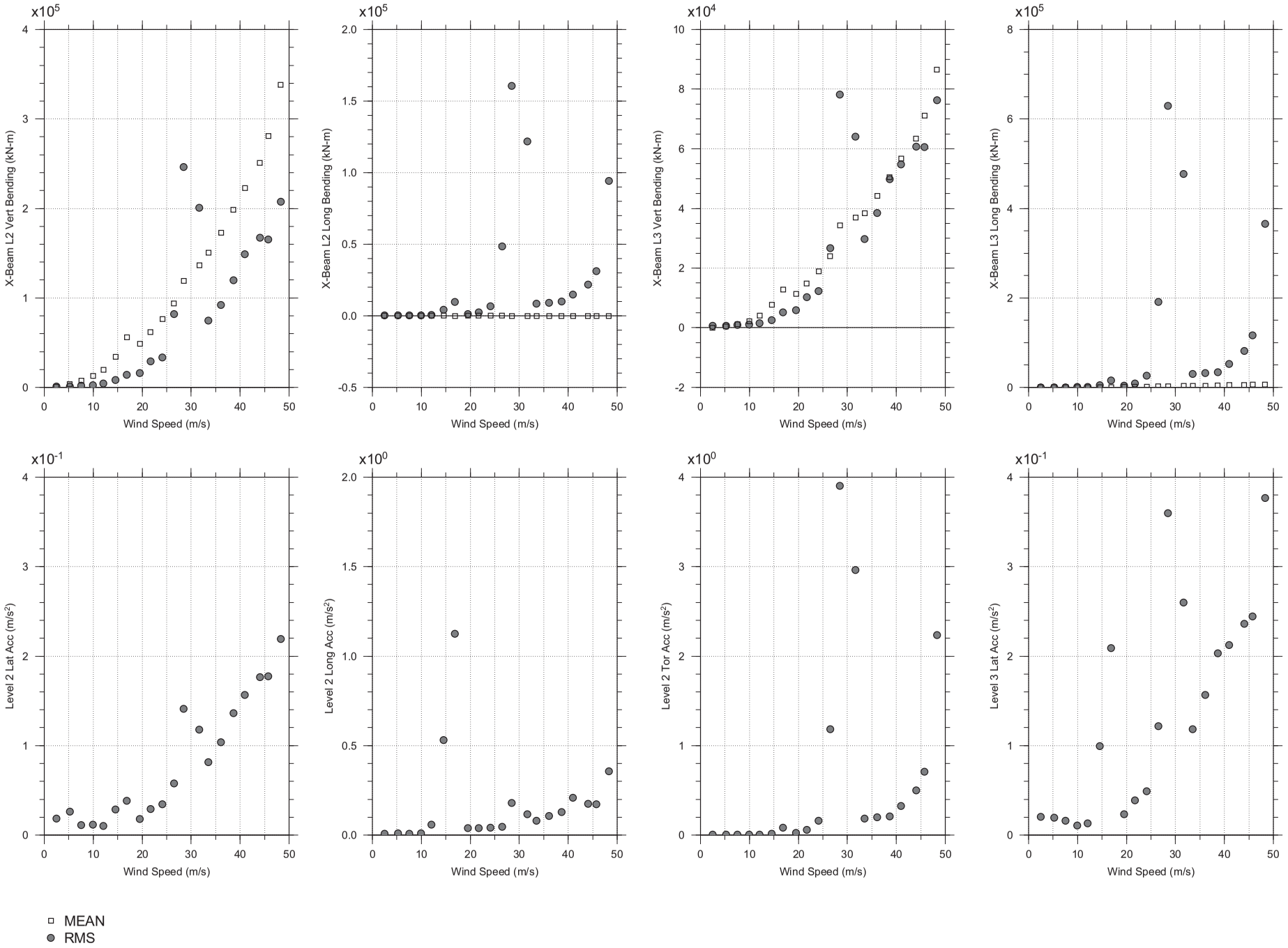

Messina Bridge, Free Standing Tower, 5 degree, Turbulent Flow

Dec. 13, 2010
tf43abdg.cl

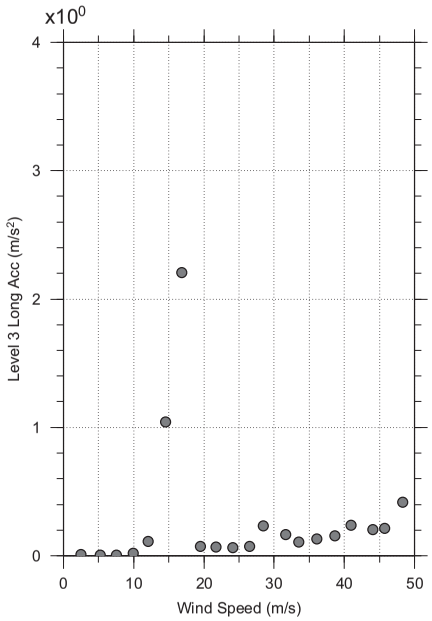

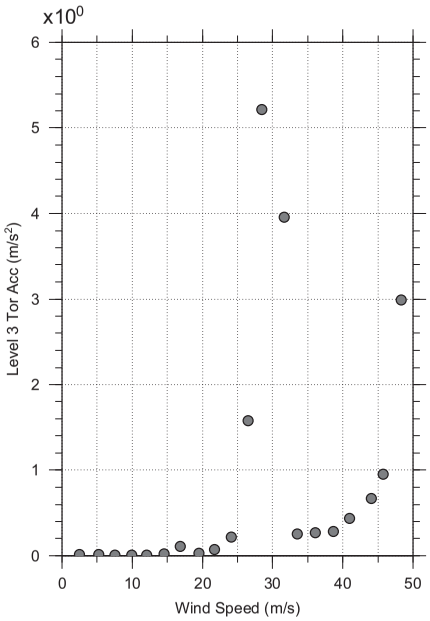

□ MEAN
● RMS

Messina Bridge, Free Standing Tower, 5 degree, Turbulent Flow

Dec. 13, 2010
tf43abdg.cl

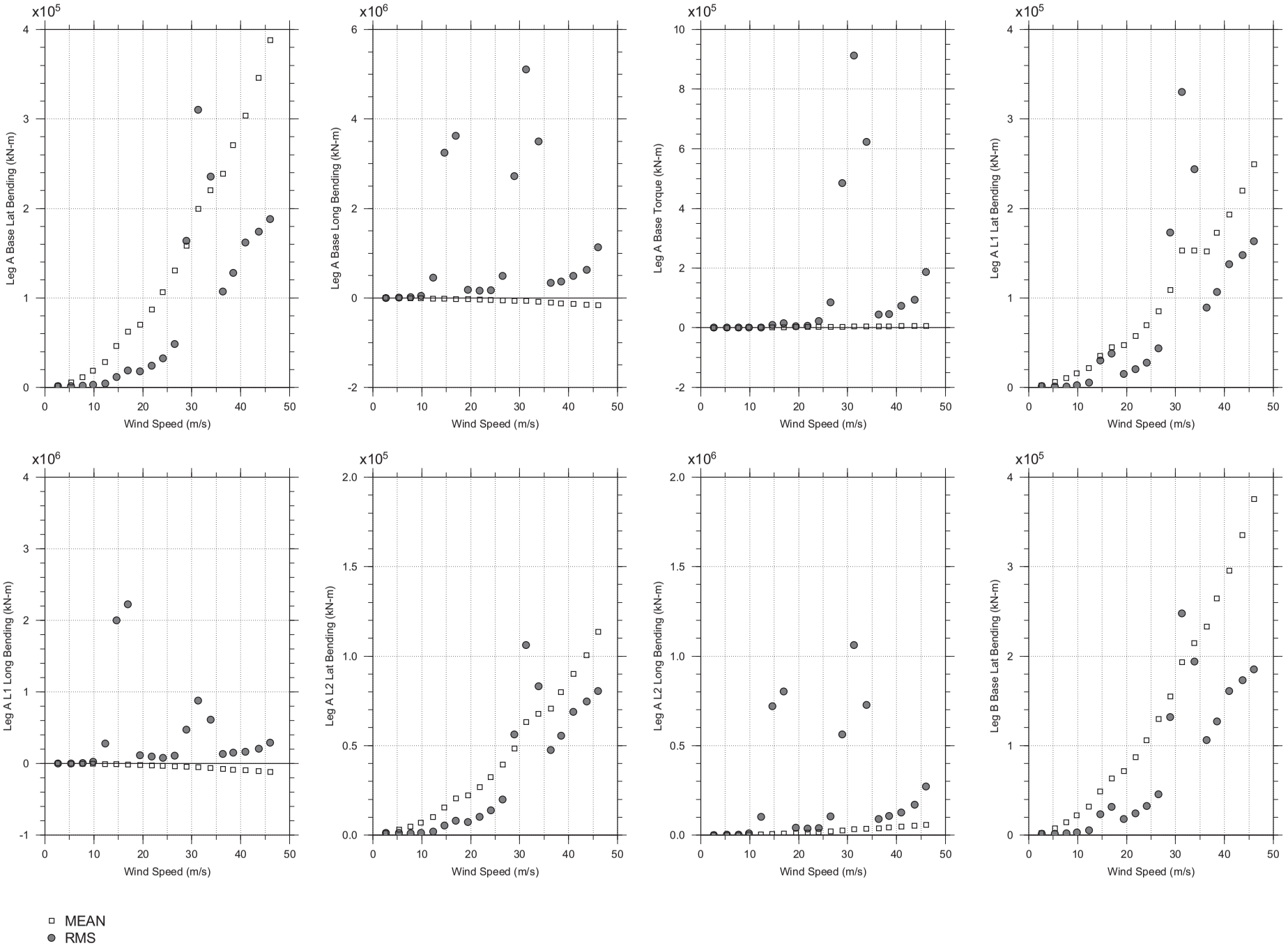

Messina Bridge, Free Standing Tower, 7.5 degree, Turbulent Flow

Dec. 13, 2010
tf44abdg.cl

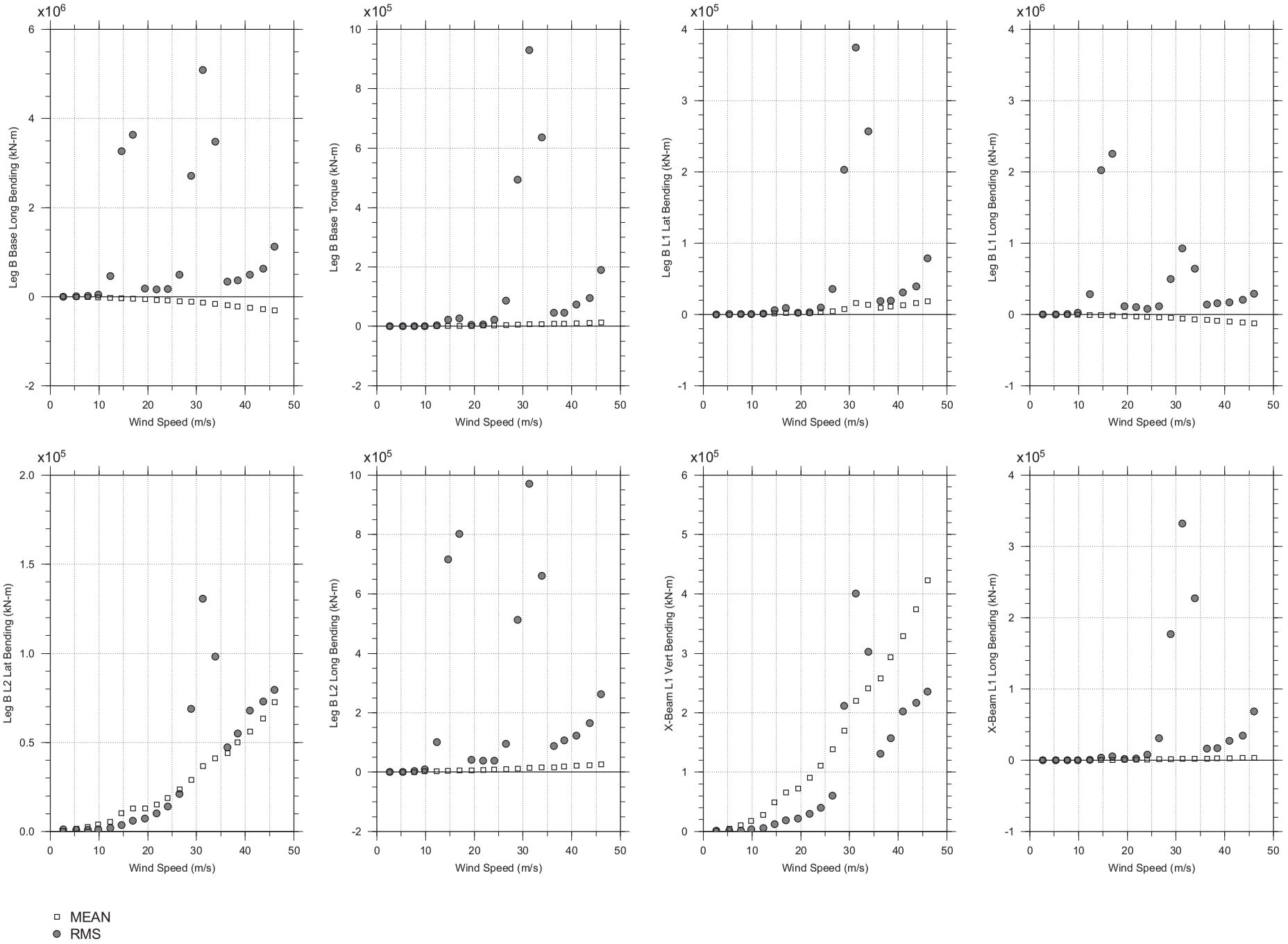

Messina Bridge, Free Standing Tower, 7.5 degree, Turbulent Flow

Dec. 13, 2010
tf44abdg.cl

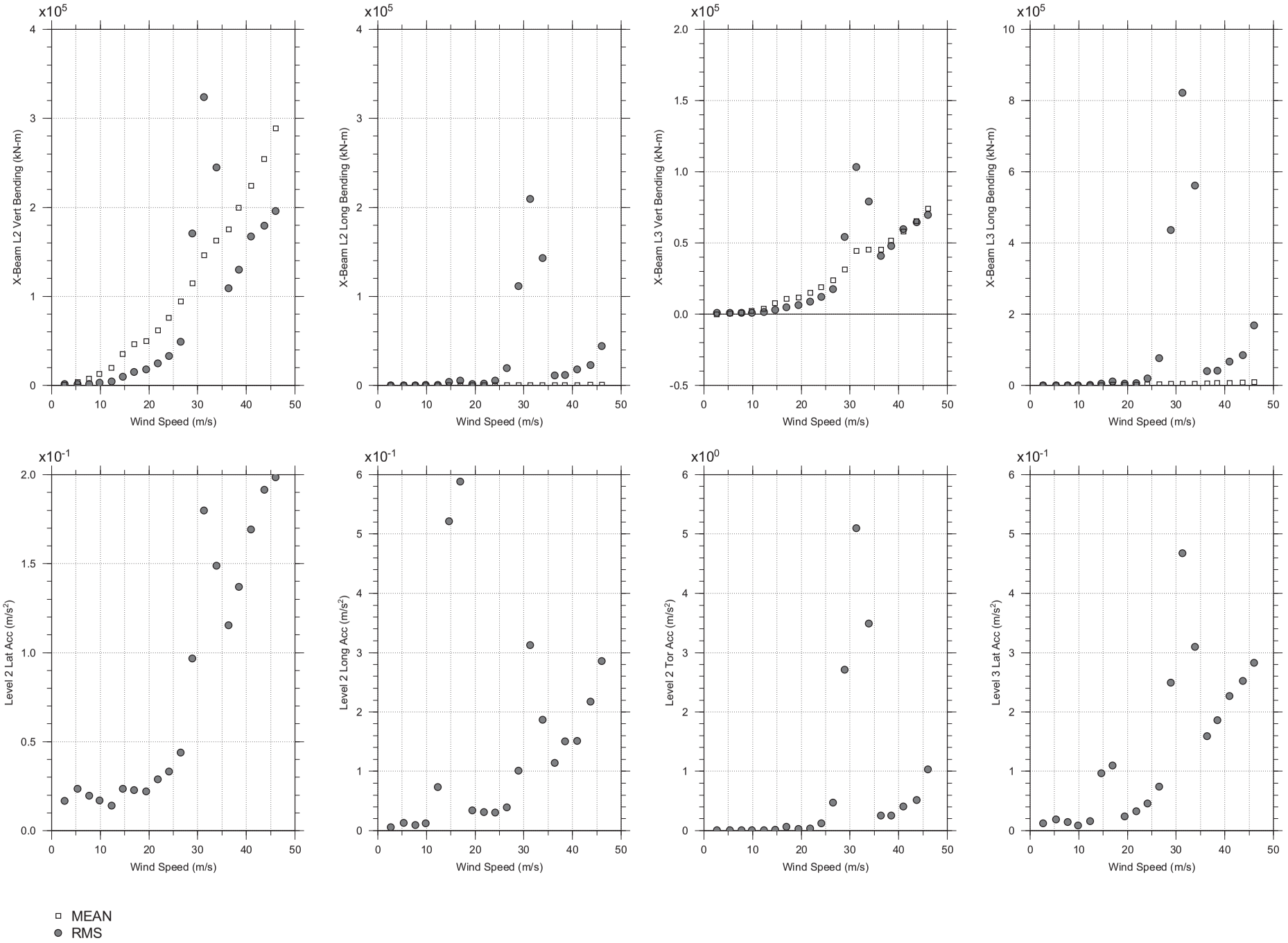

Messina Bridge, Free Standing Tower, 7.5 degree, Turbulent Flow

Dec. 13, 2010
tf44abdg.cl

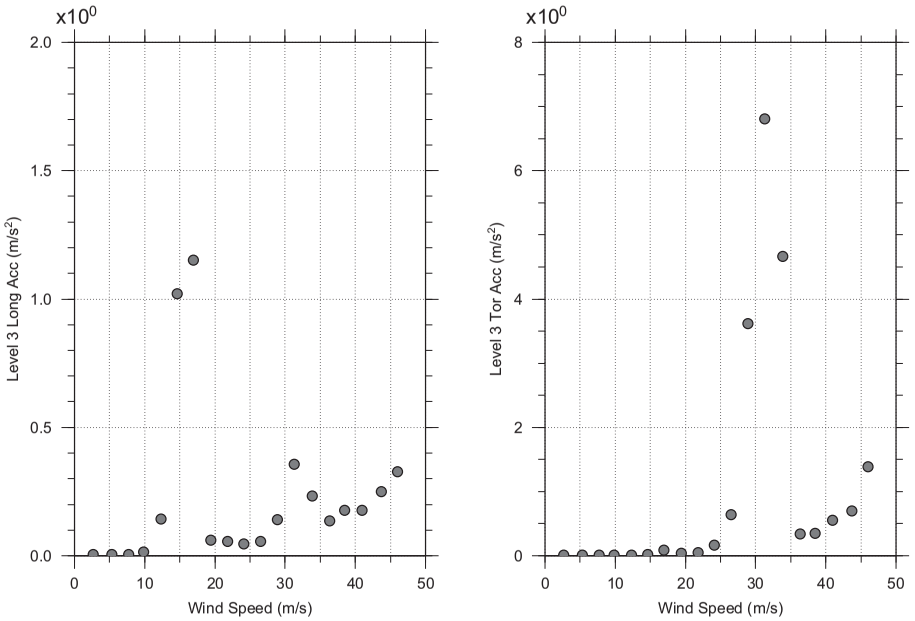

MEAN
RMS

Messina Bridge, Free Standing Tower, 7.5 degree, Turbulent Flow

Dec. 13, 2010
tf44abdg.cl

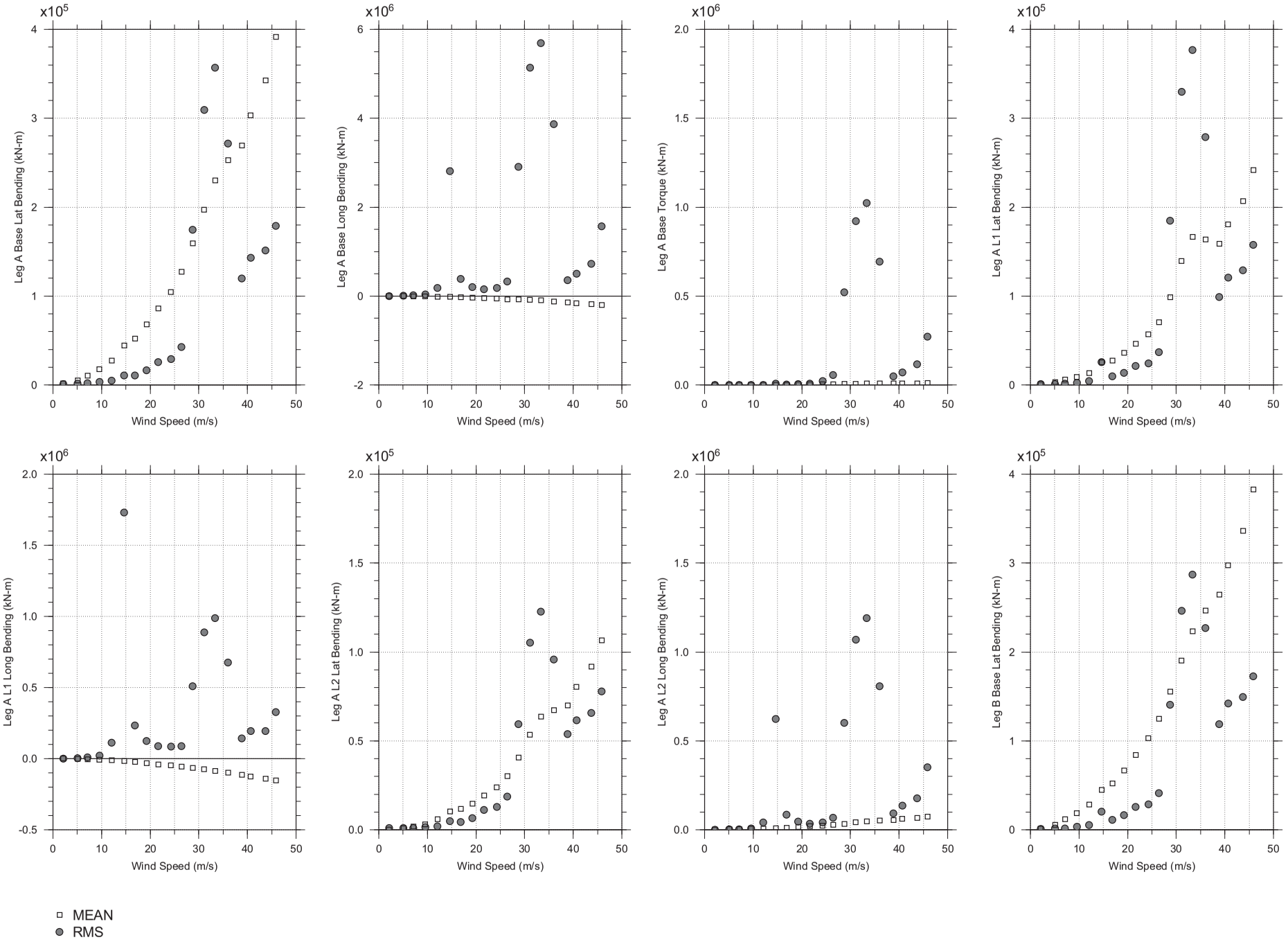

Messina Bridge, Free Standing Tower, 10 degree, Turbulent Flow

Dec. 13, 2010
tf45abdg.cl

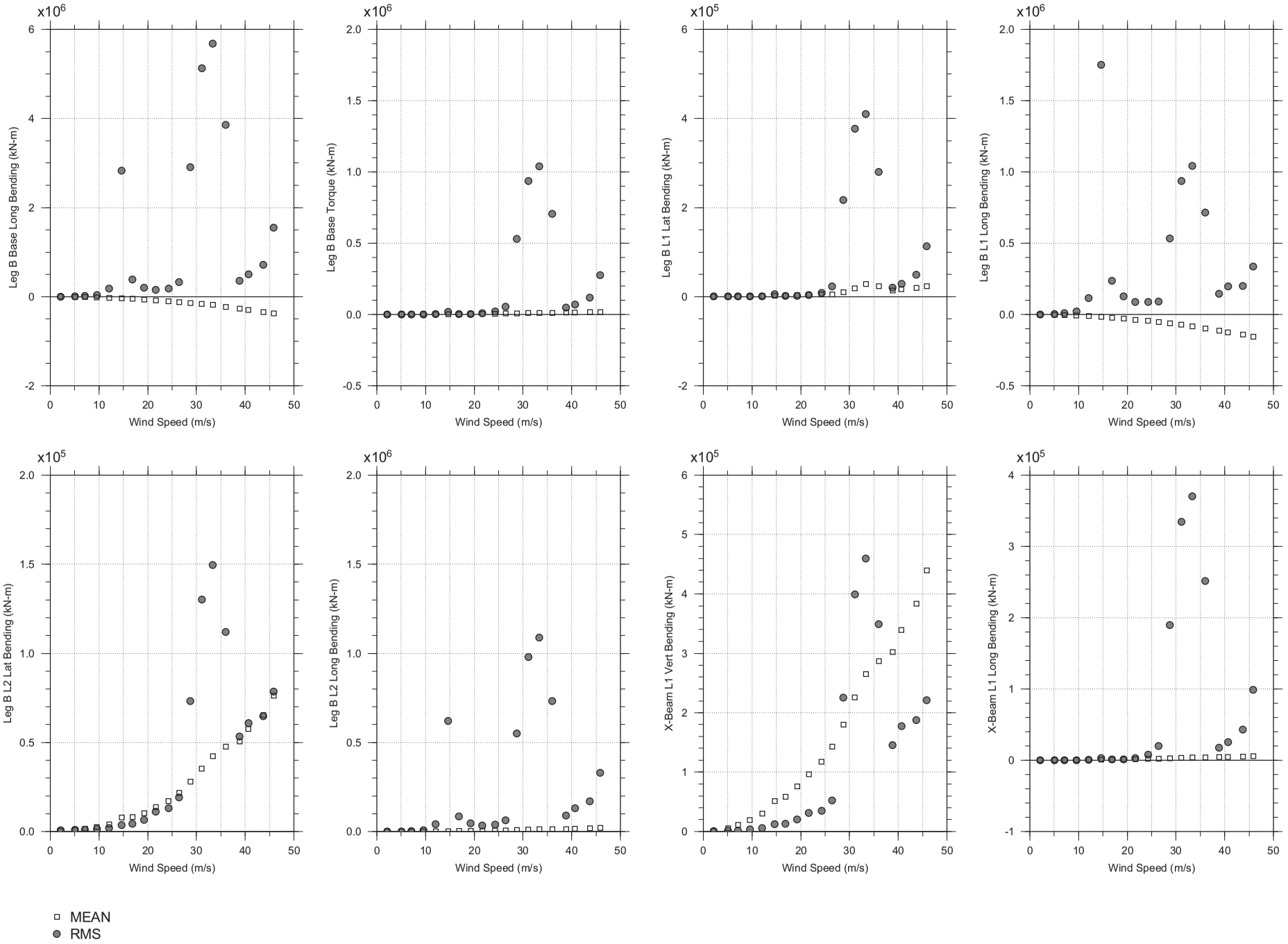

Messina Bridge, Free Standing Tower, 10 degree, Turbulent Flow

Dec. 13, 2010
tf45abdg.cl

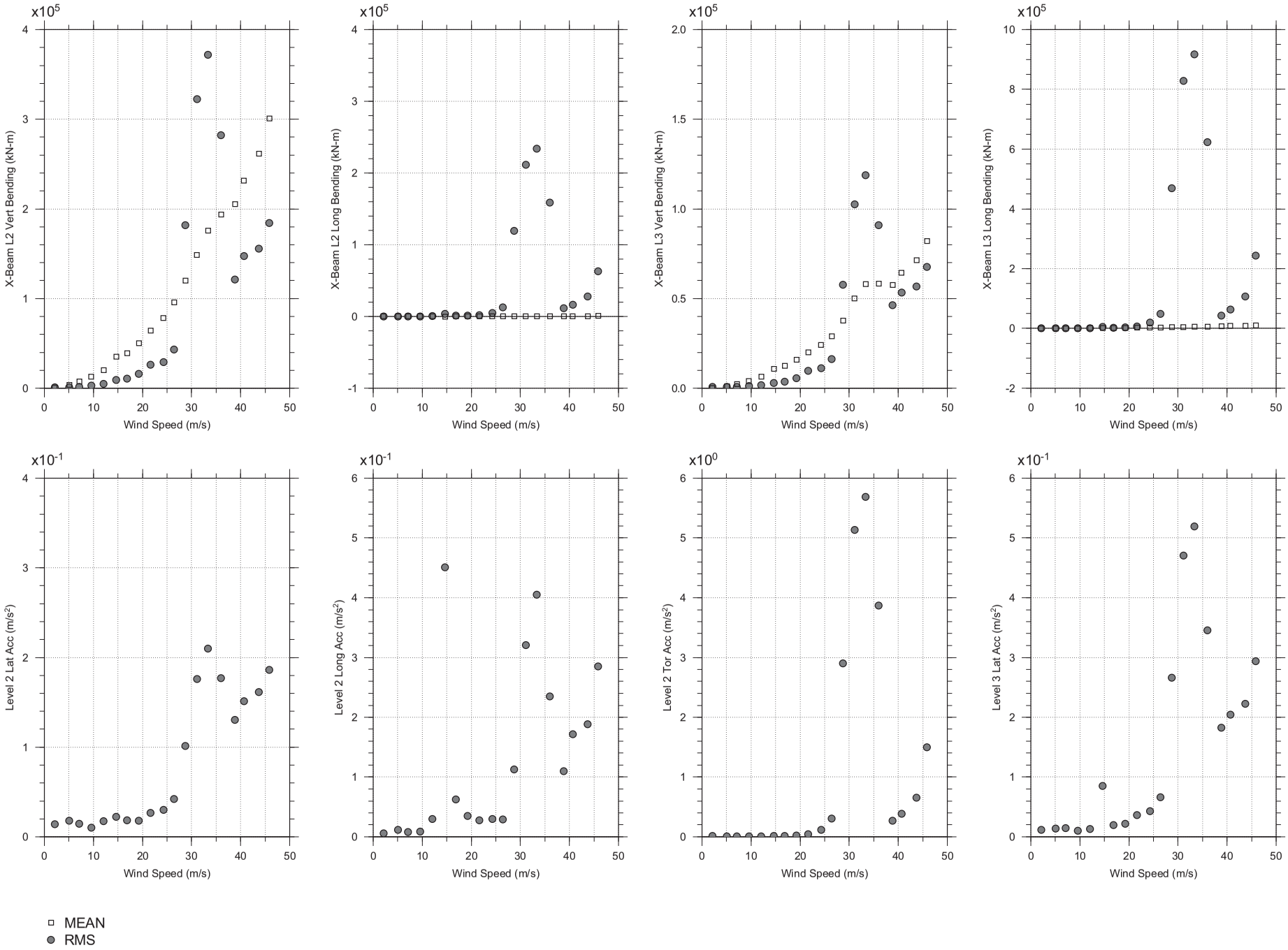

Messina Bridge, Free Standing Tower, 10 degree, Turbulent Flow

Dec. 13, 2010
tf45abdg.cl

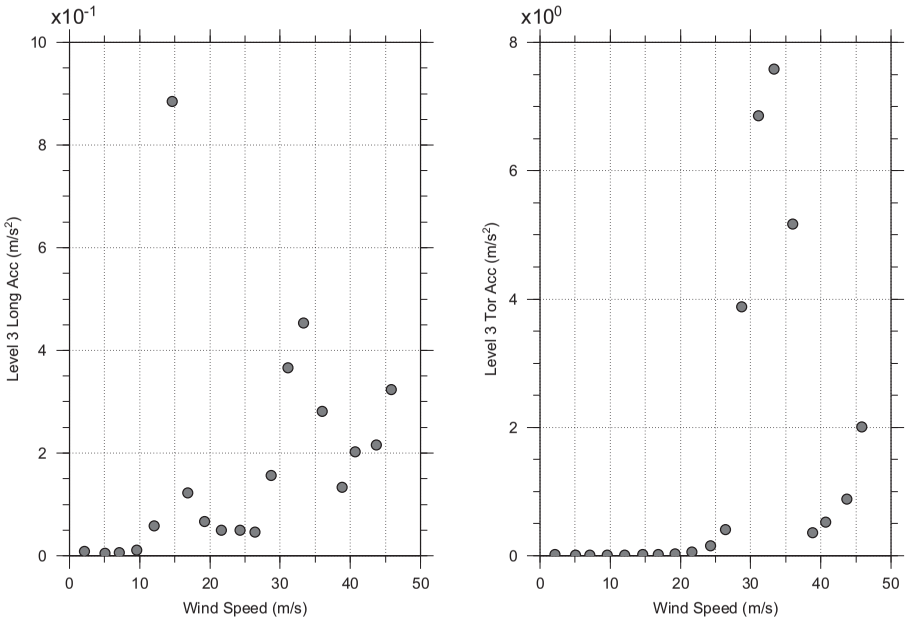

MEAN
RMS

Messina Bridge, Free Standing Tower, 10 degree, Turbulent Flow

Dec. 13, 2010
tf45abdg.cl

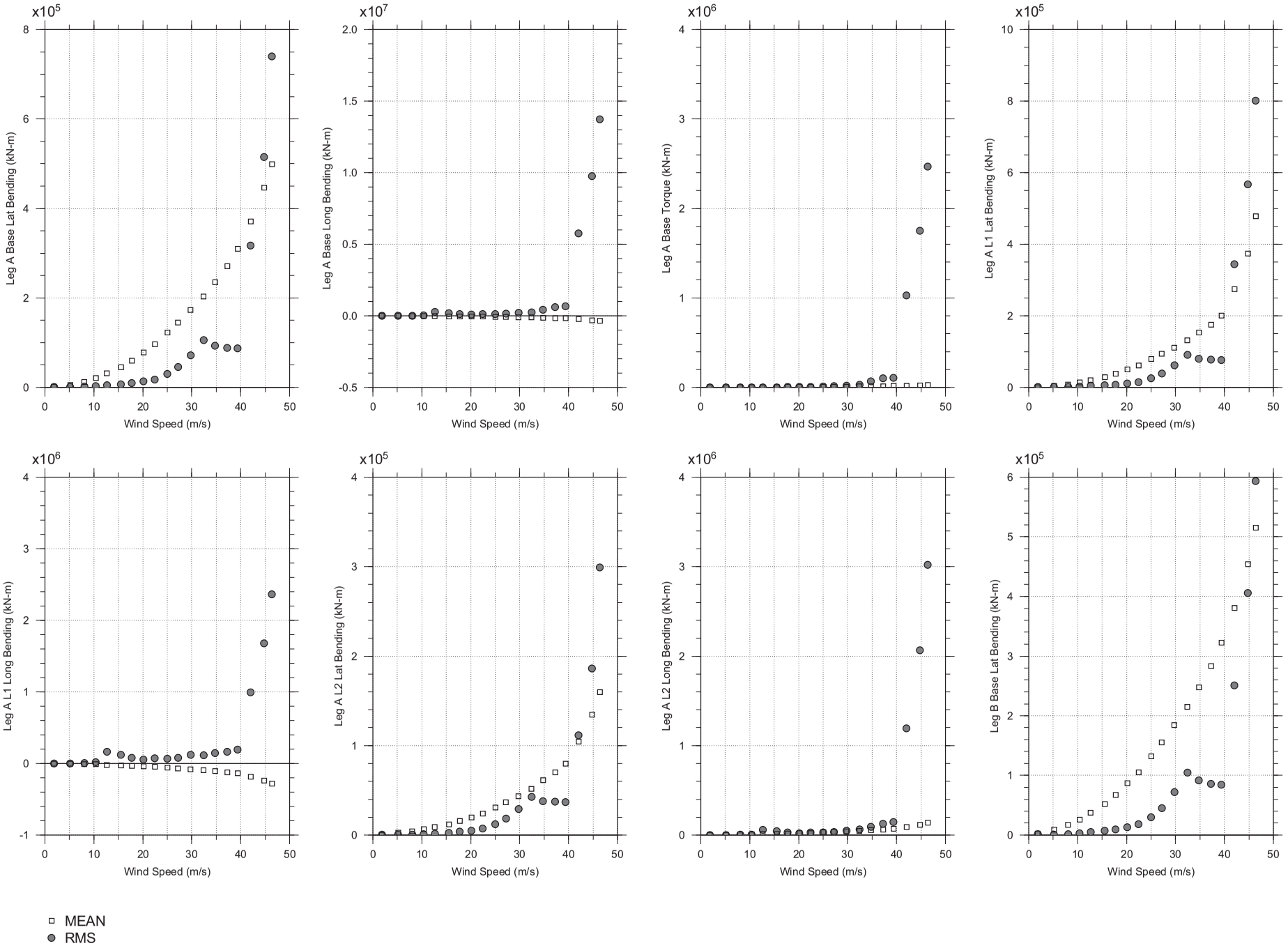

Messina Bridge, Free Standing Tower, 20 degree, Turbulent Flow

Dec. 14, 2010
tf47abdg.cl

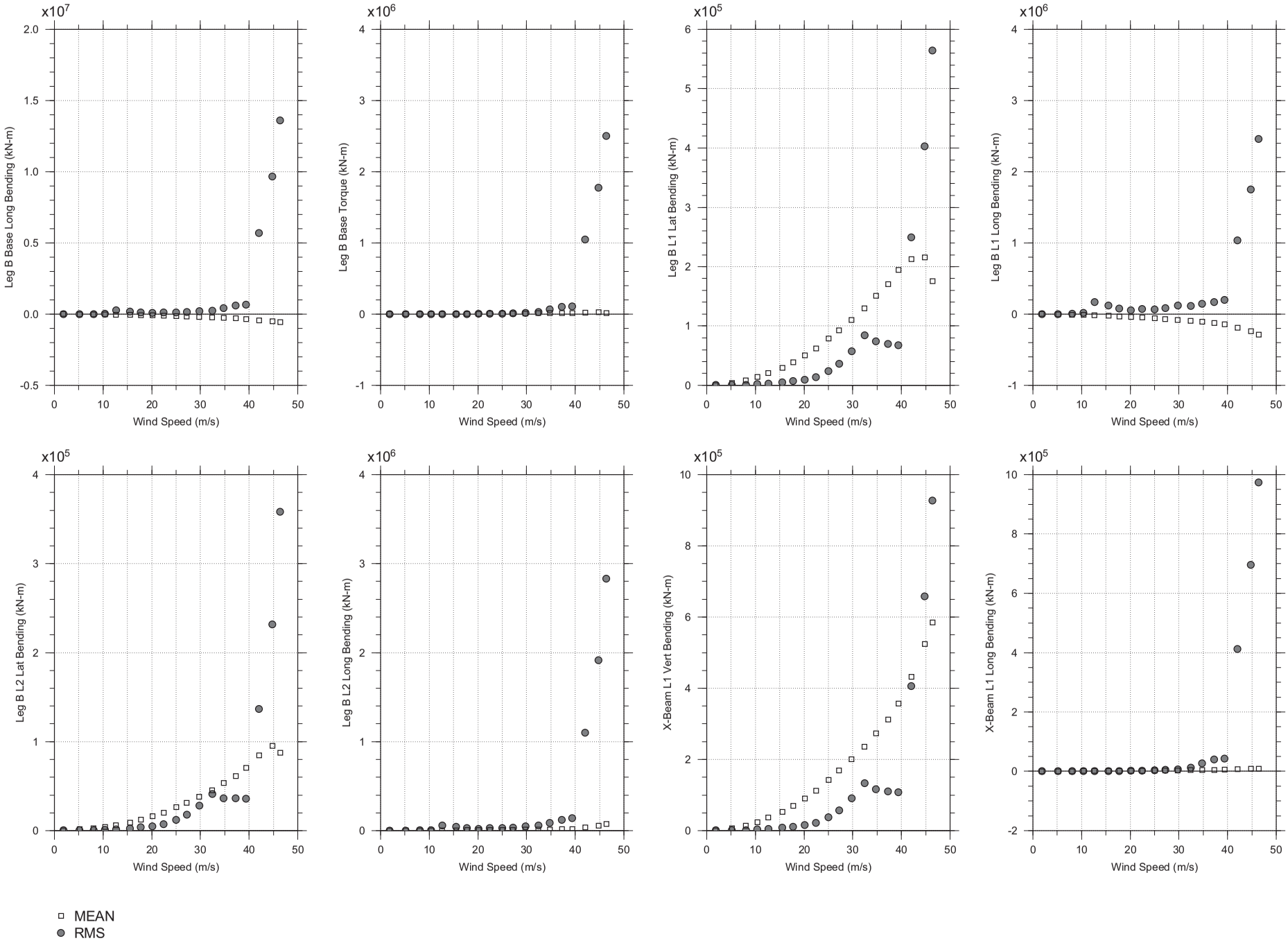

Messina Bridge, Free Standing Tower, 20 degree, Turbulent Flow

Dec. 14, 2010
tf47abdg.cl

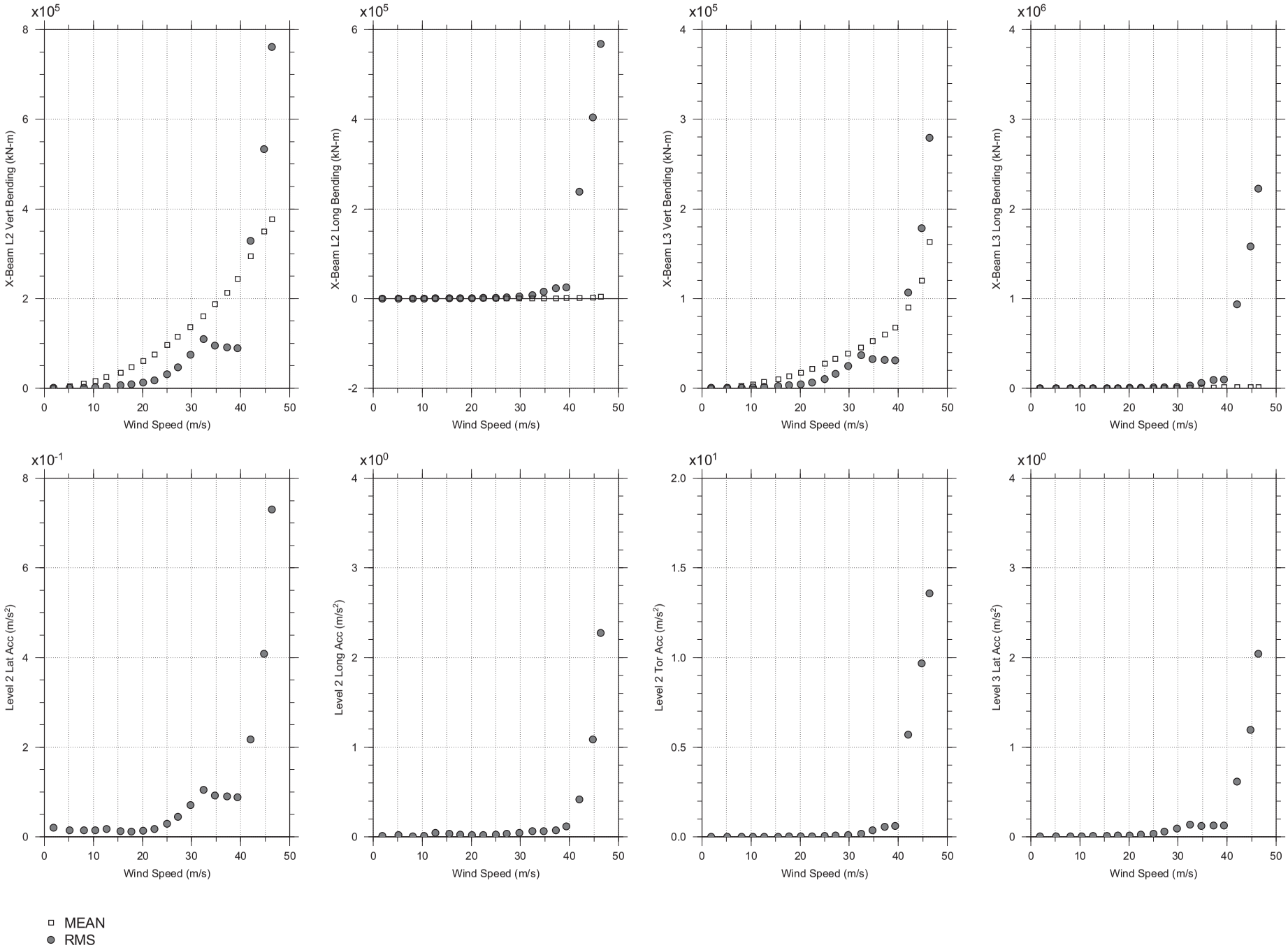

Messina Bridge, Free Standing Tower, 20 degree, Turbulent Flow

Dec. 14, 2010
tf47abdg.cl

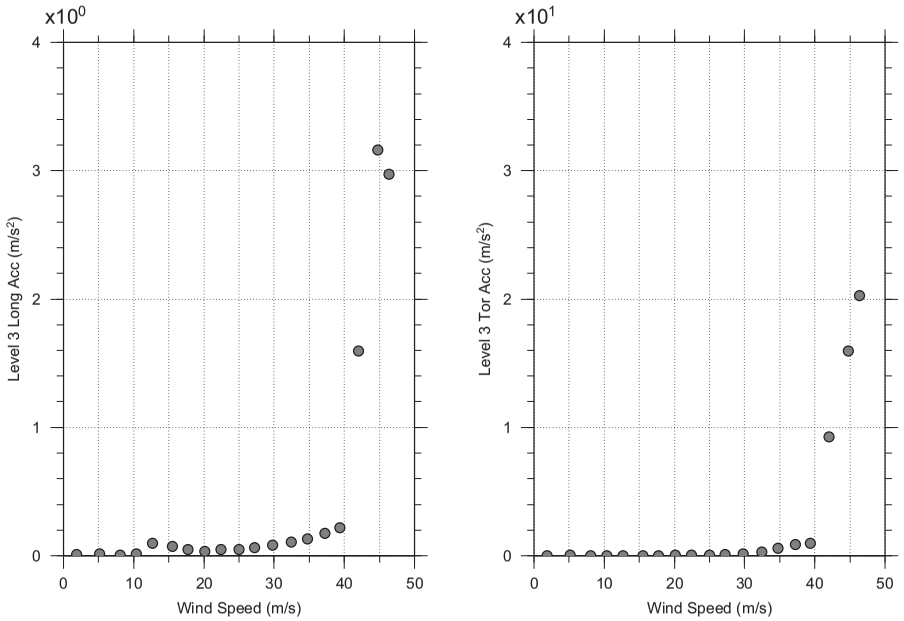

MEAN
RMS

Messina Bridge, Free Standing Tower, 20 degree, Turbulent Flow

Dec. 14, 2010
tf47abdg.cl

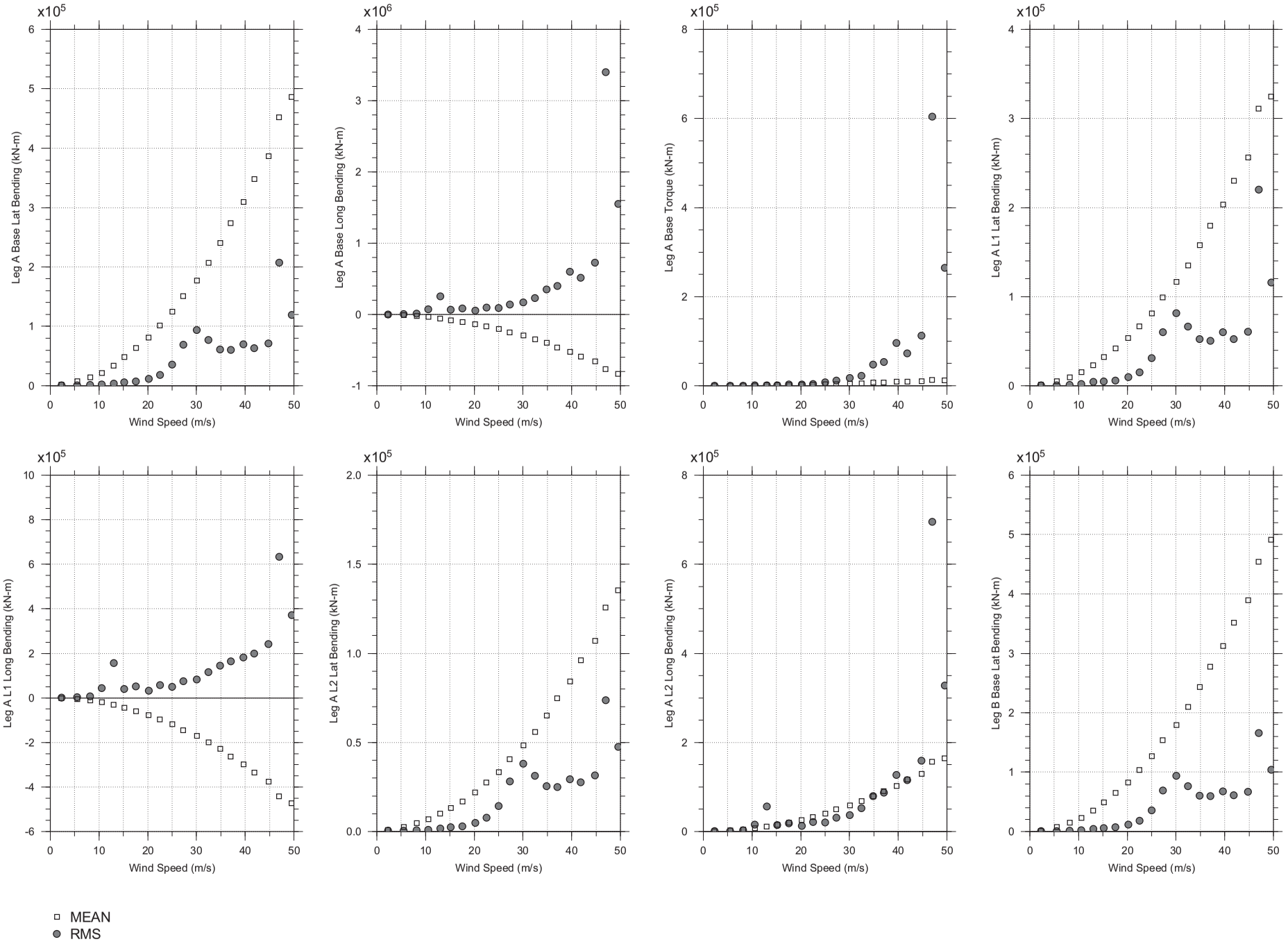

Messina Bridge, Free Standing Tower, 30 degree, Turbulent Flow

Dec. 14, 2010
tf48abdg.cl

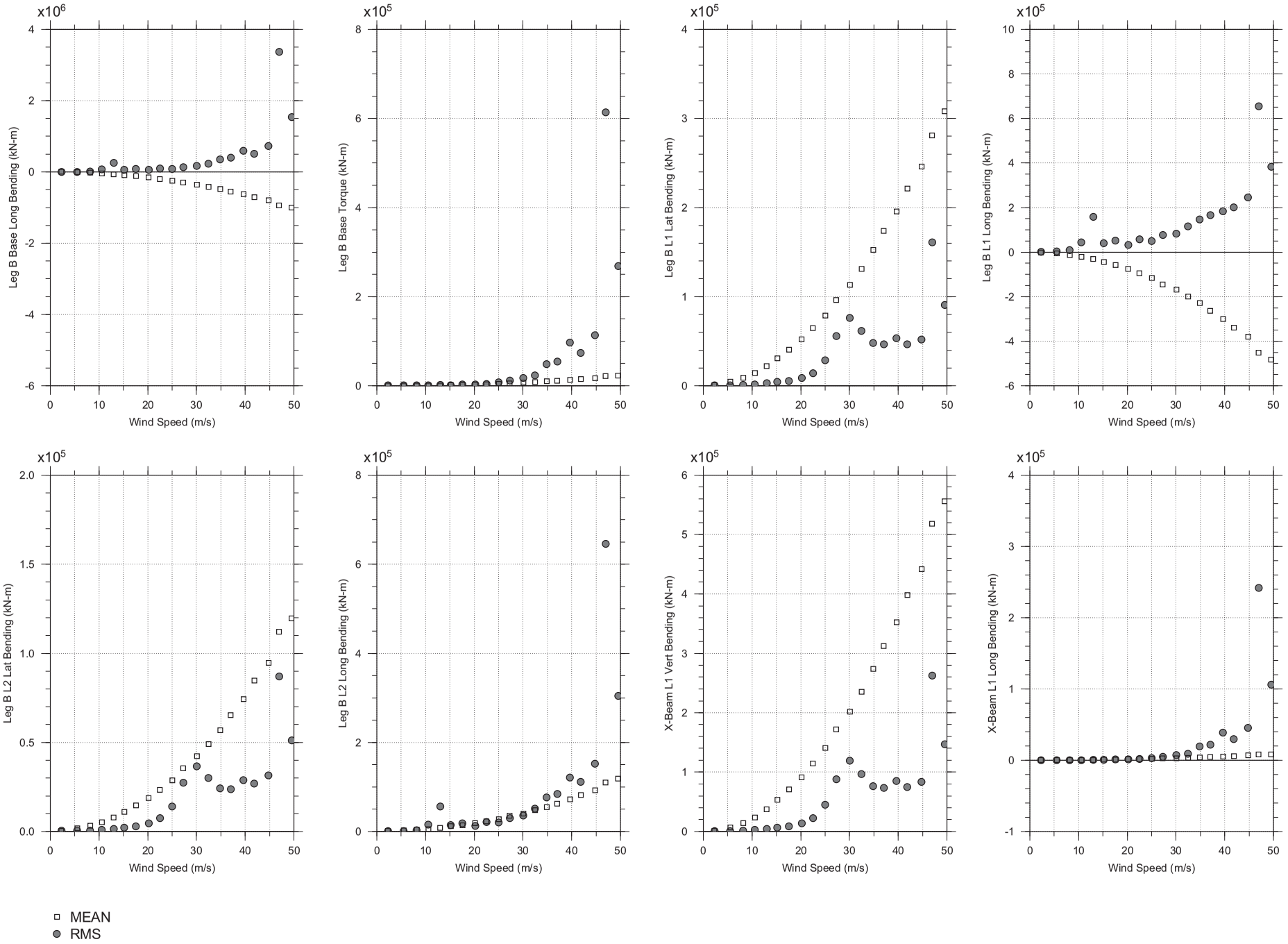

Messina Bridge, Free Standing Tower, 30 degree, Turbulent Flow

Dec. 14, 2010
tf48abdg.cl

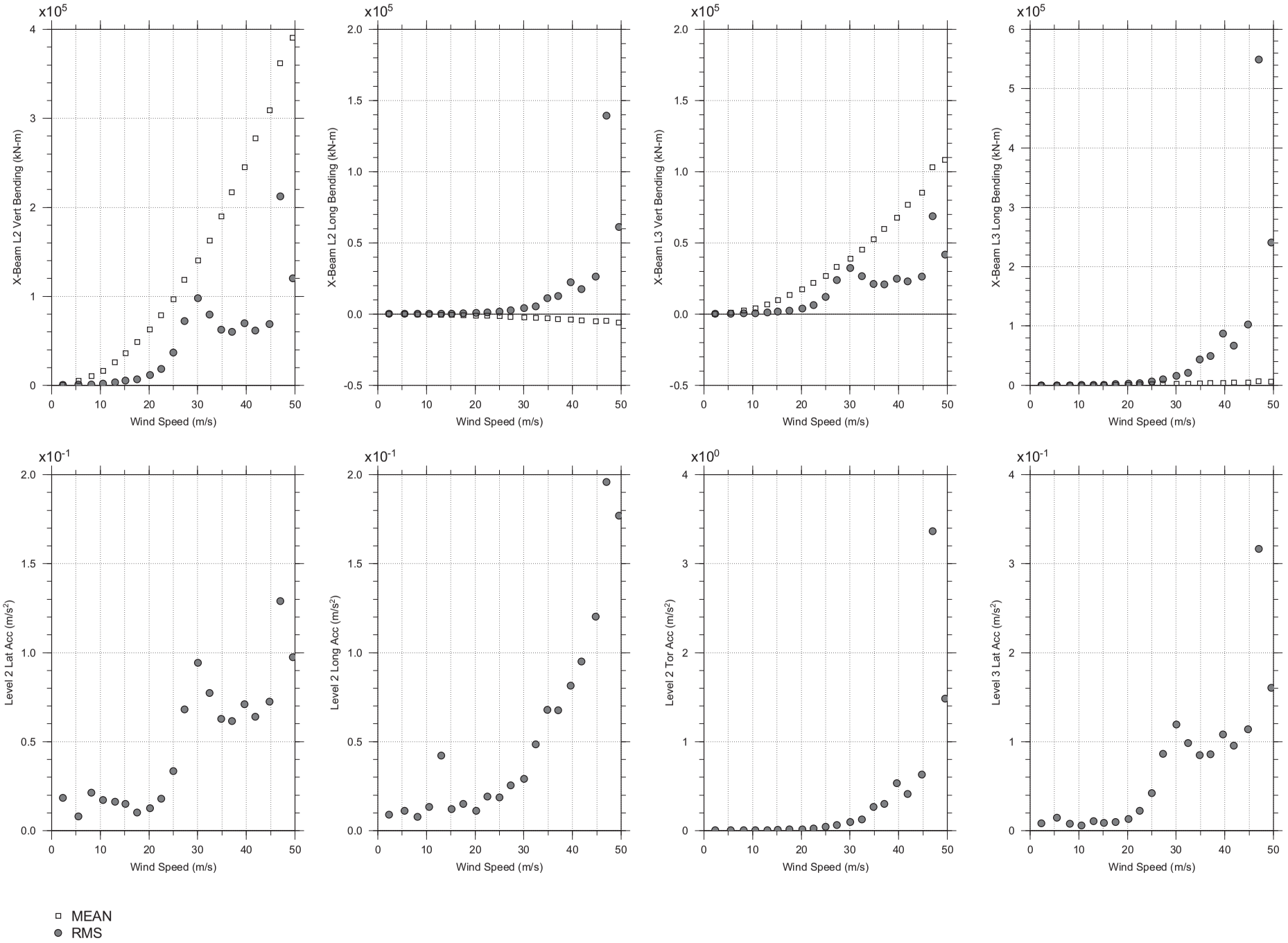

Messina Bridge, Free Standing Tower, 30 degree, Turbulent Flow

Dec. 14, 2010
tf48abdg.cl

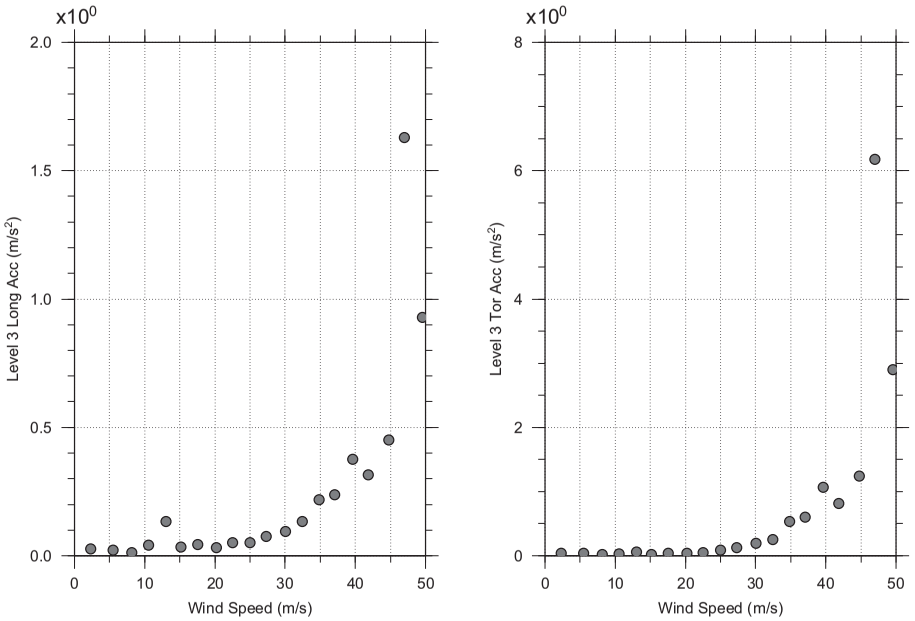

MEAN
RMS

Messina Bridge, Free Standing Tower, 30 degree, Turbulent Flow

Dec. 14, 2010
tf48abdg.cl

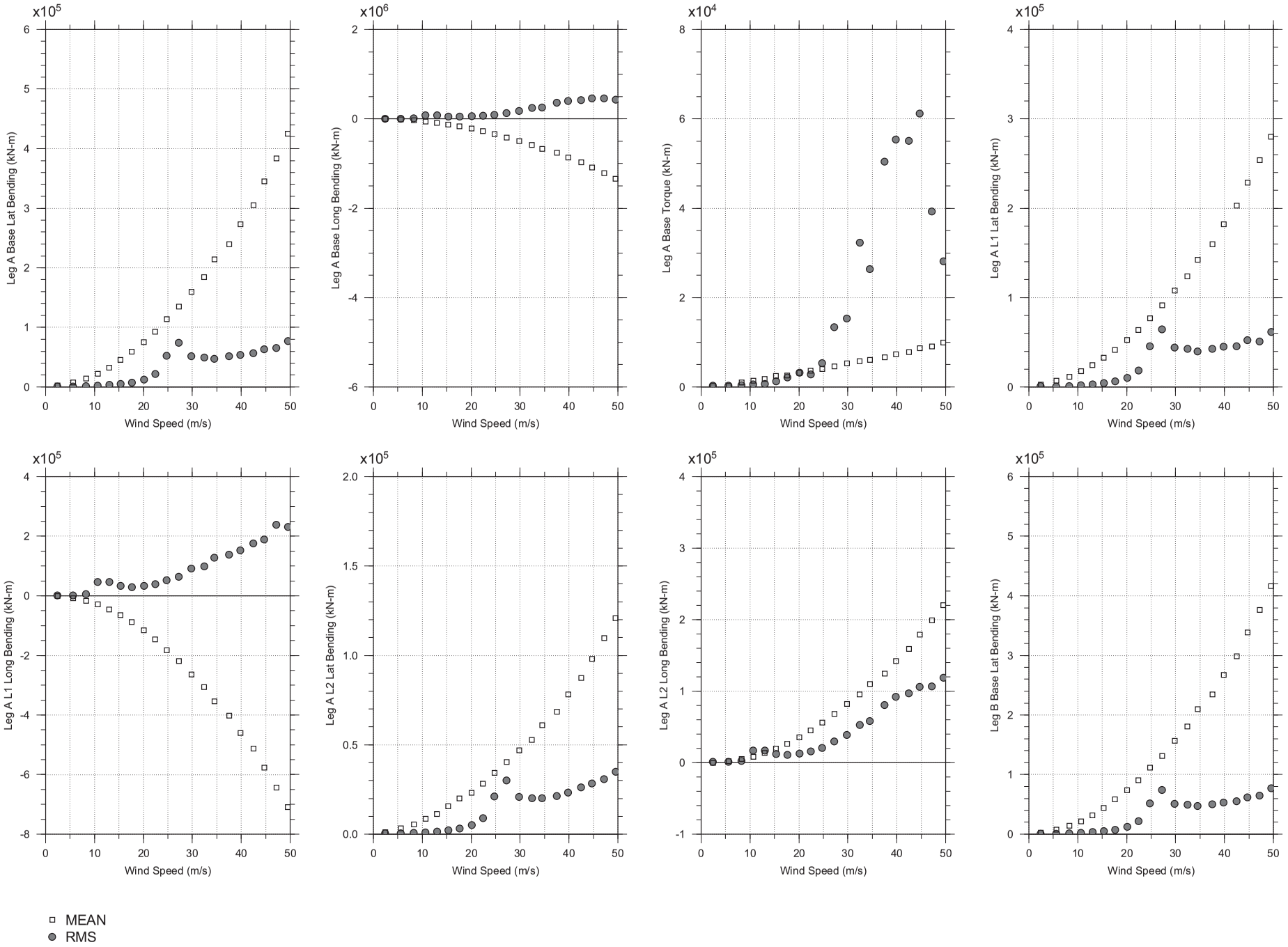

Messina Bridge, Free Standing Tower, 40 degree, Turbulent Flow

Dec. 14, 2010
tf49abdg.cl

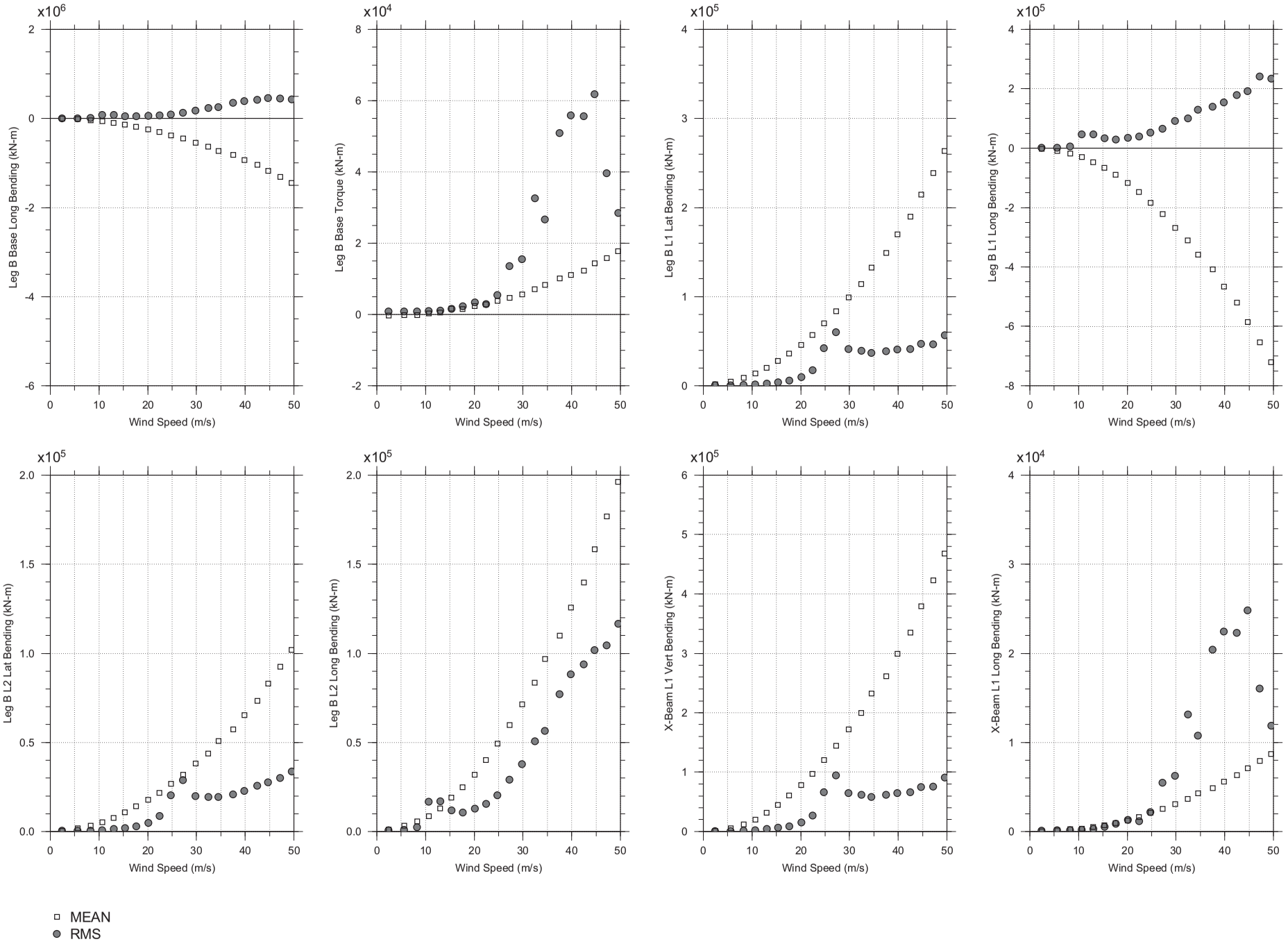

Messina Bridge, Free Standing Tower, 40 degree, Turbulent Flow

Dec. 14, 2010
tf49abdg.cl

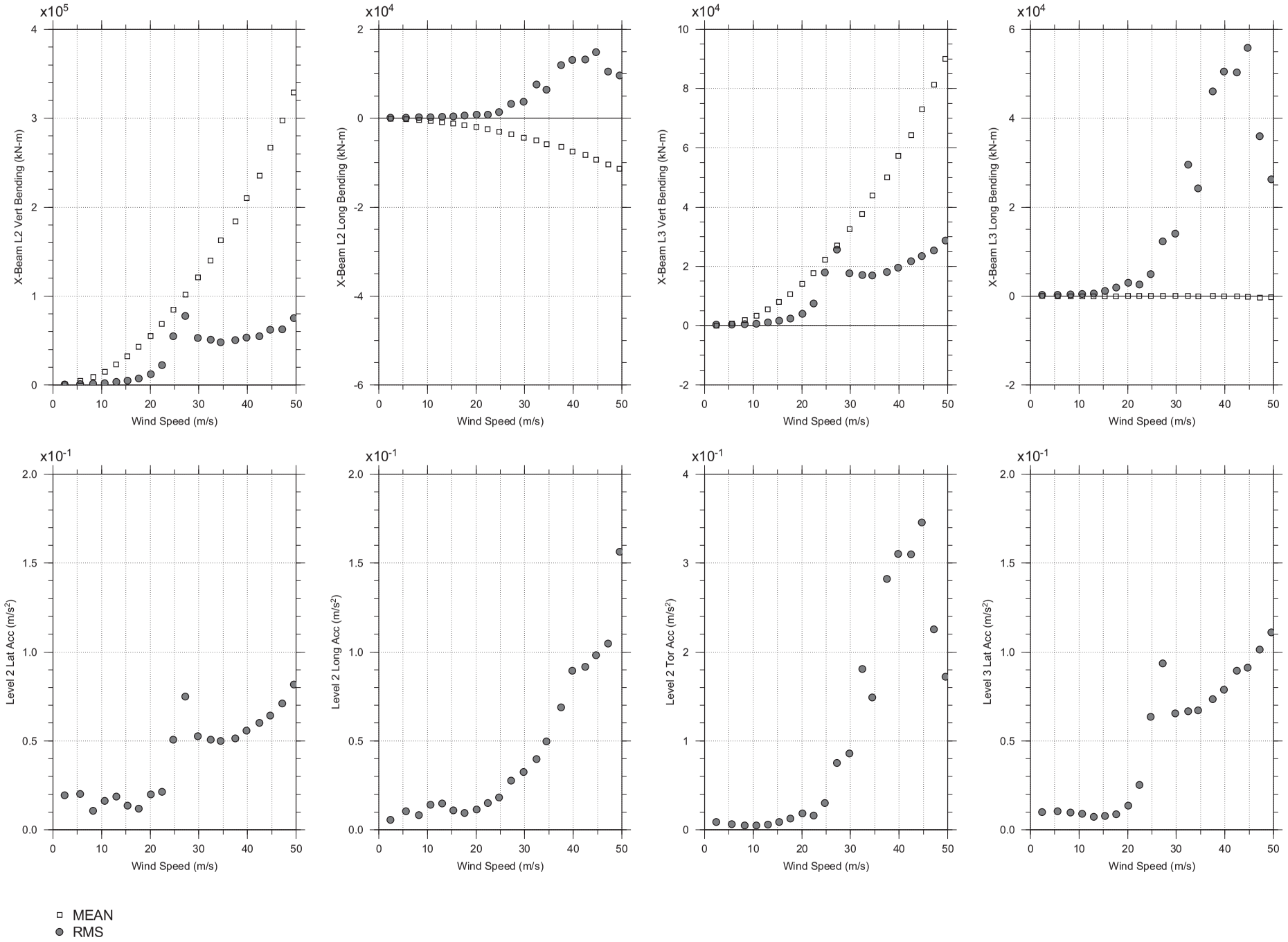

Messina Bridge, Free Standing Tower, 40 degree, Turbulent Flow

Dec. 14, 2010
tf49abdg.cl

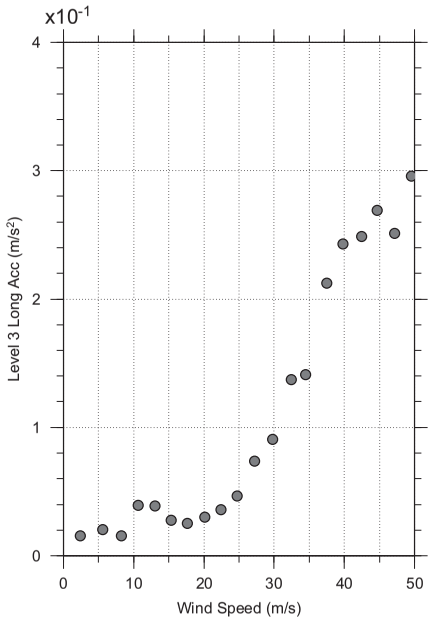

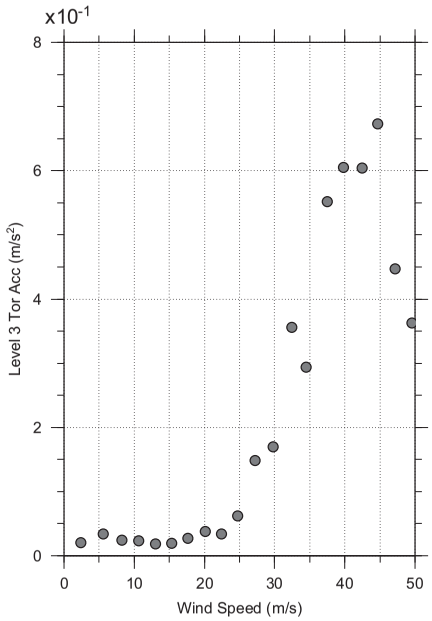

MEAN
RMS

Messina Bridge, Free Standing Tower, 40 degree, Turbulent Flow

Dec. 14, 2010
tf49abdg.cl

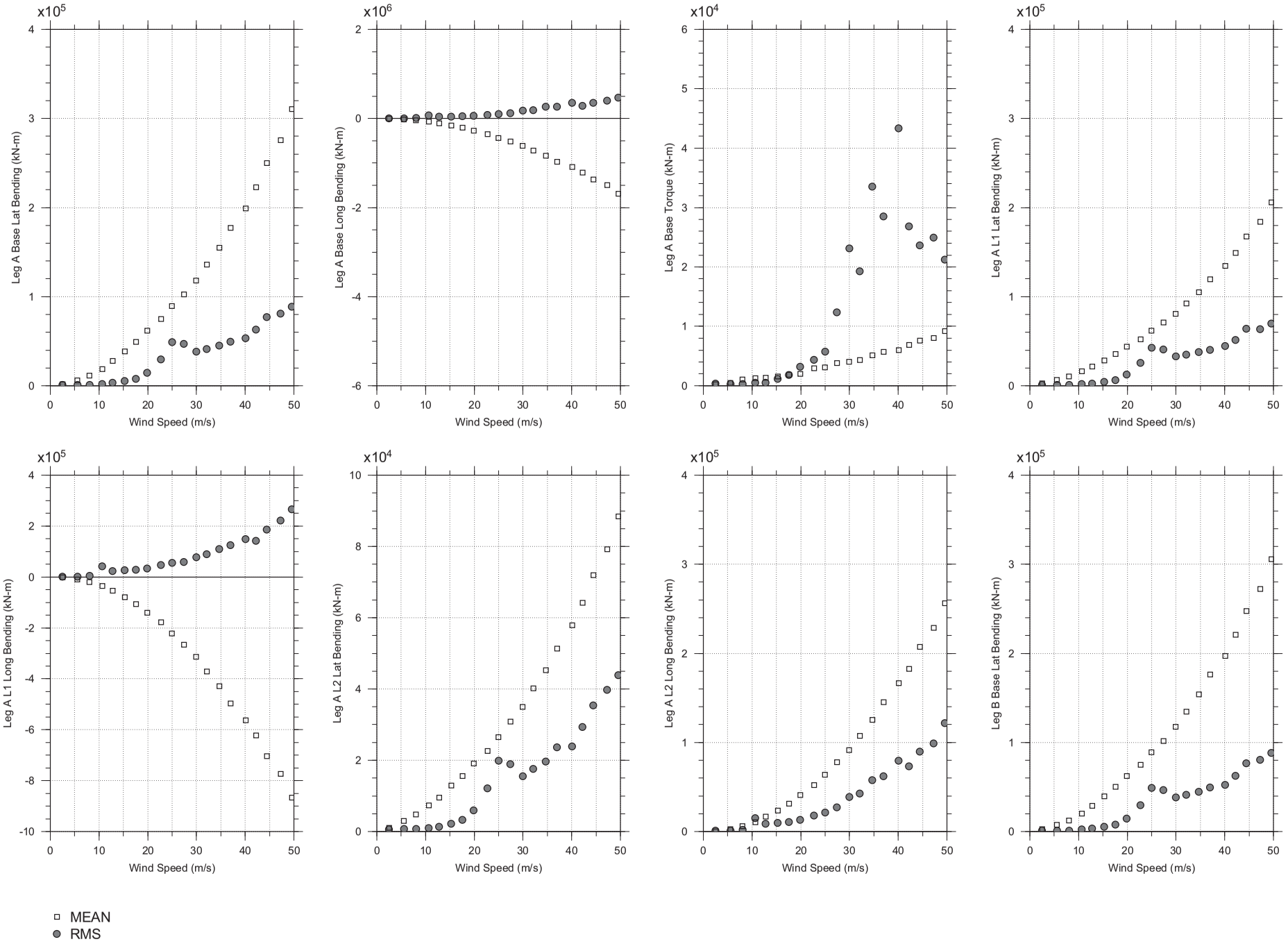

Messina Bridge, Free Standing Tower, 50 degree, Turbulent Flow

Dec. 14, 2010
tf50abdg.cl

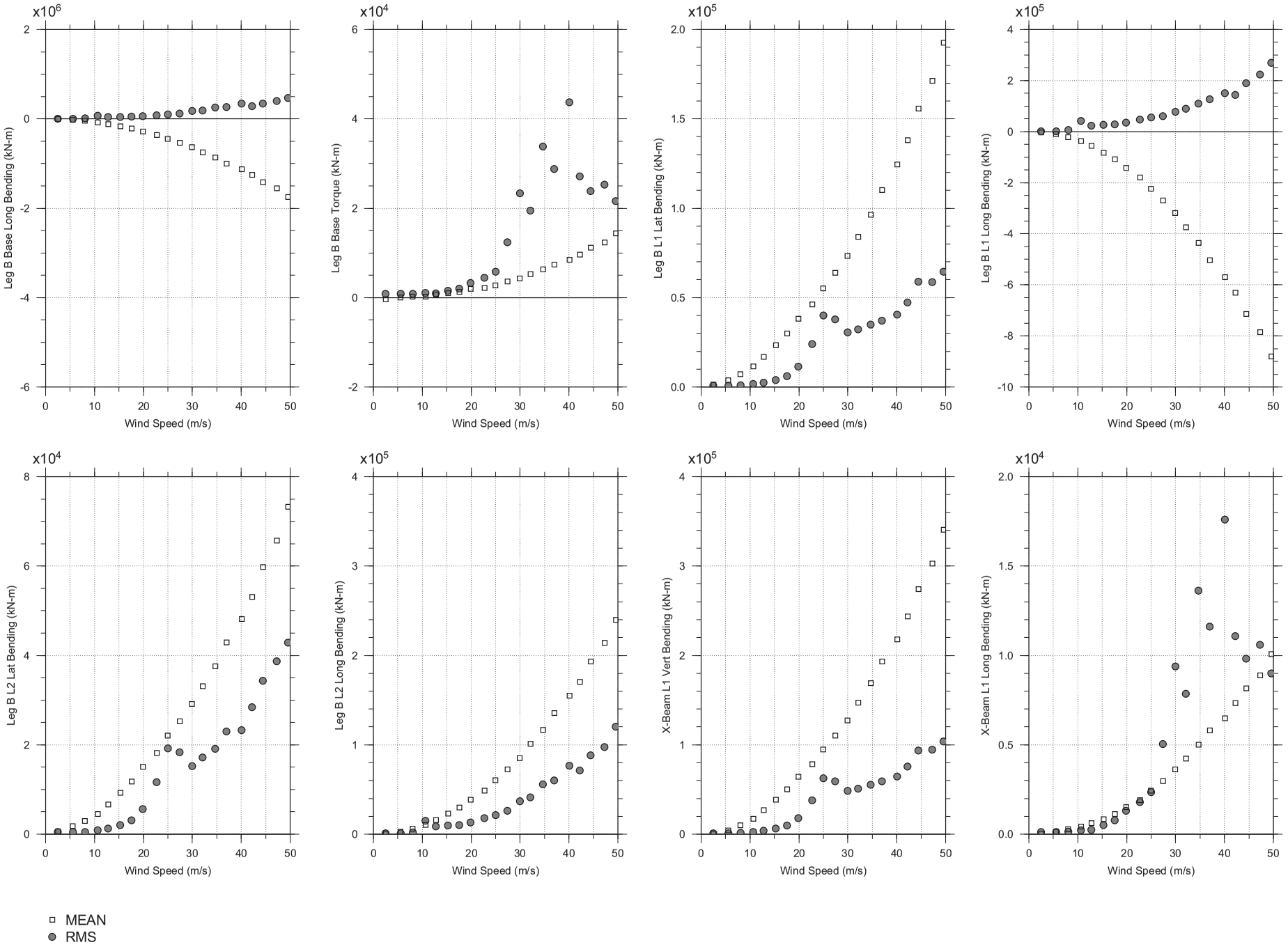

Messina Bridge, Free Standing Tower, 50 degree, Turbulent Flow

Dec. 14, 2010
tf50abdg.cl

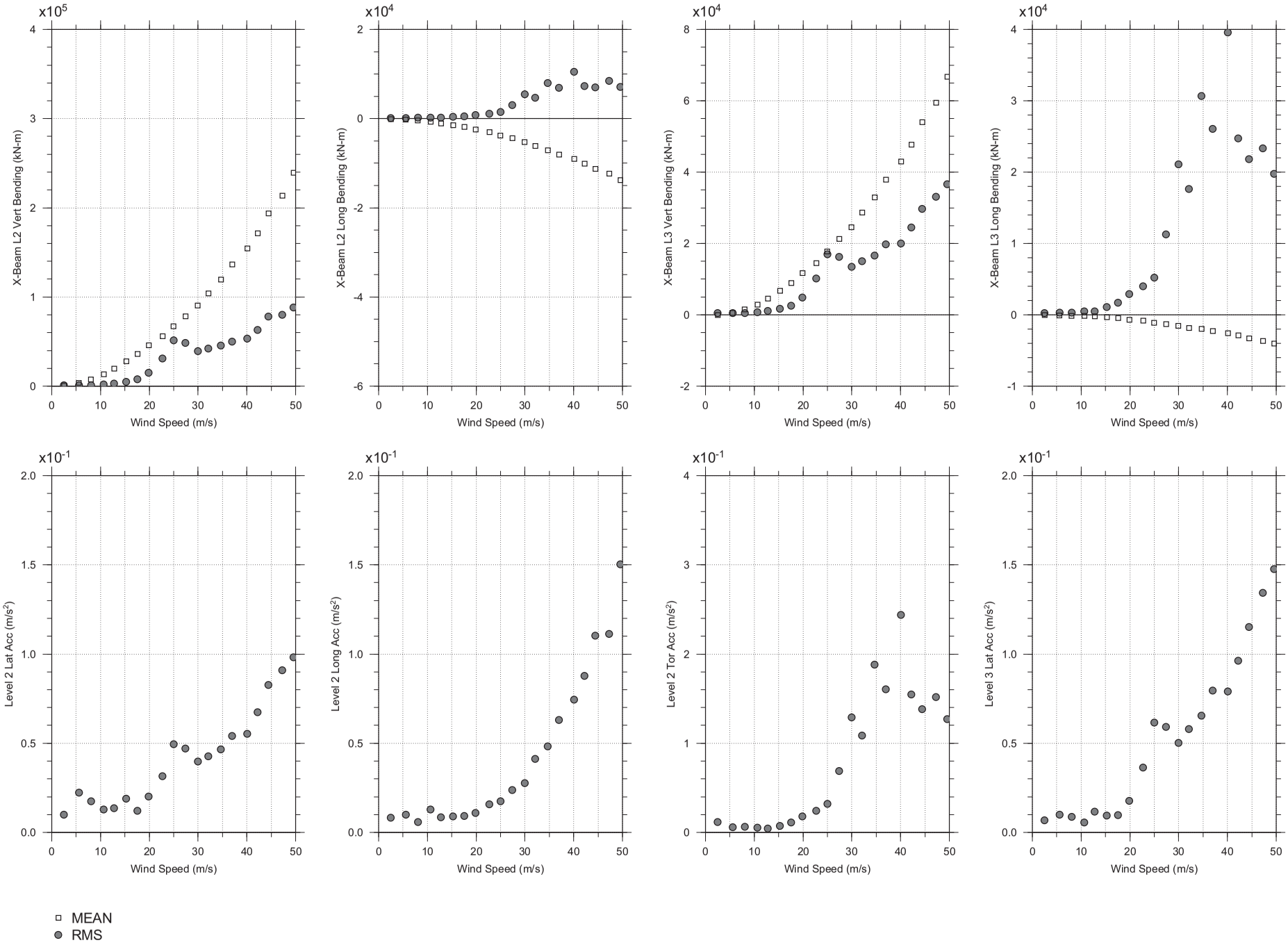

Messina Bridge, Free Standing Tower, 50 degree, Turbulent Flow

Dec. 14, 2010
tf50abdg.cl

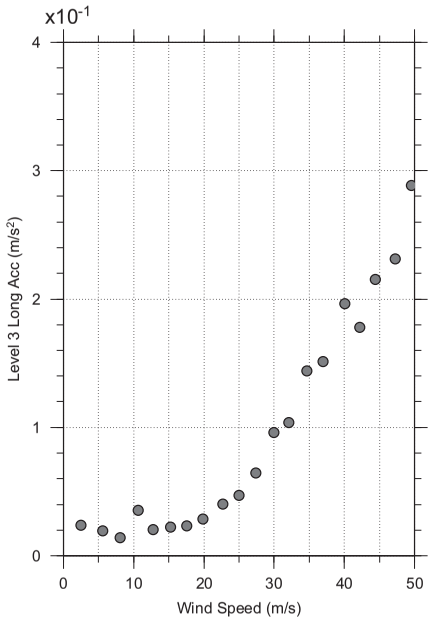

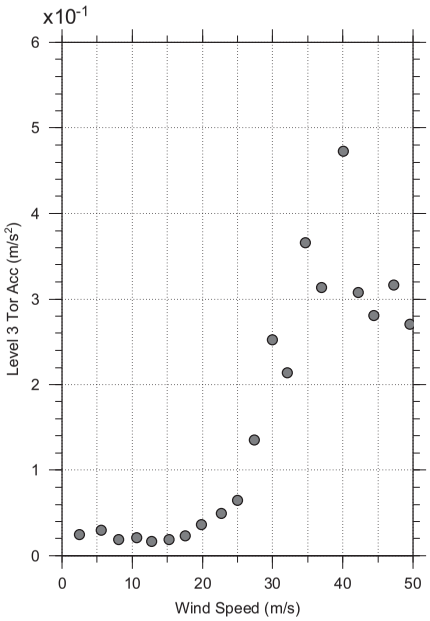

MEAN
RMS

Messina Bridge, Free Standing Tower, 50 degree, Turbulent Flow

Dec. 14, 2010
tf50abdg.cl

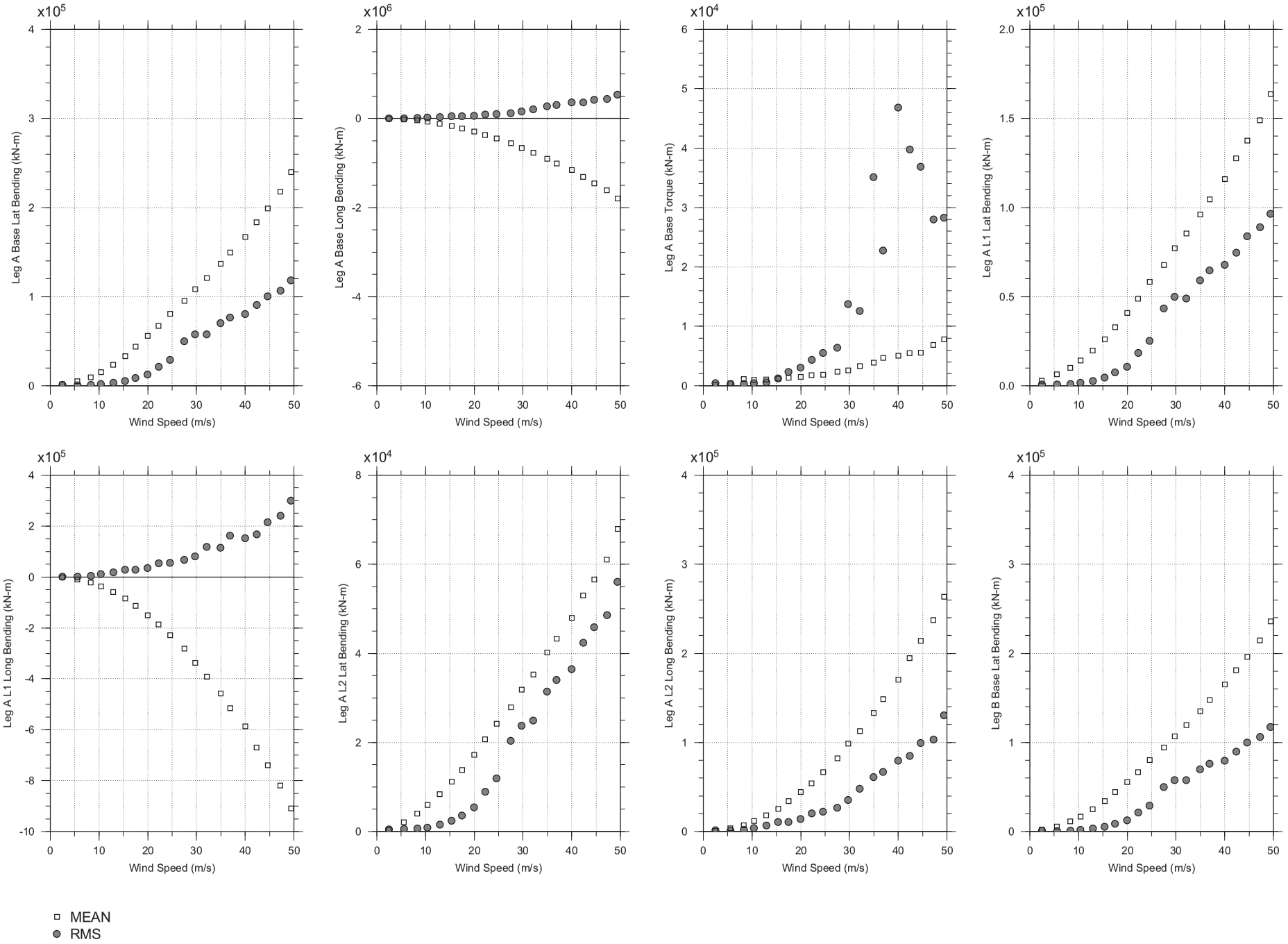

Messina Bridge, Free Standing Tower, 60 degree, Turbulent Flow

Dec. 14, 2010
tf51abdg.cl

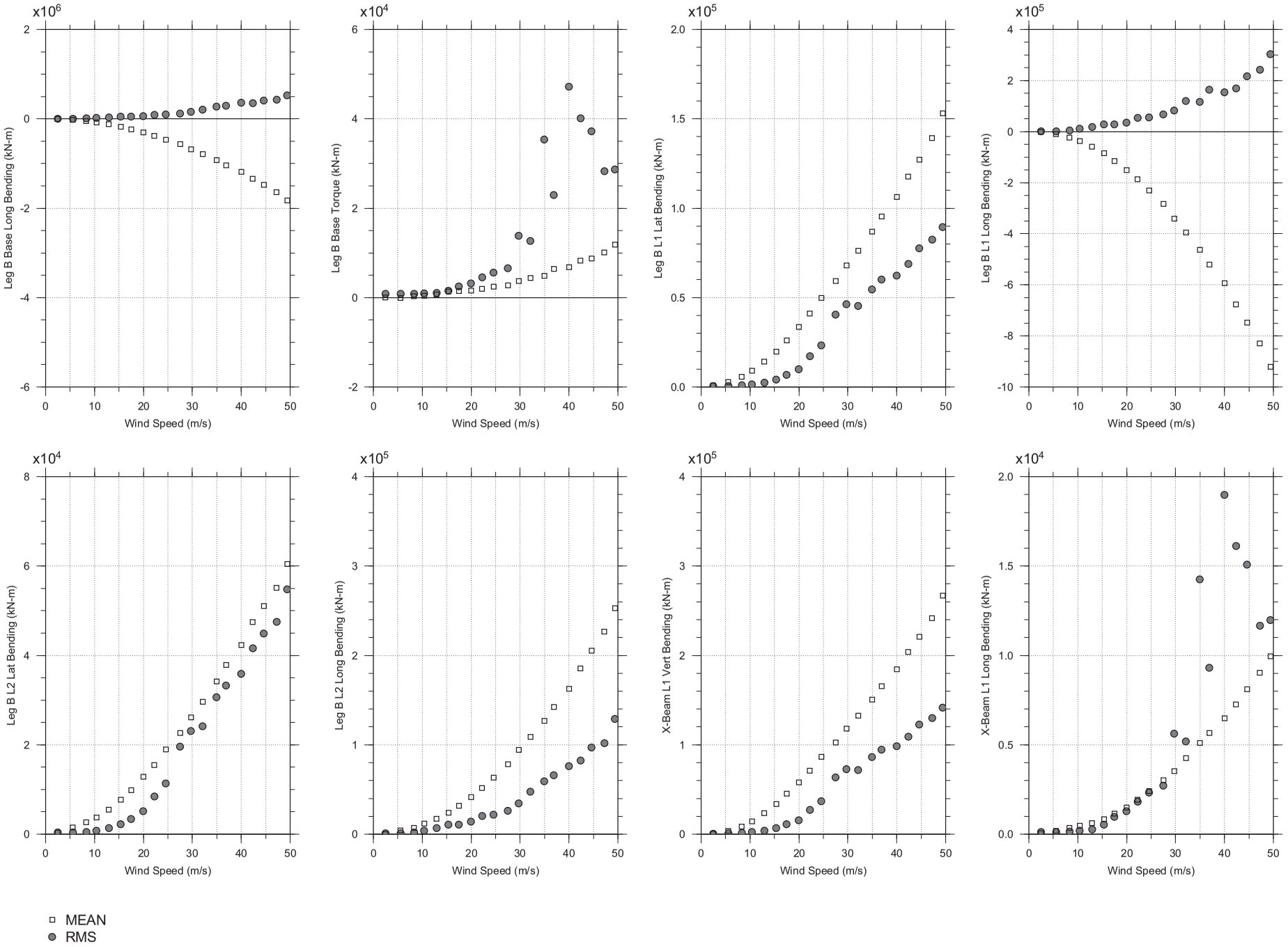

Messina Bridge, Free Standing Tower, 60 degree, Turbulent Flow

Dec. 14, 2010
tf51abdg.cl

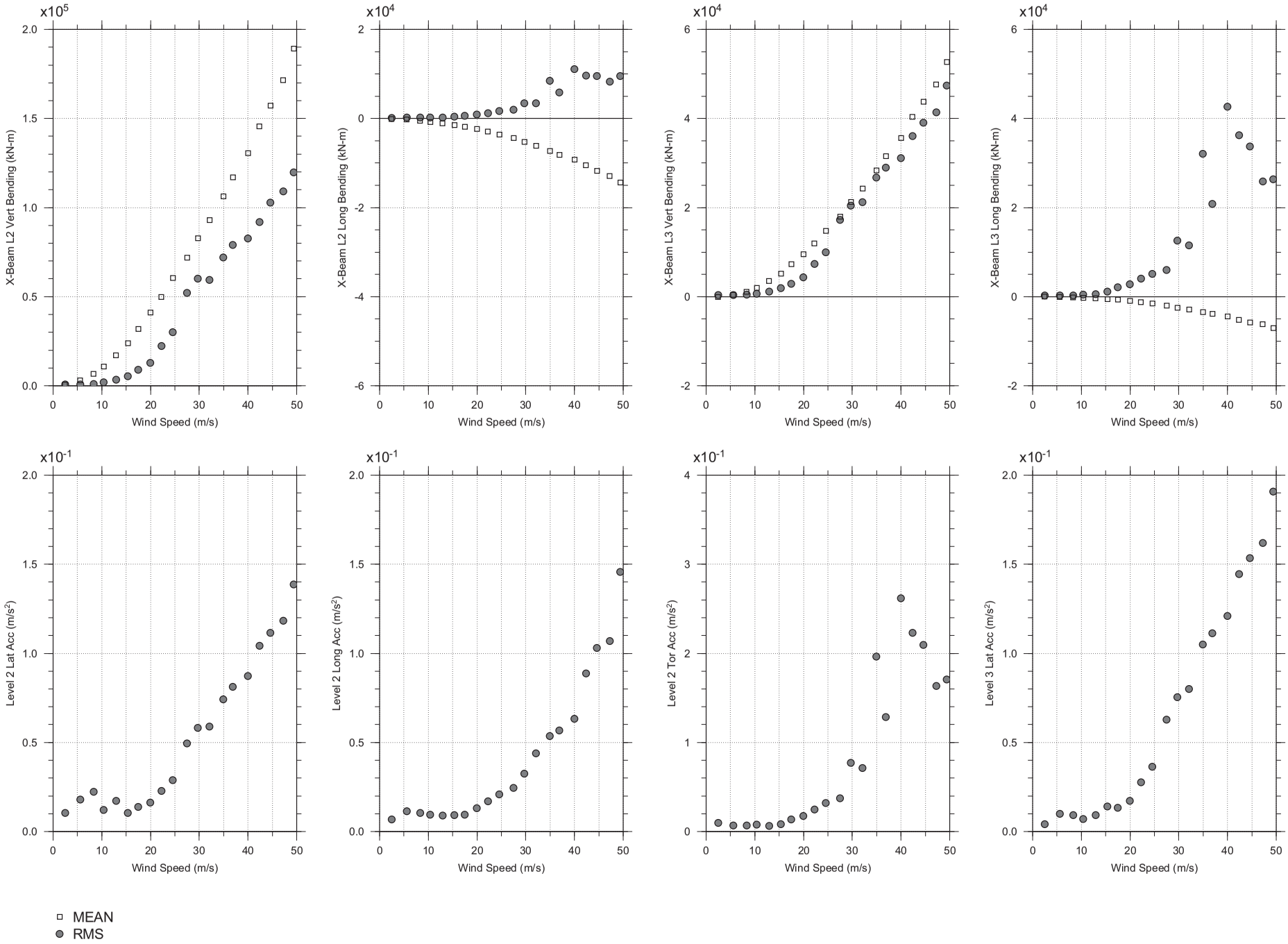

Messina Bridge, Free Standing Tower, 60 degree, Turbulent Flow

Dec. 14, 2010
tf51abdg.cl

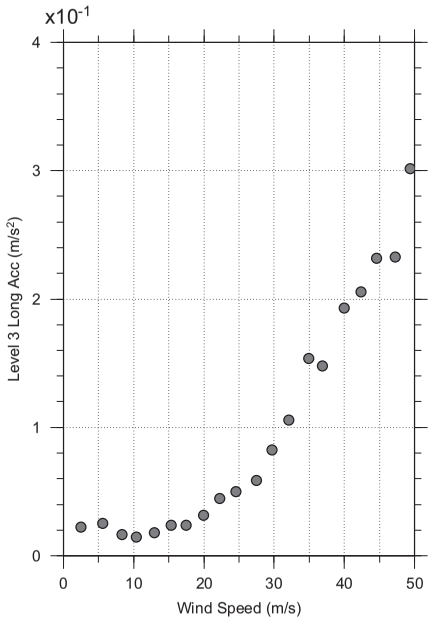

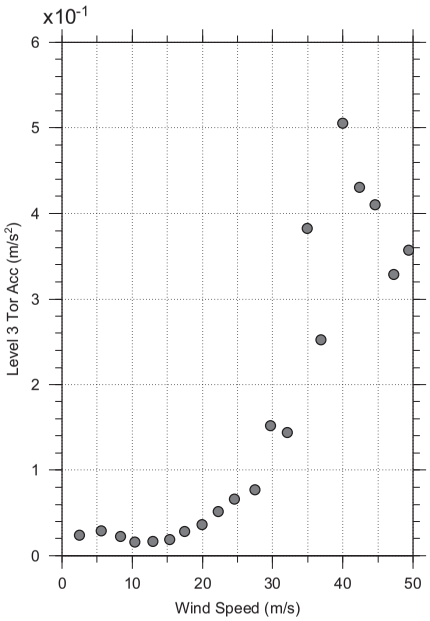

MEAN
RMS

Messina Bridge, Free Standing Tower, 60 degree, Turbulent Flow

Dec. 14, 2010
tf51abdg.cl

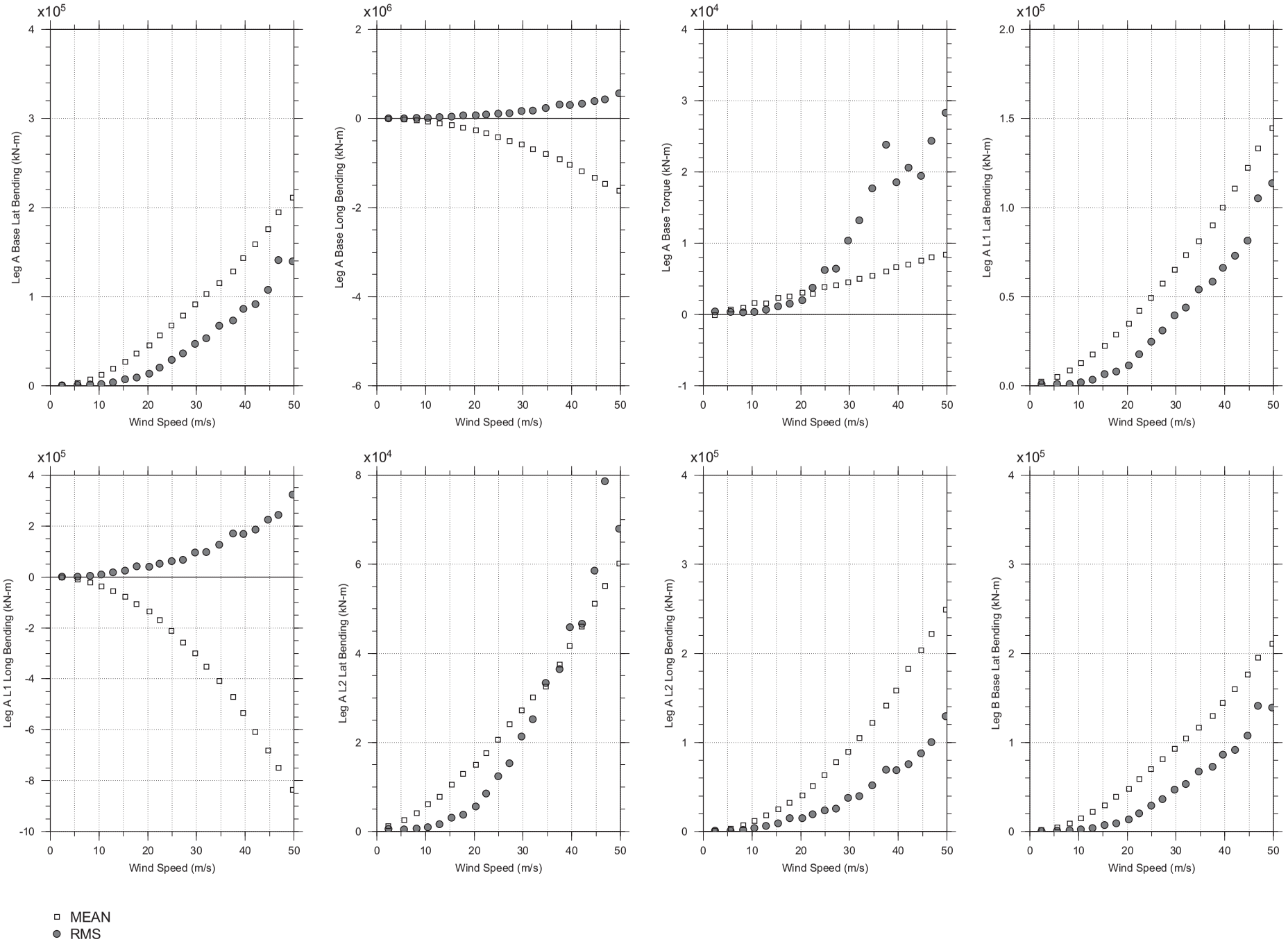

Messina Bridge, Free Standing Tower, 70 degree, Turbulent Flow

Dec. 14, 2010
tf52abdg.cl

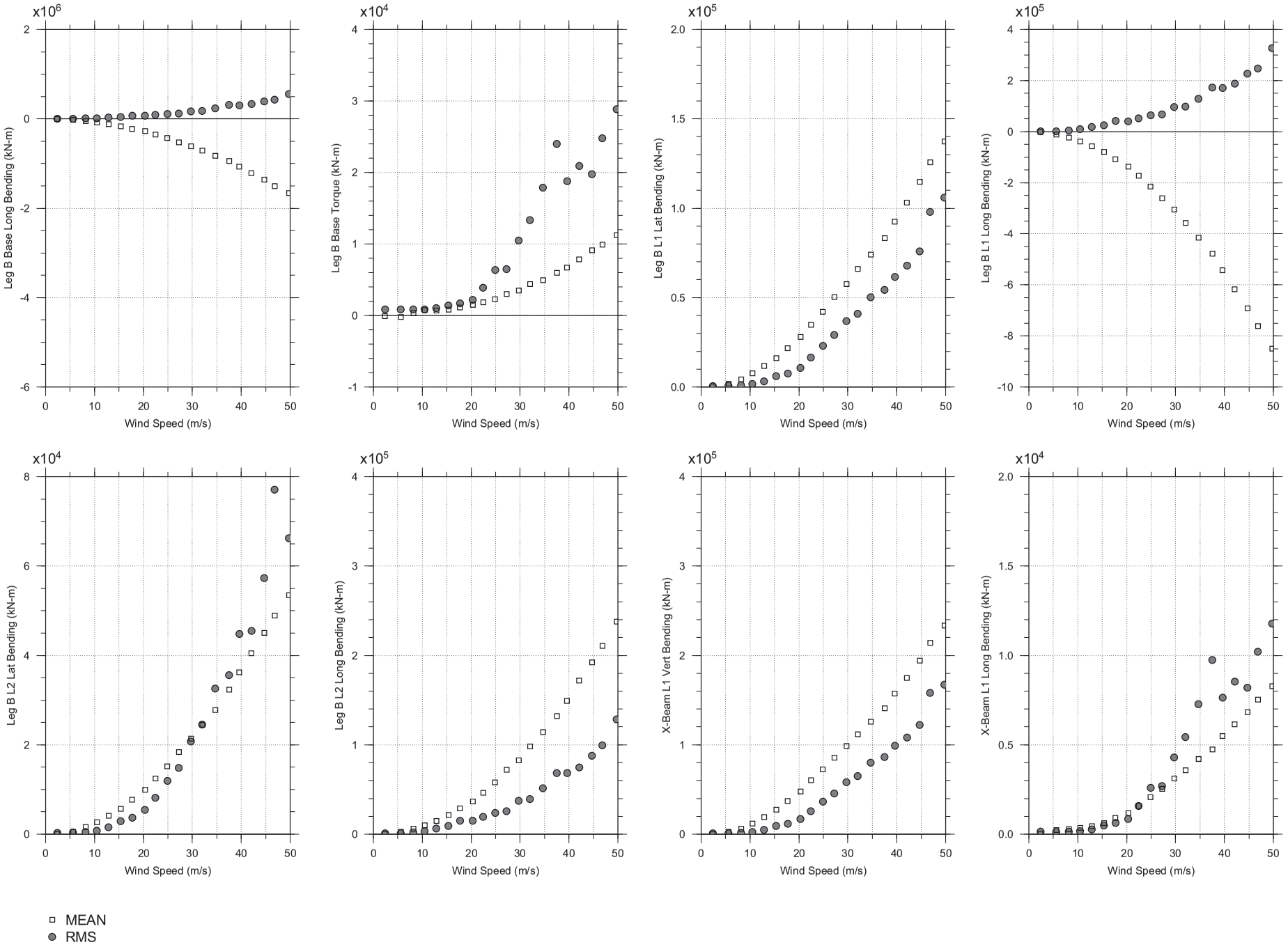

Messina Bridge, Free Standing Tower, 70 degree, Turbulent Flow

Dec. 14, 2010
tf52abdg.cl

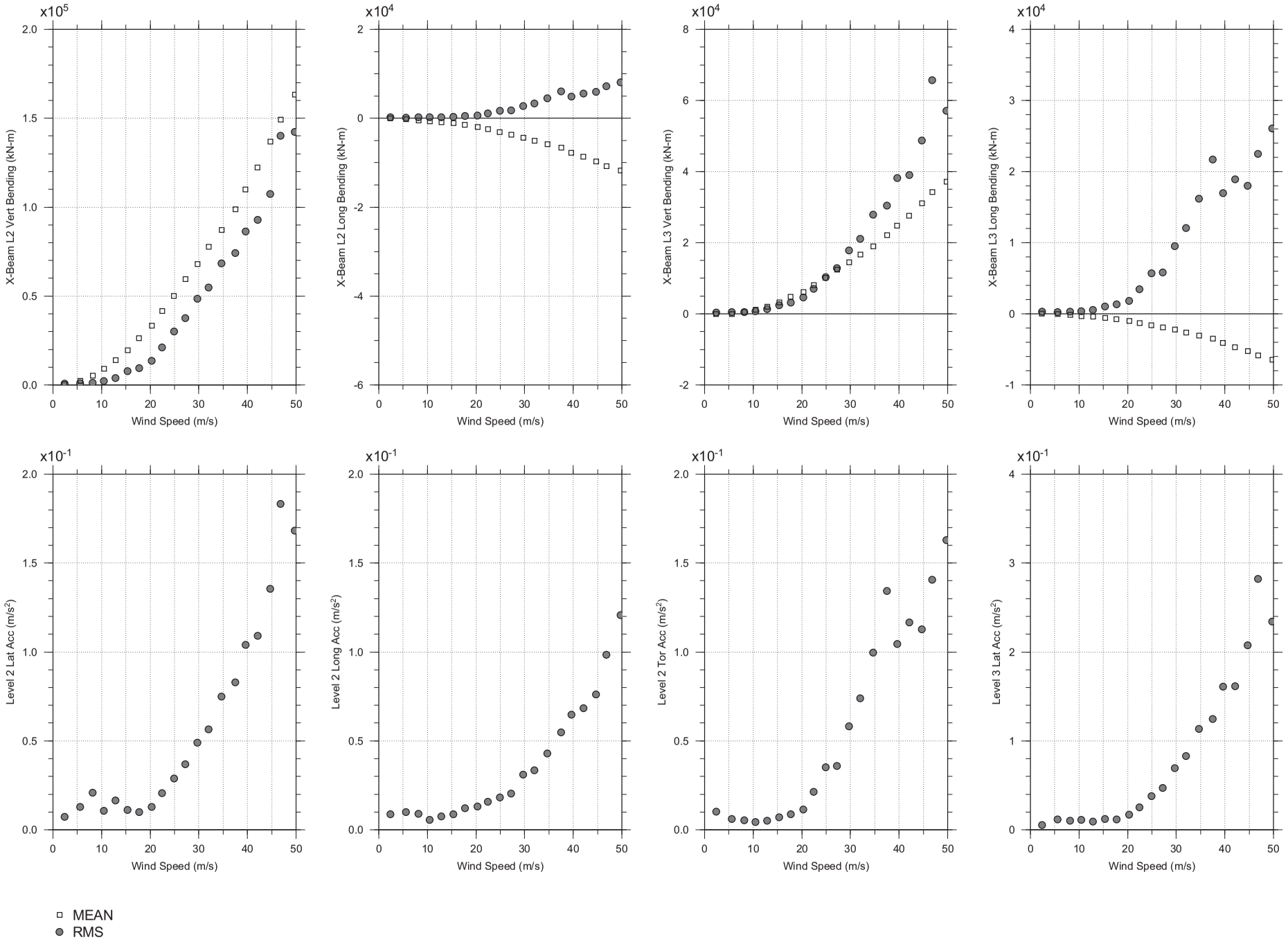

Messina Bridge, Free Standing Tower, 70 degree, Turbulent Flow

Dec. 14, 2010
tf52abdg.cl

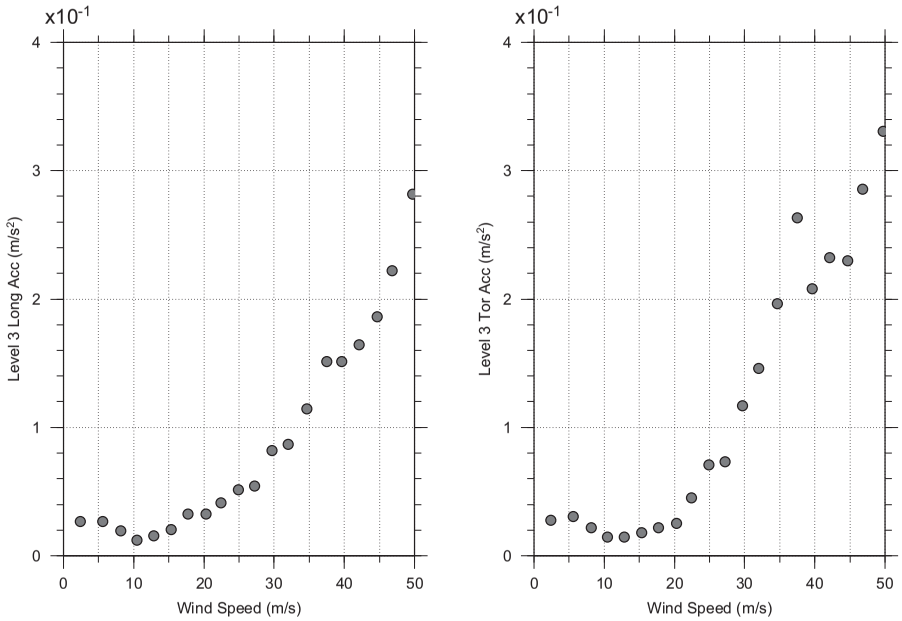

□ MEAN
● RMS

Messina Bridge, Free Standing Tower, 70 degree, Turbulent Flow

Dec. 14, 2010
tf52abdg.cl

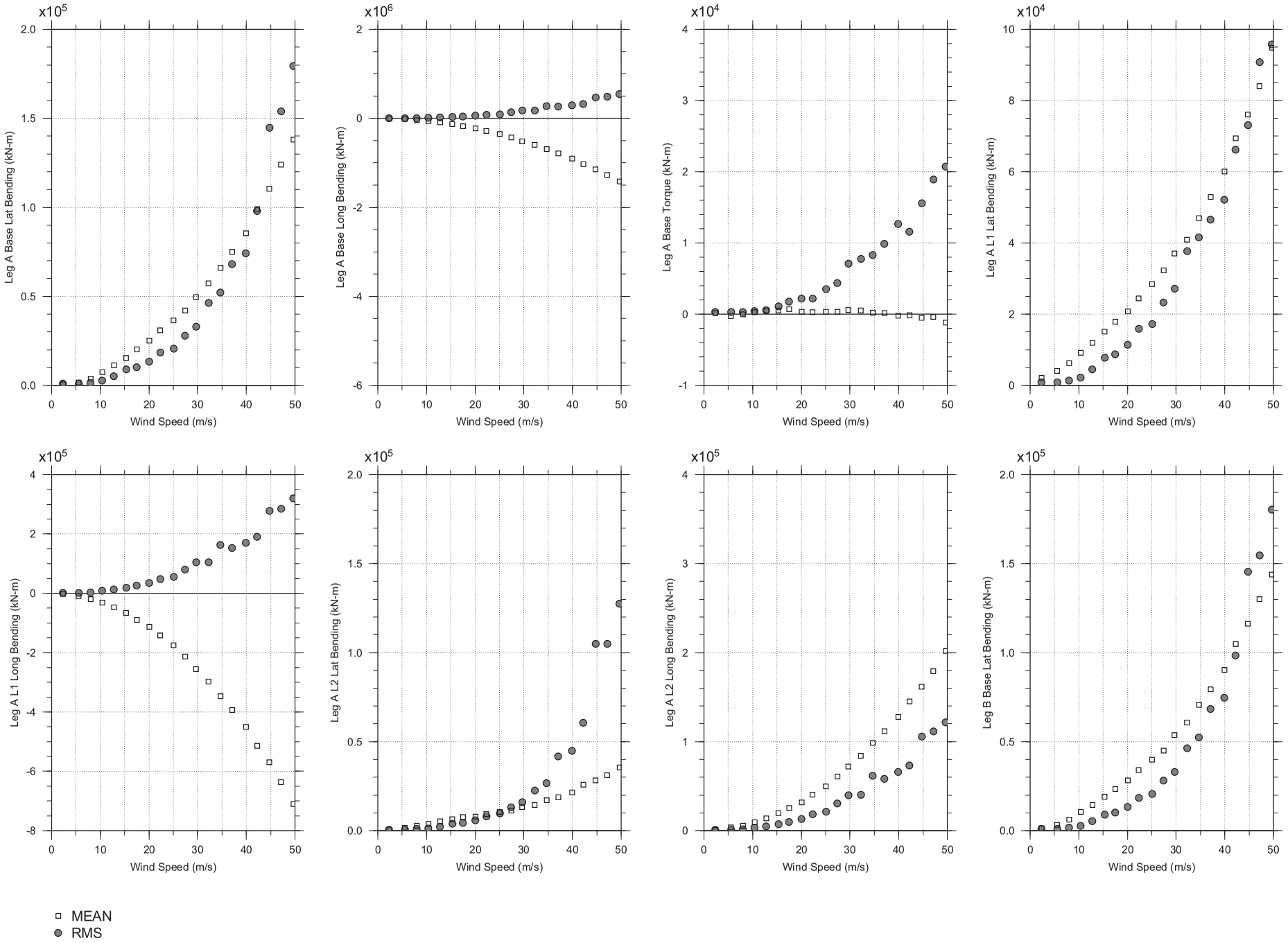

Messina Bridge, Free Standing Tower, 80 degree, Turbulent Flow

Dec. 14, 2010
tf53abdg.cl

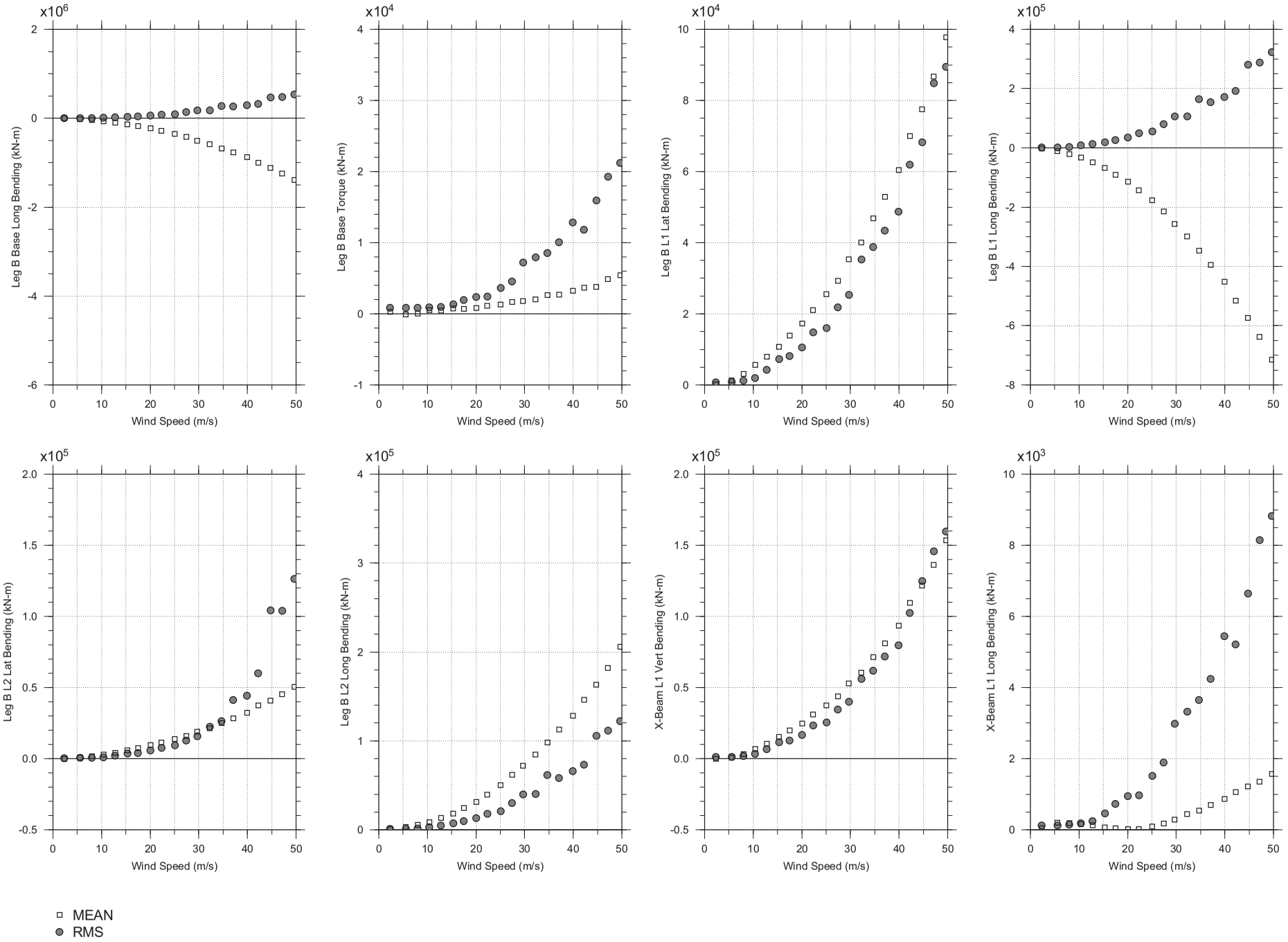

Messina Bridge, Free Standing Tower, 80 degree, Turbulent Flow

Dec. 14, 2010
tf53abdg.cl

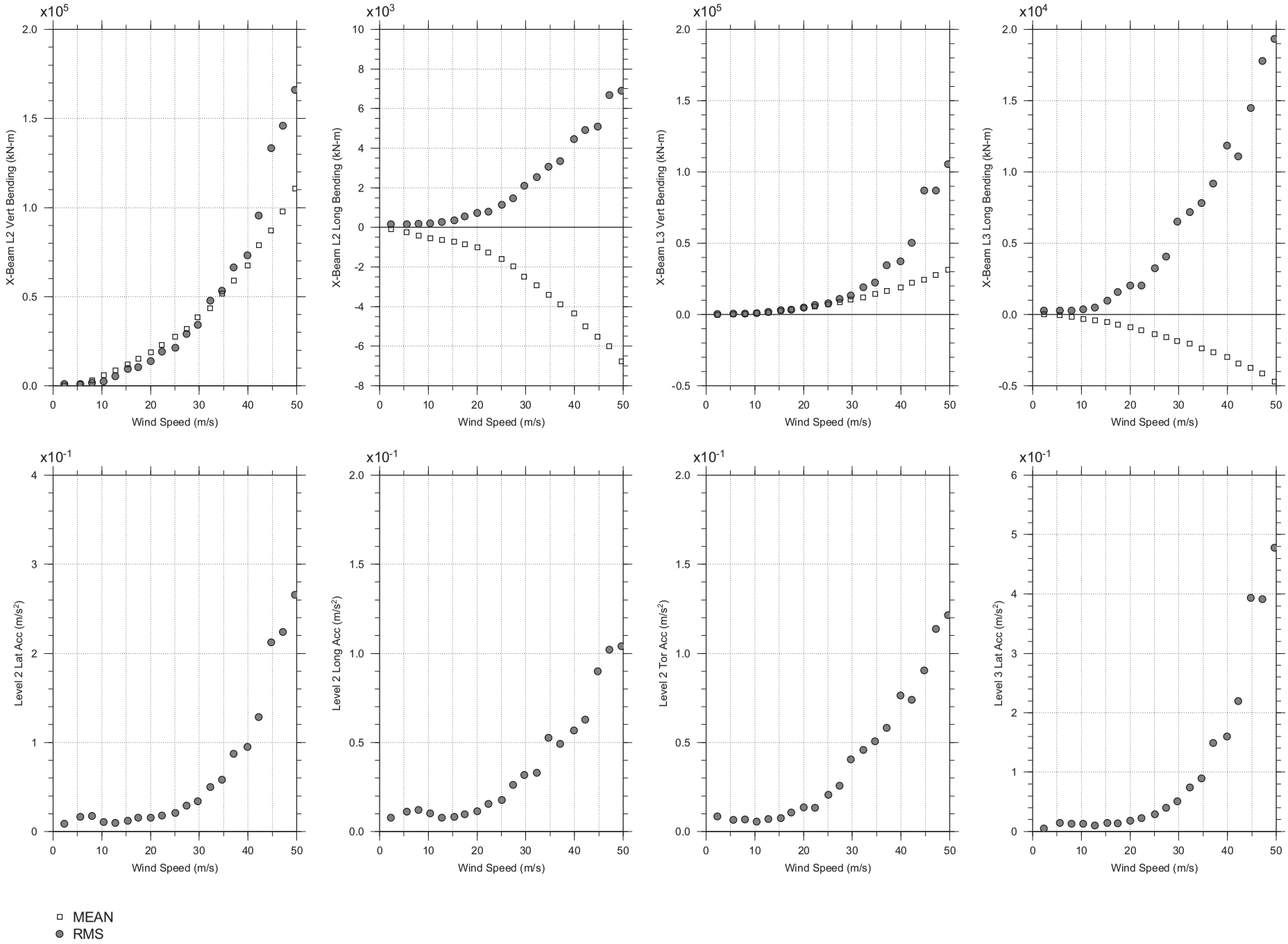

Messina Bridge, Free Standing Tower, 80 degree, Turbulent Flow

Dec. 14, 2010
tf53abdg.cl

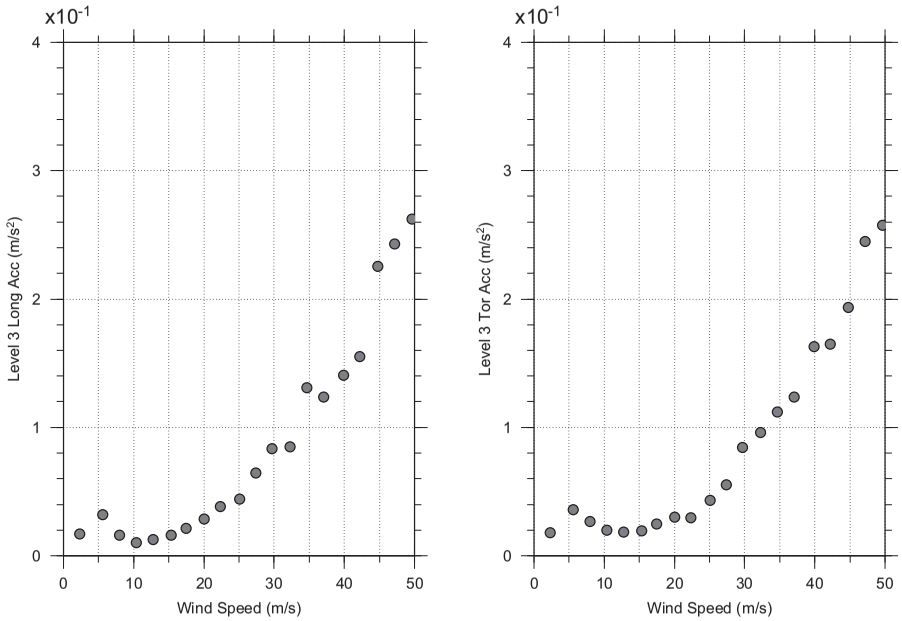

MEAN
RMS

Messina Bridge, Free Standing Tower, 80 degree, Turbulent Flow

Dec. 14, 2010
tf53abdg.cl

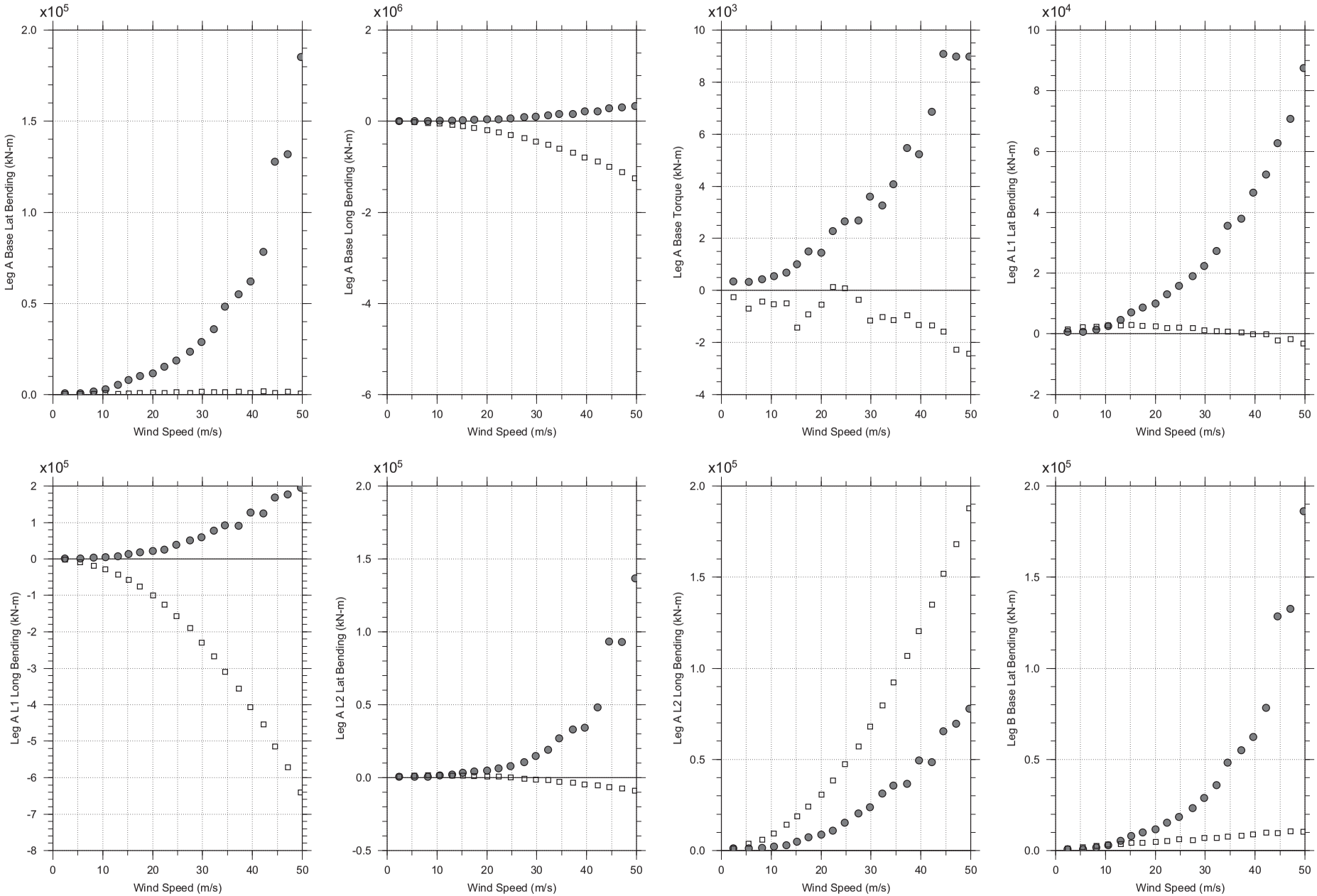

Messina Bridge, Free Standing Tower, 90 degree, Turbulent Flow

Dec. 14, 2010
tf54abdg.cl

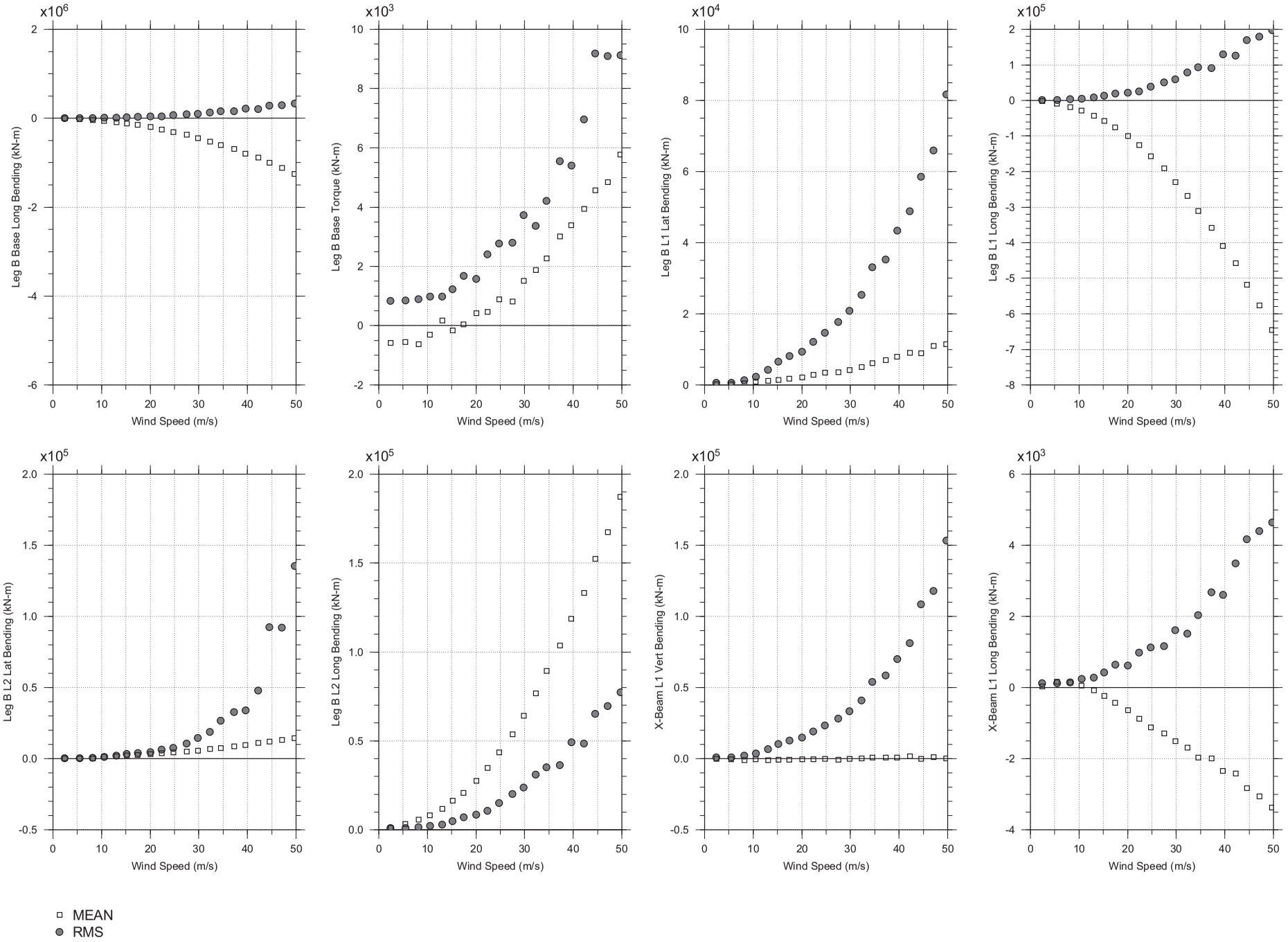

Messina Bridge, Free Standing Tower, 90 degree, Turbulent Flow

Dec. 14, 2010
tf54abdg.cl

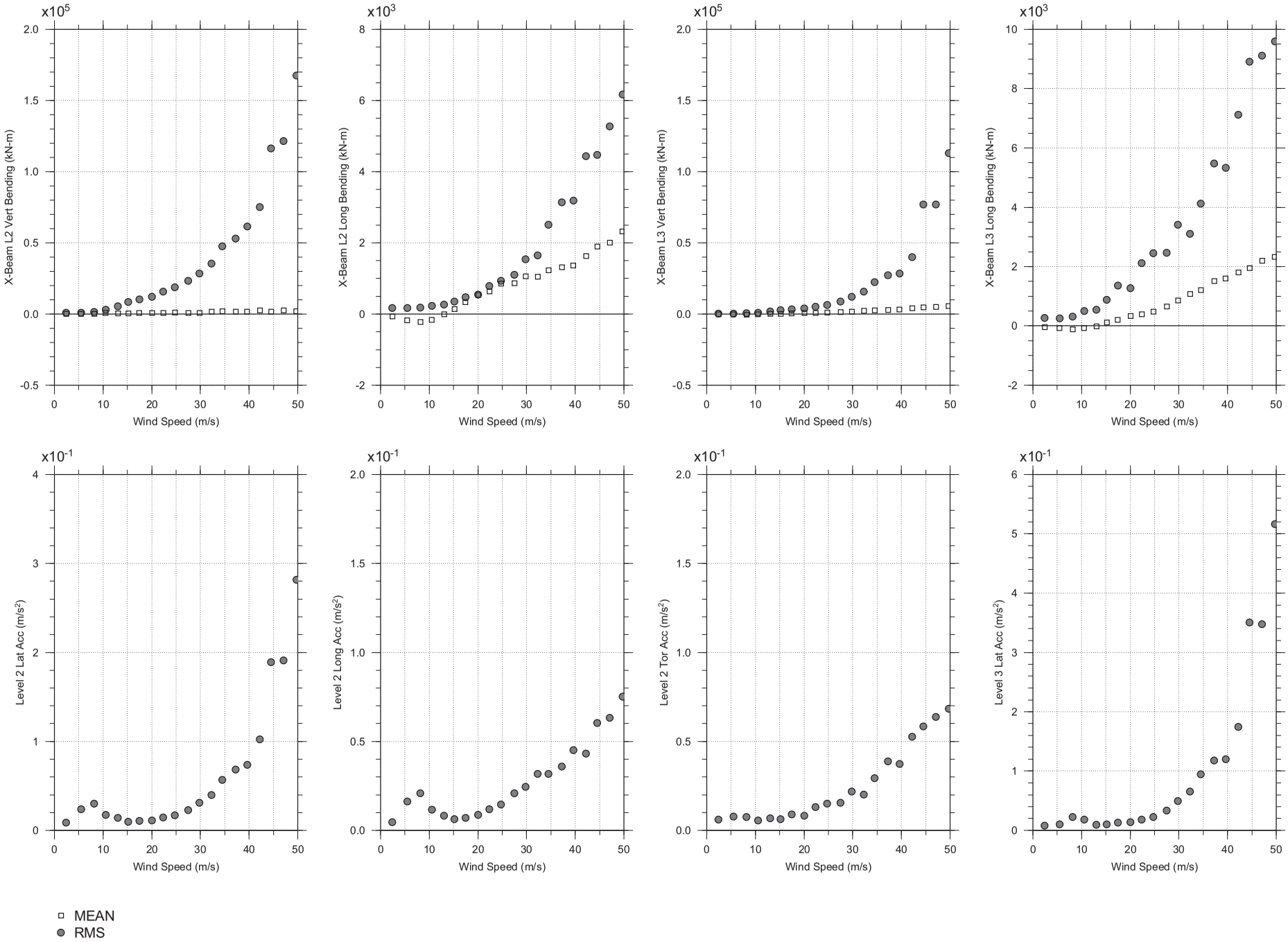

Messina Bridge, Free Standing Tower, 90 degree, Turbulent Flow

Dec. 14, 2010
tf54abdg.cl

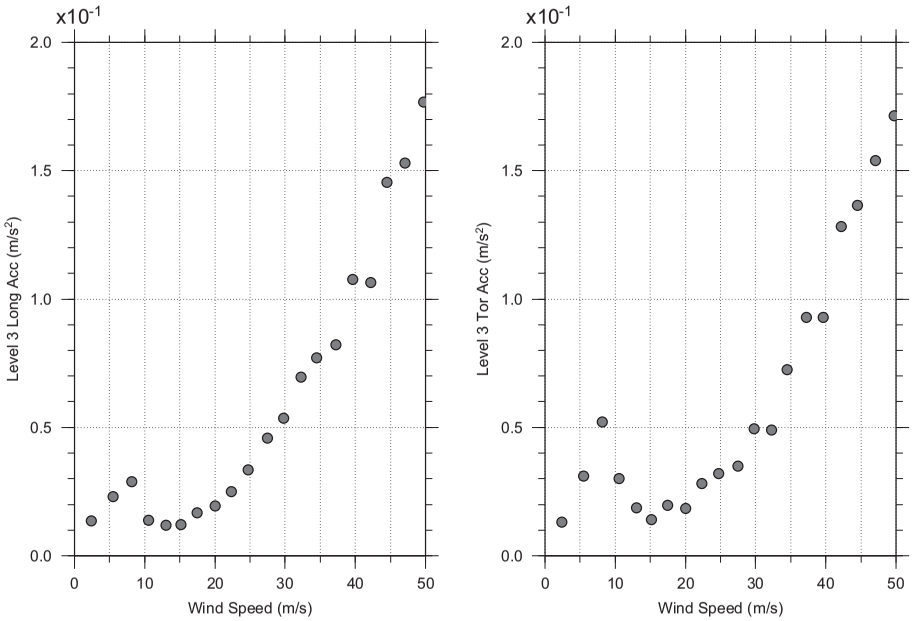

MEAN
RMS

Messina Bridge, Free Standing Tower, 90 degree, Turbulent Flow

Dec. 14, 2010
tf54abdg.cl

APPENDIX C

RESULTS OF NON-FROUDE TOWER MODEL, IN-SERVICE CONDITION

Notes:

C1. The wind speed indicated is the mean hourly wind speed in m/s at the tower height. The bending moments and torques given in the plots have the unit of kN-m. The accelerations have the unit of m/s^2. The displacements have the units of m in the longitudinal direction and degree for tower rotation.

C2. The mean and RMS (root mean square) responses are given separately in the plots. The total responses should be calculated as the mean plus or minus the RMS multiplied by the appropriate peak factor.

C3. Refer to Figure C1 for the definition of test wind angles.

C4. Refer to Figure C2 and Table C1 for the instrumentation locations and sign convention used.

C5. Table C2 summarizes the test results and corresponding test conditions.

TABLE C1 INSTRUMENTATION LOCATIONS, NON-FROUDE TOWER MODEL

Instrumentation	Instrumentation Locations
Strain Gauges (Tower Legs):	
M_x, M_y and M_Z,, Base of Leg A	Bending moments measured on Leg A at ??? m above Leg A base (or ground??)
M_x and M_y, Level 1 of Leg A	Bending moments measured on Leg A, ??? m above ???
M_x and M_y, Level 2 of Leg A	Bending moments measured on Leg A, ??? m above ???
M_x, M_y and M_Z,, Base of Leg B	Bending moments measured on Leg B at ??? m above Leg B base (or ground??)
M_x and M_y, Level 1 of Leg B	Bending moments measured on Leg B, ??? m above ???
M_x and M_y, Level 2 of Leg B	Bending moments measured on Leg B, ??? m above ???
Strain Gauges (X-Beams):	
M_z and M_x, Level 1	Bending moments measured on X-beam, ??? m from Mid location towards to Leg A
M_z and M_x, Level 2	Bending moments measured on X-beam, ??? m from Mid location towards to Leg A
M_z and M_x, Level 3	Bending moments measured on X-beam, ??? m from Mid location towards to Leg A
Accelerometers:	
x, y and Torsional accelerations, Level 2	Accelerations measured at 246.4 m above ground
x, y and Torsional accelerations, Level 3	Accelerations measured at 373.4 m above ground
Lasers (January 2011 Test only):	
x displacement and rotation, Level 2	Tower displacement along bridge axis and tower rotation measured at 238.7 m above ground
Wind Speeds:	
Deck Height	At a height of 66 m full scale above ground
Tower Height	At a height of 399 m full scale above ground
Mid Tower Height	At a height of 199 m full scale above ground
Reference Height	Where the wind speed not affected by the boundary layer of the wind tunnel floor

Notes:

1. Right-hand rule used for sign convention.
2. x – along bridge axis; y – perpendicular to bridge axis (lateral to tower).

TABLE C2 SUMMARY OF NON-FROUDE TOWER MODEL TESTS, IN SERVICE

Test Configuration	Test No.	Test Files (January 2011)	Modal Frequency (Hz) and Damping (%)			Wind Angle	Maximum Wind Speed	Level 2 Maximum Acceleration Observed		
			Long.	Lat.	Tor.	Deg	m/s	m/s^2	Direction occurred	Wind speed (m/s)
Smooth flow, inherent damping	1	M075b1E01R013 M075b1E01R036	12.95 (0.29~ 0.30)	10.10 (0.23~ 0.26)	17.99 (0.17~ 0.18)	0 (Lat.)	85	6.403	Long	50
	2	M075b1E01R014 M075b1E01R037				2.5	89	6.471	Long	50
	3	M075b1E01R015 M075b1E01R038				5	89	7.129	Long	52
	4	M075b1E01R016 M075b1E01R039				7.5	89	6.213	Long	52
	5	M075b1E01R017 M075b1E01R040				10	89	6.474	Long	54
Smooth, 0.6%	6	M075b5E01R002	12.81 (0.62~ 0.63)	10.03 (0.17~ 0.19)	17.53 (0.38~ 0.43)	0 (Lat.)	89	3.185	Long	54
Smooth flow, 1% nominal damping	7	M075b6E01R004	12.9 (1.06~ 1.08)	10.01 (0.29~ 0.34)	17.64 (0.99~ 1.10)	0 (Lat.)	89	2.295	Lat	73
	8	M075b6E01R005				2.5	89	2.423	Lat	76
	9	M075b6E01R006				5	89	3.930	Lat	76
	10	M075b6E01R007				7.5	89	4.805	Lat	76
	11	M075b6E01R008				10	89	4.289	Lat	76
Smooth flow, 2% nominal damping	12	M075b7E01R002	12.9 (1.90~ 1.93)	9.97 (0.27~ 0.33)	16.8 (1.32~ 1.66)	0 (Lat.)	85	2.687	Lat	75
	13	M075b7E01R003				2.5	88	2.374	Lat	75
	14	M075b7E01R004				5	88	4.086	Lat	75
	15	M075b7E01R005				7.5	88	4.500	Lat	75
	16	M075b7E01R006				10	88	4.181	Lat	75
Smooth flow, 4% nominal damping	17	M075b3E01R002	13.21 (3.45~ 3.64)	9.83 (1.07~ 1.12)	17.0 (1.26~ 1.40)	0 (Lat.)	79	1.418	Lat	76
	18	M075b3E01R003				2.5	79	1.138	Lat	76
	19	M075b3E01R004				10	79	3.050	Lat	79
Turbulent boundary layer flow, inherent damping	20	M075b4E02R002 M075b4E02R014	12.95 (0.29~ 0.30)	10.10 (0.23~ 0.26)	17.99 (0.17~ 0.18)	0 (Lat.)	86	5.650	Long	52
	21	M075b2E02R003 M075b2E02R018				10	84	5.250	Long	54
	22	M075b4E02R004				20	82	6.886	Tor	81
	23	M075b4E02R005				30	86	2.151	Tor	85
	24	M075b4E02R006				40	87	1.035	Tor	79
	25	M075b4E02R007				50	87	0.573	Tor	73
	26	M075b4E02R008				60	87	0.697	Tor	76
	27	M075b4E02R009				70	87	0.734	Lat	83
	28	M075b4E02R010				80	87	0.739	Lat	87
	29	M075b4E02R011				90 (Long.)	87	0.685	Lat	87

Notes:

1. Maximum wind speed is the equivalent hourly mean wind speed at the top of the tower using a velocity scale of 1:7.20, based on the longitudinal direction frequency scaling.
2. Long. = Longitudinal direction (along deck), Lat. = Transverse direction with respect to the axis of the bridge deck
3. Tests between 50 m/s and 63 m/s were skipped due to large tower responses for the inherent damping tests in smooth flow as well as Test No. 20 & 21 in turbulent boundary layer flow.

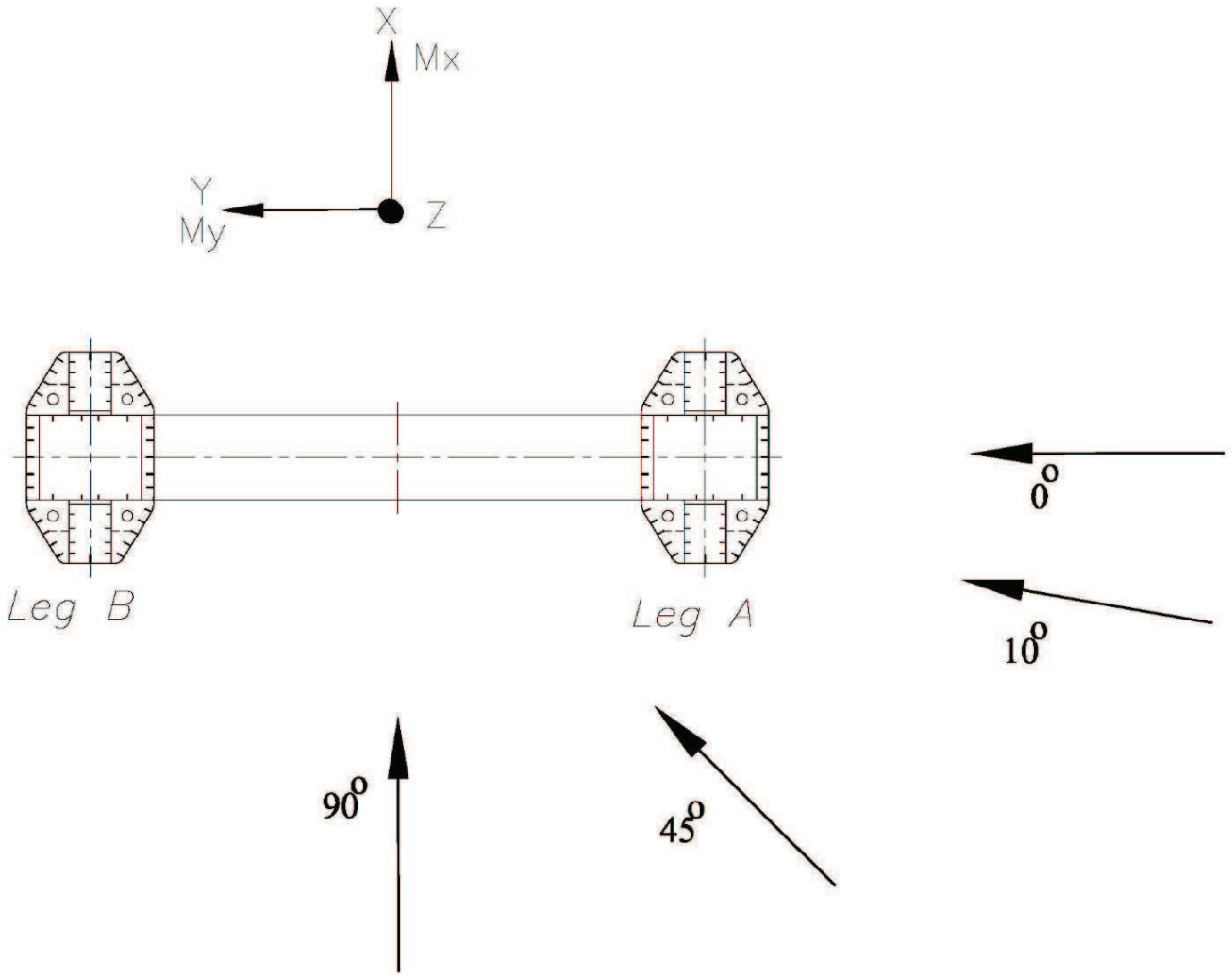

FIGURE C1 DEFINITION OF WIND ANGLES USED IN THE MESSINA TOWER TEST

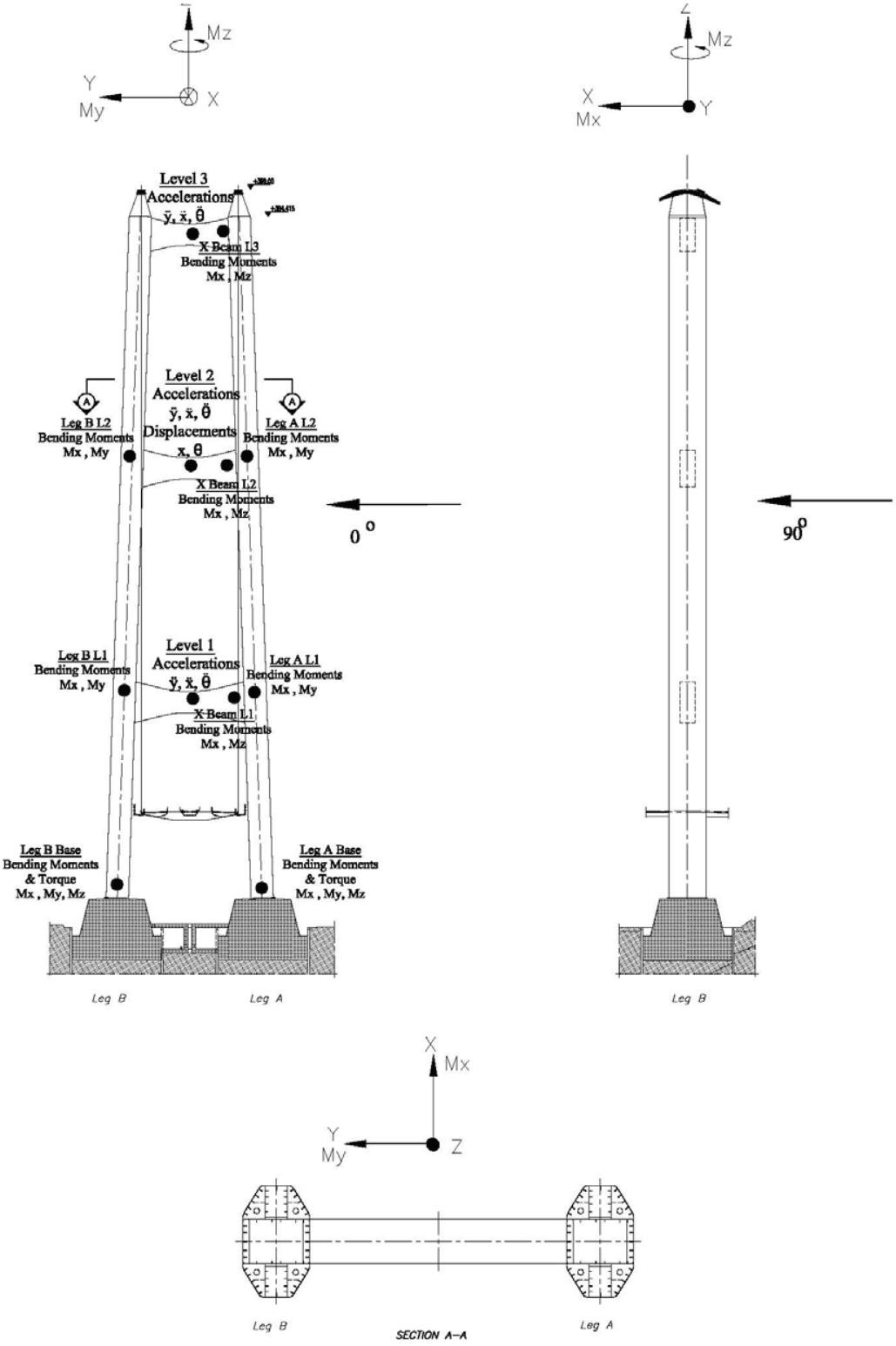

FIGURE C2 INSTRUMENTATION LOCATIONS AND SIGN CONVENTIONS USED IN THE NON-FROUDE TOWER TEST

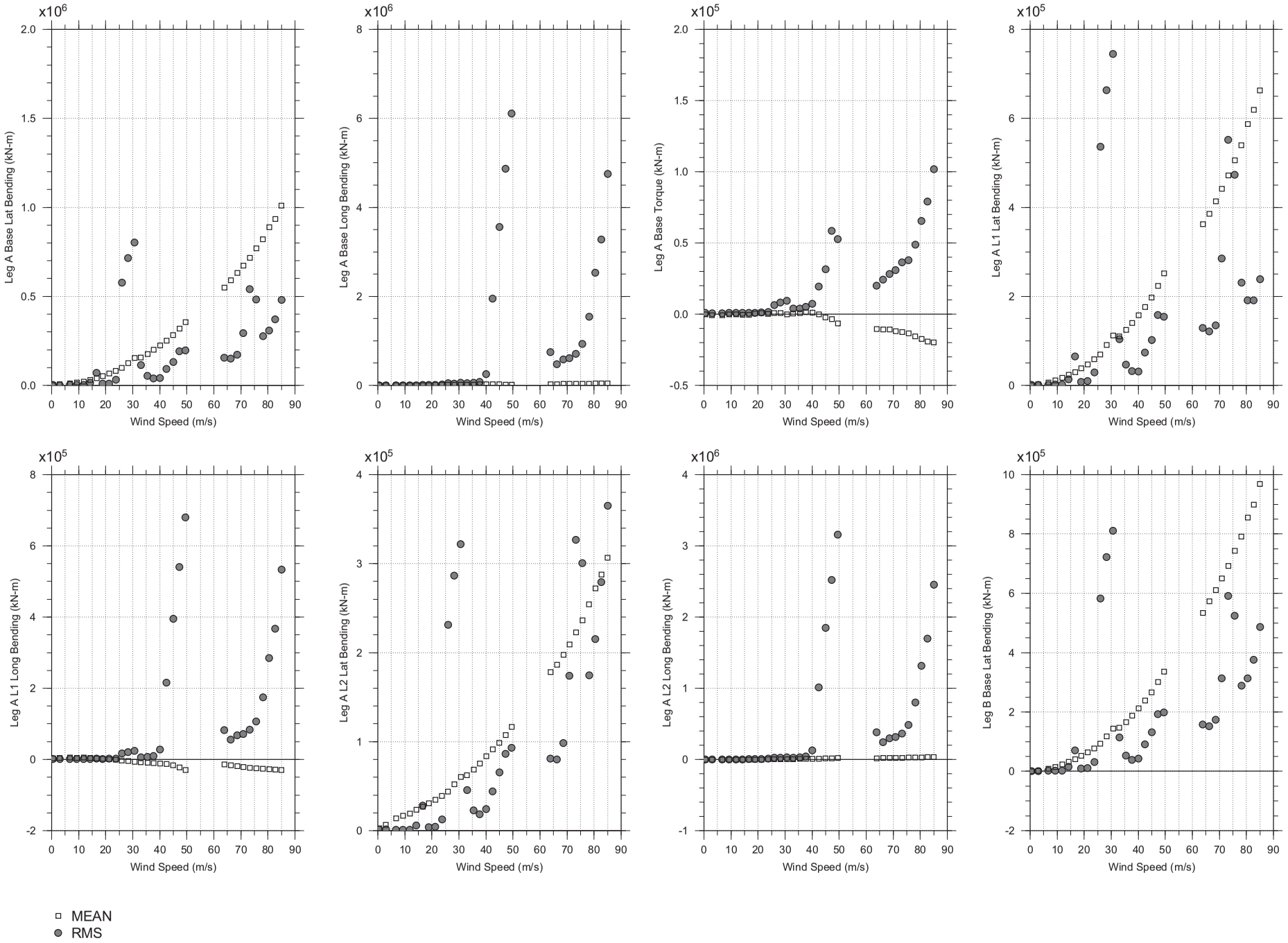

Messina Bridge, In Service Tower, 0 degree, Smooth Flow, Jan2011

Jan. 11, 2011
ti11rabdg.cl

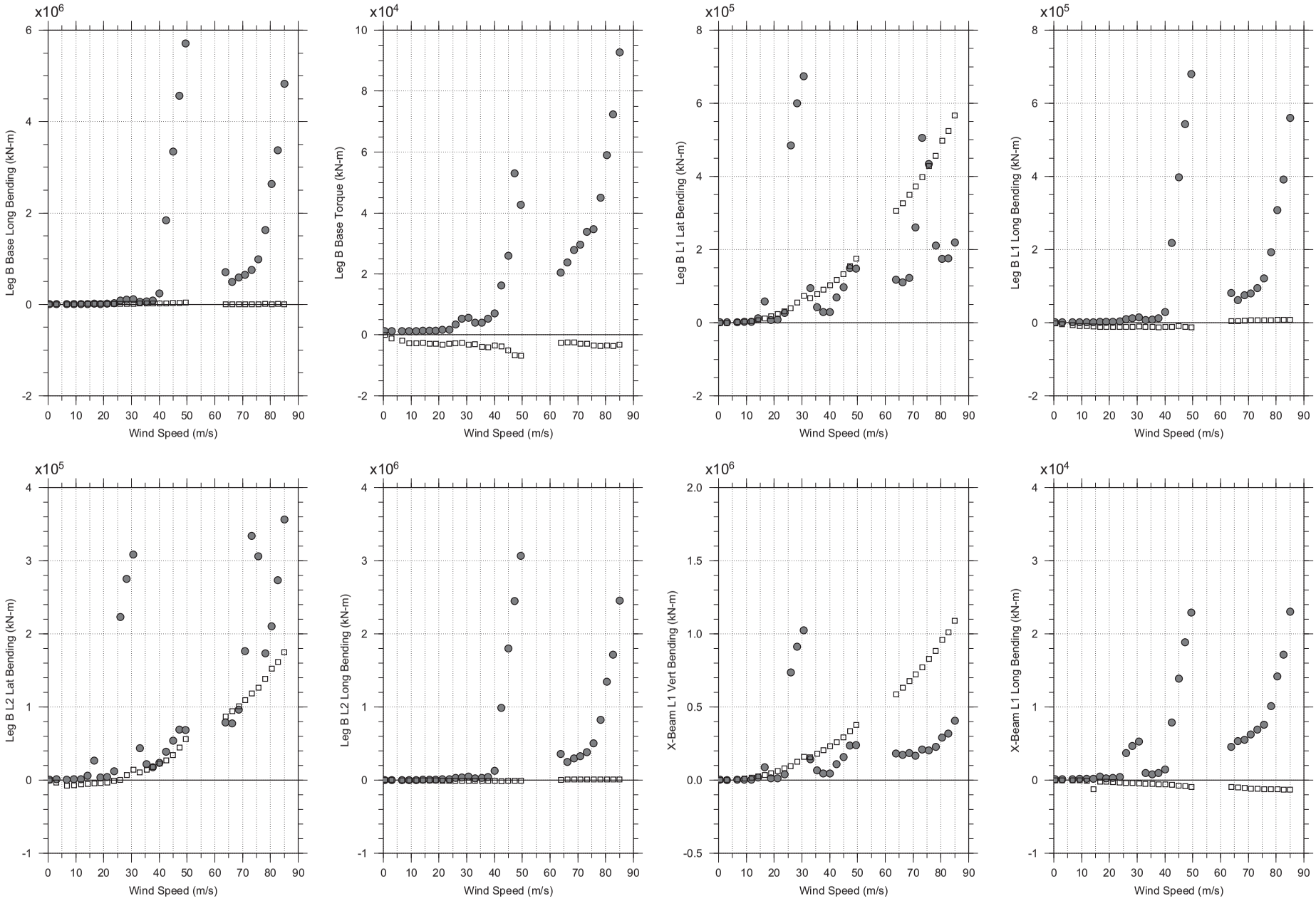

Messina Bridge, In Service Tower, 0 degree, Smooth Flow, Jan2011

Jan. 11, 2011
ti11rabdg.cl

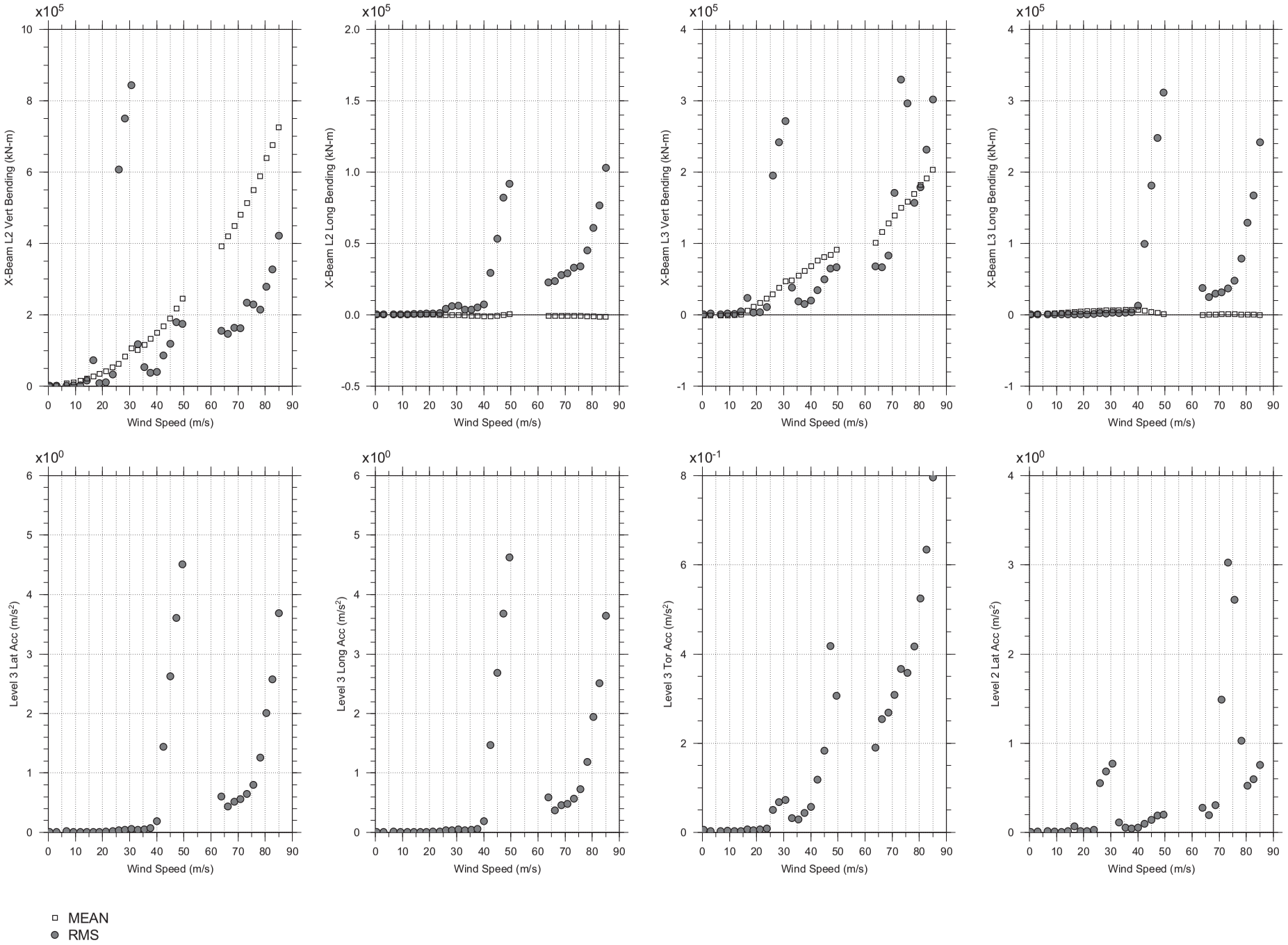

Messina Bridge, In Service Tower, 0 degree, Smooth Flow, Jan2011

Jan. 11, 2011
ti11rabdg.cl

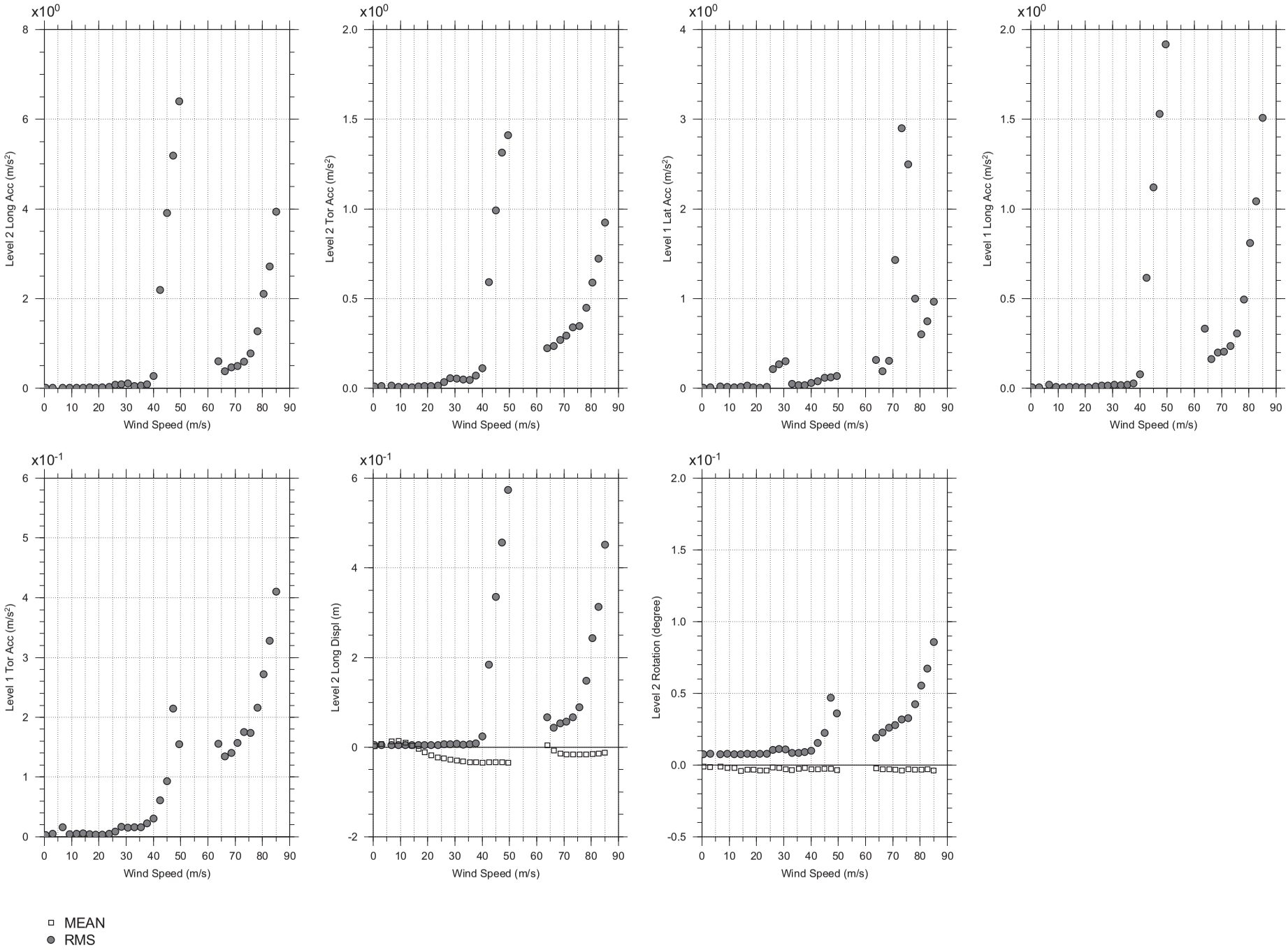

Messina Bridge, In Service Tower, 0 degree, Smooth Flow, Jan2011

Jan. 11, 2011
ti11rabdg.cl

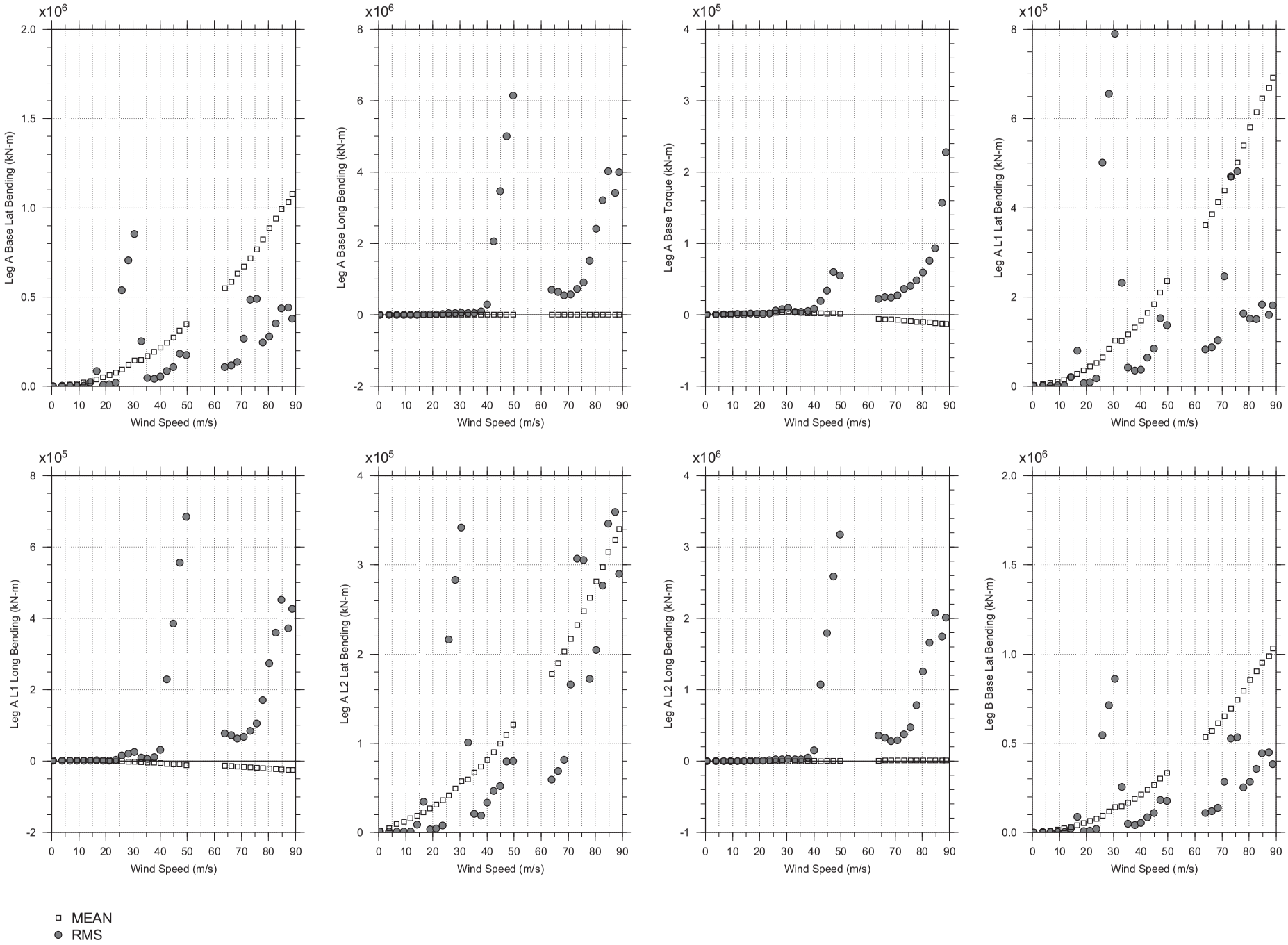

Messina Bridge, In Service Tower, 2.5 degree, Smooth Flow, Jan2011

Jan. 11, 2011
ti12rabdg.cl

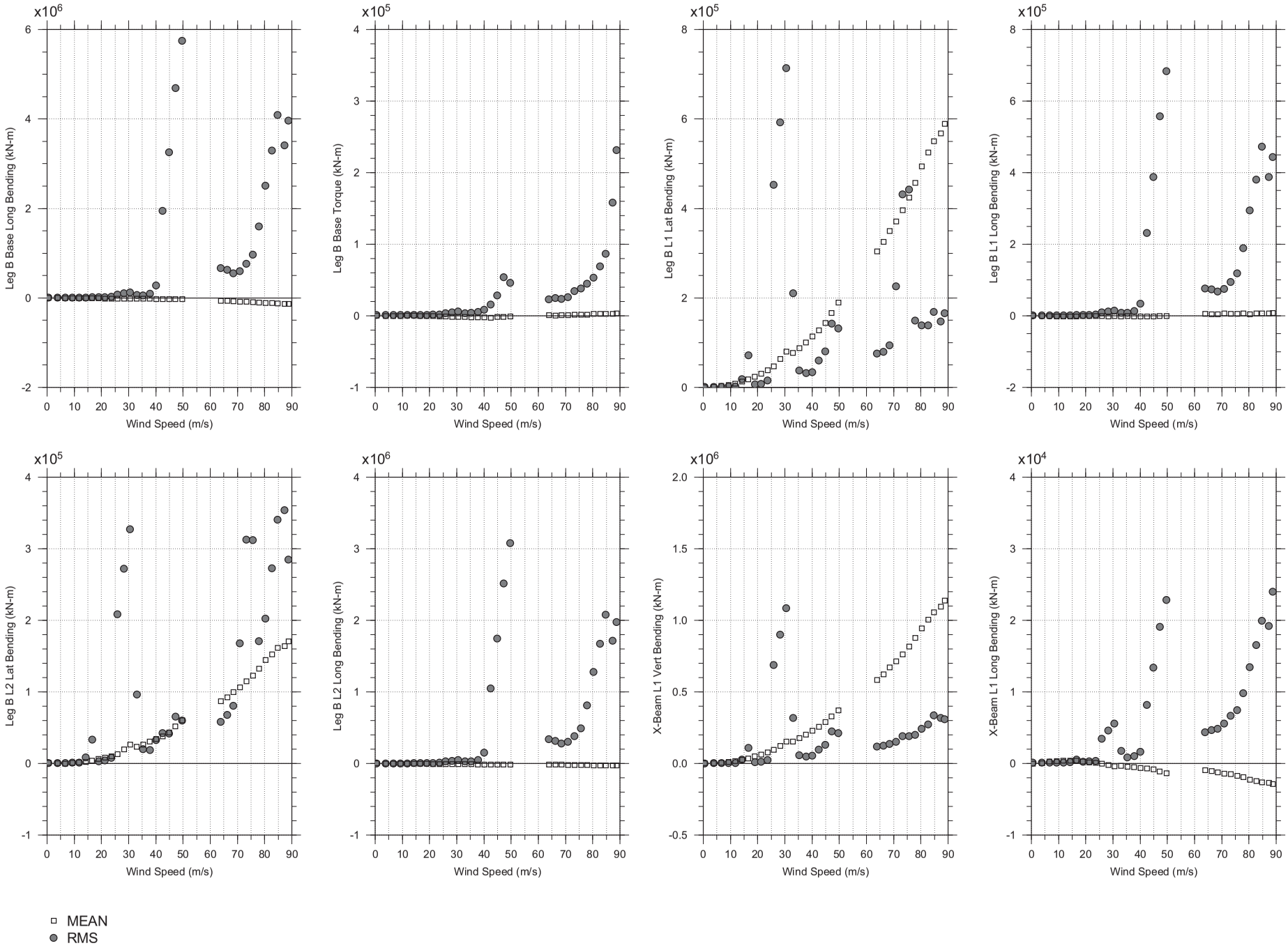

Messina Bridge, In Service Tower, 2.5 degree, Smooth Flow, Jan2011

Jan. 11, 2011
ti12rabdg.cl

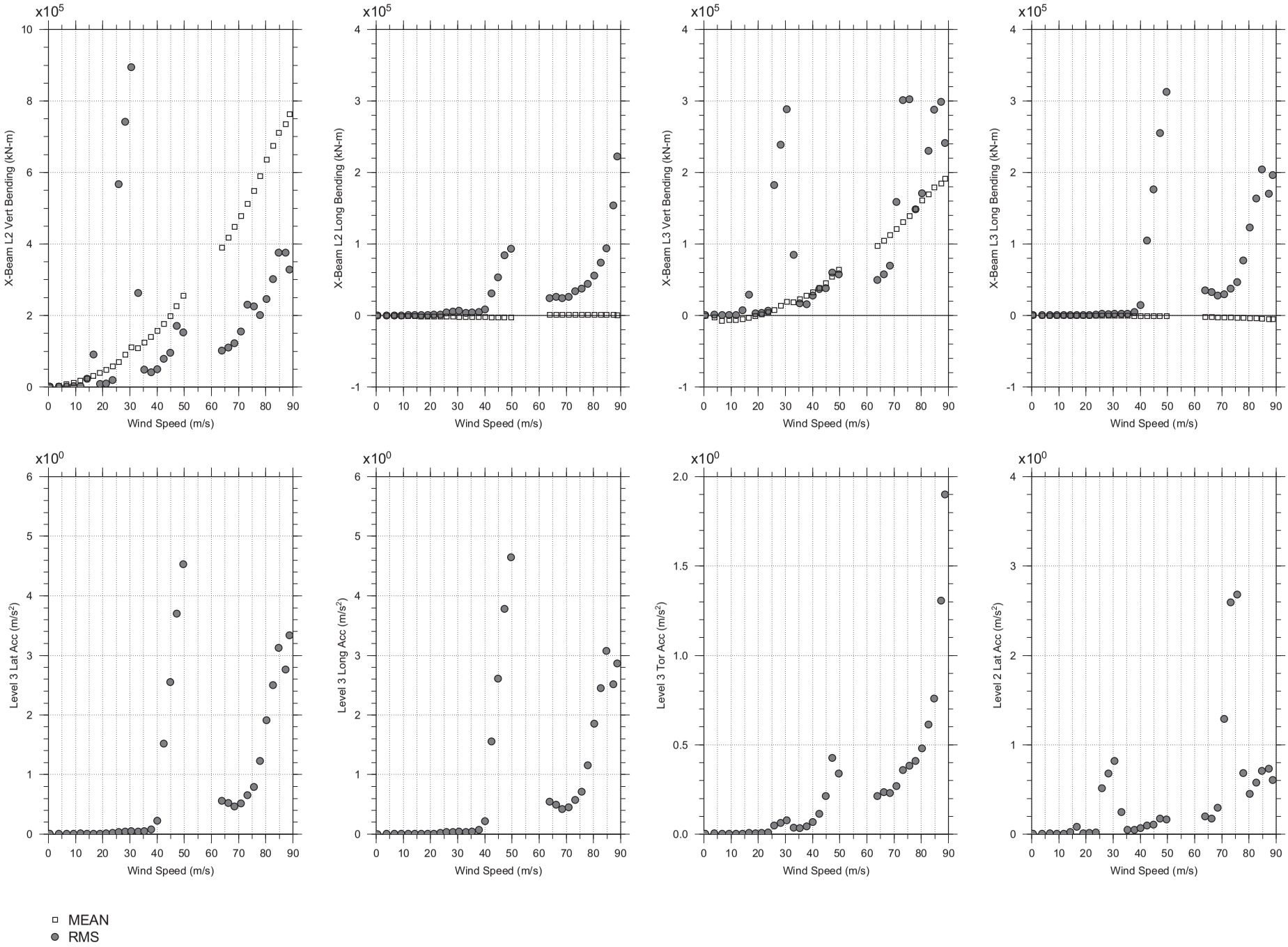

Messina Bridge, In Service Tower, 2.5 degree, Smooth Flow, Jan2011

Jan. 11, 2011
ti12rabdg.cl

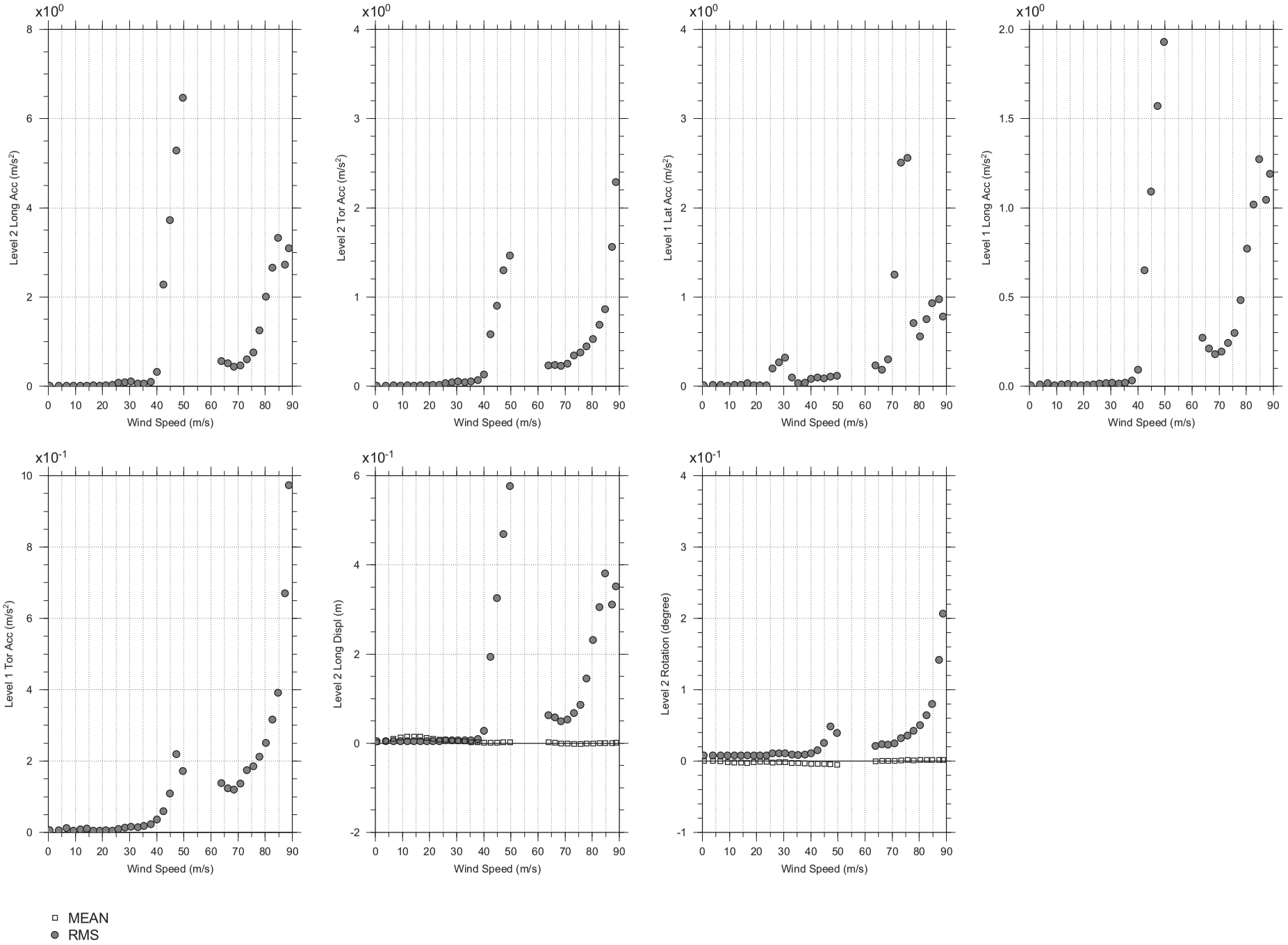

Messina Bridge, In Service Tower, 2.5 degree, Smooth Flow, Jan2011

Jan. 11, 2011
ti12rabdg.cl

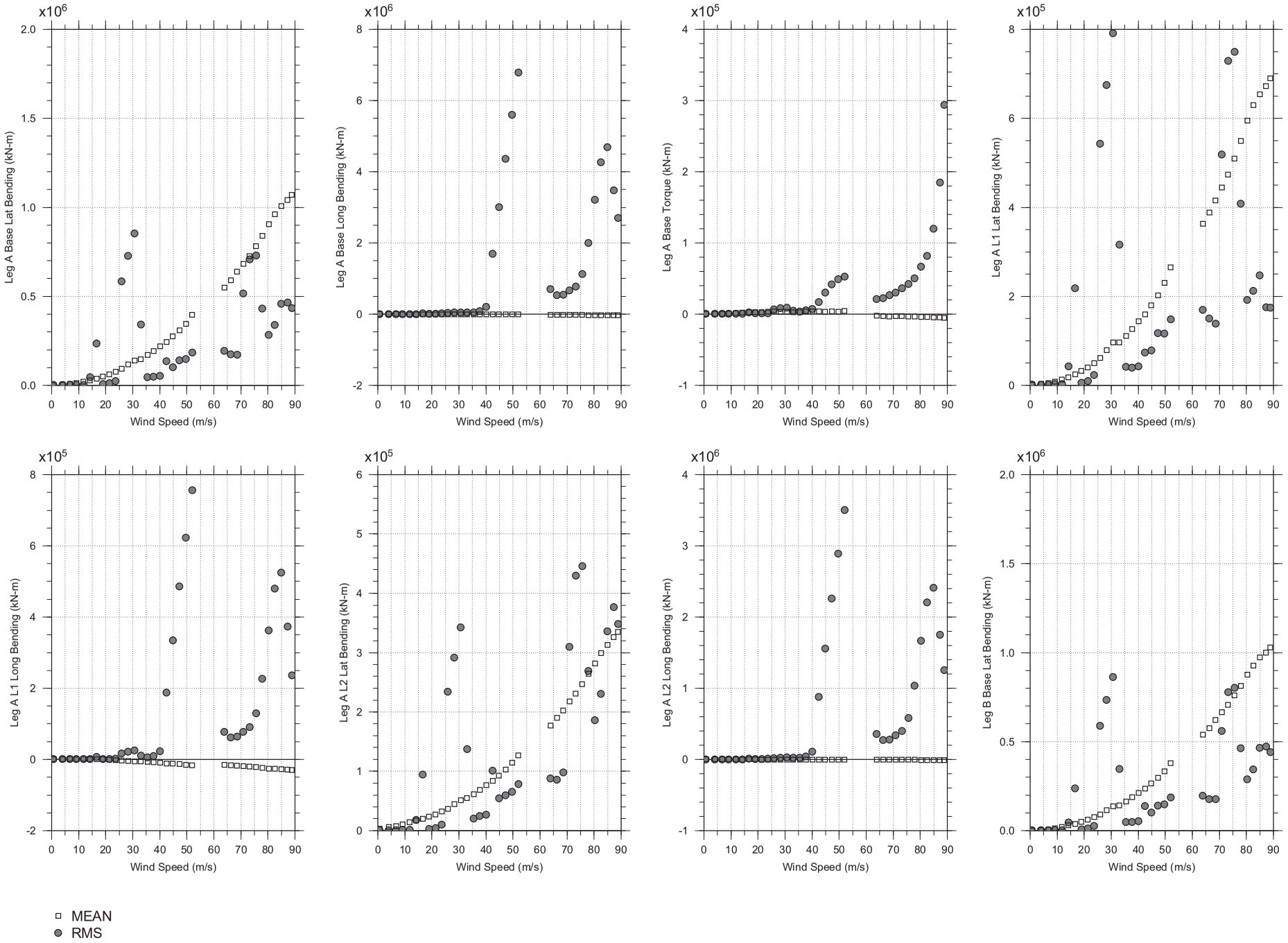

Messina Bridge, In Service Tower, 5 degree, Smooth Flow, Jan2011

Jan. 11, 2011
ti13rabdg.cl

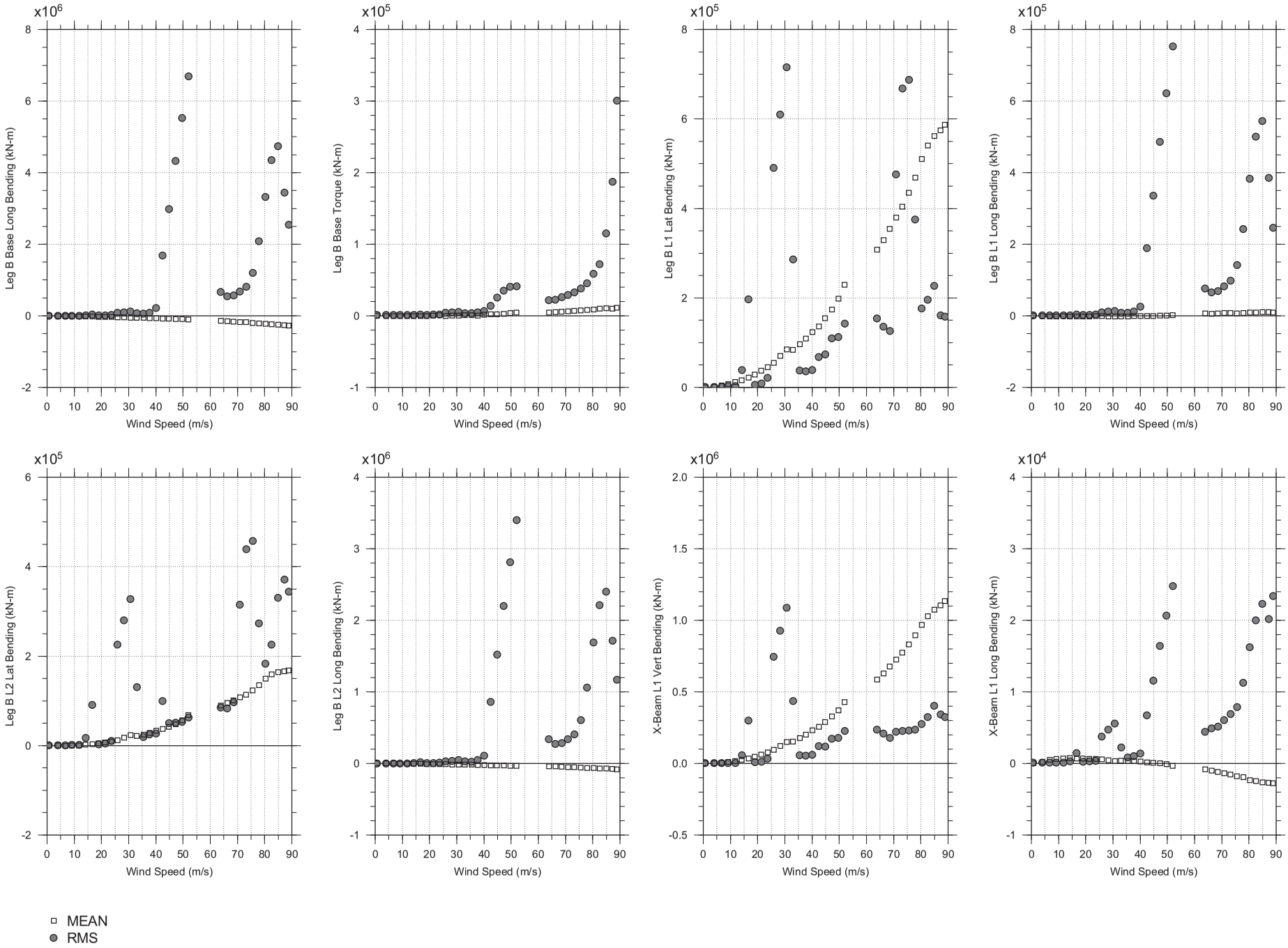

Messina Bridge, In Service Tower, 5 degree, Smooth Flow, Jan2011

Jan. 11, 2011
ti13rabdg.cl

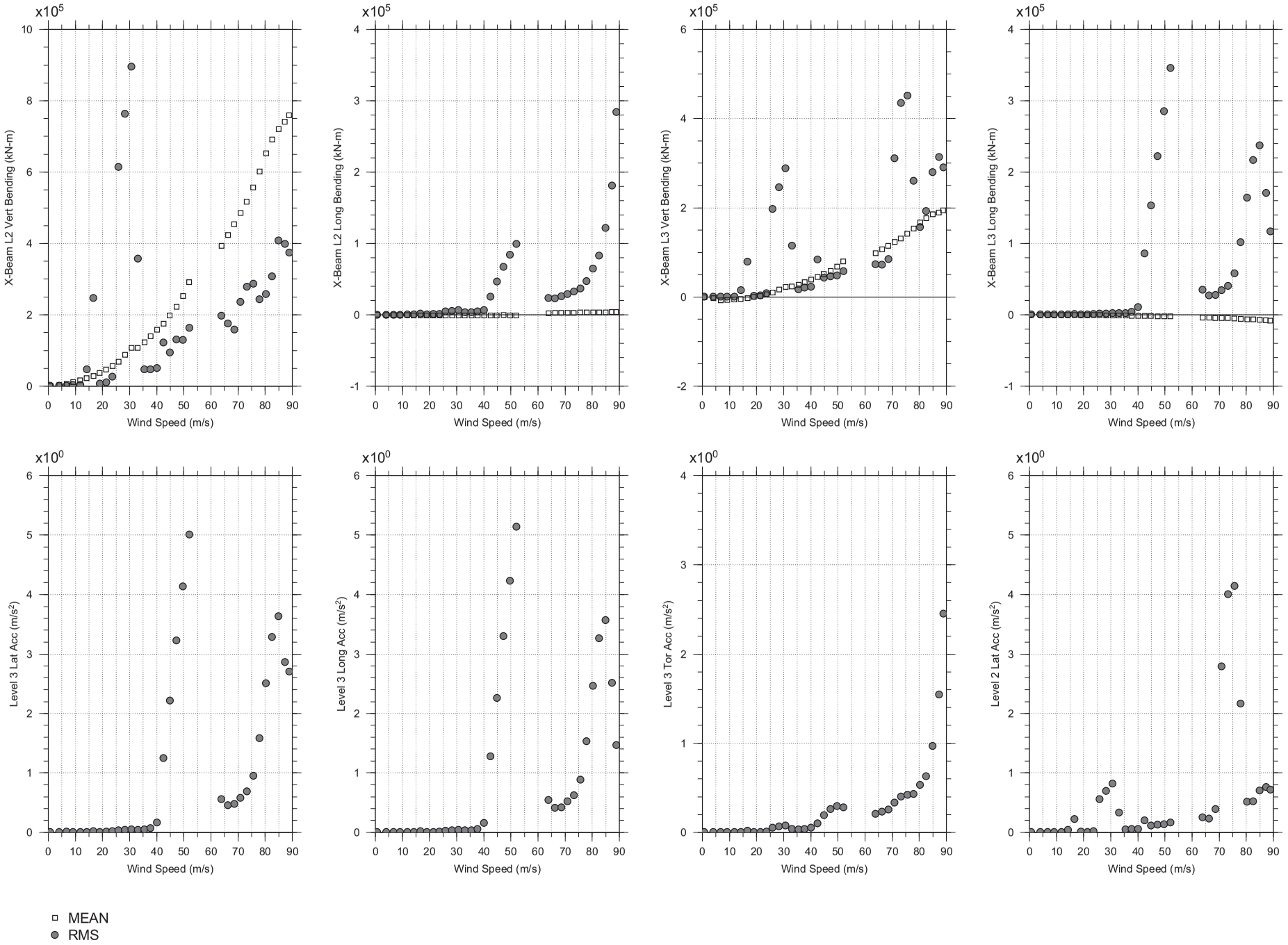

Messina Bridge, In Service Tower, 5 degree, Smooth Flow, Jan2011

Jan. 11, 2011
ti13rabdg.cl

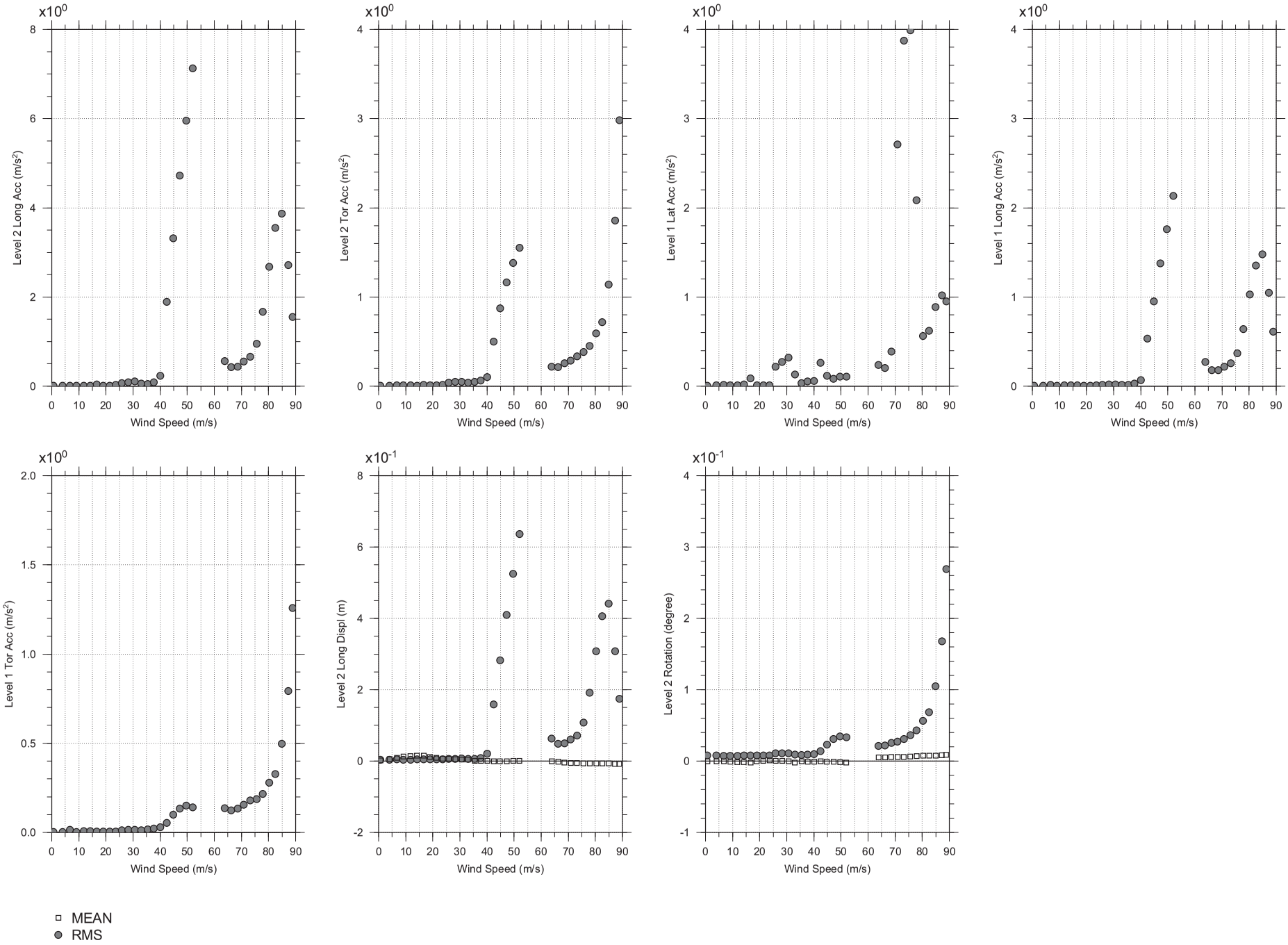

Messina Bridge, In Service Tower, 5 degree, Smooth Flow, Jan2011

Jan. 11, 2011
ti13rabdg.cl

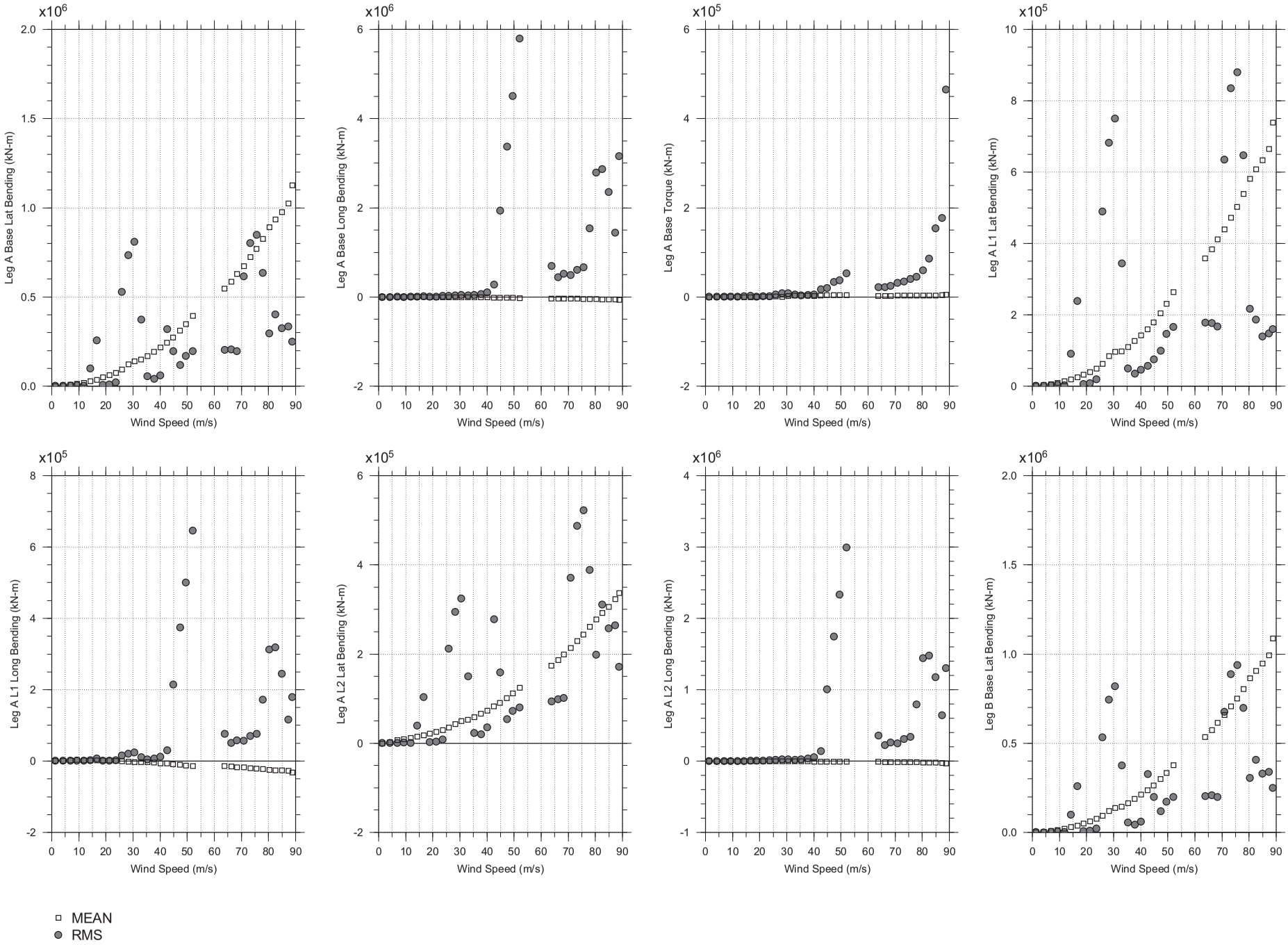

Messina Bridge, In Service Tower, 7.5 degree, Smooth Flow, Jan2011

Jan. 11, 2011
ti14rabdg.cl

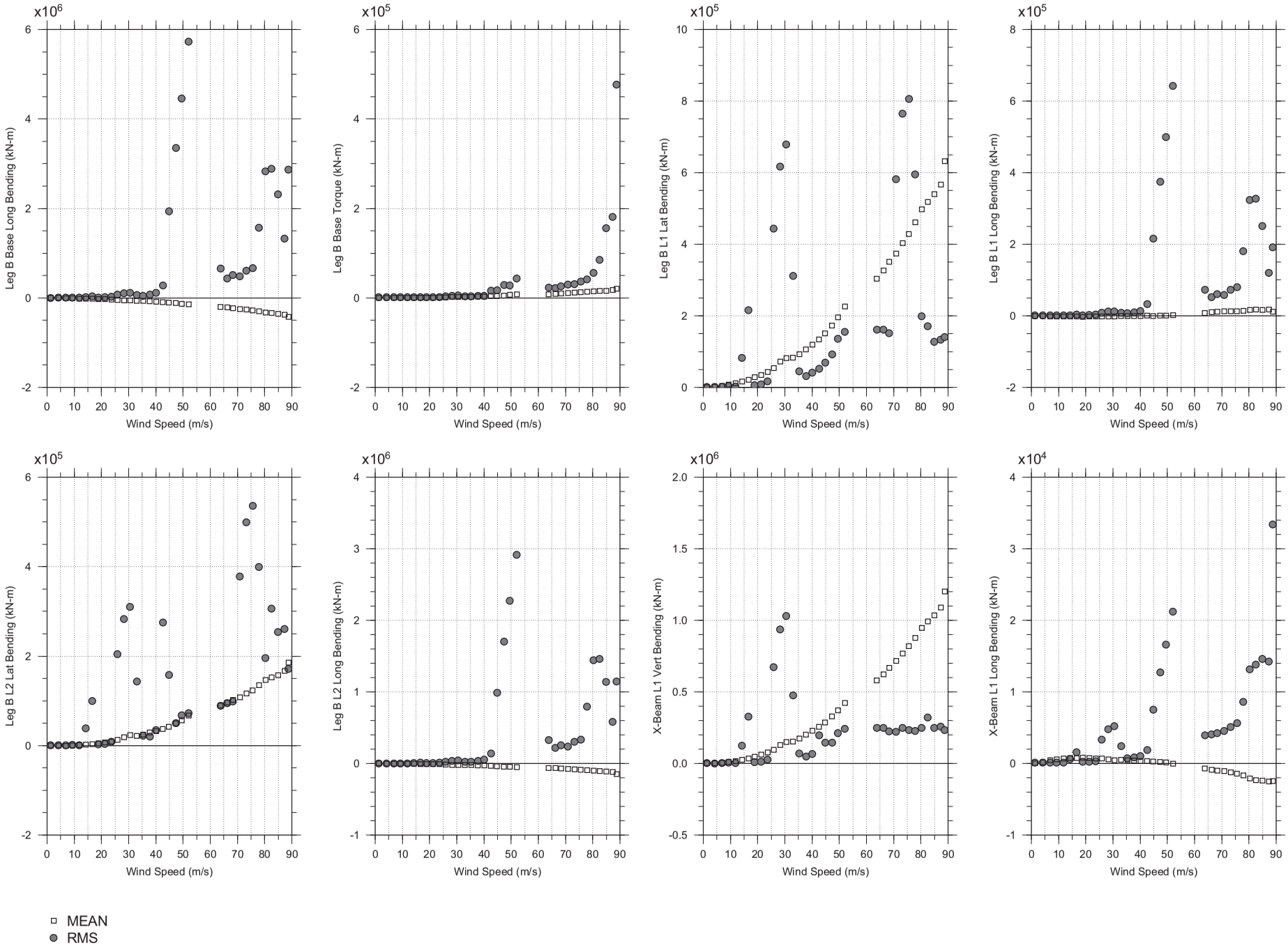

Messina Bridge, In Service Tower, 7.5 degree, Smooth Flow, Jan2011

Jan. 11, 2011
ti14rabdg.cl

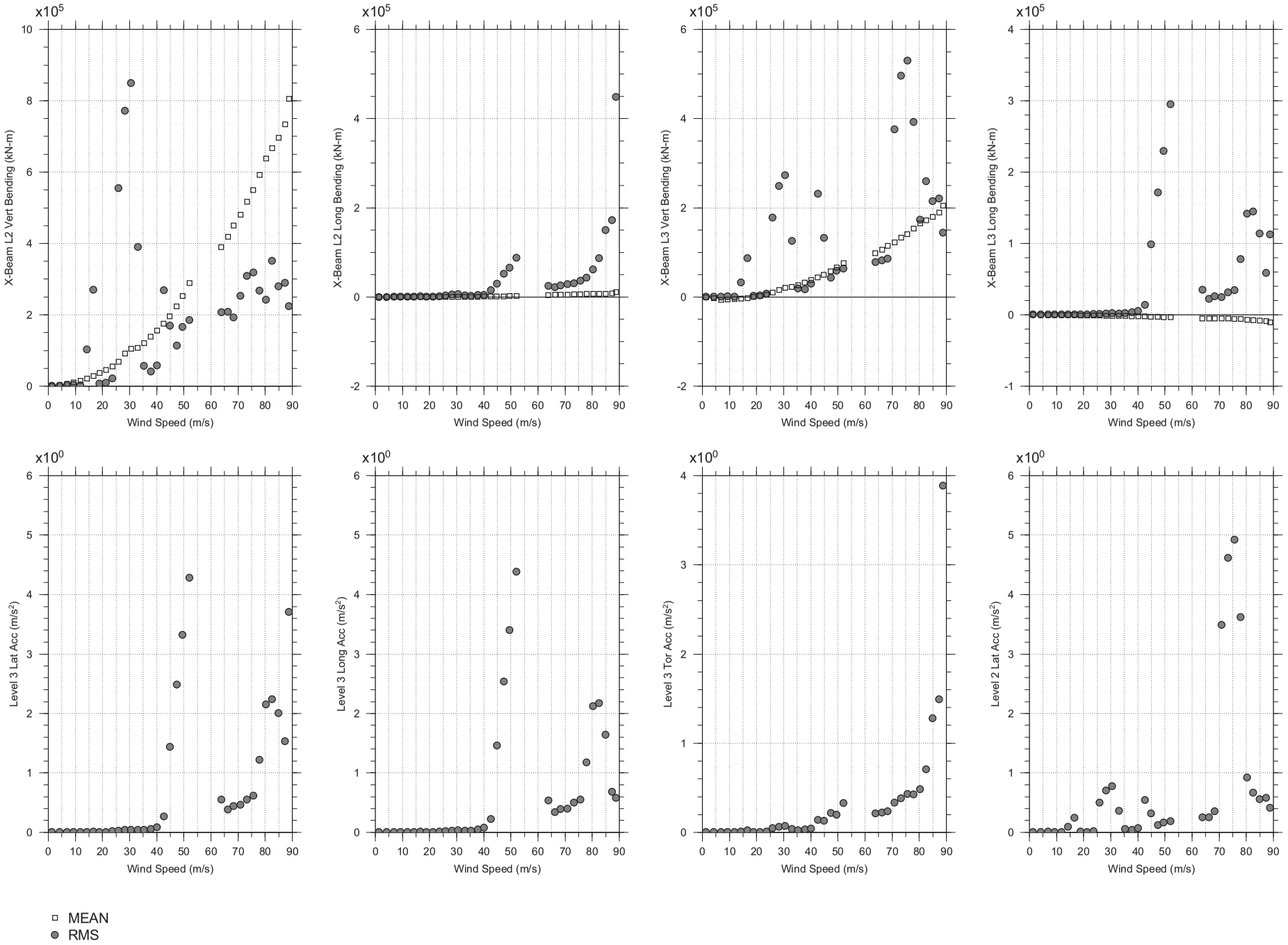

Messina Bridge, In Service Tower, 7.5 degree, Smooth Flow, Jan2011

Jan. 11, 2011
ti14rabdg.cl

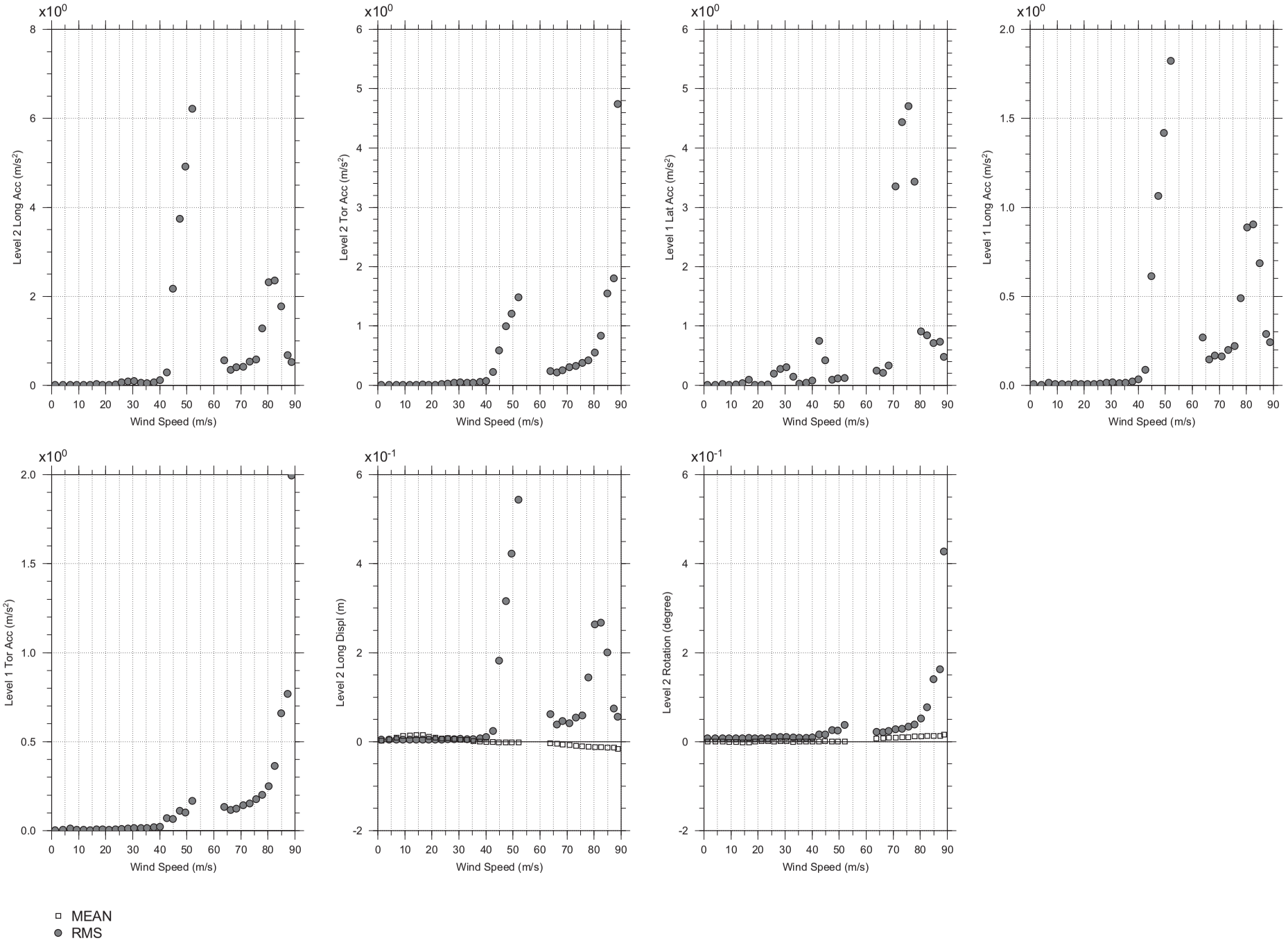

Messina Bridge, In Service Tower, 7.5 degree, Smooth Flow, Jan2011

Jan. 11, 2011
ti14rabdg.cl

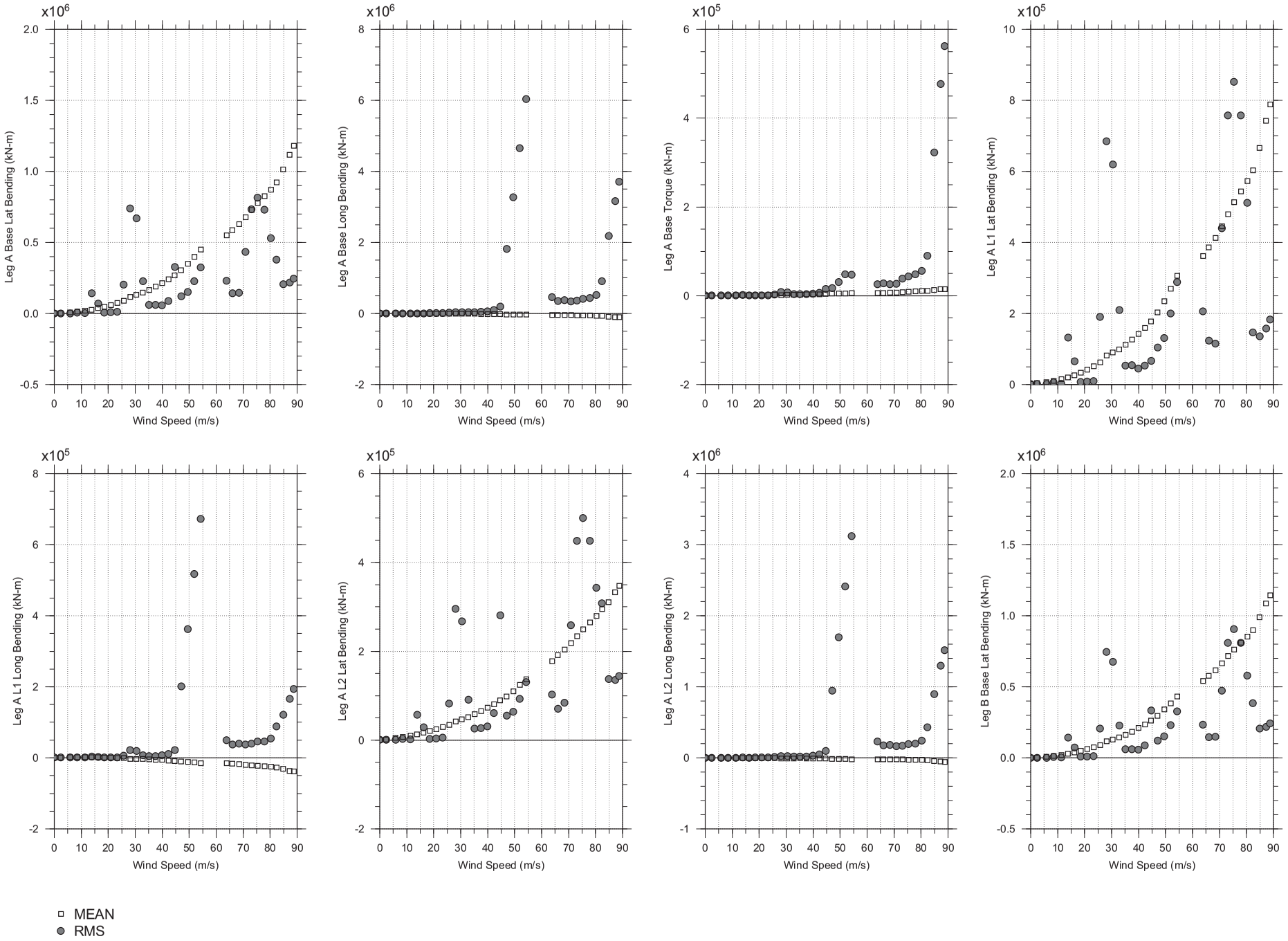

Messina Bridge, In Service Tower, 10 degree, Smooth Flow, Jan2011

Jan. 11, 2011
ti15rabdg.cl

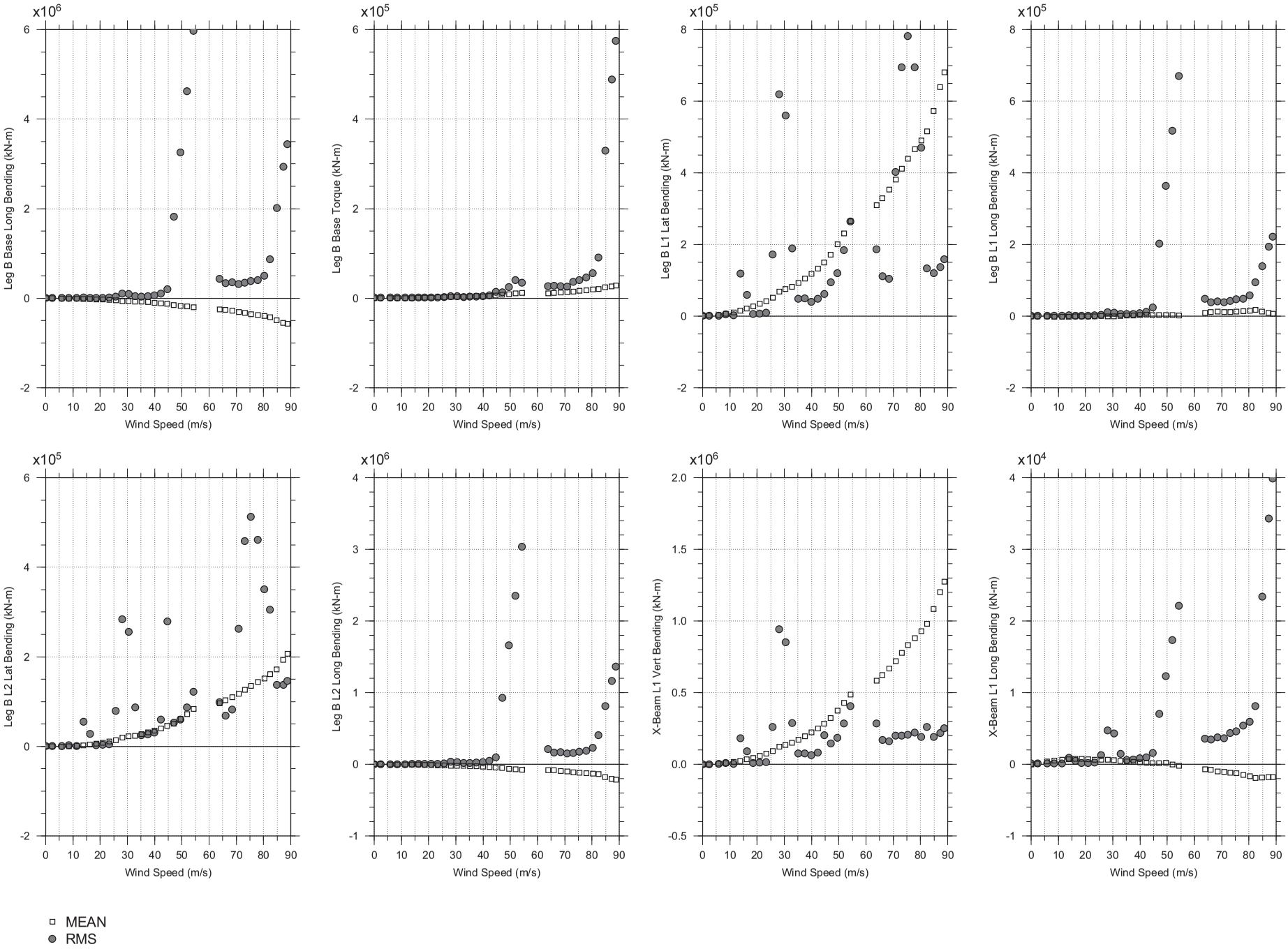

Messina Bridge, In Service Tower, 10 degree, Smooth Flow, Jan2011

Jan. 11, 2011
ti15rabdg.cl

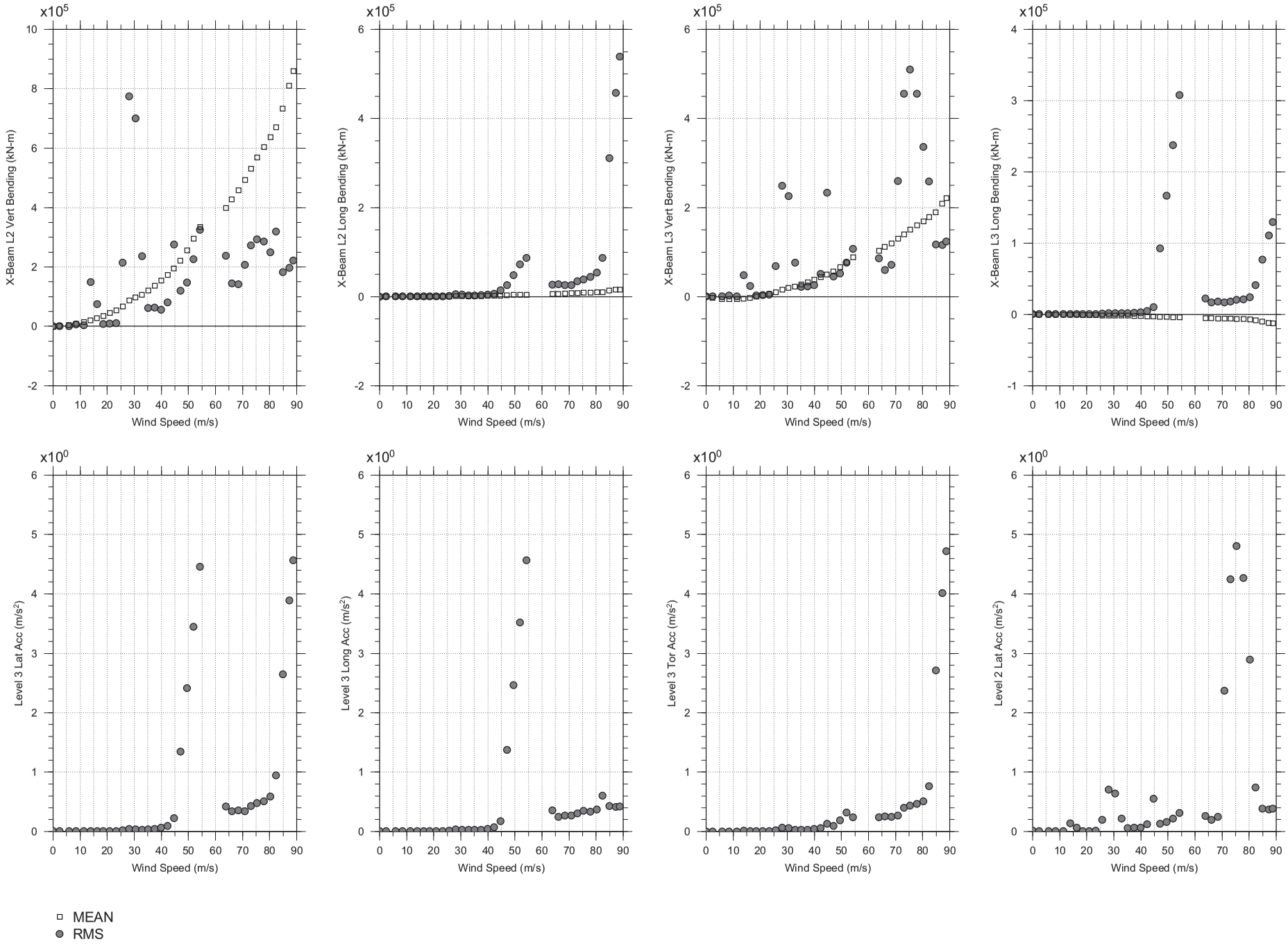

Messina Bridge, In Service Tower, 10 degree, Smooth Flow, Jan2011

Jan. 11, 2011
ti15rabdg.cl

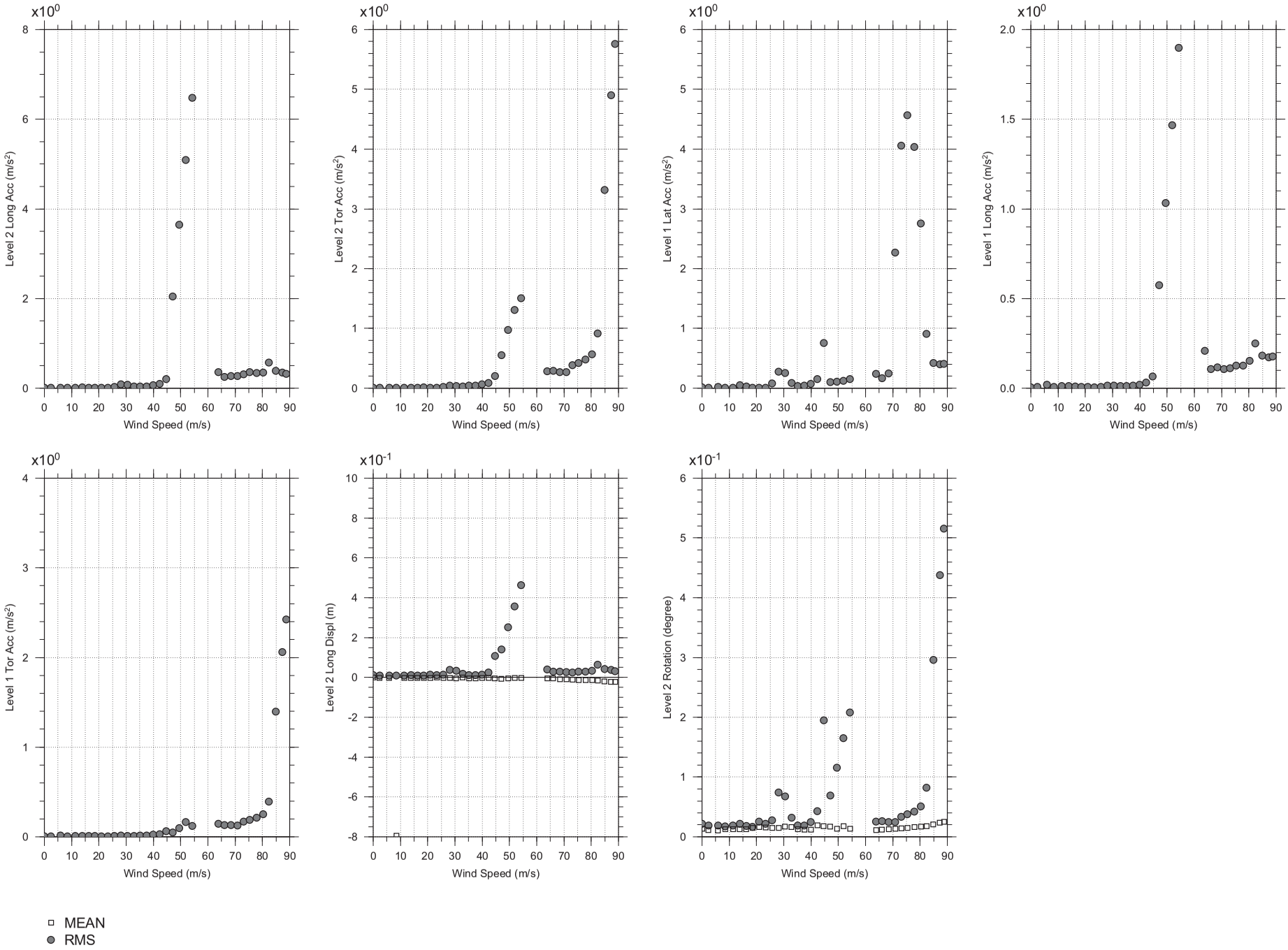

Messina Bridge, In Service Tower, 10 degree, Smooth Flow, Jan2011

Jan. 11, 2011
ti15rabdg.cl

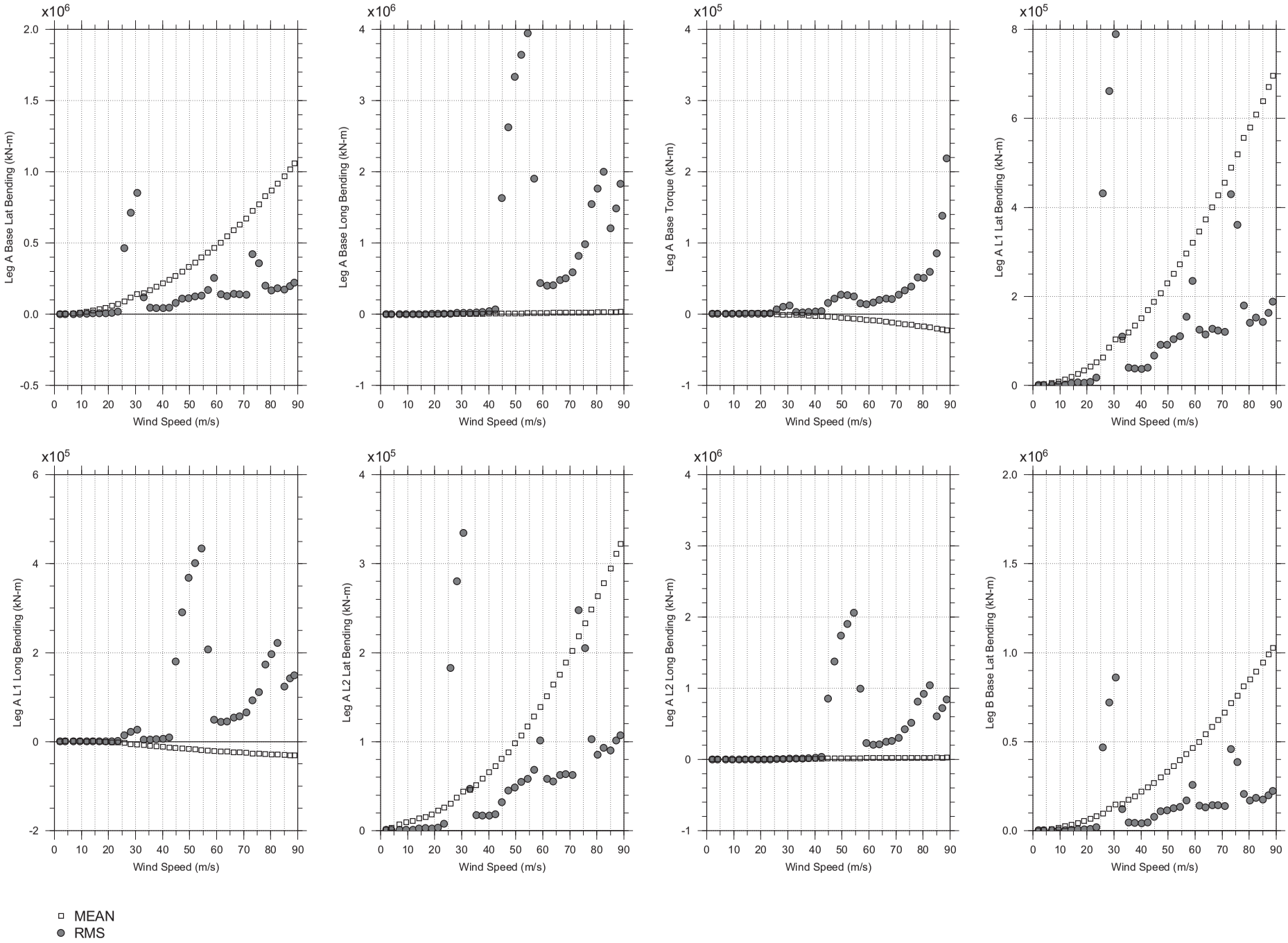

Messina Bridge, In Service Tower, 0.6% Damping, 0 degree, Smooth, Jan2011

Jan. 12, 2011
ti51abdg.cl

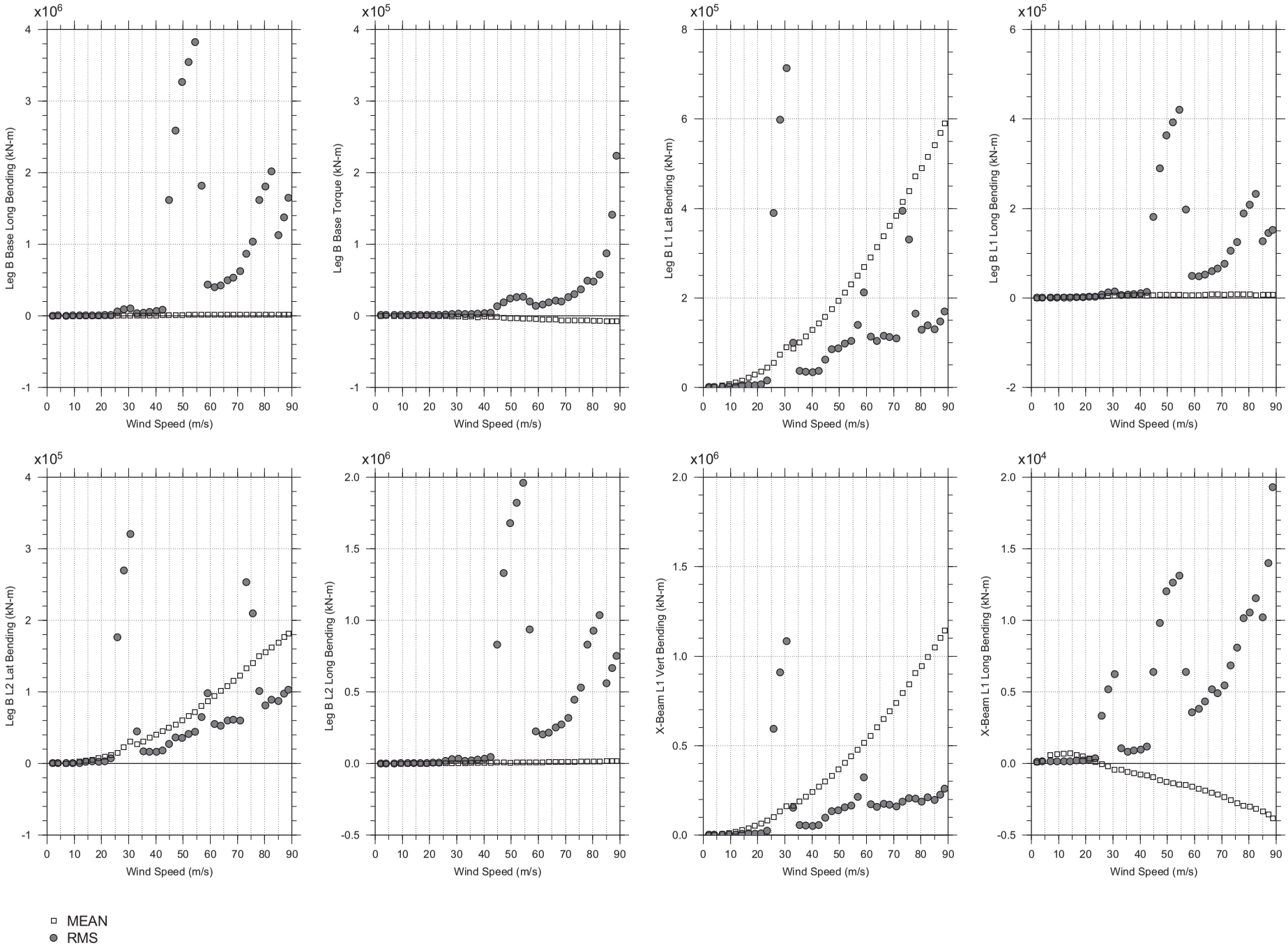

Messina Bridge, In Service Tower, 0.6% Damping, 0 degree, Smooth, Jan2011

Jan. 12, 2011
ti51abdg.cl

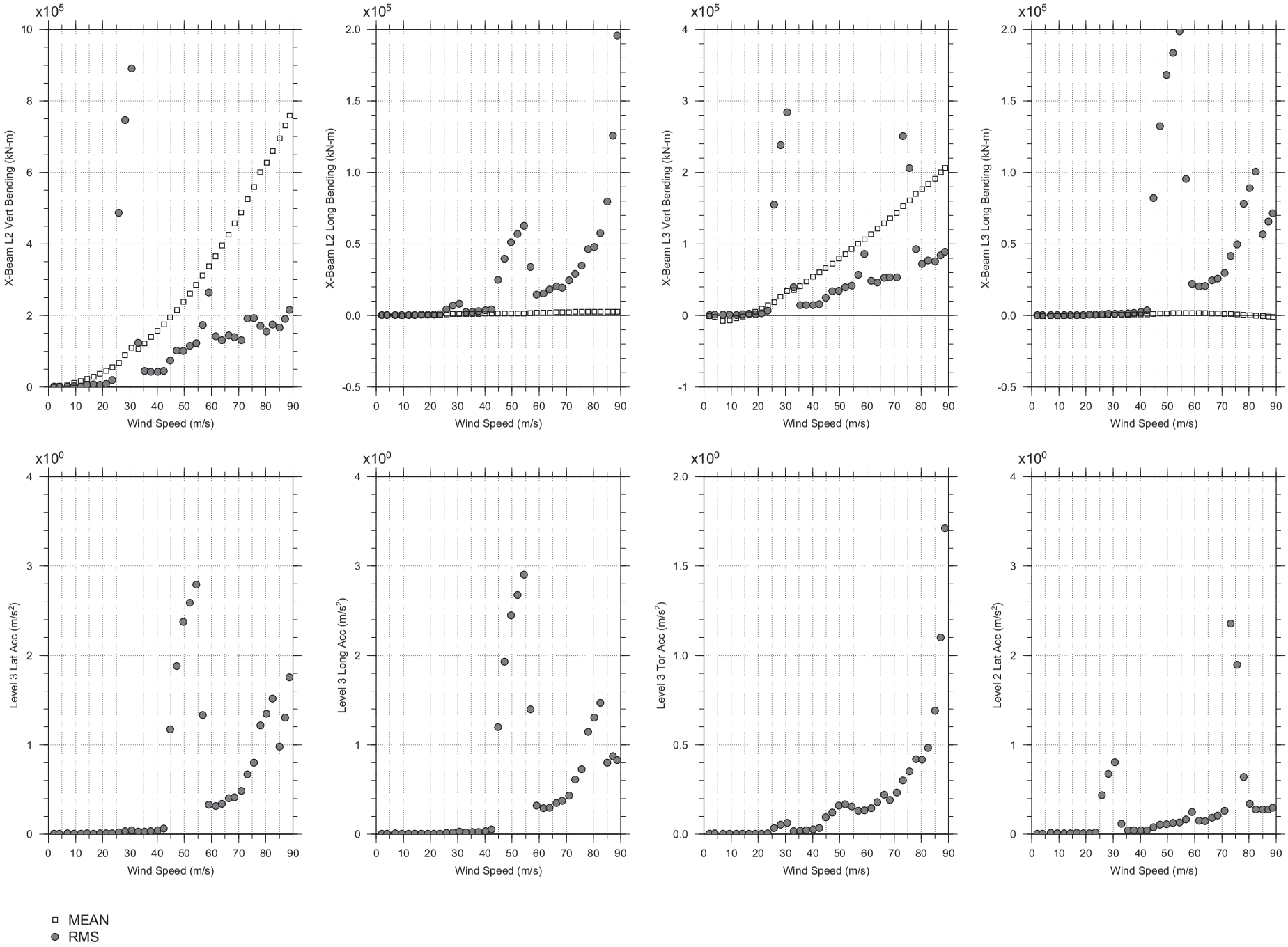

Messina Bridge, In Service Tower, 0.6% Damping, 0 degree, Smooth, Jan2011

Jan. 12, 2011
ti51abdg.cl

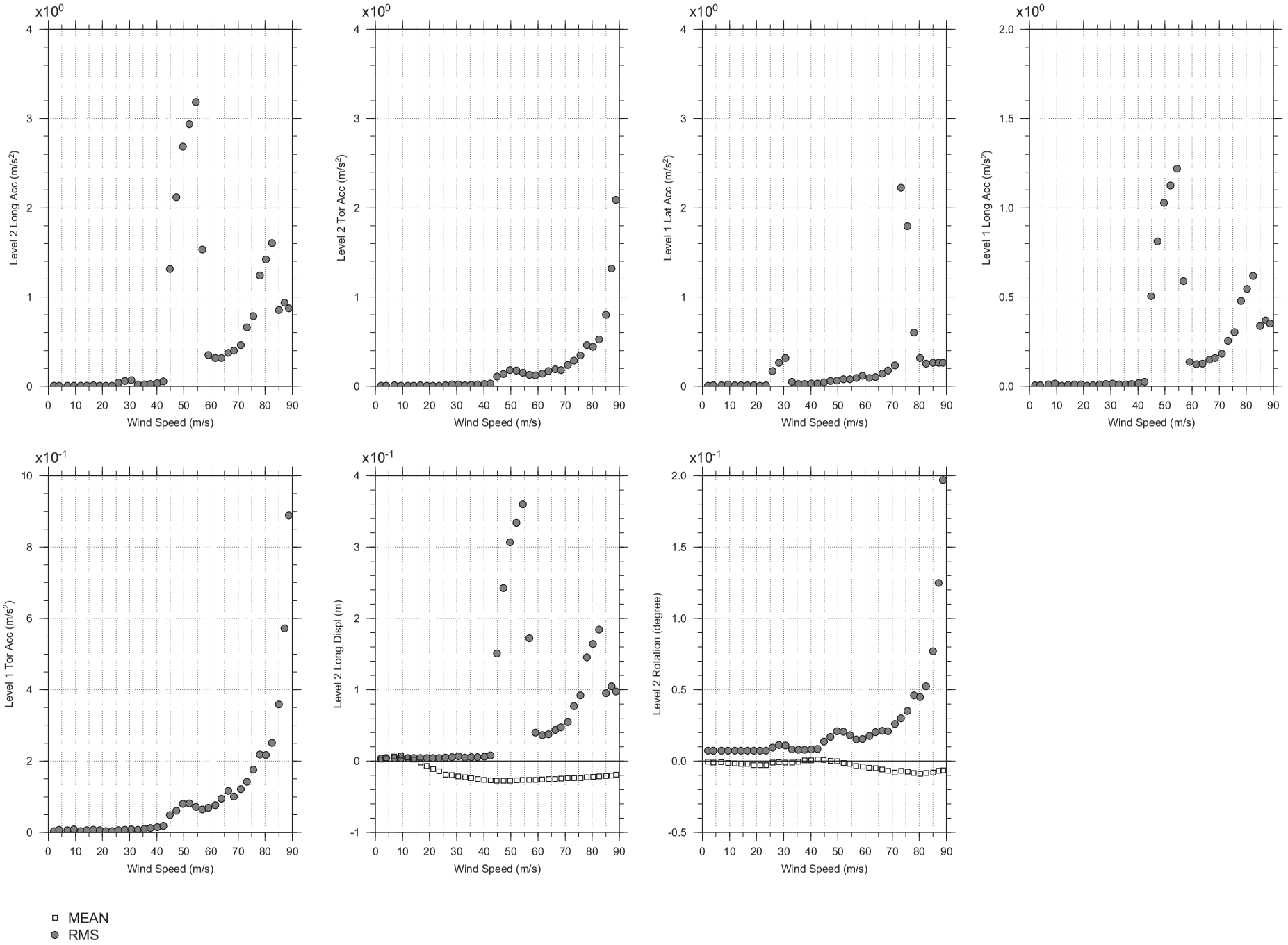

Messina Bridge, In Service Tower, 0.6% Damping, 0 degree, Smooth, Jan2011

Jan. 12, 2011
ti51abdg.cl

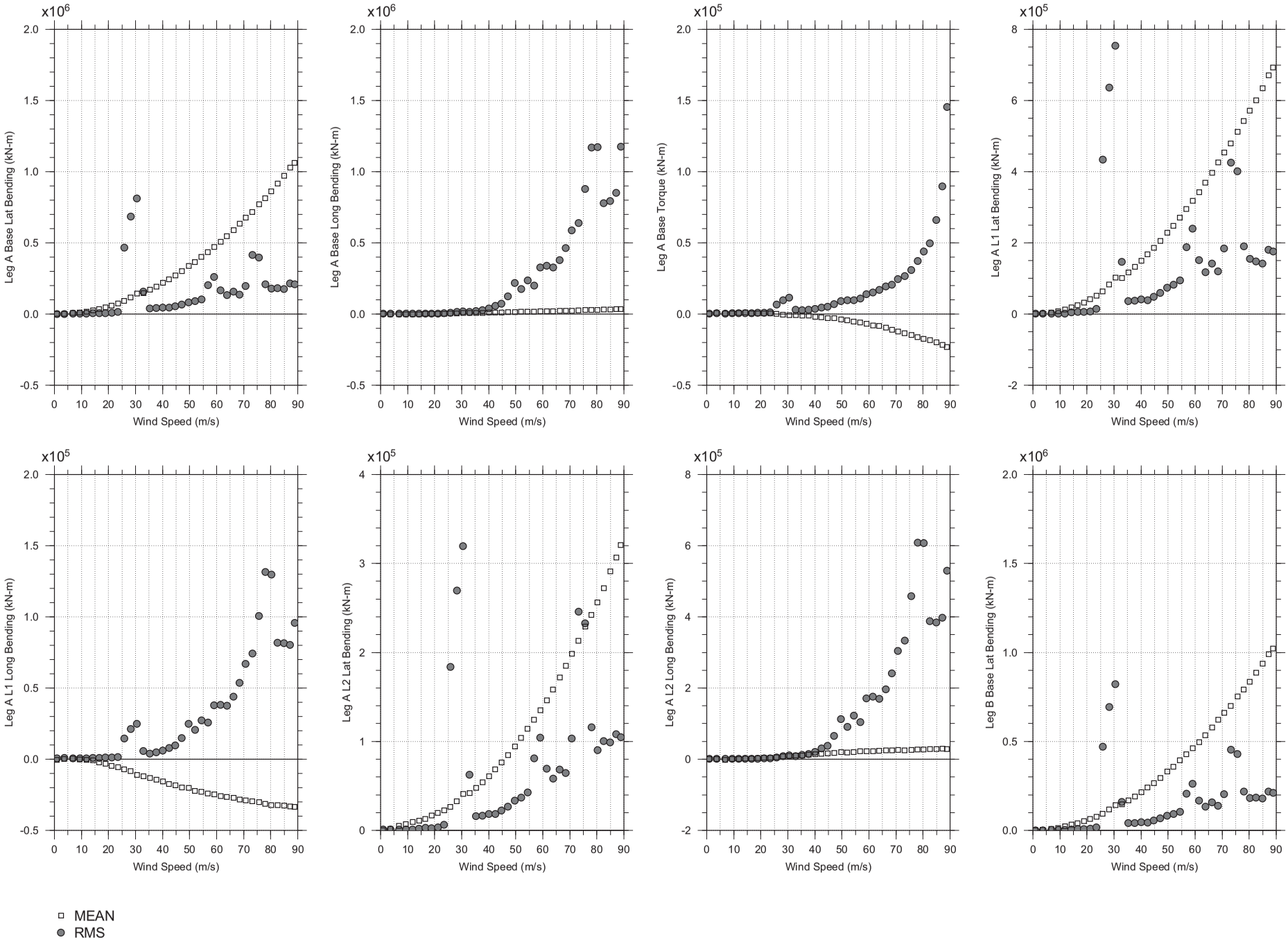

Messina Bridge, In Service Tower, 1% Damping, 0 degree, Smooth, Jan2011

Jan. 12, 2011
ti61abdg.cl

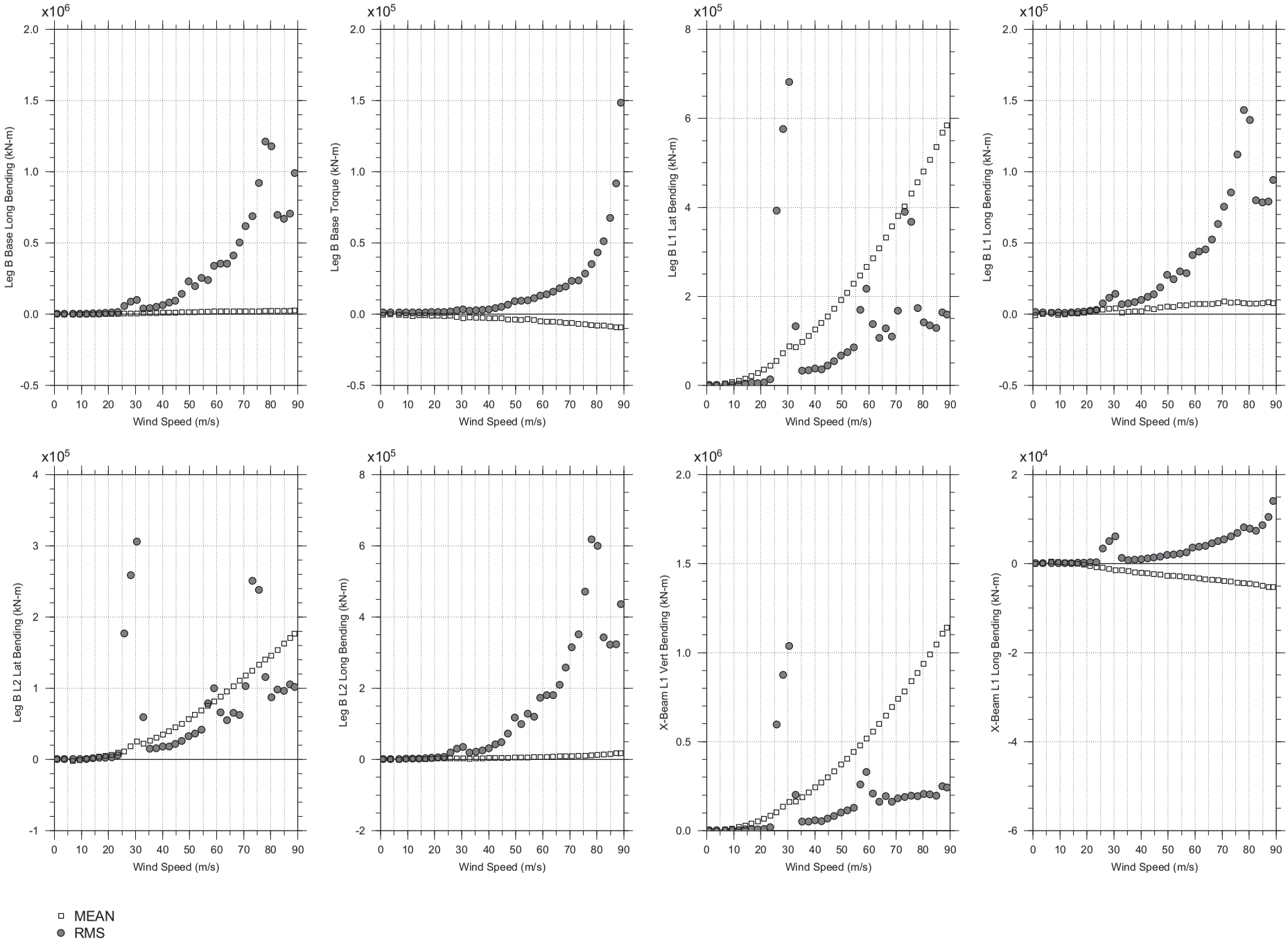

Messina Bridge, In Service Tower, 1% Damping, 0 degree, Smooth, Jan2011

Jan. 12, 2011
ti61abdg.cl

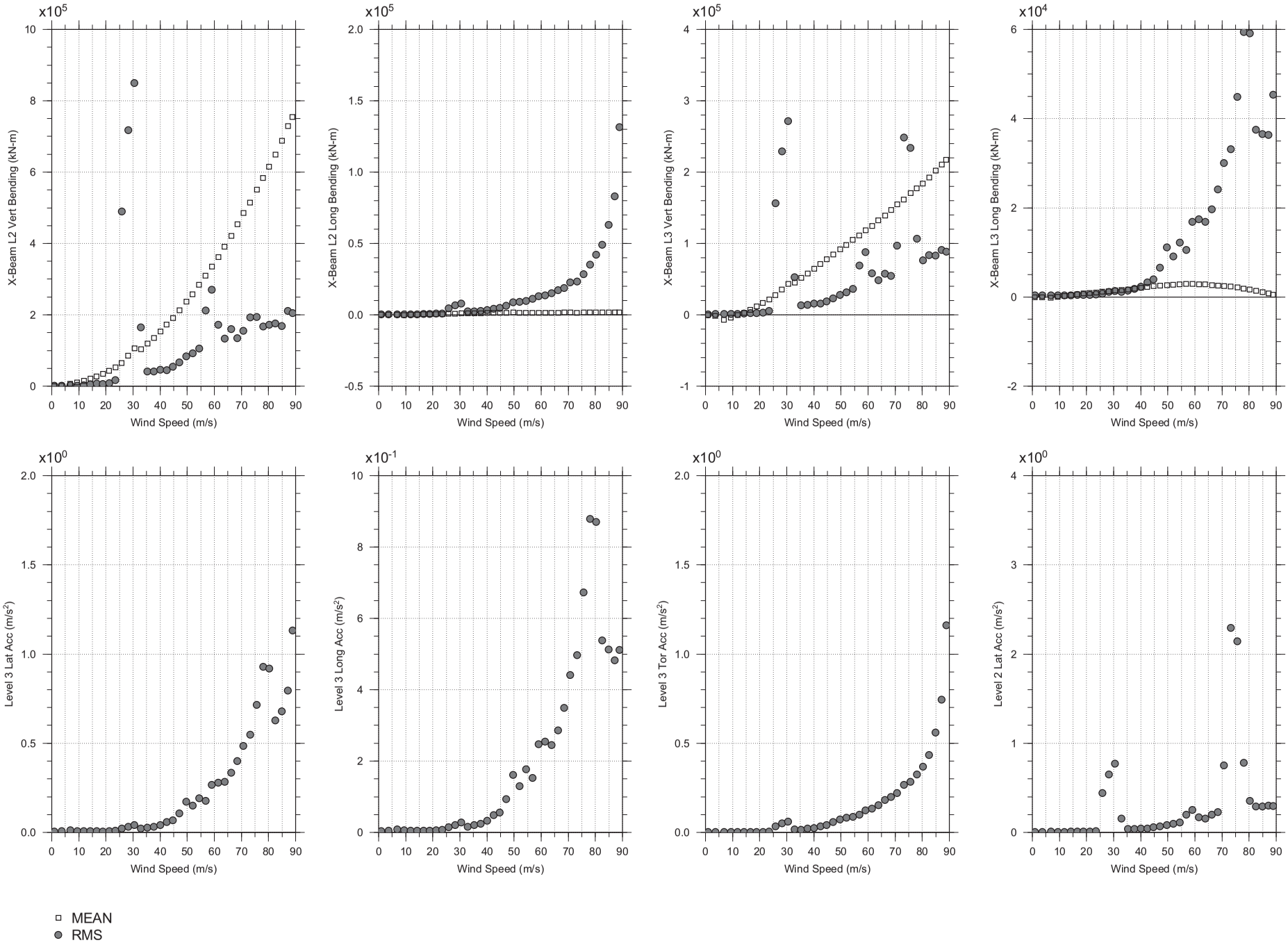

Messina Bridge, In Service Tower, 1% Damping, 0 degree, Smooth, Jan2011

Jan. 12, 2011
ti61abdg.cl

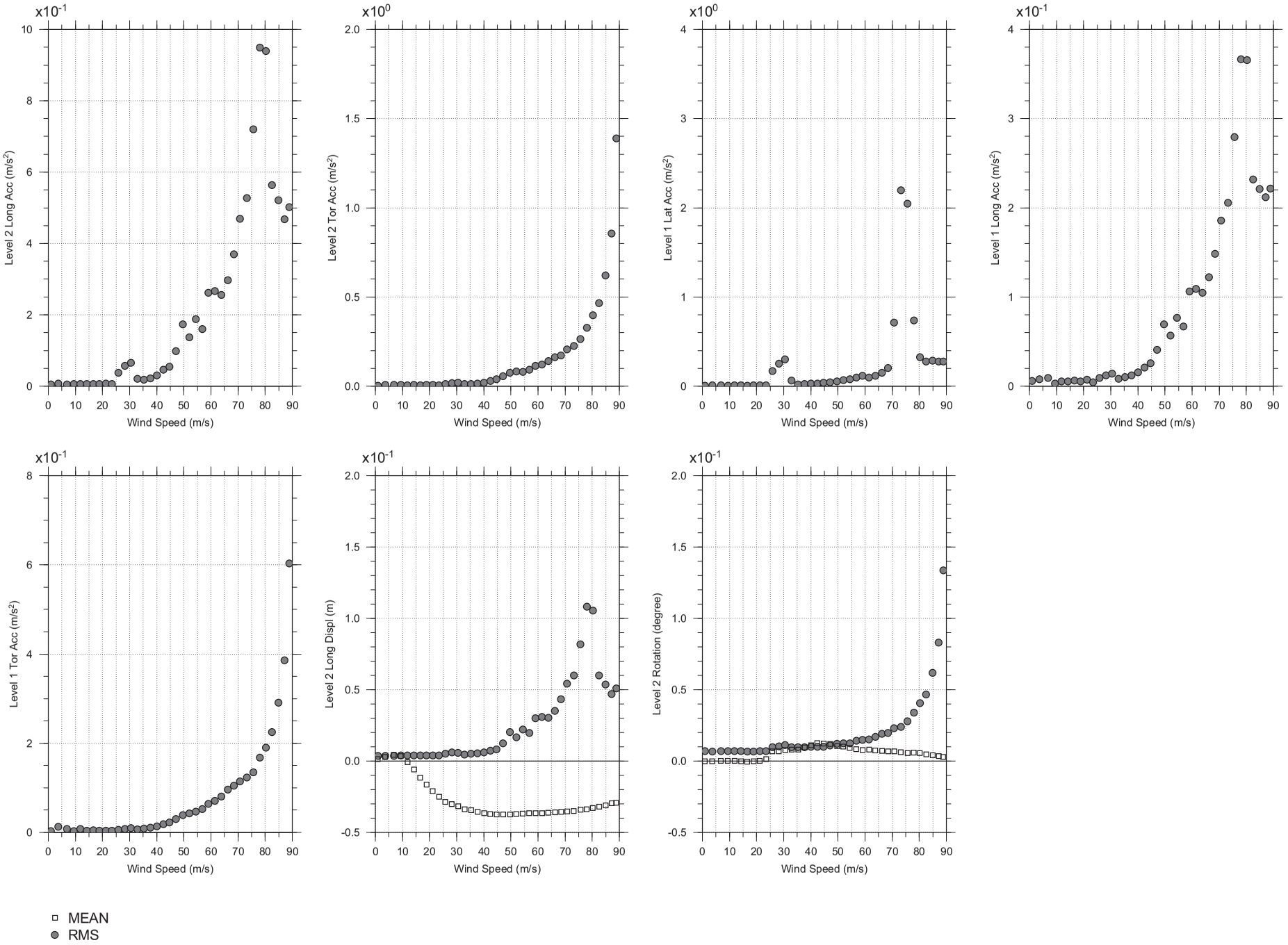

Messina Bridge, In Service Tower, 1% Damping, 0 degree, Smooth, Jan2011

Jan. 12, 2011
ti61abdg.cl

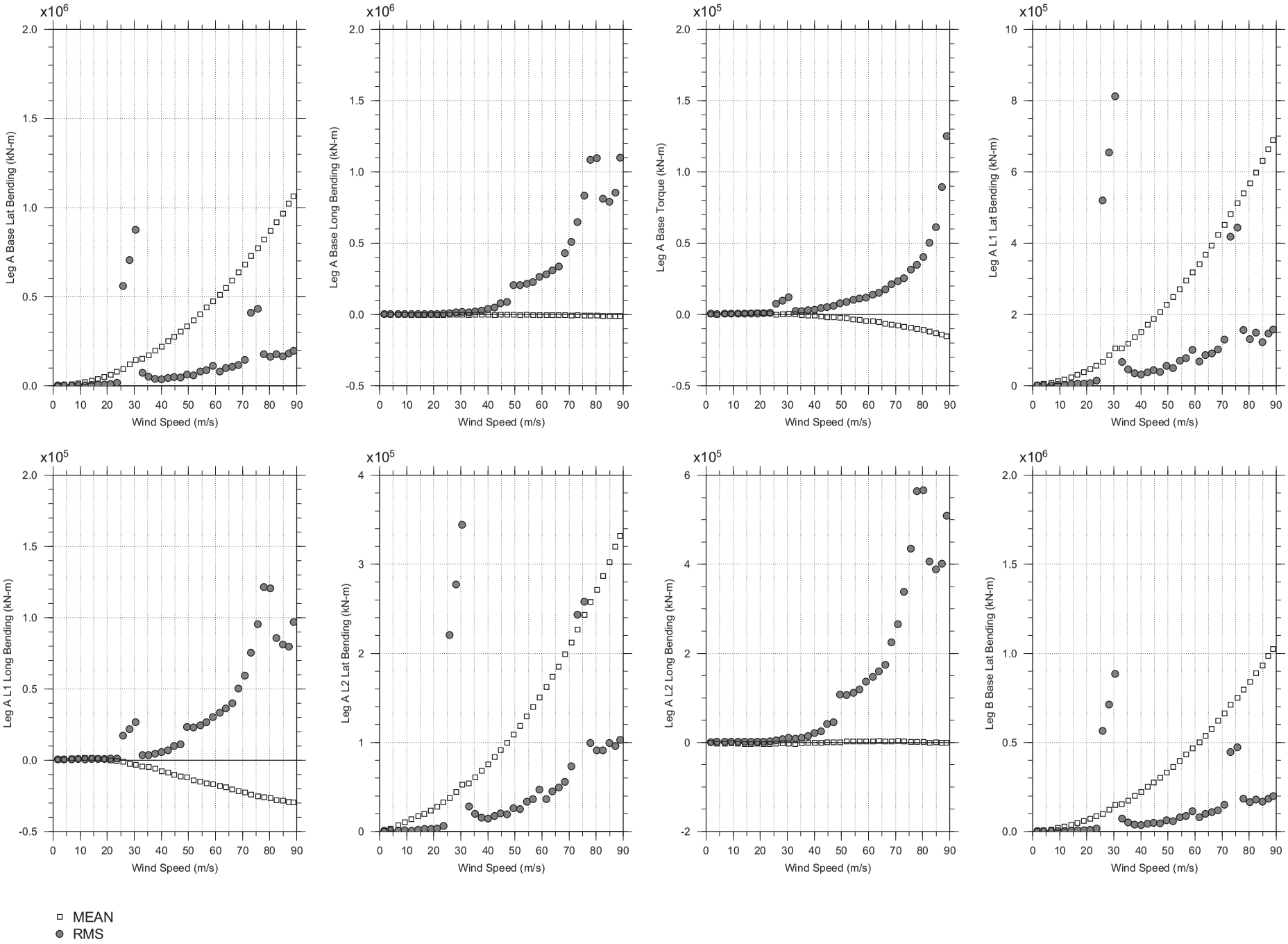

Messina Bridge, In Service Tower, 1% Damping, 2.5 degree, Smooth, Jan2011

Jan. 12, 2011
ti62abdg.cl

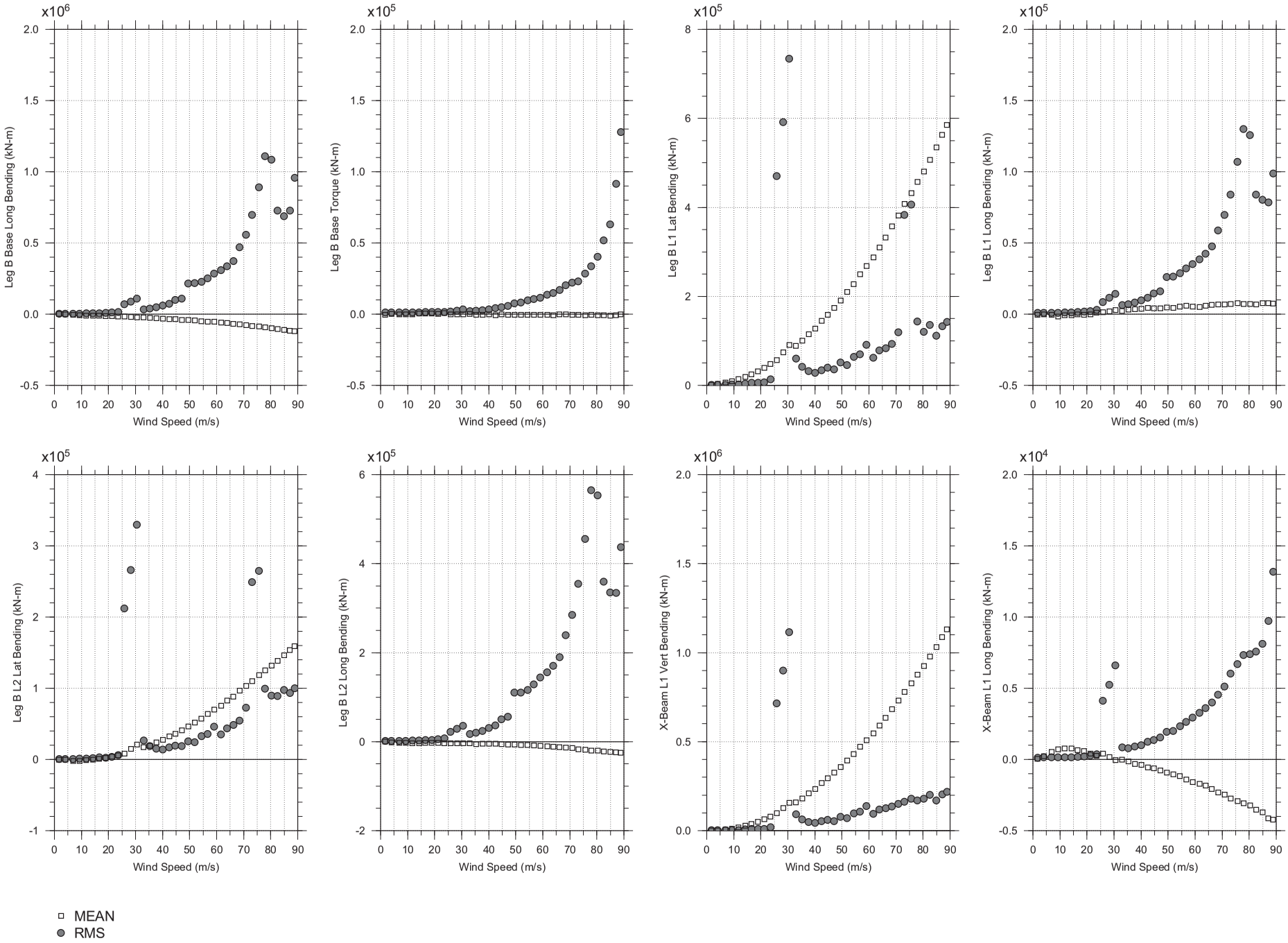

Messina Bridge, In Service Tower, 1% Damping, 2.5 degree, Smooth, Jan2011

Jan. 12, 2011
ti62abdg.cl

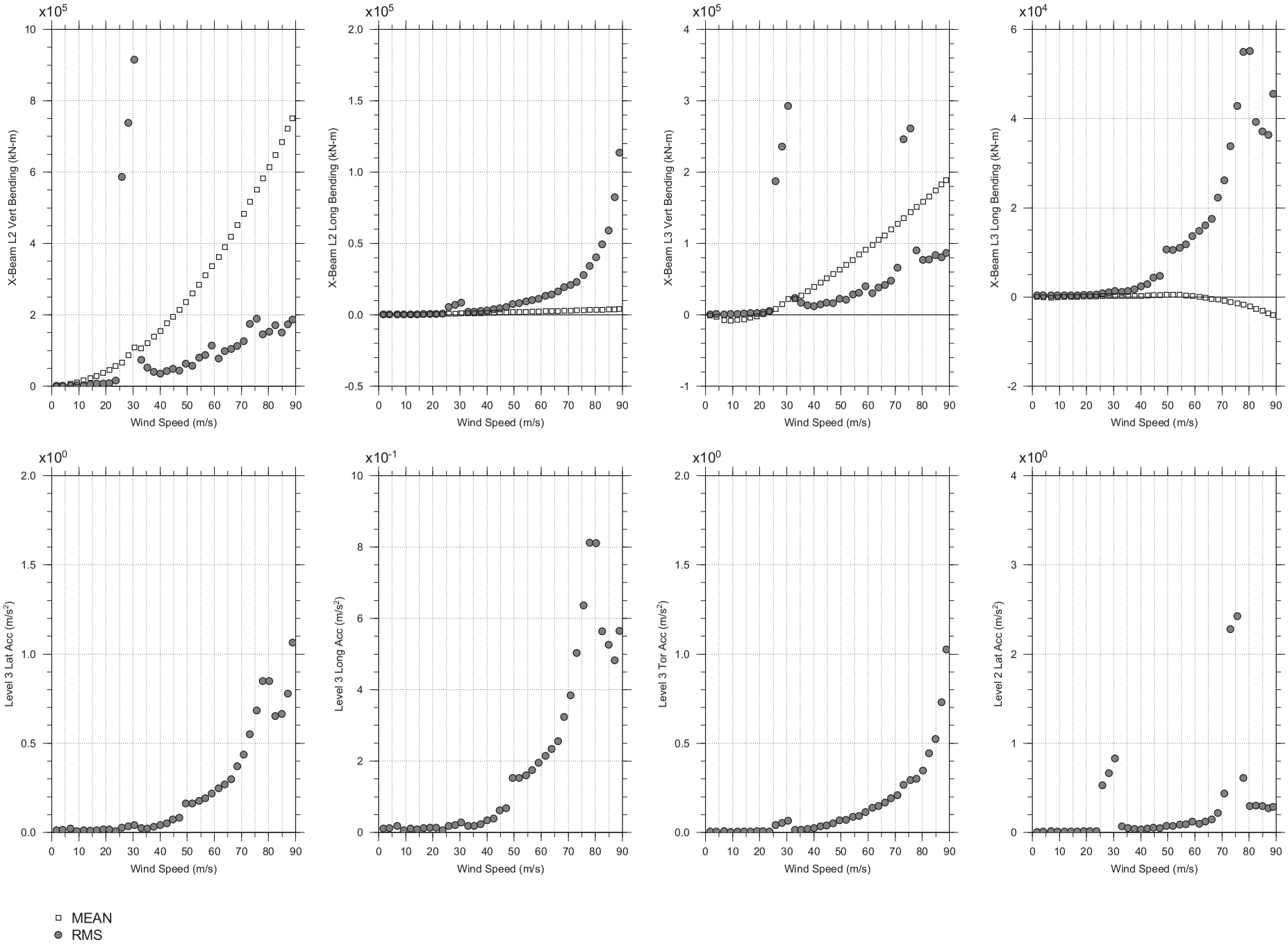

Messina Bridge, In Service Tower, 1% Damping, 2.5 degree, Smooth, Jan2011

Jan. 12, 2011
ti62abdg.cl

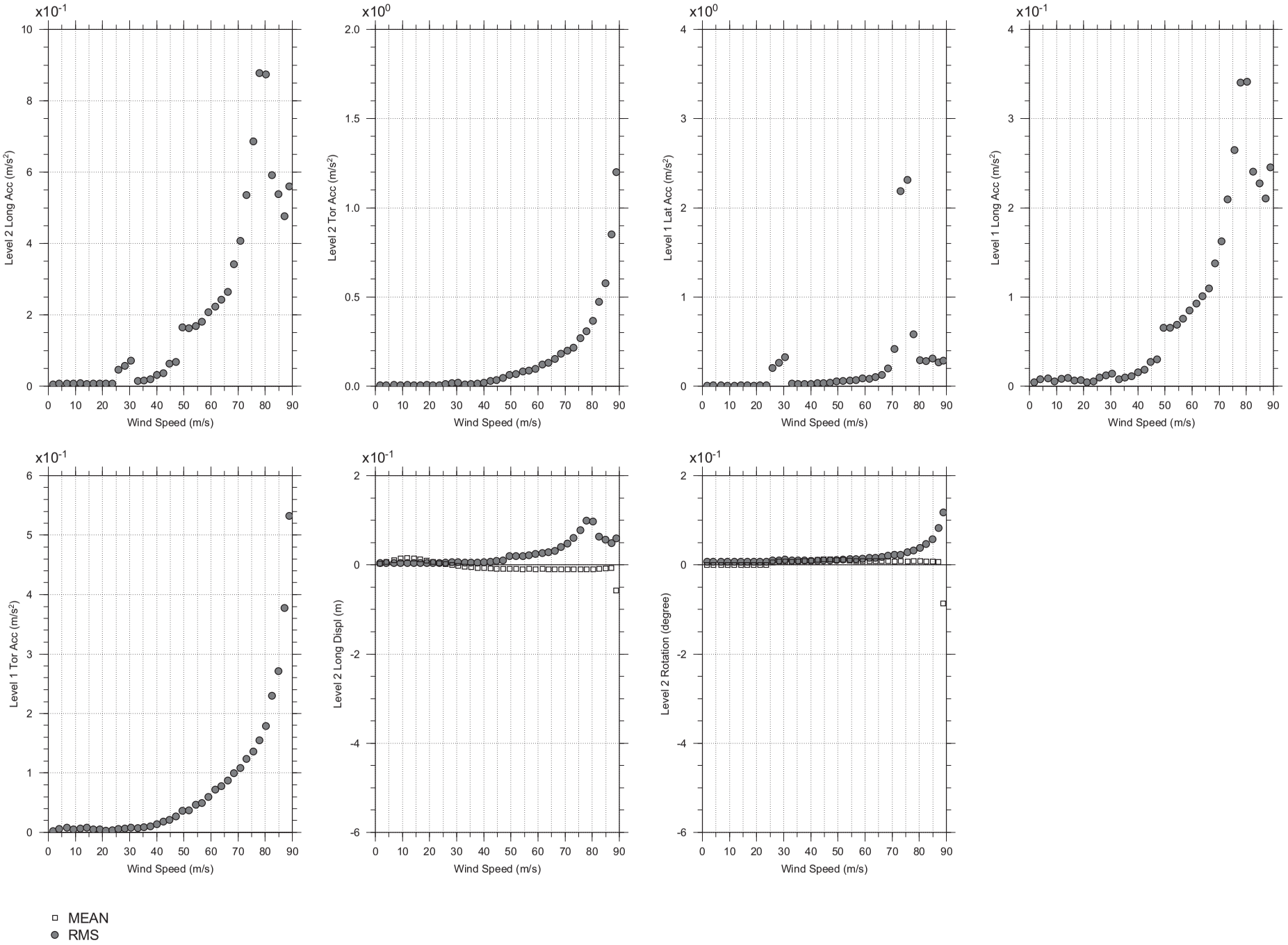

Messina Bridge, In Service Tower, 1% Damping, 2.5 degree, Smooth, Jan2011

Jan. 12, 2011
ti62abdg.cl

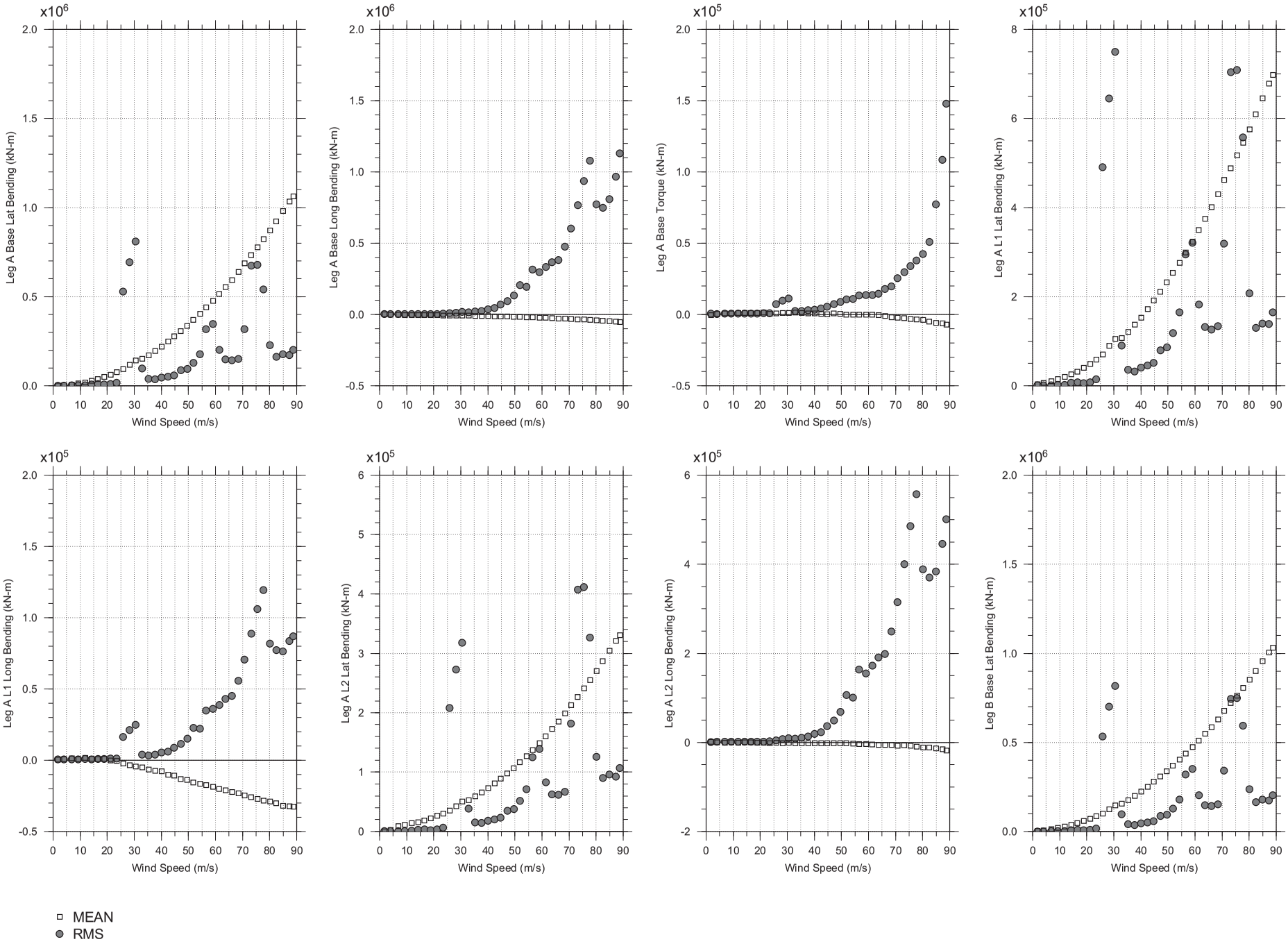

Messina Bridge, In Service Tower, 1% Damping, 5 degree, Smooth, Jan2011

Jan. 12, 2011
ti63abdg.cl

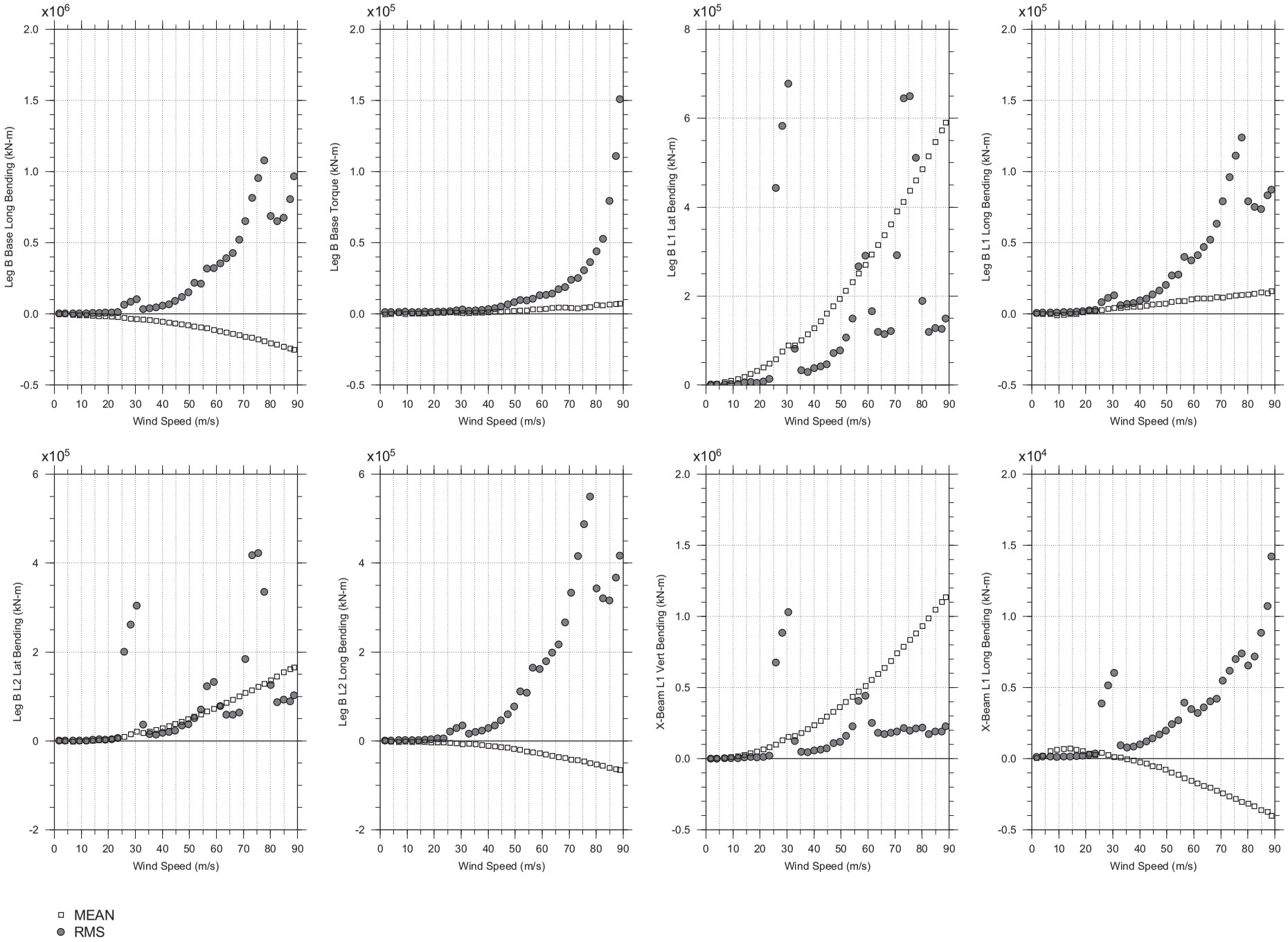

Messina Bridge, In Service Tower, 1% Damping, 5 degree, Smooth, Jan2011

Jan. 12, 2011
ti63abdg.cl

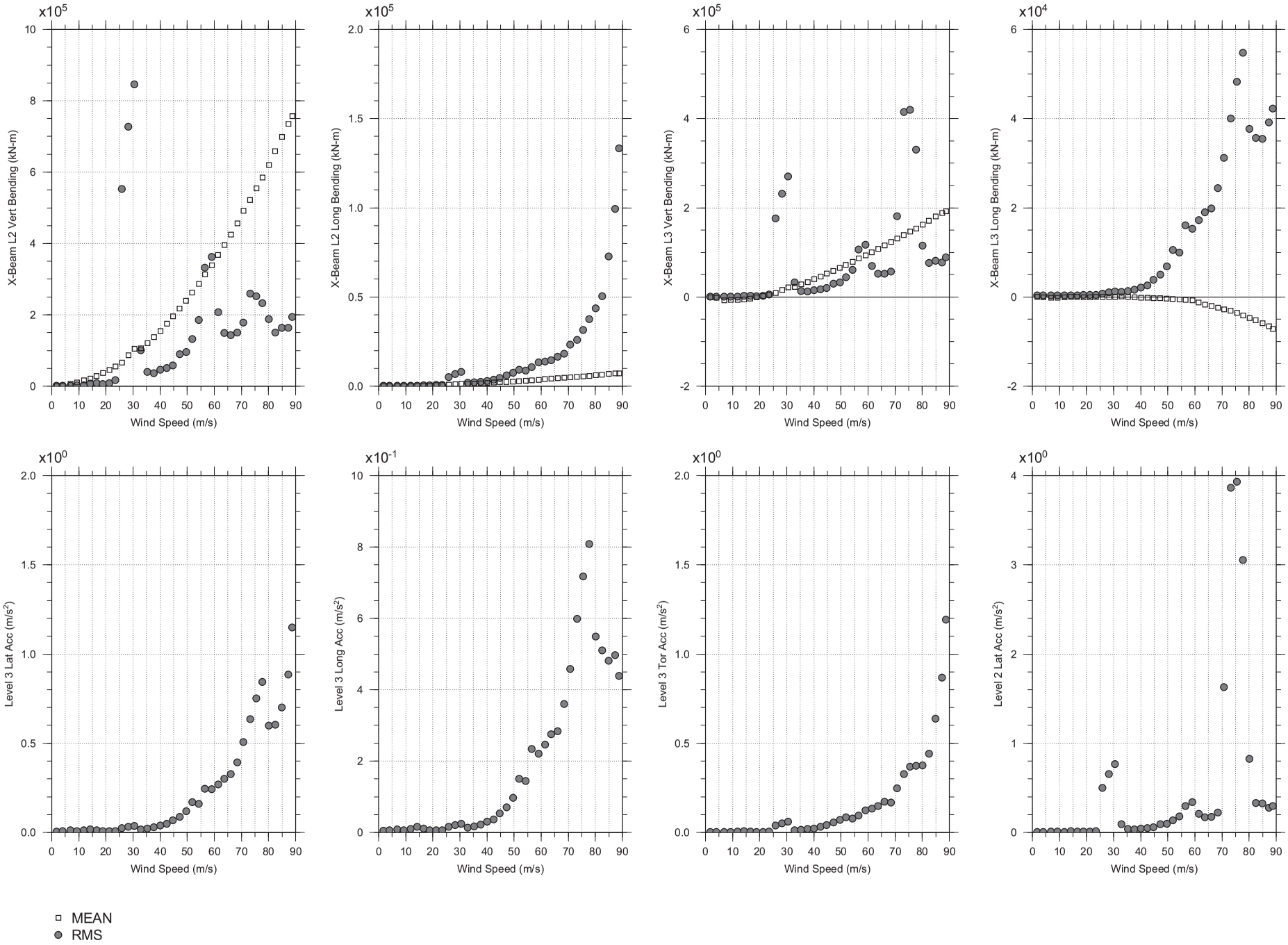

Messina Bridge, In Service Tower, 1% Damping, 5 degree, Smooth, Jan2011

Jan. 12, 2011
ti63abdg.cl

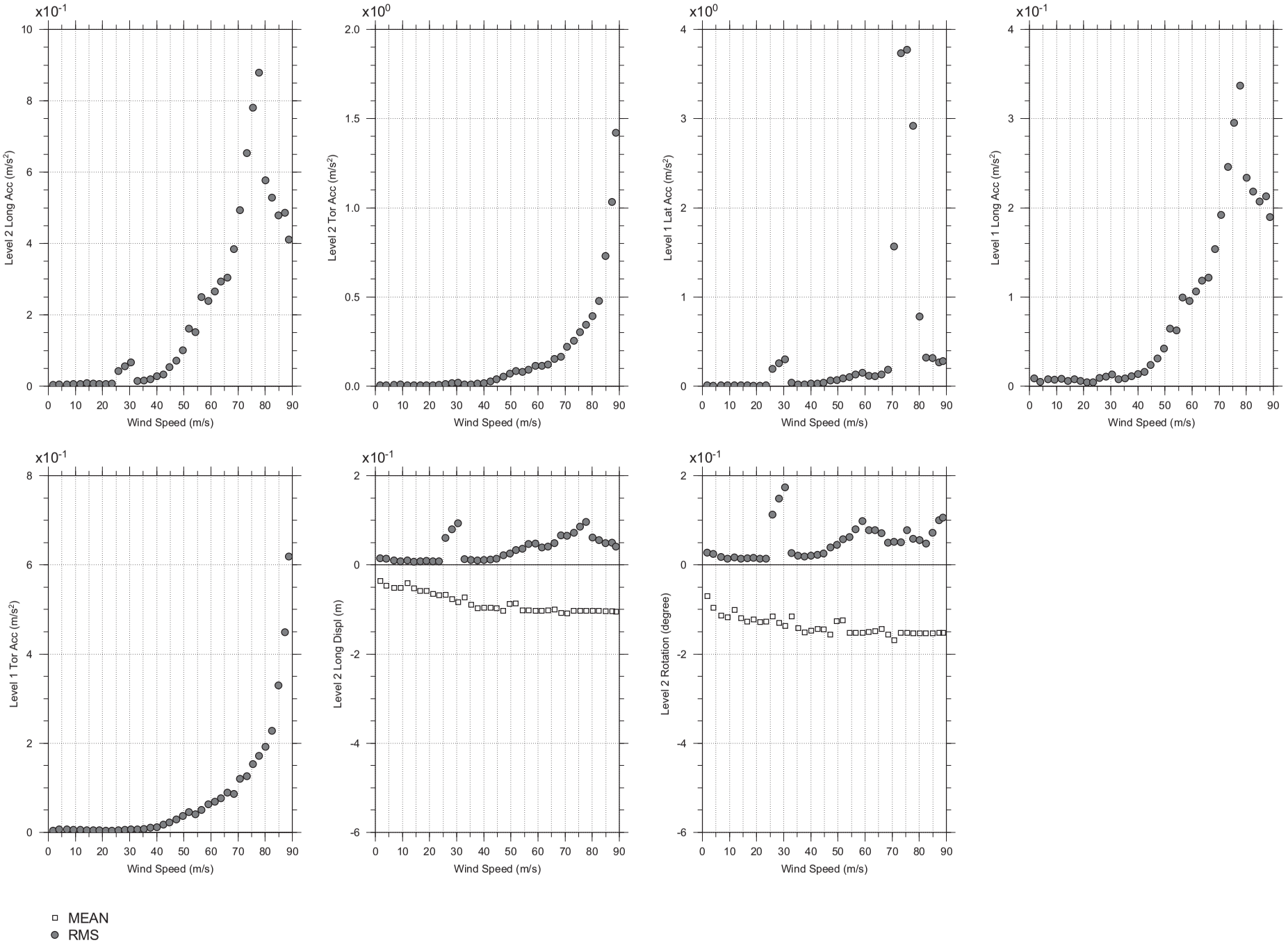

Messina Bridge, In Service Tower, 1% Damping, 5 degree, Smooth, Jan2011

Jan. 12, 2011
ti63abdg.cl

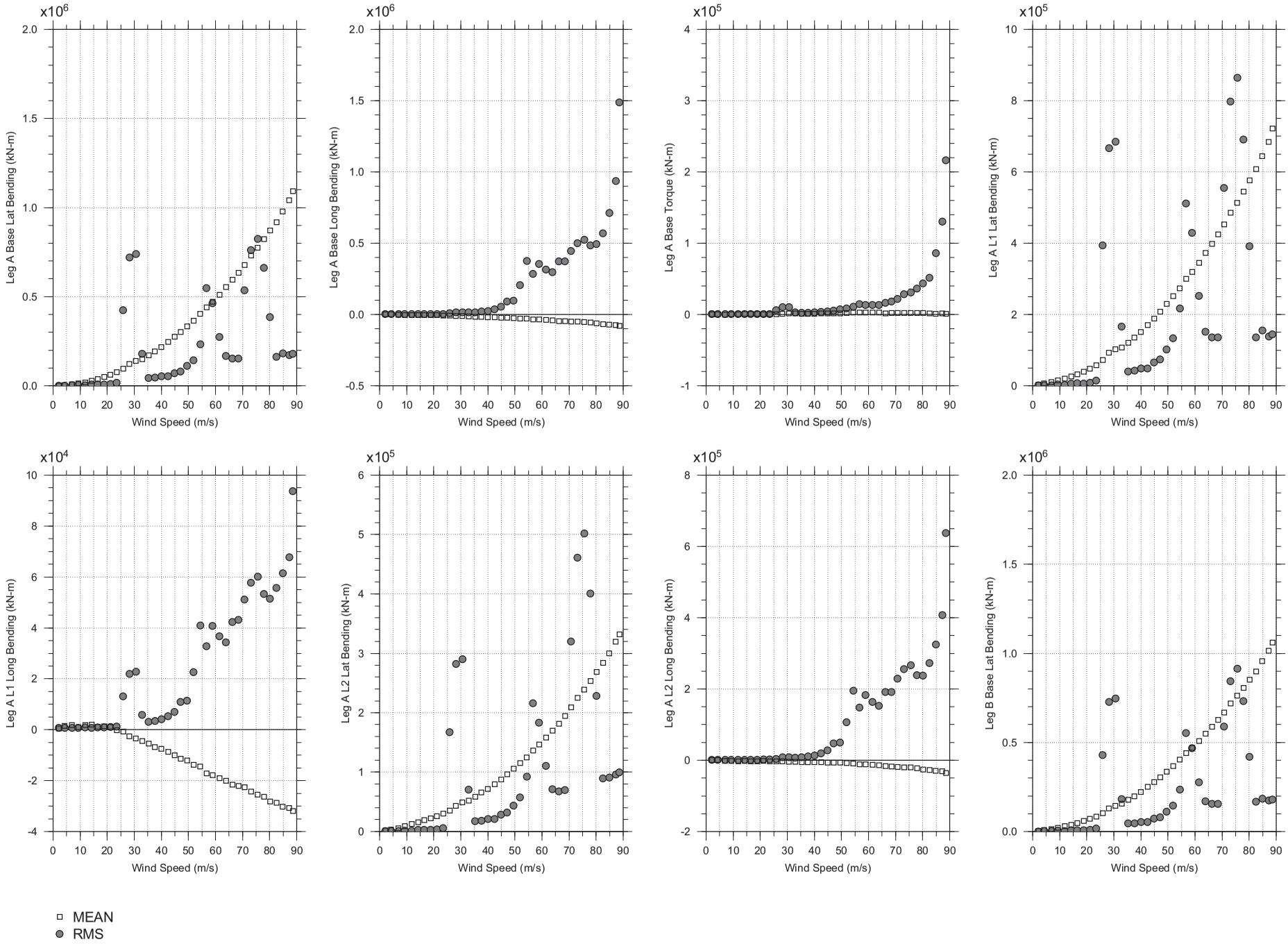

Messina Bridge, In Service Tower, 1% Damping, 7.5 degree, Smooth, Jan2011

Jan. 12, 2011
ti64abdg.cl

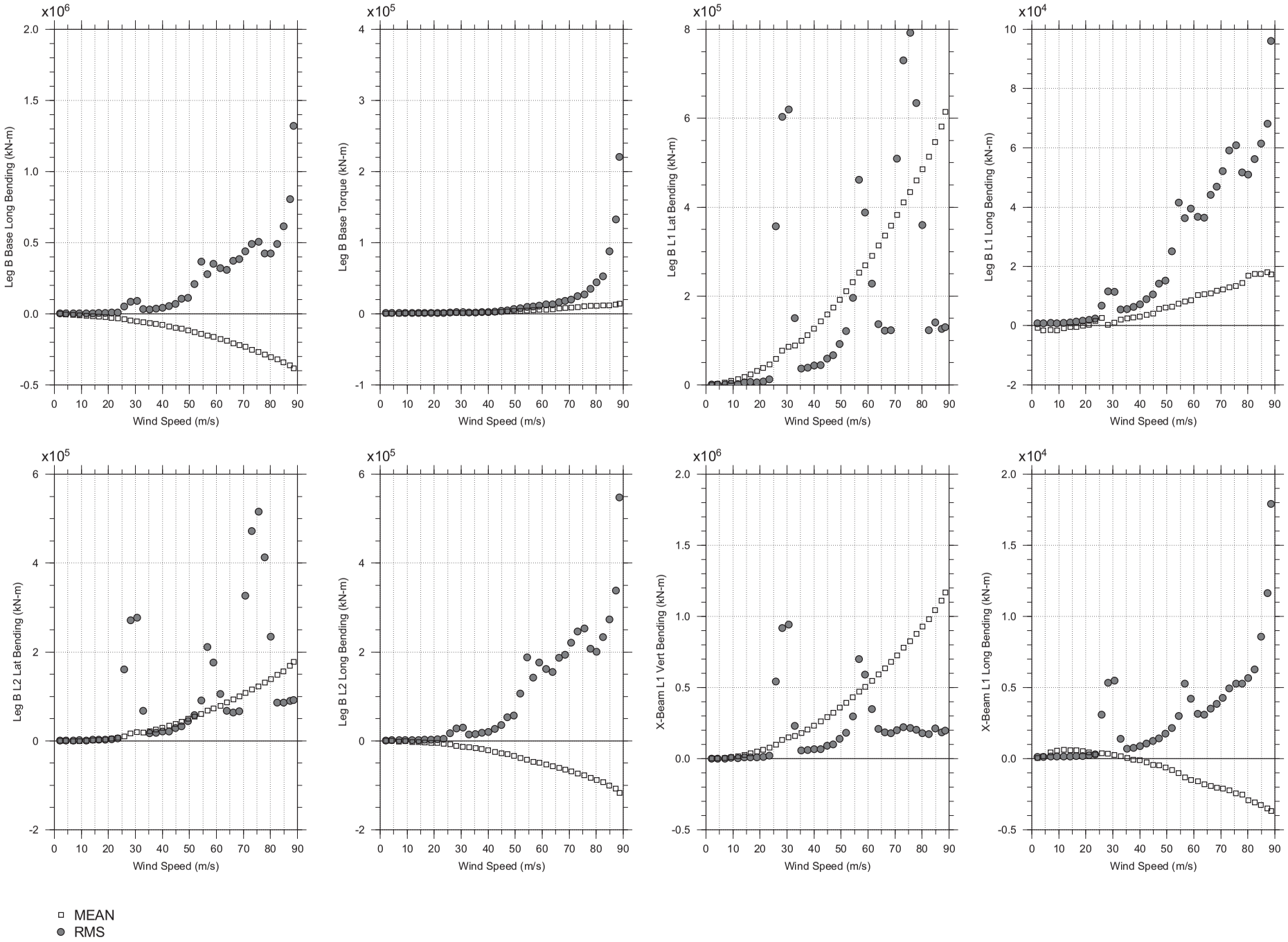

Messina Bridge, In Service Tower, 1% Damping, 7.5 degree, Smooth, Jan2011

Jan. 12, 2011
ti64abdg.cl

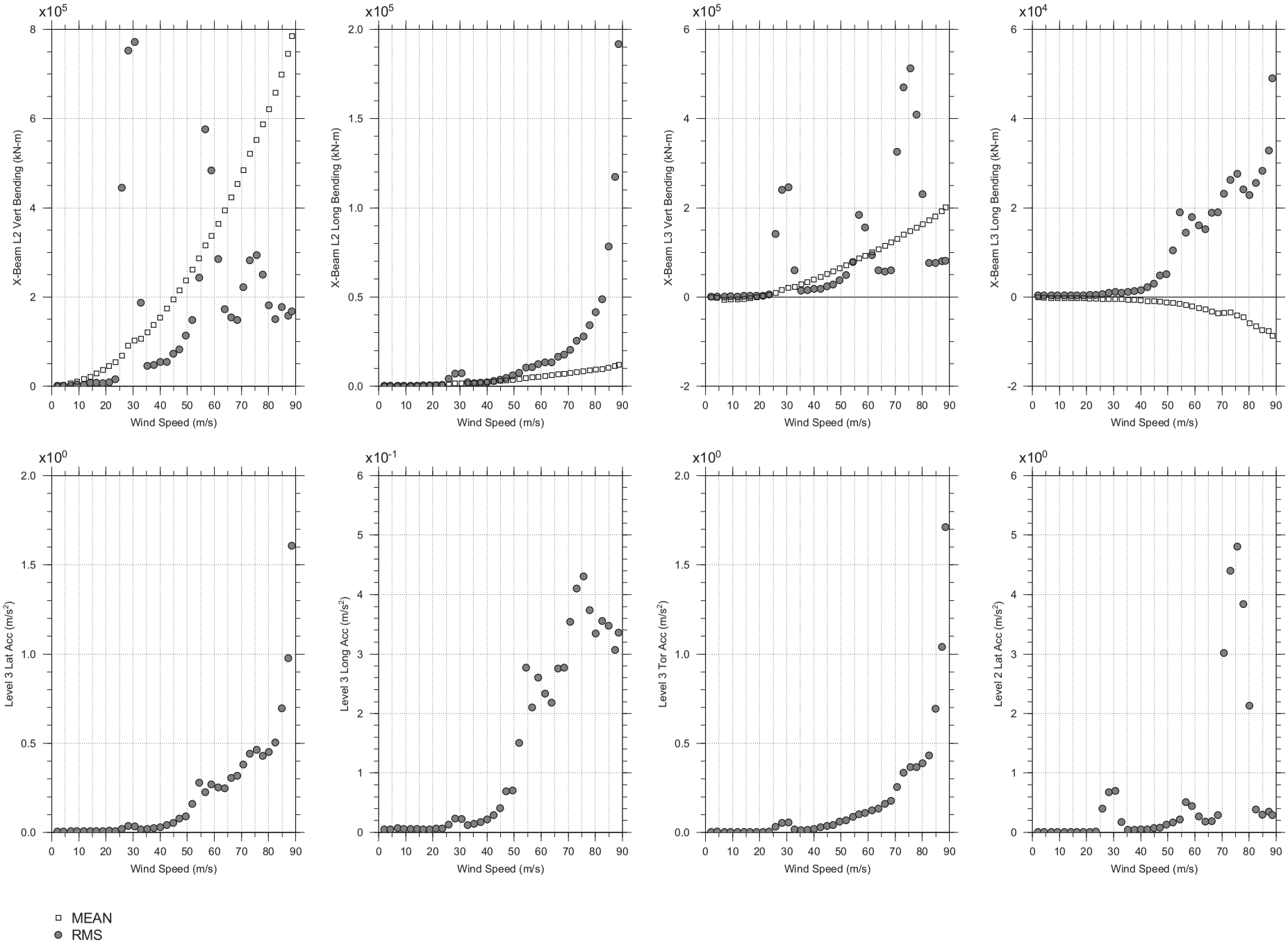

Messina Bridge, In Service Tower, 1% Damping, 7.5 degree, Smooth, Jan2011

Jan. 12, 2011
ti64abdg.cl

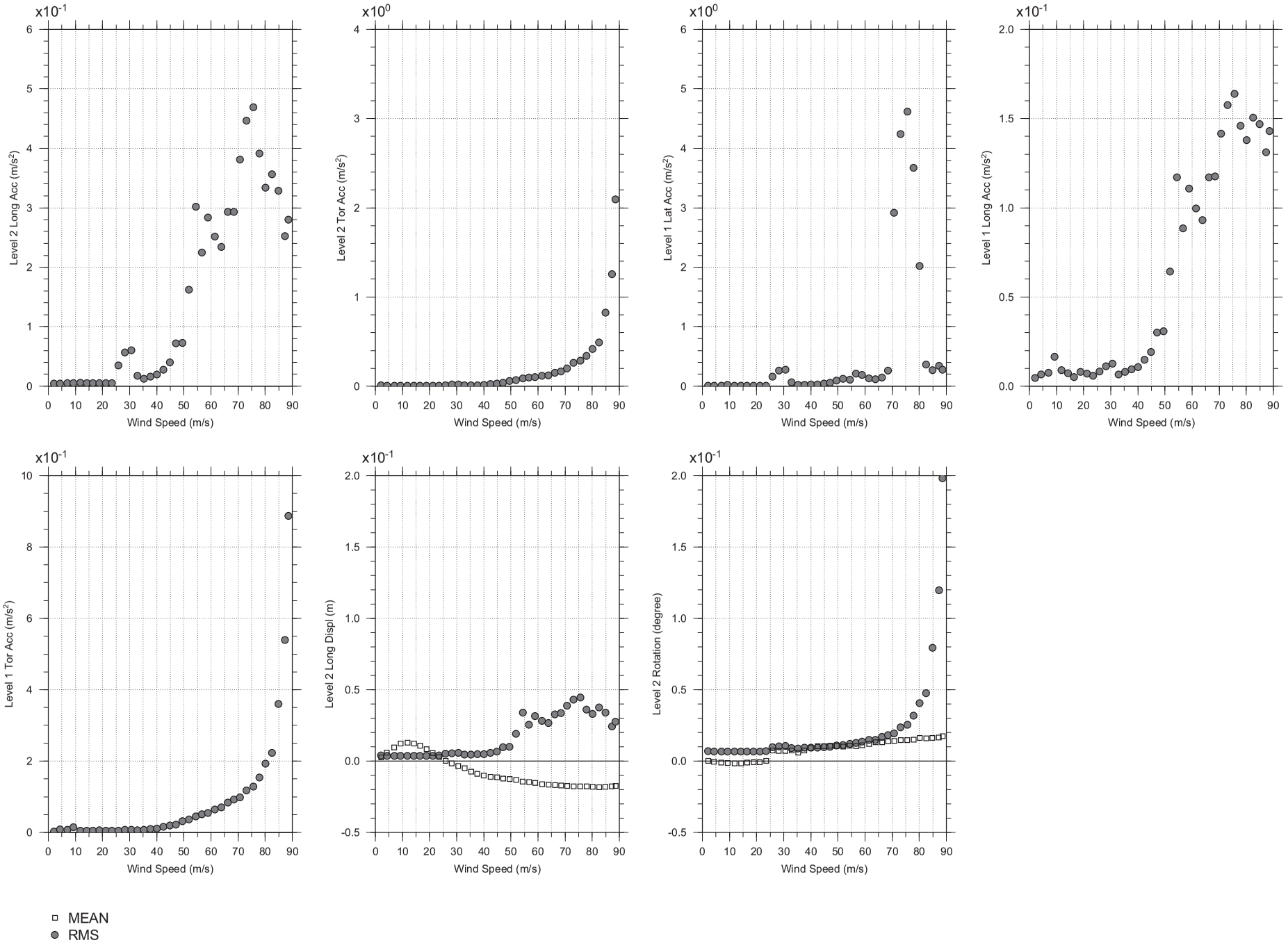

Messina Bridge, In Service Tower, 1% Damping, 7.5 degree, Smooth, Jan2011

Jan. 12, 2011
ti64abdg.cl

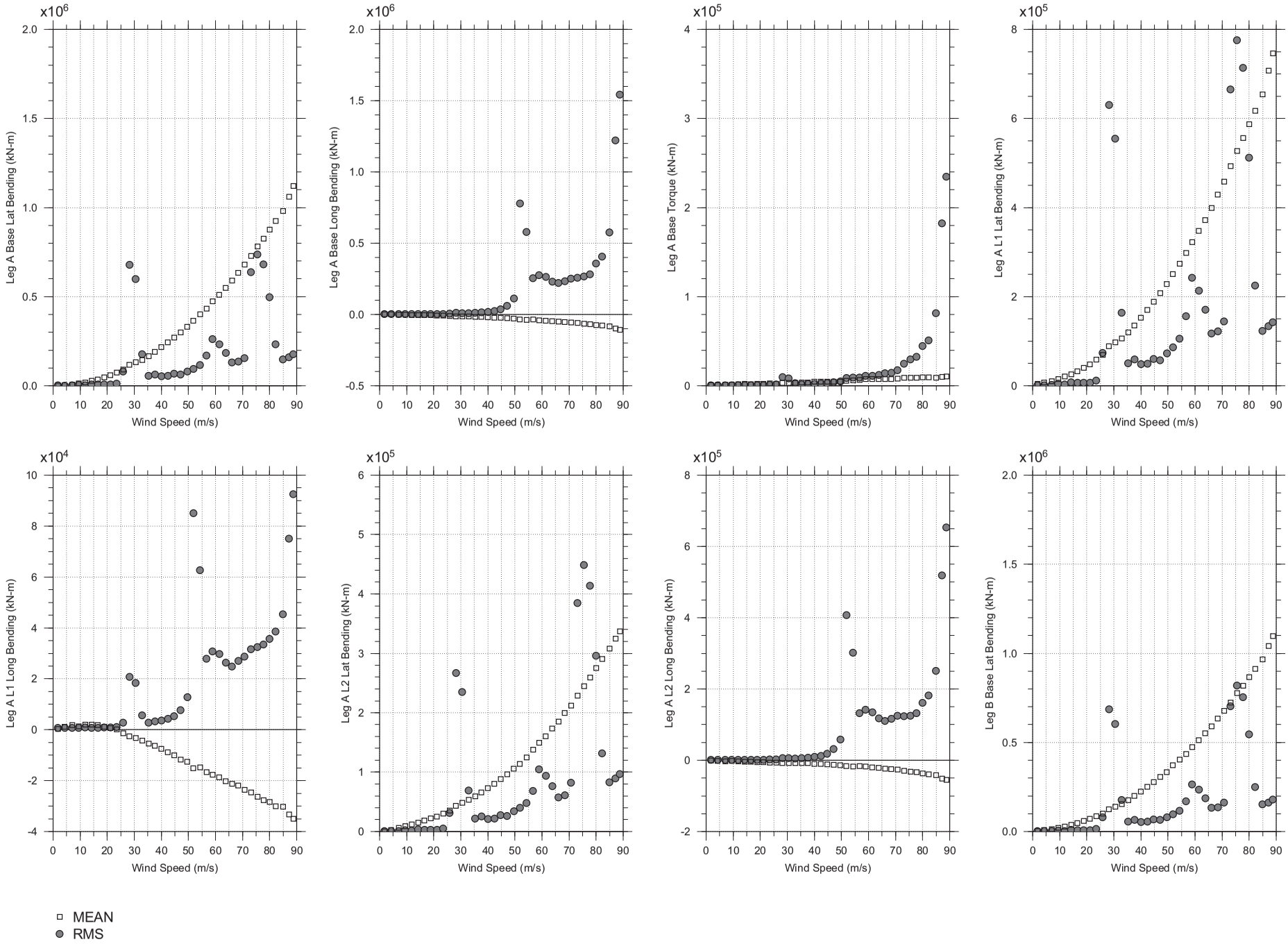

Messina Bridge, In Service Tower, 1% Damping, 10 degree, Smooth, Jan2011

Jan. 12, 2011
ti65abdg.cl

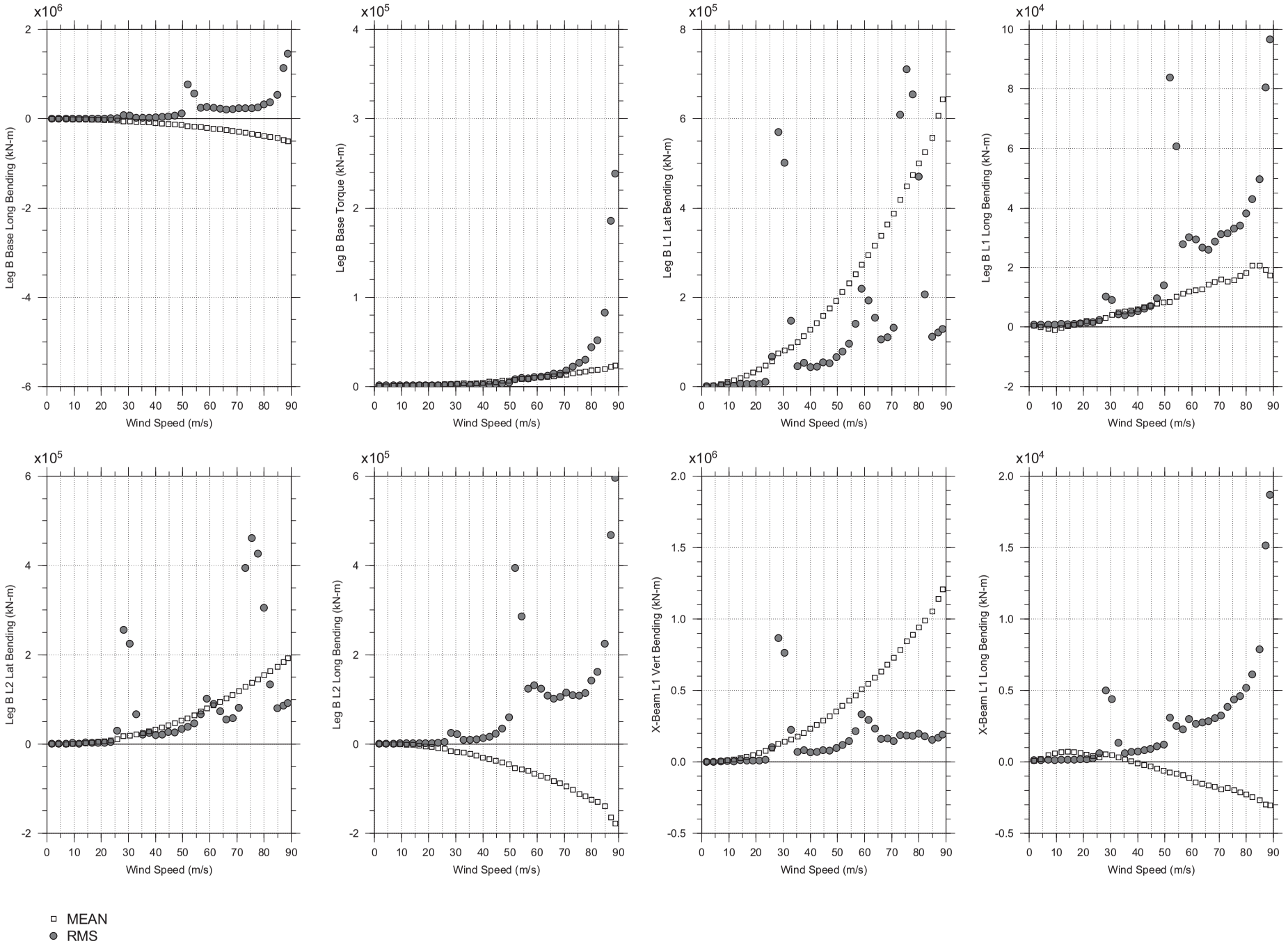

Messina Bridge, In Service Tower, 1% Damping, 10 degree, Smooth, Jan2011

Jan. 12, 2011
ti65abdg.cl

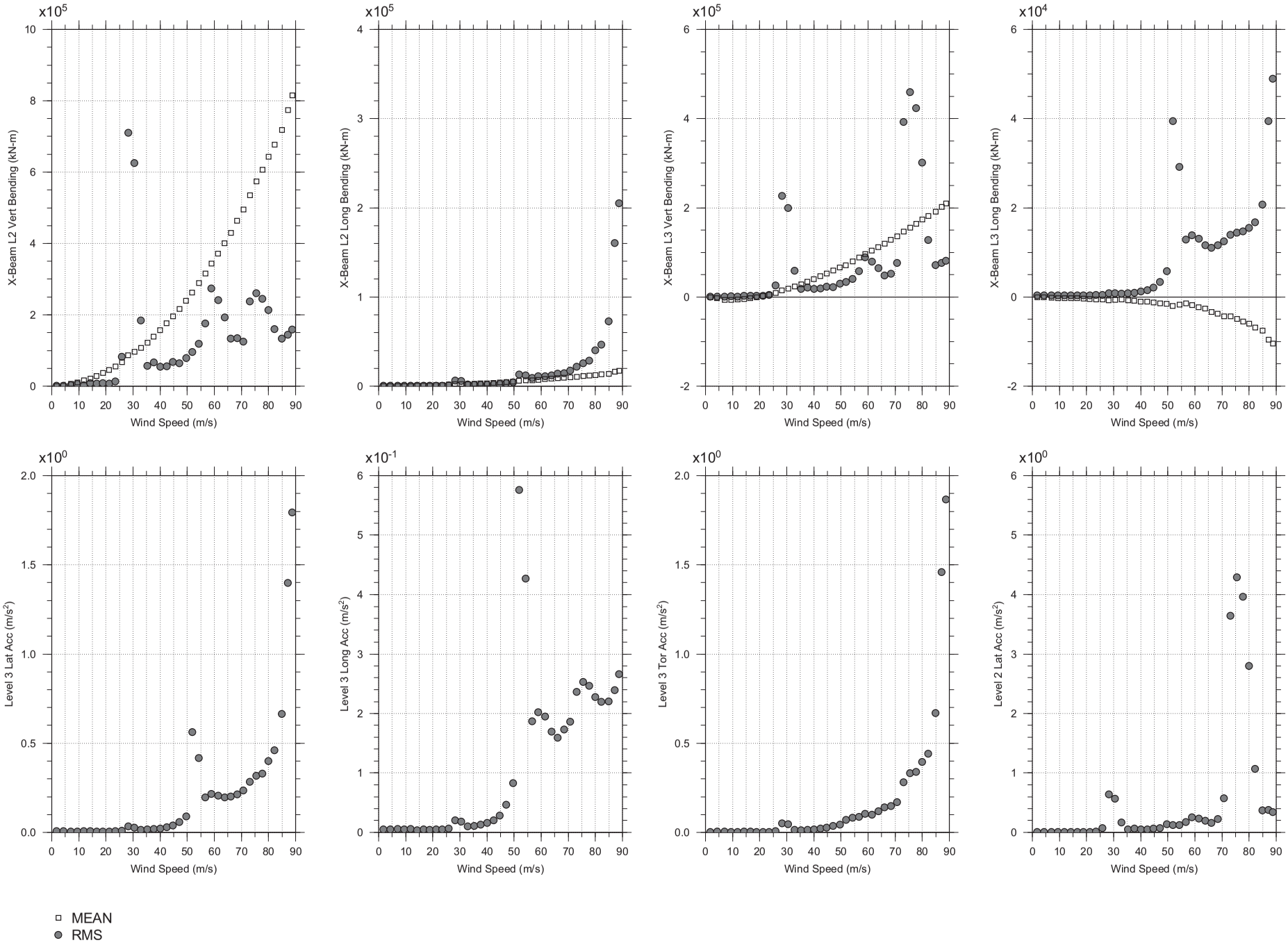

Messina Bridge, In Service Tower, 1% Damping, 10 degree, Smooth, Jan2011

Jan. 12, 2011
ti65abdg.cl

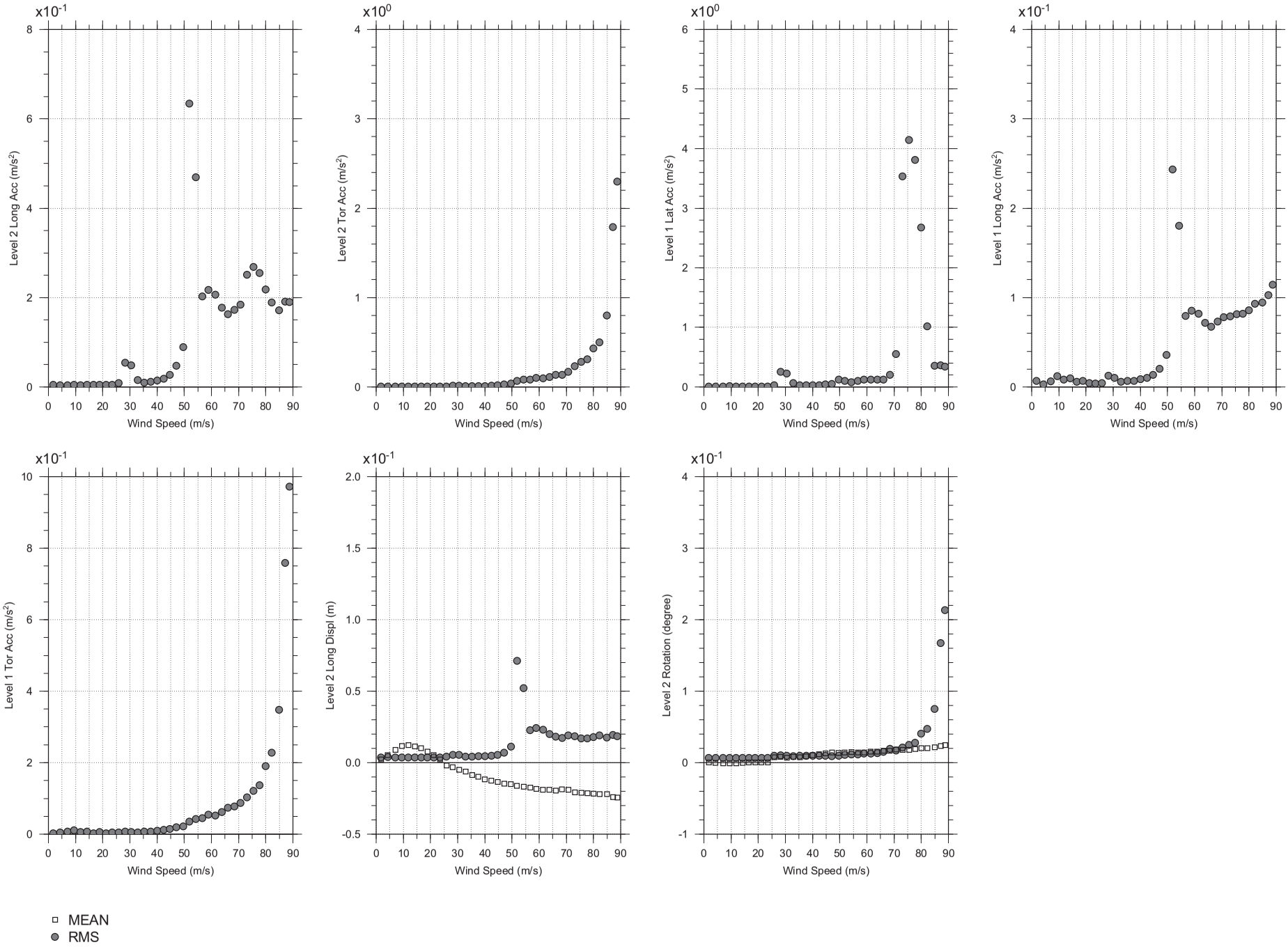

Messina Bridge, In Service Tower, 1% Damping, 10 degree, Smooth, Jan2011

Jan. 12, 2011
ti65abdg.cl

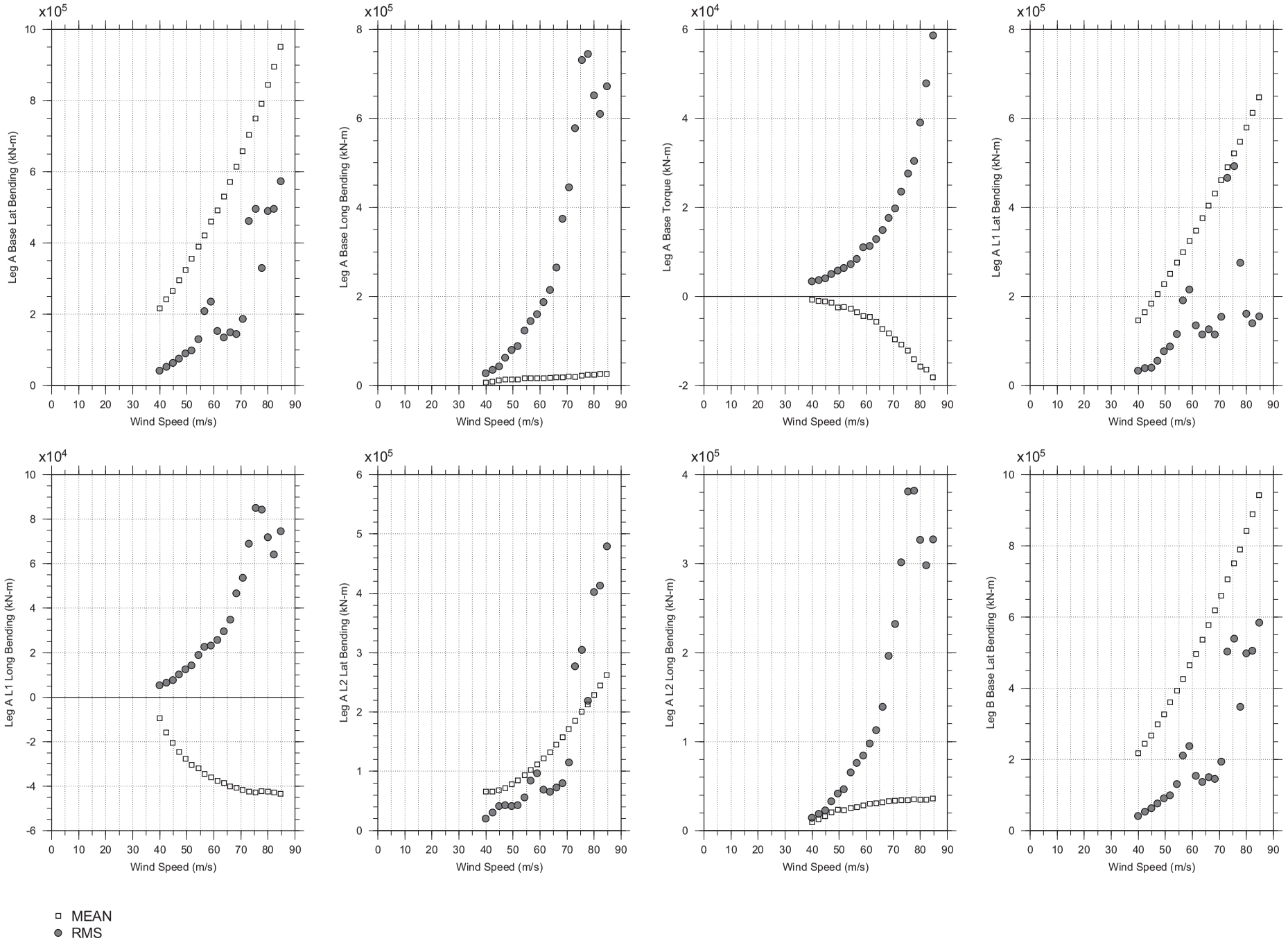

Messina Bridge, In Service Tower, 2% Damping, 0 degree, Smooth, Jan2011

Jan. 12, 2011
ti71abdg.cl

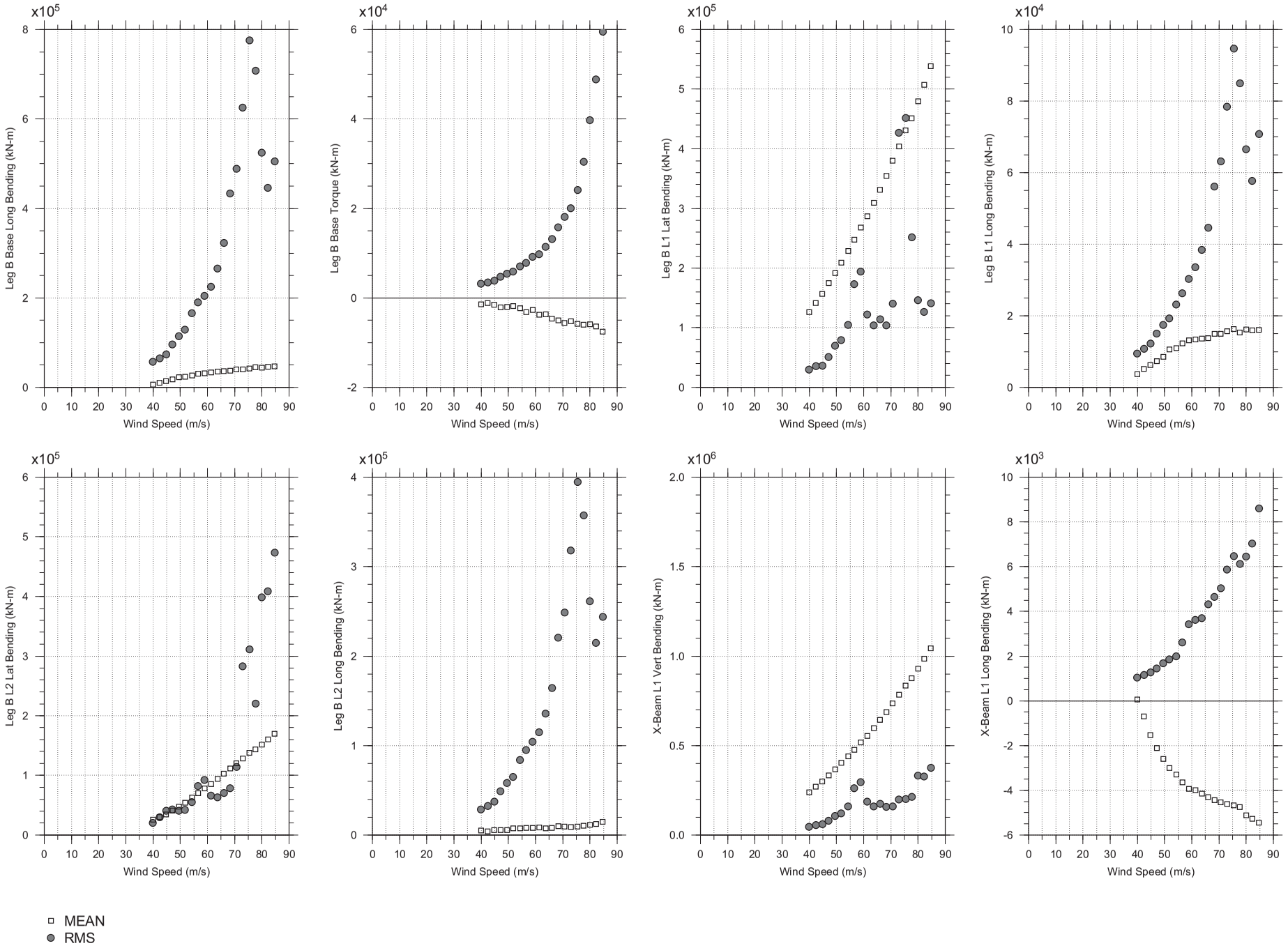

Messina Bridge, In Service Tower, 2% Damping, 0 degree, Smooth, Jan2011

Jan. 12, 2011
ti71abdg.cl

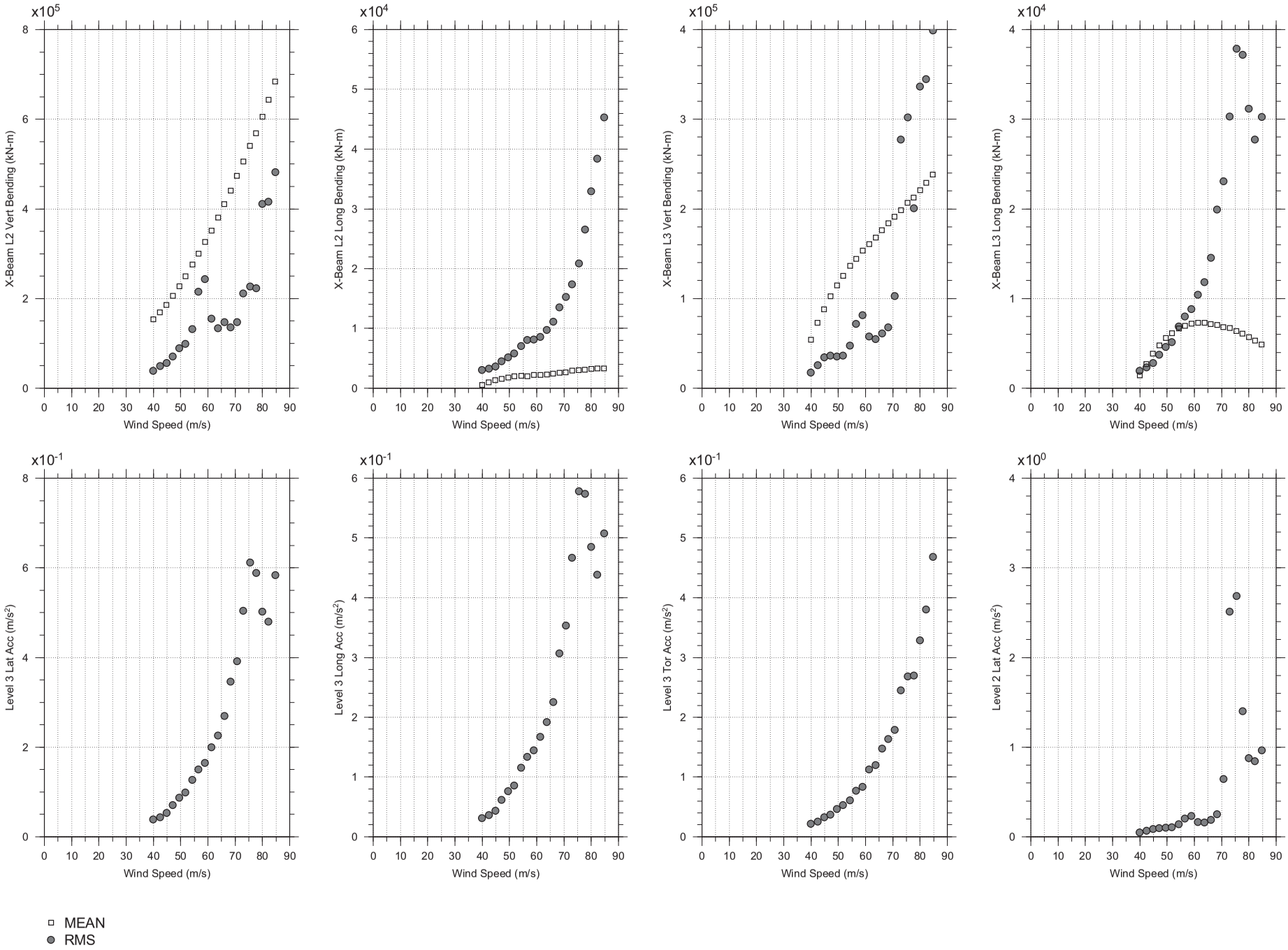

Messina Bridge, In Service Tower, 2% Damping, 0 degree, Smooth, Jan2011

Jan. 12, 2011
ti71abdg.cl

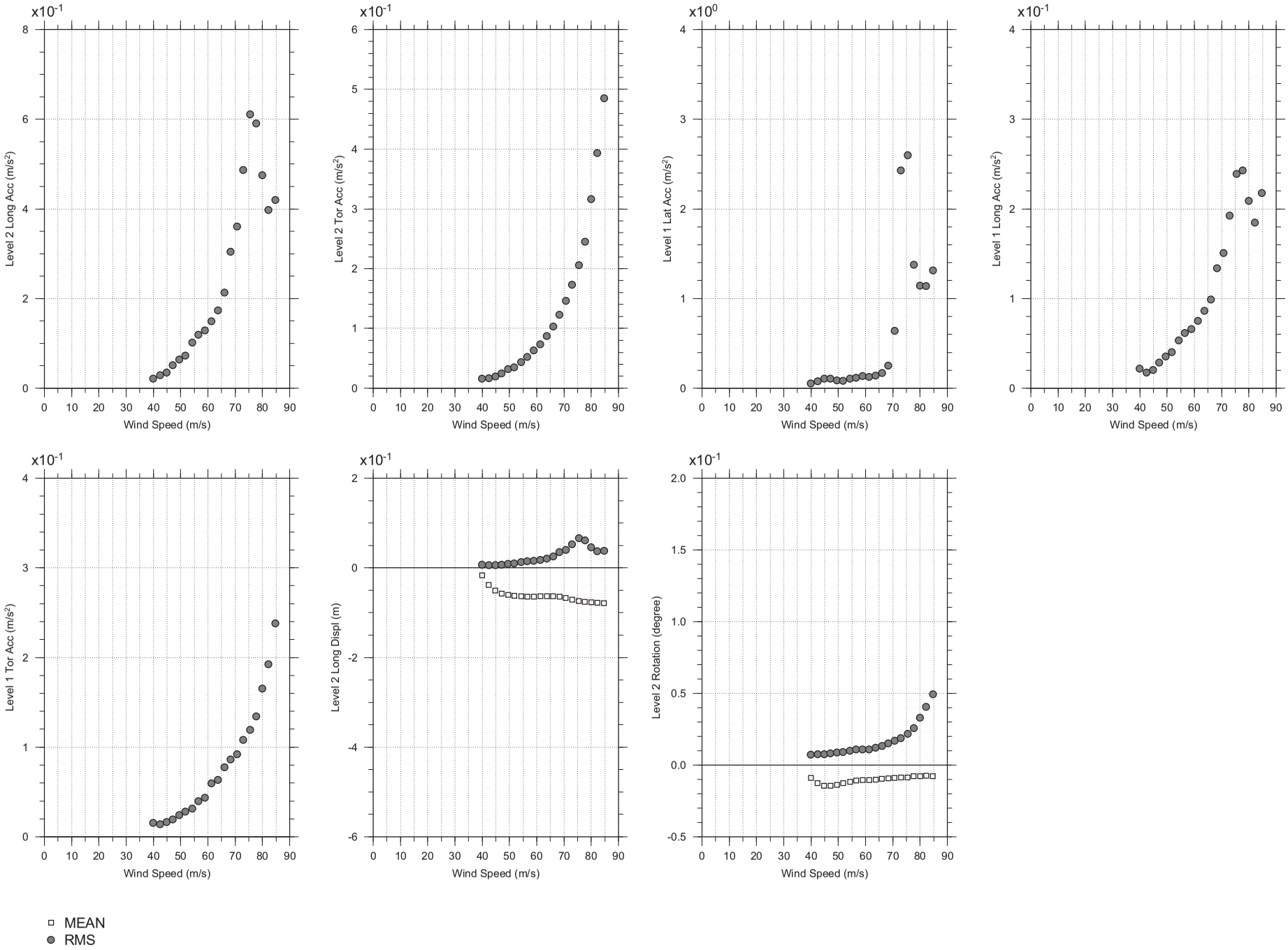

Messina Bridge, In Service Tower, 2% Damping, 0 degree, Smooth, Jan2011

Jan. 12, 2011
ti71abdg.cl

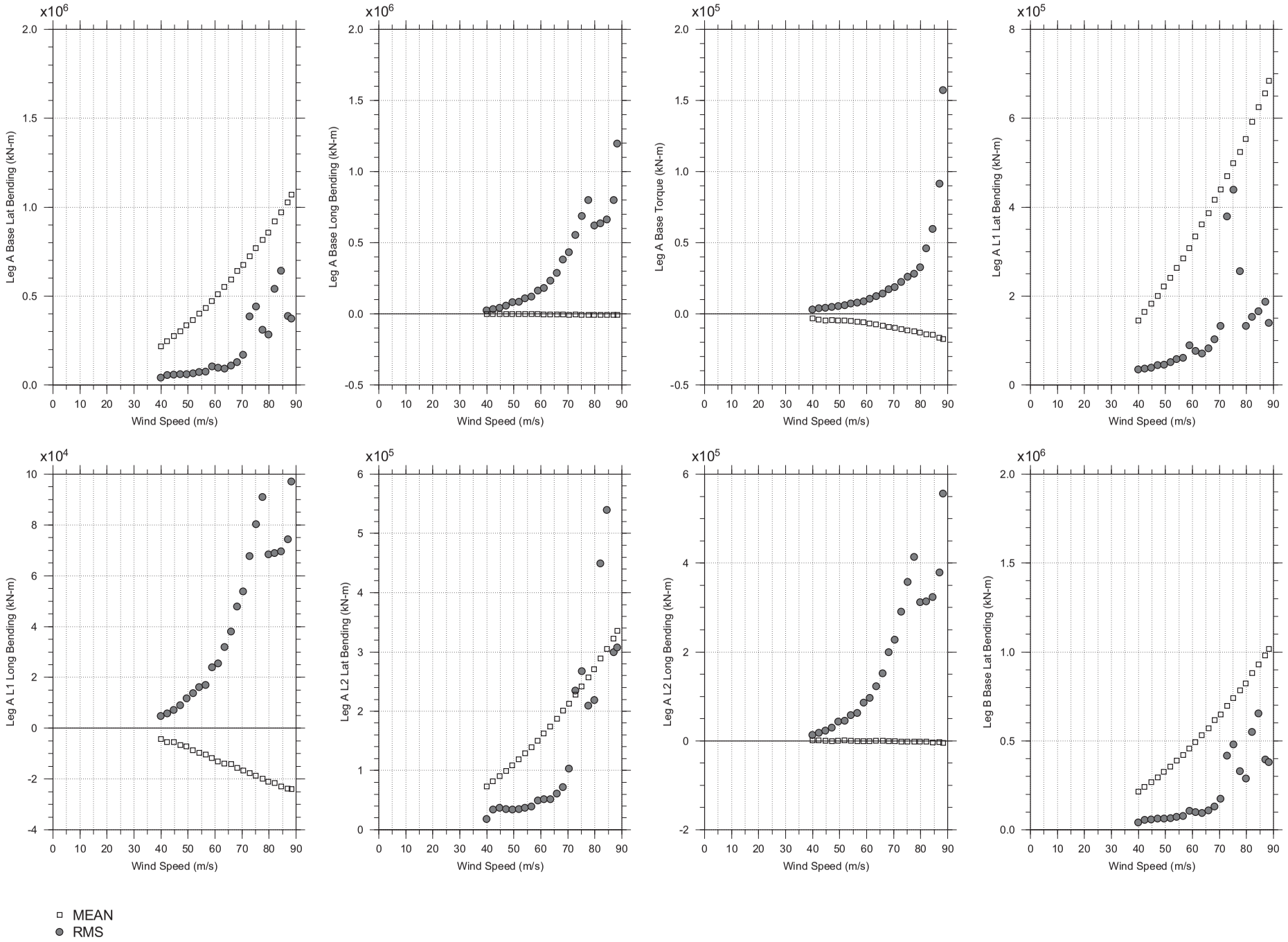

Messina Bridge, In Service Tower, 2% Damping, 2.5 degree, Smooth, Jan2011

Jan. 12, 2011
ti72abdg.cl

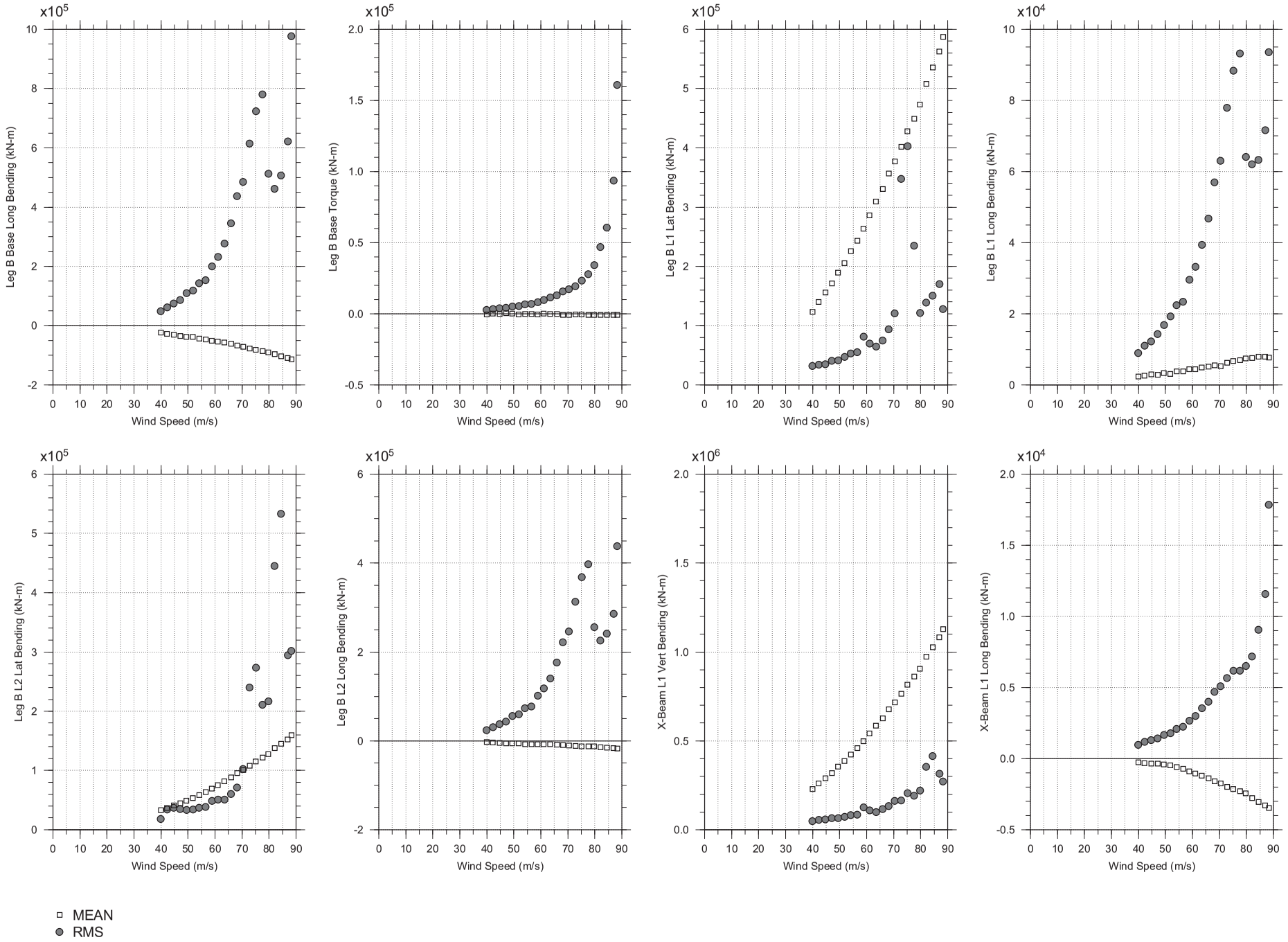

Messina Bridge, In Service Tower, 2% Damping, 2.5 degree, Smooth, Jan2011

Jan. 12, 2011
ti72abdg.cl

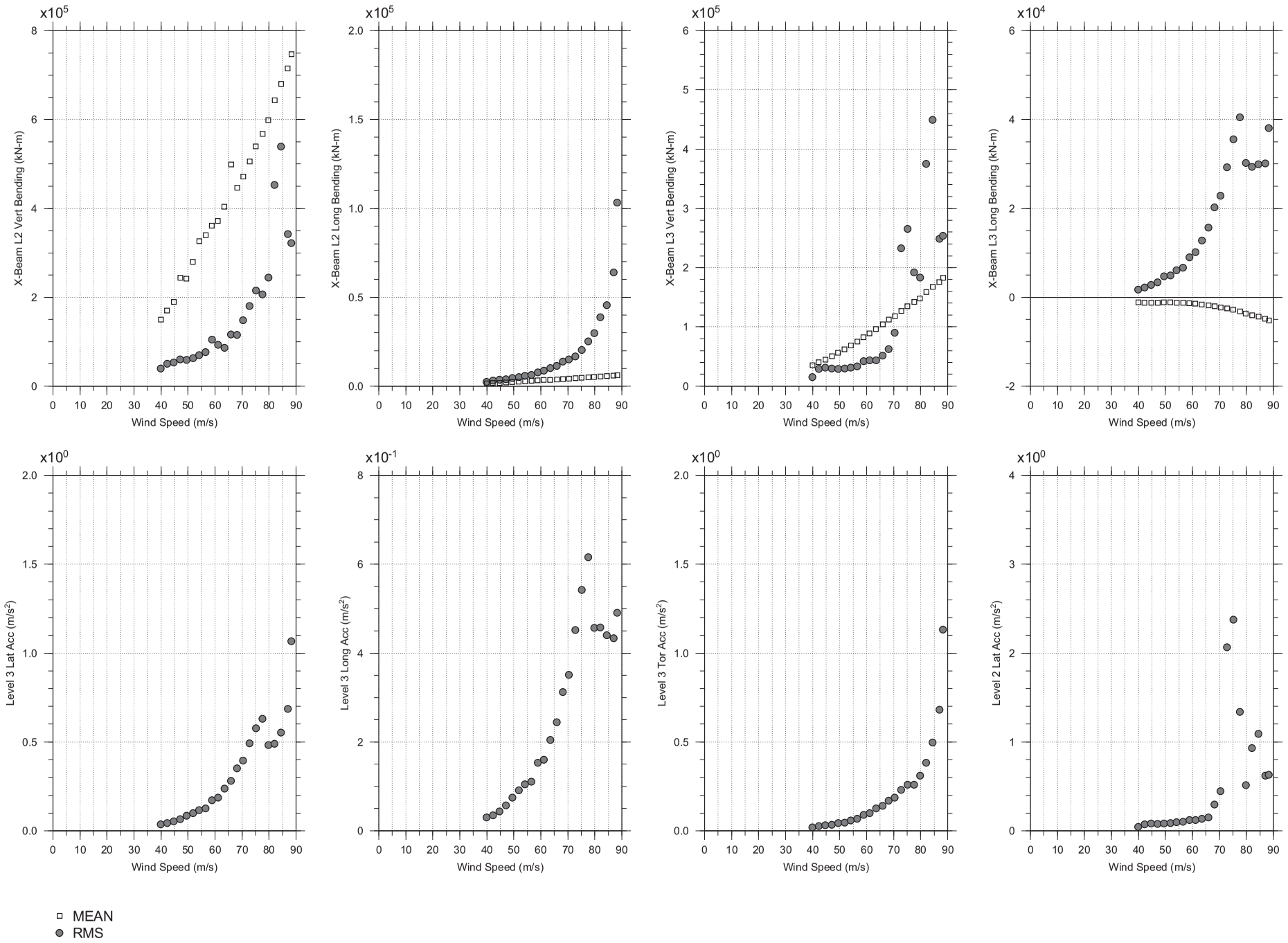

Messina Bridge, In Service Tower, 2% Damping, 2.5 degree, Smooth, Jan2011

Jan. 12, 2011
ti72abdg.cl

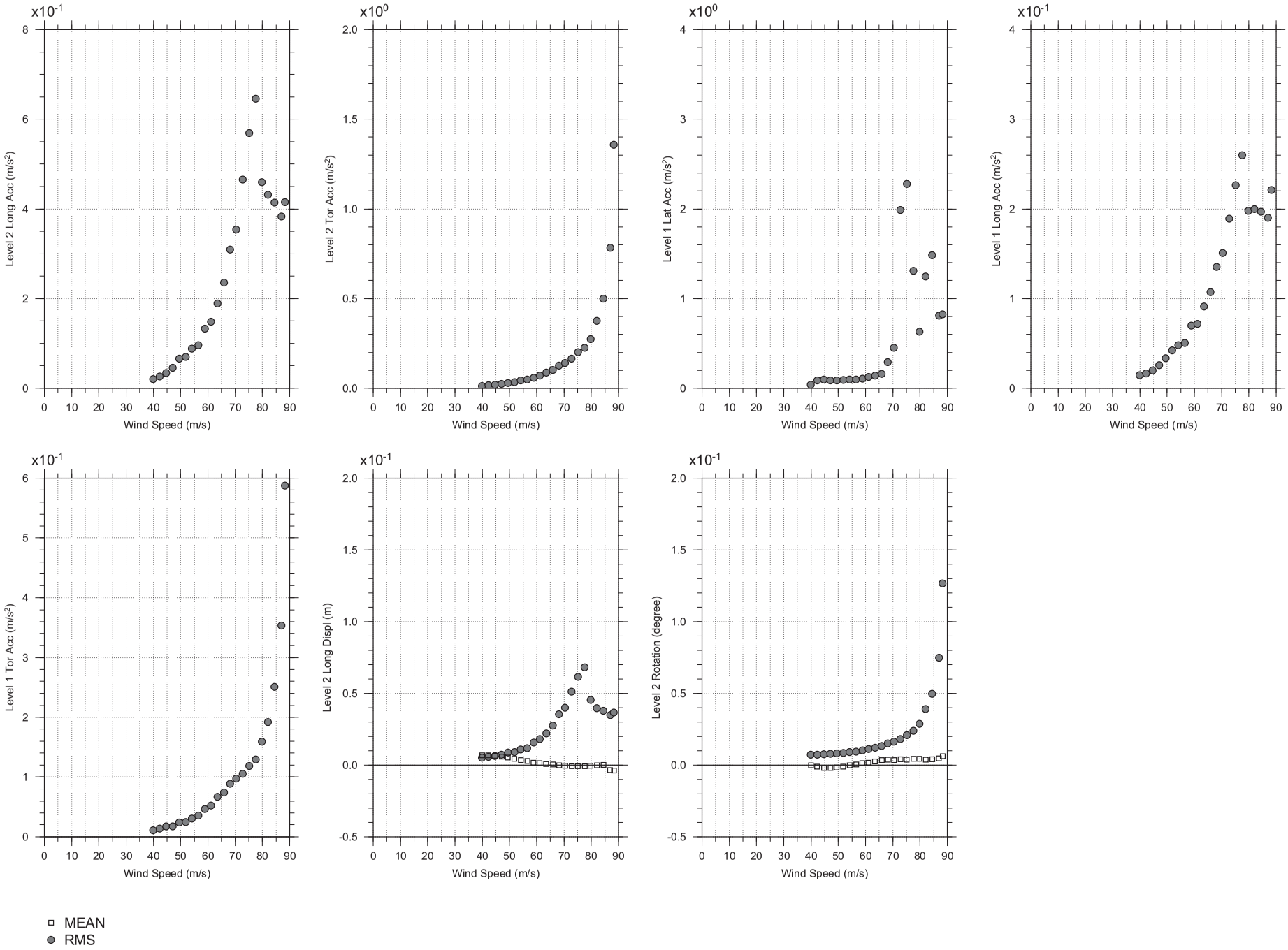

Messina Bridge, In Service Tower, 2% Damping, 2.5 degree, Smooth, Jan2011

Jan. 12, 2011
ti72abdg.cl

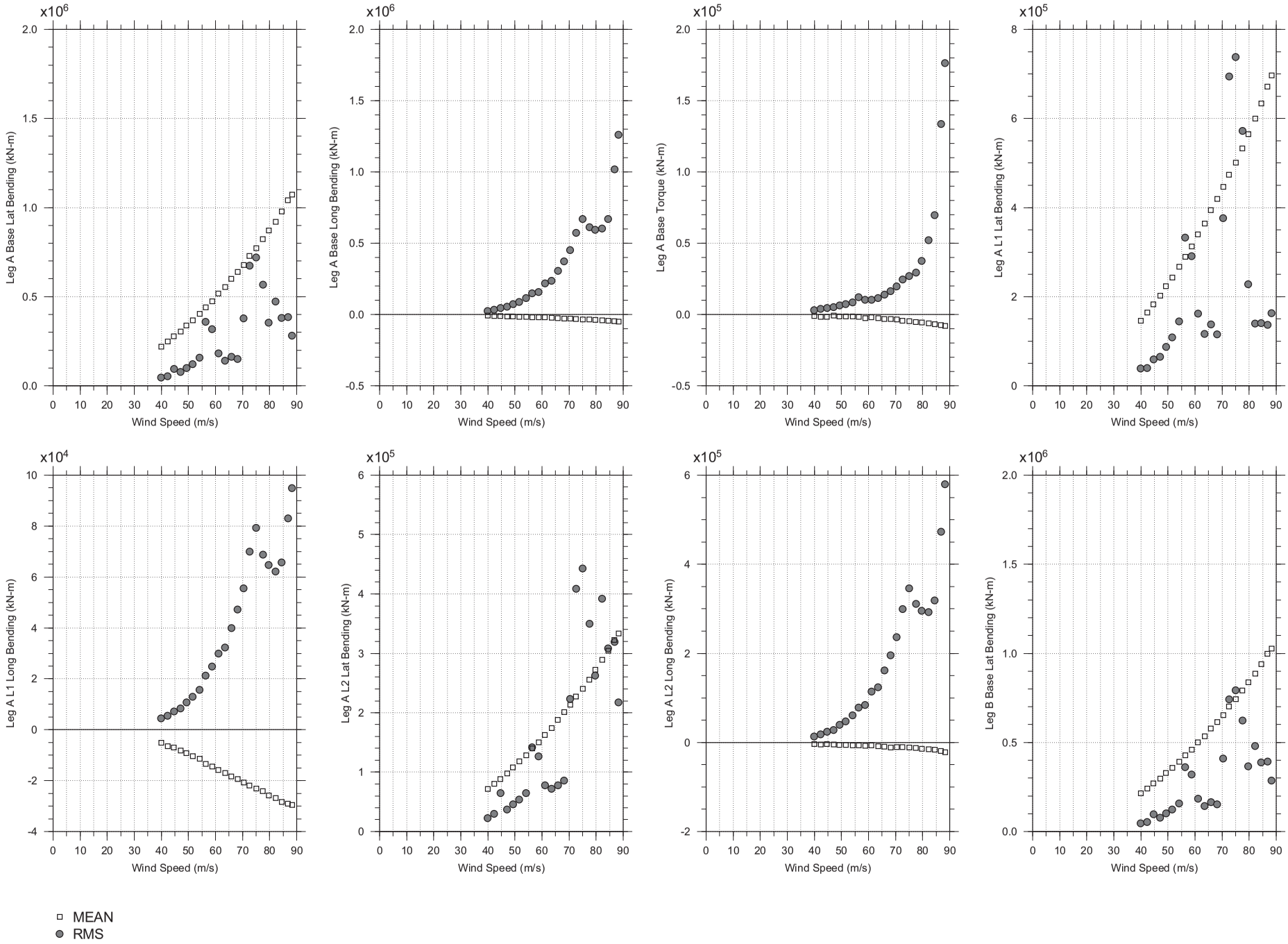

Messina Bridge, In Service Tower, 2% Damping, 5 degree, Smooth, Jan2011

Jan. 12, 2011
ti73abdg.cl

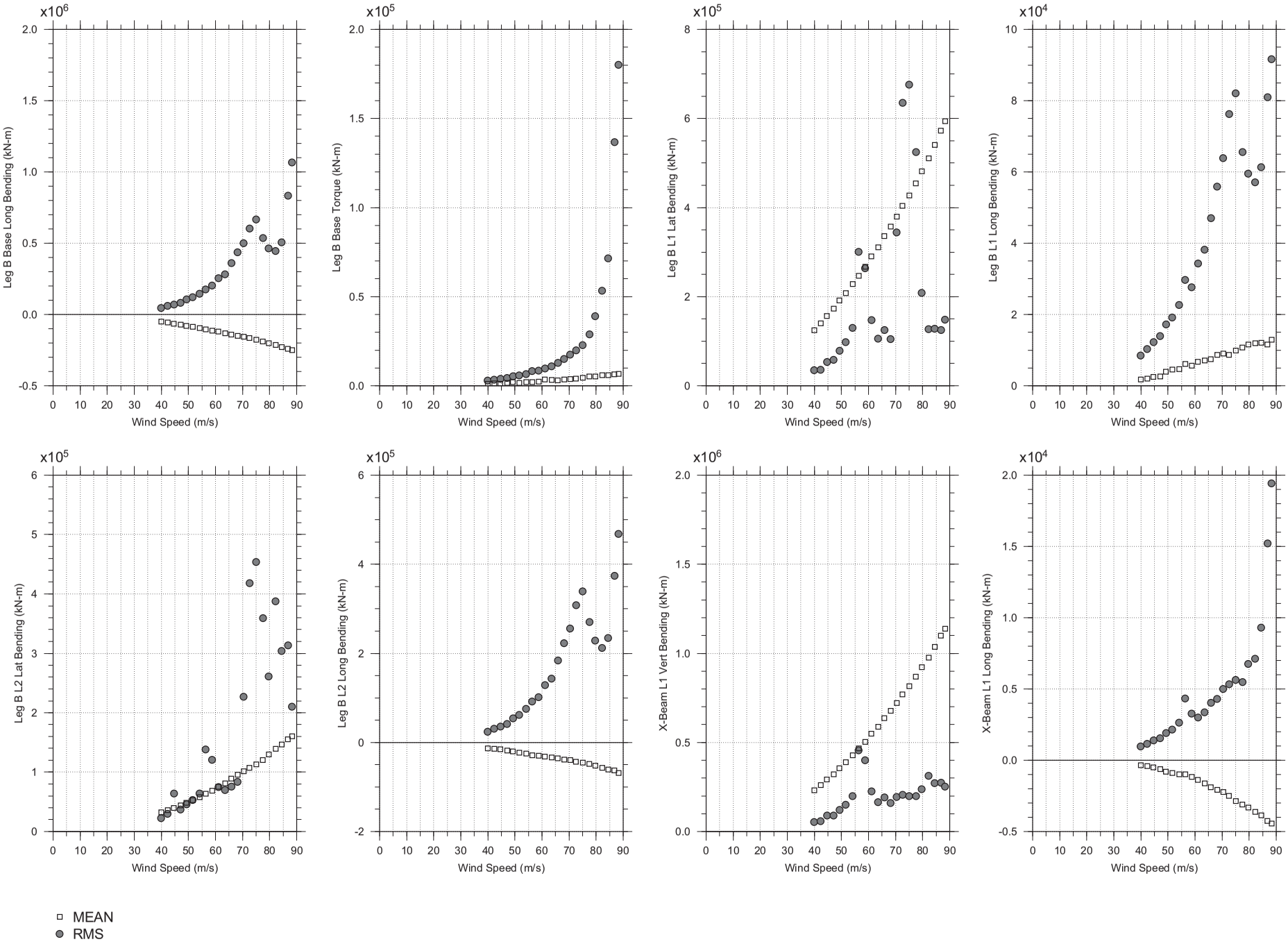

Messina Bridge, In Service Tower, 2% Damping, 5 degree, Smooth, Jan2011

Jan. 12, 2011
ti73abdg.cl

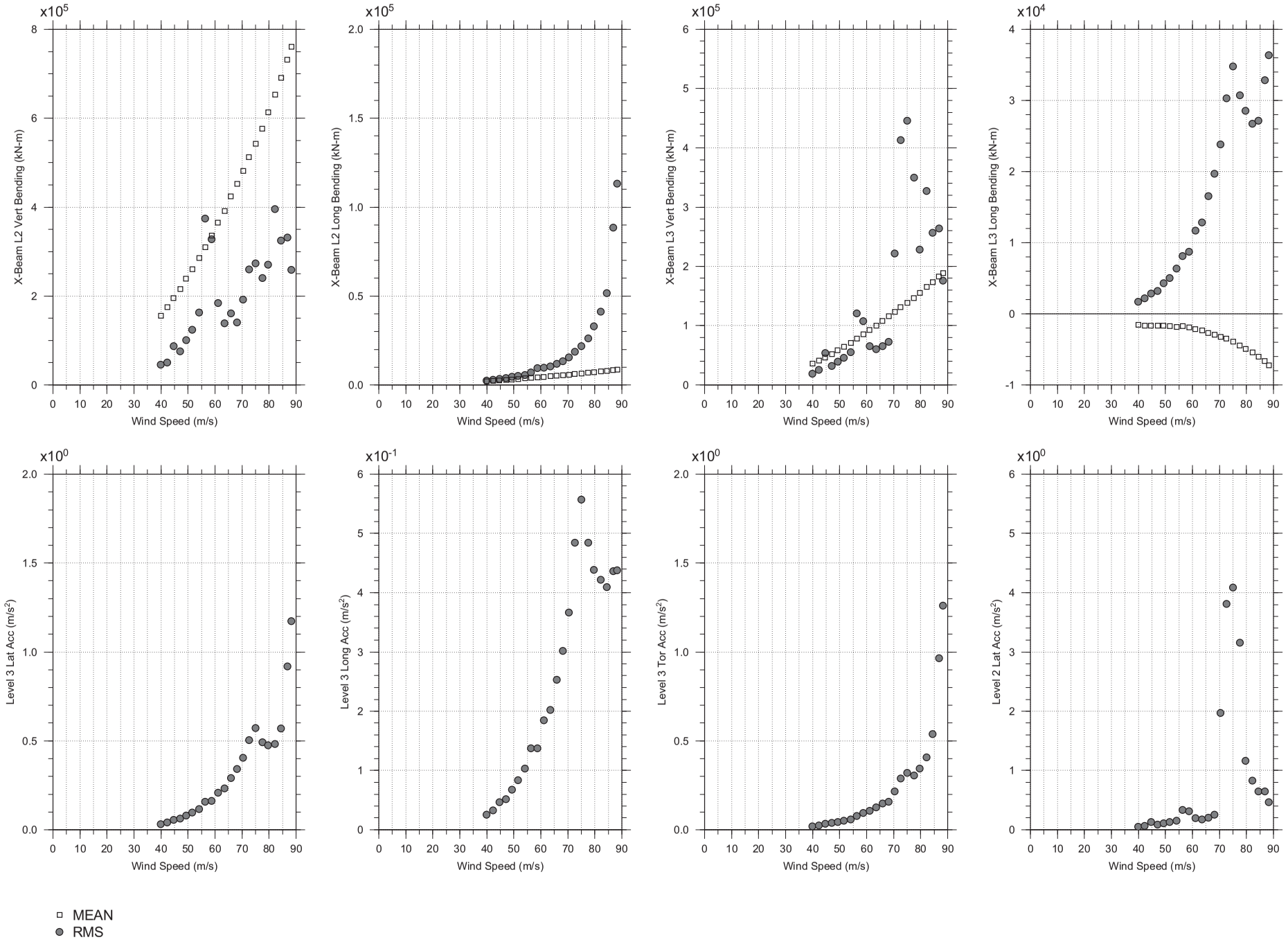

Messina Bridge, In Service Tower, 2% Damping, 5 degree, Smooth, Jan2011

Jan. 12, 2011
ti73abdg.cl

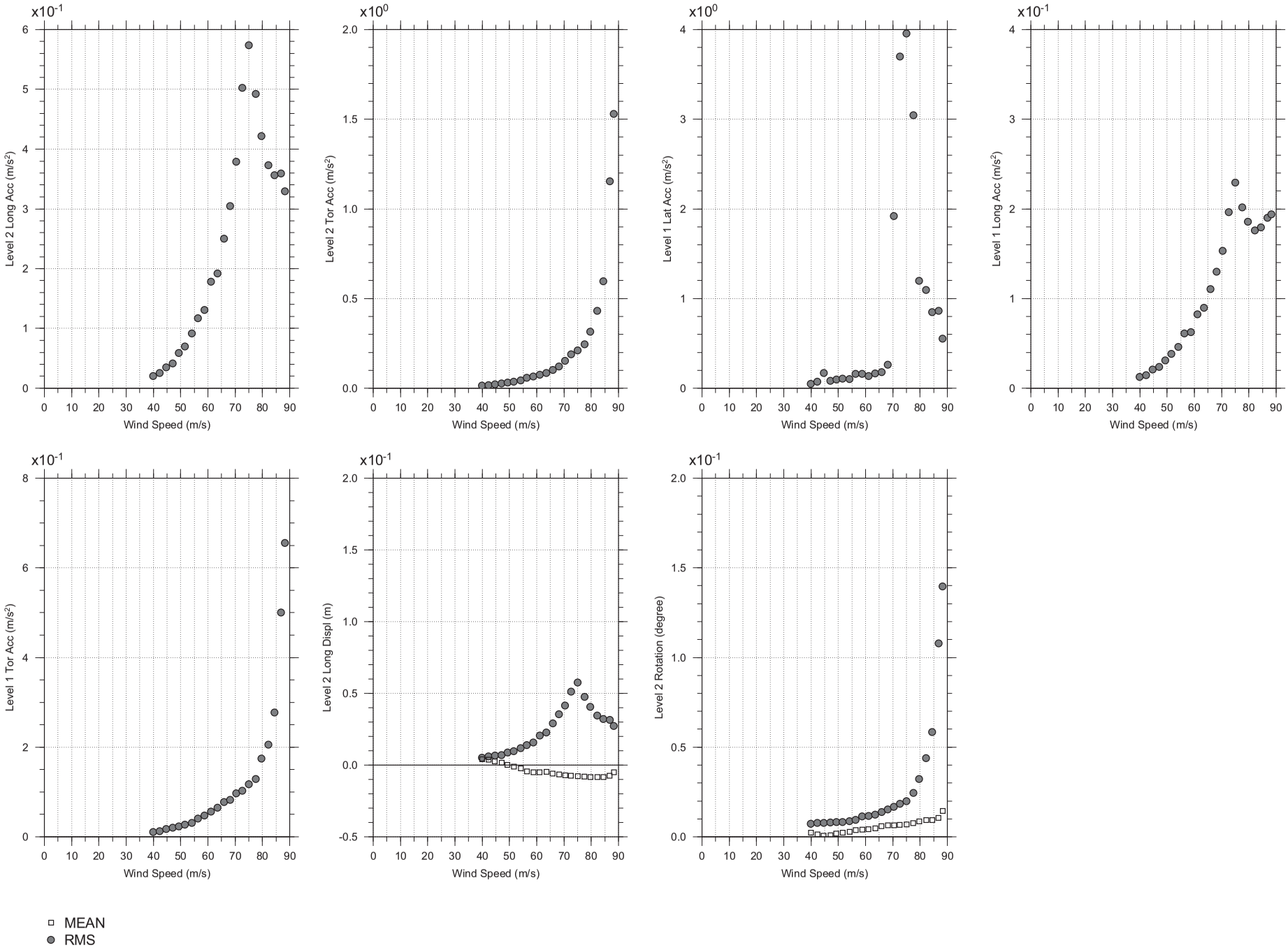

Messina Bridge, In Service Tower, 2% Damping, 5 degree, Smooth, Jan2011

Jan. 12, 2011
ti73abdg.cl

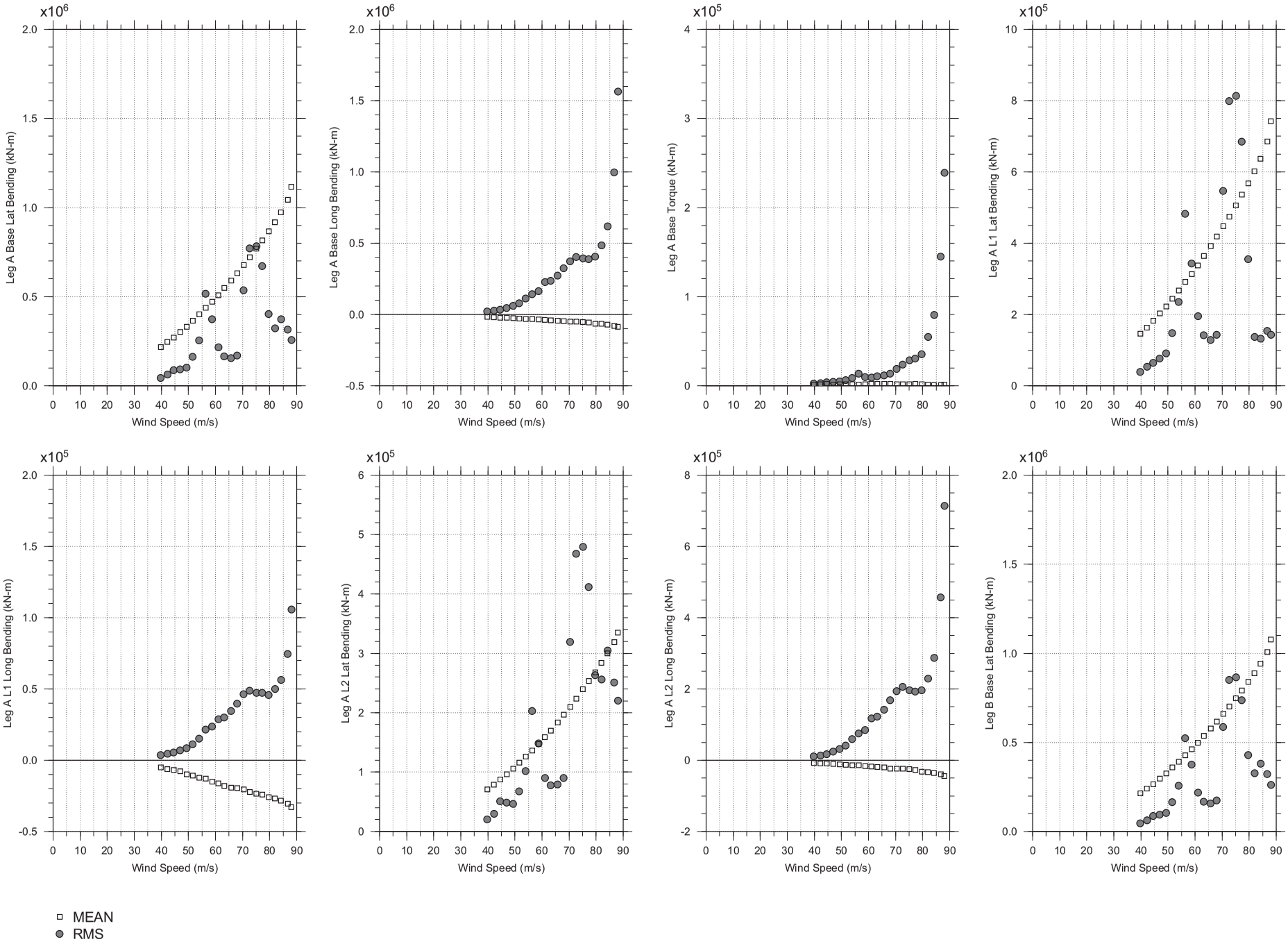

Messina Bridge, In Service Tower, 2% Damping, 7.5 degree, Smooth, Jan2011

Jan. 12, 2011
ti74abdg.cl

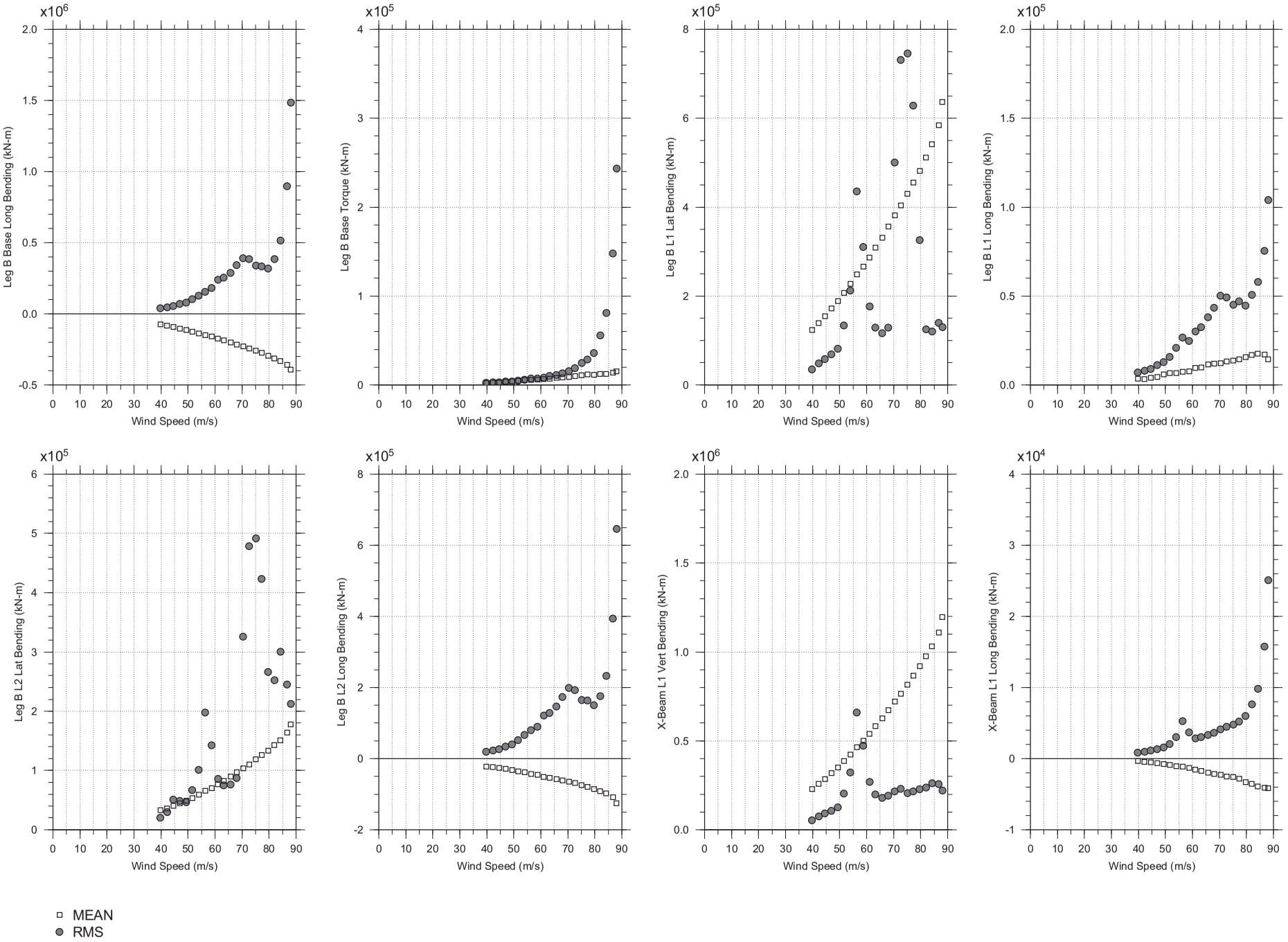

Messina Bridge, In Service Tower, 2% Damping, 7.5 degree, Smooth, Jan2011

Jan. 12, 2011
ti74abdg.cl

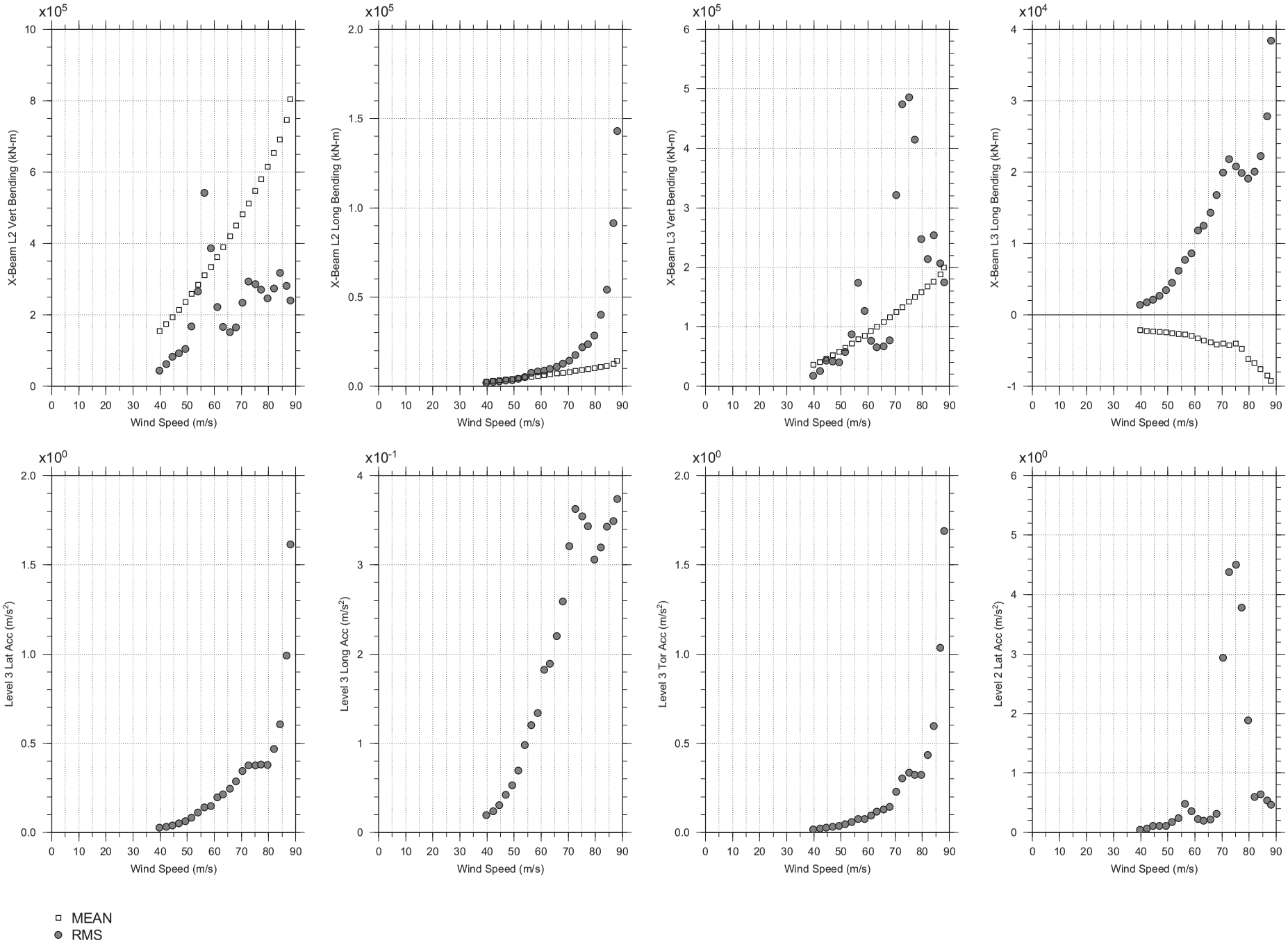

Messina Bridge, In Service Tower, 2% Damping, 7.5 degree, Smooth, Jan2011

Jan. 12, 2011
ti74abdg.cl

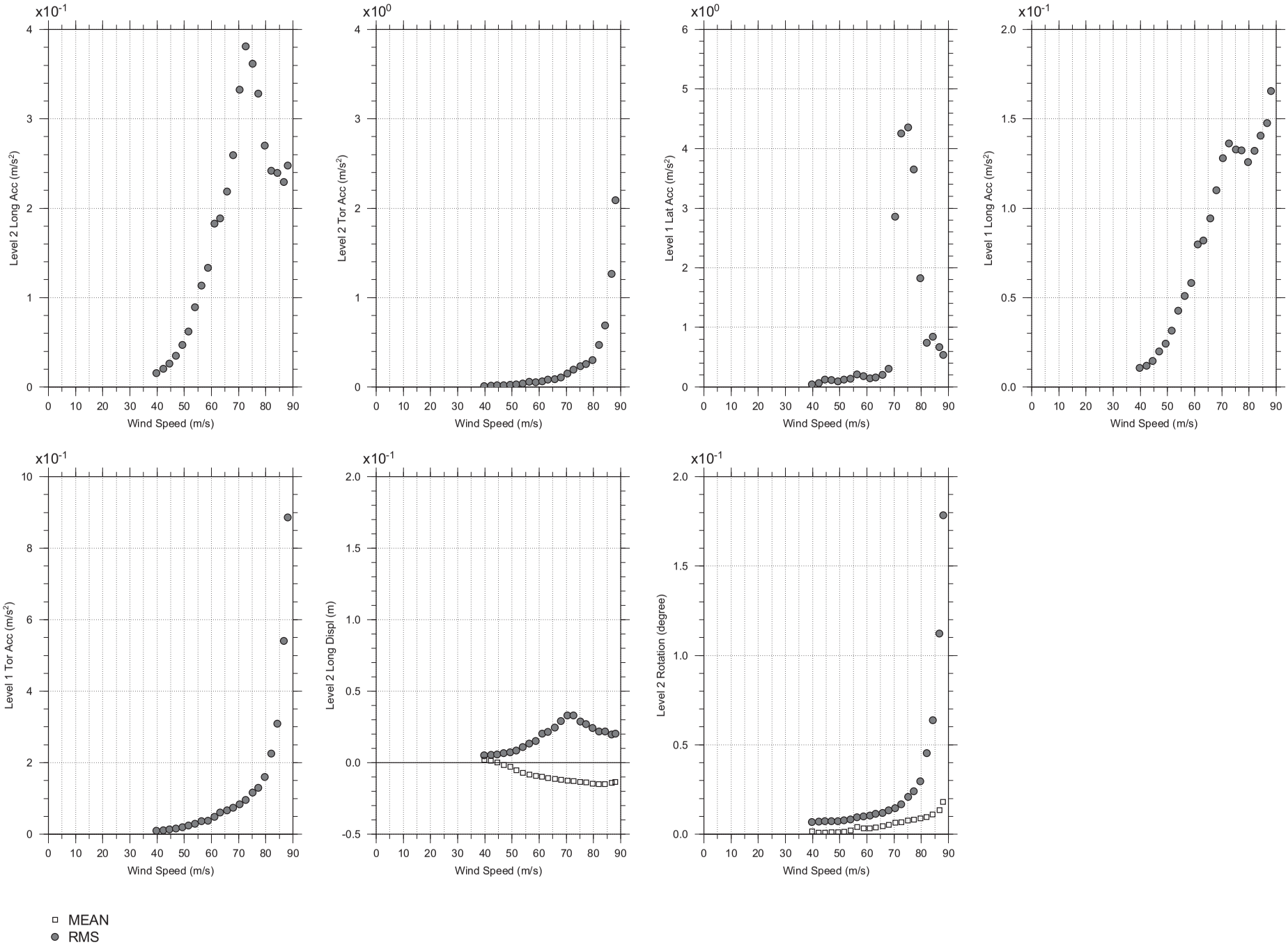

Messina Bridge, In Service Tower, 2% Damping, 7.5 degree, Smooth, Jan2011

Jan. 12, 2011
ti74abdg.cl

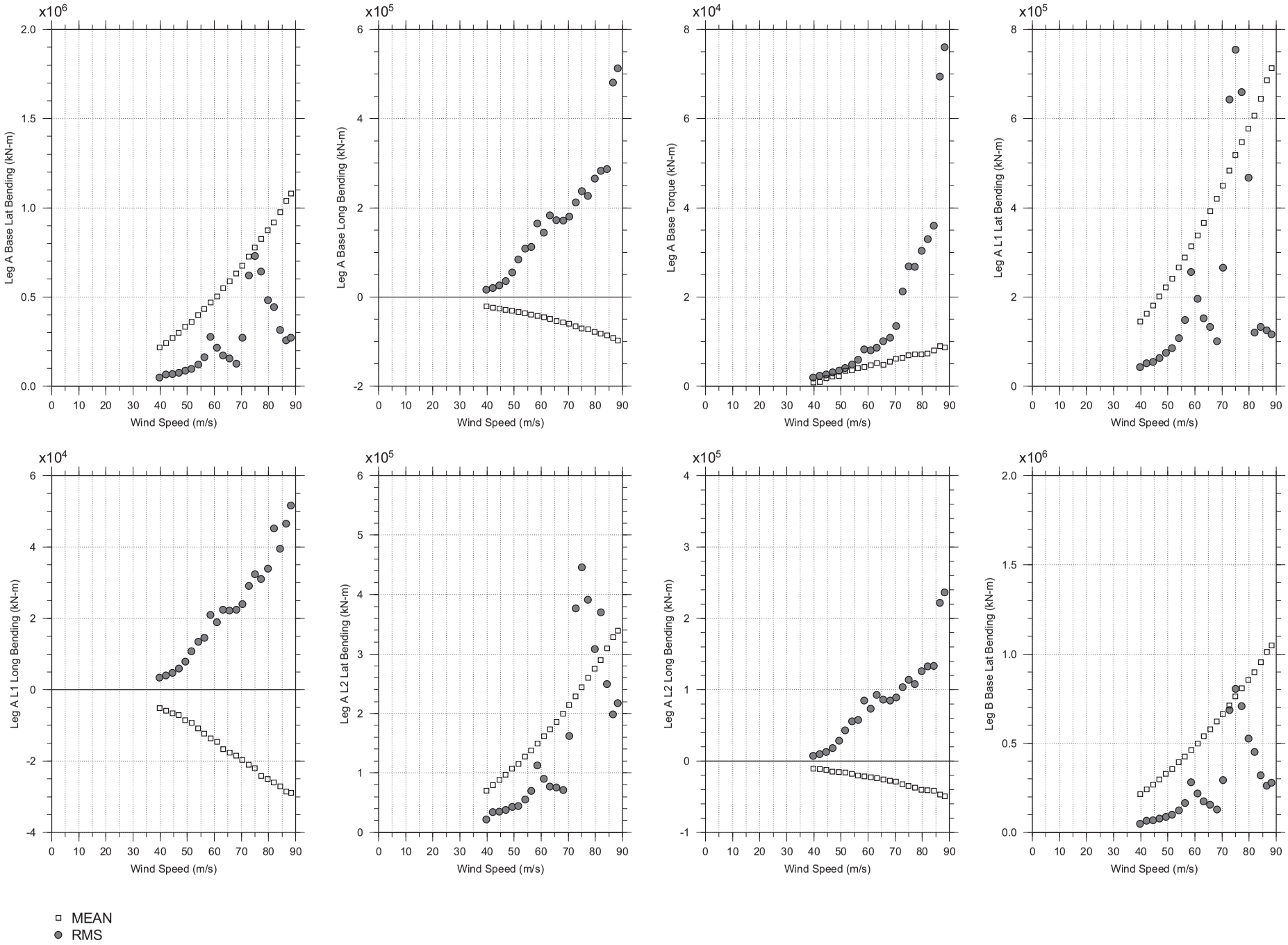

Messina Bridge, In Service Tower, 2% Damping, 10 degree, Smooth, Jan2011

Jan. 12, 2011
ti75abdg.cl

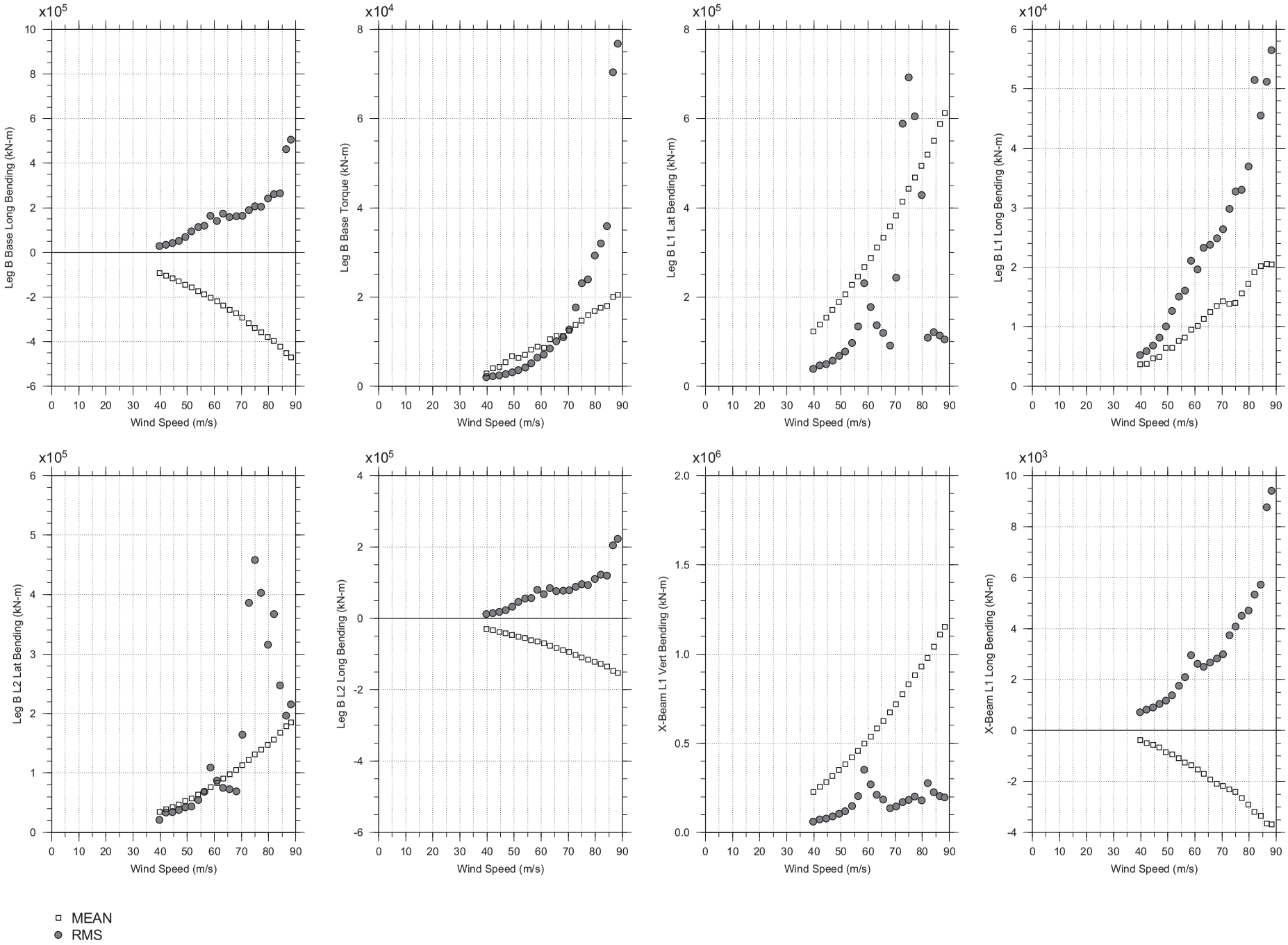

Messina Bridge, In Service Tower, 2% Damping, 10 degree, Smooth, Jan2011

Jan. 12, 2011
ti75abdg.cl

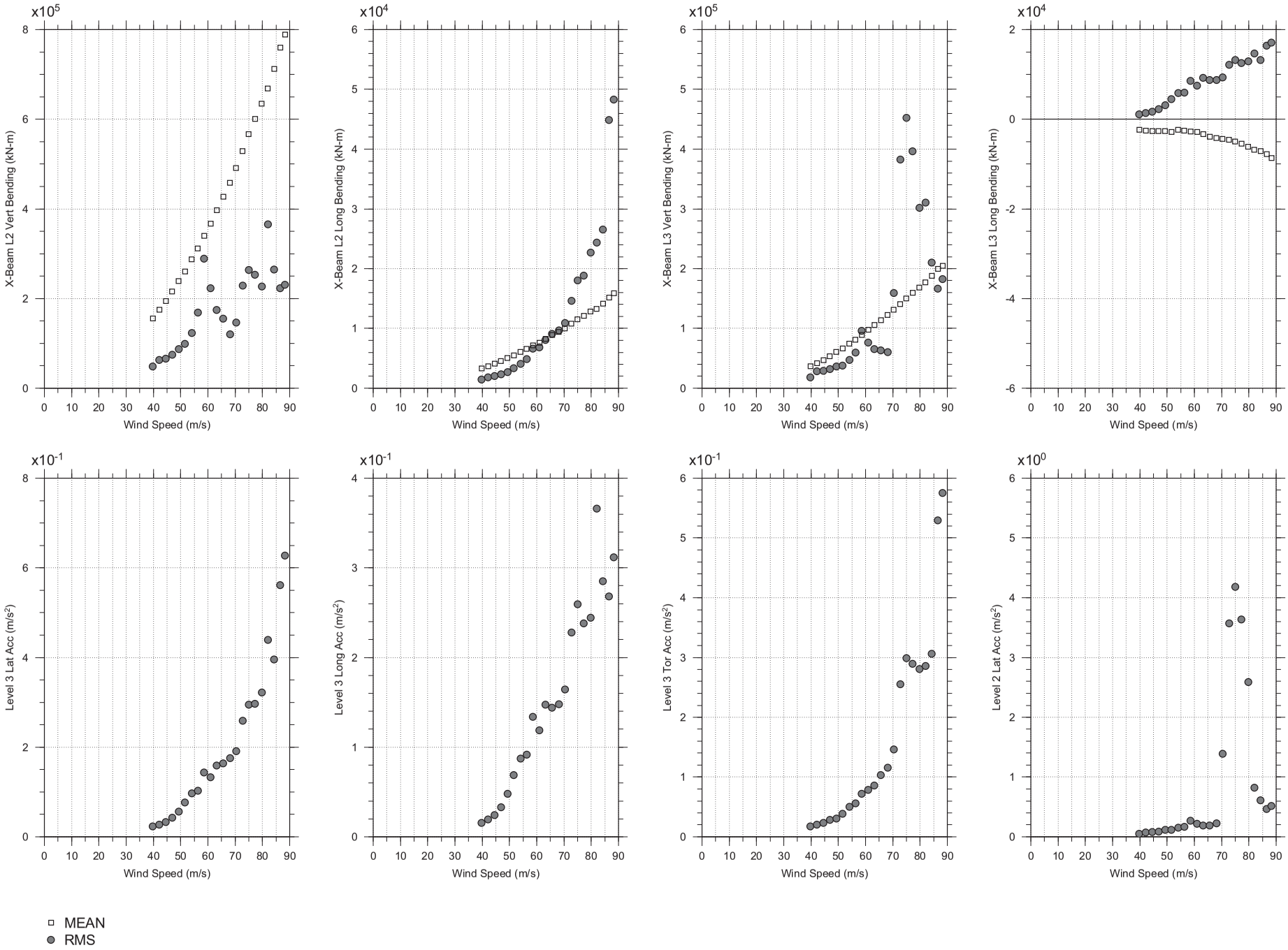

Messina Bridge, In Service Tower, 2% Damping, 10 degree, Smooth, Jan2011

Jan. 12, 2011
ti75abdg.cl

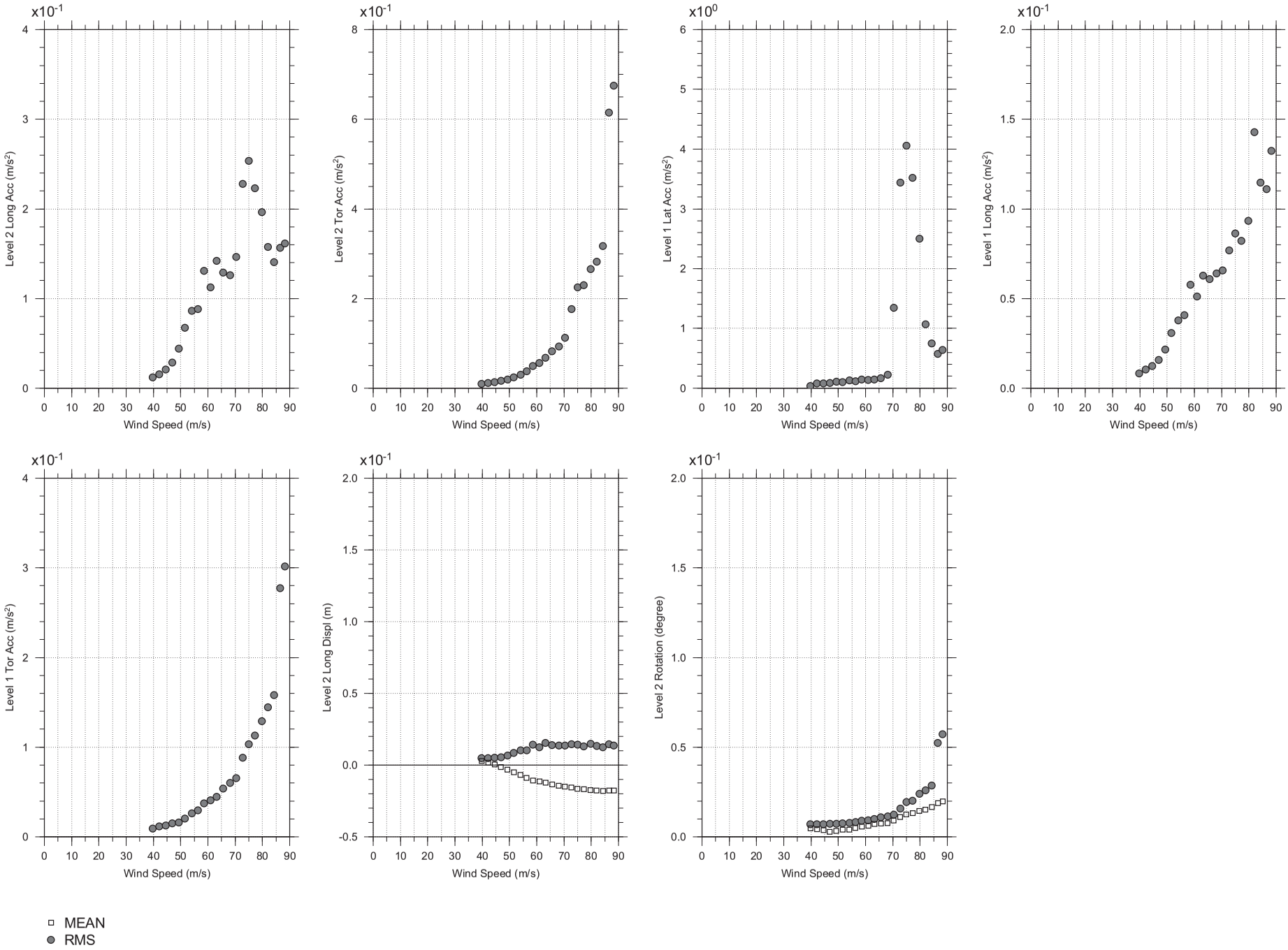

Messina Bridge, In Service Tower, 2% Damping, 10 degree, Smooth, Jan2011

Jan. 12, 2011
ti75abdg.cl

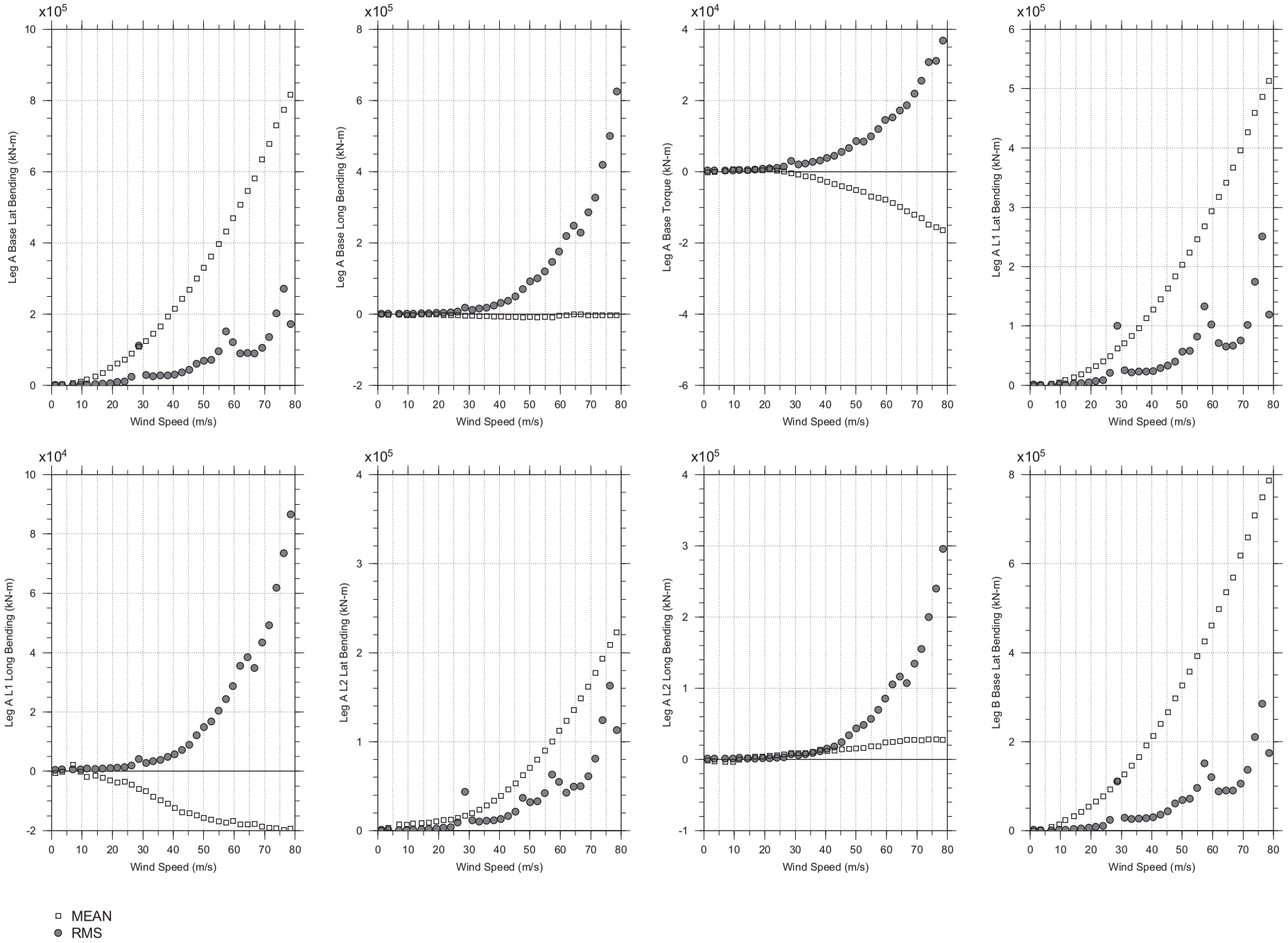

Messina Bridge, In Service Tower, 0 degree, 4% Damping, Smooth, Dec 2010

Jan. 12, 2011
ti31abdg.cl

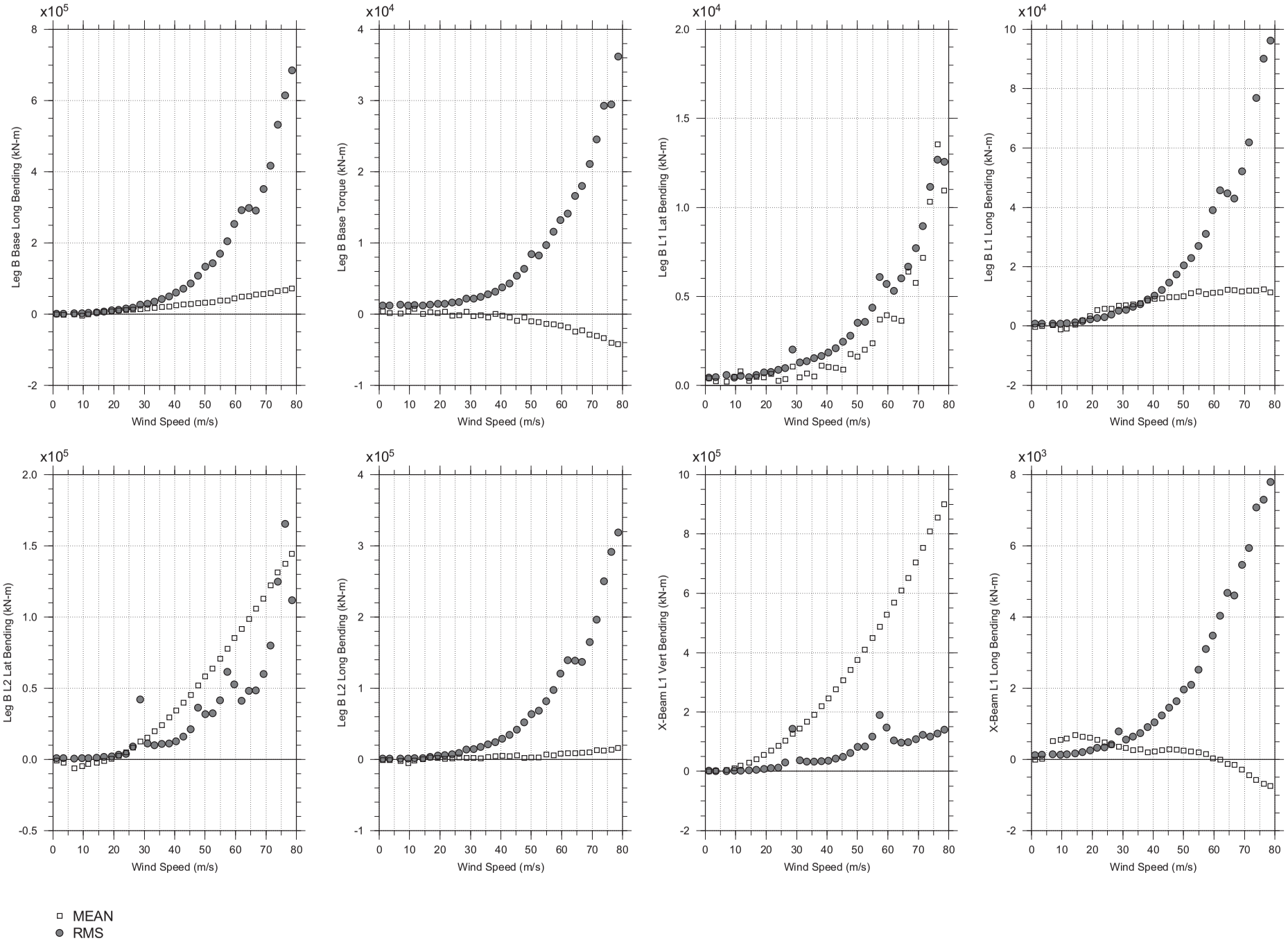

Messina Bridge, In Service Tower, 0 degree, 4% Damping, Smooth, Dec 2010

Jan. 12, 2011
ti31abdg.cl

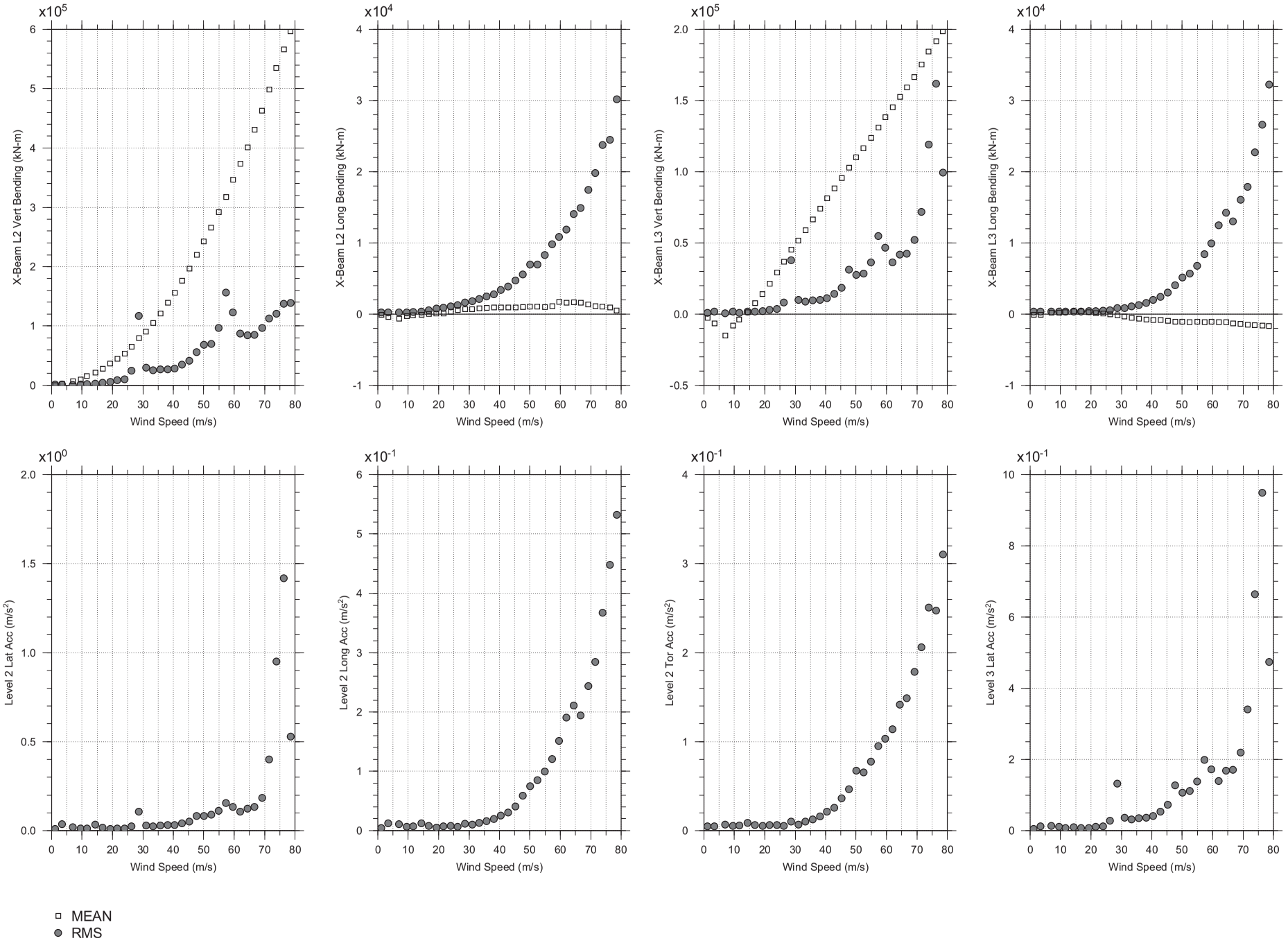

Messina Bridge, In Service Tower, 0 degree, 4% Damping, Smooth, Dec 2010

Jan. 12, 2011
ti31abdg.cl

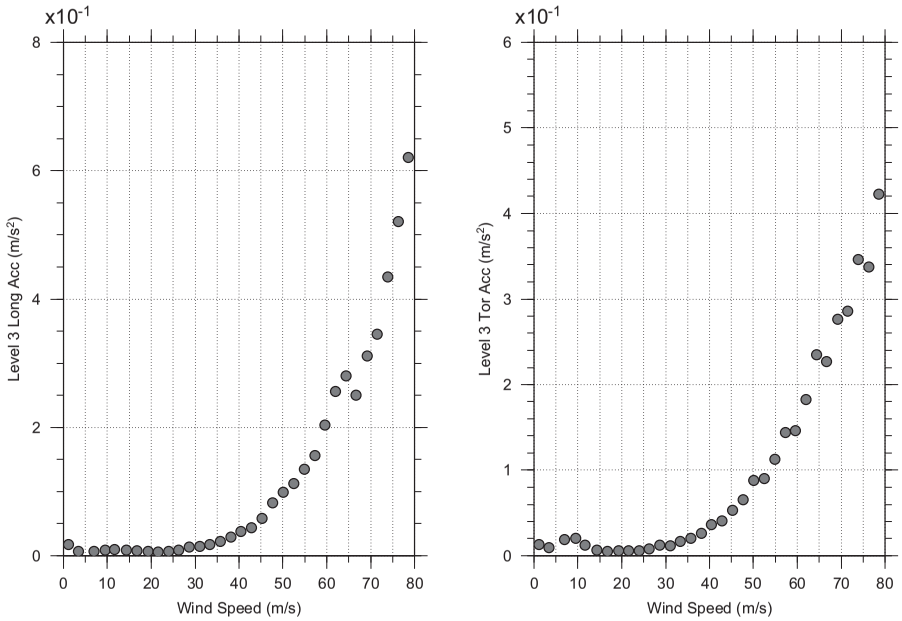

MEAN
RMS

Messina Bridge, In Service Tower, 0 degree, 4% Damping, Smooth, Dec 2010

Jan. 12, 2011
ti31abdg.cl

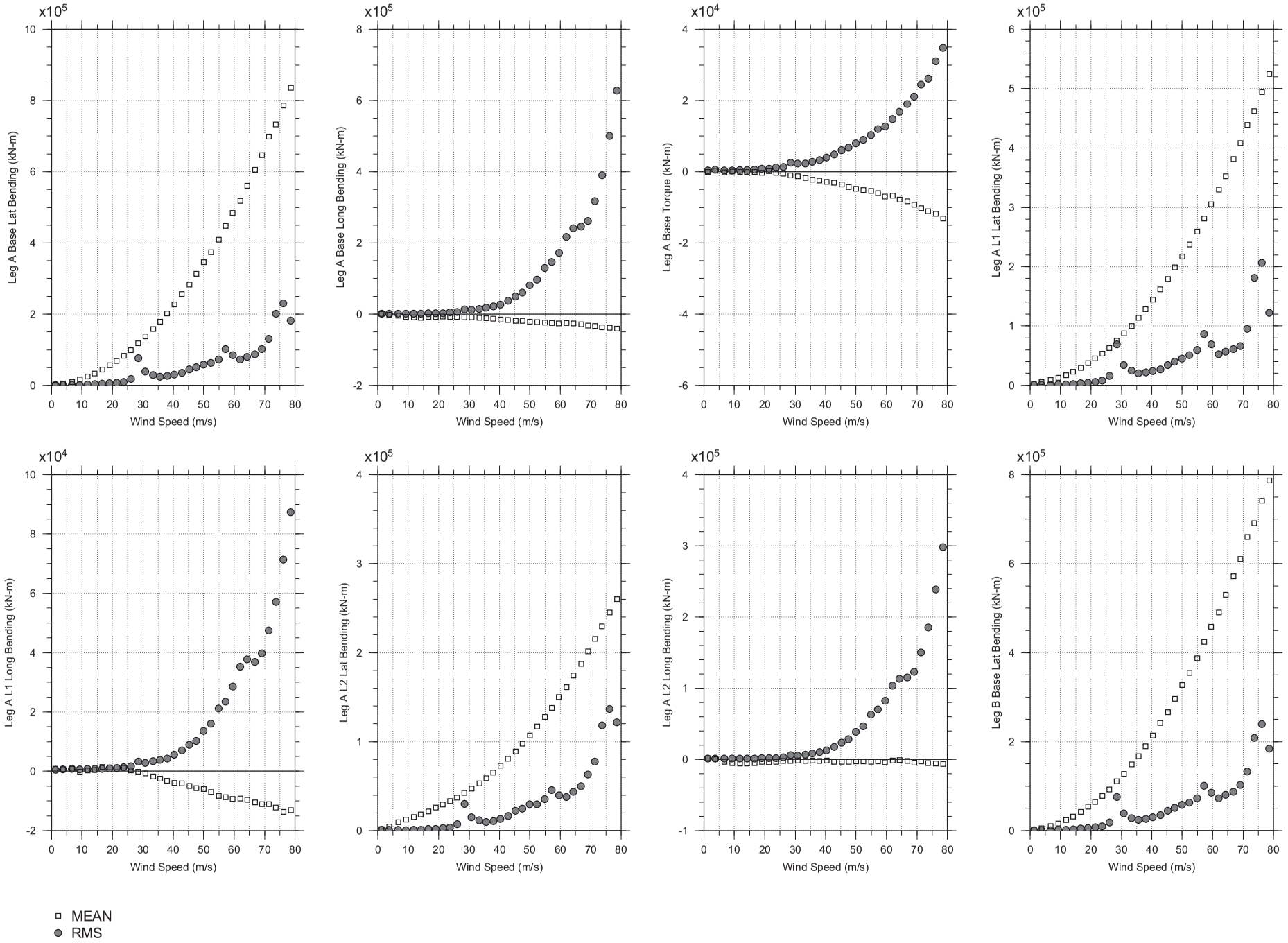

Messina Bridge, In Service Tower, 2.5 degree, 4% Damping, Smooth, Dec 2010

Jan. 12, 2011
ti32abdg.cl

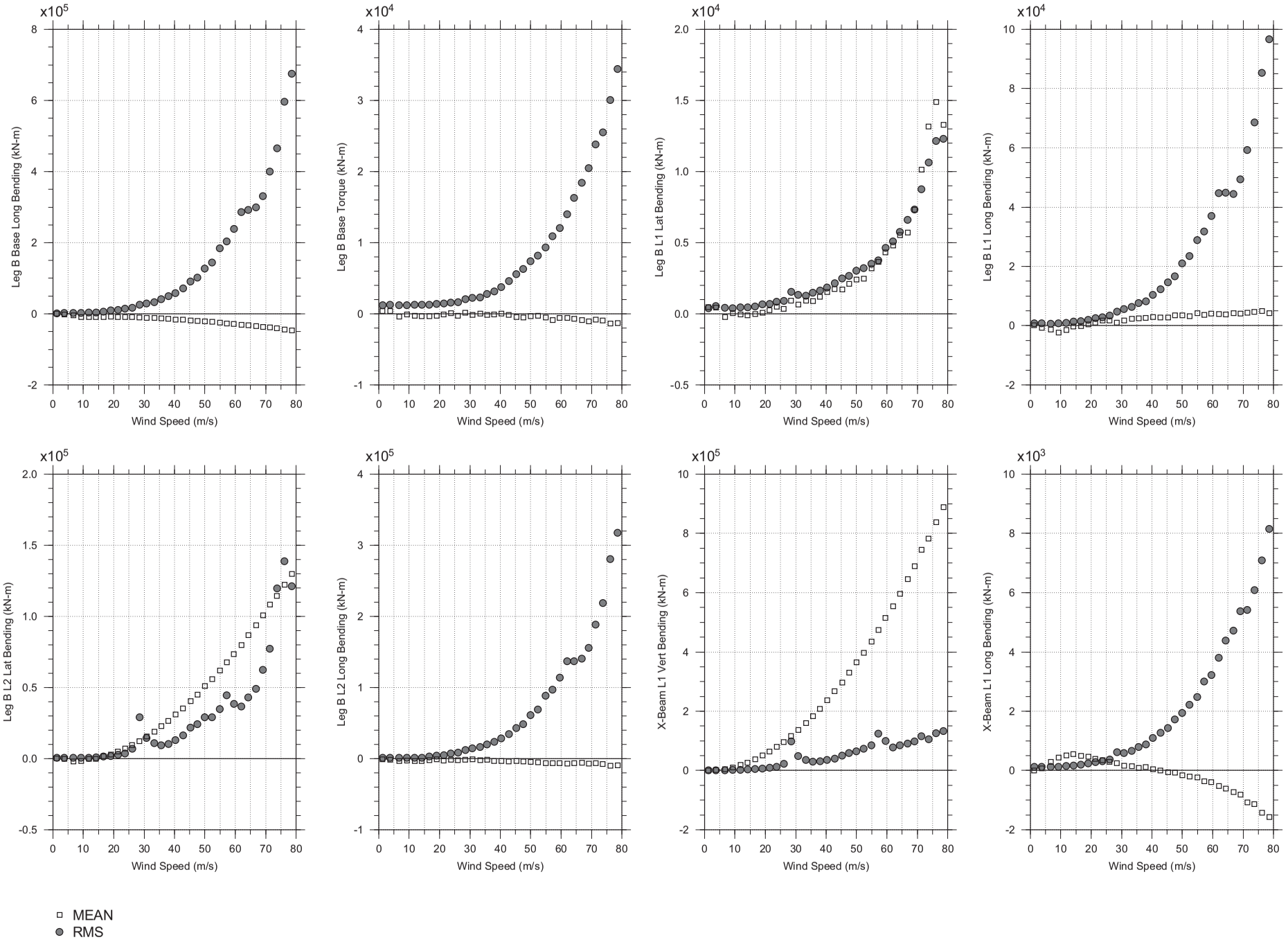

Messina Bridge, In Service Tower, 2.5 degree, 4% Damping, Smooth, Dec 2010

Jan. 12, 2011
ti32abdg.cl

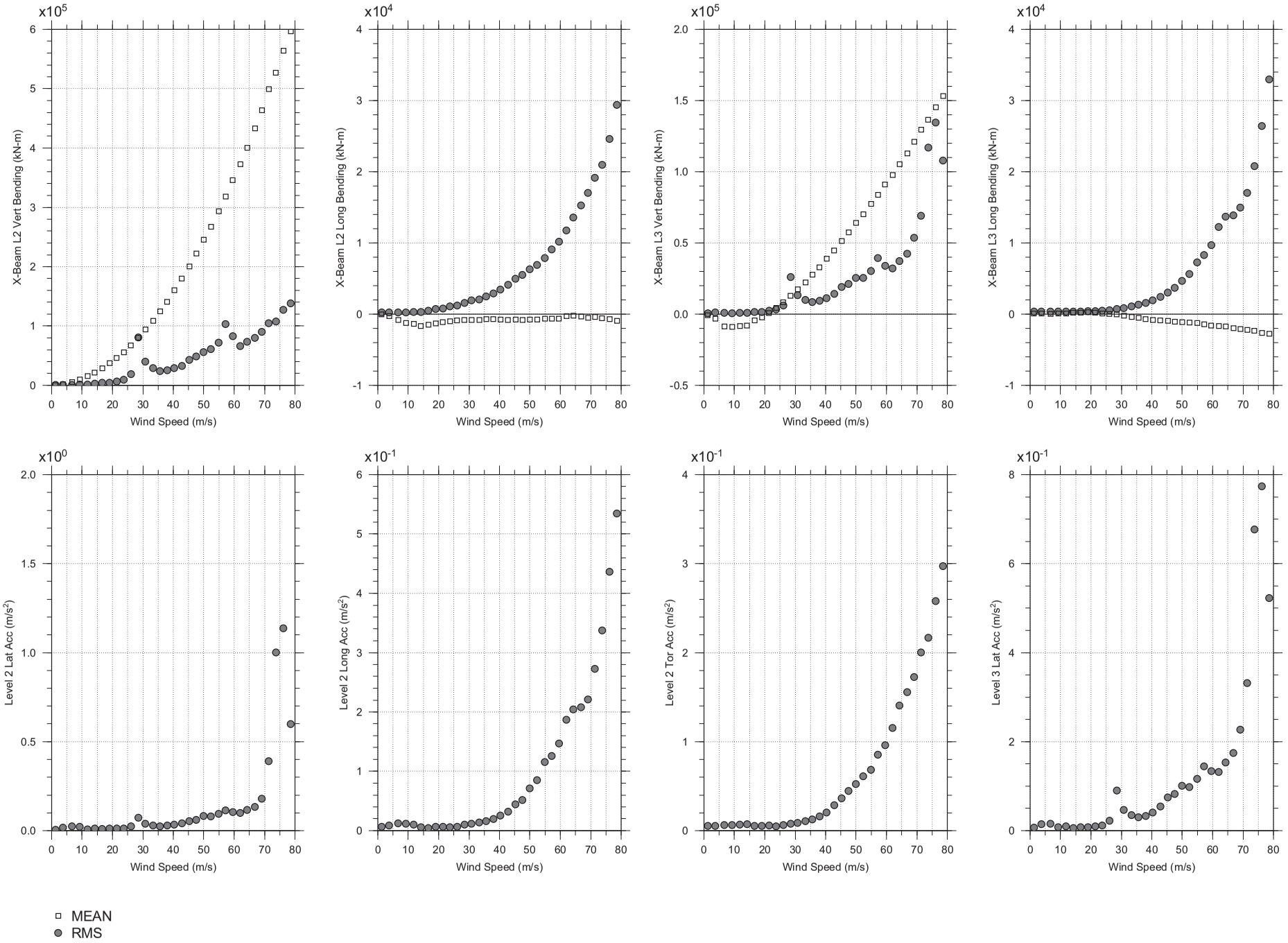

Messina Bridge, In Service Tower, 2.5 degree, 4% Damping, Smooth, Dec 2010

Jan. 12, 2011
ti32abdg.cl

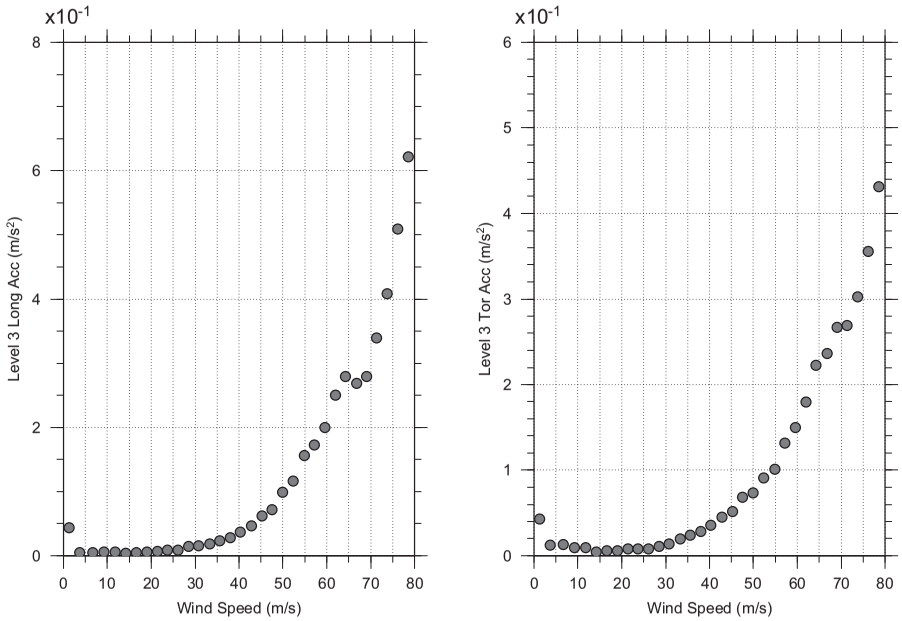

MEAN
RMS

Messina Bridge, In Service Tower, 2.5 degree, 4% Damping, Smooth, Dec 2010

Jan. 12, 2011
ti32abdg.cl

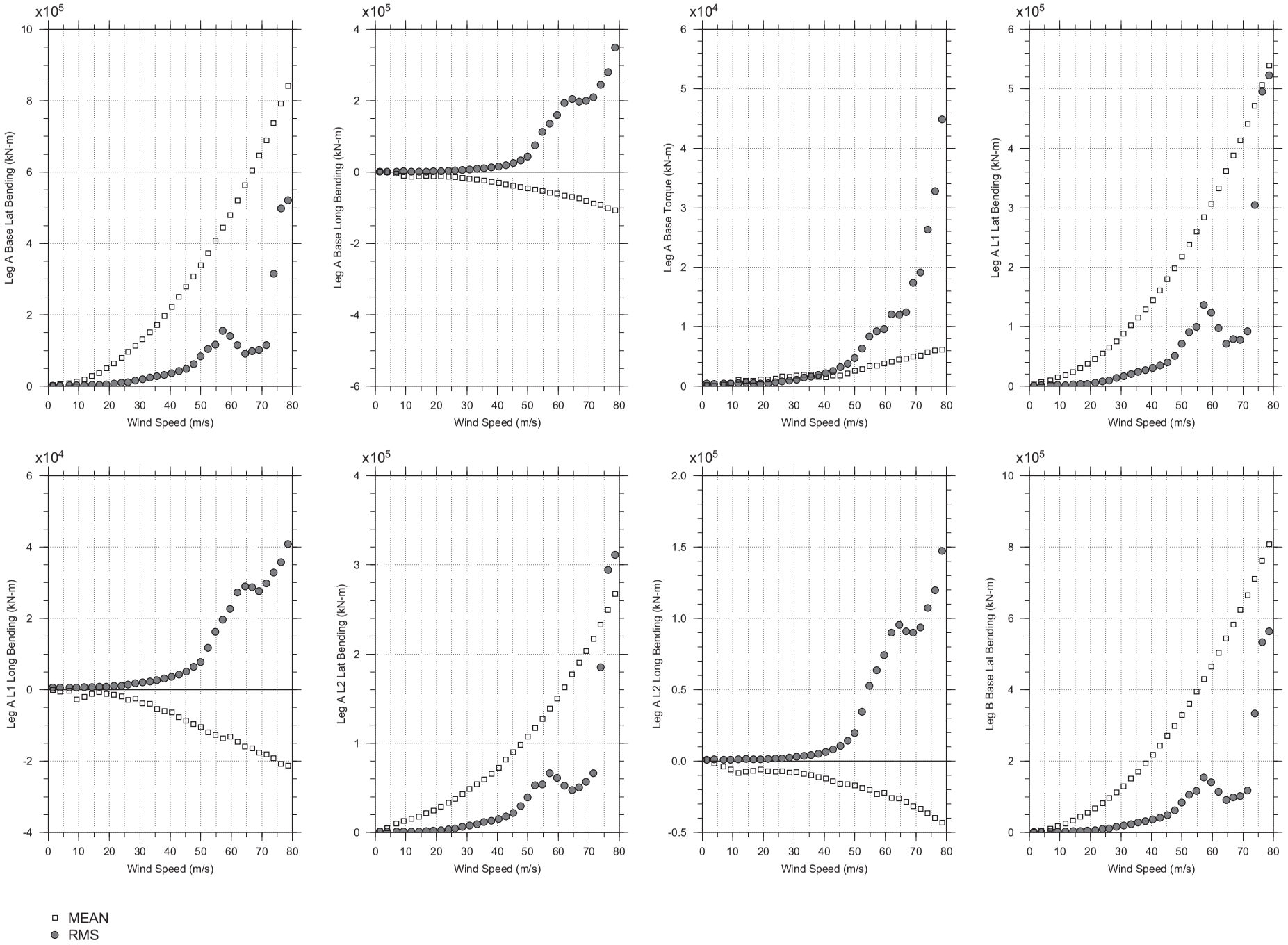

Messina Bridge, In Service Tower, 10 degree, 4% Damping, Smooth, Dec 2010

Jan. 12, 2011
ti33abdg.cl

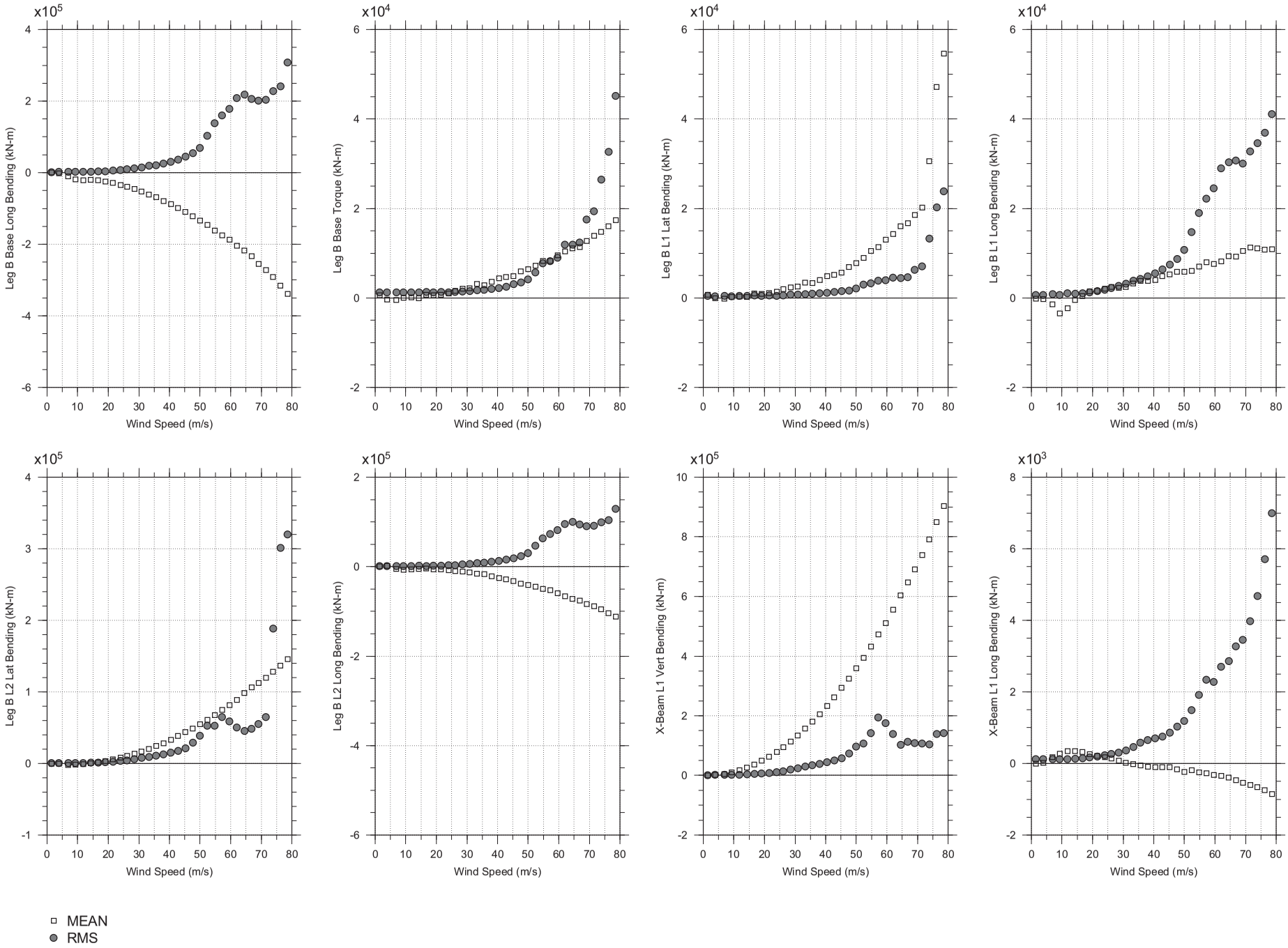

Messina Bridge, In Service Tower, 10 degree, 4% Damping, Smooth, Dec 2010

Jan. 12, 2011
ti33abdg.cl

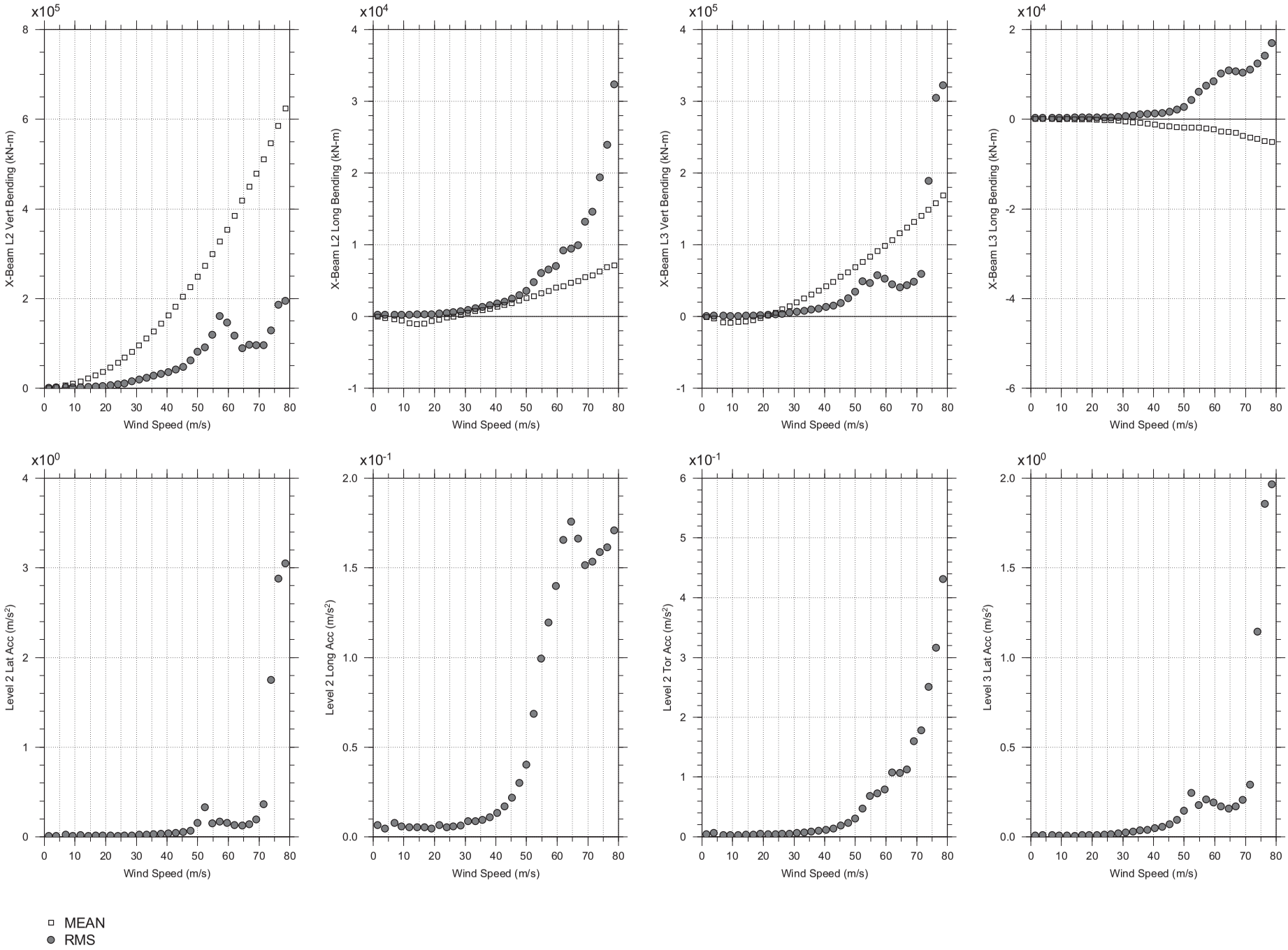

Messina Bridge, In Service Tower, 10 degree, 4% Damping, Smooth, Dec 2010

Jan. 12, 2011
ti33abdg.cl

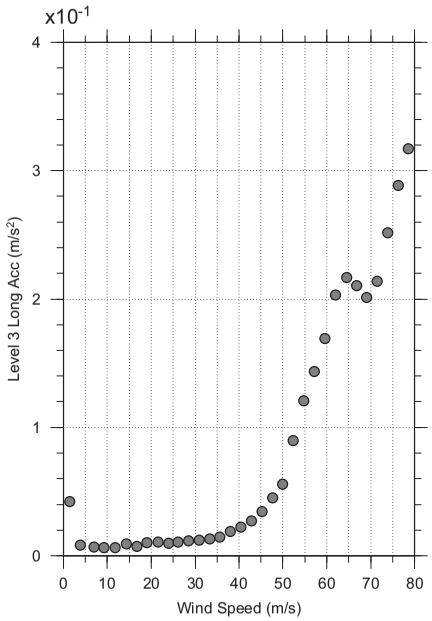

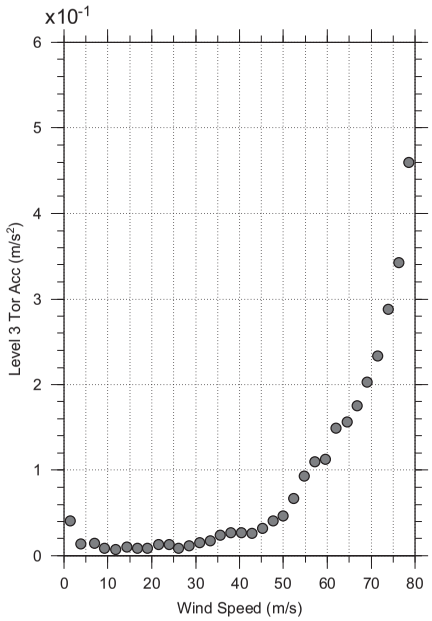

MEAN
RMS

Messina Bridge, In Service Tower, 10 degree, 4% Damping, Smooth, Dec 2010

Jan. 12, 2011
ti33abdg.cl

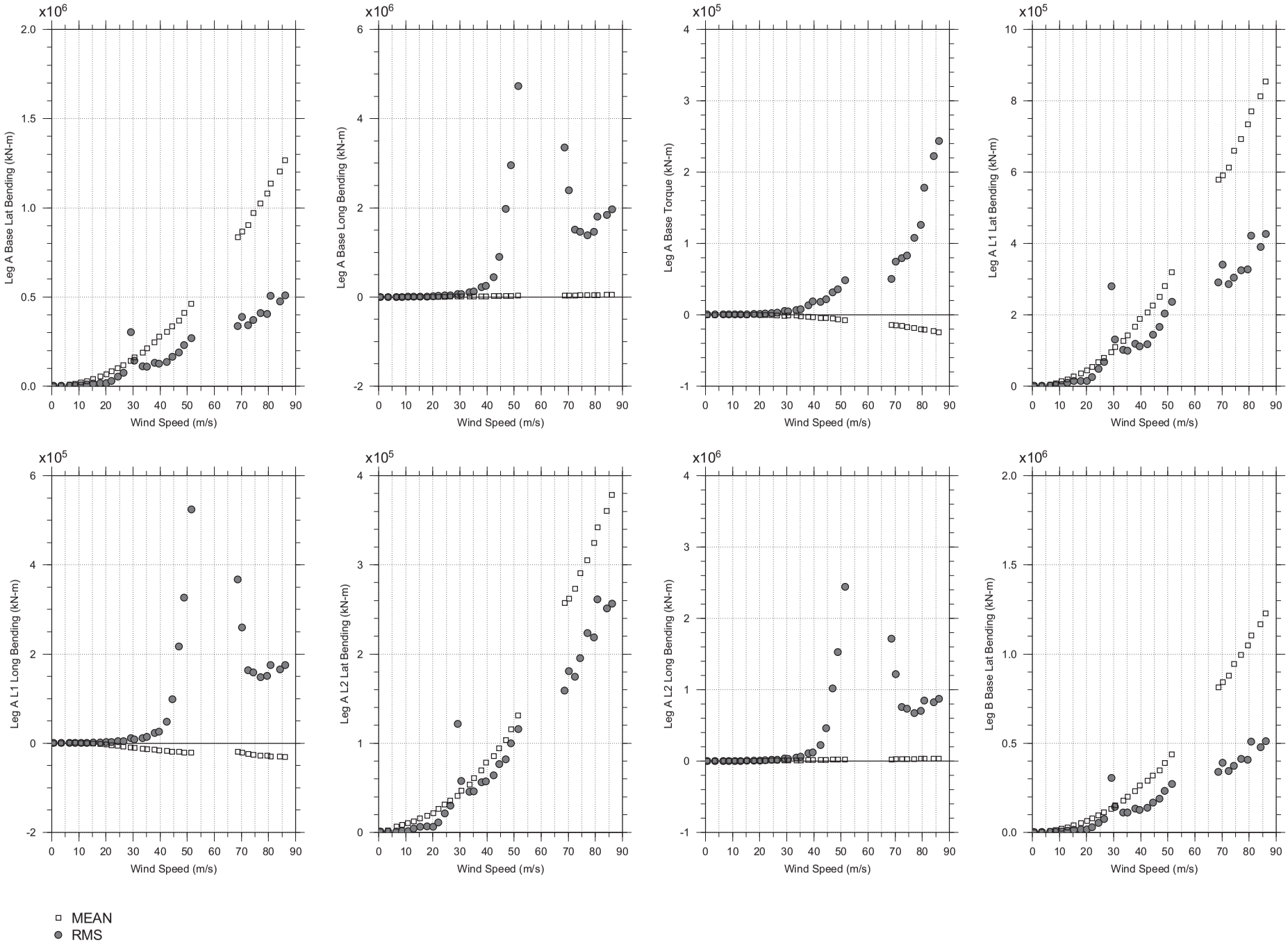

Messina Bridge, In Service Tower, 0 degree, Turbulent, Jan2011

Jan. 11, 2011
ti21rabdg.cl

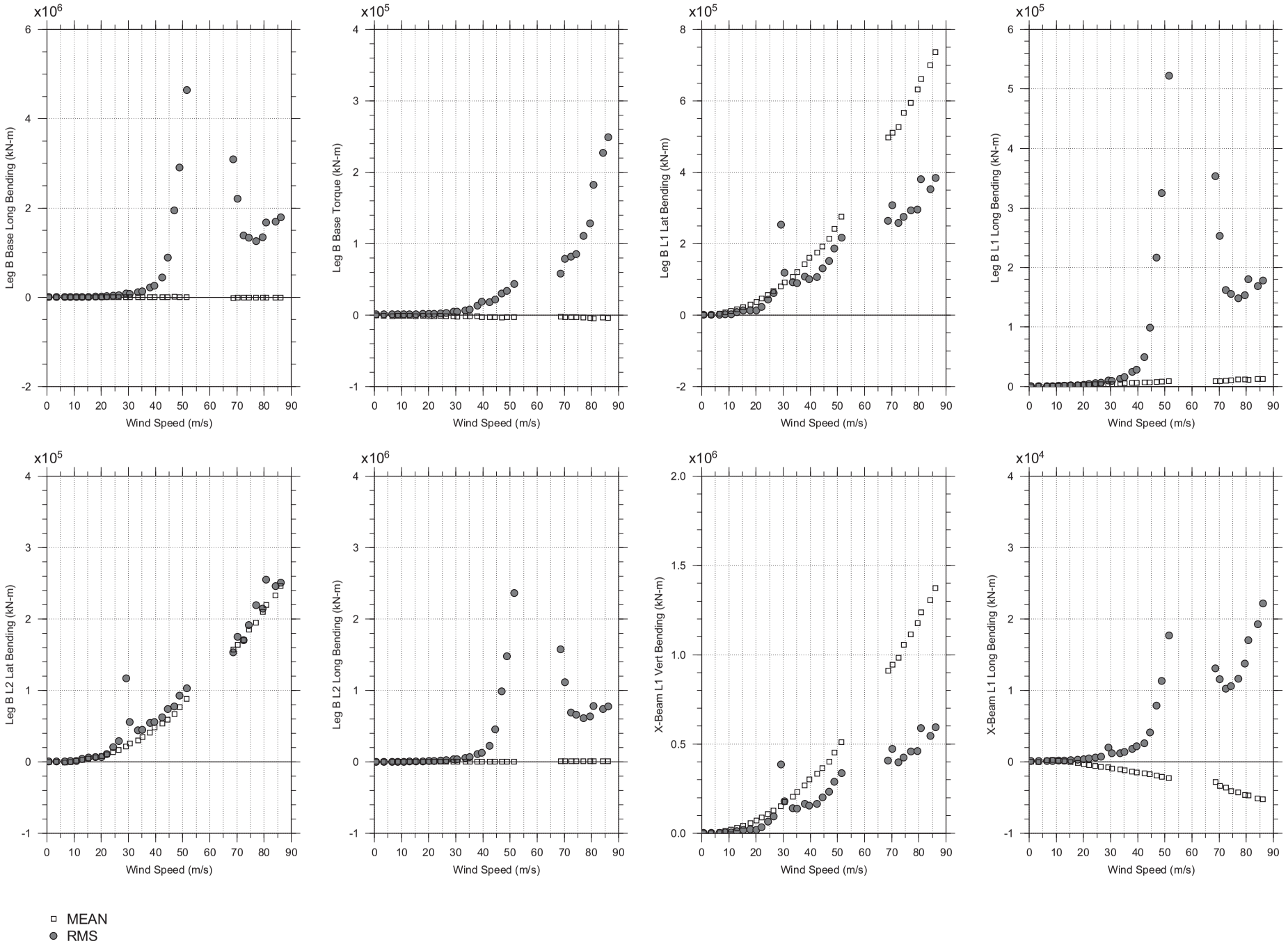

Messina Bridge, In Service Tower, 0 degree, Turbulent, Jan2011

Jan. 11, 2011
ti21rabdg.cl

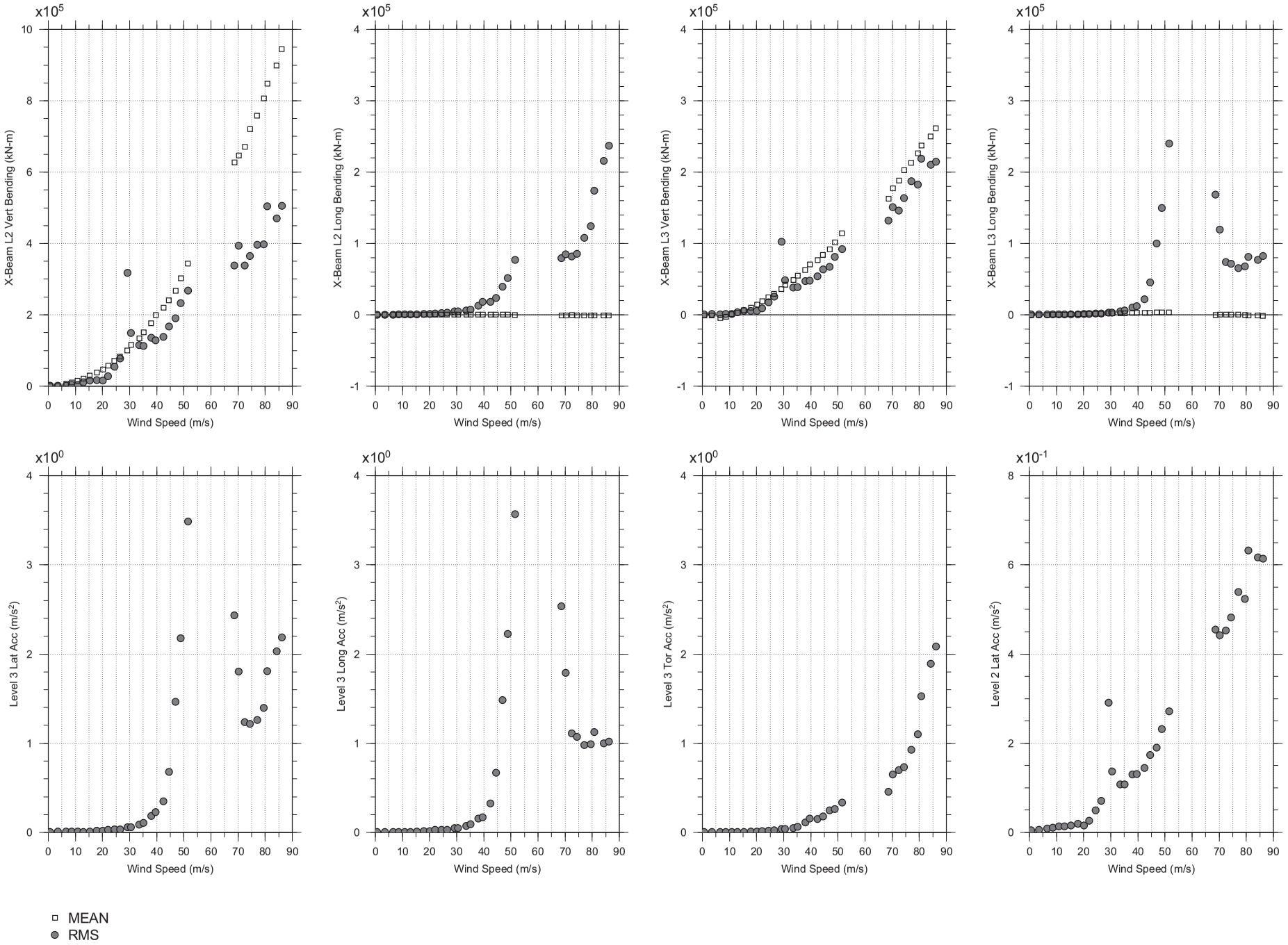

Messina Bridge, In Service Tower, 0 degree, Turbulent, Jan2011

Jan. 11, 2011
ti21rabdg.cl

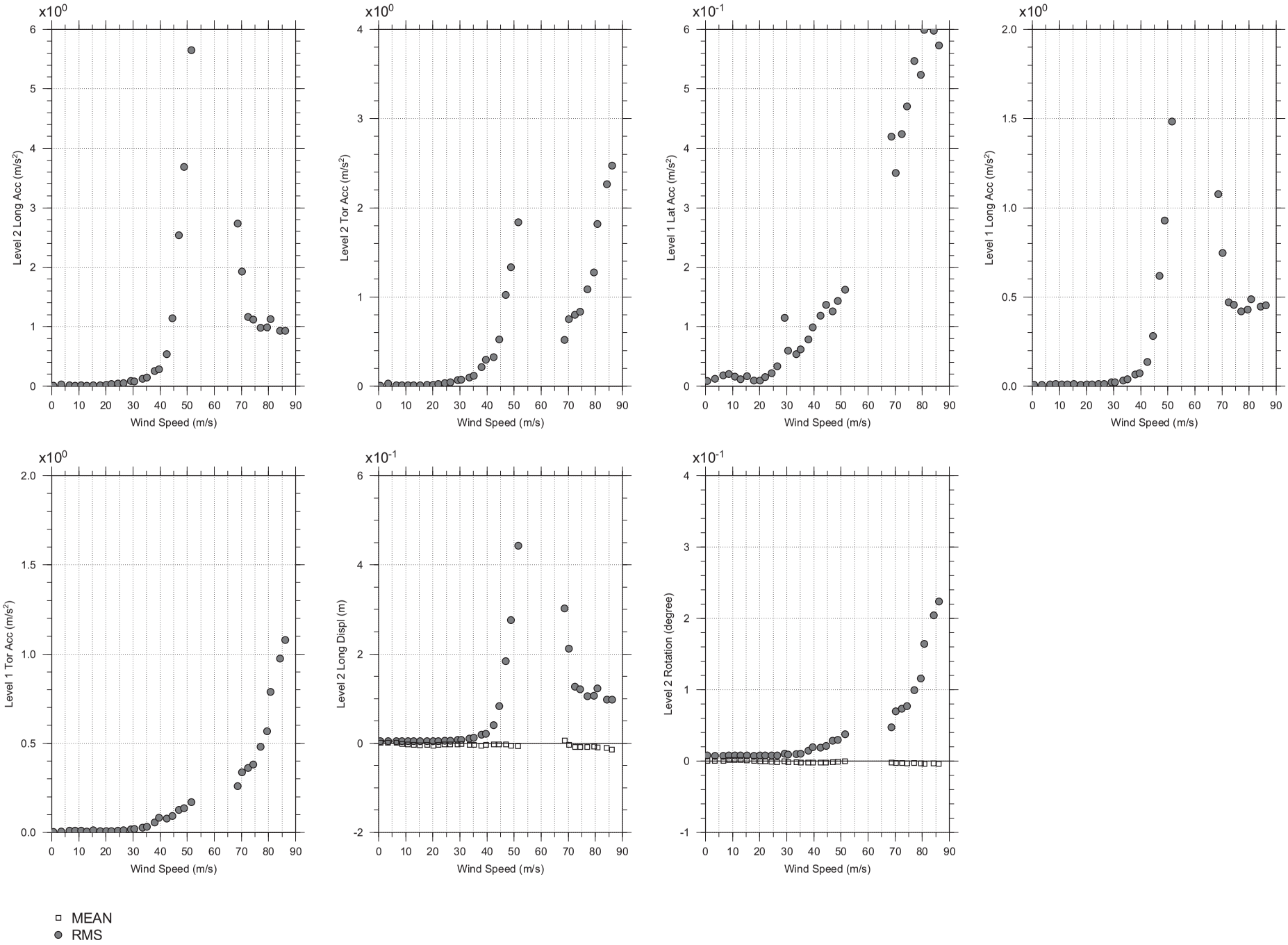

Messina Bridge, In Service Tower, 0 degree, Turbulent, Jan2011

Jan. 11, 2011
ti21rabdg.cl

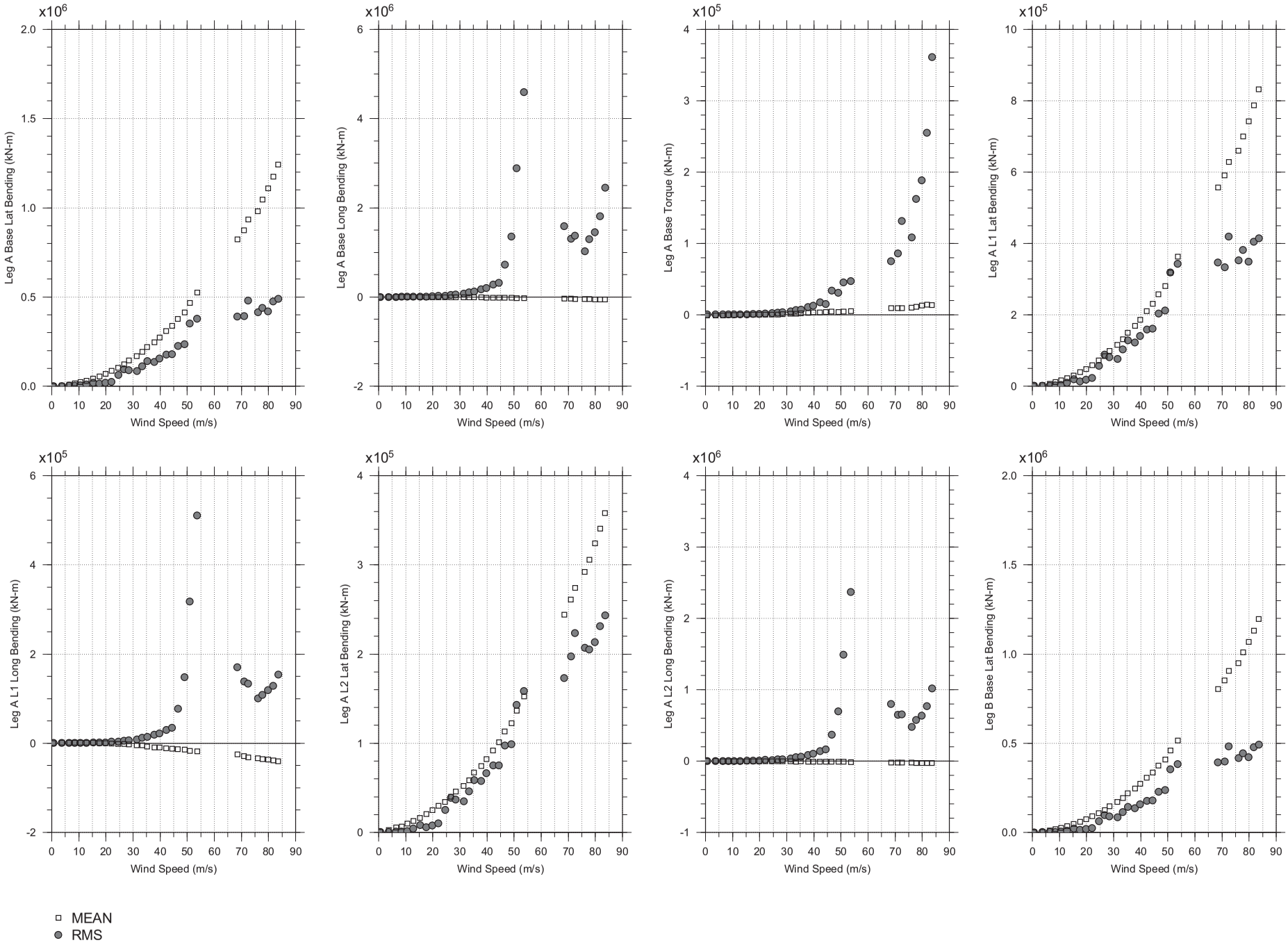

Messina Bridge, In Service Tower, 10 degree, Turbulent, Jan2011

Jan. 11, 2011
ti22rabdg.cl

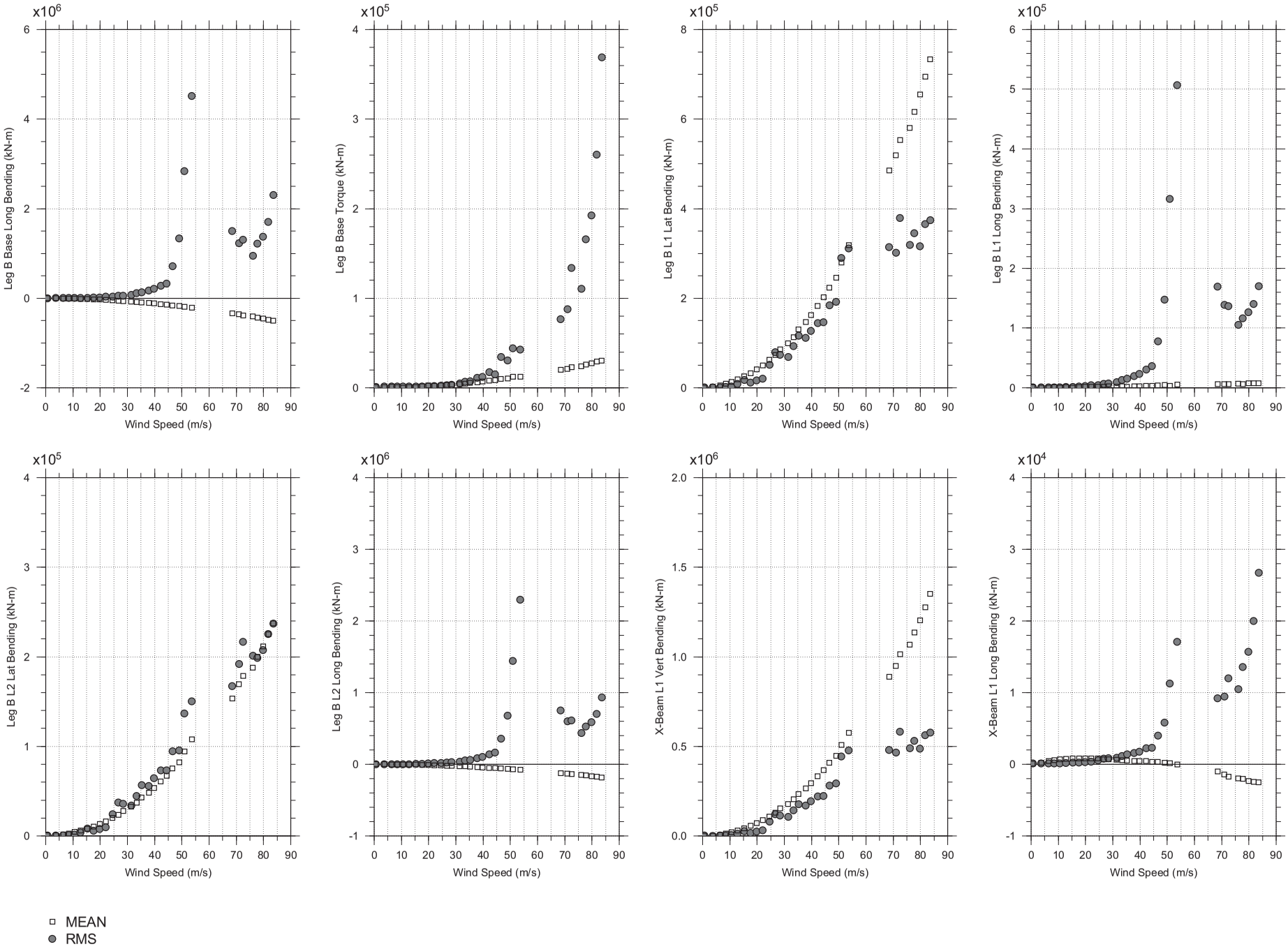

Messina Bridge, In Service Tower, 10 degree, Turbulent, Jan2011

Jan. 11, 2011
ti22rabdg.cl

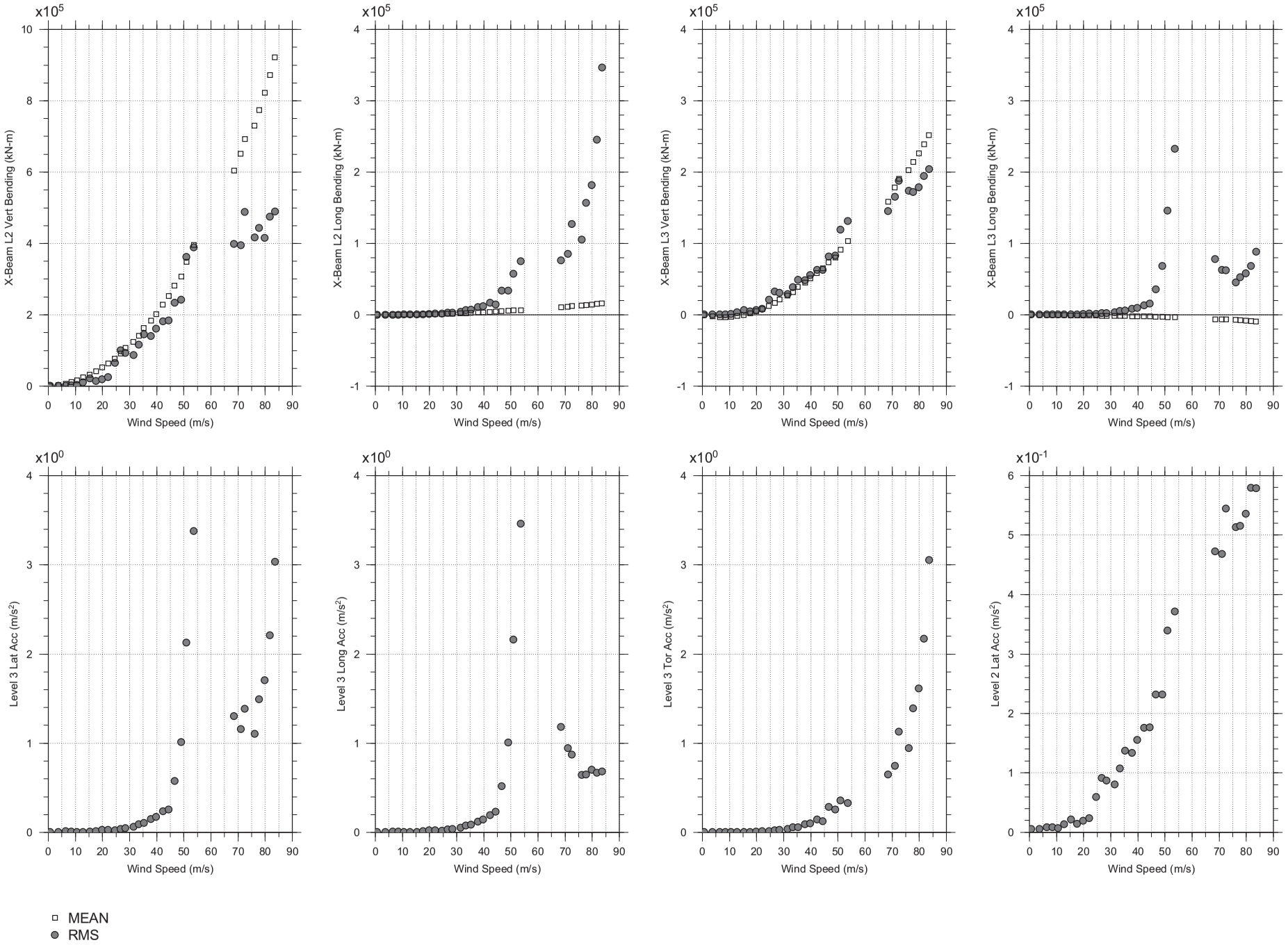

Messina Bridge, In Service Tower, 10 degree, Turbulent, Jan2011

Jan. 11, 2011
ti22rabdg.cl

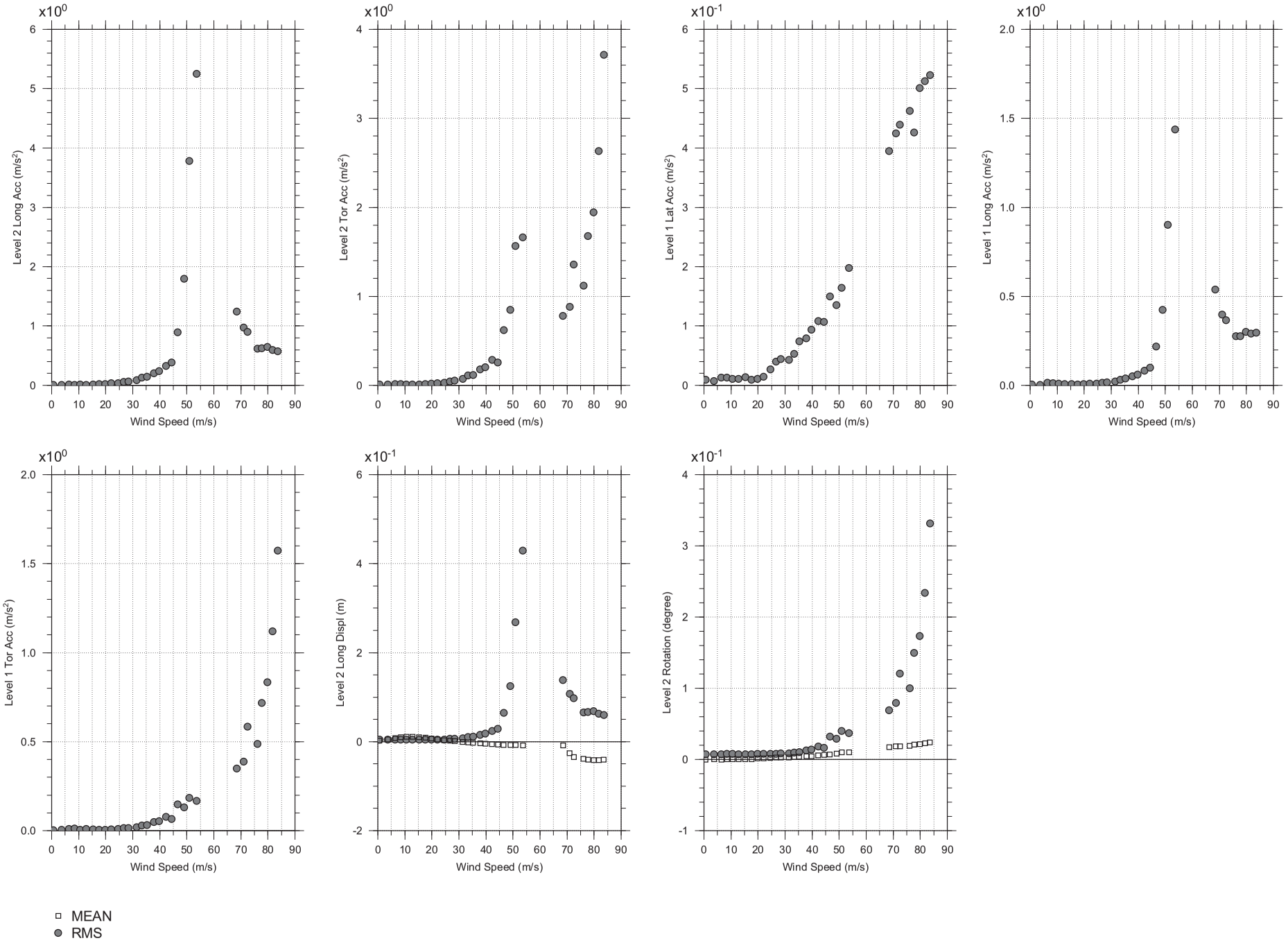

Messina Bridge, In Service Tower, 10 degree, Turbulent, Jan2011

Jan. 11, 2011
ti22rabdg.cl

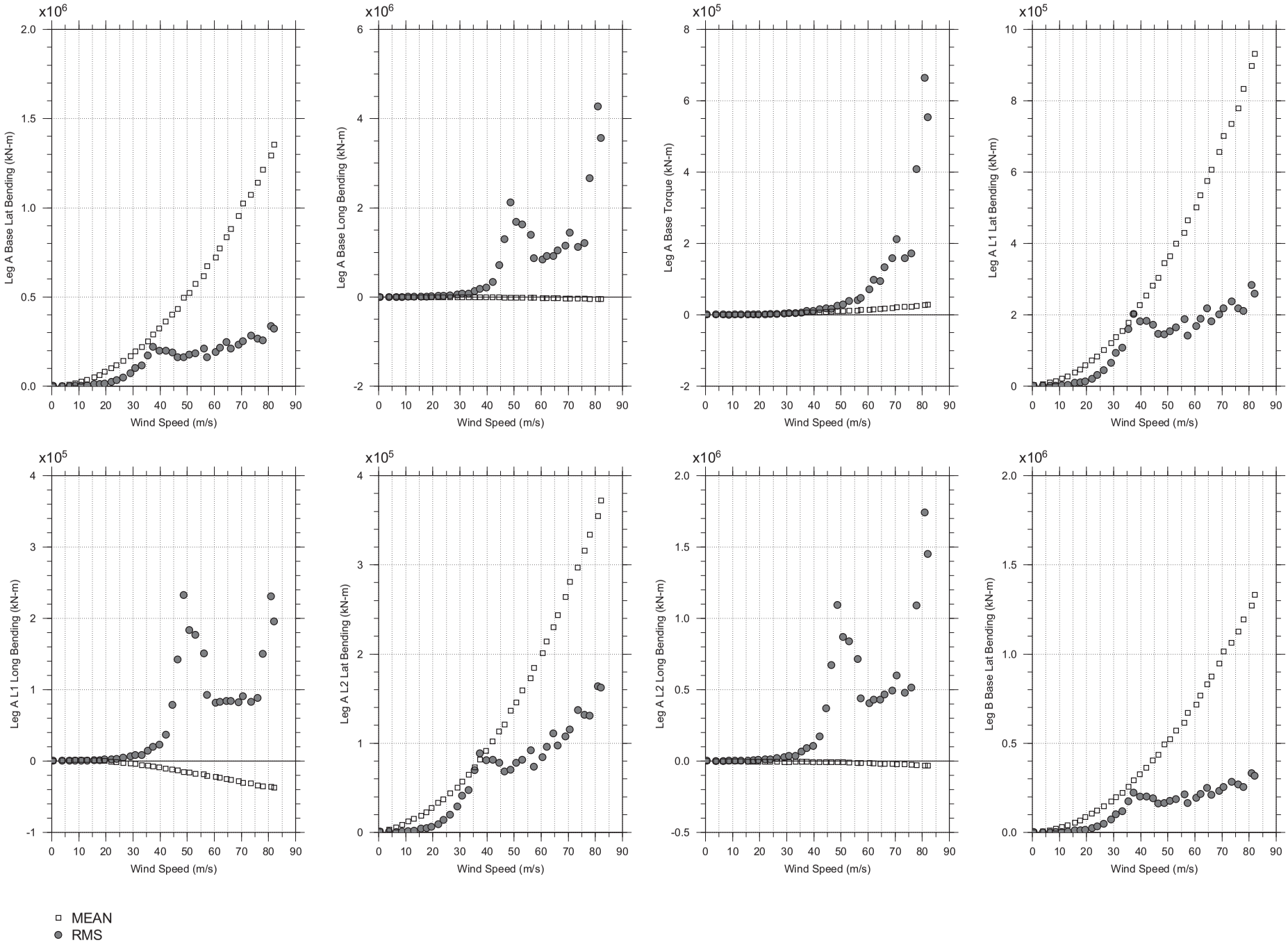

Messina Bridge, In Service Tower, 20 degree, Turbulent, Jan2011

Jan. 11, 2011
ti23abdg.cl

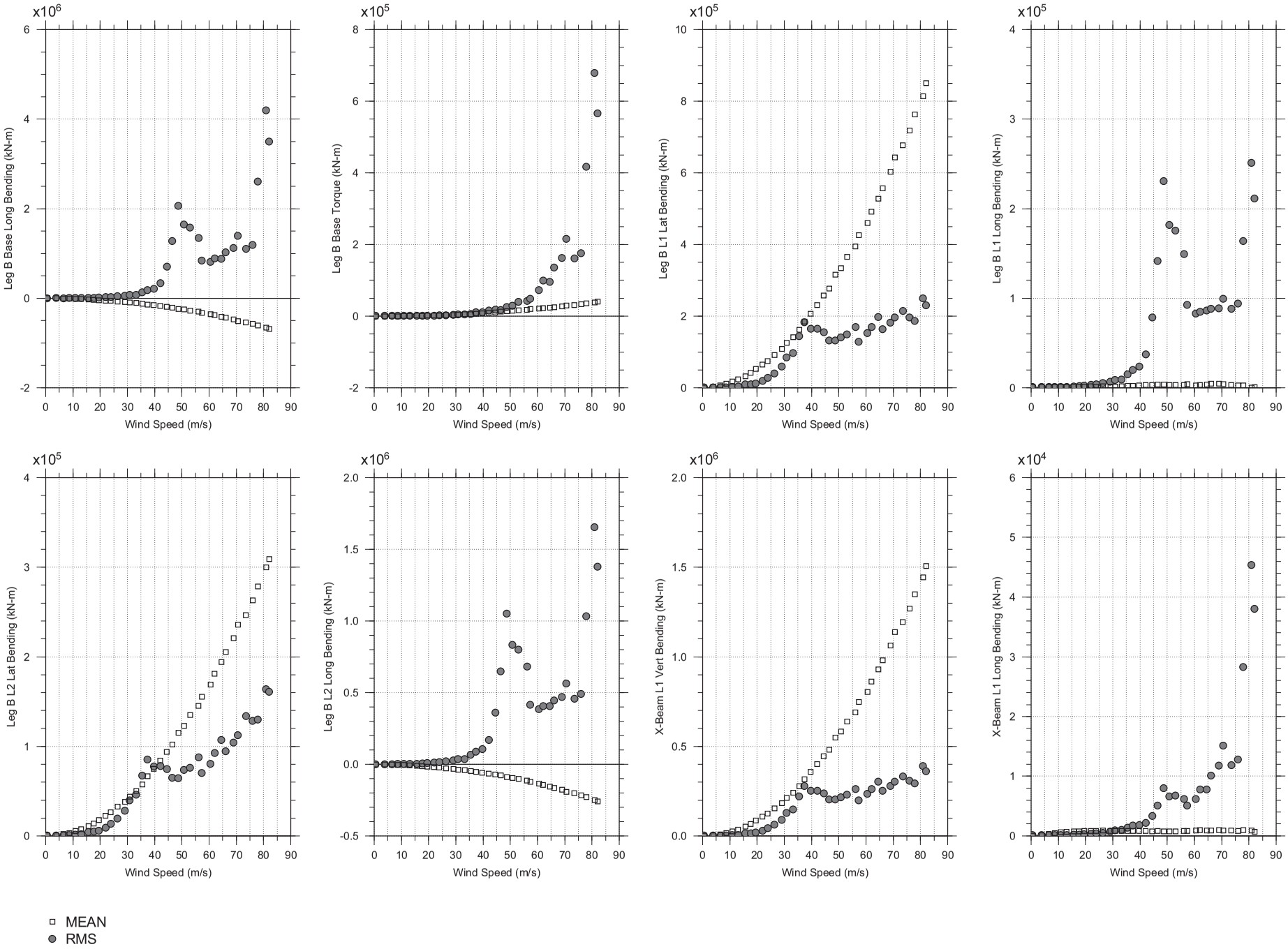

Messina Bridge, In Service Tower, 20 degree, Turbulent, Jan2011

Jan. 11, 2011
ti23abdg.cl

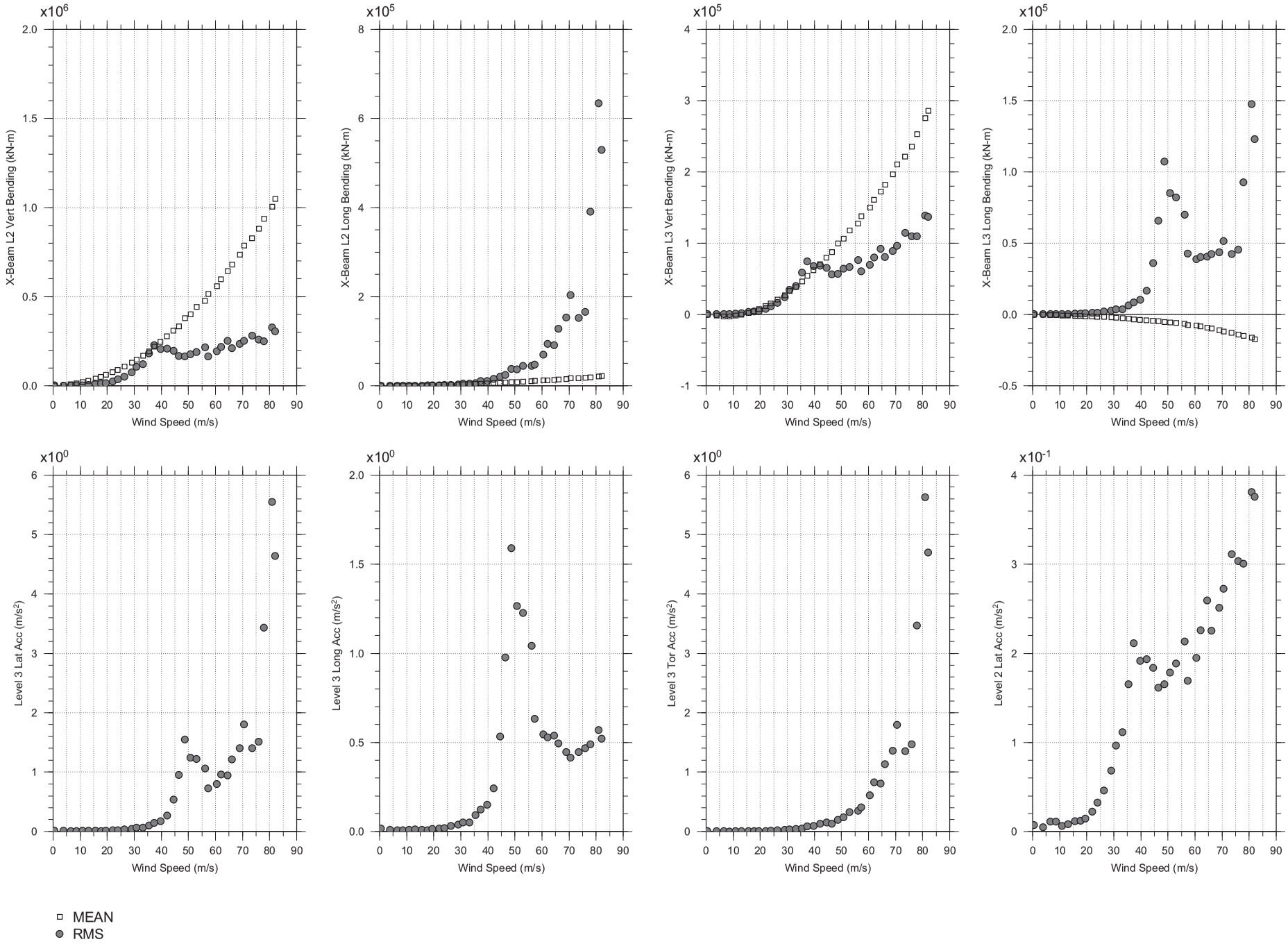

Messina Bridge, In Service Tower, 20 degree, Turbulent, Jan2011

Jan. 11, 2011
ti23abdg.cl

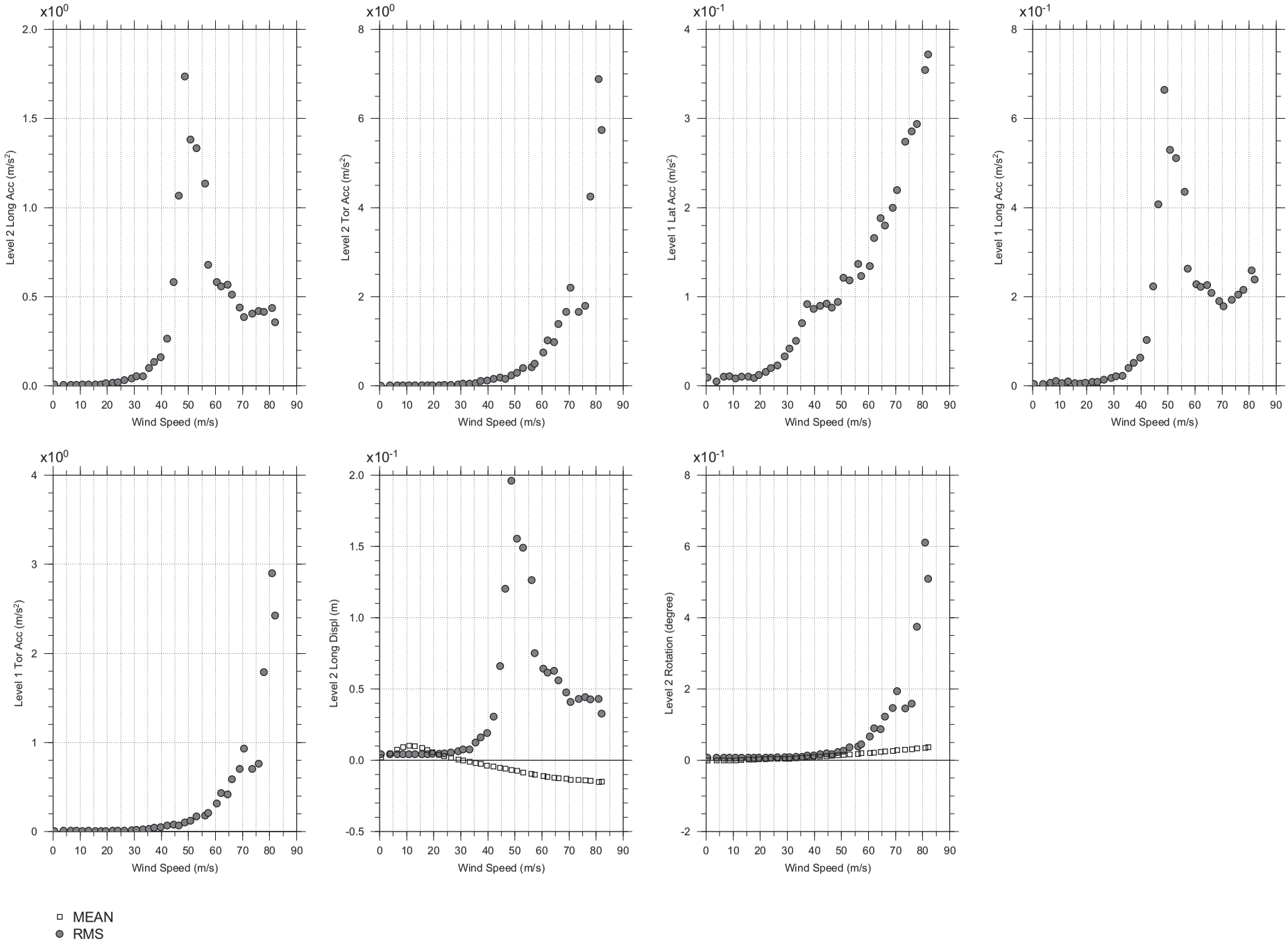

Messina Bridge, In Service Tower, 20 degree, Turbulent, Jan2011

Jan. 11, 2011
ti23abdg.cl

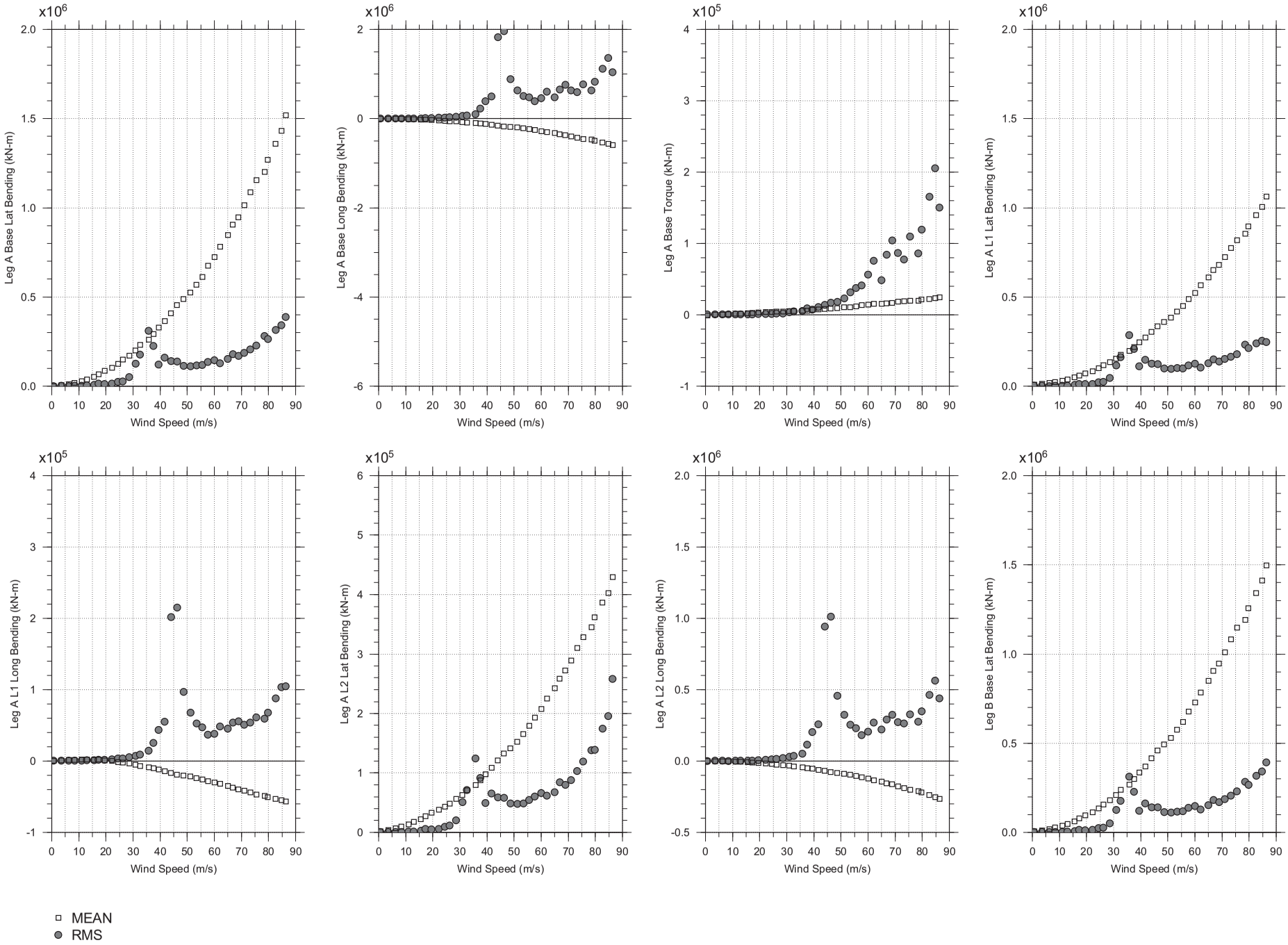

Messina Bridge, In Service Tower, 30 degree, Turbulent, Jan2011

Jan. 11, 2011
ti24abdg.cl

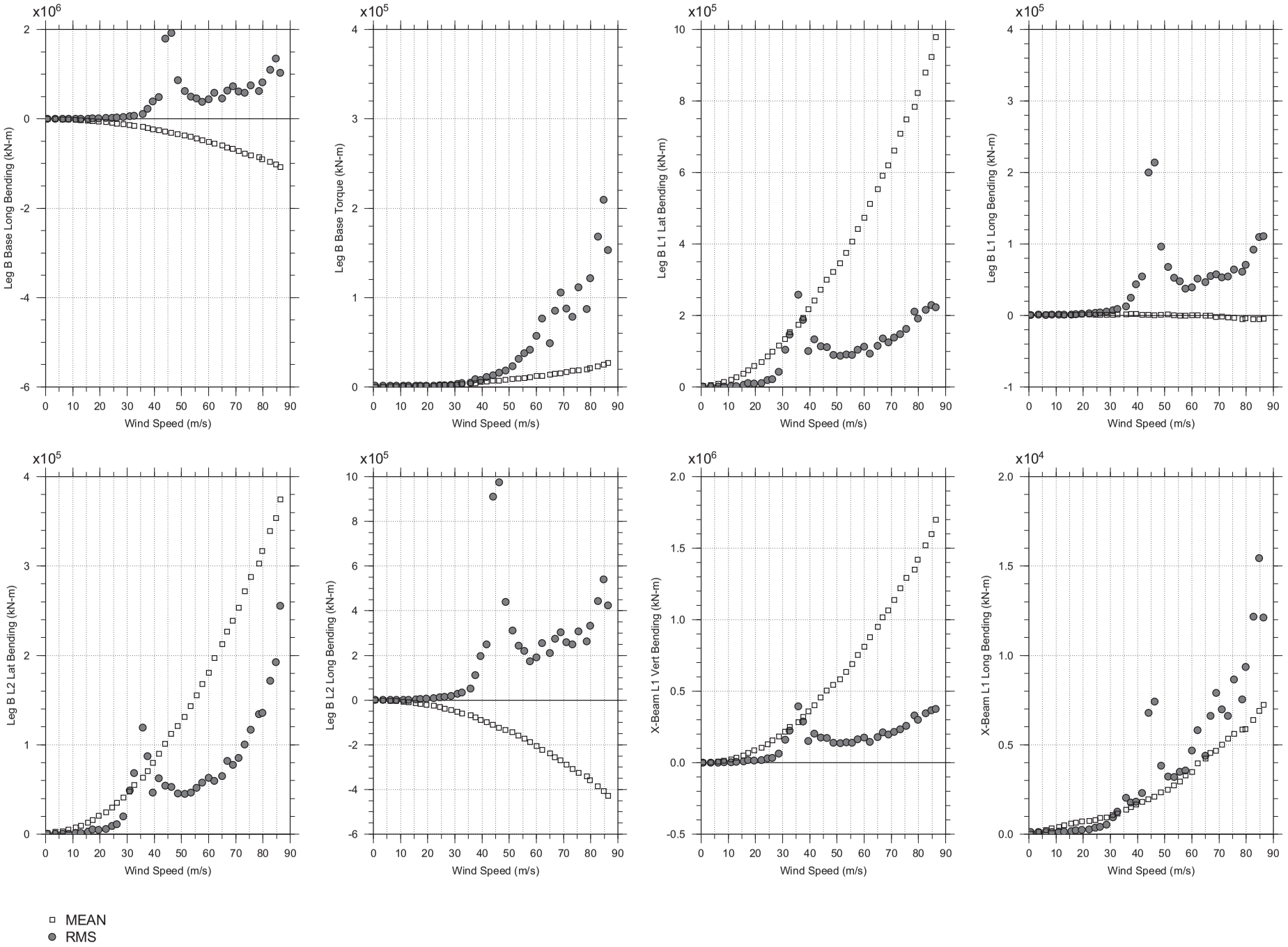

Messina Bridge, In Service Tower, 30 degree, Turbulent, Jan2011

Jan. 11, 2011
ti24abdg.cl

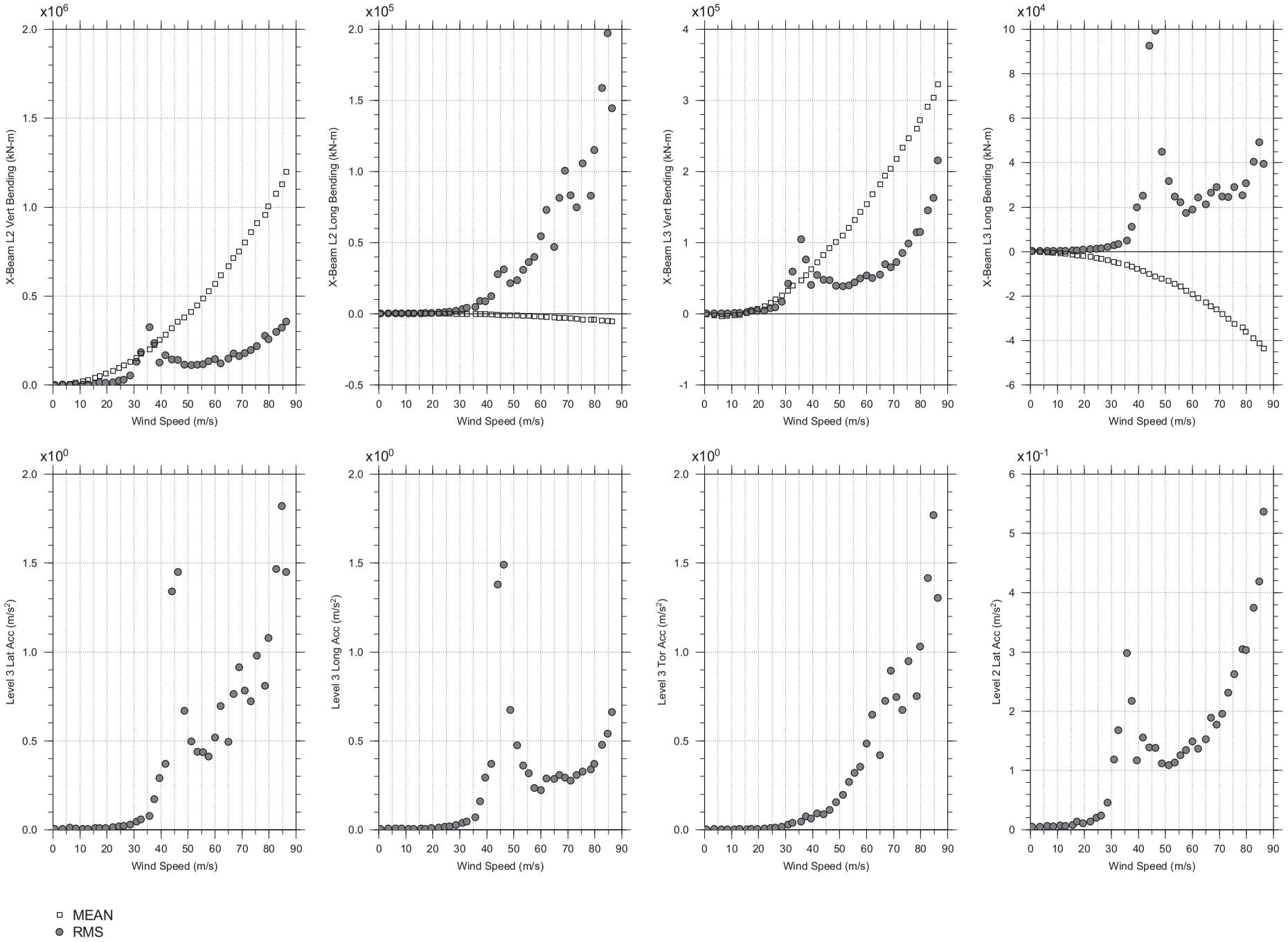

Messina Bridge, In Service Tower, 30 degree, Turbulent, Jan2011

Jan. 11, 2011
ti24abdg.cl

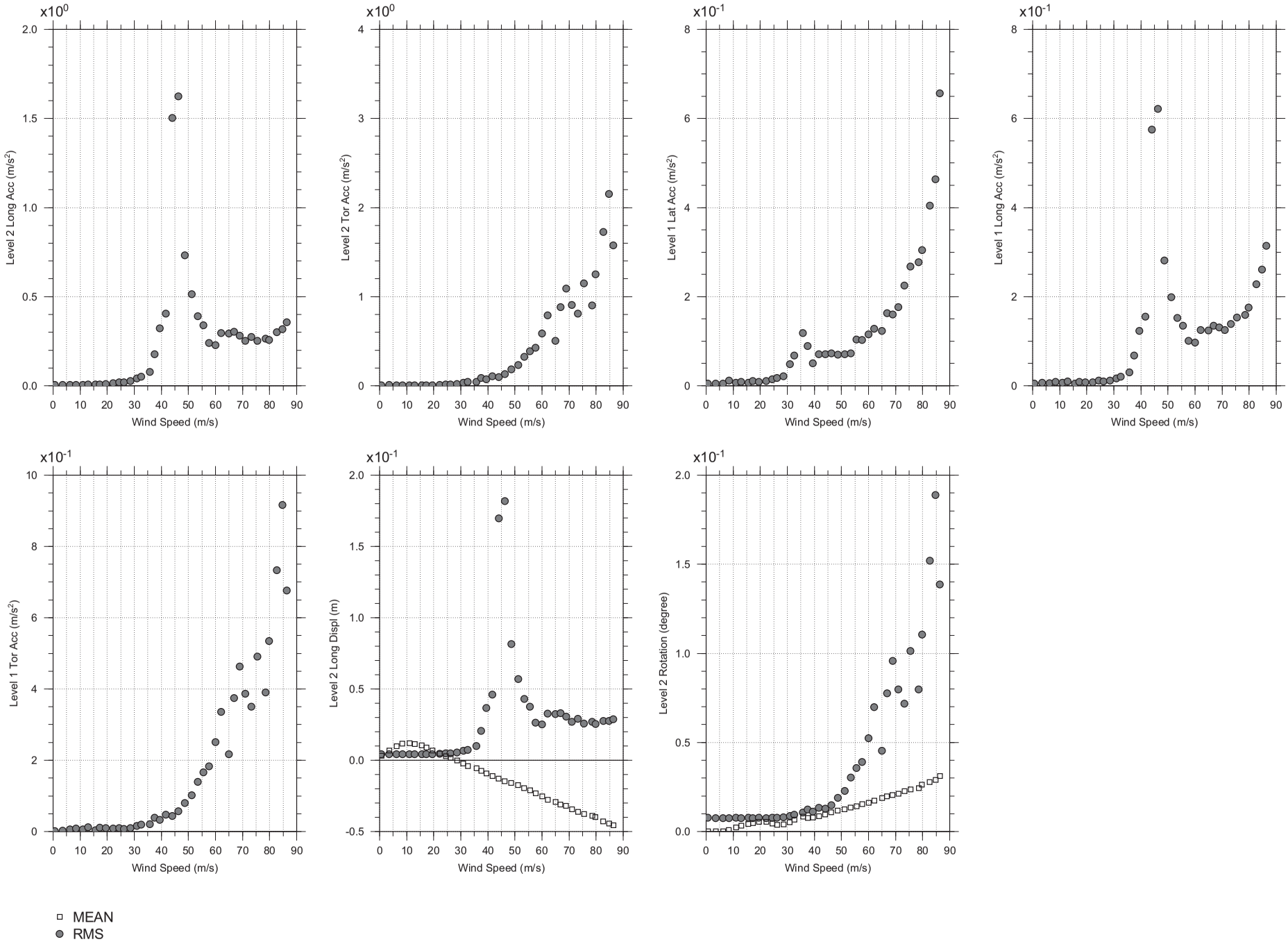

Messina Bridge, In Service Tower, 30 degree, Turbulent, Jan2011

Jan. 11, 2011
ti24abdg.cl

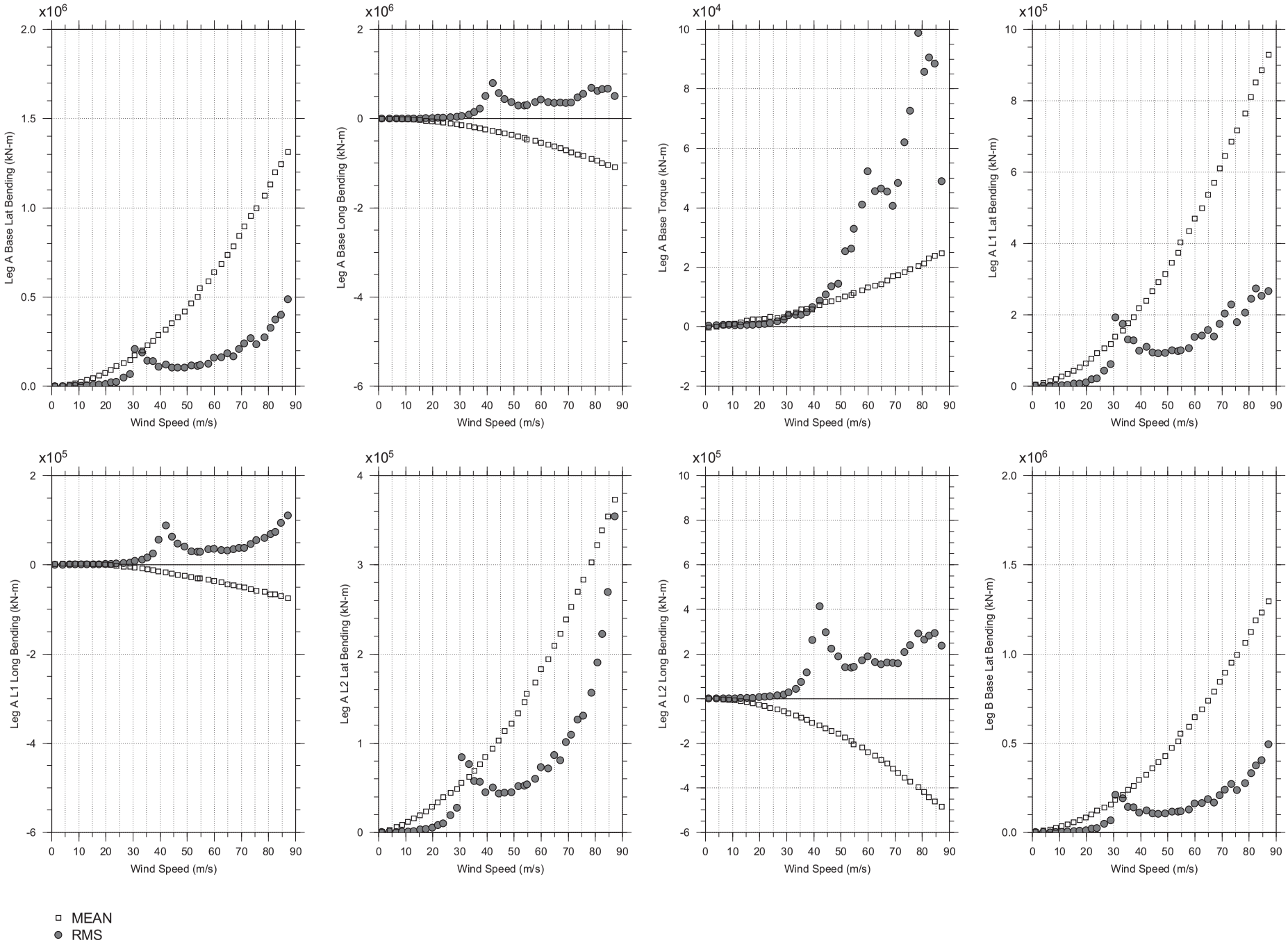

Messina Bridge, In Service Tower, 40 degree, Turbulent, Jan2011

Jan. 12, 2011
ti25abdg.cl

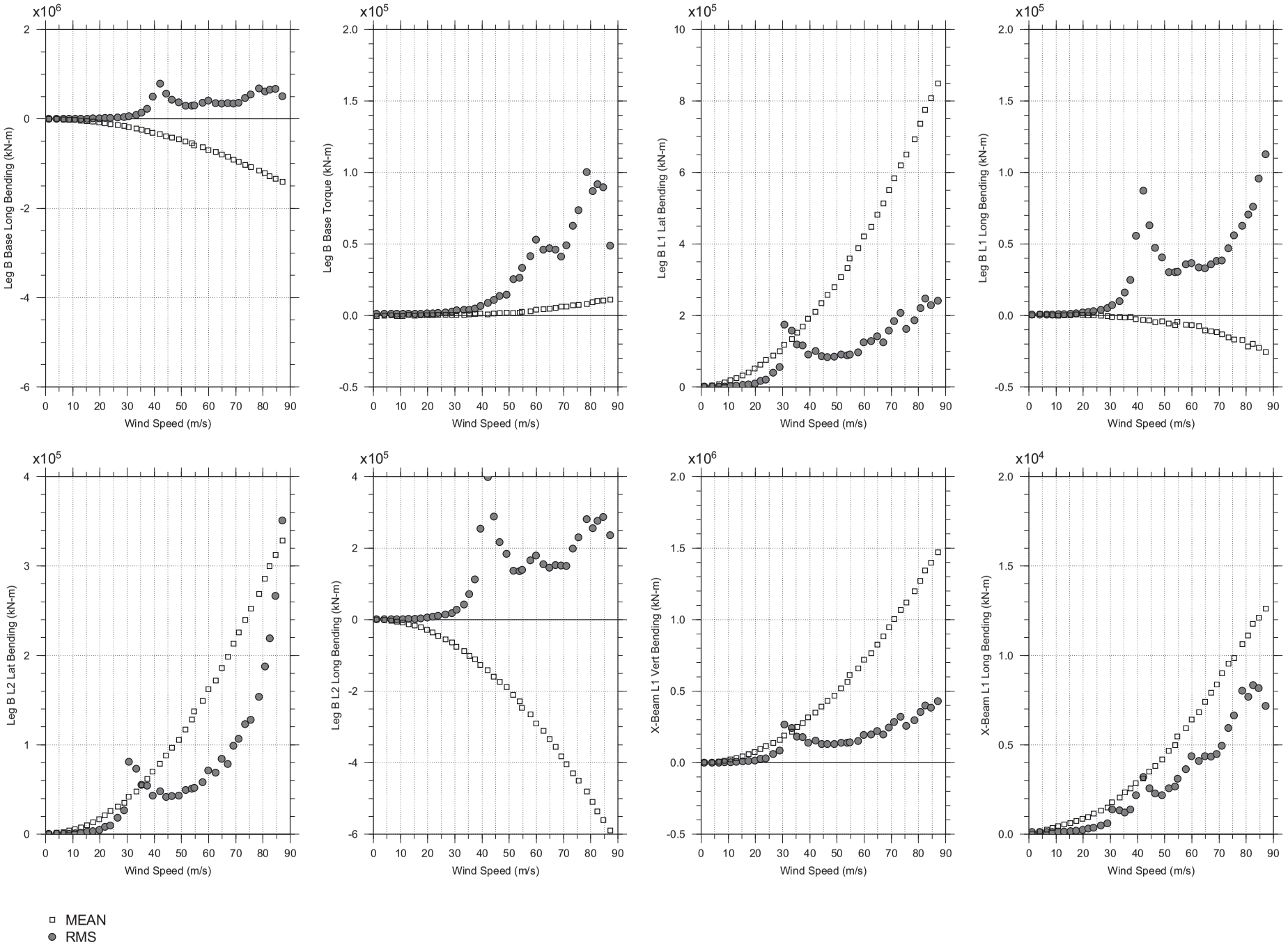

Messina Bridge, In Service Tower, 40 degree, Turbulent, Jan2011

Jan. 12, 2011
ti25abdg.cl

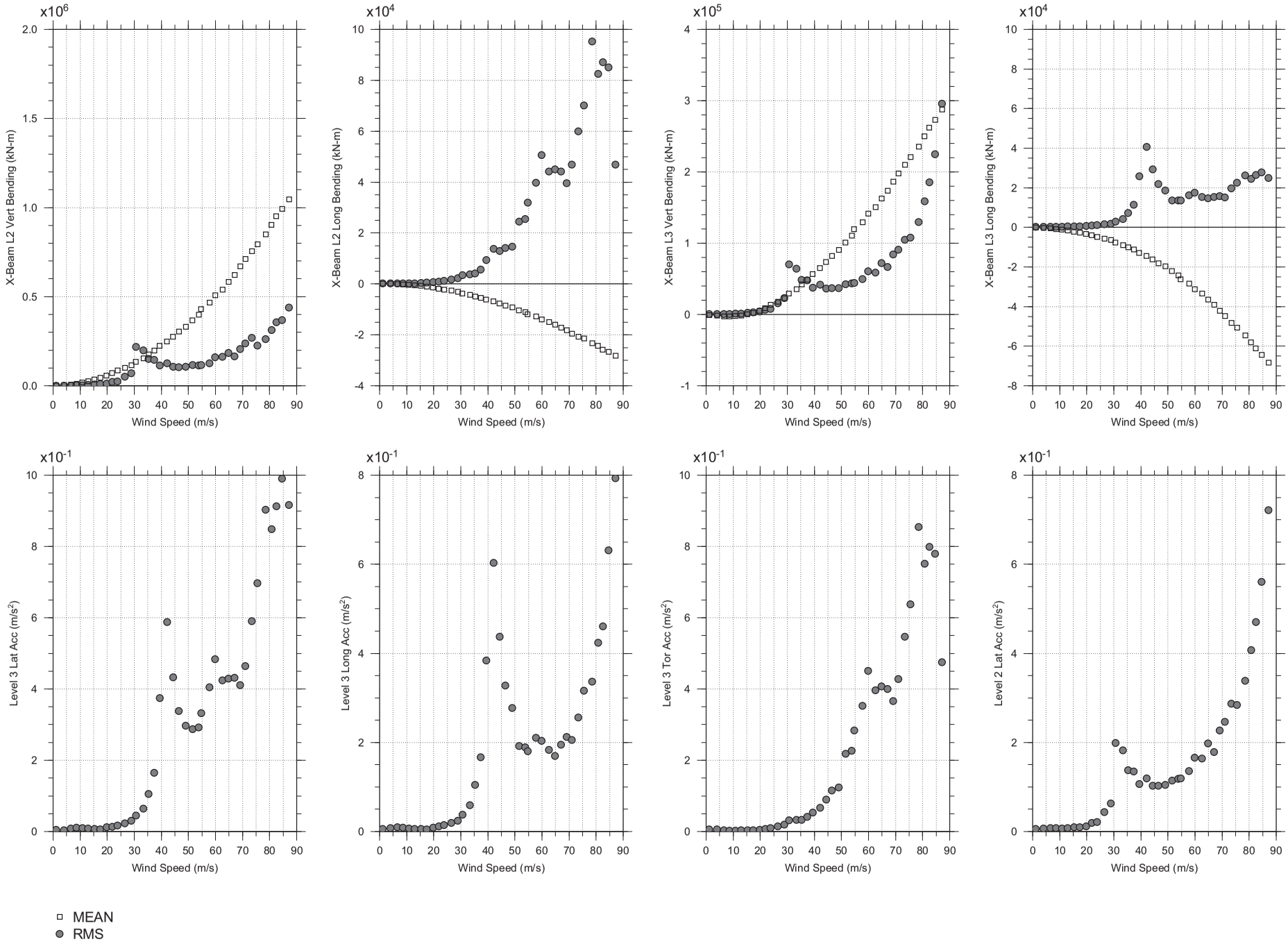

Messina Bridge, In Service Tower, 40 degree, Turbulent, Jan2011

Jan. 12, 2011
ti25abdg.cl

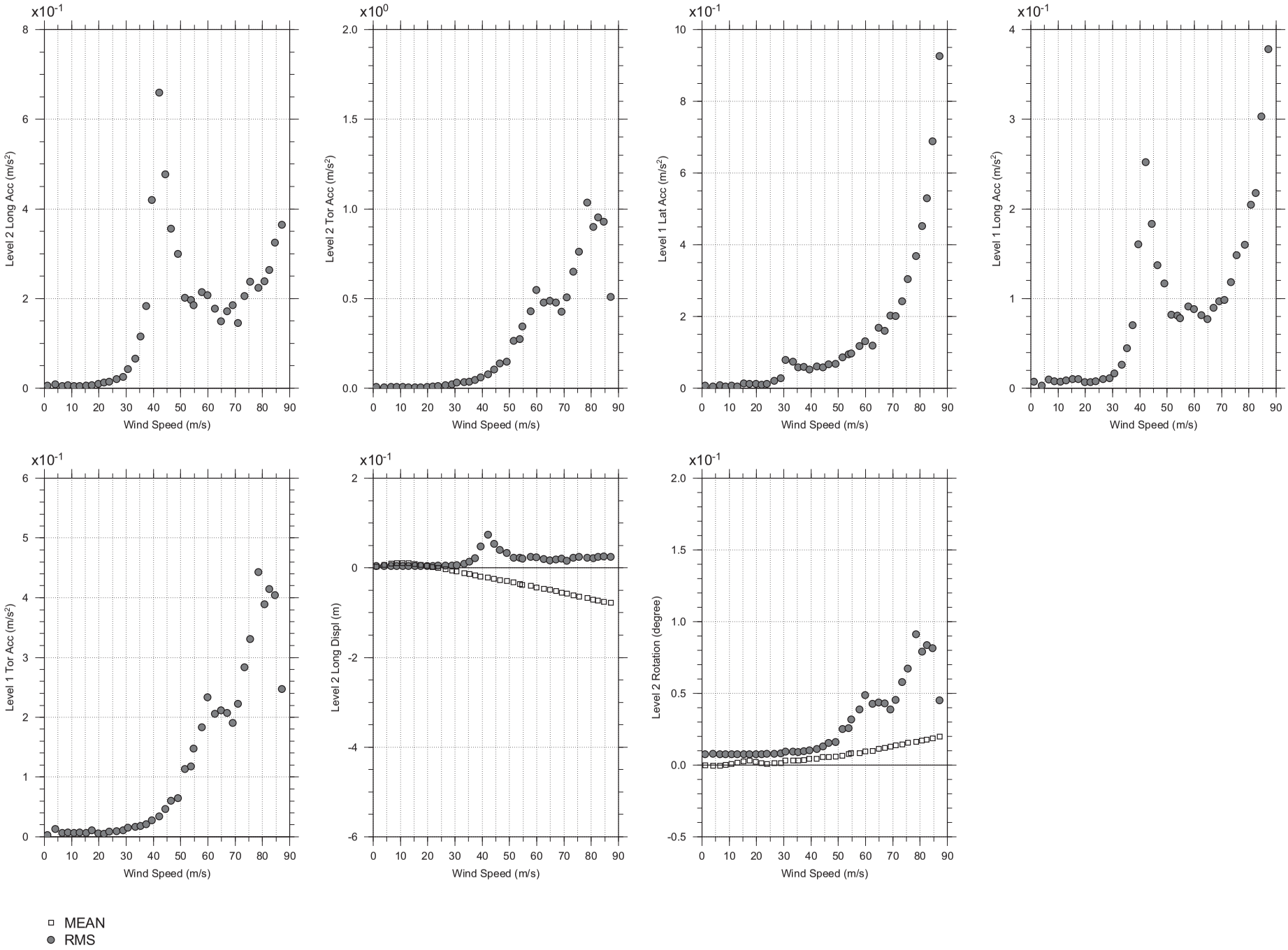

Messina Bridge, In Service Tower, 40 degree, Turbulent, Jan2011

Jan. 12, 2011
ti25abdg.cl

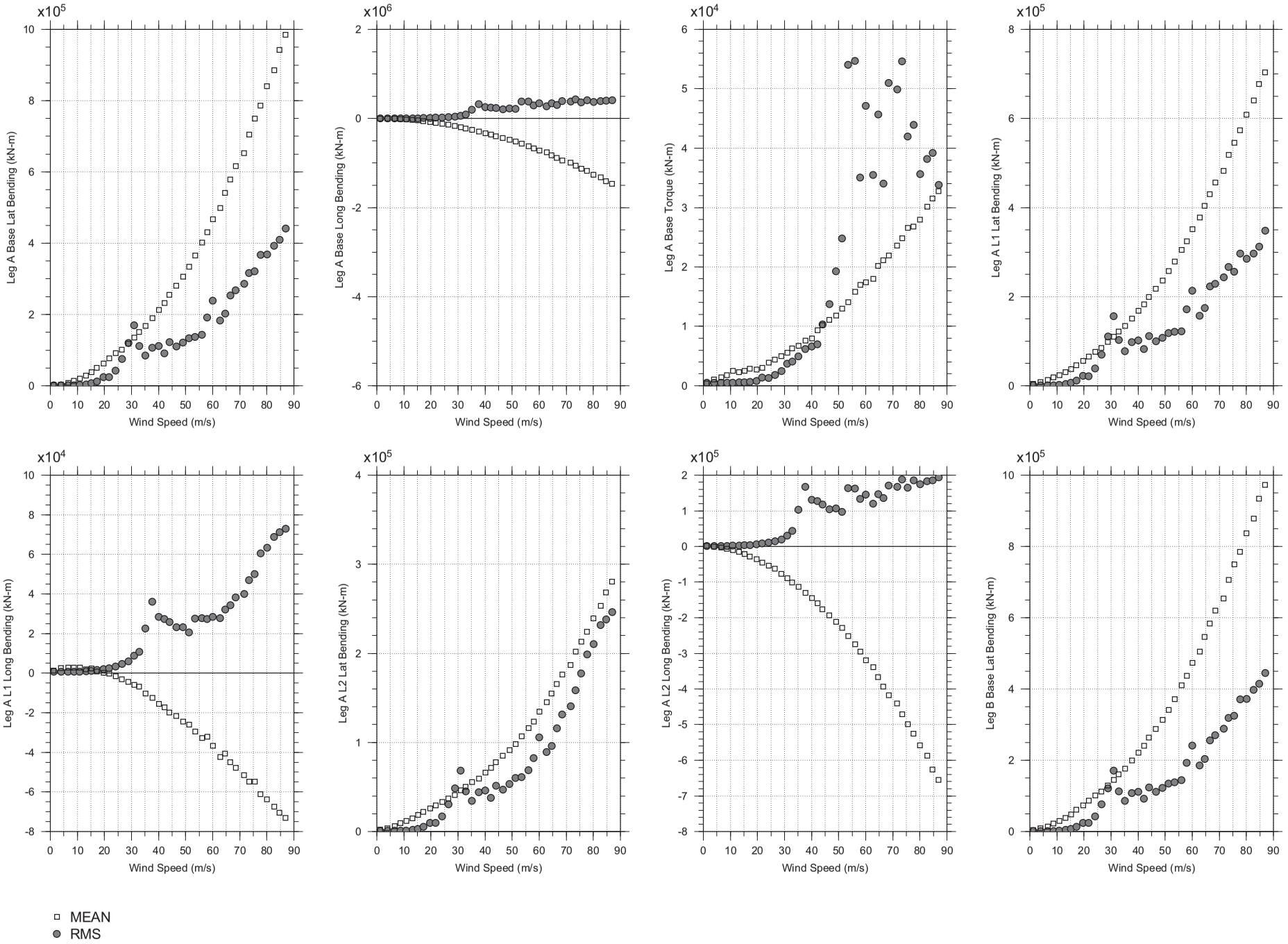

Messina Bridge, In Service Tower, 50 degree, Turbulent, Jan2011

Jan. 12, 2011
ti26abdg.cl

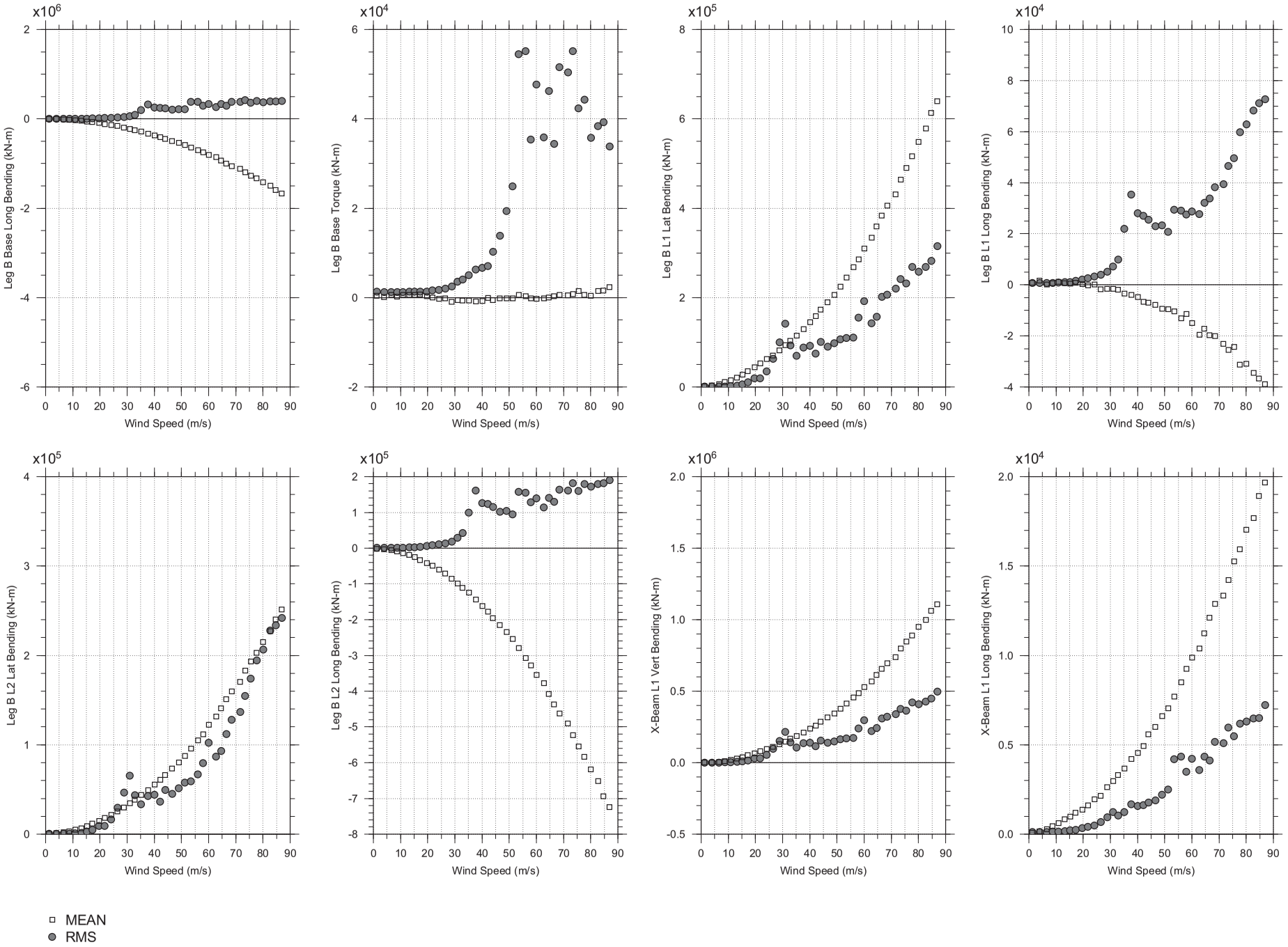

Messina Bridge, In Service Tower, 50 degree, Turbulent, Jan2011

Jan. 12, 2011
ti26abdg.cl

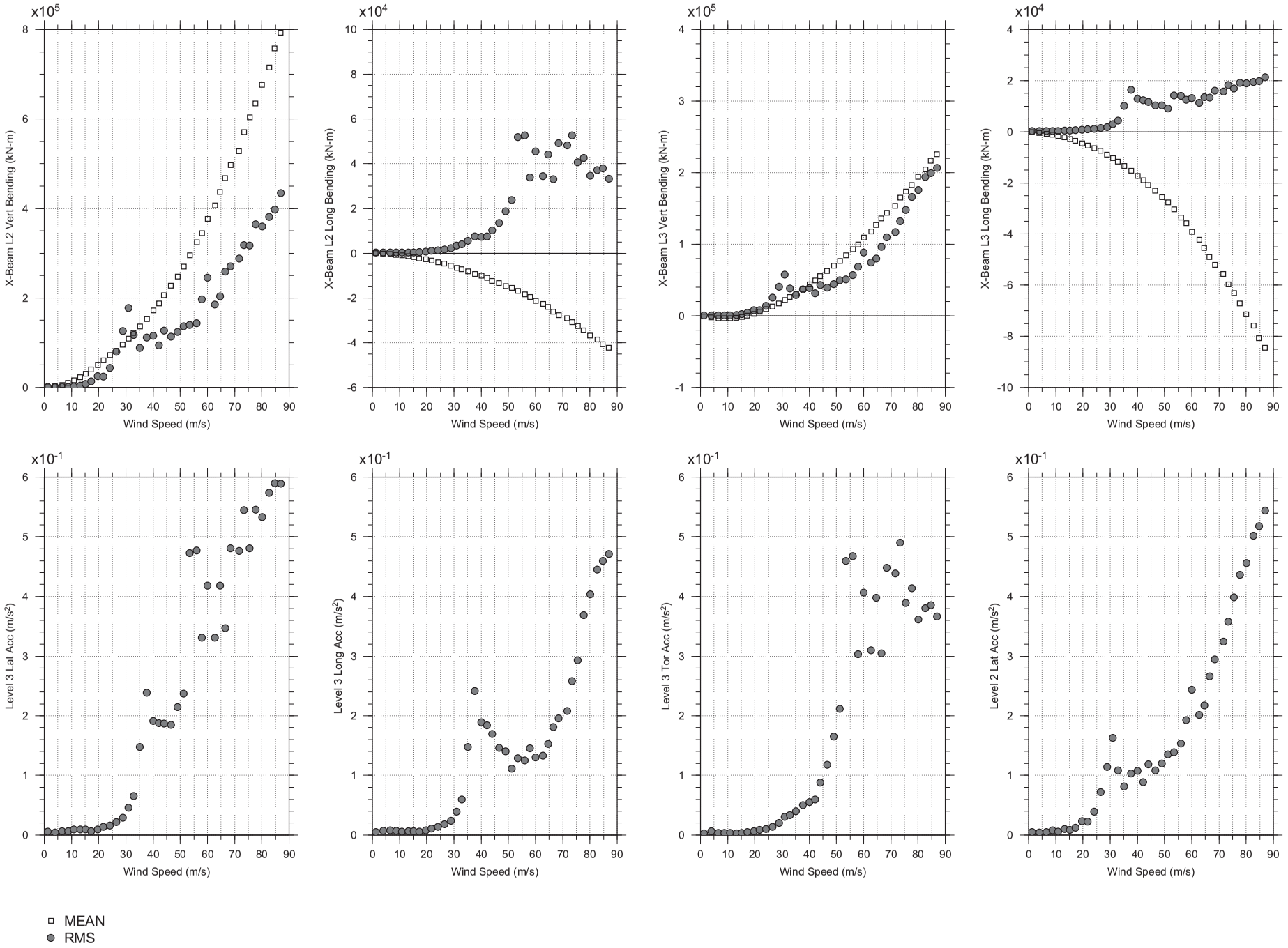

Messina Bridge, In Service Tower, 50 degree, Turbulent, Jan2011

Jan. 12, 2011
ti26abdg.cl

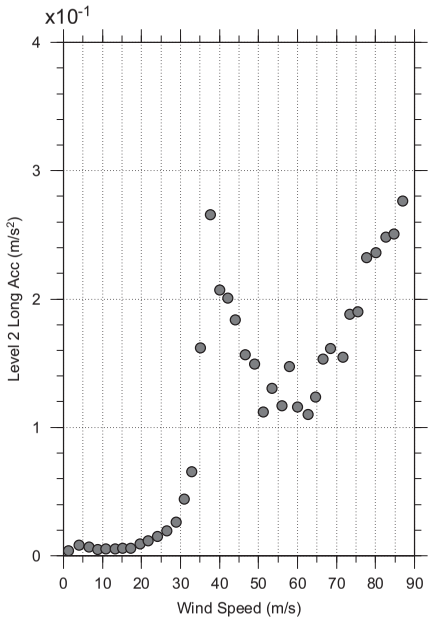

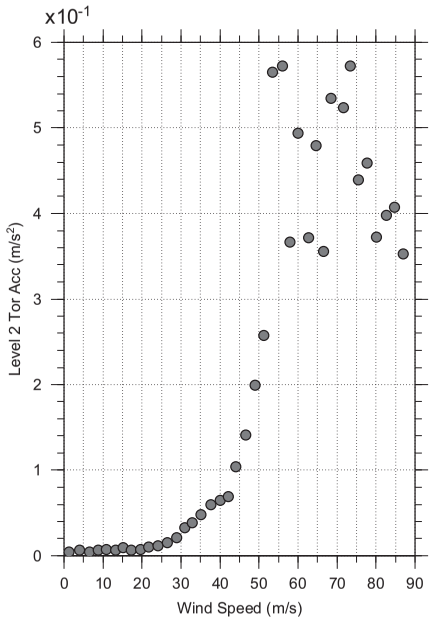

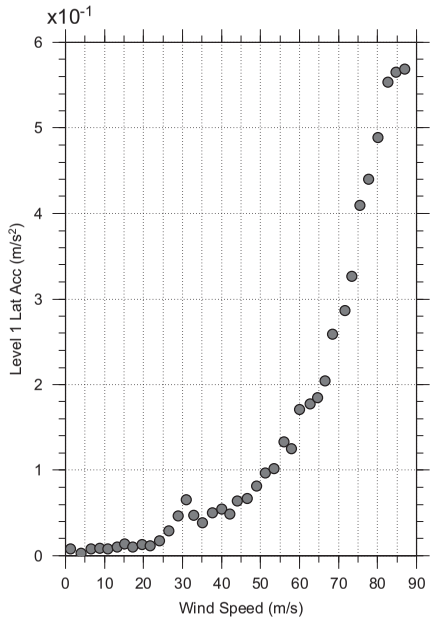

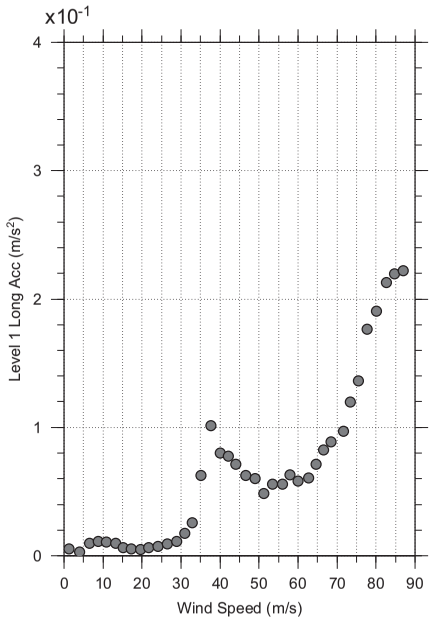

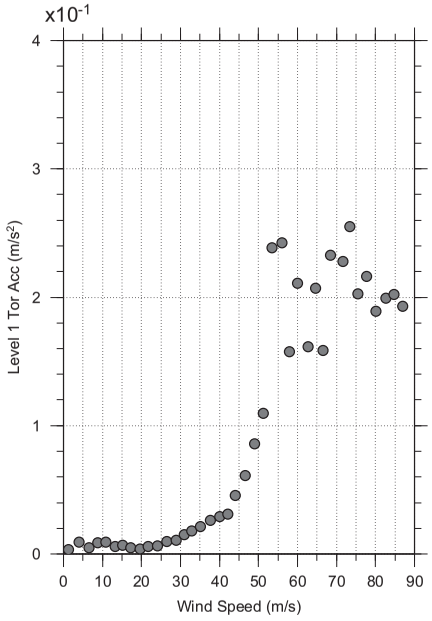

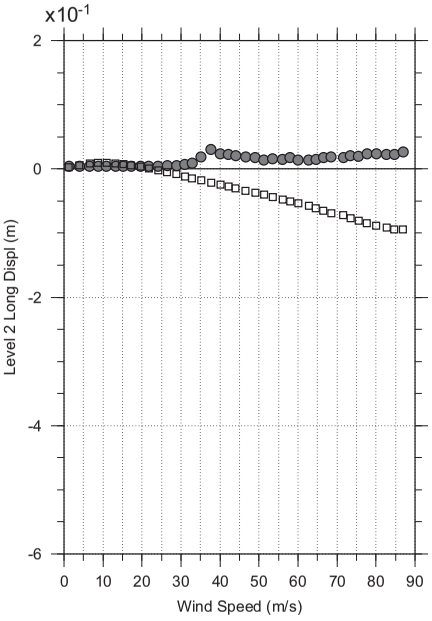

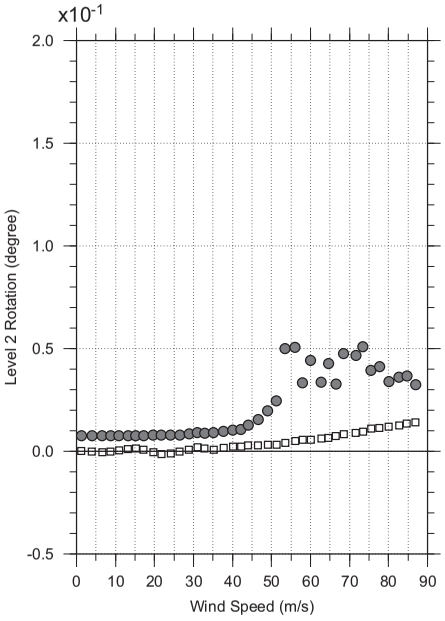

MEAN
RMS

Messina Bridge, In Service Tower, 50 degree, Turbulent, Jan2011

Jan. 12, 2011
ti26abdg.cl

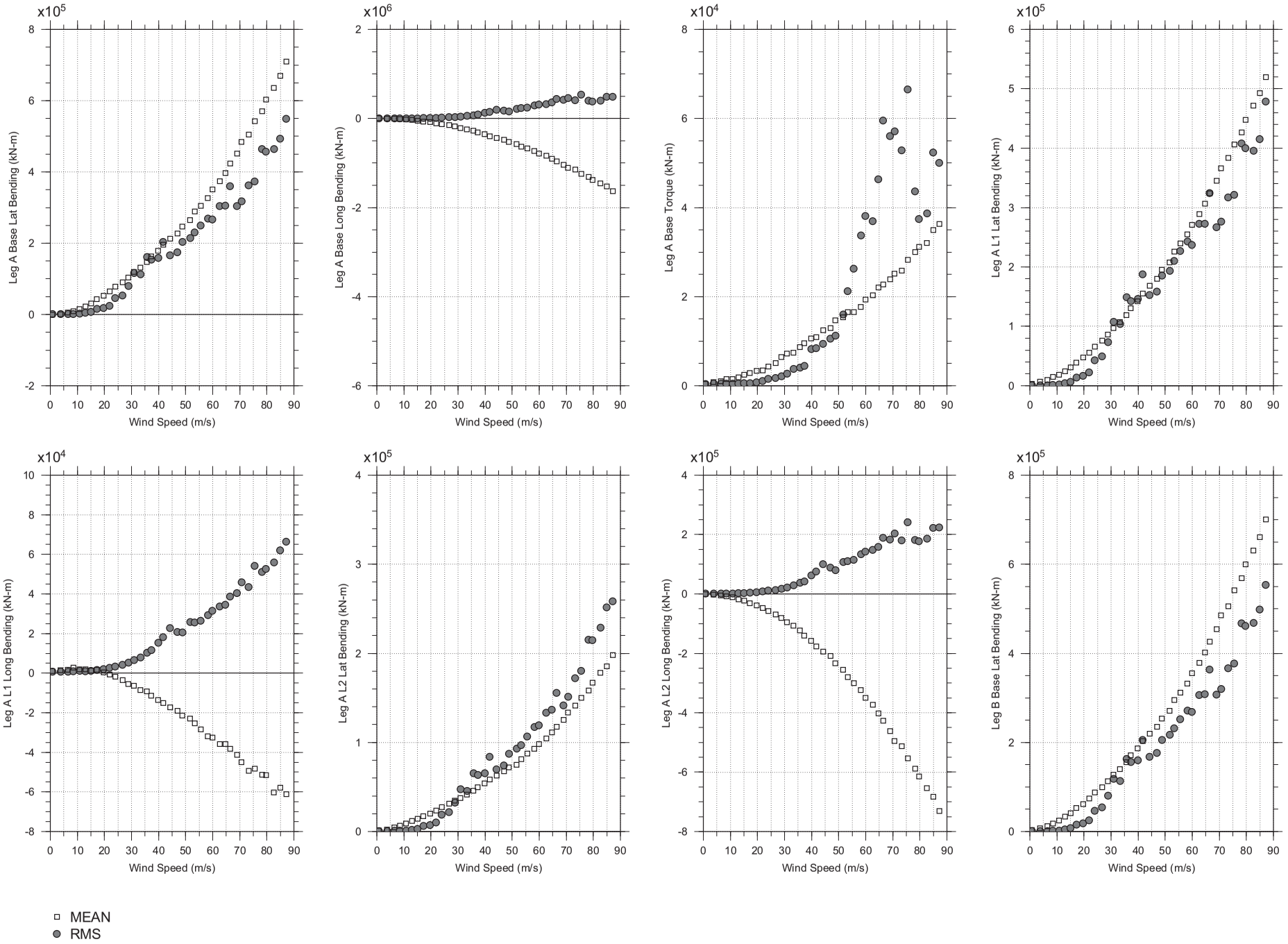

Messina Bridge, In Service Tower, 60 degree, Turbulent, Jan2011

Jan. 12, 2011
ti27abdg.cl

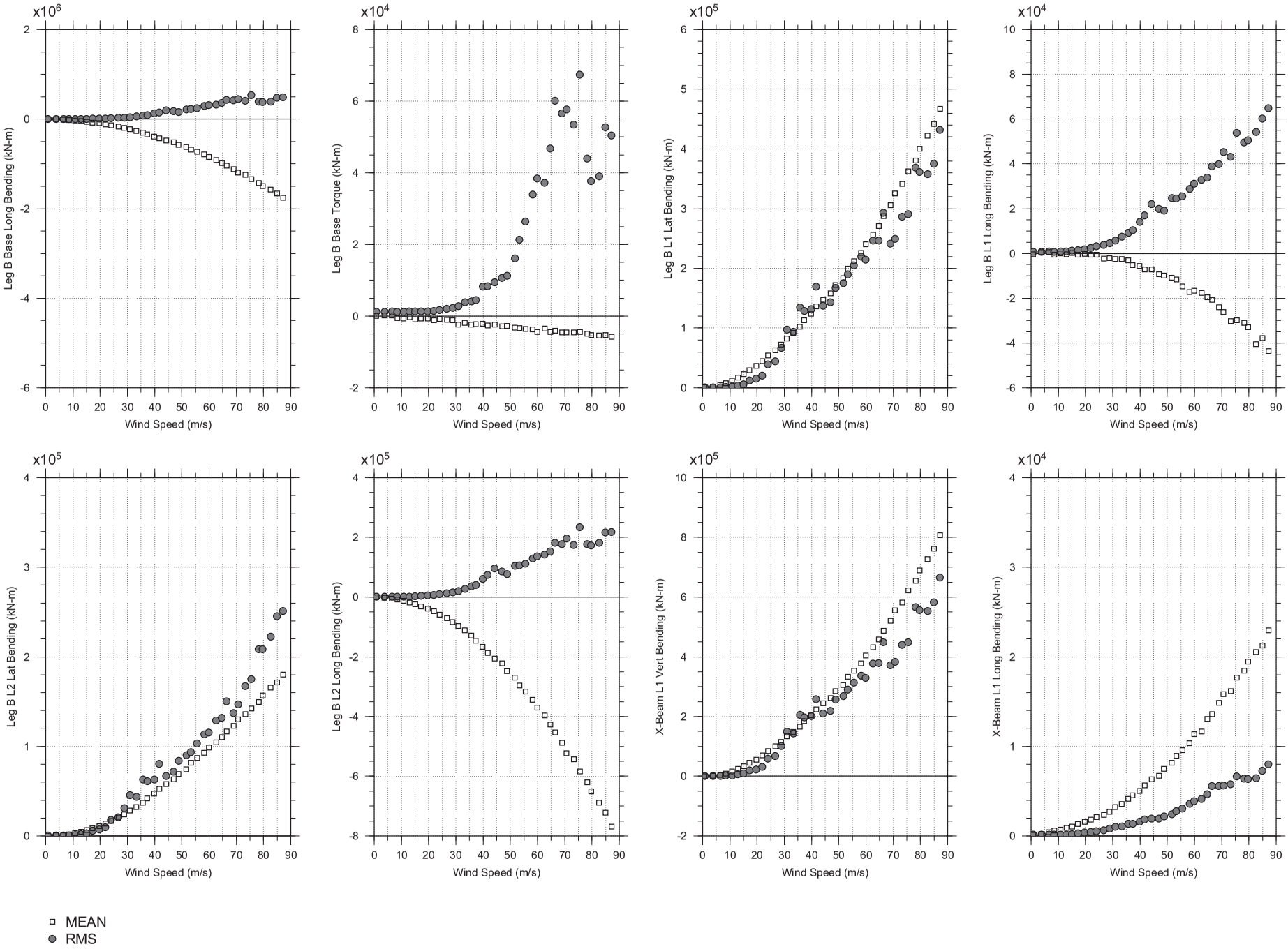

Messina Bridge, In Service Tower, 60 degree, Turbulent, Jan2011

Jan. 12, 2011
ti27abdg.cl

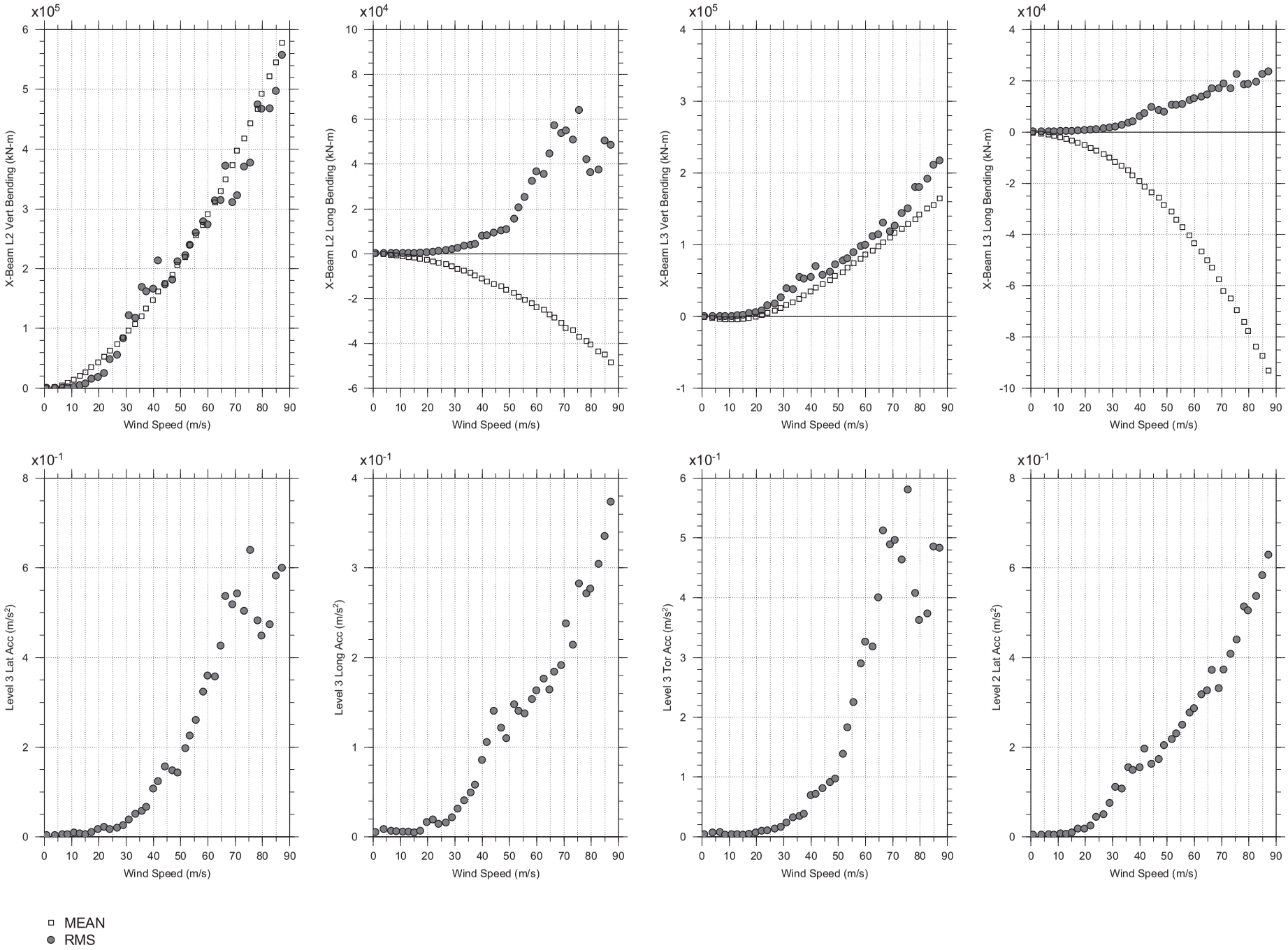

Messina Bridge, In Service Tower, 60 degree, Turbulent, Jan2011

Jan. 12, 2011
ti27abdg.cl

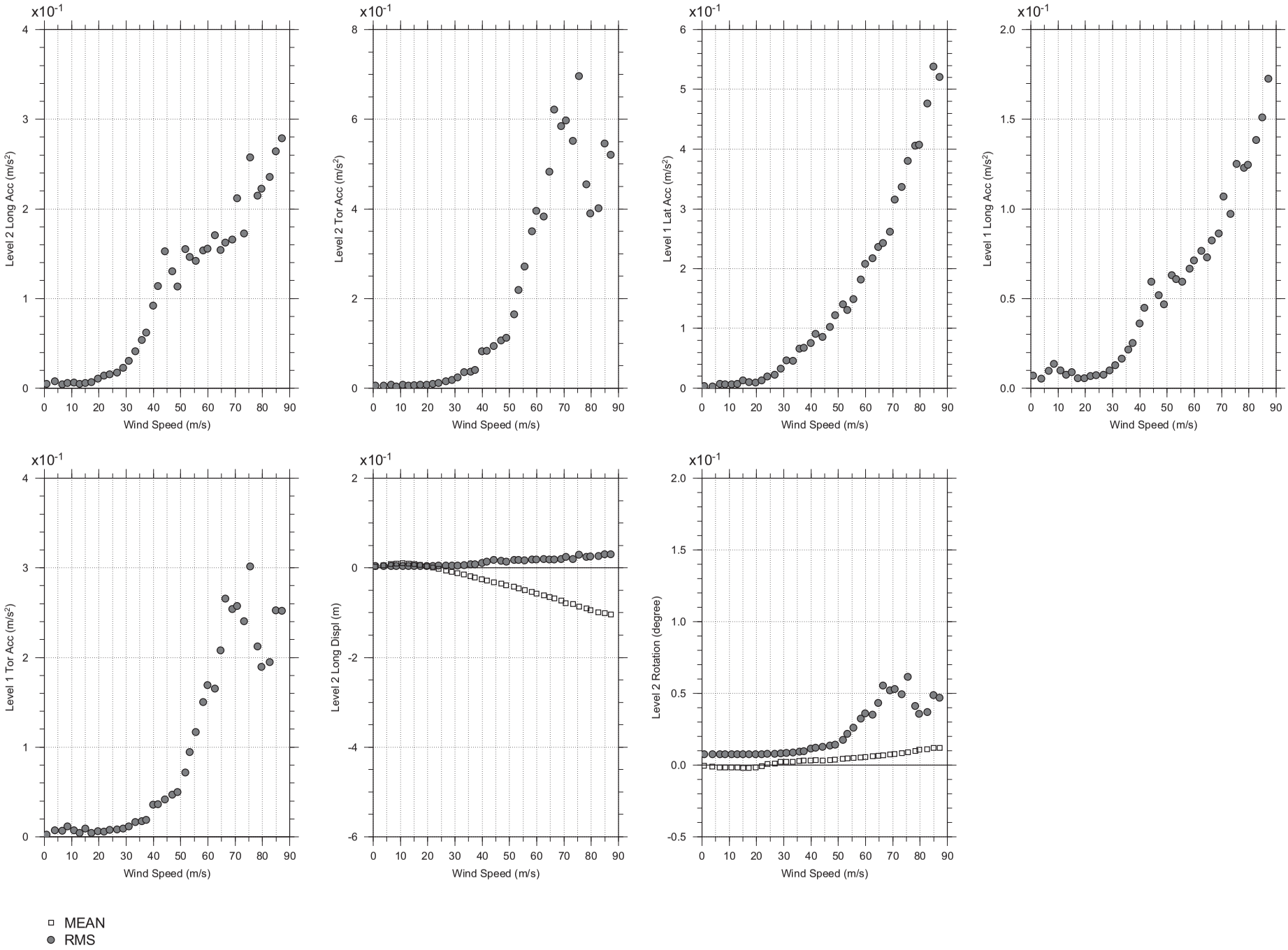

Messina Bridge, In Service Tower, 60 degree, Turbulent, Jan2011

Jan. 12, 2011
ti27abdg.cl

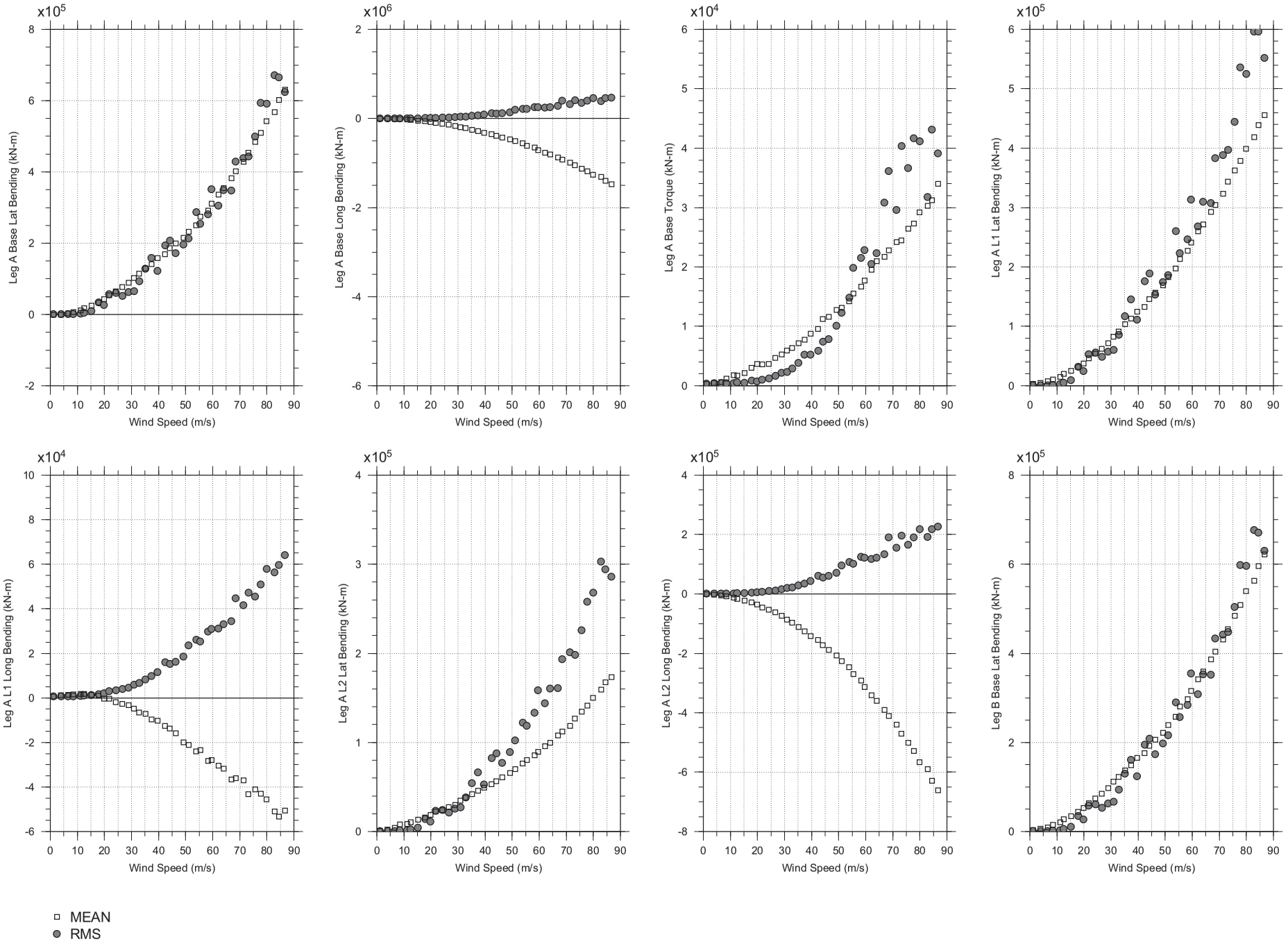

Messina Bridge, In Service Tower, 70 degree, Turbulent, Jan2011

Jan. 12, 2011
ti28abdg.cl

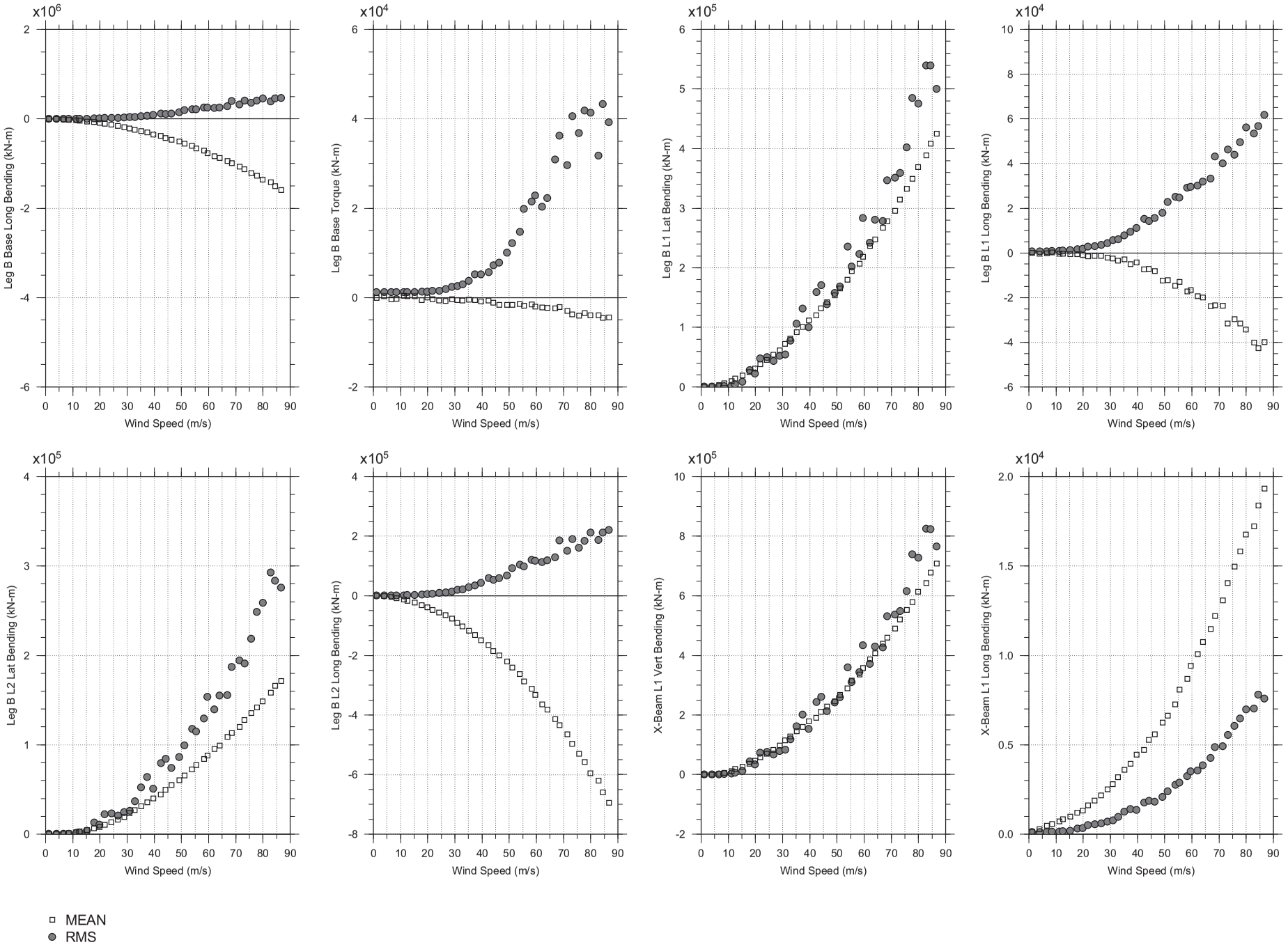

Messina Bridge, In Service Tower, 70 degree, Turbulent, Jan2011

Jan. 12, 2011
ti28abdg.cl

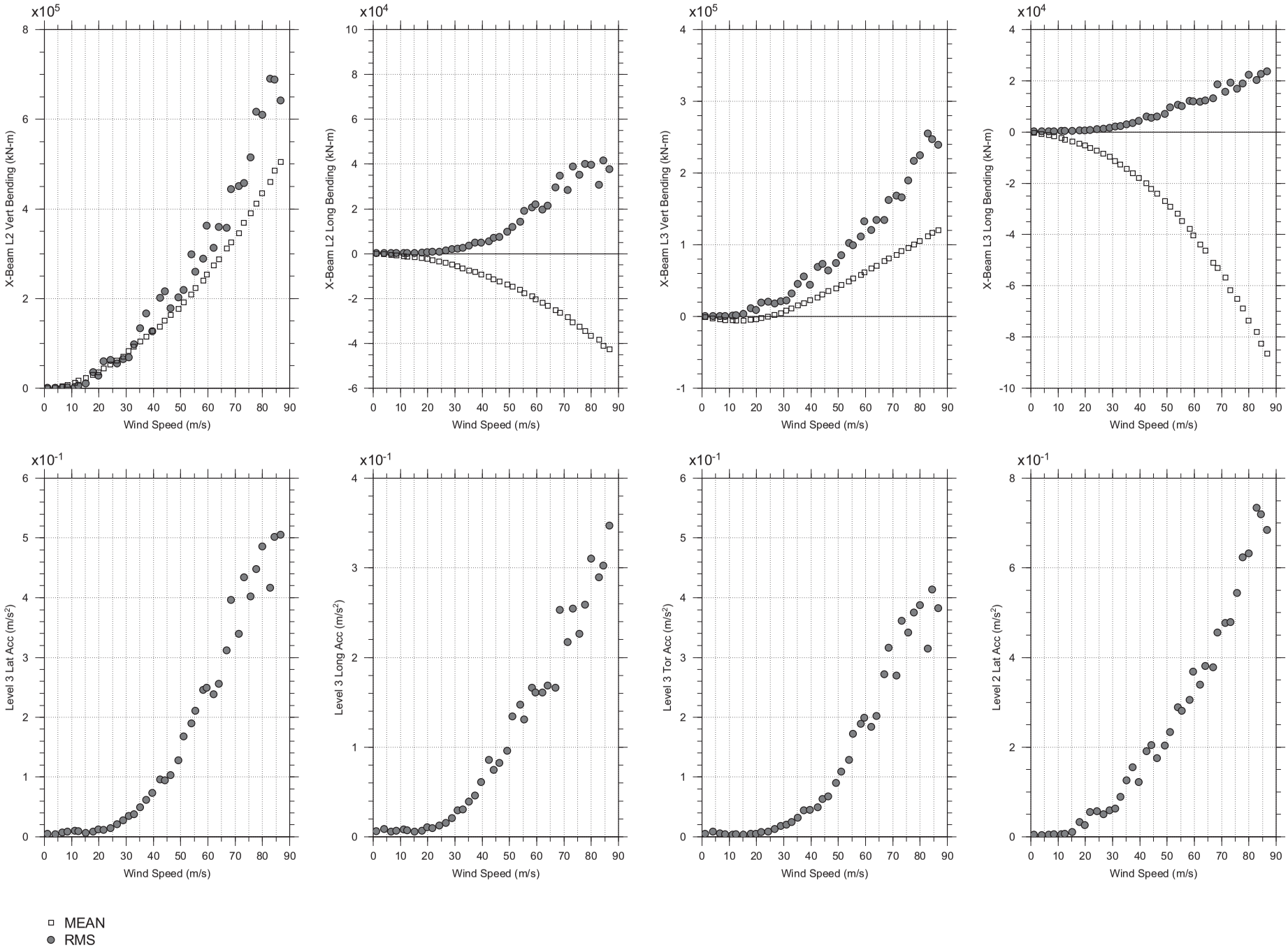

Messina Bridge, In Service Tower, 70 degree, Turbulent, Jan2011

Jan. 12, 2011
ti28abdg.cl

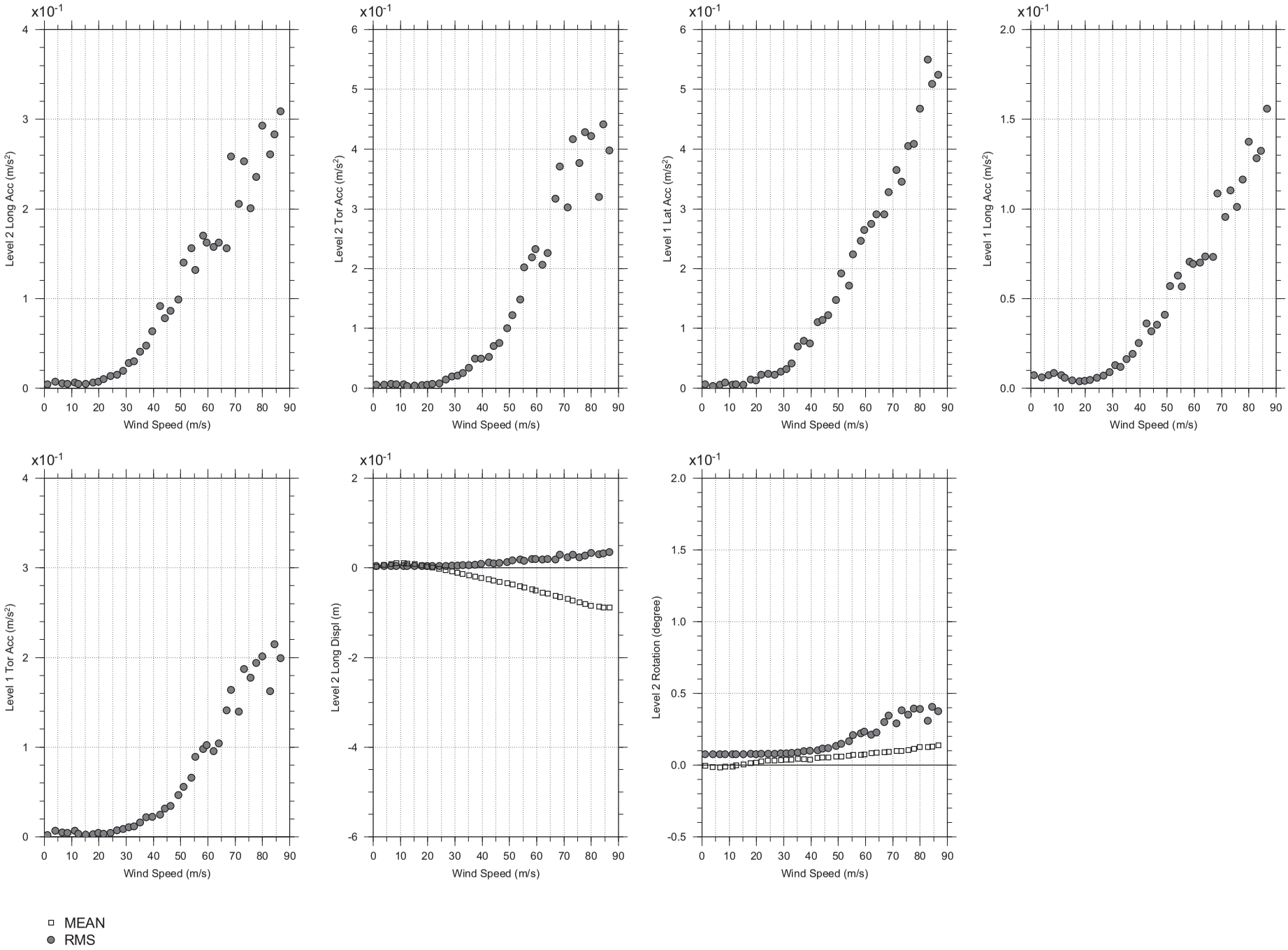

Messina Bridge, In Service Tower, 70 degree, Turbulent, Jan2011

Jan. 12, 2011
ti28abdg.cl

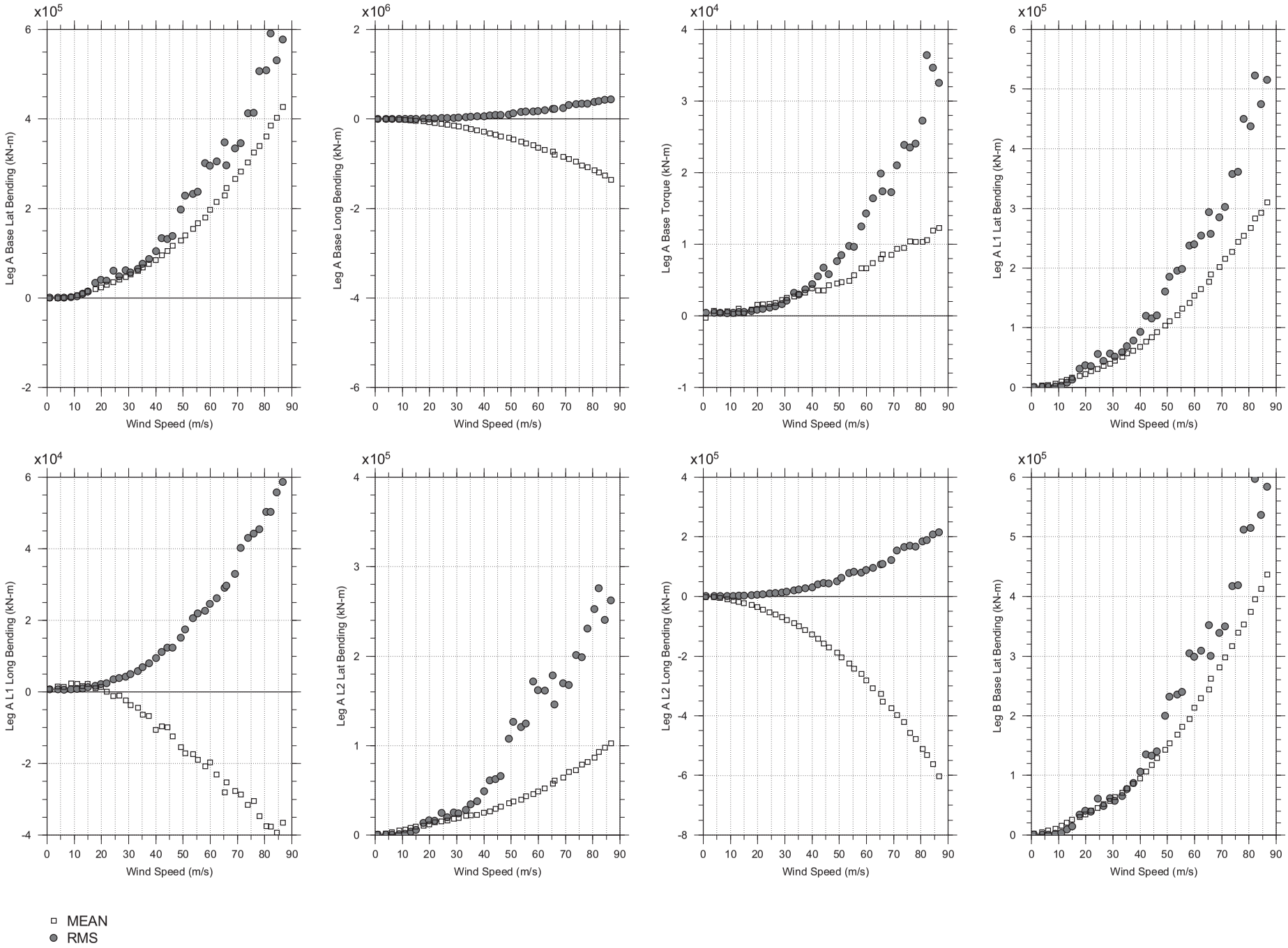

Messina Bridge, In Service Tower, 80 degree, Turbulent, Jan2011

Jan. 12, 2011
ti29abdg.cl

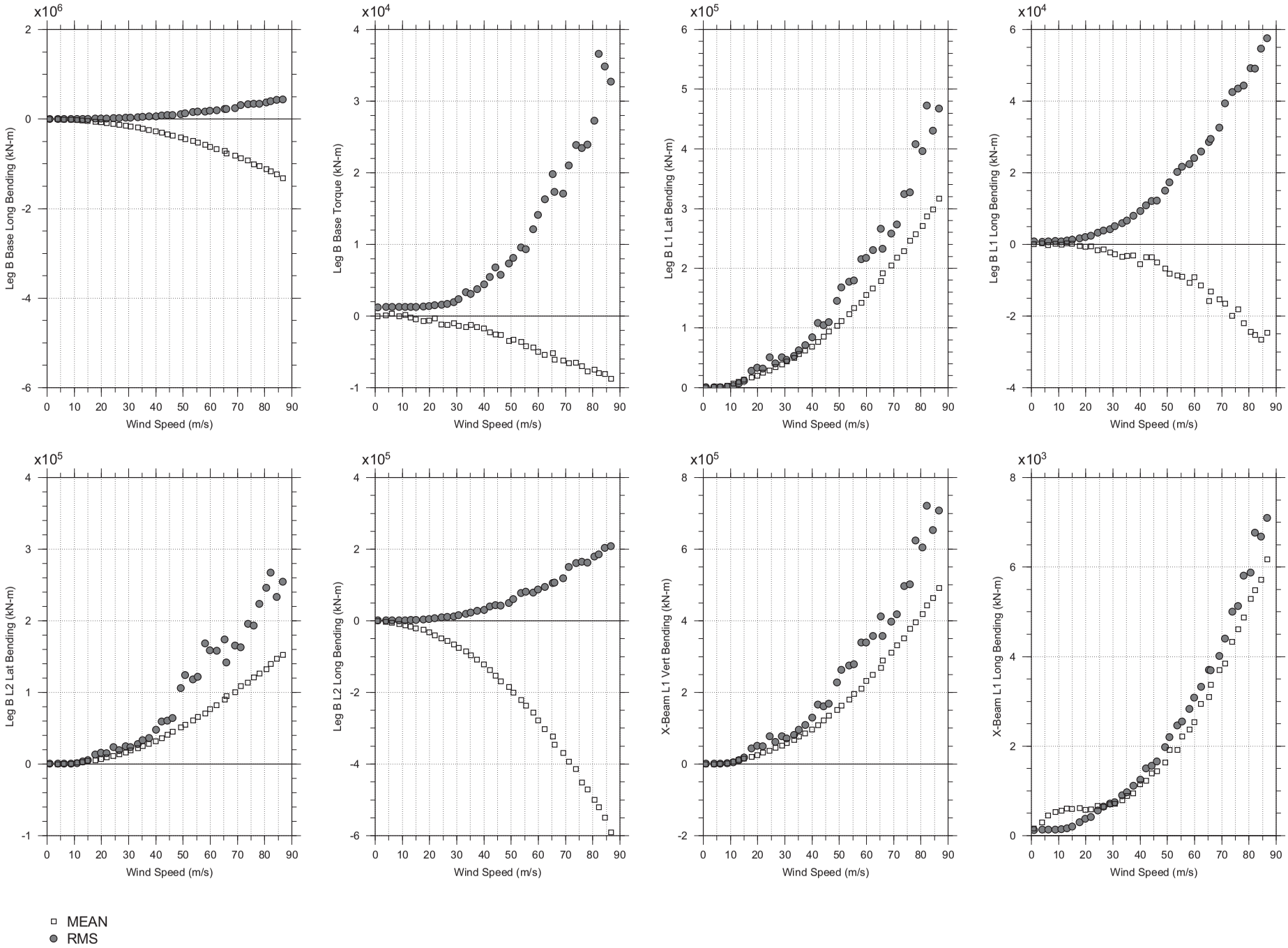

Messina Bridge, In Service Tower, 80 degree, Turbulent, Jan2011

Jan. 12, 2011
ti29abdg.cl

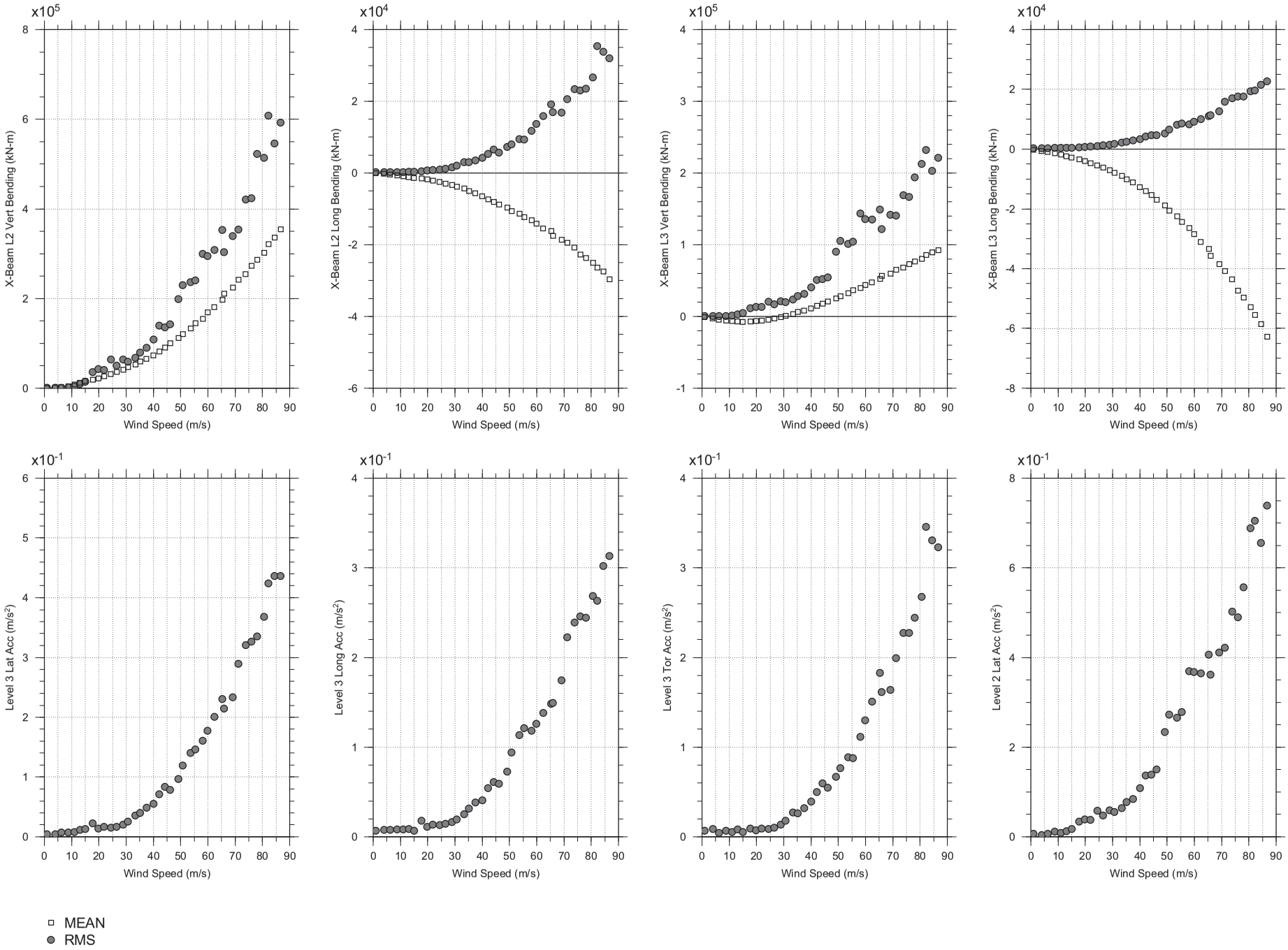

Messina Bridge, In Service Tower, 80 degree, Turbulent, Jan2011

Jan. 12, 2011
ti29abdg.cl

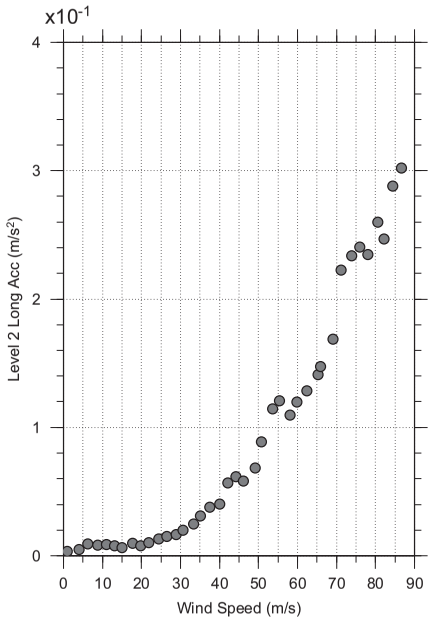

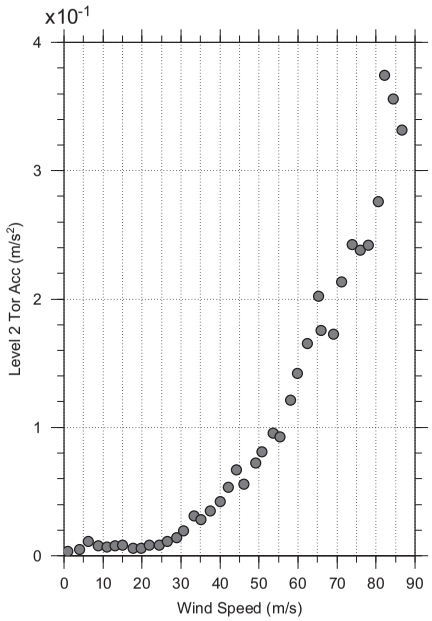

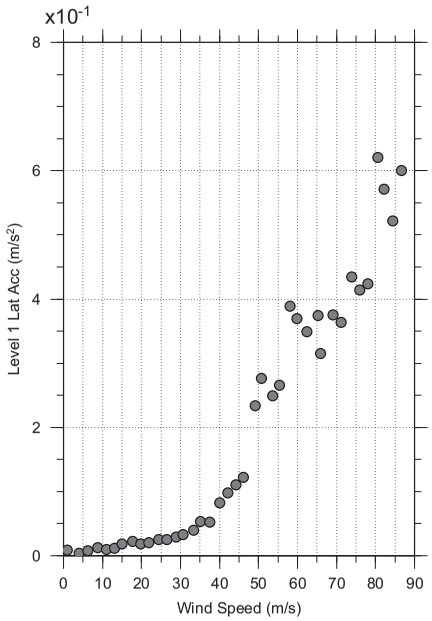

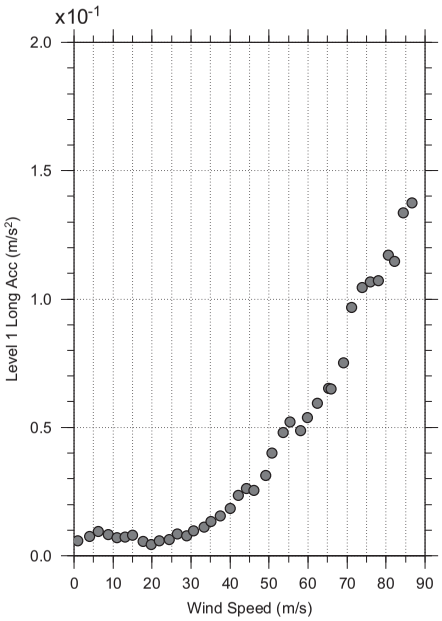

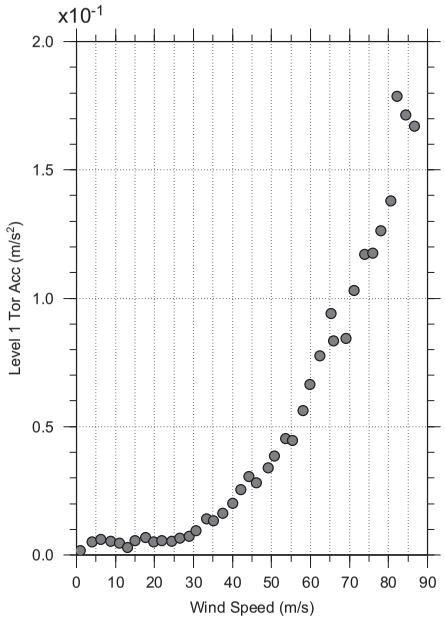

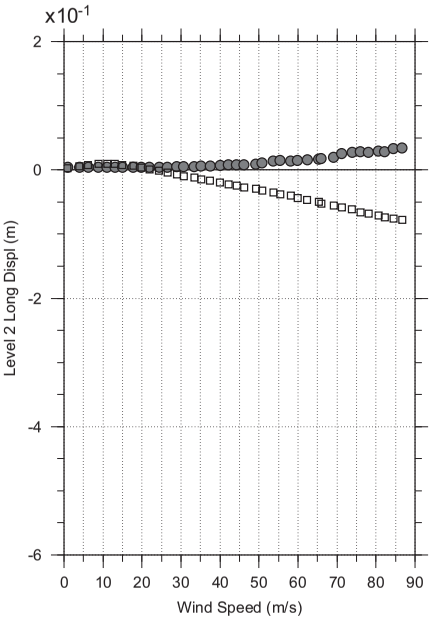

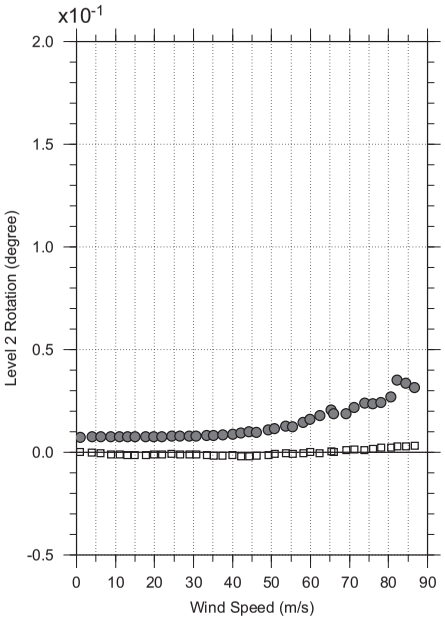

MEAN
RMS

Messina Bridge, In Service Tower, 80 degree, Turbulent, Jan2011

Jan. 12, 2011
ti29abdg.cl

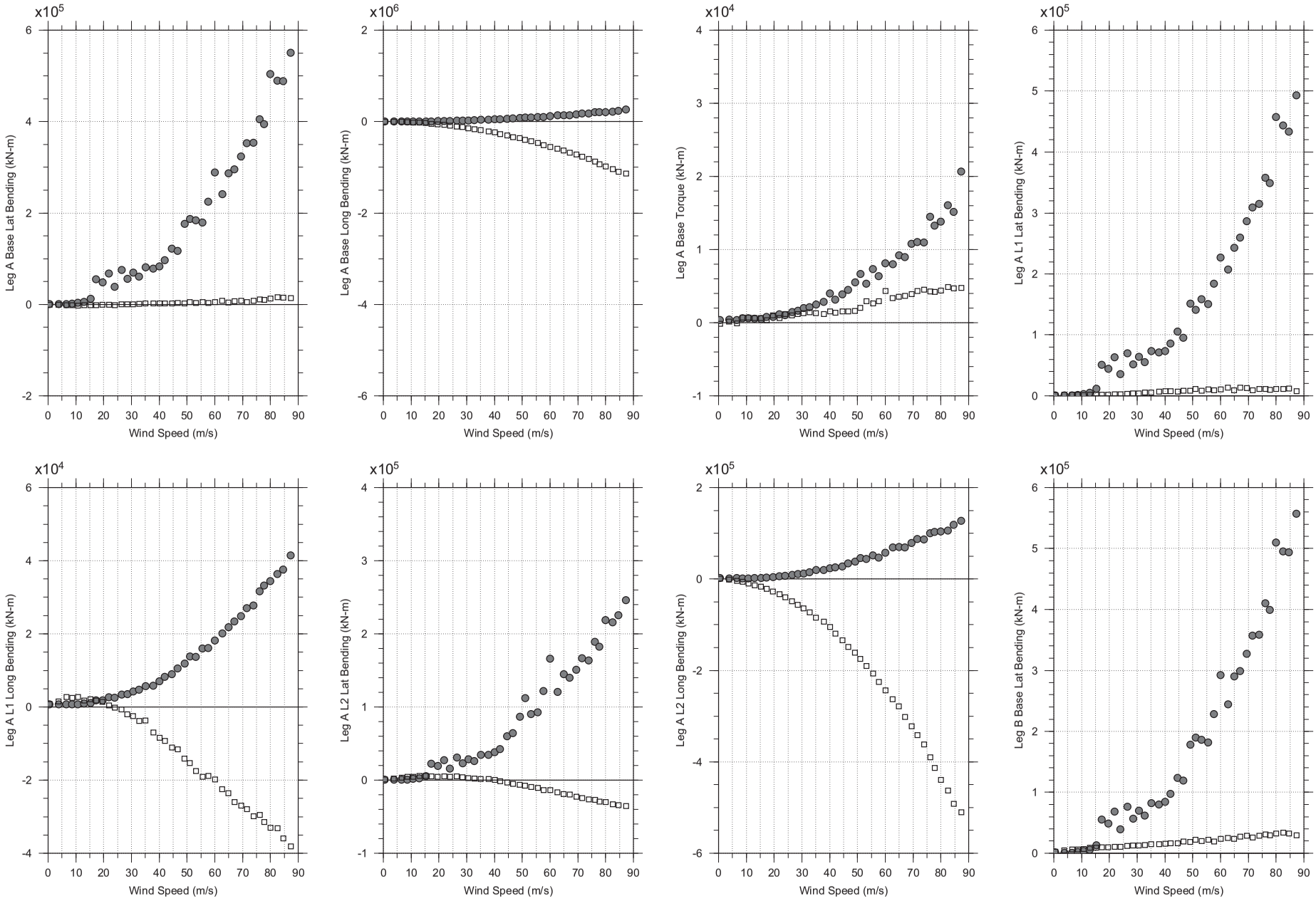

Messina Bridge, In Service Tower, 90 degree, Turbulent, Jan2011

Jan. 12, 2011
ti210abdg.cl

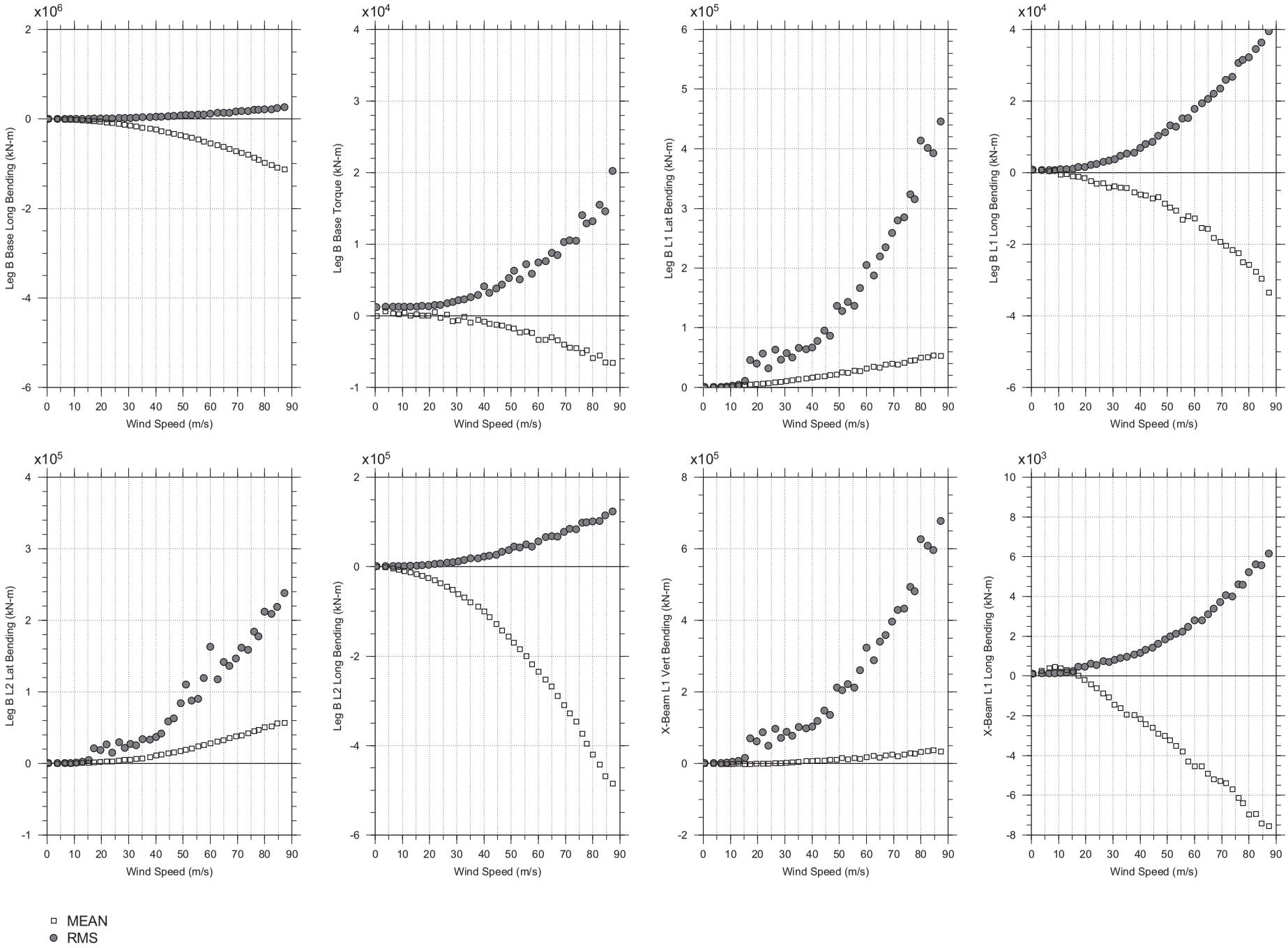

Messina Bridge, In Service Tower, 90 degree, Turbulent, Jan2011

Jan. 12, 2011
ti210abdg.cl

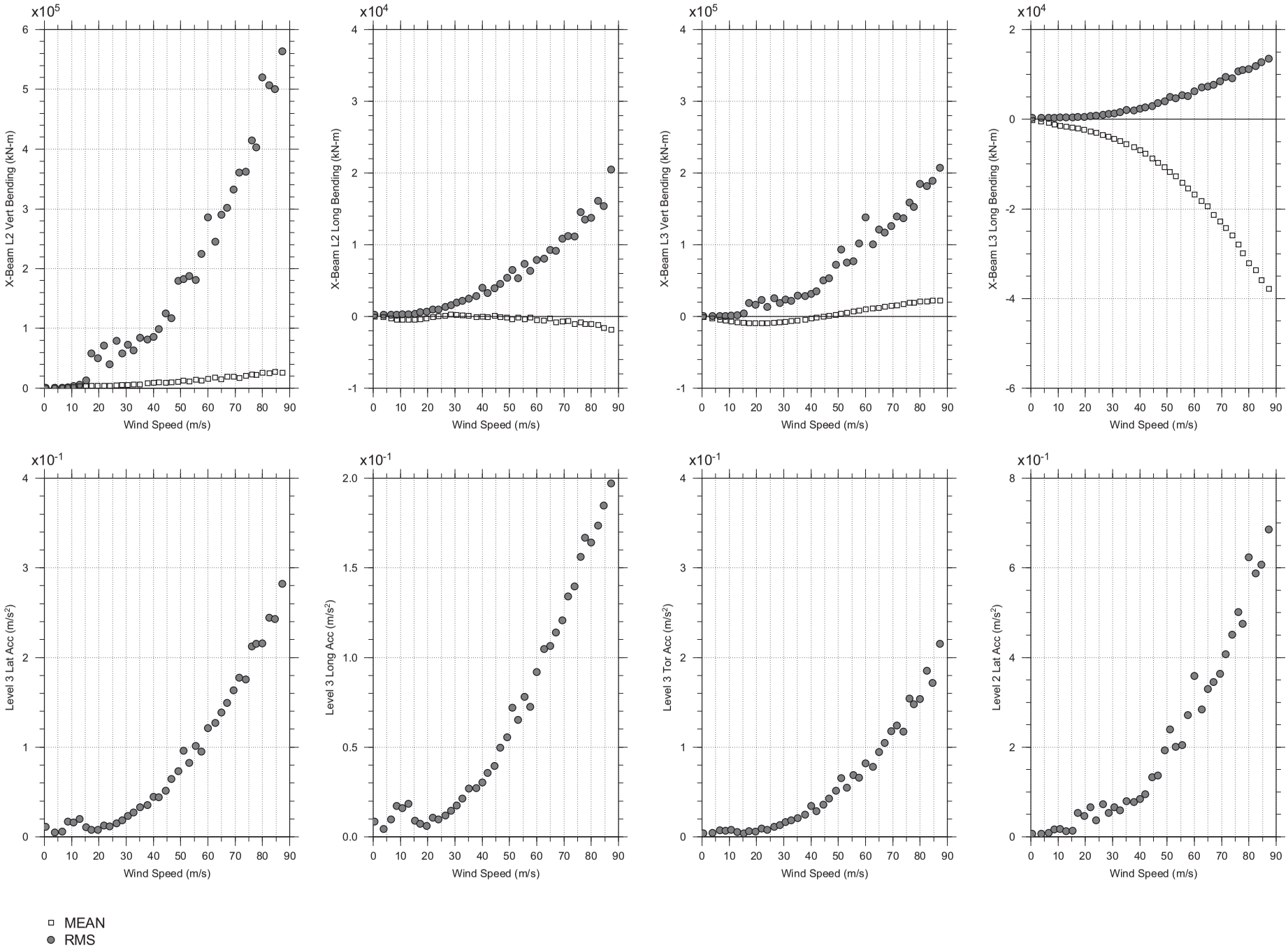

Messina Bridge, In Service Tower, 90 degree, Turbulent, Jan2011

Jan. 12, 2011
ti210abdg.cl

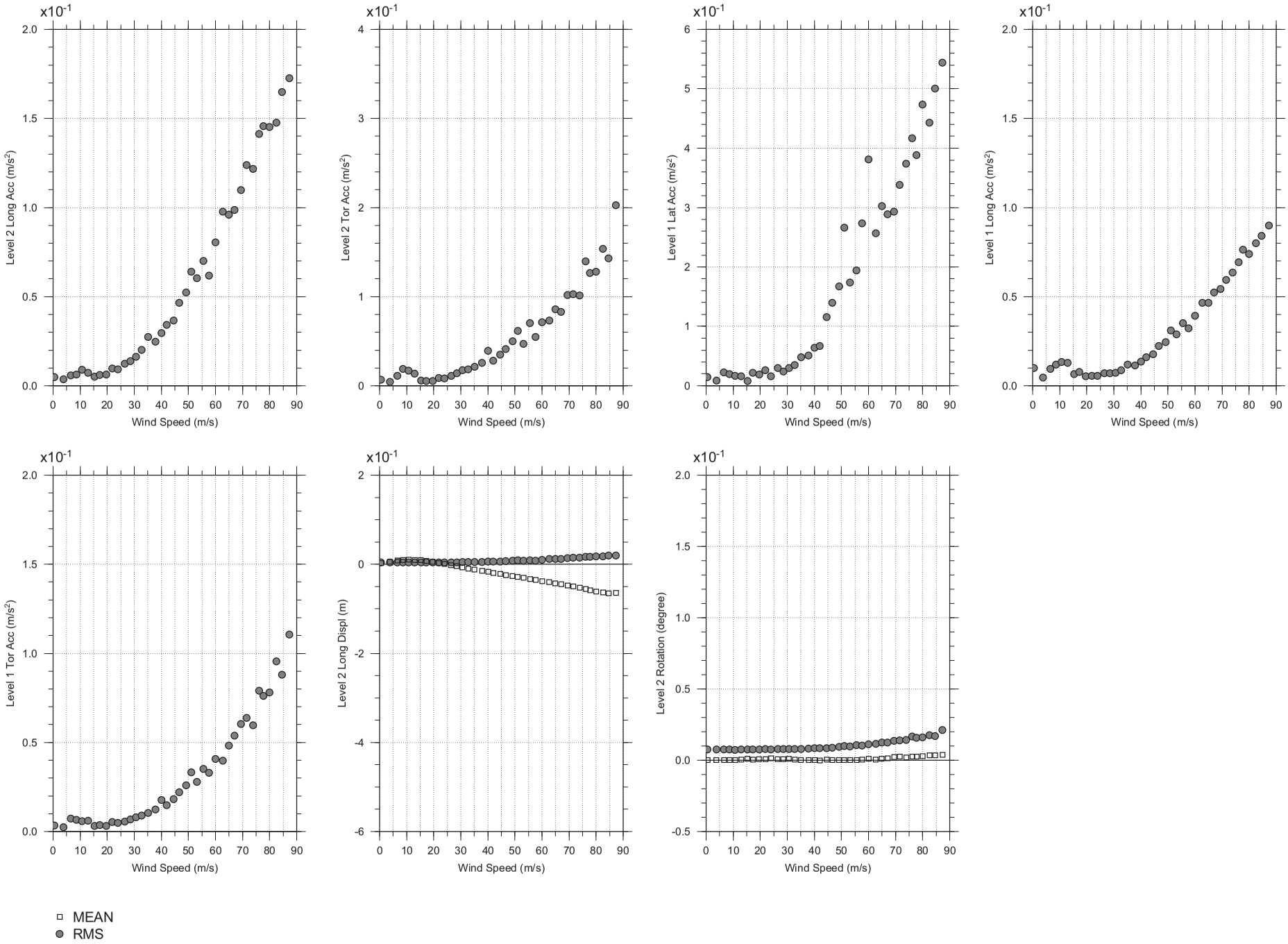

Messina Bridge, In Service Tower, 90 degree, Turbulent, Jan2011

Jan. 12, 2011
ti210abdg.cl

APPENDIX D

RESULTS OF FROUDE TOWER MODEL, CONSTRUCTION STAGE

Notes:

D1. The wind speed indicated is the mean hourly wind speed in m/s at the tower height. The bending moments and torques given in the plots have the unit of kN-m. The accelerations have the unit of m/s^2. The displacements have the units of m in the longitudinal direction and degree for tower rotation.

D2. The mean and RMS (root mean square) responses are given separately in the plots. The total responses should be calculated as the mean plus or minus the RMS multiplied by the appropriate peak factor.

D3. Refer to Figure D1 for the definition of test wind angles.

D4. Refer to Figure D2 and Table D1 for the instrumentation locations and sign convention used.

D5. Table D2 summarizes the test results and corresponding test conditions.

TABLE D1 INSTRUMENTATION LOCATIONS, FROUDE TOWER MODEL

Instrumentation	Instrumentation Locations
Accelerometers:	
x, y and Torsional accelerations, Level 1	Accelerations measured at 119.4 m above ground
x, y and Torsional accelerations, Level 2	Accelerations measured at 243.8 m above ground
x, y and Torsional accelerations, Level 3	Accelerations measured at 370.8 m above ground
Laser Deflection Transducers:	
x displacement and Rotation θ, Level 2	Displacements measured at 238.7 m above ground
Wind Speeds:	
Deck Height	At a height of 66 m full scale above ground
Tower Height	At a height of 399 m full scale above ground
Mid Tower Height	At a height of 199 m full scale above ground
Reference Height	Where the wind speed not affected by the boundary layer of the wind tunnel floor

Notes:
1. Right-hand rule used for sign convention.
2. x – along bridge axis; y – perpendicular to bridge axis (lateral to tower)

TABLE D2 SUMMARY OF FROUDE TOWER MODEL TESTS, CONSTRUCTION STAGE

Test Configuration	Test No.	Test Files	Modal Frequency (Hz) and Damping (%)			Wind Angle	Maximum Wind Speed	Level 3 Maximum Acceleration Observed		
			Long.	Lat.	Tor.	Deg	m/s	m/s^2	Direction occurred	Wind speed (m/s)
Smooth flow, inherent damping	1	M075c1E01R002	1.72 (0.16~ 0.20)	4.73 (1.21~ 1.27)	5.46 (0.08~ 0.09)	0 (Lat.)	58	7.896	Tor	34
	2	M075c1E01R003				2.5	58	8.074	Tor	36
	3	M075c1E01R009				5	58	8.659	Tor	37
	4	M075c1E01R010				7.5	58	12.629	Tor	36
	5	M075c1E01R004				10	58	12.569	Tor	36
Smooth flow, 2% nominal damping	6	M075c2E01R002	1.71 (1.90~ 1.92)	4.78 (1.25~ 1.30)	5.4 (0.97~ 1.03)	0 (Lat.)	57	3.126	Tor	57
	7	M075c2E01R003				5	57	3.384	Tor	57
	8	M075c2E01R004				10	57	0.473	Tor	57
Smooth flow, 4% nominal damping	9	M075c3E01R009	1.72 (3.98~ 3.99)	4.78 (1.24~ 1.27)	5.4 (2.14~ 2.18)	0 (Lat.)	58	1.290	Tor	58
	10	M075c3E01R010				5	57	1.487	Tor	57
	11	M075c3E01R011				10	57	0.480	Tor	57
Turbulent boundary layer flow, inherent damping	12	M075c4E02R002	1.72 (0.16~ 0.20)	4.73 (1.21~ 1.27)	5.46 (0.08~ 0.09)	0 (Lat.)	54	8.006	Tor	36
	13	M075c4E02R003				10	55	10.461	Tor	55
	14	M075c4E02R004				20	54	12.603	Tor	54
	15	M075c4E02R005				30	54	11.550	Tor	48
	16	M075c4E02R006				40	54	2.965	Tor	48
	17	M075c4E02R007				50	55	2.004	Tor	46
	18	M075c4E02R008				60	53	2.113	Tor	44
	19	M075c4E02R009				70	54	0.594	Lat	54
	20	M075c4E02R010				80	55	0.660	Lat	51
	21	M075c4E02R011				90 (Long.)	55	0.567	Lat	55

Notes:

1. Maximum wind speed is the equivalent hourly mean wind speed at the top of the tower using a velocity scale of 1:14.14.
2. Long. = Longitudinal direction (along deck), Lat. = Transverse direction with respect to the axis of the bridge deck

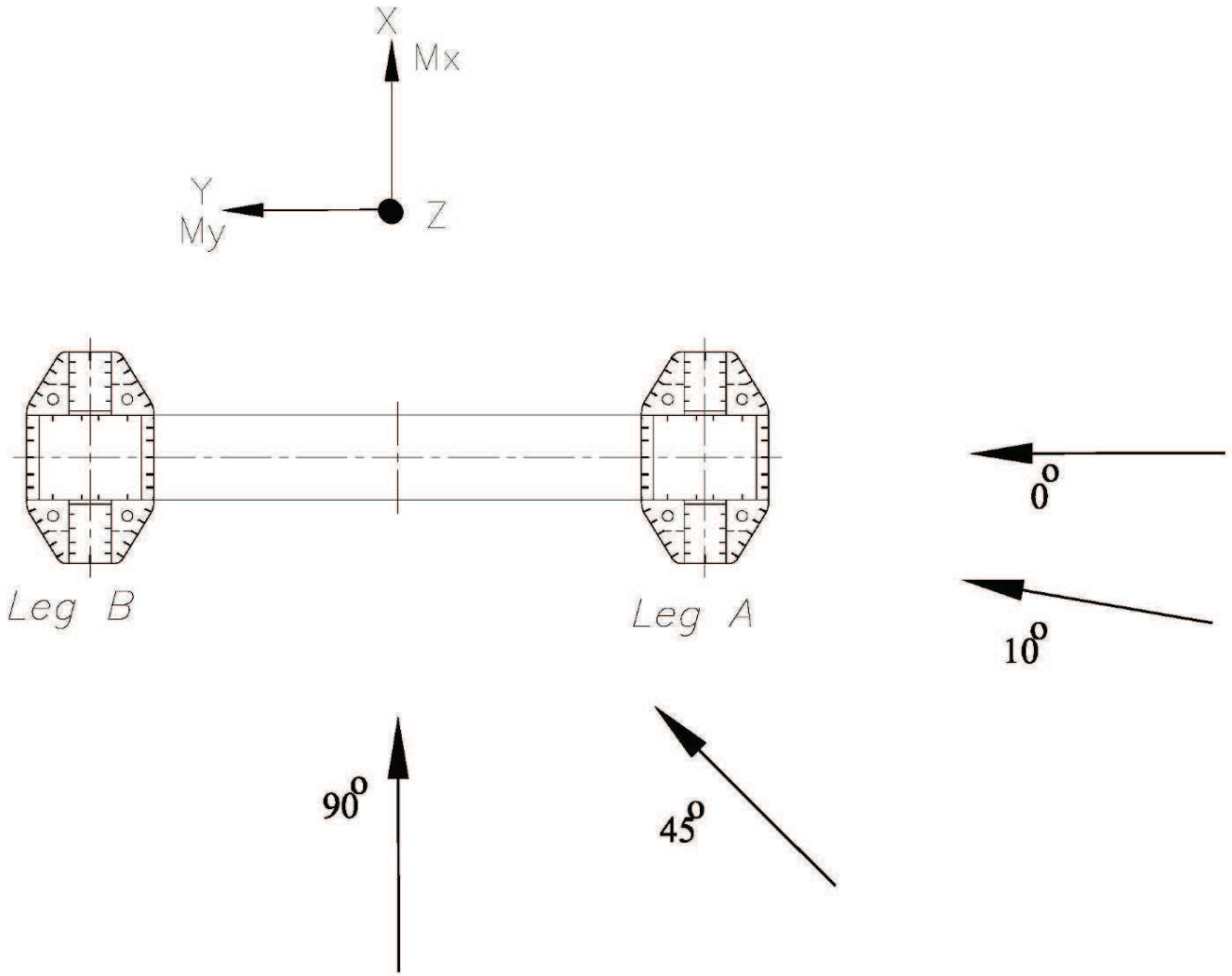

FIGURE D1 DEFINITION OF WIND ANGLES USED IN THE MESSINA TOWER TEST

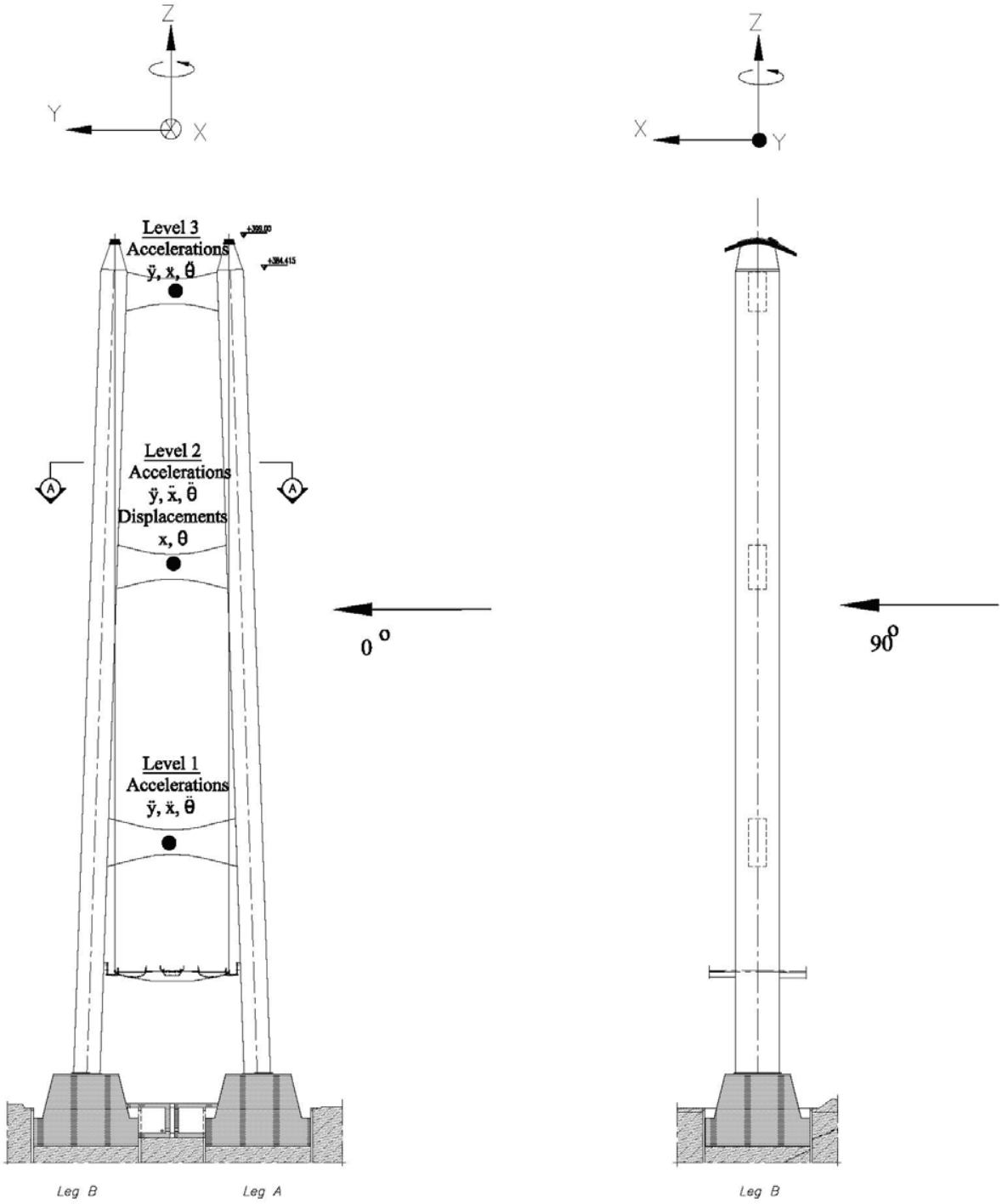

FIGURE D2 INSTRUMENTATION LOCATIONS AND SIGN CONVENTIONS USED IN THE FROUDE TOWER TEST

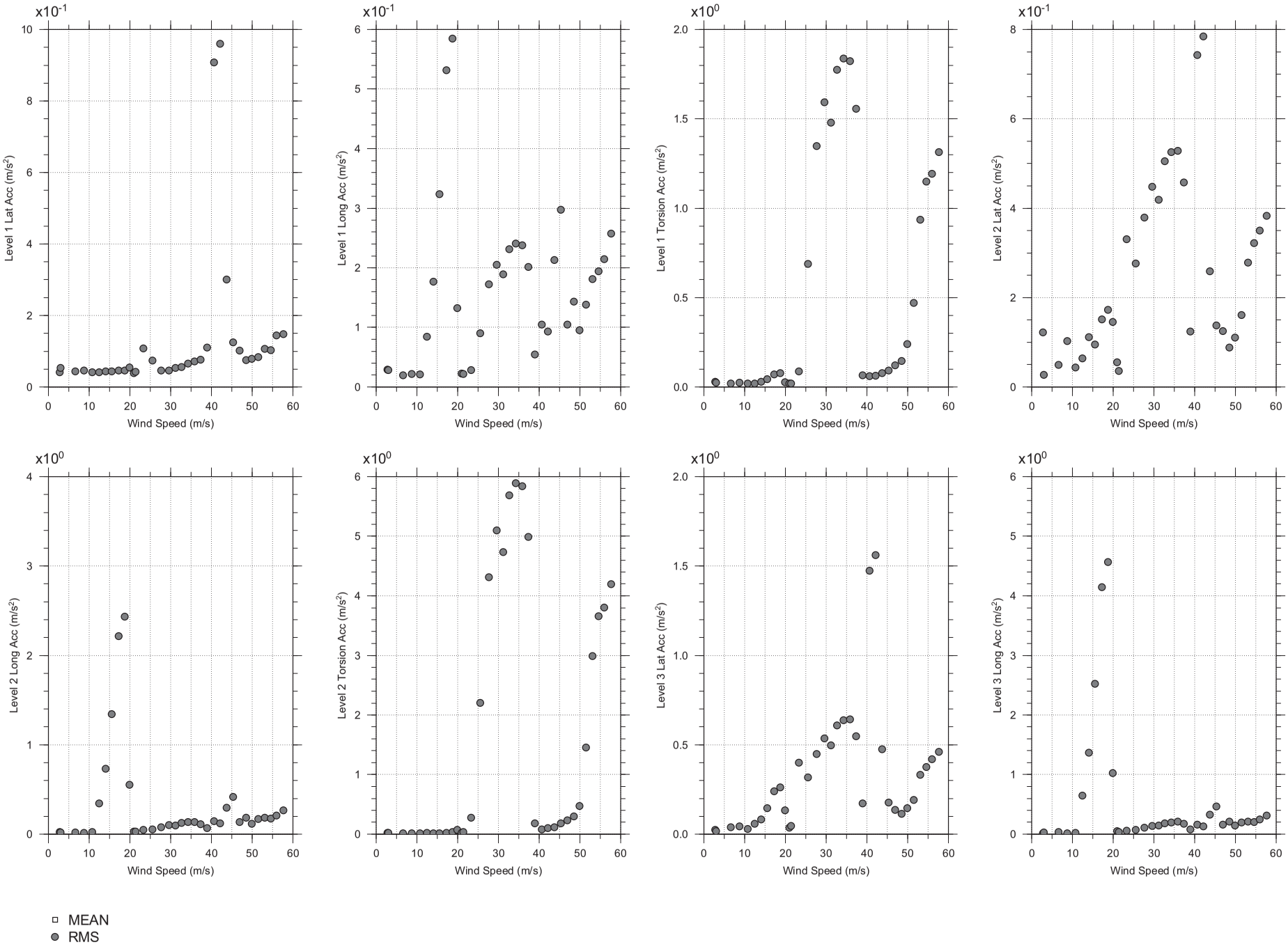

Messina Bridge, Free Standing Tower (Froude No.), 0 degree, Smooth Flow

Dec. 14, 2010
frf11abdg.cl

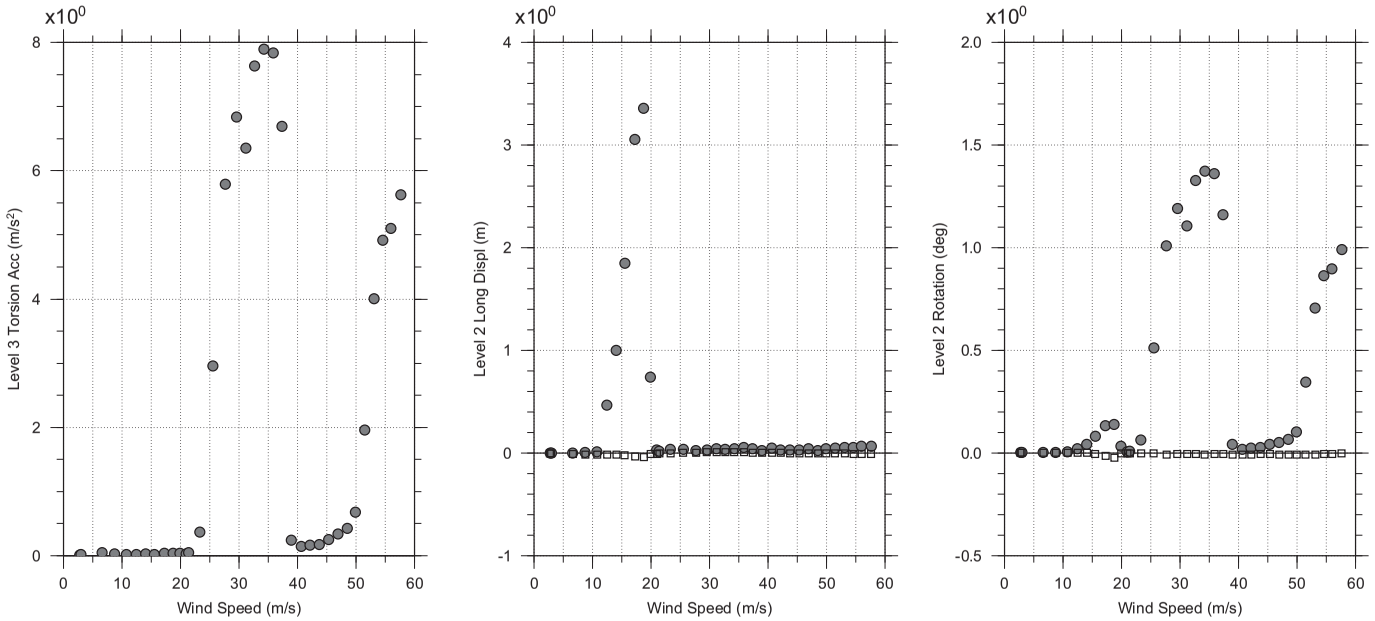

MEAN
RMS

Messina Bridge, Free Standing Tower (Froude No.), 0 degree, Smooth Flow

Dec. 14, 2010
frf11abdg.cl

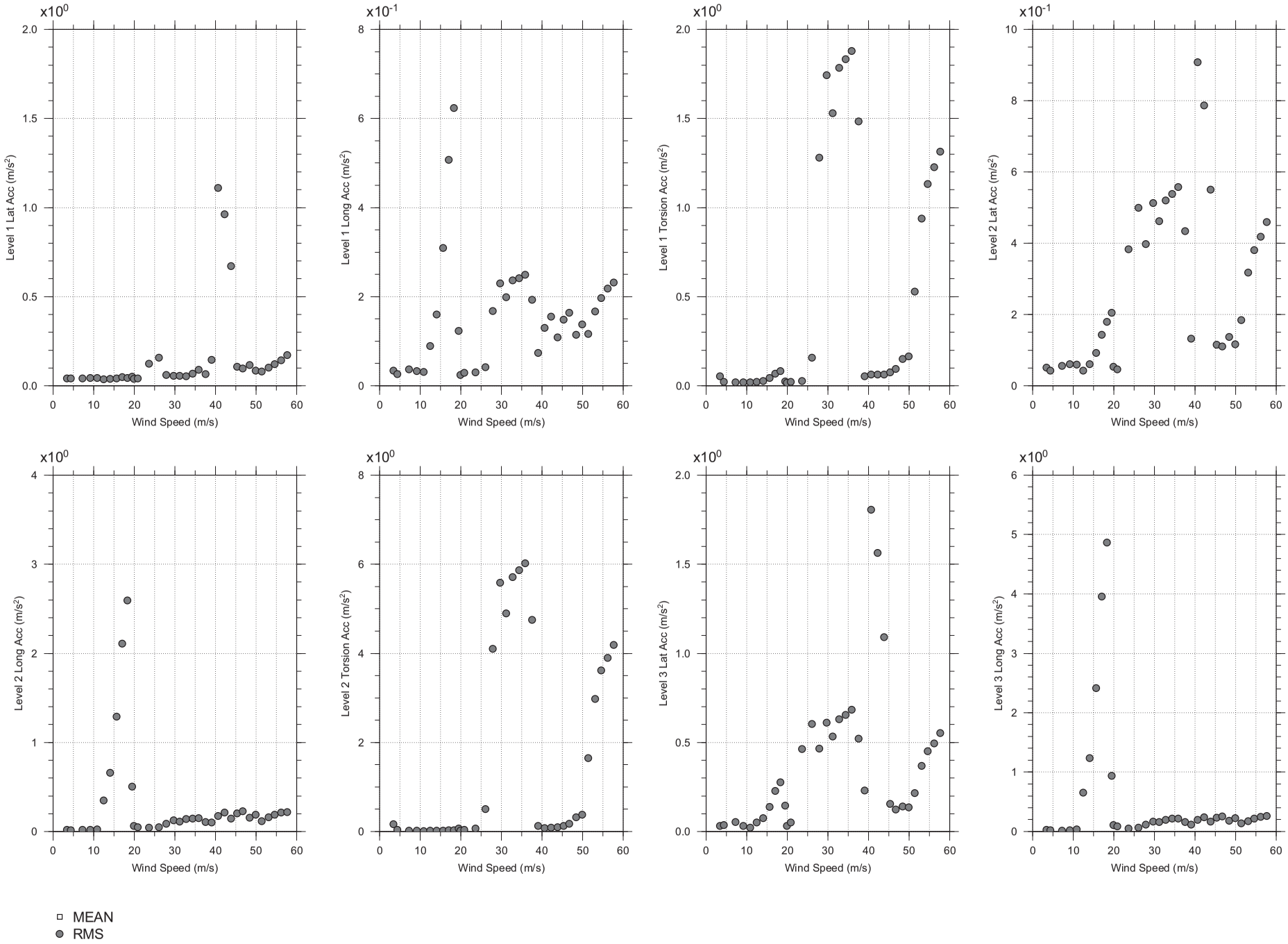

Messina Bridge, Free Standing Tower (Froude No.), 2.5 degree, Smooth Flow

Dec. 14, 2010
frf12abdg.cl

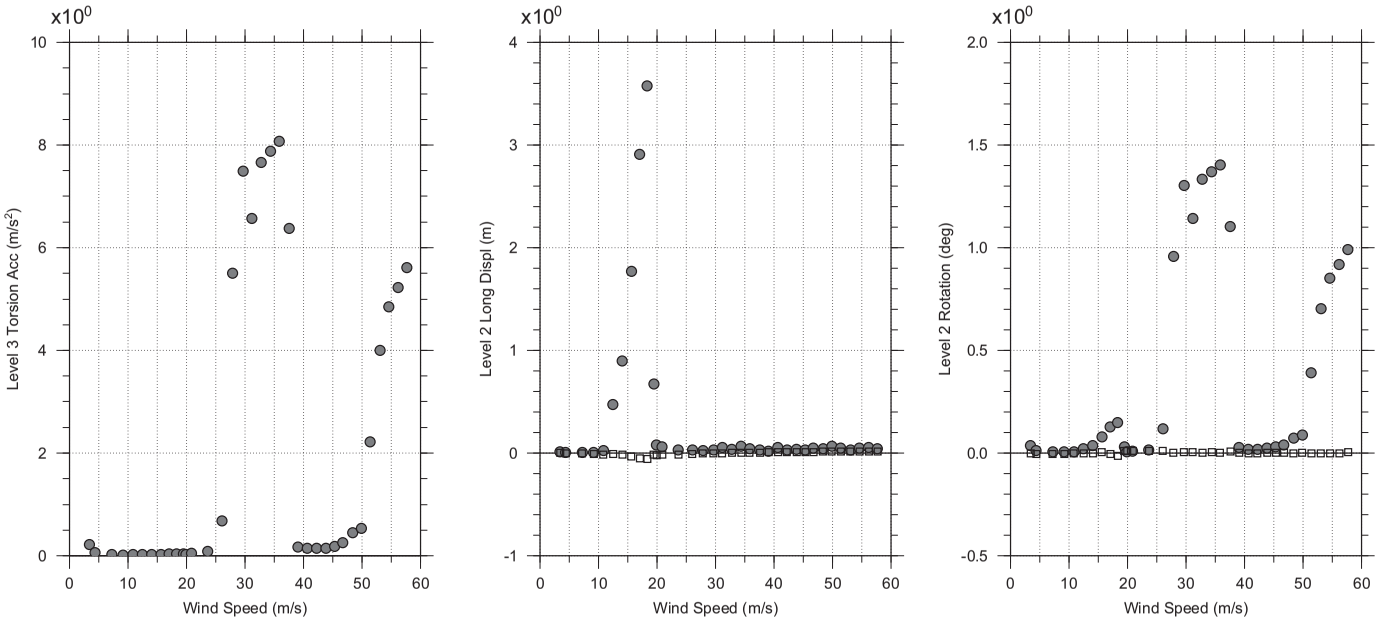

MEAN
RMS

Messina Bridge, Free Standing Tower (Froude No.), 2.5 degree, Smooth Flow

Dec. 14, 2010
frf12abdg.cl

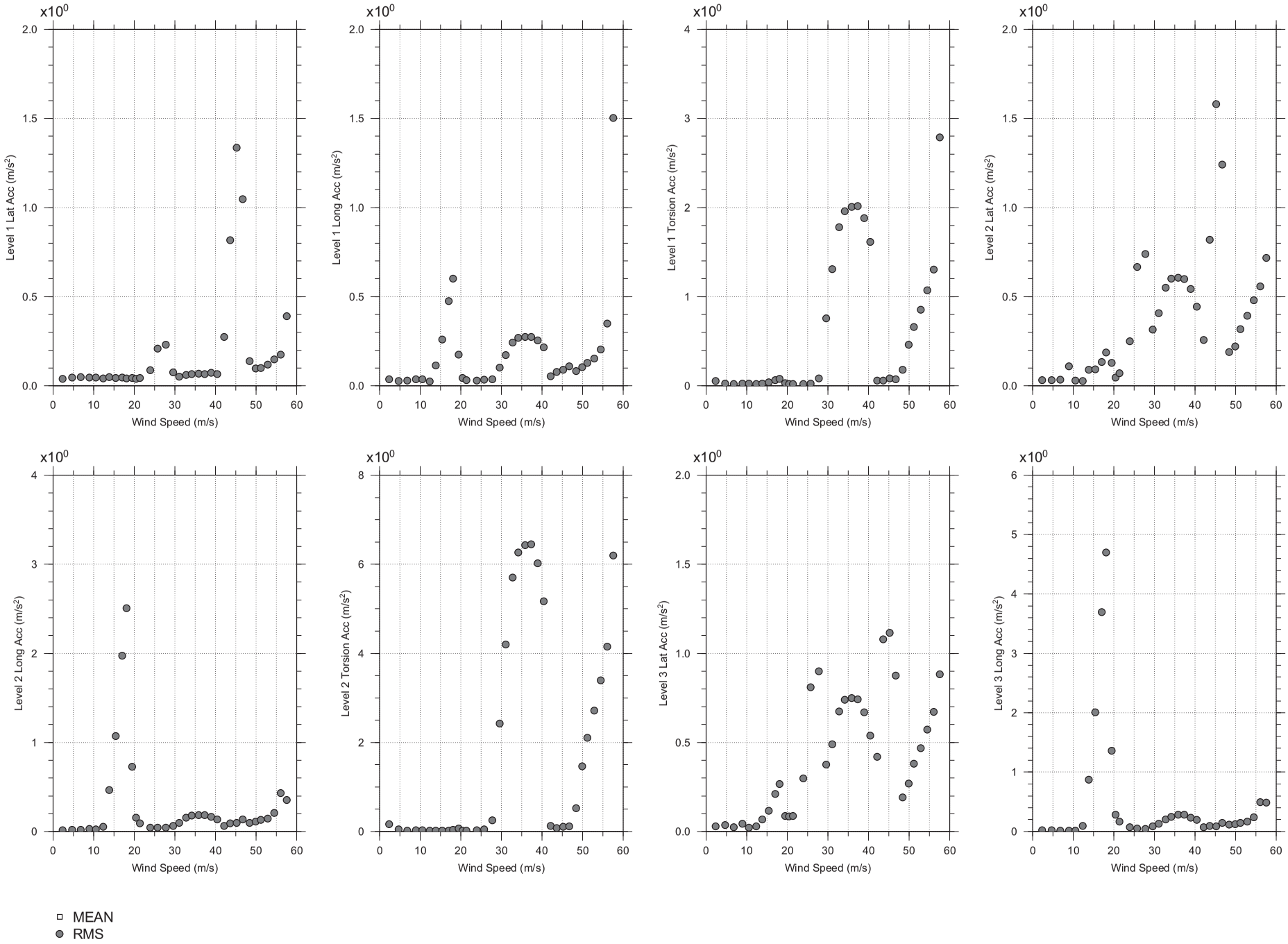

Messina Bridge, Free Standing Tower (Froude No.), 10 degree, Smooth Flow

Dec. 14, 2010
frf13abdg.cl

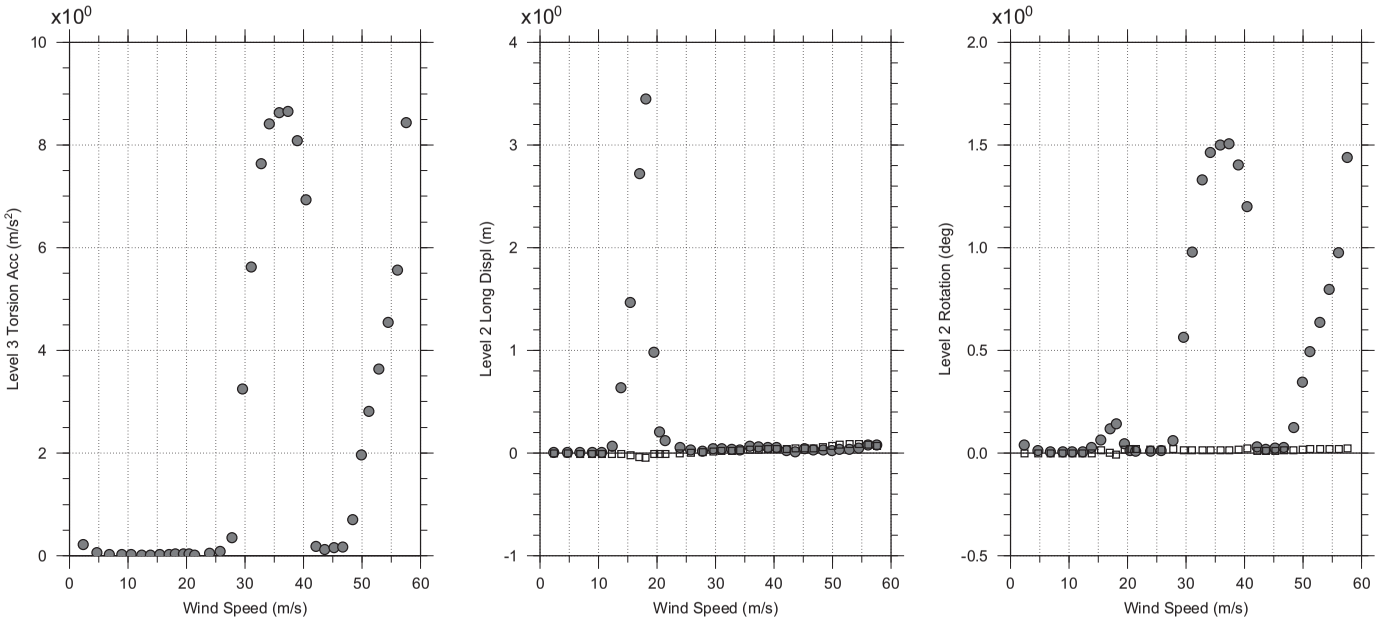

MEAN
RMS

Messina Bridge, Free Standing Tower (Froude No.), 10 degree, Smooth Flow

Dec. 14, 2010
frf13abdg.cl

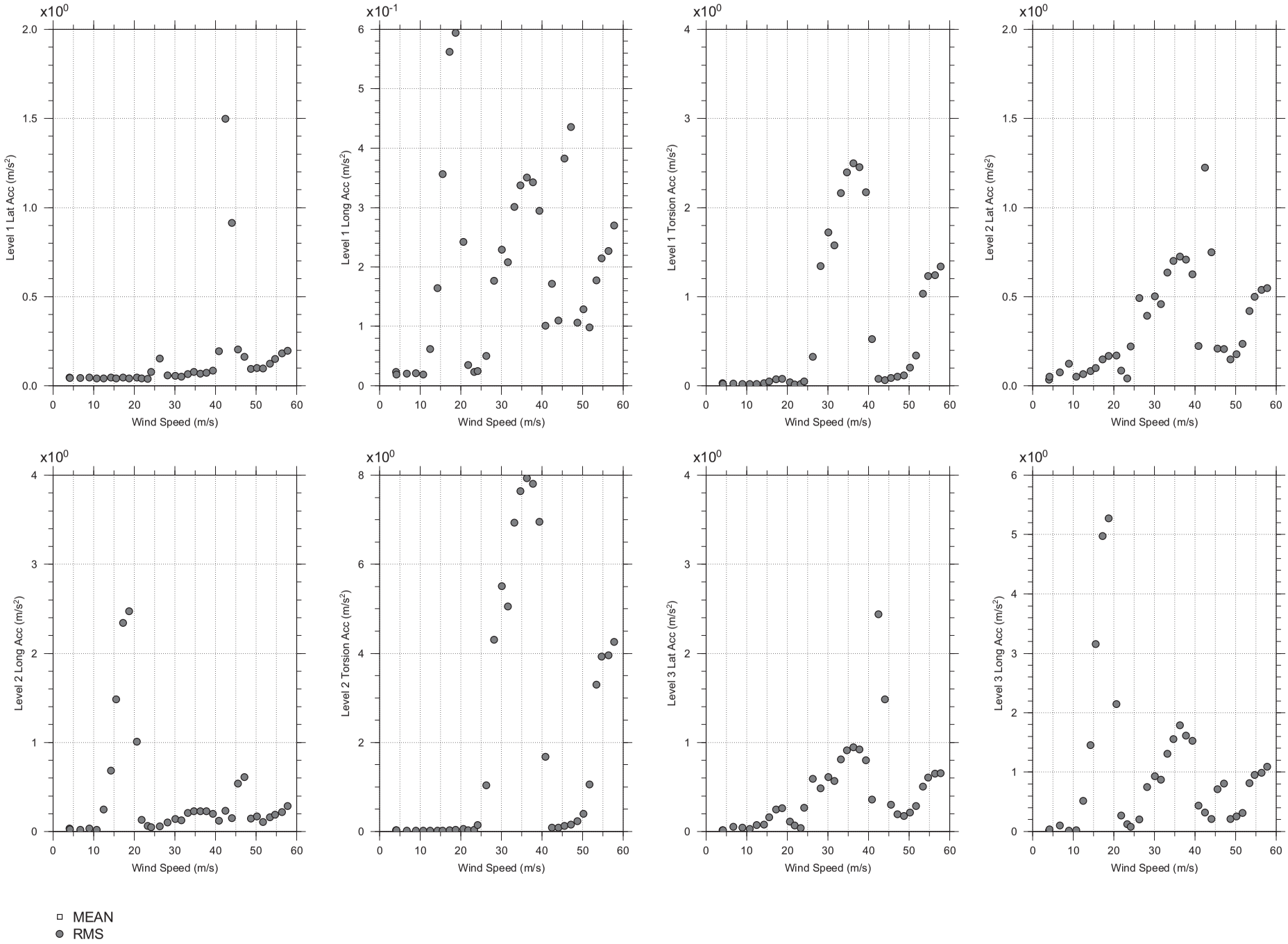

Messina Bridge, Free Standing Tower (Froude No.), 5 degree, Smooth Flow

Dec. 14, 2010
frf14abdg.cl

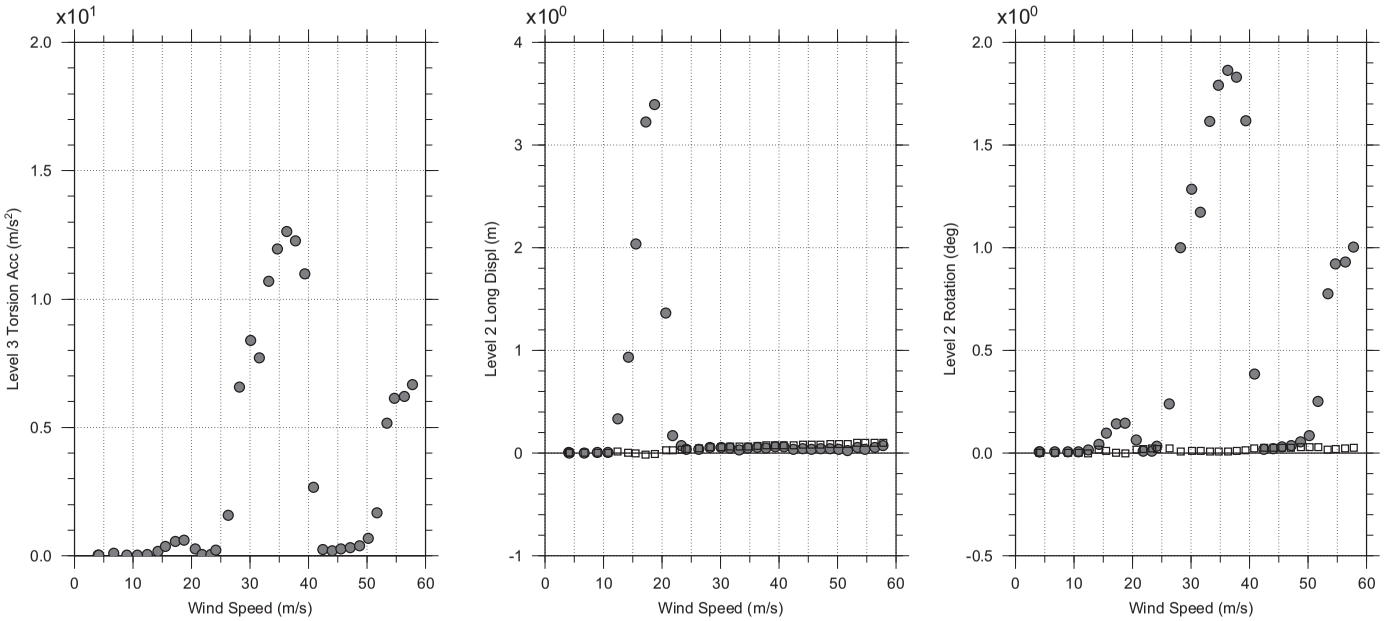

□ MEAN
● RMS

Messina Bridge, Free Standing Tower (Froude No.), 5 degree, Smooth Flow

Dec. 14, 2010
frf14abdg.cl

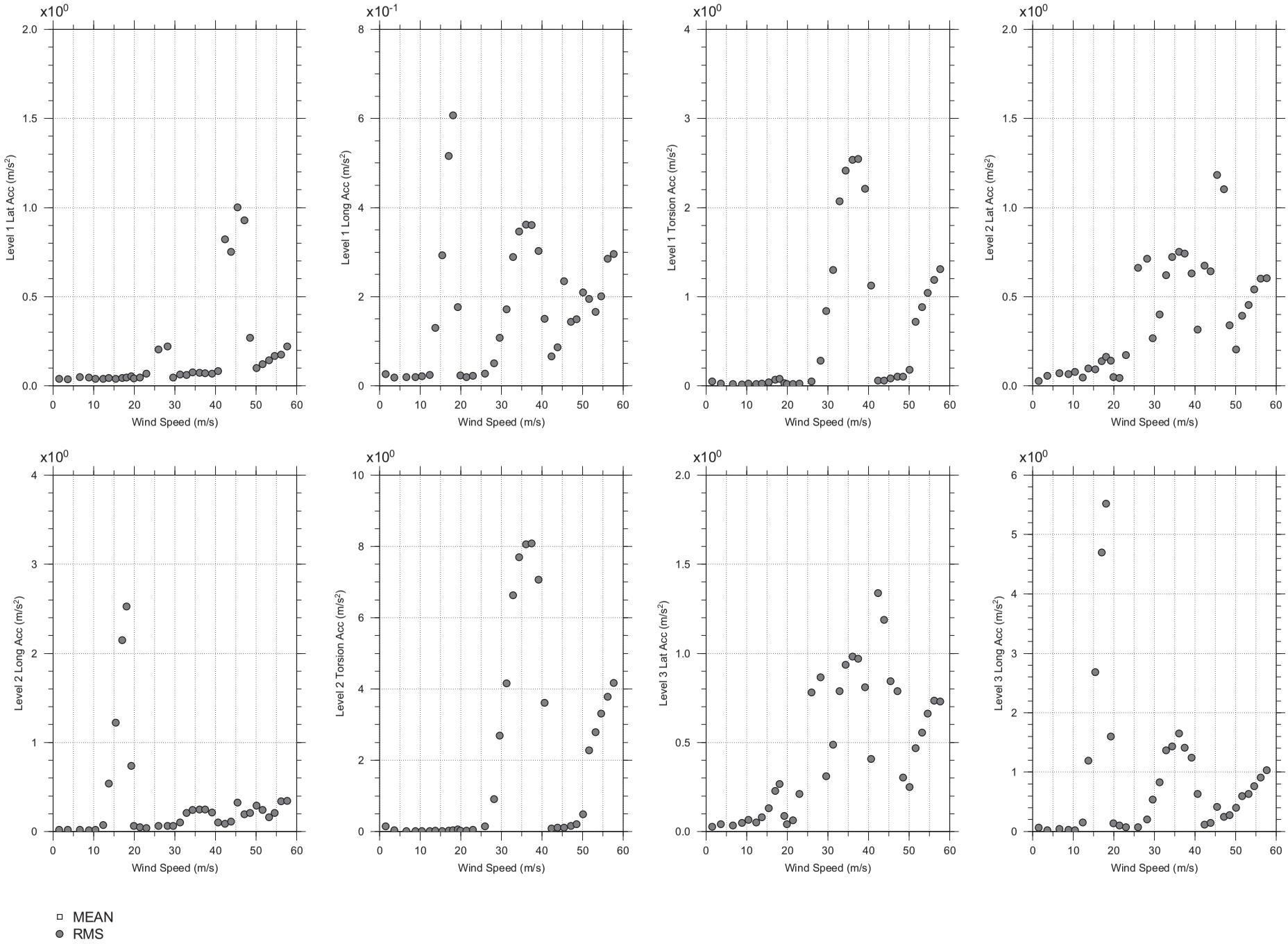

Messina Bridge, Free Standing Tower (Froude No.), 7.5 degree, Smooth Flow

Dec. 14, 2010
frf15abdg.cl

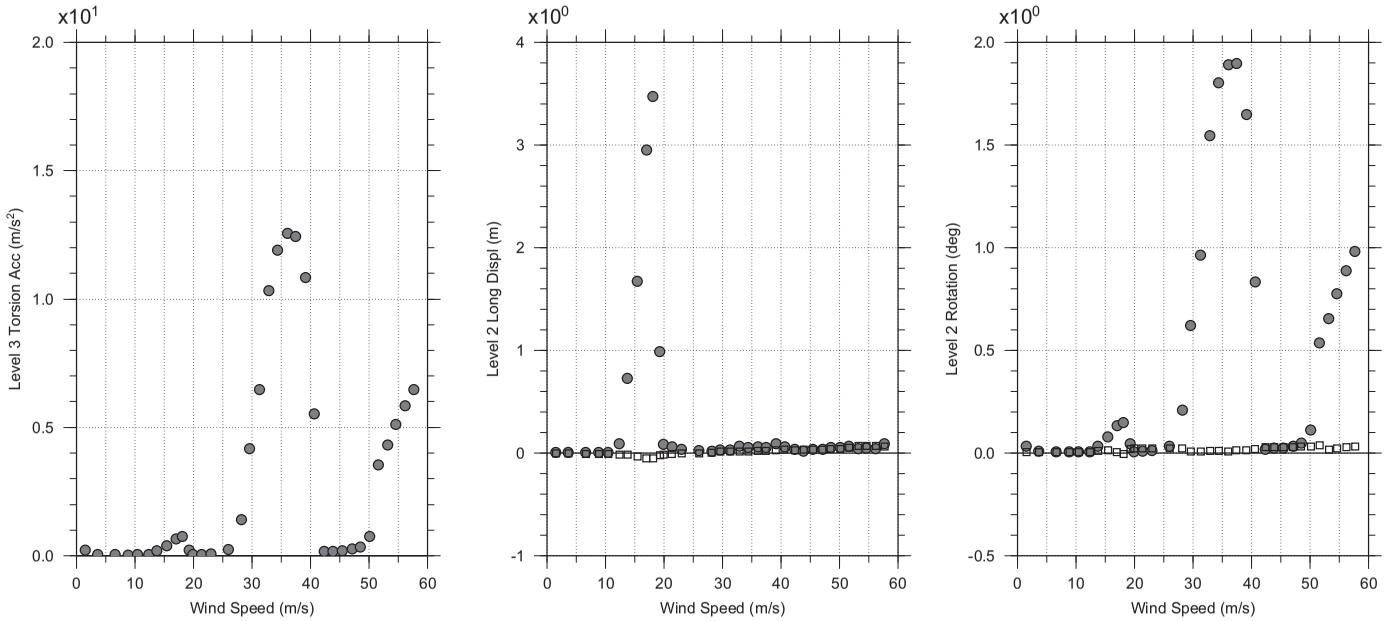

□ MEAN
● RMS

Messina Bridge, Free Standing Tower (Froude No.), 7.5 degree, Smooth Flow

Dec. 14, 2010
frf15abdg.cl

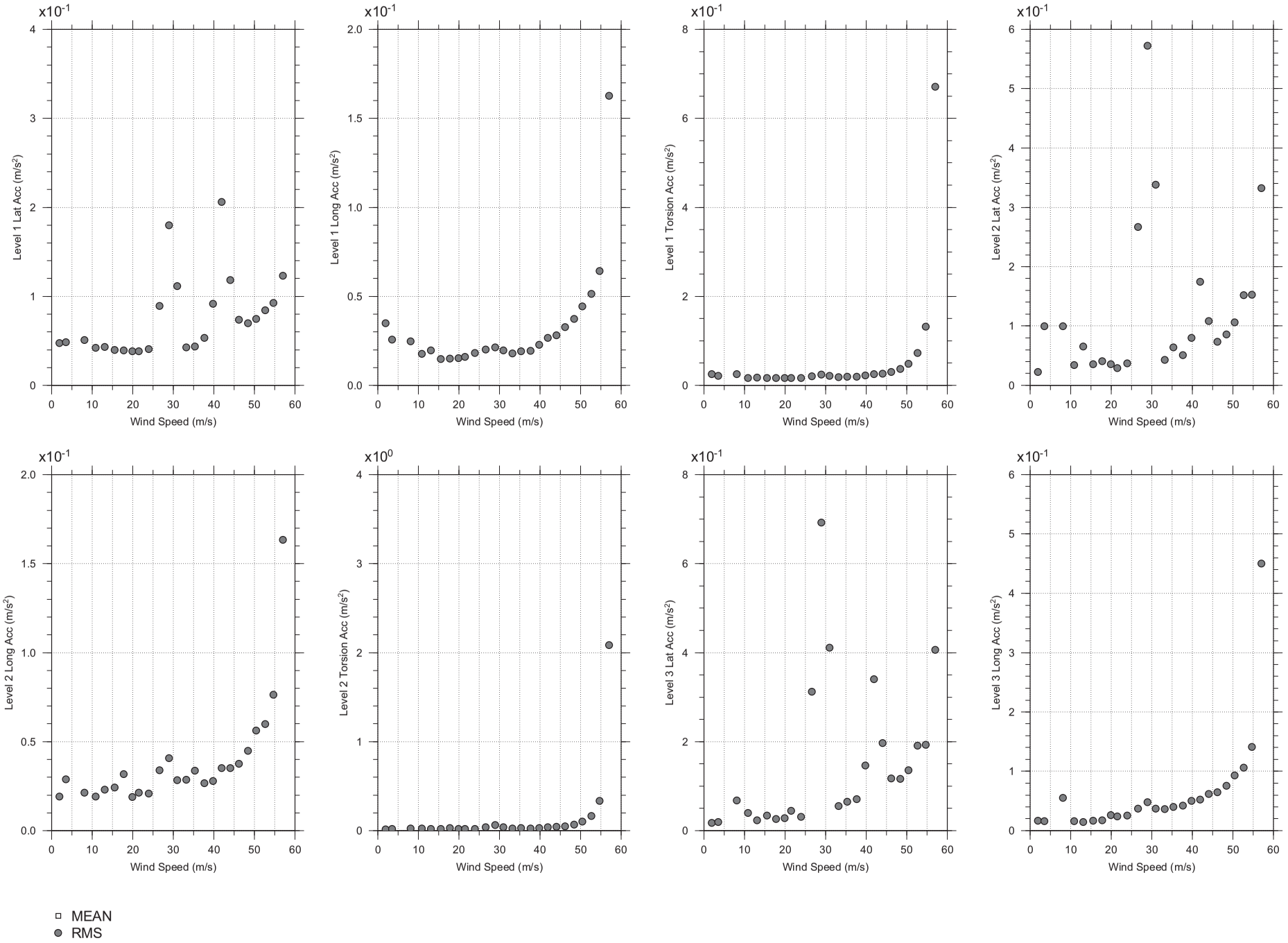

Messina Bridge, Free Standing Tower (Froude No.), 0 degree, 2% Damping, Smooth F

Dec. 14, 2010
frf21abdg.cl

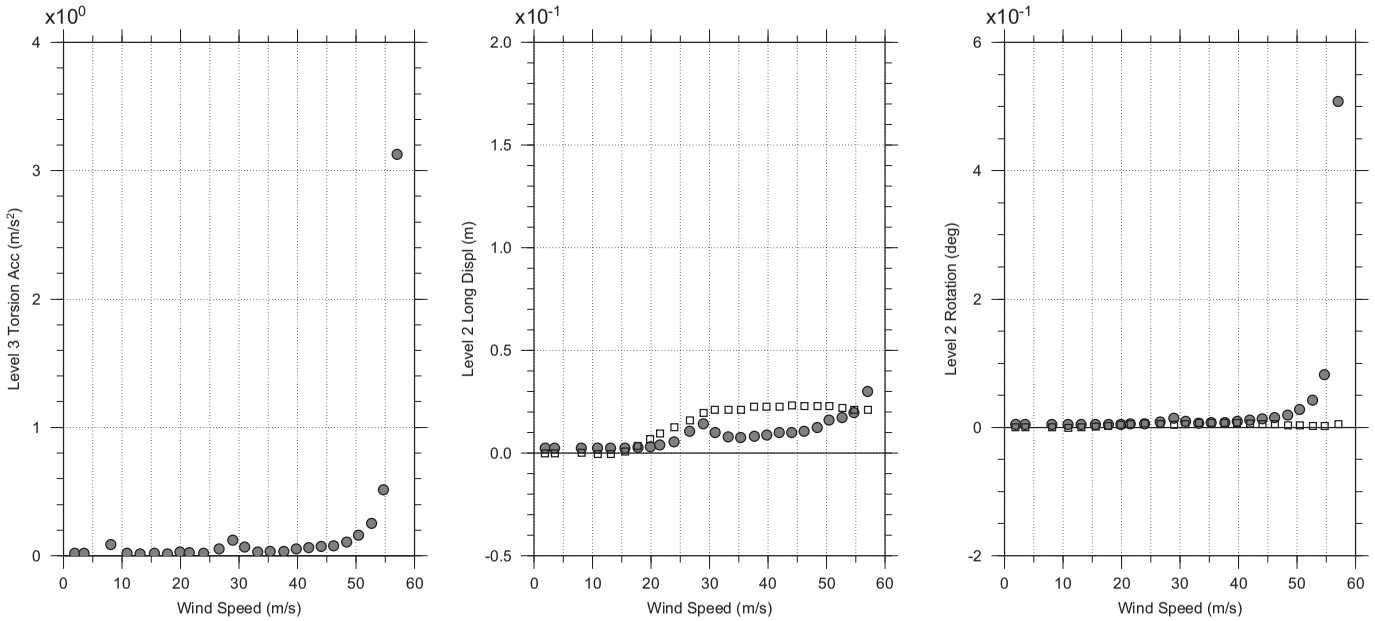

□ MEAN
● RMS

Messina Bridge, Free Standing Tower (Froude No.), 0 degree, 2% Damping, Smooth F

Dec. 14, 2010
frf21abdg.cl

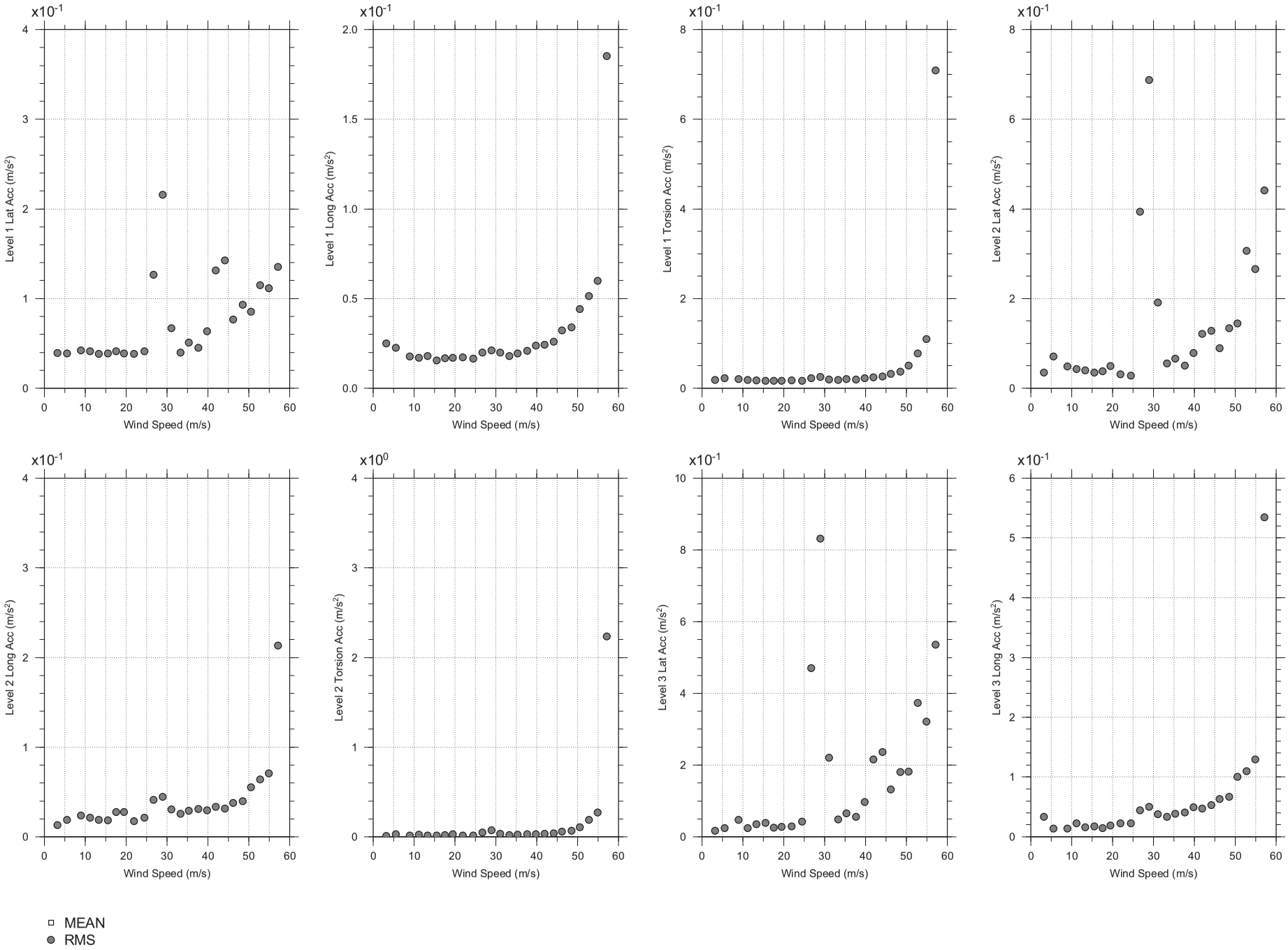

Messina Bridge, Free Standing Tower (Froude No.), 5 degree, 2% Damping, Smooth F

Dec. 14, 2010
frf22abdg.cl

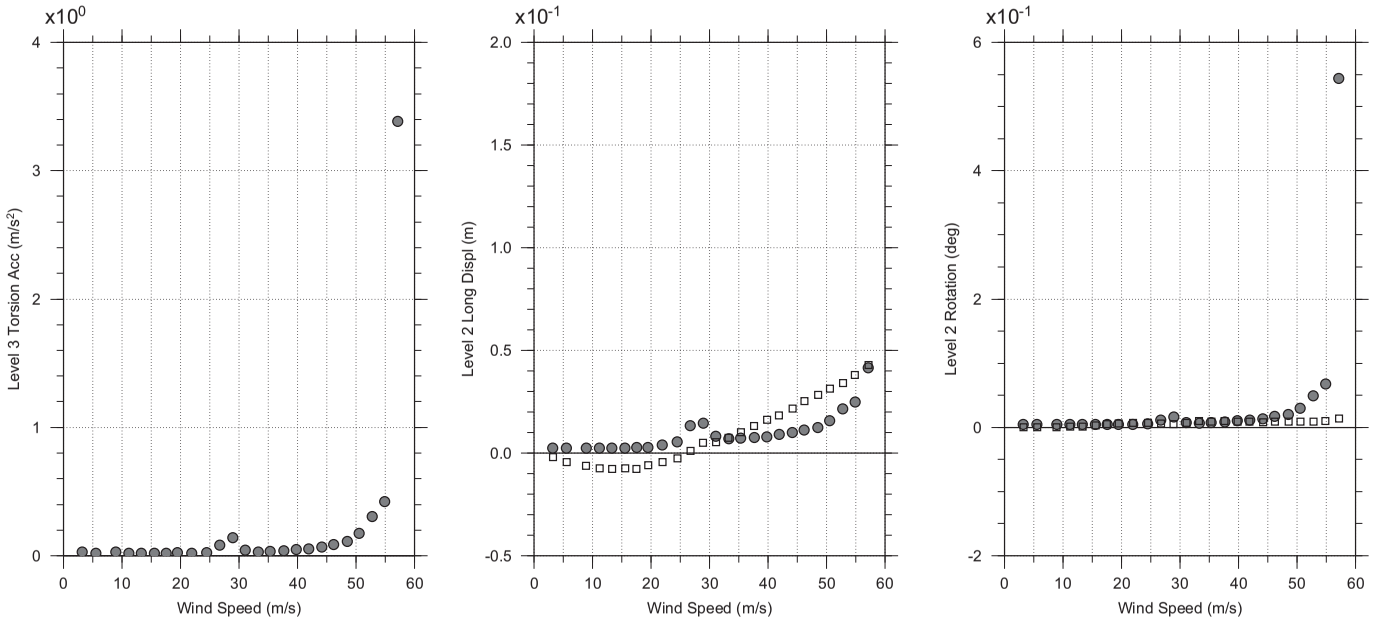

MEAN
RMS

Messina Bridge, Free Standing Tower (Froude No.), 5 degree, 2% Damping, Smooth F

Dec. 14, 2010
frf22abdg.cl

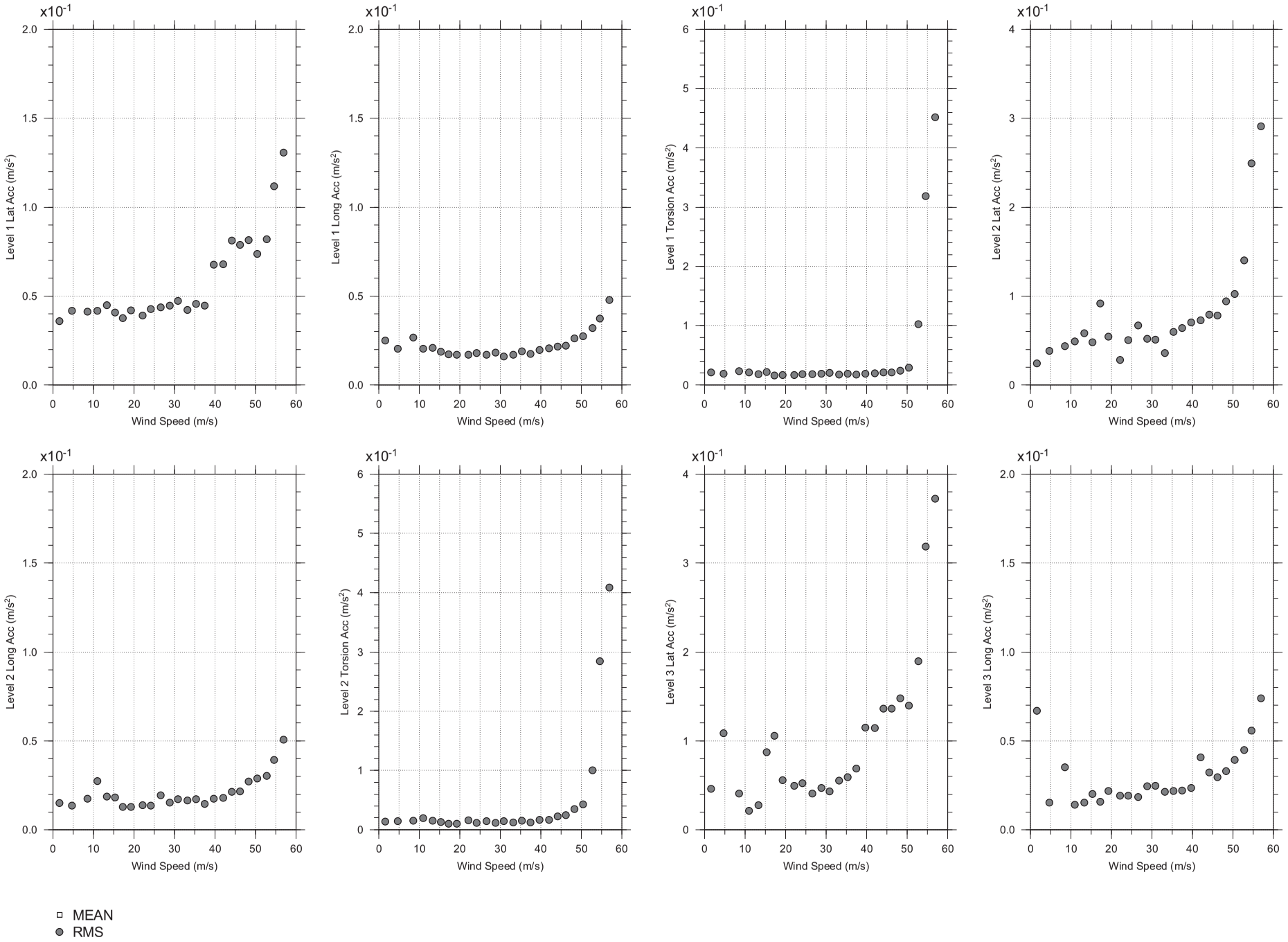

Messina Bridge, Free Standing Tower (Froude No.), 10 degree, 2% Damping, Smooth

Dec. 14, 2010
frf23abdg.cl

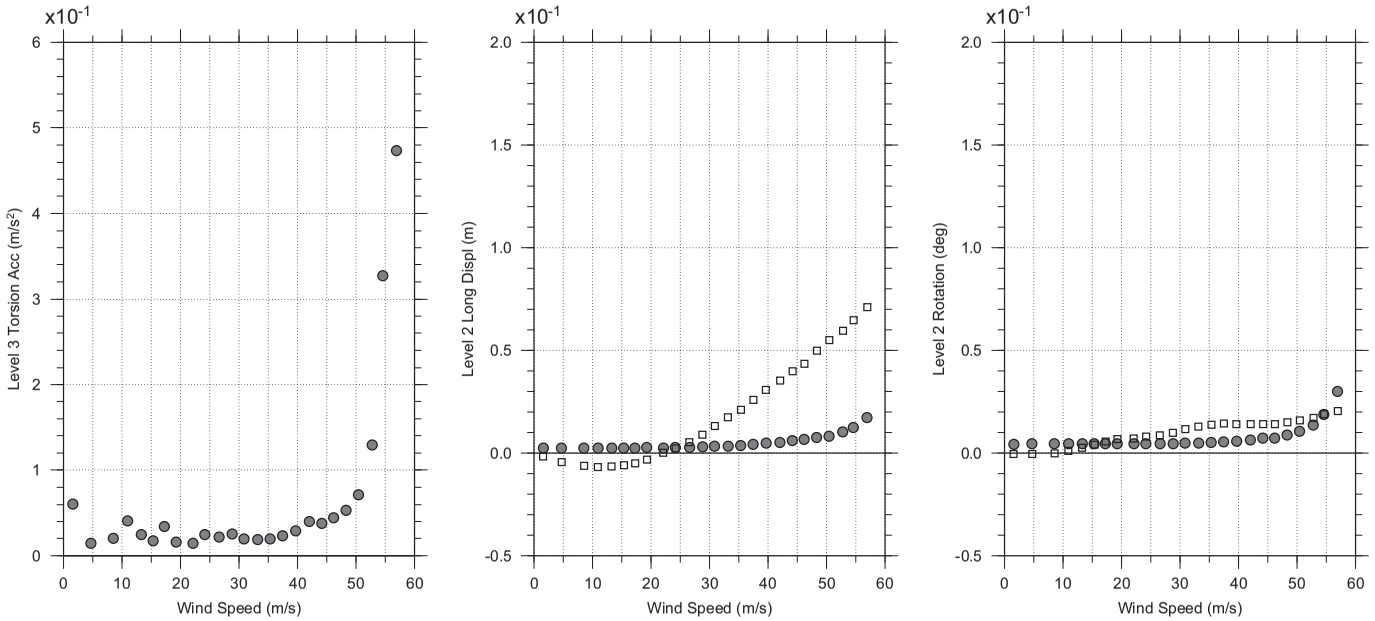

MEAN
RMS

Messina Bridge, Free Standing Tower (Froude No.), 10 degree, 2% Damping, Smooth

Dec. 14, 2010
frf23abdg.cl

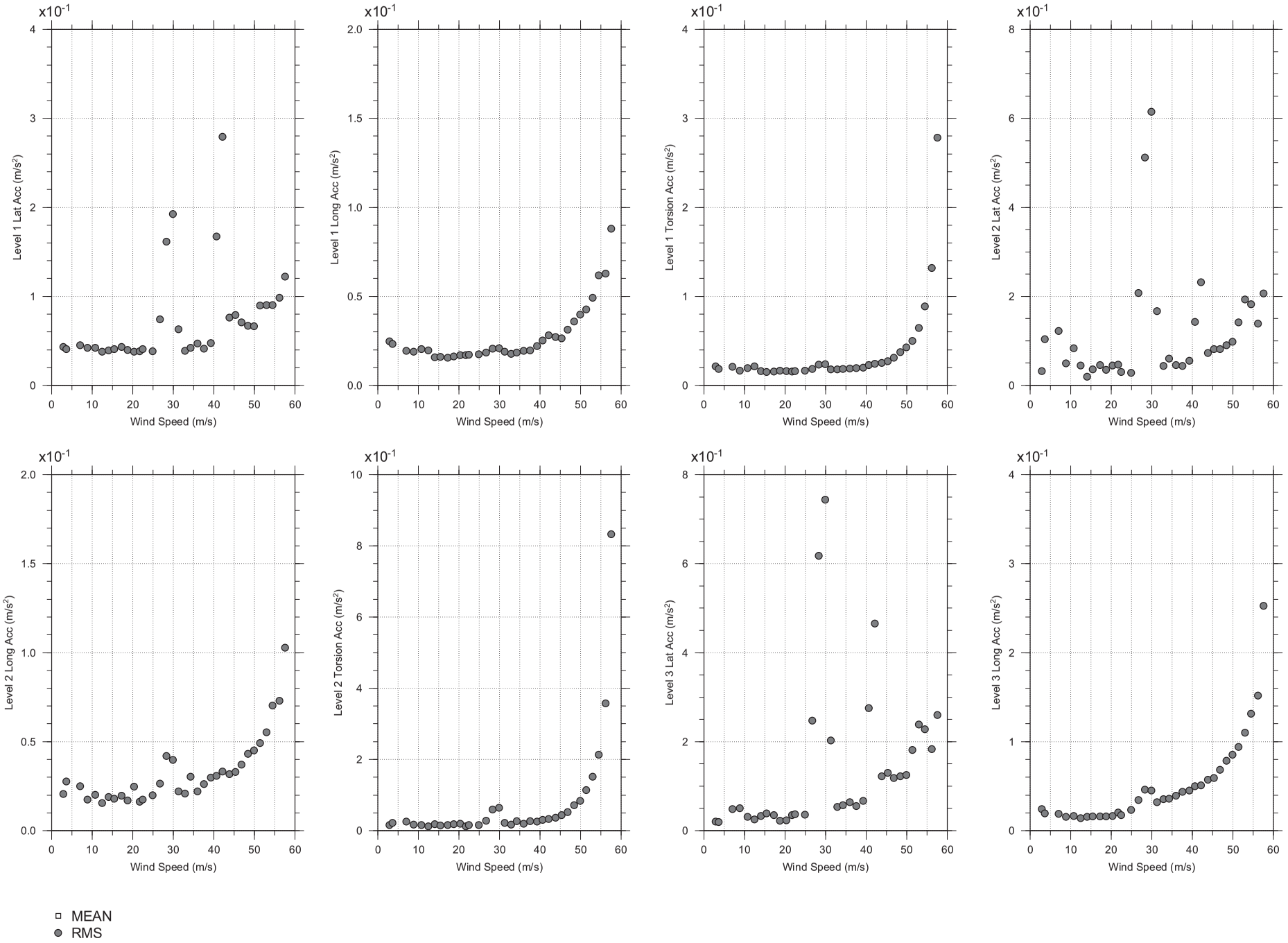

Messina Bridge, Free Standing Tower (Froude No.), 0 degree, 4% Damping, Smooth F

Dec. 14, 2010
frf31abdg.cl

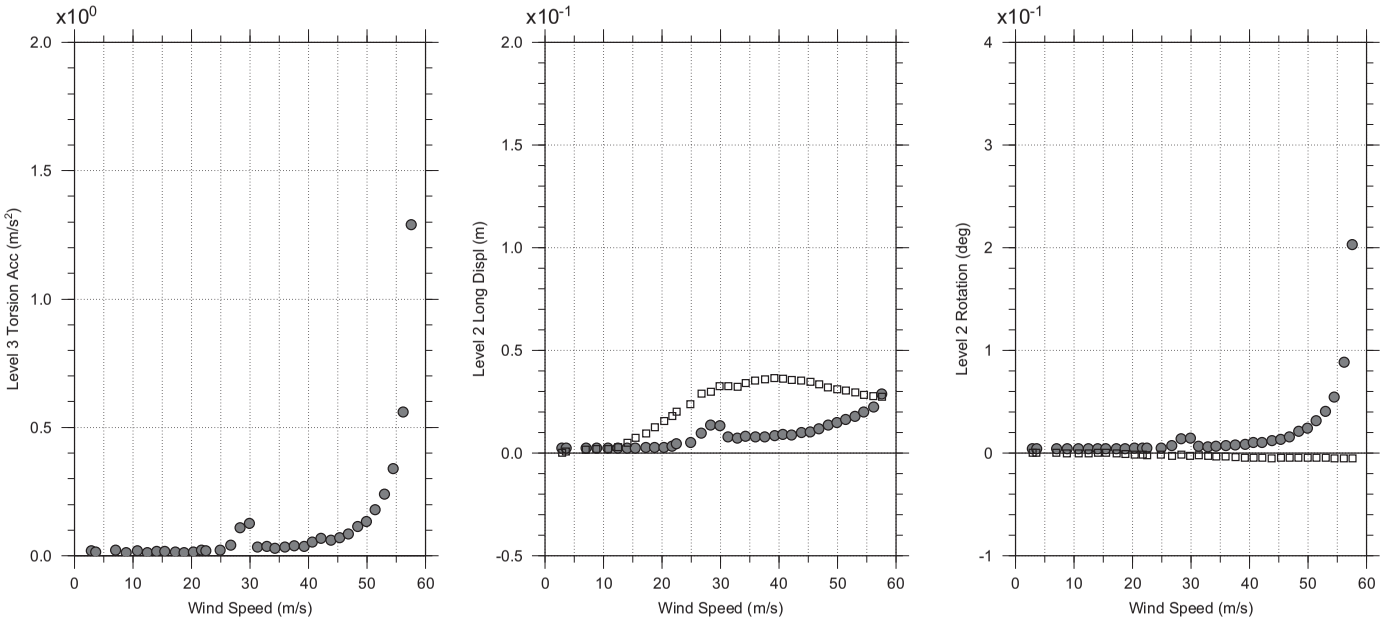

MEAN
RMS

Messina Bridge, Free Standing Tower (Froude No.), 0 degree, 4% Damping, Smooth F

Dec. 14, 2010
frf31abdg.cl

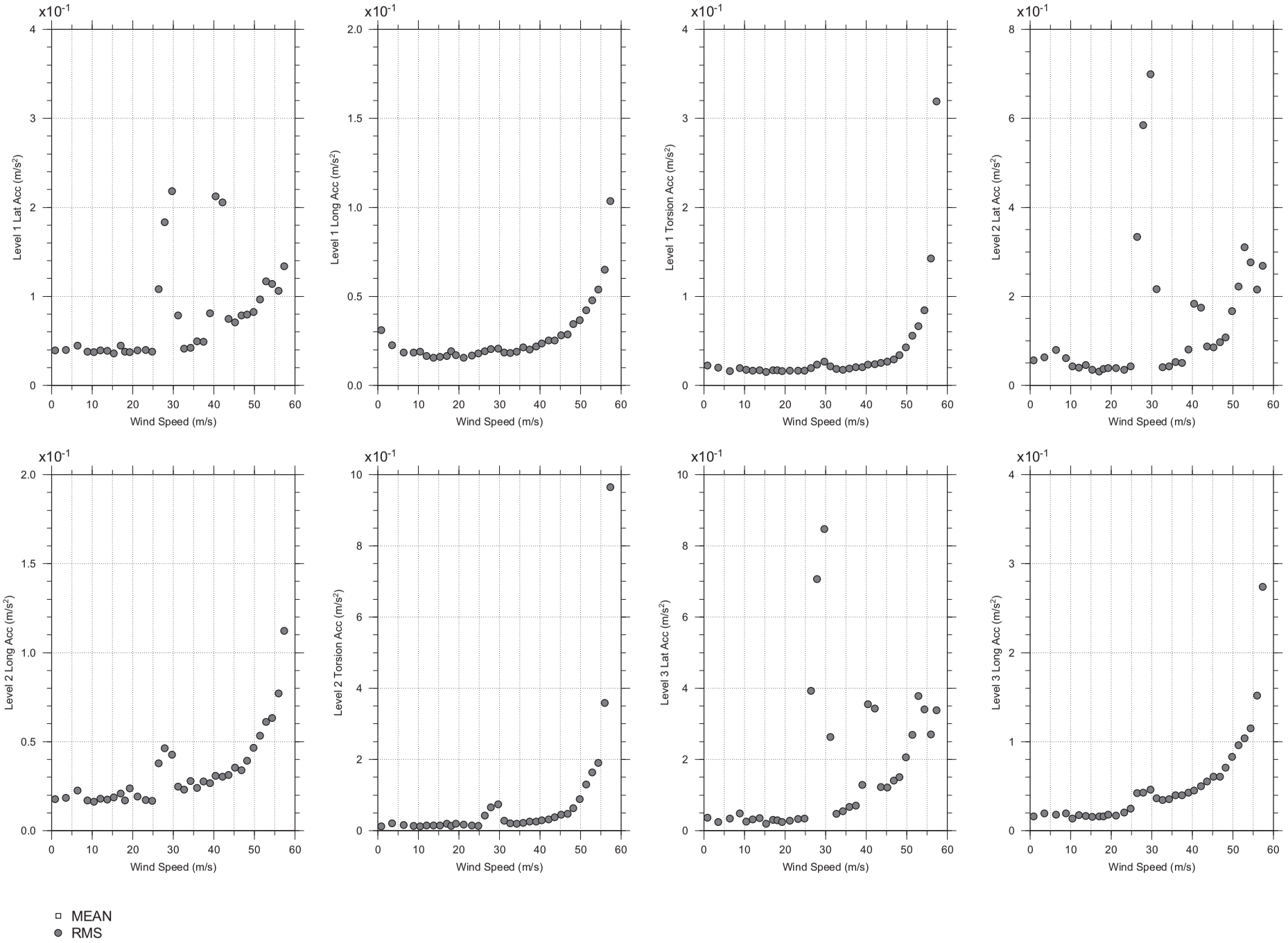

Messina Bridge, Free Standing Tower (Froude No.), 5 degree, 4% Damping, Smooth F

Dec. 14, 2010
frf32abdg.cl

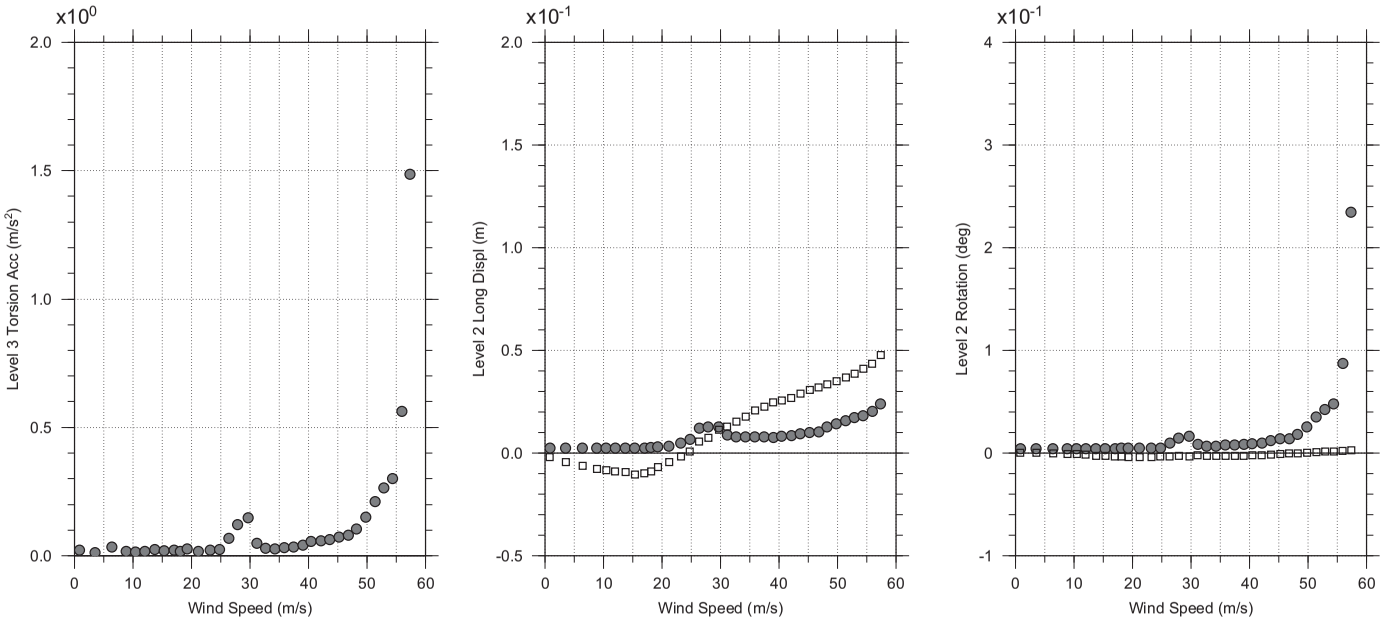

MEAN
RMS

Messina Bridge, Free Standing Tower (Froude No.), 5 degree, 4% Damping, Smooth F

Dec. 14, 2010
frf32abdg.cl

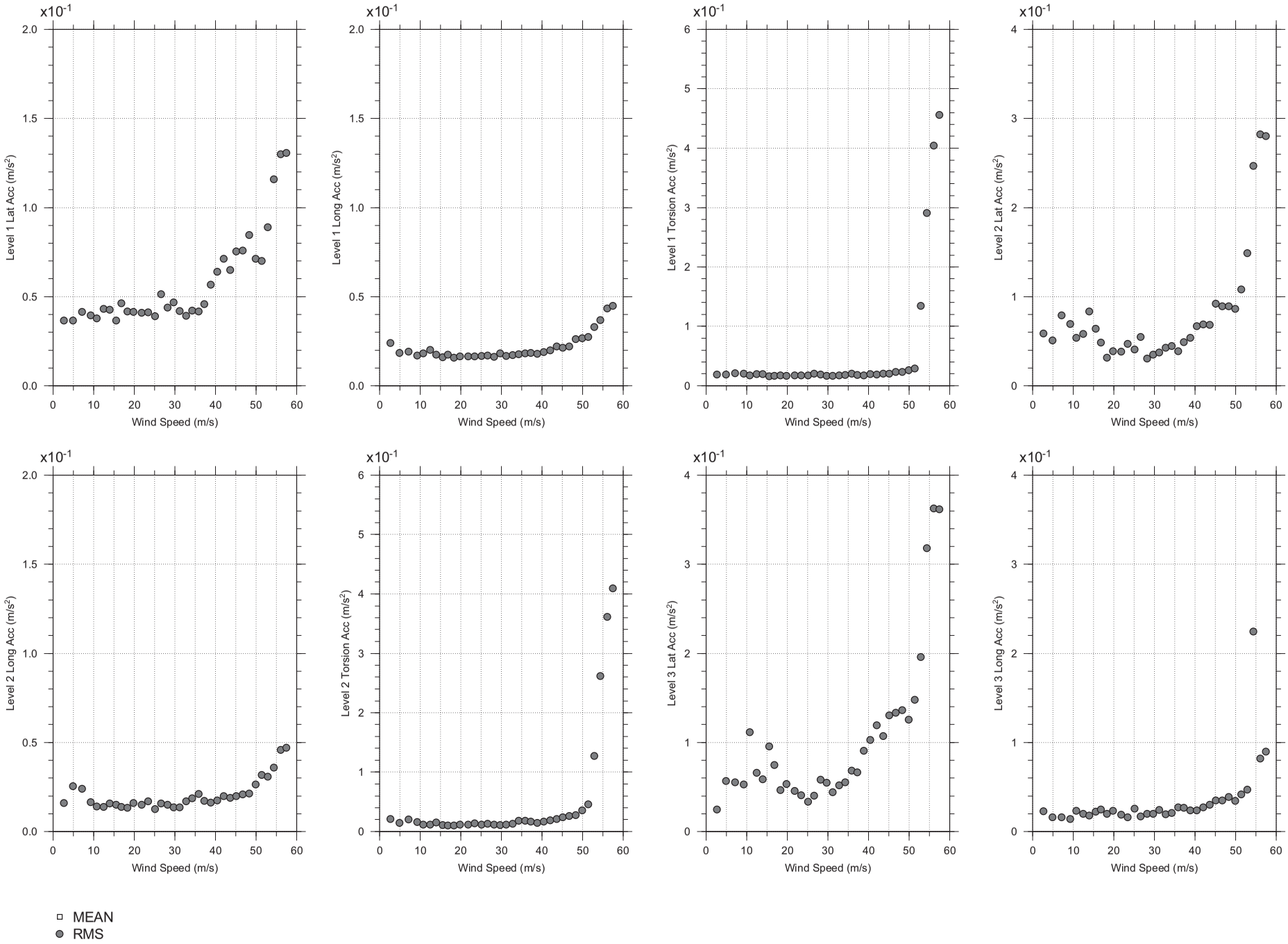

Messina Bridge, Free Standing Tower (Froude No.), 10 degree, 4% Damping, Smooth

Dec. 14, 2010
frf33abdg.cl

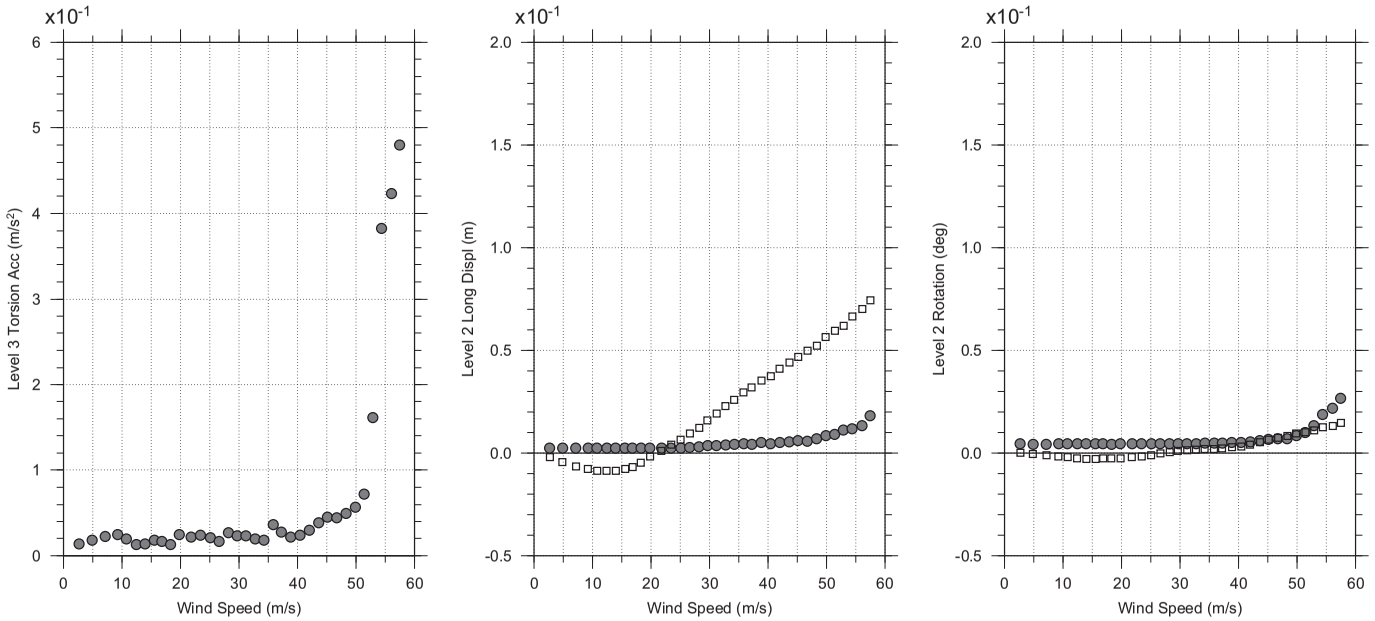

MEAN
RMS

Messina Bridge, Free Standing Tower (Froude No.), 10 degree, 4% Damping, Smooth

Dec. 14, 2010
frf33abdg.cl

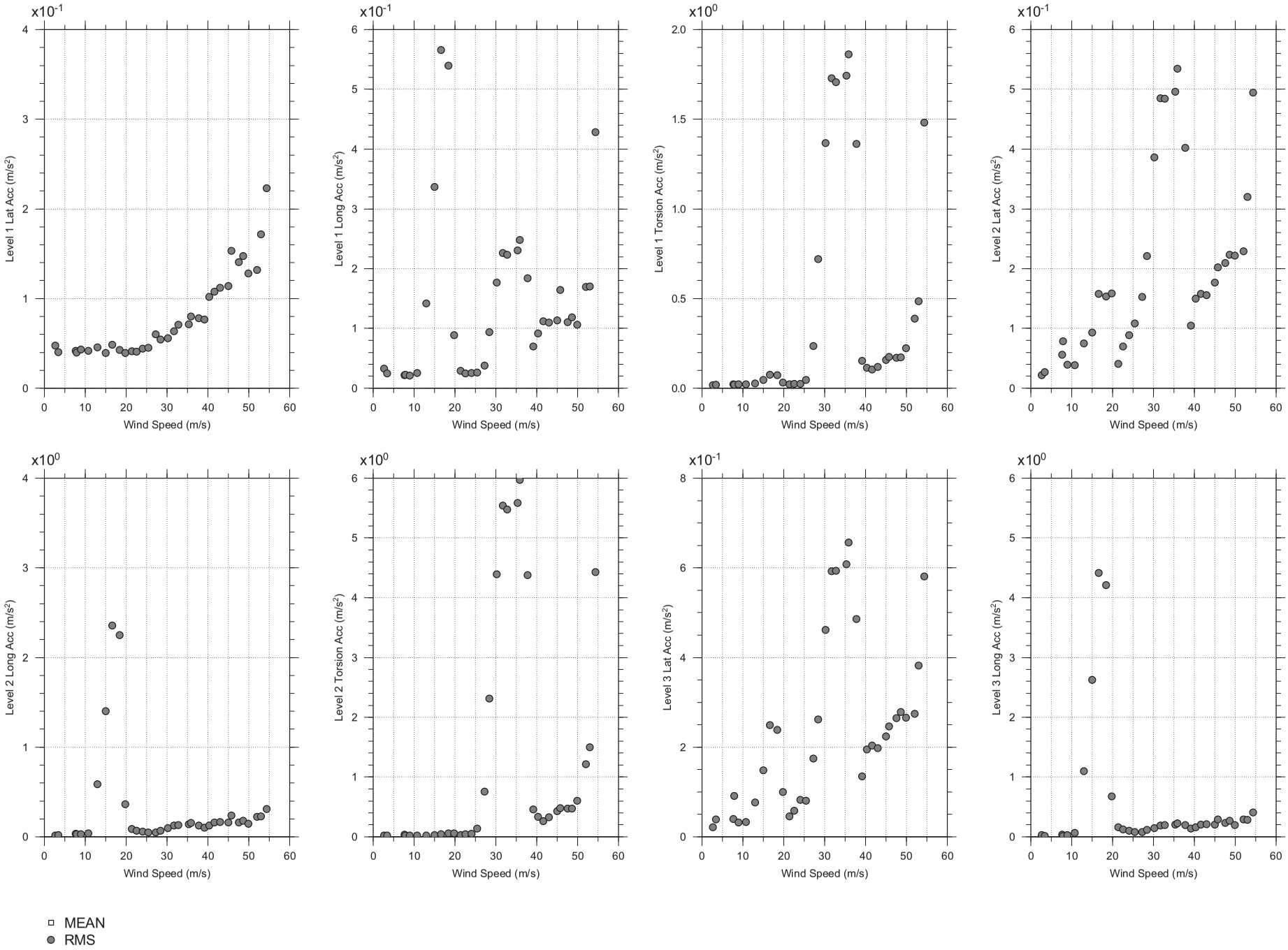

Messina Bridge, Free Standing Tower (Froude No.), 0 degree, Turbulent Flow

Dec. 14, 2010
frf41abdg.cl

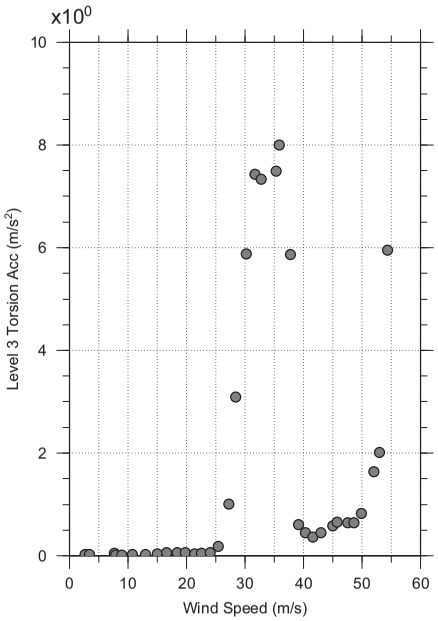

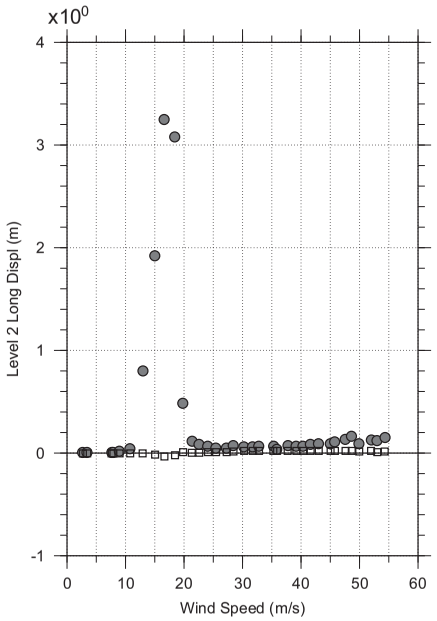

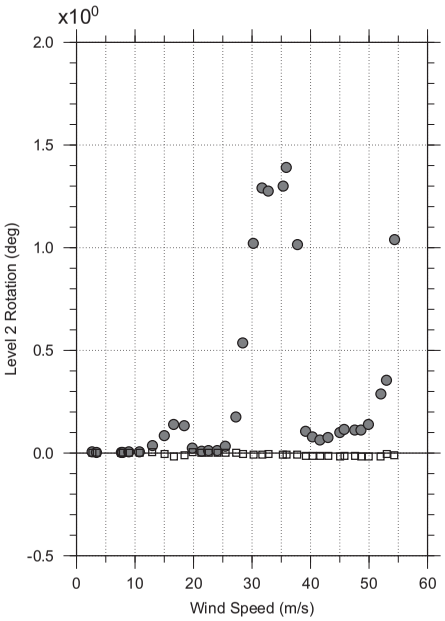

MEAN
RMS

Messina Bridge, Free Standing Tower (Froude No.), 0 degree, Turbulent Flow

Dec. 14, 2010
frf41abdg.cl

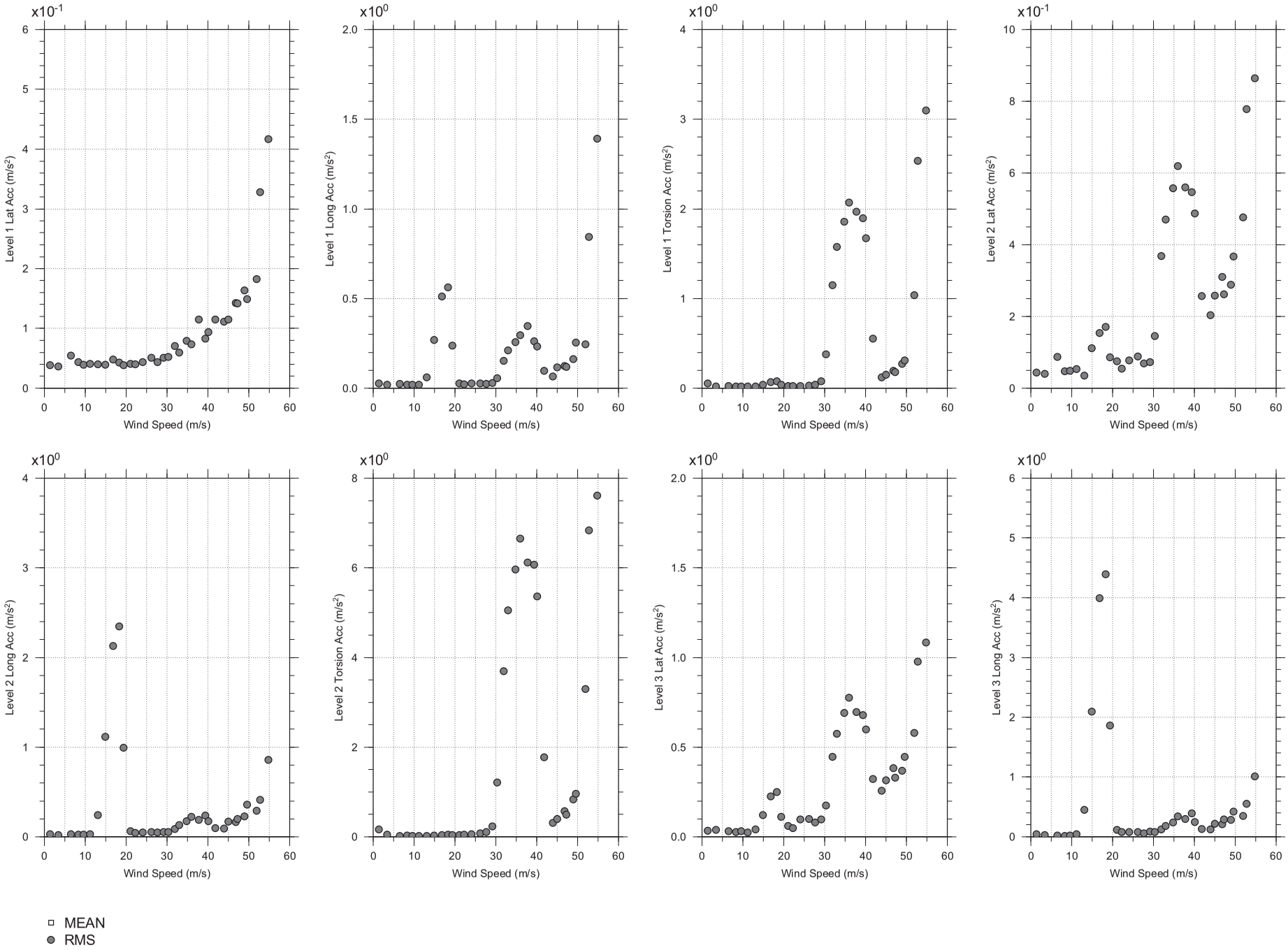

Messina Bridge, Free Standing Tower (Froude No.), 10 degree, Turbulent Flow

Dec. 14, 2010
frf42abdg.cl

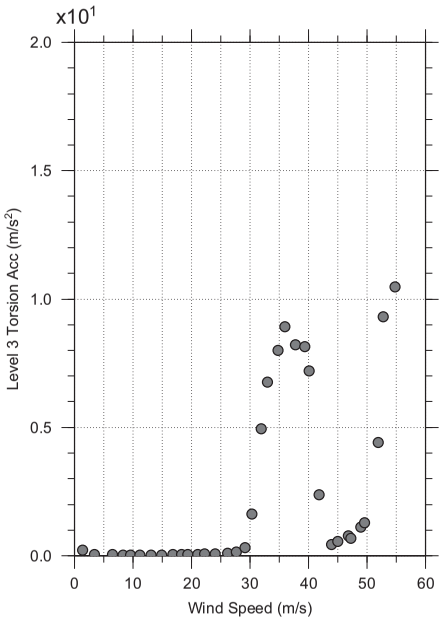

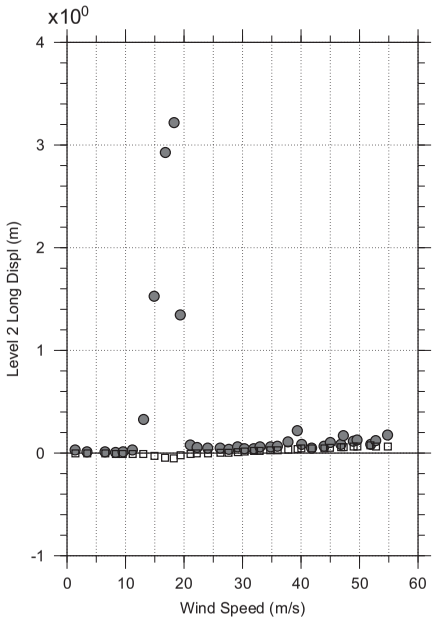

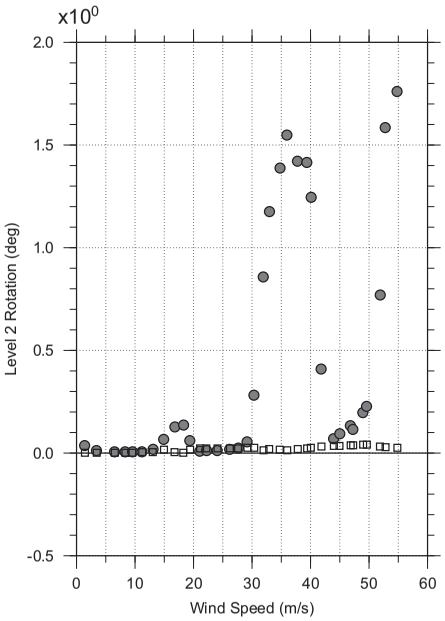

MEAN
RMS

Messina Bridge, Free Standing Tower (Froude No.), 10 degree, Turbulent Flow

Dec. 14, 2010
frf42abdg.cl

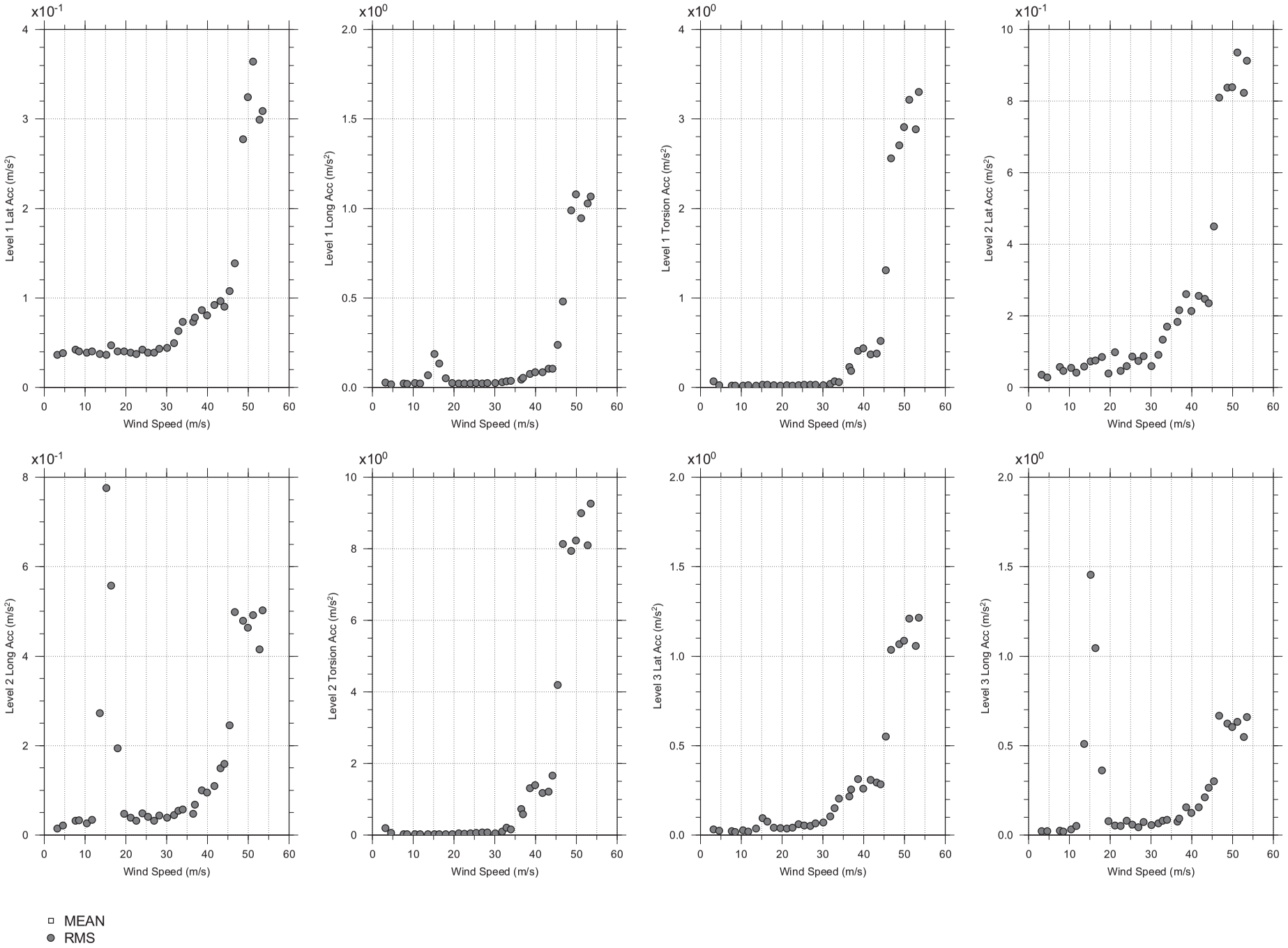

Messina Bridge, Free Standing Tower (Froude No.), 20 degree, Turbulent Flow

Dec. 14, 2010
frf43abdg.cl

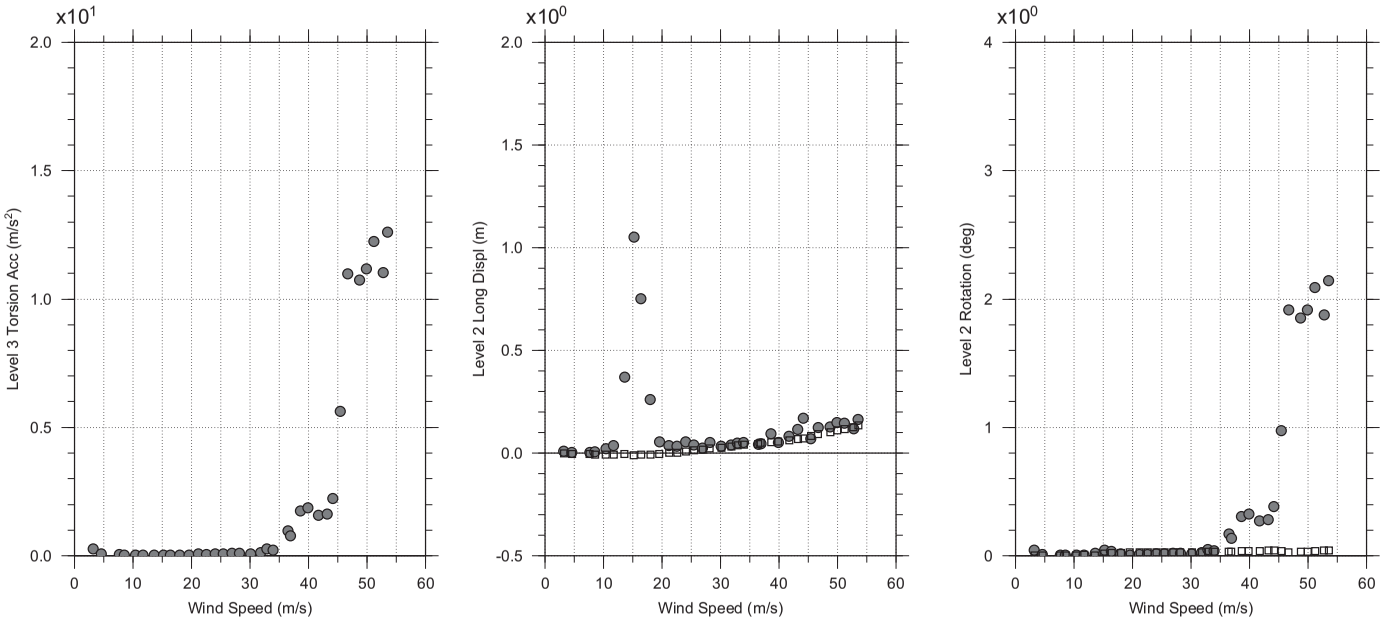

□ MEAN
● RMS

Messina Bridge, Free Standing Tower (Froude No.), 20 degree, Turbulent Flow

Dec. 14, 2010
frf43abdg.cl

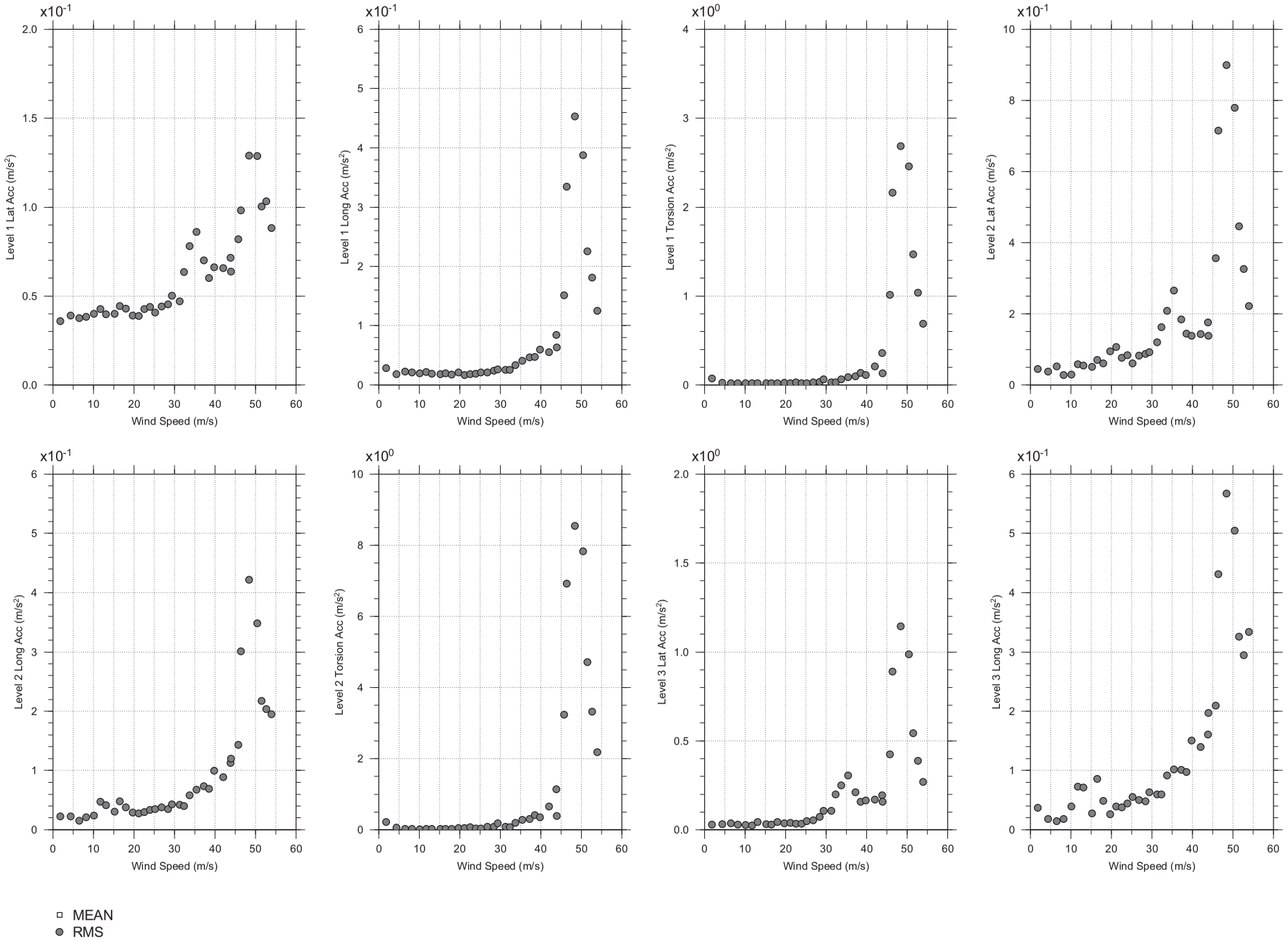

Messina Bridge, Free Standing Tower (Froude No.), 30 degree, Turbulent Flow

Dec. 14, 2010
frf44abdg.cl

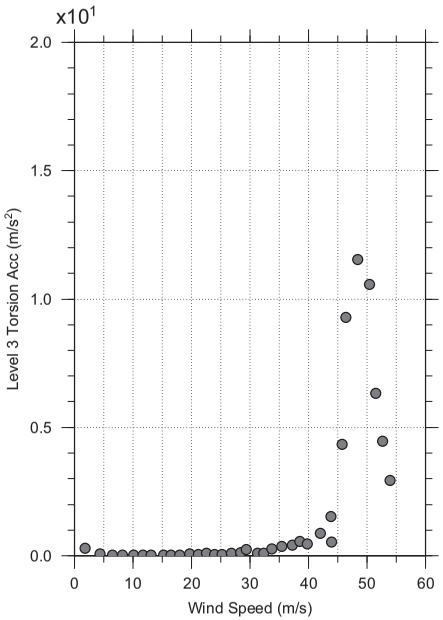

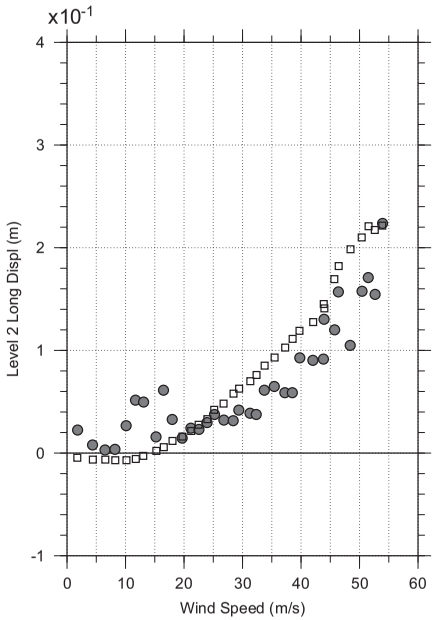

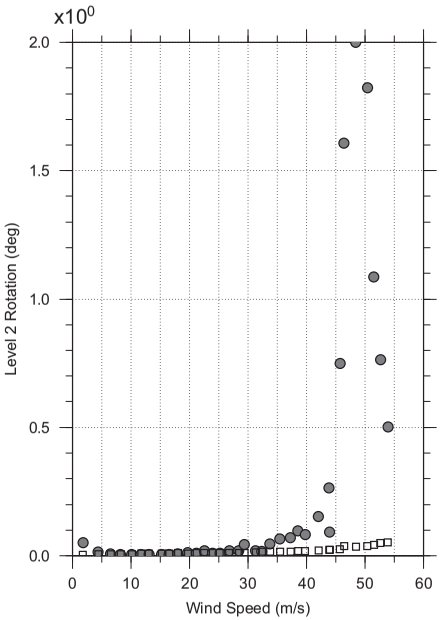

MEAN
RMS

Messina Bridge, Free Standing Tower (Froude No.), 30 degree, Turbulent Flow

Dec. 14, 2010
frf44abdg.cl

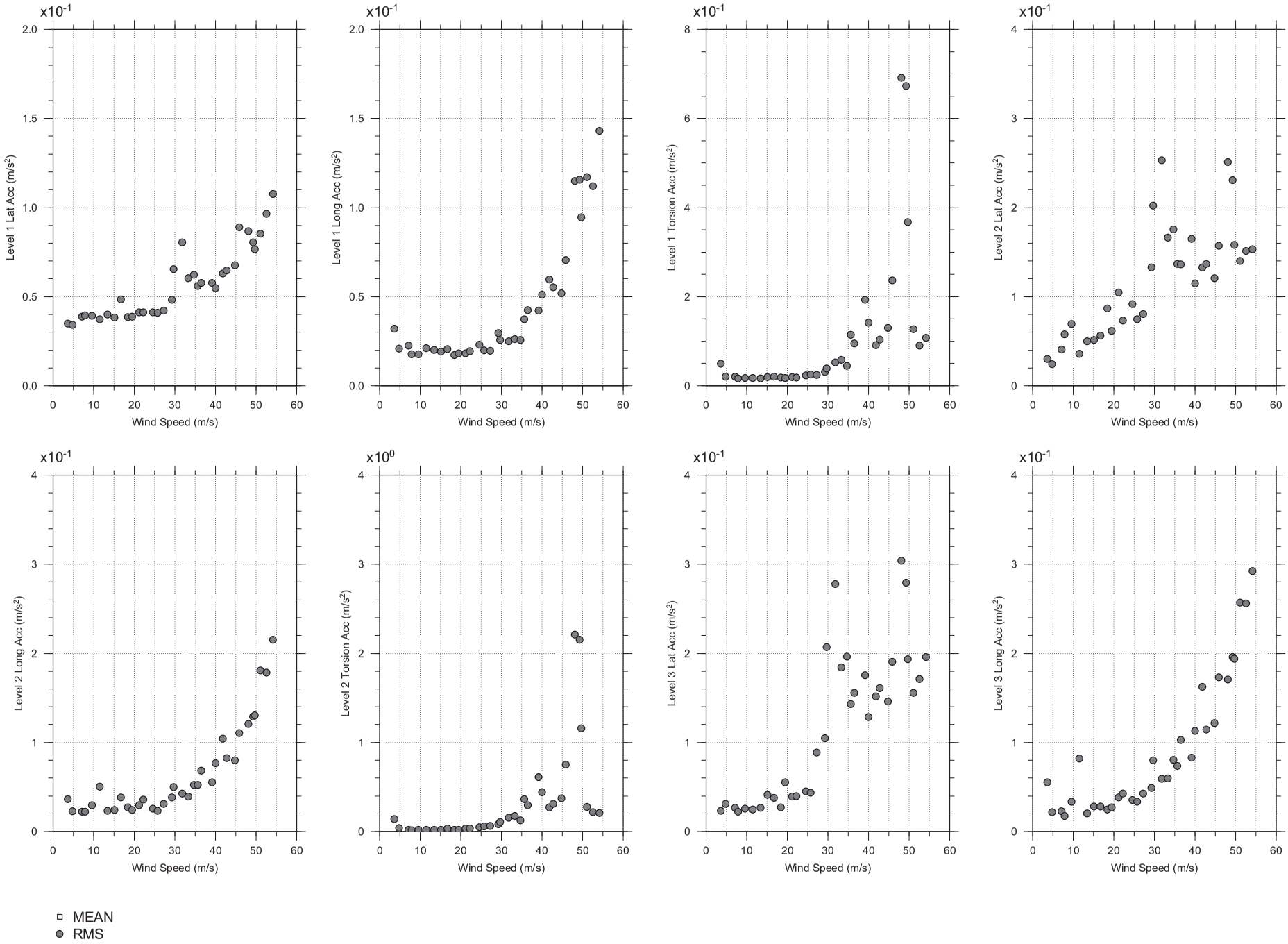

Messina Bridge, Free Standing Tower (Froude No.), 40 degree, Turbulent Flow

Dec. 14, 2010
frf45abdg.cl

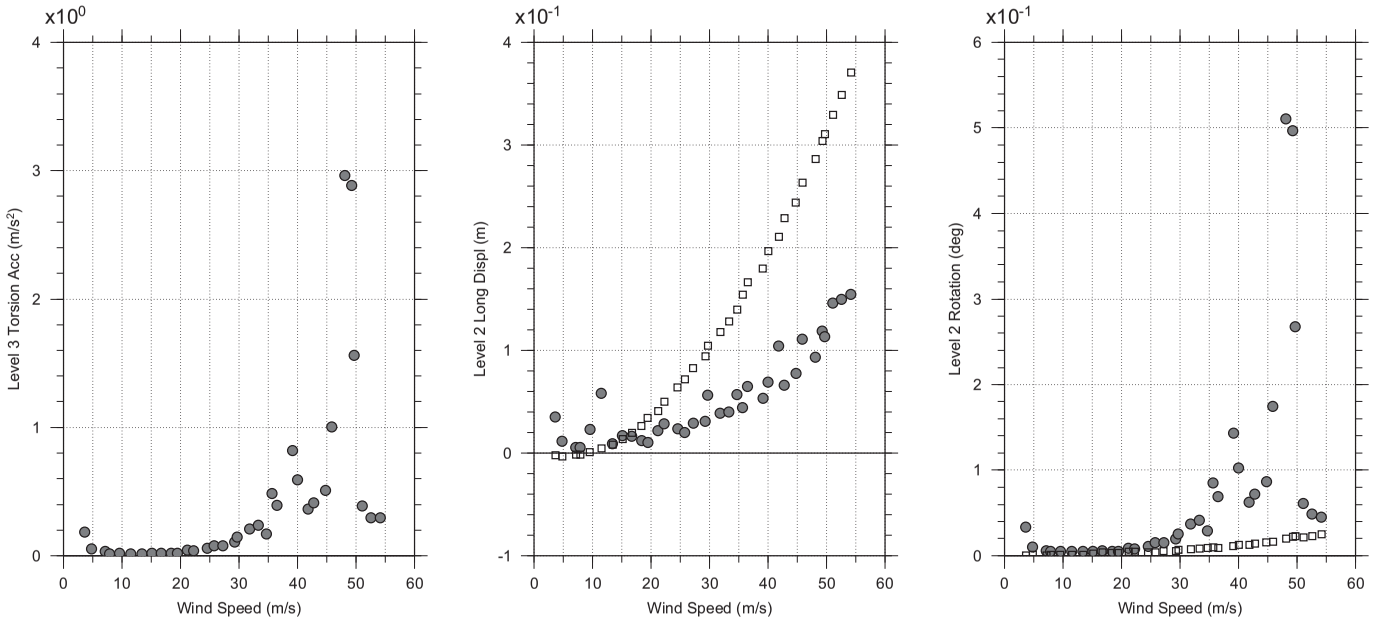

MEAN
RMS

Messina Bridge, Free Standing Tower (Froude No.), 40 degree, Turbulent Flow

Dec. 14, 2010
frf45abdg.cl

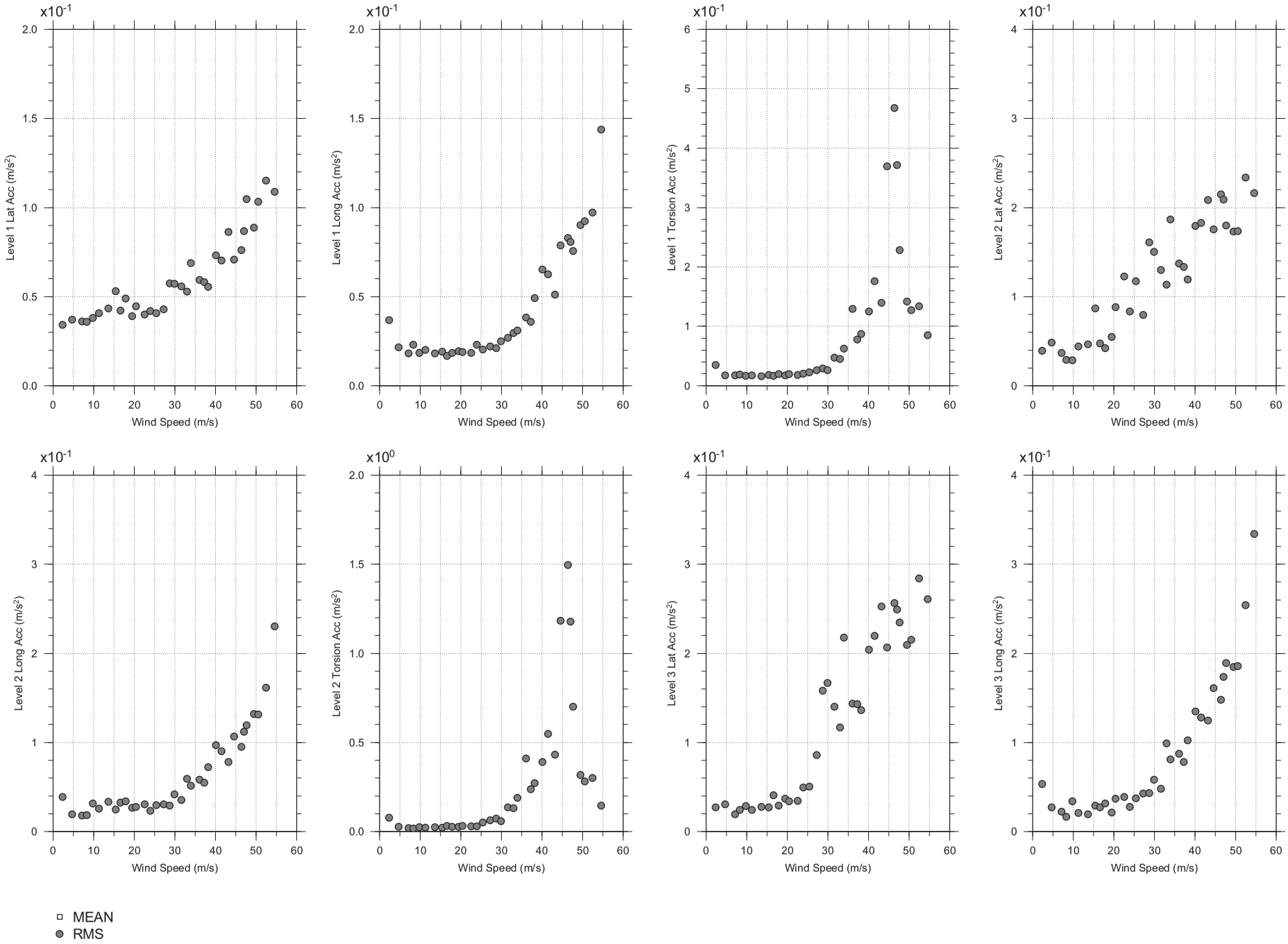

Messina Bridge, Free Standing Tower (Froude No.), 50 degree, Turbulent Flow

Dec. 14, 2010
frf46abdg.cl

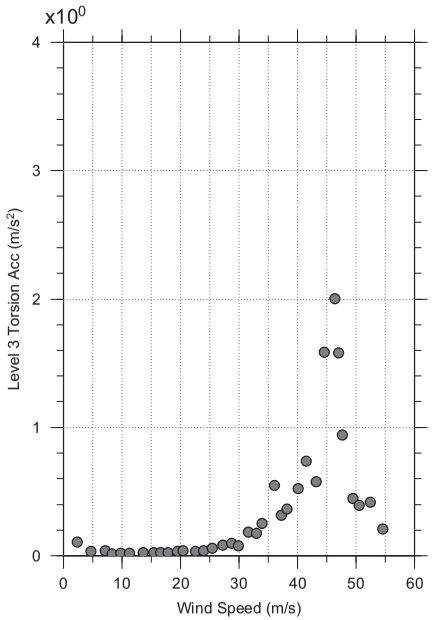

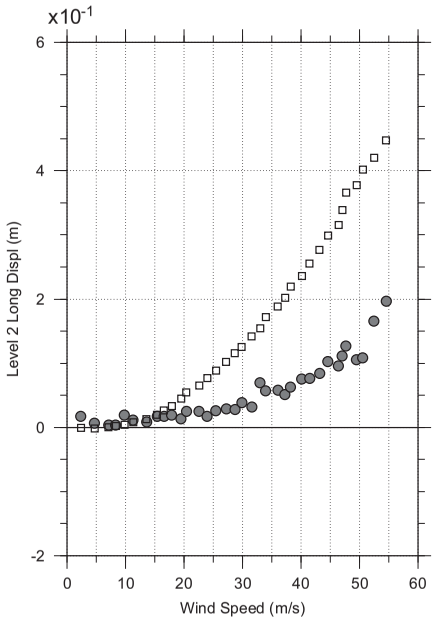

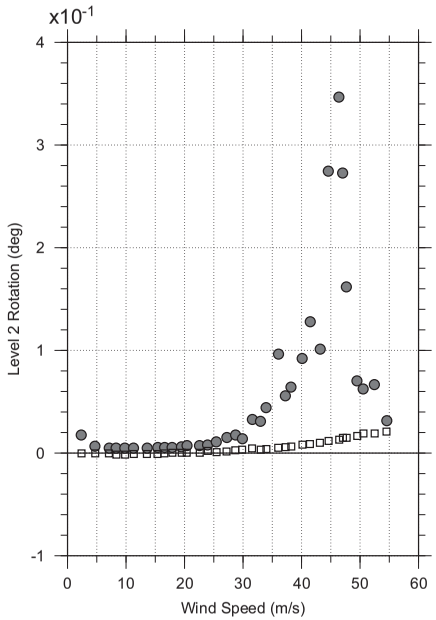

□ MEAN
● RMS

Messina Bridge, Free Standing Tower (Froude No.), 50 degree, Turbulent Flow

Dec. 14, 2010
frf46abdg.cl

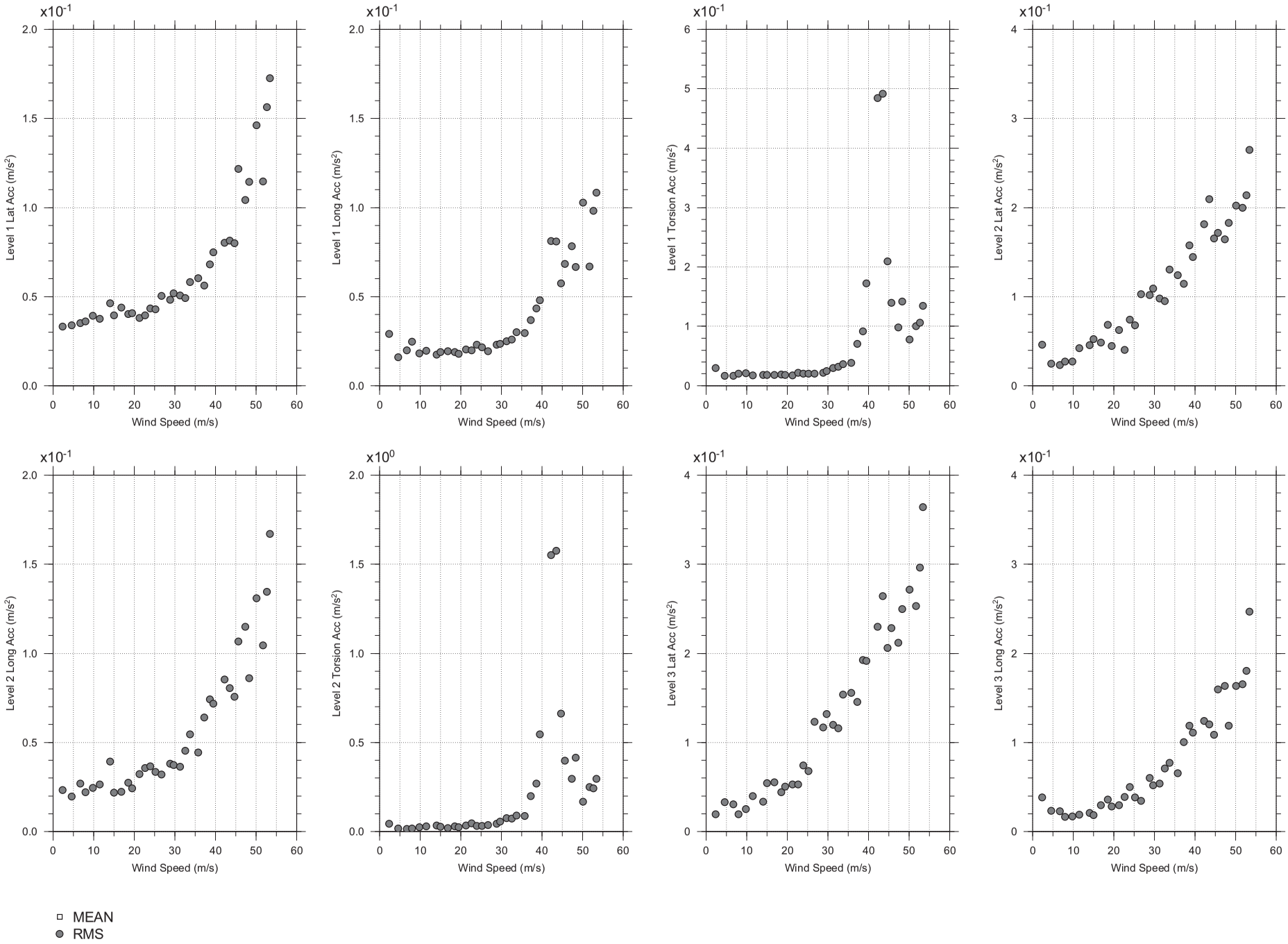

Messina Bridge, Free Standing Tower (Froude No.), 60 degree, Turbulent Flow

Dec. 14, 2010
frf47abdg.cl

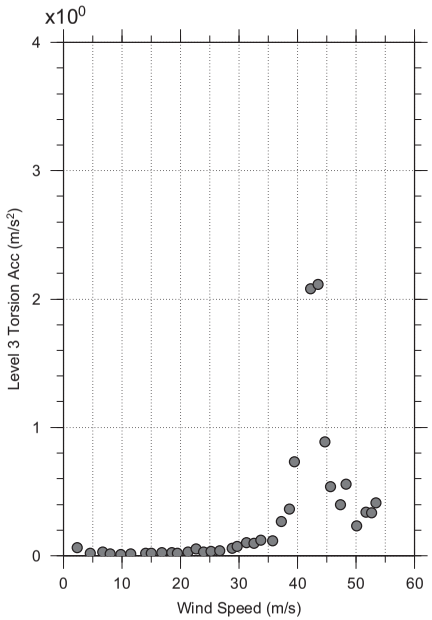

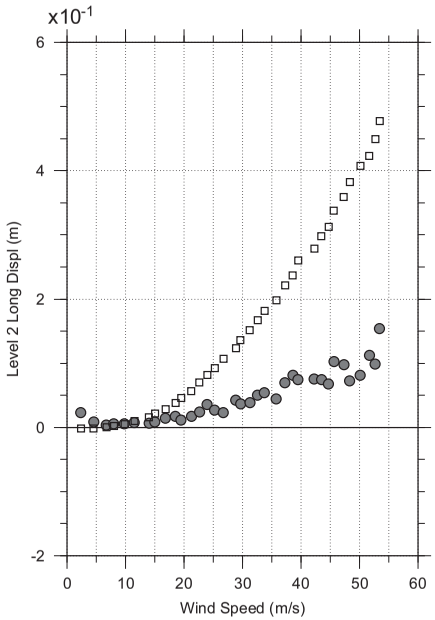

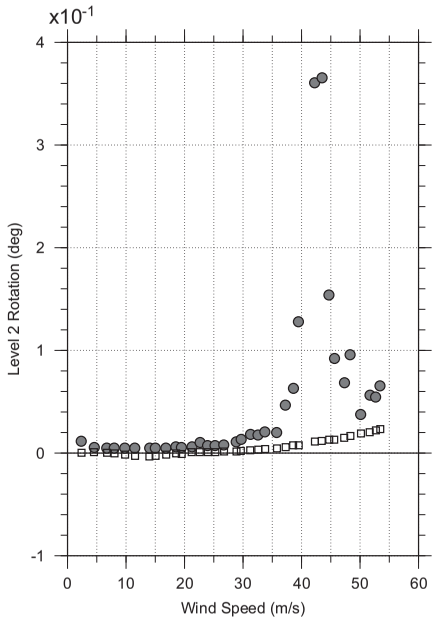

□ MEAN
● RMS

Messina Bridge, Free Standing Tower (Froude No.), 60 degree, Turbulent Flow

Dec. 14, 2010
frf47abdg.cl

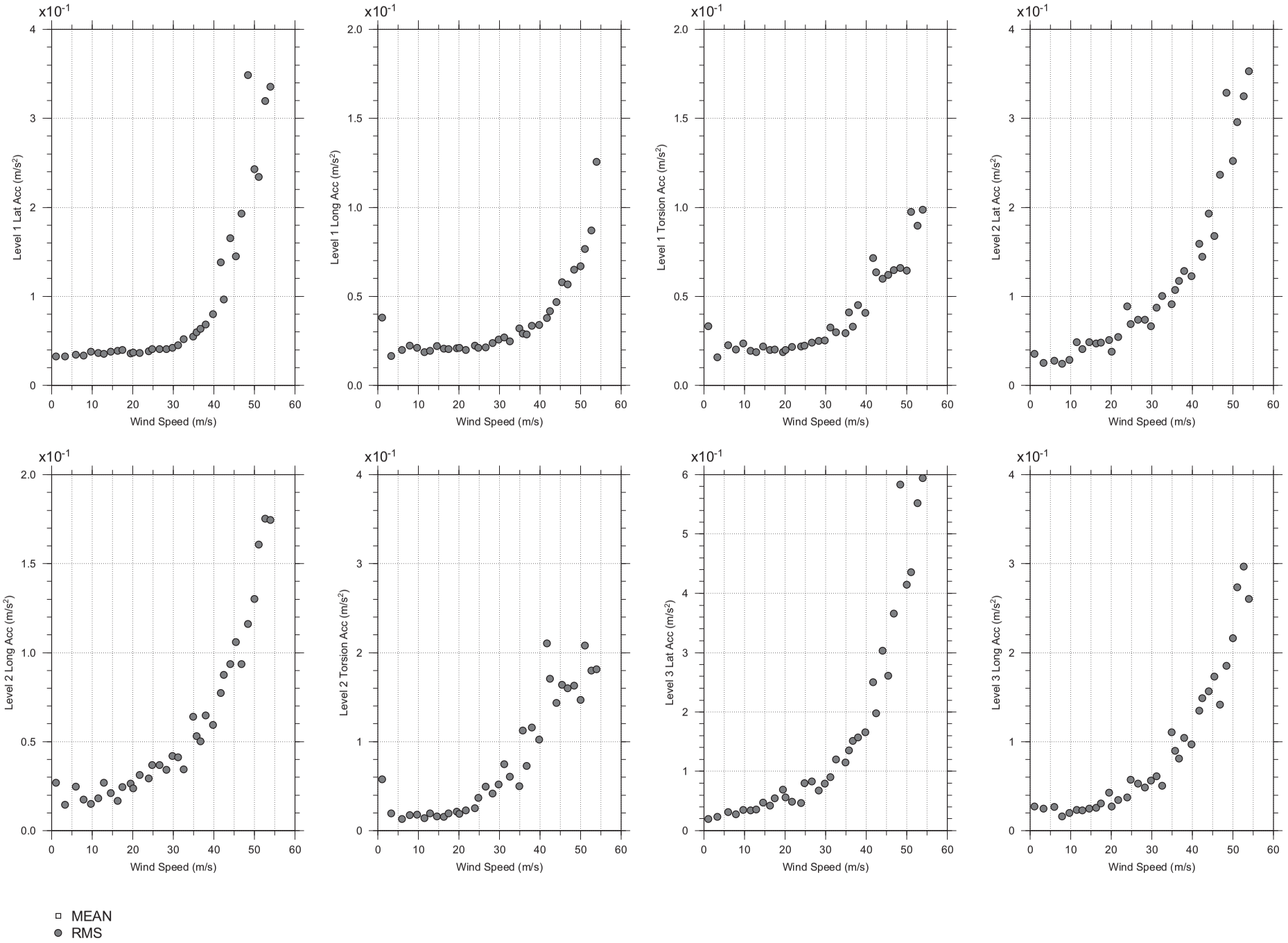

Messina Bridge, Free Standing Tower (Froude No.), 70 degree, Turbulent Flow

Dec. 14, 2010
frf48abdg.cl

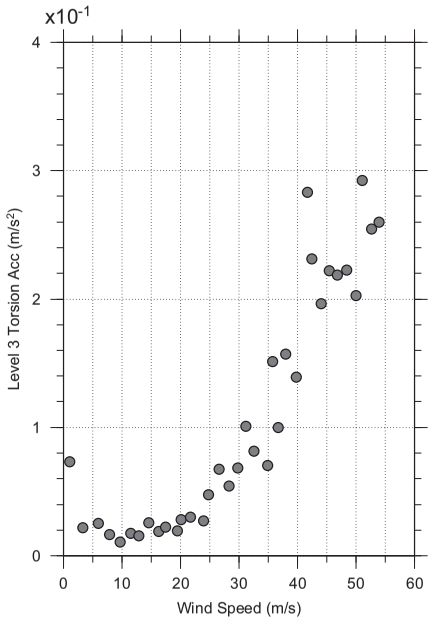

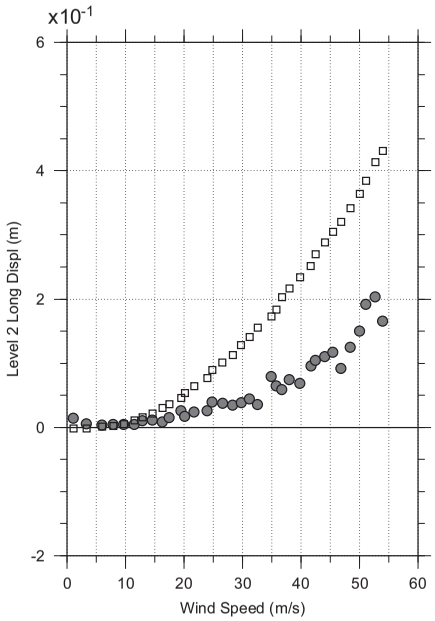

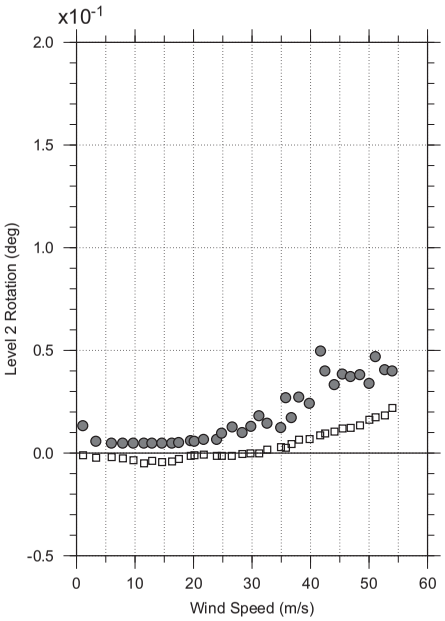

MEAN
RMS

Messina Bridge, Free Standing Tower (Froude No.), 70 degree, Turbulent Flow

Dec. 14, 2010
frf48abdg.cl

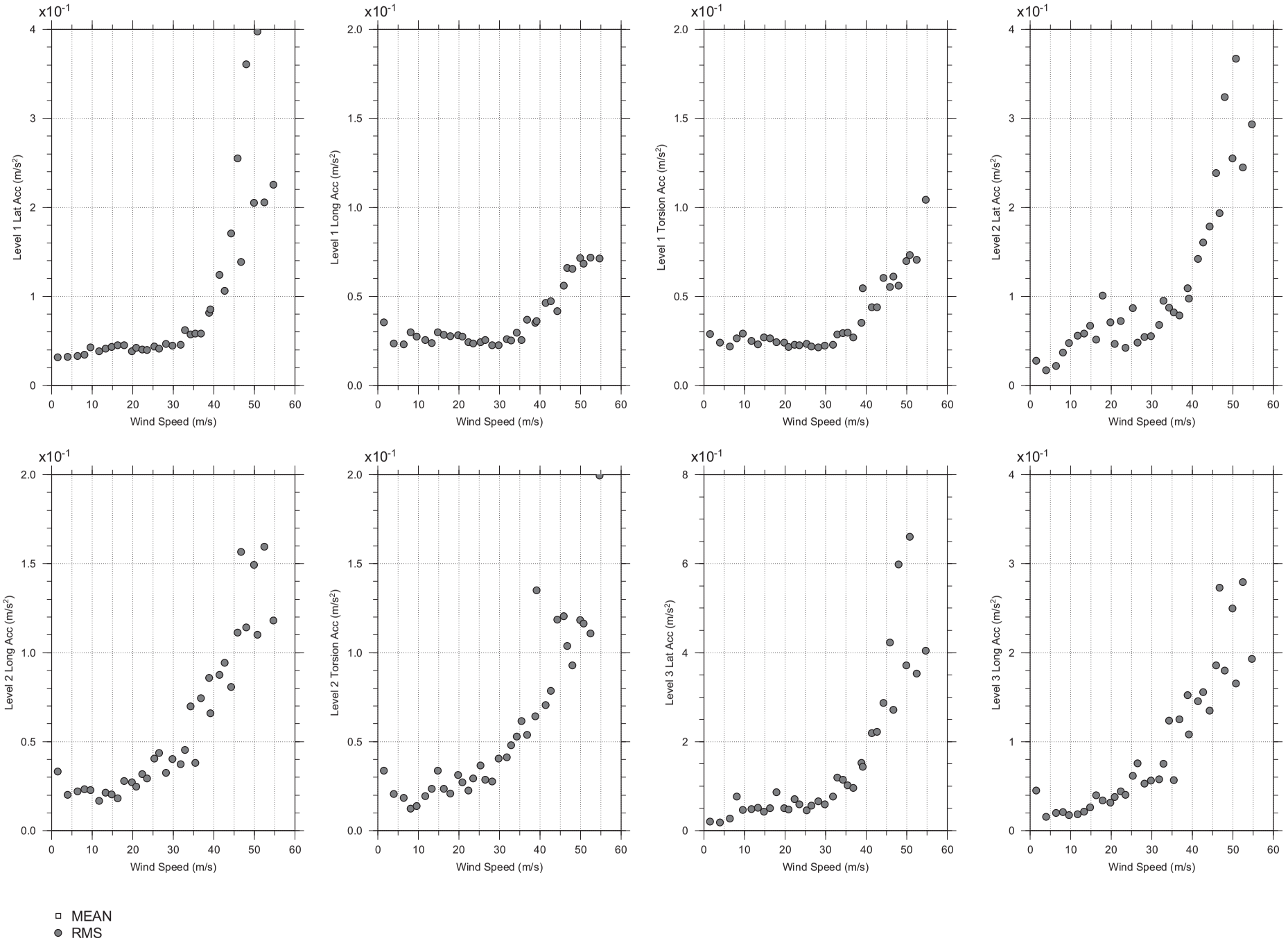

Messina Bridge, Free Standing Tower (Froude No.), 80 degree, Turbulent Flow

Dec. 14, 2010
frf49abdg.cl

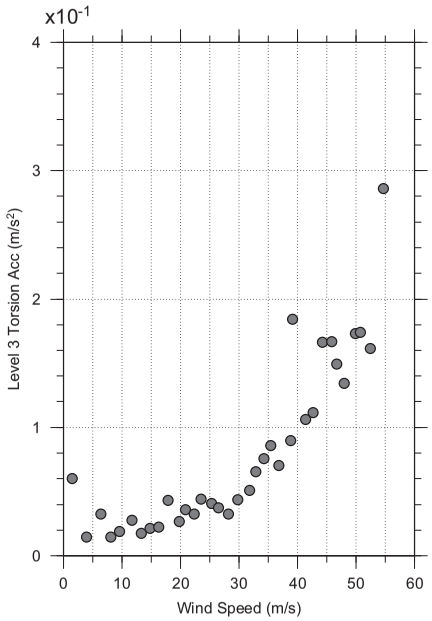

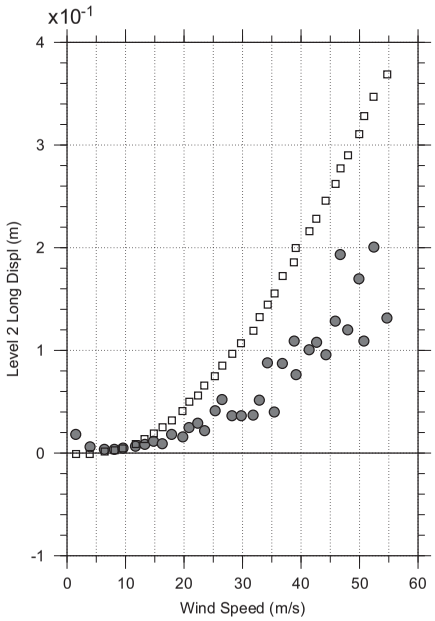

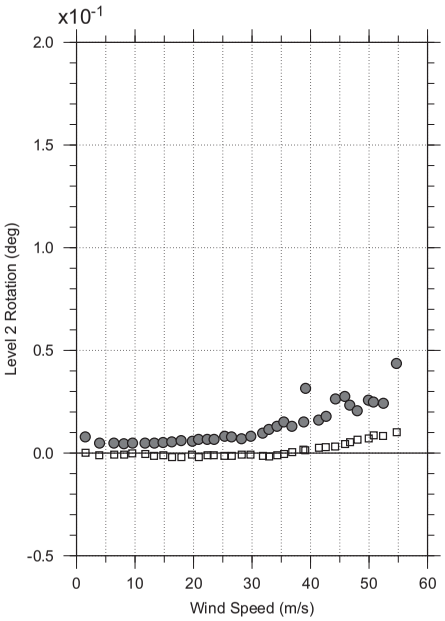

MEAN
RMS

Messina Bridge, Free Standing Tower (Froude No.), 80 degree, Turbulent Flow

Dec. 14, 2010
frf49abdg.cl

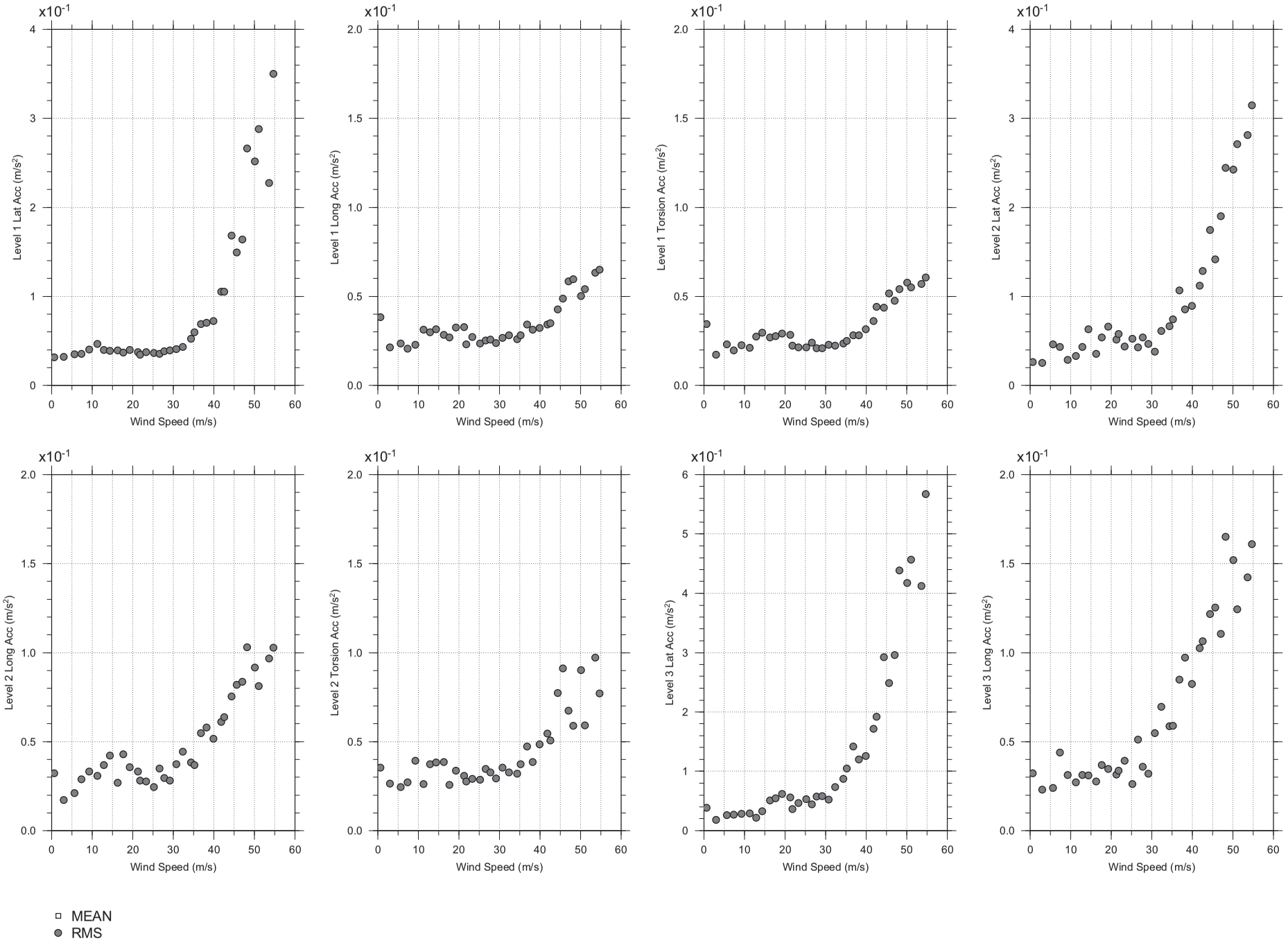

Messina Bridge, Free Standing Tower (Froude No.), 90 degree, Turbulent Flow

Dec. 14, 2010
frf50abdg.cl

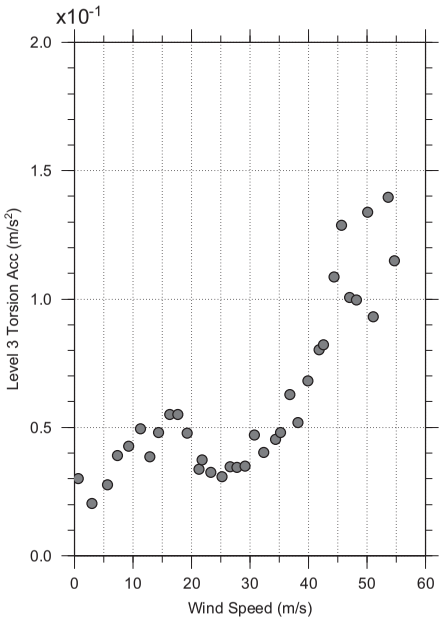

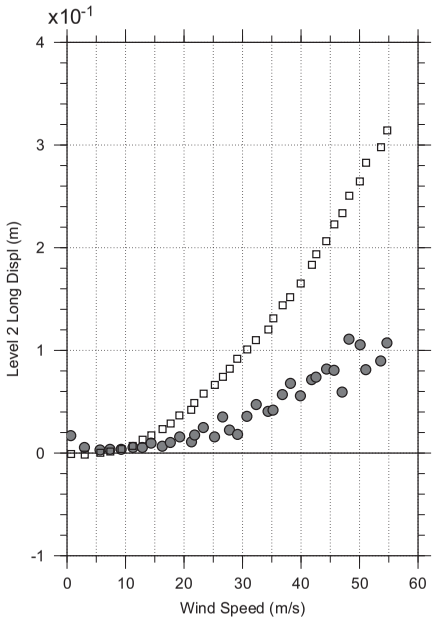

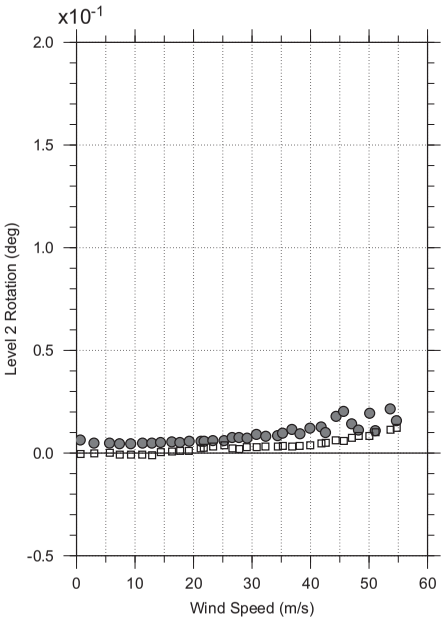

MEAN
RMS

Messina Bridge, Free Standing Tower (Froude No.), 90 degree, Turbulent Flow

Dec. 14, 2010
frf50abdg.cl

APPENDIX E

RESULTS OF FROUDE TOWER MODEL, IN-SERVICE CONDITION

Notes:

E1. The wind speed indicated is the mean hourly wind speed in m/s at the tower height. The bending moments and torques given in the plots have the unit of kN-m. The accelerations have the unit of m/s^2. The displacements have the units of m in the longitudinal direction and degree for tower rotation.

E2. The mean and RMS (root mean square) responses are given separately in the plots. The total responses should be calculated as the mean plus or minus the RMS multiplied by the appropriate peak factor.

E3. Refer to Figure E1 for the definition of test wind angles.

E4. Refer to Figure E2 and Table E1 for the instrumentation locations and sign convention used.

E5. Table E2 summarizes the test results and corresponding test conditions.

TABLE E1 INSTRUMENTATION LOCATIONS, FROUDE TOWER MODEL

Instrumentation	**Instrumentation Locations**
Accelerometers:	
x, y and Torsional accelerations, Level 1	Accelerations measured at 119.4 m above ground
x, y and Torsional accelerations, Level 2	Accelerations measured at 243.8 m above ground
x, y and Torsional accelerations, Level 3	Accelerations measured at 370.8 m above ground
Laser Deflection Transducers:	
x displacement and Rotation θ, Level 2	Displacements measured at 238.7 m above ground
Wind Speeds:	
Deck Height	At a height of 66 m full scale above ground
Tower Height	At a height of 399 m full scale above ground
Mid Tower Height	At a height of 199 m full scale above ground
Reference Height	Where the wind speed not affected by the boundary layer of the wind tunnel floor

Notes:
1. Right-hand rule used for sign convention.
2. x – along bridge axis; y – perpendicular to bridge axis (lateral to tower)

TABLE E2 SUMMARY OF FROUDE TOWER MODEL TESTS, IN SERVICE

Test Configuration	Test No.	Test Files	Modal Frequency (Hz) and Damping (%)			Wind Angle	Maximum Wind Speed	Level 2 Maximum Acceleration Observed		
			Long.	Lat.	Tor.	Deg	m/s	m/s^2	Direction occurred	Wind speed (m/s)
Smooth flow, inherent damping[3.]	1	M075d1E01R002	6.7 (0.17~ 0.18)	4.67 (0.34~ 0.35)	9.25 (0.14~ 0.16)	0 (Lat.)	81	7.938	long	53
	2	M075d1E01R003				2.5	81	8.157	long	53
	3	M075d1E01R004				5	81	8.193	long	53
	4	M075d1E01R005				7.5	81	7.441	long	53
	5	M075d1E01R006				10	81	6.418	long	53
Smooth flow, 2% nominal damping	6	M075d2E01R002	6.7 (2.07~ 2.12)	4.64 (0.30~ 0.32)	9.10 (1.58~ 1.66)	0 (Lat.)	82	2.181	Lat	77
	7	M075d2E01R003				5	82	1.637	Lat	77
	8	M075d2E01R004				10	82	0.949	Long	79
Smooth flow, 4% nominal damping	9	M075d3E01R002	6.97 (3.92~ 3.97)	4.64 (0.30~0 .34)	9.3 (2.06~ 2.08)	0 (Lat.)	82	2.126	Lat	77
	10	M075d3E01R003				5	82	1.759	Lat	77
	11	M075d3E01R004				10	82	0.898	Lat	77
Turbulent boundary layer flow, inherent damping	12	M075d4E02R002	6.7 (0.17~ 0.18)	4.67 (0.34~ 0.35)	9.25 (0.14~ 0.16)	0 (Lat.)	79	32.694	long	64
	13	M075d4E02R003				10	79	32.443	long	64
	14	M075d4E02R004				20	79	15.481	Tor	79
	15	M075d4E02R005				30	79	9.098	long	51
	16	M075d4E02R006				40	79	2.584	Tor	79
	17	M075d4E02R007				50	78	1.981	Tor	67
	18	M075d4E02R008				60	79	1.877	Tor	70
	19	M075d4E02R009				70	79	0.851	Tor	72
	20	M075d4E02R010				80	79	0.838	Lat	79
	21	M075d4E02R011				90 (Long.)	79	0.675	Lat	76

Notes:

1. Maximum wind speed is the equivalent hourly mean wind speed at the top of the tower using a velocity scale of 1:14.14.
2. Long. = Longitudinal direction (along deck), Lat. = Transverse direction with respect to the axis of the bridge deck
3. Tests between 54 m/s and 72 m/s were skipped due to large tower responses for the inherent damping tests in smooth flow.

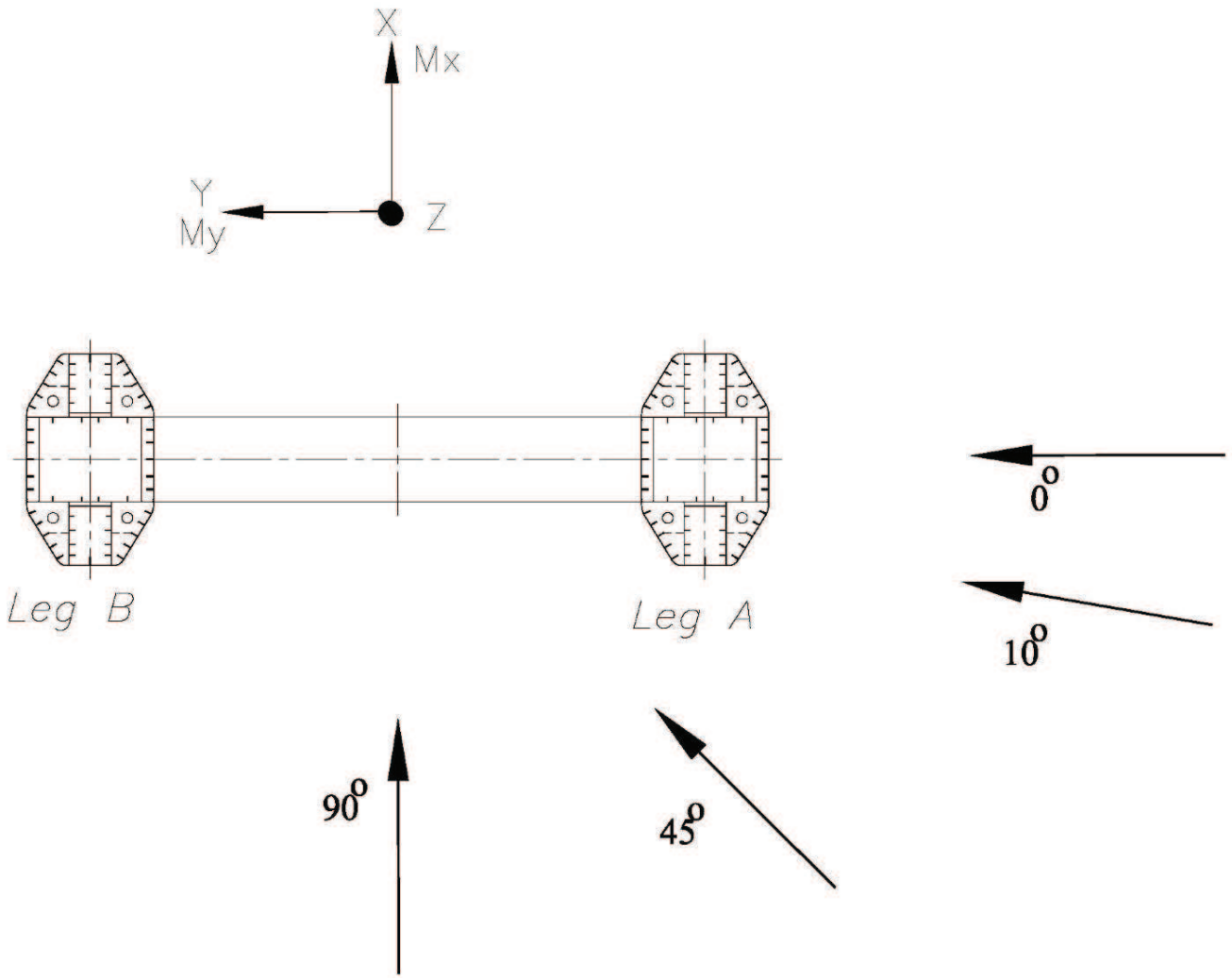

FIGURE E1 DEFINITION OF WIND ANGLES USED IN THE MESSINA TOWER TEST

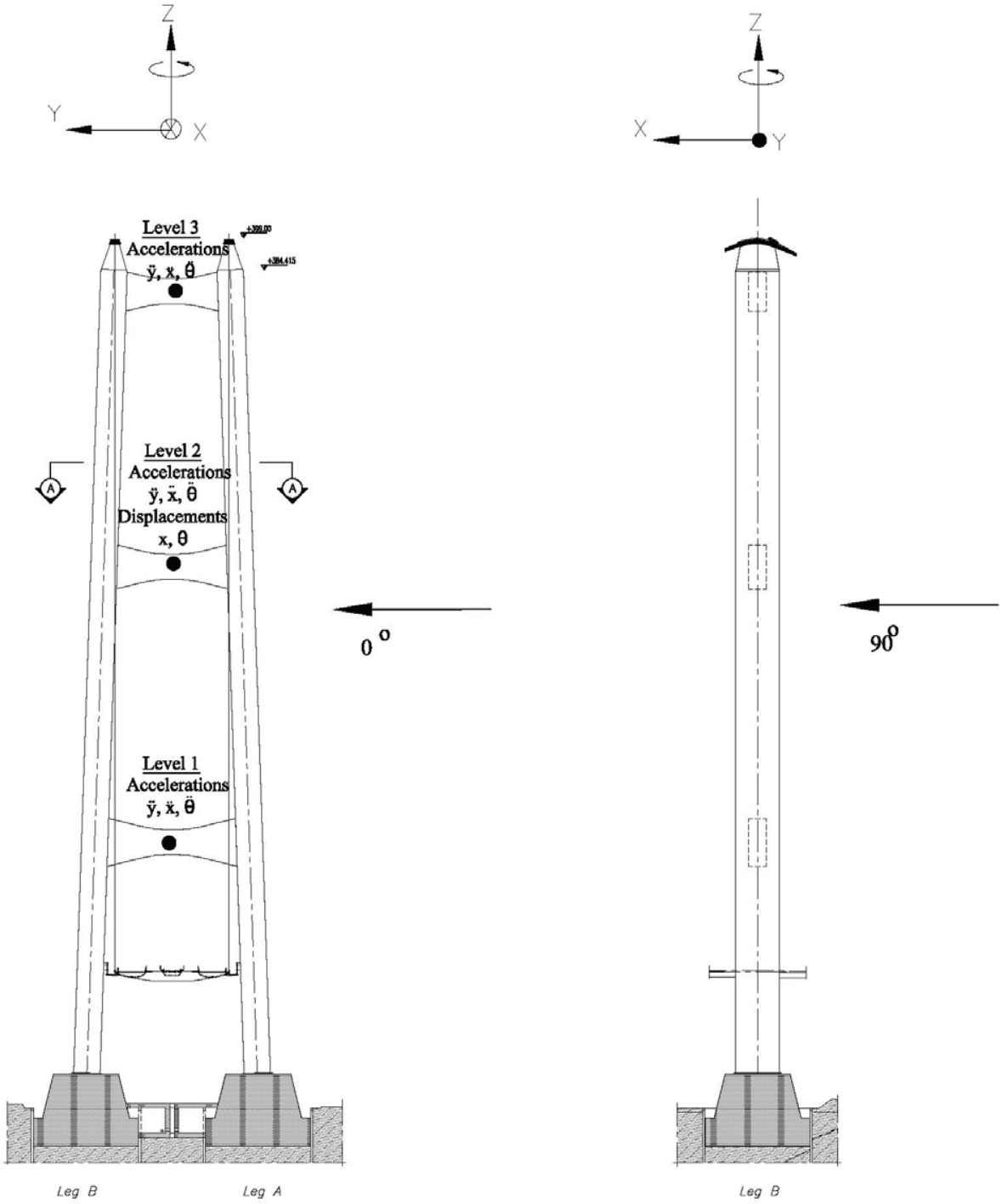

FIGURE E2 INSTRUMENTATION LOCATIONS AND SIGN CONVENTIONS USED IN THE FROUDE TOWER TEST

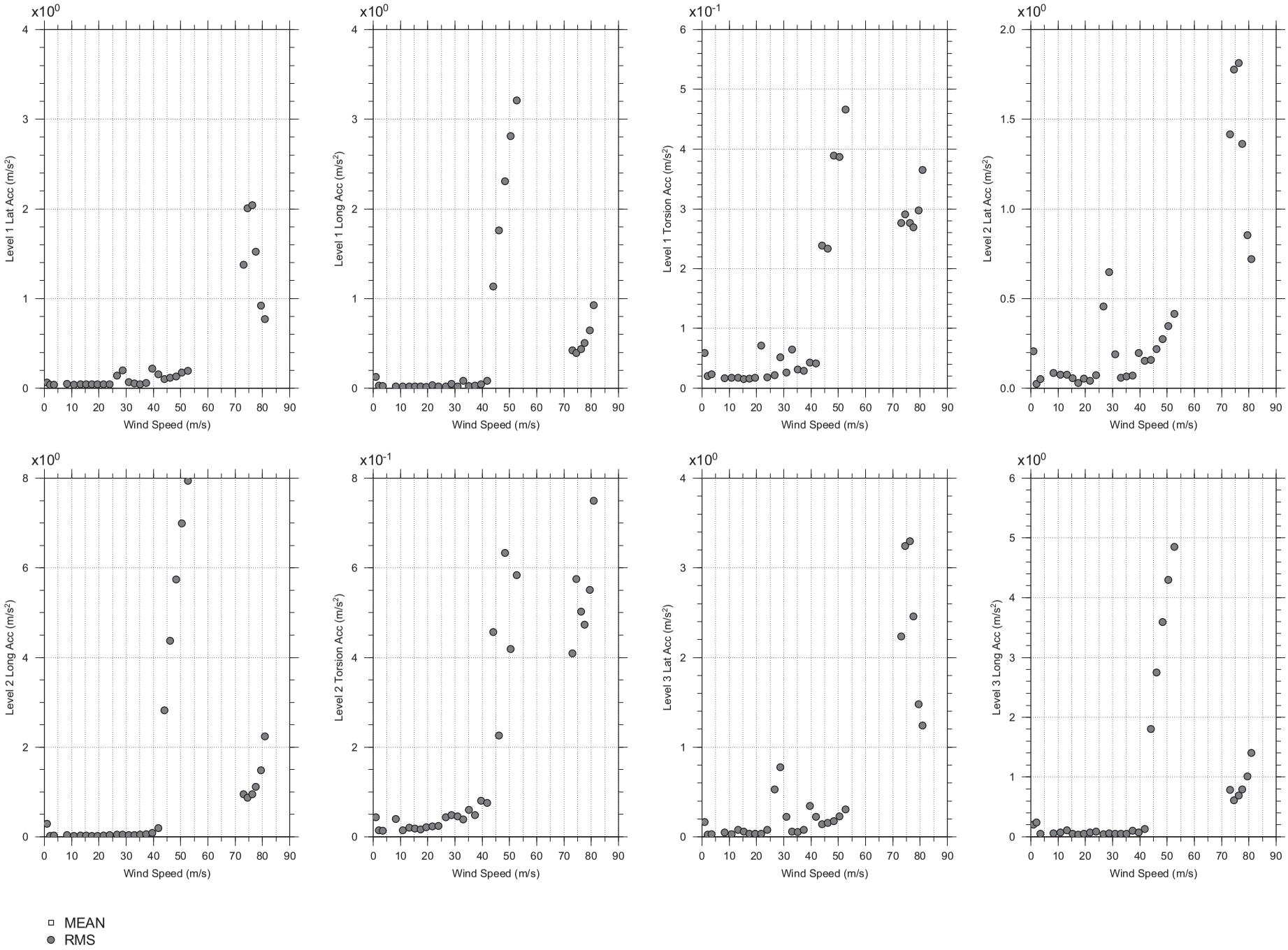

Messina Bridge, In Service Tower (Froude No.), 0 degree, Smooth Flow

Dec. 15, 2010
fri11abdg.cl

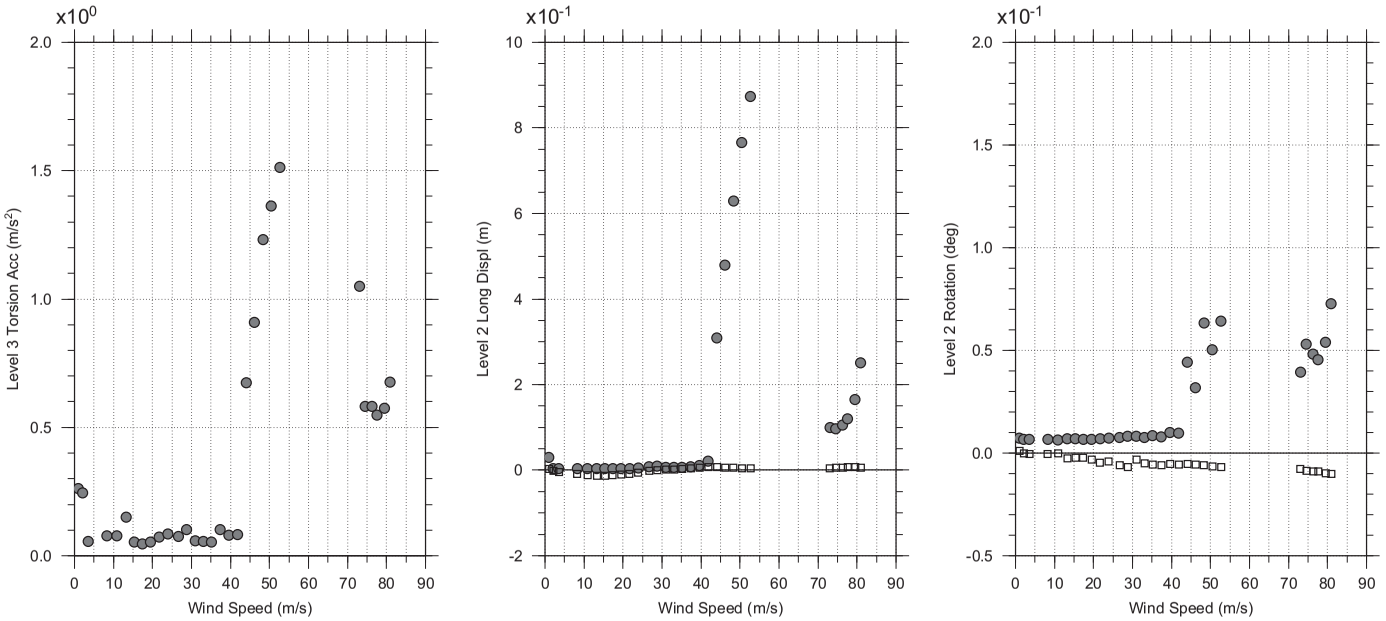

MEAN
RMS

Messina Bridge, In Service Tower (Froude No.), 0 degree, Smooth Flow

Dec. 15, 2010
fri11abdg.cl

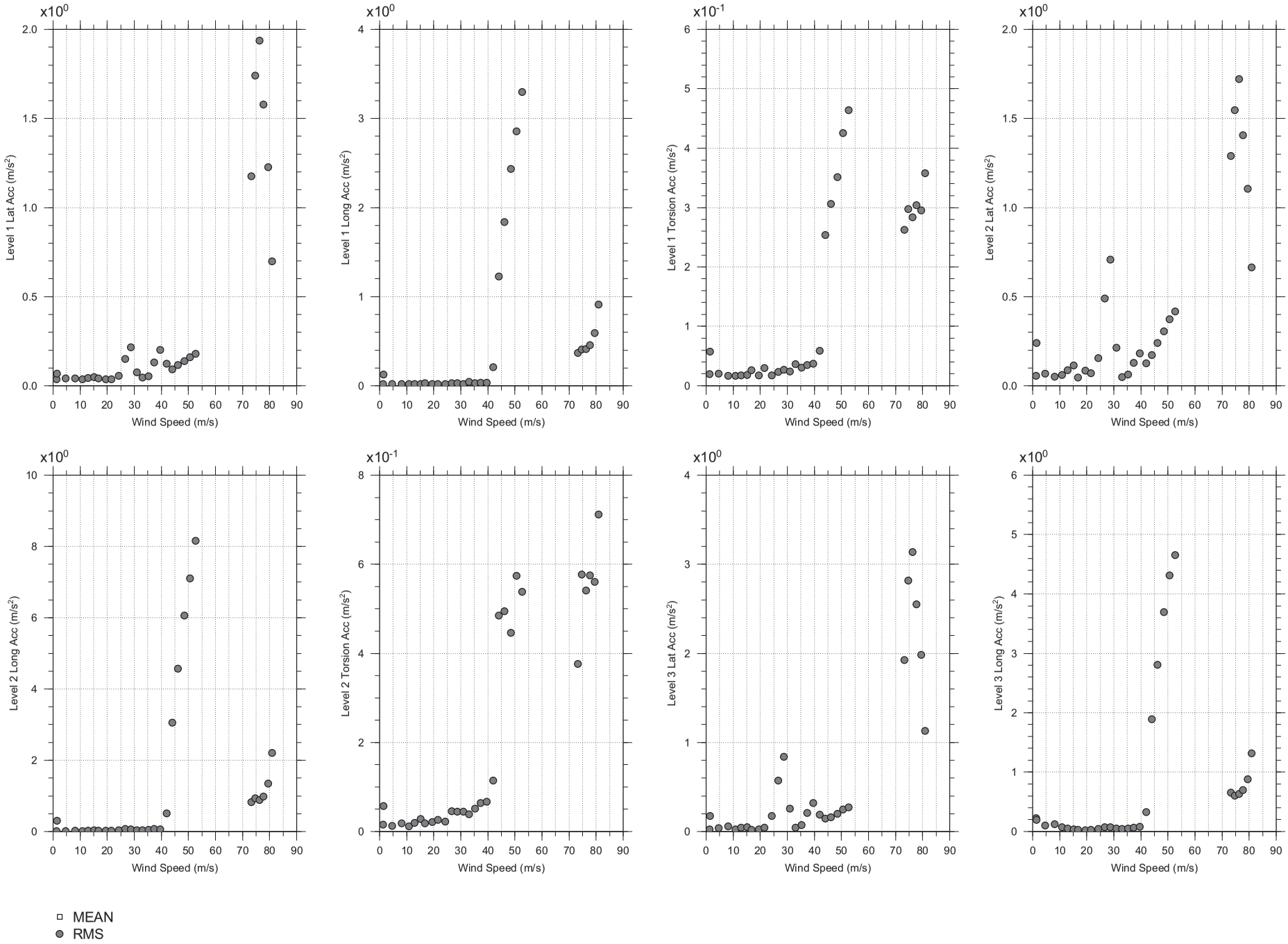

Messina Bridge, In Service Tower (Froude No.), 2.5 degree, Smooth Flow

Dec. 15, 2010
fri12abdg.cl

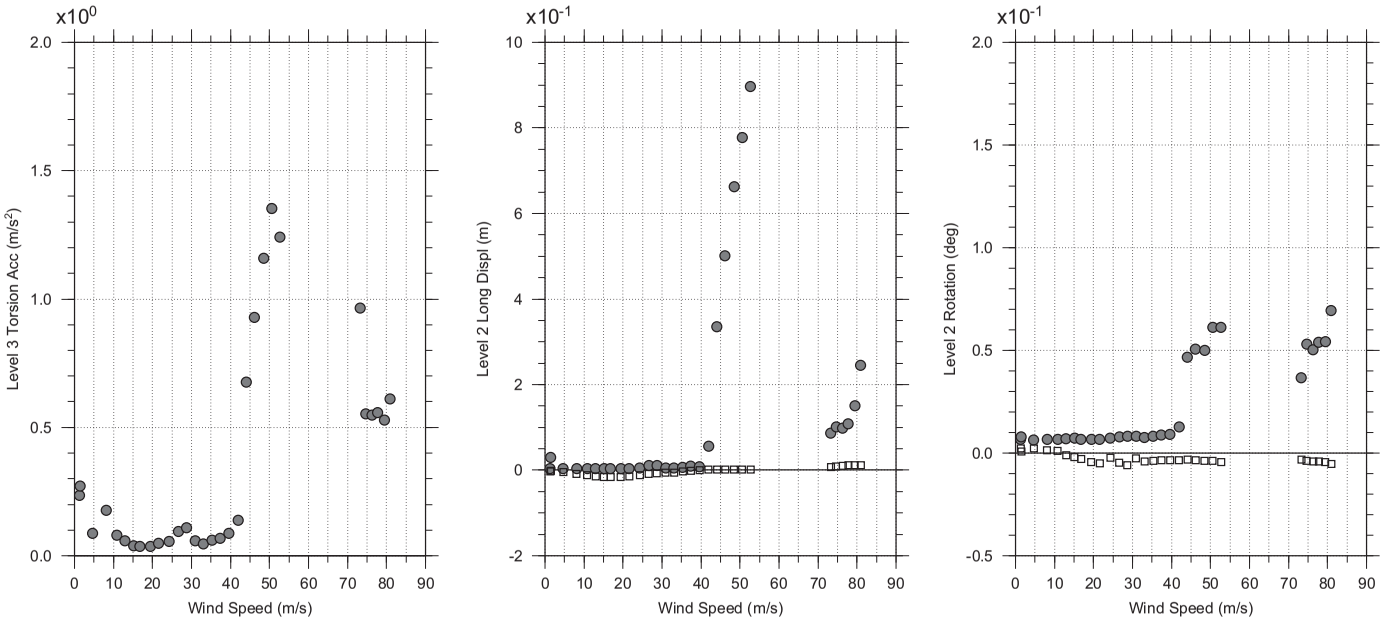

MEAN
RMS

Messina Bridge, In Service Tower (Froude No.), 2.5 degree, Smooth Flow

Dec. 15, 2010
fri12abdg.cl

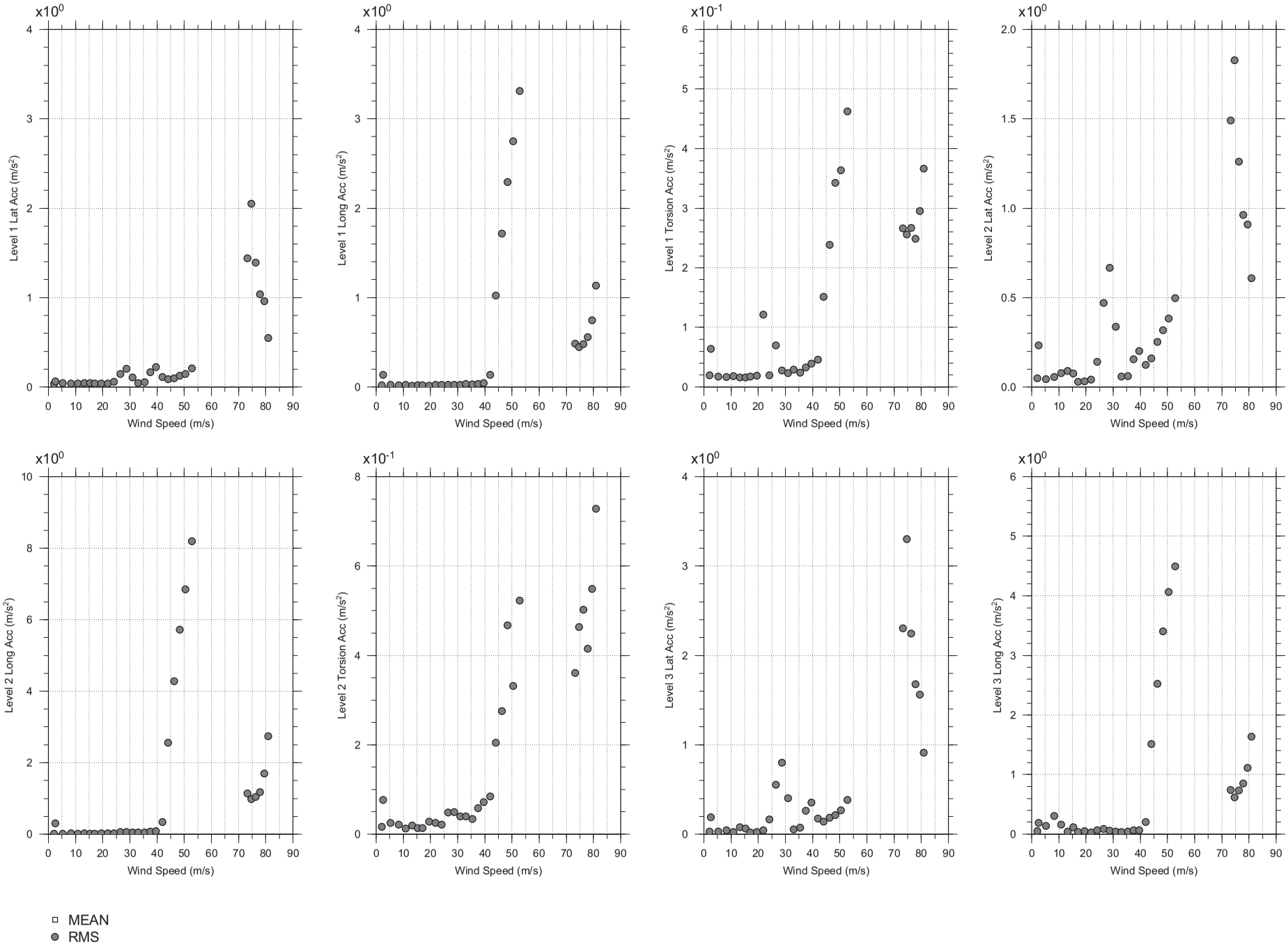

Messina Bridge, In Service Tower (Froude No.), 5 degree, Smooth Flow

Dec. 15, 2010
fri13abdg.cl

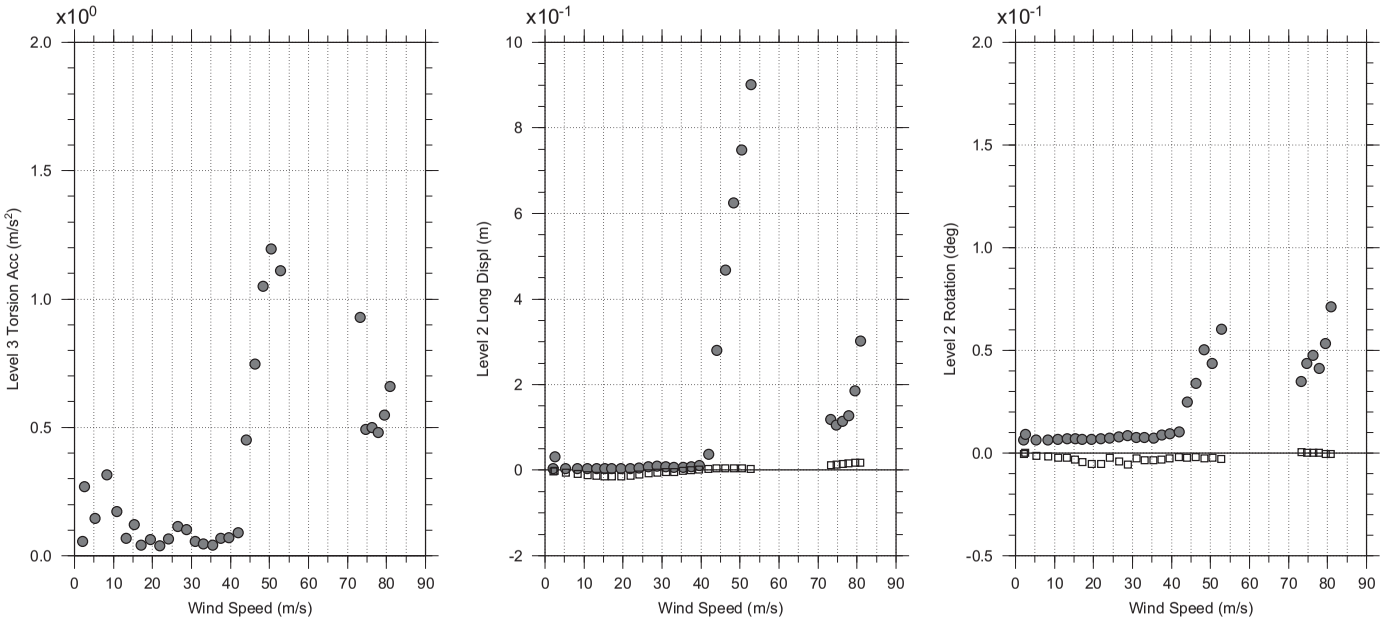

MEAN
RMS

Messina Bridge, In Service Tower (Froude No.), 5 degree, Smooth Flow

Dec. 15, 2010
fri13abdg.cl

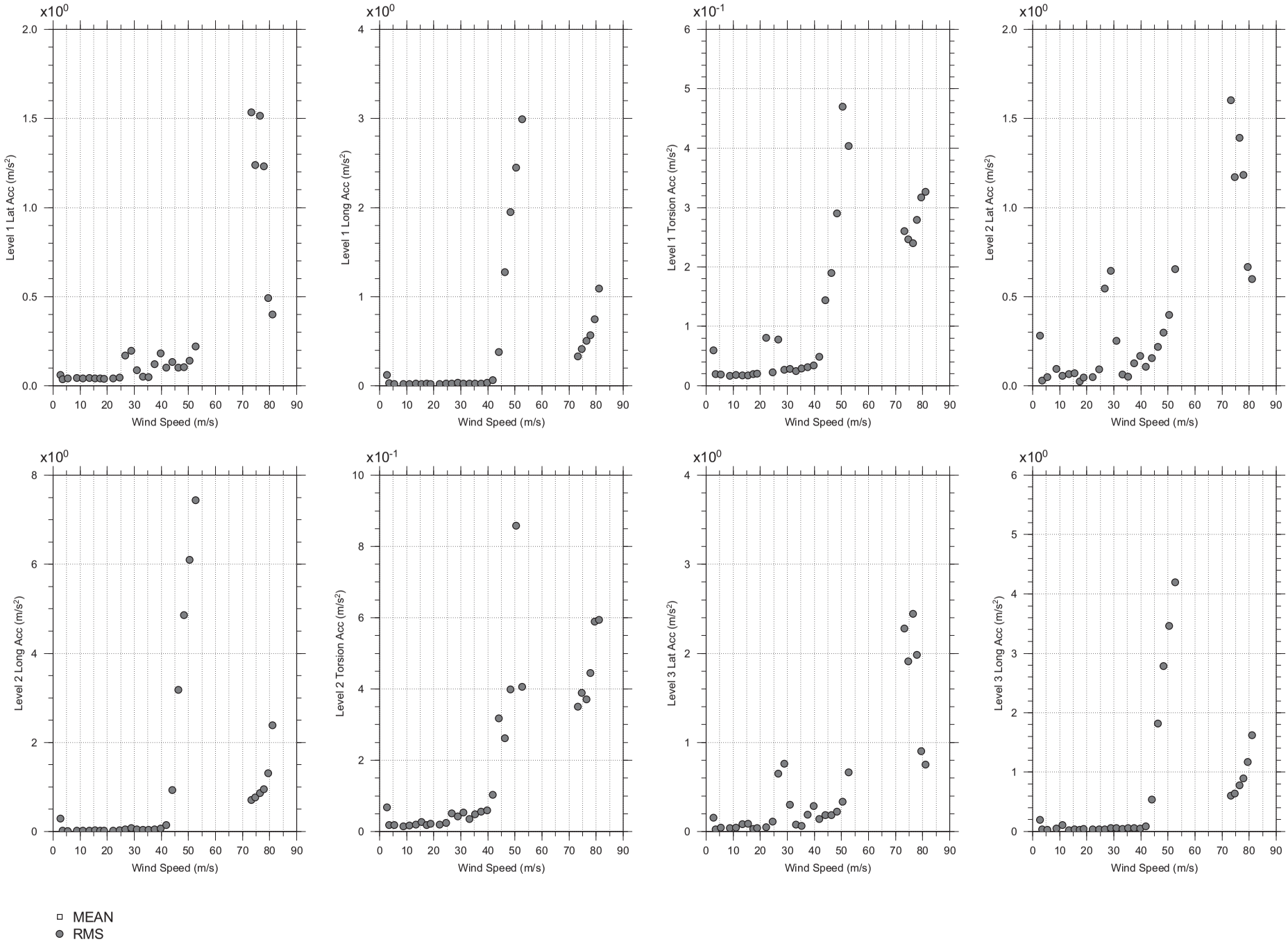

Messina Bridge, In Service Tower (Froude No.), 7.5 degree, Smooth Flow

Dec. 15, 2010
fri14abdg.cl

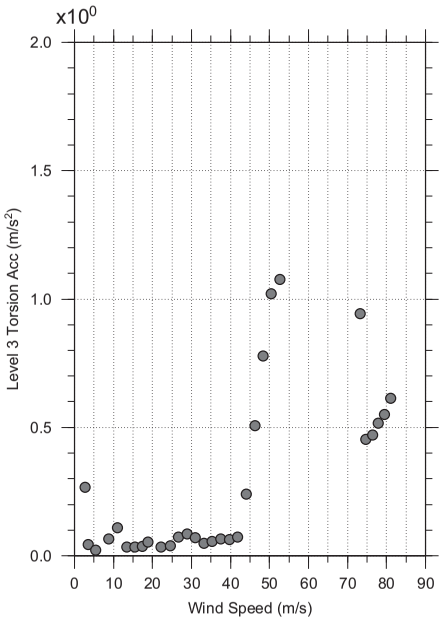

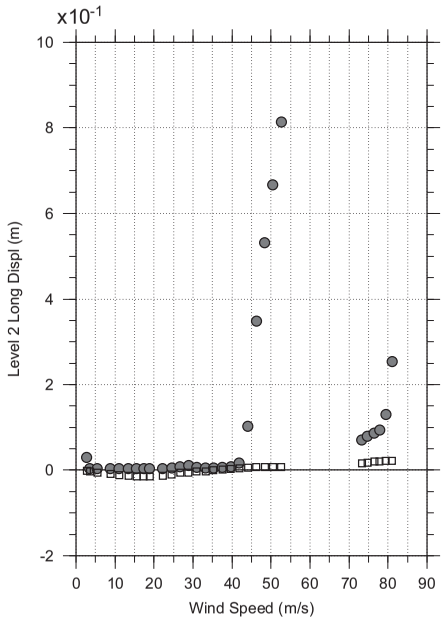

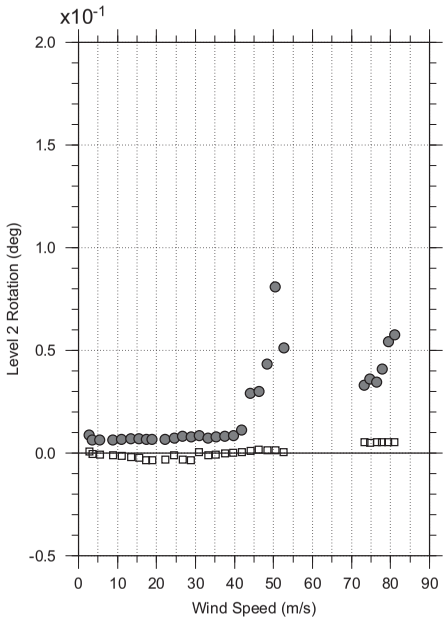

MEAN
RMS

Messina Bridge, In Service Tower (Froude No.), 7.5 degree, Smooth Flow

Dec. 15, 2010
fri14abdg.cl

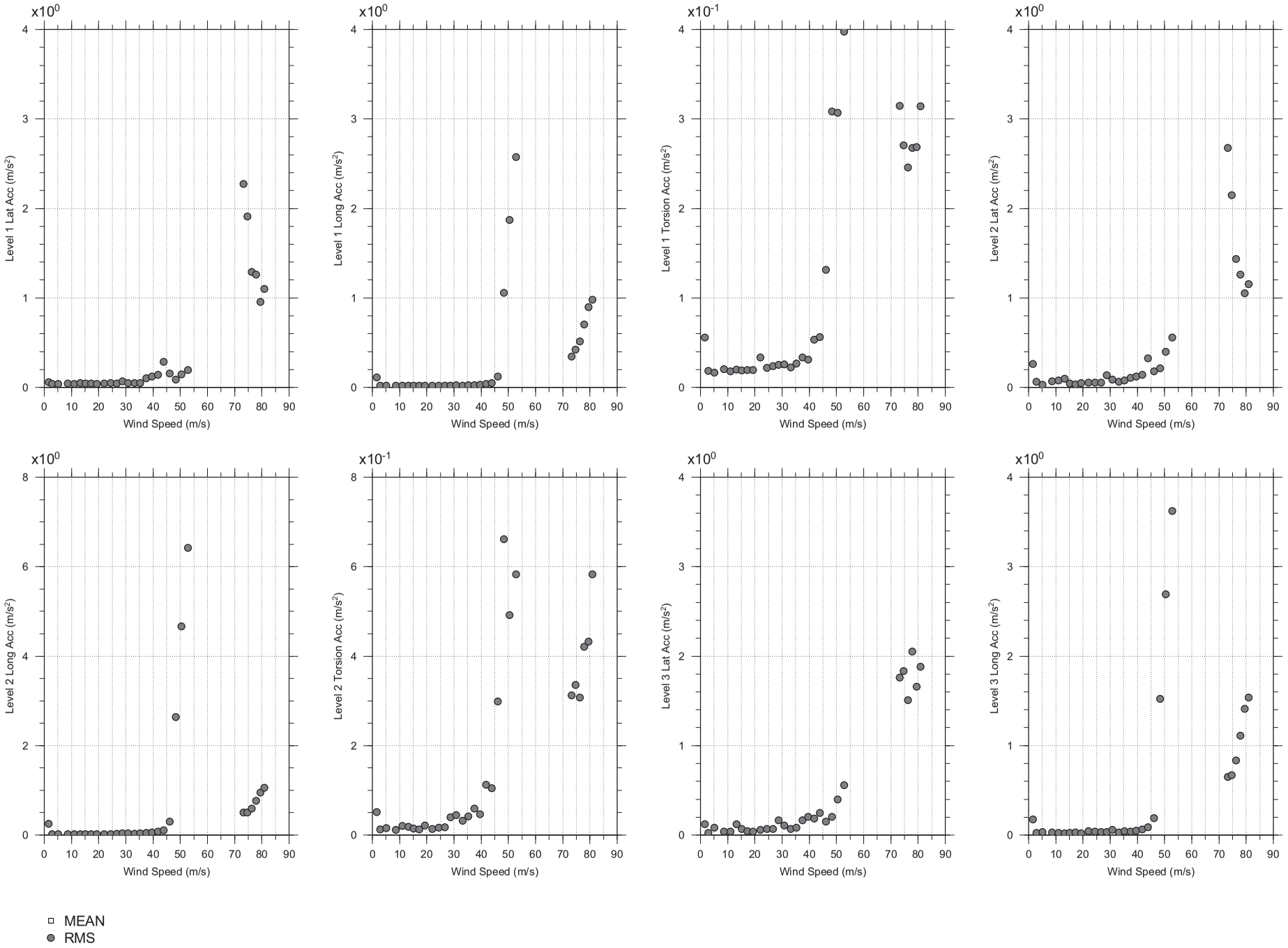

Messina Bridge, In Service Tower (Froude No.), 10 degree, Smooth Flow

Dec. 16, 2010
fri15abdg.cl

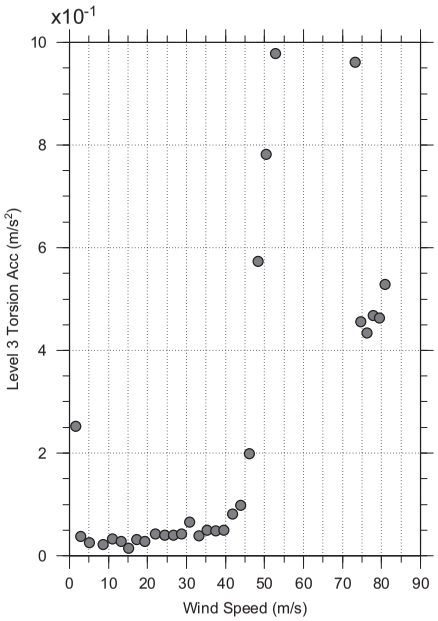

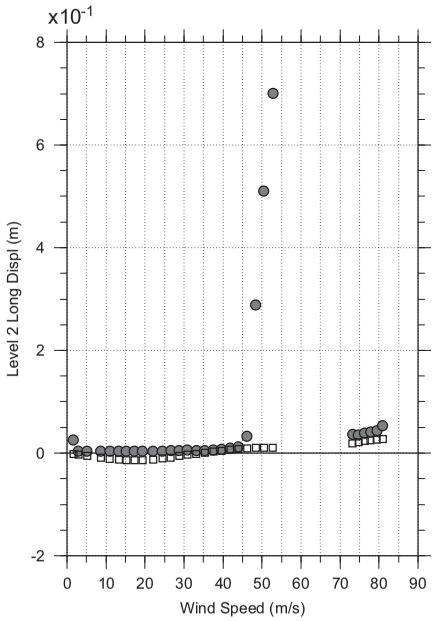

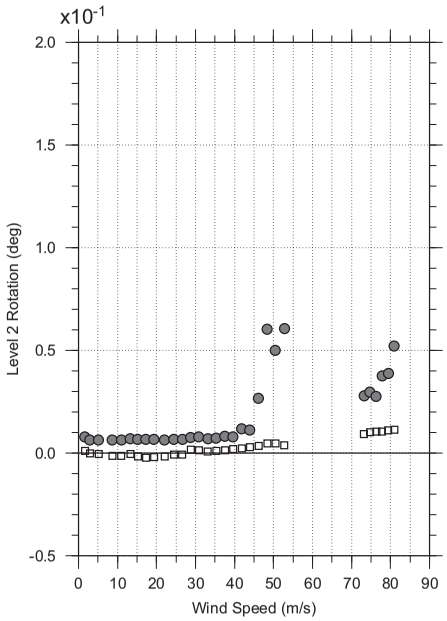

MEAN
RMS

Messina Bridge, In Service Tower (Froude No.), 10 degree, Smooth Flow

Dec. 16, 2010
fri15abdg.cl

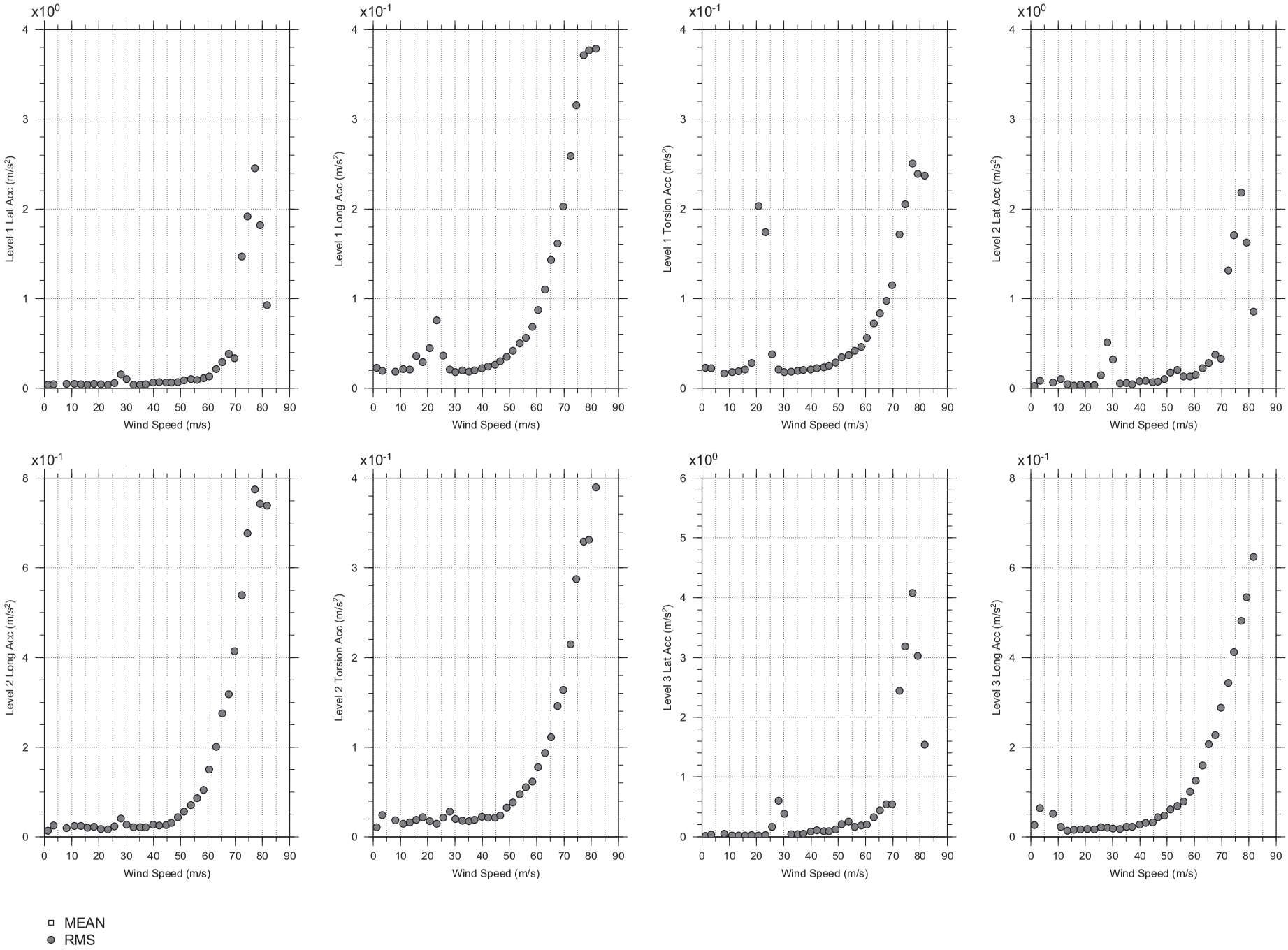

Messina Bridge, In Service Tower (Froude No.), 0 degree, 2% Damping, Smooth Flow

Dec. 16, 2010
fri21abdg.cl

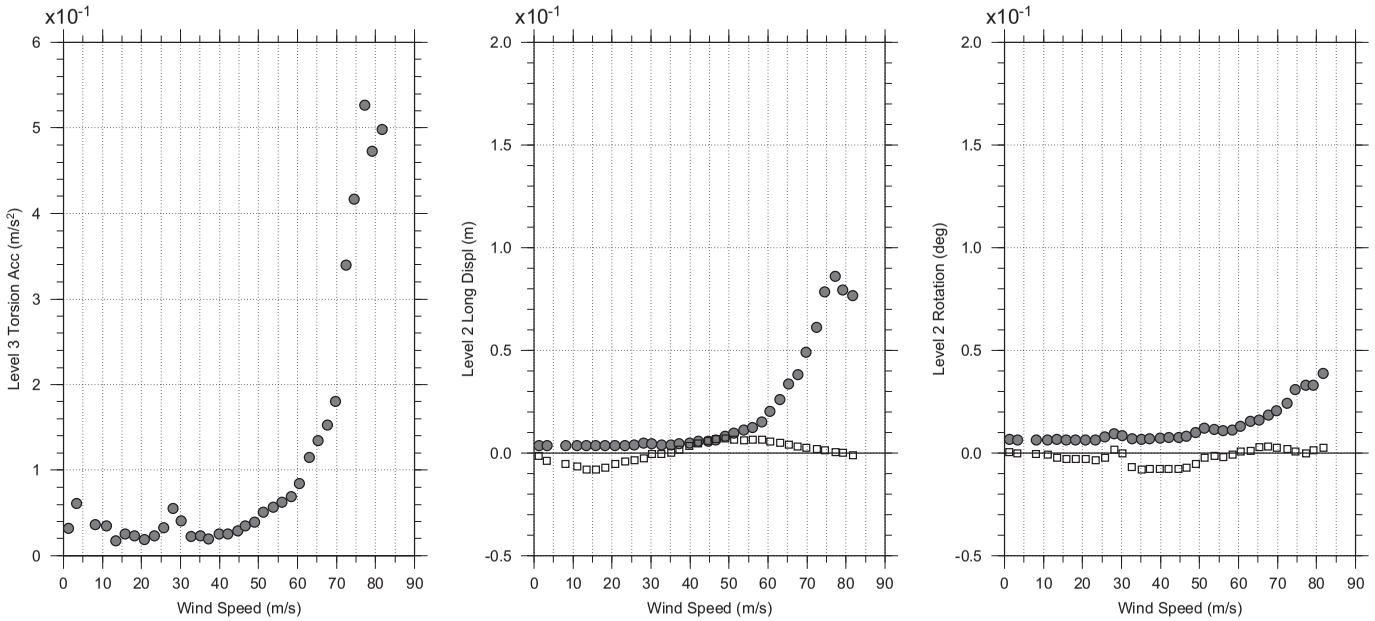

MEAN
RMS

Messina Bridge, In Service Tower (Froude No.), 0 degree, 2% Damping, Smooth Flow

Dec. 16, 2010
fri21abdg.cl

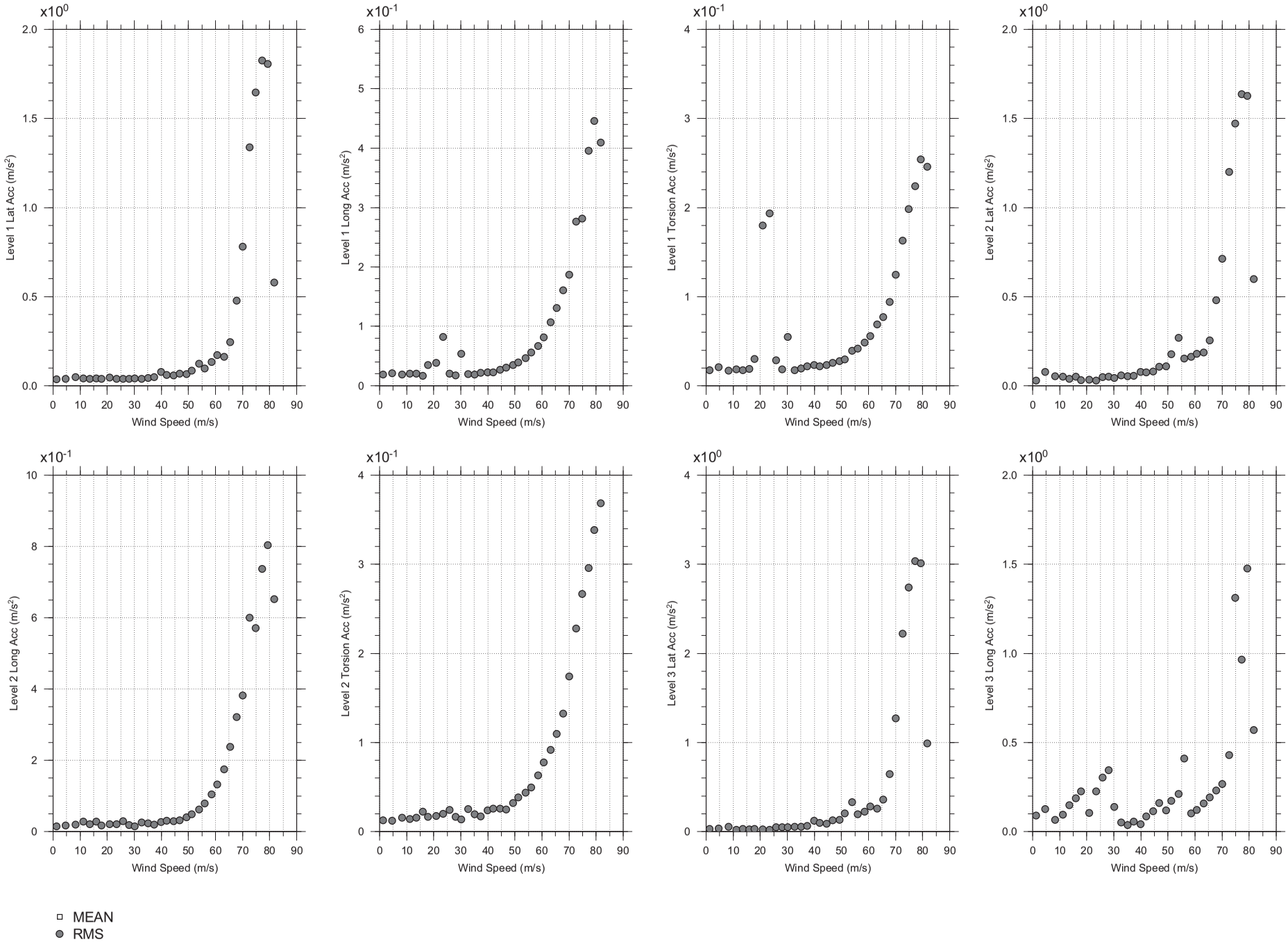

Messina Bridge, In Service Tower (Froude No.), 5 degree, 2% Damping, Smooth Flow

Dec. 16, 2010
fri22abdg.cl

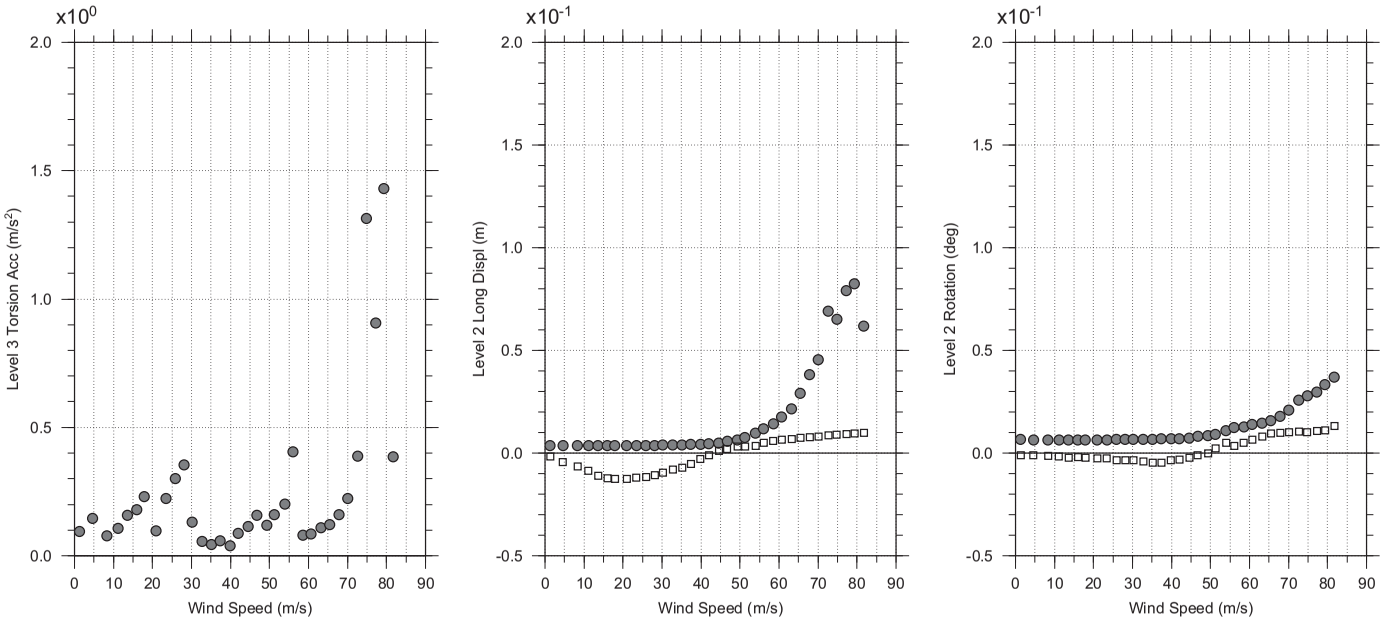

MEAN
RMS

Messina Bridge, In Service Tower (Froude No.), 5 degree, 2% Damping, Smooth Flow

Dec. 16, 2010
fri22abdg.cl

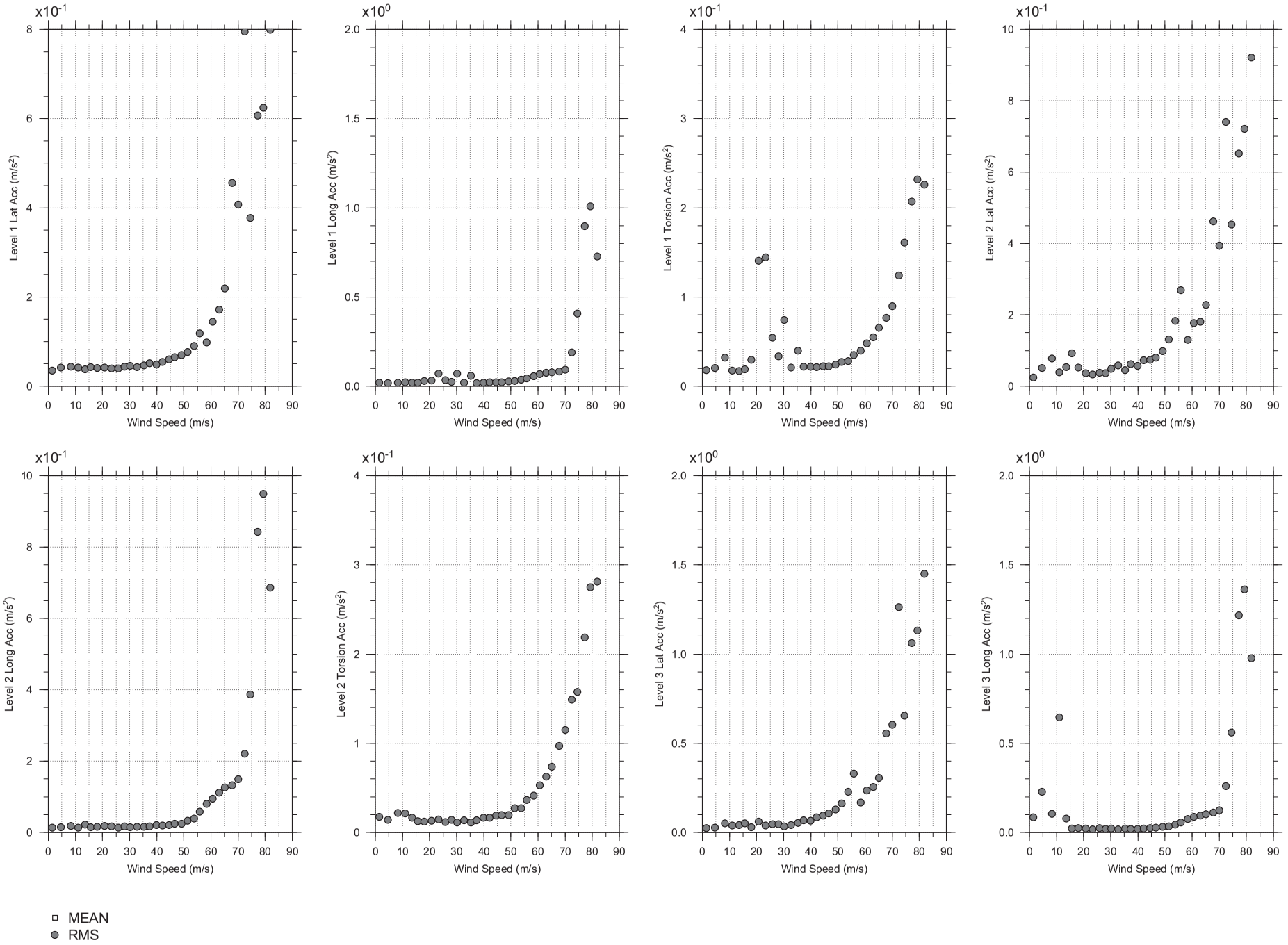

Messina Bridge, In Service Tower (Froude No.), 10 degree, 2% Damping, Smooth Flo

Dec. 16, 2010
fri23abdg.cl

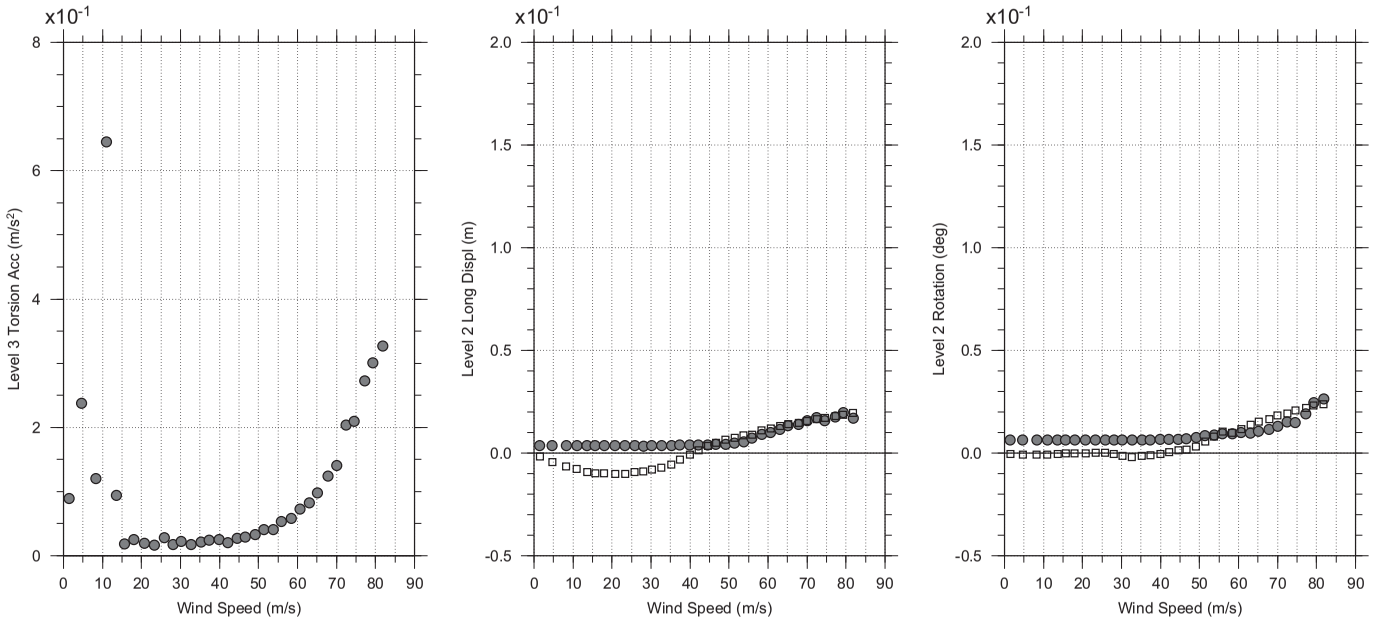

MEAN
RMS

Messina Bridge, In Service Tower (Froude No.), 10 degree, 2% Damping, Smooth Flo

Dec. 16, 2010
fri23abdg.cl

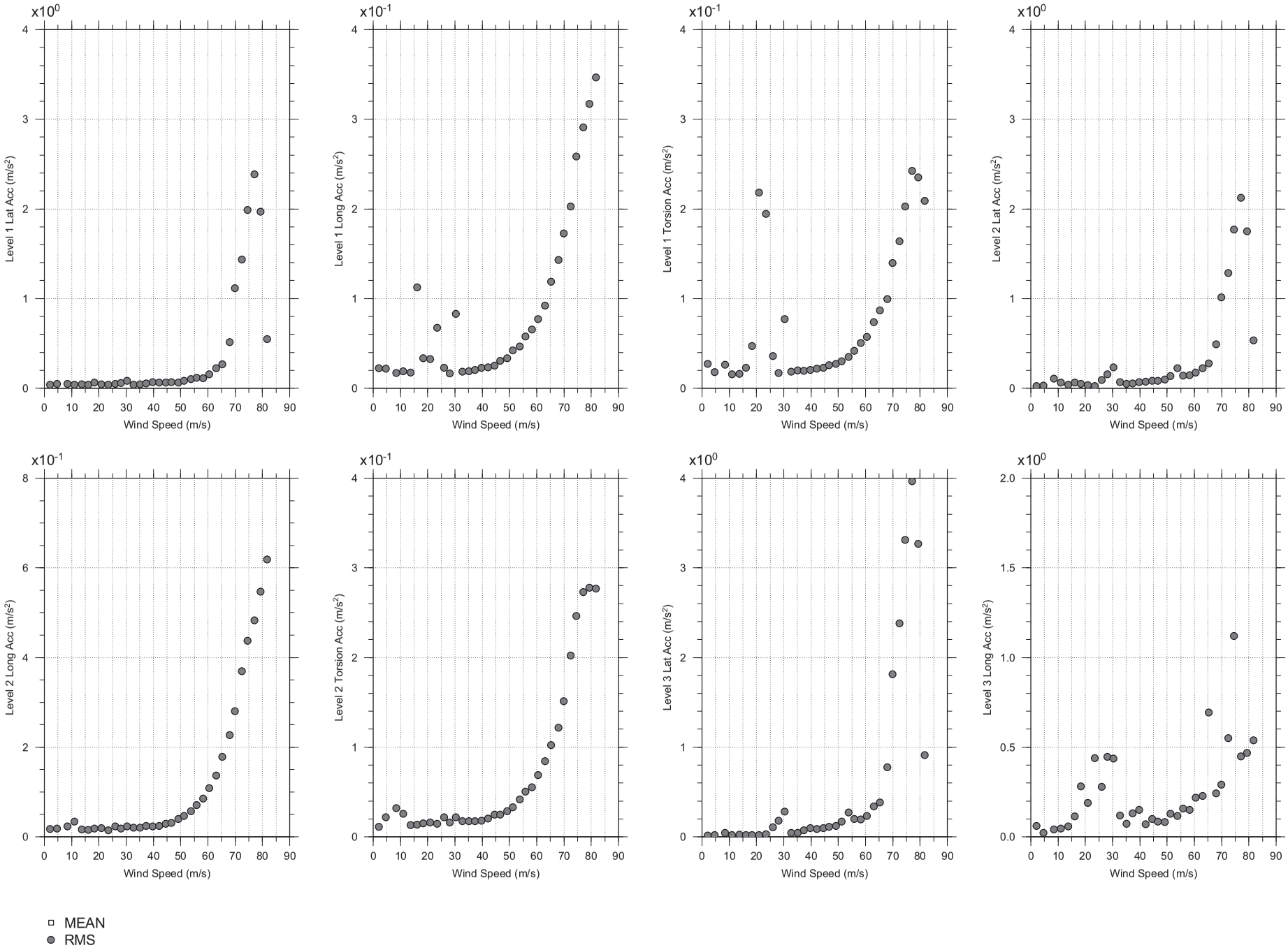

Messina Bridge, In Service Tower (Froude No.), 0 degree, 4% Damping, Smooth Flow

Dec. 16, 2010
fri31abdg.cl

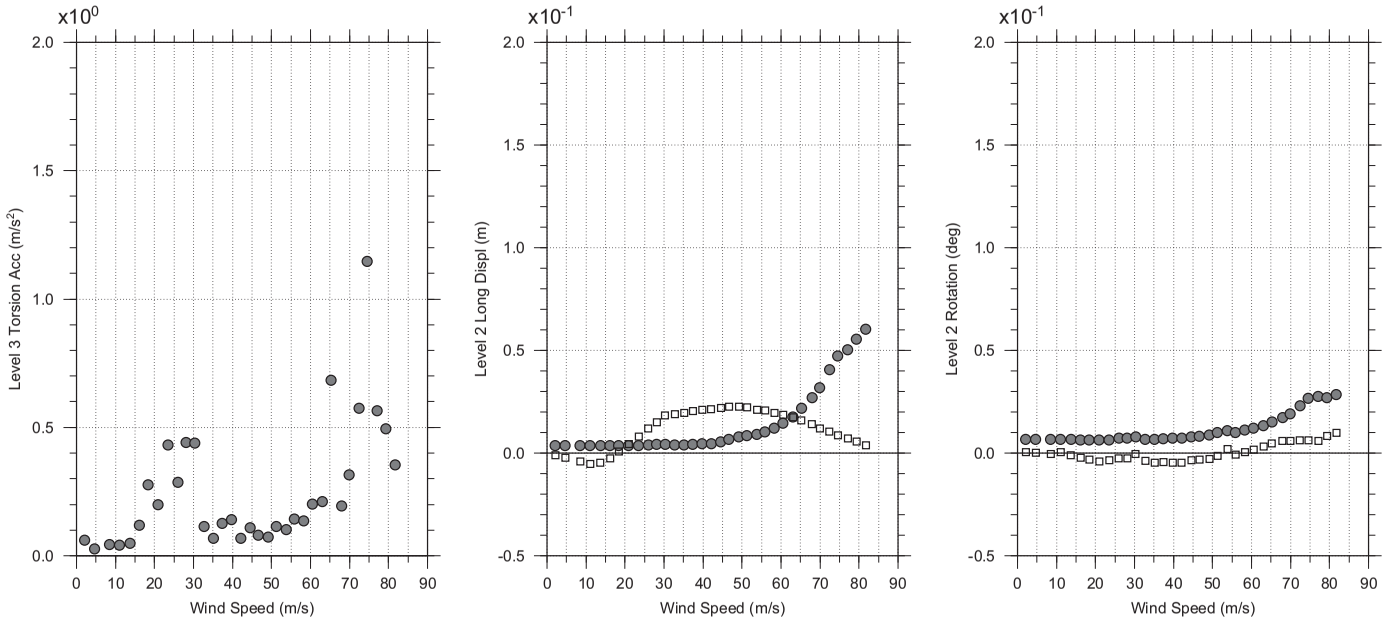

MEAN
RMS

Messina Bridge, In Service Tower (Froude No.), 0 degree, 4% Damping, Smooth Flow

Dec. 16, 2010
fri31abdg.cl

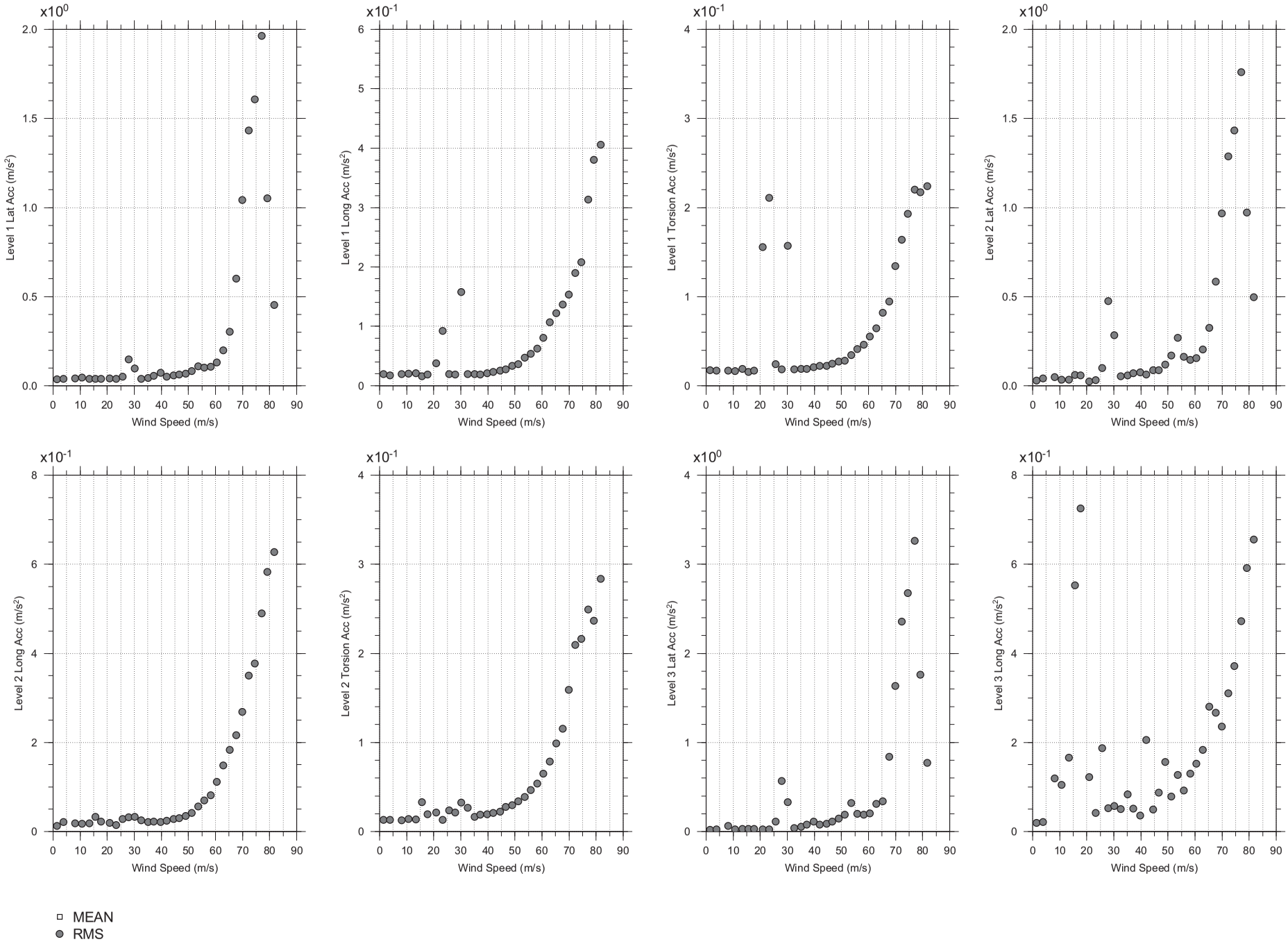

Messina Bridge, In Service Tower (Froude No.), 5 degree, 4% Damping, Smooth Flow

Dec. 16, 2010
fri32abdg.cl

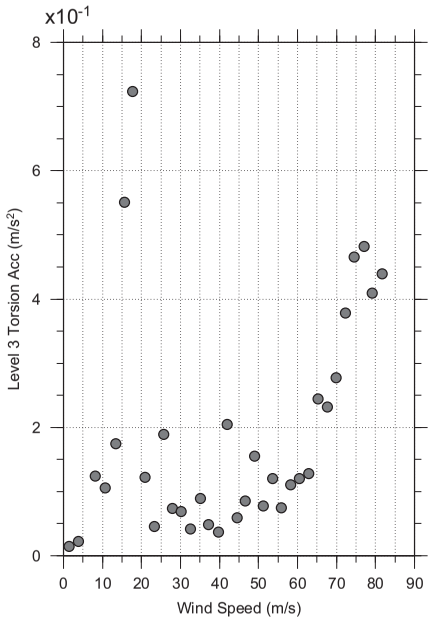

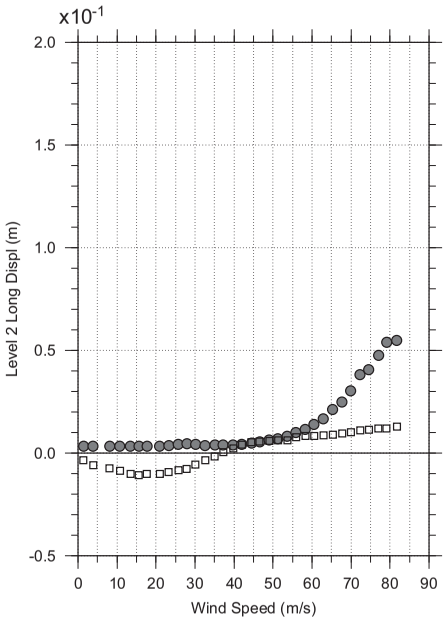

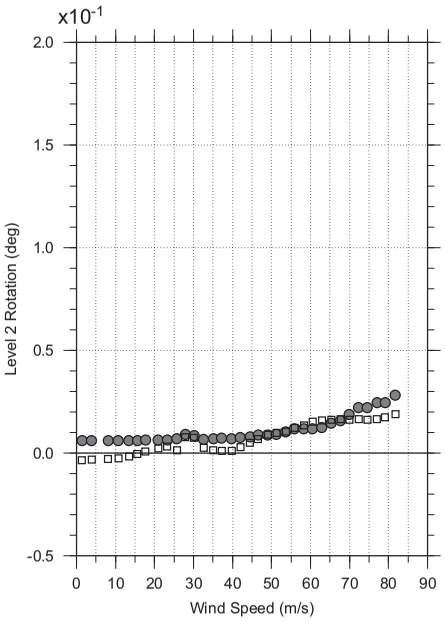

MEAN
RMS

Messina Bridge, In Service Tower (Froude No.), 5 degree, 4% Damping, Smooth Flow

Dec. 16, 2010
fri32abdg.cl

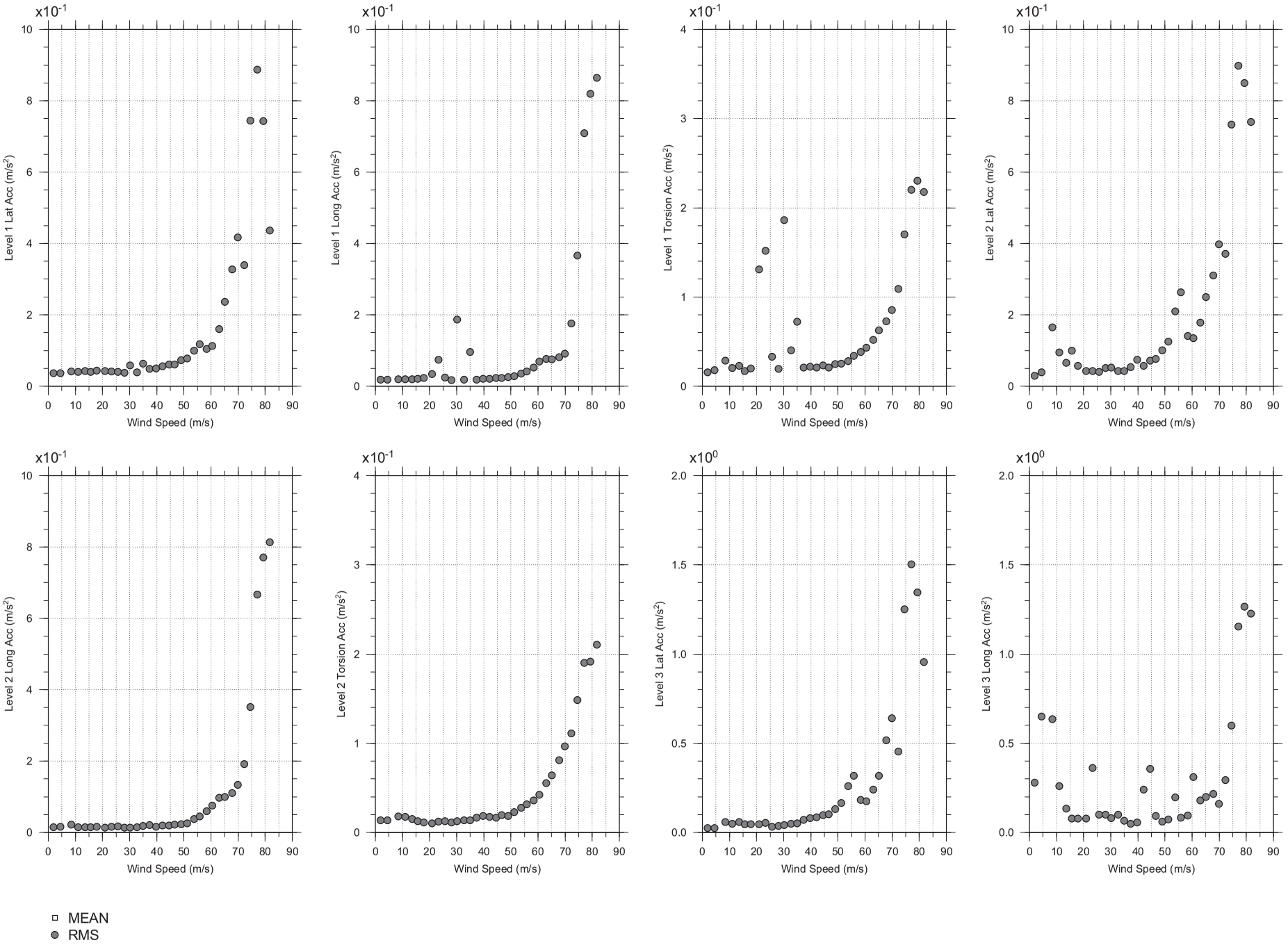

Messina Bridge, In Service Tower (Froude No.), 10 degree, 4% Damping, Smooth Flo

Dec. 16, 2010
fri33abdg.cl

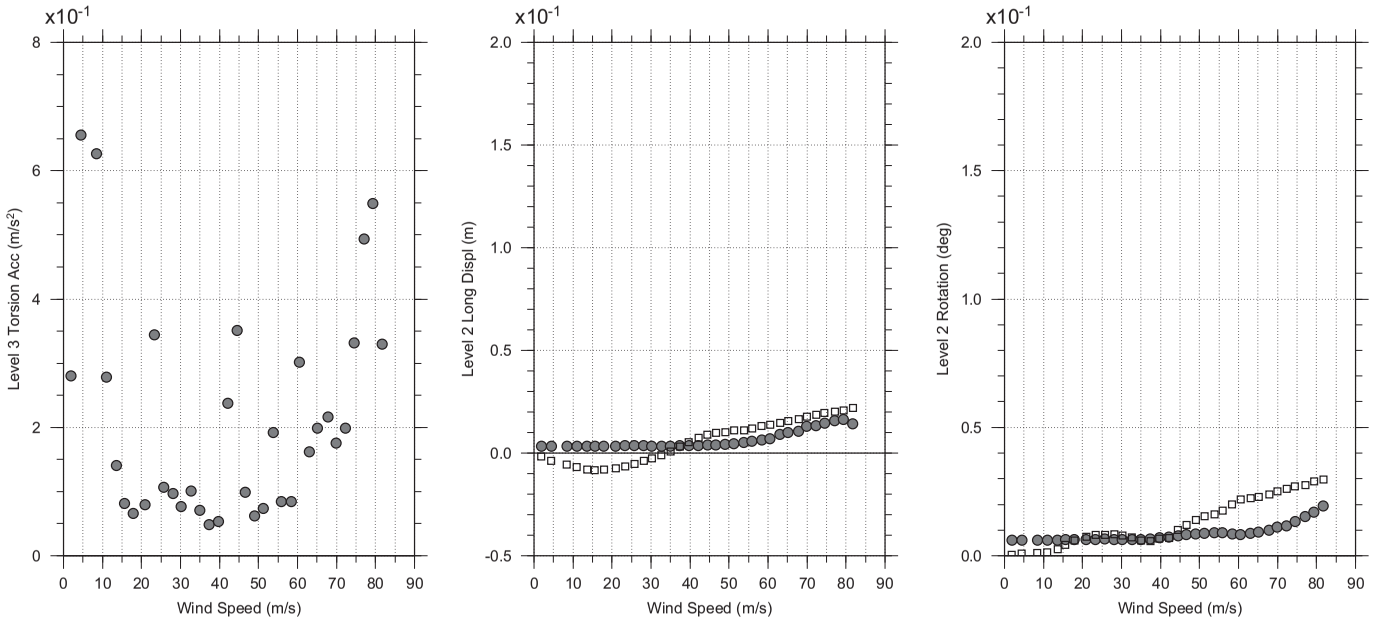

MEAN
RMS

Messina Bridge, In Service Tower (Froude No.), 10 degree, 4% Damping, Smooth Flo

Dec. 16, 2010
fri33abdg.cl

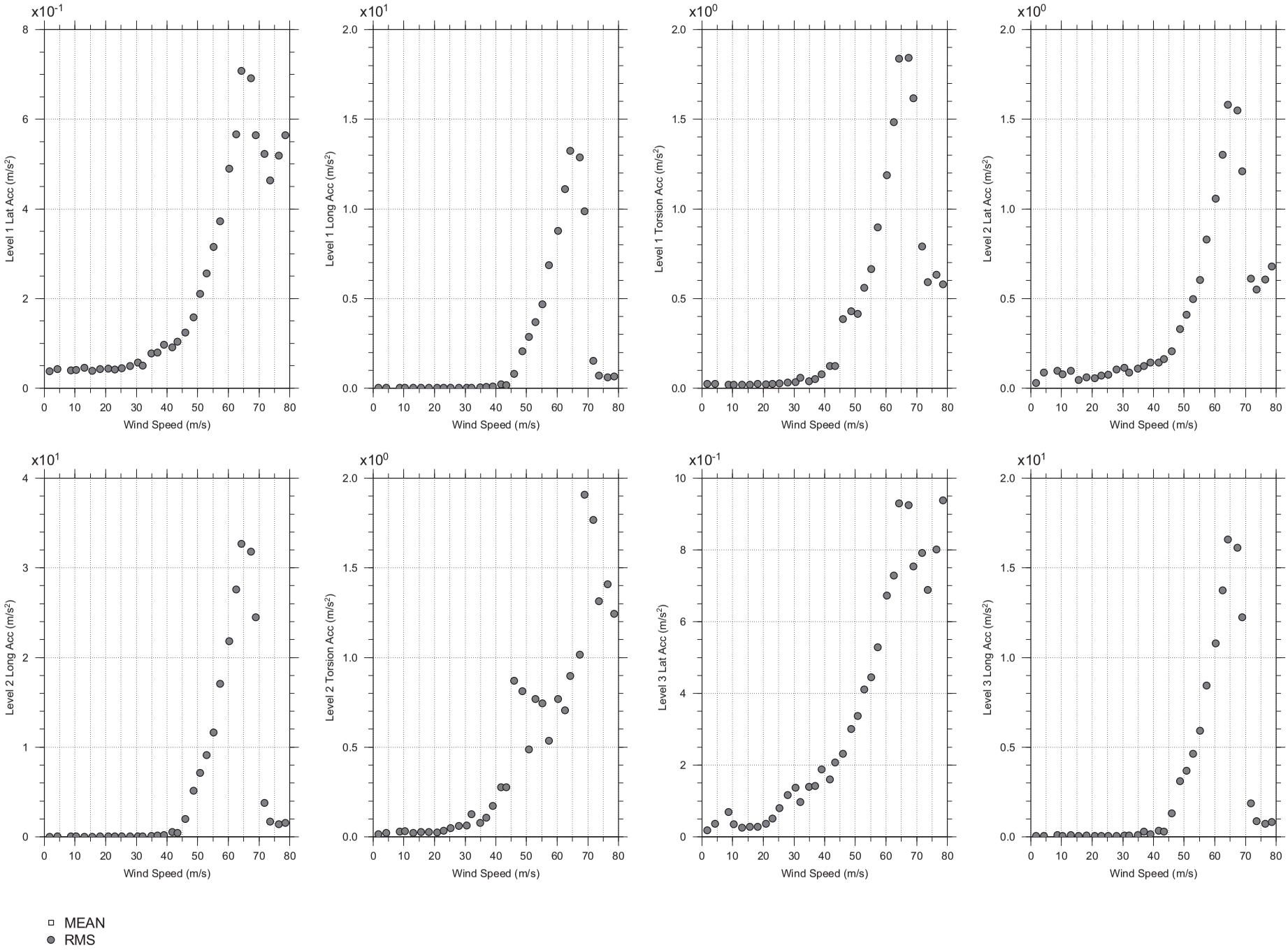

Messina Bridge, In Service Tower (Froude No.), 0 degree, Turbulent Flow

Dec. 16, 2010
fri41abdg.cl

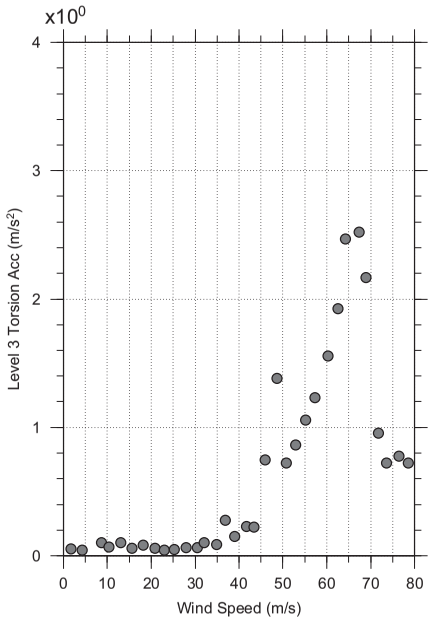

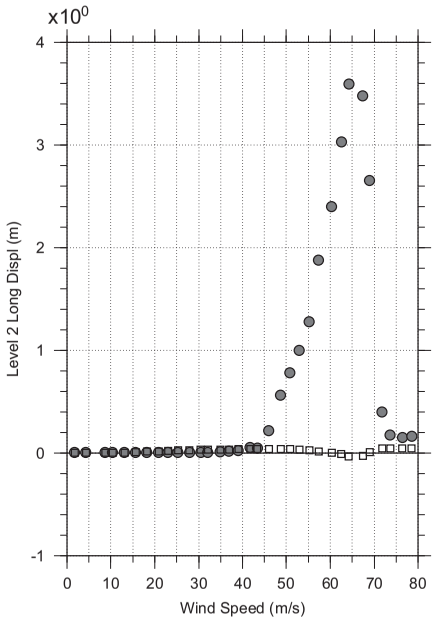

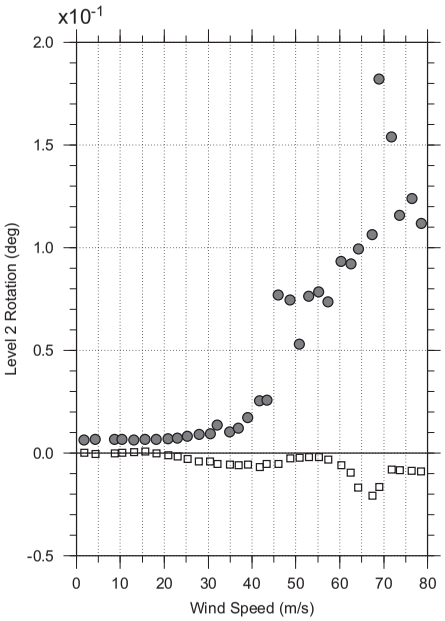

MEAN
RMS

Messina Bridge, In Service Tower (Froude No.), 0 degree, Turbulent Flow

Dec. 16, 2010
fri41abdg.cl

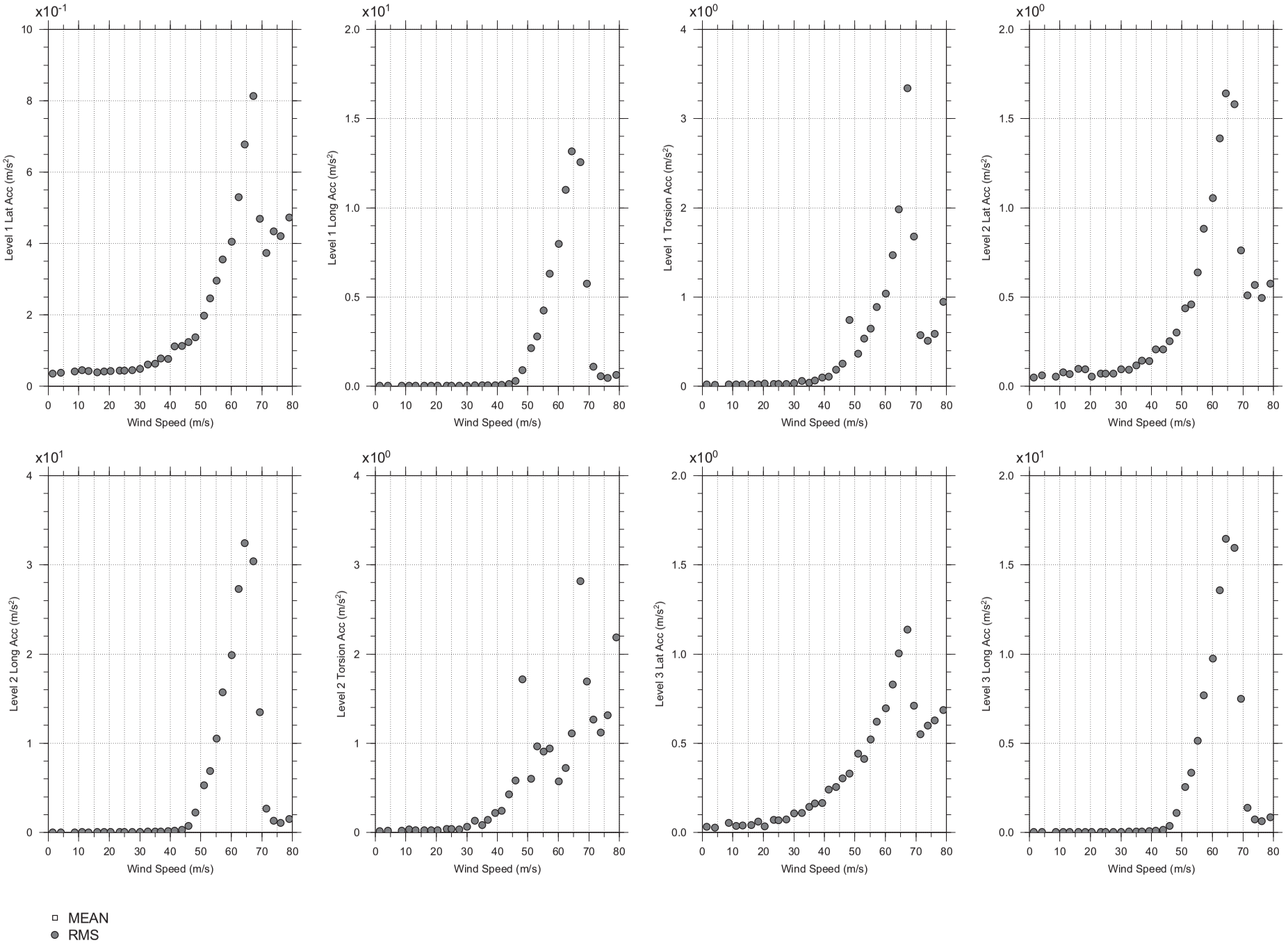

Messina Bridge, In Service Tower (Froude No.), 10 degree, Turbulent Flow

Dec. 16, 2010
fri42abdg.cl

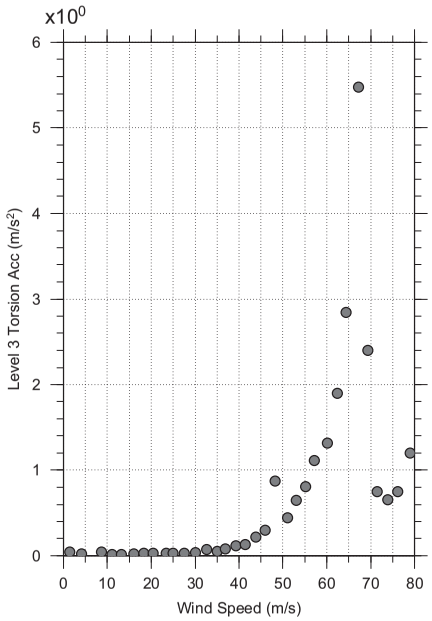

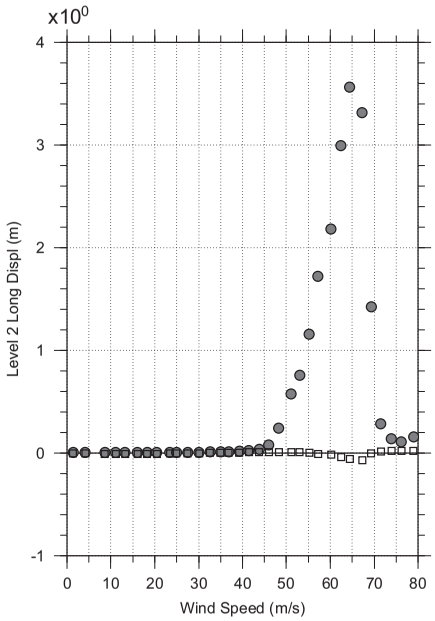

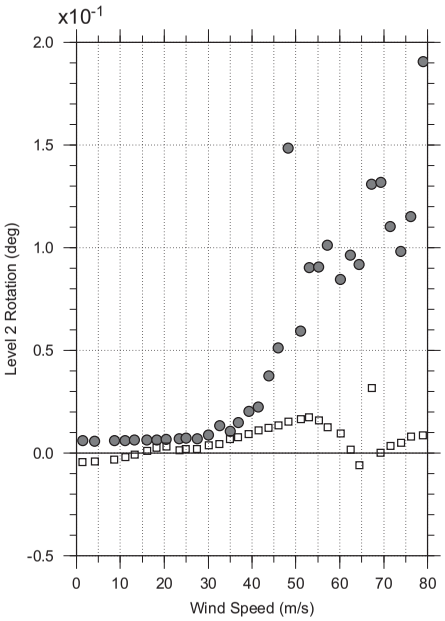

MEAN
RMS

Messina Bridge, In Service Tower (Froude No.), 10 degree, Turbulent Flow

Dec. 16, 2010
fri42abdg.cl

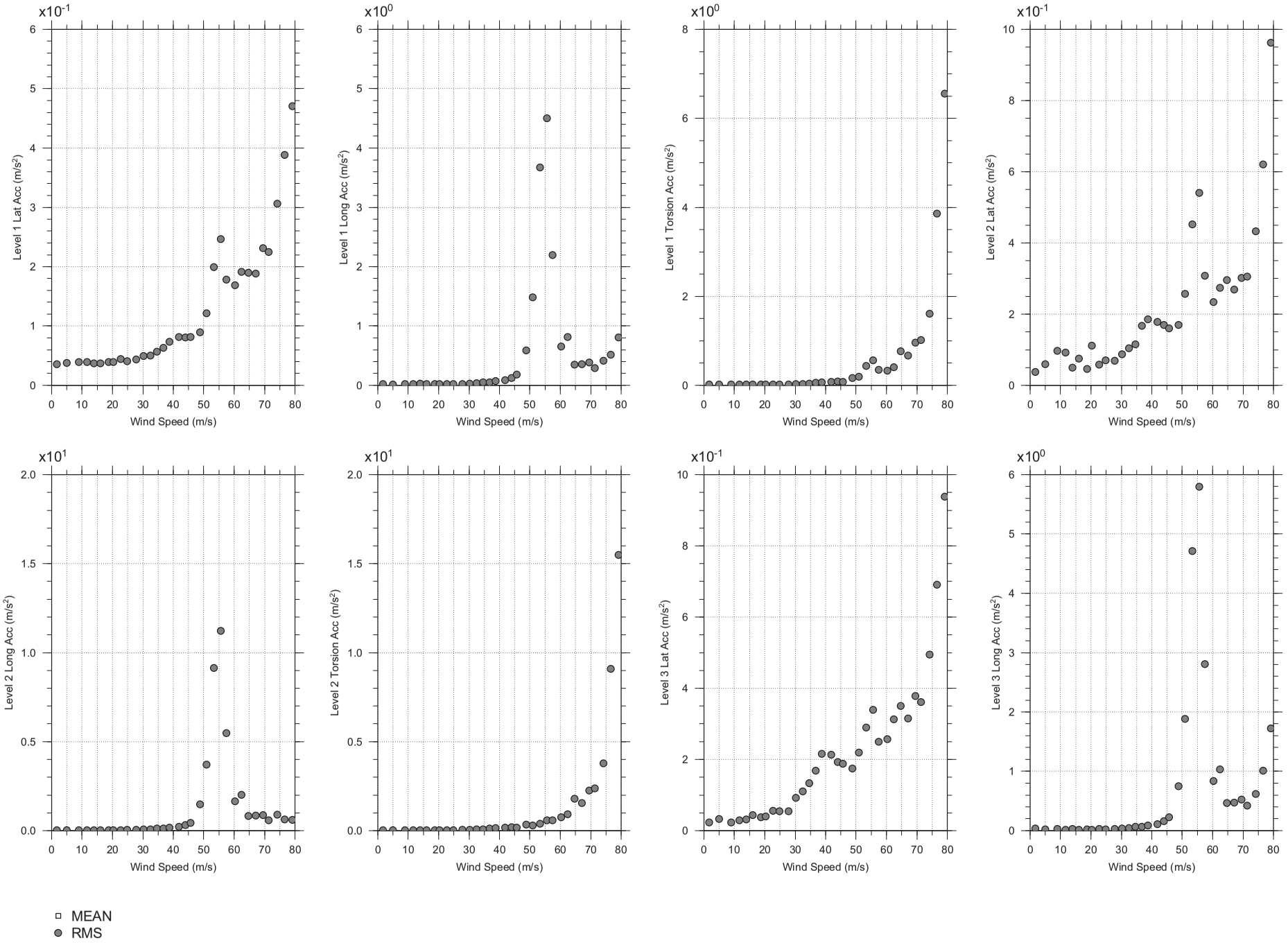

Messina Bridge, In Service Tower (Froude No.), 20 degree, Turbulent Flow

Dec. 16, 2010
fri43abdg.cl

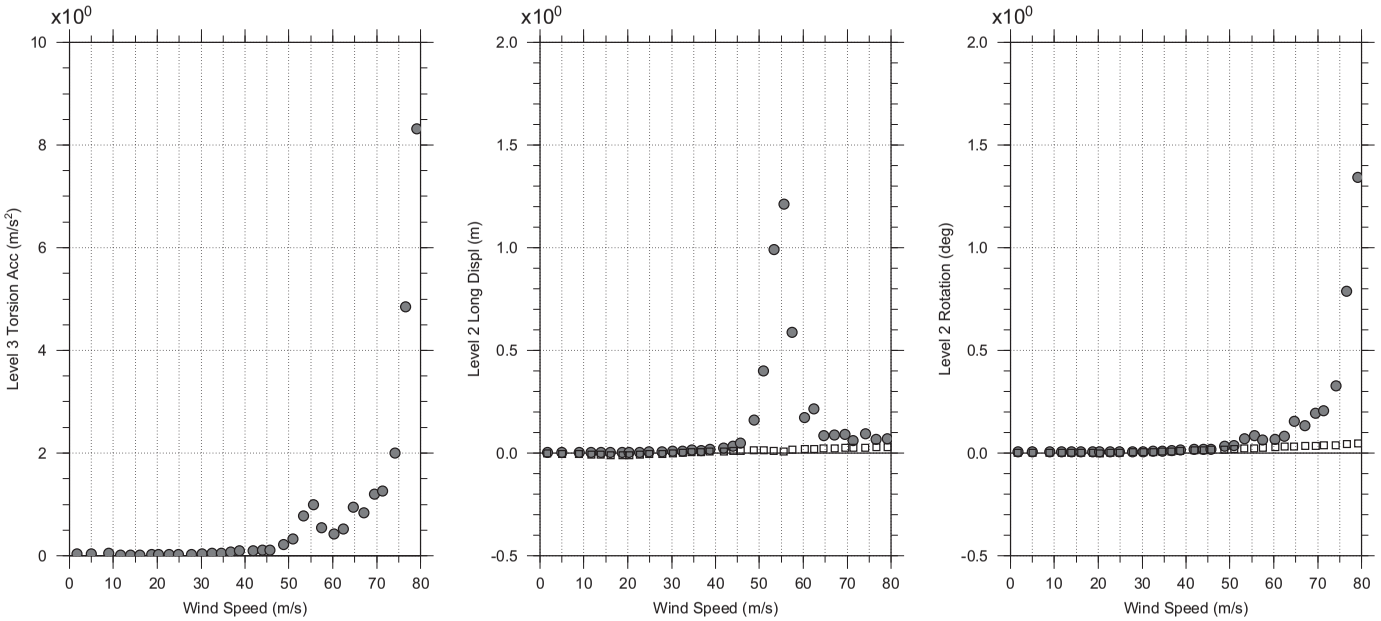

MEAN
RMS

Messina Bridge, In Service Tower (Froude No.), 20 degree, Turbulent Flow

Dec. 16, 2010
fri43abdg.cl

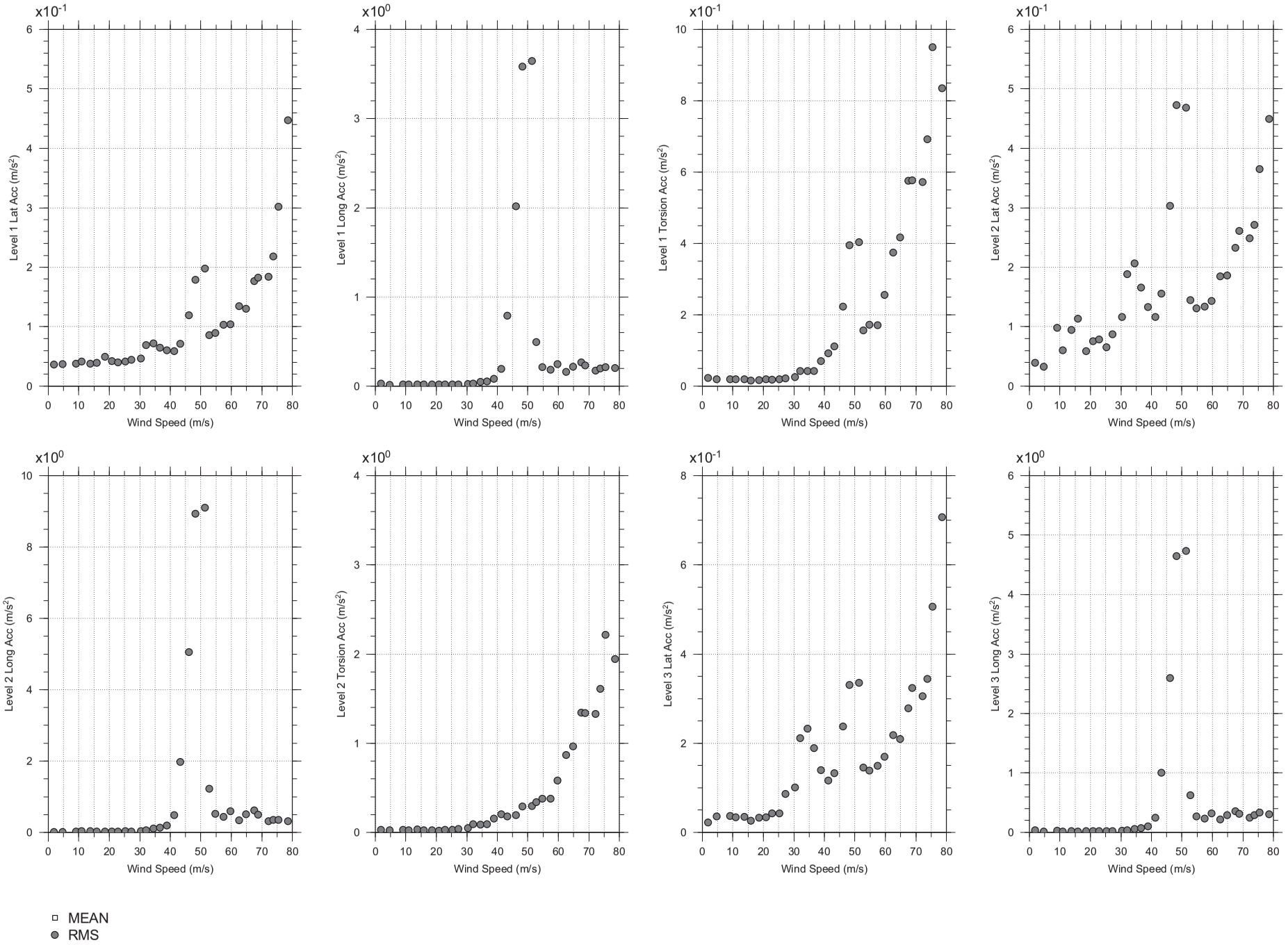

Messina Bridge, In Service Tower (Froude No.), 30 degree, Turbulent Flow

Dec. 16, 2010
fri44abdg.cl

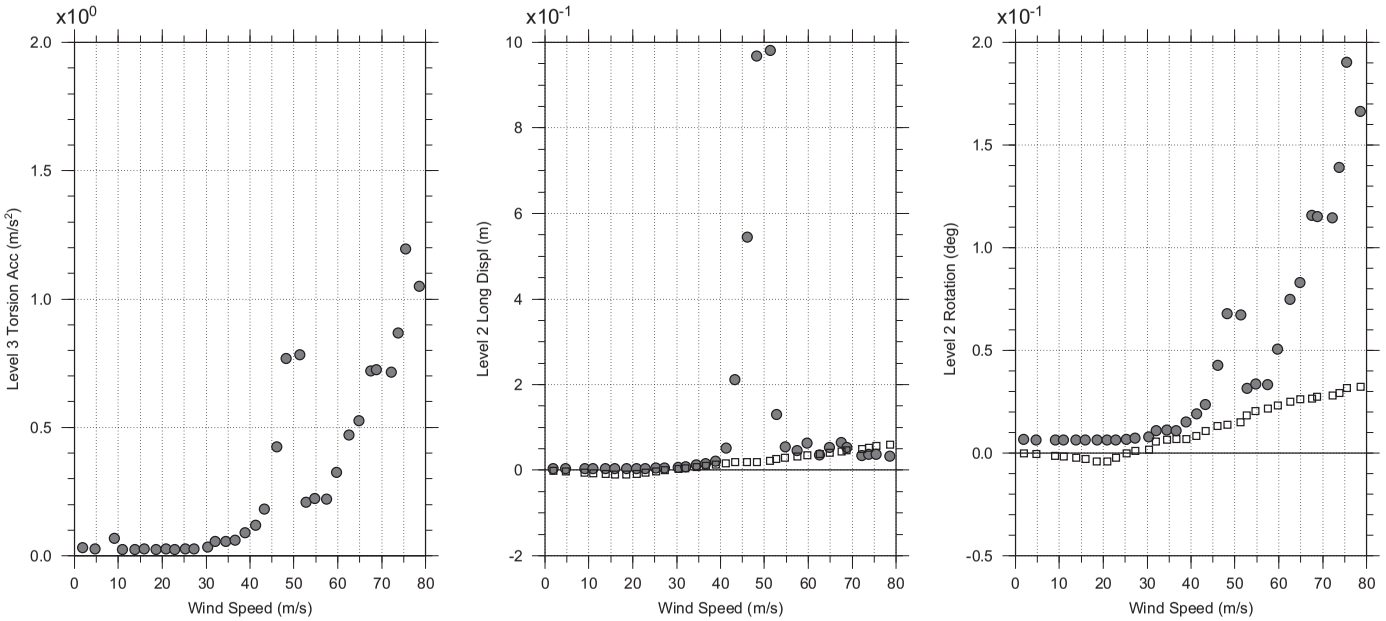

MEAN
RMS

Messina Bridge, In Service Tower (Froude No.), 30 degree, Turbulent Flow

Dec. 16, 2010
fri44abdg.cl

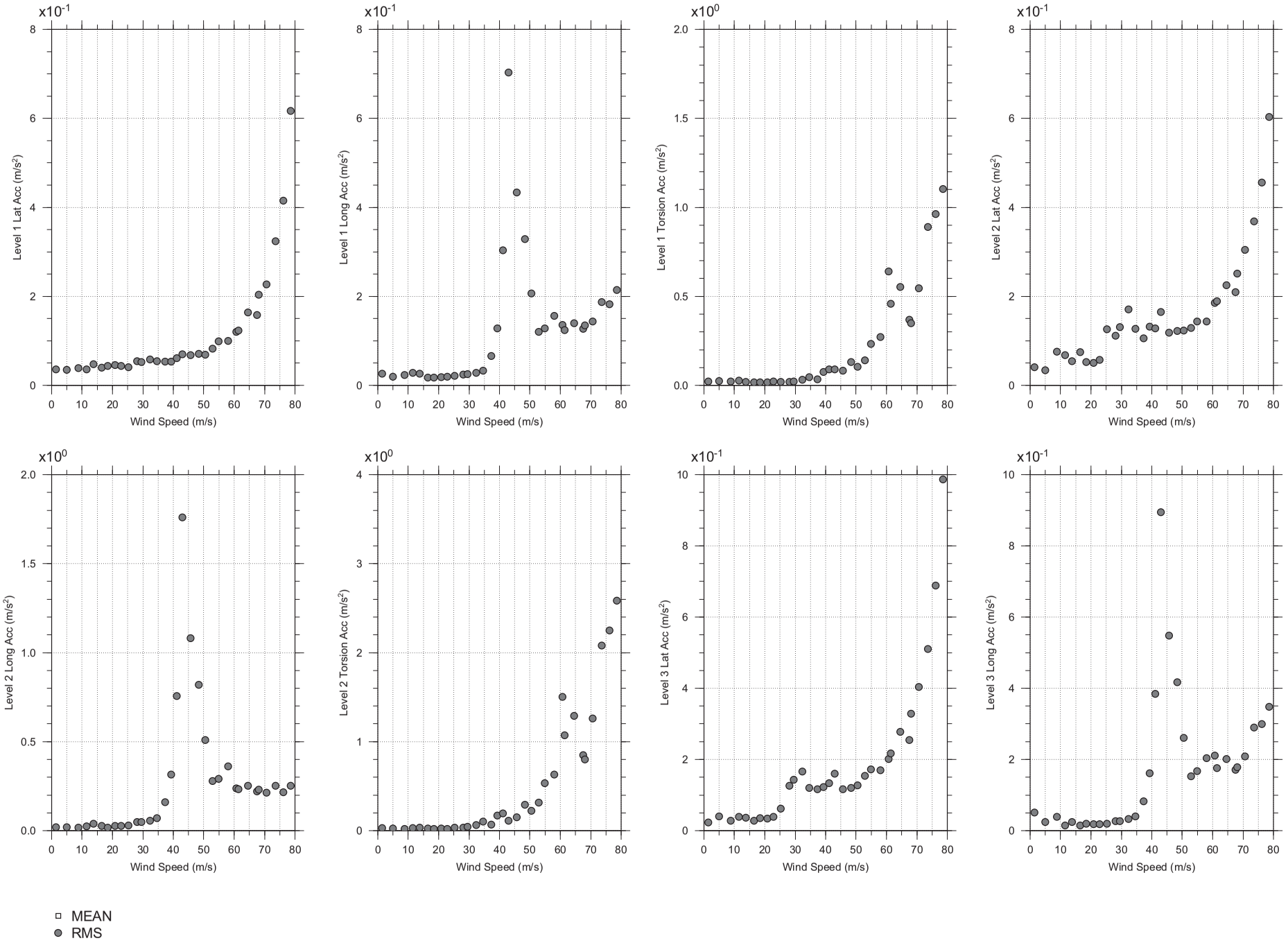

Messina Bridge, In Service Tower (Froude No.), 40 degree, Turbulent Flow

Dec. 16, 2010
fri45abdg.cl

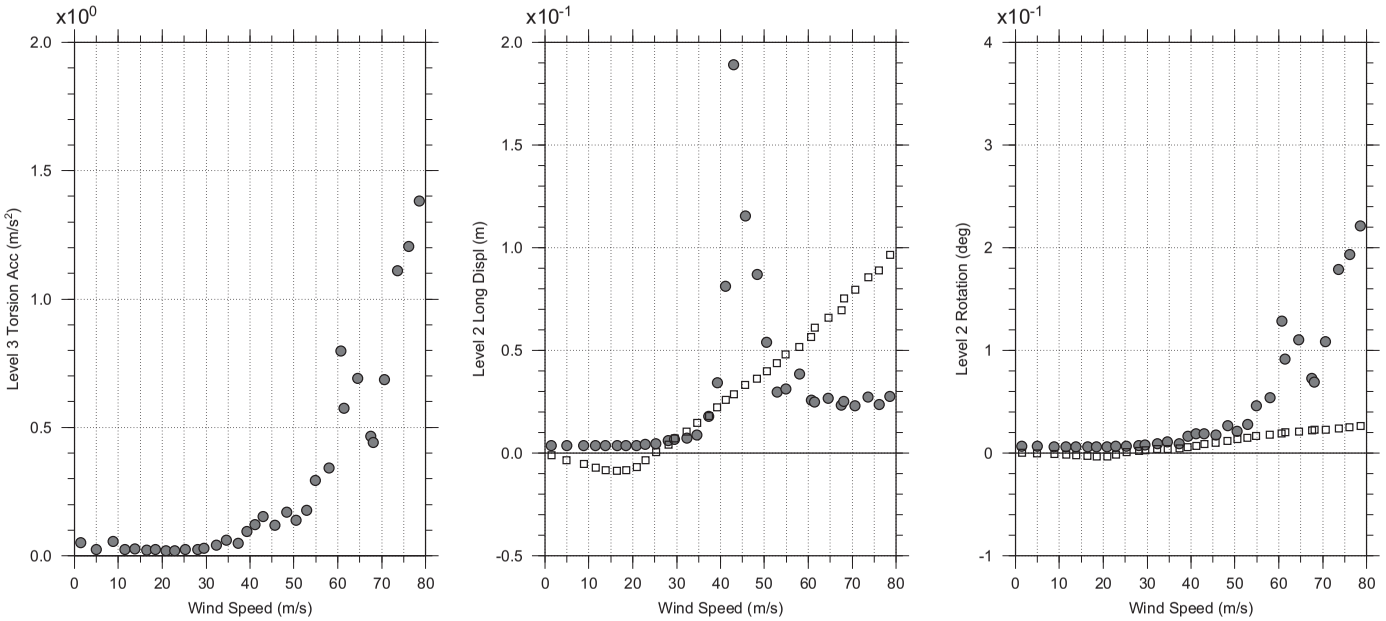

MEAN
RMS

Messina Bridge, In Service Tower (Froude No.), 40 degree, Turbulent Flow

Dec. 16, 2010
fri45abdg.cl

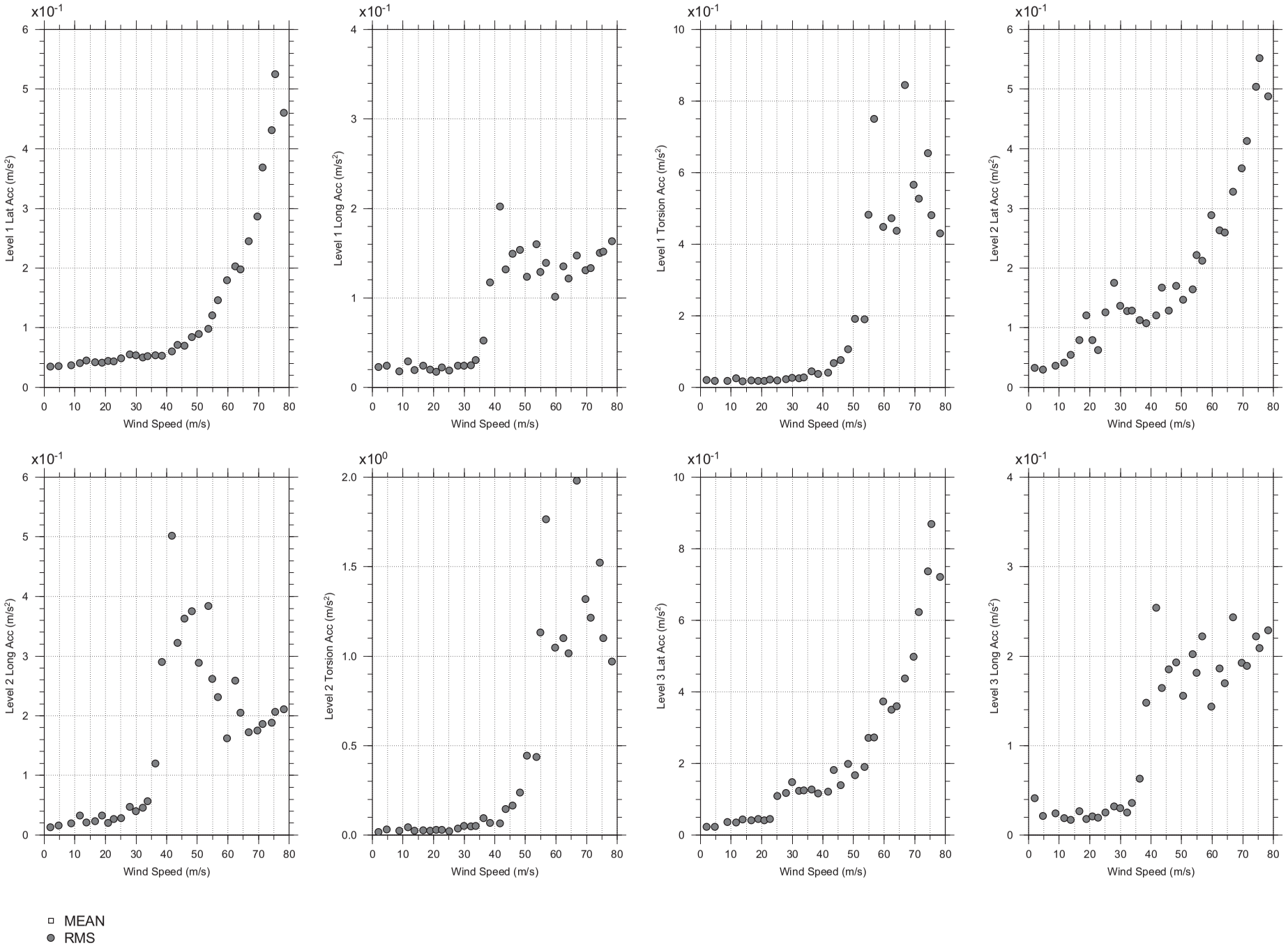

Messina Bridge, In Service Tower (Froude No.), 50 degree, Turbulent Flow

Dec. 16, 2010
fri46abdg.cl

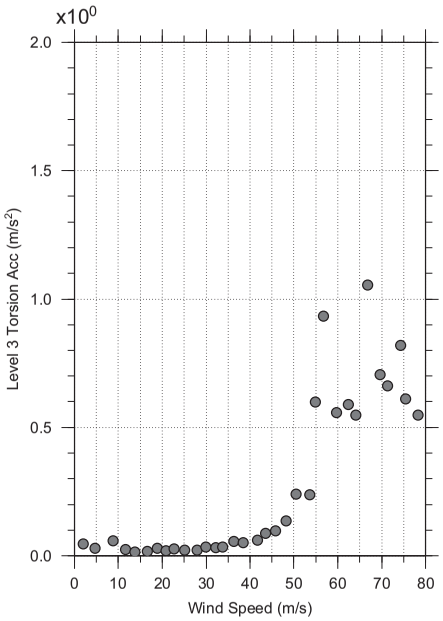

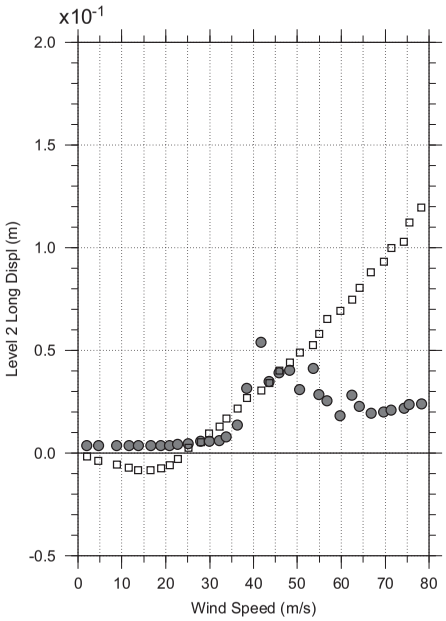

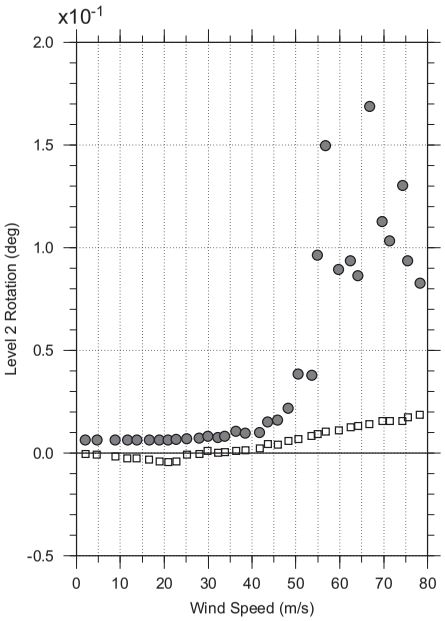

MEAN
RMS

Messina Bridge, In Service Tower (Froude No.), 50 degree, Turbulent Flow

Dec. 16, 2010
fri46abdg.cl

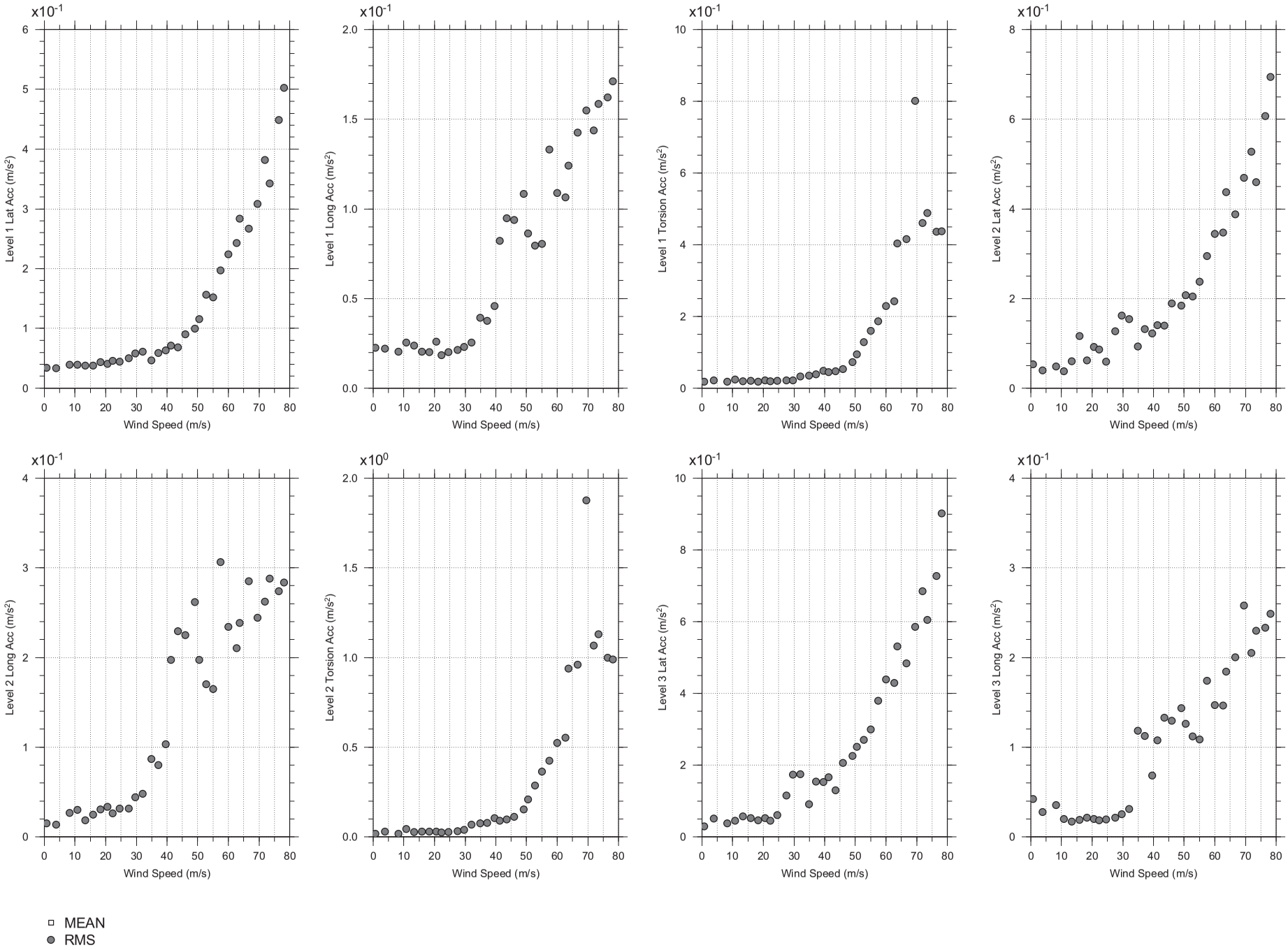

Messina Bridge, In Service Tower (Froude No.), 60 degree, Turbulent Flow

Dec. 16, 2010
fri47abdg.cl

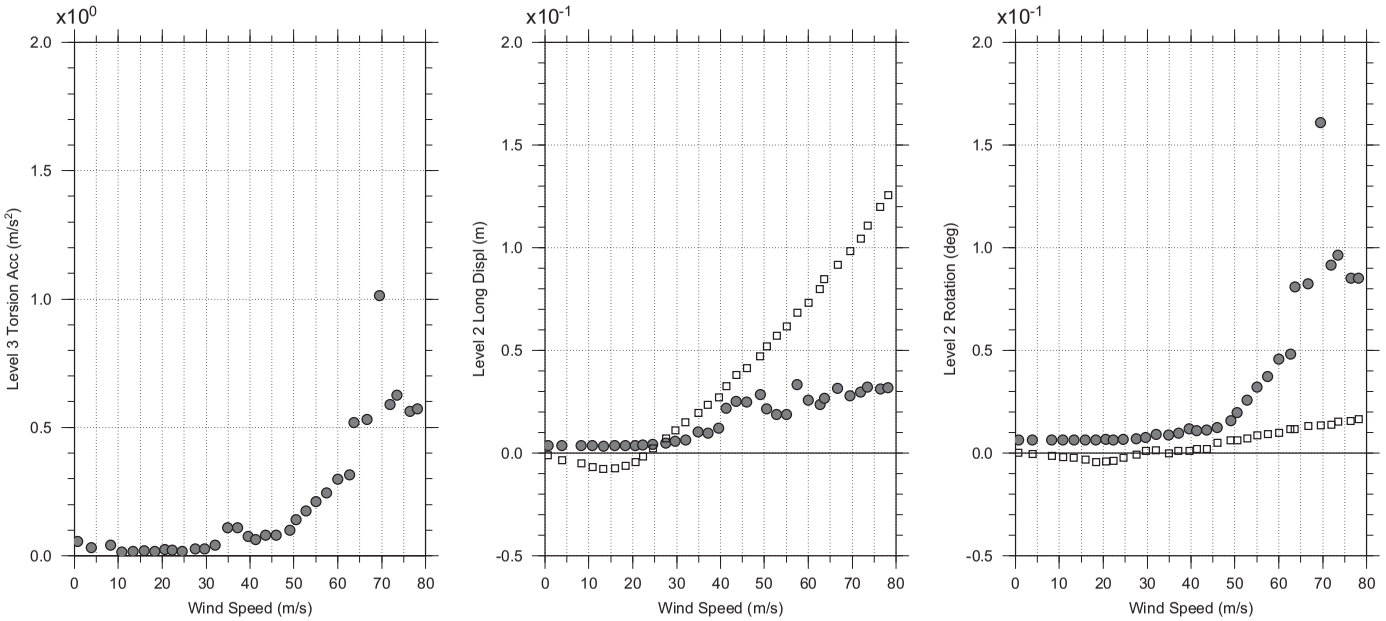

MEAN
RMS

Messina Bridge, In Service Tower (Froude No.), 60 degree, Turbulent Flow

Dec. 16, 2010
fri47abdg.cl

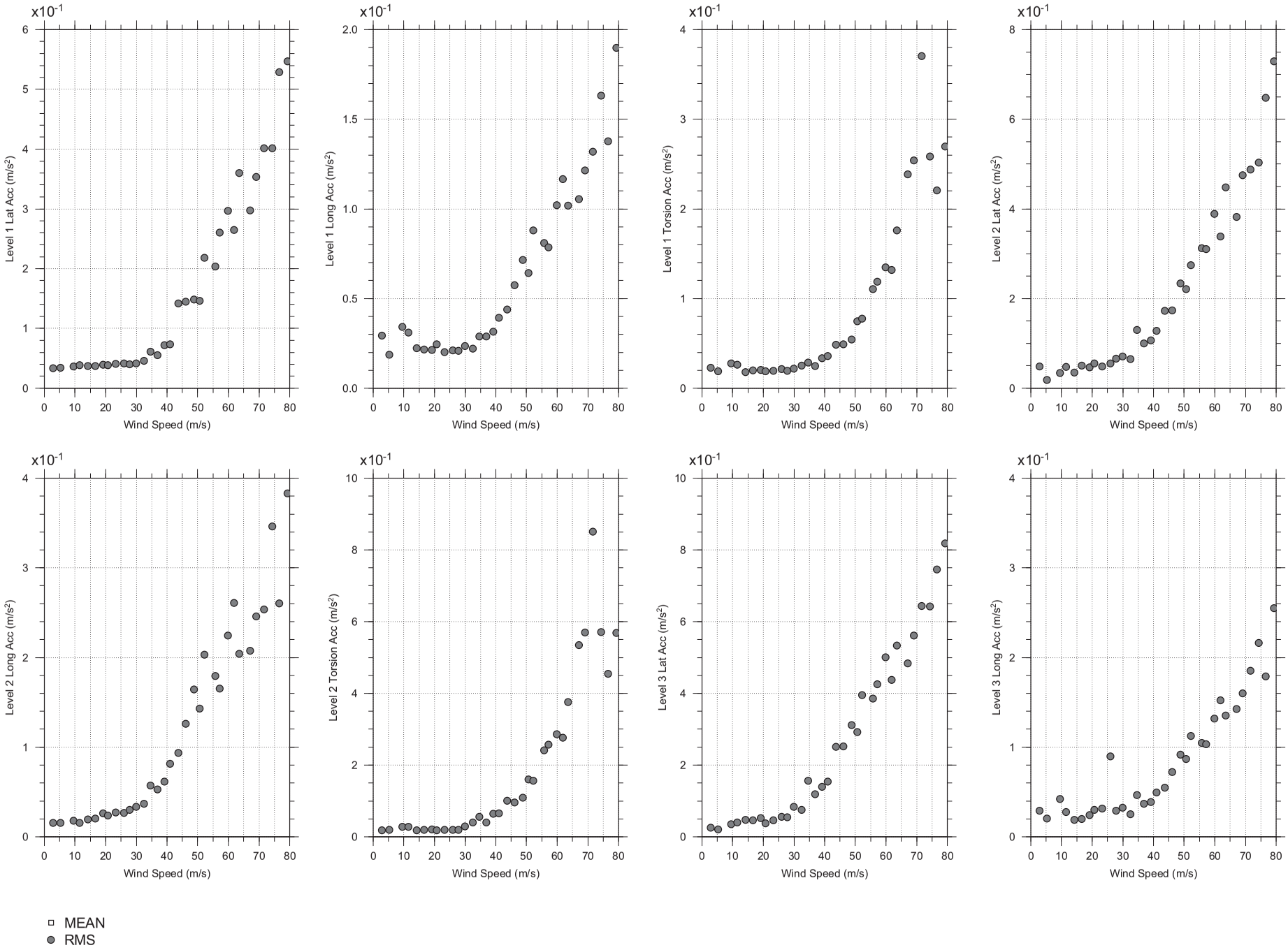

Messina Bridge, In Service Tower (Froude No.), 70 degree, Turbulent Flow

Dec. 16, 2010
fri48abdg.cl

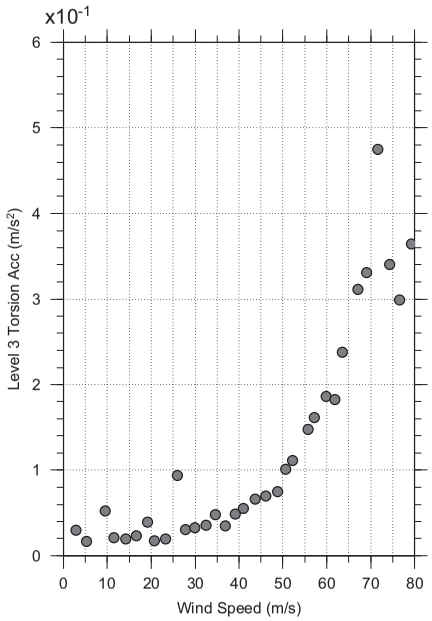

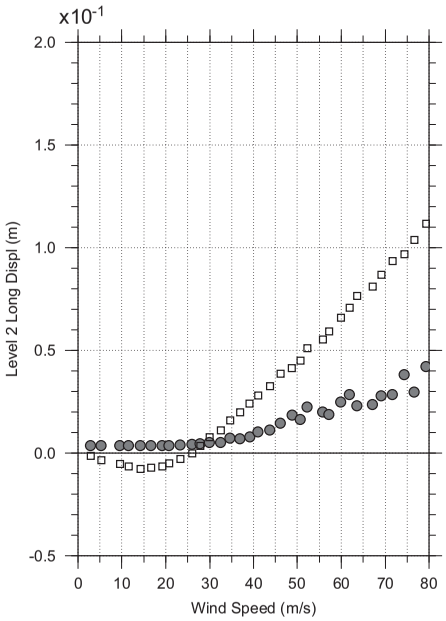

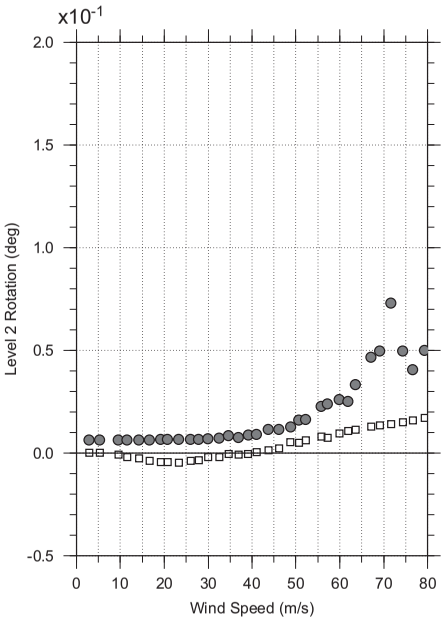

MEAN
RMS

Messina Bridge, In Service Tower (Froude No.), 70 degree, Turbulent Flow

Dec. 16, 2010
fri48abdg.cl

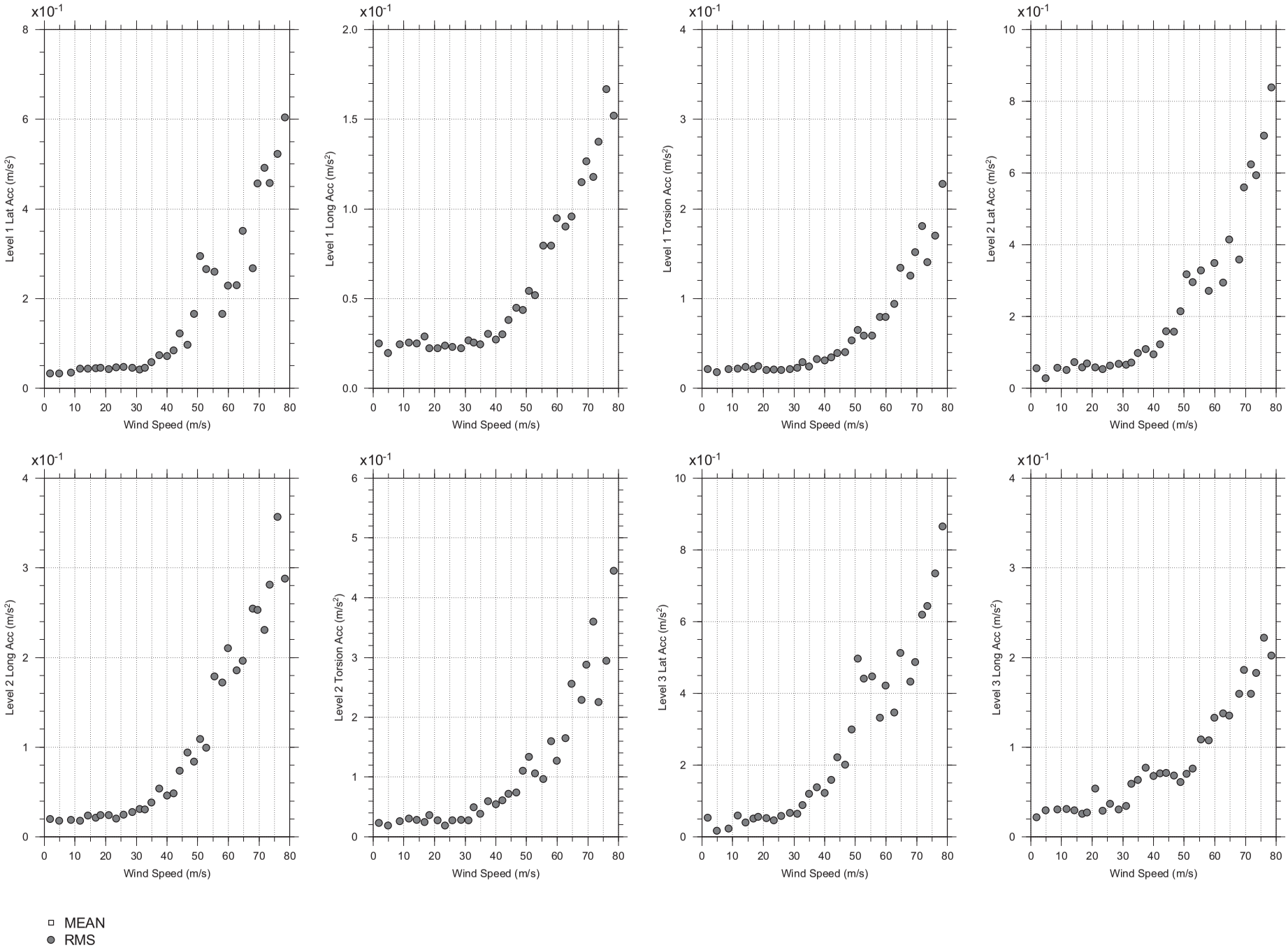

Messina Bridge, In Service Tower (Froude No.), 80 degree, Turbulent Flow

Dec. 16, 2010
fri49abdg.cl

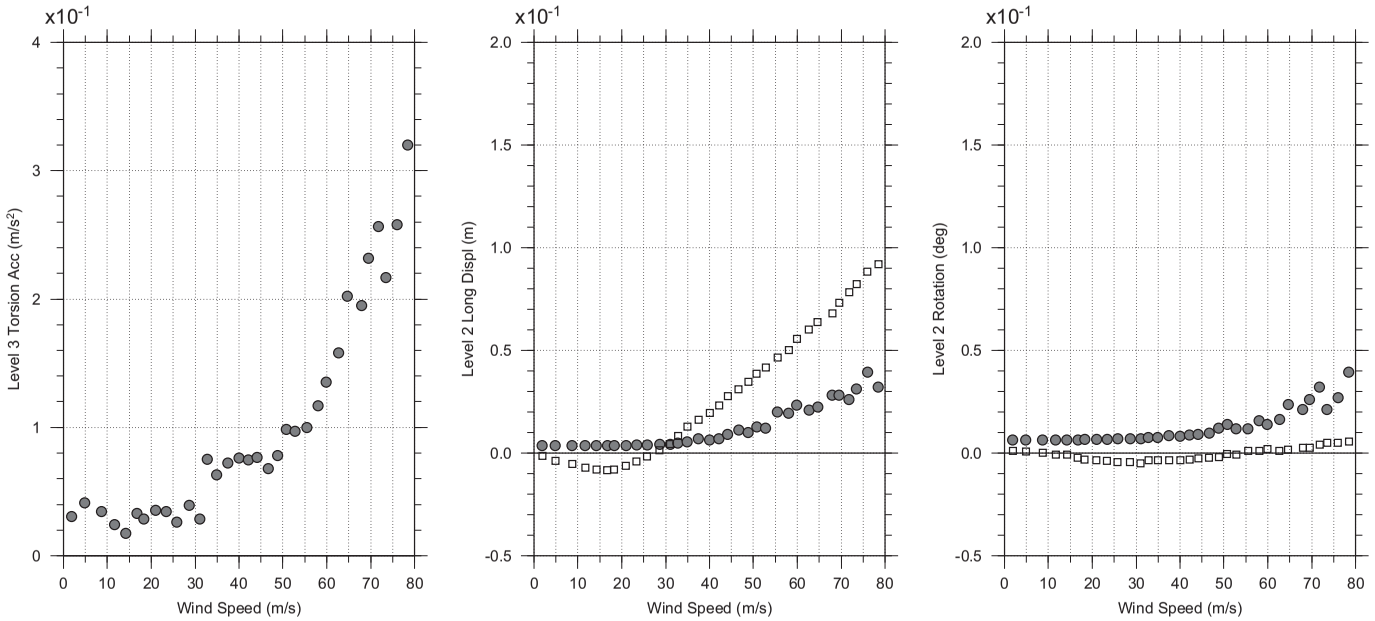

MEAN
RMS

Messina Bridge, In Service Tower (Froude No.), 80 degree, Turbulent Flow

Dec. 16, 2010
fri49abdg.cl

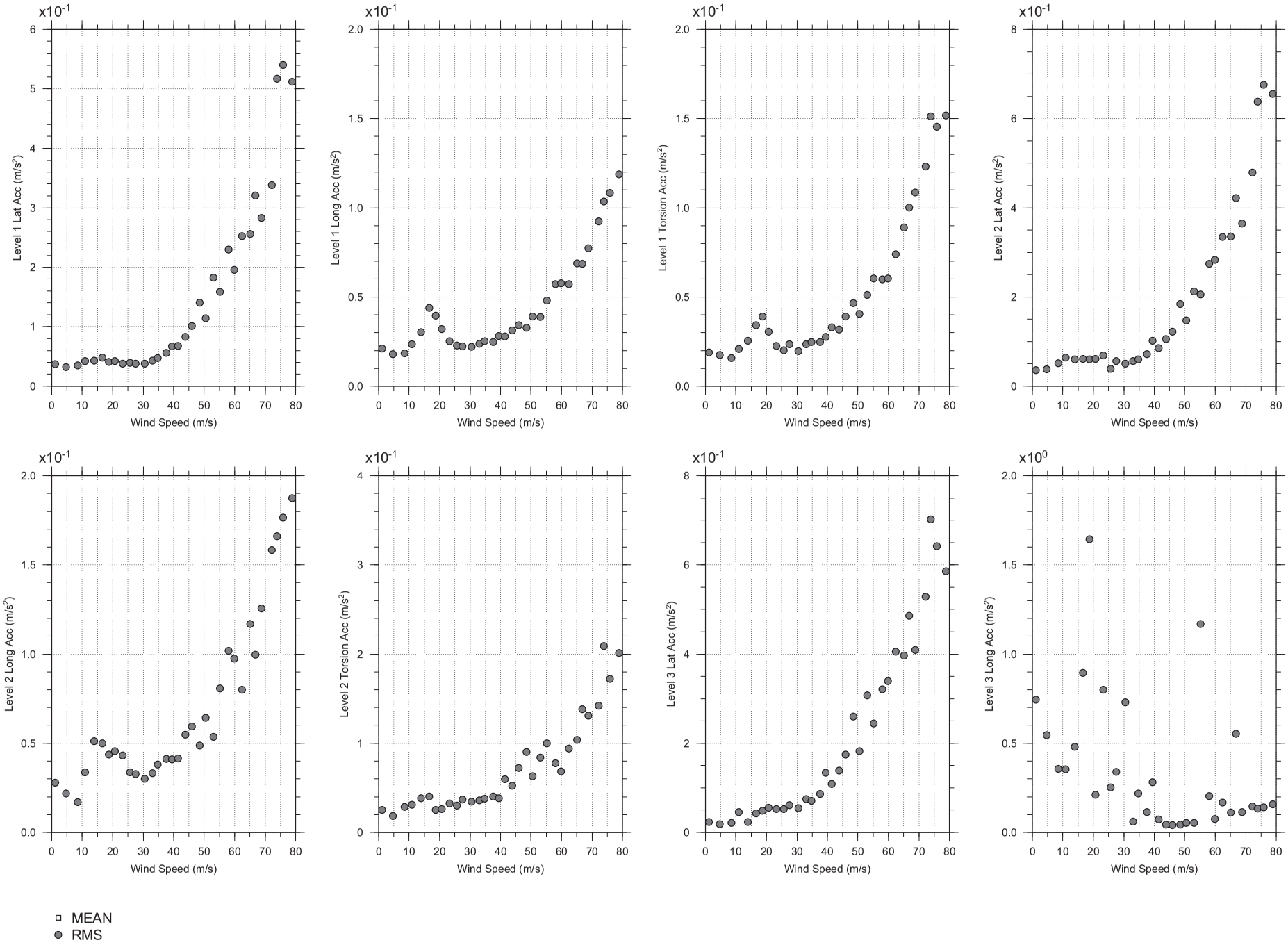

Messina Bridge, In Service Tower (Froude No.), 90 degree, Turbulent Flow

Dec. 16, 2010
fri50abdg.cl

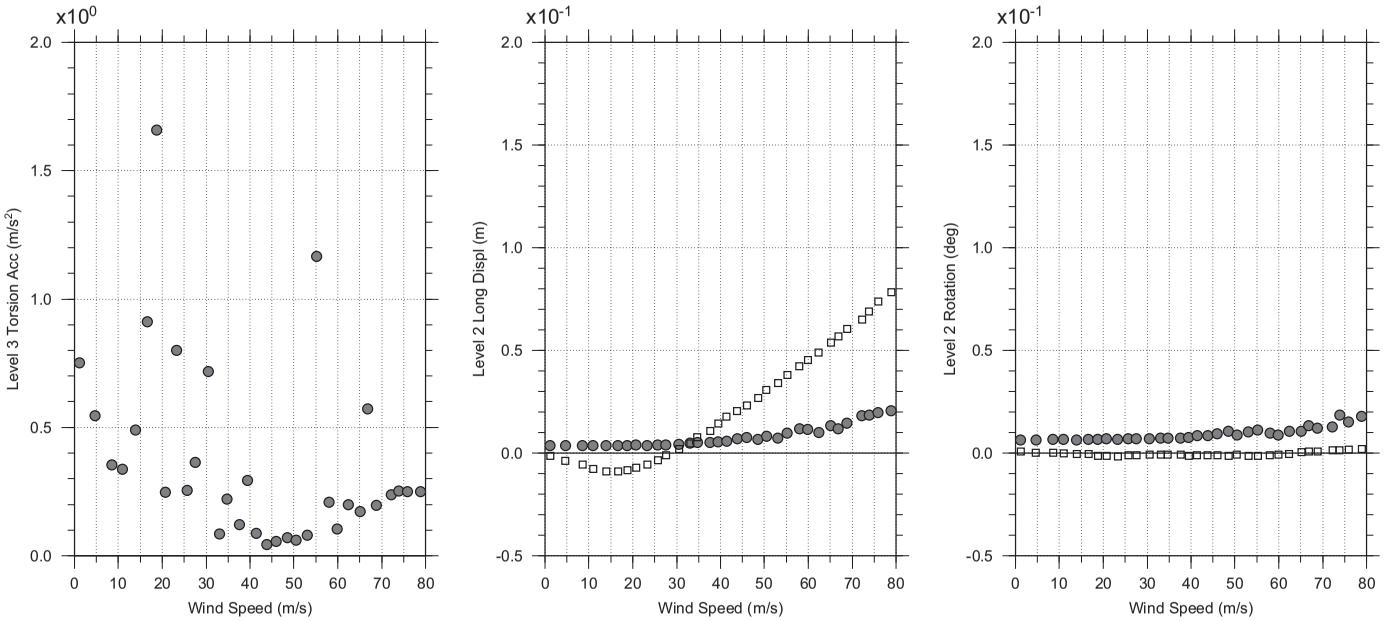

MEAN
RMS

Messina Bridge, In Service Tower (Froude No.), 90 degree, Turbulent Flow

Dec. 16, 2010
fri50abdg.cl

APPENDIX F

MODE SHAPES, FREQUENCIES AND DAMPING TRACES OF THE MESSINA TOWER MODELS

Notes:

a) Longitudinal

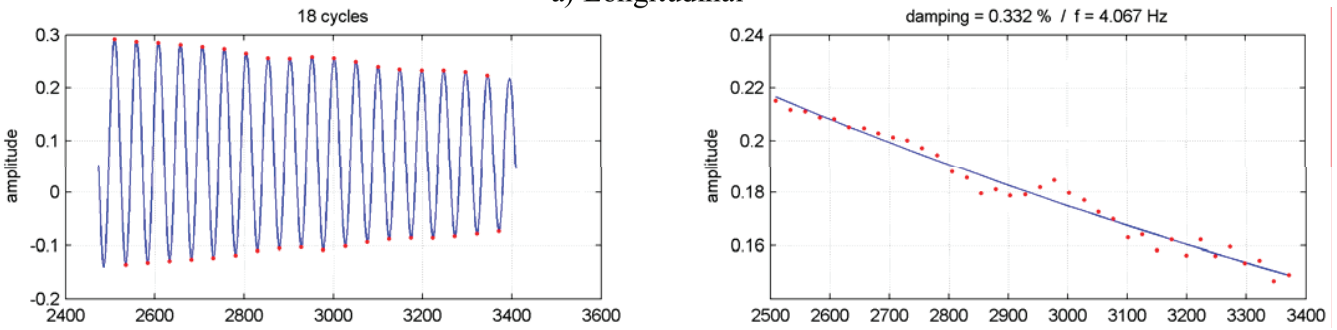

b) Torsion

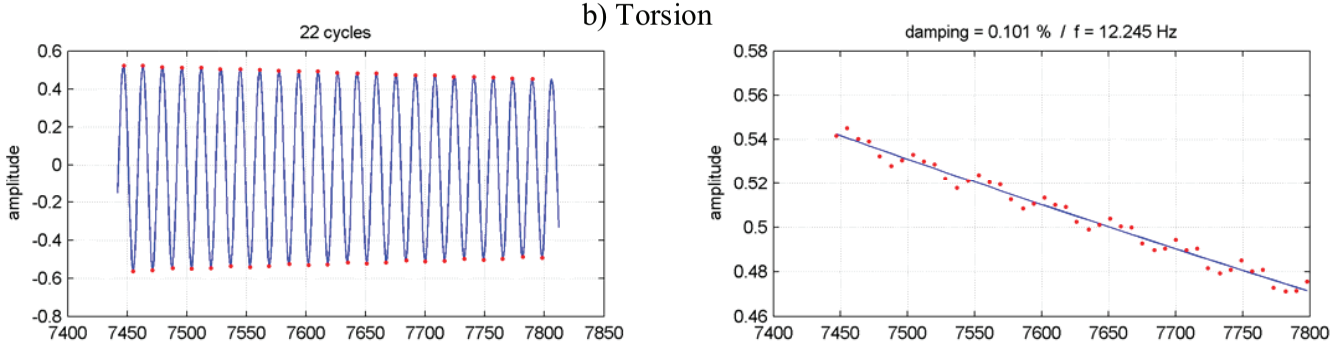

c) Lateral

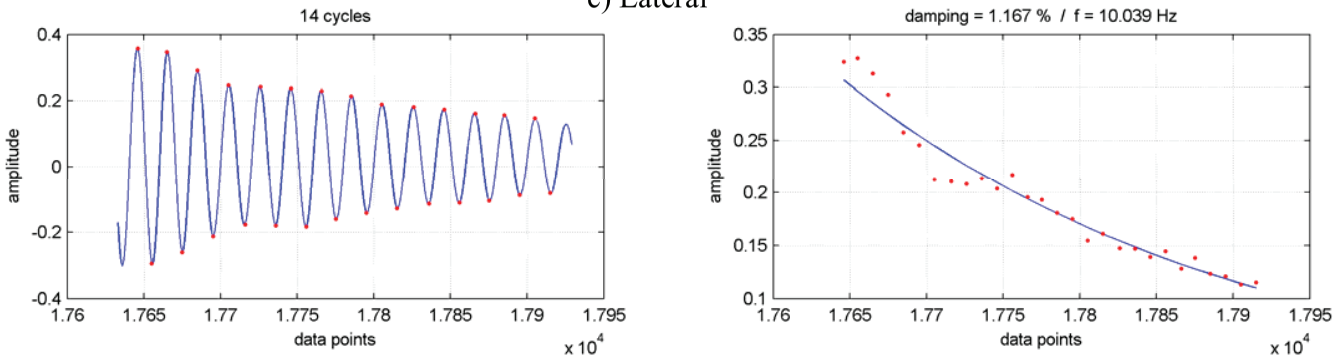

Figure 1 Non-Froude Scale Inherent Damping Free Standing Tower

a) Longitudinal

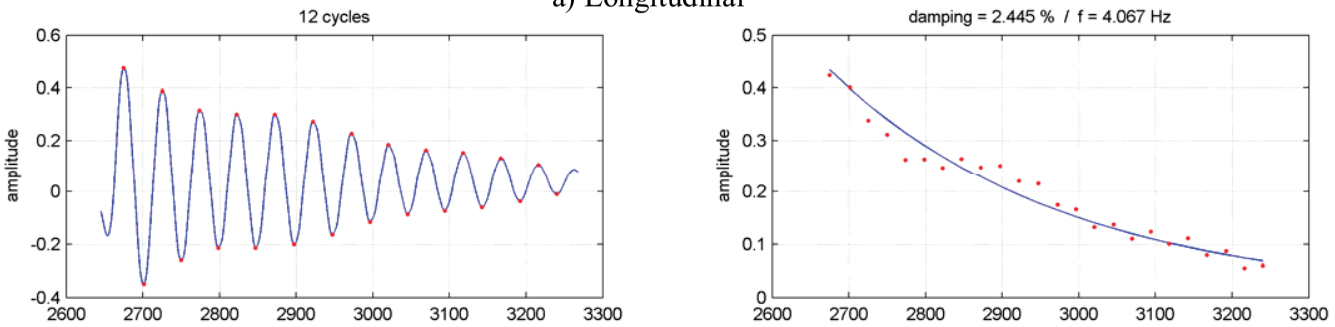

b) Torsion

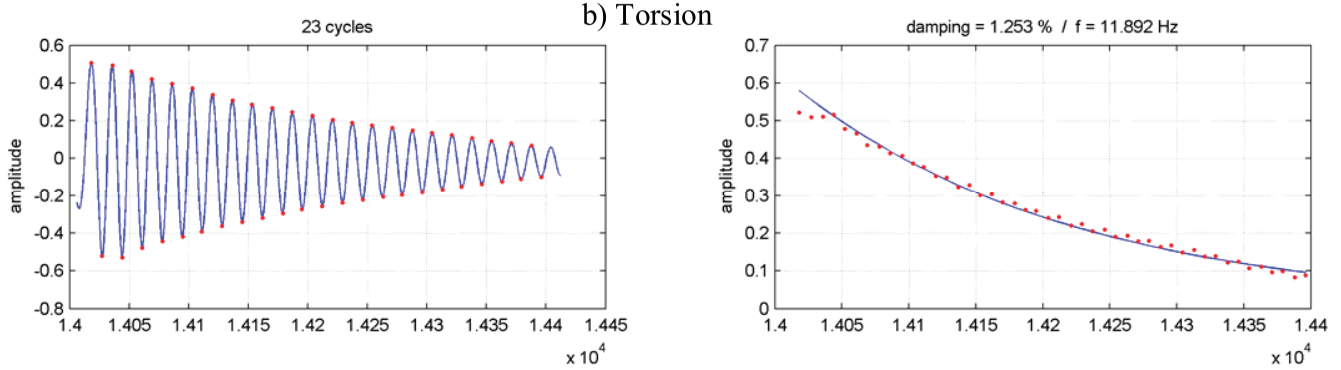

c) Lateral

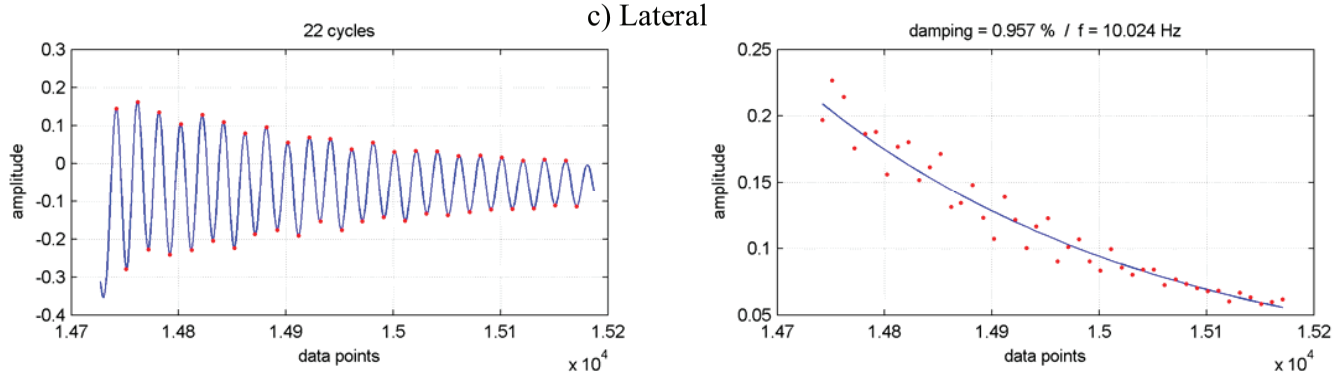

Figure 2 Non-Froude Scale 2% Nominal Damping Free Standing Tower

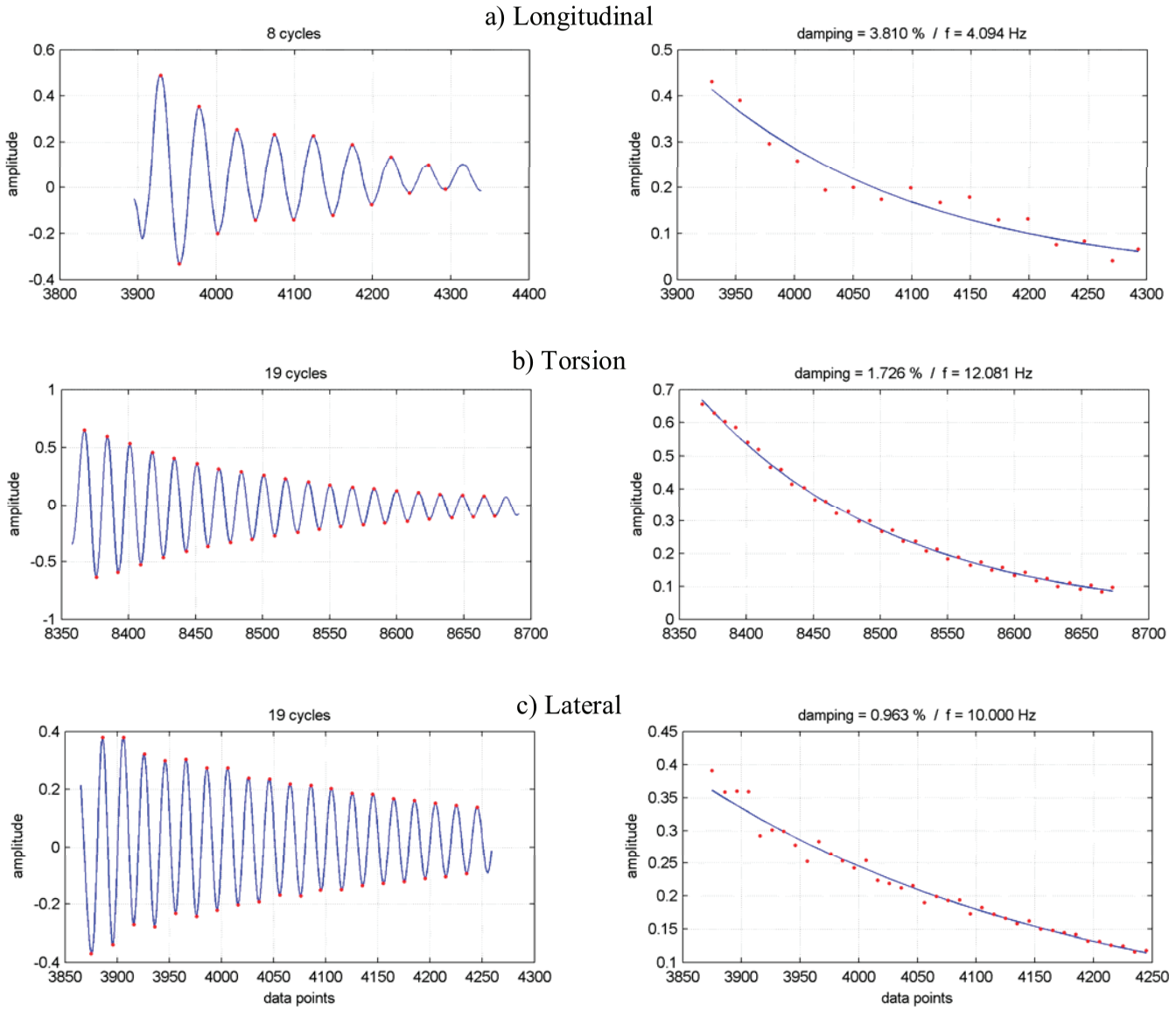

Figure 3 Non-Froude Scale 4% Nominal Damping Free Standing Tower

a) Longitudinal

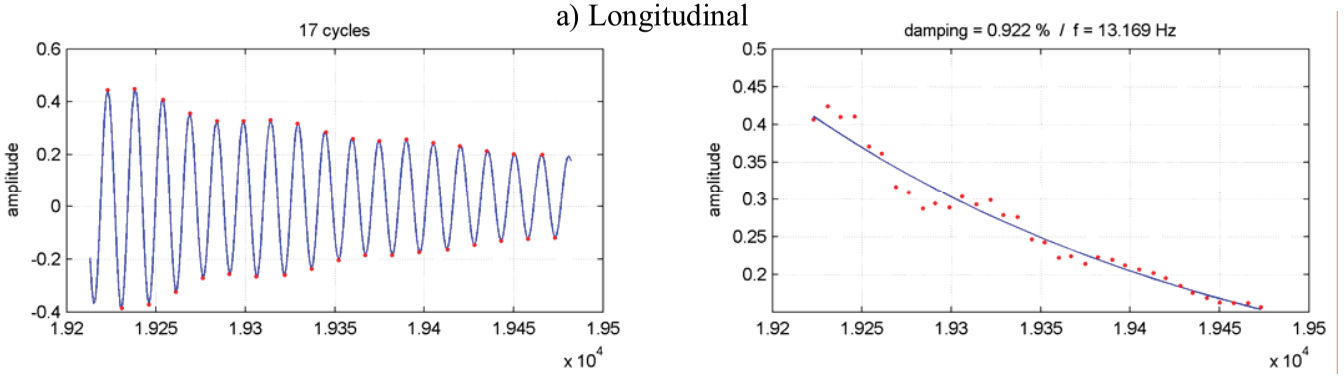

b) Torsion

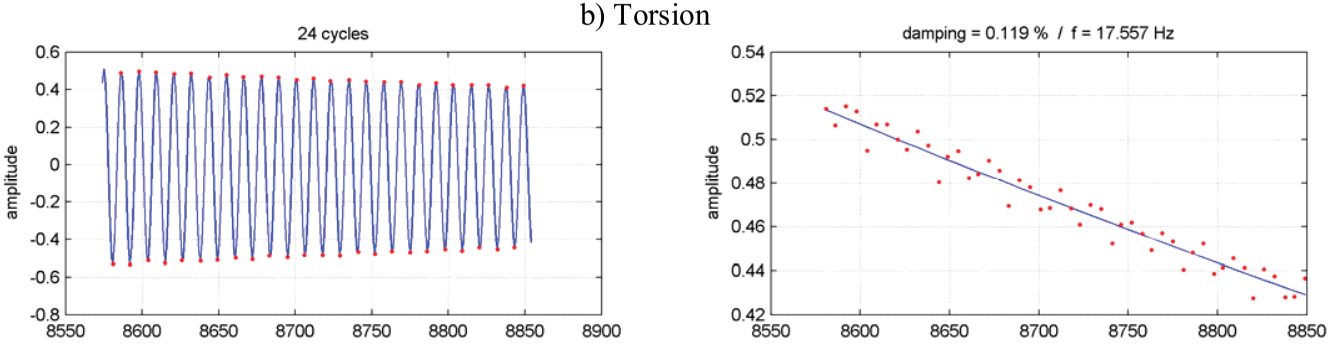

c) Lateral

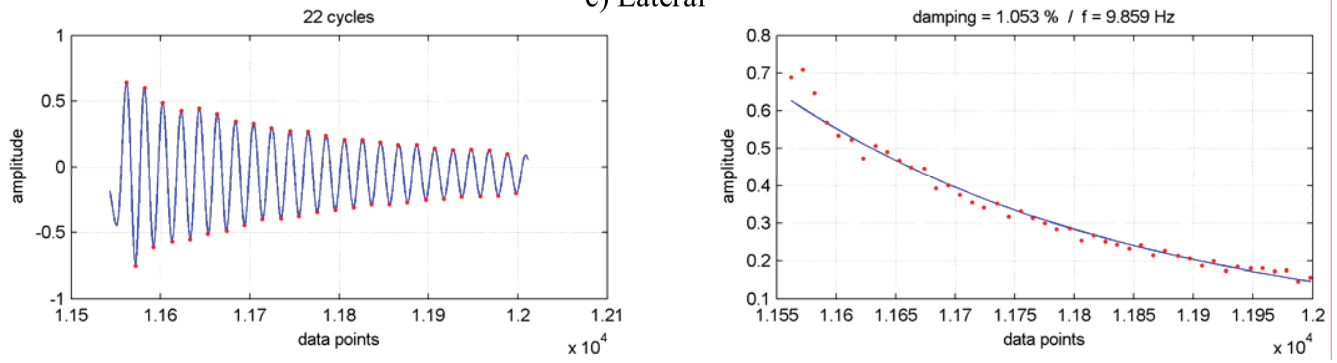

Figure 4 Non-Froude Scale Inherent Damping In-service Tower

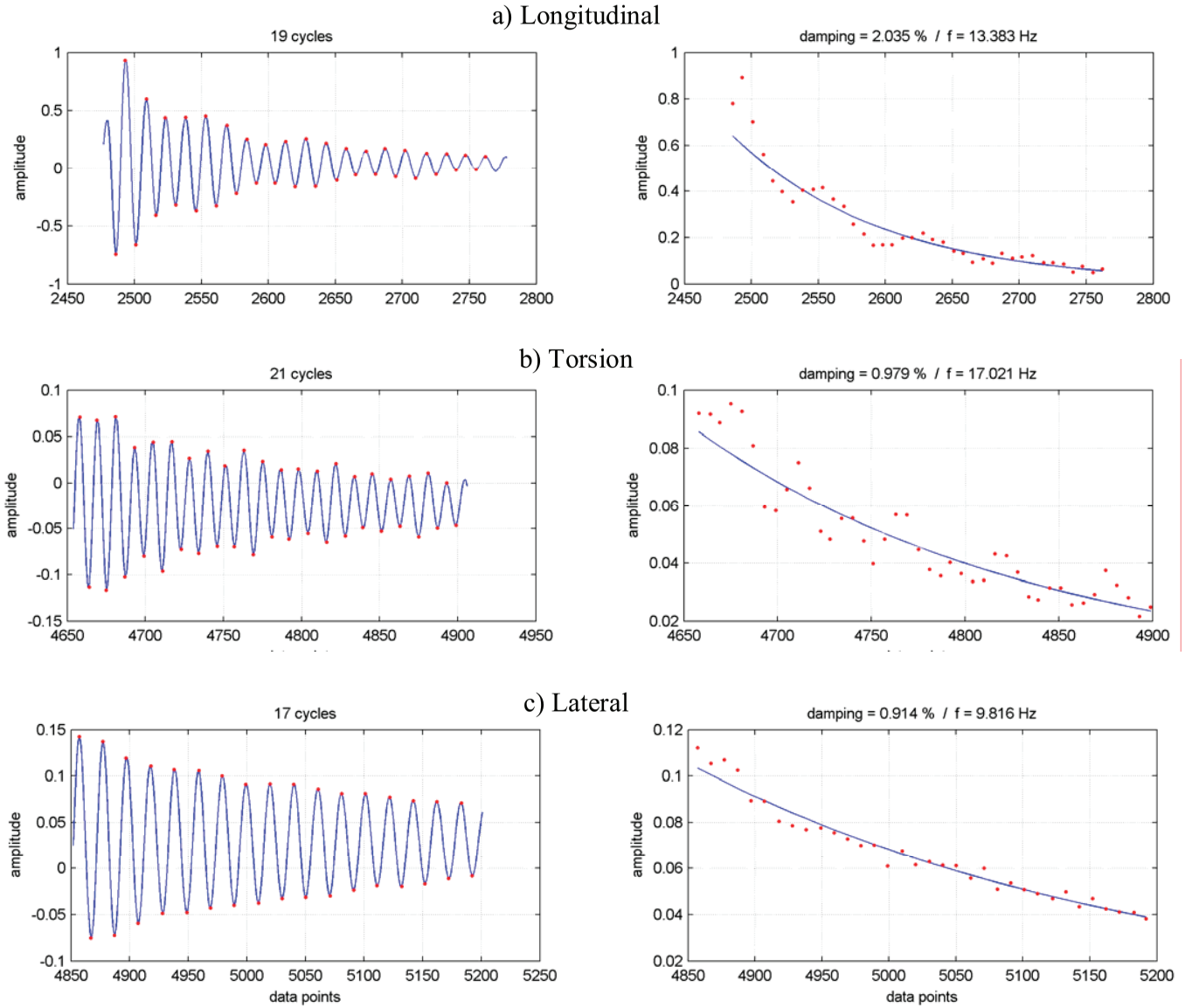

Figure 5 Non-Froude Scale 2% Nominal Damping In-service Tower

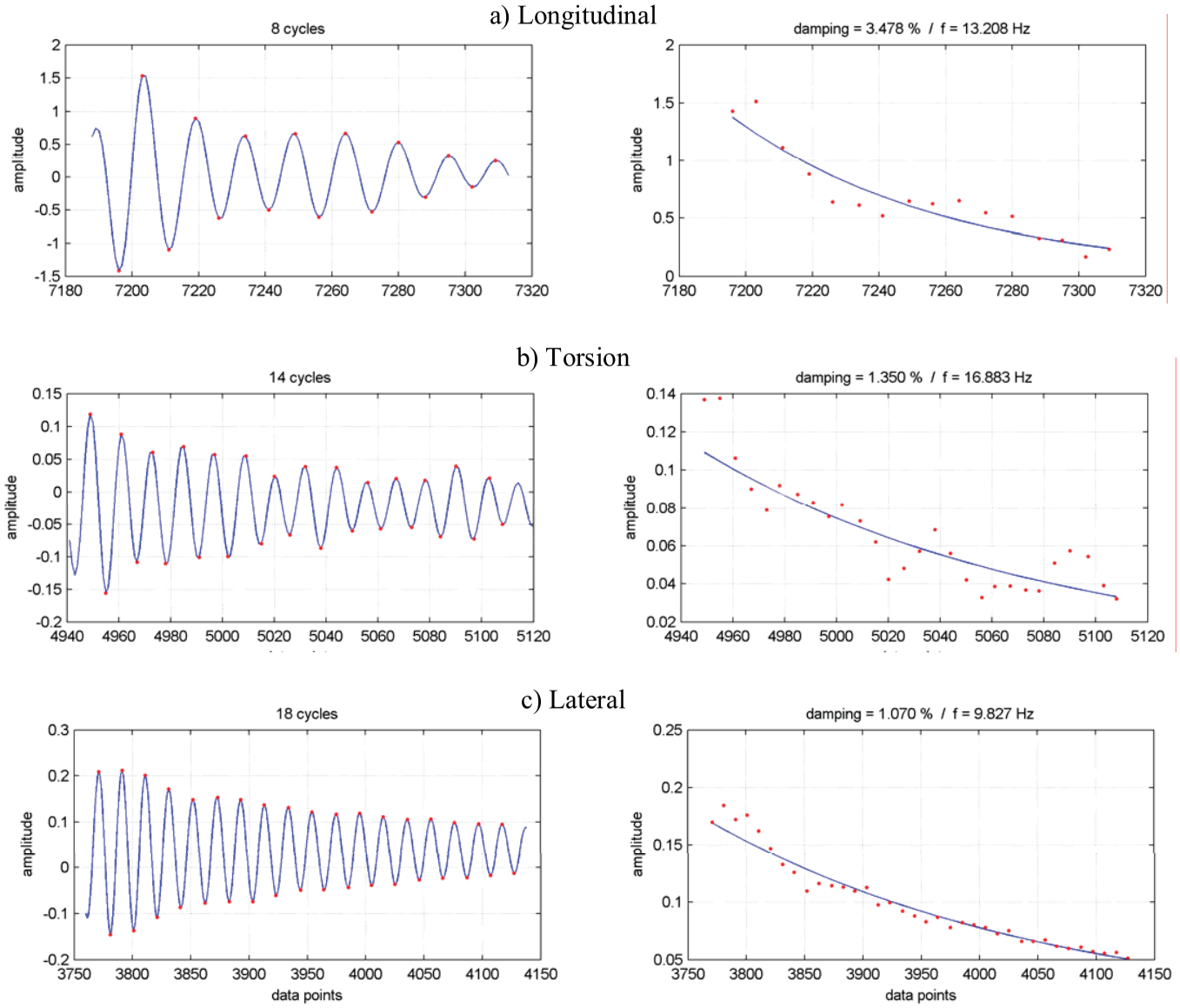

Figure 6 Non-Froude Scale 4% Nominal Damping In-Service Tower

a) Longitudinal

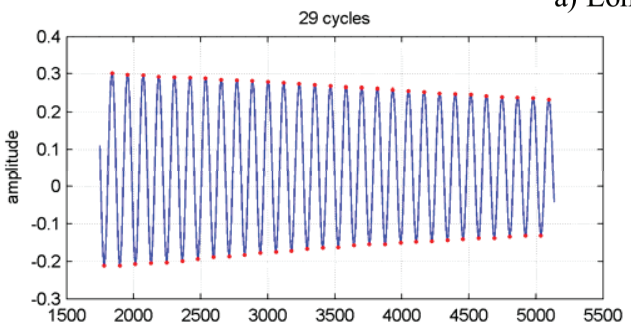

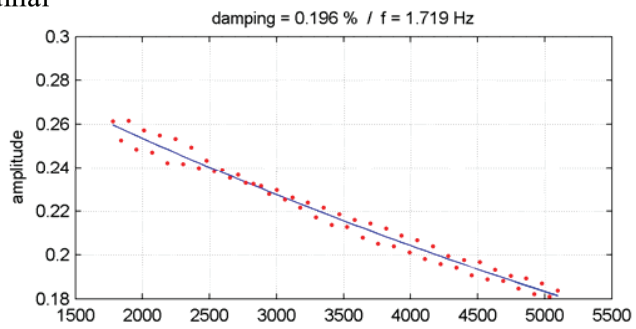

b) Torsion

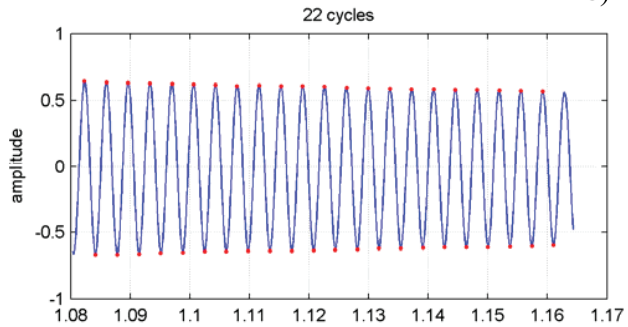

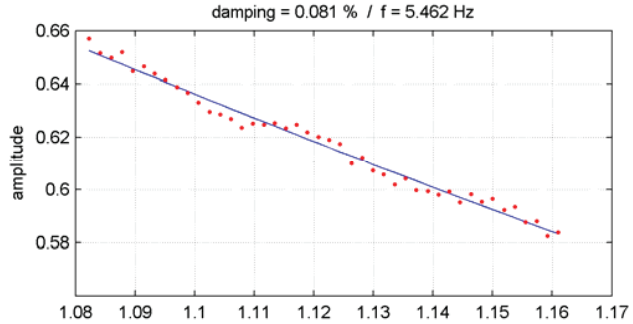

c) Lateral

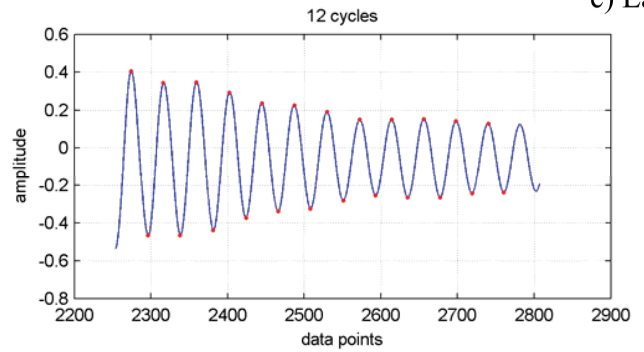

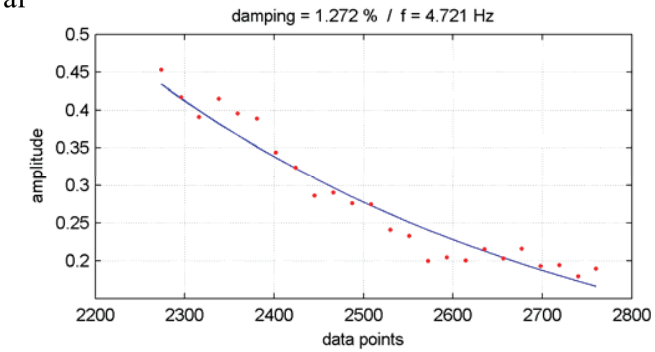

Figure 7 Froude Scale Inherent Damping Free Standing Tower

a) Longitudinal

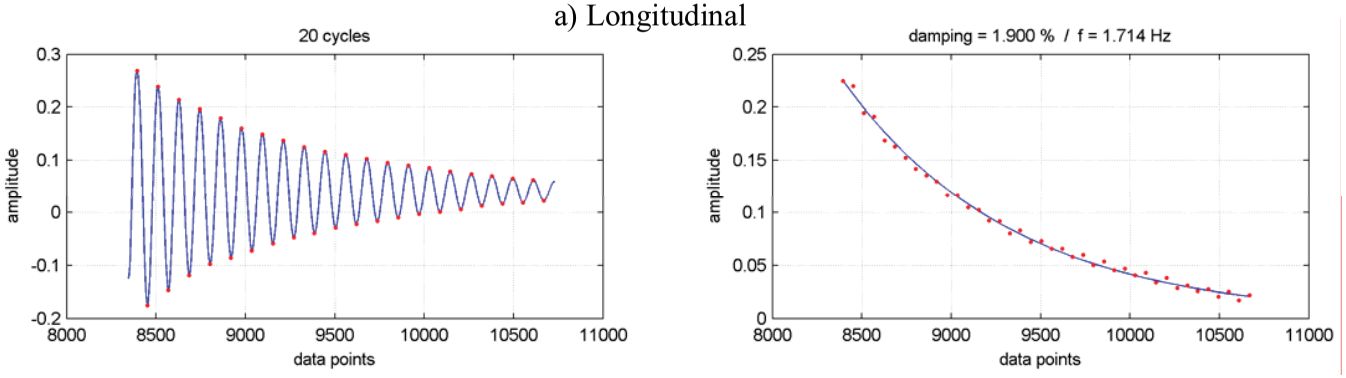

b) Torsion

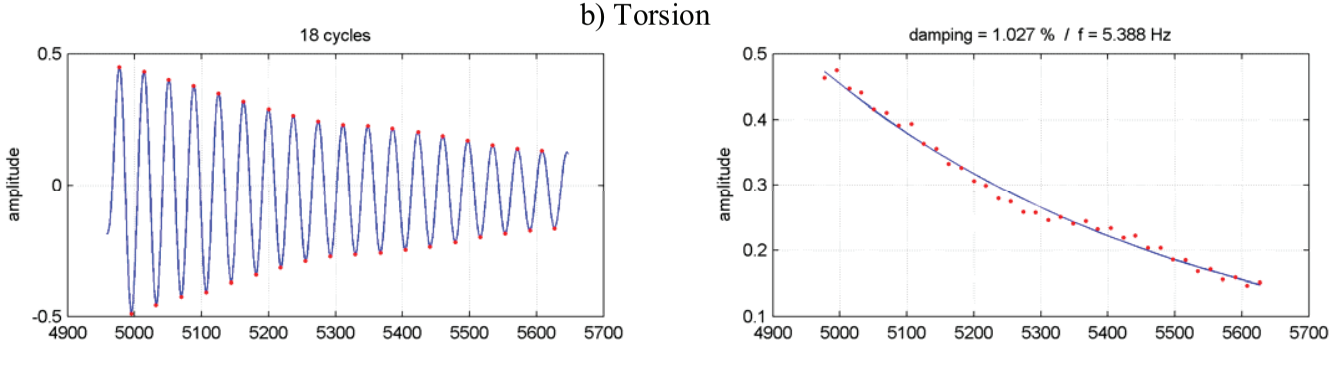

c) Lateral

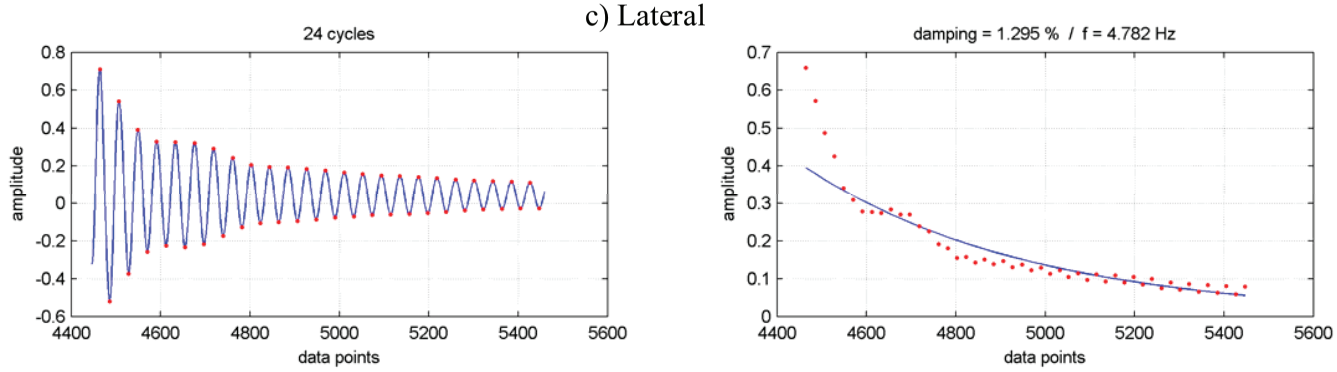

Figure 8 Froude Scale 2% Nominal Damping Free Standing Tower

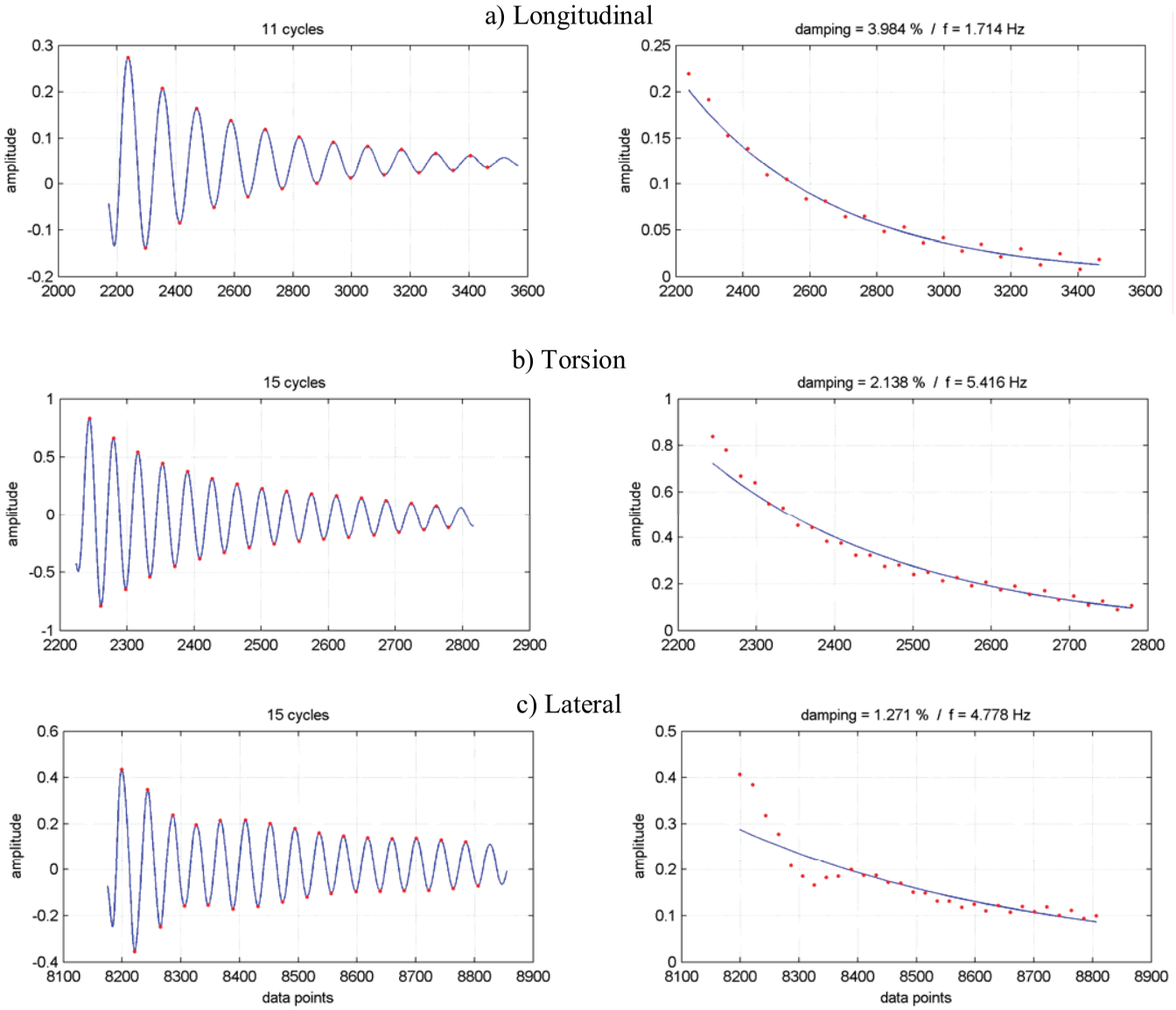

Figure 9 Froude Scale 4% Nominal Damping Free Standing Tower

a) Longitudinal

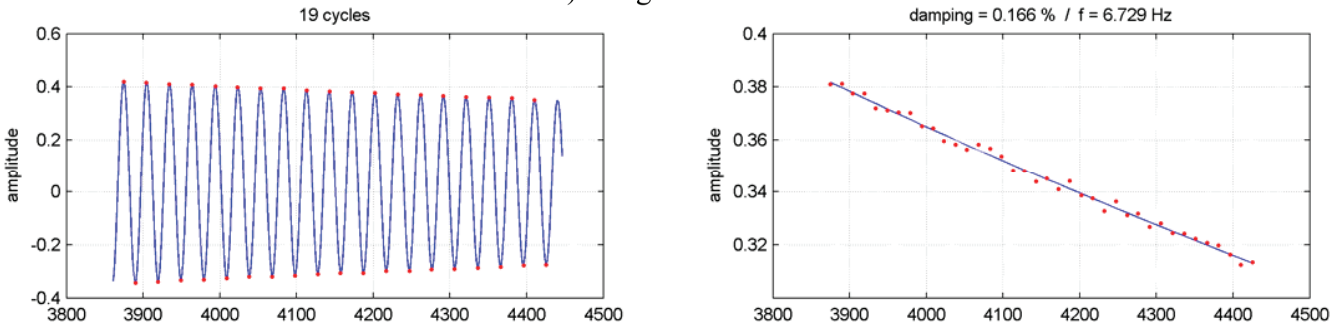

b) Torsion

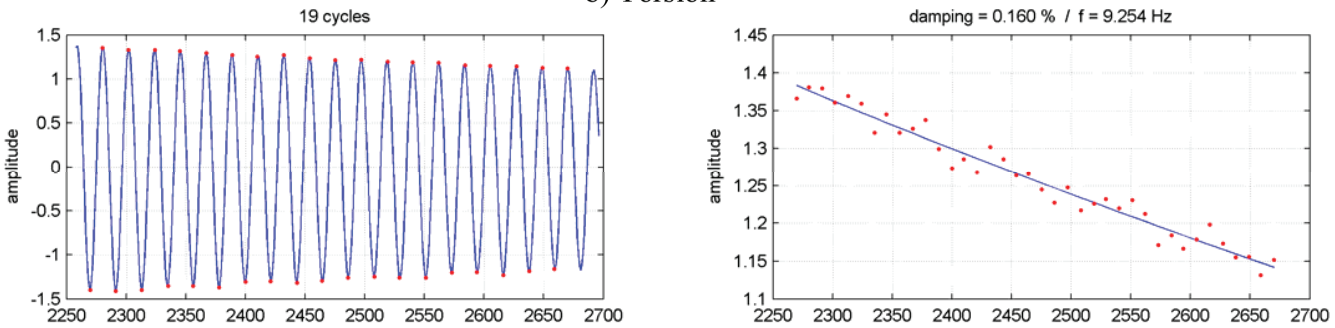

c) Lateral

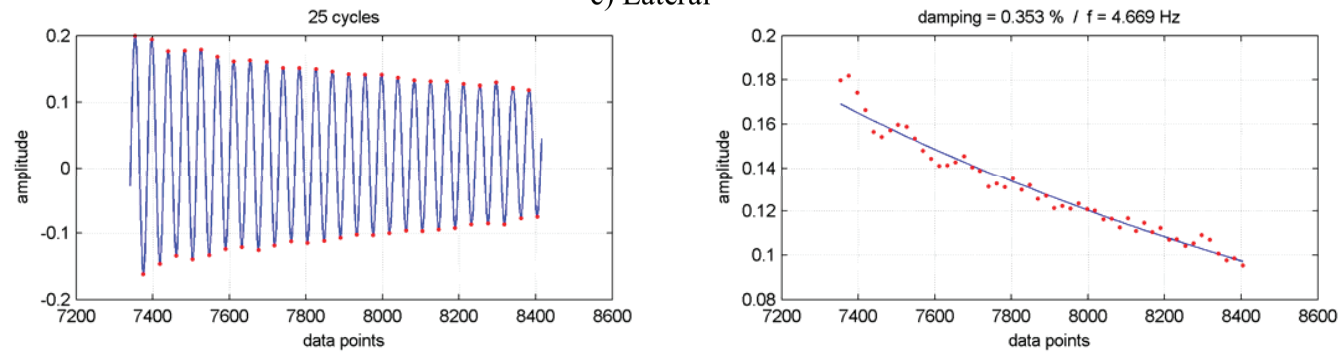

Figure 10 Froude Scale Inherent Damping In-service Tower

a) Longitudinal

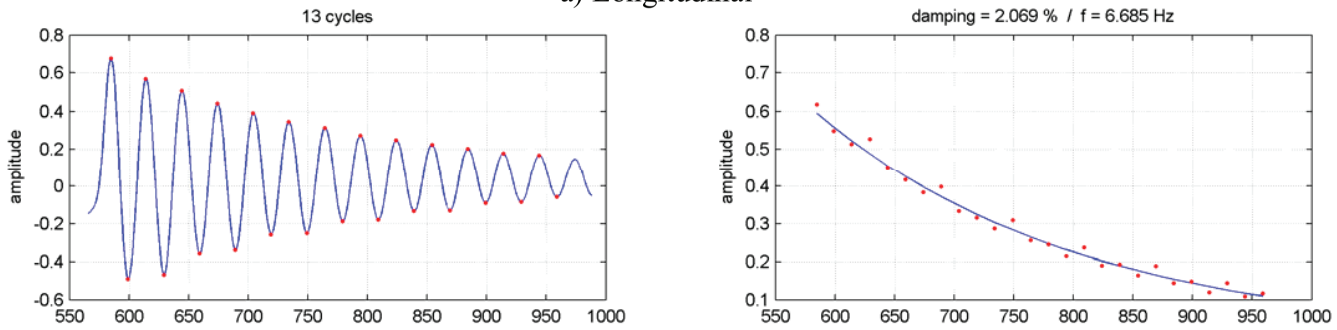

b) Torsion

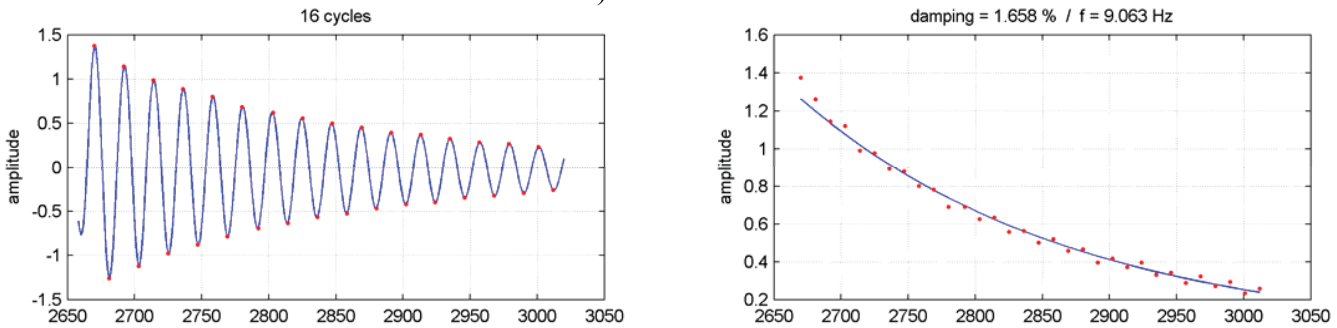

c) Lateral

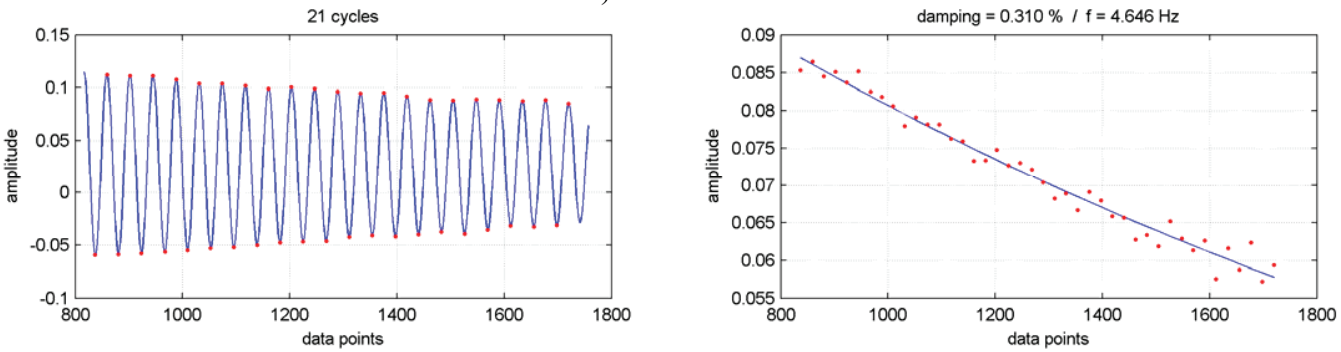

Figure 11 Froude Scale 2% Nominal Damping In-service Tower

a) Longitudinal

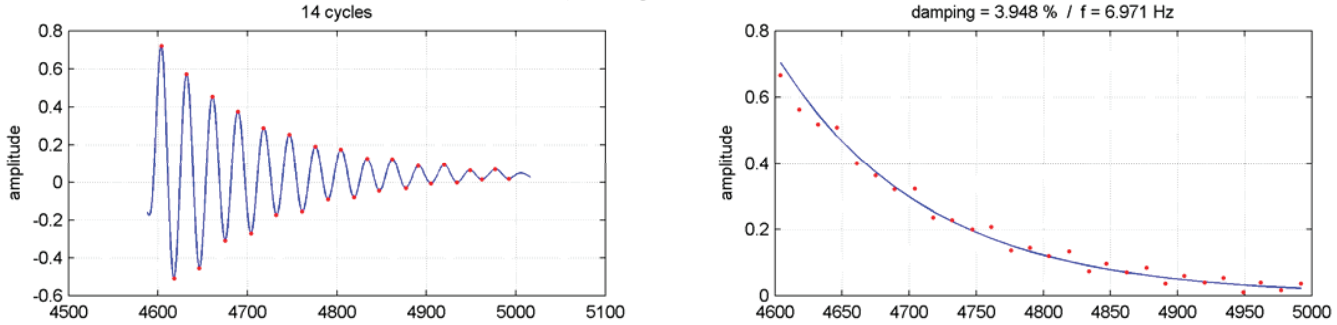

b) Torsion

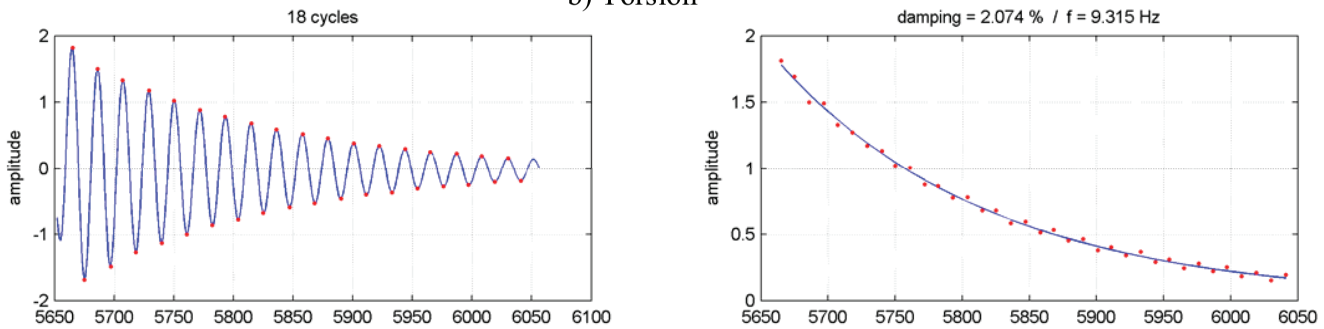

c) Lateral

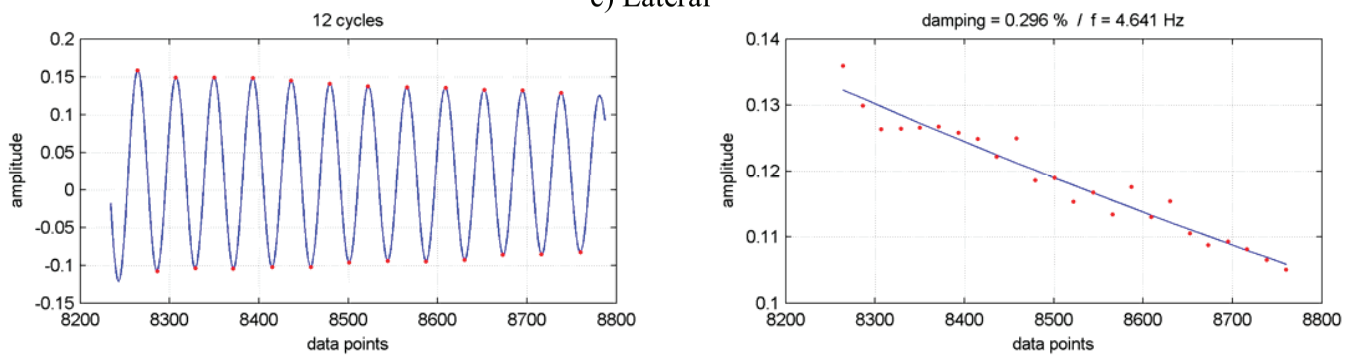

Figure 12 Froude Scale 4% Nominal Damping In-service Tower

a) Longitudinal

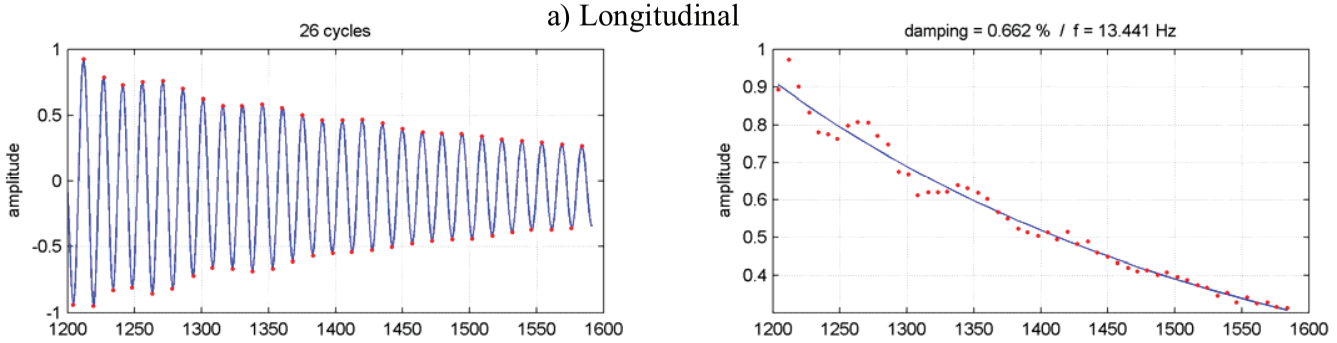

b) Torsion

c) Lateral

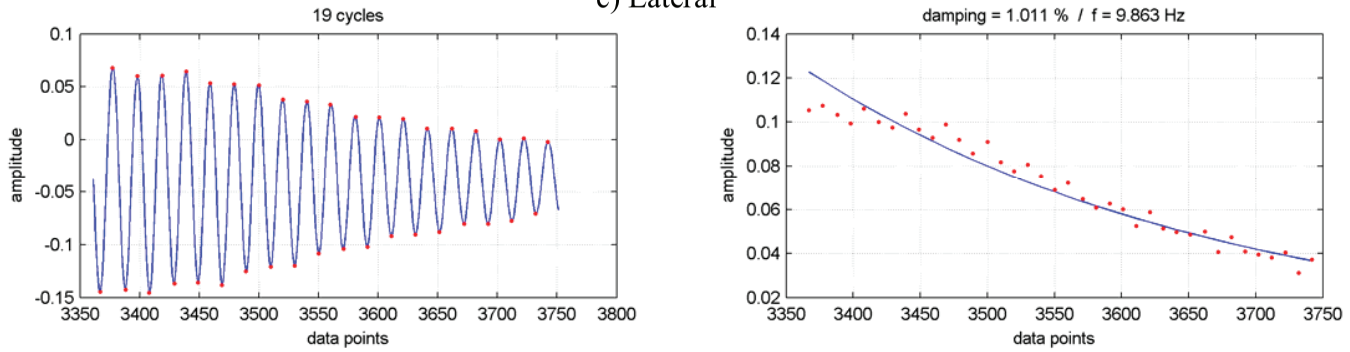

Figure 13 Non-Froude Scale High Inherent Damping In-service Tower – 0.66% Pier Base Unrestrained (R001P009)

a) Longitudinal

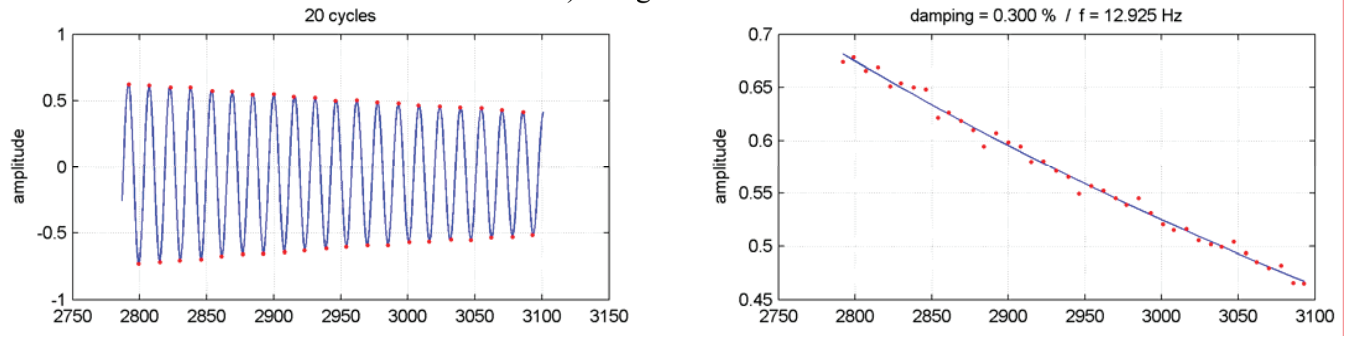

b) Torsion

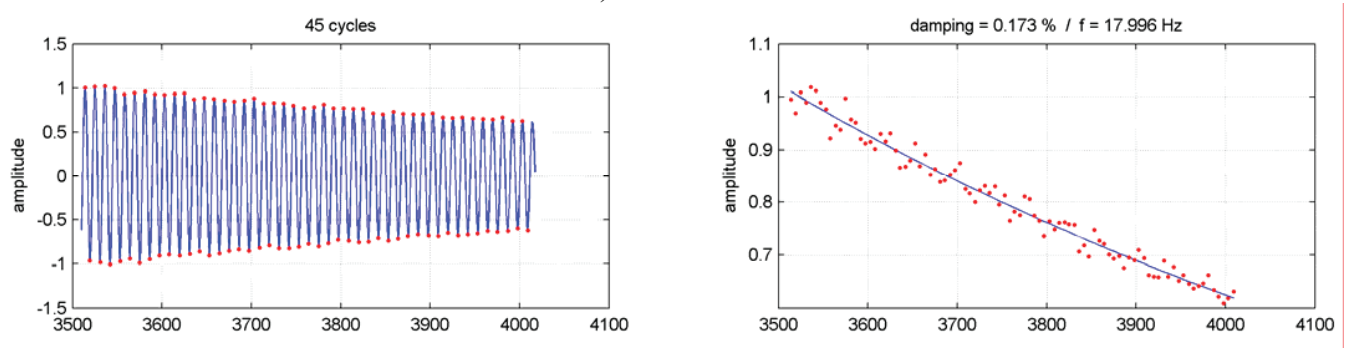

c) Lateral

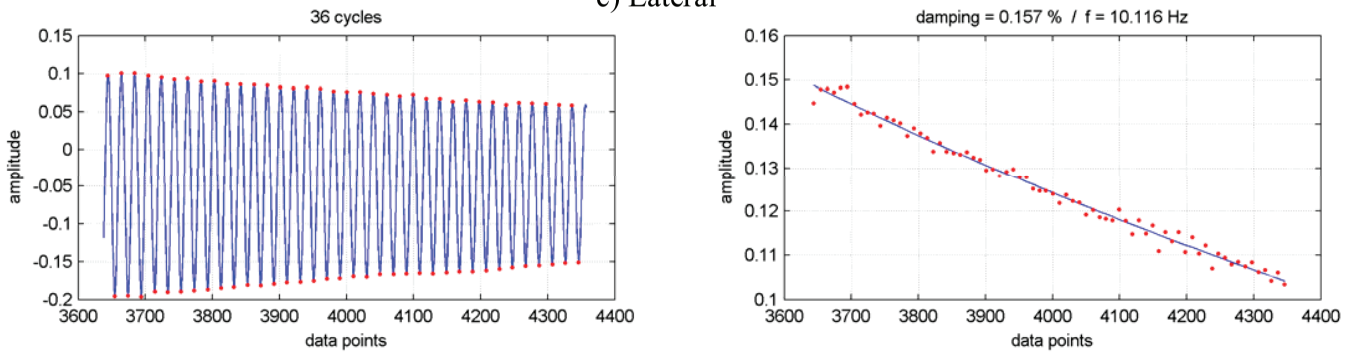

Figure 14 Non-Froude Scale Low Inherent Damping In-service Tower – 0.3% Pier Base Restrained (R003P001-3)

a) Longitudinal

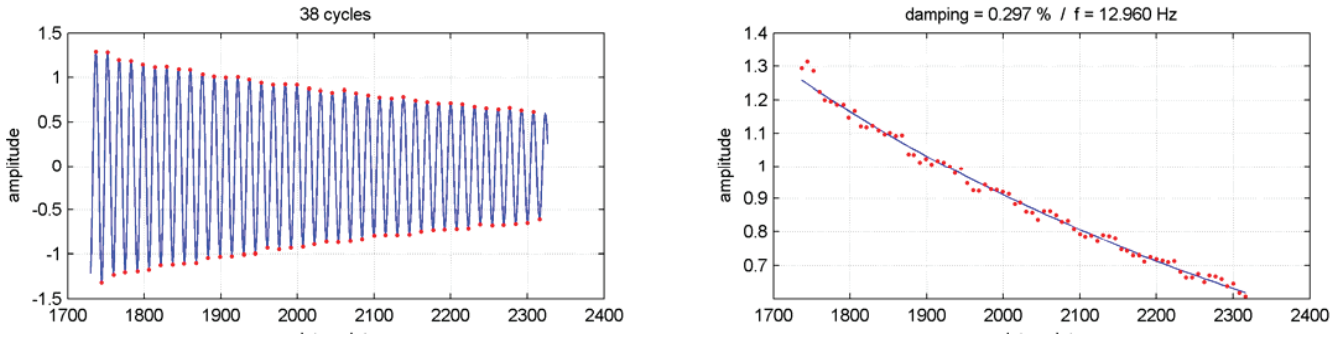

b) Torsion

c) Lateral

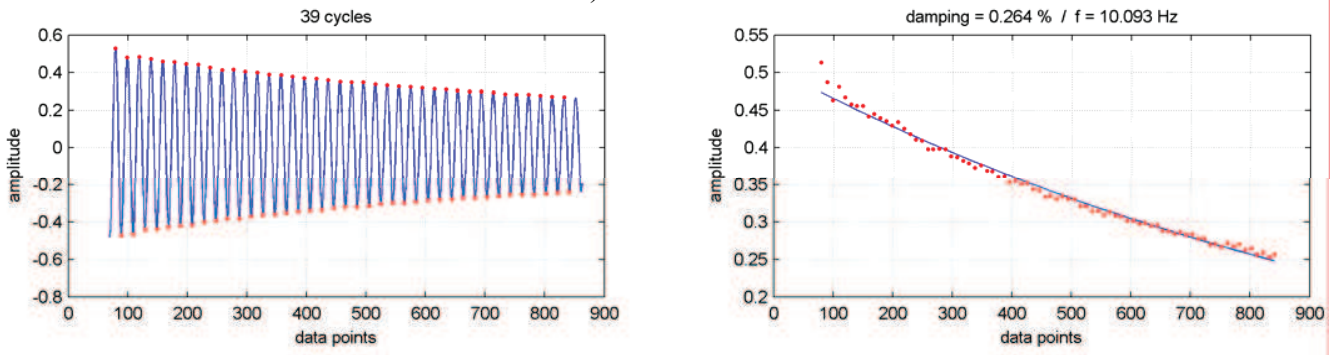

Figure 14 Non-Froude Scale Low Inherent Damping In-service Tower – 0.3% Pier Base Restrained (R004P001-3)

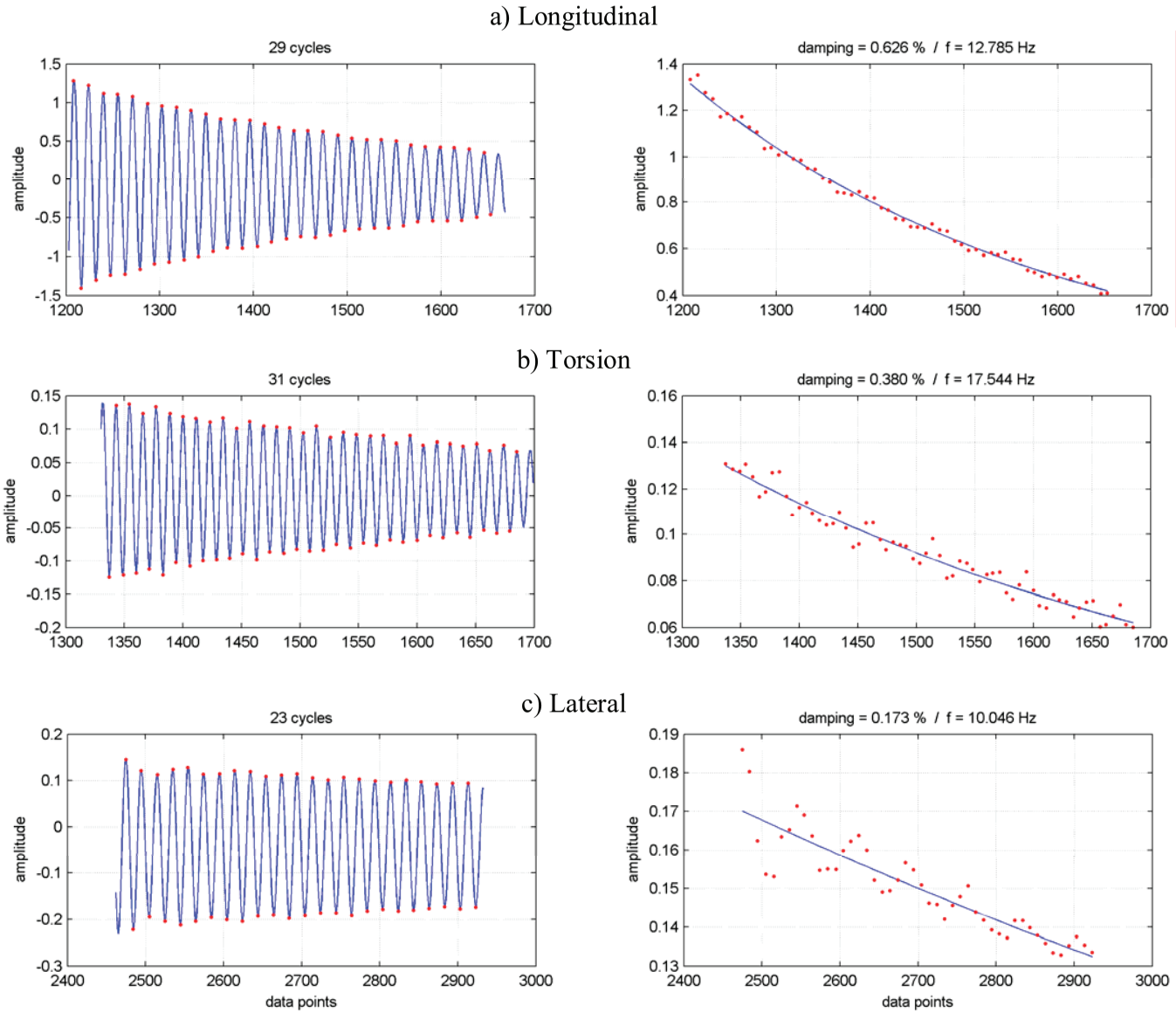

Figure 15 Non-Froude Scale 0.6% Damping In-service Tower – 0.63% Small Dampers, Pier Base Restrained (R005P006)

a) Longitudinal

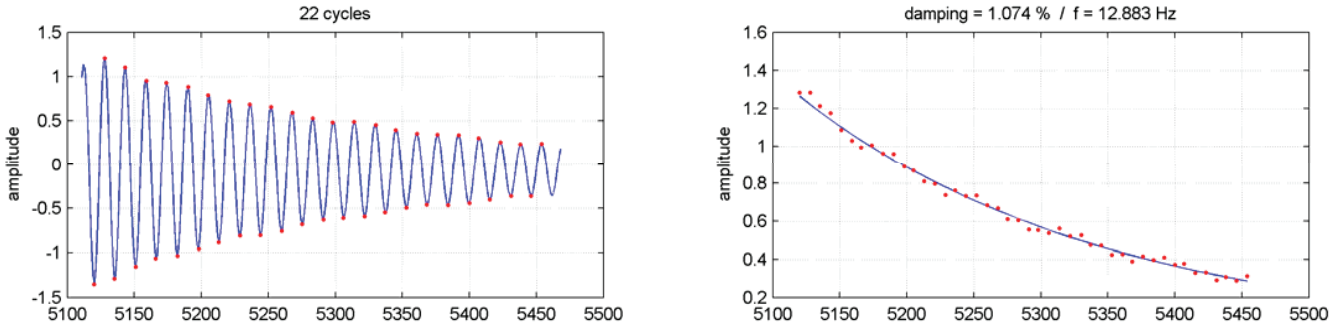

b) Torsion

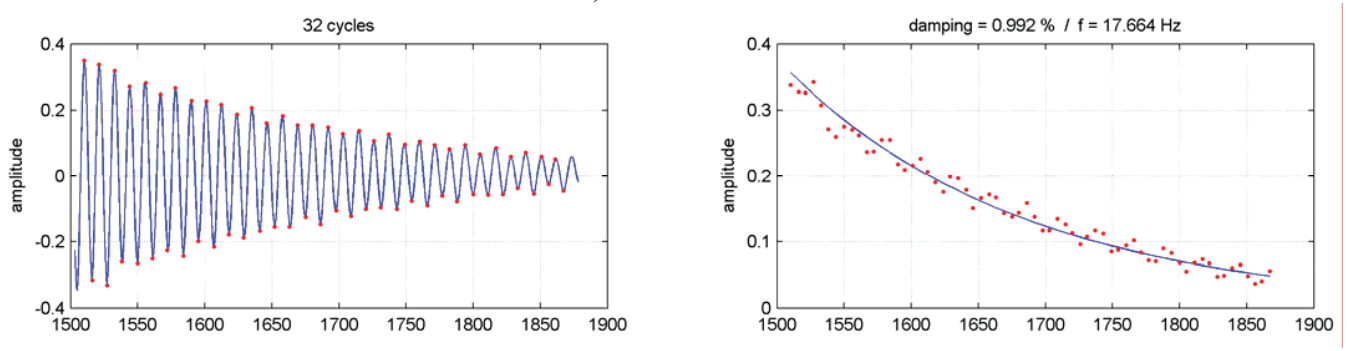

c) Lateral

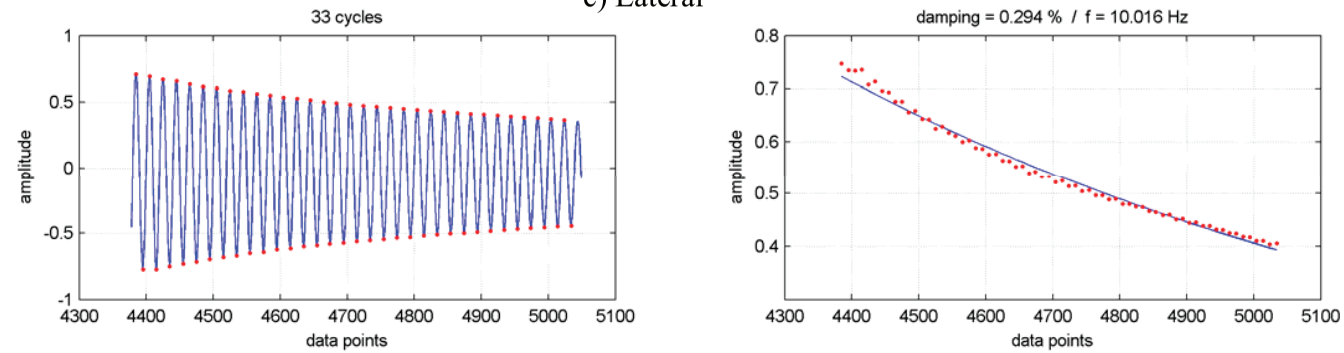

Figure 16 Non-Froude Scale 1.1% Damping In-service Tower – 1.07% Small Dampers, Pier Base Restrained (R006P001-3)

a) Longitudinal

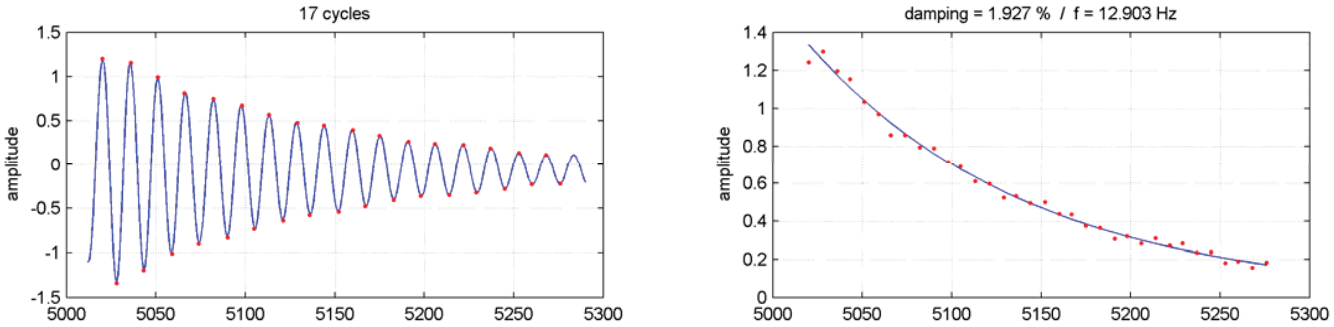

b) Torsion

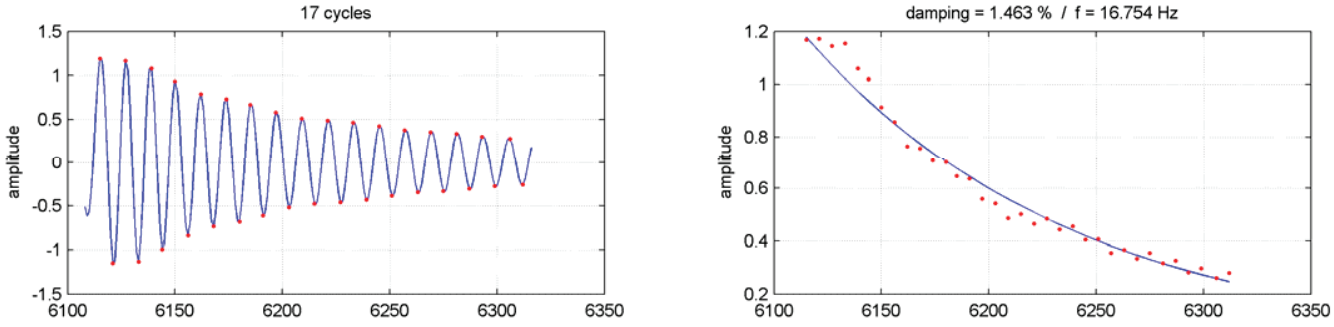

c) Lateral

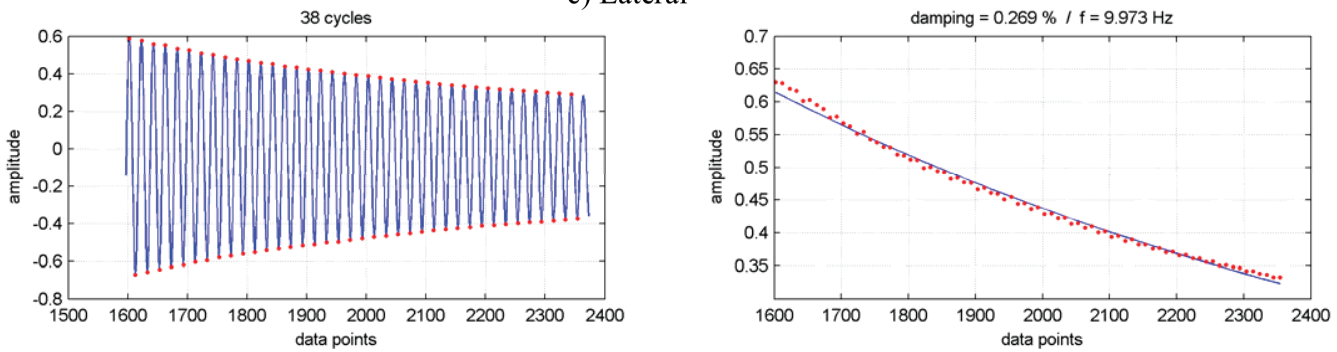

Figure 16 Non-Froude Scale 2% Damping In-service Tower – 1.93% - 4 Small Dampers, Pier Base Restrained (R007P001-3)

a) Longitudinal

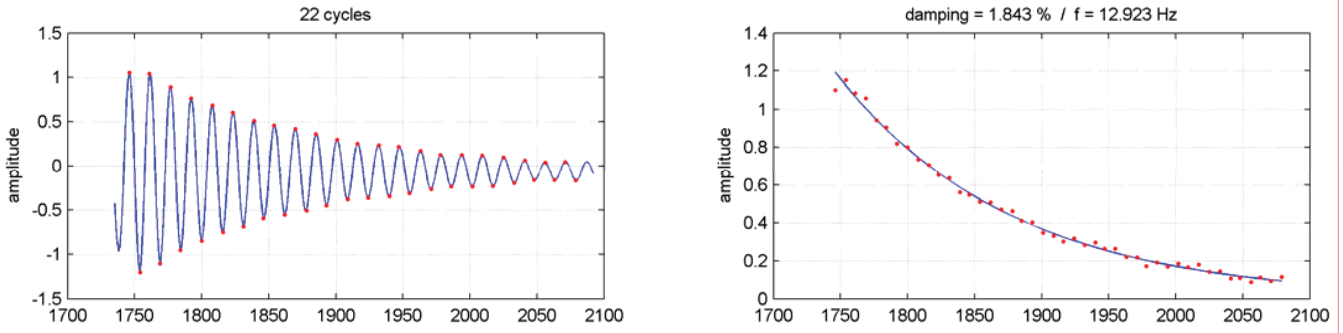

b) Torsion

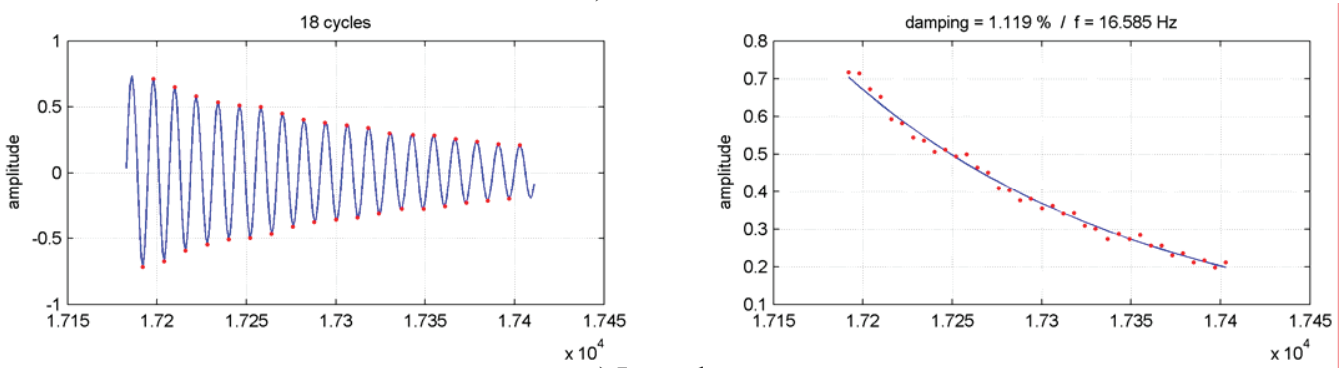

c) Lateral

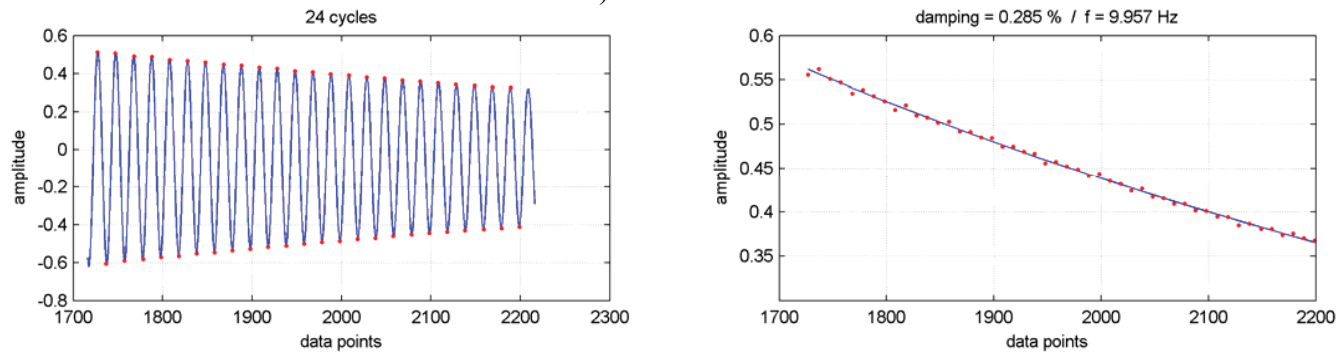

Figure 16 Non-Froude Scale 2% Damping In-service Tower – 1.93% - 4 Small Dampers, Pier Base Restrained (Repeat) (R008P001-3)